

PHOTOGRAPH THIS SHEET

DTIC FILE COPY

AD-A223 988

DTIC ACCESSION NUMBER

LEVEL

INVENTORY

AFOSR TR-90 0742

DOCUMENT IDENTIFICATION

4 AUG 1984

DISTRIBUTION STATEMENT A

Approved for public release;
Distribution Unlimited

DISTRIBUTION STATEMENT

ACCESSION FOR	
NTIS	GRA&I
DTIC	TRAC
UNANNOUNCED	
JUSTIFICATION	
BY	
DISTRIBUTION/	
AVAILABILITY CODES	
DISTRIBUTION	AVAILABILITY AND/OR SPECIAL
A-1	

DISTRIBUTION STAMP

DTIC
COPY
INSPECTED
6

DTIC
ELECTE
JUN 28 1990
S E D

DATE ACCESSIONED

DATE RETURNED

00 05 21 001

DATE RECEIVED IN DTIC

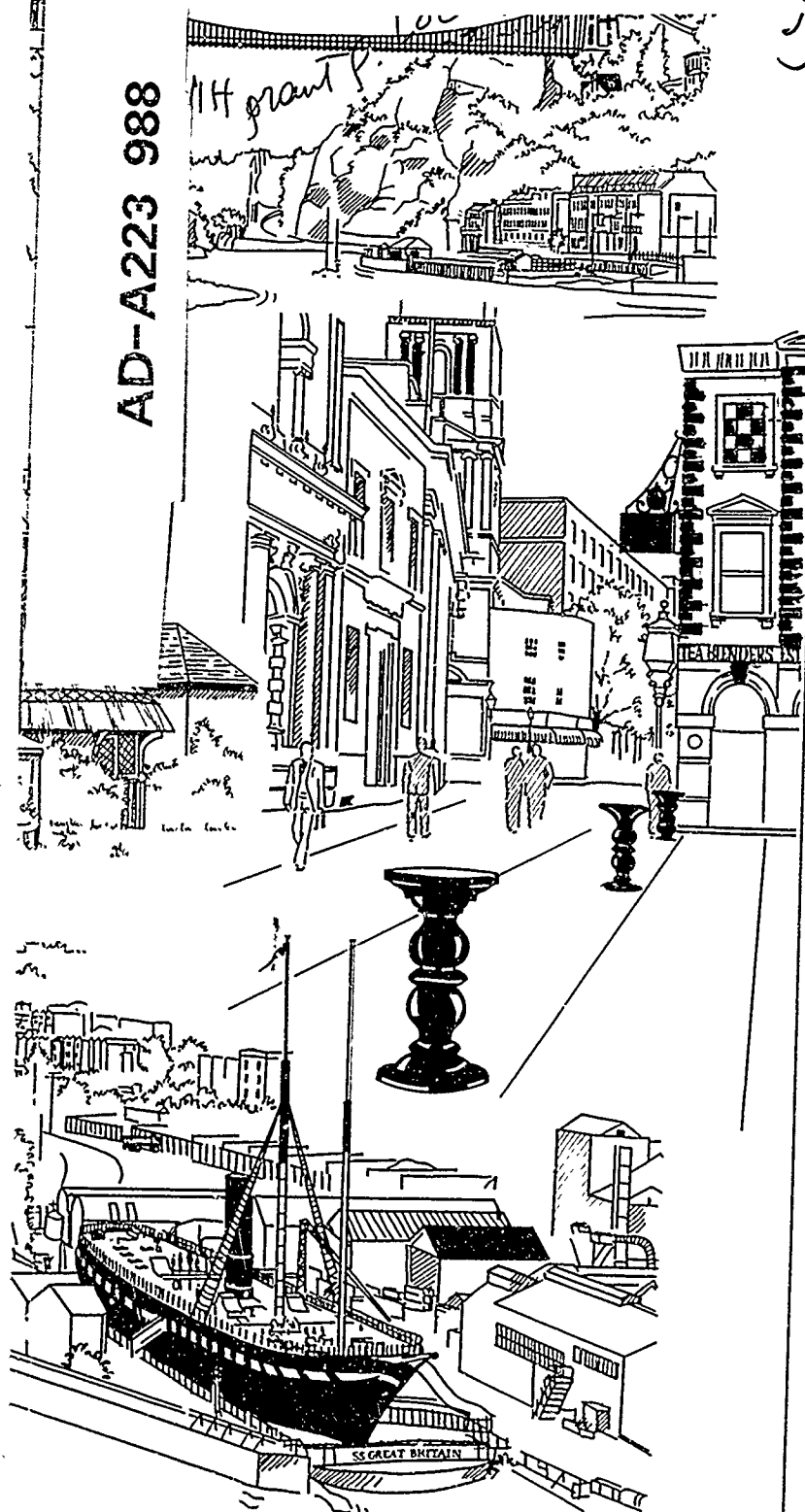
REGISTERED OR CERTIFIED NUMBER

PHOTOGRAPH THIS SHEET AND RETURN TO DTIC-FDAC

Hb (Köln) for Brunvic

AEOSR-TR- 90 0742

AD-A223 988



90 06 27 114

EISINGER

International
Union for
Pure and Applied
Biophysics
and
The Royal Society
of London

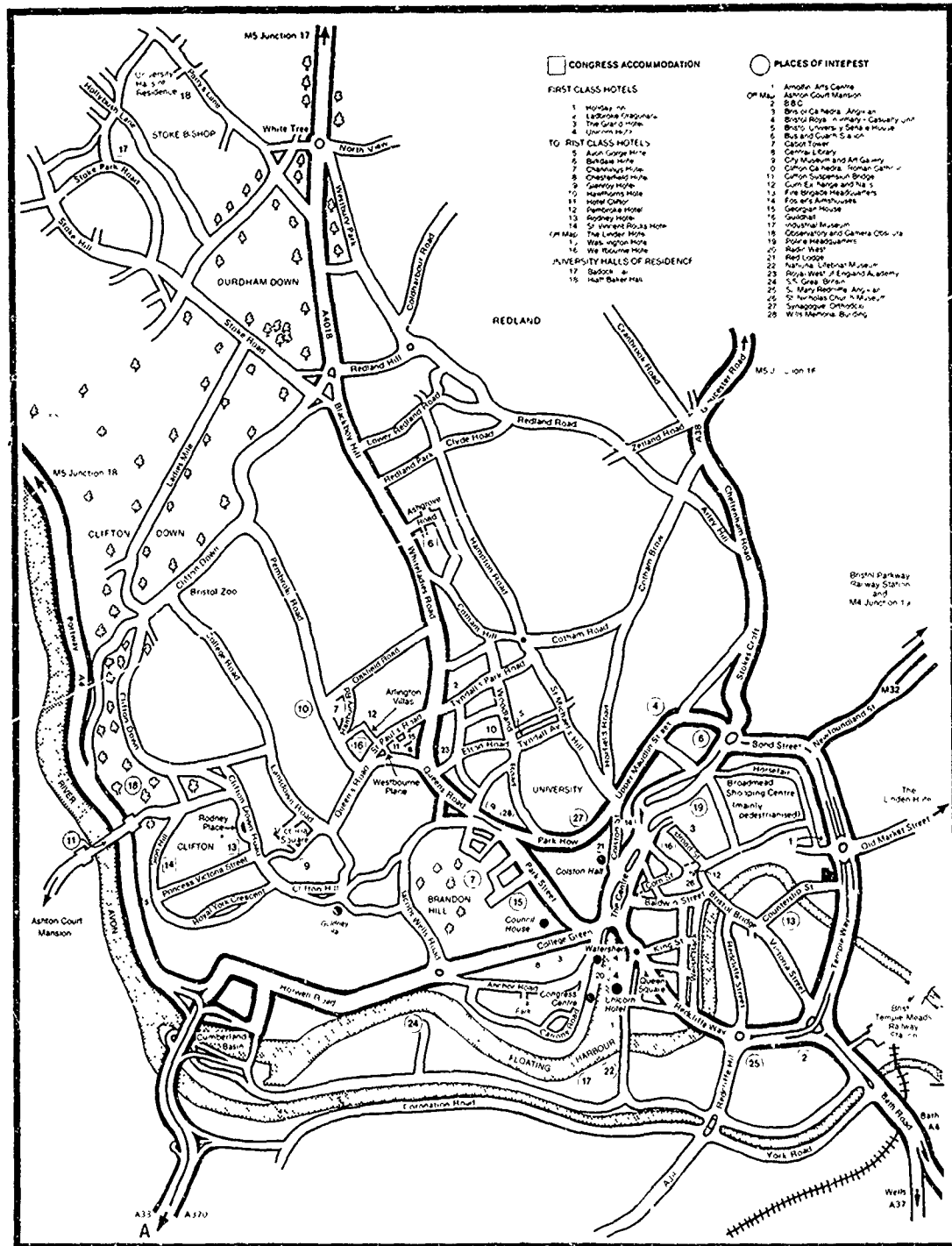


8th
International
Biophysics
Congress

The Floating Harbour
Bristol
United Kingdom
29 July - 4 August
1984

Final Programme
and
Book of Abstracts

THE CITY OF BRISTOL



Congress Venues around the Floating Harbour

Congress Centre
(City Docks Centre)

Canons Road
Bristol

Colston Hall
(Main Hall)

Colston Street
Bristol

Council House
(Conference Hall)

College Green
Bristol

Unicorn Hotel
(Trident Suite)

Prince Street
Bristol

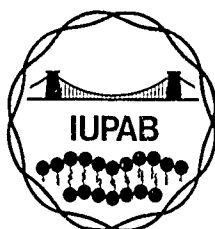
Watershed
(Cinema 1)

Canons Road
Bristol

REPORT DOCUMENTATION PAGE			Form Approved OMB No. 0704-0188	
<small>PUBLIC RELEASE UNDER E.O. 12958: THIS REPORT IS CLASSIFIED TO PROTECT THE NATIONAL DEFENSE AND THE LIFE OF THE UNITED STATES. IT IS THE POLICY OF THE GOVERNMENT TO MAKE THIS INFORMATION AVAILABLE TO THE PUBLIC AS SOON AS IT IS DETERMINED THAT IT IS NOT NECESSARY TO PROTECT THE NATIONAL DEFENSE AND THE LIFE OF THE UNITED STATES. IT IS THE POLICY OF THE GOVERNMENT TO MAKE THIS INFORMATION AVAILABLE TO THE PUBLIC AS SOON AS IT IS DETERMINED THAT IT IS NOT NECESSARY TO PROTECT THE NATIONAL DEFENSE AND THE LIFE OF THE UNITED STATES. IT IS THE POLICY OF THE GOVERNMENT TO MAKE THIS INFORMATION AVAILABLE TO THE PUBLIC AS SOON AS IT IS DETERMINED THAT IT IS NOT NECESSARY TO PROTECT THE NATIONAL DEFENSE AND THE LIFE OF THE UNITED STATES.</small>				
1. AGENCY USE ONLY (Leave blank)	2. REPORT DATE February 3, 1986	3. REPORT TYPE AND DATES COVERED Final/29/07/84-4/8/84		
4. TITLE AND SUBTITLE PROSPECTUS FOR SUPPORT OF A TRAVEL GRANT PROGRAM FOR THE VIII INTERNATIONAL BIOPHYSICS CONGRESS		5. FUNDING NUMBERS AFOSR-84-0110		
6. AUTHOR(S) Dr. Lee D Peachey				
7. PERFORMING ORGANIZATION NAME(S) AND ADDRESS(ES) Biophysical Society Office 9650 Rockville Pike Bethesda, MD 20814		8. PERFORMING ORGANIZATION REPORT NUMBER 61102F 2312/A3		
9. SPONSORING / MONITORING AGENCY NAME(S) AND ADDRESS(ES) AFOSR BLDG 410 BAFB DC 20332-6448		10. SPONSORING / MONITORING AGENCY REPORT NUMBER AFOSR-TR- 90 0742		
11. SUPPLEMENTARY NOTES				
12a. DISTRIBUTION / AVAILABILITY STATEMENT Approved for public release; distribution is unlimited.		12b. DISTRIBUTION CODE		
13. ABSTRACT (Maximum 200 words) The scientific programme comprised four plenary lectures, twentieth-eight Symposia with invited Speakers and Oral Presentations selected from Poster Contrigutions, and Poster Sessions. The Scientific Programme took place over a period of six days commencing on Sunday 29 july and finishing on Friday 03 August, 1984. Each day's Scientific Contributions were published as abstracts.				
14. SUBJECT TERMS		15. NUMBER OF PAGES		
		16. PRICE CODE		
17. SECURITY CLASSIFICATION OF REPORT unclassified	18. SECURITY CLASSIFICATION OF THIS PAGE unclassified	19. SECURITY CLASSIFICATION OF ABSTRACT	20. LIMITATION OF ABSTRACT	

AFOSR-TR 90-0742

8th International Biophysics Congress



The Floating Harbour
Bristol, United Kingdom
29 July - 04 August 1984

CONTENTS

Map of the City of Bristol	Inside Front Cover
Acknowledgements	3
The Week's Programme at a Glance	4
General Information	6
Congress Social Programme	9
Congress Scientific Programme	14
Sunday 29 July (white pages)	15
Monday 30 July (green pages)	17
Tuesday 31 July (cream pages)	89
Wednesday 01 August (white pages)	161
Thursday 02 August (blue pages)	175
Friday 03 August (pink pages)	247
A-Z Index of Presenting Authors	319
Satellite Meetings in Bristol	324
Congress Exhibitors	326
The Congress Centre at a Glance	330
Floor Plans of the Congress Centre	Inside Back Cover

Acknowledgements

Congress Sponsors

International Union for Pure and Applied Biophysics

I.U.P.A.B. Council Members

R.D. Keynes (President)	A.R. Gopal-Ayengar
S. Estrada O (Vice President)	C. Helene
B. Pullman (Vice President)	G.R. Ivanitsky
S. Ebashi (Hon. Vice President)	S. Maricic
K. Wuthrich (Secretary General)	L.D. Peachey
M. Baltscheffsky	W.E. Reichardt
M. Brunori	R. Villegas
L.C.M. De Maeyer	A. Wada
H. Eisenberg	

The Royal Society of London

Steering Committee

R.D. Keynes (Chairman)	W. Fuller
H.C. Watson (Secretary General)	M.J. Holwill
A.C.T. North (Treasurer)	C.F. Phelps
R.H. Adrian	D.C. Phillips
E.D.T. Atkins	D.C. Smith

Scientific Programme Committee

W. Fuller (Chairman)	J.R. Mallard
S.D. Dover (Secretary)	S. Neidle
E.D.T. Atkins	A.C.T. North
D.M. Blow	R.H. Pain
H. Gutfreund	D.C. Phillips
B. Katz	R.T. Tregear
R.D. Keynes	H.C. Watson
A. Klug	R.J.P. Williams

Local Committee

H.C. Watson (Chairman)	A. Keller
E.D.T. Atkins (Secretary)	A.A. Marsh
D. Carleton	J.H.M. Parry
H.V.S. Cornwell	V. Robinson
E.J. Davies	R.C. Thomas
H. Gutfreund	

Congress Hosts

The City of Bristol

The University of Bristol

The Congress Sponsors would like to thank the City and the University for accepting their invitation to act as Hosts to the Congress and its delegates.

Congress Supporters

*The Congress Sponsors gratefully
acknowledge the support of*

Amersham International plc
Cadbury Schweppes plc
Hewlett - Packard Ltd
Kelco/AIL International Ltd
Perkin - Elmer Ltd
RHM Research Ltd
The British Biophysical Society
The Leverhulme Trust
The Wellcome Trust
Wates Foundation

The Week's Programme at a Glance

Sunday - 29 July

Registration
Congress Centre

Delegates and Accompanying
Persons register in person
for the 8th International
Biophysics Congress
throughout the morning and
afternoon

Evening

The 8th International
Biophysics Congress will be
officially opened at the
Colston Hall in the early
evening

Colston Hall
Opening Ceremony

followed by

Plenary Lecture
B. Sakmann

and for Accompanying
Persons

Orientation Session
"An Introduction to Bristol"

Bristol University
Welcoming Receptions
Wills Memorial Building
and
Goldney Hall

(Buffet Dinner will be served
to residents in the University
Halls of Residence after the
Reception).

Monday - 30 July

Morning Symposia

Colston Hall
Chemical and Electrical
Regulation of Ion Channels

Council House
NMR in Vivo

Unicorn Hotel
Polymorphism and
Structural Transitions in
Nucleic Acids

Watershed
Food Biophysics

Afternoon Symposia

Council House
Nucleic Acid-Protein
Interactions

Unicorn Hotel
Processing and Control of
Visual Information

Watershed
Connective Tissue and
Bone

Poster Sessions Congress Centre

Chromatin Structure and
Function -- Molecular
Evolution -- Folding,
Dynamics and Solvation of
Macromolecules --
Electrostatic Effects in
Protein Function --
Viruses -- Dissipative
Structures and Pattern
Formation in Biological
Systems -- Rheology of
Cell Membrane

Social Programme

Bristol Heritage Walk
Bristol Waterfront Cruise
Bristol City Sightseeing
Tour
Bath
Bristol Heritage Walk

Evening

"Pub Crawl" Cruise
Caldicot Castle Banquet
Harvey's Wine Museum

Tuesday - 31 July

Morning Symposia

Colston Hall
Mechanisms of Transport
across Membranes

Council House
Cytoskeleton

Unicorn Hotel
Chromatin Structure and
Function

Watershed
Affinity Group Meeting on
Structure of Food
Biopolymers

Afternoon Symposia

Council House
Cross-Bridge Mechanisms
and Muscle Contraction

Unicorn Hotel
Education in Biophysics

Watershed
Viruses

Colston Hall
Plenary Lecture
E.H. Land

Poster Sessions Congress Centre

Polymorphism and
Structural Transitions
in Nucleic Acids --
Nucleic Acid-Protein
Interactions --
Metal-Proteins and
Electron Transfer --
Polysaccharides and
Glycoproteins --
Connective Tissue and
Bone -- Photosynthesis
-- Category 29: General

Social Programme

Bristol Heritage Walk
Bristol Waterfront
Cruise
Bristol City Sight-
seeing Tour
Slimbridge and the
Cotswolds
Butterflies and
Sherborne Castle
Bristol Heritage walk
Corsham Court

Evening

Caldicot Castle Banquet
Chequer's Inn Cruise
Theatre Royal in Bath -
"HMS Pinafore"
Harvey's Wine Museum
Classical Music Recital

Wednesday - 01 August

Morning Symposia

Colston Hall
Folding, Dynamics and
Solvation of
Macromolecules (Part 1)

Council House
Image Reconstruction

Unicorn Hotel
Dissipative Structures and
Pattern Formation in
Biological Systems

Watershed
Affinity Group Meeting on
Structure of Food
Biopolymers

Afternoon at Leisure
apart from
I.U.P.A.B. General
Assembly
Watershed

Social Programme
including
Evening Activities

Britol Hentage Walk
Bristol Waterfront Cruise
Brecon Beacons and Cardiff
Castle Banquet
Warwick Castle and Royal
Shakespeare Theatre
SS Great Britain
Bath
Bath and Theatre Royal in
Bath - "HMS Pinafore"
Wells, Glastonbury and
Shropshire's Clider Farm
Big Pit and Cardiff Castle
Banquet
Royal Shakespeare Theatre
"Richard III"
Theatre Royal in Bath - "
"HMS Pinafore"
Chequer's Inn Cruise
Harvey's Wine Museum

Thursday - 02 August

Morning Symposia

Colston Hall
Folding, Dynamics and
Solvation of
Macromolecules (Part 2)

Council House
Photosynthesis

Unicorn Hotel
Medical Imaging

Watershed
Affinity Group Meeting on
Structure of Food
Biopolymers

Afternoon Symposia

Council House
Molecular Evolution

Unicorn Hotel
Metal-Proteins and
Electron Transfer

Watershed
Polysaccharides and
Glycoproteins

Colston Hall
Plenary Lecture
A. Finkelstein

Poster Sessions Congress Centre

Cross-Bridge Mechanisms
and Muscle Contraction --
Cytoskeleton -- Electric
Field Effects in Cell
Membranes -- Photo and
Auditory Receptors --
Applications of Synchrotron
Radiation -- Developments
in Microscopy -- Image
Reconstruction --
Processing and Control of
Visual Information --
Environmental Biophysics
-- Education in Biophysics

Social Programme

Bristol Hentage Walk
Bristol Waterfront Cruise
Bath
Longleat
Chewton Cheese Dairy
Bristol Hentage Walk
Bowood

Evening

Official Congress Dinner
Grand Hotel

Friday - 03 August

Morning Symposia

Colston Hall
Electrostatic Effects in
Protein Function

Council House
Photo and Auditory
Receptors

Unicorn Hotel
Applications of
Synchrotron Radiation

Watershed
Rheology of Cell
Membrane

Afternoon Symposia

Council House
Electric Field Effects in
Cell Membranes

Unicorn Hotel
Developments in
Microscopy

Watershed
Environmental Biophysics

Colston Hall
Plenary Lecture
P.L. Privalov

followed by
Closing Ceremony

Poster Sessions Congress Centre

Chemical and Electrical
Regulation of Ion
Channels -- Mechanisms
of Transport across
Membranes -- Food
Biophysics -- NMR
in Vivo -- Medical
Imaging

Social Programme

Bristol Hentage Walk
Bristol Waterfront
Cruise
Wells and Glastonbury
Lacock and Bradford-on-
Avon

Evening

(Dinner will be served to residents in
the University Halls of Residence before
the Reception).

City of Bristol Civic Reception
Ashton Court Mansion

General Information

Banks

The Congress Secretariat was unable to persuade any U.K. Clearing Bank to establish a Banking counter in the Congress Centre. However, branches of all major Clearing Banks are located in Corn Street and these offer foreign exchange facilities during banking hours from Monday to Friday between 09.30 and 15.30.

Foreign Exchange facilities are available, at the Unicom Hotel, between 09.00 and 19.00 on both Saturday 28 July and Sunday 29 July to all delegates on production of evidence that they are associated with the Congress. During the rest of the week only those delegates who are residents at the Unicom Hotel may use these facilities.

Car Parking

There are numerous car parking spaces in the car park opposite the Congress Centre. The car park's vehicle entrance is on Anchor Road, but pedestrians can enter and leave the car park through a gate on Canon's Road, immediately opposite the main entrance to the Congress Centre. The fee for parking for the whole day is £1.00, and the ticket dispensing machines require 10p and 50p coins.

The small car park on the quayside, adjacent to the Congress Centre, is for permit holders only.

Free car parking facilities are available at the University Halls of Residence. Drivers are asked to ensure that, when parking, they do not block or impede the progress of Congress coaches.

Congress Centre

The Congress Centre has been designed as a "Common Room" or Club, with Bar and Restaurant facilities, where delegates can relax between symposia and meet up with friends and accompanying persons. It is also the location for the Poster Sessions, the Congress Exhibitors, the Congress Secretariat and the I.U.P.A.B. Secretariat.

Its official address is The City Docks Centre, Canon's Road, Bristol. It will remain open:

SUNDAY 29 JULY	08.30 hours – 19.00 hours
MONDAY through THURSDAY	08.30 hours – 21.00 hours
FRIDAY 03 AUGUST	08.30 hours – 17.30 hours

Congress Coaches

Congress coaches operate a regular shuttle service between the Congress Centre and the University Halls of Residence. Full details of this service are given in the Congress coach timetable, a separate leaflet included in the document wallet given to each delegate.

Congress coaches will board and disembark passengers for the shuttle service and the Social Programme activities at the main entrance to the Congress Centre, which is on Canon's Road.

Congress coaches, terminating at the University Halls of Residence, will turn around in the car park between Badock and Hiatt Baker Halls where they will disembark/board residents of Badock Hall before proceeding to the entrance of Hiatt Baker Hall to board residents from that Hall.

Congress Exhibition

The Congress Exhibition located on the ground floor of the Congress Centre will be open
MONDAY through FRIDAY 09.00 hours – 17.30 hours
Descriptions of the companies and their products are given in the "Congress Exhibitors" section, and their locations are shown on the floor plan at the back of this book

Congress Secretariat

The Congress Secretariat, located on the ground floor of the Congress Centre will be open:
SUNDAY through FRIDAY 09.00 hours – 17.30 hours

The main emphasis on Sunday 29 July will be on the provision of full Registration Documentation for all delegates and the settlement of any outstanding financial items. Registration desks have been allocated in geographical groupings in proportion to the number of delegates from those areas, with several desks set aside for the registration of Speakers and Travel Fellows. Reservations for Congress accommodation and Social Programme activities will be looked after at separate desks.

On Monday 30 July the Congress Secretariat desks will be re-organised into four sections:

- Congress Secretariat Information – General Information and Assistance including looking after Lost Property and dispensing tea and coffee vouchers
- New Registrations – including the issue of Exhibition Visitor Passes
- Congress Accommodation – including Travel Enquiries and finally
- Social Programme Reservations

If delegates and accompanying persons have any problems, please ask – the Congress Secretariat staff are here to help

Congress Scientific Secretariat

Full details are contained in the "Congress Scientific Programme – Introduction" section

Delegate Name Lists

Computer printouts showing delegates' names and addresses are available for inspection at the Congress Secretariat Information Desk, and delegates are welcome to use a dedicated V.D.U. terminal to interrogate the name and address file

Medical Emergencies

Delegates and accompanying persons can be treated under the normal provisions for overseas visitors made by the National Health Service. Delegates resident in hotels and University Halls should ask their hotel or University Hall management to contact a local General Practitioner (family doctor) on their behalf.

The nearest Accident and Emergency Department to the Congress Centre is the Casualty Unit at the Bristol Royal Infirmary, Marlborough Street, Bristol, which is shown on the map of the City of Bristol on the inside front cover of this book at location ④.

Messages

Noticeboards, displaying all public announcements, are situated on the ground floor of the Congress Centre, opposite the Congress Secretariat desks.

Private messages, for friends and colleagues, and incoming mail will be deposited in the Message Boxes, lettered A – Z, in the same location.

Paper, envelopes, drawing pins, photocopying etc. can be obtained from the Congress Secretariat for these purposes. To ensure that full use is made of these facilities, delegates are asked to routinely check the Noticeboards and Message Boxes.

Name Badges

Delegates and accompanying persons are asked to wear their name badges during the Congress. Unless badges are worn, admittance to the Congress Centre, Symposia, Plenary Lectures and other events will not be permitted.

Coloured dots on the name badges indicate a particular role in the Congress:

I.U.P.A.B. Council Members and Congress Organising Committee Members	Red
Symposia Chairmen and Speakers	Green
Congress Exhibitors	Yellow
Accompanying Persons	Blue

Post Office

The nearest Post Office to the Congress Centre is situated on the corner of Prince Street and Redcliffe Way, near the Unicorn Hotel.

Refreshments in the Congress Centre

Ground Floor – Lounge Bar and Quayside Bar

The following opening hours will be in operation for these two bars:
SUNDAY 29 JULY 08.30 hours – 19.00 hours
MONDAY through THURSDAY 08.30 hours – 21.00 hours
FRIDAY 03 AUGUST 08.30 hours – 17.30 hours
Delegates can relax, either inside the Congress Centre or on the Quayside, and enjoy light refreshments including tea, coffee and soft drinks. During licencing hours, at times to be advised, a full bar service will be in operation.

A fruit and ice cream stall will also be in operation.

First Floor – Restaurant and Bar

An informal Restaurant will be open:
SUNDAY through FRIDAY 10.00 hours – 17.30 hours
serving tea, coffee and soft drinks. Beer and wine by the glass will also be available within licenced hours, which have yet to be advised.

Each day the Restaurant will feature a range of light lunches, served buffet style, between 12.00 and 14.30, and in the afternoon, during Poster Sessions, speciality afternoon teas, for example strawberries and cream and Devonshire cream teas, will be available from 14.30.

Please note that waiter service will not be available in the Congress Centre.

Restaurants and Public Houses

The leaflet "Bristol by Night", included in the document wallet given to each delegate, gives the addresses of a wide variety of restaurants and public houses in Bristol.

The majority of restaurants in Bristol are closed on Sunday evenings. Hence residents at the University Halls are having a Buffet Dinner at 20.30 on Sunday 29 July after the Welcoming Reception, and delegates staying in hotels are advised to make arrangements to eat in their hotels on this night.

The "Public House" is a peculiarly British institution enabling those over eighteen years of age to purchase and consume alcoholic beverage on the premises during lunchtime and in the evening. Most pubs now serve food during lunchtime. In the dawn of female emancipation, enterprising publicans started to feature in their establishments a Lounge Bar (the "Smooth") where ladies were permitted, and a Public Bar (the "Rough") where the men were free to continue telling saucy jokes, play darts and engage in all sorts of other manly endeavour. As we all know, ladies are equal, so if during the Congress you come across a public house with two bars remember that the drinks in the public bar are cheaper. The bye-laws governing opening hours are even more arcane, but can be summarised reasonably accurately as follows:

Lunchtime Opening

MONDAY through SATURDAY 10.30 hours – 14.30 hours
SUNDAY 12.00 hours – 14.00 hours

Evening Opening

MONDAY through FRIDAY 17.30 hours – 22.30 hours
FRIDAY and SATURDAY 17.30 hours – 23.00 hours
SUNDAY 19.00 hours – 22.30 hours

Since there are numerous variations even around this basic pattern, as you can imagine, the average Brit is forced to rely on some subconscious collective folk memory in order to get him in and out of pubs at approximately the right time.

Symposia Venues

The venues being used for Symposia and Plenary Lectures are all within walking distance of the Congress Centre. The picturesque route being along the quayside to the Centre, rather than along Canon's Road.

The approximate seating capacities of the Symposia venues, which can be located on the map of the City of Bristol on the inside front cover of this book, are as follows:

Colston Hall	– Main Hall	1800
Council House	– Conference Hall	500
Unicorn Hotel	– Trident Suite	300
Watershed	– Cinema 1	200

Taxis

Despite the operation of Congress coaches, delegates may require taxi services. Two of the largest taxi operators, who offer a 24 hour service, are:

Streamline Black and White Taxis Limited

Telephone: Bristol 24001

ACE Taxis Limited

Telephone: Bristol 777477

Taxis are limited to carrying four passengers each, and a typical fare for a journey from the Congress Centre to the University Halls of Residence would be in the region of £2.50 to £3.00 plus a 10% ± tip at the passengers discretion. Please note that publication by the Congress does not imply recommendation.

Telephones

There are two, coin operated, public telephones situated in the foyer of the Congress Centre, beside the main staircase. To call a number in Bristol dial the number only. To call a number outside Bristol check the area dialling code.

The following Congress Secretariat telephone numbers are available for incoming telephone calls only.

SUNDAY through FRIDAY 09.00 hours – 17.30 hours

Congress Secretariat Information

Telephone: Bristol 272208

Social Programme Reservations

Telephone: Bristol 272207

Please note that these numbers are subject to final verification upon installation 24 hours before the start of the Congress. In the event of difficulty, please dial 100 and ask the telephone operator for assistance.

In the event of a real emergency, the "Fire", "Police" or Ambulance service may be summoned by dialling the numbers 999 and asking the telephone operator for the Emergency Service required. No money is needed to place such a call. Delegates are however cautioned that it is a punishable offence to waste the time of these emergency services and that these services must not be alerted unless there is a very serious risk of injury or damage occurring to persons or property without such immediate assistance.

9th International Biophysics Congress – Jerusalem – 1987

A representative of the Organising Committee, for the 9th Congress in Jerusalem in 1987, will be available, between Monday afternoon 30 July and Friday 03 August, at the Congress Secretariat desk to answer questions and receive suggestions from delegates. The 9th Congress will be receiving a Delegate Name and Address List, but it would be helpful if delegates could indicate to the representative any likely change of address and their interest in attending the 1987 Congress.

University Halls of Residence

The Congress Secretariat will maintain offices in Hiatt Baker Hall and Badock Hall throughout SUNDAY 29 JULY and also

08.00 hours – 10.00 hours EVERY MORNING

from 16.30 hours EVERY AFTERNOON

from MONDAY 30 JULY through to FRIDAY 03 AUGUST

Delegates are asked to routinely check the Congress Secretariat Noticeboards in the Halls of Residence for any announcements.

Full English Breakfast will be served every morning between 07.45 hours and 08.30 hours and dinner will be served to residents on Saturday 28 July, Sunday 29 July and Friday 03 August. Catering at other times will not be available.

Tea and coffee making facilities are available and Licensed Bars will be open in both Badock Hall and Hiatt Baker Hall until 23.00 hours every evening.

Delegates are encouraged to board the Congress coaches for the journey to the Congress Centre as soon as possible after the coaching operation starts at 08.15 hours every morning. This will enable all residents to arrive in time for the start of the morning Symposia. If a large number of residents choose to delay their departure from the University Halls until closer to 09.00 hours, it is highly likely that many of these delegates will miss the start of the morning sessions.

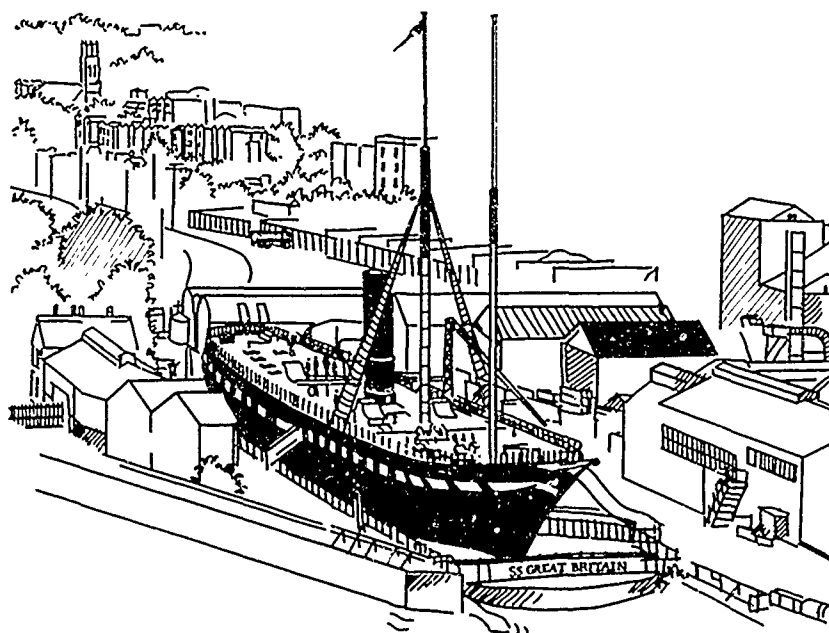
The Congress Secretariat staff at the University Halls can be contacted during the above office hours on the following telephone numbers:

Hiatt Baker Hall

Telephone: Bristol 681432

Badock Hall

Telephone: Bristol 681459



Congress Social Programme

Participation on all Congress Social Programme activities is by ticket only - since places on all activities are finite. Tickets and further information on prices, where applicable, may be obtained from the Social Programme Reservations desk, staffed by the Congress Secretariat, on the ground floor of the Congress Centre. Telephone enquires can be made on the local Bristol telephone number 272207 during office hours 09.00 - 17.30.

By Invitation

Bristol University Welcoming Receptions A01

The Chancellor of Bristol University, Professor Dorothy Hodgkin, has kindly invited delegates and accompanying persons to Welcoming Receptions at Bristol University on Sunday 29 July at 19.00, after the Plenary Lecture/Orientation Session in the Colston Hall.

In the Orangery at Goldney Hall for Residents staying at the University Halls and in the Linden Hotel.

Congress coaches will be available outside the Colston Hall from 18.30 for the journey to Goldney Hall, and will then be available to drive participants to the University Hall of Residence in time for dinner, which will be available for residents between 20.30 and 21.30, and to the Linden Hotel.

In the Great Hall of the Wills Memorial Building for all other delegates and accompanying persons.

It is a short walk to College Green and then up Park Street to the Wills Memorial Building, at the junction of Park Row and Park Street, and guides will be on hand to help with directions. No coach transport will be provided after the reception and participants will be free to make their own arrangements for dinner.

City of Bristol Civic Reception F07

The Right Honourable The Lord Mayor of Bristol, Councillor Claude Draper, has kindly invited delegates and accompanying persons to a Civic Reception on Friday 03 August. This farewell gathering for the Congress will be held in the house and grounds of the Ashton Court Mansion in the late evening from 21.00

Congress coaches will be available from 20.30 to collect participants, after they have had dinner, from their hotels and University Halls, and will then be available to return them at the end of the evening.

(Dinner will be available for residents at University Halls between 19.00 and 20.00 on this evening).

Official Congress Dinner

E08 E09

The OFFICIAL CONGRESS DINNER will be held at The Grand Hotel on Thursday 02 August. The 3-course menu E08 will include Baron of Beef piped in by a Scottish piper. An alternative vegetarian menu E09 will be available for those who have indicated this preference. Wine will be served with the meal.

Dress is informal, but gentlemen are asked to wear jackets and ties. Everyone is asked to assemble in Ballroom and Duchess Suite at 19.30 for dinner at 20.00 in the Wessex Suite.

A Cash Bar will be available for pre and after-dinner drinks, and similarly liquors may be ordered when the coffee is served.

Congress coaches will be available from 19.00 to collect participants from their hotels and University Halls, and will then be available to return them at the end of the evening.

Accompanying Persons

An Orientation Session for accompanying persons will take place on Sunday 29 July at 17.45 in the Little Theatre in the Colston Hall after the Opening Ceremony. This short presentation "Make the most of your stay with us - An Introduction to Bristol" has been specially designed by the City of Bristol Publicity and Information Office and the Corps of Guides in order to familiarise accompanying persons with the wide variety of things to do and places to see in and around Bristol.

Two special activities have been arranged for the enjoyment and interest of accompanying persons. These activities which take place every day, are informal and designed to give accompanying persons the opportunity to meet in a relaxed atmosphere. Both the Bristol Heritage Walks and the Bristol Waterfront Cruises commence from and return to the Congress Centre.

Bristol Heritage Walk B01 B05 C01 C06 D01 E01 E06 F01

These walks will enable participants to see a little of Bristol's particular charm, which lies in the variety of its architecture spanning 1,000 years. The morning walks last approximately 1½ hours. These walks include views of St. Mary Redcliffe (said by Elizabeth I to be 'the fairest church in all her realm'), the famous Nails and the picturesque Christmas Steps. The afternoon walks take about 2½ hours, and also include walking out of the city centre to the Cabot Tower from where there are magnificent views over the city.

Bristol Waterfront Cruise B02 C02 D02 E02 F02

Cruise aboard a traditional riverboat around the waterfront from which John Cabot set sail in 1497 to discover the continent of America. Bristol's subsequent prosperity depended on the ships and men who traded for cod in Newfoundland, sherry in Portugal, slaves in West Africa, and rum and molasses in the Caribbean. The cruise views the city from this perspective, then moors at the National Lifeboat Museum and the Industrial Museum, before continuing on to visit the S.S. Great Britain.

The Social Programme activities are coded alpha-numerically, for ease of reference, since this follows the style and format used in the Congress second circular. The Congress Social Programme Diary on page 13 uses these codes to highlight individual transport arrangements.

Daytime and Evening Activities

A wide variety of social activities has been arranged for delegates and accompanying persons which includes visits to magnificent castles and stately homes, drives through beautiful countryside and charming villages, visits to the theatre and a concert, and dining out in memorable surroundings.

The details of the tours are shown below in alphabetical order and in the Congress Social Programme Diary. All activities commence from the Congress Centre and participants are returned by free coach service, unless otherwise stated, to their hotel, University Hall of Residence or the Congress Centre as they desire. Guide books and entrance fees where applicable, are included in the charge for each activity. These activities are fully escorted and include local guides where appropriate

Bath and the Theatre Royal in Bath - "H.M.S. Pinafore" - *New Sadler's Wells Opera* B04 C10 D06 D07 D11 E03

Bath, one of the loveliest cities in Britain, grew up around the hot spring baths built by the Romans. The mineral waters proved so popular, that by the 18th Century, Bath had become the most fashionable inland resort to which all 'society' flocked led by the flamboyant Beau Nash. During this time, the elegant parks, crescents and Georgian houses, which give Bath its charming character, were built. Pulteney Bridge, lined with shops, is a particularly fine piece of architecture. Bath Abbey, which dates from 1499 is a most impressive building.

The two half-day tours D06 and E03 will visit the major attractions of Bath, by coach and on foot. The full day tour B04 includes visits to the main attractions plus the Costume Museum and Bath Carriage Museum, and will give participants a chance to wander round this delightful city and do some souvenir hunting.

Built in 1805, the Theatre Royal in Bath is one of Britain's oldest and most beautiful theatres. This is an opportunity to enjoy a performance of Gilbert and Sullivan's comic opera, with Nickolas Grace starring as Sir Joseph Porter, the insufferable Lord of Admiralty. So join Little Buttercup and the Jolly Jack Tars to give three cheers and one cheer more, for the captain of "HMS Pinafore." Theatre tickets and a cold buffet are included in the cost of tours C10, D07 and D11.

Bit Pit (Blaenavon) and Cardiff Castle Banquet D09

The Big Pit in Blaenavon was a South Wales coal mine for over one hundred years. Its life as a working pit ceased in 1980, and now it is a monument to the generations of Welsh miners who have spent their lives hewing coal from its seams. Visitors, equipped with safety helmets and cap lamps, can descend to the bottom of the 300 ft shaft - an unforgettable experience and an insight into the psychology of these proud "valley" people. (It is recommended that stout shoes and warm clothing are worn for this tour.) Then on to Cardiff, a major sea port and the capital of the Principality of Wales. Dine in mediaeval splendour in the Banquet Hall at Cardiff Castle, originally the site of a Roman fort and then a Norman castle. Guests are served traditional Welsh food, with red wine and mead (fermented honey) included in the price, and serenaded by a harpist and Welsh folk singers.

Bowood E07

An afternoon excursion to Bowood, the home of the Earl of Sherborne. The building is an outstanding example of 18th

Century architecture. Over half the house is open to the public including Robert Adam's famous library and the laboratory in which Dr. Joseph Priestley discovered oxygen gas in 1774. The park, laid out to the plans of 'Capability' Brown is one of the finest examples of the English style of landscape gardening

Brecon Beacons and Cardiff Castle Banquet D03

This is an ideal opportunity in the middle of the week to spend the day in the clear mountain air of South Wales. Stopping first at ruined Tintern Abbey, immortalised by Wordsworth, and then on to the historic market town of Monmouth on the Rivers Wye and Monnow, before entering the Brecon Beacons National Park, a magnificent area of hill country, 1000 feet above sea level, then descending the evocative Taff and Rhondda Valleys to Cardiff, the capital of the Principality of Wales (Remember to bring stout walking shoes.) Lunch is included at an inn in Monmouth and dinner will be a mediaeval banquet at Cardiff Castle - please see D09 for further details.

Bristol City Sightseeing Tour B03 C03

Two opportunities for participants to enjoy a morning's coach tour around Bristol, orientating themselves with the City's landmarks and learning more about its history. Participants will visit the famous Victorian Brunel's Suspension Bridge and his ironship, the S.S. Great Britain, the "village" of Clifton and the Downs

Butterflies at Compton House & Sherborne Castle C05

In the setting of Compton House and its grounds, participants see some of the world's most beautiful butterflies and moths, alive and flying in exotic surroundings of jungle plants. Lullingstone Silk Farm is another part of the attractions at Compton House. Lullingstone English silk has been supplied to the Royal Family for two coronations and many other Royal occasions.

Built for Sir Walter Raleigh in 1594, and the home of the Digby family since 1617, Sherborne Castle is a fascinating historic house with fine furniture, paintings and porcelain. The castle is set in a natural amphitheatre of wooded hills. In the parkland is a large ornamental lake, a home for many varieties of waterfowl. This delightful full day tour includes lunch.

Caldicot Castle Banquet B08 C08

Monday 30 July B08 and Tuesday 31 July C08 are the occasions to enjoy a traditional mediaeval banquet and be entertained by the "High Steward of the Court of Caldicot" and his minstrels. The four course banquet, served by "wenches" in mediaeval costume, includes Welsh broth, spare ribs of lamb, roast chicken basted in wine and honey and "creamed lover's well" and jugs of wine and Lindsfarne mead. Caldicot is a lovely old castle on the Welsh borders only half an hour's drive from Bristol.

Chewton Cheese Dairy E05

At Pnory Farm, Chewton Mendip, traditional cheese making can be seen every morning. Over the centuries commercial methods

of producing Cheddar have changed beyond recognition; but Chewton Cheddar is still made in the old way that first made Cheddar cheese famous. The milk comes every morning from the dairy's own cows and is carefully made by hand into cylindrical cheeses. A traditional 'Ploughman's' lunch at Pnory Farm is included on this four hour tour.

Classical Music Recital C12

An opportunity to listen to a fortepiano and violin recital in the splendid Great Hall of the Wills Memorial Building in the early evening on Tuesday 31 July.

Kenneth Mobbs and John Holloway will perform a selection of pieces including sonatas by Bach, Beethoven and Mozart. You are asked to be seated in the Great Hall by 19.00 hours at the latest. The Congress will not be providing coach transport either before or after the Recital

Corsham Court C07

A pleasant afternoon's visit to Corsham Court which was originally a Royal Manor in the days of the Saxon Kings. It was bought by the Methuen family in 1745 and has been the subject of architectural alterations by Nash and Bellamy. The spacious gardens, with many fine specimens, were laid out by 'Capability' Brown. The House is now also the home of the Bath Academy of Art

Chequer's Inn Cruise C09 D12

Take a romantic evening cruise up the River Avon on either Tuesday 31 July C09 or Wednesday 01 August D12 - leave the city behind and moor at a delightful riverside pub - The Chequer's Inn at Hanham. Enjoys a delicious 3 course dinner, including a glass of wine, at the Chequer's Inn before returning to Bristol by coach.

Harvey's Wine Museum B09 C11 D13

The Museum - the birthplace of Harvey's famous Bristol Cream Sherry - is the only one of its kind in Great Britain. It tells the story of how wines are made and displays the artices used in their production, serving and drinking - throughout it reflects Harvey's fine traditions and reputation. Of these three evening sherry tasting visits, B09 on Monday 30 July visits the Wine Museum only, while C11 and D13 on Tuesday 31 July and Wednesday 01 August also include a 3 course dinner at Harvey's fashionable restaurant.

Lacock and Bradford-on-Avon F06

Lacock Abbey was founded in 1232, and much of its 13th and 15th Century architecture has survived. The Abbey was converted into a Tudor dwelling house by Sir William Sharington. Since 1944, the National Trust has owned most of the village of Lacock, including old weavers' houses, an inn and a pack horse bridge. This delightful afternoon tour returns to Bristol via the attractive town of Bradford-on-Avon where the Church of St. Lawrence, one of the finest Saxon churches in England, is located.

Longleat E04

The full day tour to Longleat will give participants the chance to visit this remarkable showpiece, with extensive parkland and transformed into a Safari Park where lions, tigers, wolves, giraffes, zebras and other animals roam at will. The fine Elizabethan mansion of Longleat is the seat of the Marquis of Bath. The house has great mullioned windows, classic pillars, turrets and balustrades. The state rooms contain beautiful furniture, tapestries, fine pictures, costumes and superb libraries.

The tour will include a morning coach drive through the Safari Park, a buffet lunch and a guided tour of the house in the afternoon.

"Pub Crawl" Cruise B07

A "pub crawl" is a relaxed British pastime, which is best treated as a non-competitive sport. Originally a purely male affair, nowadays both sexes, provided they are over the age of 18 years, are welcome to participate. Participants imbibe one glass of ale, or other alcoholic beverage of their choice, at every "public house" they encounter during the course of the evening. The term "legless" invariably describes how participants feel at the end of the evening and hence the title "pub crawl"

To add a novel twist to the game, participants will voyage on a river boat between public houses and at the end of the evening coaches will carry the bodies back to their hotels and University Halls

IMPORTANT - The alcoholic beverages are not included in the price

Slimbridge & the Cotswolds C04

Slimbridge, founded by Sir Peter Scott, has the largest and the most varied collection of wildfowl in the world: over 2,500 birds of some 180 different species. At the Slimbridge Centre there are displays showing the extensive and varied work of the Wildfowl Trust. The tour returns to Bristol through the lovely hills and pretty villages of the Cotswolds.

SS Great Britain D05

This afternoon boat trip around Bristol Docks includes a visit to Brunel's SS Great Britain, launched in 1843. It was the first ocean-going propeller-driven ship. Near the SS Great Britain, the Bristol Industrial Museum is located. The museum houses exhibits illustrating Bristol's history in transport, including a unique steam carriage of 1897. The museum is linked to the SS Great Britain by a short railway line.

Warwick Castle & Royal Shakespeare Theatre - "Richard III" D04 D10

Warwick Castle is reputed to be the finest mediaeval castle in England. Surrounded by gracious parkland, the castle occupies a perfect setting on the banks of the River Avon. Within its massive walls and battlements there are magnificent state rooms and collections of armour, pictures and furniture.

Stratford-on-Avon has many Shakespearean associations, including the birthplace of the playwright, New Place, the site of his last home, and Holy Trinity Church where he is buried.

The full day tour D04 includes a visit en route to Bourton-on-the-Water and lunch at Warwick Castle. The afternoon tour D10 joins D04 for a performance of "Richard III" at the Royal Shakespeare Theatre, with dinner afterwards at the Box Tree restaurant.

This controversial history play, which ends with the Lancastrian victory over King Richard at Bosworth field, opened this summer to high critical acclaim for Antony Sher's brilliant interpretation of the mind within the deformed body of a king, whom Shakespeare implicates in the murder of the young Princes in the Tower.

Theatre tickets are included in the price of both tours.

Wells, Glastonbury & Sheppy's Cider Farm D08 F03

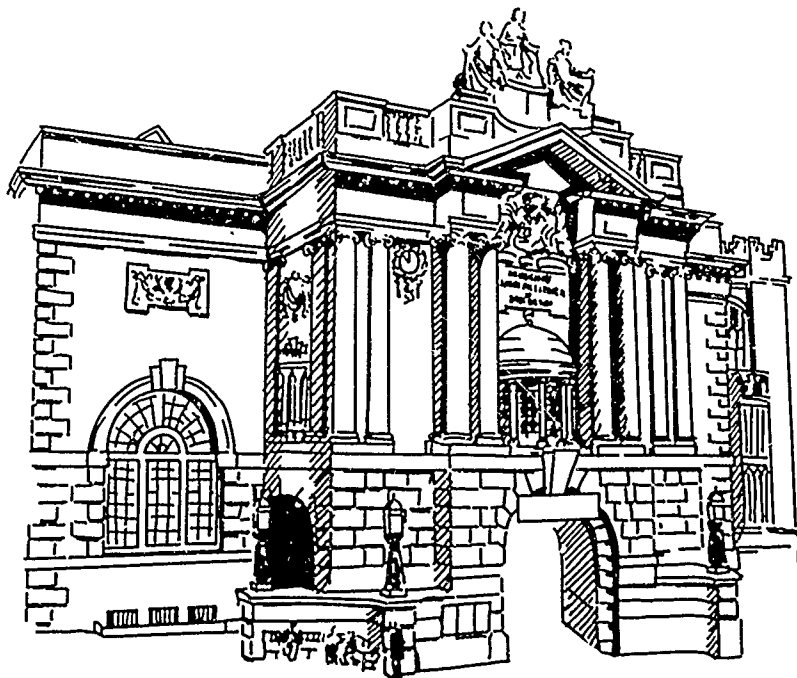
Wells Cathedral is one of the most beautiful in England. The west front of the Cathedral carries 237 mediaeval groups of sculpture extending across the whole facade. No other building in Europe can provide such an array of sculptured figures.

Glastonbury Abbey is the oldest religious foundation in the British Isles. Its origin and date are unknown. It is believed to have been visited by St. Patrick in the 5th Century. Myth and legend are part of the history of Glastonbury: the stories of Joseph of Arimathea and King Arthur have strong connections with the Abbey.

Sheppy's Farm at Bradford-on-Tone is one of the few remaining centres of traditional cider making. The tour round Sheppy's includes a visit to the apple orchards by tractor and trailer and a look round the cellars, press room and the "Farm and Cider Museum".

The morning tour F03 visits Wells and Glastonbury, while the afternoon tour D08 includes Wells, Glastonbury and Sheppy's Cider Farm and finishes off with dinner in Taunton.

*The City Museum
and Art Gallery*



Congress Social Programme Diary

Please refer to your Social Programme tickets for exact Joining Instructions.

Date	All activities start at the Congress Centre unless otherwise advised. Please see below.	Activity Start Time	Code	Activity	Meals Included	Approx. Finish Time	Activities Finish As Advised Below At Either or Both	
							Congress Centre	Hotels/ Uni. Halls
Sunday 29 July	After Plenary Lecture/Orientation Session, it is a short walk from the Colston Hall to the Wills Memorial Building	1900	A01	Brs of University Welcoming Reception in the Great Hall of the Wills Memorial Building	R	2000		Wills Memorial Building - No Coach Transport Provided
	After Plenary Lecture/Orientation Session, Congress Coaches will depart from the Colston Hall for the journey to Goldney Hall.	1900		in the Orangery at Goldney Hall	R	2000		Congress Coaches will return participants to the University Halls
Monday 30 July		0930	B01	Bristol Heritage Walk		1100	•	
		0930	B02	Bristol Waterfront Cruise		1230	•	
		0930	B03	Bristol City Sightseeing Tour		1230	•	
		0930	B04	Bath		1630	•	
		1400	B05	Bristol Heritage Walk		1600	•	
		1900	L07	Pub Crawl Cruise	R	2300		
		1830	B09	Caldicot Castle Banquet	D	2330		
		1900	B09	Harvey's Wine Museum	R	2030		
Tuesday 31 July	The Congress will not be providing coach transport for C12. Participants should make their own way to the Wills Memorial Building	0930	C01	Bristol Heritage Walk		1100	•	
		0930	C02	Bristol Waterfront Cruise		1230	•	
		0930	C03	Bristol City Sightseeing Tour		1230	•	
		0930	C04	Sandridge and the Cotswolds		1230	•	
		0930	C05	Butterflies and Sherborne Castle		1700	•	
		1400	C06	Bristol Heritage Walk	L	1600	•	
		1400	C07	Corsham Court		1700	•	
		1830	C08	Caldicot Castle Banquet	D	2330	•	
		1900	C09	Chequer's Inn Cruise	D	2330	•	
		1830	C10	Theatre Royal in Bath - "HMS Pinafore"	D	2330	•	
		1900	C11	Harvey's Wine Museum	D	2230	•	
		1900	C12	Classical Music Recital in the Great Hall of the Wills Memorial Building		2030		Wills Memorial Building - No Coach Transport Provided
Wednesday 01 August		0930	D01	Bristol Heritage Walk		1100	•	
		0930	D02	Bristol Waterfront Cruise		1230	•	
		0930	D03	Brecon Beacons and Cardiff Castle Banquet	LD	2330		
		0930	D04	Warwick Castle and Royal Shakespeare Theatre	LD	0100		
		1400	D05	SS Great Britain		1700	•	
		1400	D06	Bath		1700	•	
		1400	D07	Bath and Theatre Royal in Bath - "HMS Pinafore"	D	2330	•	
		1400	D08	Wells Glastonbury & Shepp's Cider Farm	D	2330	•	
		1400	D09	Big Pit and Cardiff Castle Banquet	D	2330	•	
		1400	D10	Royal Shakespeare Theatre - "Richard III"	D	0100	•	
		1830	D11	Theatre Royal in Bath - "HMS Pinafore"	D	2330	•	
		1900	D12	Chequer's Inn Cruise	D	2330	•	
		1900	D13	Harvey's Wine Museum	D	2230	•	
Thursday 02 August	Congress coaches will collect participants on E08/E09 from their hotels and University Halls commencing 1900 hours.	0930	E01	Bristol Heritage Walk		1100	•	
		0930	E02	Bristol Waterfront Cruise		1230	•	
		0930	E03	Bath		1230	•	
		0930	E04	Longleat	L	1600	•	
		1100	E05	Chester Cheese Dairy	L	1500	•	
		1400	E06	Bristol Heritage Walk		1600	•	
		1400	E07	Bowood		1700	•	
		1930	E08	Congress Dinner	D	2300		
			E09	Roast Beef Menu Alternative Vegetarian Menu in the Wessex Suite at the Grand Hotel				
Friday 03 August	Congress coaches will collect participants on F07 from their Hotels and University Halls commencing 2030 hours.	0900	F01	Bristol Heritage Walk		1030	•	
		0900	F02	Bristol Waterfront Cruise		1200	•	
		0900	F03	Wells and Glastonbury		1200	•	
		1300	F06	Lacock and Bradford-on-Avon		1600	•	
		2100	F07	City of Bristol Civic Reception in the House and Grounds of Ashton Court Mansion	R	2300		

Key to "Meals Included" L = Lunch D = Dinner R = Refreshments

Where there is a choice (shown above right by a •) of finishing an activity at either the Congress Centre or the Hotels/University Halls of Residence participants should make their wishes known to the Tour Escort/Driver at an early opportunity so that the route can be planned accordingly

Congress Scientific Programme

Introduction

The Scientific Programme comprises four Plenary Lectures, twenty-eight Symposia with invited Speakers and Oral Presentations selected from Poster Contributions, and Poster Sessions. The Scientific Programme takes place over a period of six days commencing on Sunday 29 July and finishing on Friday 03 August. Each day's Scientific Contributions are published in the following pages, where different coloured paper has been used to emphasise the different days of the week.

Congress Scientific Secretariat

The Congress Scientific Secretariat is open every day of the Congress between 09 00 hours and 17.30 hours and is situated on the first floor of the Congress Centre. Its location is shown on the floor plan at the back of this book

Assistance to Speakers

Technicians will be on hand in the Symposia venues, 30 minutes before the start of each Symposium and Plenary Lecture, and also during the mid-point breaks for tea and coffee, to give advice and assistance as Speakers familiarise themselves with the audio visual equipment available

Speakers, who intend using 35 mm slide projection to illustrate their talk, are invited to collect a carousel from the Congress Scientific Secretariat 24 hours before their talk, so that they can load their slides at leisure. These carousels should be returned empty to the Technician at the end of the Symposium or Plenary Lecture. (Please note that the technicians will not be available to assist Speakers load their slides into the carousels).

Tea and Coffee Vouchers

A voucher system will be introduced for the payment of tea and coffee in the Symposia venues, during the mid-point breaks announced by Symposia Chairmen.

These tea and coffee vouchers should be purchased, in advance, from the Congress Secretariat Information desk on the ground floor of the Congress Centre, and should be handed over to the catering staff in the Symposia venues in exchange for a cup of tea or coffee. These vouchers must be purchased in advance since the caterers cannot accept cash.

Posters Sessions

"When Is my Poster Session"

Contributions, including those selected for oral presentation, will be presented in the form of a poster at the Poster Sessions, which will cover the same twenty-eight topics as the Symposia Contributions, which are not amenable to such categorisation, will be presented at a special Poster Session "Category 29: General". The different topics which will be covered on each of the four Poster Session days, between 09.00 hours and 17.15 hours, are shown on the timetables for Monday, Tuesday, Thursday and Friday.

"Where Is my Poster Board"

An A - Z Index of Authors has been provided, at the back of this book, to enable presenting authors to locate the page number on which their abstract appears.

Each page then shows the day on which a Poster Session on a particular topic category takes place and also, top left corner above each abstract, the poster board number which has been allocated to each contribution on that day.

If your abstract has not been published, you should ask the Congress Scientific Secretariat to allocate a poster board to you.

you will, if possible, be allocated a poster board within the section reserved for Published Abstracts on your topic category, and you will be given a "Late Entry" sign to emphasise to other delegates that they will not have had the opportunity to read your abstract in the Book of Abstracts.

There are two hundred and eighty-two poster boards, numbered 001 - 282, on the first floor of the Congress Centre. Their location is shown on the floor plan at the back of this book

"How do I present my Poster"

Each poster board is 125 cm (4 ft) wide and 75 cm (2 ft 6 in) deep, with its number in the top left hand corner. The Congress Scientific Secretariat will provide presenting authors with drawing pins to put up their posters.

Each poster must be labelled at the top with the abstract title, the names of the presenting author and any co-authors, and the address of the Institution where the research was carried out. The lettering for this section should be at least 2.5 cm high. A copy of the abstract should be attached to the top left hand corner. Typed material should be in a large type face, hand lettering should be at least 1 cm high, while charts and illustrations should be simply but boldly drawn.

Presenting authors are asked to observe the following time schedule for Poster Sessions:

09.00 - 09.30

Presenting authors should set up their posters before the start of the morning's Symposia

09.30 - 14.00

Delegates are welcome to examine the posters at their leisure

14.00 - 17.00

Presenting authors should attend their posters throughout the afternoon discussion period

17.00 - 17.15

Presenting authors must take down their posters (Please note that the Congress Scientific Secretariat cannot be responsible for, or be expected to store, poster material).

Oral Presentations

Speakers, whose poster contributions have been chosen for Oral Presentation at the relevant Symposium, are shown by name and poster no. on each day's timetable. The headline "Oral Presentation" is used in this book and on poster boards during Poster Sessions to highlight their contributions

Sunday 29 July

Registration

Congress Centre
09.00 - 16.00

The Congress Secretariat, situated on the Ground Floor of the Congress Centre, will be open until 16.00 hours for delegates to register in person and collect a copy of the Final Programme and Book of Abstracts, their name badge and tickets for the Social Programme.

Delegates and accompanying persons should be seated in the Colston Hall (Main Hall), either in the "Stalls" on the Ground Floor or in the "Balcony" on the First Floor, by 16.55 hours in time for the start of the Opening Ceremony.

Opening Ceremony

Colston Hall - Main Hall
17.00 - 17.30

Welcome Address by
The Right Honourable the Lord Mayor of Bristol,
Councillor Claude Draper

Response by Professor R.D. Keynes F.R.S.
The President of the International Union for Pure and
Applied Biophysics

Opening Address by the Guest of Honour
The Chancellor of Bristol University, Professor Dorothy
Hodgkin O.M., F.R.S.

In attendance, the trumpeters and footmen of the City of
Bristol.

Intermission

17.30 - 17.45

Accompanying persons move to the Little Theatre on the
Ground Floor of the Colston Hall.

Plenary Lecture

Colston Hall - Main Hall
17.45 - 18.30

Delegates only

"Ion Transport through Single Membrane Pores in
Biological Membranes"

B. Sakmann (Göttingen)

The British Biophysical Society Lecture

Orientation Session

Colston Hall - Little Theatre
17.45 - 18.30 *Accompanying Persons only*

"Make the most of your stay with us - An Introduction to
Bristol"

A presentation by the City of Bristol Publicity and Information
Office and the Corps of Guides.

Delegates and accompanying persons will be able to meet up
in the foyer of the Colston Hall, when the Plenary Lecture and
Orientation Session finish.

Bristol University Welcoming Receptions

The Chancellor of Bristol University has kindly invited
delegates and accompanying persons to Welcoming
Receptions.

Goldney Hall - Bristol University
19.00 - 20.00

Those staying at the University Halls and the Linden Hotel
should board the Congress coaches which will be parked
outside the Colston Hall for the short drive to Goldney Hall,
where their reception in the attractive surroundings of the
Orangery is to be held.

Congress coaches will be available after the reception at
Goldney Hall to take delegates and accompanying persons to
the University Halls of Residence in time for their buffet dinner
which will be available between 20.30 and 21.30 for residents

Wills Memorial Building - Bristol University

19.00 - 20.00

All other delegates and accompanying persons are invited to
attend their reception in the Great Hall of the University. This
is a short walk to College Green and up Park Street to the
Wills Memorial Building, one of the city's landmarks at the
junction of Park Row and Park Street. Guides will be on hand
to help direct you.

Delegates and accompanying persons, who are staying in
hotels, are advised to make arrangements to eat in their
hotels, since many of the city's restaurants are closed on
Sunday nights.

ION TRANSPORT THROUGH SINGLE MEMBRANE PORES IN BIOLOGICAL MEMBRANES
B. Sakmann, Abt. Neurobiologie, Max-Planck-Institut für biophysikalische Chemie, Am Faßberg, D-3400 Göttingen, F.R.G.

Transmitter and voltage activated membrane currents observed in biological membranes are composed of many 'elementary' current contributions each of a few Picoamperes (10^{-12} A) in size which reflects the opening and closing of a single transmembrane channel or pore. Such elementary currents can be measured directly by restricting the current measurement to a small area ($5-10 \mu\text{m}^2$) of membrane. The membrane patch is electrically and mechanically isolated from the rest of the cell membrane. It spans the tip of a glass-pipette; ion composition on both faces of the membrane and the voltage across the membrane patch can be changed at will.

So far all channels examined by this method activated either by a ligand or by membrane voltage exhibit steplike elementary currents. They reflect the opening and closing of a single ion channel. Two classes of questions can be examined with single channel recording. One is related to the mechanism of ion transport through the open channel. The current step amplitude is measured as a function of concentration of the permeating ion and membrane voltage. The other class is related to the mechanism of opening and closing of the channel. The distributions of duration of current steps and the intervals between adjacent steps can be used to derive a plausible reaction mechanism governing the switching of the channel.

A particularly well examined membrane channel is the Acetylcholine Receptor-channel which transports monovalent cations. It is a pentameric transmembrane protein which is switched on and off by the transmitter acetylcholine (ACh). The distribution of current step sizes made with AChR-channels in skeletal muscle indicates that this channel can adopt several conductance states. Transport of Na^+ through the open channel can be described by a simple 2B1S model. In physiological ion concentration the channel is nearly saturated. The distribution of durations of current steps and intervals between them shows that the AChR channel can adopt two different open states of the same conductance but largely different life times (300 μsec and 3-4 msec). The channel also adopts, in the presence of ligand, at least five closed states with life times ranging from 20 μsec to >10 sec. The dependence of the distribution time constants on ACh concentration and on the nature of the ligand shows that the AChR channel opens with high efficiency once the receptor is doubly liganded. The opening rate β exceeds the closing rate α nearly 50fold. An estimate of the intrinsic dissociation constant K_D for ACh binding to the receptor is in the order of 100 μM . The combination of a high K_D value and a high β/α ratio is characteristic for a receptor-channel at a rapidly transmitting excitatory synapse.

Essentially similar observations are made on transmitter gated ionic channels present in the soma membrane of neurones from the central nervous system which transport anions and which are gated by GABA or Glycine, the transmitters at inhibitory synapse. The various parameters describing ion transport and channel gating are fingerprints for a given molecular species of ion channel. They will be helpful to relate functional properties of ion channels to their molecular structure.

Monday 30 July

Symposia

09.30 - 12.30

Chemical and Electrical Regulation of Ion Channels

NMR in Vivo

Polymorphism and Structural Transitions in Nucleic Acids

Food Biophysics

14.00 - 17.00

Nucleic Acid-Protein Interactions

Processing and Control of Visual Information

Connective Tissue and Bone

Poster Sessions

Chromatin Structure and Function

Molecular Evolution

Folding, Dynamics and Solvation of Macromolecules

Electrostatic Effects in Protein Function

Viruses

Dissipative Structures and Pattern Formation in
Biological Systems

Rheology of Cell Membrane

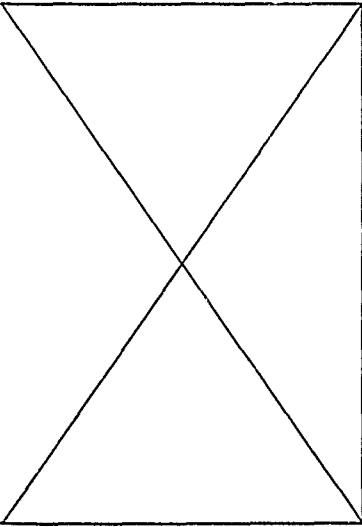


*The "Nails" or 17th century
trading tables in Corn Street
- believed to be the origin of
the phrase "To pay on the
nail".*

Monday 30 July

Colston Hall Main Hall	Council House Conference Hall	Unicorn Hotel Trident Suite
Chemical and Electrical Regulation of Ion Channels Chairman: R.D. Keynes (Cambridge) Speakers: C.F. Stevens (Yale) F. Bezanilla (California) F.J. Sigworth (Gottingen) and Authors of Posters F.B. Conti (045) P.G. Kostyuk (014)	NMR in Vivo Chairman: G.K. Radda (Oxford) Speakers: R.G. Shulman (Yale) J. Schaefer (Monsanto) G.K. Radda (Oxford) and Authors of Posters G. Navon (270) A. Haase (267)	Polymorphism and Structural Transitions in Nucleic Acids Chairman: S. Arnott (Purdue) Speakers: S. Arnott (Purdue) Z. Shakked (Weizmann) D.J. Patel (Bell) V.I. Ivanov (Moscow) and Author of Poster L.R. Hallam (045)
12.30 Morning Coffee 10.50-11.10	Morning Coffee 10.50-11.10	Morning Coffee 10.50-11.10

Break for Lunch (90 Minutes)

14.00 	Nucleic Acid-Protein Interactions Chairman: C. Helene (Paris) Speakers: B.W. Matthews (Oregon) R. Giege (Strasbourg) R. Kaptein (Groningen) and Authors of Posters M.R. Sanderson (078) K. Morikawa (079)	Processing and Control of Visual Information Chairman: W. Reichardt (Tubingen) Speakers: T.N. Wiesel (Rockefeller) M. Ito (Tokyo) B. Julesz (Bell) and Authors of Posters Y.J. Wang (236) S. Endo (235)
17.00 17.15	Afternoon Tea 15.20-15.40	Afternoon Tea 15.20-15.40

Timetable

<p>Watershed Cinema 1</p>	<p>Congress Centre First Floor</p> <p>Presenting Authors should set up their Posters before the start of Today's Symposia</p>
<p>Food Biophysics</p> <p>Co-Chairmen: A.J. Bailey (MRI Bristol) P.J. Lillford (Unilever, Colworth)</p> <p>Speakers: G.W. Offer (Bristol) P. Walstra (Netherlands) F. Franks (Cambridge)</p> <p>Morning Coffee 10.50-11.10</p>	<p>Poster Sessions</p> <p>Chromatin Structure and Function Poster Nos: 001-024</p> <p>Molecular Evolution Poster Nos: 025-042</p> <p>Folding, Dynamics and Solvation of Macromolecules Poster Nos: 043-198</p> <p>Electrostatic Effects in Protein Function Poster Nos: 199-216</p> <p>Viruses Poster Nos: 217-228</p> <p>Dissipative Structures and Pattern Formation in Biological Systems Poster Nos: 229-246</p> <p>Rheology of Cell Membrane Poster Nos: 247-282</p>
<p>Connective Tissue and Bone</p> <p>Chairman: J. Engel (Basel)</p> <p>Speakers: A. Miller (Edinburgh) W. Traub (Weizmann) J. Engel (Basel) and Authors of Posters D.A. Torchia (176) C.C. Danielsen (175)</p> <p>Afternoon Tea 15.20-15.40</p>	<p>Presenting Authors should attend their Posters throughout the Afternoon Discussion Period.</p> <p>Presenting Authors must take down their Posters</p>

Symposium on Chemical and Electrical Regulation of Ion Channels

ESTIMATES OF OCCUPANCY PROBABILITIES FOR STATES OF THE MAMMALIAN SODIUM CHANNEL FROM SINGLE CHANNEL RECORDINGS

C.F. Stevens, Section of Molecular Neurobiology, Yale University School of Medicine, 333 Cedar St., New Haven, CT, USA.

We have used the single channel recording method to study cell-attached membrane patches containing only a few (one to four) sodium channels. Most of our experiments used mouse neuroblastoma cells. We measure: single channel current magnitude, dwell time in the open state, number of channel openings per depolarization epoch, and latency to first channel opening after onset of the depolarization. We further estimate the occupancy probability of four operationally defined states: (1) the open state, (2) a state (or group of states) immediately adjacent to the open state, (3) the inactivated state (or states), and (4) all other states. Occupancy of the open state is determined directly, occupancy of the inactivated state is estimated by prepulse inactivation experiments, occupancy of the adjacent state is evaluated from the derivative of the distribution function for first entry into the open state, and the occupancy of other all other states is obtained from conservation of probability.

Our main conclusions are: (1) Sodium channel behavior can, for the level of resolution in our experiments, be accurately described in terms of a simple four state system. (2) Inactivation rates for closed states is less than that for the open state. (3) Inactivation rate from the open state is voltage independent, but rates of inactivation from closed states vary with membrane potential. (4) There is only a single open state. (5) Transitions between states are consistent with an exponential dependence of rates on voltage.

Symposium on Chemical and Electrical Regulation of Ion Channels

VOLTAGE DEPENDENCE OF THE SODIUM AND GATING CURRENTS.

F. Bezanilla, J. R. Stimers and R. E. Taylor. Department of Physiology, UCLA Laboratory of Biophysics NINCDS, NIH and Marine Biological Laboratory, Woods Hole, U.S.A.

The activation and inactivation of the sodium conductance have been represented as a multistep model with data derived from several voltage clamp protocols to study sodium and gating currents in the squid giant axon. The first series of experiments was a study of the relationship between charge vs. voltage (Q-V) and fraction of open channels vs. voltage (f-V) curves. The Q-V curve shows significant voltage dependent charge movement at potentials more negative than -70 mV (the "bump") but most of the charge moves between -70 and +50 mV. In axons with inactivation intact, the f-V curve, estimated as the peak sodium current divided by the instantaneous current, is a sigmoid curve that rises at potentials more positive and more steeply than the Q-V curve. A comparison of the normalized Q-V and f-V curves shows that the f-V curve lies below the Q-V curve at negative potentials but crosses the Q-V curve at 0 mV. When the experiments were repeated using pronase to remove fast inactivation, we found that the f-V curve is always less than the Q-V curve but they saturate together at large depolarizations, a result consistent with the notion that all the charge is associated with sodium channel gating. The total charge moved between -150 mV and 50 mV is about $1800 \text{ e}^-/\mu\text{m}^2$ and it is not significantly different from the charge measured in axons with inactivation intact. The second series of experiments correlated the time shift of the sodium current and the gating current when the initial potential was varied. Hyperpolarizing prepulses delay both currents the same amount and depolarizing prepulses decrease the lag in the sodium current turn-on and shorten gating current decay. The correlation of the time shift of both currents is paralleled by an extra charge movement occurring in the region of potentials more negative than -70 mV. This extra charge movement corresponds to the extra "bump" of the Q-V curve observed in the negative region of potentials. The third series of experiments was a study of the early events in sodium activation. Gating currents were recorded with improved time resolution to decide upon the presence of rising phase. We found that some axons do not show a rising phase and in the axons in which it is present, the capacitive current shows a slow component. We are able to decrease or abolish the rising phase along with the slow component of the capacitive current making the external solution hypertonic with respect to the internal solution. The results are consistent with the idea that the rising phase (and the slow component of the capacitive transient) are produced by a distributed series resistance in the periaxonal space and the conclusion is that if the sodium gating current has a rising phase it must be shorter than 5 to 10 microseconds.

These results have allowed us to propose a multistate model of the sodium channel which has the following characteristics. 1) There are several closed steps that occur as transitions in the negative voltage range. These steps are responsible for the lag of the sodium current turn-on and the sodium and gating current time shifts seen with prepulses. 2) The transition from the most closed state to the next closed state is as fast or perhaps faster than the next transition to explain the absence of rising phase. 3) The inactivation of the conductance is the result of an interaction of the activating gating particle and the inactivating particle which results in an stabilization of the inactivating particle when the activating gating particle is near to the open position. 4) The transition of the inactivating particle is slightly voltage dependent but it contributes a negligible gating current of its own. This voltage dependence explain the crossover of the Q-V and f-V curves in axons with intact inactivation.

Supported by USPHS Grant GM30376.

Symposium on Chemical and Electrical Regulation of Ion Channels

PROTEIN DYNAMICS OBSERVED IN REAL TIME: CURRENT FLUCTUATIONS IN 'OPEN' IONIC CHANNELS.

F.J. Sigworth, Max-Planck-Institut für biophysikalische Chemie, Postfach 2841, Göttingen, F.R.G.

A single ionic channel typically transports 10^7 ions/sec across a cell membrane. Considerable changes in this flux are expected to result from small changes in the electrostatic or chemical environment of the ion pathway; thus the current through a channel could be used to report certain small motions of the channel molecule provided that the motions are fairly slow, and that the current can be measured with sufficient resolution. The patch-clamp technique for recording membrane currents presently has a background noise level of ~ 100 elementary charges rms (in the range 1-10 kHz) and is in fact sensitive enough to detect the "shot noise" fluctuations due to the random passage of ions through a channel. An investigation of currents in acetylcholine receptor channels shows fluctuations that are considerably larger than expected from shot noise and which probably arise from internal motions of the receptor protein.

For the experiments, primary cultured rat muscle cells (myoballs) were used, and patch recordings were made in cell-attached as well as cell-free configurations (Hamill et al., Pflügers Arch., 391:85, 1981). At fairly low temperature (7°) the acetylcholine receptors in these cells carry currents of 2.2 pA and have a mean open time of 30 ms. Power spectra of the fluctuations were computed by taking the difference of spectra computed from segments when one channel was open and from baseline segments. The spectra show a flat high-frequency asymptote (to 10 kHz) but a large low-frequency excess, which can be well fitted by a single Lorentzian component with a corner frequency in the range of several hundred Hertz.

This low-frequency component can be readily seen in appropriately-filtered experimental records. Its amplitude scales with membrane potential like a conductance fluctuation, and represents a rms variation of about 3 %. The fluctuations probably arise from internal motions of the receptor rather than, say, lateral diffusion in the membrane because (1) the relaxation time (but not the amplitude) of the fluctuations is as highly temperature-dependent as the channel open time ($Q_{10} \approx 3$); and, (2) the spectrum is unlike that expected for an unrestricted diffusion process.

Analysis of the amplitude distribution of the slow fluctuations shows that they do not arise from stepwise transitions between two levels of conductance, but must come from a multi-step or continuous variation. A statistical test for coupling between the fluctuations and the channel open-close transitions was negative, placing an upper bound of about $kT/2$ on the coupling energy between the processes. Reducing the ionic strength however causes the fluctuations to become relatively larger; this suggests that they may arise through electrostatic interactions which become larger when ionic shielding is reduced.

The high-frequency asymptote of the spectrum was typically 3 - 6 times the density expected for shot noise. In cases where the value was large, an analysis of the amplitude distribution showed that it partly resulted from brief (~ 10 μ s) interruptions in the channel current. In cases where the high-frequency density was only about 3 times the shot noise level, the amplitude distribution was indistinguishable from Gaussian, suggesting that the underlying process is very rapid (< 2 μ s) and might in fact represent fluctuations in channel structure on the time scale of ion transport (~ 100 ns).

Monday 30 July Council House-Conference Hall 09.30-12.30

Symposium on NMR in Vivo

^{31}P , ^{13}C and ^1H HIGH RESOLUTION STUDIES IN VIVO. K.L. Behar, O.A.C. Petroff,⁺ J.A. den Hollander, M. Stromski, H.P. Hetherington, D.L. Rothman, J.W. Prichard⁺ and R.G. Shulman, Departments of Molecular Biophysics and Biochemistry and Neurology⁺, Yale University, New Haven, CT 06511.

We have followed metabolism in the brain of the living rats and rabbits by ^{31}P , ^{13}C and ^1H high resolution NMR. It has been possible to follow ATP, PCr, P_i and pH by ^{31}P NMR, glutamate and lactate by ^{13}C NMR and about one dozen metabolites by proton NMR including lactate, N-acetyl-aspartate, glutamate, glutamine, phosphorylcholine, phosphocreatine, creatine and γ -amino-butyric acid. The effects of hypoxia, hypoglycemia and status epilepticus upon these metabolites has been followed in real time with resolution ranging from 1 to 6 minutes. Double tuned surface coils have enabled us to switch back and forth between nuclei giving essentially simultaneous determination of metabolic levels. During hypoglycemic coma it is possible to observe via ^{31}P NMR severe reductions in the PCr and ATP levels with consequent increase in the P_i levels while at the same time the ^1H NMR spectra shows reductions in glutamate and glutamine levels and consequent increases in the aspartate levels. After glucose infusion the EEG returned to normal and the ^{31}P and ^1H spectra also returned towards their control values. However the PCr/ P_i ratio did not recover fully while in the ^1H spectra the glutamine levels remained low.

In the ^{13}C spectra it has been particularly useful to have a double tuned ^{13}C - ^1H surface coil. This has been used to observe ^{13}C NMR spectra while alternately decoupling the proton during normal ^{13}C data accumulation. It has also been possible, using spin echoes, to obtain proton observe carbon decouple spectra of glutamate and other metabolites during and after infusion of 90% enriched 1- ^{13}C glucose.

Monday 30 July Council House-Conference Hall 09.30-12.30

Symposium on NMR in Vivo

**CROSS-POLARIZATION MAGIC-ANGLE SPINNING C-13 AND
N-15 NMR OF INTACT PLANT AND BACTERIAL CELLS**

**J. Schaefer, J. R. Garbow, E. O. Stejskal and R. A. McKay;
Monsanto Company, St. Louis, Missouri, USA**

Cross polarization is a sensitivity enhancement technique which relies upon static dipolar coupling between an abundant reservoir of magnetization (typically protons) and a rare-spin system (such as ^{13}C or ^{15}N). The resulting rare-spin nmr spectrum is usually obtained with magic-angle spinning for resolution enhancement. Cross-polarization signals arise only from those components of in vivo plant or bacterial cells which are at least partially immobilized. The technique therefore complements the use of Fourier transform ^{13}C or ^{15}N nmr which is sensitive to the mobile soluble pools of in vivo cellular systems. Cross-polarization nmr can be performed on either viable (wet) cells or lyophilized materials. We have used in vivo cross polarization nmr in two ways recently: (1) to measure the metabolism of single- and double-labeled amino acids and the incorporation (via multiple pathways) of the metabolites into insoluble proteins; and (2) to measure the dynamics of specific labels in bacterial cell-wall proteins. The latter experiments involve dipolar rotational spin echoes to characterize the extent to which microscopic molecular motions in the (nearly) solid state average N-H dipolar couplings. This information will ultimately help us to quantify the effect of peptidoglycan cross linking on cell-wall rigidity.

Symposium on NMR in Vivo.

³¹P NUCLEAR MAGNETIC RESONANCE FROM CELLS AND TISSUES.

G.K. Radda, Department of Biochemistry, University of Oxford, South Parks Road, Oxford, OX1 3QU.

During the past ten years, it became possible to record high resolution NMR spectra from intact cells, isolated tissues and organs, selected regions of laboratory animals and even humans. In general, mobile small metabolites are detectable and identifiable from the resonances given by nuclei like ³¹P, ¹H and ¹³C.

Using ³¹P NMR the most abundant phosphorus-containing metabolites (e.g. phosphocreatine, ATP, ADP, AMP, P_i sugar phosphates) are simultaneously observed and quantified in a matter of minutes. In addition, the position of the P_i resonance depends on the state of ionization of the phosphate group which in turn is determined by the pH of the medium. Thus the P_i signal from within the cell gives us a read-out of intracellular pH.

A technique called saturation transfer offers a unique way for study in vivo enzymology. The unidirectional fluxes through some enzyme catalysed processes can be measured even when the system is in a steady state or equilibrium. Thus using ³¹P NMR, the major bioenergetic processes of the cell can be investigated.

Several examples of how ³¹P NMR gives us new insights into "molecular cell biology" will be given.

In isolated renal tubules, the distribution of H⁺ ions between the cytoplasm and mitochondrion has been investigated by comparison of the pH values measured by ³¹P NMR (measuring cytoplasmic pH) and by the distribution of weak acids (e.g. DMO) which reflects an average pH over all compartments.

In perfused organs, such as the heart and kidney, the flux of ATP synthesis can be measured directly by NMR. When the observed values are compared with the O₂ consumed, we can obtain true in vivo P:O ratios and relate these to phosphorylation potentials and work. In the kidney comparison of the rate of ATP turnover with Na⁺ uptake gives the unexpected conclusion that the Na⁺/ATP ratio is considerably higher than 3.

In live animals we are now able to focus the NMR observation on specific organs. For example, measurement of the ATP synthetase rate in the brain of rats gives a P:O ratio close to 3. The creatine kinase catalysed conversion of phosphocreatine to ATP is about 5 times faster than ATP utilization. The effect of hypoxia, hypocapnia and other conditions (e.g. shock) on the energy metabolism of the brain can be readily observed. The role of creatine kinase in the control of energy coupling became clear from the examination of animal muscles in which phosphocreatine was largely replaced by phospho-quanidino-propionic acid.

The energetics of human muscle in limbs has also been examined in over 300 control examinations and in more than 250 patients with muscle disorders or symptoms. We can now quantitatively relate ATP utilization to work, determine the relative importance of oxidative vs. glycolytic contribution to ATP production during exercise, observe the point at which the switch to glycogenolysis takes place and measure the rate of oxidative phosphorylation.

Detailed examination of these parameters in many pathological states gives us for the first time a non-invasive handle on cellular biochemistry in humans, both in limbs and other organs of the body such as brain.

Symposium on Polymorphism and Structural Transitions in Nucleic Acids

BASE SEQUENCE EFFECTS ON THE SURFACE OF POLYMERIC DNA.

Struther Arnott, R. Chandrasekaran, R-G. He, R. C. Millane, H-S. Park, L. C. Puigjaner and J. K. Walker, Department of Biological Sciences, Purdue University, West Lafayette, Indiana, U.S.A.

Fibrous polynucleotide duplexes are very polymorphic. This is observed both with general sequence DNAs and with synthetic DNAs, such as poly d(GC)·poly d(GC) and poly d(AC)·poly d(GT) (with their A, B and Z forms), poly d(AT)·poly d(AT) (with A, B and D forms), and poly d(A)·poly d(T) (with its heteronomous or H form). The Z forms of poly d(GC)·poly d(CG) and poly d(AC)·poly d(GT) dramatically reflect their dinucleotide chemical structures in their secondary structures by having quite differently puckered furanose rings and different backbone conformations in alternate nucleotides.

It is of no little interest to determine whether or not the base sequences within a polymeric DNA duplex are indicated on the surface by features of the sugar-phosphate backbone. If they are, then regulatory proteins and enzymes which have to bind to specific DNA sequences might more easily recognize their host sequences. Detailed analyses of various allomorphs of poly d(AT)·poly d(AT), poly d(IC)·poly d(IC) and poly d(GC)·poly d(GC) in uniaxially oriented polycrystalline fibers show that the dinucleoside monophosphate 5'RpY3', where 5'R is a purine and Y3' is a pyrimidine, have either *t*, *t* or *t*, *g*- conformations at C3'- O3', O3'- P which lead to similar orientations of phosphate groups. On the other hand, 5'YpR3' dinucleoside monophosphates commonly have *g*-, *t* conformations which are associated with markedly different orientation of the phosphate group. Studies of the more complex structures poly d(ACC)·poly d(GGT) and of a pleiomorphic form of poly d(AT)·poly d(AT) where the repeated secondary structural motifs are hexanucleotides reveal further details of the surface "wrinkles" on DNA and allow us to explore whether and to what extent the variations within the structures of crystallized DNA fragments are manifested in long polymers and are sequence dependent. In the case of poly d(A)·poly d(T), the chemical distinctiveness of the two antiparallel strands is amplified by the fact that the sugar rings in each strand are puckered differently -- C2'-*endo* in poly d(T) and C3'-*endo* in poly d(A). Similar structures may be present in some DNA-RNA hybrids. Such heteronomous duplexes have unusually pronounced directional properties.

Symposium on Polymorphism and Structural Transitions in Nucleic Acids**CONFORMATIONAL VARIABILITY OF THE DNA-DOUBLE HELIX AS OBSERVED IN CRYSTAL STRUCTURES OF OLIGONUCLEOTIDES****Z. Shakked, Weizmann Institute of Science, Rehovot, Israel**

X-ray analyses of single crystals of oligonucleotides carried out in recent years have yielded structural information at nearly atomic resolution on three structural forms: Two right-handed structures similar to the well established A- and B-DNA double helices, and a left-handed double helix, Z-DNA, discovered so far in self-complementary alternating sequences of purine and pyrimidine bases. Both the A- and B-type structures demonstrate a wide range of conformational variability of the DNA double helix which is strongly dependent on base composition and sequence.

Our comparative study of the A-type structures indicates that interactions between the bases are the primary driving force for inducing local variations in the double helix. Favorable stacking arrangements of successive base pairs are achieved by concerted changes in the backbone torsion angles and the orientation about the glycosidic bonds. This finding appears to be relevant also to the B-DNA-type structure and may be a general feature of other forms of DNA.

An attempt has been made to understand the base-stacking variability observed in the A- and B-type structures in terms of stacking energies derived by atom-atom potential energy calculations. These calculations indicate that sequence-dependent variability in A- and B-DNA structures is a consequence of the equipartitioning of the van der Waals stacking energy along the double helix. The observed local changes in the relative orientation of adjacent base pairs result in decreasing the overall stacking energy and minimizing the energy differences between various helical steps.

Monday 30 July

Unicorn Hotel-Trident Suite

09.30-12.30

Symposium on Polymorphism and Structural Transitions in Nucleic Acids

DNA CONFORMATION DYNAMICS AND INTERACTIONS IN SOLUTION.

D. J. Patel¹, S. A. Kozlowski¹ and D. R. Hare², ¹AT&T Bell Laboratories, Murray Hill, New Jersey and ²Biochemistry Department, Columbia University, New York, New York.

High resolution NMR investigations have been undertaken to define the conformation, dynamics and interactions in DNA duplexes and their modified analogs containing one to two turns of helix. Nucleic acid conformations are deduced from a distance geometry analysis of all proton-proton distances of less than 5 angstroms evaluated from two dimensional nuclear Overhauser effect measurements. Nucleic acid dynamics are probed from inversion recovery kinetic measurements of the resolved and assigned imino protons to measure hydrogen exchange rates and activation barriers in DNA duplexes at the individual base pair level. Our presentation will focus on a few topics from the following areas of research currently underway in our laboratory. (1) The sequence dependence of the conformation and dynamics of DNA with special emphasis on the role of counterion, solvent and temperature. (2) The structural details of chain folding in hairpin and bulge loop formation and the conformational and hydrogen exchange characteristics at the junction between right- and left-handed DNAs. (3) The conformation and dynamics at and adjacent to purine-pyrimidine, purine-purine and pyrimidine-pyrimidine base pair mismatches, as well as helix interruption sites containing an extra purine or pyrimidine base imbedded in DNA duplexes. (4) The structure at the site of guanosine modification with alkylating agents and aromatic carcinogens and the elucidation of alternate pairing modes to delineate the origin of transition and transversion errors in replication. (5) The sequence specificity of drug-DNA complexes and the conformational details at and adjacent to intercalation and groove binding sites.

Symposium on Polymorphism and Structural Transitions in Nucleic Acids

THREE-STATE DIAGRAM FOR DNA

V.I. Ivanov, D.Yu. Krylov and E.E. MinyatInstitute of Molecular Biology, Academy of Sciences of the USSR,
Moscow, USSR

The study of the triple equilibria (A,B,coil) and (A,B,Z) makes it possible to obtain interconnection between thermodynamic parameters of different co-operative transitions in DNA(1). Melting of DNA, poly d(A-T) and poly d(A-BrU) was performed in a broad interval of trifluoroethanol (TFE) concentrations including those of the B to A transition range. A branch, which characterizes the helix-coil equilibrium, has a universal shape for different DNAs and the polynucleotides: melting temperature is minimum near 30% TFE and increases sharply within the region of the A form stability (>65% TFE). The B-A equilibrium depends on temperature only slightly. The slope angles of the branches in the vicinity of the triple point (A,B,coil) allow estimating the co-operativity length of the B-A transition: it proves to be of the order of 20 base pairs for DNA and the polynucleotides. Due to the finite transition widths a peculiar situation, not studied up to now, is realized in our cases, at which three different conformations may be present in one polymeric molecule. This results in some new effects, predicted by a theory (2), such as the increase in width of the melting curves within the B-A transition interval. It thus appears that the phase diagram method may become very informative approach to the studies of DNA metamorphosis in solution.

(1) V.I. Ivanov, D.Yu. Krylov, E.E. Minyat, L.E. Minchenkova, J. Biomolecular Structure and Dynamics 1, 453-460 (1983).

(2) M.D. Frank-Kamenetskii and G.I. Chogovadze, J. Biomolecular Structure and Dynamics No.5 (1984), in press.

Symposium on Food Biophysics

STRUCTURAL CHANGES IN MUSCLE IN RIGOR AND MEAT PROCESSING

G.W. Offer, J.A. Trinick, C.A. Voyle, D.J. Restall, P.D. Jolley, R.E. Jeacocke, N.J. Parsons and P.J. Knight

AFRC Meat Research Institute, Langford, Bristol, U.K.

Muscle contains 75% water, but this value can change substantially post-mortem, particularly when meat is processed. Such changes are economically important and affect the eating quality. The largest water compartment in muscle is the myofibrils. We are testing the hypothesis that losses or gains in the water content of meat are due to changes in the volume of the myofibrils caused by shrinking or swelling of the filament lattice.

After muscle enters the rigor state, an aqueous solution of sarcoplasmic proteins, known as drip, slowly oozes from the cut ends of the fibres. This arises because the fibres shrink away from their endomysial sheaths leaving water-filled channels. The force responsible for driving water along the channels could either be gravitational or generated by the connective tissue. Studies on skinned muscle fibres have shown that the shrinkage of the fibres has two causes: (a) the fall in pH from 7 down to about 5.5 due to glycolysis (b) the entry of the fibre into the rigor state. We are investigating by X-ray diffraction whether the filament lattice also shrinks in intact muscle.

When meat is processed, it is treated with sodium chloride and often also with polyphosphate. This causes a substantial uptake of water (typically 5 to 40%), much of which is retained on cooking. During massaging or tumbling, a sticky exudate consisting of fibre fragments and extracted myofibrillar proteins, especially myosin, forms on the surface of the meat pieces and binds them together after cooking. We have shown that isolated myofibrils swell substantially under salt conditions similar to those used for meat processing and myosin may be extracted from the A-band. At pH 5.5, 0.6 to 0.8 M NaCl causes swelling of myofibrils at constant sarcomere length. The centre of the A-band is sometimes extracted. The addition of 10 mM pyrophosphate reduces the concentration of sodium chloride required for swelling and causes the A-band to be extracted completely beginning from its ends. Although myofibrils always swelled under these conditions, there was considerable variation in its extent, in the degree of extraction of the A-band and in the degree of expansion of the I-band. We are testing the proposition that the variation is due to differences between fibre types or to weakening of the Z-line by proteolysis.

We are also examining whether the same structural changes occur in blocks of meat. We find that while no A-band extraction occurs with salt alone, substantial extraction occurs in the presence of pyrophosphate. The Z-lines become fragmented after treatment, consistent with their being broken by myofibrillar expansion.

The mechanism by which salt induces swelling of the myofibrils remains to be elucidated, but is likely to be due to a combination of increased long-range electrostatic forces between filaments combined with removal of one or more transverse structural constraints. Raising the chloride concentration would be expected to cause substantially increased screening of the charges and it is possible that the principal effect is to increase the radii of the charges about the thick and thin filament axes.

On cooking of unprocessed meat, the weight loss can be up to 40% and the meat shrinks substantially both along and transverse to the fibre axis. Single muscle fibres shrink transversely when heated to temperatures between 40 and 60°C. We have now shown that when heated to temperatures above 65°C, single fibres also shrink longitudinally very rapidly and develop force. Isolated myofibrils, like fibres, shrink in both directions. Transverse sections of muscle cooked to temperatures up to 90°C show that the fibres have shrunk still further than in rigor, leaving a much bigger gap between them and their endomysial sheaths. We suppose that the lateral shrinkage of meat is caused by the thermal contraction of the connective tissue network forcing the fluid in this gap out to the cut ends. We are currently investigating the relative contributions of myofibrils and collagen to the longitudinal shrinkage.

Symposium on Food Biophysics

COLLOIDAL ASPECTS OF FOOD DISPERSIONS

P. Walstra, Department of Food Science, Agricultural University, Wageningen, the Netherlands.

Most liquid foods are dispersions and most particles in these dispersions (e.g. cells, cell fragments, starch granules, protein aggregates, emulsion droplets, crystals) are of colloidal size, viz. 10^{-8} - 10^{-4} m. If the particles are not small by nature, they are made so, for instance to slow down sedimentation or to speed up diffusion. Colloidal interactions therefore are manifest and they affect (1) product properties, such as physical stability and rheological behaviour, and (2) ease of processing, e.g. phase separation. Physical instability may relate to sedimentation (or creaming), flocculation and coalescence; these changes often occur simultaneously and they affect each other. Flocculation often precedes coalescence; both are for the greater part determined by colloidal interaction, and they enhance sedimentation. A satisfactory theory for coalescence is not available, but the other changes can often be predicted.

Colloidal interaction forces between similar particles always include Van der Waals attraction and nearly always electrostatic repulsion. Both can be calculated with some accuracy for homogeneous particles of simple shape from material constants and measurable parameters. Steric repulsion caused by protruding molecular chains in Brownian motion, for instance from adsorbed macromolecules, is much more difficult to predict. Moreover its existence complicates calculation of the other forces. Steric repulsion by macromolecules does not prevent contact, so that bridging between particles may occur, for instance by formation of -S-S-linkages between adsorbed proteins. Hydrodynamic interactions should also be taken into account and this is fairly straightforward for smooth particles, but adsorbed macromolecules, again, make it much more difficult.

Most foods are aqueous systems: ionic strength is usually 10^{-2} - 10^{-1} mol.m⁻³, which gives a Debye length (thickness of the diffuse double layer) of 1 - 3 nm, and the surface potential of most particles is fairly small. This implies that electrostatic repulsion mostly is insufficient to prevent flocculation, and steric repulsion is an important factor. Calculation of colloidal interaction in foods is thus difficult, also because of the following. (1) Particles show a wide range in composition, hence properties. (2) Several substances are present that can be adsorbed, notably proteins; most proteins behave neither as flexible macromolecules, nor as rigid entities, and their conformation after adsorption is difficult to predict. (3) Particles often show a wide range in size and shape. (4) Volume fraction of dispersed phase is too high to neglect multiple-particle interactions. (5) Conditions in a food often change with time by enzymic or chemical reactions. Despite these complications calculations, if only giving an order of magnitude or a trend when changing conditions, are often possible and useful: they may forestall much trial and error in product or process development. Amelioration of the theory of steric repulsion would be most welcome.

Often, weak attraction prevails, causing flocculation. In the absence of agitation and sedimentation, flocculation leads to formation of a continuous network, hence a gel, albeit a weak gel. Existence of a gel implies physical stability, as long as it does not show syneresis; syneresis occurs if the colloidal interactions are very weak. Rheological properties of the gel primarily depend on its inhomogeneity and methods for characterizing such structures need to be developed. Some progress has been achieved with a gel built of protein aggregates, employing permeability and rheological measurements. The latter should be carried out at very small stresses. Unfortunately, rheological theory is as yet confined to small deformation (linear behaviour), while large deformation (yield behaviour) often occurs in practice.

The way in which a dispersion is made may greatly affect its properties, since thermodynamic equilibrium is never reached or even approximated. In the fairly simple case of making protein-stabilized emulsions, factors governing droplet size and composition of the adsorbed layer are now qualitatively understood. Colloidal interactions, hydrodynamic forces and dynamic surface properties all come into play. Extension of this work to the formation of dispersions of solid-like particles would be useful; it should include a careful consideration of the different processes involved and their time scales.

Symposium on Food Biophysics

EQUILIBRIA, METASTABILITY AND DYNAMICS IN COMPLEX AQUEOUS SYSTEMS: THE DANGERS OF OVERSIMPLIFICATION.

F. Franks. Department of Botany, University of Cambridge, Cambridge, U.K.

The physical and chemical processes which form the basis of life resemble those which the food processor employs to preserve and/or simulate the *in vivo* textures of plant and animal tissues or to create novel textures with the aid of simpler and cheaper raw materials.

One of the basic tenets common to physiology and food processing is that the methodology of equilibrium thermodynamics is usually inapplicable. Although a sound knowledge of solid/liquid phase relationships is a *sine qua non* for an intelligent exploitation of the desirable properties of materials, such as structure, texture and rheology, this knowledge alone is insufficient for the design of commercially useful products or for an understanding of physiological processes. Indeed, it is usually left to the experience and ingenuity of the processor to achieve a combination of thermodynamic *instability* and physical/mechanical *stability*.

Ice cream manufacture graphically illustrates this principle: To achieve the desired end it is necessary to process a mixture of ingredients in such a way that the final state does not correspond to the stable equilibrium state, but that the compounded and frozen mix can be maintained in its metastable state for a sufficiently long period. What is sufficient depends largely on the end use of the product. In the storage of seeds (also under conditions of metastability) such a period is measured in years, whereas in the storage of ice cream it is measured in weeks.

In terms of physico-chemical principles the compounded system must be prevented from reaching its state of minimum free energy. In practice this is achieved by the interposition of a kinetic activation barrier, designed to retard the rate of achievement of equilibrium. Thus, the rate of coalescence of emulsified droplets, leading to an eventual phase separation, can be retarded by providing a repulsive interaction between the droplets and/or increasing the viscosity of the continuous phase, thus reducing the collision rate.

In aqueous systems at subfreezing temperatures the stable water phase is ice. Depending on the particular process and system, it may be desirable or essential to inhibit freezing altogether, or to let it proceed to a given extent, but to control the type and concentration of ice crystals formed. Both objectives involve the creation of thermodynamically metastable states which must then be "frozen-in" to achieve the desired storage life. In the absence of such stabilization ice will tend to recrystallize, additional ice may be formed, other components may crystallize and deleterious chemical reactions may occur as a result of increasing freeze concentration. The physical parameters which govern the production and control of metastable water include undercooling, supersaturation, nucleation, crystal growth, vitrification, recrystallization, maturation and melting. The practical limits are set by the thermal and diffusional properties of water. Of all the parameters mentioned, melting alone is a thermodynamic equilibrium process (i.e. it can be described by thermodynamic state functions). The same parameters are also involved in the phenomena associated with freeze tolerance and freeze resistance of living organisms. Attempts to rationalize such phenomena in terms of equilibria (e.g. so-called water binding) may provide acceptable correlations but are futile and can be shown to be so.

Before applying the tools which were developed to account for chemical equilibria, e.g. activity and activity coefficients, equilibrium constants, standard states, cyclic processes, it is well to ensure that the system under study is in fact one to which such methods can be applied. Usually it is not, and there are several classic examples of the absurd conclusions to which such simplistic reasoning can lead. Even the laws of irreversible thermodynamics are usually not applicable, because the metastable states involved in physiology and technology are far removed from equilibrium. However, a better appreciation of the kinetic aspects of metastability will help to provide a proper theoretical basis.

Monday 30 July Council House-Conference Hall 14.00-17.00

Symposium on Nucleic Acid-Protein Interactions

CRYSTALLOGRAPHIC STUDIES OF NUCLEIC ACID/PROTEIN INTERACTIONS.

B.W. Matthews, Institute of Molecular Biology and Department of Physics,
University of Oregon, Eugene, Oregon

The structures of three proteins that regulate gene expression have been determined recently in different laboratories and suggest how these proteins may bind to their specific recognition sites on the DNA (Takeda et al. Science (1983) 221, 1020-1026). One protein (Cro) is a repressor of gene expression, the second (CAP) usually stimulates gene expression and the third (λ repressor) can act as either a repressor or activator. Each of the proteins is dimeric and contains a pair of two-fold-related α -helices that could be placed within successive major grooves of the DNA.

The three proteins contain a substructure consisting of two consecutive α -helices that is virtually identical in each case. Structural and amino acid sequence comparisons suggest that this bihelical fold occurs in a number of proteins that regulate gene expression. DNA-protein recognition appears to be based primarily on a network of hydrogen bonds as well as other interactions between side-chains of the protein and the parts of the base-pairs exposed within the major groove of the DNA.

It appears that the DNA maintains a right-handed Watson-Crick B-form when either Cro, CAP or λ repressor is bound, although some bending or other deformation may occur. In addition to the crystallographic structure determinations, independent evidence for the modes of interaction of the three proteins with DNA has come from chemical modification studies, from NMR, from the analysis of mutant proteins and from electrostatics calculations.

Symposium on Nucleic Acid-Protein Interactions

INTERACTIONS BETWEEN TRANSFER RNAs AND AMINOACYL-tRNA SYNTHETASES : STRUCTURAL ASPECTS.

R. GIEGE, C. FLORENTZ, D. KERN, B. LORBER, P. ROMBY, V.V. VLASSOV, J.P. EBEL, G. ZACCAI *, J.C. THIERRY and D. MORAS, Institut de Biologie Moléculaire et Cellulaire du CNRS, 15 rue Descartes, Strasbourg, France

Aminoacyl-tRNA synthetases catalyse the specific attachment of aminoacids to their cognate tRNAs in a process which partly governs the correctness of protein biosynthesis. The aspartic acid system from the yeast *Saccharomyces cerevisiae*, formed by tRNA^{Asp} (a short extra-loop tRNA; MW=24,160) and aspartyl-tRNA synthetase (a α_2 dimeric enzyme with 2 binding sites; MW=125,000) was chosen as a model for studying the protein-nucleic acid interactions because both macromolecules have been crystallized and the three-dimensional structure of the tRNA is known at high resolution (Moras, Comarmond, Fischer, Weiss, Thierry, Ebel and Giegé, *Nature*, 286, 1980, 669-674). Structural data will be compared to those obtained in the phenylalanine and valine systems where the synthetases are of tetrameric ($\alpha_2\beta_2$; MW=270,000) and monomeric (α ; MW=130,000) nature, respectively.

The phosphate reactivity towards ethylnitrosourea of native tRNA was compared to that of tRNA bound to synthetases. The methodology involves end-labelling of tRNA, statistical alkylation splitting of the RNA chain at the modified positions, and monitoring of the modification patterns by rapid sequencing gels. Protections by the different synthetases were essentially found in the anticodon stem and loop of the tRNAs. The exact localizations of the protected phosphates are system dependent : 5' side in tRNA^{Asp}, 3' side in tRNA^{Val}, both sides in tRNA^{Phe}. Other protected phosphates in tRNA^{Asp} are found at the junction of the 5' side of the aminoacid acceptor stem with the D-stem, in the extra-arm and the 5' side of the T-stem. The chemical approach did not allow to detect conformational changes in complexed tRNAs. Experiments with the tRNA-like structure of turnip yellow mosaic virus, efficiently chargeable by valyl-tRNA synthetase, emphasize (i) the importance of the anticodon stem in recognition (the most important interaction sites occur at similar positions than in tRNA^{Val}), (ii) the non-absolute requirement of the canonical structure of the aminoacid accepting stem in this process (the tRNA-like structure possesses an additional loop at its 3' terminus).

Contrast variation experiments by small angle neutron scattering indicate different structural organizations in tRNA/synthetase complexes. tRNA^{Asp} binds at the surface of aspartyl-tRNA synthetase while tRNA^{Val} is buried in valyl-tRNA synthetase.

Binding of tRNA and tRNA-like structures to synthetases in the presence of high amount of ammonium sulfate ($\approx 2M$) has been demonstrated by different physical methods. It was shown that the tRNA aminoacylation activity remains efficient under these conditions. Control experiments confirmed that NaCl or KCl at high concentration abolish binding and aminoacylation activities. These results suggest that besides electrostatic effects, hydrophobic interactions can stabilize functional tRNA/synthetase complexes.

Advantage of the ammonium sulfate effects has been taken to crystallize the complex between aspartyl-tRNA synthetase and two molecules of tRNA^{Asp} (Lorber, Giegé, Ebel, Berthet, Thierry and Moras, *J. Biol. Chem.* 258, 1983, 8429-8435). The cubic crystals (space group 1432, $a=354\text{\AA}$), although particularly soft, are suitable for diffraction studies up to 7Å resolution.

*Institut Laue Langevin, Grenoble, France

Monday 30 July Council House-Conference Hall 14.00-17.00

Symposium on Nucleic Acid-Protein Interactions

**THE STRUCTURE OF LAC REPRESSOR HEADPIECE AND ITS INTERACTION WITH
LAC OPERATOR DNA: A NMR VIEW.**

R. Kaptein, E.R.P. Zuiderweg, W.F. van Gunsteren, R. Boelens and R.M. Scheek.
Dept. of Physical Chemistry, University of Groningen, Groningen, the Netherlands.

With the aim of investigating the nature of specific protein-DNA interactions we have embarked on a NMR study of the DNA binding domain (headpiece) of lac repressor and its interaction with synthetic lac operator DNA fragments. No crystal structures are available for these molecules. Employing two-dimensional (2D) NMR spectroscopy we have assigned ca. 95% of the backbone amide and C $_{\alpha}$ protons and the majority of the side chain protons of the headpiece (collaboration with K. Wüthrich).

In the ^1H 2D NOE spectrum approximately 200 NOE (Nuclear Overhauser Enhancement), cross peaks could be assigned to specific pairs of protons. These NOE's, which occur only between protons which are separated by less than ca. 4Å, provide the basis for a determination of the solution structure of the headpiece.

The following procedure was used. First, the secondary structure was delineated from the distance constraints set by the NOE's. It appears that the headpiece contains three α -helices (segments 6-12, 17-25 and 35-45) connected by regions of irregular structure. Then a crude model for the 3D structure was constructed, which satisfies most of the distance constraints. The next step is the refinement of this crude structure. For this we have devised a method based on the molecular dynamics (MD) procedure in which the conventional potential energy terms were augmented by quasi-potentials forcing the molecule to satisfy the NOE distance constraints. After a 25 ps MD run a significantly improved structure was obtained which is compatible with 95% of the distance constraints. This structure shows a high degree of homology with cI repressor of bacteriophage lambda for which a crystal structure has been determined.

A particularly interesting feature is that the second α -helix contains several polar surface residues, that are well positioned to act as hydrogen bond donors or acceptors in a complex with DNA. Recent photo-CIDNP NMR studies support earlier genetic evidence that amino acid residues in this helix are involved in DNA recognition.

Symposium on Processing and Control of Visual Information

CLUSTERED INTRINSIC CONNECTIONS AND FUNCTIONAL ARCHITECTURE OF THE VISUAL CORTEX. T.N. Wiesel, C.D. Gilbert, D. Ts'o, Laboratory of Neurobiology, The Rockefeller University, New York, NY, USA.

The intrinsic connections of the cortex have long been known to run vertically, across the cortical layers. We have found that individual neurons in the cat primary visual cortex can communicate over surprisingly long distances horizontally (up to 4 mm), in directions parallel to the cortical surface.¹ For all of the cells having widespread projections, the collaterals within their axonal fields were distributed in repeating clusters, with an average periodicity of about 1 mm. This pattern of extensive clustered projections has been revealed by combining the techniques of intracellular recording and injection of horseradish peroxidase with three-dimensional computer graphic reconstructions. The clustering pattern was most apparent when the cells were rotated to present a top view of the cortex. The axonal fields of all our injected cells were asymmetric, extending for greater distances along one cortical axis than along the orthogonal axis. When axons projected to more than one layer, the clusters in the deeper layer tended to be located under those in the upper layer, suggesting a relationship between the clustering phenomenon and columnar cortical architecture.

We have begun experiments to investigate the relationship between the physiological connectivity of pairs of cells, as shown by cross-correlation methods,² and the cells' receptive fields properties. Recordings in cat and monkey striate cortex from two independently manipulated extracellular electrodes were processed by window discriminators and fed into a digital computer programmed to perform real-time auto- and cross-correlations with high temporal resolution. The first step was to map the orientation columns electrophysiologically in a limited region of cortex. Using one roving electrode and one fixed electrode, this map provided a systematic means for studying connectivity between spatially separate regions of various orientation specificities. Preliminary results in both the monkey and the cat showed that units separated by .2 mm or more with overlapping receptive fields but differing in receptive field properties such as orientation, ocular dominance or directionality had responses which tended not to be correlated. At these distances, pockets of units exhibiting correlated firing had receptive field properties that matched. However, not all regions of units with matching receptive field properties showed correlated responses. The correlograms obtained suggest that horizontal interactions at these distances are excitatory. These findings provide physiological evidence for a functional contribution of horizontal connections and are consistent with anatomical demonstrations of the clustered nature or horizontal connectivity in the visual cortex.

1. Gilbert, C.D., Wiesel, T.N., J. Neuroscience 3:1116-1133, 1983.
2. Perkel, H., Gerstein, G.L., and Moore, G.P., Biophysical J. 7:419-440, 1967.

This work was supported by National Institutes of Health Grants NS16189, EY05253, and EY07042.

Symposium on Processing and Control of Visual Information

CEREBELLAR NEURONAL MECHANISMS OF VISUO-MOTOR CONTROL

Masao Ito Department of Physiology, Faculty of Medicine, University of Tokyo, Bunkyo-ku, Tokyo, Japan

Visual information is conveyed by numerous subcortical and cortical pathways and serves various types of motor control, ranging from reflexes to voluntary movements. It provides a stimulus which drives a motor system to perform a movement on one hand, but it also serves for feeding back the end-effect of a performed movement to the motor system on the other. The visual feedback would exert two different actions on the motor system; it acts to correct instantaneously any erroneous performance of the motor system in the manner of feedback control, or it acts to modify the dynamic characteristics of the motor system toward improvement of its performance in the manner of adaptive control. These multiple roles of visual information in motor control are typically represented in the neuronal mechanisms of cerebellar control of movements. For example, the optokinetic response (OKR) is a reflex eye movement which follows a relatively slow movement of the visual surroundings. It is a typical negative feedback control where visual information provides both the driving stimulus and the negative feedback. The brain stem pathway for this reflex is attached with a sidepath through the cerebellar flocculus which receives visual information through mossy fiber afferents and which in turn sends output signals of Purkinje cells to relay cells of the reflex. This flocculus sidepath is provided with another visual input through climbing fiber afferents. The author proposes that retinal slip signals conveyed by the climbing fiber pathway represent control error signals involved in the performance of the OKR and that barrage of visual climbing fiber signals leads to modification of signal transfer characteristics across the flocculus sidepath and consequently to modification of the dynamic characteristics of the whole OKR system. This hypothesis is consistent with the modifiable neuronal network model proposed by Marr (1969) and Albus (1971), and is supported by three lines of experimental data; 1) responsiveness of Purkinje cells to mossy fiber inputs undergoes a long-term depression when the mossy fiber signals collide with climbing fiber signals on the same Purkinje cells (Ito, Sakurai and Tongroach, 1982); 2) ablation of the flocculus abolishes adaptive modification of the OKR that normally occurs under sustained optokinetic stimulation (Nagao, 1983); 3) responsiveness of floccular Purkinje cells to optokinetic stimuli is modified in parallel with the adaptive modification of the OKR (Nagao, 1984). Similar role of the visual climbing fiber signals is apparent in another system for the vestibulo-ocular reflex (VOR) which is driven by vestibular signals and which operates without feedback. Vision serves the VOR system only through a climbing fiber pathway by modifying the signal transfer characteristics of the floccular sidepath attached to the VOR arc (Ito, 1972). Ample experimental evidence is now available for this flocculus hypothesis of the VOR control (Ito, 1982). The adaptive control system model of the cerebellum, developed in studies of the VOR and OKR, may be extended to account for other types of visuo-motor control such as saccades, eye-head coordination and smooth pursuit eye movements. Similar consideration may apply to visually guided pointing and tracking movements which represent goal-oriented voluntary motor control. Central pathways dedicated to these controls are more complex than reflex arcs. Nevertheless, reviewing of accumulated anatomical data on afferent and efferent connections of the cerebellum suggests that these central pathways are equipped with modifiable cerebellar sidepaths which are calibrated according to control error signals conveyed by climbing fiber pathways. The adaptive control system model, however, is unsatisfactory for accounting for the motor learning, i.e., progressive improvement of voluntary motor control through repeated trials. Such progressive improvement can be achieved only with the aid of a memory device which stores information from preceding trials, in addition to adaptive mechanisms which refer only to experiences within a trial. Identification of neural structures devoted to such memory device is an interesting subject of cerebellar physiology.

Symposium on Processing and Control of Visual Information

A TEXTON THEORY OF PREATTENTIVE VISION AND TEXTURE PERCEPTION

B. Julesz, AT&T Bell Laboratories, Murray Hill, NJ, USA

When the human visual system is prevented from detailed scrutiny by presenting patterns for a brief duration or by overloading the system with an aggregate of patterns (textures) only the preattentive mode of vision operates (Julesz & Bergen, 1983). This preattentive visual system cannot process complex forms, yet can, almost instantaneously, regardless of the number of patterns, thus parallel, detect differences in a few local conspicuous features across the entire visual field. These features, called "textons" (Julesz, 1980, 1981), are elongated blobs (e.g. rectangles, ellipses, or line segments) with specific properties, including color, angular orientation, width, length, binocular and movement disparity, and flicker rate. Although many of these textons resemble the "trigger features" of cortical neurons or the "conspicuous features" proposed by psychologists and researchers in artificial intelligence, they have been isolated during 20 years of research using statistically constrained textures. This research showed that texture discrimination cannot be the result of stochastic or topological processing, but must be based on local processing by texton detectors. For line segments, their ends-of-lines (terminators) and their crossings are also textons. Only differences in the textons or in their density (number) can be preattentively detected, while the positional relationship between neighboring textons passes unnoticed. This kind of exact positional information is the essence of form perception, and can be extracted only by a time-consuming and spatially restricted process that is called "focal attention" (Julesz & Bergen, 1983; Treisman & Gelade, 1980). The aperture of focal attention can be very narrow, even restricted to a minute portion of the fovea, and shifting this aperture around requires about 50 msec (i.e. four times faster than scanning with eye movements). Thus preattentive vision points out those loci of texton differences that should be attended to. Only in the aperture of focal attention are the adjacent textons glued together, yielding unlimited number of forms. Accordingly, the preconscious system of preattentive vision contains basic elements, the textons, while the conscious system of attention, limited to a narrow aperture, has no elements since any shape in this aperture can be learned and recognized.

B. Julesz, Spatial Nonlinearities in the Instantaneous Perception of Textures with Identical Power Spectra, Phil. Trans. R. Soc. Lond. B, 290 (1980), pp. 83-94.

B. Julesz, Textons, the Elements of Texture Perception, and Their Interactions, Nature 290 (March 12, 1981), pp. 91-97.

B. Julesz & J. R. Bergen, Textons, the Fundamental Elements in Preattentive Vision and Perception of Textures, Bell Syst. Tech. J. 62, No. 6, July-August, 1619-1645 (1983).

A. Treisman & G. Gelade, A Feature-Integration Theory of Attention, Cognitive Psychol. 12 (1980), pp. 97-136.

Monday 30 July

Watershed-Cinema 1

14.00-17.00

Symposium on Connective Tissue and Bone

STRUCTURE OF COLLAGEN IN ANIMAL CONNECTIVE TISSUE

A Miller, Biochemistry Department, Edinburgh, E Y Jones, Molecular Biophysics Laboratory, Oxford, R D B Fraser, T P Macrae & E Suzuki, CSIRO, Melbourne.

The different genetic types of collagen will be described as will the structure of the triple helical molecule as refined from X-ray fibre diffraction data. Then the problem of determination of molecular arrangement in native tissues will be discussed. The various models proposed for molecular arrangement of type I collagen will be compared and an account given of the quasi-hexagonal model. A detailed analysis of the X-ray diffraction patterns from native type I collagen fibres will be used to provide a quantitative description of the quasi-hexagonal model. Parameters such as molecular positions, azimuthal orientation and axial shift can be estimated from the diffraction patterns. These parameters refer to the helix main-chain. Side-chain conformations can then be built in by molecular graphics and the predicted X-ray pattern for the complete model compared with the observed pattern.

Monday 30 July

Watershed-Cinema 1

14.00-17.00

Symposium on Connective Tissue and Bone

**STRUCTURAL STUDIES OF PROTEIN-MINERAL RELATIONSHIPS IN CALCIFIED
CONNECTIVE TISSUES.**

W. Traub, S. Weiner and A. Jodaikin, Weizmann Institute of Science, Rehovot,
Israel and Y. Talmon, Technion, Haifa, Israel.

Over 40 different minerals have been identified in biological systems, involving some 30 different phyla. Biomineralised tissues are generally formed by the initial elaboration of an organic matrix, consisting mainly of proteins, and the subsequent growth in it of mineral crystals characteristic of the tissue. We have been studying the structures of such matrices and their roles in mediating mineralisation in a variety of animals, using mainly X-ray and electron diffraction.

Proteins in shells of the three main classes of molluscs were found to form β -pleated-sheet structures and show the same specific alignment of protein chains with aragonite crystal axes. Proteins in rat tooth enamel also contain β pleated sheets, which show a structural alignment with the hydroxyapatite crystals. The proteins in these and other mineralised tissues comprise two major classes; one composed of predominantly non-polar amino acid residues, which may serve as a framework, and the other, rich in acidic and polar residues, which may serve to determine the specific structure and microarchitecture of the mineral crystals. Our structural results suggest that the acidic proteins may include nucleation sites where mineral crystallites are formed by epitaxial growth.

Symposium on Connective Tissue and Bone

COLLAGENS, MULTIDOMAIN GLYCOPROTEINS AND PROTEOGLYCANS OF THE BASEMENT MEMBRANE.
J. Engel, R. Timpl and H. Hörmann, University of Basel, Klingelbergstrasse 70,
Basel/Switzerland and Max-Planck-Institut für Biochemie, Martinsried b. München/
Germany.

Basement membranes are extracellular 30 to 150nm thick sheet-like structures which separate epithelia cell layers from connective tissue and surround nerve and muscle cells. They serve as scaffolds for forming and maintaining cellular organization and tissue structure, act as barriers for cells and large proteins but allow filtration of small molecules. Basement membranes consist of collagens, glycoproteins and proteoglycans. Various electron microscopic techniques (rotary shadowing, negative staining, scanning transmission microscopy) as well as physical measurements in solution (sedimentation, diffusion, sedimentation equilibrium, light scattering) were applied for an elucidation of the shapes, domain organization and assembly of these components. A general approach was the fragmentation of the large multidomain proteins by limited digestion with proteinase. Circular dichroism and thermal melting profiles helped to discriminate domains of different conformation.

The major basement membrane collagen IV consists of a N-terminal short (60 nm) triple helical segment which is separated from the 330 nm long main collagen helix by a short non collageneous region. The main helix is terminated by a 85 kDa globular domain. Collagen IV forms a chicken-wire like net-work by an antiparallel association of the N-terminal helices of four monomers and the C-terminal globules of two monomers. Flexible regions in collagen IV and its assembly products were localized by a newly developed analysis of electron micrographs.

An abundant non-collageneous protein is laminin (1000 kDa) which consists of three 200 kDa- and one 400 kDa-chains. Laminin has the shape of an asymmetric cross with three short (36 nm) arms and a long (77 nm) arm. Rod-like segments and seven globular domains were distinguished and partially isolated by fragmentation. Various domains exhibited different types of secondary structure. For example rod-like segments of the long arm were α -helical whereas the domain at the tip of the long arm exhibited β -structure. The latter bound heparin and heparan sulfate proteoglycan and a globular domain originating from a short arm exhibited cell binding activity. The elongated and flexible structures of laminin and a functionally related protein fibronectin are well suited for bridging distant binding sites located at collagen glycosaminoglycans, cell surfaces and other components. Fibronectin (440 kDa) consists of two almost identical flexible arms which are disulfide linked at their C-terminal end. Each arm is composed of about 30 (!) small domains of 4 to 10 kDa. PH and ionic strength dependent changes of shape were observed and explained by internal association of segments of rather different isoelectric point in the same molecule. Recently a small proteoglycan (130 kDa) of the basement membrane was isolated. It was found to consist of four to five heparan sulfate chains connected to a small (5 to 10 kDa) protein core and interacted with laminin and the globular domain of collagen IV.

Engel, J., Odermatt, E., Engel, A., Madri, J.A., Furthmayr, H., Rohde, H. and Timpl, R., J. Mol. Biol. 150, 97-120 (1981)

Hofmann, H., Voss, T., Kühn, K. and Engel, J., J. Mol. Biol. 172, 325-343 (1984)

Marcovic, Z., Lustig, A., Engel, J., Richter, H. and Hörmann, H., Hoppe-Seyler's Z. Physiol. Chem. 364, 1795-1804 (1983).

Weber, S., Engel, J., Wiedemann, H., Glanville, R.W. and Timpl, R., Eur. J. Biochem., in press.

Posters on Chromatin Structure and Function

001

SPECIFIC DNA-BOUND LIPIDS AS POSSIBLE LINKERS BETWEEN DNA SUBUNITS AND SITES OF APPLICATION OF IONIZING RADIATION
N.B. Strazhevskaya, Inst. Biol. Physics, USSR Acad. Sci., Pushchino, USSR

Using the methods of viscosimetry, sedimentation, light scattering, circular dichroism, microcalorimetry, thin layer chromatography it was shown: 1. The presence of chromosomal lipids, composition of which depends on the activity of the genome, in supramolecular DNA (SM DNA), isolated from various eukaryotic cells (rat, mouse, pigeon, loach, cancer). 2. Participation of these lipids, in particular cardiolipin, in regulation of SM DNA transcription. 3. An important role of these lipids in organization of SM systems of DNA: enzymatic removal of lipids, but not proteins, from SM DNA of various eukaryotic cells results in a release of DNA subunits of size $100 \cdot 10^6$ Da, which is close to the size of replicon. 4. Radiation effect in vivo is realized in lipid component of SM DNA with high yield (10^4 lipid molecules per 10^4 ev) and accompanied with a release of DNA subunits with m.w. of $100 \cdot 10^6$ Da. It was suggested that lipids in SM DNA are an essential structural-functional component and may be linkers between DNA subunits, and play an important role in realization of radiation effect in vivo.

003

THE ROLE OF HISTONE H1* IN CHROMATIN STRUCTURE
J.L. Girardet, J. Roche and C. Gorka, DRF/BNC, CEN/G, Grenoble (France)

The structural role of H1* is studied by means of melting experiments, circular dichroism, light scattering and nuclease digestion. Chromatin samples are obtained from liver of adult mouse, adult rat and new-born mouse, where H1* represents respectively 20 %, 7 % and 3 % of total histones H1. The melting experiments and the determination of the repeat length do not show any significant differences for the three kinds of chromatin. However, the winding of DNA determined by the molar ellipticity at 282 nm, as well as the ability of chromatin to condense upon the effect of ionic strength are function of the H1* amount. These data suggest that the differences observed between the micrococcal nuclease activity when H1* is present, are related to an increased condensation induced by H1*. An apparent discrepancy with the results obtained on reconstituted chromatin samples is explained.

005

DISTRIBUTION OF TISSUE SPECIFIC TIGHTLY BOUND NON-HISTONE PROTEINS IN REPEATING STRUCTURE OF CHROMATIN

F. Altieri, P. Allegra, R.I. Lonigro and P. Cafafa, Institute of Biochemistry, Faculty of Pharmacy, University of Rome, Italy, and Center of Molecular Biology, Consiglio Nazionale delle Ricerche

Tightly bound non-histone proteins have been extracted from whole chromatin and core particles prepared from pig liver and kidney. We have investigated, by bidimensional gel electrophoresis, the distribution of this protein class in the repeating structure of chromatin. Our results reveal that non-histone proteins tightly bound to DNA are an heterogeneous protein class. Some of them, particularly in the core particles, appear to be common for both tissues, though having differences in their isoelectric point. This may be attributed to postsynthetic modifications. We have calculated that only 10% of core particles are associated with this protein class. In this 10% fraction there is on an average one tightly bound protein per core particle. Proteins which are surely tissue specific have high molecular weight (ranging from 130,000 to 70,000 in liver and more than 130,000 in kidney) and isoelectric point more basic in kidney. These proteins are located in the spacer regions and that could be probably related to the regulative role of these regions.

002

PHYSICAL STUDIES OF CHROMATIN-HIGHER ORDER STRUCTURE
S.P. Dunn, J.P. Baldwin, B.G. Carpenter, H.W.E. Rattle, D.Z. Staynov and E.M. Boulter, Biophysics Laboratory, Portsmouth Polytechnic, White Swan Road, Portsmouth, U.K.

We have studied the folding of polynucleosomes as a function of ionic strength and chain length by neutron and x-ray scattering, photon correlation spectroscopy, and sedimentation. Neutron and x-ray results on long (>50 nucleosome) chains may be summarised as follows:

source of material	ionic strength	radius of gyration	mass/unit length (nucleosomes/nm)
chicken	40 mM NaCl	10.2 nm	0.35
erythrocyte	80 mM NaCl	11.3 nm	0.54
	1.2 mM Mg^{++}	12.5 nm	0.8
calf thymus	1.0 mM Mg^{++}	10.8 nm	0.42
	1.2 mM Mg^{++}	11.3 nm	0.62

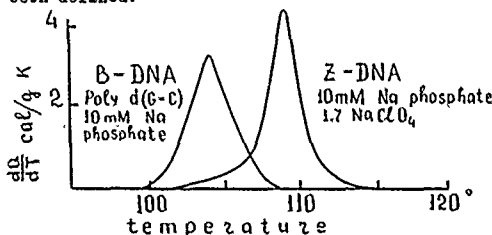
Photon correlation measurements on polynucleosomes of defined lengths from 24-60 nucleosomes agree with neutron scattering results in indicating a spring-like helical folding; the diameter remains approximately constant with increasing ionic strength above 20 mM NaCl, but with pitch steadily reducing to a final value ~ 10 nm. The data may be interpreted in terms of non-sequential arrangements of the nucleosomes in the coil as in the model of Staynov (Int. J. Biol. Macromol. 5 3-9 1983).

004

MICROCALORIMETRIC INVESTIGATION OF CHROMATIN, NUCLEOSOME, NUCLEOSOME CORE, AND DNA DENATURATION PROCESS.

J.R. Monaseldidze, B.L. Andronikashvili and Z.I. Chanchalashvili, Institute of Physics Academy of Sciences of the Georgian SSR, Tbilisi, USSR

It has been shown that the character of mononucleosome and nucleosome core particle denaturation process is determined to a considerable extent by the DNA double helix length. The study of mononucleosome, nucleosome core particle and the whole chromatin renaturation process allows to suggest that they all have different denaturation mechanisms. The thermodynamic characteristics of nucleosome DNA and poly d(G-C)d(G-C) have been defined.



006

THE ROLE OF INTRACELLULAR PROTEINASES IN THE CELL CYCLE OF EUKARYOTES

P. Schauer, M. Korbeltik¹, A. Suhar², J. Škrk³, V. Turk² and M. Likar, Institute of Microbiology, Medical Faculty, Ljubljana, ¹R. P. Šković Institute, Zagreb, ²J. Stefan Institute, Ljubljana ³Institute of Oncology, Ljubljana, Yugoslavia

Purified intracellular proteinases, specifically neutral serine proteinase and cathepsin H, were added to the media of Chinese hamster lung fibroblasts *in vitro*. In one series of experiments the effect of added proteinases on the specific activities of various intracellular proteinases was analysed. It was demonstrated that addition of one type of proteinase affects not only the level of activity of this enzyme in the cell, but also modifies the activity of other intracellular proteinases.

In the other series of experiments the effects of added proteinases on the colony forming ability of synchronized populations of Chinese hamster cells was measured after various durations of exposure in different phases of cell cycle. It appears that both neutral serine proteinase and cathepsin H can have either stimulatory or inhibitory effect on colony formation, depending on the time and duration of exposure.

Posters on Chromatin Structure and Function

007

DISTRIBUTION OF CYCLIC AMP PHOSPHODIESTERASE ON PIG LIVER CHROMATIN
G. Lupidi, A. Ferraro, E. Riva, Department of Cellular Biology, University of Camerino, Institute of Biological Chemistry, University of Roma La Sapienza, CNR Center of Molecular Biology, Roma, Italy

In view of the possible involvement of cyclic AMP phosphodiesterase in the regulation of chromatin activity, the localization of the enzyme was studied in different chromatin fractions. Fractions enriched in transcriptionally active chromatin from whole pig chromatin were prepared according to Gottesfeld et al. Proc. Nat. Acad. Sci. (1974) 71, 2193, by a partial hydrolysis with DNase II. The "active" fraction, which accounted for 4% of total chromatin appeared three to four times enriched in cyclic AMP phosphodiesterase activity when compared to the "inactive" fraction. These results suggest that this enzyme takes part in the regulatory mechanism of chromatin transcription.

Supported by grant MPI

009

MICRO RAMAN SPECTROMETRY OF INTACT CHINESE HAMSTER CHROMOSOMES J. Greve, F.F.M. de Mul and A.G.M. van Helie, Department of Applied Physics, Twente University of Technology, P.O. Box 217, Enschede, The Netherlands.

A home-made Raman microspectrometer was used to study pelleted Chinese hamster chromosomes both by normal Raman scattering and by surface enhanced Raman scattering. The chromosome pellet appeared to suffer no damage of the focused laser beam and good reproducible spectra could be recorded in a short time. From the protein part of the spectrum follows that a considerable contribution from non-histone proteins is present. The protein conformation is a mixture of α -helix and random coil conformation. The DNA of the chromosomes is in the B-conformation, no indication of the presence of Z-DNA was obtained. Moreover no splitting of the 1096 cm^{-1} phosphate backbone stretch vibration was observed. In surface enhanced Raman scattering experiments enhancement of some lines could be shown. Especially the Raman lines due to DNA base adenine at 730 cm^{-1} and the Raman lines due to adenine, thymine, cytosine and guanine at 1310 - 1385 cm^{-1} showed a considerable enhancement.

011

STRUCTURE OF THE TETRAMERIC (H3/H4)₂ 146 bp AND HEXAMERIC (H3/H4)₂(H2A/H2B)₂ 146 bp SUB-NUCLEOSOMAL PARTICLES
C.M. Read, J.P. Baldwin and C. Crane-Robinson, Biophysics Laboratories, Portsmouth Polytechnic, St Michael's Building, White Swan Road, Portsmouth, Hants, UK.

As models for intermediates in chromatin processing, tetrameric and hexameric particles were prepared by depletion of core particles using 250 mM NaCl, 4M urea in the presence of a cation exchange resin, followed by sucrose gradient separation. The composition of the depleted particles was determined by histone/histone crosslinking and sedimentation equilibrium. $S_{20,w}$ values were 6.82 and 9.08 S respectively. Small angle neutron scattering from the tetramer showed radii of gyration R_g of DNA and protein to be 5.02 and 3.47 nm. R_g DNA for core particles was measured as 4.98 nm and it is concluded that this depleted particle is as compact as the core particle. This was confirmed from calculation of the maximum dimension of the tetramer, 12.5 nm, again very close to that of the core particle. Optical melting of tetramer particle showed 54 bp strongly bound to histone and 20 bp more weakly bound. In the hexamer an extra 20 bp are strongly bound to histone. Digestion of tetramer particles both unlabelled and 5'-labelled with 32P, using DNase I and micrococcal nuclease, indicated that 70 bp, centrally located, are partially protected. Exonuclease III digests tetramer particles only slowly, implying histone contacts at the ends of the DNA. We conclude that the tetramer particle has 13/4 turns of superhelical DNA with the histone bound to the central 70 bp plus about 10 bp at each end of the DNA.

008

SOLVENT INTERACTIONS IN B12 COENZYME CRYSTAL HYDRATE.
F. Vovelle, J.M. Goodfellow, J.L. Finney, H.F.J. Savage and P. Barnes, Department of Crystallography, Birkbeck College, University of London, Malet Street, London WC1 7HX, U.K.

Both ordered and disordered solvent networks of vitamin B12 coenzyme crystal hydrate are generated by Monte Carlo simulation techniques. Five different potential energy functions are used to model water-water and water-solute interactions. Each of these simulations is compared with the experimental structure which is well characterized in both solvent regions. The results are analysed in terms of structural properties of water network such as mean water oxygen and hydrogen positions, coordination of each water molecule and maxima of the probability density map (PD).

The following is found: (1) Reasonable agreement is obtained between predicted and experimental positions in the ordered region whatever the potential function used. (2) In the disordered channel region, only EMP1 potential reflects the experimental data. (3) In the channel region different hydrogen bond networks may be predicted in different asymmetric units so, it is essential to simulate more than one asymmetric unit to look at the disorder in the solvent region. (4) PD maps are very useful for picturing the disordered regions, but there is no significant difference between the hydrogen bond networks calculated from average predicted solvent molecule positions and those obtained from the maxima of the PD maps.

010

PERTURBATION OF DNA REPLICATION BY SODIUM ARSENITE

F.H. Yew and P.T. Yeh, Dept. of Zoology, National Taiwan University, Taipei, Taiwan, ROC.

Sodium arsenite is known to raise sister chromatid exchange rate in cultured cells and to cause cancer in human. It also acts synergistically with UV and mitomycin C on cell toxicity, mutation rate and chromosome aberration. There is no evidence of direct interaction between arsenite and DNA. However, in the presence of 100 μM arsenite, the distribution of H³-thymidine label (5min) on nascent DNA sedimentation profile in alkaline sucrose gradient is different from that of control, which suggests that an alteration in the stationary state population of various replicative intermediates has occurred. The perturbation is accompanied by an increase of nucleoid sedimentation rate which reflects the change in the superhelicity of nuclear DNA as verified by ethidium bromide titration. The effect of arsenite is maximal after 30min incubation then reaches a new stationary state when the exposure time is prolonged.

012

STUDY ON *E. coli* LETHALITY AFTER OXIDATION OF INDOLE-3-ACETIC ACID

Maricilda P. De Mello^a, Sonia M. De Toledo^a, Luciana C.C. Leite^b, Adelaide Faljon-Alarico^b, and Nelson Duran^b, Department of Chemistry, Fundação Universidade Estadual de Maringá, C.P. 331, Maringá, CEP 87.100, PR, Brazil^a; Universidade Estadual de Campinas, Campinas, SP, Brazil^b; Universidade Estadual de São Paulo, SP, Brazil^c.

E. coli 248(vt) cells under treatment with indole-3-acetic acid/Peroxidase/O₂ system are protected from damage by excited state species (triplet Indole-3-Aldehyde and Singlet Oxygen) generated in this reaction. This protection occurs only in the first 10 minutes of interaction, after this period a rapid lethality is observed. *E. coli* 871 (Rec A), 1069 (uvr B) and 877 (pol A) cells present a more pronounced effect. Histidine and guanosine (efficient singlet oxygen traps) show 50% of protection. Similar results are obtained with a sensitizer such as Acridine Orange. Using the *E. coli* HB 101, pBR 322 plasmid, strand scission can be detected after treatment with enzymatic system leaving 20% of supercoiled form and 80% of linear form. Guanosine and tryptophan protect 50% and 60% while mannitol (an OH[•] trap) protects 40%. These results indicate that the lethality is related to the presence of Singlet Oxygen and OH[•] species. The role of tRNA in *E. coli* as precursor of Singlet Oxygen is tested by energy transfer from 4-thiouridine to DNA by an unknown mechanism. The K_{SV} value for this process is about 10⁴ M⁻¹. Support by: CNPq, FAPESP, FINEP and UNESP/PRUD.

Monday 30 July Congress Centre-first floor. Posters 013-018

Posters on Chromatin Structure and Function

013 ORAL PRESENTATION

THE LAYERED ORGANIZATION OF NUCLEOSOMES IN 30 NM CHROMATIN FIBERS. J.A. Subirana, Sebastián Muñoz-Guerra, Joan Aymami, Unidad de Química Macromolecular del C.S.I.C., Barcelona, Spain
Michael Radermacher and Joachim Frank, Center for Laboratories and Research, N.Y. State Dept. of Health, Albany, New York, USA

The 30 nm chromatin fibers from sea cucumber sperm and chicken erythrocytes were investigated by electron microscopy and three-dimensional reconstruction. For four fibers, the positions of individual nucleosomes were determined by fitting spheres to the reconstructed three-dimensional stain density distribution. The average distance between neighbouring nucleosomes is close to 11 nm. The longitudinal periodicity of 10-11 nm apparent in the fibers is found to originate from a grouping of the nucleosomes into disks, each containing 5-6 nucleosomes. The chromatin fiber appears to be formed from closely stacked disks. The nucleosomes may be connected either as a regularly distorted helix or as a layered zigzag. The frequent observation of constrictions in the fiber makes a zigzag connectivity more likely.

This work was supported, in part, by NIH grant 1 RO 1 GM 29169 and by grant 219 from the Comisión Asesora de Investigación Científica y Técnica.

015

CHROMATIN ORGANIZATION AND REPLICATION PROFILE OF A MOUSE INTERSPERSED REPEATED DNA SEQUENCE. Nancy Lynn Rosenberg and Douglas L. Vizard, Physics Dept., MDAH, U. of Tx., Houston, Tx. 77030.

The interspersed repeated sequences of the mouse genome can be revealed by length resolution of S1 nuclease-treated reassociated DNA. The major interspersed repeat, MIF-1, is characterized by a sequence that is segmentally heterogeneous, but, nevertheless, is distinguished by a highly conserved length, 6Kbp. Vizard et al have mapped a Hind III 400 bp genomic fragment into MIF-1. We found that although the temporal replication profile of MIF-1 resembles that of total DNA, the replication of MIF-1 lags by approximately 20 minutes behind total DNA replication. Using a combination of DNP (deoxyribonucleoprotein) electrophoresis and hybridization techniques, we have also shown that MIF-1 is associated with a higher order chromatin structure. Experiments utilizing second dimension DNA and protein electrophoresis are in progress to determine the nature of this chromatin structure.

017 ORAL PRESENTATION

CONFORMATIONAL TRANSITION OF CHROMATIN TO THE HIGHER ORDER STRUCTURE AND INTERACTIONS WITH DIVALENT IONS. H. Eisenberg, J. Ausio, N. Borochov, K.O. Greulich, D. Seger and E. Wachtel Department of Polymer Research, The Weizmann Institute of Science, Rehovot 76 100, Israel

We have studied the reversible transition of chromatin fragments, carefully isolated from chicken erythrocyte nuclei, from the "10 nm" fiber, at very low ionic strength, to the "30 nm" solenoid higher order structure, following increase of NaCl concentration to 75 mM or MgCl₂ to 0.3 mM. From the angular dependence of scattered light from chromatin fractions (containing between $N_z = 22$ to 53 nucleosomes per chain) we calculate 5.7 nucleosomes per solenoid turn, assuming a rigid cylindrical closely packed higher order structure (the pitch was taken to be 11 nm and the radius of the cylinder 13 nm). Frictional coefficients were calculated using the same parameters. They were found to be significantly lower than the experimental values derived from ultracentrifugation and quasielastic light scattering, allowing the possibility of a more extended and flexible structure. Small angle X-ray scattering reinforces the latter view. Two distinct slopes in the Porod cross-section plots of folded chromatin lead to a description of chromatin folding in terms of mixtures of lower order and higher order structures, depending on ionic conditions. We have also investigated the interaction of other divalent ions with chromatin towards a closer understanding of the role of metal ions in the cell nucleus. The first row transition metal ion chlorides led to compaction and subsequently precipitation at a significantly lower concentration than the alkali earth metal ion chlorides.

014

YEAST TWO-MICROMETER MINICHROMOSOME STRUCTURE

C. Shalitin and A. Vishlitzky, Department of Biology, Technion - Israel Institute of Technology, Haifa, Israel.

Metrizamide gradients have been used to separate 2- μ m minichromosomes from nuclear chromatin. We used two yeast strains: Pep 4-3 cir⁺ (containing 2- μ m DNA molecules) and CB 11 cir⁻ (lacking 2- μ m DNA). Cellular chromatin released from CB 11 cir⁻ nuclei banded in metrizamide gradients at a density of 1.185 g/cm³. On the other hand, the DNA from pep 4-3 cir⁺ cells showed two major DNA peaks (1.16 g/cm³ and 1.18 g/cm³). DNA was extracted from the two peak fractions, run on agarose gels and blotted onto nitrocellulose. The blot was hybridized with two probes: 1) ³²P-nick translated p82-6B containing 1.5 copies 2- μ m DNA (from J. Hartley), 2) ³²P-nick translated pJHC11 containing *S. cerevisiae* ribosomal DNA. The autoradiogram showed that DNA extracted from chromatin banding at a density of 1.16 g/cm³ hybridized with p82-6B DNA. Thus the DNA peak at 1.16 g/cm³ contained 2- μ m chromatin free of contaminating cellular chromatin whereas the DNA banding at 1.18 g/cm³ contained ribosomal genes. Our results suggest a lower ratio of histones to DNA in 2- μ m minichromosomes as compared with genomic chromatin. This finding was further substantiated by analysis of histones bound to the chromatin and by electron microscopy. The procedure described herein may be useful for the isolation and characterization of other yeast minichromosomes.

016

CONFORMATIONAL SIMILARITIES AMONG VARIOUS SIGNAL PEPTIDE SEQUENCES: Ch. Mohan Rao and D. Balasubramanian, Centre for Cellular and Molecular Biology, RRL Campus, Hyderabad 500 007, India.

Many secreted proteins are biosynthesised as precursors containing a N-terminal 15-40 residue 'signal' peptide sequence that aids in anchoring the preprotein to the membrane, where the signal sequence is cleaved by a signal peptidase thereby secreting the processed protein. While there is no perceptible sequence homology among them, many signal sequences are seen to have lys or arg close to their N-terminal end, several hydrophobic residues in the middle and pro near the cleavage site. We have therefore looked for any commonality in the folding pattern of over 78 signal peptides, both in their entire sequence and in their various fragments. We used the Eisenberg method which quantifies the conformational correlation between any two peptide sequences based on the hydrophobicity parameters of the residues. Over 66% of the peptides cross-correlate to better than 0.4 correlation coefficient value suggesting overall conformational similarity among their total sequences. Similar analysis of the first 12 residues of each of these again suggests a folding similarity of this fragment. When the last 5 residues were likewise analysed, some conformational flexibility was indicated. The results suggest that a major portion of each of the signal sequences might adopt similar chain conformations and that the processable ends might display some variation.

018

THE FOLDING MODE OF INTERPHASE MAMMALIAN DNA.

B. Cavazza, V. Trefiletti, M. Pala; C. Balbi and E. Patrone, Cntr. for Macromol. Studies, CNR, C.so Europa, and Nat. Inst. for Cancer Res., V.le Benedetto XV, Genoa, Italy.

It has been recently reported by our group that higher-order structure of interphase chromatin conforms to a coiled-coil organization; the path of DNA along the 30 nm fibre, however, has still to be recognized. Hepatocytes were lysed (0.2% Sarkosyl, 20 mM Na₂EDTA, 2M NaCl, pH 10) on cellulose triacetate filters; after washing and extraction the material consisted of naked DNA and a few proteins from the nuclear matrix. E.M. investigation has been carried out according to the method already described (Cavazza et al. J. Cell Sci. 62, 81, 1983). The DNA fibres are supercoiled and unwind at several points, clearly revealing a multistrand organization. 2-mercaptoethanol induces sharp kinks at regularly spaced loci along the single filaments. The torsional stress is completely released by ethidium intercalation. Giant, cage-like structures result, their main morphological features being inflection points in which four subfibres converge, as well as short regions where two subfibres interwind. The path of DNA can be unambiguously followed over a length up to 100 μ m. Our observations lead to a simple scheme of the folding mode of interphase DNA: very long fibres can be generated by local interwinding. This scheme offers a possible interpretation of the mechanism of synchronized initiation of DNA synthesis.

Monday 30 July Congress Centre-first floor. Posters 019-024

Posters on Chromatin Structure and Function

019

INTERACTION BETWEEN NON-HISTONE PROTEIN HMG14 AND HISTONE DIMER H2A.H2B

E. Espel^{1,2}, J. Bernués¹, P. Martínez^{1,3}, E. Querol¹

¹Institut Biologia Fonamental "V. Villar Palasí"

²Facultat de Veterinària. ³Dept. Biol. Cel.

Universitat Autònoma Barcelona. BELLATERRA. Spain

The interaction between non-histone proteins HMG14 and HMG17 and histone oligomers H2A.H2B and H3.H4₂ has been studied in free solution by chemical crosslinking with Dimethyl-3,3'-Dithiobispropionimidate (DTP), Dimethyl Suberimidate (DMS) and 1-Ethyl-3-(3-Dimethylaminopropyl)Carbodiimide (EDAC). One and two-dimensional electrophoretic patterns of the crosslinking products show the presence of bands indicating that HMG14 interacts with histone dimer but not with histone tetramer. The interaction seems to be preferentially, although not only, ionic (a band of interaction is seen even at 0.4M NaCl). The more likely stoichiometry of the interaction is HMG14/(H2A.H2B)₂ (1:1) as determined by means of two-dimensional electrophoresis. In the case of HMG 17 no bands of complexes with core histones are detected.

021

A SIMPLE THEORY FOR DNA ELUTION FROM FILTERS

C. Balbi, S. Parodi, M. Pala, B. Cavazza, V. Trefiletti and E. Patrone, Cntr. for Macromol. Studies, CNR, C.so Europa and Nat. Inst. for Cancer Res., V.le Benedetto XV, Genoa, Italy.

DNA chain scission, induced both in vitro and in vivo by various agents, is an event of great biological relevance; although the damage is currently evaluated by empirical membrane separation techniques, the results are quite reproducible and the sensitivity as high as 1 single strand break/10⁹ Daltons. We outline a simple theory of the filtration of coiled macromolecules through porous membranes, treated at the quasi-equilibrium. The basic transport equation $J_i = c_i(1 - \sigma_i)J_v$ is solved by considering that the value of σ_i , the reflection coefficient of component i , ($1 \leq i \leq N$), is given by $(1 - K_i f_i)$, where K_i is the partition constant between pore and solution, a function of the conformational entropy loss of the coil, and f_i accounts for the frictional force experienced by a particle moving along the pore. Hydrodynamic forces overcome diffusion so that the volume filled up with solute is $V_s = \sum n_i^4 / 3\pi(R_{Gi})^3$ where R_{Gi} is the i th radius of gyration. The solution of the resulting set of N differential equations gives n_i , the number of molecules of component i remaining on the filter, as a function of the elution volume V . The theory demonstrates that the process is governed by the average dimensions of the coil, so affording a universal calibration of filter elution methods, in excellent agreement with the experiments.

023

020

ORIENTATION OF NUCLEOSOMES IN THE HIGHER ORDER STRUCTURE OF CHROMATIN.

D. Staynov, A. Thorne, S. Dunn and C. Crane-Robinson, Biophysics Laboratories, Portsmouth Polytechnic, St Michael's Building, White Swan Road, Portsmouth PO1 2DT, UK.

DNA nuclease digestion patterns of whole nuclei were used to study the orientation of nucleosomes in the 30 nm fibre of chromatin. Large molecules like DNaseI and DNaseII cannot penetrate the fibre and digest only those parts of DNA which are exposed on the outside of the fibre. Thus the DNA digestion pattern depends strongly on the orientation of nucleosomes and the position of the linker DNA.

Experimentally obtained digestion patterns were compared with computer simulations based on various possible nucleosomal arrangements. It was found that:

1. Nucleosomes are not uniformly exposed towards the "surface" of the fibre but alternate within a limited angle.
2. The periodicity of alternation is 2 and does not depend on the DNA linker length.
3. There is no periodicity in the exposure of the DNA linkers and they are less accessible to nucleases than if they were on the outside of the fibre.
4. The "double nucleosome repeat" and the "half nucleosome repeat" patterns obtained by digestions with DNaseI and DNaseII respectively are determined by the same periodical exposure of DNA.

Only a very limited range of possible higher order structures are accommodated by the results.

022

DIFFERENTIAL SCANNING CALORIMETRY (DSC) OF INTERPHASE NUCLEI. STRUCTURAL INTERPRETATION OF THE THERMAL TRANSITION.

V. Trefiletti, C. Balbi, M.L. Abelson, B. Cavazza, S. Parodi and E. Patrone, Cntr. for Macromol. Studies, CNR, C.so Europa, and Nat. Inst. for Cancer Res., V.le Benedetto XV, Genoa, Italy

The melting of chromatin from intact rat liver nuclei has been investigated by DSC. The thermal profiles show four main transitions centred around 332, 350, 365, 380 K respectively (V. Trefiletti et al. Science 219, 176 (1983)). The transition enthalpy is a function of both the degree of degradation and of salt concentration and drug intercalation. By assuming that each peak arises from the denaturation of a distinct molecular domain, according to an all-or-none process, it is possible to gain detailed information on the free-energy differences among conformations. Limited micrococcal nuclease digestion leads to the disappearance of the 380 K peak, which can be related to the melting of higher order structures of chromatin, as confirmed by the parallel enthalpy increase of the 365 K transition. Interestingly, the response of both the 365 and 380 K peaks to ethidium intercalation is biphasic, their enthalpy values passing through a sharp maximum and minimum, respectively, at a drug concentration equal to 10 µg/ml. This result indicates that interphase chromatin is supercoiled and simple thermodynamic considerations lead to a zero order estimate of the mean superhelical density for nuclei under native conditions.

024

Monday 30 July Congress Centre-first floor. Posters 025-030

Posters on Molecular Evolution

025

THE MITOCHONDRIAL DNA: AN INFORMATIONAL ANALYSIS

M.I. Granero-Porati, and A. Porati, Dipartimento di Fisica, Università di Parma, Via D'Azeglio 85, Parma, ITALIA.

The recent availability of a great number of polynucleotide sequences, also of mitochondrial origin, allowed us to examine, with the aid of the computer, the more significant informational parameters of many DNA sequences, in order to assign an evolutionary meaning. In particular, we used the well known indexes D_1 and D_2 (divergence from equiprobability and divergence from independence) and R (redundancy) related to the so-called S-Entropy, $H = - \sum p_i \log p_i$, introduced by Shannon and applied to the study of the structure of languages. These indexes were also used by Gatlin in the context of biological languages. We also considered the application of informational parameters, more suitable for short sequences, derived from the so-called "k-Entropy" introduced by Kolmogorov. Our research concerns the study of the mitochondrial DNA sequences from various organisms and the sequences of genes (both nuclear and mitochondrial) coding for the same protein. The results indicate that sequences of mitochondrial origin are "similar" (from the point of view of information theory) to the bacterial ones, supporting the idea of symbiotic origin of these organelles.

027 ORAL PRESENTATION

PRIMITIVE RIBOSOMES, D.P. Burza, D.S. Tewari, B. Nag, A.K. Srivastava and S. Srivastava, Molecular Biology Unit, Department of Biochemistry, Institute of Medical Sciences, Banaras Hindu University, Varanasi-221005, U.P., India.

It has been demonstrated in this laboratory that RNA-RNA interaction plays the major role in the association of the ribosomal subunits of *E. coli*. The evidences are based on the binary complex formation between 16S and 23S RNAs under certain specific conditions (Burza et al., Proc. Natl. Acad. Sci., U.S.A., 80, 4875, 1983) and ketoxal treatment of 36S and 50S ribosomes as well as naked 16S and 23S RNAs (Nag and Burza, communicated). Ketoxal treatment has also shown the existence of two populations of 23S RNA and there are indications that the two may be directly involved in the EF-G-dependent translocation of peptidyl tRNA on the ribosome. It has also been possible to demonstrate the ribosome-like activity of 16S, 23S RNA complex with the addition of 5S RNA and a limited number of proteins. The following activities which are rather weak have so far been shown: (i) poly U binding (ii) poly U-dependent binding of phenylalanyl tRNA and (iii) N-acetyl phenylalanyl tRNA (iv) EF-G-dependent GTPase activity (v) peptidyl transferase activity (vi) protein reaction and (vi) polyphenylalanine synthesis. These results support the concept of Crick (J. Mol. Biol., 38, 367, 1968) and Orgel (J. Mol. Biol., 38, 381, 1968) that ribosomal RNAs might have acted as primitive ribosomes.

029

"INTERSUBUNIT CONTACTS IN COOPERATIVE, DIMERIC HEMOGLOBINS".

A. Boffi, F. Ascoli, J. Hermans and E. Chiancone, C.N.R. Centre of Molecular Biology, Institute of Chemistry Faculty of Medicine, University "La Sapienza", Rome, Italy.

The dimeric, cooperative hemoglobin component present in the red cells of Arctid mollusks (*Anadara scapharca*) is made up by two identical polypeptide chains and may thus represent an intermediate stage in evolution from myoglobins to tetrameric hemoglobins.

Identification of the intersubunit contact regions in these dimeric hemoglobins has been attempted given the lack of crystallographic data. The primary sequence has been compared with that of sea lamprey hemoglobin (a monomer which dimerizes when deoxygenated) and horse hemoglobin. The significant differences in the distribution of polar and hydrophobic residues at the contact regions characteristic of the tetrameric proteins indicate that dimers of the type $\alpha\beta$ - $\beta\alpha$ and $\alpha\beta$ - $\beta\alpha$ would not be extremely stable. The formation of interchain crosslinks by reaction of *Scapharca* hemoglobin with bifunctional reagents and the identification of the side chains that have reacted on each half of the molecule have therefore been used to determine spatial relationships of neighbouring aminoacids.

Interchain crosslinking increases the oxygen affinity of the molecule.

026

A STUDY OF HEMOGLOBIN FROM XENOPUS LAEVIS AND ITS EVOLUTIONARY SIGNIFICANCE

S.G. Condò, A. Bellelli, M. Lunadea, B. Giardina and M. Brunori, Inst. of Chemistry, Faculty of Medicine, University of Rome, Rome, Italy.

The evolution of oxygen carrying proteins has led to the development of mechanisms to optimize the function in relation to the specific requirements of the organism. In an attempt to elucidate the logics of this process we have carried out an extensive comparative investigation of the structure and function of hemoglobins, and recently have studied the respiratory proteins from *Xenopus laevis*, whose primary structure is now available. Hemoglobin from *X. laevis* has been characterized in its equilibrium and kinetic properties; it has also been splitted into α and β chains which have been separated in the native state and characterized from a functional stand point. Some features of this protein may be traced to some of the amino acid residues occupying specific positions in the primary structure; for example the Root effect, an extreme reduction of oxygen affinity at low pH values (which *Xenopus* hemoglobin shares with some fish hemoglobins) is attributed to the presence of a Ser residue in the $\beta 93$ (occupied by Cys in mammalian hemoglobins). These and other observations suggest some caution in accepting, without reservations, the conclusions reached through comparative evaluation of amino acid substitutions which have been carried out overlooking the functional role of specific residues in the protein. In this case in fact every substitution has the same weight and is independent of functional considerations which may be crucial to selection.

028

CELLULAR DIFFERENTIATION- LAMARCKIAN VS DARWINIAN MODEL

A. Ladislav, Institute of Microbiology, Videnská 270, Prague 8, Czechoslovakia

The analysis of cellular differentiation in the hemopoietic system was performed on the assumption of cellular differentiation analogy to evolution with different types of fully differentiated cells being analogous to organisms belonging to different species. Darwinian explanations of evolution emphasize the importance of random, occurring gene mutations as a source of diversity, and selection as a means by which environmental factors can impose some order on the process. On the other hand Lamarckian model emphasizes the major phases of cellular differentiation are based on differential gene expression in response to external stimuli. In this spirit one can treat Darwinian model as a thermodynamic system far from equilibrium /stochastic description/ wherein the order is created through fluctuations. In contrast Lamarckian model can be considered as nonlinear dynamical system with dissipation /deterministic description/ possessing a strange attractor. The pros and cons of both models are analyzed on the theoretical and experimental evidences to be known. It is argued the Lamarckian model is more appropriate to describe the hemopoiesis.

030

PIGEON EGG-WHITE LYSOZYME AND ITS STRUCTURAL RELATEDNESS TO OTHER TYPE C LYSOZYMES

L. Menéndez-Arias, G. González de Buitrago and R. Rodríguez, Dpt. Biochemistry, Fac. Sciences, Complutense Univ., Madrid-3.

Pigeon lysozyme has been purified and characterized as a type c lysozyme. However, it was found that pigeon and chicken lysozymes had different immunological characteristics and a high number of amino acid differences at the N-terminal region.

New data on the primary structure will be reported. Apart from the classical methods of structural comparison of homologous proteins, based on the alignment of sequences, we have studied the structural homology among type c lysozymes at different levels:

- Prediction of the secondary structure. This was done by using the methods described by Chou & Fasman and Lin. According to these, a different pattern of secondary structure for Anatid lysozymes c and Phasianoid lysozymes c was obtained.

- Tertiary structure was compared by using methods dealing with the hydrophobic character of the proteins and prediction of antigenic determinants. Application of these methods to the structural comparison of pigeon lysozyme will also be reported, discussing their advantages in the study of protein evolution.

Posters on Molecular Evolution

031

FOUR DIFFERENT TYPES IN PROTEINS REVEALED BY AN ANALYSIS OF AMINO ACID COMPOSITION DATA
K. Hishikawa, Y. Kubota and T. Ooi, Institute for Chemical Research, Kyoto University, Uji, Kyoto-fu 611, Japan

A protein can be expressed as a point in the "composition space" of 18 orthogonal axes, each representing the content of amino acid. We have analysed the distribution of 356 proteins in this space to see whether it reflects the difference in general properties of the protein. It was found that the amino acid composition of a protein has clear correlations with its biological properties, i.e., enzyme or nonenzyme, and intra- or extracellular type. Hence we classified proteins into four types of intracellular enzyme (I), intracellular nonenzyme (II), extracellular enzyme (III), and extracellular nonenzyme (IV). In the composition space, proteins are separated well from each other depending on the four groups. Moreover, the folding type of a protein also correlates with the four groups; intracellular enzymes (I) are characterized with the α/β type, nonenzymes (II) with α , and extracellular proteins (III and IV) with β and α/β . This parallelism among three different features of the protein, composition, biological nature and folding type, suggests that the distinction into the four groups is a basic framework in the protein taxonomy reflecting the evolutionary history.

033

A chaos model for appearance of life

J. Vincze and Z. Vincze
Dept. Biophysics, Cluj, Rumania

The life is originated from the sea-water containing organic molecules. The movement of the organic molecules can be considered as an undamped, generated, unharmonic oscillator. Sufficiently numerous collisions result in a chaotic movement. Making computer analysis, it was found, that following some thousands of iteration constant quadratic mapping can be observed in a given area. Collaterally, chaotic parts of the space are also present where the particles are not arranged along the trajectory, but they are scattered. The system crosses the points of chaotic territories in a random manner. Adjoining to the chaotic areas fine chain of elliptical points can also be found indicating the presence of macroaggregates which are sufficiently stable to compose consensuata. According to the classical theory the probability of protein-formation from 20 amino acids is in the order of 10^{-171} . The chaos-theory reduces the probability, since some hundred thousands of iteration makes the protein-formation possible. The chaotic character of the "primary ocean" excludes the necessity of external, accidental factors.

The experiences and calculations suggest chaotic and regular movements to be present at the same time, constructing a complicated living structure, being able to reproduce itself on a finer and finer scale.

035

EARLY REPTILIAN DIVERGENCE OF OVOMACROGLOBULIN

A. Ikai, M. Nishigai, M. Kikuchi, T. Osada & H. Arakawa, Dept. Of Biophysics and Biochemistry, Faculty of Science, The University of Tokyo, Hongo, Tokyo, Japan

We have recently shown that chicken ovomacroglobulin (ONG) has a strong affinity to various endoproteases and a tetrameric structure, both highly reminiscent of the characteristics of human serum α_2 -macroglobulin (α_2 -M)(1). In our subsequent work, ONG homologues were purified from the egg white of crocodiles(2), snakes and turtles. At the level of the sea turtle, a descendant of the oldest reptilian subclass, Anapsida, serum α_2 -M and ONG were distinct and immunologically non-crossreactive proteins. Since serum α_2 -M homologues were identified in the piscine, amphibian, reptilian and mammalian blood(3) we think that the divergence of ONG from α_2 -M took place in an early stage of reptilian evolution or earlier.

Binding of proteases to the purified ONG's caused a dramatic change in the latter's quaternary structure and their resistance to thermal denaturation. Protease binding to human α_2 -M exposes 4 sulphydryl (SH) groups but the same treatment exposed 2 and 0 SH's in crocodilian and chicken ONG's, respectively. Complete denaturation in SDS exposed 4 and less than 0.3 SH's in the respective two ONG's. Electron microscopic studies also showed a significant structural divergence of ONG's within themselves and from α_2 -M.

- (1) Kitamoto, et al., J. Biochem. 92 1679-1682 (1982)
- (2) Ikai, et al., J. Biochem. 93 121-127 (1983)
- (3) Starkey & Barrett, Biochem. J. 205 91-95 (1982)

032 ORAL PRESENTATION

THE tRNA-CYCLE AND ITS RELATION TO THE RATE AND ACCURACY OF PROTEIN SYNTHESIS

H. Liljenström, G. von Heijne and J. Johansson, Research group on theoretical biophysics, Department of Theoretical Physics, Royal Institute of Technology, Stockholm, SWEDEN.

We have constructed a kinetic model of the tRNA-cycle, and studied how the rate of protein synthesis depends on the size of the different tRNA pools (free tRNA, acylated tRNA, Tu-bound tRNA etc.) We have also looked at how different species compete with each other and what happens if a certain pool is suddenly changed. Of particular interest is how this substrate competition affects the accuracy and overall efficiency of the protein synthesis. Finally, we have used the model to study the effect of varying the relative tRNA levels in a system with constant codon frequencies in an attempt to find reasons for the experimentally observed proportionality between tRNA levels and codon frequencies. This kind of study is important for the understanding of how an effective protein synthesis apparatus has been developed during evolution. It is of great importance for the survival of the cell and for its competition capacity, that it has a system with optimized accuracy and growth rate, and the tRNA-cycle is a key factor in such a system.

034

STRUCTURAL AND FUNCTIONAL RELATIONSHIPS OF THE VARIABLE DOMAINS OF MHC ANTIGENS AND OTHER IMMUNOGLOBULIN RELATED MOLECULES, M. Kanehisa and C. DeLisi, Lab. of Mathematical Biology, Nat. Cancer Inst., NIH, Bethesda, MD 20205, U.S.A.

The class I and class II major histocompatibility complex (MHC) antigens contain N-terminal variable domains which are believed to lack significant sequence homologies to immunoglobulin variable domains. However, there are instances where the sequence is partially homologous to immunoglobulin variable domains; e.g. E-beta is homologous to Ig-kappa around the second cysteine. We have performed a thorough search for local homologies of all immunoglobulin related proteins and their genes, and quantified the degree and location of sequence similarities. Namely, the relationship is analyzed not for the entire sequences of variable domains, but for possible separate segments which may indicate both evolutionary and structural/functional relations. In fact, the pattern of appearance of local homologies is often correlated with the immunoglobulin framework (FR) regions. For example, Thy-1 contains homologies in FR1 and FR3 but not in FR2, while the T-cell receptor δ 6T1 contains good homologies in FR2 as well. The local homology search is then combined with the structural prediction algorithms, and the locations of allotypic variations in MHC antigens are superimposed on the predicted structure.

036

CHARACTERIZATION OF THE E. COLI GENOME BY STATISTICAL ANALYSIS OF TNA SEQUENCES, R.D. BLANE and P.W. HINDS, Dept. Biochemistry, Univ. of Maine, Orono, Maine USA.

A table of codon probabilities for each of the 64 triplets has been produced from analysis of 61 coding sequences totalling 103,100 bp from *E. coli*. The results are distinctly nonrandom and serve as a basis for a computer program that identifies reading frame segments in *E. coli* sequences. The program works by moving weighted averages of codon probabilities down the sequence for each of three reading frames. Codon probabilities in *E. coli* coding segments are approximately 70% higher than in non-coding segments, so that genes or fragments of genes are readily identified. Average codon probabilities for known genes show a bimodal distribution when plotted against the number of base pairs exhibiting that average. This means that some genes are significantly more susceptible to post-transcriptional influences of the nonrandom pattern. We suspect that both evolutionary age and function affect the level of codon bias in genes. The codon pattern is species specific. We also observe the genome-wide presence of a non-random oligonucleotide pattern. We propose these patterns to be the consequence of functional factors as well as duplication-divergence events during the evolution of the *E. coli* genome, and which perpetuate the codon bias, as well as the oligonucleotide bias in non-coding segments. The latter process would provide a selective advantage, since divergence events following gene duplication would begin with a sequence enriched in species-specific codons, greatly facilitating the development of new genes.

Monday 30 July Congress Centre-first floor. Posters 037-042

Posters on Molecular Evolution

037

A NOVEL SPECIES OF CRYSTALLIN IN THE FROG LENS
G.G.Gause, Jr., S.I. Tomarev, R.D. Zinovieva and
S.N. Dolgilevich, Institute of Developmental
Biology, USSR Academy of Sciences, Moscow, USSR

A recombinant DNA clone coding for a major
35 kDa polypeptide from the frog (*Rana temporaria*)
eye lens has been isolated and sequenced. The se-
quence 889 nucleotides in length (without counting
poly(A) tract and connectors) shows no homology
with the sequences coding for other major classes
of crystallins: α -, β -, γ - and δ -. The sequence does
not contain any internally duplicated regions. The
35 kDa polypeptide coded by the clone was termed
 ξ -crystallin. It may well be unique for the frog.
The ξ -crystallin mRNA is 1200 nucleotides in
length and about 3/4 of its coding region is pre-
sented in the cloned cDNA (225 amino acids in the
derived amino acid sequence). ξ -crystallin cDNA
probe has been found to hybridize with heterologo-
us (human) DNA probably because the cDNA contains
a genomic repeat conservative in evolution. Predic-
tion of ξ -crystallin secondary structure has de-
monstrated the presence mainly of β -strands with
only a few α -helical regions. Procedure developed
to preparatively isolate ξ -crystallin makes use
of a combination of DEAE- and phosphocellulose
column chromatography and yields an electrophore-
tically homogeneous preparation of this polypep-
tide.

039

038

PRIMORDIAL GENETIC CODE.

M.A. Soto and J. Tohá. Lab. Biophysics, Dept. Phy-
sics, Univ. of Chile, Santiago, Chile.

It is assumed that at the origins of the gene-
tic information some biopolymers were formed, being
most probably conserved, those characterized by: an
automorphic replication, the maximum information
content and a high stability. Starting from these
conditions we analyze the evolution of the genetic
code up to the present solution. It turns out that
this solution corresponds to the application of the
optimization principle of storing information to
the present genetic code. For a given system $N = p^n$
(n number of amino acids, p base of the code and n
number of positions) the optimum is attained for
 $p = e$ (Achinowicz et al., 1981). The present solution
 $e_3 = 20$ amino acids, probably emerged with the res-
trictions mentioned before, in such a way that:
1) It began with a mononucleotide representation of
the 4 early amino acids. 2) It evolved to a dege-
nerated code of nucleotide doublets, necessary dis-
posed in automorphic tetramers. At this stage, $e_2 =$
7.39 (7 to 8 amino acids) are codified by 16 dege-
nerated doublets. 3) It appeared the present day
code of 20 amino acids and 64 triplets, where all
the conditions were attained arriving to the ideal
 $e_3 = 20$ amino acids. the automorphic structure gave
origin to the double strand, the organization con-
tains a maximum of information. None of the Inter-
mediate steps can be considered an adequate solution.

040

041

042

Monday 30 July Congress Centre-first floor. Posters 043-048

Posters on Folding, Dynamics and Solvation of Macromolecules

043

THE DEPENDENCE OF DNA HYDRATION ON BASE COMPOSITION AND THE ROLE OF THE DNA HYDRATE SHELL HETEROGENEITY IN THERMAL AND CONFORMATIONAL PROPERTIES OF THE DOUBLE HELIX

G.M. Mrevlishvili, G.Sh. Japaridze, V.M. Sokhadze, D.A. Tetishvili, Yu.G. Sharimanov, Inst. of Physics, Acad. of Sci. of the Georgian SSR, 380077, Tbilisi, USSR.

Low-temperature microcalorimetry techniques have been used to investigate water-DNA interactions. It has been established that the solvent structure around DNA double helix is heterogeneous. Water state is very sensitive to base composition and sequence; a strict correlation between the number of water molecules in internal (n') and external (n'') hydrate layers and the GC-base pairs content is revealed: $n = n' + n'' = 28.0 - 0.12(\%GC)$, $n' = 12.0 - 0.06(\%GC)$ (in MHO/MBP). It is shown that at B-Z transitions occurring in poly-(dG-dC)-poly-(dG-dC) solutions abrupt changes in polymer hydration and bulk water properties take place. The DNA heat capacity in low-temperature range (4-40K) also depends on the hydration parameters of double helix. It is stated that the structural heterogeneity of the water around the double helix, which depends on the base composition and sequence, should play an important role in the recognition processes.

045

HIGH PRESSURE STUDIES OF CYTOCHROME P-450 SPIN AND SUBSTRATE BINDING EQUILIBRIA M. T. Fisher, S. F. Scarlata, and S. G. Sligar, Univ. of Illinois, Urbana, Illinois, USA.

The effects of high pressure (0-2000 atm) on the spin and substrate binding equilibria of cytochrome P-450 isolated from *Pseudomonas putida* have been determined. The high spin ($S=5/2$) to low spin ($S=1/2$) spin equilibria of the ferric hemoprotein was monitored by UV-VIS spectroscopy at various substrate concentrations. High levels of d-camphor (99.5% saturation, 50 mM TrisCl, pH 7.2, 100 mM KCl) prevented the pressure induced high spin to low spin transition observed at less than saturating substrate concentrations. These optical changes were reversible at pressures to 1000 atm, whereas above 1000 atm a gradual increase in the formation of the inactive P-420 form of the cytochrome was observed as quantitated by the reduced carbon monoxide adduct. Detailed analysis in terms of a thermodynamic linkage model demonstrates that the "spin state shift" observed with increasing pressure is due to the dissociation of substrate from the active site of the cytochrome. Thus the observed spectral change as a function of pressure can be used to determine the volume change accompanying substrate binding. With camphor and the *Pseudomonas* P-450, a volume change of 34 ml/mole (58 Å³/molecule) was measured. This indicates a substantial conformational change of the protein upon camphor ligation. Analysis of the binding equilibria with camphor analogs as a function of pressure are also presented.

047

SOLUTION CONFORMATIONS OF POSTSYNAPTIC NEUROTOXINS AND OF MEMBRANOTOXINS OF ELAPID AND HYDROPHID SNAKES.

K.A. Muskat and Khait, Weizmann Inst. Rehovot, Israel, K. Hayashi, Gifu Univ. Gifu, Japan and N. Tanaka, Tohoku Univ. Sendai, Japan.

The exposure of side chains of tyrosine, histidine, and tryptophan in snake venom neurotoxins (short and long) and in membranotoxins was studied by photo-CIDNP at 270 MHz. The accessibility probe is the 10-carboxyethylflavin triplet. Trp 29 is accessible in all neurotoxins while Tyr 25 is practically inaccessible. Tyr 39 in cobrotoxin and Tyr 55 in α -bungarotoxin are accessible. His 6 (revised sequence) is inaccessible in the erabutoxins while His 26 is only very weakly accessible. His 22 of α -cobratoxin is inaccessible as are His 4 and 68 in α -bungarotoxin and His 4 of cobrotoxin. His 33 of cobrotoxin is accessible. The rigidity order α -bungarotoxin > α -cobratoxin > erabutoxins, with respect to the unfolding effect of 7M urea was deduced. In the present study, in the membranotoxins studied (cardiotoxin and its analogs I, II and IV as well as cytotoxin I and II) the two tyrosines Tyr 25 and Tyr 58 are only weakly accessible. The present studies allow deductions to be made about the accessibilities in analogous systems. Thus, the accessibility of His 33 and the inaccessibility of His 4 in cobrotoxin can be used to deduce the conformations of these residues in a large group of neurotoxins.

044

SIMULATIONLESS EVALUATION OF THE ROTATIONAL CORRELATION TIME FOR SLOWLY TUMBLING, PROTEIN-BOUNDED SPIN LABELS (SL): APPLICATION TO MODIFIED ALBUMIN

E.A. Protescu, V. V. Grecu, A. Enulescu, D. Onica Central Institute of Physics and Faculty of Physics, Bucharest - Magurele, Romania.

In order to get relative values of the "spectroscopic" rotational correlation time τ_R from the ESR spectra of slowly tumbling, proteins-bounded SL, the simplified method proposed by Hare et al. (BBA 555, 388, 1979) was extended from spherically symmetric to weakly/moderately anisotropic motion, by approximating τ_R with $(\tau_L \tau_T)^{1/2}$ (τ_L , τ_T - longitudinal and transversal correlation times). For glutaraldehyde-treated and control rabbit serum albumin (GA-RSA and RSA) labeled with maleimide SL, we found a mean ratio $\tau_R(\text{GA-RSA})/\tau_R(\text{RSA}) \approx 6.5$, in good agreement with the "molecular" correlation times ratio, $\tau_C(\text{GA-RSA})/\tau_C(\text{RSA}) \approx 8.5$, as evaluated from gel-filtration data by the Stokes-Einstein equation. This result supports the extension of the method and shows, in addition to the qualitative ordering of "mobilities" ($2A_{zz}$ splittings), that the SL definitely reports the protein polymerization - and not a conformational modification, as for the *in vitro* quasi-physiologically "aged" albumin (A-RSA) (where $\tau_R(\text{A-RSA})/\tau_R(\text{RSA}) \approx 0.3$). Accordingly, the antigenic similarity of GA-RSA and A-RSA (Onica et al., *Immunochimistry* 15, 947, 1978) is not correlated with the macromolecular structure.

046

MOLECULAR STRUCTURE OF ELASTINS

V. Renuopalakrishnan and D.A. Keith, Orthopaedic Research Lab., Harvard Med. Sch., Childrens Hospital Med. Ctr., Boston, MA 02115, USA.

Elastin, a hydrophobic and highly cross linked protein occupies a unique place in the connective tissue architecture and function. Only recently 90% of the primary structure of pig tropoelastin has been determined. Structure of elastin at all levels is poorly understood. Currently two different concepts of elastin structure are in vogue: an amorphous three dimensional network structure based on classical rubber theory of elasticity and a β -spiral model with α -helical segment in the cross-linking region, which attempt to relate the macromolecular structure with function. In the present study, FT-IR, FT-IR Photoacoustic, and Laser Raman spectroscopic studies on the structure of elastins from bovine ligamentum nuchae and ear cartilage with markedly different amino acid compositions are discussed. Bovine ear cartilage elastin contains reduced amounts of hydrophobic residues. Two important conclusions emerge from this study: A. Observed vibrations of the peptide moiety are consistent with a molecular structure containing β -turns and B. Based on the observed vibrations and the structural interpretations thereof, the elastin from the two tissues are likely to assume different secondary structures consistent with the differences in their amino acid compositions. Presently, we are determining the % of various secondary structures present in elastin to propose a working model for elastins in the two different tissues.

048

SYNTHESIS OF UNCHARGED BUTYL-AGAROSIS FOR PROTEIN ADSORPTION BY THE TRESYLCHLORIDE METHOD

A. Demiroglou and H.P. Jennissen

Institut für Physiologie, Physiologische Chemie & Ernährungsphysiologie der Universität München, Veterinärstr. 13, D-8090 München 22, West Germany

Sephacrose 4B was activated by the tresylchloride method [1]. Tresylation appears to involve a two-phase mechanism according to time. Tresyl-Sepharose was coupled to n -(1-¹⁴C)-butylmercaptan in an alkaline medium (butyl-S-Sepharose). A quantitative coupling of butylmercaptan was achieved after ca. 60 minutes yielding gels containing from 2-100 $\mu\text{mol/ml}$ packed gel. The degree of substitution is a non-linear function of the tresylchloride concentration employed for activation indicating a cooperative activation mechanism or an alteration of agarose structure. Although the gel volume can decrease by ca. 30% at high degrees of substitution the microscopic ultrastructure of Sepharose 4B is conserved.

The adsorption of phosphorylase b was measured at high ionic strength [2]. Apparent equilibrium is reached after 90-120 minutes. The measured isotherms corresponded to the Freundlich type. In comparison to butyl-agaroses (butyl-N-Sepharose) synthesized by the CNBr activation method [2] the above synthesized butyl-agaroses adsorb up to a magnitude more protein at low degrees of substitution.

1. Mosbach, K. and Nilsson, K. (1981) *Biochem. Biophys. Res. Commun.* 102, 449

2. Jennissen, H.P. (1976) *Biochemistry* 15, 5683

Monday 30 July Congress Centre-first floor. Posters 049-054

Posters on Folding, Dynamics and Solvation of Macromolecules

049

MACROSCOPIC DIFFUSION OF COUNTERIONS
IN DNA SOLUTION Lars Nilsson and
Lars Nordenskiöld, Div. of Physical Chemistry,
Univ. of Stockholm, SWEDEN.

The macroscopic diffusion of counterions in double helical calf thymus DNA solutions has been measured by ^7Li FT-NMR self diffusion experiments as a function of salt (LiCl and MgCl_2). The effective diffusion constant D^* is smaller than its value in a DNA-free solution but approaches the free value upon titration with salt. Based on the steady-state Smoluchowski diffusion equation and the Poisson-Boltzmann cylindrical cell model, a theoretical expression for the ratio γ^*/D_0 has been derived. Numerical calculations of D^*/D_0 based on this model are compared with the experimental results and found to be in close agreement over a large salt concentration range.

051

MOLECULAR DYNAMICS SIMULATION OF PARVALBUMIN WITH A MULTIPLE TIME STEP METHOD

O. Teleman, P. Ahlström and B. Jönsson,
Div. Physical Chemistry 2, Chemical Centre,
POB 740, S-220 07 Lund, Sweden

A molecular dynamics method was used to simulate the dynamic behaviour of the carp muscle calcium binding regulatory protein parvalbumin, which is homologous with the calcium binding proteins calmodulin and troponin C. The two calcium binding sites were both occupied in the simulation, and the X-ray structure was used as starting conformation.

The simulation was made by means of a multiple time step method in which the bond forces were evaluated every 0.2 fs whereas angular and nonbonded interactions were evaluated every 1.0 fs. Semiempirical potential functions were used. The methyl and methylene groups were treated as extended atoms whereas polar hydrogens were treated explicitly in order to account for hydrogen bonds. Typically the simulation of 1 ps required 480 CPU-sec. on a CRAY-TS.

The dynamics were simulated in vacuo for 130 ps. The results indicate that the protein contracts during the simulation at the same time as the external side chains are folded on to the surface.

053

SEGMENTAL MOTION OF BOVINE SERUM ALBUMIN
P. Denšar and M. Schara, J. Stefan Institute,
Ljubljana, Yugoslavia.

Electron paramagnetic resonance (EPR) was used to separate the slow and fast mobility of the spin labeled proteins. Albumin molecules dissolved in buffer exert the rotational Brownian diffusion which is slow compared to the segmental motion. In membranes, where the overall mobility of protein molecules is slow and strongly hindered, only the segmental mobility is left to influence the EPR line shape. The experimental spectra for the buffer dissolved spin labeled protein and the corresponding lipid protein complexes were evaluated by comparison with the calculated EPR spectra. The model used considers a slow isotropic motion to which a fast hindered mobility is superimposed. The spectra, reconstructed with respect to the variable rotational correlation times and steric hindrances which influence the calculated line shapes of the spectra, do describe the dynamics of albumin in various environments at different temperatures.

050

DISORDERED WATER STRUCTURE IN CRYSTALS OF THE VITAMIN B_2 CO-ENZYME H. Savage, National Bureau of Standards, Washington, D.C., and National Institutes of Health, Bethesda, MD., U.S.A

The distribution of the water molecules in the above crystals has been analyzed, using both high resolution neutron (0.95 Å) and X-ray (to 0.92 Å and 1.1 Å) diffraction. The resulting models were extensively refined using the methods of least squares and Fourier synthesis--the final R factors were 0.085 (neutron), 0.088 (X-ray 1) and 0.134 (X-ray, 2). During the refinement, a large number of water sites (mostly disordered) and an acetone molecule were identified for all the neutron and electron density, situated in the solvent regions. Several alternative water networks were formulated from the better defined (stable) solvent sites and were seen to extend throughout all the solvent regions of the crystal. Some of the more dynamic aspects of the solvent structure were also examined in terms of the continuous solvent density observed around and between the more stable sites. The geometrical details of the interactions of the disordered water molecules with polar and non-polar groups and other water molecules within the solvent networks have been studied. Indications are, that in addition to participating in standard 2 centered hydrogen bonding networks, the waters are also involved in 3 or 4 centered interactions where the noncovalent H---X donor distances lie within the range of 2.1 to 2.5 Å. Monte Carlo computer simulation calculations have also been performed for the solvent in this macromolecular system and the results are described by F. Vovelle, J.M. Goodfellow, J.L. Finney, and P. Barnes in this volume.

052

WHAT IS A DECISIVE FACTOR STABILIZING THE α -HELICAL CONFORMATION OF C-PEPTIDE: A SALT BRIDGE OR HYDROPHOBIC INTERACTIONS?

K. Padlecz, A. Bierzynski, Dept. of Biophysics, Polish Acad. of Sciences, ul. Rakowiecka 36, C-532 Warszawa, POLAND, K. Sobocińska, G. Kupryszewski, Inst. of Chemistry, Univ. of Gdańsk, ul. Sobieskiego 18, 80-952 Gdańsk, POLAND.

C-peptide /KETAAAKFERQNHse/ is a 13 amino acid long N-terminal fragment of RNase A. Even in aqueous solutions it shows a strikingly high content of the α -helical conformation /~20% at 3°C, pH=5.3/. It was shown /A. Bierzynski, P. S. Kim, R. L. Baldwin, Proc. Natl. Acad. Sci. 79 /1982/, 2470/ that the salt bridge between His¹² and Glu⁹ is at least partly responsible for the stability of the helix. If it is a decisive factor we can expect the peptide AEAHAAEAHse, in which two His-Glu salt bridges may be formed, to exist predominantly in the α -helical conformation. To have synthesized this peptide and investigated it by CD, UV and NMR spectroscopy, at temp. below 6°C, pH 2-6 the peptide remains in random coil conformation. This result provides a strong evidence that the His¹²-Glu⁹ salt bridge, although of some importance, is not the main factor inducing the helical structure in C-peptide. The hydrophobic interactions of Ile8 and/or Lys7 side chains with Ala 4 and 5 may be crucial. To test this hypothesis we have synthesized two analogues of C-peptide with either Lys7 or Ile8 substituted by an alanine residue. Investigation of these peptides is now in progress.

054

HIGH RESOLUTION C-13 AND N-15 SOLID-STATE NMR STUDY OF PURPLE MEMBRANE

K.-H. Spohn and R. Kimmich, Sektion Kernresonanzspektroskopie, Universität Ulm, Oberer Eselsberg, Ulm, Fed. Rep. Germany

Monday 30 July Congress Centre-first floor. Posters 055-060

Posters on Folding, Dynamics and Solvation of Macromolecules

055

Isocyanide Binding to Myoglobin. Effect of the Protein Matrix. G.M. Giacometti, A. Cao, D. Anderluzzi, K.H. Winterhalter, and E.E. Di Iorio.

Dept. Biology, University of Padua, Italy and Lab. of Biochemistry I, E.T.H., Zurich, Switzerland.

Equilibrium and kinetic properties for the binding of various isocyanides to two myoglobins differing in their structure around the active site, were investigated at different temperatures above 0° C. Methyl, ethyl, isopropyl and tertbutyl isocyanides were chosen as ligands in view of the steric arrangement of their alkyl groups. Sperm Whale and *Aplysia* myoglobins were used because of the well established differences in their heme-pocket geometry. Despite the negative enthalpy of ligand binding at equilibrium, the apparent quantum efficiency for laser photolysis is found to increase with temperature at different extents in the two proteins and in relation to the bulkiness of the isocyanide alkyl groups. This finding is interpreted in terms of a temperature dependence of the ligand distribution between pocket and solvent. Such a distribution is correlated to the rate of ligand escaping from the pocket to the solvent relative to the geminate recombination.

057

Two Dimensional Lattices of Hybrid Bacteriorhodopsin Molecules

J.-L. Pegg, J. Trewhella*, S.E. Cechman, and D.M. Engelman Yale University, Dept. of Molecular Biophysics and Biochemistry, CT, USA, and *Los Alamos National Laboratories, NM, USA.

Analysis of bacteriorhodopsin structure by electron microscopy indicates that about 3/4 of the protein mass is located in the lipid bilayer in the form of seven transmembrane α -helices (1 & refs. therein). An active proton pump has been reconstituted from two chymotryptic fragments (2 & refs. therein). Free energy calculations suggest that these fragments comprise respectively two and five of the transmembrane helices (3). We have established conditions under which a two-dimensional crystal lattice dissociating to at least 6 Å is formed starting from the two purified chymotryptic fragments. We are attempting to locate the two fragments in the structure by studying neutron diffraction from lattices of hybrid bacteriorhodopsin molecules reconstituted from one hydrogenated and one deuterated fragment. This information, combined with earlier measurements in which specific classes of aminoacids were deuterated (4,5), should permit to establish the location of α -helical sequence segments in the structural map.

1. Lelifer, D., & Henderson, R., *J. Mol. Biol.* **162**, 451-466 (1983)
2. Liso, M.-L., London, R., & Khorana, H.G., *J. Biol. Chem.* **258**, 9948-9955 (1983)
3. Engelman, D.M., Goldman, A., & Steltz, T.A., *Methods in Enzymology*, **88**, 812-838 (1982)
4. Engelman, D.M., & Zaccari, G., *Proc. Nat. Acad. Sci. USA* **77**, 5894-5898 (1980)
5. Trewhella, J., Andersson, S., Fox, R., Cogoli, E., S. Khan, Engelman, D.M., & Zaccari, G., *Biophys. J.* **42**, 233-242 (1983)

059

APPLICATIONS OF H-NMR TO TRANSFORMATIONS OF FIBRINOGEN SOLUTIONS BY COAGULATION AND FIBRINOLYSIS.

Y. Tanaka, S. Nakaya, R. Nonjo, Y. Yoshida and S. Yama, Dept. of Physiol., Sch. of Med., Iwate Med. Univ., Morioka, JAPAN

Fibrinogen in solution of water (D₂O in 10% for NMR field lock) was made into fibrin gel by coagulation and the gel was lysed to sol by fibrinolysis. In each stage, water protons were examined on 3 fundamental parameters of the NMR (FT-spectrum at 4.78 ± 0.01 ppm; the relaxation time, T₁ & T₂) by using a Bruker's 60 MHz H-NMR-spectrometer with a magnet which was set in a room (size 30x2 m, temperature 24 ± 0.5 °C, humidity 40 ± 5%). Those values were measured to within 3% deviations from the mean by adjusting the 1000 pulse width between 10.4 and 10.6 micro-sec for each sample. At the coagulation stage, 0.5 ml borate-saline buffer solutions of 1 to 10 mg/ml fibrinogen (Miles-Sankyo's, 10% clottable) were taken into the 20 mm tubes. To some of them were added 0.3 ml solution of thrombin (Kochi's) to make the gel within 10 minutes. To others were added a few drops of human serum (our clinic's) diluted with an SX solution (Lederle's Variadex) and also 0.3 ml of thrombin solution to make the sol in from 0.3 to 10 hours. With an increase of fibrinogen in each stage, the size of the FT-spectrum decreased in the height but less remarkably in the area and then increased in the width especially for the gel, while both T₁ and T₂ decreased exponentially and approached a plateau. The T₁ changed from 3.40 to 2.27 sec, though there was little difference among those of 3 stages. However, the T₂ changed from 2.50 to 0.18 sec for the gel, to 0.40 for the solution and to 0.40 for the sol, suggesting that the principal protein changed in the solution as well as in the quality by coagulation and fibrinolysis.

056 ORAL PRESENTATION

FOURIER TRANSFORM DIELECTRIC SPECTROMETRY OF BIOPOLYMERS

M. Froeyen and L. Hellemaans, Department of Chemistry, University of Leuven, Celestijnenlaan 200 D, Leuven, Belgium.

Dielectric probing of rapidly reacting biopolymers dissolved in water cannot be accomplished in the frequency domain over a wide enough band in a sufficiently short time. By measuring the response to short voltage pulses in the time domain enough information is collected to reconstruct the dielectric relaxation spectra, and to follow simultaneously the evolution of the concentration of the dipolar species in real time. This paper describes our technique to measure the response digitally at sampling rates up to 20 MHz, and to recover the transfer function of the sample by fast Fourier transform methods; it illustrates some of the experimental difficulties, such as finite rise time of the pulse, electrode polarization effects, and finding the balance conditions of the bridge circuit. The performance of the instrument is tested with simulator circuits composed of resistors and capacitors. Measurements of aqueous bovine serum albumin at different ionic strength show the present limits of detection. Dilution experiments in a stopped-flow apparatus emphasize the challenging qualities of this uncommon research tool.

058

PROTEIN UNFOLDING BY COLD AND EFFECT OF AL₂O₃ SURFACE ON THE FOLDING/UNFOLDING PHENOMENA

V. Vučelić, R.P. Bray, D. Vučelić, Institute of General and Physical Chemistry, Belgrade University, Department of Physical Chemistry, Faculty of Sciences and Mathematics, Belgrade University, Belgrade, Yugoslavia

Protein folding/unfolding phenomena have been examined by differential scanning calorimetry (DSC). After unfolding "by cold" the protein molecules from the solution were spontaneously adsorbed on the Al₂O₃ surface of the DSC aluminum pan. Temperature behaviour of this system was investigated in the range 220 - 400 K. Although, all three examined proteins (lysozyme, lac repressor headpiece, albumine), are very different, one common pattern was obtained. During heating the first effect, at 273 K, is protein adsorption (an exothermic DSC peak). Cooperative desorption from the surface occurs in the range 330 - 350 K depending on the examined protein (an endothermic peak). Desorption is followed by the two consecutive processes. Fast folding in the solution of unfolded protein molecules from the Al₂O₃ surface (exothermic peak 340 - 370 K range). Folded protein molecules unstable at that high temperature undergo again fast unfolding (endothermic peak 360 - 400 K). Albumine desorption from the Al₂O₃ surface is a process with two distinguished peaks and expressed fine structures.

060

THERMAL PROPERTIES OF MELANINS

B. Simonović, V. Vučelić, T. Wilczok*, J. Hranisavljević and D. Vučelić, Institute of General and Phys. Chemistry, Belgrade University; Dept. of Phys. Chem., Faculty of Sciences and Mathematics, Belgrade University, Belgrade Yugoslavia; *Silesian Med. Acad., Inst. of Chemistry and Physics, Sosnowiec, Poland

Thermal properties of natural and synthetic melanins have been investigated by differential scanning calorimetry (DSC) and nuclear magnetic resonance (NMR) in the temperature range 230 - 450 K. Samples of melanins were isolated from banana peels, human hair and bovine eye or were synthesized from tyrosine, DOPA, tyramine, epinephrine and catechol. The low temperature (300-350 K) broad endothermic transitions with characteristic patterns for the corresponding melanins were obtained. The transitions are reversible with long thermal relaxation times (20 - 30 h). That phenomena could be used for identification of melanine samples from different sources. In the same temperature region, NMR results show a T₂ with long relaxation time (T₂ = 1 μs) in addition to the invariant short relaxation time (T₂ = 10 μs). Both results support the hypothesis of subunit layer stacking in the melanin nucleus.

061

ROLE OF THE PHOSPHATE BINDING SITE IN AN ACTIVE SITE OF RABBIT MUSCLE ALDOLASE. (Part 2), H. OGATA, Division of Chemistry and Biochemistry, The School of Allied Health Science, Yamaguchi University, UBE, Yamaguchi-ken, Japan.

Rabbit muscle aldolase has two binding sites for phosphate groups of substrates in an active site. Alkanediol monoglycolate bisphosphoric esters ($P-O-CH_2-CO-O-(CH_2)_n-O-P$) ($n=1, 2$), analogues of substrate FDP, alkanediol bisphosphates, and alkanol monophosphates were synthesized and used for probing its active site. The inhibitor constant (K_i) was lowest when the maximum distance between the phosphorus atoms of the bisphosphate was brought close to that of FDP. The binding constant estimated from difference spectra correlated well with K_i values for the substrate analogues, (Ogata et al. BBA 742 (1983)384-390).

1H NMR spectrum of the synthesized compound ($n=3$) indicated two peaks for the phosphate groups of this compound. Each peak was shifted and broadened differently by the addition of aldolase (Kobayashi et al. Seikagaku 53(1983)684). It has been suggested that the binding constants between each binding site for phosphate and a phosphate group of the substrates can be determined in the various conditions.

The synthesized phosphate compounds protected aldolase against deterioration by proteases, but several monophosphates increased the deterioration of aldolase by proteases. The structures of the phosphate compounds were sensitive to charge for protection of aldolase against these enzymes.

Role of the phosphate binding site in an active site will be discussed.

063

PRIMARY STRUCTURE AND ANTIPROTEOLYTIC ACTIVITY OF A NEW KUNITZ-TYPE INHIBITOR FROM BOVINE SPLEEN

F. Ascoli, E. Fioretti, G. Iacopino, D. Barra and F. Bossa, Department of Cell Biology, University of Camerino, CNR Center of Molecular Biology, Institute of Biochemistry, University of Rome, Italy.

The primary structure of a Kunitz-type protease inhibitor (inhibitor II) isolated from bovine spleen has been completely elucidated. The molecule contains 58 aminoacids in a single polypeptide chain. Its sequence indicates a strong structural homology to the known bovine pancreatic trypsin inhibitor (BPTI), which is also present in the same tissue: only 6 residues are changed. UV-CD spectra have provided information on the secondary structure, similar to that of BPTI, and on the environments of the aromatic residues and of the three disulfide bridges. The association constants of inhibitor II with bovine trypsin and chymotrypsin, and porcine kallikrein have been determined and compared with those of BPTI with the same proteases. On the basis of the known structure of the BPTI-kallikrein complex, it may be inferred that the aminoacid substitutions found can reasonably account for the reduced strength of the binding of inhibitor II to porcine kallikrein.

065

HEMOGLOBIN STRUCTURE CHANGES PROBED BY TRANSIENT SPECTROSCOPY

J. Hofrichter, E. R. Henry, J. H. Sommer and W. A. Eaton, NIH, Bethesda, MD; M. Ikeda-Saito and T. Yonetani, U. of Pennsylvania, Philadelphia, PA, USA

Rapid structural changes in hemoglobin A are probed by measuring accurate, time-resolved, absorption spectra. The spectrum of deoxyhemoglobin in the Soret band is used to probe the protein structure at the heme binding site. Three structural relaxations are observed. The first, occurring at ~ 100 ns, takes place concomitant with 'geminate' rebinding of the photodissociated ligand. Several lines of evidence, including recent studies of iron-cobalt hybrid hemoglobins, show that this structural relaxation is localized in individual chains of the tetrameric Hb molecule. It is not yet possible to determine to what extent it is linked to the geminate rebinding reaction. A second relaxation is observed at 1-2 μ s. Data on the $\alpha(Co)(Fe)$ hybrid suggest that the $\alpha(Co)$ subunits are slightly altered during this relaxation, but much larger changes are seen in the $\beta(Fe)$ spectrum. In $\alpha(Fe)\beta(Co)$, the spectral changes in this relaxation are confined to the $\alpha(Fe)$ chains. In the quaternary relaxation at 20 μ s the spectra of both α and β hemes show changes of roughly equal magnitude, independent of the position of the Co substitution. Accordingly, the 1st structural change can be viewed as a pure tertiary relaxation, resulting from changes in heme stereochemistry on ligand dissociation. Structural information appears to be propagated from the β to the α chain in the second relaxation, but the perturbation is small compared to that which results from the change in quaternary structure.

062

HEME GEOMETRY AND CO REACTIVITY IN MONOMERIC HEMOPROTEINS

M. Brunori, P. Ascenzi, M. Coletta and T.G. Traylor, CNR Center for Molecular Biology, Institutes of Chemistry and Biochemistry, Faculty of Medicine, University of Rome "La Sapienza", Rome, Italy.

The effect of pH on the spectral properties and the second-order rate constant of CO binding for several monomeric hemoproteins is reported. With the exception of Chironomus thummi thummi erythrocyte and Aplysia limacina myoglobin, the latter in the absence of acetic acid, which are pH independent from pH 2.5 to 9, in sperm whale, horse, Dermochelys coriacea and Coryphaena hippurus myoglobins, lowering pH brings about an increase of the second-order rate constant which is complete at pH 2 and can be described by the protonation of a single group with a pK_a around 3. Moreover, with the exception of Aplysia limacina myoglobin, in the absence of acetic acid, all hemoproteins investigated display, before the pH induced denaturation can occur, a transient deoxy spectrum very similar to the deoxy tetracoordinated protoheme. Such a pH dependent spectral and kinetic behaviour closely resembles that observed in chelated heme model compounds and attributed to the protonation of the proximal histidine with the subsequent cleavage of the fifth axial bond of the Fe atom in the deoxygenated derivative. Within this model, the energy involved in the movement of the deoxy Fe atom toward the heme plane turns out to be the crucial step in determining the height of the activation barrier in the dynamic pathway of CO binding to monomeric hemoproteins.

064

ASSEMBLY OF HORSE SPLEEN APOFERRITIN SUBUNITS

E. Chiancone, S. Stefanini and P. Vecchini, CNR Center of Molecular Biology, Institutes of Chemistry and Biochemistry, Faculty of Medicine, University "La Sapienza", Rome, Italy.

The association of the 24 subunits of mammalian apoferritins yields an extremely stable polymer which dissociates only at extremes of pH. The subunits obtained upon acid dissociation of horse spleen apoferritin (0.2M glycine-HCl buffer at pH 1.8) reassemble into whole molecules when exposed to pH values around neutrality in the presence of mercaptoethanol. A detailed study of the reassembly reaction by sedimentation velocity has brought out that increasing pH values in the range 3.0 - 4.5 differentially stabilize intermediates of increasing molecular weight, i.e. subunit dimers, trimers and tetramers, and that polymer formation begins at pH values above 3.2. Changes in the folding of the polypeptide chains and in the environment of aromatic residues take place in the different stages of the reassembly reaction as indicated by circular dichroism measurements. The stable reassembly intermediates correspond to the expected ones on the basis of the intersubunit packing observed by X-ray crystallography.

066

pH-INDUCED UNFOLDING OF THE CONSTANT FRAGMENT OF THIOPHOSPHOLIPID LIGHT CHAIN

Y. Ashikari, Y. Arata and K. Hwanguchi, Dept. of Biology, Faculty of Science, Osaka Univ., Osaka, Japan

The conformations and stabilities of the intact C_L , reduced C_L , and reduced and alkylated C_L were studied. The C_L fragment was obtained by digestion of a type λ Bence Jones protein with papain. The results of measurements of circular dichroism, fluorescence, ultraviolet absorption, n.m.r., and titration of SH groups showed that on reduction of the intrachain disulfide bond no significant change occurs in the conformation of the C_L fragment, but that reduction followed alkylation results in extensive unfolding of the protein molecule. The pH-induced unfolding of the reduced C_L was compared with that of the intact C_L . The unfolding equilibria by acid were explained assuming that the same ionizable groups participate in the unfolding for the reduced C_L as well as for the intact C_L in the same way and that the stability of the intact C_L is 100 times greater than that of the reduced C_L . The unfolding equilibria and kinetics of the reduced C_L by alkali were explained assuming that the reduced C_L molecule can no longer assume the folded conformation when either or both SH groups ionize.

Posters on Folding, Dynamics and Solvation of Macromolecules

067

BIOPOLYMERS DYNAMICS STUDIED BY RAYLEIGH SCATTERING OF MOSSBAUER RADIATION (RSMR).
V.I. Goldanskii, Yu.F. Krupnyanskii, I.V. Kurinov,
I.V. Sharkevich, T.V. Zhuravlyova, I.P. Suzdalev.
Institute of Chemical Physics, Academy of
sciences, Moscow, USSR.

Incoherent RSMR due to an inherent excellent energetic resolution ($\sim 10^{-3}$ eV) provides the possibility to study real individual motions of atoms or fragments of biopolymers with a relatively low frequencies ($\sim 10^7$ and higher). Temperature dependencies of the elastic fraction (f_R) for metmyoglobin, trypsin, chromatophore membranes, human serum albumin (HSA) and DNA with different hydration degree (h) were studied. The peculiar feature of the obtained results for samples with $h \approx 0.3$ is the abrupt decrease of f_R above some critical temperature $T \approx 200$ K. Values of the overall m.s.d. $\langle r^2 \rangle$ for all biopolymers at $h=1$ ($T=300$ K) become close to 1 Å. RSMR spectra were measured for HSA samples with a different water content ($h=0.05; 0.68; 1.1$). Spectrum of HSA with $h=1.1$ shows the specific line broadening which is an evidence for the existence of different types of motion, with different correlation times: $\sim 10^{-7}$ sec; $\sim 10^{-8}$ sec; and $> 10^{-9}$ sec. The obtained results may be interpreted in the frame of glass-like model for biopolymers.

069

PROTEIN ADSORPTION HYSTERESIS ON TWO-DIMENSIONAL HYDROPHOBIC BINDING-SITE LATTICES
Herbert P. Jennissen

Institut für Physiologie, Physiologische Chemie & Ernährungsphysiologie der Universität München, Veterinärstr. 13,
D-8000 München 22, West Germany

In protein adsorption hysteresis the dependent variable (surface concentration of protein) fails to retrace the values traversed in the forward process when the direction of change of the independent variable (bulk equilibrium concentration) is reversed [1]. This type of hysteresis should not be confused with the hysteresis concept of Frieden [2]. In adsorption hysteresis of the enzyme phosphotyrase b on butyl Sepharose the system persists in trajectories distinct from the reversible change trajectory, as found e.g. for the reversible dissociation of a gas, indicative of long-lived metastable states and thermodynamic irreversibility. The dissipated (irreversible) Gibbs free energy derived from closed adsorption-desorption loops lies between -2 and -12 kJ/(mol x K) depending on the surface concentration of immobilized butyl residues. The mechanism of protein adsorption hysteresis [3] probably involves conformational changes and rearrangement effects of the protein on the gel surface leading to an increase in the number of interacting immobilized residues.

1. Jennissen, H.P. and Botzet, G. (1979) Int. J. Biolog. Macromolecules 1, 171-179
2. Frieden, C. (1979) Ann. Rev. Biochem. 48, 471-489
3. Jennissen, H.P. (1983) in Affinity Chromatography and Biological Recognition (Chaiken, L.M., Wilchek, M. and Parikh, I. eds.), pp 282-290, Academic Press, New York

071

^{19}F NMR INVESTIGATION OF SONICATED UNILAMELLAR VESICLES AND HUMAN ERYTHROCYTE MEMBRANES M. Wu, S. R. Dowd, V. Simplaceanu, and C. Ho, Department of Biological Sciences, Carnegie-Mellon University, Pittsburgh, PA, U.S.A.

Dimyristoylphosphatidylcholine (DMPC) labeled with a CF_2 group in the 4, 8, or 12 position of the 2-acyl chain has been studied by ^{19}F NMR at 282.4 MHz from 26°-42°C in both sonicated vesicles and human erythrocyte membranes. The ^{19}F NMR spectra obtained from vesicles exhibit two resolved ^{19}F signals with different linewidths. At lower temperatures, the linewidths of the broader component increase dramatically with 2-(4,4- $^{19}\text{F}_2$)DMPC the largest and 2-(12,12- $^{19}\text{F}_2$)DMPC the smallest. A quantitative line shape analysis is possible by using experimental chemical shift anisotropy ($\Delta\sigma$) and internuclear F-F vector order parameter (S_{FF}) values obtained from the de-Paking of the powder spectrum of multilamellar liposomes. It can be concluded that either the rate of tumbling and/or the lateral diffusion of the inside and outside layers is different, or the two layers have different S_{FF} profiles. Synthetic lipid is incorporated into erythrocyte ghosts by exchange with sonicated vesicles using bovine liver PC exchange protein. The powder-pattern spectra of the erythrocyte ghosts show much larger $\Delta\sigma$ and S_{FF} values than those of the phospholipid dispersions. They are, however, comparable to spectra obtained for ^{19}F -labeled DMPC in the presence of 30% cholesterol. These results demonstrate that ^{19}F -labeled lipids can be incorporated into erythrocyte membrane. Due to the sensitivity of the ^{19}F anisotropic chemical shift to the environment, ^{19}F NMR provides a valuable tool for membrane studies. (Supported by grants from the NIH and NSF).

068

CHARACTERIZATION OF THE TRANSITION STATE OF THE LYSOZYME UNFOLDING S. Segawa, M. Sugihara, K. Kume and S. Kuroda
Sch. of Sci., Kansai Gakuin Univ., Nishinomiya, Japan

Kinetics of lysozyme unfolding has been investigated in solutions containing different kinds of denaturants, in order to characterize the transition state of unfolding in terms of protein-solvent interactions. By applying the thermodynamic relations to the parameters of the activation processes, we obtained results that the change in specific heat for the unfolding process is nearly equal to zero, and that the activation enthalpies of the unfolding processes in various denaturant solutions are the same as each other. The effects of intrachain cross-linking and inhibitor binding on the refolding rate were also studied. The former greatly accelerates the refolding rate but the latter has little effect. All these results suggest consistently that the transition state is similar to the native one. The structural fluctuations in the folded state are important to the unfolding transition. We studied the effect of cross-linking on the fluctuations in the folded state of lysozyme. Hydrogen exchange rates for the peptide NH groups were measured in 4.0 M LiBr solution by the IR method at pH 5.4 for intact lysozyme and at pH 7.8 for cross-linked one. The exchange rate for cross-linked lysozyme was smaller than that for intact one by about two orders of magnitude, if we took into account the difference in pH. The exchange mechanism was the low activation energy process ($\Delta H^\ddagger 35$ kcal/mol). These preliminary results seem to suggest that cross-linking greatly decreases the extent of structural fluctuations.

070

PICOSECOND RELAXATIONS IN PROTEINS OBSERVED BY MM-WAVE SPECTROSCOPY

A. Poglitsch, F. Kremer, L. Genzel, Max-Planck-Institut für Festkörperforschung, Stuttgart, Fed. Rep. Germany

Dynamic processes on a picosecond time scale, as predicted for biological macromolecules, can be studied with dielectric spectroscopy at mm-wave frequencies by use of the newly developed oversized-cavity technique. It provides for broadband spectroscopy in the frequency range from 30 GHz to 300 GHz and at temperatures between 4.2 K and 400 K. Measurements on hemoglobin, poly-L-alanine and lysozyme will be presented. For the dried materials, a nearly linear increase with frequency and an exponential increase with temperature of the absorption coefficient is observed between 50 K and 300 K. This frequency and temperature dependence is described by relaxation processes in asymmetric double well potentials with relaxation times in the picosecond range. Hydration, as investigated for lysozyme, yields an additional absorption which arises only above 120 K. Its frequency independence indicates relaxation rates for the bound water that are small compared to mm-wave frequencies. Thereby the contribution of bound water can be distinguished from the fast intrinsic processes. An assignment of these picosecond relaxations to the NH...OC hydrogen bond of the peptide backbone is suggested.

072

A PROTON NOE INVESTIGATION OF THE CONFORMATIONS OF THE HEME POCKETS IN LIGATED HUMAN HEMOGLOBIN. Claudio Dalvit and Chien Ho, Department of Biological Sciences, Carnegie-Mellon University, Pittsburgh, PA 15213, U.S.A.

Proton nuclear Overhauser effect (NOE) measurements have been used extensively to investigate the detailed conformations of peptides, proteins, and nucleic acids in the solution state. However, much of the published work has dealt with molecules of molecular weight less than 15,000. It is generally thought that specific NOEs cannot be observed in larger molecules (due to spin diffusion) and NOE is of little use in conformational studies of such systems. By using truncated driven NOE with short irradiation time, specific effects are observed in several proton resonances arising from the heme groups and from amino acid residues situated in the vicinity of the ligand binding site (such as residues E7 histidine and E11 valine) of the α and β chains of human normal adult hemoglobin (Hb A), a protein of molecular weight of 65,000. In addition, 2-dimensional homonuclear J-correlated NMR and spin-echo experiments as well as theoretical ring-current calculations have confirmed the above-mentioned spectral assignments obtained by the 1-dimensional NOE experiments. These new results not only have permitted us to map the heme pockets and to study the conformational differences in the heme pockets between O₂ and CO forms of Hb A, but also have demonstrated that the technique of truncated driven NOE can be used to investigate the detailed conformations of selected regions in larger macromolecules heretofore thought not feasible. [Supported by research grants from the NIH (HL-24525) and the NSF (82-08829)].

Monday 30 July Congress Centre-first floor. Posters 073-078

Posters on Folding, Dynamics and Solvation of Macromolecules

073

LIMITED PROTEOLYSIS AS A TOOL FOR DETECTING EXPOSURE AND FLEXIBILITY IN GLOBULAR PROTEINS: STUDIES ON THERMOLYSIN. C. Vita, D. Dalzoppo, G. Fassina and A. Fontana, Inst. of Organic Chemistry, Biopolymer Res. Centre of CNR, Univ. of Padua, Padua, Italy.

Limited proteolysis of thermolysin with subtilisin results in cleavages at the NH₂-terminal end between Thr-4 and Ser-5 and at an exposed loop 220-228 between Thr-224 and Glu-225 as well as Glu-225 and Asp-226. Thermal autolysis of thermolysin leads to cleavage at the same loop, followed by a slower cleavage at the hinge peptide (at Leu-155 and Ile-156) between the two structural domains 1-157 and 158-316. In the presence of 10 mM EDTA at pH 7.2, fast autolysis occurs at region 195-205, which is involved in the binding of Ca(4) in the native protein. Of interest, these cleavages of the polypeptide chain of thermolysin do not lead to unfolding or dissociation, so that it was possible to isolate and characterize "nicked" thermolysin species constituted by a strong association of two as well as three fragments. These results correlate well with the known three-dimensional structure of thermolysin and, in particular, with the location of the sites of the polypeptide chain characterized by highest mobility in native thermolysin, as recently determined by X-ray crystallography (Holmes, M.A. and Matthews, B.W. (1982) *J. Mol. Biol.* 160, 623-639).

075

REACTION KINETICS OF GLYCOGEN PHOSPHORYLASES α AND β BY FLOW-QUENCH METHOD.

T. Nakamura and H. Kihara, Department of Physics, Jichi Medical School, Minamikawachi, Tochigi-ken JAPAN

Reaction of glycogen phosphorylases α and β with glucose-1-phosphate and maltoheptaose was surveyed by flow-quench method. In the case of phosphorylase α , reaction curve against time shows a time lag of c.a. 20 s. It is qualitatively in good agreement with the relaxation time obtained by stopped-flow X-ray scattering (H. Kihara et al. unpublished). On the other hand, in the case of phosphorylase β , the reaction curve shows no time lag in sec order. Results implies that phosphorylase α takes tetramer-dimer interconversion through its reaction course, whereas phosphorylase β does not take any tetrameric forms through its reaction course, since tetramer-dimer interconversion of phosphorylases α and β is slow enough to be detected by our flow-quench device.

077

APPLICATIONS OF H-NMR TO AQUEOUS SOLUTIONS OF URINE COMPONENTS S. Nakaya, Y. Tanaka, R. Honjo, Y. Yoshida and S. Yagi, Dept. of Physiol., Sch. of Med., Iate Med. Univ., Morioka, JAPAN

Aqueous solutions of NaCl, KCl and urea were prepared each in the 20 mm NMR-tube as a 5 ml aliquot of differing concentration (0.1 to 5 M) by dissolving pure reagents (Wako's for NaCl & KCl, Nakarai's for urea) in water and adding 0.5 ml D₂O for NMR field lock, and then were examined each on 3 fundamental parameters of the NMR by using a Bruker's 80 MHz H-NMR spectrometer with a magnet which was set in a room (size 30x2 m, temperature 24 \pm 0.5 °C, humidity 40 \pm 5 %). Each FT-spectrum taken by checking the 180° pulse width between 96.6 and 148.0 micro-sec showed a single peak at 4.78 \pm 0.01 ppm, of which the relaxation time was obtained in T₁ and T₂. With an increase of the concentration, especially at lower concentrations, the spectrum decreased the size in the area but not so much in the height and then in the width showed the decrease going along a hyperbolic curve deeper for urea than that for NaCl and KCl. Similarly, at lower concentrations, T₂ decreased remarkably from 3.81 \pm 0.75 sec of pure water, resulting in a hyperbolic curve, to 0.33 \pm 0.07 sec at 5 M for urea, to 2.47 \pm 0.17 at 0.4 M for NaCl and to 2.03 \pm 0.25 at 0.1 M for KCl. At higher concentrations of NaCl and KCl, the T₂ showed no more significant decrease but rather a tendency for KCl to increase. On the other hand, T₁ values among the different components were not significantly different from those of pure water (3.34 \pm 0.24 sec). The results suggested the behavior in the NMR of those different urine components corresponding to their physical properties (specific gravity, viscosity, ...) dependent on the extent of solvation.

074

TRYPTOPHAN OXIDATION KINETICS IN MIXTURES OF HYDROGEN PEROXIDE, BICARBONATE AND DIOXANE

R.P. Bray, S. Raičević, L. Weglarz, J. Hranisavljević, D. Vučelić Inst. of General and Phys. Chemistry, Belgrade University *Silesian Med. Acad., Inst. of Chemistry and Physics, Sosnowiec, Poland; Dept. of Phys. Chem., Faculty of Sciences and Mathem. Belgrade University

The kinetics of oxidation of tryptophan to oxindoleacetaline have been monitored spectrally at various concentrations of hydrogen peroxide, ammonium bicarbonate and dioxane. In one series of experiments, tryptophan and hydrogen peroxide were kept constant in 0.4, 0.8, 1.0 and 1.2 M bicarbonate solutions containing 0, 2, 4, 8 and 12% dioxane for each bicarbonate concentration. Plots of $\ln(A^{230}/A^{300})$ versus time gave linear semi-log plots typical for a pseudo-first order reaction at 1.0 and 1.2 M bicarbonate in the presence of dioxane. In contrast, biphasic kinetics with a slow initial rate followed by a faster rate were obtained at 0.4 and 0.8 M bicarbonate in the presence or absence of dioxane. Thus, conditions of high bicarbonate concentration (1.0-1.2 M) were preferable due to the pseudo-first order kinetics and the faster rate order kinetics and the faster rate of reaction. At such bicarbonate levels, tryptophan oxidation kinetics were extensively studied at various hydrogen peroxide and dioxane concentrations.

076

NMR RELAXATION, FLUORESCENCE DEPOLARIZATION AND PROTEIN DYNAMICS: THEORY AND EXPERIMENT. Attila Szabo, Laboratory of Chemical Physics, NIDDK, NIH, Bethesda, MD, USA.

Nuclear magnetic relaxation and time-resolved fluorescence depolarization of probes attached to macromolecules or embedded in membranes reflect the internal dynamics of these systems. How should one analyze such experiments to extract their unique information content and how do these results compare with the predictions of molecular dynamics simulations? For NMR, the uniqueness problem for fast local motions can be solved in a rigorous and simple way once it is realized that the information content of such experiments is completely specified by two model independent quantities: a generalized order parameter and an effective correlation time which are measures of the spatial restriction and the time scale of the motion, respectively. In order to interpret fluorescence studies where the time dependence of the anisotropy depends on excitation frequency and/or the total intensity is multiexponential, we have developed a comprehensive formalism that treats both excited state and orientational dynamics in a unified way. Our approach readily handles not only the overall and internal reorientation of probes but also such complications as energy transfer, heterogeneity and the interconversion of excited states with different emission characteristics. Illustrative applications to the analysis of experimental data will be presented and the results will be used to show that molecular dynamics simulations for pancreatic trypsin inhibitor predict generally smaller motional amplitudes than detected experimentally. Several possible explanations for this discrepancy will be examined.

078

CATALYTICALLY DEFECTIVE SEMISYNTHETIC RIBONUCLEASES. M.S. Stern, M.S. Doscher, P.D. Martin and B.F.P. Edwards, Dept. of Biochem., Wayne State Univ. Sch. Med., 540 E. Canfield St., Detroit, MI 48201, U.S.A.

The fully active semisynthetic enzyme formed by the non-covalent interaction of residues 1 through 118 of bovine pancreatic ribonuclease (RNase A) and a synthetic tetradecapeptide containing residues 111 through 124 of the enzyme allows methodical study of the role of several residues at or near the active site of the molecule. Refined structures at 2.0 Å of the parent enzyme (RNase 1-118:111-124)(R=0.23) and a catalytically defective (13% active at pH 6.0) analog in which leucine replaces phenylalanine-120 (R=0.24) have been obtained. In the fully active parent enzyme, active-site residue histidine-119 occupies two positions, one clearly exterior to the active site (interior \rightarrow exterior is achieved by an approximately 180° rotation about the α -8 bond of this residue); the occupancy of the exterior position is roughly twice that of the interior position. In the leucine-120 analog, only the exterior site is occupied. No other differences of comparable magnitude exist between the two structures; histidine-12 and lysine-41 positions are not detectably different.

A second, catalytically defective (1.6% active against cytidine-2',3'-cyclic phosphate at pH 5.8) analog has been obtained by replacing aspartic acid-121 with asparagine. Further kinetic characterization of the enzyme is underway as are attempts to grow diffraction-quality crystals. (Supported in part by funds from NIH Grant 05384.)

Monday 30 July Congress Centre-first floor. Posters 079-084

Posters on Folding, Dynamics and Solvation of Macromolecules

079

PROTEIN FOLDING - A NEW APPROACH AND ALGORITHM. A.S. Kolaskar, V. Ramabrahmam and B.V.J. Reddy

Crystal structural data of large number of globular proteins have been analyzed. This analyses have been used to categorise secondary structures in two types. Type I of secondary structures are formed due to intrinsic preference of constituent amino acids and type II are formed mainly due to tertiary interactions. Further, potential values are derived not only for single residue but also for pair of residues using probability of occurrence values in (ϕ, ψ) - Ramachandran plot. These pair of amino acid residue potentials were used to predict rough three dimensional structure of protein from primary structure without going through the step of predicting secondary structures. Our results are quite encouraging. Thus, for the first time a simple method has been developed which can predict three dimensional structure of globular proteins and can be used on home computers.

These studies along with our studies on analysis of c-DNA sequence data indicate that the rate at which polypeptide chain is elongated on ribosome is an important factor in determining the three dimensional structure of the molecule and not only its primary structure. The information of usage of particular codon for coding an amino acid must therefore be incorporated in prediction scheme. Our results are discussed to show the correlation between codon usage and conformation of amino acid residue in protein.

081

STOCHASTIC DESCRIPTION OF SEGMENT MOTION IN BIOLOGICAL MACROMOLECULES

C. Blomberg and O. Edholm, Department of Theoretical Physics, Royal Institute of Technology, S-100 44 Stockholm, Sweden.

It is a desirable goal when describing dynamics of biological macromolecules to extract simple basic mechanisms governing the motion. Such a mechanism would be the movement of a comparatively small segment of the molecule. A way to describe such motion is to use stochastic equations where a small number of degrees of freedom are treated explicitly while most of them are considered merely as a random background. The simplest case, that of diffusion along a one-dimensional reaction coordinate across a barrier is often not sufficient to give a good description in complicated systems. We study the barrier passage problem in several dimensions involving potentials of saddle point shape but also of more complicated structure. We also consider generalisations of simple Brownian motion theory that are necessary to give a proper description of the random background in these systems. This forms a basis for the interpretation of experimental data from e. g. NMR that contain information about the dynamics. We primarily consider lipid molecules in membranes because of their comparative simplicity and that a large amount of experimental data are available but our methods are also applicable to other types of large molecules.

083

QUATERNARY STRUCTURE CHANGES IN ASPARTATE TRANSCARBAMYLASE STUDIED BY X-RAY SCATTERING - SIGNAL TRANSMISSION FOLLOWING EFFECTOR BINDING

Patrick TAUC¹, Patrice VACHETTE², Guy "CRVE", Peter JONES³ and Michael MOODY³.

¹Laboratoire d'Enzymologie, C.N.R.S. 91190 Gif-sur-Yvette, France; ²J.L.U.R.E, Université Paris-Sud, 91405 ORSAY, France and ³J.E.M.S.L. 6900 Heidelberg, West Germany.

The effect of binding ATP or CTP to ATCase was studied by X-ray solution scattering using a synchrotron radiation X-ray source. Binding of substrate analogues produces a substantial change of solution scattering pattern (Moody et al., 1979), allowing us to monitor the proportion of the different quaternary structure states present in solution. In the initial solution this proportion was made roughly unity by adding carbamyl phosphate and succinate, or N-(phosphonacetyl)-L-aspartate (PALA). ATP or CTP were then added, and their effect on the proportion of the different quaternary structure states was followed. We find that when carbamyl phosphate and succinate were used, ATP or CTP had a clear effect. However when PALA was used, ATP had no detectable effect while CTP might cause a weak change in the scattering pattern. This result supports the explanation of Tauc et al. (1982), that the effect of nucleotides is essentially (exclusively in the case of ATP) on the affinity at the active sites for substrate and not a direct one on the quaternary structure equilibrium. Tauc P., Leconte C., Kerbiriou, D., Thiry, L. and Hervé, G. (1982) J. Mol. Biol. 155, 155-168. Moody, M.F., Vachette, P. and Foote, A.M., (1979) J. Mol. Biol., 133, 517-532.

080

ELECTROSTATIC AND HYDROPHOBIC DEHYDRATION OF THE ACTIVE SITE OF ACETYLCHOLINESTERASE

M.R. Pavlič, Institute of Biochemistry, School of Medicine, Ljubljana, Yugoslavia

It was found recently in our laboratory that the acceleration of acylation of cholinesterases by some cations results from a dehydration of the active sites under the influence of accelerators; the best accelerators are Li^+ and tetramethylammonium and tetraethylammonium. In order to get an insight into the nature of dehydration, the acylation of acetylcholinesterase in the presence and absence of accelerators was investigated at various temperatures. Making use of the usual thermodynamic equations, some characteristic thermodynamic quantities were determined. It was found that all accelerators increase the entropy of activation of the acylation; Li^+ increases also the enthalpy of activation whereas tetramethylammonium and tetraethylammonium do not change this quantity. These and some other results indicate that the dehydration of the active site of acetylcholinesterase results from a reorientation of water in the active site; in the case of Li^+ the reorientation is electrostatic and in the case of tetramethylammonium and tetraethylammonium it is hydrophobic.

082

NMR STUDIES ON THE DENATURATION OF LYSOZYME

M. Sheinblatt, Department of Chemistry, Tel-Aviv University, 69978 Ramat Aviv, Israel

NMR, as well as photospectroscopy studies on the denaturation of lysozyme in the presence of some of its specific inhibitors is reported.

The NMR measurements of both the enzyme and the inhibitor molecules indicate that in the presence of bound inhibitor molecules, the enzyme is more resistant to the effect of the denaturant agent (GuHCl) as compared to the free enzyme. This observation is discussed in terms of the denaturation process.

084

DYNAMIC SOLVENT ACCESSIBILITY OF BPTI AND OF THE BPTI-TRYPSIN COMPLEX. C. Woodward, E. Tüchsen & V. Copie, Biochemistry Dept., Univ. of Minnesota, St. Paul, Minnesota 55108 U.S.A.

Solvent isotope exchange of peptide amide protons and of internal water demonstrate that regions of bovine pancreatic trypsin inhibitor (BPTI) and BPTI-trypsin that are buried in the static crystal structure have some accessibility to solvent in the dynamic solution structure. Exchange kinetics for 39 of the 53 backbone NH's in BPTI, determined over a wide range of pH and temperature, indicate that: 1) Chemical exchange involves O-protonation, and the probability of exposure to solvent of peptide O and N atoms are determined from the catalytic rate constants. 2) BPTI surface NH's exchange slower than small peptide NH's, indicating that NH's with finite static accessibility and no internal H-bonding are shielded in the solution structure. 3) Among the NH's in the β -sheet core, the NH's of residues 21-23 are qualitatively slower exchanging. 4) The effect on BPTI exchange rates from binding of trypsin is highly localized. Solvent exchange of buried H_2O water molecules in BPTI-trypsin has been measured by a technique involving rapid dialysis and mass spectrometry. The BPTI-trypsin crystal structure has 33 buried water molecules. ^{18}O label remaining with the complex after 30 sec. corresponds to 4-8 H_2O /molecule of complex.

Monday 30 July Congress Centre-first floor. Posters 085-090

Posters on Folding, Dynamics and Solvation of Macromolecules

085

STUDIES ON THE DISSOCIATION OF $\alpha\beta$ DIMERS OF HEMOGLOBIN A. J.R. Shaeffer, M.J. McDonald, S.M. Turci, D.M. Dinda, and H.F. Bunn, The Center for Blood Research, and Brigham and Women's Hospital, Boston, Mass., USA.

Adult human hemoglobin tetramers (HbA = $\alpha_2\beta_2$) dissociate into, and exist in equilibrium with, small amounts of $\alpha\beta$ dimers. To determine if $\alpha\beta$ dimers dissociate into α and β monomers, isolated ^3H - α chains (~ 0.1 mg/ml) were incubated with either 0.1, 1, or 10 mg/ml of unlabeled CO-HbA in 0.01 M $\text{PO}_4(\text{K}^+)$ pH 7.0 at 25°C for several days. Samples were withdrawn at various times, and the free α monomers and HbA tetramers were separated by electrophoresis on cellulose acetate or chromatography on DEAE-cellulose. Radioactivity analysis showed a slow, steady transfer of ^3H - α chains into HbA (e.g., $\sim 55\%$ of ^3H - α chain cpm were incorporated into HbA, 10 mg/ml, after 72 h). The initial rate of this transfer increased directly with the calculated concentration of $\alpha\beta$ dimer. Additional evidence (e.g., separation of the globin chains on a CM-cellulose column in 8 M urea or Sephadex chromatography in 0.10 M NaCl) showed that the ^3H -cpm in HbA were in intact α chains that were an integral part of, and not adsorbed to, the tetramer. In a complementary experiment, unlabeled α chains (~ 6 mg/ml) were incubated with 12 mg/ml of ^3H -HbA (α/β cpm ratio = 0.28), and 5% of the ^3H -HbA cpm were transferred into free α chains after 240 h. These results show there was an exchange of α chains between free monomers and those in HbA subunits and were used to calculate a rate constant k for the dissociation of $\alpha\beta$ dimers into α and β monomers of $\sim 7 \times 10^{-3} \text{ h}^{-1}$.

087

ON THE ELECTRICAL INTERACTION IN BIOFLUIDS

J.R. Grigera, F. Vericat and L. Blum. *Instituto de Física de Líquidos y Sistemas Biológicos (IFLYSIB), 1900 La Plata, Argentina. **Department of Physics, University of Puerto Rico, Rio Piedras, Puerto Rico 00931.

The effect of the ions on the forces between charged groups of macromolecules is considered. It is pointed out that the main action of the ions is due to the charge screening. This screening can be included in the Coulomb's law as an effective dielectric permittivity and will depend on the salinity of the medium in such a way that departures from the physiological concentration could disturb the force balance. The screening effectivity can be roughly quantified by a time and a length. The time being a measure of how fast the rearrangement of the ions take place, while the length gives an idea of the size of the ion cloud around the charges. In this work the former is estimated through the Maxwell's relaxation time and the latter using the Mean Spherical Approximation (MSA). The computed screening length for a number of salts allows to order the ions in a series that resembles the well known Hofmeister series.

089

MUCONATE LACTONISING ENZYME AT 6.5 Å RESOLUTION

A. Goldman, D. L. Ollis and T. A. Steitz, Department of Molecular Biophysics and Biochemistry, Yale University, New Haven, Connecticut, U. S. A.

We have obtained crystals of Mucenate Lactonising Enzyme from *Pseudomonas putida* which diffract to better than 2.4 Å resolution. The enzyme has a molecular weight of 40 kD, and contains one Manganese atom per monomer. The cell dimensions are: 139.3 by 139.3 by 84.1 Å in the space group I4, giving a V_m of 2.5 Å³ per Dalton, assuming two monomers in the asymmetric unit. The two monomers are related by a non-crystallographic two-fold axis, which is perpendicular to the crystallographic four-fold axis, and is inclined at an angle of 24 degrees to the x-axis.

Using two heavy-atom derivatives, $\text{Sn}(\text{Ac})_4$ and $\text{K}_2\text{Pt}(\text{NO}_2)_4$, we have calculated a map at 6.5 Å resolution. Symmetry-averaging and molecular replacement have improved the map; the final figure of merit is above 0.8. This map shows that the enzyme is a tightly-packed octamer with D₄ symmetry, with more intra-octamer than inter-octamer contacts. This contradicts earlier solution measurements (1), which indicated that the oligomeric molecular weight was 240 to 255 kD, consistent with the enzyme being a hexamer. We are currently collecting data to high resolution and will use molecular replacement to improve that map.

(1) G. Avigard et al, J. Mol. Biol., 89, 651-662 (1974)

086

EFFECTIVE INTER-RESIDUE CONTACT ENERGIES FROM PROTEIN CRYSTAL STRUCTURES. S. Miyazawa and R. L. Jernigan, Lab. of Math. Biol., NCI, Nat. Inst. of Health, Bethesda, Maryland, USA

Contact energies for proteins in solution are estimated from the numbers of residue-residue contacts observed in crystal structures on the basis of the quasi-chemical approximation with an approximate treatment of the effects of chain connectivity. A protein is regarded as a close-packed mixture of unconnected residues and effective solvent molecules whose size is the average size of a residue. A basic assumption is that the average characteristics of residue-residue contacts formed in a large number of protein crystal structures reflect actual differences of interactions among residues, as if contacts among residues and solvent molecules in each protein were in quasi-chemical equilibrium. The number of effective solvent molecules for each protein is chosen to yield the number of residue-residue contacts equal to its expected value for the hypothetical case of hard sphere repulsions. A residue is represented by the center of its side chain atom positions, and contacting residues are defined to be close pairs within a distance of 6.5 Å; nearest neighbor pairs along a chain are excluded. Coordination numbers, for each type of residue and solvent, are estimated and used to evaluate the numbers of residue-solvent and solvent-solvent contacts. Estimated contact energies have reasonable residue-type dependences; e.g., non-polar-in and polar-out are seen as well as the segregation between these residue groups. There is a linear relationship between the average contact energies for non-polar residues and their hydrophobicities reported by Nozaki and Tanford.

088

ESR STUDIES ON IRRADIATED SINGLE CRYSTALS OF OXYMYOGLOBIN

W. Leibl, W. Nitschke and J. Hüttermann, Inst. f. Biophysik und Phys. Biochemie, Universität Regensburg

X-Irradiation of single crystals (type A) of oxymyoglobin at 77 K results in electron addition to the Fe-O₂ unit. Besides the nitrosyl, the superoxide derivative that is formed is the only species whose paramagnetism does not stem from the metal ion.

An ESR crystallographic study was pursued with the dioxygen ligand enriched to 30% in ¹⁷O and with ⁵⁷Fe-substituted myoglobin. There are two spectroscopically distinct FeO₂⁻ species. For the more abundant species, F I, the g-tensor (2.23, 2.13, 1.97), the ¹⁷O Hf-tensor (-27, 16, 6 G) and the ⁵⁷Fe Hf-tensor (16, 6, 5 G) were determined showing most of the unpaired spin density in the iron d₂ and d₃ orbitals with an oxygen π -orbital population of approximately .3 mainly in the "in plane" orbital. The resulting Fe-ligand geometry was found to be strongly tilted with a bond angle of 118°, the O-O direction pointing towards the distal histidine.

Upon annealing the samples above 180 K two new paramagnetic centers were irreversibly formed, possibly as a result of protonation of the ligand. Both secondary species and the other primary center showed no ¹⁷O Hf-splitting suggesting a shift of spin density to the iron. Possible interactions between the ligand and the protein moiety are discussed.

090

The impact of hydration patterns observed in oligonucleotide crystals on our view of the stabilisation of different DNA conformations.

Olga Kennard, Maxine McCall and Joseph Nachman, University Chemical Laboratory, Cambridge, U.K. and Dov Rabinovich and Zippora Shakked, The Weizmann Institute of Science, Rehovot, Israel.

Oligonucleotides generally crystallise with only 40-60% DNA per cell volume, the remainder of the cell being taken up by water and counter-ions. At a resolution of around 2 Å it is possible to identify, with some confidence, a substantial number of water molecules particularly in the first hydration shell, and thus study the water structure around the DNA double helix.

The hydration pattern observed in two isomorphous A-type octamers with different base sequence [d(GGTATACC) and d(GGGGCCCC)] will be described. The results will be compared with the hydration of the B-dodecamer d(CGCGAATTCGCG) (1) and used to re-examine our views on the role of water in B to A transitions and conformational stabilisation.

(1) H. Drew and R.L. Dickerson, J. Mol. Biol. (1981) 151, 535-556

Monday 30 July Congress Centre-first floor. Posters 091-096

Posters on Folding, Dynamics and Solvation of Macromolecules

091

A Comparison of Iron and Heme Pocket Dynamics in Oxyhemoglobin, Carbonmonoxymyoglobin and Deoxyhemoglobin. Abraham Levy and Joseph M. Rifkin. The Johns Hopkins University, Department of Physics, Baltimore, MD 21218 and Laboratory of Cellular & Molecular Biology, NIH/NIH, Baltimore, MD 21224.

Mossbauer spectroscopy has been applied to the study of the dynamics of heme proteins¹⁻³. We report here a comparative study of the dynamics of the iron sites of horse hemoglobin in the Oxy, Carbonmonoxy and Deoxy forms. The mean square displacement $\langle x^2 \rangle$ as a function of the temperature, T, is inferred through the temperature dependence of the Lamb-Mossbauer factor of the compounds. The Mossbauer spectra performed on ⁵⁷Fe enriched horse hemoglobin indicate a more flexible structure at the iron site for carbonmonoxymyoglobin than oxyhemoglobin even though both have the same quaternary R structure. Surprisingly the iron sites in oxyhemoglobin exhibits a more rigid structure even than the deoxyhemoglobin T structure. The differences in these dynamics will be discussed in terms of the geometry of ligand coordination and the possible influence of amino acid side-chains in the distal heme pocket. The relevance of heme pocket dynamics to the binding of different ligands and the cooperative interactions between subunits will be considered.

1. H. Keller & P.G. Debrunner (1980) Phys. Rev. Letters **45**, 68-71.
2. G. Parak, E.N. Prolov, R.L. Mossbauer & V.I. Goldanski (1981) J. Mol. Biol. **145**, 825-833.
3. A. Levy, K. Alston & J.M. Rifkin (1984) J. Biomolec. Struct. & Dynam. **1**, 1299-1309.

093

IMPLICATIONS OF A SUCCESSFUL MODEL FOR SICKLE HEMOGLOBIN NUCLEATION AND ASSEMBLY F. A. Ferrone, Department of Physics Drexel University, Philadelphia, Pennsylvania, USA

We have recently developed a double nucleation model to provide a quantitative explanation of the significant aspects of the self-assembly of sickle hemoglobin.¹ In this model, polymerization proceeds via two nucleation-controlled paths: Homogeneous nucleation of polymers, and heterogeneous nucleation onto the surface of other polymers. This model correctly reproduces the strong but varying time, temperature, and concentration dependence of the reaction. The overall success of the model now permits the prediction of intracellular delay times in the presence of oxygen so as to devise strategies for dealing with this disease. The model also succeeds in describing homogeneous nucleation kinetics in simple thermodynamic terms. This allows us to analyze the nucleation of other assembly systems (actin, collagen, keratin, tubulin) in similar terms.

1. F.A. Ferrone, J. Hofrichter, H.R. Sunshine and W.A. Eaton, Biophys. J. **32** 361 (1980) and F. A. Ferrone, J. Hofrichter and W.A. Eaton, to be published

095

CORRELATIONS BETWEEN SOLVATION AND X-RAY AND SEDIMENTATION DATA FOR PROTEINS IN SOLUTION

H. Pessen and T.F. Kumosinski, Eastern Regional Res. Cntr., U.S.D.A., 600 E. Mermaid Lane, Philadelphia, Pa., U.S.A.

Molecular modeling from X-ray crystallographic coordinates has shown that protein surfaces possess clefts, grooves, channels, and protuberances. Proteins, however, function in an aqueous environment where, unlike in the crystal, they are fully hydrated, with surfaces consequently modified. Hydrodynamic methods, dependent on surface topography, traditionally have been employed in this context, but correlations have been marginal. A method is presented for calculation of sedimentation coefficients ($s_{20,w}$) from solution small-angle X-ray scattering (SAXS) data (hydrated volume, V , radius of gyration, R_G , and surface-to-volume ratio, S/V). For a data base of 20 globular macromolecules, $s_{20,w}$ could be predicted with good accuracy when two departures from customary practice were followed: (i) to calculate required Stokes radii, V was used, not the partial specific volume, and (ii) an equivalent axial ratio used in Perrin's equation to calculate frictional coefficients was a function of both S/V and R_G , instead of R_G and V alone; this gives the requisite weight to the surface irregularities. In this way it was possible also to estimate solution-structure axial ratios and R_G with only $s_{20,w}$, molecular weight, and partial specific volume of the protein known. Comparison of parameters from SAXS with those from X-ray coordinates clearly shows hydrated volumes larger, and surface areas smaller, in solution than in the crystal. These findings are compatible with bound water residing largely in crevices and grooves.

092

MOLECULAR GRAPHICS AS AN AID IN THE INTERPRETATION OF THE FLUORESCENCE OF PROTEINS.

C. Haydock, L. W. Engel, C. O. Barry* and F. G. Prendergast, F. G., Department of Pharmacology, Mayo Foundation, Rochester, MN and *Computer Systems Lab, Washington University, St. Louis, MO, U.S.A.

We have measured fluorescence spectra, lifetimes, and anisotropy in several proteins of known crystal structure. In an effort to understand the fluorescence evinced by these proteins, we used the "extra-radius" molecular graphics method (Barry, C. O., J. Mol. Graphics, submitted) to depict the environments of the fluorophores in the protein matrix. The results show that fluorescence spectra and lifetimes cannot be interpreted simply in terms of water accessibility or location in the protein matrix. Factors determining measured fluorescence lifetimes (as compared to radiative lifetimes) are difficult to discern. Further, sites designated as hydrophobic by virtue of their effect on the fluorescence of adsorbed fluorophores are often very polar in nature. The "extra-radius" graphics method allows an assessment to be made of the apparent volume available to the fluorophore to move. The results support inferences drawn from steady-state, time-resolved and lifetime-resolved anisotropy data regarding tryptophan mobility and also corroborate inferences made from molecular mechanics simulations on picosecond motions.

094

DYNAMIC EFFECTS IN ENZYME CATALYSIS

M. Compiani, T. Fonseca, P. Grigolini, R. Serra, TEMA S.p.A., Viale Aldo Moro 38, Bologna, Italy.

We discuss a generalization of Kramers' stochastic approach to chemical reaction rates, for the treatment of macromolecular catalytic effects. The generalization is two-fold. First, we consider the non-white noise case, where the system's behaviour is described by a generalized Langevin equation, and we show that reaction rates can actually increase in the overdamped regime. The upper limit for the reaction rate is given by transition state theory. Second, we introduce a coupling among the reaction coordinate and other non-reactive modes. Besides the well known reduction of the effective potential barrier, such coupling produces interesting dynamic phenomena which can be studied by using the Adiabatic Elimination Procedure (AEP), if we assume that the reaction coordinate relaxes more slowly than the non-reactive degrees of freedom. We thus obtain an evolution equation for the probability density of only the reaction coordinate. It is shown that the reaction rate can increase by several orders of magnitude. We also show that the use of different projection operators leads to different dynamic behaviours, because it physically corresponds to the choice of different initial conditions.

096

HYDROPHOBIC ANIONS AND CONFORMATION OF BASIC POLY- α -AMINOACIDS

G. Ebert and H. Lukasch, Fachbereich Physikalische Chemie-Polymer- Philipps Universität, D-3550 Marburg(L)

Very recently it could be shown by Senō et al. (1) that the surfactant Bis(2-ethyl-hexyl)-sulfo-succinate (AOT) induces the formation of ordered structures like α -helix and β -structure in aqueous solutions of some basic poly-aminoacids. Ethane-sulfonate is not effective in this regard and one can conclude, that the strong hydrophobic interactions of the AOT-octylgroups are necessary for an interaction with the polycations strong enough for inducing a conformation change.

Because perfluorinated alkyl groups show an enhanced hydrophobicity compared with the nonfluorinated ones we studied the influence of trifluoromethylsulfonate and other perfluorinated alkylsulfonates on the conformation of some basic poly- α -aminoacids. It was found that $CF_3SO_3^-$ induces the formation of α -helix and β -structure whereas $CH_3SO_3^-$ does not. Therefore one can assume that - supported by the electrostatic interactions with the charged polypeptide sidegroups - a micell-like aggregation of the strong hydrophobic fluorinated anions along the poly- α -aminoacid molecules occur. (1) Senō, M., Noritomi, H., Kuroyanagi, Y., Iwamoto, K., Ebert, G., Colloid & Polymer Sci., (in press)

Monday 30 July Congress Centre-first floor. Posters 097-102

Posters on Folding, Dynamics and Solvation of Macromolecules

097

CALCULATION OF CONFORMATIONAL CHANGES FOR DIRECTED MUTAGENESIS IN A GLOBULAR PROTEIN

S. Yoshioki, Yatsushiro National College of Technology, Yatsushiro 866, and M. Katsuyama and N. Go, Department of Physics, Faculty of Science, Kyushu University, Fukuoka 812, Japan

Recently a very fast algorithm has been developed to calculate the first and second derivatives of the empirical conformational energy function of a protein molecule in which bond lengths and bond angles are treated as fixed and only dihedral angles are treated as independent variables. By using the first and second derivatives thus calculable we can minimize the conformational energy function rapidly to locate local minima corresponding to stable conformations. This method is applied to calculate subtle conformational changes that occur in a small globular protein, bovine pancreatic trypsin inhibitor, when an amino acid substitution is made. A minimum energy conformation of this protein molecule is first calculated by starting the energy minimization from the X-ray structure. Then a directed sidechain is replaced by another one in this minimum energy conformation and the energy minimization is carried out again in this mutated molecule. Such calculations have been carried out for fifteen different amino acid substitutions. Analysis of the results indicates that about one half of the molecule is rather rigid, i.e., does not change local conformation appreciable, for the substitutions but the other half which contains the site to bind to trypsin is flexible.

099

SOLVENT ANALYSIS FOR THE PROTEIN CRAMBIN FROM NEUTRON X-RAY DIFFRACTION STUDIES. Martha M. Teeter Department of Chem., Boston University, Boston, MA 02215 USA.

The small, hydrophobic plant protein crambin (MW=4700) forms crystals which diffract to 0.88 Å. Models refined against x-ray data at 0.945 Å (Hendrickson & Teeter, unpublished) and against neutron data at 1.5 Å for crystals in D₂O are now available.

Crambin crystals contain 32% solvent. More than 80% of this solvent is ordered. Despite the fact that crystals were grown from 60% ethanol, very little ethanol (about 7%) has been located in the crystals. Most of the water found at the surface of crambin is bound to polar groups at the surface. These molecules connect donor and acceptors on the protein lines.

However, a cluster of waters at a hydrophobic inter-molecular interface, sandwiched between charged protein side chains, forms a pentagonal array around a methyl group on the surface. Analysis of the contacts between molecules in the cluster and surrounding atoms suggests the proximity to the hydrophobic surface leads the pentagonal array to form more water-water associations than protein contacts.

Solvent molecules in crambin crystals form about twice as many water bonds to backbone-C=O as to -NH, in agreement with results for other proteins. 58 primary waters, 12 secondary shell waters and 3 tertiary waters have been located in the crystals. The detailed geometry of the solvent, i.e. the number and lengths of bonds formed with other atoms, will be described.

101

RECOGNITION OF PROTEIN SUPER-SECONDARY STRUCTURE

William R. Taylor and Janet M. Thornton
Laboratory of Molecular Biology
Department of Crystallography
Birkbeck College, London, WC1E 7HX

With the increasing number of known protein structures, several well-defined sub-assemblies of local secondary structure have been found to occur very frequently. These recurrent motifs, which have been termed super-secondary structure are probably energetically favourable, possibly provide stable nucleation centres and certainly dominate the tertiary folds of most globular proteins. The super-secondary structures identified so far include the right-handed $\beta\alpha\beta$ unit and the β -hairpin.

A procedure to recognise super-secondary structure in protein sequences is described in which idealised templates, derived from known super-secondary structures, are used to locate probable sites by matching with secondary structure probability and hydrophobic profiles. We applied the method to the identification of $\beta\alpha\beta$ units (Taylor & Thornton (1984) JMB 173 487) and β -hairpins. The location of super-secondary structure was then used to refine the original (Garnier et al.) secondary structure prediction resulting in almost 9% improvement in prediction accuracy for the $\beta\alpha\beta$ type proteins and 11% for the all- β proteins. Most importantly, the overall pattern of predicted secondary structure agrees very well with observation with over 80% of structures correctly located.

A recent extension of the method to incorporate sequence specific templates of the type described by Hol (Nature, 1983) is also described.

098

APPARENT IRREVERSIBILITY OF THE UNFOLDING-REFOLDING OF HOPSE MUSCLE PHOSPHOGLYCERATE KINASE. CHARACTERISATION OF TRAPPED SPECIES UNDER CRITICAL CONDITIONS.

A. Mitraki, J.M. Betton, M. Desmadril & J.M. Yon, Laboratoire d'Enzymologie Physicochimique & Moléculaire, Bât. 433, Université de Paris-Sud, Orsay, France

The denaturation-renaturation of phosphoglycerate kinase has been studied under equilibrium conditions and the kinetics of the process were analysed. The results indicated that intermediates occur during the unfolding-refolding process. In the present work, we have tried to characterize intermediates trapped under critical Gdn-HCl concentrations. Indeed, a "trough" was observed in the recovery of enzyme activity and was maximum for a Gdn-HCl concentration of 0.8M. Structural studies suggest that the trapped inactive species were partially folded: 1) C.D. spectra indicated that about 25 % of helical structure was irreversibly unfolded 2) fluorescence spectrum of the inactive species was similar to the spectrum of an intermediate which was kinetically characterized 3) three more-SH groups became rapidly titratable by Nbs2. However, these species were able to interact with substrates since 3PG as well as nucleotides modified conditions of irreversibility.

100

SOME CENTRAL QUESTIONS ABOUT PROTEIN FOLDING.

D. B. Wetlauffer, Department of Chemistry, University of Delaware, Newark, DE 19716, USA.

Is the structure of a protein dependent on its assembly process?--Or is it process-independent?

Is folding just unfolding run backwards?

Does reversibility of folding prove that the process is thermodynamically controlled?

What is the connection between the equilibrium population of intermediates in a folding/unfolding reaction, and the intermediate population in flux?

Alternative answers to these several questions will be examined, some old and new experiments discussed, and conclusions developed.

102

A POTENTIAL INCLUDING POLARISABILITY FOR PROTEIN-WATER ENERGY CALCULATIONS.

J. Baum and J.L. Finney, Department of Crystallography, Birkbeck College, Malet Street, London WC1E 7HX, UK

Our understanding of biomolecular interactions at the molecular level can be greatly improved through realistic accurate energy calculations. Most empirical potentials now used do not include induction energies and so the electrostatic term, which is of major importance, has serious inaccuracies. We have investigated the use of quantum chemistry programs in providing accurate data for fitting an electrostatic model of protein-water interactions including polarisability to handle environmental effects.

Large basis set test calculations have been carried out initially for the water dimer hydrogen bond, at both SCF and CI levels. The accuracy of energy data from such calculations is shown to be rather poor, with errors greater than kT, which is 10% of the total interaction energy.

The basis set dependence of the electrostatic potential was investigated for water, ammonia and formaldehyde using minimal to near Hartree-Fock basis sets. Convergence of the pure SCF potentials is very slow. However, using a point dipole approximation to correct for deviation of the molecular dipoles from experimental values, it was found that using a double-zeta or larger basis set the major differences between potentials could be explained by slight differences in orientation. Including CI did not significantly improve results. Dipole corrected potential data are now being used to fit a charge and dipole model with polarisability for a protein-water potential.

Monday 30 July Congress Centre-first floor. Posters 103-108

Posters on Folding, Dynamics and Solvation of Macromolecules

103

ENERGY LEVEL DISTRIBUTIONS IN HIGH-SPIN FERRIC MYOGLOBIN: SOLUTION STATE COMPARED WITH THE CRYSTALLINE STATE.
A.S. Brill, F. G. Fleming, P. D. Levin and R. Thorkildsen, Dept. of Physics, Univ. of Virginia, Charlottesville, VA USA.
Several independent EPR measurements at cryogenic temperatures have been used to quantify the energies and widths of a four level crystal field model of the ferric ion in aquozuglobin: 1) absorption in the g=6 region (in frozen solution), 2) variation in hyperfine component line width in the heme plane (from single crystal orientation study), 3) temperature dependence of the spin-lattice relaxation rate giving the best single exponential fit to power saturation recovery, 4) residuals between actual recovery curves and the best single exponential fits. The rms width of Δ_1 (energy of the first excited electronic state, a spin quartet) is remarkably (within $\pm 10\%$) the same in solution and crystal. The next pair of states (also quartet, orbitally degenerate in the axial approximation) has an average energy Δ_2 which is about 3 times greater than Δ_1 . Because the effect upon zero-field splitting of a change in one of these energies is inversely proportional to the square of the energy, the rms width of the average Δ_2 is relatively poorly constrained. The site is rhombic; the rms width of the separation in energy of the two Δ_2 levels is well-determined and is five to seven times greater in solution than in the crystal. The difference, between solution and crystal, in the distribution of the orientation of the proximal imidazole relative to the heme plane is likely to be an important factor in this effect.

105

PROTEIN FOLDING AND PROTEIN DYNAMICS BY HYDROGEN EXCHANGE STUDIES OF INDIVIDUAL AMIDES IN HEN LYSOZYME
B.W. Sigurskjold¹, M. Delopierre², J. Stockwell², C.M. Dobson² and F.M. Poulsen¹
¹Carlsberg Laboratory, Department of Chemistry, Valby, Denmark. ²Inorganic Chemistry Laboratory, Oxford, England.
The dynamic properties of a protein structure can be monitored by the kinetics of the hydrogen exchange reaction of individual amides in the peptide backbone. In hen lysozyme the solvent exchange reaction at the amides in the α -helix A and the amides of the larger β -pleated sheet region has been studied using ¹H-NMR-spectroscopy. The dynamics of the reversible folding/unfolding processes of hen lysozyme has been analyzed at these specific sites, and the results suggest that there are at least one intermediary state in the folding pathway.
The hydrogen exchange reaction has also been employed in studies comparing the dynamic properties in the crystal and the solution form of the protein. This comparison reveals significant differences between crystal and solution in certain sites and close similarity in others. These results will be discussed in terms of protein dynamics and solvent accessibility in the two states.

107

DOES A LYOPHILIZED PROTEIN UNDERGO PERIODIC CONFORMATIONAL TRANSITIONS AFTER BEING DISSOLVED?
E.L. Coo, C.B. Kherlakian, and Gh. Daouk, Dept. of Biochemistry, American Univ. of Beirut, Lebanon.
During the first hour after solution of lyophilized glucose-6-phosphate dehydrogenase (*L. mesenteroides*) to a final concentration of 2 g% protein in 40 mM Tris-Cl, pH 7.0, at 25°C, there are periods of change in the rate of H-D exchange, specific rotation at 436nm, and the relative velocities of the enzymatic reaction with NAD and NADP. The H-D exchange, estimated from the Amide II IR absorption band, accelerates between 20 and 30 min, suggesting a period of unfolding protein structure. Specific rotation decreases from -62° at 5 min to -65.5° at 25 min, and then increases again. The ratio of velocities (NAD/NADP) appears to oscillate, exhibiting a maximum of 1.8 at 10 min, a minimum of 1.6 at 20 min, and a subsequent maximum and minimum at 37 and 85 min, resp. The presence of saturating levels of NAD (40 mM) or NADP (0.5 mM) in the solution shifts the timing of these phenomena. The duration of a wave is directly proportional to the time at the midpoint of the wave for all three parameters and for enzyme with or without the presence of coenzyme, an observation which supports the validity of the data, even though individual variations are near the limits of error. Such a proportionality would imply a system relaxing in a hyperbolic rather than an exponential fashion. (Highly purified enzyme donated by Dr. L.H.Hsu of Worthington Biochemical Corp.; supported by grants from A.U.B. Med Echl and the Diana Tamari Sabbagh Fund.)

104

MOLECULAR DYNAMICS OF THE AVIAN PANCREATIC POLYPEPTIDE MONOMER
P. Krüger, W. Straßburger, A. Wollmer, RWTH Aachen, Germany, W.F. van Gunsteren, University of Groningen, The Netherlands.
Molecular dynamics simulation techniques were used to compare avian pancreatic polypeptide (aPP) hormone both in the environments existing in the crystal (van Gunsteren, unpublished) and in solution. Motivation was twofold: 1) It is of obvious interest whether aPP, as suggested by CD spectroscopy, is stable as an independent monomer in solution - since in the crystal it exists as a dimer (coordinates from Birkbeck College, London) and 2) never before have these techniques been applied to a solvated polypeptide with highly ordered main chain conformation. The rms fluctuations for all atoms of the solvated monomer turned out to be of the same order of magnitude as calculated for a single monomer in the crystal ($\leq 0.8\text{\AA}$). In the solvent run all H bonds of the α -helix backbone were reproduced and maintained over the full time span. The main chain dihedral angles more or less exhibit 3 different patterns of fluctuation corresponding to the 3 types of secondary structure present. (poly-proline helix: short relaxation and non-correlated fluctuations; β -bond: possible fluctuation, but with period exceeding the time span; α -helix: fluctuations with a period of $\approx 0.1\text{ps}$).

106

PREDICTION OF THE THREE-DIMENSIONAL STRUCTURE OF THE SIS VIRAL ONCOGENE COMMON SEQUENCE WITH HUMAN PLATELET-DERIVED GROWTH FACTOR.
B. Robson*, E. Platt*, P. Finn*, J.F. Gibrat* and J. Garnier*.
^{*}Theoretical Biochemistry, School of Medicine, University of Manchester-Manchester, England.
^{*}Laboratoire de Biochimie Physique, INRA, BAT. 433 - Université de Paris Sud - ORSAY - FRANCE.
It has recently been reported that the sequence of the SIS oncogene of Simian Sarcoma virus (SVSIS) and of human platelet-derived growth factor (PDGF) are very similar, establishing the most solid link yet between the mitogenic actions of growth factors and the transforming proteins of retroviruses. To investigate molecular mechanisms of transformation we have undertaken the prediction of the three-dimensional structure of the common sequence between the two proteins (160 Amino Acid residues) through energy minimization (by a Simplex method) of a starting conformation of phi and psi angles predicted by a new version of the method of Garnier, Osguthorpe and Robson. To reduce computing time, various procedures have been applied including computer graphic system.
The predicted structure is in agreement with the known antigenic sites obtained from synthetic peptide immunization reported by other authors.

108

INTERACTION OF APOCYTOCHROME C WITH LIPID VESICLES: CONFORMATIONAL CHANGES AND BILAYER FUSION ARE CHARGE DEPENDENT
Raj Mohan¹, Anne Walter² and Robert Blumenthal¹
¹University of Strasbourg, France; ²LKEN, NHLBI, NIH; ³LTH, NCI, NIH, Bethesda, MD 20205, USA
Apocytochrome c, an extremely basic protein (pI=10.5) is the non-heme precursor to the mitochondrial protein, cytochrome c. Its conformation in solution and in the presence of lipid vesicles was assessed from circular dichroism (CD) spectra in the far UV. Measurements were done at 25°C of apocytochrome c (3.7 μM) in 10 mM phosphate buffer in the absence and presence of small unilamellar vesicles (0 - 0.13 mM total lipid). Apocytochrome c was found in an essentially random coil in aqueous solution over the pH range 5 - 11.5. This spectrum was unchanged when vesicles composed of the zwitterionic lipid phosphatidylcholine (PC) were added but converted immediately to a typical α -helix spectrum in the presence of vesicles containing the acidic lipid phosphatidylserine (PS) (100% PS or PS:PC, 1:1) lipid. The conditions associated with apocytochrome c conformational changes from random coil to α -helix correlated with optimal conditions for protein-induced vesicle-vesicle fusion.

Monday 30 July Congress Centre-first floor. Posters 109-114

Posters on Folding, Dynamics and Solvation of Macromolecules

109

NMR STUDIES OF DOMAIN STRUCTURE AND MOBILITY IN THE PYRUVATE DEHYDROGENASE MULTIZYME COMPLEX.

G.C.K. Roberts, R.N. Perham and L.C. Packman, National Institute for Medical Research, Mill Hill, London, U.K., and Dept. of Biochemistry, University of Cambridge, U.K.
The pyruvate dehydrogenase complexes ($M_r 6 \times 10^6$ - 10×10^6) consist of multiple copies of three enzymes. The E2 (lipoate acetyltransferase) component forms a structural core to which the E1 and E3 components are bound. It also carries the lipoic acid residue(s) which serve to transfer the substrate between the separate active sites.
 1H NMR spectra of the complexes from *E. coli* and *B. stearothermophilus* show numbers of relatively sharp resonances, indicating the existence of a region of substantial polypeptide chain mobility. Selective proteolysis experiments allow us to localise this mobility, which involves ca. 100 and ca. 50 residues/protomer in the two complexes, to the region of the E2 subunit containing the lipoyl groups. We have shown that in the *Bacillus* complex, the lipoyl groups are attached to a small (~65 residue) folded domain which is linked to the major part of the E2 component by a long flexible arm. Analysis of the nucleotide sequence of the *E. coli* E2 gene (J. Guest) confirms and extends the conclusions drawn from the selective proteolysis/NMR experiments.
The unusual structure of the E2 protein permits a striking coupling of the active sites in the multienzyme complex.

111

EXPONENTIAL GROWTH CURVES IN HEMOGLOBIN S. G.W. Christoph and R.W. Briehl, A. Einstein College of Med., Bronx, N.Y.

The reversible polymerization of deoxyhemoglobin S into long rods and the resultant gelation has many similarities to other macromolecular polymerizations. The original three stage model for gelation (homogeneous nucleation, rod growth, and alignment) explains the delay time and its concentration and temperature dependence, but predicts that reaction fraction, f , develops as a power law in time. Reaction progress, beginning at about $f=10^{-6}$, was measured by light scattering in which the effects of high optical density, long rod non-ideality, multiple scattering, monomer depletion, and back reaction were minimized or corrected for. Long rod form factors in the scattering equation permit f to be directly followed, because scattering is independent of rod length.

Progress curves were exponential up to $f=0.4$. Therefore growth rates were proportional to the mass of polymer. This suggests surface dependent heterogeneous nucleation and hence a double nucleation model, as proposed previously for other reasons by Ferrone et al. (Biophys. J. 32:361 (1980)). Growth rates and delay time have similar thermodynamic activation parameters and concentration dependence. This evidence supports the view, implied in the double nucleation model, that delay and growth stages are mechanistically identical, differing only in amount of polymer present. Very early in the reaction, progress curves of the form $\cosh(kt)-1$ were observed, also as predicted by the double nucleation mechanism. Supported by grants HL 28303 and 07451 from the NIH and a grant from the N.Y. Heart Association.

113

EXPERIMENTAL EVIDENCE OF THE HIERARCHIC ORGANIZATION OF GLOBULAR PROTEINS: INDEPENDENT FOLDING OF COOH-TERMINAL FRAGMENTS OF THERMOLYSIN. D. Daizoppo, C. Vita and A. Fontana, Inst. of Organic Chemistry, Biopolymer Res. Centre of CNR, Univ. of Padua, Padua, Italy.

We have previously shown that the COOH-terminal BrCN fragments 121-316 and 206-316 of thermolysin are able to refold into a stable native-like structure. We now report the results of limited proteolysis of these fragments, with the aim to identify the minimum size of a fragment able to fold by itself. Proteolysis with subtilisin, chymotrypsin, thermolysin and trypsin allowed to isolate to homogeneity eight different subfragments which can be grouped in two sets of peptides, i.e. (218-222)-316 and (252-255)-316. These subfragments are able to acquire a stable conformation of native-like characteristics, as judged by quantitative analysis of secondary structure from far-ultraviolet circular dichroism spectra and immunochemical properties using rabbit anti-thermolysin antibodies. From the kinetics of the proteolytic digestion it is concluded that proteases lead to a stepwise degradation of the fragments from their NH₂-terminal region. These results provide evidence that it is possible to isolate stable subdomain structures and correlate well with predictions of stable subfragments of the COOH-terminal structural domain 158-316 of thermolysin (A.A. Rashin, private communication).

110

INTERMEDIATES IN THE FOLDING OF RIBONUCLEASE A

R. G. Biringer and A. L. Fink, Division of Natural Sciences, University of California, Santa Cruz, California, USA.

The folding of ribonuclease A has been investigated using aqueous methanol cryosolvents and subzero temperatures. The presence of the relatively more hydrophobic cosolvent results in the stabilization of partially-folded intermediate states. These can be observed under equilibrium thermal unfolding conditions by a variety of techniques, including NMR and circular dichroism, and are consistent with the loss of tertiary structure before (i.e. at a lower temperature than) secondary structure. The kinetics of refolding at -15°C of some nitro-tyrosine derivatives of RNase A were compared to those for unmodified protein. Inhibitor binding and catalytic activity were also studied as a function of refolding kinetics. In each case the process was multiphasic, and revealed that different regions of the protein folded at different rates. A model for refolding, taking proline isomerization into consideration, has been developed. The experimental observations are interpreted in terms of two partially-folded intermediate states which have properties rather similar to the native state.

112 ORAL PRESENTATION

CRYSTALLOGRAPHIC STRUCTURE OF PIG PANCREAS α -AMYLASE (2.9 Å RESOLUTION). By G. Buisson, E. Dué, D.R.F., GEN-G, C.E.A., 85 X, 38041 Grenoble Cedex, France. R. Haser, F. Payan, C.R.M.C.2, Campus de Luminy Case 913, 13288 Marseille Cedex 9 France.

The structure of Pig Pancreas α -Amylase (PPA) ($M_r=53,000$) was solved at 2.9 Å resolution. The electron-density map obtained from multiple isomorphous replacement was improved by a density-modification procedure. The resulting map was interpretable in terms of the amino acid sequence. P.P.A. contains two domains: a larger N-terminal domain (residues 1-410) with a 8-stranded singly wound parallel β -barrel and a smaller C-terminal domain (residues 411-496) with essentially β -sheets. The main chain arrangement in P.P.A. is roughly similar to that in Taka-amylase A. The activator Cl^- ion is located at the center of the β_2 barrel (as shown by Br^- substitution). The essential Ca^{2+} ion maintains one stretch of the polypeptide chain in the vicinity of the β -barrel, which would explain why it is "essential" for the integrity of the 3D structure of P.P.A. The re-interpretation of previous substrate analogues binding experiments (Acta Cryst. (1980) B36,416-421) indicates which amino acids are involved in substrate binding. The active site cleft is located at the carboxyl end of the β -barrel and is delineated by residues constant in all α -amylases sequenced so far. The secondary binding site is formed by residues belonging to the two domains.

114

PROTON NMR STUDIES OF THE FOLDING AND UNFOLDING OF PROTEINS C.H. Dobson, P.A. Evans and R.O. Fox, Inorganic Chemistry Laboratory, South Parks Road, Oxford OX1 3QR, UK.

Many resonances in the 1H NMR spectrum of the native state of hen lysozyme are now assigned. Changes in the spectrum of lysozyme as the temperature is varied through the denaturation transition are readily observed. The enthalpy of denaturation measured by monitoring the intensities of resonances in the native and denatured states agree well with values from calorimetric methods. Magnetization transfer techniques have enabled assignments in the spectrum of the denatured protein to be made by correlating resonances with those in the spectrum of the native protein using one- and two-dimensional methods. These techniques have also enabled the kinetics of the folding and unfolding reactions to be measured, and the apparent activation energies of the two processes to be determined. In conjunction with hydrogen exchange measurements this has enabled the conformation state of the denatured as well as the native protein to be explored. The approach has been extended to examine staphylococcal nuclease where it has been possible to measure the kinetics of interconversion between the denatured state and different states of the native protein. Nuclease mutants produced by primer directed mutagenesis are under study to elucidate the role of proline isomerism in nuclease stability and folding kinetics. The significance of these results for protein folding is discussed.

Monday 30 July Congress Centre-first floor. Posters 115-120

Posters on Folding, Dynamics and Solvation of Macromolecules

115

REPEATING MOTIFS IN THE TAIL FIBRES OF T4 AND T7 PHAGES CAN BE FOLDED INTO CROSS- β AND α -HELICAL STRUCTURES
N.M. Green, National Institute for Medical Research, Mill Hill, London NW7 1AA, UK.

Segments of sequences of phage tail fibre proteins have repeating motifs analysable in structural terms (cf. the cross- β structure of the adenovirus fibre, Green et al., EMBO J. 2, 1357 (1983)). The distal portion of T4 gene 37 also has a cross- β structure broadly consistent with its sequence (Oliver & Crowther, J. Mol. Biol. 153, 545 (1981)). Closer examination of its C-terminal fine tip (160 x 18 Å) showed a 9-residue (x 14) repeating motif, analysable in terms of a 4-residue polar sequence (e.g. DSHS) alternating with a 5-residue sequence (e.g. TVAG) with hydrophobic residues at 2 and 4 and glycine at 5. Models were constructed with alternating 4-residue β -turns, the extra residue forming a β -bulge opposite the glycine. Most of the hydrophobic residues could be aligned on one surface of this structure and were buried when a dimeric fibre was formed, the fibre axis being the dyad. Although each repeat has only two residues in extended β -configuration, the resulting structure has the required 4.7 Å repeat. The sequence of the distal segment of the T7 fibre is also consistent with a cross- β structure. However, the proximal arm of the fibre (175 Å) has a 7-residue repeat (x 17) with hydrophobic residues at 4 and 7. This implies a coiled coil α -helical dimer of the tropomyosin type.

117

NEUTRON DIFFRACTION STUDIES OF TORTOISE EGG-WHITE LYSOZYME
C.C.F. Blake, S.T. Evans, and S.A. Mason, Laboratory of Molecular Biophysics, Department of Zoology, Oxford and Institute Laue-Langevin, Grenoble, France.

Large (2.5-3.0 cm³) crystals of Tortoise Egg White Lysozyme (TEWL) have been grown and investigated using the technique of neutron diffraction with a view to comparing the solvent structure and exchange properties with that of Triclinic Lysozyme (Bentley, G.A., Delepiere, M., Dobson, C.M., Mason, S.A., Poulsen, F.M., and Wedin, R.E., J. Mol. Biol. (1983) 170, 243-247). Data were collected at the Institute Laue-Langevin, Grenoble, France, using a single counter 4-circle diffractometer to a resolution of 2.8 Å on a crystal that had been soaked in deuterated mother liquor for five weeks prior to data collection, and to 3.5 Å on a crystal grown directly from D₂O. Using the Hendrickson-Konnert restrained least squares refinement program, the X-ray structure of TEWL (Palford, W.C.A., (1981) in Refinement of Protein Structures (Machin, P.A., Cabell, J.W. and Elder, M. eds.) pp. 69-71 SERC, Daresbury Laboratory, Warrington) is being refined against the neutron data, and preliminary results show that the pattern of amide proton exchange is very similar to that found for Triclinic Lysozyme. Further analysis is in progress.

119

¹³C NUCLEAR MAGNETIC RESONANCE STUDIES OF M13 COAT PROTEIN.
Gillian D. Henry, Joel H. Weiner and Brian D. Sykes, Department of Biochemistry, University of Alberta, Edmonton, Canada

The major coat protein of the filamentous coliphage M13 is a 59 residue polypeptide chain which spans the inner membrane of *E. coli* during infection. It thus represents a good model system for the study of the structure and dynamics of an integral membrane protein. ¹³C NMR, which offers many advantages to such an investigation, is limited by the low natural abundance of the ¹³C nucleus (1.1%). Inclusion of a specifically enriched amino acid in the culture medium, however, yields phage with a coat protein selectively labeled at predetermined sites.

¹³C natural abundance spectra of coat protein in deoxycholate micelles have shown clearly that regions of differential flexibility occur. A broad overview of the molecule has been obtained by incorporation of 3-[¹³C]alanine, which contributes 10 of the 59 residues in a fairly even distribution along the polypeptide chain. The conformation appears largely independent of the nature of the solubilising detergent (deoxycholate or SDS). The N-terminal and penultimate residues (ala-1 and ala-49) have been identified, and can be used as environmental probes in model membranes. T1, T2 and NOE data have been analysed using the model free approach of Lipari and Szabo (JACS 104 4546-4559).

Protein backbone motions have also been studied by incorporation of lysine, phenylalanine, proline and tyrosine labeled at the carbonyl carbon. These residues occur singly (proline) or in localized groups (e.g. lysine), and have allowed investigation of precise regions of the molecule.

116

AN X-RAY DIFFRACTION STUDY OF A PEPTIDE HORMONE DEAMINO-OXYTOCIN. By T.L. Blundell, S. Cooper, J.-L. Li, J.E. Pitts, I.J. Tickle, A.C. Treharne and S.P. Wood, Laboratory of Molecular Biology, Department of Crystallography, Birkbeck College, University of London, London WC1E 7HX, U.K.; V.J. Hruby, Department of Chemistry, University of Arizona, Tucson, Arizona 85721, U.S.A. and H.R. Wyssbrod, Department of Physiology and Biophysics, Mount Sinai Medical Centre, New York 10029, U.S.A.

Oxytocin is a nona-peptide hormone composed of a twenty membered ring and acyclic tail. It acts hormonally on the uterus and mammary glands by eliciting smooth muscle contraction. Deamino-oxytocin, which is more potent in most tests than the natural hormone, was crystallised from 20% ethanol. The data was collected to 1.2 Å resolution (after Low; Science 151, 1552 (1966)). 6-seleno deamino-oxytocin was crystallised isomorphously from water and data was collected to 1.92 Å resolution. The phases were calculated using anomalous and isomorphous differences. The models were refined using SHELX and RESTRAIN (Moss, Morfey, Hance, Stanford and Borkakoti). The structure contains two β -turns, a type II turn involving residues 2 to 5 and a type I β -turn involving residues 6 to 9. There is some conformational disorder in the disulphide bridge. The crystal structure is compared to conformations from NMR and other spectroscopic studies in water and DMSO in terms of binding to neurophysin and receptors.

118

COMPUTER SIMULATION OF PROTEIN FOLDING PATHWAYS

R.L. Somorjai, Division of Chemistry, NRC, Ottawa, Ontario, Canada, M.K. Ali and L. Solheim, Department of Physics, Univ. of Lethbridge, Lethbridge, Alta., Canada

A conceptually novel simulation strategy of protein folding is presented. As in actual experiments, folding-unfolding is induced by systematically changing the protein's environment (e.g. temperature, pH, solvent, etc.). This is implemented computationally by an effective potential formulation: the influence of the environment is represented only through the explicit parametrization of the protein's interaction potentials. Folding pathways are traceable by changing the parameters between their extremes (i.e. from random coil values to native ones). Each new set of parameters represents a new protein-environment system, and each system is to be reequilibrated, using a constant temperature (canonical ensemble) molecular dynamics (MD) method. In preliminary tests we used simple pseudo-atom residue-residue potentials, parametrized by a single "folding" parameter τ . Temperature is the other folding parameter. Both were varied. In particular, the relevance of various folding concepts was tested by changing τ nonuniformly, the rate depending on the range of residue-residue separation along the backbone. Such simplifications are appropriate for discovering relevant qualitative features of the folding process. BPTI was the test protein. A large number of long (500-1000 psec) equilibrated MD runs were created and the trajectories subjected to both local and global analysis. Denatured BPTI was successfully folded into a globular shape and a movie of the folding pathway was produced.

120

INTERNAL DYNAMICS OF HEN EGG-WHITE LYSOZYME. C.B. Post, P.

Artymuk, C.M. Dobson, D.C. Phillips, and M. Karplus, Chemistry Dept, Harvard University, Mass, USA; Molecular Biophysics and Inorganic Chemistry Laboratory, Oxford, UK.

The internal motions of hen egg-white lysozyme (HEWL) have been studied by molecular dynamics (MD) simulation and compared with the results from proton NMR and X-ray crystallography. Three MD trajectories of HEWL were computed with the Harvard University program CHARMM on a CRAY-1S computer at Daresbury Laboratory. Two trajectories were of native HEWL and 53 water molecules, while the third was of HEWL and 35 waters plus the substrate hexa-N-acetylglucosamine (NAG). The variation in the positional fluctuations from the simulations have been related to the structural features of HEWL. In the MD results, there is a correspondence between mobility and secondary structure; residues from the α -helical and β -sheet regions have, in general, smaller fluctuations than those in the intervening random-coil regions. This is in accord with the X-ray temperature factors. The mobilities of some residues differ substantially between the unbound and bound lysozyme trajectories. NMR relaxation rates (cross-relaxation, T_1 and T_2) calculated from the MD simulations differ significantly from the results expected for isotropic, rigid rotation of lysozyme due to the internal motions of residues. The predictions from the trajectories are compared with the available proton NMR relaxation data. The mobilities of residues determined from NMR and from the simulation are discussed in terms of the protein and structured water environment and the effects due to bound (NAG)₆.

Monday 30 July Congress Centre-first floor. Posters 121-126

Posters on Folding, Dynamics and Solvation of Macromolecules

121

CALCULATION OF PROTEIN CONFORMATIONS BY DISTANCE CONSTRAINTS
M. Braun and N. Go, Department of Physics, Kyushu University
Fukuoka, Japan

A new efficient algorithm was developed to calculate protein conformations which satisfy a given set of distance constraints. The program can be used for regularization of X-ray structures to standard bond lengths and bond angles or for the calculation of protein conformations by given experimental or simulated proton-proton distance constraints. The program was successfully applied for proteins up to 240 residues where all atoms are included in the calculations. Trypsin inhibitor, lysozyme and elastase were regularized. The RMSD values for structures generated from the X-ray dihedral angles are 3.6Å, 10.5Å and 10.9Å for these proteins. After regularization the corresponding RMSD values are 0.2Å, 0.3Å and 0.3Å. From the regularized trypsin inhibitor structure different proton-proton distance constraints sets were extracted to evaluate the possible restrictions of these constraints on the tertiary structure. By using all exact proton-proton distances up to 5Å excluding the intra-residue contacts and by starting from 10 randomly chosen initial conformations with RMSD values ranging from 10Å to 20Å, the minimizer converged to the regularized structure with final RMSD values of 0.1Å. We conclude that knowledge of all short proton-proton distances in globular proteins determines almost uniquely the tertiary structure of protein domains. By using short range distances with an accuracy of 0.5Å and an upper limit of 5Å for the long range distances, we can reconstruct the regularized structure with RMSD of 1Å to 2Å.

123

EFFECTS OF UREA AND AMMONIUM SULPHATE (AmSO_4) ON *S. AUREUS* PENICILLINASE

C. Mitchinson, R.H. Pain, Department of Biochemistry,
University of Newcastle upon Tyne, U.K.

The reversible urea denaturation of *S. aureus* penicillinase was studied in the presence and absence of AmSO_4 , and the non-coincidence of the transition followed by different probes confirms the existence of a helical intermediate (II) in the (un)folding;

(Native) $\text{N} \rightleftharpoons \text{H} \rightleftharpoons \text{U}$ (Unfolded)

AmSO_4 shifts both transitions to concentrations of urea greater by 5.3 M/mol. AmSO_4 but has markedly different effects on the free energies of stabilization of states N and H in the absence of denaturant: $-\Delta G_{\text{N},0}$ is increased by 61 kJ/mol. and $-\Delta G_{\text{H},0}$ by 20 kJ/mol. per mole AmSO_4 . AmSO_4 has a dramatic effect on the unfolding rate constant of the $\text{N} \rightleftharpoons \text{H}$ transition, 1.40 M AmSO_4 decreasing it by a factor of more than 10^{11} , whilst having little effect on the refolding rate. The effects of AmSO_4 and the characteristics of the transitions in urea and in guanidinium chloride support a model for the unfolding of penicillinase in which the separation of virtually intact folding units, held together by mainly apolar interactions, is followed by their gross unfolding, with concomitant loss of secondary structure.

125

EVIDENCE FOR A TRANSIENT INTERMEDIATE IN THE REFOLDING OF DENATURED THIOREDOXIN. Robert Kelley and Earle Stellwagen,
Department of Biochemistry, University of Iowa, Iowa City,
Iowa 52242.

The monomeric protein thioredoxin from *E. coli* is reversibly denatured in a single cooperative transition between 2 M and 3 M guanidine hydrochloride (Gdn) at pH 7 and 25°. The kinetics of the refolding of denatured thioredoxin were observed by the increase in tryptophan fluorescence quenching following dilution of the Gdn by stopped flow mixing. Refolding in 2 M Gdn occurs in three kinetic phases having relaxation times of about 500, 15 and 1 sec accounting for 80%, 10% and 10%, respectively, of the fluorescence change. The slowest phase has an activation energy of 22 kcal/mole and is generated in the denatured state. These features suggest that the slowest phase results from isomerization of a peptide bond of proline 76 which is about 80% trans in the denatured state and 100% cis in the native protein. The fractional amplitude of the slowest phase diminishes to 20% in a single transition centered at 1.5 M Gdn. By contrast, kinetic measurements of far ultraviolet ellipticity and of biofunction obtained by manual mixing indicate that 0% and 80%, respectively, of the refolding amplitude occurs in a slow phase. These observations together with the results obtained from manual multi-mixing protocols, urea gradient electrophoresis measurements, and model simulations are consistent with the view that a folding intermediate transiently accumulates during the refolding of thioredoxin in low [Gdn]. The stability of this intermediate to Gdn is similar to that of thioredoxin having its single intrachain disulfide bond cleaved. (Supported by USPHS research grant GM22109.)

122

ESR AND ENDOR STUDIES ON IRRADIATED-FROZEN SOLUTIONS OF OXYHEMOGLOBIN AND OXYMYOGLOBIN

R. Kappl, M. Hohn-Berlage and J. Huttermann, Inst. f. Biophys.
U. Phys. Biochem., Universität Regensburg

Frozen solutions of oxyhemoglobin and oxymyoglobin, X-irradiated at 77 K, exhibit distinct EPR-spectra of rhombic symmetry which were assigned to electron-adduct-centers formed at the FeO_2 -unit in the α -, β -chains and in myoglobin X- and Q-band measurements verified the g-factor assignment of the centers. Between 77 K and 250 K the irreversible formation of secondary centers in polycrystalline and glassy solutions and differences between the systems were characterized. Upon irradiation down to 4 K no precursors of the centers could be found. The formation of the centers upon UV-irradiation at 77 K and Fe(III)-aquomet-Mb reduction studies are indicative for a direct effect in the protein moiety and subsequent e⁻-conduction to the heme-center. ¹H-ENDOR studies were pursued on primary and secondary centers to resolve hydrogen bonds. Depending on the field position 2 to 6 couplings were observed. 5 of these had magnitudes between 0.5 MHz and 4.1 MHz and showed no effect upon H-D exchange. One exchangeable anisotropic coupling amounted to 11 MHz for the primary Mb- and α -center. It was assigned to the proton of H₂ of the distal histidine. For the secondary centers this coupling could not be resolved. ¹⁴N-ENDOR studies revealed a number of lines in the frequency range 1 MHz to 7 MHz, which were assigned to pyrrol and histidine nitrogens, showing significant spectral changes between the primary and secondary centers.

124

COMPARATIVE ¹H-NMR STUDIES ON THE WATER STRUCTURE IN SOFT CONTACT LENS AND PROTEIN GEL. S. Hayano, H. Amano, K. Kawai, K. Takahashi, M. Sogami*, S. Nagaoka*, S. Era*, K. Kuwata*, H. Watarai** and K. Shiga**, Dept. of Ophthalmol., *Dept. of Physiol., Sch. of Med., Gifu Univ., Gifu, Japan and **Nat. Inst. for Physiol. Sci., Okazaki, Japan

The water structure in soft contact lenses (SCL) (HEMA derivatives) were studied using 360MHz ¹H-NMR spectra. T₁(H₂O) and cross relaxation time (T₁ρ(H₂O)) obtained by irradiation at -4.00 ppm from TSP at 3H₂/2π = 69Hz. A rod-shaped SCL (4.8 X 20 mm) with a center hole for a D₂O capillary was inserted into 5 mm NMR tube, after removing H₂O on the surface by an inert tissue paper. A sharp and a broad H₂O spectra were observed at 4.74 ppm and 4.47 ~ 4.52 ppm, respectively, at 25°. T₁(H₂O, 4.74 ppm) and T₁(H₂O, 4.47 ~ 4.52 ppm) were 2.7 ~ 2.8 sec and 0.56 ~ 0.62 sec respectively. T₁ρ(H₂O, 4.74 ppm) and T₁ρ(H₂O, 4.47 ~ 4.52 ppm) were 1.5 ~ 2.9 sec and 0.35 ~ 0.37 sec, respectively. Spin diffusion from polymer matrix to H₂O might indicate the interaction between polymer and H₂O. Though a sharp H₂O signal was decreased by soaking the rod-shaped SCL into D₂O for 10 min., a broad H₂O signal was not affected. So, a broad H₂O signal might correspond to the strongly bound H₂O with polymer matrix. On the other hand, HDO signal in the modified plasma albumin gel did not show any significant chemical shift.

126

DNA INTERMOLECULAR INTERACTIONS AND SOLVENT VISCOSITY
J.V. Ostashevsky* and C.S. Lange*, *The Brooklyn Hospital, and
**SUNY Downstate Medical Center, Brooklyn, N.Y., U.S.A.

The effect of solvent viscosity (η_s) on the shape of the concentration dependence of the principal and total recoils in creep-recovery viscoelasticity experiments has been studied for T4c DNA-glycerol-water solutions. The range of DNA concentration (c) was 2-50 µg/ml, glycerol, 70-80% v/v; T₄, 275 - 325°K; salt, 5 mM - 1 M NaCl. We found a linear proportionality of both recoils to DNA concentration could be obtained at high η_s . At low η_s , the c-dependence was nonlinear, approaching saturation at higher c. For a given concentration, the ratio of high- to low- η_s recoil values was found to equal 1/K, where K is dependent on ionic strength, but not η_s and T. For a given solution, both recoils showed a narrow (~2° width) temperature transition between their high- and low- η_s constant values. The limiting viscosity of DNA molecules did not change across the transition.

The above results suggest: (1) the recoil transition from high- to low- η_s values is due to collisions between DNA molecules, and (2) an absence of intermolecular collisions if η_s exceeds a critical value (η_{crit}). This η_{crit} depends on the ionic strength because of the electrostatic expansion of DNA molecules. The large size, the higher η_s must be to prevent collisions. Below η_{crit} , collisions are controlled by K, which is the product of the diffusion coefficient (D) and the retardation time (τ) of DNA molecules. K is independent of η_s and T because D is proportional to T/ η_s , while τ is proportional to η_s /T.

Monday 30 July Congress Centre-first floor. Posters 127-132

Posters on Folding, Dynamics and Solvation of Macromolecules

127

NMR STUDY OF THE RATE AND MECHANISM OF HEME REORIENTATION AS A PROBE OF HEMOPROTEIN DYNAMICS

G. N. La Mar, H. Toi and Y. Yamamoto, Department of Chemistry, University of California, Davis, California, USA

We have used proton NMR spectroscopy of paramagnetic forms of both myoglobin and hemoglobin to demonstrate that, contrary to current hypotheses, both proteins exhibit heme disorder (~5-10%) with respect to rotation about the α - γ meso axes. Preliminary O_2 binding data reveal that the O_2 affinity in sperm whale Mb is dramatically influenced by the heme orientation. By carrying out the reaction between apoprotein and heme or heme- O_2 within an NMR tube, we have also shown that the initial products for both Mb and Hb are the proteins with completely disordered heme. In contrast to findings based on optical spectroscopy of both Mb and Hb reconstitution, we find that the time course to yield the native protein is many hours rather than a few milliseconds. In the case of Mb, we have determined the rate of equilibration of the heme, which has a sharp minimum at neutral pH and depends critically on heme 2,4-substituents and protein chain origin. Although the rate determining step in the reorientation is demonstrated to involve the rupture of the axial ligand bonds in the heme pocket, the equilibration rate is much faster than the heme self-exchange rate. This requires that the heme does not leave a protein "cage" during the reorientation. Thus this intramolecular reorientation represents an internal motion which requires the largest protein structural fluctuations documented to date for a hemoprotein.

129

INVESTIGATION OF THE PATHWAY OF PROTEIN FOLDING BY NON-RADIATIVE ENERGY TRANSFER MEASUREMENTS

¹D. Amir, ¹D.P. Levy and ^{1,2}E. Haas, ¹Dept. of Life Sciences, Bar-Ilan Univ. Ramat-Gan and ²Depts. of Biophysics and Chemical Physics, Weizmann Institute of Science, Rehovot, Israel.

Non-radiative energy transfer measurements are used to investigate the pathway of protein folding. Intramolecular distance distributions and dynamic and static segmental flexibilities are obtained from donor fluorescence decay curves. In combination with site-directed labeling procedures this method allows characterization of the conformations of defined segments of partially ordered states of protein derivatives within the refolding transition. A series of bovine pancreatic trypsin inhibitor (BPTI) derivatives was prepared, each specifically labeled by a single donor and a single acceptor chromophore at a pair of its amino groups. All the derivatives were purified by HPLC and characterized by peptide mapping. Using these derivatives intramolecular distance distributions of several segments in the BPTI molecule were determined in the native, unfolded and partially folded states. The kinetics of conformational changes of each labeled segment occurring during the unfolding/refolding transitions are currently being measured. The combination of data obtained by these methods from all the labeled derivatives will allow detailed analysis of the sequence of events and intermediate conformations comprising the folding pathway of BPTI.

131

THE EFFECT OF ORGANIC COSOLVENTS ON THE DIMER-TETRAMER EQUILIBRIUM OF HUMAN HAEMOGLOBIN.

A. Cupane, E. Vitranò and L. Cordone, Istituto di Fisica and GNFM (CNR), Via Archirafi 36, Palermo - Italy.

In order to further investigate the role of protein-solvent interactions in the conformational and functional stability of biological macromolecules, we have studied the effect of organic cosolvents (monohydric alcohols and formamide) on the dimer-tetramer equilibrium of human haemoglobin. The study was performed by measuring the dependence of the oxygen affinity upon haemoglobin concentration in a 100-fold concentration range, from $3 \times 10^{-6} M$ to $3 \times 10^{-4} M$ on a hepc basis. The data were analyzed in terms of a modified Monod-Wyman-Changeux model in which the equilibrium (tetramer) \rightleftharpoons 2 dimer+dimor was taken into account; this allowed to obtain the dimer-tetramer equilibrium constant (K). The organic cosolvents were found to affect the dimer-tetramer equilibrium through two main contributions: 1) bulk-electrostatic contributions, linearly related to the variation of the bulk dielectric constant of the solvent and 2) non-bulk-electrostatic (hydrophobic) contributions, related to the decreased free energy needed to expose hydrophobic surfaces to the solvent when organic cosolvents are present in the solution medium. This indicates that in the (tetramer) \rightleftharpoons 2 dimer+dimor transition electrostatic bonds are broken and hydrophobic surfaces are exposed to the solvent.

128

DYNAMICS AT THE ACTIVE SITE OF α -CHYMOTRYPSIN STUDIED BY ^{19}F AND 2H NMR

S.J. Hammond and J.T. Gerig, Department of Chemistry, University of California, Santa Barbara, CA 93106, U.S.A.

An aryl ester of N-acetyl- α -aza-p-fluorophenylalanine stoichiometrically acylates α -chymotrypsin to give a reasonably stable, catalytically inactive protein which resembles the transient acylenzyme intermediate formed during cleavage of a phenylalanyl substrate by chymotrypsin. This protein, and an analogue in which the p-fluorophenyl ring is specifically deuterated, have been studied by ^{19}F NMR and 2H NMR. Analysis of fluorine spin-lattice relaxation data and ^{19}F 2H nuclear Overhauser effects, measured as a function of radiofrequency, indicates that rotation of the fluorophenyl ring of the inhibitor is slow relative to overall protein tumbling. The observed linewidth of the deuterium resonance also shows that the fluorophenyl ring is considerably immobilized by the protein structure at the active site. However, the observed fluorine linewidths are larger than those predicted from our analysis of nuclear relaxation. Experiments demonstrate that this additional broadening does not result from heterogeneity of the protein; it may be due to an exchange of the fluorophenyl ring between environments characterized by different chemical shifts.

130

LOW FREQUENCY VIBRATION ASSOCIATED WITH THE OPEN AND CLOSED MOTION OF THE TWO DOMAINS IN PAPAIN

Y.Y. Sun, R.Y. Yan, F.J. Lu, C.L. Jone, Theoretical Molecular Biophysics Group, Chinese University of Science and Technology, Hefei, Anhui, China.

Papain is a proteolytic enzyme consisted of 212 residues. There are two domains situated to the right and left of a cleft in the molecule. The active site Cys-25 and His-159 lie at the surface of this dividing cleft. It is assumed that the bending motion of papain around the axis paralleled to the cleft in the presence of solvent is determined by the Langevin equation for a damped harmonic oscillation. Using the empirical energy function with the simplified model of protein, the hinge bending potential energy curve was calculated. After fitting to this curve, it was found that the motion is "overdamped". If absence of random forces, the domains would relax to their equilibrium position without oscillating. The relaxation time $\tau_{rel} = 4.4 \times 10^{-10}$ sec. Actually the domain overcomes random force due to collisions with the surrounding solvent, so the domain fluctuation is expected to be governed on the overdamped decay behavior.

132

KINETICS OF HEME CAVITY PROTON EXCHANGE IN SPERM WHALE AND HORSE MYOGLOBIN

J.T.J. Leconte and G.N. La Mar, Dept. of Chemistry, Univ. of California, Davis, CA, USA

Dynamic aspects of the heme pocket of myoglobin (Mb) from Sperm Whale (SW) and Horse were investigated by evaluating the rate of exchange of selected cavity NH protons as a function of pH. The rates were obtained for the met-cyano proteins by 1H NMR spectroscopy at 360 MHz through linewidth analysis and saturation transfer experiments. The HisF8N,H (proximal His) and HisF62N,H (on the proximal side) exhibit similar rate profiles and values in SW Mb and Horse Mb. However, the Horse Mb HisE7N,H (distal His) undergoes both acid and base catalyses whereas the same NH group in SW Mb shows acid catalysis only. The heme pockets of SW Mb and Horse Mb differ by one residue, at position CD3, but are structurally the same otherwise; CD3 obstructs a possible channel to the distal face of the heme in SW Mb (ArgCD3) but to a lesser degree in Horse Mb (LysCD3). Hence, it is suggested that hydroxyl ions penetrate readily the Horse Mb heme pocket through an opening located at the level of residue CD3. Support for this hypothesis is provided by the X-ray structure of met-aryl SW Mb where the bulky ligand, by displacing ArgCD3, opens a way to the distal side. Our findings offer a rationalization for the faster on and off rates of isocyanide binding in Horse Mb versus SW Mb in spite of similar equilibrium constants. The observed exchange behaviors reflect local phenomena and do not correlate with the folded macrostate stability of the proteins considered.

Monday 30 July Congress Centre-first floor. Posters 133-138

Posters on Folding, Dynamics and Solvation of Macromolecules

133

SCREENING MUTANT PROTEINS FOR ALTERED FOLDING PROPERTIES
B.T. Hall and F.H. Ziegler, Biochemistry and Molecular Biology
University of Texas Medical School, Houston, Texas, U.S.A.
Polyacrylamide slab gel electrophoresis similar to that described by Creighton (J. Mol. Biol. 129: 235) has been used to screen mutant forms of yeast cytochrome c for altered folding behavior. The gels contain a denaturing gradient of 0.50% formamide perpendicular to the direction of electrophoresis such that fixed and stained gels provide a record of electrophoretic mobility throughout the unfolding transition zone. It is shown that the oxidized form of the wild type protein folds reversibly and that folding-unfolding is fast compared to the time of electrophoresis. A non-equilibrium experiment shows that reduced cytochrome c is more stable (or unfolds more slowly than the oxidized form) and may provide an approach to estimating differences in thermodynamic stability between the two forms. For mutant proteins the gels provide information on the following: 1) Is folding-unfolding reversible? 2) Are rates of folding-unfolding slower in the mutant? 3) What is the difference in thermodynamic stability between the mutant and wild type protein?

134

Comparative Studies of Native and Circular Bovine Pancreatic Trypsin Inhibitor by ¹H NMR
M.J. Chazin, D.P. Goldenberg* and K. Wüthrich,
Institut für Molekularbiologie und Biophysik,
ETH-Hönggerberg, CH-8093 Zürich, Switzerland,
* Med. Res. Council Center, Univ. Med. Sch.,
Hills Road, Cambridge, U.K.

A circular derivative of bovine pancreatic trypsin inhibitor (BPTI), with the C- and N-termini covalently linked (cBPTI), has been studied by spectroscopic techniques in solution. The outstanding stability of the globular conformation of BPTI is preserved in cBPTI. The frequencies of 180° flips for corresponding aromatic rings are nearly identical, and there is also close coincidence of corresponding amide proton exchange rates in the two proteins. In the fingerprint region of the ¹H COSY spectra in H₂O almost all amide proton-C^α-proton cross peaks in BPTI and cBPTI are superimposable, showing that the bulk of the secondary structure of BPTI is preserved in the circular derivative. Overall, conformational differences are thus strictly localized to the polypeptide segment which corresponds to the C- and N-terminal regions of native BPTI. The spatial structure and internal mobility of this molecular region are further investigated by measurements of intramolecular ¹H-¹H distance constraints with NOESY experiments and spin-spin coupling constants with high resolution, phase sensitive, double quantum filtered COSY experiments.

135

RESOLUTION OF HUMAN MERCAPT- AND NONMERCAPTALBUMIN BY HIGH-PERFORMANCE LIQUID CHROMATOGRAPHY (HPLC). M. Sogami, S. Nagaoka, S. Era, K. Kuwata and K. Noguchi*, Dept. of Physiol., Sch. of Med., Gifu Univ., Gifu, Japan and *Techn. Develop. Labor., Asahi Chemical Industry Co., Ltd., Yako, Kawasaki-Ku, Kawasaki, Japan
Human serum albumin (HSA) is the mixture of mercaptalbumin (HMA) and nonmercaptalbumin (HNA). During HPLC studies on HSA using various kinds of gel-exclusion chromatography columns with an UV-monitor (UV) and a low-angle laser light scattering photometer (LS) (632.8 nm), we found a covalent HPLC column (Asahi Pak GS-520H, 0.75 X 200 cm, 0.10 M Na phosphate buffer, 0.30 M NaCl, pH 6.86) for the analysis of fraction of HMA, HNA. HPLC profile of HSA from GS-520H column showed two peaks. Weight-average molecular weights of the principal and the secondary peaks in HPLC profile of HSA obtained by UV and LS data were 66K. Various kinds of PNA prepared by the intermolecular SH-S-S exchange reaction with cystine or oxidized glutathione, HNA(CYS) or HNA(GLUT) exactly corresponded to the secondary peak in HPLC profile of HSA. An elution volume of synthesized HSA dimer was quite different from those of the principal and the secondary peaks. The tightly bound lipid impurities, such as fatty acid did not show any effect on HPLC profile of HSA from Asahi Pak GS-520H column. So, the principal and the secondary peaks in HPLC profile of HSA might be HMA and HNA, respectively. Mechanism for the separation of HMA and HNA might be due to weak resin-HSA interaction which is extremely sensitive to the microenvironment of CYS-34 of HSA.

136

¹H-NMR STUDIES ON THE WATER STRUCTURE IN THE GEL OF MODIFIED BOVINE PLASMA ALBUMIN (BPA*). M. Sogami, S. Nagaoka, J. Shigemitsu, S. Era, K. Kuwata, H. Watari*, K. Shiga* and K. Aizawa*, Dept. of Physiol., Sch. of Med., Gifu Univ., Gifu, Japan, *Natl. Inst. for Physiol. Sci., Okazaki, Japan and **Dept. of Chemistry, Fac. of Sci., Kyoto Univ., Kyoto, Japan
Bovine plasma albumin Fr. V (BPA) has known to contain a small amount of proteolytic enzyme. The enzyme cleaves the peptide bonds of BPA around pI 4.0 between Glu-392 and Cys-435 in one or two portions. The resultant BPA (BPA*) has a tendency to form clear gel above 8%. The water structure inside of the gel was studied using 360MHz ¹H-NMR by measuring T₁, T₂ and cross relaxation time of the saturation transfer method (spin diffusion). The gel showed a similar spectrum to that of the F-form except for slightly broad H₂O signal. The saturation transfer experiment from the irradiated protein moiety to H₂O revealed the strong cross relaxation between the protein and the surrounding water molecules which may be strongly immobilized. Both T₁ and T₂ of H₂O in the gel were remarkably shorter than those of proteolytic enzyme-free bovine mercaptalbumin (BMA) solution and supported the results of the cross relaxation experiments. From the gel concentration-dependent T₁ change, the hydration of the gel state BPA* was calculated to be more than 8g/g BPA* which was 6 folds higher than that of BMA solution.

137

INTRAMOLECULAR SULFHYDRYL-DISULFIDE EXCHANGE REACTION OF BOVINE PLASMA ALBUMIN - N-A ISOMERIZATION. K. Kuwata, S. Era, S. Nagaoka, M. Sogami, H. Inouye* and S. Sakata*, Dept. of Physiol., *3rd Dept. of Int. Med., Sch. of Med., Gifu Univ., Gifu Japan
Bovine mercaptalbumin (M) when incubated at alkaline pH isomerizes to a new component (A). The reaction is sulfhydryl (CYS-34) catalyzed and reversible (Sogami et al. (1969) and Nikkel et al. (1971)). The influence of ionic strength on the N-A isomerization was studied by a moving boundary electrophoresis. The N-A isomerization was suppressed by an increase of the ionic strength generally and especially by the small amount of Ca²⁺ due to chelate formation (Saroff et al. (1962)). The measurement of the relaxation time of the N-A isomerization in 0.15 M KCl at pH 8.6 at 35°C reveals that the life span of bovine plasma albumin in vivo was controlled by the N-A isomerization. The N-A isomerization was the multi-step reaction. In glutathione oxidation-reduction buffer (GSH/GSSG = 0.3 mM/0.03 mM) without added salt at pH 8.6 at 25°C in air, the rate of the N-A isomerization was notably increased and at an early state of the reaction two peak of the A-form was observed in a moving-boundary electrophoresis. In oxidation-reduction buffer system, the rate of the N-A isomerization was more strongly dependent on the oxidation-reduction potential than the concentration of the reduced glutathione.

138

FOLDING OF HISTONES H1. INFLUENCE OF N- AND C- DOMAINS ON THE GLOBULAR HEAD.

F. Morán, R. Caballero, B.A. Fernandez and F. Montero, Dept. of Biochemistry, Faculty of Chemistry, Univ. Complutense, Madrid, Spain.

The controlled tryptic digestion of H1 from both calf thymus and *C. capitata* has been followed by circular dichroism in the near and far UV, difference spectroscopy and fluorescence emission spectroscopy. The presence of two tyrosine residues, as well as the specific fluorescence properties of one of them at low pH for insect histone H1 (1), has been used to follow from another perspective the conformational transition of the globular region as tryptic digestion occurs. These studies show that the hydrolysis of N- and C- domains of the H1 molecule have influence on both secondary and tertiary structure of the globular region. The kinetic analysis of the variation of the α -helix content, $\Delta\epsilon$ and quantum yield of fluorescence, show two different contributions: the fast one correspond to the influence of the hydrolysis of the non structured domains on the globular one; and the slow process is due to the hydrolysis of this structured region.

(1) J. Jordano, J.L. Barbero, F. Montero and L. Franco, J. Biol. Chem. 258, 315-320 (1983).

Monday 30 July Congress Centre-first floor. Posters 139-144

Posters on Folding, Dynamics and Solvation of Macromolecules

139

HIGH-PERFORMANCE LIQUID CHROMATOGRAPHIC (HPLC) STUDIES ON ALBUMIN IN HUMAN AQUEOUS HUMOUR. K. Takahashi, K. Kawai, S. Hayano, K. Kuwata*, S. Era*, S. Nagaoka*, M. Sogami*, Dept. of Ophthalmol., *Dept. of Physiol., Sch. of Med., Gifu Univ., Gifu, Japan

Samples of human aqueous humour with corresponding samples of blood serum were obtained from 20 patients with cataract. HPLC analyses on PGP 2000 (Asahi Pak GS-520H, 0.75 X 200 cm) with a UV-monitor or on JASCO Fine Pak 102F (0.72 X 100 cm) with a multichannel detector at neutral pH. HPLC profile of human aqueous humour from 102F column (only molecular sieve) showed albumin (66K) and lower mol. weight components with λ_{max} of 260 ~ 265 nm. In the HPLC profile of serum, the later component was not observed. HPLC analysis of serum on PGP 2000 column resolved serum albumin into two components, human mercaptalbumin (HMA) and nonmercaptalbumin (HNA). Fraction of HMA in samples of blood serum of 20 patients (50 ~ 80 years) was 0.7 ~ 0.5. However, major part of albumin in human aqueous humour was found to be HNA. HNA in the chamber aqueous might be produced by an intermolecular SH-S-S exchange reaction between HMA and oxidized forms of sulfa-containing amino acids, such as cystine, oxidized glutathione. The conversion of HMA to HNA might decrease the concentration of free oxidized forms of sulfa-containing amino acids in the chamber aqueous.

141

CONFORMATIONAL CHANGES OF BOVINE PLASMA ALBUMIN PRIOR TO THE SALTING-OUT IN CONCENTRATED SALT SOLUTION. M. Sogami, H. Inoue, S. Nagaoka and S. Era*, Dept. of Physiol., Sch. of Med., Gifu Univ., Gifu, Japan

The N-F transition of bovine plasma albumin (BPA) in concentrated salt solution was studied using a pH-solubility profile (salting-out), $[\alpha]_{233}$ and tryptophyl fluorescence (F_{350}) with excitation wavelength of 290 nm. It was postulated by Foster's group (1965) that the solubility (salting-out) curve as a function of pH could be explained quantitatively on the basis that the F-form was an extremely low solubility which is virtually independent of pH, while the N-form appears to be extremely soluble. By working at very low protein concentration, it is possible to measure F_{350} and $[\alpha]_{233}$ of BPA as a function of pH under salting-out condition. A slight decrease in $[\alpha]_{233}$ was observed before starting the salting-out in concentrated KCl and NH₄Cl solutions. However, such a slight decrease in $[\alpha]_{233}$ is too small to conclude conformational changes of BPA before starting the salting-out. In 0.50 M or 1.00 M KCl (no salting-out), the major decrease in F_{350} (~40%) was complete at the initial part of the N-F transition (N-F₁). By working at very low protein concentration, ~40% decrease in F_{350} was observed before starting the salting-out in 2.00 M KCl or 3.00 M NH₄Cl and no further change over the salting-out pH range. So, BPA shows definite changes of conformation prior to the starting of salting-out in acidic concentrated salt solutions.

143

The Inactivation Kinetics of Trypsin by Its Specific Inhibitors. J.-M. Zhou and C.-L. Tsou, Inst. Biophysics, Chinese Acad. Sci., Beijing, China.

Although the binding stoichiometry and binding kinetics of trypsin with its specific inhibitors have been extensively studied, the activity change during the association of the enzyme with the inhibitor has received but little attention. The classical way of following activity changes by taking aliquots and making enzyme assay cannot be reliably applied to the fast inhibition reactions between trypsin and some of the inhibitors. This has now been measured by the novel approach developed in this laboratory by following the substrate reaction in presence of the inhibitor (Tian & Tsou, 1982, Biochemistry, 21, 1028). The hydrolysis of benzoylarginine ethyl ester in presence of the inhibitor has been followed and the bimolecular rate constants for the inhibition of trypsin with the pancreatic, ovomucoid and soya bean inhibitors have been found at pH 7.8 and 25°C to be 3×10^4 , 1×10^5 and 3×10^5 M⁻¹s⁻¹ respectively. Kinetic analysis of the effect of substrate concentration on the rate constants shows that the inhibitions by the pancreatic and ovomucoid inhibitors are of the competitive and non-complexing type whereas the mechanism of the inhibition by the soya bean inhibitor is much more complex and may involve a number of intermediate steps.

140

¹H-NMR STUDIES ON VARIOUS CONFORMATIONAL STATES OF BOVINE MERCAPTALBUMIN (BMA). S. Nagaoka, S. Era, K. Kuwata, M. Sogami, K. Shiga*, H. Watarai* and K. Akasaka**, Dept. of Physiol., Sch. of Med., Gifu Univ., Gifu, Japan, *Natl. Inst. for Physiol. Sci., Okazaki, Japan and **Dept. of Chem. Fac. of Sci., Kyoto Univ., Kyoto, Japan

BMA has various conformational states, such as E(pd 3.02) F(pd 4.03), N(pd 4.5 ~ 7.0) and B(pd 9.4) in 0.10 M NaCl. An increase of BMA concentration in the F-form caused ¹H-NMR spectral changes (360MHz) in parts of aliphatic and histidine signals which were substantiated by gel formation, but no in the N-form. From the ¹H-NMR studies, the N- and B-forms showed the typical shape being ascribed to the rigid internal structure, while the F- and E-forms appeared to lose partly their rigid structure. In saturation transfer experiments by irradiation either at -7.18 ppm or 2.40 ppm from H₂O, the cross relaxation time (T₁) from the irradiated moiety to typically assigned side chain protons were evaluated. T₁ values of the F- and E-forms were 2 ~ 3 folds greater than those of the N- and B-forms. ¹H-NMR spectra and T₁ values of the F-form indicated that a partial loss of the secondary structures and very slight increase in the intrinsic viscosity in the N-F transition lead to increase the mobility of side chains, that is, "the side chain melting or disorder". The side chain disorder in the N-F transition is similar to those in cytochrome c and poly L-glutamate reported by Dr. Mada's group (1981).

142

PICOSECOND DYNAMICS OF ACTIVE SITE CYS-25 IN FAFAIN. R. Y. Y. Shi and C. X. Liang Theoretical Molecular Biophysics Group, Chinese University of Science and Technology, Hefei, Anhui, China.

Fafain is a proteolytic enzyme consisted of 217 residues. For the full understanding of the structure and function, it is essential to have a knowledge not only of the average position of the atoms, but also of the magnitudes and time scales of the fluctuations about the average position. The molecular dynamics simulation has been used to investigate the picosecond dynamics of active site Cys-5 at 300°K in Fafain. In the 10 picosecond trajectory of every extended atoms in Cys-5, the root mean square fluctuations about the average positions. The average fluctuations for these six atoms is 0.1 Å. After performing the cumulative analysis, we got the power spectrum too, which specify the rotational character of Cys-5 in picosecond time scales. The frequencies correspond to the higher power spectrum are between 0.1 GHz ~ 10 GHz.

144

THE INCOMPLETELY DENATURED STATE OF GLOBULAR PROTEINS

S. Kidokoro, R. Hanai, K. Nagayama, A. Wada, Department of Physics, Faculty of Science, University of Tokyo, Bunkyo-ku, Tokyo, Japan

From the measurement of near and far ultraviolet circular dichroism, fluorescence, nuclear magnetic resonance, and calorimetry of globular proteins such as lysozyme, carbonic anhydrase B, ribonuclease A and pepsinogen in various solution conditions, we classified the conformational states of these proteins broadly into three states, that is, native state, random coil state, and incompletely denatured state (ID state). In the ID state, the tertiary structure of native state is almost broken while some secondary structures are retained, which are not necessarily same as in native state. Although lysozyme exhibits one-step transition and pepsinogen shows an equilibrium intermediate during guanidine hydrochloride (GuHCl) denaturation, the temperature-GuHCl state-diagrams of these proteins are found to be almost same and consist of these three states. We consider that denatured protein in water could still have secondary structures, and when the concentrated denaturant such as GuHCl exists at low temperature, the secondary structures would be broken by the binding of denaturant and the protein is unfolded to random coil state.

Monday 30 July Congress Centre-first floor. Posters 145-150

Posters on Folding, Dynamics and Solvation of Macromolecules

145

VIBRATIONAL CIRCULAR DICHROISM OF POLYPEPTIDES
T.A. Keiderling, A.C. Son, U. Narayanan, S. Yasui,
A. Annamalai, Department of Chemistry, University
of Illinois at Chicago, Box 4348, Chicago,
Illinois 60680 / USA

Vibrational circular dichroism (VCD) spectra of polypeptides in both the α -helical and β -sheet conformations have been obtained in solution and films. The data for Amide I and A bands have very good signal-to-noise ratio and show characteristic features for each conformation. Some of the signs and magnitudes are not in agreement with previous theoretical predictions. Film VCD for extended polypeptides is very sample dependent; however, for globular proteins, such data matches the solution results. Preliminary results on oligopeptides and polynucleotides will be discussed. These shorter segments yield less easily characterized VCD due to the proportionally larger end effects.

147

NONMERCAPT-MERCAPT CONVERSION OF HUMAN SERUM ALBUMIN (HSA) BY HEMODIALYSIS. M. Sogami, S. Era, S. Nagaoka, K. Kida, K. Kuwata, K. Miura*, H. Inouye*, E. Suzuki*, S. Hayano** and S. Sawada***, Dept. of Physiol., *3rd Dept. of Int. Med., Sch. of Med., Gifu Univ., Gifu, Japan; **Hayatoku Hospital, Gifu, Japan and ***Sawada Hospital, Gifu, Japan

HSA is the mixture of mercaptalbumin (HSA) and nonmercaptalbumin (HNA). The SH group of HSA acts as a scavenger for heavy metal ions, such as Hg^{2+} . Another role of the SH group is the intramolecular SH-S-S exchange reaction, resulting in the molecular ageing of HSA (see a separate poster from our group). We recently developed a new high-performance liquid chromatography system (HPLC) for the resolution of HSA and HNA at neutral pH (Asahi Pak GS-520H, 0.75 X 200 cm). Using a new HPLC, fraction of HSA (f_{HSA}) of healthy male adults was 0.76 ± 0.025 . In hemodialysis patients, f_{HSA} before dialysis and mean value of [f_{HSA} after dialysis) - (f_{HSA} before dialysis)] were 0.45 ± 0.077 ($n = 112$) and 0.16 ± 0.054 ($n = 100$). We found the nonmercapt-mercapt conversion (HNA \rightarrow HSA) during hemodialysis and the mercapt-nonmercapt conversion (HSA \rightarrow HNA) after hemodialysis in hemodialysis patients, indicating HNA being "a covalent carrier protein" for sulfa-containing amino acids, such as cysteine, homocysteine.

149

AGGREGATION OF MELITTIN IN MEDIUM - DEPENDENT
B. Chandani, & D. Balasubramanian, Centre for Cellular and Molecular Biology, Hyderabad, India.

The membrane-lytic bee venom peptide, melittin, is shown to exist as monomers, tetramers or other aggregates depending upon its environment. At pH 7 it is monomeric and unordered, and the circular dichroism of its lone tryptophan is negligible in the aromatic region. The tetramers of melittin formed upon 2M NaCl or upon 0.2M phosphate addition at pH 7 (form T_1) are largely helical and display well-defined aromatic region ellipticities ($\sim 90^\circ$). Melittin also tetramerizes beyond pH 10 into form T_{II} with a secondary structure similar to T_1 but displays weaker aromatic ellipticity ($\sim 20^\circ$). These aromatic circular dichroism results, along with the reported NMR spectral differences, indicate different protomer arrangements and tryptophan environment/mobility between forms T_1 and T_{II} . We have found melittin to also aggregate in aqueous sodium dodecyl sulphate (SDS) solutions to form mixed aggregates (e.g. at SDS:melittin ratio 13:1) with distinctly enhanced aromatic ellipticity compared to T_1 . As the SDS:melittin ratio is increased to upto 70, the secondary structure remains unaltered while the aromatic ellipticity and sedimentation coefficient decrease. These indicate a decrease in the number of melittin molecules per mixed aggregate, until at excess SDS, monomeric helical melittin is obtained. This same form is seen when melittin is included in inverted micelles of Aerosol OT in isooctane (0.2% water), but when the water content is increased to 0.9%, the aromatic ellipticity doubles due to melittin aggregation and phase separation. Such aggregates of melittin in these membrane-mimetic media would appear more relevant to the study of its function than T_1 or T_{II} .

146

QUENCHING OF TRYPTOPHAN PHOSPHORESCENCE IN ALCOHOL DEHYDROGENASE FROM HORSE LIVER AND ITS TEMPERATURE DEPENDENCE
N. Barbov and J. Feltelson, Department of Physical Chemistry, The Hebrew University of Jerusalem, Jerusalem 91904, Israel.

The phosphorescence of Alcohol Dehydrogenase from Horse Liver (LADH) can be observed at room temperature. The quenching of this long-lived light emission, which comes from a tryptophan residue well buried within the interior of the enzyme structure was measured. The rate constant for the quenching by the small oxygen molecule and by the I^- ion were found to be $1.4 \times 10^8 \text{ M}^{-1} \text{sec}^{-1}$ and $10^8 \text{ M}^{-1} \text{sec}^{-1}$ respectively at room temperature. The same quenching rate constant was obtained both by steady state and by triplet lifetime measurements, i.e. a dynamic process and no ground state complex is involved in the quenching. The temperature dependence of the quenching yields an activation energy of about 14 kcal/mole. This activation energy and the meaning of the accompanying large pre-exponential factor in the Arrhenius equation, $A = 10^{10} \text{ M}^{-1} \text{sec}^{-1}$, are discussed in terms of a model in which the quencher threads its way through the protein network. It is proposed that the diffusion of the quencher is made possible by temporal "melting" of local structures within the protein. These temporarily disordered locations provide on the one hand channels for the diffusing quencher molecule and on the other hand cause the entropy of activation in $k_q = A_{diff} \exp(\Delta S^\ddagger/R) \exp(-\Delta H^\ddagger/RT)$ to assume a large positive value.

148

THE STRUCTURAL TRANSITION OF BOVINE PLASMA ALBUMIN (BPA) WITH THE SIDE CHAIN MELTING — THE N-F TRANSITION. S. Era, K. Kuwata, S. Nagaoka and M. Sogami, Dept. of Physiol., Sch. of Med., Gifu Univ., Gifu, Japan

The N-F transition (0.10 M KCl, pH 3.75-4.45) of BPA is the structural transition with decrease in α -helix content, very slight increase in the intrinsic viscosity and the side chain melting indicated by the Scatchard's plot of acid-titration data with correction for protein surface potential and by the $^1\text{H-NMR}$ spectra of the F-form. The structural transitions of ferri cytochrome c and poly-L-glutamate with the side chain melting were reported by Wada's group (1981). BPA-detergent (sodium dodecyl sulfate) complex, AD_m was studied using tryptophyl fluorescence measurements, such as peak in fluorescence (λ_{MAX}), fluorescence polarization (1/P), rotational relaxation time (τ_{TRP}) and CD-resolved secondary structure. λ_{MAX} , 1/P, τ_{TRP} and CD-resolved secondary structures of AD_m ($m \leq 8$) showed characteristic changes in the N-F transition. Those of AD_m ($m = 10 \sim 12$) did not show any significant changes in the N-F transition region expected by the corrected Scatchard's plot and only showed characteristic changes in the acid-expansion. The corrected Scatchard's plot of AD_{12} clearly indicated the side chain melting as AD_0 , that is, the transition of ionic bondings between positively and negatively charged side chains to those between small ions and side chains. So, the N-F transition of AD_{10} or AD_{12} might be the structural transition with the side chain melting and without any changes in the secondary structures.

150

DYNAMICS OF STREPTOKINASE SPATIAL STRUCTURE IN SOLUTION
V.N. Nikandrov, G.V. Vorobyova, N.I. Garbus, V.P. Golubovich, Byelorussian Res. Inst. of Epidemiology and Microbiology, Pogin Street, Minsk, USSR

Arising from the possible role of tyrosine and tryptophane residues of streptokinase (SK) in plasminogen activation SK structure changes have been studied in aqueous solution by methods of tryptophano luminescence and circular dichroism. Four tryptophane residues are localized in SK molecule "pockets", which bring the positive charge. PK changes from 3 to 9 do not influence their state. At the range of pH from 2 to 12 the SK secondary structure is represented by an unordered form α -helices β -beads β -structures (mainly, antiparallel). At the range of pH from 2 to 5 the part of parallel β -structures significantly increases and at pH > 5 the part of α -helices and β -structures reduces. At pH > 12 irreversible despiralization of the molecule and decrease of the part of parallel β -structures most stable for SK are observed. The increase of NaCl concentration up to 1.5M only somewhat changes the molecule surface in the region of "pockets". Urea (8M) and guanidine-HCl (6M) cause the molecule despiralization. Unlike the urea the guanidine-HCl action is irreversible. The studied physico-chemical factors excluding external effect do not appear to influence the SK molecule sites near tryptophane residues.

Monday 30 July Congress Centre-first floor. Posters 151-156

Posters on Folding, Dynamics and Solvation of Macromolecules

151

STUDIES OF ANTIBIOTIC/PEPTIDE COMPLEXES: IMPLICATIONS FOR PROTEIN BINDING

M.P. Williamson and D.H. Williams, Univ. Chem. Lab., Lensfield Rd., Cambridge, UK.

Vancomycin and ristocetin are peptide antibiotics which act by binding to cell wall peptidoglycans terminating in the sequence -D-Ala-D-Ala. Their structures and those of their complexes with Ac-D-Ala-D-Ala and Ac-Lys-D-Ala-D-Ala are well characterised and provide the basis for studies of the effect of mobility on the thermodynamics and kinetics of complex formation. Evidence to be presented, largely from nmr studies using the nuclear Overhauser effect, shows that the binding site of ristocetin for the carboxylate terminus of the peptide is fairly rigid, with hydrophobic walls and a bottom lined with amide nitrogens, which are thus in a very unusual environment and can form strong hydrogen bonds. By contrast vancomycin is flexible, and in the absence of peptide exists largely in an extended conformation; on addition of Ac-D-Ala-D-Ala it folds up into the same unusual carboxylate pocket as ristocetin. The consequence is that the rate of formation of the complex is much faster for vancomycin, but the binding constant is larger for ristocetin. Obvious implications for enzyme/substrate complexes are drawn.

153

SOLVENT-PERTURBATION FLUOROMETRY OF GLOBULAR PROTEINS: ESTIMATION OF SURFACE TRYPTOPHAN RESIDUES IN BACTERIORHODOPSIN

M.V. Sherman, R.J. Plotkin and K. Boyd, Dept. of Physical Sciences, Chicago State University, Chicago, IL 60628, USA.

The broad fluorescence emission from Trp residues of aq. suspensions of bacteriorhodopsin in its native purple membrane may be resolved into contributions characteristic of exposed residues in addition to those typical of a hydrophobic environment. Addition of glycerol to the suspending medium results in an enhancement of the fluorescence. Examination of the glycerol effect for nine other Trp-containing proteins reveals a linear correlation between fluorescence enhancement and literature values for fractional Trp exposure. Glycerol is considered to have little effect on polypeptide conformation and its role in the observed phenomenon may be attributed to viscosity-dependent inhibition of fluorescence quenching which results from solvent relaxation around the nascent dipole moment of the excited state of exposed Trp. It is proposed that glycerol-perturbation fluorometry may be a generally applicable sensitive method for the estimation of surface regions of protein polypeptide chains under conditions that are close to physiological. When applied to bacteriorhodopsin, it gives a value for the exposed fraction of fluorescent Trp of .50±.15 that is in good agreement with other estimates. (Research supported by NIH grants EY02219 and RR08043 and NSF grant PCM-8303454.)

155

TRIPLE POINT BEHAVIOUR OF MUTANT HUMAN HAEMOGLOBINS

Stanley J. Gill and Brough Richey, Department of Chemistry, University of Colorado, Boulder, Colorado, 80309

A recent crystallographic observation by Brzozowski et al. shows that half-oxygenated haemoglobin crystals exist. At first sight this would seem to imply the discovery of a unique structural species defined by the presence of two bound oxygen molecules. However, the formation of crystals with a specific degree of ligation is predicted to occur when two distinct crystalline phases coexist, namely at the triple point. It seems likely that the crystals studied by Brzozowski et al. were selected from a mixture of T and R crystalline forms obtained under conditions where the triple point existed. The partial pressure of oxygen at the triple point has been calculated from the results of Haire et al. to be 55 torr for HbA under these conditions. At this pressure the solid T form is 58% saturated and the solid R form is 99.9% saturated. This corresponds notably well with the half-saturated T state crystals found by Brzozowski et al. Similar calculations on the mutant haemoglobins HbC and HbS show that their crystalline T forms should be 33 and 74% saturated at their triple points of 19 and 108 torr, respectively. This work was supported by NIH grant HL22325.

1. Brzozowski, A., Derewenda, Z., Dodson, E., Dodson, G., Grabowski, M., Liddington, R., Skarzynski, T., and Valiely, D. Nature 307, 74-76 (1984)
2. Haire, R. N., Tisel, W. A., Niazi, G., Rosenberg, A., Gill, S. J., and Richey, B. Biochem. Biophys. Res. Comm. 101, 177-182 (1981)

152 ORAL PRESENTATION

CORRELATION OF SUBSTITUTED AMINO ACID RESIDUES WITH CONFORMATIONAL STABILITY IN EIGHT PROTEINS VARIOUSLY SUBSTITUTED AT AN IDENTICAL UNIQUE POSITION

K. Yutani, K. Ogasahara, & Y. Sugino*, Inst. Protein Res., Osaka Univ., Suita Osaka Japan and *Kansai Medical Univ., Hirakata Osaka Japan

In order to elucidate the role of individual amino acid residues in conformational stabilization of a protein, the stabilities of the wild-type tryptophan synthase α -subunit from *E. coli* and its seven mutant proteins substituted by single amino acid residues at the same position were compared. The mutant proteins have Gln, Met, Val, Tyr, Leu, Ser, or Lys in place of Glu in the wild-type protein at Position 49.

The results indicate that (1) the conformational stabilities of the studied proteins increase linearly with hydrophobicity of the substituted residues (except Tyr) and the coefficient of this linear dependence is 2.3, 3.4, and 1.2 at pH 5.5, 7.0, and 9.0, respectively and (2) charged groups (Lys or Glu) at Position 49 serve as destabilizing factor when ionized in acid or alkaline region.

154

α -HELIX FORMATION BY SHORT PEPTIDES IN WATER

R.L. Baldwin, K.R. Shoemaker, P.S. Kim and D.N. Bems, Department of Biochemistry, Stanford University Medical Center, Stanford, CA, USA; Eunice York and J.M. Stewart, Department of Biochemistry, University of Colorado Medical School, Denver, CO, USA; and I.M. Chaiken, Laboratory of Chemical Biology, NIH, Bethesda, MD, USA.

Peptides of 20 residues or less are predicted not to form α -helices in water, regardless of amino acid composition, according to the Zimm-Bragg equation and "host-guest" data for helix formation. Nevertheless the C-peptide of ribonuclease A (residues 1-13) and related peptides show partial helix formation in water near 0°C. Charged groups play a major role, as shown by the pH dependence of helix stability. Some of us proposed that a Glu 9⁺...His 12⁺ salt bridge may stabilize the C-peptide helix, and we have now tested this with chemical analogues of C-peptide. The substitution Glu 9⁺→Leu slightly enhances helix stability, in contrast to the prediction of the salt bridge model. Allowing a second salt bridge (Glu 2⁺...His 5⁺) to be made via the substitution Ala 5⁺→His strongly reduces helix stability, again in contrast to the predicted effect. We conclude that the unexpected stability of the C-peptide helix is not caused by a Glu 9⁺...His 12⁺ salt bridge.

156

FLUOROMETRIC AND CIRCULAR DICHROIC STUDIES ON THE ACID-INDUCED ISOMERIZATION OF BOVINE PLASMA ALBUMIN-1-ANILINO-8-NAPHTHALENE SULFONATE COMPLEX (BPA-ANS)_{1,0}

S. Era, S. Ogura, K. Kida, K. Kuwata, S. Nagaoka and M. Sogami, Dept. of Physiol., Sch. of Med., Gifu Univ., Gifu, Japan

The acid-induced isomerization of BPA-ANS_{1,0} was studied using fluorescence intensity (F_{460}), fluorescence polarization (1/P), peak in fluorescence (λ_{MAX}), fluorescence lifetime (τ_F) and induced ANS CD spectra. In 0.02 M or 0.05 M NaClO₄, the pH-profiles of fluorescence data were extremely simple and correlated exactly with the N-F transition and the acid-expansion (F-E). Increase in F_{460} , decrease in 1/P and blue shift were observed in the N-F transition (0.02 M NaClO₄, pH 3.2-3.9) or the N-F₁ transition (0.05 M NaClO₄, pH 3.6-4.2). Slight decrease in F_{460} and slight increase in 1/P were observed below pH 2.5 (the acid-expansion). Induced ANS CD spectra were obtained using difference CD between BPA and BPA-ANS_{1,0}. Induced ANS CD spectra showed two positive bands at 250~258 and 340~345 nm and one negative band at 280 nm. Large increases in $[\theta]_{280}$ and F_{460} were exactly correlated with the N-F transition. Rotational strengths at 280 nm in the N-, F- and E-forms were -0.434, -0.089 and -0.161 DBM, respectively. The bound ANS might be in a markedly asymmetric environment in the N form and a less asymmetric in the F-form, resulting in the increase in F_{460} .

Monday 30 July Congress Centre-first floor. Posters 157-162

Posters on Folding, Dynamics and Solvation of Macromolecules

157

CHROMATOGRAPHY AS A NEW MEANS FOR EVALUATING BASIC MOLECULAR STRUCTURE PARAMETERS.
H. Waldmann-Meyer, Institute of Physical Chemistry, Technical University of Denmark, Copenhagen-Lyngby.

Chromatographic partition is a diffusion process and thus depends upon the molecular Stokes' radius R_s . The Geometrical Exclusion Model (GEM)¹ predicts that for GLASSES $K_D = (1 - R_s/R_p)^2$ and for GELS $K_{AV} = [1 - R_s/(R_p \cos \phi)]^3$. Here, R_p is the cavity radius, ϕ a cone angle and $k^2 = K_D/K_{AV}$. Both eqs. have been thoroughly validated by data for native and denatured proteins, polysaccharides and polymers. The R_s values agree with physical measurements. For any molecule, $R_s = M^x A^y$, where x and y are well defined, structure-specific constants, widely different for ellipsoids, rods and flexible coils. For the first two, x and/or y contain V and $f/f_0(M)$, while for coils they comprise the expansion factor α , effective bond-length b and monomer weight M_0 . Replacing R_s in the above eqs., we get the linear GEM-plot: $-\log(1 - K_D^2)$ [glass] or $-\log(1 - K_{AV}^3)$ [gel] vs. $\log M$. The slope = $-x$ and the y-intercept = $-\log(A/R_p \cos \phi)$ or $-\log(A/R_p \cos \phi)$. The slope will often be known a priori, so that only few experiments are needed for calibration. Thus, homologous substances give a straight line from which the hydrodynamic structure, axial ratio, ideality (via α), length b , diffusion coefficient and gyration radius may be determined. No other single technique is able to provide as many essential data as exclusion chromatography.

¹ H. Waldmann-Meyer, in "Chromatography of Synthetic and Biological Polymers", Vol. I, R. Epton, ed., E. Horwood, 1978.

159

ENERGETICS OF ALLOSTERIC REGULATION IN E. COLI ASPARTATE TRANSCARBAMYLASE. N. Allowell, Dept. Biol., Wesleyan Univ. Middletown, CT USA; J. Matthew, Genex Corp., Gaithersburg, MD USA; J. Wild, Dept. Biochem. Biophys. Texas A&M College Station, TX USA.

E. coli aspartate transcarbamylase is a dodecamer composed of 2 c_3 (catalytic) and 3 r_2 (regulatory) subunits. Allosteric regulation depends upon transmission of signals between active sites and between active and regulatory sites. The following approaches have been taken towards elucidating the allosteric mechanism. (a) Reaction and differential scanning microcalorimetry have been used to define the thermodynamics of ligand binding and assembly. Results indicate that linked proton binding makes a major contribution to the energetics of binding substrates and nucleotide effectors. (b) The discrete charge static solvent accessibility model of Gurd and coworkers has been used to characterize ionizable groups perturbed by intermolecular interactions and to evaluate the role of electrostatic effects in docking substrates and assembly. Results indicate that a positive potential energy surface surrounds the active site while a negative potential energy surface is associated with r_2 . (c) Classical hydrogen exchange experiments show that both assembly and ligand binding to isolated subunits produce large changes in solvent accessibility. Medium resolution methods utilizing HPLC are being used to identify perturbed regions. (d) The relationship between structure, physical properties, and function is being explored with single site mutants. Replacing Tyr 165 in c_3 with Phe has a large effect on the allosteric properties of $c_3 r_6$.

161

CIRCULAR DICHROISM AND FLUORESCENCE STUDIES ON THE METAL (Zn^{2+} AND Ca^{2+}) INDUCED CONFORMATIONAL CHANGES IN S-100 PROTEINS. R.S. Muni and C.M. Kay, MRC Group in Protein Structure and Function, Department of Biochemistry, University of Alberta, Edmonton, Canada T6G 2H7

The effect of Zn^{2+} binding on the CD spectra of brain specific S-100a and S-100b calcium binding proteins has been examined. In the presence of Zn^{2+} , S-100a undergoes a conformational change and the decrease in ellipticity at 222nm, as a result of Zn^{2+} addition, was nearly 1300 deg.cm².dmol⁻¹, whereas with S-100b there was no significant conformational change. Ca^{2+} was able to bind to S-100 proteins in the presence of Zn^{2+} and the two metal ion binding sites on the protein appear to be different. Ca^{2+} and Zn^{2+} induce different environments around the tyrosine residues in S-100a, whereas with S-100b, similar changes were observed using either metal. Zn^{2+} has a pronounced effect on the secondary structure and the aromatic environment of S-100a but with S-100b it has only a subtle effect on the microenvironment of the aromatic groups. The sulfhydryl fluorophore N-(1-pyrenyl)iodoacetamide was used to study the possible involvement of sulfhydryl groups in metal binding. Among the 3 sulfhydryl groups in S-100a only one was labelled in 0.1M Tris, 1mM EDTA, pH 7.5 medium. When the protein was excited at 344nm, the emission maximum occurred at 385nm. Addition of Ca^{2+} caused nearly 30% quenching in fluorescence intensity at 385nm. Zn^{2+} addition resulted in an increase in fluorescence intensity, suggesting that the microenvironment around the sulfhydryl group is sensitive to the presence of these metal ions. (Supported by MRC of Canada and AMFMR)

158

SOLVENT STRUCTURE IN PROTEIN CRYSTALS

P.V. Artyukov, D.I. Stuart, C.C.F. Blake and W.C.A. Pulford, Laboratory of Molecular Biophysics, Department of Zoology, Oxford, UK.

Analysis of the solvent structure of a number of well refined high resolution protein structures shows that the water molecules can be divided in four distinct classes:

1. Ordered waters making more than one hydrogen bond to protein: these are as well ordered as the protein itself and occupy similar binding sites in homologous molecules.
2. Ordered waters making only one direct H bond to protein - these are less ordered than the protein.
3. Those not directly H bonded to protein. These are less ordered still.
4. Bulk water, usually comprising 60-80% of the solvent in the crystal characterized by low featureless electron density.

For human and tortoise lysozyme molecules contact area calculations indicate that the proportion of the protein surface covered by ordered waters is about 75% and the interactions with the protein have been examined in detail. Even in the absence of a detailed model for the waters in classes 1 to 3 simple models can be constructed for the disordered solvent, either directly, using a continuum of electron density or, by Babinet's principle, from the complementary scattering of the solvent which is displaced by the ordered components of the crystal. Furthermore the use of such models facilitates analysis of these ordered components.

160

SOLVENT NETWORKS IN NUCLEOTIDE CRYSTALS

P.L. Howell and J.M. Goodfellow, Department of Crystallography, Birkbeck College, Malet Street, London, UK.

Solvent is known to play an important role in the stability and transitions of nucleic acid helices. We are using computer simulation techniques to study the energetics of the water molecule-nucleic acid interactions and the effect of counter-ions in nucleotide crystal hydrate crystals. This enables detailed comparisons of the predicted solvent structures to be compared with well-characterised experimental data from crystallographic studies. Initial studies have shown that the force fields, used originally to study amino acid interactions, can be used in the simulation of solvent around nucleotides and that the cooperative effects are important in these interactions. Further studies are being undertaken to show the effect of modifications to the potential energy functions to obtain better agreement with experiment. These include the explicit use of solute hydrogen atoms both on all relevant 'heavy' atoms and attached to polar groups only. Results on the inclusion of solvent networks with (a) counter-ions such as Na⁺ and NH₄⁺ in nucleotides and (b) drugs such as proflavin in the dinucleotide dCpC will also be presented.

162

HYDRATION-RELATED CONFORMATION AND FLEXIBILITY CHANGES ARE NECESSARY FOR LYSOZYME ACTIVITY: Philip L. Poole and John L. Finney, Crystallography Department, Birkbeck College, Malet Street, London.

Dry hen egg white lysozyme is inactive. Activity begins when water is added to a hydration of about 0.7 g water/g protein. Using direct difference IR, Raman, and NMR techniques, we have investigated the hydration process and possible conformational and dynamical changes that may occur as water is slowly added to the dried protein. The direct difference IR allows us to follow the hydration of some specific atom groups (amides I and II, acidic and polar side chains). The acidic groups hydrate fast at low hydration while the maximum hydration rates of the polar side and main chain groups occur at higher hydrations of about 0.04-0.07 g/g. NMR back exchange results suggest a "loosening up" of the molecule occurs at about 0.07-0.10 g/g, at which hydration the enzyme gains sufficient flexibility for buried amide hydrogens to exchange. A small hump in the IR feature corresponding to water uptake of the amide II atom group is also seen at this hydration. This increased (hydration-dependent) flexibility is argued to facilitate subsequent (possibly small) conformation changes detected by our Raman Spectroscopy results. These changes are all complete before the onset of enzyme activity. We conclude that a minimum water content (less than monolayer coverage) is a necessary "lubricant" which facilitates molecular flexibility. This flexibility then permits small conformational changes which, together with the flexibility itself, is necessary for lysozyme function. Recent inelastic neutron scattering Expts are consistent with this protein "loosening up" model.

Monday 30 July Congress Centre-first floor. Posters 163-168

Posters on Folding, Dynamics and Solvation of Macromolecules

163

COMPARISON OF EXPERIMENTAL X-RAY DATA WITH COMPUTER SIMULATION OF THE DYNAMICS FOR LYSOZYME

J. Stockwell, C. Post, P.J. Artymus, C.M. Dobson, M.Karplus and D.C. Phillips, Laboratory of Molecular Biophysics, Department of Zoology, Oxford, U.K.

A 100 ps molecular dynamics simulation on hen egg-white lysozyme (HEWL) and a 50 ps simulation on HEWL plus the substrate hexa-N-acetyl glucosamine have been performed using CHARMM, on the former SERC CRAY computer. The results are being analysed and compared with the refined temperature factors (B values) of various crystal forms of HEWL. The correlation coefficients calculated indicate that the overall correlation, between experimental and simulation rms displacements, for the whole molecule is good (correlation coeff. = 0.55 for main chain atoms of tetragonal lysozyme). The B factor maxima in the 'lips' of the active site are reproduced in the simulation. We are now continuing the analysis with reference to particular regions of secondary structure and areas of contact within the crystal.

165

Calculation of stability limits of cold labile proteins.

F. Franks, Dept. of Botany, Univ. of Cambridge, Cambridge.

The stability profile of globular proteins is indicative of two limiting temperatures between which the native state is stable. Heat denaturation is of little biological significance but cold inactivation is implicated in the observed effects of chill and freezing on many living organisms. The low temperature order/disorder transition is also of theoretical interest. At any given pH, $\Delta G(T)$ appears to have a parabolic shape. The thermodynamic conditions for a parabolic $\Delta G(T)$ relationship have been analysed in terms of $C_p(T)$ and $C_v(T)$, where C is the heat capacity and N and D refer to the native and denatured state respectively. In particular, two special cases have been considered: 1) ΔC is independent of temperature and 2) C_p is independent of temperature, but $C_v(T) = C_p - k(T/T^*)^N$ where T^* is the temperature corresponding to maximum stability.

The results have been applied to lysozyme, the only protein for which separate C_p and C_v data are available.

167

PROTEIN DYNAMICS STUDIED BY INELASTIC NEUTRON SCATTERING (INS)

S. Cusack¹, J. Smith², U. Pezzocca², B. Brooks², M. Karplus², J. L. Finney¹ (1: ILL, Av. des Martyrs, Grenoble, France, 2: Dept. Chem., Harvard Univ., Oxford St., Cambridge, Mass., U.S.A. 3: Dept. Crystallography, Birkbeck College, Malet St., London, U.K.)

We report theoretical and experimental work on INS by bovine pancreatic trypsin inhibitor (BPTI) which allows us to draw detailed conclusions concerning the intramolecular motions involved in protein INS.

1) Theoretical studies using the results of a normal mode analysis of BPTI show that alone-phonon scattering is dominated by the frequency distribution, $g(\omega)$, of the protein. $b(\omega)$ can be obtained by extrapolation to zero momentum transfer. c) multiphonon scattering complicates the extraction of $g(\omega)$. d) scattering from different parts of the protein varies considerably.

2) Experimentally obtained INS spectra of BPTI are analysed in order to extract $g(\omega)$, evaluate the effects of solvent and of intramolecular anharmonicity on INS spectra and assess the sensitivity of INS spectra to modelling differences within the harmonic approximation.

164

THERMODYNAMIC INVESTIGATIONS OF CYTOCHROME b_5 UNFOLDING

W. Pfeil and P. Bendzko, Central Institute of Molecular Biology, Acad. Sci. GDR, 1115 Berlin, German Democratic Republic.

Cytochrome b_5 unfolding was investigated by scanning microcalorimetry in order to get insight into the molecular organization of membrane proteins. Melting profiles and thermodynamic quantities of (i) the tryptic and the chymotryptic fragment (res. 1-90 and 1-97 resp.), (ii) the complete protein (res. 1-133) in the presence and in the absence of detergent, (iii) the protein incorporated in dimyristoyl phosphatidylcholine (DMPC) vesicles are compared.

The results show (1) similarity between the proteolytic fragments and small globular proteins, (2) differences between cytochrome b_5 in aqueous solution and in liposomes, (3) a number of 35±4 lipid molecules which do not contribute to the phase transition heat of DMPC, and (4) different influence of the incorporated cytochrome b_5 on the phase transition of unilamellar and multilamellar DMPC liposomes.

The thermodynamic data and independent findings are suitable for detailing a model proposed by TANFORD (1980) for the spatial arrangement of the protein within the lipid layer.

166

pH INDUCED CHANGES IN TURTLE MYOGLOBIN. O.R. Nascimento*,

M. Tabak* and O. Baffa**, Instituto de Física e Química de São Carlos, USP, São Carlos, SP, Brazil*, Faculdade de Filosofia, Ciências e Letras de Ribeirão Preto, USP, Ribeirão Preto SP, Brazil**.

The sea turtle myoglobin "Dermochelis Coriacea" (MbT) has one cysteine in the polypeptide chain. This enables the labelling of this residue with a reporter group like a spin label. The present study is an attempt to investigate the functional role of this SH group which is not generally present in other myoglobins. In the studies of MbT labelled with a maleimide spin label we observed that the protein undergoes a precipitation at acid pH when this SH group is labelled and the iron is in the low spin configuration (highly coordinated at sixth coordination site). The same behaviour was observed with MbT-H₂O not labelled with the unmodified SH group. On the other hand the MbT-CI with the unblocked SH group do not show this precipitation.

The measurement of the optical absorption at 700 nm of MbT-H₂O show a transition from the soluble to the precipitated form at pH 6.5. This phenomenon is reversible.

This study is presently extended to other ligands using turbidity and small angle X-ray scattering (SAXS) in order to understand the aggregation mechanisms defining if a protein denaturation occurs or if a polymerization is occurring as a function of pH.

Supported by CNPq, FAPESP and FINEP.

168

PROTEIN STRUCTURE BY FT-INFRARED SPECTROSCOPY: FOURIER SELF DECONVOLUTION AND CURVE FITTING

H. Susi and D. M. Byler, Eastern Regional Research Center, USDA, Philadelphia, Pennsylvania 19118 (USA)

Infrared spectroscopy is one of the oldest methods available for investigating the secondary structure of proteins and polypeptides. The first results were published in 1950 by Ambrose and Elliott (Nature 4206, 921, 1950). Until recently, however, the technique has provided merely qualitative information because absorption bands caused by substructures such as the α -helix, β -strands and turns, overlap extensively and cannot be resolved by optical techniques. The advent of FT infrared spectroscopy has made it possible to resolve the broad bands into specific components by means of Fourier self deconvolution. The individual components can be assigned to specific types of secondary structure such as the α -helix, β -strands and turns. The areas of the resolved components, evaluated with the help of a Gauss-Newton iterative process, provide quantitative information regarding the prevalence of different secondary structure elements. The approach appears to be quite successful for applications where some other physical techniques are least effective, such as in studies of β -strands and β -turns. Application to several proteins, including ribonuclease, concanavalin, and hemoglobin, is demonstrated.

Monday 30 July Congress Centre-first floor. Posters 169-174

Posters on Folding, Dynamics and Solvation of Macromolecules

169

STRUCTURE AND DYNAMICS OF AVIAN PANCREATIC POLYPEPTIDE:
X-RAY ANALYSIS AT 0.98 Å RESOLUTION
I. D. Glover, B. C. Mabbitt, J. E. Pitts, I. J. Tickle,
S. P. Wood and T. L. Blundell, Department of Crystallography
Birkbeck College, Malet Street, London, UK.

Pancreatic polypeptide is a 36 amino acid hormone synthesised in the endocrine pancreas. The molecule has a wide range of physiological activities including effects on gut motility and gastrin-like actions. Homologous peptides have been isolated from pig intestine and brain tissue. X-ray analysis of avian pancreatic polypeptide (aPP) at 1.4 Å has defined a globular structure comprising a polyproline II-like helix (residues 1-8) and an α -helix (residues 14-32). These helices interact via hydrophobic contacts to produce a compact and stable tertiary fold. However, the C-terminal region (residues 33-36) displays some flexibility in the crystal lattice. aPP forms symmetrical dimers mainly through hydrophobic interactions, and in the crystals aPP dimers are cross-linked in the lattice by zinc ions. Circular dichroism studies show that the hydrophobic interactions between helices are maintained by the monomer in solution.

We have recently extended the resolution of the X-ray analysis to 0.98 Å. This ultra high resolution allows systematic study of distortions in the α -helix, of the organisation of water around the polypeptide, and the location of hydrogen atoms. These results have been correlated with information obtained from NMR solution studies in order to characterise further the dynamic behaviour of aPP. Preliminary results are also reported from crystallographic studies of aPP, the homologous pancreatic polypeptide isolated from bovine tissue.

171

ENERGY DIRECTED FORMATION OF STRUCTURAL FEATURES OF FIBROUS AND GLOBULAR PROTEINS. H.A. Scheraga, Baker Laboratory of Chemistry, Cornell University, Ithaca, New York, U.S.A.

The formation of the structural features of folded fibrous and globular proteins by energy minimization is illustrated, and the computed results are verified by experimental tests. Thus, the interactions leading to the screw sense (handedness of twist) of α -helices and β -sheets have been identified. The interactions leading to the observed (low-energy) packing modes of assemblies of α -helices, in homopolymers, copolymers, collagen-like poly(tripeptides), and a three-helical portion of myoglobin, have also been identified. Work is in progress to obtain minimum-energy structures of: assemblies of α -helices in bacterial rhodopsin, and packing of α -helices against β -sheets, of β -sheets against β -sheets, and of β - α - β structures. A molecular treatment of the helix-coil transition and a statistical mechanical treatment of the β -sheet-coil transition have been developed and applied to experimental data. Finally, the combination of a build-up procedure, distance constraints, and energy minimization is leading to native structures of open-chain and cyclic oligopeptides, and fibrous and globular proteins.

173

DYNAMICS OF BOVINE β -TRYPSIN-BPTI ASSOCIATION.
NON-EQUIVALENCE OF PROFLAVINE AND BENZAMIDINE BINDING SITES AT THE ENZYME ACTIVE CENTER.
E. Monagatti, M. Guarnieri, M. Bolognesi, P. Ascenzi and G. Amiconi, Inst. of Pharmaceutical Chemistry, Univ. of Ferrara; Inst. of Crystallography, Univ. of Pavia; Inst. of Chemistry, Univ. of Rome "La Sapienza"; Italy.

The reaction of bovine β -trypsin (trypsin) with the bovine basic pancreatic trypsin inhibitor (BPTI), is a multistage process. In fact, the apparent rates of the adduct formation determined by proflavine displacement are higher than those measured by the intrinsic optical density changes in the uv region and the latter are greater than those resulted by both benzamidine displacement and the loss of the enzymatic activity, which are identical. In spite of the competitive inhibition of trypsin by both benzamidine and proflavine, the two spectroscopic probes show very different displacement rates and mechanisms of interaction. In particular, BPTI binding to the enzyme involves a ternary proflavine:trypsin:BPTI transient, while, on the contrary, benzamidine displacement may be treated as a simple competition event. As a whole, the experimental evidence suggests that the two probes bind at non-coincident regions of the trypsin active center: benzamidine occupies the enzyme specificity pocket, while proflavine, not attracted by the negatively charged Asp189, interacts possibly with a subsite close to the catalytic triad of the enzyme (as suggested by its competitive inhibition). The realization that proflavine and benzamidine look at different aspects of the adduct formation improves the prospects of understanding of this multistage process by resolving it in discrete steps.

170

SINGLE RESIDUE MUTANTS REVEAL CHARACTERISTICS OF A FOLDING INTERMEDIATE IN β -LACTAMASE
R.H. Pain and S. Craig, Dept. Biochemistry, Univ. Newcastle upon Tyne, NE1 7RU, UK.

β -lactamase from *S.aureus* unfolds reversibly and shows a stable intermediate state, H. Urea gradient gel electrophoresis reveals a further transient state, I, which interconverts rapidly with state H but slowly with the native state, N. [Creighton, T.E. & Pain, R.H. (1980) J.Mol.Biol. 137, 431] State I is only slightly less compact than state N. By contrast, two mutant β -lactamases, P2(Thr40 to Ile) and P54(Asp148 to Asn) show fast refolding from state H by c.d. and by urea gradient gel electrophoresis. The folded state of these mutants show closely similar secondary structure to the wild type enzyme but less order in the tyrosine environment. Like the wild type enzyme they unfold reversibly to intermediate states indistinguishable from state H which in turn interconverts rapidly with the fully unfolded state. Differential sedimentation shows them to be slightly more expanded than the wild type enzyme although more compact than state H. We conclude that recovery of the active native state in the mutants is blocked at a state similar to I. This state has native-like secondary structure but is not quite as condensed as state N. This supports a folding model where folding units containing native-like secondary structure collapse to a compact pseudo globular state, which then reshuffles to exclude remaining trapped solvent and to gain the native state.

172 ORAL PRESENTATION

THE EFFECT OF SUBSTITUTION OF EVOLUTIONARILY INVARIANT RESIDUES OF CYTOCHROME c ON ENTHALPY-ENTROPY COMPENSATION IN FOLDING. E. Poerio, R. Taniuchi and M. Juillerat, NIH, Bethesda, MD USA and Univ. of Geneva, Geneva, Switzerland

Using a biologically active three-fragment complex system of horse cytochrome c containing heme fragment residues 1 to 25 (1-25)H and apofragments (28-38) and (39-104), it has been found that replacement of invariant Leu 32 with Ile, Val or Phe profoundly affects the binding force while substitution of variant Leu 35 with Ile has no significant effect (Juillerat and Taniuchi, (1983) Abstracts, 15th FEBS Meeting, Brussels, p. 214). In the present studies invariant Pro 30 of fragment (28-38) was replaced with glycine and invariant Gly 34 with serine or alanine by chemical synthesis. The thermodynamic values for dissociation from the complex of the previous and the present analogs were determined using equilibrium dialysis or reduction of the complex with ascorbate and van't Hoff plots. The results have indicated a) the enthalpy-entropy compensation in dissociation of (28-38) or the analogs is similar between the ferric and the ferrous complex, b) the degree of this enthalpy-entropy compensation dramatically decreases in replacement of invariant Pro 30, Leu 32 and Gly 34 while the effect of replacement of variant Leu 35 with Ile is small, c) the balance of the enthalpy-entropy compensation also decreases the magnitude of ΔG° in substitution of the invariant residues but keeps it essentially constant in replacement of variant Leu 35 with Ile. Further investigation suggests that substitution of the invariant residue would also influence thermodynamics of ligation of methionine 80 to the heme iron in the complex.

174

THERMAL ANALYSIS OF X-IRRADIATED DNA AND OTHER MACROMOLECULES
C.L. Greenstock, Medical Biophysics Branch, Atomic Energy of Canada Limited, Pinawa, Manitoba, Canada R0E 1L0.

Alterations in the structure and conformational integrity of DNA, phospholipids and other macromolecules in aqueous solution, arising from undetected chemical changes following irradiation, are being measured using thermal analysis. These conformational changes also alter the thermal sensitivity of irradiated macromolecules. The thermal denaturation of DNA and other macromolecules is being studied by absorbance spectroscopy, differential scanning calorimetry and melting point analysis. The unwinding or 'melting' temperature for the thermal denaturation of DNA irradiated in aqueous solution, as monitored spectrophotometrically using the hyperchromic effect, shows a linear decrease with dose of $\sim 0.1^\circ\text{C}/\text{Gy}$. The stabilizing conditions of high-salt protect DNA against both radiation-induced and thermal denaturation.

Changes in the melting point of macromolecules following irradiation also reflect their structural integrity and conformational changes. Phospholipids and nucleic acids have higher melting points after irradiation, possibly because of free-radical induced cross-linking. Phospholipids with saturated and unsaturated fatty acids, exhibit a two-component melting point profile, the lower-temperature transition being the most radiosensitive. DNA extracted from aqueous solution irradiated at a concentration of 10 µg/ml shows a 10°C increase in melting point after a dose of 300 Gy. This type of structural alteration has a higher radiosensitivity than base damage, strand breaks or other chemical changes measured by conventional analytical techniques.

Monday 30 July Congress Centre-first floor. Posters 175-180

Posters on Folding, Dynamics and Solvation of Macromolecules

175

MERCURIAL-PROMOTED Zn^{2+} RELEASE FROM *E. COLI* ASPARTATE TRANSCARBAMOYLASE, A. Ginsburg, S.H. Reece, H.K. Schachman, and J.B. Hunt, Nat. Heart, Lung & Blood Inst., Nat. Inst. Health, Bethesda, MD, U.S.A.

The release of Zn^{2+} from aspartate transcarbamoylase (ATCase; cgr6) upon challenge by p-hydroxymercuriphenylsulfonate (PHPS) has been studied using the sensitive, high-affinity metallochromic indicator 4-(2-pyridylazo)resorcinol at pH 7.0. When the -SH group of each c chain is protected, 1 Zn^{2+} is released for every 4 eq of PHPS added to ATCase during titration of the 24 -SH groups of r chains. Moreover the release of Zn^{2+} is a linear function of PHPS added, indicating that the rate-limiting step in Zn^{2+} release is mercurial attack on the first of the 4 -SH groups bonded tetrahedrally to Zn^{2+} near c/r contacts. Dissociation of ATCase is linked to Zn^{2+} release and mercaptide bond formation; e.g., upon addition of 4 eq of PHPS in the absence of phosphate, 1/6th of ATCase is dissociated to c3 and r2 subunits at ~83% of the rate of Zn^{2+} release. Up to 4 eq of PHPS/ATCase, the release of Zn^{2+} is first-order in [PHPS] and is virtually independent of [ATCase] with an activation energy (E_a) of 75 kJ/mol. At large excesses of PHPS, stopped-flow traces show a lag period followed by pseudo-first-order release of Zn^{2+} from ATCase and the reaction order in [PHPS] = ~1.3. Under these conditions, PHPS has a chaotropic effect on ATCase and E_a is lower. A participation of nonthiol protein groups of ATCase in mercurial binding is suggested by kinetic data. Furthermore, mercurial-promoted Zn^{2+} release is > 3000-fold faster from r2 subunits than from ATCase.

177

IMINO- AND AMINO-PROTON EXCHANGE WITH 1H_2O : QUANTITATIVE ANALYSIS OF 2D-EXCHANGE NMR SPECTRA OF DNA FRAGMENTS IN 1H_2O

R.M. Scheek, R. Boelens, M. Koning, K. Dijkstra and R. Kaptein, Department of Physical Chemistry, University of Groningen, The Netherlands

Two-dimensional exchange NMR spectroscopy at 360 MHz was used to study the imino- and amino-protons of small DNA fragments in 1H_2O . The experiment consists of two non-selective 90° rf pulses, separated by the variable time t_1 , and followed by a short (5 ms) homogeneity-spoil pulse at the beginning of the mixing period τ_m (15-50 ms). For detection a selective 45° - 45° pulse sequence was used to suppress the large 1H_2O signal. NOE cross peaks involving imino- and amino-protons provide a systematic way to obtain the resonance assignments of these protons. Their rates of exchange with 1H_2O were determined by measuring the initial build-up rates of the corresponding exchange cross peaks at the 1H_2O frequency. Activation energies were estimated for AT and GC imino-proton exchange with 1H_2O in a 8 bp DNA fragment. The method compares favourably with those based on relaxation time measurements. The effect of lac-repressor head-piece binding on the imino-proton exchange in a 14 bp lac operator fragment was studied by this technique.

179

HYDROGEN ISOTOPE EXCHANGE AT PROTEIN SURFACES

E. Iuchsen and C.K. Woodward, Univ. of Minnesota, Dept. of Biochem., 1479 Gortner Ave., St. Paul, MN 55108, U.S.A.

Recently, proton exchange (HX) kinetics at varying pH were measured for 25 assigned peptide CONH groups at the molecular surface of BPII. In disagreement with traditional HX theory which predicts equal structural shielding for acid and base catalyzed HX, it was found that while base catalyzed HX is correlated with accessibility to water of the NH, acid catalyzed HX is rather correlated with accessibility of the carbonyl O. For many of the 25 CONH's, NH is exposed to water and the carbonyl O is buried. Consequently, for these acid catalyzed HX is relatively more shielded than base catalyzed HX resulting in rate minima at lower pH (occasionally pH < 1) than for fully solvated model compounds (pH_{min} ~ 3.5). These findings suggest a chemical mechanism for the acid catalyzed HX that involves a rate limiting carbonyl O protonation step.

The present experiments are aimed at identifying CONH groups with pH_{min} > 3. Resonances for these are resolved in 100 MHz PMR spectra of BPII samples prepared by a selective 1H labeling procedure. Rates of HX are measured in D_2O at 25° (peak intensity vs. time). In general, simple first order catalysis by D^+ and OH^- is observed. The pH_{min}'s are as high as 4.4 (for Lys15-CONH-Ala16). Also, a previously amide proton (in the Asp43 side chain) has pH_{min} ~ 4.8. For all peptide CONH's with high pH_{min} the carbonyl ^{18}O is exposed to water and NH is buried. These data strongly support an O-protonation mechanism.

176

TWO DIMENSIONAL FOURIER TRANSFORM NUCLEAR MAGNETIC RESONANCE STUDIES OF RIBOSOMAL PROTEIN E-L30.

F.J.M. van de Ven, S.H. de Bruin and C.W. Hilbers, Department of Biophysical Chemistry, University of Nijmegen, Toernooiveld, 6525 ED Nijmegen, The Netherlands.

2D-FT 1H NMR methods have been used to investigate the structure in solution of ribosomal protein L30 isolated from *E. coli* MRE 600. The resonances of protons of glycines, serines, alanines, valines, isoleucines, threonines, histidines, phenylalanine 52 and asparagine 48 could be identified using Correlated Spectroscopy (COSY), Nuclear Overhauser Enhancement Spectroscopy (NOESY), J-resolved spectroscopy, Relayed Coherence transfer and Double Quantum Spectroscopy. Making use of nuclear Overhauser Effects occurring between resonances of peptide-bond amide protons and protons of residues preceding and/or following the peptide-bond it was possible to determine nearest neighbour relationships between amino acid residues. By comparing these neighbour-pairs with the known amino acid sequence of the protein sequential resonance assignments became available for many residues. Furthermore the occurrence of α -helices and β -sheets in the molecule could be established. Finally, NOESY spectra were searched for cross-peaks indicating interresidue interactions. Several interactions were found between residues which were far apart in the sequence; these allowed the elucidation of elements of the tertiary structure of the protein. Especially antiparallel β -strands gave rise to several outstanding spectral features.

178

QUANTITATIVE ANALYSIS OF THE NUCLEAR OVERHAUSER EFFECT IN BIOLOGICAL MACROMOLECULES BY 2D 1H -NMR R. Boelens, R.M. Scheek and R. Kaptein, Laboratory for Physical Chemistry, University of Groningen, Nijenborgh 16, 9747 AG Groningen, The Netherlands

One of the most useful parameters for structure analysis of biological macromolecules by NMR is the proton-proton NOE effect. In 2D-NOE spectra separate cross peaks can be assigned to distinct pairs of protons. 2D-integration of the pure-absorption cross peaks in interlevel experiments with different mixing times τ_m gives the initial build-up rate of the NOE intensity for a large number of proton pairs. For large rigid molecules this rate is directly related to the distance r_{ij} between these protons: $k_{ij} = \text{constant}/r_{ij}^6$. The constant (depending on the rotation correlation time of the molecule) is calibrated by measuring cross peaks of protons with fixed distances. If protons are coupled by a through-bond-exchange interaction, zero quantum coherences can be separated from the NOE cross peaks by incrementing the mixing time as proposed by Macura et al. (J. Mag. Res. 46 (1982) 269). The method was applied to small 7-14 bp DNA fragments and initial rates were estimated with mixing times < 100 ms. The fixed cytidine H5-H6 distance of 0.24 nm was used as calibration and found to be constant within 0.005 nm for cytidines at different positions in the fragments, indicating their rigidity. Distances between a large number of proton pairs (intra- and internucleotide) indicate that the fragments are mainly in a B-DNA conformation. Accurate distances were obtained only < 0.3 nm, while at greater distances second order NOE's contributed considerably.

180

ANHARMONICITY AND PROTEIN REFINEMENT

J. Kurian, M. Varplus*, R.M. Levy* and G.A. Petsko*, Departments of Chemistry, Massachusetts Inst. of Technology, Cambridge, MA02139*, Harvard University, Cambridge MA02138, Rutgers University, New Brunswick NJ08903, U.S.A.

Molecular Dynamics (M.D.) simulations are used to study the effects of anharmonicity and anisotropy of the atomic dynamics on crystallographic protein refinement. Time-averaged X-Ray diffraction intensities, calculated from M.D. simulations of myoglobin, are input to a least-squares, reciprocal-space refinement program, PROLSQ (Konert & Hendrickson) the resulting structure and temperature-factors are compared with those calculated directly from the simulation and the sources of error are analysed. The model used to calculate intensities neglects correlations in the dynamics and hence the diffracted intensity is given by the square of the Fourier transform of the time-averaged electron density in a unit cell. We find that many atoms have multiple peaks in their probability distribution functions and these atoms have errors on the order of 30-80% in the refined temperature factors and 0.5-2.0 Å in their refined positions. This is due to the refinement fitting one or two of the peaks in the distribution and neglecting the rest. For many of the residues that exhibit this sort of behaviour the use of stereochemical restraints is inconsistent with the average dynamics structure. Finally, we have examined experimental difference-fourier maps for myoglobin at 300K and 80K and find evidence for many of the alternate side-chain conformations predicted by the simulations.

Monday 30 July Congress Centre-first floor. Posters 181-186

Posters on Folding, Dynamics and Solvation of Macromolecules

181

STUDY OF THE INFLUENCE OF pH ON THE PAPAIN-KINETICS.

T. Sasmito, J. Demeester and A. Lauwers, State University of Gent, Laboratorium voor Algemene Biochemie en Fysische Farmacie, Wolterslaan 16, B-9000 Gent, Belgium.

The influence of Dimethylsulfoxide (DMSO) on the papain catalysed hydrolysis of the small synthetic substrate Nα-Benzoylarginine-p-nitroanilide (BAPA) has been investigated. BAPA has two stereoisomeric forms (D and L). Its solubility is greatly enhanced by adding DMSO, a solvent with only small influences on dielectric constant of the solutions.

By the kinetics investigations, it could be shown that the hydrolysis of the substrate L-BAPA by papain is competitively inhibited by D-BAPA and non-competitively by DMSO and that both inhibitors act independently. DMSO also effects the ionizations of the amino acids in the active site of papain. Indeed, from the pH influences on the reaction rates could be concluded that the effect of DMSO is strongly dependent on the state of papain, i.e. if the enzyme is bound or not bound to the L-BAPA-molecule. The following empirical equations were optimised for the pH optima for the free enzyme and the enzyme-substrate complex respectively:

$\text{pH}_{\text{opt},E} = 7.41 + 0.141(\text{DMSO})$ and $\text{pH}_{\text{opt},ES} = 7.23 + 0.280(\text{DMSO})$

At the common intersection point, $(\text{DMSO}) = 1.25\text{M}$ and $\text{pH} = 7.58$, pH optimum will not be changed by variations in substrate and DMSO concentrations.

182

ESTIMATION OF EFFECTIVE INTER-RESIDUE CONTACT ENERGIES FROM PROTEIN CRYSTAL STRUCTURES

Sanzo Miyazawa and Robert L. Jernigan, Building 10, Room 4B-56, Laboratory of Mathematical Biology, DCBD, MCI, National Institutes of Health, Bethesda, MD 20205 USA

Effective inter-residue contact energies for proteins in solution are estimated from the numbers of residue-residue contacts observed in crystal structures of globular proteins. Employing a lattice model, each residue of a protein is assumed to occupy a site in a lattice, and vacant sites are regarded to be occupied by an effective solvent molecule whose size is equal to the average size of a residue. A limit to the size of the system in terms of the number of lattice sites or the number of effective solvent molecules, is imposed, and the system is regarded as the mixture of unconnected residues and effective solvent molecules. The quasi-chemical approximation, that contact pair formation resembles a chemical reaction, is applied to this system to relate the statistical averages of the numbers of contacts to the contact energies. The estimated values of contact energies have reasonable residue-type dependences, reflecting residue distributions in protein crystals; non-polar-residue-in and polar-residue-out are seen as well as the segregation of those residue groups. In addition, there is a linear relationship between the average contact energies for non-polar residues and their hydrophobicities reported by Nozaki and Tanford.

183

184

185

186

Monday 30 July Congress Centre-first floor. Posters 187-192

Posters on Folding, Dynamics and Solvation of Macromolecules

187

188

189

190

191

192

Monday 30 July Congress Centre-first floor. Posters 193-198

Posters on Folding, Dynamics and Solvation of Macromolecules

193

194

195

196

197

198

Monday 30 July Congress Centre-first floor. Posters 199-204

Posters on Electrostatic Effects in Protein Function

199

ELECTROSTATIC EFFECTS ON HYDROGEN EXCHANGE IN PROTEINS.
M. Delepierre, C.M. Dobson, M. Karplus, F.M. Poulsen,
S.J. States and R.E. Wedin.
Department of Chemistry, Harvard University,
Cambridge, Mass. USA.
Inorganic Chemistry laboratory, Oxford University,
Oxford, England.

The assignments of many amides and tryptophan hydrogens in the proton NMR spectrum of lysozyme have been made. Using these, the rate of exchange of the individual hydrogen have been determined under a variety of conditions. The results demonstrate that the pH curve for each hydrogen is unique and is different from the pH curve for simple compounds. Under certain conditions and particularly for the more exposed hydrogens the pH dependences correlate well with calculations involving electrostatic effects. This implies that the exchange takes place from a state of the protein closely similar to that of the native protein and that local fluctuations provide the mechanism for exchange. That the behaviour under other conditions cannot be correlated with the electrostatic consideration, is interpreted to be a consequence of exchange taking place under these conditions from a state of the protein different from the native state. The observation that local electrostatic effects can lead to unique pH dependencies for hydrogen exchange rates suggest that hydrogen exchange studies may increase the understanding of electrostatic interaction in proteins, a subject of direct relevance to protein stability and enzyme catalysis.

201

A NUMERICAL METHOD FOR STUDYING PROTEIN ELECTROSTATICS
J. Warwicker, Department of Biochemistry, Bristol
University, Bristol, UK.

A review has been made of the methods available for calculating electrostatic interactions in solutions of bio-molecules. The continuum electrostatic problem with irregular boundaries has been solved, using the method of Finite Differences. This numerical solution technique has been applied to the α -helix dipole charge arrays of several enzymes of alternating α/β structure. It was found that large positive potentials from the helix dipoles exist in the active site cleft regions, where negatively charged substrates are bound.

The continuum electrostatic method has been extended to include regions of solvent that saturate in the high electric fields adjacent to the polar side-chain charges of a protein, thus giving dielectric values less than bulk. In addition, counter-ion concentrations responding to the Boltzmann occupation factor at high electric potential, rather than the linearised Debye-Huckel term, are accounted for. Calculations have been performed on the full helix dipole, polar side-chain charge array of the glycolytic enzyme phosphoglycerate mutase, for a number of different solvent/counter-ion models. A positive potential field, of significant size with respect to kT/e , is found in the enzyme active site cleft for all of these calculations. It is suggested that the long-range attractive field between enzyme and substrate counter-acts desolvation forces.

203

VISUALIZATION OF ENZYMES RECOGNIZING ELECTRO-
STATICALLY THEIR SUBSTRATES, INHIBITORS AND CO-
FACTORS H. Nakamura, Dept. Appl. Phys., Fac. Engineering,
Univ. Tokyo, Hongo, Tokyo, JAPAN.

Electrostatic potentials of several enzymes and their guest molecules of substrates, inhibitors and/or co-factors (DFR-NADPH-MTX, LDH-NAD, GPD-NAD, FXN-FMN and LY2-NAM-NAG-NAM) were calculated individually, and illustrated as colour codes on their tertiary structures using a raster computer graphic technique. Two kinds of potential surfaces were illustrated; (1) a host potential on a guest molecule (H-on-G potential: electrostatic potential due to the host enzyme on the van der Waals surface of the guest molecule) and (2) a guest potential on a guest molecule (G-on-G potential: the potential due to the guest molecule on the surface of the guest molecule itself). The potentials were calculated using Mulliken net charges, which were given by *ab-initio* MO calculations (Gaussian 70), and the molecular graphic program TERAS was used for the illustration. It was found that each H-on-G potential has in the most cases reversed characteristics of the corresponding G-on-G potential, indicating the electrostatic force is essential in the recognition of each guest molecule. Previously, such mutual complementarity had been qualitatively described as the chemical terms of salt bridges and hydrogen bonds, but now it is quantitatively understood as one of the physical properties of the biomolecules.

200

MODELING THE MAGNETIC CIRCULAR DICHROISM OF LOW SYMMETRY
CUPRIC SITES B.S. Gerstman and A.S. Brill, Dept. of Physics,
Univ. of Virginia, Charlottesville, Virginia, U.S.A.

We describe the use of hybrid atomic orbital models of the cupric ion in low symmetry sites for the calculation of MCD spectra. This simple model was originally used to explain other spectroscopic data from (cupric) blue proteins. Two fold spin degeneracy of the ground state and spin-orbit mixing of excited electronic states produce C-terms that dominate the MCD spectra below 100K. Such effects have been observed experimentally in a blue copper protein and in cytochrome oxidase (C. Greenwood, B. Hill, D. Barber, D. Eglinton, A. Thomson, Biochem. J., 215, 1983).

Excited state energies not only determine the positioning of MCD bands but also influence strengths. If spin-orbit coupling of excited states with the ground state is neglected, the sum of C-values over all transitions is zero. With the assumption that vibrational intensities for each transition are equal, C-values summing to zero would result in MCD spectra that are nearly balanced with respect to the baseline, in contrast to experimental data. However, when admixing of the ground state with excited states by spin-orbit coupling is included, the sum of C-values is no longer zero and MCD spectra become imbalanced. We report on the formulation of these effects and on factors important to the imbalancing. Spectra, simulated with parameters of the model consistent with other data (absorption, CD, EPR), are presented that are in good qualitative agreement with experimental MCD data.

202

CALCULATIONS OF CHANGES IN REDOX POTENTIALS: CYTOCHROME C551
N.K. Rogers, G.R. Moore and M.J.E. Sternberg, Laboratory of
Molecular Biophysics, Department of Zoology, South Parks
Road, Oxford and Inorganic Chemistry Laboratory, South Parks
Road, Oxford.

An equal mixture of oxidised and reduced Cytochrome C551 experiences a change in the potential of the haem iron, when one of the propionates attached to the haem is ionised. This process has been followed by Moore (1983) and the change is 65mV, which corresponds to an effective dielectric between the propionate and the iron of 27. It has been possible to use the algorithm of Warwicker and Watson (1982) to calculate the change in the potential at the haem iron arising from the change in ionisation of the propionate. This gives the extra work required to oxidise or reduce the iron. Arginine 47 is in very close contact with the propionate and is implicated in the ionisation mechanism. The effective dielectric that we calculate between the propionate and the iron is 21. In comparison with other commonly used dielectric models the agreement is very good.

References:

Moore G.R. FEBS Letters, 1983, 161, 171-175.
Warwicker J. and Watson H.C. J. Mol. Biol., 1982, 151, 671-679.

204

CHARGE MEASUREMENTS ON MYOSIN THREADS

P.H. Cooke, E.M. Bartels, G.F. Elliott, R.A. Hughes, and
K. Jennison, Open University Research Unit, Oxford, U.K..

The importance of ion-binding effects in muscle contraction is exemplified by the role of divalent cations in activation processes. Donnan potentials, measured with KCl-filled microelectrodes, have revealed large changes in protein charge associated with relaxation, rigor and contraction in the A and I bands of glycerinated muscle. To clarify the mechanism of charge changes, Donnan potentials were measured from extruded threads of gels containing purified rabbit muscle myosin and the rod subfragment. The threads simulate some of the essential structural features of the A band in muscle as determined by electron microscopy and X-ray diffraction. The molecular charge changes of myosin and myosin rod in threads are qualitatively similar to the pattern of charge changes in the A band: fixed charge varies with ionic strength of the solution phase and with [ATP]. In "relaxing" solutions containing 2.5 mM ATP, the fixed charge on myosin and myosin rod decreases by 20-40% at ionic strengths from 0.03 to 0.12 M, and the volume of myosin threads increases by up to 40%. The results indicate that significant changes in net electrical charge on myosin and rod in gels are effected by solutions which regulate the functional state of muscle.

Monday 30 July Congress Centre-first floor. Posters 205-210

Posters on Electrostatic Effects in Protein Function

205

IONIC STRENGTH DEPENDENT POSITIVE COOPERATIVITY BETWEEN CALCIUM BINDING SITES IN CALMODULIN: TERBIUM LUMINESCENCE
R. MOHAN, Max Planck Institute for Biophysical Chemistry, Göttingen, West-Germany

Tb³⁺ luminescence titration of Ca²⁺-free brush border calmodulin (1x10⁻⁶ M) shows specific binding of two Tb³⁺ ions to high affinity sites III and IV. At neutral pH and low ionic strengths (I = 0.003 to 0.13) the two sites are equivalent and independent while at physiological and higher ionic strengths the binding, with an asymmetric sigmoidal curve, is positive cooperative of a sequential nature. The origin for the conformational mobility is a Debye type shielded electrostatic term as assessed by effects of ionic strength on binding coefficients.

The conformational changes upon cooperative binding is gleaned from the intensity and gem (dissymetry) values of circularly polarized luminescence (CPL) part of the total luminescence (TL) of Tb³⁺. A comparison of CPL on Tb³⁺ titration against calmodulin at low and high ionic strengths shows that gem is a constant at low ionic strengths while at high ionic strengths, upon cooperative binding of the second Tb³⁺ ion there is no additional CPL, although the Tb³⁺ TL is enhanced. A detailed analysis of Tb³⁺ luminescence titration curves shows that both tyrosines (TYR 99 and TYR 138) and both bound Tb³⁺ ions are involved in the energy transfer process of sensitized Tb³⁺ luminescence at all the ionic strength used.

207 ORAL PRESENTATION

HOW TO CALCULATE ELECTROSTATIC ENERGIES IN PROTEINS
S.T. Russell, A.K. Churg and A. Warshel, Dept. of Chemistry, University of Southern California 90089-0482.

Various approaches for electrostatic calculations in proteins are analysed and compared. An examination of macroscopic approaches demonstrates that the model of Tanford and Kirkwood, which treats proteins as non polar spheres, is inconsistent with experimental facts. It is also shown that a recent modification of the Tanford-Kirkwood model, using solvent accessibility is inconsistent with its own assumptions and with basic electrostatic theory. The examination of microscopic models is concentrated on calculations of intrinsic pK_a's in BPTI using the protein structure. It is shown that calculations that use only the protein permanent dipoles can underestimate the stabilization of charged groups by up to 50 kcal/mol. It is then shown that only calculations that include the permanent and induced dipoles of the protein and the surrounding water molecules can give reasonable results. An extremely effective model that includes all these factors is described. The model is based on a refinement of a previous microscopic dielectric approach¹. The protein induced dipoles are simulated by a self consistent iterative approach and the surrounding water molecules are simulated by effective self consistent average dipoles (with average orientations determined from molecular dynamics simulations). This model is shown to provide reliable electrostatic energies for ions and ion pairs in proteins.

1) A. Warshel, Acc. Chem. Res. 14, 284 (1981).

209

STRUCTURAL AND SOLVENT EFFECTS ON THE REACTIVITY OF OXYGEN WITH 2-OXAZOLIN-5-ONES DERIVED FROM ALPHA AMINO ACIDS. C.A. Chusqui,* H. Rodriguez,**, J. Merritt,* A. Marquez,** and L. Zagal,**. *Medical Biophysics Branch, Atomic Energy of Canada Limited Research Company, Whiteshell Nuclear Research Establishment, Pinawa, MB, Canada, R0E 1L0, and **Departamento de Ciencias Farmacéuticas, Fac. Ciencias Básicas y Farmacéuticas, Univ. of Chile, Santiago, Chile.

Oxazolinones are produced by dehydration of N-acylamino acids. Their reactivity toward oxygen is critically dependent on structural factors as well as solvent effects. For instance, the substitution at position 4 of the heterocyclic ring (originally the alpha carbon in the amino acid) is of primary importance since a reaction takes place only if a hydrogen is present at that position. The reaction proceeds through tautomeric forms in which the hydrogen shifts to the carbonyl and imino groups in the ring, a process that is greatly influenced by solvent characteristics. The type of products formed is also dependent on structural characteristics of the substituents that control the reaction to produce oxidation products or dimerization products. In the present work, the reactions of oxygen with 2-phenyl-4-ethyl-2-oxazolin-5-one (I), 2,4-diphenyl-2-oxazolin-5-one (II) and 2-p-methoxyphenyl-4-phenyl-2-oxazolin-5-one (III) in dimethylsulfoxide (DMSO) dimethylformamide (DMF) and tetrahydrofuran (THF) were analyzed. The results show that, while (I) yielded mainly an imide derivative and CO₂, oxazolinones II and III formed dimeric products. It was also observed that the rate of reaction depends on the polarity of the solvent.

206

INVESTIGATION OF THE DIELECTRIC PROPERTIES OF HUMAN HEMOGLOBIN DURING OXYGENATION. S. Takashima, Department of Bioengineering, D-3, University of Pennsylvania, Philadelphia, PA, USA

The dielectric properties of human hemoglobin were reinvestigated at various stages of oxygenation. The measurements were carried out between 10 KHz and 5 MHz using highly purified and defoamed hemoglobin samples. The input voltages were kept as low as possible. The dielectric increments measured at various oxygen partial pressures show two maxima at 2.5 mmHg and 20 mmHg respectively and a minimum at 7.5 mmHg. This result is in agreement with those obtained by Takashima and Luury years ago. The dielectric dispersion curve of partially oxygenated hemoglobin consists of two clearly separated relaxation curves. One of these, which is observed around 1 MHz is identical with that of fully oxygenated hemoglobin. The second curve is found around 30-40 KHz. In view of the very different time constant of this additional dispersion, it is inferred that the origin of this relaxation may be a charge transfer between subunits rather than conformation changes of hemoglobin molecules. These observations indicate that intermediate forms with a highly asymmetric charge distribution would appear during the oxygenation of hemoglobin. The author is partially supported by ONR N00014-82-K-0321.

208 ORAL PRESENTATION

CHARGE DISTRIBUTIONS IN PROTEINS
D.J. Barlow and J.M. Thornton, Department of Crystallography, Birkbeck College, London, UK.

The charged group distributions for 32 proteins of known 3D structure have been analysed. To assess how symmetrically the charged groups are arranged, charge polarity vectors were calculated, considering only the positions of charges and neglecting their actual sign. The results show that most proteins have symmetric or random distributions of charged groups; very few have asymmetric distributions. Electric dipole moments were also calculated for the proteins, using both formal and partial charges. The analysis indicates that for the majority of proteins: (1) the permanent charge distribution accounts for almost all of the dipole. (2) peptide dipoles contribute little to the overall dipole (except in the case of the α/β proteins) and (3) the dipoles are small considering the size of the molecules. Preliminary studies have been made on several specific proteins, to relate the magnitude and direction of the electric dipoles to the molecules' function. To assist in this work we have developed an interactive projection algorithm for use on a colour computer graphics system. The Hammer projection maps produced by the program, allow the entire charged group distribution for a protein to be shown on a single figure, so that clusters and interaction sites are easily identified.

210

CHARGE CALCULATIONS IN MOLECULAR MECHANICS
B.D. Hudson and R.J. Abraham, The Robert Robinson Laboratories, The University of Liverpool, Liverpool L69 3BX and W.A. Thomas, Roche Products Ltd., P.O. Box 8, Welwyn Garden City, Herts AL7 3AY

A previously published scheme of estimating atomic charges in haloalkanes, based on atomic electronegativities and polarisabilities, has been extended to include all common functional groups in proteins. This is done by the explicit inclusion of the effects of mesomeric charge transference. Good agreement between the observed and calculated dipole moments for a range of model compounds has been found. Charged species can be treated by 1) the addition of integral charges to the relevant atoms and 2) a dependence of the atomic electronegativity with atomic charge. The scheme predicts a gradual spreading out of the excess charge in contrast to the CNDO picture of charge alternation. For the zwitterionic forms of Glycine, and α and β alanine, the scheme gives calculated dipole moments in good agreement with observed values in H₂O solution. The full set of charges for all the charged and uncharged amino acid residues should be of use in molecular mechanics calculations of enzyme systems.

Monday 30 July Congress Centre-first floor. Posters 211-216

Posters on Electrostatic Effects in Protein Function

211

THEORETICAL STUDIES OF CATALYTIC PATHWAYS.

F. Sussman*, J. Moulton and M.N.G. James*, Department of Crystallography, Birkbeck College, London W1C, UK*, and Biochemistry Department, University of Alberta, Edmonton, Alberta, Canada*.

A semi-classical method which in principle can include the influence of all the residues of an enzyme onto the catalytic pathway has been applied to the study of serine proteases. The accuracy and scope of such a method was checked in small model systems. We then used this method to test hypothesis proposed from X-ray crystallographic and other biophysical as well as biochemical experiments. The test system to which we applied our methodology was a well characterised serine protease, *Protease A* from streptomyces *Griseus* (SGPA). Specifically we were interested to understand the role of the triad of residues that participate directly into the enzymatic process: Aspartic acid, Histidine and Serine, and how the bulk of the protein influences these residues so as to lower the energetic barriers. This program was carried out by analysing the resulting energies and electron-density distributions.

213

MONTE CARLO STUDY OF LIPID BILAYER PACKING CHARACTERISTICS, USING THE DISTRIBUTED ARRAY PROCESSOR. T.J.Coe, A.J.G.Hay, D.Melville, H.L.Scott Physics Dept., University of Southampton, SO9 5NH, U.K.

Radial distribution functions for pure lipid and lipid-protein systems are obtained, assuming both systems to be hard disc fluids. This approach is motivated by Scott's Statistical Mechanical Theory of Bilayer Membranes, which successfully uses the molecular projections onto the Bilayer Plane as the interacting species(1). In this first paper, we assume circular projections of different radius for the lipids and proteins. The packing of this purely random system is examined in detail. We are extending our investigation to include a) ellipsoidal lipid molecular projections b) phenomenological lipid-protein and protein-protein interactions. The computational aspects of this calculation are somewhat novel. By mapping real space onto the processor array, and utilizing the inherent parallelism of this machine we are able to include large numbers of molecules. This allows us to use physiologically relevant protein concentrations, while still maintaining good protein statistics.

(1) Scott H.L. (1981) *Biochim. Biophys. Acta* 643, 161-167

215

ELECTROSTATIC INTERACTIONS IN THE BINDING OF METHOTREXATE AND TRIMETHOPRIM ANALOGUES TO DIHYDROFOLATE REDUCTASE

A. A. Bevan, B. Birdsall, G.C.K. Roberts, National Institute for Medical Research, Mill Hill, London, U.K., H.T.A. Cheung, University of Sydney, and J. Kompa, Hoffmann-La Roche, Basle.

We have used ¹H, ¹³C and ¹⁵N nmr to study electrostatic interactions between antifolate drugs and their 'target', dihydrofolate reductase. Trimethoprim is shown to be protonated on N1 when bound to the enzyme, and the 2,4-diaminopyrimidine ring binds in the same way as the corresponding part of methotrexate, forming a hydrogen bond from N1 to the carboxylate of Asp 26. The dynamics of this hydrogen bond were studied by measurements of the exchange of the N1-H with solvent.

The γ-carboxylate of methotrexate forms an ion-pair with His 28, and the accompanying change in pK of the histidine has been measured by nmr. Studies of the binding of methotrexate amides lead to estimates of the energetic contribution of this interaction and that between the γ-carboxylate and Arg 57.

Computer graphics methods, based on the crystal structure determined by Matthews et al, have been used to design a trimethoprim analogue having a dicarboxylic acid substituent intended to bind to Arg 57 and His 26. Nmr studies indicate that this compound does bind as predicted, and it is found to bind 1000-fold more tightly than the parent compound.

212

COMPUTER SIMULATION OF TRIMETHOPRIM - DHFR INTERACTION

C.R. Beddell, Wellcome Research Laboratories, Langley Court, Beckenham, Kent, England.

The enzyme dihydrofolate reductase (DHFR) is a target for certain anticancer, antiparasitic and antibacterial drugs. DHFRs from vertebrate and bacterial sources are homologous and also similar in three dimensional architecture.

Nevertheless, the antibacterial drug trimethoprim can bind to bacterial enzyme about 3000 times more tightly than to vertebrate enzyme. It is established by crystallography and NMR that trimethoprim adopts basically two different types of conformation when bound, according to enzyme type. It seemed appropriate to test whether a simple molecular mechanics simulation of the interaction would reproduce this observation. The simulation used the computer program ENERGY (North, A.C.T., University of Leeds) and the general procedures of Pottier, E.A. (D.Phil. thesis (1983), University of Leeds) to estimate electrostatic and van der Waals interactions. Crystallographic atomic coordinates for trimethoprim complexed with (1) *E. coli* DHFR, (2) *E. coli* DHFR and NADPH (Chapman J.N., Beckenham), (3) hen DHFR and NADPH (Matthews, D.A., La Jolla), (4) L1210 (mouse) DHFR and NADPH (Stammers D.K., Beckenham) were used to define the four binding sites containing comparable regions of enzyme structure. In each site, trimethoprim was positioned in each type of conformation, and a minimum potential energy of binding was obtained by energy minimisation. For each of the four binding sites, the trimethoprim conformer calculated to bind with minimum energy was of the crystallographically observed type.

214

ON THE PRIMARY SULPHATE AND PHOSPHATE BINDING SITES IN YEAST PHOSPHOGLYCERATE KINASE M Larsson-Rafniewicz and M M Khamis, Dept. Chem. & Mol. Biol., Swedish Univ. Agric. Sci., Uppsala, and B Schierbeck, Dept. Biochem. & Biophys., Chalmers Techn. Highschool, Göteborg, SWEDEN.

The phosphoglycerate kinase reaction with MgATP and 3-P-glycerate as substrates can kinetically be described by a random equilibrium mechanism. A ping-pong mechanism has been suggested as an alternative (phosphoryl intermediate) but in all cases the due results have been shown to arise from artefacts. Many anions activate at lower and inhibit at higher concentrations. Most pronounced effects are obtained by the sulphate ion. Detailed studies reveal that the sulphate ion as an activator does not affect substrate binding. As an inhibitor it competes with both the substrates. More recent studies on phosphate effects reveal that even if sulphate and phosphate ions are similar they show quite different inhibition patterns. Phosphate is strictly noncompetitive inhibitor of MgATP and mixed noncompetitive and competitive inhibitor of 3-P-glycerate. Still a Webb and Theorell-Yonetani plot indicate exclusive binding of the inhibiting sulphate and phosphate ions to the enzyme. If the results reflect a part of the "trigger mechanism" suggested by Watson et al (1) is worth while to take into consideration. An extended positive center in the enzyme exists close to the site of the 3-phosphate of a presumed D-triose when binding to the enzyme (1). Triphosphosphate is strictly competitive with 3-P-glycerate and a mixed inhibitor with Mg ATP.

1/. EMBO J. (1982) 1, 1635.

216

Posters on Viruses

217

STRUCTURAL STUDIES OF NATIVE ADENOVIRUS AND ASSEMBLY MUTANTS

C. Berthet-Colominas¹, C. Devaux^{1,2}, B. Jacrot¹ and P.A. Timmins²; EMBL, Grenoble¹, INSERM Lille² and Institut Laue-Langevin, Grenoble¹, France.

X-ray and neutron scattering techniques have been used to investigate the distribution of protein and DNA in adenovirus. The neutron scattering studies have led to a model describing the radial distribution of DNA and protein in the virus as well as determining the molecular weight. Complementary neutron experiments on the thermosensitive mutant ts112, which lacks specific proteins and most of the DNA, allow us to determine the radial location of these missing components in the native particle. The X-ray studies have given details of the packing of the major protein (the hexon) in the viral coat and indicate a rather looser packing than previously believed. A broad reflection centered at $1/29 \text{ \AA}^{-1}$ is not explained by the protein packing but staining with Hg_2Cl_2 enhances this reflection, suggesting that it is due to the DNA packing in the nucleo-protein core. This hypothesis is confirmed by the absence of this reflection in the mutant ts112.

219

ELECTRON SPIN RESONANCE STUDIES ON THE LIPID BILAYER OF INFLUENZA VIRUS. P.J. Sizer, A. Miller, Department of Molecular Biophysics, & A. Watts, Department of Biochemistry, University of Oxford, U.K.

Synthetic fatty acids and phospholipids containing the nitroxide free-radical reporter group have been introduced into the lipid matrix of the influenza A virion. Electron spin resonance measurements have confirmed the bilayer structure proposed for the lipid of the virus. Incorporation of either a sterol or phospholipid spin-label analogue gives a two-component spectrum; one component indicating lipids undergoing slow-exchange with the bulk lipid. This result is thought to indicate that the annulus of lipid that surrounds the integral membrane proteins of the viral bilayer is relatively immobilized relative to the bulk lipid through lipid-protein interactions. Approximately 10% of the total lipid is immobilized, and if this is taken to be the average distribution of a typical lipid in the bilayer, a measurement of 11Å for the average hydrophobic radius of the protein may be estimated using the molar lipid to protein ratio obtained from neutron diffraction studies. When a fatty acid spin-label is introduced into the lipid bilayer, the proportion of lipid immobilized is about 40%. This may reflect a positive selection for fatty acids by the protein in its lipid annulus; the immobilization due to either non-covalent interactions or possibly covalent linkages as reported in other viruses.

221

ISOLATION OF A CYANOBACTERIAL MUTANT RESISTANT TO THE VIRUS N-11

A. Vaishampayan and Anupama Sahay, faculty of Science, University of Bihar, Muzaffarpur, India.

In the cyanobacterium *Nostoc muscorum* the occurrence of spontaneous as well as nitroguanine-mutants resistant to the virus N-11, has been reported by Padhy and Singh (1976, *Arch. Virol.*, 52, 85-90). We hereby report the isolation of another mutant of *N. muscorum* resistant to a typical virus which affects the vegetative cells as well as the nitrogen-fixing apparatus, i.e., heterocysts on solid medium at a temperature strictly above 32°C. The nature of this virus has been although not fully established yet it has been found to cause a very rapid lysis (within 12-16 h) of the cyanobacterial cells. Through ultra violet-irradiation, using a 'Phillips' germicidal lamp emitting mostly at 2537Å with a dose rate of approximately 90 ergs/mm²/sec at a distance of 7 inches from the lamp, a mutant of this host organism has been isolated which has been found 100% resistant to the virus in question (designated as N-11), even at high-temperatures ranging between 32 to 40°C. The frequencies of spontaneous and uv-induced mutations of this kind in *N. muscorum* have been found to be of the order of $2.88 \pm 0.12 \times 10^{-8}$ and $1.35 \pm 0.66 \times 10^{-7}$ respectively, reverting back to the wild type mostly at the pace of 1.2 to 3.3/109.

218 ORAL PRESENTATION

FURTHER OBSERVATIONS ON THE STRUCTURE OF NARCISSUS MOSAIC VIRUS PARTICLES

J H Low¹, P Tollin¹ and H R Wilson¹

¹Carnegie Laboratory of Physics, University of Dundee, Dundee DD1 4HN

²Physics Department, University of Stirling, Stirling FK9 4LA
Narcissus mosaic virus (NMV) is a member of the potex group. NMV particles are elongated and flexuous with a length of ~550 nm and a diameter of ~14 nm. X-ray diffraction studies and optical diffraction from electron micrographs can be interpreted in terms of a helical arrangement of protein subunits, with $5q + 4$ subunits in 5 turns of the helix, where q is an integer lying in the range $6 \leq q \leq 9$. (Tollin et al. 1968, 1975; Bancroft et al. 1980). In order to determine q more precisely, we have made preliminary Fourier transform calculations from the NMV micrographs and also made molecular volume calculations based on the amino acid composition of RNA content. These results give firm evidence in favour of $q = 8$, which supports the hypothesis that the number of protein subunits per turn of the helix in the potex viruses is close to, but slightly less than 9, and that different viruses in the group differ in the fractional departure from 9 (Richardson et al. 1981).

References

- P Tollin, H R Wilson & D W Young, *J.Mol.Biol.* 34 189 (1968)
P Tollin, H R Wilson & W P Mowat, *J.Gen.Virol.* 29 331 (1975)
J B Bancroft, G T Hills & J F Richardson, *J.Gen.Virol.* 50 451 (1980)
J F Richardson, P Tollin & J B Bancroft, *Virology* 112, 34 (1981).

220

PRELIMINARY DATA ON THE STRUCTURE OF THE FIBRE PROTEIN OF ADENOVIRUS TYPE 2. C. Devaux¹, C. Berthet-Colominas², P.A. Timmins², P. Boulanger¹ and B. Jacrot². Laboratoire de Virologie Moléculaire INSERM-LILLE¹, European Molecular Biology Laboratory, Grenoble², Institut Laue-Langevin², Grenoble, FRANCE.

Crystals of the fibre protein of Adenovirus type 2 have been obtained by precipitation from polyethylene glycol. They are thin platelets (about 10-20 µm thick). Small crystals have been analysed with electron microscopy and X-ray powder diffraction, showing the most likely space group to be P321 with a unit cell $77 \times 77 \times 590 \text{ \AA}$. Measurement of crystal density shows that, if the space group is correct, the fibre must be a dimer. A model for the molecular packing in the crystal has been deduced. The largest crystals obtained diffract up to at least 3Å resolution.

Biochemical analysis indicates that the fibre in the crystals has been proteolysed, possibly from the C-terminal.

222

HEAT-INDUCED TRANSITIONS IN BACTERIOPHAGE T4 PROTEINS

G.R.Ivanitsky, V.L.Shnyrov and O.D.Veprintseva, Inst.Biol.Phys.,USSR Acad.Sci., Pushchino, USSR

An interaction between the phage and the host cell, as well as some physical or chemical factors (e.g. heat) induce contraction of the phage sheath. The contraction is irreversible and has been characterized by a considerable change in free energy. The contribution of enthalpy into the free energy change was studied by scanning microcalorimetry. Electron microscopic analysis has shown the sheath contracts at 70±2°C. Calorimetric curve of the phage T4B ghosts has only endothermic peaks with maxima at 52, 70, 80 and 88°C. A peak with the maximum at 70°C corresponds to the tail sheath contraction. However, this correlation was also observed on thermograms of the ghosts precontracted by treatment with urea or alkali. So, the process of the tail reorganization, in fact, cannot be characterized by considerable changes in enthalpy. Heat generation observed in a number of our experiments and by other authors results from a side process and is due to unspecific irreversible aggregation induced by heat. Heat and alkali treatment of the phages in the solutions of low ionic strength leads to the normal tail reorganization. In the solutions with ionic strength equal to 0.1 and higher the untransformed baseplate, being separated from the contracted sheath, often remains contact with the tail core.

Posters on Viruses

223

SELF-ASSEMBLY OF BROME MOSAIC VIRUS. C. Berthet-Colominas¹, M. Cuillel¹, M. Koch², P. Vachette³ and B. Jacrot¹. E.M.B.L., Grenoble, FRANCE¹, E.M.B.L., Hamburg, GERMANY, LURE Orsay, FRANCE³.

The kinetics of self-assembly of Brome Mosaic Virus (BMV) capsid has been studied by X-ray and light-scattering. In the absence of RNA at pH=7, 0.5M KCl, BMV protein is solubilized as small molecular weight subunits; lowering the pH to 5 induces a crystallization of the protein into empty capsids. Structural studies of these initial and final states of polymerization have been already published. The plot of light-scattering intensity at 90° versus time of polymerization could be interpreted as a superposition of two exponentials with decay coefficients depending on the concentration of the protein. Using X-ray Synchrotron Radiation, scattering curves on solutions at 0.8 mg/ml, 4 mg/ml and 12 mg/ml have been collected at different times of the assembly process. After about 1.5 sec (at 4 mg/ml concentration) the appearance of maxima and minima in the scattering curve indicates the presence of capsids in the solution. Cryo-Electron Microscopy performed on a sample, unfixed, unstained and frozen 4 minutes after the start of polymerization allowed the observation of an heterogeneous population of capsids all of the same radius but some being completely filled and others in intermediate states of filling. This result leads to the analysis of the X-ray scattering curves by a linear combination of the scattering curves of thick spherical shells having openings of different sizes. From these theoretical curves we derive a model to fit our experimental data. The interpretation is currently under way.

225

STRUCTURAL INVESTIGATIONS ON IRIDESCENT VIRUS

S.K. Burley, R.J. Grencall, A. Miller, C. Nave, M.T. Stubbs, Laboratory of Molecular Biophysics, Department of Zoology, University of Oxford, South Parks Road, Oxford. OX1 3PS, UK.

Small-angle neutron & X-ray scattering have been used to investigate various aspects of the structural organization of a cytoplasmic deoxyribovirus, iridescent virus type 29. The neutron data allows the determination of the radial distribution of DNA, lipid, & protein. A new low density external shell of filamentous protein has been discovered. A shell model is proposed, of three spherical shells consisting of a nucleoprotein core, a lipid bilayer, & protein, & one icosahedral shell of protein. A Debye calculation is used to model the icosahedral outer shell.

224

INTERACTION BETWEEN OLIGONUCLEOTIDES AND PROTEIN, STUDIED IN A SPHERICAL PLANT VIRUS

J. Kruse, G. Vriend, B.J.M. Verduin and M.A. Hemminga, Agricultural University, Wageningen, The Netherlands.

The protein-RNA interaction in cowpea chlorotic mottle virus, an icosahedral plant virus, has an important effect on the mobility of the N-terminal arm of the protein subunits. Binding experiments, using synthetic oligo-nucleotides have been carried out to investigate the differences between the three types of subunits that are present in icosahedral particles with a triangulation number equal to three. The binding has been studied with NMR and ultracentrifugation techniques. The role of the N-terminal arm has been emphasized using mixtures of protein subunits lacking the N-terminus and ordinary protein subunits, which are reconstituted together into empty, viruslike spherical particles.

226

227

228

Monday 30 July Congress Centre-first floor. Posters 229-234

Posters on Dissipative Structures and Pattern Formation in Biological Systems

229

RADIATIONLESS TRANSITIONS IN A SUBSTRATE-ENZYME COMPLEXES DUE TO DEFORMATION ENERGY RECUPERATION IN CONFORMATION DEGREES OF FREEDOM
V.A. Novarsky, N.P. Perelman, I.Sh. Averbukh, Applied Physics Inst., Acad. Sci. of Moldavian SSR, Kishinev, USSR

The main idea of the paper presented is the following: due to the intermode binding of the enzyme reaction (ER) coordinate with the low frequency conformational degrees of freedom of enzyme molecule the process rate of the SE complex conversion into the PE complex essentially depends on the excitation level of the conformation degrees of freedom. In the simplest case such a binding is provided by the bilinear form interaction. The energy of the ER activation depends on conformation coordinates in a parametric way. The averaging over the conformation states provides the decrease of the activation energy up to its complete disappearance which ensures the exponential growth of the ER rate.

The cases of different relations between binding and decay rates of SE complexes are analysed and the model of enzyme catalysis as the kinetic phase transition is constructed.

231

ATTRACTORS AND BIFURCATIONS IN NEURAL DYNAMICS
K. Aihara*, G. Matsumoto**, M. Kotani* and T. Utsunomiya***
*Tokyo Denki Univ., Kanda, Chiyoda-ku, Tokyo, Japan,
**Electrotechnical Lab., Tr. Kuba, Ibaraki, Japan, and
***Tokyo Univ. of Sci., Chiba, Japan.

Attractors and bifurcations in neural dynamics have been numerically analyzed by the Hodgkin-Huxley equations from the viewpoint of nonlinear and nonequilibrium dynamics. Further, the dynamics has been physiologically verified by experiments on squid giant axons.

The attractors and the bifurcations analyzed in this research are summarized as follows: (1) a limit cycle of self-sustained repetitive firing and Hopf bifurcations with decreasing the external concentrations of the divalent cations (Ca and Mg) and at the same time increasing the differences between the internal and external concentrations of the monovalent cations (Na and K), (2) Two stable steady-states and saddle-node bifurcations with increasing the external concentration of potassium, and (3) strange attractors and several routes to the turbulent oscillations in periodically forced neural oscillators. In the case of (2), the bifurcation set in parameter space is complex because Hopf bifurcation set coexists with the cusp catastrophe set. The routes to the chaotic oscillations of (3) so far observed in the neural dynamics are successive period-doubling bifurcations, intermittency, collapse of a torus and alternating periodic-chaotic transitions.

233 ORAL PRESENTATION

TEMPORAL EVOLUTION OF CONVECTION PATTERNS IN PROTEIN SOLUTIONS AND CYTOPLASMIC MEDIA
S.C. Müller, Th. Plesser and B. Hess
Max-Planck-Institut für Ernährungsphysiologie, Rheinlanddamm 201, 4600 Dortmund 1, FRG

The temporal evolution of convective pattern formation is studied in a protein solution (albumin) and in cytoplasm extracted from yeast cells containing up to 60 g/l protein. The samples are placed in a petri dish with a diameter of 3.2 cm resulting in a layer depth of 0.18 cm. The patterns are investigated by optical transmission and dark-field techniques. The dark-field method indicates gradients of refractive index provoked by variation in temperature and chemical composition. Starting from a homogeneous state the formation of initially rod like structures and their transition to a network of polygons are observed. The time period for the onset of structure evolution depends on the protein content of the solution. A limiting value of the protein content is found below which no pattern can be detected. The existence of a threshold for pattern formation is discussed on the basis of the Marangoni instability resulting from surface tension driven convection. The experiments emphasize the importance of hydrodynamics for the process of spatial patterning as previously observed at NADH specific wavelengths in a thin layer of periodically glycolyzing yeast extract.

230

ON THE STRUCTURAL COMPLEXITY OF BIOSTRUCTURES
G. Yagil, Department of Cell Biology, The Weizmann Institute of Science, Rehovot, Israel

Biomolecules and large bioassemblies vary enormously in the complexity of their structures. While self assembly processes have been found to be sufficient for directing the assembly of simple structures, more involved mechanisms have to be involved for the assembly of more complex biopatterns, including several common bacteriophages.

It is therefore important to have quantitative procedures for the assessment of the complexity of biostructures. This paper describes such a procedure. The basic proposal is to evaluate complexity by counting the number of independent numerical instructions necessary to specify a given structure in real space. A set of formal rules for evaluating structural complexity is presented. The procedure is applied to a series of biostructures ranging from a simple biomolecule like adenine, through a cellular structure like the nucleosome, to a quasiorganism like the Tobacco Mosaic Virus (TMV). It is found that a correlation exists between the structural complexity of a biopattern and the genomic requirements for its formation. Complexity analysis can serve thus as a tool for assessing genomic requirements for pattern formation.

232

MODULATION-INDUCED TIME PATTERNS IN A GLYCOLYTIC MODEL SYSTEM WITH PERIODIC SUBSTRATE INPUT
M. Markus, H. Becher and B. Hess
Max-Planck-Institut für Ernährungsphysiologie, Rheinlanddamm 201, 4600 Dortmund, FRG

Glycolysis under periodic substrate input flux is investigated with a two-enzyme model. A great variety of time patterns is obtained upon variation of the input flux amplitude A and frequency ω [1]. The transitions between these patterns often display "hysteresis" loops, i.e. the transitions occur at different values of A (or ω) depending on whether A (or ω) is increased or decreased [2].

The introduction of additional bifurcation parameters by sinusoidal variation of A or ω (modulation) enormously enriches the time pattern diversity. We obtain modulation-induced chaotic attractors having a considerable higher degree of randomness (higher Liapunov dimension) than the chaotic attractors without modulation. Furthermore, intermittency is induced by slowly modulating A or ω in the neighbourhood of a bifurcation, provided the modulation covers the interval of A (or ω) where hysteresis, if any, takes place.

- [1] B. Hess & M. Markus (1984) in: "Synergetics from Microscopic to Macroscopic Order" (E. Fröhland, ed.) Springer-Verlag, Berlin
- [2] M. Markus & B. Hess (1984) Proc. Natl. Acad. Sci. USA, in the press.

234

TWO-DIMENSIONAL CHIRAL CRYSTALS OF PHOSPHOLIPID
R. M. Weis and H. M. McConnell, Stauffer Laboratory for Physical Chemistry, Stanford University, Stanford, California USA, 94305

Solid phase domains of dipalmitoylphosphatidylcholine (DPPE) coexist with fluid phase DPPE in monolayers at the air/water interface under specified conditions of average molecular area and temperature. The partitioning of several fluorescent lipid analog probes between the solid and fluid phases has made this observation possible by epifluorescence optical microscopy. Compression of the monolayer causes the solid phase domains to grow at the expense of the fluid phase. The shape of the domains is a sensitive function of the compression rate. Previous work has shown that under slow rates of compression periodic arrays of round solid phase domains form in a continuous fluid phase. At relatively rapid rates of compression, of the order of a 2% decrease in area per second, chiral domains are formed. The handedness of the domains is directly related to the enantiomeric configuration of the lipids in the monolayer. Domains with a three fold rotation axis are formed most often, although domains with 2, 4, 5 & 6 fold rotation symmetry are also observed. These chiral domains provide direct evidence for long range orientational order in two-dimensional crystals.

McConnell, H. M. et al. 1984, Proc. Natl. Acad. Sci. USA, 81, XXXX-XXXX.

This work has been supported by Grant NSF PCM 8021993 and DoD Equipment Grant DAAG29-83-G-0095 to H.M.M. and a fellowship to R.M.W. from the Fannie & John Hertz Foundation.

Monday 30 July Congress Centre-first floor. Posters 235-240

Posters on Dissipative Structures and Pattern Formation in Biological Systems

235

THE "LOOSE STRUCTURE" THEORY FOR LIVING STATE.
A NECESSARY CONDITION FOR DISSIPATIVE STRUCTURES
R.K. Mishra, Department of Biophysics, All India
Institute of Medical Sciences, New Delhi-110029,
INDIA.

In a series of papers necessary and sufficient conditions for structure formation and dissipation by internal energy flows in living organisms are described. These are (1) choice of certain atoms and bonds; (2) "Loose structure" - a structure in which conformational barriers are relevantly low and approximately equal to energies of association; (3) nonlinear couplings; (4) open system away from equilibrium; (5) internal pumps, and lastly and importantly (6) large flux of elementary excitations, all reducible to a bosonic formalism, and the presence of a radiation field. A unified view and correspondence to experimental facts will be presented.

Refs.

1. Living State, Ed. (R.K. Mishra), Wiley Eastern (under publication, April, 1984).
2. Living State II, Ed. (R.K. Mishra), World Scientific Publishers, July, 1984.
3. The Living State XII, Role of Excitons in Biological Structures and the Chemical Bond (in Janibel Symposium), 1984.

237

DISSIPATIVE STRUCTURES AS VEHICLES FOR MACROMOLECULAR TRANSPORT,
S.N. Preston, M.D. Cooper, G. Checkley and T.C. Laurent, Dept. of
Biochemistry, Monash Univ., Clayton, Vic., Australia.

Finger-like flow structures (dissipative structures) may develop on the formation of free liquid boundaries in concentrated multicomponent aqueous systems containing concentration gradients of polymeric solutes. These convective structures move at rates in excess of 10 μ m/hr and may act as vehicles for the rapid transport of high molecular weight solutes, cells and colloidal particles. The nature of the phenomena is such that counter-current flows are observed allowing for simultaneous transport of material in opposing directions. The observed transport of macromolecular species is increased up to $\times 10^3$ normal diffusional rates whilst the behaviour of low molecular weight solutes remains relatively unaltered. We have proposed that the formation of the structures is a multi-step process. The initial step has been demonstrated to involve the formation of a local density inversion at the boundary due to cross (coupled) diffusion between solutes. The cross diffusion between polymeric solutes is primarily due to excluded volume interactions. The relationship of the type of boundary interface (whether diffusional or countercurrent structured flow) to the magnitude of the diffusion mediated inversion and the nature of the molecular interactions have been investigated in a number of different systems having direct biological interest. We have demonstrated the formation of dissipative structures in systems undergoing (a) enzymic depolymerisation, (b) self aggregation and (c) association-dissociation reactions. (1) Preston *et al.*, Nature 287, 499 (1980), (2) Cooper and Preston, Biochem. Int. 3, 337 (1981), (3) Cooper and Preston, Adv. Polym. Sci. 55, 105 (1984), (4) Series of papers on the phenomenology, Preston *et al.*, J. Phys. Chem. 87, 648-661 (1983) and on the mechanism, Cooper *et al.*, J. Phys. Chem. 87, 667 (1983), and 88 (1984).

239

BIOLOGICAL STRUCTURES AS A RESULT OF A COLLECTIVE DYNAMICS
S. Doglia, E. Del Giudice and M. Milani, Department of
Physics of the University, Via Celoria 16, Milan, Italy.

A dynamical description of biological systems at a microscopic level responsible for ordering processes is presented. The collective dynamics of the system is alternatively conservative (vibrational solitons on biomolecular chains) and dissipative (coherent electric polarization waves). The dissipative dynamics provides a mechanism for the spontaneous production of ordered structures in living systems. Two specific cases will be considered: cytoskeleton structures in cell cytoplasm and rouleaux formation among erythrocytes mediated by polymer formation. Polymerization process of actin and fibrinogen will be discussed in terms of nonlinearities in the refractive index of the medium (Kerr birefringence of monomers). The organization produced in the system is the consequence of non linear propagation of coherent electric waves (self focusing) and of the induced ponderomotive forces.

References

1. L. Del Giudice, S. Doglia, M. Milani: "A Collective Dynamics of Metabolically Active Cells", Physica Scripta 26, 232 ('82)
2. E. Del Giudice, S. Doglia, M. Milani: "Actin Polymerization in Cell Cytoplasm" in the Application of Laser Light Scattering to the Study of Biological Motion, eds. J.C. Larnshaw & M.W. Steer, Plenum (1983).
3. E. Del Giudice, S. Doglia, M. Milani: "Self-focusing of Fröhlich Waves and Cytoskeleton Dynamics", Phys. Lett. 90A, 104 (1982).

236

THE IDENTIFICATION OF DETERMINISTIC CHAOS IN ISOPOTENTIAL EXCITABLE MEMBRANES, M.A. Muhsen, Department of Physiology, The University, Leeds LS2 9HQ, U.K.

Irregular, non-periodic changes in membrane potential may result from random processes, or from strictly deterministic nonlinear processes that show extreme sensitivity to initial conditions and possess a strange attractor. Such deterministic chaos may be produced by a sinusoidally forced nonlinear oscillator, such as the excitation equation for an excitable membrane. Numerical solutions of sinusoidally forced axonal and cardiac membrane excitation equations are used to obtain examples of chaotic activity. n -dimensional portraits of the strange attractors are constructed from the vectors $\{V(t), V(t+T), \dots, V(t+(n-1)T)\}$ from computed solutions $V(t)$ and a time delay T , and their self-similarity is demonstrated. Since this method only requires $V(t)$ it may be applied to identify chaos in experimentally recorded membrane potential signals.

238

NEW TYPES OF DISSIPATIVE STRUCTURES

V.I. Krinsky, K.I. Agladze, A.V. Panfilov, A.M. Pertsov
A.N. Rudenko, Inst. Biol. Physics USSR Acad. Sci.,
142292 Pushchino, USSR

The dissipative structures on two- and three-dimensional active media have been studied experimentally. The following patterns have been found in thin layers of a chemical active medium:

- 1) Multiarmed rotating vortices with the topological charge $N=2,3$ and 4. They proved to be stable, the rotation being observed up to complete exhaustion of the chemical reagents. The decay of a vortex with $N=2$ into two simple vortices was also observed.
- 2) Chaotic structures produced by proliferating vortices when interacting with the stationary hexagonal convection cells. Numerical calculations of a three-dimensional active medium described by the Fitz-Hugh-Nagumo equation resulted in:
- 3) Twisted scroll. It is unstable in a homogeneous medium and degrades rapidly to a simple one. In a nonhomogeneous medium, the twisted scroll becomes stable, its filament being directed down the parameter gradient.
- 4) Scroll ring. It turned out to be unstationary, the shortening of its thread and the drift along the symmetry axis being observed.
- 5) Twisted scroll wave with similar properties.

240 ORAL PRESENTATION

CHAOS AND OTHER TEMPORAL SELF-ORGANIZATIONS IN COUPLED ENZYME-CATALYZED SYSTEMS. Li Yue-xian, Ding Ba-fu and Xu Jing-hua, Shanghai Institute of Biochemistry, Academia Sinica, Shanghai, China.

This paper is a study of the dynamic behaviours of the coupled biochemical model systems containing two instability generating mechanisms. The system, we studied in detail, consists of two allosteric enzymes coupled in series, the first is inhibited by its substrates and second activated by its products. It can exhibit all known patterns of temporal self-organization: periodic oscillation, bistability, hard excitation, birhythmicity, periodic doubling bifurcation leading to chaos, etc.. The relationship between these modes of dynamic behaviour is analyzed as a function of the control parameter. All the four possible combinations of the two instability generating mechanisms are discussed and the reason is given to how the instability mechanisms cooperate to induce these behaviours. The fact that three out of the four systems are able to exhibit such phenomena shows that these behaviours are of frequent occurrence in coupled enzyme catalyzed systems.

Monday 30 July Congress Centre-first floor. Posters 241-246

Posters on Dissipative Structures and Pattern Formation in Biological Systems

241

ABNORMAL RESPONSES AND CHAOS IN EXCITABLE MEMBRANE MODELS
T.R. Chay, Department of Biological Sciences, University of
Pittsburgh, Pittsburgh, PA USA.

Using the Hodgkin-Huxley type model of neurons, β -cells, and myocardial fibers, we have studied periodic as well as aperiodic behavior in the self-sustained oscillations. Numerical solutions reveal a variety of patterns in response to variation in temperature, ionic compositions, chemicals, and the strength of applied depolarizing current. These include regimes of repetitive beating and bursting modes and, in the transition between these modes, aperiodic responses. We have analyzed the chaotic pattern formation with a bifurcation analysis. We have also studied it in the context of a one-variable, discrete-time representation of the dynamics. *This work was supported by NSF PCM82 15583.

242

243

244

245

246

Monday 30 July Congress Centre-first floor. Posters 247-252

Posters on Rheology of Cell Membrane

247

A STUDY OF THE INFLUENCES OF A SURFACTANT (SODIUM DESOXYCHOLATE) ON LIPOsome MEMBRANES MADE FROM EGG YOLK LECITHIN

P.M. Wang, Department of Bioengineering, Huazhong University of Science and Technology, Wuhan, Hubei, China.

A recent advance in membrane research is the discovery that Ca^{2+} ions can induce the liposomes to take a helical form, and that surface active substances such as Triton X-100, Tween-80, etc. can induce liposomes to readily form tubular and helical structures. We report here that sodium desoxycholate, a surfactant which exists in bile, can also induce the liposomes made from egg yolk lecithin to form helical structures. Due to the sliding movement between the two winding tubes of a double helix, the simple helical liposomes can grow slowly to form complicated helical and superhelical liposomes, or, growing in another way, it can unlance the helix. The surfactant, i.e. sodium desoxycholate influences differently from Ca^{2+} , because sodium desoxycholate impels, or promotes, increased fluidity of the membrane. This conclusion is consistent with NMR findings. In this paper the author presents his hypothesis that lipid molecules circulate on the plane of the membrane in given conditions.

249

LIPID PEROXIDATION AND FLUIDITY OF TUMOUR MEMBRANES.

M. Marotti, P. Cavatorta, G. Sartor, M.B. Ferrari, C. Zannoni, T. Calotini, Inst. Biol. Chemistry, Univ. Parma, Via Gramsci 14, Parma, Italy, *Inst. Physic. Chemistry, Univ. Bologna, V.le Risorgimento, Bologna, Italy, *Inst. Gen. Pathol., Univ. Cattolica, Largo F.Vito, Roma, Italy.

Quantitation studies of the change in membrane structure induced by lipid peroxidation were carried out on microsomes isolated from the fast growing Morris hepatoma 3924 and rat liver used as control. Peroxidation was induced by using xanthine oxidase. Membrane fluidity was evaluated by measuring static fluorescence anisotropy (r) and fluorescence lifetime of DPH incorporated into the membranes. After 5 and 10 minutes of peroxidation the correlation time of DPH in control membranes was noticeably increased. As for tumour membranes, different anisotropy values were observed in the conditions of peroxidation used. However, the contribution of the lifetimes in the equation used to evaluate the correlation times virtually cancelled such differences, that is no difference in fluidity could be calculated for tumour membranes. These findings point out the importance of lifetime determination in evaluating dynamic parameters of biological membranes, and the inadequacy of static measurements of r alone for the same purposes. Finally DPH correlation time increases with the degree of peroxidation of membranes underlining the importance of this biological process in determining order and fluidity of the membranes.

251

DIRECT VS. INDIRECT EFFECTS OF PEG AND DEXTRAN ON LIPOsome GROWTH.

R.L. MacDonald, Dept. Biochem., Mol. Biol. and Cell Biol., Northwestern Univ., Evanston, IL 60201, USA.

This study was begun to determine whether the commonly used cell fusogen, polyethylene glycol (PEG), fuses membranes by interacting with them directly or indirectly—e.g., by dehydrating the membranes. Fluid phase, phosphatidylcholine vesicles in 10 mM HEPES, pH 7, labeled with the fluorescence energy transferring probes, dansyl PE and DiI-C₁₈ or RhPE, were mixed with unlabeled vesicles and exposed to various concentrations of 15,000–20,000 M PEG. Liposomes were either mixed directly with the PEG solutions or dialyzed against the PEG solutions. After dilution with 10 mM HEPES, PEG-treated vesicles were measured for fluorescence energy transfer and absorbance at 400 nm to assess vesicle growth. Liposomes grew to the same extent, whether directly mixed or dialyzed against PEG solutions. Limit-sonicated vesicles grew more than uni- to paucilamellar, 120–140 nm vesicles, which, in turn, grew more than multilamellar vesicles. Since PEG could fuse membranes by interacting with them indirectly, experiments were repeated with another polymer with similarly high osmotic activity and impermeance to dialysis tubing—i.e., 40,000 M dextran. Energy transfer and turbidity measurements revealed that vesicles dialyzed against dextran grew as much as vesicles exposed to PEG but more than those exposed to dextran by direct mixing. This result indicates that dextran, unlike PEG, can interact directly with vesicles to inhibit that growth which its high osmotic activity would otherwise induce. Electron microscopy of the various vesicle preparations corroborated these findings.

248

PHASE BEHAVIORS OF SATURATION TRANSFER ESR SIGNALS AT HIGH MICROWAVE FIELD

H. WATARI and Y. SHIMOYAMA* Dept. Molecular Physiol., Natl. Inst. Physiol. Sciences, Okazaki 444, Japan and *Dept. Physics, Hokkaido Univ. of Education, Hakodate 040, Japan. Spin labeling electron spin resonance (ESR) spectroscopy has been widely applied to study molecular motion of biomolecules. Saturation transfer (ST) spectroscopy has been developed using adiabatic rapid passage technique to investigate molecular motion having a rotational correlation time slower than the rigid limit. The phase behavior of ESR spectrum is studied using the second harmonic absorption (V_2) spectrum of the spin label (2,2,6,6-tetramethyl-piperidine-1-oxyl) in glycerol-water solution at room temperature. In this conditions the observed ESR spectra are in the fast tumbling domain, which is not the usual ST-ESR regime. Upon application of an intense microwave field (0.508 G), a pronounced nonzero component is observed at the modulation phase where the peak-to-peak amplitude is expected to be zero. This component is the ST spectrum which is latent at the phases giving intense V_2 signals. A single integration of the obtained spectrum yields a significant integrated value, as reported by Evans. However, this integrated value is found to vary in a sinusoidal manner when the angle of the instrumental phase changes. A phase discrepancy is obtained to be 70 degrees between the variations of the peak-to-peak amplitude and the integrated value. This fact indicates that the phase is varied with the amplitude by changing the magnetic field. These led to the concept of vector ESR.

250

PLASMA MEMBRANE FLUIDITY MAY BE SPECIFICALLY STUDIED IN INTACT LIVING CELLS USING NON-PERMANENT FLUORESCENT PROBES SUCH AS TMA-DPH

G. LAUSTRIAT, C. DUFOURTAIL and J.G. KUHRY, Laboratoire de Physique de l'U.E.R. des Sciences Pharmaceutiques, Equipe de Recherche Associée au C.N.R.S. (N° 551), B.P. 10, 67048 Strasbourg Cedex, France.

Fluorescence intensity measurements and fluorescence microscopy data showed that TMA-DPH (trimethylammonium diphe nylhexatriene), a cationic derivative of the fluorescence polarization probe DPH, has a considerably different behavior in L929 cultured cells than does its parent molecule. In contrast to DPH, it incorporates very rapidly in the plasma membranes of the treated cells, and remains specifically localized on the cell surface for about 30 min., thus yielding specific information on the plasma membrane fluidity. Interpretation of the results must nevertheless take into account that TMA-DPH is not totally incorporated into the membrane during the cell treatment and that an equilibrium takes place between the free and bound forms of the probe.

252

TRANSLATIONAL DIFFUSION OF LARGE INTEGRAL PROTEINS IN ARTIFICIAL PHOSPHOLIPID BILAYER MEMBRANES.

W. L. C. Vaz, Max-Planck-Institut für biophysikalische Chemie, Göttingen, F. R. G.

The fluorescence recovery after photobleaching technique has been used to study the translational diffusion of several integral membrane proteins in phospholipid bilayer membranes in the liquid crystalline phase. The proteins examined were: glycophorin (1), bovine rhodopsin and sarcoplasmic reticulum Ca^{++} -ATPase (2), acetylcholine receptor in its monomeric and covalently cross-linked oligomeric forms (3,4), and wheat germ agglutinin-aggregated glycophorin. The translational diffusion coefficients for all of the above proteins fall in the range of $1-4 \times 10^{-8}$ cm²/s (maximum temperature examined was 37°C). The range of radii of these proteins in the plane of the membrane is between ~1 and ~6 nm. This experimentally observed weak dependence of the translational diffusion coefficient upon the diffusing protein radius confirms the prediction of the continuum fluid hydrodynamic model of Saffman (5) for the diffusion in thin viscous fluid sheets.

(1) Vaz, W. L. C., et al (1981) Biochemistry 20, 1392; (2) Vaz, W. L. C., et al (1982) Biochemistry 21, 5608; (3) Criado, M. et al (1982) Biochemistry 21, 5750; (4) Vaz, W. L. C., & Criado, M. (1984) submitted; (5) Saffman, P. G. (1976) J. Fluid Mech 73, 593

Monday 30 July Congress Centre-first floor. Posters 253-258

Posters on Rheology of Cell Membrane

253

RBC DEFORMABILITY EVALUATION BY VISCOMETRY AND FILTRATION RELATED TO MORPHOLOGICAL RBC CHANGES.
C. Lacombe, C. Berling, C. Bucherer and J.C. Lelièvre, Unité de Biologie, Département de Biophysique, CHU Pitié-Salpêtrière, Paris, France.

The aim of this paper is to compare two methods to quantify RBC (Red Blood Cell) deformability, viscometry and filtration, for stored RBC and artificially modified RBC.

(i) viscometry : rheological experiments are performed with a servo control Couette viscometer type device with coaxial cylinders. It allows to record the shear thinning curves in the range 0.01 s^{-1} to 25 s^{-1} . Viscometric data are analysed by means of phenomenological rheological model which gives an index of deformability D_v .

(ii) filtration : we use Hanss' hemorheometer. The results are given in term of a filtration index D_f .

This study was carrying out on the following blood samples :

- blood samples stored as packed cells in CPD
- blood samples artificially modified by an echinocytic agent.

The indices of deformability D_v and D_f are compared and interpreted according to morphological RBC changes controlled under microscope.

255

ROTATIONAL MOTION OF HUMAN RED CELL MEMBRANE PROTEINS
N. Wakayama, Y. Kawasaki and T. Saitoh, Mitsubishi-Kasei Institute of Life Sciences, Machida-shi, Tokyo, Japan

Rotational motion of the membrane proteins of human red cell was studied by delayed fluorescence anisotropy decay method. Red cells were collected from freshly drawn blood and labelled with eosin maleimide. Labelled ghosts were obtained by lysing the labelled cells in a hypotonic solution. Delayed fluorescence was generated with a N_2 laser pumped dye laser as an exciting pulsed light and detected with a gated photomultiplier and recorded in a multichannel analyzer.

Delayed fluorescence anisotropy was studied under various physical conditions and in the presence of various drugs. Several drugs were found which strongly affect the rotational motion of the labelled proteins (mainly consisting of band 3 proteins). Triton X-100 strongly affects the rotational motion of the protein in peculiar way. In the presence of 0.01% Triton the rotational motion is slightly enhanced, whereas at 0.035% the proteins seemed to be immobile in the time range of 5 msec. In the presence of 0.1% Triton, the anisotropy decayed quite rapidly after the excitation. From these results, it was suggested that at 0.01% Triton, the membrane protein motion is enhanced slightly within the membrane and at 0.035% they are enabled to migrate within the membrane and aggregate. At 0.1% Triton, the membrane proteins are mostly solubilized.

257

EFFECT OF CATIONS AND OF FREEZE-THAWING ON AN AQUEOUS SUSPENSION OF PHOSPHOLIPID UNILAMELLAR VESICLES, C. Landry*, M. Correia, R.M. Leblanc* and J. Aghion, Département de Botanique (B-22), U of Liège, Belgium and *CRP, UQTR, Trois-Rivières, Québec, Canada.

In the presence of di- or tri-valent cations at room temperature, the average size of asolectin vesicles suspended in water increases (as shown by turbidity measurements and sepharose filtration). By contrast, phosphatidylcholine (PC) vesicles remain unchanged in the same conditions. Since the PC vesicles have a net superficial charge of 0, it is hypothesized that asolectin vesicles bear a negative superficial charge and that cations neutralize the charges, leading to vesicle-aggregation.

The possibility of some perturbation of the aqueous halo of the vesicles is not to be excluded because a cycle of freeze-thawing of the suspensions (liquid N_2 then room temperature) also leads to an increase of the vesicle-size; the freeze-thaw affects similarly asolectin and PC vesicles. Moreover, glycerol protects the vesicles against such a treatment and monovalent cations (ineffective at room temperature) enhance the effect of the freezing and thawing. Such results do not preclude that the size-increase of the vesicles is due to membrane fusion instead of aggregation.

Acknowledgements : Due to Belgian I.R.S.I.A., to the Belgian-Québec cooperation and to the Actions Concertées de l'Etat Belge.

254

STUDIES ON THE MELANOSOMAL MEMBRANE FROM BOVINE EYES
E. Casali, P. Cavatorta, P.R. Crippa, E. Ferrari, A.S. Ito, G. Sar to: and A. Vecchi, Department of Physics and Institute of Biological Chemistry, University of Parma, Italy.

Pure melanosomal membranes were obtained for the first time in order to study both their composition and physical properties by fluorescence spectroscopy. Purified melanosomes from eye tissues were separated by sucrose gradient centrifugation and, after rapid decompression in N_2 , it was possible to isolate their membranes, as verified by electron microscopy.

After incorporation of the probe DPH, we studied both the static fluorescence anisotropy and the fluorescence time decay in the temperature range $10-40^\circ\text{C}$. The emission decay curves were fitted by a non linear least square method with a two-exponential decay with the principal component showing a half life of about 10 ns.

The fluorescence anisotropy and the microviscosity calculated by a Perrin-type equation have given values decreasing monotonically vs. the temperature, comparable with previous data obtained with other biological membranes.

256

NMR AND SPECTROFLUORIMETRIC STUDIES OF GAMMA-IRRADIATED MODEL AND NATURAL MEMBRANES.

F. Ianzini, L. Guidoni, P.L. Indovina, V. Viti
Laboratorio di Fisica, Istituto Superiore di Sanità, Roma Italy

In recent years membrane damage by ionizing irradiation has been suggested as partially responsible for cell death (1).

Reported and discussed herein are some chemical and structural modifications induced in synthetic phosphatidylcholine multilayer liposomes and erythrocyte ghosts after γ -irradiation. Changes in DPH probe fluorescence properties are reported, e.g. DPH fluorescence anisotropy increases in liposomes (2) and decreases in erythrocyte ghosts. Conducted ^1H and ^2H NMR studies of free, bound and trapped water indicate that γ -irradiation induces variations in dynamic structure and quantity ratios.

Changes at bilayer surface and within the hydrophobic core of membranes are also reported and discussed.

References

- 1) A. Cole-Proc. 7th International Congress of Radiation Research, B3/R Amsterdam, July 3-8, 1983.
- 2) F. Ianzini, L. Guidoni, P.L. Indovina, V. Viti, G. Erriu, S. Onnis, P. Randaccio-Radiation Research, In press.

258 ORAL PRESENTATION

SLOW MOTIONAL DOMAIN IN THE ORIENTED MULTILAYERS AS REVEALED BY SATURATION TRANSFER ESR SPECTROSCOPY

Y. Shimoyama and H. Watarai* Department of Physics, Hokkaido University of Education, Hakodate 040, Japan, and *Department of Molecular Physiology, National Institute for Physiological Sciences, Okazaki 444, Japan.

The saturation transfer electron spin resonance (ST-ESR) spectra was successfully applied to the spin labeled oriented multilayer membranes of egg yolk phosphatidylcholine (EYPC), dipalmitoylphosphatidylcholine (DPPE) and dimyristoylphosphatidylcholine (DMPC) in order to explore molecular order and motion of the lipid membrane organisations. The spectra varies with an angle between the membrane film surface and applied magnetic field, yielding that the lipid membrane forms two-dimensional layered structures. The motional parameters were characterized by means of the relationship between the peak height ratio and rotational correlation time. In the case of DPPE oriented multilayers, correlation times at temperatures below the gel-liquid crystalline phase transition point (ca. 313 K) were found to be in the range of 10^{-8} to 10^{-9} sec. The lipid motion in the EYPC multilayer membranes at temperatures between 233 K to 273 K was determined by the correlation times, obtaining the same range as DPPE membranes below the transition point. The integration method has been developed in order to determine the dynamical behavior of the lipid ensemble in the oriented membranes. Upon addition of cholesterol, an anisotropic structure of correlation times was found in the gel-phase of the DMPC multilayer membranes.

Monday 30 July Congress Centre-first floor. Posters 259-264

Posters on Rheology of Cell Membrane

259

RED BLOOD CELL SHAPES

B. Zekš and S. Svetina, Institute of Biophysics, Medical Faculty and J. Stefan Institute, Ljubljana, Yugoslavia

A normal red blood cell is of a discocyte shape and changes its form under the influence of various agents into stomatocytes, echinocytes, etc. The bilayer couple hypothesis, which assumes that the cell membrane consists of two monolayers which are tightly connected but can slide over each other has been used to study these transformations. The shape of the cell is determined by minimizing the membrane elastic bending energy at constant membrane area (A), constant difference of the areas of the outer and inner monolayers (ΔA) and constant cell volume (V). The discocyte shape corresponds to the absolute minimum of the elastic bending energy and physiological V and ΔA . A decreased ΔA induces a discocyte-stomatocyte second order phase transition and an increase in ΔA should lead to echinocytes. The agents acting on the red blood cell by changing ΔA affect both the shape of the cells and their hemolytic properties because of the indirect effect on the maximum cell volume (V_m). The proposed model elucidates the mechanism causing the difference between the fast and slow hemolysis. For fast hemolysis ΔA is fixed and V_m is smaller than the volume of a sphere (V_0) with given A , while on a larger time scale ΔA can adjust to its minimal energy value and hemolysis starts at $V = V_0$.

260

Twisting in the excited state: Time-resolved fluorescence in diphenylhexatriene (DPH).

A.G. Szabo, P. Cavatorta, C. Zannoni, L. Masotti, S. Yamashita. Div. Biol. Sci., Nat. Res. Council, Ottawa Canada.

The polyene, all trans-DPH has been used extensively as a fluorescence probe of lipid and membrane structure. It is important that its excited state properties be satisfactorily elucidated in order to correctly interpret experiments in which it is used as a probe of lipid order and dynamics. We have conducted fluorescence decay experiments to determine the kinetics of the singlet state deactivation processes of DPH. In non-viscous, non-polar solvents DPH fluorescence decays with single exponential kinetics. In viscous, non-polar solvents the fluorescence decays with double exponential kinetics, with the pre-exponential of one term having a negative value. These results indicate that DPH is twisting in the excited state and that this twisting is affected by the viscosity of the medium. Comparable experiments have been conducted with DPH in liposomes and SUV's of DMPC and DPPC. The results show that in the gel phase bilayers the DPH probe is unable to undergo this twisting motion. These results will be presented and the implications for DPH-membrane studies will be discussed.

261

EFFECT OF OSMOLARITY AND CELL SHAPE ON LIGAND DIFFUSION AND BINDING TO INTRAERYTHROCYTIC HEMOGLOBIN.

M. COLETTA¹, S. Giardinà², G. Amiconi³, M. Brunori³, P. Gualtieri¹ and P.A. Benedetti¹; ¹Center for Molecular Biology CNR, Inst. of Chemistry, Fac. of Medicine, Univ. of Rome "La Sapienza" Rome; and ²Inst. of Biophysics, CNR, Pisa - ITALY.

The diffusion-controlled rate of CO binding to intraerythrocytic hemoglobin has been studied in single red blood cells using a scanning microspectrophotometer. In order to investigate the effect of intracellular hemoglobin concentration and cellular shape on the kinetics of CO binding, measurements have been carried out at different osmotic pressures, using red blood cells from *Canis lupus familiaris*. These erythrocytes, which are smaller than human red cells and have a different shape, are known to remain intact even at an osmolarity 6 times lower than isotonic conditions (280-290 mOsm/l), swelling up to twice their normal volume.

The results show that for these erythrocytes diffusion of CO through an unstirred layer of solvent around the cell membrane, proposed to be the main rate-limiting step for the reaction of ligands with intracellular hemoglobin in human red blood cells, may not be the only factor which affects the CO binding kinetics to intraerythrocytic hemoglobin in small red blood cells.

MOSM ~ 50!

262

THE EFFECT OF AQUEOUS PHASE VISCOSITY ON THE LATERAL DIFFUSION OF PLASMA MEMBRANE MOLECULES.

P.J. Kurtz, W.W. Carley and W.W. Webb, School of Applied and Engineering Physics, Clark Hall, Cornell University, Ithaca, NY 14853, United States of America

Most membrane proteins diffuse significantly slower in cell membranes than predicted by the continuum hydrodynamic theory for homogeneous viscous membranes (Saffman, P.G., J. Fluid Mech. 73:593-602 (1976)). This discrepancy is commonly attributed to constraints due to interactions with the cytoskeleton; however the continuum theory neglects the effect of the sections of membrane proteins which project into the extracellular fluid. We have studied this interaction by measuring the lateral diffusion of 3,3'-diiodoacetylcarboxyanine (dII), Acetyl-Rhodamine-Stearoyl-Dextran (AcRSD) and Rhodamine Sulfonyl Chloride (Texas Red) protein conjugates in the presence of additives which enhance the external viscosity. The experiments were carried out on NRK cells and on NRK cell blebs using the method of fluorescence photobleaching recovery. We find that lateral diffusion of all three probes on cells is independent of external viscosity over a wide range of viscosities. Diffusion coefficients on NRK cell blebs approach the theoretical viscous membrane value. AcRSD diffuses significantly slower on blebs as the external viscosity is increased. Diffusion inhibition by external viscosity can be compared with a modification of the continuum theory in which the projecting protein sections are appropriately modeled, based on the work of Hughes, B.D., Pailthorpe, B.A. and White, L.R. (J. Fluid Mech. 110:349-372 (1981)).

263

ANCHORAGE DEPENDENT CELLS ATTACH TO MICROCARRIER BEADS IN MICROGRAVITY. D.R. Morrison¹, A. Cogoli², A. Tschopp² and M.L. Lewis³; (a) NASA/Johnson Space Center and (c) Technology Incorporated, Houston, TX, U.S.A., and (b) Laboratorium für Biochemie, ETH-Zentrum, CH-8032 Zurich, Switzerland.

The attachment of cells to growth surfaces on Earth is normally affected by the settling of cells onto surfaces of flasks or other culture vessels. Using microcarrier beads and attachment dependent cultured human embryonic kidney cells, we have shown that cells adhere to growth surfaces, flatten and proliferate in the absence of gravity. In two experiments, one aboard the Space Transportation System (STS), Shuttle flight 7, under ambient cabin temperature and the second aboard STS-8 in a 37°C cell culture incubator, cells were mixed with microcarrier beads on orbit. In the second experiment at times, 5 min. and 2.5, 13.5 and 24.5 hours after mixing, cells were fixed by injecting glutaraldehyde. After return to Earth, cell-to-bead attachment was evaluated by counting beads with cells attached, numbers of cells per bead and the number of unattached cells. Attachment characteristics were visualized using a scanning electron microscope. Although no apparent differences were seen in the manner in which cells attached to beads in microgravity compared to the ground control experiment, the flight experiment appeared to have more beads with cells attached and a greater proportion of cells attached. This trend will be investigated in future experiments.

These findings suggest an instantaneous "hit" attachment phenomenon and clearly show that cell cultures may be seeded in the environment of space for culture of cells in microgravity.

264

LATERAL DIFFUSION CHARACTERISTICS OF IONIC CHANNELS AND LECTIN BINDING SITES IN FROG SKELETAL MUSCLE MEMBRANE.

Richard E. Weiss, Walter Stühmer & Wolfhard Almers, Physiol. & Biophys. Dept., Univ. of Washington, Seattle, WA, USA.

The lateral mobility of Na and K channels in surface membrane of *Rana temporaria* muscle was studied by the patch clamp method of Stühmer & Almers (1982, PNAS, 79:946). K channels were found to be relatively immobile with a diffusion coefficient (D) $\leq 5 \times 10^{-12}$ cm²/s. As previously reported (Stühmer & Almers, 1982), Na channels were also immobile, $D \leq 10^{-12}$ cm²/s. For lectin studies, bundles of 1-3 muscle fibers were dissected and incubated for 20-45 min with the fluorescein-conjugated lectin wheat germ agglutinin (WGA). WGA bound tightly to the sarcolemma and/or basal lamina since the fiber retained a stable fluorescence for > 3 hrs after lectin washout. Mobility of WGA receptors in the plane of the cell surface was measured with "fluorescence recovery after photobleaching," using a 5-7 μ m diameter spot of blue light. Measurements were made at 22°C in Ringer and in a relaxing solution (RS) containing no Ca²⁺, 20 mM EGTA and 96 mM KCl. Recovery of fluorescence in RS was well fitted with $D = 4.7 \times 10^{-11}$ cm²/s ($\pm 0.6 \times 10^{-11}$ cm²/s S.E.M., n=12). The mobile fraction of WGA receptors was 65% \pm 7% (S.E.M., n=12). Recovery time courses in Ringer varied widely. Preirradiation of the sarcolemma with ultraviolet light (2-3 J/cm² at 289 or 302 nm) had no measurable effect on the mobility of WGA receptors. This argues against the possibility that the immobility of Na and K channels in frog muscle sarcolemma is a result of UV irradiation. Supported by grants from the NIH (AM-17803 to WA and AM-06915 to REM) and the MDA.

Monday 30 July Congress Centre-first floor. Posters 265-270

Posters on Rheology of Cell Membrane

265 ORAL PRESENTATION

SUPPORTED PHOSPHOLIPID BILAYERS

L. K. Tamm and H. M. McConnell

Stauffer Laboratory for Physical Chemistry, Stanford, CA USA
Single phospholipid bilayers of DPPC, DMPC and DOPC have been prepared on various hydrophilic substrates, namely oxidized silicon, quartz and glass. Two phospholipid monolayers were sequentially transferred from an air-water interface to the solid support by using a modified Langmuir-Blodgett technique. Epifluorescence microscopy and fluorescence photobleaching were used to provide a first physical characterization of the supported phospholipid bilayers. The following observations lead us to conclude that single planar bilayers have indeed been formed on the solid supports and that the physical properties of these model membranes resemble those in other model systems very closely: (i) For compressed monolayers the lipid transfer ratio from the air-water interface to the substrate is nearly 1. (ii) On oxidized silicon the fluorescence intensity of a bilayer is twice that of a monolayer. (iii) Lateral diffusion coefficients are of the order of $1-8 \times 10^{-8} \text{ cm}^2/\text{s}$ in "fluid" membranes for both leaflets of the lipid bilayers. (iv) Supported DPPC bilayers on silicon exhibit two sharp phase transitions at about 32 and 40°C, close to the well-known pretransition ($L_{\beta}' \rightarrow P_{\beta}'$) and chain melting phase transition ($P_{\beta}' \rightarrow L_{\alpha}$) in multibilayers. Supported phospholipid bilayers are stable only in a certain pressure-temperature regime. Excess lateral pressure or excess tension leads to a "collapse" (tubular and spherical liposomes) or defect structures (membrane holes), respectively. Supported phospholipid bilayers are useful for studying the binding kinetics and surface diffusion of antibodies.

267

SPIN-LABEL STUDIES ON THE PROPERTIES OF PHOSPHATIDYLCHOLINE-CHOLESTEROL MEMBRANES. Akihiro Kusumi, Witold K. Subczynski*, Marta Pasenkiewicz-Gierula* and James S. Hyde, National Biomedical ESR Center, Medical College of Wisconsin, Milwaukee, WI 53226, USA. * on leave from the Institute of Molecular Biology, Jagiellonian University, 31-001 Krakow, Poland.

We report three major findings on phosphatidylcholine-cholesterol membranes in this presentation. (1) Very small amounts of cholesterol (cholesterol/dipalmitoyl-phosphatidylcholine = 1/3,000 - 1/30,000 molar ratio) cause a dramatic increase in the mobility of 5-doxyl stearic acid spin label (5-SASL, 1/400, molar ratio) in the gel-phase membranes. Cholesterol at low concentrations also greatly increases the rate of approach to equilibrium after temperature-jump (cooling) across the pretransition. (2) In the fluid phase, the mobility of 5-SASL decreases monotonically in proportion to the mole fraction of cholesterol in unsaturated phosphatidylcholine membranes. In the fluid phase of saturated phosphatidylcholine membranes, the mobility of 5-SASL decreases up to a certain mole fraction of cholesterol (which depends on the temperature) and then increases with the further addition of cholesterol. (3) Cholesterol increases the accessibility of water to the hydrophilic loci of various phosphatidylcholine membranes.

(Supported in part by NIH grants RR-01008 and GM-22923, and the Liposome Company postdoctoral fellowship to A.K.)

269

EVIDENCE FOR MORE THAN ONE PHOSPHOLIPID DOMAIN IN BIOLOGICAL MEMBRANES; A P-31 NMR STUDY, Philip L. Yeagle*, Barry S. Selinsky and Arlene D. Albert, Department of Biochemistry, SUNY/Buffalo, Buffalo, NY, USA.

P-31 nuclear magnetic resonance (NMR) has been used to investigate the properties of phospholipid headgroups in biological membranes. In particular, the influence of protein has been studied. Membranes from muscle sarcoplasmic reticulum, from retinal rod outer segment disks, and from human erythrocytes have been investigated. P-31 NMR has shown that in the first two membranes at least two overlapping resonances have been detected. This is interpreted in terms of two phospholipid headgroup environments which are in slow exchange with each other on the msec timescale. Recombined membranes containing the major proteins of these two membranes demonstrate that the presence of two environments is dependent upon protein. The populations of the two environments are shown to be correlated with the environment of the membrane, the state of the protein, and the functionality of the protein. No such effects are noted for the intact erythrocyte membrane.

The exchange rate of phospholipids between the two environments has been directly measured at 1 s⁻¹ (supported by NIH HL23853 and EY03328).

266

FORMATION OF HELICAL LIPOSOMES UNDER VARIOUS CONDITIONS

K.C. Lin, P.M. Wang, P.S. Zheng and S.C. Liu, Dept. Biophysics, Beijing Medical College, Beijing, China.

Liposomes in the form of tubes, single and double helices and superhelices can be formed with various kinds of phospholipids or binary systems thereof after evaporating, hydrating and vortexing. In systems containing cardiolipin (CL), cations (e.g. Ca²⁺, Mg²⁺ etc.) are effective in inducing helices mainly in 10-80 mole% of CL above the transition temperature of its partner in a pH range 6-8. These liposomes are multilayered as shown by scanning or freeze-fracture electron microscope.

With surface active substances, phospholipids can form tubes and sometimes helices more easily, provided that part of a liposome is in close contact with the glass slide. Fluorescence polarization measurement showed that surface active substances reduced the fluidity and flow activation energy ΔE of liposomes. An asymmetry surface tension hypothesis is postulated to explain this phenomenon.

268

RHEOLOGY OF THE PLANT PLASMA MEMBRANE

J. Wolfe, M.F. Dowgert, W.J. Gordon-Kamm and P.L. Steponkus, School of Physics, Univ. New South Wales, Sydney, Australia and Dept. Agronomy, Cornell Univ., Ithaca NY, U.S.A.

The rheology of the plasma membrane of isolated rye protoplasts was measured by micropipette aspiration. Over periods of about 1s., the material in the membrane is conserved and it acts like a two-dimensional fluid with negligible viscosity: changes in area are proportional to changes in tension γ with an area elastic modulus of 200 mN.m⁻¹. The membrane ruptures under tensions of 4 to 6 mN.m⁻¹ (depending on time of exposure) limiting elastic stretching to 2 or 3%. Much larger area changes are possible over longer periods by the transfer of membrane material to or from a cytoplasmic reservoir. The membrane has a characteristic resting tension, γ_r , which is typically 0.1 mN.m⁻¹ and is, at most, weakly dependent on changes in area. Light and electron microscopy shows that when a protoplast is contracted osmotically, the initially flaccid membrane loses area by endocytotic vesiculation until it becomes spherical and regain γ_r . When $\gamma > \gamma_r$, reservoir material is incorporated into the membrane. The incorporation rate is a strong function of γ , as is the probability of lysis. The survival by protoplasts of osmotic expansions depends on the rate and extent of incorporation of new material into the membrane. An analytic solution for $\gamma(t)$ during an osmotic expansion has been found.

270

ERYTHROCYTE MEMBRANE INJURY AND RECOVERY DURING HYPOTONIC HAEMOLYSIS

S. Eskelinen, Department of Physiology, University of Oulu, SF-90220 Oulu, Finland.

In hypotonic NaCl media, the erythrocyte membrane is injured during sphering in a manner such that potassium will leak out and, probably, sodium flows in, but a lesser degree. The spherical shape remains, while the potassium release and degree of haemolysis increase during the course of time. In fact, the cell membrane is in a state in which any additional disturbance will cause haemolysis. On the contrary, in the presence of lysophosphatidylcholine (LPC) the potassium release and haemolysis do not increase in respect to time but remain at their 2-minute levels. Hence, it is suggested that LPC prevents the membrane injury or allows the membrane to recover. LPC protects erythrocytes even against colloid osmotic lysis in an isotonic NaCl medium, when the cells have been treated with nystatin. Thus, the maximal volume is not the most important parameter in the mechanism of haemolysis and its prevention, but the permeability properties of the cell membrane are more important. Maximal protection is achieved with a LPC concentration which evokes vesicle release in an isotonic NaCl medium. Alterations in the lipid bilayer-cytoskeleton interactions and in the organization of the lipid bilayer are, therefore suggested to lie behind the protection.

Posters on Rheology of Cell Membrane

271

FOURIER TRANSFORM INFRARED SPECTROSCOPIC STUDIES OF LIPID-PROTEIN INTERACTION
R. Mendelsohn, G. Andrieu and M. Jaworsky, Dept. of Chemistry, Rutgers University, Newark, New Jersey, USA.

Vibrational spectroscopy has been used to monitor the conformation of phospholipids reconstituted into model membrane systems with Glycophorin (erythrocyte membrane) or CaATPase (rabbit sarcoplasmic reticulum).

High precision (0.03 cm^{-1}) FT-IR measurements of acyl chain CH_2 stretching frequencies as a function of temperature are used to construct lipid melting curves. The effect of glycophorin on saturated phosphatidylcholines or phosphatidylserine is to reduce the midpoint temperature of and broaden the gel-liquid crystal phase transition. No evidence is obtained for an immobilized lipid component. Reconstitution of CaATPase with DPPC reveals a similar perturbation, in which the onset of melting correlates well with the onset of ATPase activity. This confirms a suggestion that a liquid crystalline environment is required for optimal protein function.

Use of acyl chain perdeuterated lipids as one component of a binary lipid mixture permits studies of the thermal behavior of each lipid in ternary complexes composed of two lipids plus protein. The ability of membrane proteins to select a particular lipid was shown in two separate systems, CaATPase/DPPC- d_{67} /DOPC and Glycophorin/DPPC- d_{67} /PS. In each case, the lower melting lipid demonstrated a preferential association with protein. Current work centers around FT-IR determination of membrane protein secondary structure.

273

LIPID CHAIN DYNAMICS AND PHASE COEXISTENCE IN PHOSPHATIDYLETHANOLAMINE MEMBRANES. J.-H. Sachse, A. Watts and D. Marsh, Max-Planck-Institut für biophysikalische Chemie, D-3400 Göttingen, Fed. Rep. Germany.

ESR studies on the dynamics of dimyristoyl phosphatidylethanolamine (DMPE) bilayer membranes in the fluid, gel and phase transition regions ($T_m = 49^\circ\text{C}$) have been made using 6 different positional isomers of PE spin-labelled in the $\text{sn}-2$ chain. Comparison of the chain order parameters ($S = \langle \cos^2\theta - 1/2 \rangle$) with those of the corresponding phosphatidylcholine label isomers in dipalmitoyl phosphatidylcholine bilayers ($T_m = 41^\circ\text{C}$) reveals a considerable decrease in amplitude of chain motion in the DMPE bilayers for all chain segments. Since the comparison is made on a reduced temperature scale, this indicates a pronounced chain stiffening (on a $T_m/10^3$ timescale), arising from the different headgroup interactions in PE bilayers. This is equivalent to the effect of a $\sim 10^\circ\text{C}$ temperature shift on the bilayer chain motion. In the gel phase, saturation transfer ESR studies ($10^{-3} - 10^{-7}$ s) also reveal a considerable reduction in motion relative to PC and a torsional gradient in chain motion. In the transition region ($\sim 47^\circ - 50^\circ\text{C}$) 2 co-existing spectra are observed, characteristic of different motional states. Intersubtraction of spectra at different temperatures indicates that the lower mobility state converts to the higher mobility state, and yields the degree of conversion with increasing temperature, through the transition. With the 5-C positional isomer a further coexistence is observed in the range $41^\circ - 48^\circ\text{C}$, indicating the existence of incipient pretransitional effects in PE bilayers.

275

The Lateral Fluidity of Intact Erythrocyte Membranes by Use of an Excimer Probe. Fluorimetry of Turbid and Absorbant Samples, Josef Eisinger and Jorge Flores, AT&T Bell Laboratories, Murray Hill, New Jersey 07974

While fluorescence techniques are often employed in membrane model systems, the difficulties encountered in the quantitation of fluorescence intensity and polarization of strongly absorbant and scattering samples have largely prevented their use in the study of intact cells. We have developed and tested a concentration titration method which permit the use of any optical probe including fluidity probes and hemoglobin proximity probes, in intact cell systems. An illustration of the technique is the measurement of the lateral mobility of 1-pyrene-hexadecanoic acid (PHD) in the outer leaflet of the lipid bilayer of intact erythrocytes. The location of the probe was determined by resonance energy transfer between PHD and the cytosol hemoglobin (Eisinger & Flores, Biophys. J. 41, 367, 1983). The PHD excimer or monomer yields (I) extrapolated to zero hematocrit ($h=0$) were measured by plotting $\log(I/h)$ versus h . This simple procedure is based on the experimentally verified expectation that for $h \leq 0.01$, $I = (\text{constant}) \cdot nh \phi \exp(-\alpha h)$; where n = probes per cell and α is an effective extinction coefficient which is a function of the scattering and absorption properties of the cells at the excitation and emission wavelengths and the fluorometer's configuration. ϕ is the fluorophores' *in situ* quantum yield. The first 10^6 probes per cell are almost immobile, while the next 2×10^6 were characterized by a lateral diffusion coefficient (D) of 12 and $19 \times 10^{-9} \text{ cm}^2/\text{s}$ for intact cells and ghosts, respectively (21°C). These values of D , obtained by use of a random walk model, show that the lateral fluidity of the membrane is perturbed by osmotic lysis. The activation energy of D (E_a) was 3.5 kcal/M° , considerably less than the E_a determined by fluorescence photo-bleaching recovery (FPR) (Bloem & Webb, Biophys. J. 42, 295, 1983). This may be related to the fact that the diffusion distance for FPR experiments is $\sim 500 \text{ nm}$, a distance which spans many membrane proteins, while the present method is sensitive to diffusion over $\sim 3 \text{ nm}$, which is of the order of the inter-protein spacing.

272

PREDICTION OF ERYTHROCYTE MECHANICAL PROPERTIES SHAPE AND SHAPE TRANSFORMATION

B. T. Stokke, A. Mikkelsen and A. Elgsaeter, Division of Biophysics, University of Trondheim. N-7034 Trondheim-NTH Norway

The human erythrocyte has no nucleus and no transcellular cytoskeleton. The erythrocyte mechanical properties are therefore assumed to be determined by the plasma membrane alone. The main features of the molecular organization of the erythrocyte plasma membrane are a fluid lipid bilayer with an apposed spectrin meshwork on the cytoplasmic surface. Based on current knowledge of the physical properties of the various constituents of this plasma membrane we have carried out a statistical thermodynamic and numerical analysis of its physical properties. Our analysis suggests that the membrane skeleton may be described as a swollen, ionic gel. Recent discoveries of phase transitions and critical phenomena in such gels make this concept particularly interesting. Our membrane model can account for all the major intrinsic material properties of the red cell, and is the first membrane model that can quantitatively account for all the commonly observed shapes and shape transformations of erythrocytes.

274

DIFFERENT LYMPHOCYTE MEMBRANE PROTEINS REVEAL DIFFERENT SENSITIVITIES TO MOBILITY-MODULATION BY LOCALIZED CONCAVALIN-A BINDING.

Yoav I. Henis, Department of Biochemistry, The George S. Wise Faculty of Life Sciences, Tel Aviv University, Tel Aviv, Israel.

We have employed fluorescence photobleaching recovery to demonstrate selective immobilization of lymphocyte membrane proteins by localized concanavalin A (ConA) binding to the cell surface. Localized ConA binding was achieved by the binding of ConA coupled to paraformaldehyde-fixed platelets to mouse spleen lymphocytes. The effect of the localized cross-linking of ConA-receptors on the mobility of specific membrane proteins at regions distal to the ConA-platelets was investigated. The diffusion of surface immunoglobulins (sIg) was inhibited above a threshold coverage (12%) of the upper lymphocyte surface by ConA-platelets. This modulation propagates through cytoskeletal interactions, as evidenced by its synergistic reversal by the action of colchicine and cytochalasin B. In contrast, no effect is observed on the diffusion and aggregation of H-2K^a antigens labeled with a fluorescent monoclonal antibody. These results indicate specificity in the interactions of membrane proteins with the cytoskeleton. This specificity enables a selective response of different membrane proteins to the ConA anchorage-modulation.

276

Monday 30 July Congress Centre-first floor. Posters 277-282

Posters on Rheology of Cell Membrane

277

278

279

280

281

282

Tuesday 31 July

Symposia

09.30 - 12.30

Mechanisms of Transport across Membranes

Cytoskeleton

Chromatin Structure and Function

Affinity Group Meeting on Structure of Food
Biopolymers

14.00 - 17.00

Cross-Bridge Mechanisms and Muscle Contraction

Education in Biophysics

Viruses

Plenary Lecture

17.15 - 18.30

"Continuing Studies in Retinex Theory"

E.H. Land (Rowland Institute)

Poster Sessions

Polymorphism and Structural Transitions in Nucleic Acids

Nucleic Acid-Protein Interactions

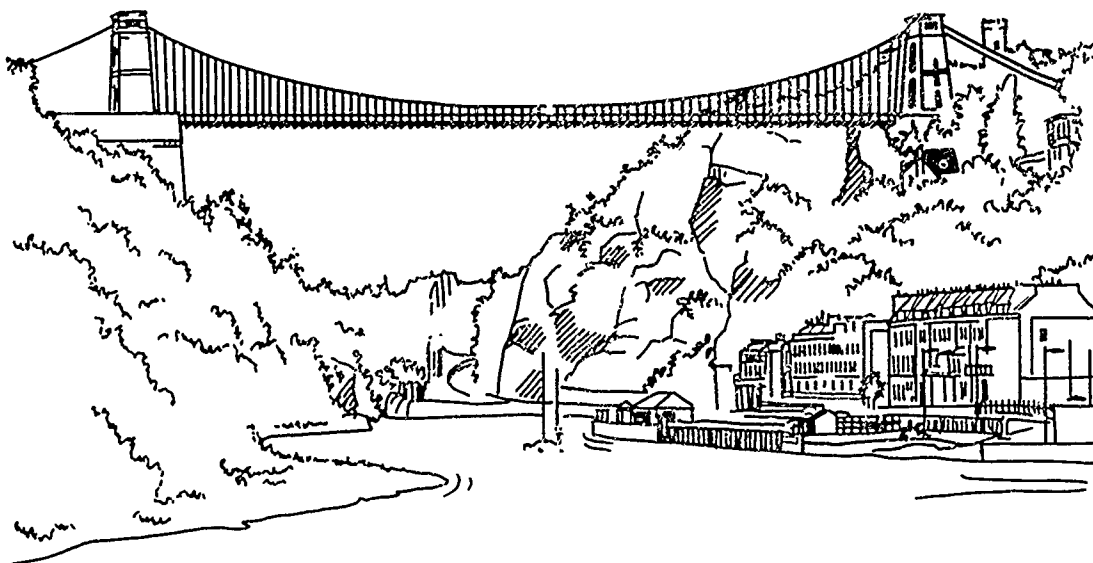
Metal-Protein and Electron Transfer

Polysaccharides and Glycoproteins

Connective Tissue and Bone

Photosynthesis

Category 29: General



The Clifton Suspension Bridge

Tuesday 31 July

Colston Hall Main Hall	Council House Conference Hall	Unicorn Hotel Trident Suite
09.30		
Mechanisms of Transport Across Membranes Co-Chairmen: I.M. Glynn (Cambridge) S Estrada-O (Mexico) Speakers: M.J.A. Tanner (Bristol) F. Palmieri (Bari, Italy) I.M. Glynn (Cambridge) L. De Meis (Rio de Janeiro) and Authors of Posters H. Gogelein (164) M.J. Avison (192)	Cytoskeleton Chairman: K. Weber (Göttingen) Speakers: K. Weber (Göttingen) I.R. Gibbons (Hawaii) S.N. Timasheff (Branders) and Authors of Posters E. Lierns (095) D.A.D. Parry (079)	Chromatin Structure and Function Chairman: G. Felsenfeld (NIH) Speakers: G. Felsenfeld (NIH) T. Koller (Zurich) T.J. Richmond (Cambridge) and Authors of Posters H. Eisenberg (017) J.A. Subirana (013)
12.30		
Morning Coffee 10.50-11.10	Morning Coffee 10.50-11.10	Morning Coffee 10.50-11.10

Break for Lunch (90 Minutes)

14.00	Cross-Bridge Mechanisms and Muscle Contraction Chairman: H.E. Huxley (Cambridge) Speakers: H.E. Huxley (Cambridge) Y.E. Goldman (Pennsylvania) R. Cooke (California) and Author of Poster T. Yanagida (001)	Education in Biophysics Chairman: M. Anbar (Buffalo) Speakers: M. Anbar (Buffalo) S. Mascarenhas (Brazil) J.G. Norby (Denmark) A.C.T. North (Leeds) C. Sybesma (Brussels)
17.00	Afternoon Tea 15.20-15.40	Afternoon Tea 15.20-15.40
17.15		
18.30	Continuing Studies in Retinex Theory Plenary Lecture by E.H. Land (Rowland Institute)	

Timetable

Watershed Cinema 1	Congress Centre First Floor	
	Presenting Authors should set up their Posters before the start of Today's Symposia	09.00
		09.30
Affinity Group Meeting on Structure of Food Biopolymers Chairman: G. Stainsby (Leeds) Speakers: J. Edelman (RHM Research) E.D.T. Atkins (Bristol) J.M.V. Blanshard (Nottingham) D.G. Dalgleish (Hannah, Ayr) E. Dickinson (Leeds) E. Tornberg (Kävlinge) S.B. Ross-Murphy (Unilever, Colworth)	Poster Sessions Polymorphism and Structural Transitions in Nucleic Acids Poster Nos: 001-054 Nucleic Acid-Protein Interactions Poster Nos: 055-090 Metal-Proteins and Electron Transfer Poster Nos: 091-144 Polysaccharides and Glycoproteins Poster Nos: 145-162 Connective Tissue and Bone Poster Nos: 163-186 Photosynthesis Poster Nos: 187-216 Category 29: General Poster Nos: 217-276	12.30
Morning Coffee 10.50-11.10		
		14.00
Viruses Chairman: D.C. Wiley (Harvard) Speakers: D.C. Wiley (Harvard) B. Jacrot (Grenoble) K. Simons (Heidelberg) and Authors of Posters H.R. Wilson (218) B.J.M. Verduin	Presenting Authors should attend their Posters throughout the Afternoon Discussion Period.	
Afternoon Tea 15.20-15.40		17.00
	Presenting Authors must take down their Posters	17.15
		18.30

Symposium on Mechanisms of Transport Across Membranes

THE STRUCTURE OF THE ERYTHROCYTE ANION TRANSPORT PROTEIN AND A POSSIBLE MECHANISM.

M.J.A. Tanner and C.J. Brock, Department of Biochemistry,
University of Bristol, Bristol, U.K.

Small monovalent anions equilibrate very rapidly across the red cell membrane by a process which involves the strict one-for-one exchange of anions. This transport is mediated by the most abundant integral membrane protein of the erythrocyte (band 3) and occurs by a sequential 'ping-pong' carrier mechanism in which the anion transport site on the protein is available alternately at the extracellular and cytoplasmic sides of the membrane. The anion transport protein has an apparent molecular weight of 100,000 and consists of two domains with very different properties. The N-terminal 40,000 dalton domain is situated within the erythrocyte cytoplasm, has regions which are very rich in acidic amino acids and has sequence characteristics similar to that of soluble proteins. This domain forms the attachment site of the erythrocyte cytoskeleton and also binds many peripheral membrane proteins. The C-terminal 55,000 dalton membrane-bound domain is glycosylated and carries out anion transport. Studies with impermeant protein labelling agents have shown that the polypeptide traverses the membrane several times in this hydrophobic portion. It is likely that the anion transporting structure is formed from a bundle of transmembrane α -helices. We have been studying the amino acid sequence and sites of binding of anion transport inhibitors in this region of the protein. A portion of the sequence which represents two of the transmembrane α -helices has been determined. The orientation of this sequence with respect to the membrane has been established by determining the sites of extracellular lactoperoxidase-mediated radioiodination and the sites of extracellular proteolysis. The intracellular portion of this sequence contains a cluster of six basic residues and a lysine residue in this cluster selectively reacts with the anion transport inhibitor, phenylisothiocyanate. This region may form a part of the intracellular anion binding site. The structural features of this sequence suggest a possible molecular model for the mechanism of anion transport. We assume the protein contains a cluster of transmembrane α -helices with a core filled with amino side chains through which anions are transported rather than a water filled channel. Anions are translocated between spatially separated anion binding sites at the two surfaces of the membrane by the rearrangement of a series of intra-membrane charge pairs of acidic and basic residues, the anion being transferred between basic residues in the core of the protein. In this mechanism the translocation process generates an anion transport site alternately in the two anion binding domains at the surfaces of the membrane thus imposing a sequential exchange transport mechanism on the anion transport process. The amino acid sequence so far elucidated shows that some polar amino acids (serine, threonine) are probably located in the membrane interior. Their distribution on the surface of the transmembrane helices suggest that these side chains may be directed towards the core of the protein where they could modify the environment around the anion-translocating charge-pairs.

Symposium on Mechanisms of Transport Across Membranes

ISOLATION AND RECONSTITUTION OF THE MITOCHONDRIAL PHOSPHATE CARRIER PROTEIN

F. Palmieri, Institute of Biochemistry, Faculty of Pharmacy,
University of Bari, Bari, Italy

The N-ethylmaleimide-sensitive electroneutral phosphate/proton symporter of the inner mitochondrial membrane catalyzes the uptake of inorganic phosphate required for oxidative phosphorylation. The mitochondrial phosphate carrier, isolated by solubilization of mitochondria in non-ionic detergents and chromatography on hydroxylapatite, contains not only the ADP/ATP carrier and the phosphate carrier but altogether at least 5 protein bands in the Mr-region of 30000-35000, as shown by high resolution SDS gel electrophoresis. Several attempts to further purify the phosphate carrier by chromatography on Celite, on Mersalyl-Ultrogel and by using Triton X-114 instead of Triton X-100, were partially successful to remove the ADP/ATP carrier, but they failed to decrease the number of protein bands. We have now identified the phosphate carrier protein with only one band (Mr 33000) of the 5 protein bands present in the hydroxylapatite pass-through and have isolated it with 2 methods: a) by using an organomercurial agarose column after hydroxylapatite, and b) by collecting the very first part of the pass-through of a dry hydroxylapatite column to which a cardiolipin-supplemented mitochondrial extract has been applied. Crosslinking studies of the phosphate carrier isolated from pig and beef heart mitochondria indicate that the purified protein is a dimer of approx. Mr 68000. A polarity of 50% is calculated from the aminoacid composition.

The isolated phosphate carrier protein, after incorporation into liposomes by the freeze-thaw-sonication procedure, is able to catalyze both the unidirectional transport of phosphate (uptake or efflux) and the exchange between the intra- and extraliposomal phosphate. In the solubilized state the phosphate carrier is very sensitive to various parameters, e.g. high detergent concentrations, high ionic strength, high pH, freezing and incubation at 25°C. Once the detergent-solubilized carrier is reincorporated into liposomes, it becomes rather stable. The inhibition of the carrier by Triton can be largely prevented or reversed by cardiolipin suggesting a removal of this phospholipid by the detergent. Cardiolipin is the only phospholipid tested, including acidic and unsaturated ones, which markedly increases the elution of the phosphate carrier protein from hydroxylapatite. Furthermore, by comparing the effect of various lipid compositions of liposomes on the reconstituted exchange, it was found that the highest activities are obtained after reconstitution with liposomes containing 5% cardiolipin. These results suggest a specific interaction of the phosphate carrier protein with cardiolipin. The $^{32}\text{Pi}/\text{Pi}$ exchange in reconstituted proteoliposomes follows a first order kinetics similarly as found in mitochondria. The Arrhenius plot of the temperature-dependence of the reconstituted phosphate exchange shows a break at 27°C with an E_a of 16 Kcal/mol in the lower temperature range. The Lineweaver-Burk analysis of the exchange reveals hyperbolic saturation characteristics with a K_m between 2.0 and 2.5 mM for external Pi very close to that found in mitochondria. The transport of phosphate in proteoliposomes is inhibited by SH-blocking reagents and not by inhibitors of other mitochondrial anion transport systems. Substrates of other carriers have also no effect. Both the uptake and the efflux of phosphate are dependent on the transmembrane ΔpH as shown by changing the intra- or the extraliposomal pH and by the use of ionophores. Thus the reconstituted mitochondrial phosphate carrier exhibits properties very similar to those described in the original membrane.

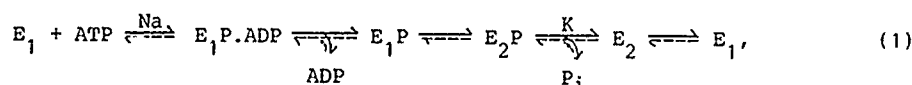
Symposium on Mechanisms of Transport Across Membranes

OCCLUSION OF SODIUM AND POTASSIUM IONS BY THE Na,K-ATPase; THE ROLE OF THE OCCLUDED-ION FORMS IN THE PUMP CYCLE

I.M. Glynn and D.E. Richards. Physiological Laboratory, University of Cambridge, Cambridge, U.K.

Because, in its normal cycle, the Na,K-ATPase transports three Na ions outwards and two K ions inwards, across the cell membrane, it has long seemed likely that intermediate states of the Na,K-ATPase exist in which Na or K ions are occluded within the enzyme.

The normal cycle is thought to consist of the steps:



where $E_1\text{P}$ and $E_2\text{P}$ are two conformations of the phosphorylated enzyme (sensitive, respectively, to ADP and to K) and E_1 and E_2 are two conformations of the dephosphoenzyme. Na ions are needed for phosphorylation by ATP; K ions greatly accelerate the hydrolysis of $E_2\text{P}$; and the conversion of E_2 to E_1 is very slow in the absence of ATP, but fast when ATP is bound to a low-affinity site on E_2 .

We now have evidence that phosphorylation of the enzyme by ATP leads to the occlusion of three Na ions within $E_1\text{P}$, and that hydrolysis of $E_2\text{P}$ leads to the occlusion of (probably) two K ions within E_2 . The evidence comes from experiments in which the enzyme is forced rapidly through cation exchange columns after having been exposed to ^{22}Na or ^{42}K (or, more conveniently, ^{86}Rb) in conditions leading to the formation, but not to the breakdown, of the hypothetical occluded-ion forms. If the time spent on the columns is small compared with the time-constants of the reactions that release the occluded ions, the occluded ions will be carried through the resin by the enzyme and will appear in the effluent. To demonstrate the occlusion of Na ions, it is necessary to pretreat the enzyme with α -chymotrypsin or with N-ethyl maleimide (procedures which largely block the conversion of $E_1\text{P}$ to $E_2\text{P}$), and also to ensure that no ADP is present, since this would dephosphorylate the $E_1\text{P}$. To demonstrate the occlusion of K or Rb ions, it is necessary to stabilize the enzyme in the E_2 form by excluding ATP or Na ions in high concentration (since these would convert the enzyme into the E_1 form), and also excluding P_i (which would phosphorylate the enzyme and release the occluded ions).

Examination of equation 1 shows that each of the occluded-ion forms can be approached by two routes, one involving the transfer of a phospho group and the other involving only a change in conformation — of the phosphoenzyme, in the case of Na; of the dephosphoenzyme, in the case of K or Rb. There is indirect, but strong, evidence that it is intracellular Na ions that become trapped in $E_1\text{P}$ on phosphorylation, and that the release of Na ions from $E_2\text{P}$ is to the extracellular solution. Similarly, there is indirect, but strong, evidence that it is extracellular K ions that become trapped in E_2 when $E_2\text{P}$ is hydrolysed in the presence of K, and that the release of K ions from E_1 is to the intracellular solution. For both Na and K, therefore, the two routes to the occluded-ion forms, coupled back to back, provide pathways from one side of the membrane to the other; and the properties of these pathways account for many of the features of the fluxes of Na and of K through the membrane under both physiological and other conditions.

When P_i and Mg are added to enzyme which is in the E_2 form and which contains occluded Rb, there is a rapid release of all of the occluded Rb, provided that the suspending medium contains no free Rb or other K congener. If free Rb, or other K congener, is present, however, only 50% of the Rb is released rapidly. Na antagonises this effect of Rb. The explanation of the effect is not known, but it may reflect interaction between the two halves of the dimeric enzyme.

Although a good deal is now known about the molecular structure of the enzyme, it is not yet possible to relate the reactions leading to the occlusion or release of the alkali-metal ions to this structure.

Symposium on Mechanisms of Transport Across Membranes

SYNTHESIS OF ATP BY THE SARCOPLASMIC RETICULUM ATPase IN ABSENCE OF IONIC GRADIENT.

L. de Meis. Instituto de Ciências Biomédicas, Dept. de Bioquímica, Universidade Federal do Rio de Janeiro, C. Universitária, I. Fundão, Rio de Janeiro, RJ, Brasil.

Vesicles derived from the sarcoplasmic reticulum skeletal muscle can drive a continuous synthesis of ATP when a Ca^{2+} gradient is formed across the vesicle membranes (Makinose, M. and Hasselbach, W., FEBS Lett. 1971, 12, 271). Synthesis of ATP is initiated by phosphorylation of the membrane-bound ATPase by P_i , forming an acylphosphoprotein. This is followed by the transfer of the phosphate from the phosphoenzyme to ADP, leading to the synthesis of ATP. The ATPase can be phosphorylated by P_i in the absence of a Ca^{2+} gradient when incubated in a medium without Ca. This phosphoenzyme is referred to as "low energy" because it does not transfer its phosphate to ADP. However, in the absence of a Ca^{2+} gradient, synthesis of ATP after a single catalytic cycle can be attained if, after phosphorylation by P_i , ADP and a high Ca^{2+} (10 mM) are added to the medium. This indicates that the phosphoenzyme is converted from "low energy" into "high energy" when transferred from a medium without Ca^{2+} to a medium containing high Ca^{2+} . Phosphorylation by P_i and conversion of the phosphoenzyme from low into high energy is mediated by the asymmetrical binding of Ca^{2+} on the two sides of the membrane. The affinity of the Ca^{2+} binding sites varies with pH. Thus, ATP synthesis can be attained in the absence of ion gradients and at constant Ca^{2+} concentration (0.6 mM) by varying the pH of the medium from 5.5 to 8.0. Conversion of the phosphoenzyme from low energy into high energy can also be attained by varying the water activity of medium by means of different organic solvents. In this case, synthesis of ATP is attained without gradients in a medium where pH and Ca^{2+} concentrations are maintained constant.

George et al (Biochim.Biophys.Acta, 1970, 223, 1) proposed that the energy of hydrolysis of a compound is determined by the difference of solvation energies of reactant and products. The data obtained with the SR-ATPase can be interpreted according to the concept of solvation energy. A variation of either Ca^{2+} concentration, pH or water activity can lead to a change of solvation energy of product and reactant. For instance, the solvation of P_i will depend on the water activity of the medium (organic solvent), its ionization (H_2PO_4^- or HPO_4^{2-}) and whether it is free or forming complexes with divalent cations. In order to explore this possibility the K_{eq} of hydrolysis of pyrophosphate, a compound similar to ATP, was measured in solutions adjusted to different pH values, different Mg^{2+} and Ca^{2+} concentrations and in the presence of different organic solvents. It was found that the K_{eq} may vary from a value higher than 4×10^3 to a value as low as 3. The two steps transitions which permit the sarcoplasmic reticulum ATPase to catalyze the synthesis of ATP also promote a large decrease in the observed K_{eq} for pyrophosphate hydrolysis.

Symposium on Cytoskeleton

MOLECULAR ASPECTS OF THE CYTOSKELETON; STRUCTURE AND FUNCTION OF INTERMEDIATE FILAMENTS, K. Weber, Max Planck Institute for Biophysical Chemistry, Goettingen, FRG.

Most vertebrate cell types contain in addition to microtubules and microfilaments extensive displays of intermediate filaments (IF), often also called 100 Å filaments. Whereas microtubules and F-actin are based on globular subunits IF contain rod-like protofilamentous units. Their α -type X-ray diffraction pattern predicts coiled-coil arrays, which are now documentable by sequence data and correlated biochemical properties (see below). Here I shall try to summarize current efforts directed towards a molecular understanding of the IF structure. In addition I shall follow up the cell- and tissue-specific expression pattern of the 5 subclasses as a diagnostic tool in pathology.

Amino acid sequences in conjunction with the biochemical characterization of isolated domains are instrumental in our concepts of intermediate filament structure and the understanding of the diversity of IF proteins. They provide the basis of a topographical model, which accounts for most aspects of molecular variability (polypeptide length, charge, solubility and different requirements for polymer formation) while keeping a common structural theme. A related highly α -helical rod-like domain (about 310 residues) able to form interpolypeptide coiled-coils is flanked by the non- α -helical terminal domains hypervariable both in sequence and in length. This model identifies the hard α -keratins of wool as a special set of epithelial (cyto)keratins thus drawing their well known structural properties into the common concept developed for IF proteins. The protofilamentous unit is by many criteria not based on the predicted triple-stranded rope but rather on a double-stranded coiled-coil. Recent experiments on the neurofilament triplet proteins show that the IF model can accommodate molecules of extreme length (M_{app} 160K, 200K), since the extra mass is located into long and curious carboxyterminal extensions of polypeptides which in their aminoterminal part are bona fide IF proteins.

The histologically meaningful cell- and tissue-specific subclassification of IF made originally by polyclonal antibodies is fully verified by sequence data and consolidated by an increasing bank of monoclonal antibodies, each specific for only one IF protein (vimentin, desmin, GFA, neurofilament 68K, 160K, 200K, cytokeratin 18). In the case of epithelial (cyto)keratins monoclonal antibodies can be either extremely specific recognizing only a single polypeptide or can cover to a various extent a few, several or many components. Such antibodies selected for their specificity on human IFs are very useful in surgical pathology to distinguish different tumor types difficult to segregate by conventional histological techniques. Thus basic cell biological research on IFs has a useful application in applied medical problems. Preliminary epitope mapping experiments will be discussed because of several structural implications.

Symposium on Cytoskeleton

THE ROLE OF DYNEIN IN MICROTUBULE-BASED MOTILITY.

L. R. Gibbons, Pacific Biomedical Research Center, University of Hawaii, Honolulu, Hawaii, USA.

Dynein ATPase occurs as 20-25 nm projections, called "arms", disposed along the length of the microtubules in cilia, sperm flagella, and many motile cytoplasmic microtubular systems, where it is responsible for transducing the chemical energy of ATP hydrolysis into functional mechanical work. In most cases studied, the dynein arms constitute crossbridges between two adjacent microtubules, with each crossbridge a complex structure of $M_r = 1.3-1.9 \times 10^6$. One end of each bridge is attached by a functional site that undergoes cyclic detachment and reattachment concurrent with the binding and hydrolysis of molecules of ATP, while the other end is attached by a stable structural site. The crossbridge cycling induced by ATP results in relative sliding movement between the two bridged tubules. In most organelles, this sliding is coordinated and opposed by resistive structures that convert it into bending waves that propagate along the organelle, but under appropriate conditions continuous longitudinal movement at velocities up to $10-15 \mu\text{m sec}^{-1}$ can be demonstrated.

Extraction of demembrated sea urchin sperm flagella with 0.6 M NaCl solubilizes selectively the outer arms on the doublet tubules. The resultant soluble dynein 1 consists of 21S particles ($M_r = 1.3 \times 10^6$) comprised of 9 distinct polypeptides--the α and β heavy chains ($M_r \sim 420,000$), 3 intermediate chains ($M_r = 85,000-115,000$) and 4 light chains ($M_r = 15,000-25,000$). Structural examination by scanning transmission electron microscopy shows that the 21S dynein 1 particle consists of two compact globular heads joined by a slender stalk. Freshly extracted dynein 1 has a low latent specific ATPase activity and can be shown to retain functional capability by its ability to restore the beat frequency of dynein-depleted sperm flagella. The ATPase latency is the result of a relatively slow product release step in the enzyme kinetic pathway and is necessary for mechanochemical energy conversion.

Fractionation of dynein 1 at low ionic strength yields two ATPase-containing subunits, sedimenting at 12S and 14S, that consist principally of the α heavy chain, and the β heavy chain with intermediate chains 2 and 3, respectively. About 90% of the ATPase activity is associated with the β /intermediate chain subunit, and about 10% with the α chain subunit. Reformation of a 21S particle occurs when a mixture of the α and β subunit preparations is returned to 0.6 M NaCl, but not with either of the subunit preparations separately, suggesting strongly that each 21S particle forming an outer arm contains both an α and a β heavy chain. Neither the α nor the β chain subunit appears functionally competent by itself, as judged by its ability to restore beat frequency. However, the β chain subunit does appear able to block the manifestation of frequency restoration of subsequently added intact dynein 1 in a manner that is gradually reversed over 2-8 min in the presence of ATP.

Extended tryptic or chymotryptic digestion of either whole solubilized dynein 1 or the separated β /intermediate chain subunit leads to formation of a protease-resistant particle, termed Fragment 1A, of $M_r \sim 380,000$. This Fragment 1A retains high ATPase activity, and is composed principally of two polypeptides ($M_r = 120,000$ and $190,000$) derived from the original β heavy chain. No analogous protease-resistant fragment appears to be formed upon digestion of the α subunit. Digestion of unextracted flagella with trypsin to a stage at which the α chain is substantially digested but the β chain remains mostly intact, enables a large amount of the dynein 1 to be solubilized by 3 mM ATP at physiological salt concentration, indicating that the affinity of the salt-sensitive structural bond of the outer arm to the tubule is diminished substantially by the early stages of digestion of the α chain.

The overall evidence is consistent with a model of the outer arm in which the α and β heavy chains each constitute one of the two globular heads. The heads appear to play distinct functional roles, with the β head being the one principally responsible for the cyclic ATP-driven detachment/reattachment to successive sites on the adjacent tubule, which is the primary mechanism of mechanochemical energy transduction.

Symposium on Cytoskeleton

ON THE MECHANISM OF TUBULIN SELF-ASSEMBLY INTO MICROTUBULES Serge N. Timasheff, José Manuel Andreu and Octavio Monasterio, Graduate Department of Biochemistry, Brandeis University, Waltham, MA, USA.

The mechanism of assembly of pure tubulin into microtubules was probed by comparison with the self-assembly of the tubulin-colchicine complex. All studies were done in pH 7.0 phosphate buffer with calf brain tubulin prepared by the modified Weisenberg procedure (Lee et al., J. Biol. Chem. (1973) 248, 7253). A strong analogy was found between the two polymerization processes. Both reactions can be described thermodynamically in terms of a nucleated polymerization. The end products, however, have different morphologies, the cooperative polymerization of the tubulin-colchicine complex leading to filamentous or sheet-like structures, rather than microtubules. In both cases, the polymerization requires the presence of magnesium ions and GTP; both are inhibited by calcium ions, GDP and low temperatures. Analysis in terms of the Wyman linkage theory showed the uptake of one Mg^{2+} and one H^+ per tubulin α - β heterodimer added to both growing structures. Addition of the heterodimer in both cases is an endothermic reaction, characterized by a positive change in standard entropy and a negative change in heat capacity (for microtubule formation, $\Delta C_p = -1500 \text{ cal deg}^{-1} \text{ mol}^{-1}$, $\Delta S^0 = 30 \text{ e.u. at } 37^\circ\text{C}$; for the tubulin-colchicine complex, $\Delta C_p = -1200 \text{ cal deg}^{-1} \text{ mol}^{-1}$, $\Delta S^0 = 35 \text{ e.u. at } 37^\circ\text{C}$). The sole major difference found was in the pattern of GTPase activity: in microtubule growth, addition of a tubulin dimer generates a slow GTPase activity, while the enzymic activity present in the tubulin-colchicine complex was not affected by polymerization. Both polymerizations were weakened by an increase in ionic strength, although, in the case of microtubules, the effects of sodium and potassium salts were not identical, suggesting ion specificity. Thus the critical concentrations in 10 mM NaCl and KCl were 10.7 and 7.5 μM , respectively, in the presence of 12 mM $MgCl_2$. The absolute requirement of GTP for assembly was scrutinized by the use of analogues. Replacement of the E-site GTP by the non-hydrolyzable analogue, CMP-P(CH_2)P, resulted in a protein which assembled readily into microtubules that were easily reversed by cold temperature and calcium ions. This reaction was fully endothermic, with no exothermic step detected in differential heat capacity microcalorimetry (H.-J. Hinz and S.N. Timasheff, unpublished). Fluorination of the γ -phosphate on the E-site GTP resulted in inhibition of assembly, indicating that addition of a tubulin α - β heterodimer to the growing end of a microtubule requires that the γ -phosphate on the nucleotide be ionizable. (This work was supported by NIH grants GM-14603 and CA-16707.)

Symposium on Chromatin Structure and Function

CHROMATIN IN THE NEIGHBORHOOD OF TRANSCRIPTIONALLY ACTIVE GENES. G. Felsenfeld, J.M. Nickol, B.M. Emerson, J.D. McGhee, D. Jackson, Laboratory of Molecular Biology, National Institute of Arthritis, Diabetes, and Digestive and Kidney Diseases, National Institutes of Health, Bethesda, Maryland, USA.

Most of the DNA within the eukaryotic nucleus is packaged in nucleosomes, which are in turn folded into the solenoidal array that comprises the 30 nm thick chromatin fiber. When a gene is expressed, a variety of changes occur in the chromatin structure in the neighborhood of the gene. We have used the adult β globin gene of chicken erythrocytes to study such changes. Even when isolated from embryonic erythrocytes that are active in the production of β globin messenger RNA, most of the DNA in the neighborhood of the gene is complexed with histones. Sequences coding for the globin gene are represented at levels close to genomic abundance in nucleosome monomer fractions prepared from erythrocyte nuclei. The hydrodynamic properties of the particles containing globin DNA can be studied by combining sucrose gradient sedimentation with "dot blot" hybridization methods. In this way, it is possible to show that these particles behave, to a first approximation, like normal nucleosomes, although some interesting differences are observed. Despite these similarities to bulk chromatin, the β globin region also displays important differences. The entire gene is unusually sensitive to digestion by nucleases, and there is a nuclease-hypersensitive domain in the 5' flanking region, extending from about -70 to -270 nucleotides from the starting point of transcription. We are able to show that this domain, which contains DNA sequence elements important for regulation of globin gene expression, is free of nucleosomes. We have studied the physical properties of the DNA of this region, and show that it contains a run of sixteen G residues which, when present in supercoiled plasmids, is unusually sensitive to the single-strand-specific S1 nuclease. We have also searched for factors that might be associated with the DNA of this region within chromatin. We find that erythrocyte nuclei contain a factor which, when recombined with globin DNA and histones, confers nuclease hypersensitivity on the 5' flanking region. Partially purified column fractions that are active in generation of hypersensitivity have been used in filter binding assays with restriction fragments from the β globin gene region. These fractions specifically retain on the filter the DNA of the hypersensitive domain. The filter binding assay has been used to estimate the abundance of the factor within the nucleus, and to measure its association constant for binding to DNA.

Symposium on Chromatin Structure and Function

ARE THERE NUCLEOSOMES IN HYPERACTIVE GENES?

Th. Koller, Institute for Cell Biology, Swiss Federal Institute of Technology, Zürich, Switzerland.

Since the discovery of the nucleosome in 1973 no consensus has evolved with regard to the presence or absence of nucleosomes, or other histone-DNA complexes in transcribing chromatin. We have been concentrating on chromatin structure in gene systems which are likely to be very active in transcription. The following assays were used, where possible in parallel on the same material: Micrococcal nuclease digestion, accessibility of chromatin to restriction enzymes with a 6 base-pair recognition sequence (DNA in inactive chromatin is inaccessible according to our observations) electron microscopy and psoralen-crosslinking of chromatin-DNA. So far, we have studied the chromatin structure of the ribosomal genes of *Xenopus laevis* oocytes (Labhart and Koller, 1982) and of *Dictyostelium discoideum* (Ness et al., 1983; Sogo et al., 1984), as well as a secretory protein gene in salivary glands of *Chironomus* larvae (Widmer et al., 1984). Our cumulative results are best explained by a model in which in hyperactive genes nucleosomes are not present. We further speculate that during the passage of RNA polymerase most of the histones, at least histones in stoichiometric amounts, are not bound to the DNA (Labhart et al., 1983). However, this speculation has yet to be proven.

Labhart, P. and Koller, Th. (1982): Structure of the active nucleolar chromatin of *Xenopus laevis* oocytes. *Cell* 28, 279-292.

Labhart, P., Ness, P., Banz, E., Parish, R. and Koller, Th. (1983): Model for the structure of the active nucleolar chromatin. *Cold Spring Harbor Symp. Quant. Biol.* 47, 557-564.

Ness, P.J., Labhart, P., Banz, E., Koller, Th. and Parish, R.W. (1983): Chromatin structure along the ribosomal DNA: regional differences and changes accompanying cell differentiation. *J. Mol. Biol.* 166, 361-381.

Sogo, J.M., Ness, P.J., Widmer, R.M., Parish, R.W. and Koller, Th. (1984): Psoralen-crosslinking of DNA as a probe for the structure of active nucleolar chromatin. *J. Mol. Biol.*, submitted.

Widmer, R.M., Lucchini, R., Lezzi, M., Sogo, J.M., Edström, J.E. and Koller, Th. (1984): Chromatin structure of a hyperactive secretory protein gene of *Chironomus*. *EMBO J.*, submitted.

Symposium on Chromatin Structure and Function

THE STRUCTURE OF THE NUCLEOSOME CORE PARTICLE OF CHROMATIN AT 7Å RESOLUTION

T.J. Richmond, J.T. Finch, B. Rushton, D. Rhodes and A. Klug,
MRC Laboratory of Molecular Biology, University Postgraduate Medical School,
Hills Road, Cambridge, U.K.

The nucleosome is the fundamental structural unit of the chromatin in eukaryotic cells. It has a composition of approximately 200 base pairs of DNA, an octamer of the core histones, and the outer histone, H1. The nucleosome core particle is released from chromatin by nuclease digestion, and consists of 146(±2) base pairs of DNA wrapped around the core histone octamer in approximately 1.8 turns of a superhelix. The octamer itself is assembled from a tetramer of a pair of each of the histones H3 and H4, and two dimers of the histones H2A and H2B.

X-ray crystallography has been used to determine the structure of the nucleosome core particle to a resolution of 7 Å. The crystals are in the orthorhombic space group $P2_12_12_1$ having unit cell dimensions of $a=107.5$, $b=184$, and $c=110.5$ Å with one particle of 206,000 daltons per asymmetric unit. Cluster compounds containing several heavy atoms were used in conjunction with the method of multiple isomorphous replacement to solve the structure. Several other procedures were necessary to offset the difficulties due to the large asymmetric unit and variation in the cell dimensions.

The current electron density map is in general agreement with the results of past crystallographic studies, but it also reveals many structural features unobserved at lower resolution. The disk shaped particle is approximately 57 Å high and 106 Å in diameter. It has been verified that the double helix is of the right-handed B-form arranged in a left-handed superhelix with a pitch of approximately 30 Å. The DNA is not uniformly wrapped around the histone octamer, but exhibits several tight bends or possible kinks along the superhelix. The sites of greatest curvature in the superhelix occur adjacent to points where histones H3 or H4 make substantial contact with a minor groove that is directed to the interior of the particle. At no point along the DNA superhelix does the protein density appear to wrap around the double helix nor does it penetrate between the turns of the superhelix. In general, the protein contacts with the DNA are confined to the inner face of the superhelix, where interactions are made on nearly every turn of the double helix. The distortions from a regular superhelical structure may impart a DNA sequence dependency on chromatin superstructure. The points of tightest bending are well correlated with the sites of DNase I protection and dimethylsulfate reaction enhancement of the core particle DNA.

The greater part of the individual histone domains are clearly defined in the electron density map. The histone assignments that were deduced from chemical crosslinking data and the previous low resolution model are consistent with the protein domains seen now, the H3 histone dimer having been identified with a heavy atom label. The halves of the H3-H4 tetramer and the central turn of the DNA superhelix are well related by a non-crystallographic symmetry axis. However as a consequence of inter-nucleosomal DNA-H2A associations in the crystal, the H2A-H2B dimers which reside on opposite faces of the core particle do not maintain the molecular dyad symmetry visible in the tetramer region. The dislocation of one of the H2A-H2B dimers suggest a disassembly pathway for the octamer which may be of biological importance. The observed positions of the H2A dimers in the core particle would appear to affect the path of the linker DNA as it enters and exits the nucleosome.

Affinity Group Meeting on Structure of Food Biopolymers

POLYSACCHARIDE INTERACTIONS IN ORIENTED GELS

E.D.T. Atkins, H.H. Willis Physics Laboratory, Royal Fort, University of Bristol, Bristol, England.

X-ray diffraction methods have been used to examine oriented fibres prepared from concentrated solutions and gels of polysaccharides. Analysis of the diffraction spectra together with computerised model building procedures provide information on the geometry, conformation and association of polysaccharide chains in these oriented samples.

In certain cases the X-ray derived periodicities, particularly those generated along the polysaccharide chains, do not bear a straightforward relationship with values expected from our knowledge of the stereochemistry of the chemical sequence. The extra cellular microbial polysaccharide curdlan is an example where a successful solution has been found. However, in the case of gellan gum serious problems still exist and a variety of model structures have to be considered. The stereochemical consequences and wider implications will be discussed. The repeating tetrasaccharide repeat is approximately 2nm in length but the observed X-ray diffraction periodicities have a value of 0.94nm, less than half that expected. Various contracted single helices and the classes of intertwined multistand helices will be illustrated and contrasted.

RECENT DIFFRACTION STUDIES OF STARCH GRANULE STRUCTURE

John M.V. Blanchard, David L. Wild and David R. Bates, Department of Applied Biochemistry and Food Science, School of Agriculture, Sutton Bonington, Loughborough LE12 5RD

Theoretical X-ray powder diffraction patterns have been calculated based on the published atomic coordinates of the crystal structures of A- and B-amyloses. There appear to be differences between the calculated spectra and the experimental powder diffraction patterns obtained from A- and B-starches. Possible explanations for these differences will be considered. At the supermolecular level, the recent use of small angle X-ray (SAXS) and small angle neutron (SANS) scattering has given valuable insight into long range order within the granule and points to a regular periodicity of approx. 100Å. By examining the scattering of suitably prepared wheat starch granules in an appropriate D₂O/H₂O mixture, it has proved possible to demonstrate a further periodicity at 150-160Å for which lipid is believed to be responsible. The implications of these structural observations on gelatinization, particularly when monitored by the dynamic small angle light scattering technique will be discussed.

THE STRUCTURE OF CASEIN MICELLES

D.G. Dalgleish, The Hannah Research Institute, Ayr, Scotland, U.K.

Casein micelles of bovine milk are composed of proteins of four different structures, together with calcium phosphate, calcium ions and small amounts of citrate and have radii of up to 200nm. The structure is highly porous, allowing relatively free passage of protein in and out of the structure. Stability is achieved by a surface containing κ-casein, which contains a hydrophobic moiety, and may achieve its action by steric stabilization. Destabilization and aggregation of the micelles may be achieved by the action of proteases, by addition of alcohol, or by heating, all of which affect the micelle structure in different ways. The concept of the micelle as a system in dynamic equilibrium, rather than a fixed structure requires consideration to explain the changes brought about which lead to instability. Caseins, in molecular or micellar form are excellent emulsifiers, and the mechanism of the interaction between casein, especially in the micellar form, and lipid surfaces requires the postulation of further structural changes in the micelle to explain the behaviour of emulsified particles with respect to destabilizing phenomena.

GELATIN + CASEINATE AT THE OIL-WATER INTERFACE

S. M. Chesworth, E. Dickinson, B. S. Murray, D. J. Pogson, A. Searle and G. Stainsby, Procter Department of Food Science, University of Leeds, U. K.

Interfacial tensions and viscoelasticities of mixed adsorbed films of gelatin + sodium caseinate have been measured at 25°C as a function of time at the n-hexadecane-water interface (pH 7.2, ionic strength 0.005 M). At a constant bulk protein concentration (10⁻³ wt %), the time to develop a steady-state surface pressure (~20 min) is much less than that over which is observed a steady increase in surface shear modulus and surface viscosity. Initial changes in surface pressure (< 3 min) are sensitive to protein concentration, but not to protein composition. At longer times (> 10 min), the gelatin and caseinate components make predominant contributions to the surface rheology and pressure respectively. The mechanical properties of the mixed films are not simple averages of those of the 'pure' protein films.

Mixtures of the same gelatin and caseinate samples have been used to make emulsions of a vegetable oil in water. An analysis of the supernatant and cream layers following emulsion centrifugation gives an estimate of the proportions of the two proteins in bulk and adsorbed phases. Stabilities of emulsions containing gelatin + caseinate (pH 7.2, ionic strength 0.005-2.0 M) have been measured for comparison with stabilities of emulsions containing gelatin and caseinate alone at the same protein load and phase volume ratio.

FILM AND EMULSION FORMATION OF SOME FOOD PROTEINS

E. Tornberg, Swedish Meat Research Institute, Kävlinge, Sweden.

This paper will review results obtained on surface coverage of proteins, on the formation of protein stabilised emulsions, and coalescence stability of these emulsions. The protein preparations studied were sodium caseinate, whey protein, blood plasma, soy protein and sarcoplasmic proteins.

The surface film formation of the proteins has been followed by measuring the kinetics of the interfacial tension decay. It has been analyzed in terms of distinguishable rate-determining steps, diffusion- and penetration-controlled adsorption of proteins. Depending on whether diffusion or penetration is the rate controlling step during adsorption, different protein membranes are formed. This will be shown for varying initial protein subphase concentrations, for different proteins and interfaces, and for a variety in charge density of the proteins.

Protein stabilized emulsions have been characterized with regard to oil particle size distribution and the amount of protein adsorbed per unit area of fat surface (protein load). The former property of the emulsion is mainly governed by the emulsifying conditions. The protein load is largely determined by the protein/oil surface area ratio, the protein used, the charge density and by the occurrence of recoalescence during emulsion formation.

Coalescence, measured as percentage oil extracted by hexane, decreased with an increase in fat surface area. No straightforward relationship has been observed between the coalescence stability of the emulsions and the protein load.

NON-LINEAR VISCOELASTICITY IN POLYSACCHARIDE SOLUTIONS

R.K. Richardson and S.B. Ross-Murphy, Unilever Research, Colworth Laboratory, Sharnbrook, Bedford.

Dynamic oscillatory, steady shear, time evolution of stress in start shear and its recovery, the strain dependence of stress relaxation and other non-linear viscoelastic measurements may be used to investigate the similarity and the differences of response observed in 'entanglement networks' and 'weak gel network' ('thixotropic') polysaccharide solutions. The former type of behaviour, observed for example for aqueous solutions of guar galactomannan, follow the expected behaviour including Cox-Merz superposition of $\eta^*(\omega)$, $\eta'(\dot{\gamma})$ in the same way as most solutions of synthetic polymers in organic solvents. By contrast, 'weak gel' systems here exemplified by solutions of the microbial polysaccharide xanthan, have properties much more akin to those observed for colloidal dispersions (i.e. Bingham-like flow properties). In the above cases of guar and xanthan, viscoelastic properties will be related to the flexibility of the original polysaccharide, and the nature of the intermolecular entanglements/interactions. Particularly for the polyelectrolyte xanthan, the viscoelastic properties depend not only upon the ionic strength of the solvent, but also upon the nature of the counterion species.

Tuesday 31 July Council House-Conference Hall 14.00-17.00

Symposium on Cross-Bridge Mechanisms and Muscle Contraction

TIME-RESOLVED X-RAY DIFFRACTION STUDIES OF STRUCTURAL CHANGES IN MUSCLE DURING ACTIVATION AND CONTRACTION

H.E. Huxley, M. Kress, A.R. Faruqi (MRC Laboratory of Molecular Biology, Cambridge), M.H.J. Koch & J. Hendrix (EMBL, Hamburg)

We have continued our studies on the behaviour of the low-angle X-ray diffraction diagrams from the actin and myosin filaments during contraction of striated muscle, taking advantage of the high X-ray intensity provided by the Storage Ring 'DORIS' in Hamburg and improved data-collecting facilities provided by the EMBL Outstation there. Earlier work using film and conventional X-ray sources had shown a characteristic increase in intensity on the second actin layer line at a radial spacing around 0.021 \AA^{-1} , which could be interpreted in terms of a movement of tropomyosin towards the centre of the long pitch grooves in the actin helical structure (the steric blocking mechanism). The present work confirms the existence of this substantial intensity increase, specifically associated with the active state, and shows that it occurs earlier after the stimulus than any of the other changes in the X-ray diagram that we have studied. At 5°C , the average half-time for the change was 17 msec (48 experiments). Under similar conditions, the changes in the equatorial pattern (showing crossbridge attachment) have a half-time of about 25-30 msec, while half maximum tension is reached in about 45 msec. In semitendinosus muscles stretched beyond overlap, the intensity increase on the second layer line is still observed, and can have a similar magnitude to the change at normal overlap. These results (and others) suggest that in relaxed muscle under physiological conditions, the initial attachment of crossbridges is blocked by the troponin-tropomyosin system, and that when this inhibition is removed following stimulation, attachment takes place to an initial state which does not develop tension until a further rate process (which may also be regulated by troponin/tropomyosin) has occurred. The results also indicate that tropomyosin movement takes place in response to calcium binding to troponin independently of myosin attachment. Analogous observations on the 59 \AA actin reflection indicate that part of the increase in intensity observed during contraction is associated with the activation process itself and part with cross-bridge attachment.

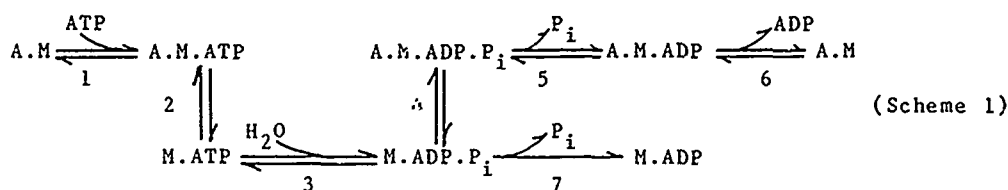
In collaborative work with R.M. Simmons we have examined the behaviour of the equatorial reflection during quick releases of otherwise isometrically contracting muscles. A very rapid increase in the side spacing of the filaments, by up to 2%, takes place when tension is removed, i.e. a substantially larger amount than would be expected from the length change of the sarcomeres. Nevertheless, only very small (1-2%) changes in the intensity of the [10] and [11] reflections are seen. The significance of these observations in terms of changes of shape or orientation of the crossbridges during their working stroke will be discussed.

Symposium on Cross-Bridge Mechanisms and Muscle Contraction

PROBING THE ACTOMYOSIN ATPASE MECHANISM IN SKELETAL MUSCLE FIBERS

Y.E. Goldman, Department of Physiology, University of Pennsylvania, Philadelphia, PA U.S.A.

Transformation of metabolic energy into mechanical work by muscle is accomplished by a cyclic interaction between myosin and actin in the contractile filaments driven by hydrolysis of ATP to ADP and orthophosphate (P_i). Scheme 1 shows the sequence of reactions which occur when isolated actomyosin splits ATP in solution.



Where M = myosin; A = actin

Our working hypothesis is that the sequence of reactions in a contracting muscle fiber is similar to Scheme 1 but regulation of some of the reactions may be altered by mechanical force generation and filament sliding. We have developed several new techniques to test this hypothesis.

Mammalian single skinned muscle fibers were put into a rigor contraction (A.M) by removing ATP. The medium contained "caged ATP", an inert compound that can be photolyzed by a pulse of ultraviolet (347 nm) laser light, to ATP and a leaving group. The step increase in ATP concentration within the fiber relaxed the rigor tension via reactions 1 and 2. These steps are rapid, independent of Ca^{2+} , and similar in rate to the corresponding reactions in experiments with the solubilized proteins.

The kinetics of reactions 3, 4 and 5 were found to be rapid compared to the overall cross-bridge cycle in photolysis experiments with Ca^{2+} present. Reaction 5 (P_i release) may be reversible in a muscle fiber whereas P_i does not readily bind to isolated actomyosin. This result suggests that cross-bridges in the A.M.ADP state are under more mechanical strain than A.M.ADP. P_i . Caged ATP photolysis experiments in the presence of ADP relate to reaction 6. ADP binds more tightly to muscle fibers than to isolated actomyosin apparently because ADP release from A.M.ADP (forward reaction 6) is much slower in fibers.

Reaction 3 was probed in muscle fibers by measuring the extent of oxygen exchange between bound product P_i and solvent labelled with the stable isotope, ^{18}O . In the absence of Ca^{2+} , there was a high degree of incorporation of solvent oxygen atoms into the product P_i indicating that reformation of M.ATP from M.ADP. P_i (reversal of reaction 3) occurs more rapidly than P_i release from M.ADP. P_i (reaction 7). In the presence of Ca^{2+} , much less ^{18}O exchange occurred suggesting that P_i release via reactions 4 and 5 occurs more rapidly than reversal of step 3.

We are improving our understanding of the relationship between the chemistry and mechanics of muscle cross-bridges. Several of the intermediate reactions, namely ATP binding, cross-bridge detachment, ATP hydrolysis, and cross-bridge reattachment occur similarly in muscle fibers as with the isolated proteins. Other reactions, namely release of P_i and ADP from the actomyosin-products complex, have very different kinetics in the fibers. This difference suggests that the product release steps are closely coupled to the force generation and control of physiological contractions. Supported by NIH grants HL15835, AM26846 and AM00745 and by MDA.

Symposium on Cross-Bridge Mechanisms and Muscle Contraction

MEASURING THE ORIENTATION AND MOTION OF MUSCLE CROSS-BRIDGES USING PARAMAGNETIC PROBES R. Cooke, M. Crowder and D. Thomas, Department of Biochemistry & Biophysics, University of California, San Francisco, San Francisco, CA 94143, IBM Instruments, San Jose, CA 95110, Department of Biochemistry, University of Minnesota Medical School, Minneapolis, MN 55455.

Current theories of muscle contraction envision a cyclic interaction in which force is generated by a change in orientation of myosin during its powerstroke. Paramagnetic probes (nitroxide spin labels) provide an excellent means to test this hypothesis since the angular distribution of the probes can be determined from EPR spectra and their rotational motion can be measured from saturation transfer (ST-EPR) spectra. We have used spin labels specifically attached to a reactive sulfhydryl on the myosin head in glycerinated rabbit psoas muscle to examine rigor, relaxed and contracting muscle fibers.

The EPR spectra of probes attached to the myosin heads of rigor fibers show that the probes are highly ordered with respect to the fiber axis and that the probes are rigid on the millisecond time scale. In relaxed fibers there is a random distribution of probe orientations, and rotational motion in the 1-10 microsecond time range. Similar disorder and mobility is observed for isolated myosin filaments and for non-overlap regions of stretched fibers, indicating that the myosin heads in relaxed fibers are detached from the actin filaments. We conclude that the myosin heads in relaxed fibers are executing large angle ($>90^\circ$) Brownian rotation in microseconds.

Addition of both ATP and calcium to fibers produces isometric contraction and spectra which consist of a superposition of the spectra obtained in rigor and relaxation. Approximately 20% of the myosin heads have probes oriented at the same angle as rigor muscle, and the probes on the remaining heads are highly disordered. ST-EPR spectra show that about 20% of the probes are rigid while 80% are undergoing Brownian rotations identical to probes in relaxed muscle. This observation supports the conclusion that the disordered fraction of probes (~80%) are on myosin heads that are not attached to actin. These EPR results have one simple interpretation: during the contractile cycle the myosin head spends approximately 80% of its time detached from actin and 20% of its time attached with probes at a fixed orientation. During isometric contraction, attached myosin cross-bridges are most probably distributed throughout the powerstroke. Thus during the powerstroke the spin probe does not undergo a change in orientation.

Force could be generated by the rotation of one domain of myosin while a second domain containing the probe remains rigidly attached to actin. Alternatively, some region of the myosin molecule could shorten during the powerstroke. The first hypothesis could be defined more precisely if we knew the position of the probes on the myosin head. Recently fluorescence energy transfer has shown that both the reactive sulfhydryl and the nucleotide site on myosin are distant (5nm or greater) from probes on actin (Takashi, 1979, Trayer et al, 1982 dos Remedios and Cooke, in press). Thus a rather large portion of the myosin head $>50\%$ does not change orientation during the powerstroke.

Recently a spin-labeled analog of ADP (SL-ADP) with the label attached to the 2' or 3' position of the ribose ring has been shown to bind in an oriented fashion to the myosin heads of rigor fibers. Relaxation of the fibers by addition of Vanadate induces disorder in the spectra of the analog. The orientation of the analog is not altered by the application of tension to rigor fibers. In these respects the probes on the nucleotide mimic those attached to the reactive sulfhydryl.

Supported by grants from the USPHS AM30868, GM27906 and AM 00051 and from the NSF PCM-8004612.

Tuesday 31 July

Unicorn Hotel-Trident Suite 14.00-17.00

Symposium on Education in Biophysics

NEW TRENDS IN THE INSTRUCTION OF BIOPHYSICS

M. Anbar, Department of Biophysical Sciences, State University of New York at Buffalo, Faculty of Health Sciences, 118 Cary Hall, Buffalo, New York, U.S.A.

Taking the situation of Biophysics in the universities in the United States into consideration, it is concluded that more relevant courses must be offered to the undergraduates and medical students.

Offering courses in applied Biophysics to make Biophysics a more attractive subject for graduate students does not mean discontinuance of conventional specialized graduate courses on a variety of fundamental biophysical topics. In fact, offering thematic undergraduate courses and applied biophysics courses is expected to result in an increased enrollment in specialized fundamental biophysics courses.

Tuesday 31 July

Unicorn Hotel-Trident Suite

14.00-17.00

Symposium on Education in Biophysics

BIOPHYSICS TEACHING FOR STUDENTS FROM DEVELOPING COUNTRIES - S.Mascarenhas, Bio physics Lab., Inst. Phys. and Chem., CP 369, S.Carlos, SP, 13560, Brazil.

The teaching of biophysics for students from developing countries is important for several reasons: 1) Biophysics is an interdisciplinary area and interdisciplinarity is an important facet of science for development; 2) Biophysics has both basic and applied possibilities thereby constituting a highly desirable activity in third world countries of different stages of development; 3) In many developing countries scientific activities in Physics have evolved through highly abstract aspects in particular attractive for the best young scientists. Biophysics, with its great amplitude and strong motivation constitutes an excellent attraction and alternative for physicists. In this paper we want to report on our experience for approximately 10 years in Brazil, Mexico and other Latin American countries on the implantation of biophysics for physicists as contrasted to "physiological" biophysics. This experience has been supplemented in the last 3 years with our activities as Director of Biophysics and Medical Physics Colleges at the International Center for Theoretical Physics (ICTP) in Trieste, an Unesco and AIEA institution. It was indeed very interesting that Prof. Abdus Salam, Nobel laureate 1979, in the field of elementary particle physics, gave full support to Biophysics programme for developing countries which is now a permanent activity of the ICTP. Participants come from all over the world, Asia, Africa, Latin-America, Oceania, Middle-East. With this experience we have found that the teaching of biophysics for developing countries present particular aspects that we summarize below:

1) At the present stage the teaching of biophysics at the graduate or post-doctoral level is the most important for developing countries where there is practically no tradition of biophysics particularly among physicists.

2) The teaching of biophysics at Institutions of non-biological areas such as Institutions or Schools of Physics, Chemistry and Engineering is extremely important not only because it is an area of great potential in view of inter-disciplinarity but because teaching of biophysics in many countries is connected to physiology or at most biochemistry and normal resistance to change to modern molecular physical aspects of biophysics is encountered.

3) The teaching of biophysics in optional courses at the undergraduate level is an important strategy for introducing biophysics from research groups centered around this new area. In fact it is our personal view that the teaching of biophysics has to come together with research motivation. This way active research groups are in a most favoured position for the teaching of biophysics. Teaching of biophysics without research motivation in particular in developing countries is faced with the dangers of alienation and lack of creativity.

4) An extended concept of biological physics encompassing molecular biophysics and medical physics is very important for the Third World. So it is our contention that Biophysics (microscopic) and Medical Physics (phenomenological) are two complementary areas though diverse techniques of teaching will have to be applied to both.

The teaching of biophysics for biological oriented institutions should in our view receive the new winds of physical biophysics and at the same time collaborate in such a way that the bio in biophysics is a reality and not only a prefix. In our contribution we plan to discuss curricular strategies we have adopted for the teaching of biophysics according to the lines broadly outlined above.

Tuesday 31 July

Unicorn Hotel-Trident Suite

14.00-17.00

Symposium on Education in Biophysics

BIOPHYSICS EDUCATION IN THE MEDICAL SCHOOLS IN DENMARK

Jens G. Nørby, Institute of Biophysics, University of Aarhus, DK-8000 Aarhus C, Denmark.

The teaching of physics and biophysics in two of the medical schools in Denmark is organized traditionally with physics in the first year and biophysics and physiology later. The third school in Aarhus has no physics course, but the biophysics course in the first year (the main topic of this communication) is based on high school (college) physics, and is custom-designed to provide a quantitative approach to biology and physiology. This is reflected in the selection of subjects taught. The course consists of 24 modules, each with a lecture and a small-group session with problem solving. The problems have the form of general physiology "case stories" designed to develop and test the students ability a) to identify a problem, b) select the relevant information, and c) apply physical and mathematical skills in solving the problem. Examples of such "case stories" will be given.

Several educational obstacles are encountered during this course, e.g. the science background of the students starting the course is variable and often poor, and the fundamental importance of quantitative, scientific thinking in the medical profession is often not appreciated. The failure rate at the final test is therefore (?) quite high: 30-55%, so that more than a third of the students require more than one attempt to pass. It will be discussed how this situation may be ameliorated without loss of the objectives and the goals of the course.

Tuesday 31 July

Unicorn Hotel-Trident Suite

14.00-17.00

Symposium on Education in Biophysics

BIOPHYSICS AS A FIRST DEGREE COURSE - THE POSITION IN THE U.K.
A.C.T. North, Astbury Department of Biophysics, University of Leeds,
Leeds LS2 9JT.

What is biophysics? Is it a proper discipline in itself? And is it a proper subject for a first degree course? Collins English Dictionary defines biophysics as "the physics of biological processes and the application of methods used in physics to biology". Such a definition in terms of longer-established disciplines perhaps implies that it cannot stand by itself; but such an implication ignores the fact that no distinct boundary can be drawn between any sciences - modern chemistry would be unthinkable without methods such as spectroscopy and crystallography that originated in physics; modern physics would be nowhere without the logical and computational tools of mathematics. Our definitions of subjects are purely an operational convenience whose need arose when universities grew sufficiently large to require subdivision into departments of specified function and when modern styles of university teaching developed, with a need to define the scope of the knowledge expected of a graduand.

It therefore seems more profitable to attempt to answer the third of my questions and, in doing so, I would draw attention to the dual aspects of the subject implied by the dictionary definition quoted above. It is not sufficient to think of biophysics as "physics-with-biology", which loses the essence of the subject, which lies in the interplay between the parent disciplines. Paradoxically, in my view, it is the addition of a third parent, chemistry, which really provides the bridge that bonds together physics and biology - chemistry as the subject that is concerned with molecular structure and with the relationships between structure and function. I would myself be inclined to use Astbury's definition of "molecular biology" - it is predominantly three-dimensional and structural ... it must concern itself with genesis and function. What "the methods used in physics" show us of biological systems is most commonly their structures and modes of organization; and "the physics of biological processes", if it is to be understood thoroughly, must usually be interpreted in terms of structure at the atomic and molecular level.

An education for a biophysicist therefore ideally requires a basic understanding of four disciplines - physics, biology, chemistry and the mathematics that underlies all exact sciences. Biophysics courses can then draw together these disciplines, showing not only how the fundamental methods and laws of physics can illuminate and explain the properties of biological systems but also how the complexity of biological systems themselves stretch our physical methods and understanding, thus providing many of the growing points of contemporary physics. A university degree course in biophysics is not just an ideal preparation for research in one of the most exciting fields of science; it is a complete scientific education that provides a rare understanding of the essential unity of scientific knowledge.

Biophysics first degree courses in the U.K.:

Aberdeen: Chemistry degree with additional courses in Biophysics

East Anglia: Unit course structure in School of Biological Sciences

King's College London: Combined physics/biology degree with specialized biophysics course units

Leeds: Integrated scheme with Biophysics, Physics, Mathematics and Chemistry courses

York: Combined physics/biology degree with specialized biophysics course units

Keele: final year option courses in physics degree

Imperial College London: final year option courses in physics degree

Symposium on Education in Biophysics

FUNDAMENTAL ISSUES OF BIOPHYSICS EDUCATION

C. Sybesma, Biophysical Laboratory, Vrije Universiteit Brussel, Pleinlaan 2, Brussels, Belgium.

A discussion about education in biophysics should address a number of fundamental issues, such as the following :

(1) Can there be agreement on a description of what biophysics really is ? ;

(2) Who needs biophysics ? ;

(3) Is it possible to design a "standard curriculum" ? ;

(4) What is the significance of biophysics teaching in developing countries ?

(1). If one talks about education in biophysics, it seems obvious that one has to agree first about what biophysics is. This is not a trivial problem, as is clearly demonstrated by the fact that, comparing educational programs in different countries, there exists a wide variety of opinions about both the subject matter and approaches to teaching. A clear-cut definition of biophysics still is difficult to give. There are some who question the need for such a definition, arguing that approaches and methods used to solve biological problems determine whether, more or less by general consent, the research is biophysical ("probably any area in biology could qualify for biophysical research"⁺). It seems, however, that there might be some agreement about a description of biophysics as the approach to biology that considers biological systems as part of the physical universe.

(2). Biophysics teaching to students who want to become biophysicists is different from biophysics teaching to students being educated for professional careers. In the former case the education should comprise a complete curriculum. In the latter case there is no general agreement. Biophysics courses in medical, pharmaceutical, agricultural, etc... curriculae sometimes are controversial. It seems, however, that the inclusion of biophysics in such curriculae (for instance as part of, or partly replacing physiology courses) might contribute to a more scientific background in the professions involved. Biophysics for physics and (bio-)chemistry students in many schools is provided as a facultative and in some as a compulsory subject. The content of such courses depends to a large extent on who is teaching them. They should at least convey the notion that biophysics is a germane division of the physical sciences.

(3). A "standard curriculum" or a "standard introduction course", comprising all topics that are considered as indispensable seems, as yet, not to exist. Some guidelines about the design of such a curriculum could be given, but local circumstances, traditions and opportunities (availability of teachers in certain areas) largely determine how such a curriculum would look like. The contents of courses for professional curriculae also are difficult to generalize.

(4). In developing countries there is a primary need for professionally educated people. Biophysics, therefore, should be taught in courses as part of professional curriculae, if necessary by guest-teachers from developed countries. It seems not advisable to encourage such countries to set up prestigious biophysics research programs, although graduate programs (coupled to research projects, perhaps) in a few major universities or institutions may be favorable, in order to educate people to teach in smaller schools. The possibility of assistance from international bodies (IUPAB, UNESCO, --- ?) supporting such programs should be examined.

⁺) A.T. Quintanilha, CEDB symposium, Mexico-City, 1981

Symposium on Viruses

THE STRUCTURE OF THE INFLUENZA VIRUS HA GLYCOPROTEIN AND ITS RECEPTOR BINDING, ANTIGENIC VARIATION, AND MEMBRANE FUSION ACTIVITIES

D. C. Wiley, M. Knossow, W. Weis and J. J. Skehel, Department of Biochemistry and Molecular Biology, Harvard University, 7 Divinity Avenue, Cambridge, MA, USA

The influenza virus haemagglutinin, the major membrane glycoprotein in the virus surface, is active in initiating infection. The HA binds the virus to a sialic acid-containing cell surface receptor of a target cell. Mutant viruses have been selected (Rogers et al. 1983, *Nature* 304, 76) with altered receptor specificity which correlates with single amino acid substitutions in the haemagglutinin. This allows us to identify the receptor binding site. Wild-type and mutant HA crystals with bound trisaccharide receptor analogs are being studied to a 3 Å resolution by X-ray diffraction difference Fourier techniques to determine how a single amino acid substitution causes the change in receptor specificity.

After the cell endocytoses the virus, the low pH of endosomes triggers the HA molecule to fuse the viral membrane to the cellular membrane which effects transfer of the viral nucleocapsid into the cytoplasm. The haemagglutinin has been observed to undergo a conformational change at the pH optimum for its membrane fusion activity (Skehel et al. 1982, *PNAS* 79, 968). The conformational change exposes a hydrophobic "fusion peptide" which was "buried" by the neutral pH conformation of the HA. One interpretation of these observations is that the haemagglutinin becomes anchored into the cell's membrane by the hydrophobic "fusion peptide" and therefore becomes a membrane protein of two membranes: that of the cell and that of the virus.

Neutralizing antibodies generated during influenza infections are directed against the HA antigen. Antigenic variation in the HA is responsible for the familiar re-occurrence of epidemics of respiratory disease in humans. By analyzing the amino acid sequence of HA's from successive epidemics and by selecting single amino acid substituted antigenic mutants by growth in monoclonal antisera, the locations of antibody binding sites are being mapped on the HA surface. The structure of an antigenic variant has been determined to 3.0 Å resolution to confirm one proposed site. The current hypothesis is that a small number of regions on the HA surface must receive mutations to generate a novel epidemic strain of the virus.

Symposium on Viruses

STRUCTURAL STUDIES ON SOME ANIMAL VIRUSES WITH NEUTRON SCATTERING

B. Jacrot, European Molecular Biology Laboratory, Grenoble, France.

Neutron scattering from virus solutions provides information on the average radial distribution of the chemical components (Proteins, Nucleic acid, lipids) inside the virion (review in Comprehensive Virology 17 (1981)). It also permits a determination of the molecular weight of the virus. The method has been applied in recent years to several animal viruses, in particular Influenza virus, Adenovirus and Semliki forest virus. The strategy to study these complex viruses is somewhat different from that used previously for the more simple and smaller plant viruses. Neutron experiments provide the same amount of data (but to a lower resolution), but the description of the virion requires more parameters; for instance in an enveloped virus one must localize the position of the lipid layer, and try to determine its thickness and protein content. Moreover the chemical composition is often not completely known. So the neutron data are more useful if combined with chemical analysis (Amino acid analysis, Phosphorus content) other physical methods (Measures of S, D, v, X rays) and electron microscopy. Such an association of techniques has been applied to the above mentioned viruses.

For Adenovirus, the analysis gives a distance between Hexons $\sim 100\text{\AA}$, a figure confirmed by X ray scattering from solution and electron microscopy in amorphous ice. Neutron data have also been collected with mutants ts 112 and ts 104. Comparison with the data from the native virus helps to localize some of the viral proteins (e.g. protein VI). Some isolated capsid proteins have also been studied, in particular the penton base, which was shown to be a trimer. The fibre has been crystallized, preliminary X ray data suggest that it is a dimer.

For Semliki forest virus, the molecular weight is determined by neutron scattering to be about 46×10^6 , a value confirmed by combination of S and D. Electron microscopy indicates clearly that the capsid is organized with a triangulation number $T=4$, which would correspond for a classical icosahedral shell to a molecular weight of 60×10^6 . The conclusion is that the capsid is organized in another way and is possibly made of 42 pentamers. The nucleocapsid is shown to be organized like a plant virus, possibly with a triangulation number $T=3$. The lipid layer is centered at 230\AA , but the model fit on neutron data does not allow an unambiguous determination of its thickness. The same ambiguity is found with influenza virus. However with Semliki one can determine the integrated scattering density in that layer and deduce a rough estimate of the protein content.

With all these viruses excellent agreement with the data can be obtained with a three or four shell model. This is the limit of the method and attempts to obtain a more detailed description are meaningless.

Symposium on Viruses

ENVELOPED VIRUSES AS TOOLS TO STUDY CELL SURFACE POLARITY IN EPITHELIAL CELLS.

K. Simons, S. Fuller and K. Matlin

European Molecular Biology Laboratory, Heidelberg, W. Germany.

Enveloped viruses have proven to be useful tools to study the mechanisms of membrane assembly in the animal cell. These viruses are simple in their make-up and hence are very well characterized. After infection, the protein-synthesizing machinery of the host cell is programmed by the viral RNA to make viral proteins exclusively and these include the viral surface glycoproteins. The net effect is the same as if the cell would divert most of its protein-synthesizing capacity towards the making of only one or two species of its own plasma membrane glycoproteins.

Our present studies are directed towards elucidating the mechanisms of establishment of cell surface polarity in epithelial cells using enveloped viruses as tools. We are studying the MDCK cell line which grows in culture as an epithelium. The plasma membrane of these cells is like all epithelial cells polarized into two domains, the apical surface membrane facing the extracellular medium and the basolateral plasma membrane separated from the other domain by a junctional complex encircling the apex of the cell. Each surface domain has a characteristic set of proteins. Rodriguez-Boulan and Pendergast (1980) have shown that in MDCK cells infected with enveloped viruses the newly synthesized viral membrane glycoproteins are inserted into one or the other surface domain. The influenza virus glycoproteins are distributed mainly to the apical domain, while the vesicular stomatitis virus G protein is inserted primarily in the basolateral domain. To establish an experimental system in which both surface domains of the MDCK cells are accessible to experimentation, we have grown the cells on nitrocellulose filters. Using filter-grown cells we have studied the transport of the virus glycoproteins to the cell surface domains. Our results suggest that sorting occurs intracellularly after terminal glycosylation has taken place.

ReferenceRodriguez-Boulan, E. and Pendergast, H. (1980) *Cell* 20, 45-54.

Plenary Lecture By E.H. Land

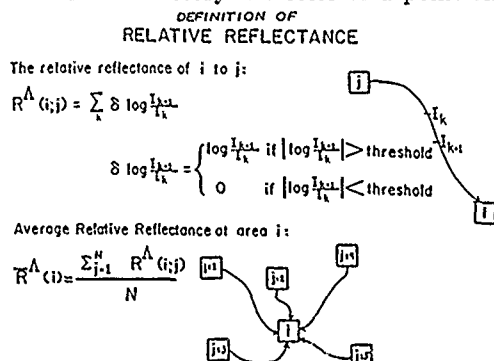
CONTINUING STUDIES IN RETINEX THEORY

E.H. Land, The Rowland Institute for Science, 100 Cambridge Parkway, Cambridge, Massachusetts, USA.

From the point of view of retinex theory the classical term, color constancy, derives from the attribution of visual color to an incorrect causal system. The classical causal system is inherently based on the ratios to each other of three fluxes at long, middle, and short wavelengths of the visual spectrum. Since it is generally observed that the colors of objects tend to change very little with variation in these ratios, there is a manifest inconsistency between the theory and the observation. This inconsistency has led to the concept of color constancy.

Clearly an approach is called for which predicts that color should not change significantly with the changes in the ratios of long, middle and short wave illuminating fluxes. If an approach can be found which not only eliminates color constancy as a problem but also at the same time predicts the color in any area in the field of view, then we will have gone a long way to a viable theory of color vision. Retinex theory represents our attempt to generate such an approach.

In retinex theory the color of a point on any object can be predicted from a computed relationship between the radiation from that point and the radiation



from all the other points in the field of view. To predict the perceived color of an area in any visual scene, the computation shown here is broken into unit areas. The relative reflectance, R , of the target area, i , is computed with respect to some other area, j , along a path drawn between the two areas using the formula shown, where Λ designates the particular waveband (long, middle or short) and I is the intensity. The threshold operation on the ratios

along the path is included in order to remove the effects of non-uniform illumination over the scene: variations gradual enough to be below threshold are dropped out. All others are considered significant and contribute to the computation. The average of many such computed relative reflectances is taken in order to determine the value we define as average relative reflectance at area i . Conceivably, this average of relative reflectances, (not fluxes) could be taken over every area in the visual field, but as few as 100 to 200 is usually sufficiently accurate. The average of relative reflectances is taken over areas from the entire visual field and not just those nearby; experiments indicate there may be nearly as much contribution from distant areas as nearby ones. As the above computation is carried out three times, once for each of the three wavebands, three numbers (designators) become associated with each unit area. These designate a point in a three-dimensional color space, a point which proves to be invariant with large changes in quantity and composition of illumination of the field of view. Experimentally it is found that if two widely separated areas in any visual scene are the same color (even when, because of non-uniform illumination, the wavelength composition reflected from them may be very different), they will be represented at the same point or closely adjacent points in this color space. Applications of the algorithm to various physiologies by co-ordinate transforms will be discussed.

The lecture will review the theory and experiments described in a paper entitled "Recent advances in retinex theory and some implications for cortical computations: Color vision and the natural image" (*Proc. Nat. Acad. Sci., USA*, Vol. 80, pp. 5163-5169, August 1983). Most of the experiments described in that paper will be shown as lecture demonstrations. Recent work by the speaker and colleagues will be illustrated by experiment: in particular (1) a device called "optimouse," which while moving across the surface of the Mondrian calculates average relative reflectance and (2) Mondrian experiments with the goldfish as a retinex animal.

Tuesday 31 July Congress Centre-first floor. Posters 001-006

Posters on Polymorphism and Structural Transitions in Nucleic Acids

001

COMPLEX FORMATION BETWEEN SANGUINARINE AND DEOXYRIBONUCLEIC ACID

M. Maiti, K. Nandi and K. Chaudhuri, Indian Institute of Chemical Biology, Calcutta - 700 032, India.

The interaction of sanguinarine, an antitumour alkaloid, with calf thymus DNA has been studied by spectrophotometry, thermal melting, viscosity, spectrofluorimetry and circular dichroism. DNA forms a complex with sanguinarine producing thereby a quenching and a bathochromic shift of the alkaloid absorption pattern. The binding isotherm was a non-linear one indicating involvement of more than one binding process in the formation of the sanguinarine-DNA complex. The fluorescence of sanguinarine bound to DNA is quenched and can be decreased by sodium, magnesium and calcium ions. The alkaloid stabilizes DNA against thermal strand separation by a significant degree. It increases the viscosity of sonicated rod-like DNA fragments and induces an unwinding-rewinding process of covalently closed superhelical DNA like ethidium bromide. Circular dichroism measurements show that the alkaloid induces conformational changes of DNA. The results indicate that sanguinarine interacts strongly with DNA by a mechanism of intercalation which probably accounts for its reported antitumour activity.

003

DNA CONDENSATION: EFFECTS OF CHARGE DENSITY

J.A. Benbasat, Dept. of Biochemistry, Univ. of British Columbia, Vancouver, B.C., Canada V6T 1W5

Bacteriophage Φ W14 DNA carries a +2 charged base, α -putrescinylnthymine. The low average charge density may affect the collapse of this DNA facilitating its exceptionally dense packaging in Φ W14. I used total intensity light scattering to determine the critical concentrations (cc) of spermidine (spd) required to induce collapse *in vitro* and quasielastic light scattering to compare the dynamics of condensed wild type and mutant Φ W14 DNAs (charge spacings 1.3-2.2Å) to T4 phage DNA (1.7Å). In accord with the counterion condensation theory of Manning (Quart. Rev. Biophys. 11 (1978)), DNAs of lower charge density require higher counterion cc; the diameters of the toroidal condensates which they form vary marginally. Specific ion effects were probed by substituting hexamine cobalt (hc) for spd. Hc induces collapse at one sixth the spd cc and condensates are 30% smaller (1100Å vs 775Å), except for wild type Φ W14 DNA which forms hc- and spd-induced condensates of similar diameters. Collapse occurs, again excepting wild type Φ W14 DNA, when ~80% of the charges on each DNA are neutralized by territorially bound spd. Thus, the driving force for condensation depends on charge density, and charge distribution may affect the critical degree of neutralization. Lowering the charge density by covalent modification beyond a threshold (as in wild type Φ W14) may result in the compression of the DNA double helix allowing more information on a genome the packagable length of which is determined by the encapsidation mechanism.

005

Quaternary Ordering of DNA by $\text{Co}(\text{NH}_3)_4\text{Cl}_2$. Yong A. Shin, Susan L. Ferrell and Gunther L. Eichhorn, Laboratory of Cellular and Molecular Biology, NIH/NIH, Baltimore, MD 21224.

The quaternary ordering of DNA is conveniently studied by CD because the anisotropic nature of DNA compaction gives rise to a large increase in the magnitude of the CD: the ψ effect, which can give (-) or (+) CD peaks. We have previously shown that metal ions can manipulate the transition $\psi(-) \rightleftharpoons \psi(+)$ (Eichhorn *et al.* (1981) *Biomolecular Stereodynamics*, II, 185). We now find that $\text{Co}(\text{NH}_3)_4\text{Cl}_2$ can induce a conformational change in polyd(AT)-polyd(AT) from $\psi(-) \rightarrow \psi(+)$. A critical amount of the cobalt complex is required to bring about this transition, and this concentration varies with the amount of NaCl present.

The cobalt-induced ψ effect can be either (+) or (-), depending on the reaction temperature, and high temperature leads to $\psi(-)$. The transition between (-) and (+) is totally reversible by temperature control. The temperature at which ψ crosses 0 is linearly dependent on the salt concentration, varying from 16° in the absence of salt to 31° in 50 mM NaCl. Beyond 150 mM, no ψ formation occurs.

$\text{Co}(\text{NH}_3)_4\text{Cl}_2$ produces no ψ effect with natural DNA, polyd(CA)-polyd(GT) and polyd(AT)-polyd(T). It produces only $\psi(+)$ with polyd(GC)-polyd(GC), and $\psi(-)$ as well as $\psi(+)$ with polyd(AT)-polyd(AT). This reagent is much more sequence-specific than polyethyleneoxide which induces the $\psi(-)$ form with all DNAs. In this respect it somewhat resembles lysine-alanine copolymers that are also capable of distinguishing among DNAs with different sequences when inducing quaternary ordered structures (Shin and Eichhorn (1984), *Biopolymers* 21, 375).

002

POLYMORPHIC STRUCTURES OF DNA INVOLVED IN GROWTH AND REPAIR OF BACTERIOPHAGE Φ X 174.

R. K. Poddar, A.R.Thakur, S.Pal and S.K.Mukherjee Biophysics Section, Physics Dept., Univ.College of Science, 92 A.P.C.Road, Calcutta, India.

The biological roles of the various unusual structural forms of DNA, observed under *in vitro* conditions, are enigmatic in most cases. We report some of our investigations on the functions of the polymorphic forms of Φ X DNA during its repair replication within the host cells. A damaged Φ X genome on its entry into the host cell is unable to produce efficiently, a superhelical circular duplex structure (RFI) and thus fails to give rise to viable progeny. This block in the production of the RFI structure may be partially removed under conditions of 'SOS repair' by the host cells. However, all RFI structure generated under such conditions do not apparently lead to production of viable progeny, suggesting possible macroheterogeneity amongst them. Experimental evidence will also be presented to show that the gene A product of Φ X 174 is able to release negative superhelical twists of the host DNA leading to reduction of its transcriptability.

004

THE BIOLOGICAL SIGNIFICANCE OF G.T/G.U MISPAIRING IN NUCLEIC ACID SECONDARY STRUCTURES

U.R. Müllert and W.M. Fitch, Department of Microbiology, East Carolina University School of Medicine, Greenville, NC 27834, and Department of Physiological Chemistry, University of Wisconsin, Madison, WI 53706.

We have computed the expected distribution of hairpin like secondary structures with small loops (3-20 bases) and uninterrupted stems and compared that to the distribution observed in the complete genomes of seven DNA viruses from animals, plants and bacteria, as well as a bacterial plasmid. The formation of G.T mismatches in the stems of these structures was allowed. Furthermore we have analyzed the distribution of such structures along the genetic maps of these genomes, specifically around the start sites of known genes. Our data reveal that mismatch containing structures with stem lengths exceeding eight base-pairs are overrepresented and non-randomly distributed, but to a much lesser degree than perfect structures of equal size. From this we deduce that G.T/G.U containing secondary structures in nucleic acids are biologically less significant than perfect ones.

006

A TIME RESOLVED FLUORESCENCE STUDY OF DAPI BINDING TO POLYNUCLEOTIDES.

P. Cavatorta, L. Masotti, A. Szabo*, M. Barcellona*, M. Avitabile*, Inst. Biol. Chemistry, Univ. Parma, Via Gramsci 14, Parma, Italy, * Div. Biol.Sci., Nat. Res. Council of Canada, Ottawa K1A 0R6, Canada, * Inst. Biol. Chemistry, Univ. Catania, Catania, Italy.

At phosphate/dye (P/D) ratio >30 the quantum yield of 4',6-diamidino-2-phenylindole.2HCl (DAPI)-DNA and DAPI-poly(d(A-T)), complexes were found to be 0.62, and 0.66, respectively. Contrary to earlier reports a fluorescence enhancement of DAPI-(d(G-C)) complexes was observed with a quantum yield of 0.22. Time resolved fluorescence measurements of complexes with a P/D ratio of 150:1 indicate that there were three fluorescent components in DAPI-DNA complexes with lifetimes of 3.86 ns, 1.79 ns, and 0.13 ns. In DAPI-poly(d(A-T)) complexes the lifetimes were 3.91 ns, 1.20 ns, and 0.11 ns. Also three components with lifetimes of 3.98 ns, 0.87 ns and 0.12ns, were found in DAPI-poly(d(G-C)) complexes. At low P/D ratios (<5) another binding form of DAPI was observed which was assigned to the interaction of one or more molecules of DAPI with one previously bound to DNA. It is concluded that DAPI does not exhibit A-T binding specificity and that at the high P/D ratios there are two types of binding having similar binding constants.

Tuesday 31 July Congress Centre-first floor. Posters 007-012

Posters on Polymorphism and Structural Transitions in Nucleic Acids

007

RESONANCE RAMAN SPECTROSCOPY OF Z-DNA

A. Laigle, B. Jollès and L. Chinsky, Institut Curie, 11, rue Pierre et Marie Curie, 75005 PARIS.

Poly(dG-dC).poly(dG-dC) in H₂O and D₂O at low salt concentration (B form) and at high salt concentration (Z form) has been studied by Raman resonance spectroscopy using two excitation wavelengths: 257 nm and 295 nm.

As resonance enhances the intensity of the lines in a proportion corresponding to the square of the molar absorption coefficient, the intensities of the lines with 295 nm wavelength excitation are enhanced of an important factor during the B to Z transition.

By comparison with the U.V. resonance Raman spectra of DNA, we conclude that resonance Raman spectroscopy allows one to characterize the B to Z transition from one line with 257 nm excitation wavelength and from three lines with 295 nm excitation. The conjoint study of these four lines should permit to observe a small fraction of base pairs being in Z form in a DNA.

008

Application of Homo- and Heteronuclear 2D NMR Methods in Structural Studies of Synthetic DNA-fragments

M. Leupin, M.H. Frey, M. Rance, S. Hyberts, W.A. Denny* and K. Wüthrich,

Institut für Molekularbiologie und Biophysik,

ETH-Hönggerberg, CH-8093 Zürich, Switzerland

* Cancer Research Laboratory, Medical School,

University of Auckland, Auckland, New Zealand

NMR studies of DNA-fragments have recently gained renewed impetus through the availability of novel, efficient techniques for sequence specific resonance assignments for hydrogen and phosphorous atoms, and for investigations of DNA solution conformations. We explore further improvements of the methods used for both resonance assignments and spatial structure determination. The following oligodeoxyribonucleotides were synthesized by the phosphotriester method in liquid phase: dTpTp, dGpCpApTpGpC, dGpCpGpTpApApCpGpC and dGpCpApTpTpApApTpGpC. These DNA-fragments were studied in the single stranded and/or duplex form by ¹H and ³¹P NMR spectroscopy. The NMR techniques used include homonuclear double quantum filtered-COSY, relayed-COSY, NOESY, and various ¹H-³¹P heteronuclear two-dimensional experiments. For all the above compounds sequence-specific resonance assignments were obtained for all hydrogen atoms, except for some H5' and H5'' sugar protons. Work is in progress using these resonance assignments for studies of the solution conformations of the DNA-fragments and of conformational rearrangements induced by sequence modifications or by intermolecular interactions with a variety of substrates.

009

ROLE OF REC GENES IN EFFICIENT GENETIC TRANSFORMATION WITH CHIMERIC PLASMIDS IN HAEMOPHILUS INFLUENZAE

Vasudha P. Joshi and N.K. Notani

Biology & Agriculture Division, Bhabha Atomic Research Centre, Trombay, Bombay 400 085, India

A high efficiency vector pJ1-8 was used to clone nov (resistance to novobiocin) gene of *H. influenzae*. Three isolates were extensively characterized. Restriction analysis indicated that nov marker is carried on a 5.5 kb BamHI fragment. None of the clones contained linked *str^r* marker. In all three isolates, the plasmid segment carries the *amp^r* marker and the chromosomal insert carries the *nov^r* marker. Transformation with all the chimeric plasmids is differential. Ratio of *nov^r*: *amp^r* transformants is about 20:1 or more and *nov^r* *amp^r* is always a fraction of *amp^r*. *rec* genes make a profound difference for transformation with the chimeric plasmids and in *Rec⁻* strains transformation is lower by two to four orders of magnitude. Input DNA undergoes degradation, fragmentation and recombination. Correlation between the molecular and genetic events will be shown.

010

MOLECULAR BASIS OF DRUG-NUCLEIC ACID INTERACTIONS

Nitish K. Sanyal, M. Roychoudhury and R.P. Ojha

Department of Physics, University of Gorakhpur, Gorakhpur-273001, INDIA

Even though extensive crystallographic and pharmacological studies of various drug-nucleic acid bindings have been reported but the mechanism and binding sites of molecular level is yet not understood. Stacking energies between the consecutive pairs are evaluated. CNDO atomic charges and dipoles have been used for computing the interaction energies. On the basis of these studies, we have developed a model for intercalation of drugs and their binding with the nucleic acid.

Interaction energies have been computed upto the second order and they consist of electrostatic, polarization, dispersion and repulsion terms. In this, intercalation and binding in the deep and shallow grooves of the DNA have been taken into account. This method is applied to some of the antibiotic drugs e.g. daunomycin, actinomycin D and Ethidium Bromide.

011

ADENINE SINGLE CRYSTALS AS MODELS FOR HORIZONTAL AND VERTICAL INTERBASE INTERACTIONS IN POLYNUCLEOTIDES

V. Prosser, V. Baumruk, O. Jelinek, J. Plasek, M. Pudlak, J. Stepanek, J. Zachova, Institute of Physics, Charles University, Prague, Czechoslovakia.

Single crystals of adenine ionic salts were grown from saturated solutions in order to obtain suitable structure models for horizontal (hydrogen bonds) and vertical (stacking) interactions between adenine residues. Combining several optical methods, the effects of different protonation and hydrogen bonds upon vibrational and electronic characteristics of adenine both in ground and excited states were investigated. The intensities and directions of *S*₀ - *S*_n transitions in adenine protonated at N1 and N7 were determined by polarized perpendicular specular reflection, the correlation between the changes of some adenine skeletal vibrations and the type of protonation was found by Raman spectroscopy. Having compared structure peculiarities of adenine crystals we concluded that their excimer luminescence is due to the interaction of polar amino group with the adjacent polarizable adenine ring as in the ground state stacking. The simple monopole-monopole estimate for the excited state interaction between stacked adenine molecules is also given.

012

Z-TRANSITION OF COVALENTLY CLOSED CIRCULAR DUPLEX (RF I) STRUCTURE OF pBR 322 DNA AT HIGH pH.

A.R. Thakur and C.R. Santra

Biophysics Section, Physics Department, University College of Science, 92 A.P.C. Road, Calcutta, INDIA.

Denaturation of covalently closed circular duplex (RF I) structure of pBR 322 DNA at high pH yields a collapsed state (RF I_c) having greater electrophoretic mobility on agarose gel even after neutralization. This form allowed less Ethidium Bromide to be intercalated but yielded a Circular Dichroic spectrum which had reduced magnitude of both positive peak at 273nm and negative peak at 245nm. Such CD spectra can arise as a possible mixture of B- and Z-DNA. S. nuclease digestion analysis show that RF I_c is nicked to RF II relaxed form at a faster rate than RF I, suggesting that the B-Z junction of RF I_c offers a favourable site. However on prolonged incubation equivalent amount of linear duplex (RF III) is not obtained from RF I_c as compared to RF I. Similarly digestion by Bam HI shows RF I_c as well as RF II obtained from it to be poorer substrates compared to usual RF I and RF II structures. The double strand nicking by the endonucleases is perhaps hindered by the presence of Z-segment.

Tuesday 31 July Congress Centre-first floor. Posters 013-018

Posters on Polymorphism and Structural Transitions in Nucleic Acids

013

STRUCTURAL STUDIES OF d(CCGG) AND d(GGCC)

Kumud Majumder and Samir K. Brahmachari,
Molecular Biophysics Unit, Indian Institute of
Science, Bangalore 560 012, INDIA.

The oligonucleotides d(CCGG) and d(GGCC), the restriction sites for *Hsp* I/Hpa II and *Bsu*/Hae III respectively, have been studied by circular dichroism (CD) spectroscopy. The CD spectra of d(CCGG) show it to have a different conformation in solution as compared to the A-DNA type conformation shown by the crystals of d(CCGG). Titration studies with spermine hydrochloride indicate that its presence in the crystallisation cocktail may be the possible reason for this difference. The d(CCGG) shows a strong negative CD band at ~285nm. However, salt and alcohol titrations rule out the possibility of a Z-type conformation. In a high salt solution, d(CCGG) shows a novel temperature dependent ordered to ordered structural transition. Such type of transition is not shown by d(GGCC). It is interesting to note that these two oligomers exist in intrinsically different conformations in solution, even though d(CCGG) and d(GGCCGGCC) have been shown to exist in similar (i.e. A-type) conformations in the crystalline state.

015

PICOSECOND SINGLE PHOTON FLUORESCENCE SPECTROSCOPY OF NUCLEIC ACIDS

R. Ritzler, F. Claessens & Gösta Lomakka, Department of Medical
Biophysics, Karolinska Institute, Stockholm, SWEDEN

Fluorescence spectroscopy of nucleic acids at room temperature has been limited by the short lifetimes of the excited states of purines and pyrimidines. Appropriate time resolution is provided by mode-locked synchronously pumped and frequency doubled dye laser pulses for the excitation of nucleoside fluorescence. With multichannel plate detectors of low transient time jitter (Hamamatsu R1565U) we have reduced the instrumental response time for single photon events to 40 ps. With a split beam instrument allowing simultaneous laser pulse and probe response detection and thus exact deconvolution, fluorescence lifetimes and rotational correlation times with uncertainties of 1-4 ps can be measured.

Time gated and background free fluorescence emission spectra of purine and pyrimidine ribo- and deoxyribonucleotides as well as of synthetic and natural DNAs were recorded at room temperature. They show emission maxima above 400 nm with a pronounced shoulder at 330 nm which is particularly pronounced with double helical structures. The lifetime spectra for various nucleotides were investigated and will be discussed in terms of singlet and triplet transitions as well as due to different conformations (stacking and hydrogen bonding) of purine and pyrimidine bases. Special references will be made to the emission and lifetime properties of modified nucleosides such as 7m-guanosine, mybutine and 2-aminoguanine.

017

TOPOLOGY OF THE TRANSITION OF DOUBLE HELICAL DNA

Asok Banerjee, Bose Institute, Calcutta, India.

The interconversion from right handed(R) to left handed(L) helical conformation in DNA is typified by the B-Z equilibrium in poly(dG-dC).poly(dG-dC), and is not strictly limited to alternating Guanine and cytosine sequences. This transition is well characterized now in solution from spectroscopic, electrophoretic, sedimentation and enzymatic measurements.

The versatile function of DNA, a deceptively simple molecule, lies in the enormous flexibility inherent in the DNA molecule^{2,3}. Yet to date neither the stereo chemical nature of drug binding to the Z-form, nor the molecular mechanism of the drug induced Z to B transition is well understood. To further our understanding in this paradigm, a model conformational analysis has been done with typical short repeating sequence DNA to assess the nature of the topological intermediate transitional conformation states. An interesting feature revealed that the base pairs in the transitional phase towards Z-DNA are turned around to a position 180° away from B-DNA position they have. Other interesting features revealed throw light on the structure function relationship of this molecule.

Reference: T.M. Jovin, F. Eckstein et al, *J. of Biomol. structure and dynamics*, Vol 1, p 60-65(1983).
2. H.M. Sobell, A. Banerjee, Cold spring har symp quant biol, 57, p 293-314(1983).
3. S. Aronoff, A. Banerjee et al, *J. Biomol. structure & dynamics*, 1, p 437-451(1983).

014

SPECTROSCOPIC STUDIES OF POLY(dA-dC).POLY(dG-dT) A, B, X AND Z CONFORMATIONS IN PRESENCE OF Na⁺, Cs⁺ AND Ni²⁺

J.A. Taboury, S. Adam, P. Bourtyre, J. Liquier and L. Taillandier, Laboratoire de Spectroscopie Biomoléculaire, Université Paris XIII, 74, rue Marcel Cachin, 93012 Bobigny Cedex, France.

The A, B, X and Z forms of Poly(dA-dC).poly(dG-dT) have been characterized by UV absorbance, circular dichroism and IR spectroscopy.

In high condensed phases, the IR spectra reflect in the case of Na⁺ the A and B form depending on the water content of the sample. The Z conformation has been observed in the presence of Ni²⁺. A new different IR spectrum is obtained in the case of Cs⁺, the corresponding geometry can be correlated to an helix belonging to the right-handed conformations.

In solution, CD results indicate that the polymer adopts a B conformation in the presence of Na⁺ and Ni²⁺, while the X conformation is observed at 6 M Cs⁺. The X and Z forms are shown to be different as the X → Z transition is followed in the presence of Cs⁺ + Ni²⁺.

The mechanisms involved in these processes are now investigated on other polynucleotide sequences.

016

THYMINE-NEIGHBOR BASE SHORT CONTACTS IN A-FORM DNA

Y. Takeda, Dept. of Food Sci., Kobe College,
Nishinomiya, Hyogo, Japan

An idea of thymine-neighbor base short contacts in A-form of DNA is proposed, which was found during molecular model building, to understand the nature of structural changes of double helical DNA.

To confirm that the unstable A-conformation needs the lateral interactions including those through some number of cross-bridges of tetramine between duplexes, X-ray studies on the precipitated complex of E.coli DNA with synthetic thermospermine were carried out by using the equipment at Univ. of Tokyo. This complex in fibers showed the ordinary transition to a crystalline A-form and yielded a semicrystalline B-form at 66% r.h., implying the good lateral interactions of the material in contrast to DNA-putrescine(diamine) complex. These are consistent with that tetramines have a strong effect of forming a cluster of cotton-like precipitates with DNA. DNA-spermidine complex in fiber showed the similar structural changes, although it tends to form dispersed aggregates. These short contacts owing to methyl group of thymine base are potentially of considerable biological interest in relation with the compaction of an isolated DNA.

018

CONFORMATION OF A STEM-LOOP STRUCTURE IN 16S RIBOSOMAL RNA

P.H. van Knippenberg and H.A. Heus, Department of Biochemistry, University of Leiden, Wassenaarseweg 64, 2333 AL Leiden, The Netherlands.

The RNA of small ribosomal subunits (16S RNA in bacteria) contains a conserved hairpin structure near its 3' end (1). Two neighbouring adenosines in the loop are dimethylated at the N⁶ position, except in kasugamycin-resistant bacteria where the methyl groups are lacking. We have isolated this section of 16S RNA from wild-type and kasugamycin-resistant *E. coli* and *B. stearothermophilus* using the bacteriophage colicin which makes a specific cleavage in the RNA. These "colicin fragments" were analysed by various techniques, including high-resolution proton NMR. The conclusions from these studies are that a conserved A-U/U-G junction in the stem represents a thermo-labile site in the helix (2,3). NOE experiments suggest that the U-G basepair is destacked from the A-U pair causing an irregularity in the stacking pattern. Comparisons of wild-type and mutant colicin fragments show, that dimethylation of the adenosines in the loop cause a destabilization of the helix proper. This is probably due to the stronger stacking tendency of m⁶Apm⁶A as compared to ApA.

Probing of the RNA conformation with base-specific chemical agents and with enzymes yielded results which agree very well with those obtained with physical methods.

1. P.H. van Knippenberg, J.M.A. van Krimpen & H.A. Heus (1984) *Nucleic Acids Res.* 12, 2595-2604.

2. P.H. van Knippenberg & H.A. Heus (1983) *J. Biomolec. Struct. and Dynamics* 1, 371-381.

Tuesday 31 July Congress Centre-first floor. Posters 019-024

Posters on Polymorphism and Structural Transitions in Nucleic Acids

019

REACTION OF CIS-DIAMMINEDICHLOROPLATINUM(II) AND DNA IN B OR Z CONFORMATION. M. Leng, J.M. Malinge and M. Ptak, Centre de Biophysique Moléculaire, C.N.R.S., 45045 Orléans cedex, France

The nature of the adducts and the conformational changes produced in poly(dG-m⁵dC).poly(dG-m⁵dC) by cis-diamminedichloroplatinum(II) (cisPt) have been studied. In the reaction of cisPt and B-DNA, the main adduct is bidendate and arises from an intrastrand crosslink between two guanine residues separated by a cytosine. This was deduced from the study of the compounds by thin layer chromatography after acid hydrolysis of the polymer. The platinated polymer is not digested by S₁ nuclease. The antibodies to Z-DNA bind to the platinated polymer with a smaller affinity than to poly(dG-br⁵dC).poly(dG-br⁵dC). The circular dichroism and the ³¹P RMN spectra differs from those of poly(dG-m⁵dC).poly(dG-m⁵dC) in Z conformation. It is concluded that the bidendate adduct induces a conformational change from the B form towards a distorted Z form.

In the reaction of cisPt and Z-DNA, a monodentate adduct is formed. This adduct stabilizes the Z conformation as shown by circular dichroism and binding to the anti Z-DNA antibodies. At room temperature, the second function of the drug can still react with small ligands as NH₄HCO₃.

021

MODELS OF HYPOTHETICAL RECOMBINATION JUNCTIONS

Stewart McGavin, Department of Chemistry, University of Dundee, Scotland, and M.E. Bosshard and C. Carlson, EMBL, Heidelberg, West Germany.

Models have been constructed of hypothetical recombination junctions (see McGavin (1977), Nash et al (1980) and Nash and Pollock (1983)) using the computer graphics system at EMBL (Heidelberg, West Germany). These are based on a suggestion of a specific pairing of duplexes to form four strand structure (McGavin (1971, 1979)). Models of an initial and final pairing and of possible intermediate stages have been constructed.

A simple model has also been devised which allows following the topological consequences of some recombination models (see Nash et al 1980, 1983). This model was designed with the above mentioned detailed molecular models in mind but may be of wider interest and could apply to any close and restricting association of duplexes (McGavin, 1984).

References

- McGavin, S. (1971), *J. Mol. Biol.*, **55**, 293-298.
McGavin, S. (1977), *Heredity*, **32**, 15-25.
McGavin, S. (1979), *J. Theor. Biol.*, **77**, 83-99.
McGavin, S. (1984), *J. Theor. Biol.*, **107**, 37-56.
Nash, H.A., Mizuchi, K., Enquist, L.W. and Weisberg, R.A. (1980), *Cold Spring Harbour Symp.*, **45**, 417-428.
Nash, H.A. and Pollock, T.J. (1983), *J. Mol. Biol.*, **170**, 19-83.

023

NMR STUDIES OF NUCLEIC ACID STRUCTURE AND DYNAMICS

B.R. Reid, D.E. Wenner, S.H. Chou, R.E. Klevit, P. Rajagopal and N.S. Ribello, Departments of Chemistry and Biochemistry, University of Washington, Seattle WA 98195, USA.

Pure tRNA species and several regulatory DNA sequences, including operators and promoters, have been studied by high-resolution 500 MHz NMR. Each base pair contributes one imino proton to the low field spectrum and these protons have been completely assigned by 1D nuclear Overhauser experiments and/or 2D NMR (NOESY) in H₂O solution. Inversion recovery experiments have been carried out to determine the helix opening rates at each base pair. Promoters are asymmetric in their base pair opening and several tRNAs contain cloverleaf secondary structure base pairs t⁺at are markedly more labile than the tertiary base pairs involved in three-dimensional folding.

2D NMR (COSY and NOESY) has been used to assign all protons except C5'H and C5''H in the EcoRI restriction sequence, the SV40 promoter, and the lambda OR3 operator. The single base pair vC3 mutant (AT5-GC5) of the OR3 operator has been studied and compared to the wild-type operator. The NOESY spectra contain cross peaks corresponding to known distances (cytosine C5H-C6H, deoxyribose C2'H-C2''H) that can be used as yardsticks for other proton-proton distances from which local structural variations can be monitored.

Supported by grants GM29764, GM32302 and Program Project GM32681 from the National Inst. Health and grant PCM8215812 from the National Science Foundation.

020

CONFORMATIONAL DYNAMICS OF OLIGONUCLEOTIDES

F. Claessens, R. Figliari, A. Gräslund & J. Chattopadhyaya^A
^ADept. Med. Biophysics, Karolinska Institute, Stockholm,
^BDept. Biophysics, Arrhenius Laboratory, Stockholm
^CDept. Microbiology, Biomedical Center, Uppsala, SWEDEN

Conformational states and transition kinetics of oligo- and polynucleotides can be studied using fluorescent nucleotides at defined positions as local structural probes. From the analysis of the lifetime spectrum and the rotational motion of the probe after excitation by a mode-locked and synchronously pumped dye laser pulse, the dynamic properties of probe and neighbouring nucleotides can be assessed with picosecond time resolution.

Here the temperature dependence of the stacking and unstacking of the fluorescence 2-aminopurine (2AP) is investigated in ribonucleotide duplets and triplets. The fluorescence decay of 2AP alone is mainly characterized by a lifetime of 10 ns while when incorporated into oligonucleotides 3 fluorescent lifetimes (8.7, 3.8 and 1.1 ns) are needed to describe the fluorescence decay of 2AP.

Anisotropy decay curves show that the rotational correlation time of 2AP alone ($\rho=130$ ps) easily can be distinguished from the A(2'p5')A(2'p5')2AP molecule ($\rho=340$ ps) when compared at the same temperature (25°C).

From comparison of the temperature dependence of lifetimes, rotational correlation times and ring current shifts obtained from high resolution NMR spectra, the dynamic properties of stacked and unstacked conformations as indicated by 2AP in various positions are deduced.

022

CD EVIDENCE THAT C-C⁺ PAIRS EXIST ALONGSIDE A-T PAIRS IN THE OLIGONUCLEOTIDE DOUBLE HELIX d(C₄A₄T₄C₄)-d(C₄A₄T₄C₄). D.M. Gray, T. Cui, and R.L. Ratliff, Program in Molecular Biology, Univ. of Texas at Dallas, Richardson, TX, USA.

It is well-known that helical structures of poly(d(C)) and poly(r(C)) contain hemiprotonated C-C⁺ base pairs. We have shown that C-C⁺ pairs also form in the alternating sequence polymer poly[d(C-T)]. It seems reasonable to assume that in these polymers the base pairs form between parallel strands. In order to test the possibility that C-C⁺ pairs can also form between antiparallel strands, we have synthesized and studied the DNA hexadecamer, C₄A₄T₄C₄. A-T pairs can form between antiparallel strands of this oligomer, but not between parallel strands. The CD characteristics of stacked A-T pairs (e.g. a negative CD band at 250 nm) and of stacked C-C⁺ pairs (e.g. a positive CD band at 285 nm) have been determined from other systems. We find that both types of CD features simultaneously appear for the C₄A₄T₄C₄ oligomer as the temperature is lowered to 0°C at pH 5 or 6 (0.5M NaCl), conditions favorable for formation of a double helix. We conclude that C-C⁺ pairs form alongside A-T pairs between antiparallel strands of the oligomer.

(This work was supported by NIH Research Grant GM19060 and Grant AT-503 from the Robert A. Welch Foundation.)

024

ALGORITHMS FOR THE STABILITY MAP OF NUCLEIC ACID SECONDARY STRUCTURE AND FOR THE SECONDARY STRUCTURE COMPOSED OF MORE THAN TWO CHAINS

A. Suyama, Y. Eguchi and A. Wada, Dept. of Physics, Univ. of Tokyo, Bunkyo-ku, Tokyo, Japan.

Two efficient and well-defined algorithms for the secondary structure of single-stranded nucleic acids have been developed. The first one is to calculate one- and two-dimensional bonding probability maps which represent stability of the secondary structure. Especially one-dimensional bonding probability map is convenient to compare with experimental enzyme accessibility and chemical modification data. By this method the secondary structure of E. coli 5S rRNA was calculated and compared with experimental enzyme accessibility and chemical modification data. In a certain condition the calculated structure well explains the experimental data. The second one is to calculate the secondary structure composed of more than two chains such as rRNA-mRNA complex. By this method the secondary structure composed of human U1 snRNA and β -globin hnRNA was obtained. It was found that U1 snRNA preferentially binds to a 5' splice site. We are now applying these methods to the secondary structures related to biologically interesting systems including a self-splicing RNA such as rRNA precursor of Tetrahymena, a complex formed from M1 RNA of RNase P and rRNA precursor, and a 16S rRNA-mRNA complex in E. coli.

Tuesday 31 July Congress Centre-first floor. Posters 025-030

Posters on Polymorphism and Structural Transitions in Nucleic Acids

025

A MECHANISM FOR CONTROL OF GENE EXPRESSION

R.C. Hopkins, Univ. of Houston-CL, Houston, Texas 77058 USA

The pairing of two homologous DNA duplexes to produce a tetraplex structure has been proposed recently as a mechanism by which semi-permanent gene inactivation and cell differentiation might occur (1). The implications of this hypothesis are far-reaching indeed: a) it provides a basis for understanding the extreme fidelity of genome maintenance in eukaryotes, b) it offers an explanation of the methylation patterns in higher organisms, and c) it suggests a fundamental mechanism in the initiation of carcinogenesis, with clear implications for drug design. Nonetheless, both a scheme for specifically pairing two homologous base pairs to form a tetrad (2) and a model of four-stranded Watson-Crick DNA (3) have been known for a long time. What is unique about the tetraplex models mentioned above is that they are based on an alternative family of double-helical models for the structure of DNA (4,5). This model family, Configuration II, preserves the base pairing scheme of the original Watson-Crick family, Configuration I, but differs in having antiparallel chains of the opposite sense. The left-handed Z-DNA forms are examples of this alternative structural family, but are not members of the topologically distinct Watson-Crick family (5). (Supported by grant E-889 from the Robert A. Welch Foundation)

1. Hopkins, R.C. (1984) *Comments Mol. & Cell. Biophys.* 2, 153
2. Lowdin, P.-O. (1964) in *Electronic Aspects of Biochemistry*, B. Pullman, ed. (Academic Press, N.Y.), p. 167.
3. McGavin, S. (1971) *J. Mol. Biol.* 55, 293.
4. Hopkins, R.C. (1981) *Science* 211, 289.
5. — (1983) *Cold Spr. Harb. Symp. Quant. Biol.* 47, 129.

027

ELECTRIC FIELD INDUCED DICHOISM OF NUCLEIC ACIDS: ALTERNATING PURINE-PYRIMIDINES

E. Charney, H-H Chen and D. C. Rau, Laboratory of Chemical Physics, NIAID, National Institutes of Health, Bethesda, MD 20205, U.S.A.

The dichroism of alternating AT and GC sequences, produced by electric-field orientation of the deoxypolymers of these compounds is used to study their polymorphic transformations and their physical and structural properties. The transient decay of the dichroism, of poly(dA-dT) of defined molecular lengths, when the orienting field is sharply cut-off (in tens of nanoseconds) shows this sequence is highly flexible compared to that of random sequence DNA. Both the transient and steady-state dichroism of poly dG-dC in the B and Z conformations conform to theoretical predictions based on their crystal and fibre x-ray determined structures. The results do not bear out inferences drawn from other dichroism studies of B-form DNA that imply that the average tilt or the propeller twist of the bases is much greater than expected from the canonical B-DNA structure calculated from the x-ray diffraction of fibres.

029

A RAMAN SPECTROSCOPY ANALYSIS OF PROMOTER AND NON-PROMOTER DNA FRAGMENTS, R. M. Martell, J. T. Harrell and S. Abhiraman, Georgia Institute of Technology, Atlanta, GA 30332 (U.S.A.)

Raman spectroscopy was employed to examine DNA restriction fragments, 69 - 144 bp., from the E. coli lactose promoter region. The 144 bp. fragment contains the binding sites for RNA polymerase, the lac repressor, and the CAP protein. The 64 bp. DNA isolates the CAP site and is identical to one end of the 144 bp. fragment. The 80 bp. DNA constitutes the other end of the 144 bp. DNA. Spectra were obtained in 0.1 M NaCl from these fragments, as well as from five heterogeneous sequence DNAs (30%-72% G-C) and the DNA polymers d(A-T)_n-d(A-T)_n, d(A)_n-d(T)_n, d(G-C)_n-(G-C)_n, and d(T-G)_n-d(C-A)_n.

A data analysis procedure was developed to evaluate Raman band height, location and width for overlapping Raman bands. This procedure generated a least squares fit of calculated curves to the experimental spectra. Intensities of over twelve Raman bands were measured relative to the 1093 cm⁻¹ diox-phosphate stretching mode. Plots of relative intensity vs. G-C content for base ring vibrations at 668, 682, 730, 750 and 782 cm⁻¹ increased or decreased as expected. Overlapping Raman bands at 791 cm⁻¹, 810 ± 5 cm⁻¹ and 835 ± 6 cm⁻¹ were required to produce the 780-850 cm⁻¹ spectral region for all DNAs. The 835 cm⁻¹ is a B-specific backbone vibration associated with a C2'-endo sugar pucker. The 810 cm⁻¹ band has been assigned to a backbone mode with the sugar ring C3'-endo. The promoter fragments have intensities consistent with their X G-C and the data from the heterogeneous sequence DNAs. Work supported by N.I.H.

026

DRUG BINDING TO Z DNA

R.H. Shafer, S.C. Brown and D.A. Wade, Department of Pharmaceutical Chemistry, University of California, San Francisco, CA. U.S.A.

The interaction of left-handed, Z DNA with several intercalators has been studied under a variety of conditions. In particular, ethidium and bis(methidium)spermine, a double intercalator, have been examined using absorption, fluorescence, circular dichroism and ³¹P NMR techniques. Results from these experiments indicate that left-handed poly(dG-dC) can bind intercalators resulting in effects on the ligand similar to those produced by complex formation with right-handed DNA. Stopped-flow studies demonstrate bimolecular kinetics for the binding of these compounds to Z DNA on a time scale similar to that observed with B DNA. This result suggests that binding occurs directly to the Z form rather than to a reverted B form of the polynucleotide. The dynamics of the drug-polynucleotide complexes in both the B and Z forms have also been examined using stopped-flow H-D exchange with fluorescence detection. Results of these experiments address the question of the local DNA conformation at the site of drug binding. Actinomycin D also appears to bind to Z DNA. These data will be discussed in terms of the biological significance of Z DNA as a drug receptor.

028

EFFECTS OF LOCAL ELECTROSTATIC FIELDS ON TRANSITION MOMENT DIRECTIONS IN 9-ETHYLGUANINE. R.W. Woody, Department of Biochemistry, Colorado State University, Fort Collins, CO, USA.

The directions of transition moments are fundamental parameters in theoretical treatments of the absorption and CD spectra of biopolymers. Absolute transition moment directions of the purine and pyrimidine bases of nucleic acids have been derived from polarized absorption spectra of single crystals. In previous studies, the effects of local electrostatic fields have been neglected. Such fields can (1) shift the energies of states relative to the gas phase due to the charge distribution upon excitation; (2) electrostatically induce mixing of states. In extreme cases, the first effect can reverse the ordering of excited states in a polar molecular crystal relative to the gas phase. The second effect can lead to reorientation of transition moments in the crystal. Both effects are expected to be most important in cases of near-degeneracy, e.g. the near-uv spectra of purines. According to MO theory, 9-ethylguanine has a large permanent dipole moment in the ground state which decreases upon excitation to the first excited state (S₁), but increases upon excitation to S₂. Calculations using several different MO parameterizations indicate that the first two excited states are brought closer together in energy and are mixed significantly in the crystal. The resulting transition moment directions agree much better with experiment than do those predicted by MO theory for the gas phase. The effect of electrostatic fields on transition moment directions must be considered in improved treatments of the optical properties of nucleic acids and proteins. Supported by a USPHS grant, GM22994.)

030

INTERACTION OF CAFFEINE WITH WATER AND DNA HYDRATION SHELL

V.Ya. Malaev, A.V. Shestopalova, A.I. Gagan and V.A. Kashpur, Institute of Radiophysics and Electronics of the Ukrainian Academy of Sciences, Kharkov, USSR

The thermal stability of DNA from calf thymus was studied spectrophotometrically as a function of caffeine concentration. At low caffeine concentration C_f, the DNA melting temperature T_m was found to increase by 2°C in comparison with T_m for pure DNA. On the contrary the increase of the caffeine concentration decreases the T_m. We supposed that such behaviour can be explained by different effects of monomer and associated caffeine forms on the water molecules surrounding DNA. The results of the Monte Carlo simulation of the monomer and dimer caffeine forms hydration in a cluster of 200 water molecules have shown that the water-water interaction around the dimer is greater than the analogous interaction around monomer. The theoretical results are in a good agreement with the experimental data on caffeine hydration in solution obtained by the dielectric method in the microwave region. We found that at relatively low concentration (C_f = 0.6%) about three water molecules are bound to each caffeine molecule. At higher concentration (C_f = 1.8%) the amount of the bound water molecules decreases to 1.5 per one caffeine molecule apparently owing to molecular association.

Tuesday 31 July Congress Centre-first floor. Posters 031-036
Posters on Polymorphism and Structural Transitions in Nucleic Acids

031

CD AND $^1\text{H-NMR}$ STUDIES OF THE B AND Z DOUBLE HELICAL STRUCTURES OF d-(C-G-m⁵C-G-C-G), COMPARISON OF THE MECHANISM OF THE B-Z, COIL TRANSITION BETWEEN d-(C-G-m⁵C-G-C-G), d-(m⁵C-G-C-G-m⁵C-G) AND d-(C-BrG-C-G-C-BrG). J.M. Neumann*, J.A. Cavaillès*, J. Taboury*, T. Huynh-Dinh**, J. Igolen** & S. Tran-Dinh*. *Service de Biophysique, Département Biologie CEN Saclay 91191 Gif / Yvette Cedex, France** Unité de Chimie Organique, Institut Pasteur 28 rue du Dr Roux 75724 Paris Cedex 15, France.

The various structures of d-(C-G-m⁵C-G-C-G) in aqueous solution have been investigated by CD and $^1\text{H-NMR}$ spectroscopies at different temperatures and salt concentrations. At room temperature, in 0.1 M NaCl, the B form is only detected whereas in 1.8 M NaCl, the B helix slowly exchanges with the Z helix (at the NMR time scale). In presence of 4M NaCl, the Z form is largely predominant at room temperature. Assignment of the Z proton signals has been achieved by saturation transfer between the B and Z signals at 1.8 M NaCl and by selective $^1\text{H-NMR}$ decoupling at 4 M NaCl. The mechanism of the transitions between the B, Z and coil forms has been also investigated; in particular, the exchange rates have been determined by measuring the NOE, T_1 and T_2 of the Z proton signals. As in the case of d(m⁵C-G-C-G-m⁵C-G), the Z helix is obtained from the B helix by intramolecular rearrangement. This mechanism is compared to that observed in the case of d-(C-BrG-C-G-C-BrG) where the Z helix is directly obtained from the coil form.

033

HYDRODYNAMIC PROPERTIES OF BROMO MOSAIC VIRUS RNA

B.M. Schoot, J.Y. Sgro and B. Jaerott, EMBL Grenoble outstation, c/o ILL 156X 38042 Grenoble Cedex France.

Sedimentation coefficients of purified BMV RNA (Mr 0.28, 0.7 and 1.0 x 10⁶ d. tons) are determined in buffers containing KCl, MgCl₂, Spermine and Spermidine. Increase in additive concentration results in increased S_{20,w} values and in an increased tendency to form aggregates. The higher the molecular weight of the RNA studied, the more pronounced are these effects.

A plot of ln S_{20,w} versus ln Mw for data obtained from BMV RNA, yeast tRNA^{phe} and from E. Coli 16S RNA in the same buffer, show that these values all fit on the same straight line. The slope of this line varies between 0.44 (10 mM Tris-acetate buffer pH 7.0) and 0.57 (200 mM KCl, 50 mM MgCl₂ and buffer). This indicates that RNA molecules undergo transitions from a rather extended to a more globular shape, with a flexible chain as intermediate. The fact that the ln S values for tRNA fits on this line may indicate that the chain consists of hydrodynamically tRNA-like subunits.

Measurements of the radius of gyration with X-rays or neutrons show that the RNA in solution is not as compact as in the virion. This shows the essential role of the coat protein in the morphogenesis of the virion.

035

LENGTH AND SALT DEPENDENCE OF OLIGONUCLEOTIDE HELIX-COIL TRANSITIONS BY MONTE CARLO.

Pamela Mills, Paul Christy, Charles Anderson, and M. T. Record, Jr., Dept. of Chemistry, University of Wisconsin, Madison, Wisconsin 53706.

The Poisson-Boltzmann (PB) cell model has often been used to calculate the radial distribution of small ions around polyelectrolytes in solution. From these distribution functions the thermodynamic properties of polyelectrolyte solutions can be calculated. The counterion condensation (CC) model for ion interactions with rod-like polyelectrolytes provides an alternative approach to the analysis of thermodynamic measurements. In order to test the accuracy of the PB and CC models at the molecular level, we have computed small ion radial distribution functions by adapting the Metropolis Monte Carlo method for a canonical ensemble to cylindrical symmetry. We have developed a perturbation approach that permits the systematic approximate evaluation of nonconfigurational thermodynamic variables (entropy and free energy).

The systems of interest are helical polymeric and oligomeric DNA in an aqueous solution containing one type of simple electrolyte. The polyelectrolyte is modeled as a uniform impenetrable cylinder having a regular discrete array of structural charges. The mobile ions are modeled as hard spheres and the solvent as a medium of a uniform dielectric constant. Only Coulombic interparticle forces are included in the simulations. We have used this model to obtain small ion distributions and thus to predict thermodynamic parameters such as the dependences of the helix-coil transition temperature of oligomeric DNA on salt concentration and chain length.

032

TEMPERATURE DEPENDENCE OF THE B-DNA TO Z-DNA TRANSITION
 Probhas Raychaudhuri, Department of Applied Mathematics, Calcutta University, Calcutta-700009, INDIA.

A dynamical model for DNA(SSS)molecule has been presented which can incorporate both right handed and left handed in a unique way. The structure of DNA molecule is then oscillating between right handed and left handed form depending on the solvent characteristics⁽¹⁾. Under ordinary conditions there are no transitions between the right handed DNA to the left handed DNA. Relatively pure B-DNA can be prepared in crystalline fibre at low temperature. In these pure substances transition leading to the equilibrium mixture of B-DNA and Z-DNA will depend on the concentration and mechanical and magnetic moment of the individual monomer in the helices. We have shown that in a DNA molecule the ratio of the numbers of B-DNA and Z-DNA is a function of temperature, which form the Boltzmann distribution is

$$X = \frac{N_{B-DNA}}{N_{Z-DNA}} = \frac{\sum_i i_{i+1} Z_{i+1}}{\sum_i i_{i+1} Z_{i+1}}$$

depending on the spin of the nucleotide, where Z_1, Z_2 are the rotational partition function for B-DNA and Z-DNA molecule at the temperature varies from 0 to ∞. The ratio varies from 0 to ∞ depending on the spin of the nucleotide. Temperature dependence of the B-DNA to Z-DNA transition has been observed recently by Patel et al.⁽²⁾ Jovin et al.⁽³⁾ Behe et al.⁽⁴⁾

REFERENCES: (1) P. Raychaudhuri, Spec. Sci. Tech., 263, 267 (1981), 2, 23, 461 (1982). (2) D. J. Patel et al. J. Biol. Chem., 257, 1413 (1982). (3) T. H. Jovin et al. Biomolecular structure and dynamics (1983). (4) K. J. Behe et al. Private communication to T. H. Jovin (1983).

034

PHOTOCHEMICAL STUDIES OF ALTERNATING DNA COPOLYMERS

S. Kumar and R. J. H. Davies, Department of Biochemistry, Medical Biology Centre, Queen's University, Belfast, N. Ireland.

A novel adenine-thymine photoadduct is produced when poly(dA-dT) is irradiated at 254nm in aqueous solution. Its formation can be detected by its specific conversion into the fluorescent heterocyclic base 1-methyl-1-deazapurin-2-one when the irradiated DNA copolymer is treated with 1 M HCl, at 100 °C, for 4 h. The 1-methyl-1-deazapurin-2-one thus generated can be isolated by high voltage paper electrophoresis or by reversed phase HPLC. Its subsequent quantitation by spectrofluorimetry permits calculation of the quantum yield of the photoreaction under the relevant experimental conditions. For single-stranded poly(dA-dT)₁ the quantum yield is approximately 5 x 10⁻⁴ mol einstein⁻¹. The yield is decreased at least five-fold in double-stranded poly(dA-dT).poly(dA-dT), showing that the photoreaction is quenched as a consequence of the conformational changes accompanying base pairing.

The possibility that analogous purine-pyrimidine photoadducts are formed in poly(dI-dC) and poly(dG-dC) was explored by irradiating these copolymers at 254nm and then analyzing their acid hydrolyzates for the presence of the expected degradation product 1-deazapurin-2-one. Negative results were obtained, however, with the single and double-stranded forms of poly(dI-dC) and the B and Z forms of poly(dG-dC).

This work was supported by the SERC.

036

STRUCTURE IN rRNA FROM E. coli BY ELECTRON MICROSCOPY.

B.K. Klein and O. Schlessinger, Department of Microbiology and Immunology, Washington University Sch. of Medicine, St. Louis, MO, USA.

The positions and sizes of the most stable loops were determined in partially denatured 16S and 23S rRNA from *E. coli*. rRNA was prepared for electron microscopy using a hyperphase containing 50% formamide, 10 mM Tris (pH 8.0), and varying concentrations of monovalent and divalent ions to adjust the amount of structure in the partially denatured molecules. The loop patterns of many molecules were then analyzed in detail to infer a composite structure. At moderate Mg²⁺ concentrations (0.5 to 2.0 mM) the consensus loop patterns fall into discrete location domains along the contour of the molecule. For 16S rRNA three loop location domains were identified, with five loops resolved well; a 5' terminal loop was particularly prominent. In 23S rRNA thirteen loops were seen in seven locations domains; four of them especially prominent. These results agree well with the models for unique secondary structure features predicted on the basis of phylogenetic comparisons and chemical and enzymatic protection studies. In addition, the relative stability of the loops show that those features most prominent in 16S and 23S rRNA are among those with the lowest predicted free energy in the secondary structure models. The loop structures showed some strong and unexpected similarities between the most stable features of secondary structure in 16S and 23S rRNAs. Both rRNAs show a stable 5' terminal loop and a set of subterminal nested loops near the 3' end.

Tuesday 31 July Congress Centre-first floor. Posters 037-042

Posters on Polymorphism and Structural Transitions in Nucleic Acids

037 EVIDENCE FOR THE EXISTENCE OF STABLE CURVATURE OF DNA IN SOLUTION

P.J. Hageman, Dept. of Biochemistry, Biophysics and Genetics, Univ. of Colorado Health Sciences Center, Denver, Colorado, USA.

Certain DNA restriction fragments derived from kinetoplast minicircles of *Trypanosoma* display substantially abnormal electrophoretic behavior when run on polyacrylamide gels. One of these restriction fragments (KP242) has been examined in detail using the technique of differential decay of birefringence (DOB). This technique consists of analyzing the difference in the rates of decay of birefringence for two DNA fragments, each comprising an identical number of base pairs, and is capable of resolving differences in length as small as one percent. The DOB approach has been used to establish that static curvature of the DNA helix is the basis of the abnormal electrophoretic behavior. Although curvature of the helix axis has been reported for duplex oligonucleotides in the crystal, this DOB study provides the first direct evidence for stable curvature of the helix axis in solution. KP242 consists of 242 base pairs in which the region giving rise to the abnormal electrophoretic behavior has been mapped to the central portion of the molecule. When KP242 is represented as a rod with a single bend at its center, the bend angle is approximately 50 degrees. Although the actual curvature is undoubtedly more complex, the once-bent rod representation provides insight as to the magnitude of the curvature.

039

X-RAY FIBRE DIFFRACTION STUDIES OF CONFORMATIONAL CHANGES IN DNA DOUBLE-HELICES USING SYNCHROTRON RADIATION, V.T. Forsyth, A. Mahendrasingam, W.J. Pigram, R.J. Greenall, C. Nave and W. Fuller, Department of Physics, University of Keele, Keele Staffs, ST5 5BG, England and SERC Daresbury Laboratory, Daresbury, Warrington, WA4 4AD, England.

The Daresbury Synchrotron Radiation Source (SRS) has been used to follow conformational changes in the DNA double-helix in oriented fibres as a function of the relative humidity of the fibre environment. For the lithium salt of the synthetic polynucleotide poly d(A-T).poly d(A-T) the relative humidity of the fibre environment was raised from about 57% to over 95% and then reduced to 57%. During this humidity variation the following conformational changes were observed: semi-crystalline C \rightarrow semi-crystalline B \rightarrow crystalline B \rightarrow semi-crystalline C. Diffraction patterns were recorded using an area detector with an exposure time of about 1 minute. In a typical run the conformational changes were observed over a period of about half an hour and recorded as 32 end-to-end one minute time-slices. The sequence of diffraction patterns was recorded on video cassette and shows the gradual appearance of diffraction spots with the transition to a new molecular conformation and packing.

For the sodium salt of poly d(A-T).poly d(A-T) we have observed the gradual transition with increasing relative humidity from the semi-crystalline C form to the crystalline A form. A number of conformational intermediates were observed corresponding to variants of the C conformation in which the pitch changed gradually from approximately 31A to the value of 28A which characterises the A form.

041

NUCLEIC ACID JUNCTIONS CAN BE ENZYMATICALLY JOINED TO FORM COVALENTLY CLOSED FIGURES, N.C. Seeman, R.-I. Ma and W.R. Kallenbach, Dept. Biol. Sci., SUNY/A, Albany, NY 12222 USA and *Dept. Biol., Univ. of Penna., Philadelphia, PA 19104 USA

We have recently shown that the minimization of sequence symmetry can yield stable immobile nucleic acid junctions formed from oligonucleotides in solution.¹ Starting with a rapid algorithm, which optimizes the sequences of component strands so that they will assume the desired junction architecture, it is now possible to carry out physical studies on a variety of stable junction complexes. It has been pointed out that nucleic acid junctions constitute valence clusters, which can be connected to form stick figure structures in space.² In each of these polygons, polyhedra or N-connected figures, the junction constitutes a vertex, while the edges are double helical nucleic acid. We have now shown that enzymatic joining of a third-rank sticky-ended junction, composed of strands containing 18, 20 and 22 residues, produces covalently closed quadrilaterals and hexagons. These equilateral structures are not necessarily planar. The ability to obtain closure with this oligomerization reaction suggests that individual junctions, with designed unique sticky ends, can be concatenated to form specified closed figures.

¹N.R. Kallenbach, R.-I. Ma and N.C. Seeman, *Nature* **305**, 829-831 (1983).

²N.C. Seeman, *J. Theor. Biol.* **92**, 237-247 (1982).

This work has been supported by grants ES-00117, GM-29554 and CA-24101 from the NIH.

038

TRANSITIONS BETWEEN LEFT-HANDED AND RIGHT-HANDED CONFORMATIONS OF THE POLY d(G-C).POLY d(G-C) DOUBLE HELIX, A. Mahendrasingam, W.J. Pigram, R.J. Greenall, T. Forsyth, C. Nave and W. Fuller, Department of Physics, University of Keele, Staffs, ST5 5BG, England and SERC Daresbury Laboratory, Daresbury, Warrington, WA4 4AD, England.

The conformation assumed by nucleic acid double-helices in oriented fibres depends critically on the water and ionic content of the fibre. We have determined the ionic content required for fibres of the potassium salt of poly d(G-C).poly d(G-C) to undergo as a function of the relative humidity the fibre environment the following series of conformational transitions: semi-crystalline B' \rightarrow crystalline A \rightarrow crystalline S \rightarrow semi-crystalline B. The S form has been interpreted in terms of a left-handed double-helix whereas the crystalline A and semi-crystalline B forms are generally accepted as right-handed conformations. The observation of such profound conformational changes as that of helix handedness within a fibre is of particular interest.

We have also observed a well-defined variation in the S conformation itself with relative humidity. Up to 92% relative humidity we observe a conformation which we designate S_I and above 92% one designated S_{II}. We have analysed the S_I and S_{II} diffraction patterns and shown that these two conformations correspond in a general way to the 2_I and 2_{II} conformations observed in single crystals of oligonucleotides containing alternating guanine and cytosine residues.

040

SPECTROSCOPIC AND THERMODYNAMIC STUDIES ON SUPER-HELICAL PLASMIDS, A. Seidl and H.-J. Hinz, Institut für Biophysik und Physikalische Biochemie, Universität Regensburg, FRG

Col E1 amp plasmid and PM2 DNA have been investigated using ultraviolet absorption, circular dichroism, isothermal and scanning microcalorimetry to elucidate the influence of superhelical structure on double helix stabilization. Characteristic differences were observed for the transition enthalpies of the linear, open circular, covalently closed superhelical, and covalently closed relaxed forms of the circular DNAs, which can be rationalized when considering the energetics and topology of superhelix formation.

042

Sequence-dependent structural variations in two right handed alternating pyrimidine-purine DNA oligomers in solution determined by NOE measurements.

G.M. Clore and A.M. Gronenborn
Division of Physical Biochemistry, National Institute for Medical Research, Mill Hill, London, U.K.

A 500 MHz ¹H-NMR study on two right handed self-complementary double stranded alternating pyrimidine-purine oligodeoxyribonucleotides, 5'd CGTACG and 5'd ACGCGCGT, is presented. Using the proton-proton nuclear Overhauser effect all proton resonances are assigned by a sequential method and a large number of interproton distances, both intra- and internucleotides are determined (113 for 5'd CGTACG and 79 for 5'd ACGCGCGT). The general procedure required to solve the three dimensional solution structures of oligonucleotides from such distance data is outlined and applied to these two oligonucleotides. In the case of both oligonucleotides it is shown that the overall solution structure is that of B DNA, namely a right handed helix with a helical rise of ~3.3 Å, ten base pairs per turn and the base pairs approximately perpendicular to the helix axis. In the case of 5'd CGTACG subtle local structural variations associated with the pyrimidine and purine nucleotides are superimposed on the overall structure but the mononucleotide repeating unit is preserved. In contrast, 5'd ACGCGCGT has a clear alternating structure with a dinucleotide repeat, alternation occurring in the local helical twist and the glycosidic bond, sugar pucker and phosphodiester backbone conformations.

Tuesday 31 July Congress Centre-first floor. Posters 043-048

Posters on Polymorphism and Structural Transitions in Nucleic Acids

043

tRNA^{Phe}: Codon-anticodon interaction. A 500 MHz ¹H-NMR study
A.M. Gronenborn¹, G.M. Clore¹, and L.W. McLaughlin²

¹ Division of Physical Biochemistry, National Institute for
Medical Research, Mill Hill, London, UK.

² Max Planck Institut für Experimentelle Medizin, Herman-Rein
Strasse 3, D-3400 Göttingen, F.R.G.

A 500 MHz ¹H-NMR study of the semi-synthetic RNA pentadecamer 5'-rCAGAC-UG₃AAAYAA³CUG comprising the anticodon loop and stem (residues 28 to 42) of yeast tRNA^{Phe} is presented. Using pre-steady state AGE measurements all exchangeable and non-exchangeable base proton resonances, all H1' ribose resonances and all methyl proton resonances are assigned and over 70 intra- and internucleotide interproton distances determined. From the distance data the solution structure of the pentadecamer is solved by model building. It is shown that the pentadecamer adopts a hairpin loop structure in solution with the loop in a 3' stacked conformation. This structure is both qualitatively and quantitatively remarkably similar to that of the anticodon loop and stem found in the crystal structures of tRNA^{Phe} with an overall root mean square difference of 1.2 Å between the interproton distances determined by NMR and X-ray crystallography. Interaction of the pentadecamer with the ribonucleoside diphosphate UpUpC, one of the codons for the amino acid phenylalanine, results only in minor perturbations in the structure of the pentadecamer and the 3' stacked conformation of the loop is preserved. The stability of the pentadecamer-UpUpC complex is approximately an order of magnitude greater than that of the tRNA^{Phe}-UpUpC complex.

045 ORAL PRESENTATION

STRUCTURAL POLYMORPHISM IN SUPERCOILED DNA: THERMODYNAMICS
AND KINETICS OF CRUCIFORM STRUCTURE

D M J Lilley & L R Hallam, Dept Biochemistry, Medical
Sciences Inst, University of Dundee, DUNDEE DD1 4HN

We have shown that inverted repeat sequences (eg, the 13bp repeat of ColEI) in negatively supercoiled DNA molecules are hypersensitive to a variety of enzyme and chemical probes, indicating cruciform extrusion. The probes include (a) Single-strand-specific nucleases (S1 nuclease, micrococcal nuclease and BAL31) which cleave the loop of the cruciform (b) Holliday structure resolvase (T4 endonuclease VII) which introduces staggered cleavages at the base of the stems and (c) Single-strand-selective reagents (bromoacetaldehyde and OsO₄).

Thermodynamics: We have prepared pure single topoisomers of a small plasmid containing the ColEI inverted repeat, and studied their reactions with S1 nuclease, BAL31, T4 endonuclease VII and OsO₄. In each case there is a sharp transition from total insensitivity to sensitivity, and the critical linking difference is probe-independent. This value correlates well with band shifts observed in electrophoresis. We may calculate the twist change (ΔT_w) on cruciform extrusion and the free energy (ΔG) of cruciform formation.

Kinetics: We prepare plasmid without cruciform structure by treatment with ethidium bromide and subsequent removal at low temperature. We assay the re-extrusion process by exposure to a given temperature, time etc, followed by a low temperature S1 nuclease or T4 endonuclease VII reaction. A critical temperature of 33°C is required for facile extrusion of the ColEI cruciform. We have calculated both enthalpy (ΔH[‡]) and entropy (ΔS[‡]) of activation.

047

044

X-RAY DIFFRACTION STUDIES OF THE D FORM OF THE POLY d(A-T).
POLY d(A-T) DOUBLE HELIX. W. Fuller, A. Mahendrasingam,
W.J. Pigram, R.J. Greenall, V.T. Forsyth and C. Nave,
Department of Physics, University of Keele, Staffs, ST5 5BG
England and SERC Daresbury Laboratory, Daresbury, Warrington,
WA4 4AD, England.

A number of quite different models have been proposed to account for the D patterns observed from the poly d(A-T). poly d(A-T) double-helix. These models differ not only in the number of nucleotide pairs per turn, but even more profoundly in the handedness of the helix. We have observed better defined diffraction patterns from the D conformation than have been reported hitherto. Some of this data has been recorded on conventional sources and some on the Daresbury Synchrotron Radiation Source (SRS) using both film and two-dimensional multi-wire proportional chamber. D patterns have been recorded from not only the sodium salt of poly d(A-T).poly d(A-T) but also the potassium, rubidium and caesium salts. This data is being analysed in terms of both right- and left-handed models. To date of the models we have built, a left-hand with 8 nucleotide-pairs per helix pitch gives the best agreement with the observed diffraction. In addition to the tetragonal form of the D conformation detailed above we have observed a hexagonal form from the potassium salt of poly d(A-T).poly d(A-T). We have not observed a D pattern from the lithium salt although another form, designated F, which may be structurally related to D has been observed.

046

048

Tuesday 31 July Congress Centre-first floor. Posters 049-054

Posters on Polymorphism and Structural Transitions in Nucleic Acids

049

050

051

052

053

054

Tuesday 31 July Congress Centre-first floor. Posters 055-060

Posters on Nucleic Acid-Protein Interactions

055

A PRESSURE-JUMP KINETIC STUDY OF ETHIDIUM BROMIDE BINDING TO SYNTHETIC DNA'S
R.B. Macgregor, Jr., R.M. Clegg, T.M. Jovin; MPI biophys. Chemie; Abt. mol. Biol.; Göttingen, FRG.
Pressure-jump chemical relaxation has been used to investigate the binding of ethidium bromide to the double-stranded synthetic polymers poly d(G-C) and poly d(A-T) in 0.1 M NaCl, 10 mM Tris, 1 mM EDTA, pH 7.2, 24°C. The base-pair/dye ratio was varied from 1/2 to 45, no evidence of excluded site interactions were seen even at the lowest ratios. The kinetics were followed by monitoring the fluorescence at wavelengths > 610 nm, excitation was at 545 nm. As the concentration of poly d(G-C) was varied between 0.5 and 45 μ M a single relaxation was observed, $\tau = 20$ to 2 msec. The association and dissociation rates were $11 \mu\text{M}^{-1}\text{s}^{-1}$ and 39s^{-1} , respectively. Assuming a one-step bimolecular mechanism, ethidium bromide binds to poly d(G-C) with a reaction volume of $\Delta V^\ddagger = -8 \text{ cm}^3\text{mol}^{-1}$. The binding of this dye with poly d(A-T) was also best characterized by a single-step bimolecular mechanism. In this case, as the DNA concentration was changed from 0.5 to 12.5 μ M the relaxation time decreased from 30 to 6 msec. The rate constant for the association of the dye with this polymer is $13 \mu\text{M}^{-1}\text{s}^{-1}$, the dissociation rate constant 17s^{-1} , and $\Delta V^\ddagger = -9 \text{ cm}^3\text{mol}^{-1}$.

057

CO-OPERATIVE BINDING OF T7 DNA POLYMERASE.
H. Rindahl, F. Watanabe*, A. Holmgren and R. Rigler*
Dept. Chemistry, Karolinska Institutet, Stockholm, Sweden.
* Dept. Medical Physics, Karolinska Institutet, Stockholm, Sweden.

The binding of T7 DNA polymerase to poly(dA-dT) and single- and double-stranded calf thymus DNA was studied by means of intrinsic tryptophan fluorescence. The number (n) of bases or base-pairs occupied by one T7 DNA polymerase molecule, the co-operative binding constant (K) and the co-operative interaction between nearest neighbours (q) were determined at various NaCl concentrations. The method used assumes co-operative and was according to Schwarz & Watanabe, (1983) J. Mol. Biol. 163, 467. T7 DNA polymerase showed co-operativity which was enhanced at salt concentrations up to 0.1 M. At higher concentrations the co-operativity of the polymerase was less salt dependent. The co-operative binding constant at 5°C and 0.05 M NaCl was $4 \times 10^4 \text{ M}^{-1}$. It decreased by a factor of six at a salt concentration of 0.30 M. In a plot of log K versus log NaCl extrapolation of the data to 1 M NaCl indicated that the enzyme-DNA interaction is of hydrophobic nature. The number of ion pairs displaced was estimated from the same plot, to be two. The DNA polymerase did not show any preference for either single- or double-stranded DNA.

059 CRAL PRESENTATION

STRUCTURAL REQUIREMENTS OF COMPEA CHLOROTIC MOTTLE VIRUS RNA AND COAT PROTEIN IN CAPSID MORPHOGENESIS.
B.J.M. Verduin, Department of Virology, Agricultural University, Binnenhaven 11, 6709 PD Wageningen, The Netherlands.

Compea chlorotic mottle virus, a spherical plant virus of which RNA and coat protein can be isolated in a native state, is used as a model system for protein-protein and protein-RNA interactions. Mixtures of coat protein (P20) and protein lacking 25 N-terminal amino acids (P17.5) formed homogeneous 28 nm capsids (T=3) with mixed composition upon dialysis from 0.3 M NaCl pH 7.5 to 5.0. All compositions including P20 could be precipitated with RNA indicating that all N-terminal arms are within reach of externally added RNA. In mixtures of capsids prepared at pH 5.0 from either P20 ($s_{20,w} = 52S$) or P17.5 ($s_{20,w} = 45S$) only capsids containing P20 were precipitated. Further removal of N-terminal amino acids (minus 41, 44 and 53) resulted in one band (M 15,000) in SDS-polyacrylamide gels. Mixtures of P17.5 and P15 in 0.3 M NaCl pH 7.5 with a molar ratio < 1 formed 18 nm capsids (T=1) after dialysing to pH 5.0. At low ionic strength pH 7.5 P20 interacted with the oligonucleotide d(ApTp)ApT (double-stranded) to form nucleoprotein particles resembling the original virus. Single stranded (Ap)₈A did not interact. P17.5 and P15 did not interact with any oligonucleotide or RNA. These experiments have been completed with NMR studies (G. Vriend) and Laser Raman spectroscopy studies (G.J. Thomas, Jr.). All data will be discussed in view of the A, B and C types of coat protein subunits observed in crystals of similar plant viruses.

056

OLIGONUCLEOTIDES COVALENTLY LINKED TO INTERCALATING AGENTS: STRUCTURE AND INTERACTIONS WITH COMPLEMENTARY SEQUENCES.

U. Asseline*, M. Delarue*, F. Toulmé*, M. Takasugi*, C. Barbier*, G. Lancelot*, J.J. Toulmé*, T. Montanav-Garestier*, N.T. Thuong* and C. Hélène*, Centre de Biophysique Moléculaire, 45045 Orléans Cedex (*), and Biophysique - Muséum, INSERM U.201, 61, Rue Buffon, 75005 PARIS, France(†)

Oligodeoxynucleotides covalently linked to intercalating agents have been synthesized. They interact selectively with their complementary sequences. Their binding strength is enhanced as compared with the parent oligodeoxynucleotide.

Absorption, fluorescence and nuclear magnetic resonance data will be presented for binding to poly(rA) and poly(dA) of oligothymidylates covalently linked to an acridine derivative. All the results available show that base pairing of the oligonucleotide with its complementary sequence is accompanied by an intercalation of the acridine ring between base pairs of the duplex sequence. The interaction depends on the length of the linker between the acridine ring and the oligonucleotide, and on the attachment site of the acridine substituent.

Preliminary data indicate that these new substances can be used as artificial repressors to block the transcription or the translation of specific genes.

058

AROMATIC COMPONENTS OF THE BINDING SITE OF A DNA SINGLE STRAND BINDING PROTEIN: THE GENE 32 PROTEIN OF BACTERIOPHAGE T4.

J.R. Casas-Finet*, R.V. Prigodich*, J.J. Toulmé*, R. Santus*, and J.E. Coleman*. (*) Laboratoire de Biophysique, ERA 951 du CNRS, Muséum National d'Histoire Naturelle, 61 rue Buffon, Paris (FRANCE); (†) Dept. of Molecular Biophysics & Biochemistry, Yale University, New Haven, Conn. (U.S.A.)

Gene 32 protein (gp32) from phage T4 binds strongly and cooperatively to single-strand nucleic acids whereas it exhibits a low affinity for native double-stranded DNA. This protein is involved in DNA replication, recombination and repair. gp32 is a monomeric polypeptidic chain of 301 amino acid residues which contains 5 Trp, 8 Tyr and 18 Phe. Its fluorescence is partially quenched in the complexes with single-stranded polynucleotides.

Tryptophyl (and cysteinyl) residues of gp32 can be selectively oxidized by Br_2^+ and $(\text{SCN})_2^+$ radical-anions produced by steady state γ -radiolysis. 2 Trp residues are readily oxidized in addition to 3 SH groups, leading to a complete inhibition of the binding properties of the gp32; these 2 Trp are fully protected in the complex formed with denatured DNA.

^1H NMR (500 MHz) spectra of an active proteolytic fragment of gp32 and its complexes with oligonucleotides of varying length show that the proton resonances of at least 1 Phe, 1 Trp and 5 Tyr shift upfield upon oligonucleotide binding.

Stacking interactions between aromatic amino acids and nucleic acid bases could explain these facts and ensure the specificity of single-strand binding (SSB) proteins for single-stranded polynucleotides.

060

PHOSPHOPEPTIDES IN HIGHLY PURIFIED CALF THYMUS DNA.

R.S. Welsh and K. Vyska, Institute of Medicine, Kernforschungsanlage, 5170 Jülich, F.R.G.

If highly purified DNA, isolated from calf thymus nuclei, is reacted with chelating agents, it cleaves into subunits accompanied by release of phosphopeptides (PPs). At the end-point of cleavage, about one half of the PPs remain bound to the DNA. In order to study the linkage of PPs to DNA, calf thymus DNA was purified to a minimum protein content, treated with ultrasonication, and then with pancreatic DNase, exonuclease III, and SI nuclease (to hydrolyze to the last nucleotide attached to the PP). The resulting material ("nucleotide-peptides") was fractionated on a Chelex column and then on DEAE Sephacel. From this the main component was hydrolyzed with Proteinase K and briefly with Pronase. Amino acid analysis of the hydrolysate revealed the presence of phosphoser, asp, glu, ser, gly, ala plus 3 components appearing after NH_4^+ . The resulting mixture was fractionated again on DEAE Sephacel, and the main component obtained was fractionated according to amino acid analysis, to collect the 3 unknown components ("nucleotide-amino acids"). By hydrolysis with 6N HCl or with snake venom diesterase and analysis, these were found to contain mainly phosphoser and a nucleotide, plus some glu and gly. From this it was concluded that the covalently bound peptide contained phosphoser, asp, ser, glu, gly, ala and that phosphoser, glu, and gly were terminal.

Tuesday 31 July Congress Centre-first floor. Posters 061-066

Posters on Nucleic Acid-Protein Interactions

061

THE LOCATIONS OF 5 PROTEINS WITHIN THE 30S RIBOSOMAL SUBUNIT OF *E. COLI*, DETERMINED BY SMALL ANGLE NEUTRON SCATTERING
M.S. Capel, M. Kjelgaard, V.R. Razakrishnan, D.M. Engelman & P.B. Moore, Dept. Molecular Biophysics & Biochemistry, Dept. Chemistry, Yale University, New Haven, Connecticut, U.S.A.

The position of the centers of mass of S14, S16, S17, S18 and S20 within the *E. coli* 30S ribosomal subunit has been determined, in solution, by small angle neutron scattering. Combined with prior data from this laboratory, the relative configuration of 17 of the 21 proteins of the 30S subunit has been specified. The map of centroids was constructed from a set of 77 interprotein distance measurements via least squares refined triangulation. In situ radii of gyration and distances between deuterated pairs of proteins (in an otherwise protonated reconstituted subunit) were derived from the second moment of the cord distribution of the deuterated pair, and the parallel axis theorem. Cord distribution functions were obtained by the conventional mixed difference method. The map of centroids is consistent with chemical crosslinking data, interprotein Förster fluorescence energy transfer measurements and the locations of surface-exposed antigenic determinants of ribosomal proteins deduced from electron microscopy. Spatial proximities within the map correlate with established cooperativities between ribosomal proteins that occur in the process of *in vitro* 30S subunit assembly. The centroid map also serves as a referent for discriminating between models of 16S rRNA tertiary structure and tRNA-ribosome interactions.

063

Two-dimensional ^1H NMR study of the λ phage O_{R3} operator.

K.D. Hahn^a, F. Buck^a, H. Rüterjans^a, B.K. Chernov^b, K.G. Skryabin^b, and M.P. Kirpichnikov^b.

^aInstitute of Biophysical Chemistry, University of Frankfurt, FRG, and ^bInstitute of Molecular Biology, USSR Academy of Sciences Moscow, USSR

The solution structure of the 17-base-pair operator O_{R3} , which is the most preferential binding site for Cro repressor of phage λ , was studied by two-dimensional NMR spectroscopy. Two-dimensional nuclear Overhauser enhancement (NOE) and homonuclear scalar coupling shift-correlated techniques made it possible to assign the resonances from the purine H-8, the pyrimidine H-6 and H-5, the thymidine methyl protons and many of the H-1', H-2' and H-2'' sugar protons to specific nucleotides in the double helix. The pattern of the observed NOE connectivities is consistent with B-form DNA. The base and sugar proton assignments provide the necessary information for further studies of the interaction of the O_{R3} operator with Cro repressor.

065

THERMODYNAMIC AND MECHANISTIC STUDIES OF THE INTERACTIONS OF RNA POLYMERASE WITH THE λ P₀ PROMOTER J.-H. Roe and M. T. Record, Jr., Depts. of Chemistry and Biochemistry, University of Wisconsin, Madison, Wisconsin, USA. 53706

Interactions of the cationic binding sites of proteins with the DNA polyanion behave at a thermodynamic level like ion exchange reactions (Record, Lohman, and deHaseth, J. Mol. Biol. (1976) 107, 145-158). Consequently both the equilibria and kinetics of these interactions are sensitive functions of the ionic environment. We have used this effect to probe the thermodynamics and mechanism of the interaction of *E. coli* RNA polymerase with the λ P₀ promoter, using the nitrocellulose filter assay. We find that approximately 20 monovalent ions are released in the formation of the transcriptionally-competent open complex at this promoter, and that the entropic contribution from release of these ions is the dominant thermodynamic driving force for complex formation under approximately physiological ionic conditions ($K_{eq} = 2.6 \times 10^{10} \text{ M}^{-1}$ at 25°C, pH 7.5, 0.20 M NaCl). At least two intermediates must exist on the pathway between the initial collision complex and the open complex, as determined from the magnitude of the salt-dependence of the overall second-order association rate constant and the negative activation energy of the overall first order dissociation reaction. The rate constants for the interconversions of these two intermediates have been accurately determined only at lower temperatures (10°-20°C). From the salt- and temperature-dependences of these rate constants, it appears that the interconversion of the intermediates proceeds by a mechanism involving the opening of the DNA originally proposed by Bock and Lohman (personal communication).

062

PHYSICO-CHEMICAL STUDIES ON THE ASSOCIATION BETWEEN *E. COLI* RNA POLYMERASE AND THE TET PROMOTER OF pBR322. EFFECT OF DNA UNWINDING ON THE FREE ENERGIE OF THE INTERACTION.

E. Bertrand, M. Schnarr, J.F. Lefèvre and M. Daune, Institut de Biologie Moléculaire et Cellulaire, Laboratoire de Biophysique, 15, rue René Descartes, Strasbourg, France.

Two different approaches were used to study the initiation of transcription by *E. coli* RNA polymerase of the tet promoter carried by supercoiled or linearized pBR322.

1) Following topoisomerase induced unwinding and separation by agarose gel electrophoresis, the specific binding of RNA polymerase to the tet promoter in 160 mM salt, was shown to lead to the release of approximately one more negative superturn at 37°C with pBR322 than with a plasmid (pBREB3) from which the tet promoter had been deleted.

2) Taking advantage of the abortive initiation method and of a fluorescent probe (UTP-γ-ANS), the initiation reaction could be followed as a function of time, the two parameters K_a (equilibrium constant of association) and k_2 (isomerization rate constant) were determined for different temperatures. The unspecific initiation was negligible in the case of pBREB3. When interpreted within the context of the classical scheme of Mac Clure, polymerase binding to the promoter appears to be stronger at 37°C in the case of linearized DNA than with one that is supercoiled.

Further the interpretation of these results requires a more elaborate model, that takes account of the energy of supercoiling.

064

TYROSINE FLUORESCENCE OF HISTONE H₁ AND H₂ - DNA COMPLEXES

C. Cuniberti, F. Pioli, B. Cavazza, E. Patrone, V. Trefiletti, Centro Studi Macromolecole Sintetiche e Naturali, CNR, Università di Genova, Genova, Italia.

Tyrosine fluorescence has been used to study the folding-unfolding equilibrium of free calf-thymus histone H₁ and its binding to DNA. Histone H₁, when acid extracted from chromatin, is devoid of structure. Secondary and tertiary structuration induced in a central core of about 80 residues on increasing the pH or on addition of salt is accompanied by an increase of the fluorescence quantum yield of the single tyrosine present in this region. The stability of the folded conformations towards thermal and chemical unfolding has been monitored by fluorescence. The binding of H₁ to DNA at neutral pH, 20°C and starting from different degrees of structuration (0-1 M NaCl) has been studied by coupling light scattering to fluorescence measurements. Different binding mechanisms may be suggested at 0 M NaCl and around physiological ionic strength. Binding to the DNA helix with folding of the protein core and the tyrosine out of contact with DNA occurs at low salt. Minimum interaction is established around 30-50 mM. At higher ionic strength the histone seems simply to work as a bridge between different DNA chains.

066

DNA TRIS-INTERCALATION : QUASI IRREVERSIBLE BINDING OF ACRIDINE TRIMER. P. Laugaa, J. Markovits, B. Gauguain, J.B. Le Pecq, and B.P. Roques. Département de Chimie Organique, Unité 266 INSERM et ERA 613 CNRS, Faculté de Pharmacie, 75006 PARIS. Laboratoire de Physicochimie Macromoléculaire, LA 147 CNRS, Institut Gustave Roussy, 94800 VILLEJUIF.

A trimer made up of 3 acridine chromophores (AcTri) linked by a charged amino-alkyl chain was designed as a potential tris-intercalating agent. The length of the linking chain was selected to allow tris-intercalation according to the excluded site model.

DNA tris-intercalation of the dye at low dye/base pair ratio was shown by measurements of both the unwinding angle of closed circular DNA and the lengthening of sonicated rod like DNA.

AcTri exhibits a high affinity ($K_{ap} = 10^9 \text{ M}^{-1}$, 1.5 M Na⁺) for poly-d(A-T) as shown by competition experiments with ethidium dimer. Kinetic studies of both the association with poly-d(A-T) and the exchange between poly-d(A-T) and sonicated calf thymus DNA have been performed as a function of the ionic strength. In 0.5 M Na⁺ the on rate constant ($k_1 = 2.1 \times 10^4 \text{ M}^{-1} \text{ s}^{-1}$) are similar to those reported for other mono or diacridines, whereas the off rate constants are much smaller ($k_{-1} = 6.5 \times 10^4 \text{ s}^{-1}$), leading to binding constants as large as $K_{ap} = 3.10^{10} \text{ M}^{-1}$. According to Record the plot of $\log(k_1/k_{-1})$ as a function of $\log(\text{Na}^+)$ yielded a straight line with a slope of 5 (i.e. 5.7 interacting charges out of 7 potential), from which a K_{ap} value of 10^{14} M^{-1} in 0.1 M Na⁺ can be computed. Such a value reaches and even goes beyond DNA affinity of regulatory proteins.

Tuesday 31 July Congress Centre-first floor. Posters 067-072

Posters on Nucleic Acid-Protein Interactions

067

Calculation of Electrostatic Orientation
and Docking Between DNA Binding Proteins and B-DNA

Jones B. Matthew and Douglas H. Chlenendorf
Genex Corporation, Science and Technology Center, 16020 Industrial Drive,
Gaithersburg, Maryland 20877 USA

Various studies have shown that the binding of DNA binding proteins with DNA is mediated by ionic interactions. Here we describe a computational study in which we examine the role of electrostatic interactions in the formation of the protein-DNA complex. To assess the role of the complementary ionic interactions we have computed the change in electrostatic free energy during association assuming a simplest case trajectory where there is no relative rotational reorientation of the molecules. The algorithm is an extension of the solvent accessibility discrete charge model¹. The use of the solvent accessibility factor in reducing charge-site interactions introduces a higher coulombic shielding. This screening can be interpreted as a high local ionic strength or alternately a higher effective dielectric constant. The computed complementary electrostatic potential surfaces will be presented as a function of separation distance. At all ionic strengths the displacement of bound sodium from the DNA minor groove plays an important role in determining the electrostatic energy of protein-DNA association. The role of this counterion redistribution in deforming the DNA will be discussed.

¹Matthew, J.B. and Richards, F.M. (1982) *Biochem J.* 21, 4989-4999.

069

REGULATION OF DNA REPLICATION AND THE *dnaA* PROTEIN OF
E. coli H.J. Eberle, M. Van de Merwe, C. Stillman,
D. Sporn and G. Kamp, Dept. Rad. Biol. and Biophys.,
Univ. Rochester, NY 14642

The *dnaA* protein is required for the initiation of DNA replication in *E. coli*. Genetic and biochemical evidence suggests that it interacts with the origin of chromosomal replication (*oriC*). Other genetic evidence suggests that *dnaA* protein also interacts with the θ subunit of RNA polymerase and may be involved in the synthesis of the primer needed for initiation at *oriC*. The recent discovery of binding sequences for *dnaA* protein at *oriC*, as well as between promoters *P*₁ and *P*₂ of the *dnaA* gene suggest that the *dnaA* protein may regulate its own synthesis, as well as function with RNA polymerase to allow primer formation at *oriC*. Our laboratory has isolated a mutant, called *PR1*, which overproduces the *dnaA* protein. The *PR1* mutation maps in the *dnaA* region of the chromosome. Transcriptional studies reveal that there are three times as many transcripts of the *dnaA* gene in *PR1* as are present in *C600*, a normal wild type *dnaA* strain. In order to determine whether the *PR1* mutation has resulted in faulty self-regulation by *dnaA* protein, the location of the *PR1* mutation within the *dnaA* region, is being more precisely determined and the expression of the *lacZ* gene, cloned behind a promoter with the *dnaA* protein binding sequence, is being examined in *PR1* and wild type *dnaA* cells.

071

STRUCTURE AND DYNAMICS OF OLIGOPEPTIDE - NUCLEIC ACID COMPLEXES.

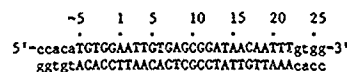
J. Fidy*, M. Takasugi and T. Montanay-Garestier, Laboratoire de Biophysique, INSERM U.201, Muséum National d'Histoire Naturelle, 61 Rue Buffon, F-75005 PARIS (France).
*Institute of Biophysics - Semmelweis Medical University BUDAPEST (Hungary).

Static and dynamic fluorescence experiments provided information on the structure of complexes formed between tetrapeptides containing a tryptophan residue and nucleic acids. Analysis of fluorescence decays of the free and the complexed peptide showed that two conformers of the peptide bind to nucleic acids, each giving a fluorescent complex(I) and a quenched complex(II). The equilibrium between the populations of the two peptide conformers is shifted upon binding. Dynamic quenching by acrylamide of the free peptide and of the fluorescent complex(I) allowed us to compare tryptophan accessibility and mobility in the fluorescent species. The quenching rate constant and the rotational correlation time were measured. In complexes(I), the tryptophan residue is fully accessible and its mobility is almost not restricted indicating no interaction between the indole ring and the nucleic acid bases. In complexes(II), the fluorescence of the tryptophan residue is completely quenched.

068

LAC OPERATOR DNA: CORRELATION OF IMINO PROTON EXCHANGE RATE WITH FUNCTION. S. Cheung, K. Arndt, and P. Lu, Department of Chemistry, University of Pennsylvania, Philadelphia, PA, USA.

The imino protons of the double helical DNA sequence containing the lactose operon operator has been examined by NMR. The intensities of the imino proton resonances as a function of increasing temperature indicate that a DNA fragment containing the operator not only melts sequentially from the ends, but also from a region inside the *lac* operator, i.e. at position 6 in:



In order to examine this phenomenon in detail, we have synthesized 3 sections of the sequence as indicated. At temperatures where proton exchange dominates the relaxation rate, it is clear that the melting effects seen at position 6 are reflected in the higher exchange rates at the GC neighbors, 5 and 7. Changes in this three base pair region, from 5 to 7, results in operator constitutive mutations.

This GTG/CAC triplet occurs in a number of DNA sites that specifically interact with proteins in prokaryotic and eukaryotic systems. (Supported by grants from the NIH)

070

HYDRODYNAMICAL STUDY OF ARTEMIA RIBOSOMAL RNAs.

K. Donceel, P. Nieuwenhuysen and J. Clauwaert, Department of Biochemistry, Antwerp University, 2610 Antwerpen, Belgium.

The conformation and structure of the small and large ribosomal subunits, as well as their interaction, is influenced by the conformation, structure and interaction of the ribosomal RNAs. Therefore, we have followed up a study of the physical properties of eukaryotic ribosomal particles with a study of the size and conformation of their RNAs free in solution. Information about the structure of the rRNAs was obtained by measuring their sedimentation coefficient at Mg^{2+} concentrations from 0 to 15 mM, in the presence of 100 mM K^+ ; this K^+ concentration turned out to be optimal to avoid aggregation. The diffusion coefficient has also been measured by photon correlation spectroscopy in fewer well-defined conditions, to confirm the sedimentation data.

For the RNA of the small subunit, the sedimentation coefficient increased drastically in a narrow range from 0 to 1 mM Mg^{2+} corresponding to a decrease of the hydrodynamic radius R_h from more than 70 nm to 12 nm. This reflects a drastic compacting of the tertiary and secondary structure of the RNA chain. For the large rRNA of the large subunit, the hydrodynamic parameters depend much less heavily on the Mg^{2+} concentration: R_h changes from 20 nm in the absence of Mg^{2+} to 14 nm at 15 mM Mg^{2+} .

The distinct difference in the hydrodynamic behaviour of the two RNAs must be related to a different secondary interaction pattern, particularly for the ends of the RNA chains.

072

NON-SPECIFIC AND SPECIFIC BINDING OF THE LEX A REPRESSOR : CIRCULAR DICHROISM AND GEL ELECTROPHORESIS MEASUREMENTS
M. Schnarr, M. Granger-Schnarr and M. Daune, Institut de Biologie Moléculaire et Cellulaire, Laboratoire de Biophysique, 15, rue René Descartes, Strasbourg, France.

The Lex A repressor of *E. coli* plays a central role in the regulation of the so-called SOS system, controlling the transcription of at least fifteen different SOS genes. Here we present results on the non-specific and specific interactions of the Lex A protein with poly [d(A-T)] and a *recA* operator containing DNA fragment. Using circular dichroism spectroscopy we find that the interaction with poly [d(A-T)] is co-operative and rather resistant to ionic strength, indicating an important non-electrostatic energy contribution, that might arise from protein-protein contacts. The conformational change of the DNA as revealed by the circular dichroism spectra is very similar, if not identical to that observed for the interaction of *lac* repressor with non-operator DNA. The specific interaction of Lex A with the operator of the *recA* gene has been studied by gel electrophoresis. At low Lex A concentrations ($< 10^{-7}$ M) a single band due to specific binding is observed. At more elevated concentrations an additional band appears, representing probably the co-operatively saturated non-specific complex.

Posters on Nucleic Acid-Protein Interactions

073

PREDICTION OF PROTEIN CODING REGIONS IN DNA SEQUENCES BY DISCRIMINANT ANALYSIS. K. Nakata, M. Kanehisa and C. Delisi, Laboratory of Mathematical Biology, NCI, NIH, Bethesda, Maryland, U.S.A.

Protein coding regions and their boundaries are known to exhibit significant patterns in DNA sequences; such as consensus sequences of promoters and splice junctions, and the periodic appearance of specific bases reflecting the non-random usage of degenerate codons. One approach to detect such patterns is the "perceptron" algorithm. It can usually achieve 100% of discrimination between correct and incorrect members after a learning procedure. However, its usefulness is limited when predicting unknown sequences, i.e. sequences not included in the learning procedure. We have developed a more general method, based on discriminant analysis, to incorporate various features and to make better predictions. By this approach we can, for example, combine, in a natural way, the values for the perceptron matrices reflecting consensus sequence patterns at the boundaries, and the base composition and periodicity.

We have applied this method to distinguish initiation sites, termination sites, exon/intron and intron/exon boundaries from merely fortuitous sequences, using the GenBank database. The combination of the perceptron and the base composition and periodicity was shown to be powerful for the prediction of the allocation of unknown sequences.

075

CYCLOC AMP RECEPTOR PROTEIN - RNA POLYMERASE INTERACTIONS. M. Pinkney and J. G. Hoggett, Department of Biology, University of York, Heslington, York, U.K.

The cyclic AMP Receptor Protein (CRP) of *E. coli* is a pleiotropic gene activator which acts, together with its allosteric effector c-AMP, to produce a stimulation of the rate of initiation of gene transcription. It has been suggested that the mechanistic basis for CRP action might be direct interaction between CRP and RNA polymerase.

Fluorescence polarization studies have been used to demonstrate and characterize interactions between fluorescein labelled CRP (F-CRP) and native RNA polymerase. The results obtained show that, under quasi-physiological conditions, F-CRP binds RNA polymerase holoenzyme in a c-AMP dependent manner; the dissociation constant in the presence of c-AMP being about $4.0 \mu\text{M dm}^{-3}$. Competition experiments suggest that binding between holoenzyme and native CRP is somewhat tighter and a tentative estimate for the dissociation constant of $0.7 \mu\text{M dm}^{-3}$ has been made.

Interactions between F-CRP and RNA polymerase core enzyme, which lacks the sigma subunit known to be important in promoter selection, appear to be c-AMP independent but are dependent upon ionic strength to the extent that they are probably negligible under physiological conditions.

Analytical ultracentrifugation studies have shown that CRP binds to monomeric rather than dimeric RNA polymerase.

077

THE STRUCTURAL ROLE OF THE RIBOSOMAL RNA OF THE SMALL SUBUNIT OF THE *E. coli* RIBOSOME BY DARK FIELD E.M.

A.P. Korn, D. Elson and P. Spitnik-Elson, Biochemistry Department, Weizmann Institute of Science, Rehovot 76100, Israel.

We have been investigating ribosome structure by dark field EM because of its high sensitivity and resolution. The small subunit consists of a conical body bearing a "head" and "collar". Treatment with uranyl acetate stains the collar as well as two additional parallel bands below it. Examination of a fragment, which lacks a double-stranded section at the 3' end of the rRNA (domain IV) demonstrated that the collar was missing and that no staining occurred here. Thus, we 1) have identified the collar as being domain IV and 2) suggest that the two other stained bands are also external double-stranded rRNA. Electron spectroscopic imaging, a technique that selectively images the element-specific information in the inelastic electrons, allows a study of the phosphorus, and therefore the nucleic acid distribution in intact subunits. It was observed that the RNA is concentrated towards the centre, with some signal appearing towards the surface in those regions which were shown to be external by uranyl acetate staining. We compared these results to protein-free RNA. In the presence of spermidine, shapes were remarkably similar to the 30S subunit though somewhat elongated. In the absence of spermidine, further elongation to about 300 Å occurred. In conclusion, it would seem that the rRNA serves as a "skeleton" to the ribosome, and that the RNA already has the potential for a large degree of folding but final compaction is effected by the ribosomal proteins but can be simulated in part by spermidine.

074

HIGH RESOLUTION ELECTRON DIFFRACTION OF tRNA CRYSTALS AND THEIR SUBSTANTIAL STABILITY TO ELECTRON IRRADIATION

Y. Fujiyoshi, Inst. for Chemical Res., Kyoto Univ., Uji, Kyoto-Fu, K. Morikawa and H. Yamagishi, Dept. of Biophysics, Faculty of Sci., Kyoto Univ. Kyoto Japan

The crystals of yeast tRNA^{Phe} have been subjected to electron microscopy using negative staining, glucose embedding technique and frozen hydrated specimen technique as representative of various polynucleotide crystals. The dimensions of the stained crystals were estimated at $a=54\pm 1\text{Å}$, $b=33.5\pm 0.5\text{Å}$ and $c=63.5\pm 0.5\text{Å}$. They are close to those of the unit cell dimensions of native crystal determined by X-ray diffractions. The comparison between the obtained images and those simulated from the drawing of the molecular model leads to the conclusion that the observed images represent the real molecular arrangements within the crystal lattice. Some parts within the unit cell seem to obstruct the penetration of uranyl ion into the internal, and this appears to give somewhat modified images of the molecules. Electron diffraction patterns with a resolution better than 4Å were obtained from a glucose embedded crystal and also frozen crystals. The fading of diffraction intensities by electron irradiation were measured for the Bragg reflections 3,4,4(14 5 0) of the glucose embedded crystal and frozen hydrated one at about 300 K and about 13K respectively. Their critical dose are 3.7 e/Å² and 42 e/Å² respectively. These measurements of radiation damage rate indicates 7 and 84 times, respectively, less susceptibility to electron exposures than that of protein crystals embedded in glucose at room temperature.

076

SPECIFIC RECOGNITION AND MECHANISM OF DNA CLEAVAGE OF THE TYPE II RESTRICTION ENZYMES HgaI and TagI.

J.A. Littlechild - Dept. of Biochemistry, University of Bristol, Bristol, U.K.

The HgaI enzyme from *Herpetosiphon giganteus* recognises a degenerate hexameric site GAGCAG in which either the second or the fifth position can be an adenine or a thymine residue. The mechanism of cleavage of the enzyme has been studied using, supercoiled DNA (pAO3(mini ColEI) and fd) with either a single palindromic or non-palindromic recognition site. Agarose gel electrophoresis is used to separate the supercoiled, open circle and linear DNA products. Differences in mechanism are observed between two sites under conditions of low Mg²⁺ and pH 5.6. The enzyme TagI has been isolated from the thermophilic bacterium *Thermus aquaticus* and it recognises and cleaves within the tetrameric site T⁺CGA. Similar studies with a DNA molecule with one recognition site (SV-40) have been used to study the enzyme mechanism. The importance of sequences outside the recognition site lead to the conclusion that AT rich sequences result in more rapid cleavage than GC. Enzyme inhibition, by methylation at the N6 of adenine by *E. coli* dam methylase can be overcome by substituting Mn²⁺ for Mg²⁺ in the reaction mixture.

Both enzymes have been purified to homogeneity and appear to be dimers.

078 ORAL PRESENTATION

STUDIES ON THE INTERACTION OF THE CYCLIC AMP RECEPTOR PROTEIN (CAP) AND RESOLVASE WITH DNA. S.S. Abdel-Meguid, I.T. Weber, P. Drost, N.D.F. Grindley, H.M.K. Murthy, T.A. Steitz, M.R. Sanderson, J.A. Rice and D.M. Crothers, Departments of (Molecular Biophysics and Biochemistry) and Chemistry, Yale University, New Haven, Connecticut.

Two DNA binding proteins and their respective DNA binding sites are being studied using X-ray crystallographic and solution techniques in order to understand protein-DNA interactions at a molecular level.

The cyclic AMP receptor protein (CAP, 45,000 D.), is being studied in complexes with DNA oligomers from the *lac* site. The X-ray crystal structure of CAP is known from previous work in this group¹.

Resolvase (M.W. 20,500 D.), the gene product of the *tnpR* gene in the $\gamma\delta$ transposon², can be cleaved into 2 domains, M.W.'s 15,300 D. (L.F.) and 5,000 D. (S.F.) by α -chymotrypsin. S.F. is the DNA binding domain and L.F. contains the catalytic site for site-specific recombination³. X-ray crystallographic studies of L.F. are in progress^{3,4}. Intact resolvase and S.F. are being studied in complexes with a DNA oligomer, which is part of a site shown by footprinting⁵ to have a high affinity for S.F.

- 1 D.B. McKay and T.A. Steitz, Nature 290, 744-749 (1981).
- 2 N.D.F. Grindley et al., Cell 30, 19-27 (1982).
- 3 P.C. Weber, D.L. Ollis, W.R. Bebrin, S.S. Abdel-Meguid, T.A. Steitz, J. Mol. Biol. 157, 689-690 (1982).
- 4 S.S. Abdel-Meguid, N. Templeton, N.D.F. Grindley and T.A. Steitz, P.N.A.S., in press.

Tuesday 31 July Congress Centre-first floor. Posters 079-084

Posters on Nucleic Acid-Protein Interactions

079 ORAL PRESENTATION

X-RAY DIFFRACTION AND ELECTRON-MICROSCOPIC STUDY OF 5 S rRNA CRYSTALS. K. Morikawa, Department of Biophysics, Faculty of Science, Kyoto University, Kyoto, Y. Fujiyoshi, K. Ishizuka, Institute for Chemical Research, Kyoto University, Kyoto, M. Kawakami and S. Takemura, Institute of Molecular Biology, Nagoya University, Nagoya, Japan.

5 S rRNA is a common constituent that is present in the larger ribosomal subunit of biological species from prokaryotes to eukaryotes. We for the first time succeeded in the crystallization of 5 S rRNA from thermophilic bacteria, *Thermus thermophilus* HB8 (Morikawa et al., FEBS Letters (1982) 165, 194-196). We have subsequently been searching for the crystals good enough to be analysed at an atomic resolution level. Up to date, 5 different types of crystals have been grown by a vapour diffusion technique and crystal data about 3 of them were determined by X-ray diffraction. At the moment, the best crystal diffracts up to 13 Å resolution level. One type of crystals was thin enough to be subjected to electron microscopy. The crystal stained with uranyl acetate was found to preserve its regularity at 17 Å resolution level. The noise filtered images of [001] and [112] projections revealed the molecular arrangements within the crystal lattice. We could construct a model explaining features of the two images consistently. The further examination about packing of the molecules into the unit cell consequently gave some implications on the overall shape of 5 S rRNA molecule.

081

3-D STRUCTURE OF DNase I AND ITS INTERACTION WITH SKELETAL MUSCLE ACTIN

D. Suck, Ch. Oefner and W. Kabsch, EMBL, Heidelberg, F.R.G.
The three-dimensional structure of bovine pancreatic deoxyribonuclease I (DNase I) has been determined at 2.5 Å resolution by X-ray diffraction from single crystals. An atomic model was fitted into the electron density using a graphics display system. DNase I is an $\alpha\beta$ -protein with two 6-stranded β -pleated sheets packed against each other forming the core of a "sandwich"-type structure. The two predominantly antiparallel β -sheets are flanked by three longer α -helices and extensive loop regions. The carbohydrate side chain attached to Asn 18 protrudes by about 15 Å from the otherwise compact molecule of approximate dimensions 45 Å x 40 Å x 35 Å. The binding site of Ca^{2+} -deoxythymidine-3',5'-bisphosphate (Ca-pdTp) has been determined by difference Fourier techniques confirming biochemical results that the active centre is close to His 131. Ca-pdTp binds at the surface of the enzyme between the two β -pleated sheets and seems to interact with several charged amino acid side chains. Active site geometry and folding pattern of DNase I are quite different from staphylococcal nuclease, the only other Ca^{2+} -dependent deoxyribonuclease whose structure is known at high resolution. In the crystals of the rabbit skeletal muscle actin:DNase I complex four contact regions were found. The DNase I residues involved in these contacts are predominantly charged or hydrophilic amino acid side chains.

083

Regulation of the Equilibria and Kinetics of Interaction of Proteins and Nucleic Acids by Inorganic Ions. M. Thomas Record, Jr., Departments of Chemistry and Biochemistry, University of Wisconsin, Madison, Wisconsin 53706 USA.

Protein-DNA interactions may be modeled at a thermodynamic level as ion exchange reactions, in which the neutralization of fixed charges on these biopolyelectrolytes upon complex formation is accompanied by a significant redistribution of the inorganic ions originally ordered in concentration gradients in the vicinity of the macromolecules. This redistribution is thermodynamically equivalent to the release of as many as 10-20 ions in the formation of a protein-DNA complex, and makes the equilibria and kinetics of the association reaction far more sensitive to the ionic environment than to the macromolecule concentrations themselves. We have used Monte Carlo methods, analytical polyelectrolyte theory and quadrupolar cation NMR to examine the distribution of small ions in the vicinity of DNA, and the thermodynamic consequences of this distribution. In addition, we have demonstrated the use of inorganic ions to probe the thermodynamics and mechanisms of the interactions of lac repressor and RNA polymerase with specific and nonspecific binding sites on DNA. The dramatically large ion effects observed in these interactions make ion concentrations the key regulatory variable for controlling these interactions *in vitro*, and strongly suggest that inorganic ions may also be an important regulator of the protein-DNA interactions in gene expression *in vivo*.

080

THE INTERACTION OF THE PFI DNA BINDING PROTEIN WITH VIRAL DNA

G.G. Kneale and R.W. Wijnandts, European Molecular Biology Laboratory, Heidelberg, F.R.G.

The DNA binding protein of P1 bacteriophage binds to the single stranded phage genome during replication, forming an intracellular nucleoprotein assembly complex. The structure of the isolated complex has been analysed by X-ray fibre diffraction, revealing an open helical assembly with 6.0 to 7.5 protein dimers per turn and a variable pitch of 45-55 Å, with the two strands of the DNA held apart by the protein dimers, each site binding 4 nucleotides of one strand. The fluorescence of the protein arises from its single tryptophan. The fluorescence depolarisation, the fluorescence lifetime and the emission spectrum of the nucleoprotein complex all differ significantly from those of free protein dimers. We have used these changes to investigate the binding of oligonucleotides and DNA to protein dimers in solution, and propose a model for the equilibrium. We show that the fluorescence properties of the complexes formed are related to the lateral association of dimers along DNA strands. The results can be correlated with the role of the protein in promoting single stranded DNA synthesis and phage assembly.

082

Low resolution neutron crystal study of the Aspartyl-tRNA-synthetase t-RNA^{Asp} complex using contrast variation.

M. Roth (ILL, Grenoble), A. Levit-Bentley (EMBL, Grenoble), D. Moras & R. Giegé (IBM, Strasbourg), France.

The H₂O/D₂O solvent contrast variation technique was applied in a single crystal study to determine the low-resolution structure of the protein and nucleic acid components of the complex. The crystals are of space-group I4₃₂, a=354 Å with one enzyme dimer and two tRNA molecules per asymmetric unit and useful data extend to 22 Å d-spacing.

A preliminary study of the variation of diffracted intensity with deuterium concentration (1) gave values for match-points of the mean scattering density of the protein and the tRNA. Using data at the match-point of the tRNA, we made a positional and rotational search with a simple model against data to 40 Å d-spacing, followed by a least-squares refinement against data to 32 Å d-spacing. The enzyme dimer was represented by two identical ellipsoids of the expected volume, related by a local 2-fold axis. The solution with the best agreement with experimental data and with the radius of gyration closest to that measured in solution corresponds to a grouping of two enzyme dimers about the [110] 2-fold axis of the crystal, thus forming a tetrameric unit with three orthogonal 2-fold axes. The refinement of the position and shape of the tRNA molecules is now in progress. The coherence of the results within the contrast variation series will serve to confirm our results.

(1) Moras, D. et al. (1983), J. Biomol. Structure & Dynamics 1, 209-223

084

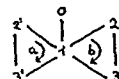
CIRCULAR DICHROISM OF THE 16S RNA CLOACIN FRAGMENT: TITRATION BY IF3. E. Wickstrom, Dept. of Chemistry, Univ. of South Florida, Tampa FL 33620 USA

IF3 is a strongly binding RNA helix destabilizing protein, which binds specifically to the initiation codon AUG, and to a 14-nucleotide sequence near the 3' end of 16S rRNA which is virtually conserved in all forms of life (Wickstrom, E. (1983) Nucleic Acids Res. 11, 2035-2052). Hence, it was of interest to examine the secondary structure of the 3' end of 16S rRNA by observing its circular dichroic (CD) spectrum, and the subsequent effects of adding IF3. The CD spectrum of the 49-nucleotide 3' terminal fragment of 16S rRNA was measured at 25°C in 10 mM Tris-HCl, pH 7.4, 100 mM NH₄Cl, 1 mM Mg(OAc)₂, 1 mM DTT, 5% glycerol, and displayed no 299 nm trough, a 269 nm peak, a 242 nm crossover, and a 225 nm trough. Upon addition of increasing amounts of IF3, the peak CD decreased smoothly by about 20% to an endpoint of >1 IF3 per RNA strand, with a peak redshift of only 2 nm. When the CD spectrum was measured in 10 mM Na₂HPO₄, pH 7.4, 1 mM EDTA, 1 mM DTT, 5% glycerol, its shape was virtually the same, but titration with IF3 decreased the peak CD by 35% to an endpoint of 2 IF3 per strand, with the same 2 nm peak redshift. The probable implications of these observations for the modes of IF3 binding to the 3' end of 16S rRNA, and for the function of IF3 in mRNA binding, will be discussed.

Posters on Nucleic Acid-Protein Interactions

085

A MODEL OF CHEMOMECHANICAL TRANSDUCTION BY DNA GIRASE.
E. Mirzaj and J. Lin, Depto. de Biofísica, Facultad de Medicina, Depto. de Física, Facultad de Humanidades y Ciencias, Montevideo, Uruguay.
The following diagram specifies a minimal model for the action of DNA Girase,



where 0,1,... are conformational states of the enzyme. The transition 0→1 represents the binding of the enzyme to the DNA. In cycle b, 1→2 describes ATP binding, 2→3 represents supercoiling events, and 3→1 describes the release of products. In cycle a the protein goes through the same states as in b but in the absence of ATP. The model has transition probabilities dependent on the linking number. As the enzyme cycles through b clockwise, DNA suffers supercoiling and generates mechanical tension. The following results are derived from this model: i) Kinetic constants of cycles a and b in general do not satisfy Wegscheider relations. ii) There is a unique stable steady state at the point where mechanical forces exactly balance the forces generated by the hydrolysis of ATP. iii) Without substrates the system behaves as a topoisomerase thus decreasing the linking number via cycle a. iv) Near the steady state the system relaxes as an Ornstein-Uhlenbeck process.

087

INTERACTION OF SUBSTRATES IN THE ACTIVE SITE OF E. COLI RNA POLYMERASE
P. Szafranski, W. J. Smagowicz and K. L. Wierzechowski
Inst. of Biochem. Biophys., Polish Acad. Sci., Warsaw
Steady-state kinetic studies of abortive initiation of transcription on the ALT7 promoter by E. coli RNA polymerase (ATP+UTP+pppApU+ppp) with use of appropriately modified substrate analogues were carried out to investigate which particular groups of the ribose moiety and triphosphate chain are involved in binding of ribonucleoside 5'-triphosphates by the enzyme. Analysis of the kinetic constants derived therefrom indicated that: (i) the triphosphate chains of the primer PuoTP and of the elongating NTP interact with some protein receptor groups through their α- and β-residues, (ii) the ribose 2'-OH of the elongating NTP is also bound to the protein, (iii) the 3'-OH of the PuoTP and the γ-phosphate of the elongating NTP are involved in an interaction between the substrates, whereby affinity of the substrates to their binding sites increases significantly, and (iv) the α- and β-phosphates of the elongating NTP also participate in this interaction. It is postulated that the interaction of substrates is mediated by the protein-bound Mg(II) ion, and a minimal molecular model of a chelate PuoTP-Mg(II)-NTP complex in the catalytic centre of the enzyme: promoter initiation complex is proposed.

089

STRUCTURAL ANALYSIS OF CRYSTALS OF RESTRICTION ENZYME/DNA COMPLEXES BY ELECTRON MICROSCOPY.
J. A. Berrigan, K. R. Leonard and F. K. Winkler.
European Molecular Biology Laboratory (EMBL)
Postfach 10.2209, Meyerhofstr. 1, D-6900 Heidelberg, F.R.G.
During work on the restriction enzyme EcoRV by X-ray diffraction, co-crystals were formed with the decanucleotide (5') CGAATTCG containing the recognition sequence (underlined). These crystals were thin enough for electron microscopy and, negatively stained with uranyl acetate, gave images with a resolution of 1.5 nm. The unit cell size is 5.4 x 6.4 nm (κ=90°), plane group pg. In glucose these crystals gave electron diffraction patterns with very good mirror and Friedel symmetry extending to 0.3 nm resolution. With the octanucleotide (5') CGAATTCG which lacked the proper recognition sequence, another crystal type was formed. This gave negatively stained images to 1.5 nm resolution and a unit cell of 7.4 x 8.4 nm (κ=90°), plane group cm. It was found that diluting the mother liquor caused these crystals to disrupt and form single layer sheets and tubes. The unit cell dimensions were unchanged, now with plane group pgg symmetry. In glucose these crystals diffracted to 0.5 nm and two arcs, presumably from the DNA base-pair stacking, were seen in the diffraction pattern at 0.34 nm and ±20° to the long axis of the crystal. We are now working on a tilt reconstruction of the single layers to define the low resolution shape and packing of the protein dimer. This, together with the electron diffraction data, may identify the DNA binding positions for the specific and non-specific complexes.

086

CHARACTERISTIC BASE SEQUENCE PATTERNS OF PROMOTER AND TERMINATOR REGIONS IN ΦX174 AND ΦD PHAGE DNAs (DNA-RNA POLYMERASE INTERACTION) J. Otsuka and T. Kunisawa, Dept. of Applied Biol. Sci., Faculty of Sci. and Technol., Sci. Univ. of Tokyo, Chiba 278, Japan.
The base sequence properties have been investigated over the entire region of ΦX174 and ΦD phage DNAs in comparison with in vivo and in vitro transcription data accumulated on these phages. The properties investigated here are distribution of recognition and firm binding sequences, palindromes, symmetrical base sequences, A + T content and the other specific sequences of three to seven bases with low frequency of occurrence. The present investigation reveals the following rules. (1) In in vivo promoters, the recognition and firm binding sequences appear with a definite base distance of 18±2 bp. (2) In in vitro promoters, the base distance between the recognition and firm binding sequences is somewhat deviated, and their promoter efficiency is under the influence of the A + T content in a wide range of about 60 bp. (3) Most terminators, especially rho-independent ones, are characterized by a homology of the G+C rich palindromes followed by a poly A+T sequence. (4) The palindrome which intervenes between the recognition and firm binding sequences much reduces the promoter efficiency, even if the set of these sequences seems to constitute a promoter site. These rules provide some insight into the molecular mechanism how E. coli RNA polymerase consisting of subunits interacts the double stranded DNA.

088

INTERACTION OF THE ANTICODON LOOP OF YEAST tRNA^{Val} WITH RIBOSOMES. AN ESR STUDY
Ivana Mervand-Burasevic, Vesna Nöthig-Laslo and Ž. Kučan
Faculty of Science and Rudjer Boskovic Institute, University of Zagreb, Zagreb, Yugoslavia
We have used yeast tRNA^{Val}, spin-labelled in 6A-37 residue with 4-amino-2,2,6,6-tetramethylpiperidine-1-oxyl, to study conformational changes caused by binding of various ligands to this macromolecule (V. Nöthig-Laslo et al. (1981) Eur. J. Biochem. 117, 263-267), as well as the contacts of the anticodon region of this tRNA with other macromolecules. The message-free binding of deacylated tRNA^{Val} to E. coli ribosomes, taking place at the P₂ site, was our first choice. The equilibrium constant of 1x10⁴ mol⁻¹ for the complex formation was determined from Scatchard plot. ESR spectrum of free tRNA^{Val}, characteristic for a rapidly-tumbling nitroxide, changes to a spectrum with extensively broadened lines in the ribosome-tRNA complex. The original spectrum can be restored upon long incubations of the complex with an excess of extraneous tRNA. ESR spectra suggest that the spin-label motion is drastically perturbed though not completely blocked in the ribosome-tRNA^{Val} complex. Since ESR spectra of a spin-label attached to the opposite, i.e. 5'-side of the anticodon loop, are only slightly perturbed by the messenger-free binding to ribosomes (Rodriguez et al. (1980) J. Biol. Chem. 255, 8116-8120), it is concluded that the two sides of the anticodon loop face entirely different environments when bound to the P-site, the 3'-side being oriented towards the surface of the ribosome, and the other side towards its environment or a large cavity.

090

PROTEIN-DNA INTERACTIONS: INFLUENCE OF POLYPEPTIDE CONFORMATION AND COMPOSITION. F. Azorin, J. L. Campos J. Aymari, J. Vives, J. Lloveras and J. A. Subirana
Unidad de Química Macromolecular del C.S.I.C., Barcelona, Spain.
R. Mayer and A. Brack, Centre de Biophysique Moléculaire du CNRS, Orleans, France.
We have studied the interaction with DNA of basic polypeptides which have different conformations. We have found that DNA in the B form can interact with polypeptides which have either an α or β conformation. In all cases the DNA maintains its B form upon interaction. The polypeptides usually maintain its original conformation, but in some cases the original conformation is lost and the polypeptide is wrapped around the DNA. We conclude that there is no single polypeptide conformation (α, β or other) which is favoured for interaction with DNA. The polypeptides we have studied are:
β conformation preserved:
Ac-Lys-Ala-Tyr-Ala-Lys-NHET
Poly(Val-Lys), Poly(Leu-Lys)
β conformation lost upon interaction:
Poly(Ala-Lys)
α conformation preserved:
Poly(Lys-Ala-Ala-Lys)
Poly(Lys-Leu-Ala)
α conformation lost:
Poly(Lys-Ala-Ala)

Tuesday 31 July Congress Centre-first floor. Posters 091-096

Posters on Metal-Proteins and Electron Transfer

091 ORAL PRESENTATION

PROTON MAGNETIC RESONANCE STUDIES OF 7Fe FERREDOXINS
K. Nagayama¹, T. Imai², D. Ohtori³, and T. Oshima⁴
¹Bionetology Lab, JEOL LTD, Nakagami, Akishima, Tokyo Japan
²Dept of Chemistry, College of Science Rikkyo, Toshima-ku Tokyo Japan
³Dept of Chemistry, School of Medicine Juntendo Univ, Chiba
⁴Lab of Chemistry for Natural Products, Tokyo Institute of Technology, Yokohama, Japan

Ferredoxins (Fd) extracted from *Thermophilus thermophilus* (Tt) *Mycobacterium smegmatis* (Ms) and *Pseudomonas ovalis* (Po) were studied by ¹H-NMR. On the basis of spectral change accompanying with redox titration, two redox centers, 3Fe and 4Fe clusters, were concluded in these ferredoxins. The order of redox potentials for each of redox centers was
3Fe: Em(Po) < Em(Tt) < Em(Ms) < 0mV (1)
4Fe: Em(Po) < Em(Tt) < Em(Ms) < -400mV (2)

The 4Fe center always showed a potential lower than that of the 3Fe center. This apparently contradicted to the notion that the 4Fe center belonged to the iron-sulfur of the HiPIP type. For Po Fd which is the most homologous to the well-known Azotobacter vinelandii Fd, this was solved by confirming the oxidizability of the 4Fe redox couple using a stoichiometric amount of oxidant. Po Fd provided a first example of the verification of the three state theory of the redox center. An excess amount of oxidant was, however, found to effect conversion of the 4Fe center to an iron center of the 3Fe type for all of the three Fds. On long term incubation in air, the converted 3Fe center showed even further change in NMR spectra.

093

CHANGES IN THE ELECTRONIC STRUCTURE OF IRON-HEME AS AFFECTED BY UV-LIGHT IRRADIATION AND LASER.

M.S. Abd El-Baset. National Research Centre.
Dokki, Cairo, Egypt.

Oxyhemoglobin ($2.6 \times 10^{-3} M$) was subjected at $23^\circ C \pm 1$ to near UV (300-420 nm) and long waves (320-390 nm) by use specific filters. The time of exposure was 5-30 min, which corresponds to $7.55-45.3 \times 10^{-3}$ joule/cm² and $5.45-32.7 \times 10^{-3}$ joule/cm². Also the same concentration of HbO₂ was subjected at $23^\circ C \pm 1$ to 0.5m volt laser (630 nm) for the same exposure time. It was found that, irradiation with near UV led to shift in Soret band for 5-10nm, towards short wavelength. Evidence of oxidation also comes from EPR signals which confirmed the loss of electron. Changes in electronic states of heme, heme-heme interaction and globin-heme interaction were much more in the case of near UV. Whereas long waves of UV besides its effect on heme parts, it caused a weakness in the noncovalent bond between globin and heme. An intermediate states and threshold were detected from spin states constant and thermodynamic parameters. Also different unfolding degrees were detected with an increase in active sites (OH⁻ receptors). The effect of laser seemed to be less effective as compared to UV irradiation. Interesting data were obtained when exposed HbCo.

095

CYTOCHROME c OXIDASE: STRUCTURE AND FUNCTION AS AN OXIDASE AND A PEROXIDASE

L. Powers, Y. Ching, Bell Laboratories, Murray Hill, NJ, USA
and B. Chance, C. Kumar, Johnson Foundation, U. of Penn, Medical School, Philadelphia, PA, USA

The structure of the resting oxidized form of this terminal enzyme in the respiratory chain, cytochrome c oxidase, has been shown by x-ray absorption spectroscopy to contain a sulfur bridge between the copper and iron of the active site which are separated by ~3.8Å. This form functions as an oxidase with the CO or O₂ bound to the reduced active site iron producing a structure similar to CO or oxy hemoglobin while the sulfur remains with the active site copper. It is this form with the sulfur bridged active site that is found in sub-mitochondrial particles and intact mitochondria and is isolated by the Yonetani method with ~90% homogeneity but not by the Hartzell-Beinert method. The pulsed form is also fully oxidized but lacks the sulfur bridged active site and the iron of the active site is structurally similar to that of the peroxidases. This form functions as a peroxidase. A stable intermediate is also formed with hydrogen and ethylhydrogen peroxide in which the active site iron structure is similar to that of the peroxidase intermediate. The active site copper does not participate in the peroxidatic role. Thus, this unique enzyme has a peroxidase activity which serves as to safeguard its main oxidase function.

092

ANTIMITOTICS INDUCE CARDIOLIPIN CLUSTERS FORMATION: POSSIBLE ROLE IN MITOCHONDRIAL ENZYME INACTIVATION.
P. Haart, R. Brasseur, E. Goormaghtigh and J.-M. Ruysschaert
Labor. Macromol. at Interfaces. CP:206/2 Brussel Free University, Brussels - Belgium, B-1050.

We recently proposed that inhibition of the last oxidation site of the respiratory chain (cytochrome c oxidase: E.C.1.9.3.1.) could participate to the Adriamycin mitochondrial toxicity (1). We demonstrate here that the formation of cardiolipin clusters induced by Adriamycin is a prerequisite to the inactivation process. Three antimitotics (Adriamycin, acridine orange, ethidium bromide) with a similar affinity ($\approx 10^6$ mole/litre) for cardiolipin were shown to affect differently the cytochrome c oxidase activity measured on beef heart mitochondria. This observation can be explained in terms of clusters formation resulting from the mode of association of the antimitotic-cardiolipin complex. The acridine orange-cardiolipin and Adriamycin-cardiolipin complexes allow the formation of cardiolipin stacked structures stabilized by antimitotic-antimitotic interaction whereas, in the ethidium bromide-cardiolipin structure, molecules are not oriented parallelly rendering stacking between cycles and consequently cardiolipin clustering very improbable. For Adriamycin, it is tempting to design new structures avoiding the lipid clusters formation but preserving the interaction with DNA. It could be another possibility to decrease the antimitotic cardiotoxicity.

(1) E. Goormaghtigh, R. Brasseur and J.-M. Ruysschaert (1982) Biochem. Biophys. Res. Commun. 104, pp. 314-320.

094

HIGH AND LOW SPIN THERMAL EQUILIBRIUM IN MET-HAEMOGLOBIN AND MET-MYOGLOBIN - DEPENDENCE WITH FREEZING VELOCITY
E. Wajnberg, H. J. Kalinowski and G. Benski¹.
¹Department of Physics, Pontificia Universidade Católica, Centro Brasileiro de Pesquisas Físicas, Rio de Janeiro, Brasil

We have used Electron Spin Resonance (ESR) to study the equilibrium mixture of the low and high spin states in haemoproteins. Measurements in the temperature range from 6K to 100K were taken in powdered samples of haemo- and myoglobin. The intensity ratio of the ESR spectra is used to measure the relative spin population of the two spin states. As the ESR intensity also depends on the spin-lattice relaxation time, the experiments were conducted under sufficient low power of the incident microwave radiation to avoid that effect. We have also observed the dependence of the ratio mixture with the freezing velocity of the sample. We have found that in the low temperature range ($T \leq 12K$) the high to low spin concentration ratio increases as the freezing velocity increases. For sufficient high temperatures ($T > 60K$) both proteins show a classical Boltzmann distribution of the spin-states, with a typical energy of 13 cm^{-1} for moderate freezing velocities ($11.5-27K/min$). This distribution is valid for the entire range of temperatures when the sample is slowly frozen ($\sim 1.5K/min$).

Research supported by CNPq

096

CYTOCHROME P450_{CAM}: ORIENTATION OF THE g-TENSORS RELATIVE TO THE HEME COMPLEX.

F. G. Debrunner, P. W. Devaney and G. C. Wagner,
Departments of Physics and Biochemistry, University of Illinois, Urbana, IL 61801 USA

Cytochrome P450_{CAM} from *Pseudomonas putida* is the first heme-thiolate monooxygenase to be crystallized. Spectroscopically, P450_{CAM} resembles the mammalian P450 cytochromes, a functionally diverse group of membrane proteins. According to the 3d electron density map of P450_{CAM} (T. Poulos et al. (1984) J. Mol. Biol. cys-134 coordinates to the heme iron in the high-spin ferric substrate complex. Based on a preliminary analysis of the x-ray data and single crystal EPR (P. W. Devaney et al., in preparation) we can infer the orientation of the Fe(III) g-tensors relative to the heme complex. The majority of the substrate adduct has $g = (7.75, 3.93, 1.80)$ with principal axes within 4° of the iron - N_{pyr} directions (x,y) and the heme normal (z). At 4.2K a minority (30%), low-spin species with $g = (1.97, 2.23, 2.40)$ is observed, which resembles the pure low-spin species, $g = (1.91, 2.24, 2.46)$, of the substrate-free enzyme. Assuming the transition to low spin does not change the orientation of the heme in the crystal, the g-values 2.40 and 2.46 are observed at 18° and 6° from z, while the g-values 1.97 and 1.91 are at 9° and 10° from x and within 2.7° and 1.9° of the heme plane, resp. The results are discussed in a ligand-field model. Supported by USGM 16406.

Tuesday 31 July Congress Centre-first floor. Posters 097-102

Posters on Metal-Proteins and Electron Transfer

097

INTERACTION BETWEEN THE TWO HEMES IN *Pseudomonas* CYTOCHROME *c* PEROXIDASE.
R. Aasa^a, N. Ellfolk^a, M. Rönnberg and T. Vänn-
gård^a, ^aDepartment of Biochemistry and Biophysics,
University of Göteborg and Chalmers Institute
of Technology, Göteborg, Sweden, and ^bDepartment of
Biochemistry, University of Helsinki, Helsinki,
Finland.

The anion binding and catalytic properties of
cytochrome *c* peroxidase from *Pseudomonas aerugi-
nosa* have been studied with optical and magnetic
resonance techniques. The high-potential (+300 mV)
c heme is always low-spin, but the low-potential
(-300 mV) *c* heme undergoes a transition from
high-spin at room temperature to low-spin at low
temperatures. Reduction of the high-potential heme
changes the EPR and proton NMR spectra of the
low-potential heme and enhances its binding of
azide, cyanide and fluoride. The reaction of
hydrogen peroxide at the low-potential heme re-
quires that the high-potential heme is reduced,
and intermediates are formed in which the high-
potential heme plays a role similar to that of the
protein radical in the yeast enzyme.

099

STRUCTURAL PARAMETERS OF PEROXIDASE-PEROXIDE INTERMEDIATES
B. Chance and L. Povers, University City Science Center,
Phila., PA 19104 and A T & T Bell Labs, Murray Hill, NJ 07974
Enzyme-substrate compounds of peroxidases serve as models
for Michaelis-Menten intermediates in enzymology (1). Their
ferryl iron models (Fe^{IV}O) as represented by ferryl
myoglobin have been useful (2). Here we report X-ray
absorption spectroscopic studies. The edge spectrum of
compounds I and II of horseradish peroxidase indicate valence
states higher than Fe^{IV}. The ratios between the
intensities of X-ray absorption at 7175 and 7200 eV appears
to be linearly related to the volume magnetic susceptibility
from low-spin to high-spin range, for 9 stable compounds and
two intermediates. A comparison of the structural properties
of compounds I, II and III as derived from their EXAFS
indicates a short Fe-Ne (proximal histidine) distance in I
and III. The corresponding Fe-Np (pyrrole-nitrogen) distance
is long, a result which differentiates the peroxidases from
oxygen transport hemoproteins and may play a pivotal role in
their reaction mechanism. Compound II differs distinctly
from compound I. The first shell peak average distances are
not as short as compound I and are similar to other low spin
derivatives. These parameters now permit a structural analysis
of the sequence of intermediates in peroxidase activity.
REFS. 1) Chance, B., J. Biol. Chem. 151:553-577 (1943) 2)
George, P. and Irvino, D. H. Biochem. J. 52:511-519 (1952) 3)
Hahn, J.E. et al. SSRL Activity Rpt. 83/01 699B (1983)
Grant Support: NIH grants GM33165 and HL18708.
The collaboration of Dr. K. G. Paul and Dr. T. Poulos is
gratefully acknowledged.

101

IRON STORAGE COMPOUND STUDY IN HEPATIC AND SPLENIC OVERLOADED
TISSUES BY MOSSBAUER SPECTROSCOPY.
J.H. Rimbart, C. Kellershohn, F. Dumas and G. Richardot,
Lab.de Biophys., Fac. Med.Necker-Enfants Malades, Paris, FRANCE.

Mössbauer spectra have been performed on lyophilized
tissue samples of normal human livers and human livers present-
ing iron overload (hemochromatosis due to hypertransfusional
therapeutic in patients with major β -thalassaemia). These
spectra are carried out at different temperatures (R.T., 77°K
and 4.2°K).

At room temperature, the spectra suggest the presence of
electric quadrupole interactions typical of a high spin ferric
iron. At 77°K, the behaviours of the spectra are strikingly
different. For the normal liver samples, we observe only quad-
rupolar interactions due to the superparamagnetic properties
of ferritin and hemosiderin. For the iron overloaded liver
samples, in addition of this typical electric doublet ($\Delta = 0.7$
mm s⁻¹, $\delta = 0.5$ mm s⁻¹), we note the presence of another component.
This one consists, on the spectra, as a doublet ($\Delta = 1.2$ mm s⁻¹,
 $\delta = 0.4$ mm s⁻¹) and a beginning of a magnetic splitting. At low
temperature (4.2°K), the magnetic splitting is complete in
all cases.

This is confirmed by Mössbauer spectra performed on chemi-
cally isolated hemosiderin samples from spleen of normal or
iron overloaded subjects. In particular, in the latter case,
we observe also this typical component characterized by a
beginning of magnetic order at higher temperature as 77°K.

These results suggest that, in the case of iron overload,
in addition of normal ferritin and hemosiderin, a new magnetic
state of iron is appearing.

098

FAILURE OF THE ALLOSTERIC MODEL FOR BOTH INITIAL AND
TERMINAL PHASES OF LIGATION IN HEMOGLOBIN. L. J.
Parkhurst, Wang Guang-Xin, T. M. Zamis, and G. Geraci,
Dept. of Chemistry, Univ. of Nebraska, Lincoln, NE
68588-0304, U.S.A.

Double mixing instrumentation and rapid quenching
techniques together with rapid protein separations have
allowed us to quantitate the distribution of CO molecules
between the alpha and beta chain hemes in the initial
phases of ligation. Once the initial sites were occupied
with CO, the remaining sites were filled with other
ligands, such as NO, or the sites were rapidly oxidized
and excess reactants removed. EPR spectroscopy on the NO
hybrids allowed the distribution of NO (and by
complementarity, CO) to be determined for the alpha and
beta sites. Azide binding was also monitored in the met
hybrids, confirming the NO EPR assignments. These
population studies showed that the alpha chain is
preferentially occupied in the initial phases of ligation.
The distribution results together with precise
spectrophotometric data near the static isosbestic point,
allow rate constants to be assigned to the individual
hememes for various models. A heterogeneous three-state model
is the minimal model for early phases of ligation. Later
photolysis and precise oxygen equilibrium studies on
valency hybrids show that the allosteric model appears to
fit terminal phases of ligation. The values required for
L, however, are in marked disagreement with values
determined from simple stopped-flow kinetics. Support:
NIH HL 15,284, NSF PCM 8003655.

100

RESONANCE RAMAN SPECTROSCOPIC STUDIES OF SIX-COORDINATE
LOW-SPIN FORMS OF HORSERADISH PEROXIDASE James Tierner,
David Reed, and Andrew Sitter, Dept. of Chemistry, Vir-
ginia Commonwealth University, Richmond, VA 23284, U.S.A.

We have obtained highly detailed resonance Raman
spectra of a number of derivatives of isoenzymes of horse-
radish peroxidase, which include among others, the alkali-
ne form, and compounds II and X obtained in mixing
experiments. Native horseradish peroxidase is believed to
contain a five-coordinate high-spin heme. Resonance Raman
spectra of the alkaline form of horseradish peroxidase are
indicative of a six-coordinate low-spin heme. It is
interesting to note that the oxidation state marker bands
of the iron(IV) hemes of horseradish peroxidase compounds
II and X are not significantly higher than those of the
low spin iron(III) derivatives.

Support is acknowledged from Research Corporation,
the Petroleum Research Fund as administered by the Ameri-
can Chemical Society, and the Jeffress Memorial Trust.

102

NMR STUDY OF pH AND METAL ION BINDING EFFECTS ON THE
BEHAVIOR OF ALBUMIN TETRAPEPTIDES A.A. Ribeiro and C.F.
Chionell, Laboratory of Molecular Biophysics, National
Institute of Environmental Health Sciences, P. O. Box 12233,
Research Triangle Park, NC 27709, USA.

¹H NMR spectroscopy has been used to investigate the pH
behavior and metal-ion binding properties of two synthetic
tetrapeptides, AspThrHisLys and AspAlaHisLys in H₂O/D₂O
mixtures. These peptide sequences respectively correspond
to the N-terminal metal-ion binding sites of bovine and human
serum albumins, proteins that are involved in the transport
of toxic metal-ions. Using 2-dimensional NMR correlated
spectroscopy we have made complete assignments of the ex-
changeable amide and non-labile side chain proton resonances
of these peptides. The chemical shifts and line shapes are
sensitive to pH. The line widths of selected backbone and
side chain resonances are also sensitive to the presence of
Cu(II) and Ni(II) ions at a given pH. Previous work on model
tripeptides has suggested that the metal-ion binding sites
of these peptides involve the α -amino nitrogen atom, two
deprotonated nitrogen atoms, the imidazole nitrogen atom and
the side chain carboxyl group of the aspartic acid. Our work
allows for the first time the direct monitoring of the back-
bone amide protons involved and the evaluation of the role
of the lysine residue in metal ion binding. We are now
extending these studies to include ¹³C NMR methods to look
directly at the carbonyl and α -methylene resonances.

Tuesday 31 July Congress Centre-first floor. Posters 103-108

Posters on Metal-Proteins and Electron Transfer

103

ENLARGED FLUORESCENCE POOL OF ONE-ELECTRON REDOX CENTERS IN OXIDATIVE PHOSPHORYLATION AND ATP SYNTHESIS REGULATION.

L.P. Lavushin, O.S. Medelina, Institute of Chemical Physics, Acad. Sci. USSR, Morigina Street, Moscow, USSR
ESR studies of intact mitochondria and SLP in flow system allow to detect energy-dependent ESR signals with $g=1.94, 1.98, 2.00, 2.02, 2.05$ (room t., 7 and 21K). These signals were present in tightly coupled mitochondria and SLP under conditions of intensive ATP synthesis or its inhibition by oligomycin or competitive inhibitor vanadate (P_i -analogue) and reverse transfer in the A/P presence. So it is essential the presence of a local one electron transport chain regulating ATP synthesis at a coupling site.

Redox state of some flavin groups in mitochondria, reversibly changed to, visible in ESR, as shown to correlate with oxidative phosphorylation intensity. In a model system, flavin-ADP- P_i photocyclized and ATP synthesis along with ADP free radicals were detected.

The photodynamic model of ATP synthesis in oxidative phosphorylation was developed according to it, an activation of A/P in active center of ATP-synthase occurs via formation of ADP phosphoryl radical, possessing a high affinity to P_i , this radical arose in one-electron local chain on triggering it by energization.

105

PROTON HYPERFINE RESONANCE ASSIGNMENTS IN CYTOCHROME C PEROXIDASE AND THE GLYCERA DIBRANCHIATA HEMOGLOBINS
James D. Satterlee, James E. Erman and Ioannis Constantinidis
Department of Chemistry, University of New Mexico;
Albuquerque, NM, 87131 USA

The physiological role of cytochrome c peroxidase is to catalyze the hydrogen peroxide oxidation of ferrocytochrome c in yeast mitochondria. This participation by peroxidase in the mitochondrial electron transport chain occurs via the electron transfer complex formed between cytochrome c and cytochrome c peroxidase. In order to compare the proposed structure of this complex with an actual solution structure we have begun to make assignments of CoP hyperfine shifted proton resonances. These include both heme and non-heme protons and are currently being extended to the protein redox complex.

Another set of proteins, the hemoglobins isolated from the monomer fraction of Glycera dibranchiata proteins, are of interest for the very important reason that one member of this group has been shown to lack the distal histidine. We will demonstrate the extent of heterogeneity which occurs in the monomer hemoglobin fraction and present our initial results of ligand studies of individual purified components. The replacement of the distal histidine by leucine dramatically affects the heme pocket ligation dynamics and we will present our most recent work on hyperfine shift assignments for both deuterium exchangeable and non-exchangeable proton resonances in the met-hemoglobins.

107

EFFECTS OF AXIAL LIGATION AND PORPHYRIN DIMERIZATION IN DISTINCT PH FORMS OF COPPER CYTOCHROME C
J.A. Shelnutt, Sandia National Laboratories,
Albuquerque, New Mexico, USA.

Unusual features of the absorption and resonance Raman spectra of copper cytochrome c ($Cu\text{-cyt-c}$) are shown to result from axial ligation in the neutral form and from dimerization of the Cu porphyrins at pH extremes. A new method of quantitatively analyzing changes in the spectra in terms of the MO parameters of the four-orbital model is successfully applied to the problem. The method correctly predicts distinct relationships between band intensities and energies for model monomeric and dimeric metalloprotoporphyrins [M(ProtoP)]. $Cu\text{-cyt-c}$ is shown to fall along these theoretical curves. At pH extremes where dimerization occurs, the $Cu\text{-cyt-c}$ point falls near the $Cu(\text{ProtoP})$ dimer, however, the point for the pH 7 form falls near $Mg(\text{ProtoP})$ and far from the $Cu(\text{ProtoP})$ monomer. The latter result is explained in terms of the effect of axial ligation on the porphyrin-metal interaction. The interpretation given is supported by resonance Raman and absorption spectroscopy of model Ni and Cu porphyrin complexes in coordinating solvents.

1. J.A. Shelnutt, K.D. Straub, P.H. Rentzepis, M. Gouterman, E.R. Davidson, Biochemistry, in press.
2. J.A. Shelnutt, L. Phys. Chem. in press.

104

MODEL STUDIES OF ELECTRON TRANSFER IN THE METAL-LIGAND/SUPEROXIDE/METAL-O₂

B. Jezowska-Trzebiatowska, P. Cadelevat, M. Ogi, Institute of Chemistry, University of Lodz, Joliot-Curie Street, Lodz, Poland

The problem of electron transfer in the model system $Cu(II)/H_2O_2/H_2O$ has been studied. The correlation between the donor-acceptor orbital steric properties of $Cu(II)$ and the steric properties of the donor or coordination site is studied by this system. The model reaction of electron transfer in the system $Cu(II)/H_2O_2/H_2O$ for its alkyl or aryl derivatives was explained. The existence of the relatively stable ternary complex metal-substrate- O_2 was proved as an intermediate in the catalytic oxidation of substrate (hydroquinone), that simulates the active centre of the oxidase.

106

Electrostatic Interactions During Electron Transfer Reactions Between c-type Cytochromes and Flavodoxin

Patricia C. Weber (Submitted by James B. Matthews)
Department of Protein Engineering
Genex Corporation, 16020 Industrial Drive
Gaithersburg, Maryland 20877 USA

Ferrocyanide c and flavodoxin semiquinone form a 1:1 electron transfer complex in vitro. The intermolecular rate of electron transfer depends on solution ionic strength with larger rate constants observed at low ionic strength. Computer modelling studies have suggested that the complex is stabilized by salt-linkages between lysine residues on horse heart cytochrome c and aspartate and glutamate residues on Clostridium pasteurianum flavodoxin (Sundgren, et al., Biochemistry (1982) 24, 6366). Using a modified Tanford-Kirkwood theory, the computed electrostatic potential surfaces of the isolated molecules were shown to be large and opposite in sign (Matthew et al., Nature (1983) 301, 169). The attraction of these charged surfaces was proposed to accelerate the reaction rate by preorienting the molecules along a productive reaction pathway and promoting their association.

Computer graphics and computational studies have been extended to include other c-type cytochromes whose electron transfer rates with flavodoxin also depend on ionic strength (Weber, et al., (1983) submitted to J. Biol. Chem.). Taken together, the kinetic and computational studies provide evidence for a positive correlation between the rate of electron transfer and the extent of positive electrostatic potential about the exposed heme edge of cytochrome c.

108

PROTEIN STRUCTURES AND THE RATES OF ELECTRON TRANSFER REACTIONS. A.K. Churg and A. Warshel, Department of Chemistry, University of Southern California

A microscopic treatment of the energetics of electron transfer (ET) between proteins is described. The calculations treat the contribution of the reorganization energy, α , to the activation energy for ET, ΔG^\ddagger , and are applied to the case of electron exchange between two cytochrome c molecules. The problem is addressed in three stages: (i) it is shown that, assuming the validity of the Marcus-Levich relation, $\Delta G^\ddagger = (\alpha + \Delta G^\circ)^2 / 4\alpha$, the observed X-ray structural differences between reduced and oxidized cytochrome c yield an estimate of α which depends on the electrostatic interaction of the redox active cofactors with the protein dipoles and is rigorously independent of the folding energy of the protein. (ii) A potential surface for electron exchange between cytochromes is constructed from the X-ray coordinates of the protein atoms. This static model gives the same values of α and ΔG^\ddagger and in (i). (iii) The reorganization component of ΔG^\ddagger for ET is evaluated by simulating the classical motion of the protein atoms (including both the protein folding and the electrostatic interactions). Preliminary results for ΔG^\ddagger derived from trajectories of the oxidized and reduced cytochromes are presented and the dynamic approach is compared to the static model. The computed value of α for electron exchange at a distance of 8 Å is 6.4 kcal/mol in the protein system, whereas the corresponding quantity is estimated to be 32 kcal/mol in water, indicating that proteins control the dielectric relaxation around redox active groups in their active sites.

Tuesday 31 July Congress Centre-first floor. Posters 109-114

Posters on Metal-Proteins and Electron Transfer

109

LATERAL MOBILITY OF FLUORESCENT DERIVATIVES OF CYTOCHROME c IN MITOCHONDRIA J.M. Vanderkooi, G. Maniara and M. Erecinska, Dept. of Biochemistry & Biophysics & Dept. of Pharmacology, University of Pennsylvania, Philadelphia PA, USA.

The technique of fluorescence recovery after photobleaching was used to examine the lateral motion of cytochrome c bound to giant (2 to 10 μ m diameter) mitochondria from the waterbug *Lethocerus indicus*. Native cytochrome c was exchanged for iron-free ('porphyrin') cytochrome c , a derivative in which the porphyrin has high quantum yield of fluorescence. In the presence of excess porphyrin cytochrome c the apparent diffusion coefficient was 6×10^{-11} cm²/sec in 0.3 M sucrose-mannitol-EDTA and 3×10^{-10} cm²/sec in 0.10 M KCl-0.10 M sucrose. At concentrations of porphyrin cytochrome c which are stoichiometric with cytochrome c oxidase, a component which showed no recovery during the time scale of measurement was observed. We make these speculations on the possible origins of the immobilized fraction: 1. cytochrome oxidase and reductase may be aggregated into large complexes, 2. the outer membrane and/or folds in the cristae may impede diffusion, 3. a protein matrix, analogous to the cytoskeleton, may also exist in mitochondria. (Supported by NIH HL18708).

111

CALORIMETRIC AND NMR STUDIES OF α -LACTALBUMIN P. Sellers, T. Drakenberg and H.J. Vogel, Dept. of Physical Chemistry 2, University of Lund, Lund, Sweden

α -Lactalbumins (α -Lac) are homologous with hen egg white lysozyme. Using proton NMR nuclear overhauser enhancement studies we have observed that the folding of the amino acid residue Ile95 with respect to Trp60 and Trp104 in the bovine and human α -Lac is identical to that of the homologous Ile98 and Trp63 and 108. The latter are part of the so-called hydrophobic box region of lysozyme. Notwithstanding such similarities these two proteins differ markedly in their capacity to bind Ca^{2+} . Proton NMR and differential scanning calorimetry studies show that Ca^{2+} - α -Lac reversibly denatures around 65°C and that the apo form is only stable up to 25°C. Calcium-43 and cadmium-113 NMR studies indicate the presence of one strong and one weak Ca^{2+} -binding site. Occupation of the strong Ca^{2+} -binding site can also be followed using titration microcalorimetry which shows that binding of Ca^{2+} to α -Lac is a strongly exothermic process, similar for Ca^{2+} binding to other calcium-binding proteins. Zn^{2+} binding to apo α -Lac occurs with a positive enthalpy change and so is completely entropy controlled. Thermodynamic parameters measured for Ca^{2+} binding to Zn^{2+} - α -Lac indicate that binding of both these cations is not necessarily mutually exclusive as had been suggested previously.

113

OXYGEN ACTIVATION BY IRON CONTAINING DIOXYGENASES J.D. Lipscomb, D.M. Arciero and J.W. Whittaker, Dept. of Biochemistry, Univ. of Minnesota, Minneapolis, MN., U.S.A. Activation of O_2 for insertion into protocatechuate (PCA) by intradiol (Fe^{3+}) dioxygenases has been proposed to require enzyme mediated substrate ketonization to promote O_2 attack on the resulting carbanion. However, binding kinetics of readily ketonized, azo-analogs of PCA to PCA 3,4 dioxygenase (3,4 PCD) suggest, instead, that PCA binds initially in the phenolic form as an Fe chelate, and that O_2 attacks this species, promoting ketonization. EPR detected, ^{51}V hyperfine broadening shows that the Fe of 3,4 PCD has at least one H_2O ligand which is displaced along with a 2nd ligand by PCA. It is now proposed that the putative ketonized intermediate is stabilized by a bond between one of the vacatable sites in the Fe ligation and the distal atom of the attacking O_2 . O_2 bond breaking and insertion probably occur in this Fe-organic peroxo species. The O_2 activation reaction catalyzed by extradiol dioxygenases such as PCA 4,5 dioxygenase appear to differ markedly. The active site Fe is ferrous and can bind NO to give an S=3/2, EPR active, species. This species is dramatically altered by PCA suggesting that both PCA and NO are bound to the Fe. No spectroscopic or kinetic experiments indicate that O_2 is bound by the Fe of resting enzyme. We suggest that O_2 activation occurs in an oxy-enzyme-substrate complex and may be again promoted by coordination of oxy species in vacatable sites of the Fe ligation. (Supported by NIGMS 24689).

110

THE CRYSTAL STRUCTURE OF MANGANESE SUPEROXIDE DISMUTASE FROM BACILLUS STEAROTHERMOPHILUS K. Karlsson, L.H. Weaver, J.D.G. Smit, R.A.auptit and J.N. Janssonius, Biozentrum, University of Basel, Klingelbergstrasse 70, CH-4056 Basel, Switzerland.

X-ray data to 2.5 Å resolution of Mn SOD, an α - β dimer from *B. stearothermophilus*, crystal form D with one 3 β -mer per asymmetric unit (Smit et al. (1977), J.Mol.Biol. 112, 491) were collected several years ago, but the phase problem could not be solved. D. Ringe and G. Petsko at M.I.T. recently solved the presumed homologous structure of Fe SOD from *Ps. ovalis* and kindly supplied us with their data. Cross- and self-rotation function runs at 4.5 Å with a new program (Karlsson, in preparation) gave consistent results, thus establishing the structural homology of the two enzymes and the orientation of the molecular dyad of Mn SOD. The molecular position was determined with the translation function. Phases from the Fe SOD dimer in the Mn SOD unit cell confirmed previously determined heavy atom positions in five derivatives. MIR phases from these were refined by local symmetry averaging using a method based on Shannon interpolation in reciprocal space (K. Karlsson, in preparation). The polypeptide chain of known sequence (Brook & Walker (1980), Biochemistry 19, 2873-2882) is being built into the resulting "best" electron density map with the use of an E & S PS 300 graphics display system. The molecule is very similar to Fe SOD and the Mn positions correspond to those of the iron atoms in Fe SOD.

112

DYNAMIC RELATIONSHIPS OF LIPID AND REDOX PROTEIN LATERAL DIFFUSION REVEALED IN MITOCHONDRIAL INNER MEMBRANES OF VARYING PROTEIN DENSITY. B. Chazotte, E.-S. Wu and C.R. Hackenbrock, Labs. for Cell Biol., NC Dept. of Anatomy, Univ. of North Carolina, Chapel Hill, NC 27514 USA

Fluorescence recovery after photobleaching (FRAP) was utilized to measure the lateral diffusion of the lipid analog 3-3' dihexyldicarbocyanine (Dil) and selected immunofluorescently labeled mitochondrial redox proteins in intact rat liver mitochondrial inner membranes. The low pH method of Schneider et al. (PNAS 79:112, 1980) was employed to enrich the inner membrane in phospholipid. The calcium fusion method of Chazotte et al. (Fed. Proc. 42:2170, 1983) was then used to fuse these enriched membranes to a diameter of 10-200 μ m which are then suitable for FRAP. Freeze fracture electron microscopy confirmed that the above membranes have randomly distributed proteins with the same density as the lipid-enriched membranes from which they are formed. Lipid lateral diffusion was found to increase as the protein density decreased. Lipid diffusion was also found to have a greater temperature dependence in native (protein dense) membranes than in pure lipid membrane systems. The temperature dependence was found to decrease as the protein density was decreased by lipid enrichment of the inner membrane. The rate at which redox proteins diffuse appears to be influenced by the overall protein density as well. These results indicate that dynamic interactions at high protein density limit the rate of lateral diffusion of the membrane components. Supported by NSF PCM79-10968 and NIH GM 28704 to CRH.

114

CRYSTALLOGRAPHIC STUDIES OF THE FERREDOXIN I FROM *Hydrogenobacter thermophilus* (Norway) J. Mossé, J.P. Astier and M. Frey, CNRS-CNRS MARSEILLE 13288 CDX 9 France.

In the sulfate-reducing bacteria from the genus *Hydrogenobacter*, ferredoxins which serve as electron carriers are associated either with the reduction of sulfate to SH_2 , or with the molecular H_2 exchanges with other bacteria through hydrogenase. The ferredoxin I from *H. thermophilus* is a direct physiological partner of a 4 heme cytochrome c_3 which behaves itself as a cofactor of the hydrogenase. The 3d structure of the c_3 from this same organism has already been determined in our laboratory (Häser et al., Nature 1979-1982, p. 806; Picot et al. J.B.C. 1982-1987, p. 1434). Ferredoxin I is a small protein (M.W. 6000) which contains one cluster of four irons and four labile sulfurs. Diffraction data from the native protein crystals (Cubic, $a = 74$ Å, S.G. P4₃2₁) were collected at 4.3 Å resolution on a diffractometer coupled to a rotating anode X-ray tube. Data collections for three potential heavy-atoms derivative (at 4.5 Å res.) are underway. Computer graphics studies have been attempted, on the basis of sequence homologies with the ferredoxin from *Hydrogenobacter thermophilus*, the 3d structure of which is already known (Adman et al. J.B.C. 1974-1983, p. 1987) they suggest that an hydrophobic zone on the surface of the molecule which surrounds the cluster as well as some close acidic residues should play a role in the recognition process with the c_3 . Collaboration with F. Guerlesquin and M. Brischi ICB-CNRS Marseille France.

Tuesday 31 July Congress Centre-first floor. Posters 115-120

Posters on Metal-Proteins and Electron Transfer

115

LIPOSOME-ENCAPSULATED HEMOGLOBIN. BIOPHYSICAL PROPERTIES OF A RED CELL SURROGATE

M.C. Farmer and B.P. Gaber, Biomolecular Optics Section, Code 6510, Naval Research Lab, Washington DC, USA.

Liposome-encapsulated hemoglobin (LEH) is being developed as an emergency resuscitation fluid. Oxygenation of LEH is reversible and cooperative, oxygen affinity can be modulated by co-encapsulation of organic phosphates. Our standard liposomal membrane composition is dimyristoyl phosphatidylcholine:cholesterol:dicetyl phosphate in a 6:4:0.5 molar ratio. A dispersion of lipids in stroma-free hemoglobin is extruded through controlled-pore size membranes to produce a nearly monodisperse suspension of largely unilamellar vesicles 0.4 microns in diameter. Repulsive forces due to the negative charge on the dicetyl phosphate prevent significant aggregation or fusion during storage. Serum free Ca^{++} levels induce reversible aggregation but not fusion. No hemolysis is detected in a suspension of erythrocytes or LEH incubated at 37 C for 8 hours. Circulation half-life of LEH averages 5.5 hours in mice presented with a volume equivalent to 30% of blood volume, with 100% survival of the mice. Circulation half-life varies with phospholipid chain length. Infusion of LEH into an isolated rabbit heart preparation yields measurements of coronary resistance which parallel those for infused erythrocytes. Viscometry measurements show the LEH to have a pattern of non-Newtonian viscosity similar to that of erythrocytes. (Supported by the Office of Naval Research.)

117

ELECTRON TRANSFER, OXYGEN ACTIVATION AND SUBSTRATE TRANSFORMATION MEDIATED BY ALKALINE HAEMIN

P.A. Adams, C. Adams, MRC Biomechanics Research Unit, Department of Chemical Pathology, University of Cape Town Medical School, Cape Town, Republic of South Africa.

Haemin at high pH in the obligatory presence of substrate (aniline), molecular oxygen and reductant (NAD(P)H) mediates oxygen activation to the HO_2^- anion, and regioselectively hydroxylates the substrate to p-aminophenol. Axial ligands of the iron (pyridine and cyanide) inhibit in a non-competitive manner with aniline. However, studies with compounds which bind by planar π bonding interactions to the tetrapyrrole ring system (N-methyl pyridinium ions) indicate that aniline interacts with two sites on the haemin, at one of which we observe competitive inhibition. Side chain modification of the haemin vinyl groups to hydrogen or methyl does not affect catalysis, however methylation of the propionic acid side chains inactivates the catalyst. We conclude that (1) interaction of aniline with haemin occurs via ring to ring π bonding interactions at either of the two pyrrole rings with propionate side chains attached (2) the propionic acid side chains must be in the anionic form for interaction and (3) the haemin-aniline interactions are necessary for electron transfer from reductant to the iron atom. Interactions of this type could provide pathways for electron transfer during oxygen activation by the cytochrome P-450 group of enzymes.

119

^{14}N NUCLEAR MAGNETIC RESONANCE STUDIES OF THE INTERACTION OF CALCIUM, YTTERBIUM, AND LUTETIUM WITH PORCINE INTESTINAL CALCIUM BINDING PROTEIN

J.G. Shelling, B.D. Sykes, and T. Hofmann, Department of Biochemistry, The University of Alberta, Edmonton, Alberta, Canada (T.H. is with the Department of Biochemistry, The University of Toronto, Toronto, Ontario, Canada).

A novel analysis of data obtained from the titration of porcine intestinal calcium binding protein, in the presence of the competing chelator EDTA, has led us to conclude that this protein binds two mole equivalents of calcium in a non-cooperative manner, with $k_{d1} \cdot k_{d2} = 1 \times 10^{-7} \text{M}$. In the presence of calcium, the protein was observed to bind one mole equivalent of the paramagnetic lanthanide ytterbium, with $k_d \cdot Yb^{3+}/k_d \cdot Ca^{2+} = 0.18$; the lanthanide-induced shifts were broad at room temperature. The observed effects of increasing temperature and KCl concentration upon the lanthanide-induced shifts supported the proposal that these resonances were broadened due to their close proximity to the ytterbium ion in the Yb^{3+} -substituted metal binding site of the protein. Further studies have shown that, in the absence of calcium, the lanthanide binding properties of the protein differ from those observed in the presence of calcium. Two mole equivalents of the trivalent lanthanide lutetium, which is similar to ytterbium in both size and other physical properties (except that it is diamagnetic), bound to the apoprotein in a sequential manner, with $k_{d1} < 10^{-6} \text{M}$ and $k_{d2} = 2 \times 10^{-4} \text{M}$. The binding of the second mole equivalent of lutetium by the protein had little effect on the proton nuclear magnetic resonance spectrum, and the presence of excess lutetium resulted in protein aggregation.

116

INDUCED CD AND METAL NMR STUDIES ON METAL-CALMODULIN AND DRUG-CALMODULIN INTERACTIONS

T. Shimizu and M. Hatano, Chem. Res. Inst. Non-Aqueous Soln. Tohoku Univ., Katahira, Sendai 980, JAPAN

Induced CD and metal NMR spectroscopies have been used to study metal-calmodulin (CaM) and drug-CaM interactions. An antipsychotic drug, trifluoperazine (TFP), gave rise to a large positive CD band at 265 nm corresponding to a absorption peak of TFP when Ca^{2+} -free CaM was added to the TFP solution. This positive peak was diminished by adding alkaline cations such as K^+ or Na^+ . In contrast, adding Ca^{2+} to the TFP-CaM solution induced a large negative CD band at 260 nm. Other bivalent cations such as Mn^{2+} , Cd^{2+} or Zn^{2+} also induced large negative CD bands of TFP. The magnitudes of the negative induced CD bands of the TFP-CaM in distilled water were much larger than those in KCl solutions. ^{43}Ca NMR band-width of the Ca^{2+} -CaM solution was markedly decreased by adding TFP, but not by K^+ . ^{25}Mg NMR band-width of the Mg^{2+} -CaM solution was markedly decreased by adding Ca^{2+} or K^+ , but not so much by TFP. ^{67}Zn NMR band-width of Zn^{2+} -CaM in K^+ solution was narrower than that in Na^+ solution. ^{67}Zn NMR band-width of the Zn^{2+} -CaM- K^+ solution was markedly decreased by adding Ca^{2+} , but that of the Zn^{2+} -CaM- Na^+ solution was not changed by adding Ca^{2+} . ^{39}K NMR band-widths of the K^+ -CaM and K^+ -CaM-TFP solutions were markedly decreased by adding Ca^{2+} . From these findings, it was suggested that (1) A negatively charged region in the CaM molecule participates in the TFP-CaM binding; (2) Mn^{2+} , Cd^{2+} and Zn^{2+} enhance the TFP-CaM binding as Ca^{2+} does; (3) K^+ , Mn^{2+} , Cd^{2+} and Zn^{2+} bind at a Ca^{2+} -high-affinity site of CaM.

118

RESONANCE RAMAN SCATTERING STUDIES OF REDUCED LOWSPIN FORMS OF CYTOCHROME OXIDASE

D. L. Rousseau, P. V. Argade and Y. C. Ching, AT&T Bell Laboratories, Murray Hill, NJ USA

Resonance Raman Scattering studies have been carried out on the fully reduced, carbon monoxide bound, and cyanide bound forms of cytochrome c oxidase. Vibrational modes are identified which characterize the spin state in the fully reduced forms of the protein. The cyanide bound form of the fully reduced enzyme has a spectrum different from that reported previously. We show that in the previously reported data partial oxidation had occurred. The cyanide bound form we detect has the spectrum expected for a low spin heme. In carbon monoxide cytochrome oxidase the Fe-CO stretching mode and the Fe-C-O bending mode have been located at 520 and 578 cm^{-1} respectively. Analysis of these frequencies shows that the CO adopts a linear but highly tilted configuration in cytochrome oxidase. In addition, we find that the proximal histidine is strained in both the fully reduced and the ligand bound forms. These findings can account for the low binding affinity of the CO to the enzyme.

120

MAGNETIC SUSCEPTIBILITY STUDIES OF SOYBEAN LIPOXYGENASE-1

L. Petersson^a, S. Slapperdel^b, M. Feiters^a, J.F.G. Vliegenhart^b
^aDept. of Biophysics, Univ. of Stockholm, Stockholm, Sweden.
^bDept. of Bio-organic Chemistry, State Univ. of Utrecht, Utrecht, The Netherlands.

Lipoxygenase (linoleate: oxygen oxidoreductase, EC1.13.11.12) is a non-heme iron dioxygenase which catalyzes the dioxygenation of poly-unsaturated fatty acids containing a 1,4-cis,cis-pentadiene system. Upon incubation of linoleic acid with soybean lipoxygenase-1 at pH 9.0, 13-L_h-hydroperoxy-9-cis,11-trans-octadecadienoic acid (13-L-HPOD) is formed almost exclusively.

Soybean lipoxygenase-1 contains one mol of iron per mol protein. The iron of the native enzyme is in the high-spin Fe(II) state. Addition of an equivalent amount of 13-L-HPOD to the native enzyme gives a yellow form which is enzymatically active. In this form roughly 75% of the iron is EPR-detectable as high-spin Fe(III). The yellow form can be reduced with linoleic acid. In an aerobic system the dioxygenation reaction is then fulfilled. Anaerobic addition of linoleic acid gives an EPR-silent enzyme form.

Magnetic susceptibility studies have been performed in the temperature range 10-170 K for different enzyme forms. The results give additional information on the spin state of the iron as well as the symmetry of the iron environment.

Tuesday 31 July Congress Centre-first floor. Posters 121-126

Posters on Metal-Proteins and Electron Transfer

121

THE HAEM STRUCTURE AND HAEM LIGANDS IN MYELOPEROXIDASE AS STUDIED BY RESONANCE RAMAN AND EPR SPECTROSCOPY
B.G.J.M. Bolscher, R. Wever and G.T. Babcock*

Lab. of Biochemistry, Univ. of Amsterdam, P.O. Box 20151, 1000 HD Amsterdam, The Netherlands and *Dept. of Chemistry, Michigan State Univ., East Lansing, Michigan 48824, U.S.A.
Myeloperoxidase from human leukocytes contains a chromophore with an unusual structure and which is covalently linked to the polypeptide chain. Both an iron-chlorin species and a porphyrin species with a formyl substituent have been suggested to be present. To establish the structure we have studied the enzyme by resonance Raman spectroscopy. The Raman spectra of myeloperoxidase under various valence and iron ligation states are complex. No evidence is found for unusual electrophilic substituents such as a formyl group in conjugation with the main chromophore. The Raman spectra show that the haem iron in the resting enzyme is six-coordinate high-spin. Binding of cyanide produces a six-coordinate low-spin species and in the ferrous form the haem iron is five-coordinate high-spin. EPR spectroscopy of nitrosyl ferrous myeloperoxidase shows that the paramagnetic centre has rhombic symmetry. A hyperfine structure is found of nine lines on the central resonance line, originating from a triplet with a hyperfine splitting of 0.69 mT superimposed upon another triplet with a hyperfine splitting of 2.34 mT. Substitution of ^{14}NO by ^{15}NO results in a hyperfine splitting of six lines ($A_1 = 3.22$ mT, $A_2 = 0.6$ mT). These results demonstrate that a nitrogen atom is present in myeloperoxidase as an axial haem ligand.

123

NMR STRUCTURAL STUDIES ON THE CALCIUM BINDING PROTEINS.
T.C. Williams, D.C. Corson, L. Lee, L.E. Kay, M.R. Bjornson and B.D. Sykes*. Department of Biochemistry and MAC Group on Protein Structure and Function, University of Alberta, Edmonton, Alberta T6G 2H7.

^1H , ^{13}C , and ^{113}Cd NMR spectroscopy, optical stopped flow methods, and lanthanide substitution have been used to characterize the structure and function of the calcium binding domains of several calcium binding proteins. Lanthanide shifted ^1H NMR spectra have been used to compare the structure in solution of the EF hands of parvalbumins from several species (Carp, Buffalo fish, Pike, rat, rabbit, Whiting, frog) which are shown to be very similar. The differences in structure can be explained in terms of the amino acid substitutions between proteins. The variation of the stoichiometry and kinetics of the binding of calcium and the lanthanide series of metal ions has allowed us to elucidate a particularly simple picture of the interactions of metal ions with the CD and EF domains of carp parvalbumin which are shown to be functionally different. Further, we have prepared specific derivatives of carp parvalbumin to investigate the role of the F helix in the E helix-calcium binding-loop-F helix domain. These derivatives involve the sequential removal of the F helix one amino acid at a time. The results indicate the important role of residue 102, and the strong interaction between the two binding sites.

125

STRUCTURAL COMPARISONS AND HEAT STABILITY IN FERREDOXINS ISOLATED FROM MESOPHILE AND THERMOPHILE BACTERIA
M. Bruschi and F. Guerlesquin, Laboratoire de Chimie Bactérienne, C.N.R.S., B.P. 71, 13277 Marseille Cedex 9, France

Ferredoxins are among the simplest iron sulfur proteins. They function as electron carriers in a number of biological oxidation reduction processes. The comparison of their amino acid sequences shows that they are phylogenetically related but they present various types of iron sulfur clusters. The study of the influence of the protein structure on the different type of cluster arrangements and on their inherent stability is in intensive development. In the sulfate reducing bacteria, *D. desulfuricans* Norway, two different ferredoxins have been characterized. FdII is a 2 (4 Fe-4 S) ferredoxin very sensitive to O_2 and to temperature fluctuations. The loss of the second cluster in *D. desulfuricans* Norway Fd I and in *D. gigas* ferredoxin is associated to the disappearance of two cysteines. In *D. gigas* ferredoxin the presence of six cysteine residues allow the same polypeptide chain to accommodate two types of iron sulfur cores, namely (4 Fe-4 S) Fd I and (3 Fe-3 S) Fd II. *D. africanus* Fd I which contains 4 cysteine residues represents the most simple case of one (4 Fe-4 S) cluster ferredoxin. The determination of the amino acid sequence of the 2 (4 Fe-4 S) clusters ferredoxin isolated from *Clostridium thermocellum* provides an example of a thermostable ferredoxin. Crystals suitable for three dimensional structure determination have been obtained both from the instable ferredoxin I from *D. desulfuricans* Norway and from the thermostable ferredoxin from *C. thermocellum*.

122

THE REACTION BETWEEN NITRITE AND HEMOGLOBIN.
INFLUENCE OF OXYGEN AND TEMPERATURE. F. Jung and B. Ebert, Inst. of Molecularbiology, Berlin-Buch DDR.

The autocatalytic oxidation of hemoglobin by nitrite was analysed. The intermediate paramagnetic species has a strong temperature dependence. The time of annihilation decreases between 10 and 30 °C about 4 times, the time of formation only 1.7 times. This explains the unusual temperature dependence of the total reaction: decrease of the reaction rate with increasing temperature for hemoglobin of rats and guinea pigs, whereas the reaction rate for human hemoglobin does not change with temperature.

If the autocatalytic reaction is quenched by antioxidants (p.e. ascorbic acid) the remaining slow oxidation of hemoglobin by nitrite is inhibited by oxygen. This reaction has a positive temperature dependence. Using a flow system, we demonstrate, that the autocatalytic reaction is not influenced by the oxygen pressure as long as the hemoglobin remains fully oxygenated. These findings support our assumption, that hemoglobin bound oxygen and also hemoglobin bound superoxide anion is essential for autocatalysis.

124

THE CRYSTAL STRUCTURE OF A 'SALT-LOVING' FERREDOXIN FROM HALOBACTERIUM OF THE DEAD SEA.
I. Shoham*, J.L. Susseman*, I. Harel* and A. Yonath*, The Weizmann Inst. of Science, Structural Chemistry, Rehovot, Israel. *NIH, NIDDK, Bethesda, Md. 20205, U.S.A.

Extrema 'halophilic' bacteria are unique in the realm of living organisms since their cellular interiors are approximately 4M in KCl. The survival of these microorganisms depends on the ability of their proteins to have adapted to their extreme environment. A 2Fe-2S ferredoxin from halobacteria of the Dead Sea has been isolated, crystallized, and is an example of an extremely halophilic protein in which 40/125 residues are aspartic or glutamic acid. Phase information was obtained by the following means: 1) a single isomorphous platinum derivative, 2) anomalous scattering of the iron-sulfur cluster, 3) real space three-dimensional search techniques using as a model the known structure of a homologous 2Fe-2S ferredoxin from the blue-green alga *S. platensis* 4) automatic enveloping, density modification, and phase extension & combination (Bhat & Blow, Acta Cryst. (1982) A38, 21-29.) and 5) least-squares refinement of a partial structure. An iterative use of these methods resulted in an electron density map at 2.2 Å resolution, from which we have been able to trace about 90% of the polypeptide chain and to see most of the side chain groups. The bulk of the halobacteria ferredoxin structure is quite similar to non-halophilic *S. platensis* ferredoxin, except for a striking addition of a highly negatively charged 22-residue segment at the amino terminus which is located far from the iron-sulfur cluster.

126

HEMOCYANIN DERIVATIVES FLUORESCENCE. M. Alviaggi, F. Ricchelli, B. Salvato Dept. of Biology, University of Padova

The two copper ions in the active site of Octopus Hc are kinetically distinct being removed in sequence by KCN. When the metal is gradually removed, the intrinsic fluorescence increases linearly and reaches the quantum yield of the apo-protein when about 50% of the metal is lost. Further removal of copper causes no further changes. This indicates that the quantum yield of the half-apo derivative is equal to that of the apo-protein, actually of the two copper ions in the active site only the fast reacting has quenching effect. The fluorescence of the Hc derivatives as compared with that of oxy-Hc (native) is

Hc	Q/Q	Hc	Q/Q
Oxy (native)	1	Half-apo	5
De-Oxy	3	Half-MET	1.7
Apo	5	MET	1.8

The decrease of the fluorescence from Apo- to Deoxy-Hc is due to the "heavy metal effect" of the fast reacting copper. The decrease from Deoxy- to Half-MET and MET Hc is due to paramagnetic effect of the "fast reacting copper". The decrease of quantum yield from metal oxidized derivatives to Oxy-Hc can be attributed to the energy transfer due to overlapping between the intrinsic fluorescence emission band (λ_{max} 330 nm) and the copper oxygen absorption band (λ_{max} 350 nm).

Tuesday 31 July Congress Centre-first floor. Posters 127-132

Posters on Metal-Proteins and Electron Transfer

127

INFLUENCE OF A DIFFUSIVE NUCLEAR COORDINATE IN VERY LARGE DISTANCE ELECTRON TRANSFER, J.H. Onuchic and J.J. Hopfield, Division of Chemistry and Chemical Engineering, California Institute of Technology, Pasadena, California, USA

The distant electron-transfers, with redox groups well separated, are essential to biological electron transfer and photosynthesis, and can be studied in chemical systems as well. The conventional theory is based on the supposition that the motion of nuclear coordinates are fast compared to a small electronic parameter, T/λ , where T is the electronic matrix element. Gross motion of protein, solvent polarization, and the motion of counter-ions are often diffusive events, and thus can have characteristic frequencies of "zero". Thus under some circumstances, there are important frequencies which must be less than any reasonable T/λ . A theoretical model able to include these slow, diffusive motions in the electron-transfer theory is developed in this work. We consider the applicability of this model to real systems.

129

THE EFFECTS OF DICYCLOHEXYLCARBODIIMIDE ON ENERGY TRANSDUCTION IN COMPLEX III (CYTOCHROME b_5 - c_1) OF THE MITOCHONDRIAL RESPIRATORY CHAIN D.S. Beattie, T. Clejan and G. Bosch, Dept Biochem, Mount Sinai School of Medicine, New York, NY, USA.

Treatment of complex III from yeast mitochondria with dicyclohexylcarbodiimide (DCCD) either before or after incorporation into proteoliposomes resulted in a loss of electrogenic proton movements without a significant decrease in the rate of electron transfer from ubiquinol to cytochrome c_1 . Similarly, addition of DCCD to rat liver mitochondria caused an inhibition of proton ejection but not electron transfer from succinate to cytochrome c_1 suggesting that DCCD may act by "uncoupling" proton translocation from electron transport. Incubation of the yeast complex III with [14 C]DCCD under these conditions resulted in a time, temperature, and concentration dependent binding of DCCD preferentially to cytochrome b and phospholipids. Pretreatment with antimycin A decreased the binding of DCCD to cytochrome b : pretreatment of the complex with DCCD affected the binding of antimycin spectrally. By contrast, [14 C]DCCD was bound to both cytochrome b and subunit VIII (plus phospholipids) of a complex III from beef heart mitochondria incubated under conditions where there was no inhibition of electron transfer. At short times of incubation and with low concentrations of DCCD, a greater binding of DCCD to cytochrome b rather than to subunit VIII was observed. These results suggest that cytochrome b may play an important role in proton translocation at this site of the respiratory chain. (supported by NIH grant HD 04007)

131

THE STABILITY OF THE COMPLEXES BETWEEN CYTOCHROME c_1 AND CYTOCHROME c_1 .

B.F. van Gelder and M.J. Tervoort, Lab. of Biochemistry, Univ. of Amsterdam, P.O. Box 20151, 1000 HD Amsterdam, Netherlands.

Complexes of monomeric bovine cytochrome c_1 and cytochrome c were isolated by means of equilibrium permeation chromatography. The stability of the complexes depended on ionic strength and on the redox states of the cytochromes, the reduced species having the higher dissociation constant (at 1-60 mM, $K_D < 1 \mu M$ for the oxidized complex, and K_D 10 μM for the reduced cytochromes).

Potentiometric titrations revealed that the midpoint potential (E_m) of isolated cytochrome c_1 was 258 ± 4 mV (20 C, pH 7.4). This value corresponds with a constant of 1.4 for the equilibrium: $\text{cyt. } c_1^{+} + \text{cyt. } c^{3+} \rightleftharpoons \text{cyt. } c_1^{2+} + \text{cyt. } c^{2+}$. The E_m of cytochrome c_1 markedly decreased in the presence of cytochrome c , in particular at low ionic strength and at high ratios of cytochrome c to c_1 (E_m 200 mV at 1-60 mM, cytochrome c , 15 μM and cytochrome c_1 , 5 μM), whereas the E_m of cytochrome c was hardly affected. The most stable complexes between cytochrome c_1 and cytochrome c were therefore the cytochromes $c_1^{2+}c^{2+}$ and the cytochromes $c_1^{3+}c^{2+}$ complexes.

Good agreement was found between the values of the measured and the simulated constants for the equilibria between the various valence states of cytochrome c_1 and cytochrome c .

128-ORAL PRESENTATION

The Multiphasic Oxidation-Reduction Kinetics of Cytochrome b . C.-L. Tsou, Inst. Biophysics, Chinese Acad. Sci., Beijing, 100080, China.

In succinate cytochrome c reductase, the reduction of cytochrome b by either succinate or duroquinol shows triphasic kinetics as followed at 562 nm. In the presence of a small amount of cytochrome c , the course of reduction of b becomes multiphasic. It has now been shown by repeated spectral scan either at low temperatures or with a rapid scan instrument at 25°C that the results obtained at the single wavelength of 562 nm indeed represent the reduction and oxidation of cytochrome b . The oxidation phase of b is shown by an almost symmetrical peak at 553 nm of reduced c_1 with hardly a trace of a shoulder at 562 nm. The multiphasic course in presence of added c terminates with a partial reduction of b as shown by a peak at 562 nm and complete oxidation of the c cytochromes. The rates of the oxidation-reduction of cytochromes b and c_1 are pH dependent increasing with increasing pH. However in the entire pH range of 6.0-9.0, the course of the reduction of cytochrome b remains triphasic with the final reduction phase begins when the reduction of c_1 approaches completion. The oxidation phase of cytochrome b could be attributed to an accumulation of an oxidant not initially present in the enzyme preparation most probably a protein bound form of ubisemiquinone.

130

EMPIRICAL RULES FOR PREDICTING ELECTRON TRANSFER RATE DEPENDENCE ON BRIDGING LIGAND STRUCTURE, D.N. Beratan and J.J. Hopfield, Dept. of Chemistry and Chemical Engineering, California Inst. of Technol., Pasadena, CA 91125, USA

Semi-empirical models have been used to study electron propagation through saturated rigid organic bridges. The model suggests that transfer rates fall exponentially with distance but that the decay length depends critically on the geometry of the bridge and the redox energies of the electron traps. The method is being used to model bond mediated electron transport in proteins and photosynthetic model compounds.

Electron transport over "pathologically" long distance may result in the inapplicability of the Born-Oppenheimer approximation in studying these reactions. Limitations of the approximation and the implications for long distance charge transfer are under study.

132

SHIFT REAGENTS FOR CALCIUM-43 NMR W.H. Braunlin and H.J. Vogel, Dept. of Physical Chemistry 7, Lund, Sweden.

The interpretation of ^{43}Ca NMR measurements of Ca^{2+} binding to proteins is complicated by the narrow natural chemical shift range of this nucleus (~ 20 ppm). In particular, $^{43}\text{Ca}^{2+}$ signals from slowly exchanging $^{43}\text{Ca}^{2+}$ sites may be obscured by overlapping signals from free or rapidly exchanging $^{43}\text{Ca}^{2+}$. In an attempt to overcome this problem we have examined the interactions of $^{43}\text{Ca}^{2+}$ with aqueous anionic shift reagents. Such reagents are complexes of small highly charged anions with paramagnetic metal ions which by virtue of their overall net negative charge interact with cationic nuclei, thereby inducing large changes in the NMR chemical shifts measured for these ions.

In our studies of the interactions of $^{43}\text{Ca}^{2+}$ with various aqueous shift reagents we found that both positive (up to +60 ppm) and negative (as much as -120 ppm) chemical shifts can be obtained. Further, we have examined in more detail the interactions of $^{43}\text{Ca}^{2+}$ with complexes of Dy^{3+} and tripolyphosphate in order to determine the conditions for obtaining optimal $^{43}\text{Ca}^{2+}$ chemical shifts. In a separate set of experiments we have demonstrated that the dysprosium tripolyphosphate complex may be employed to separate slowly from rapidly exchanging $^{43}\text{Ca}^{2+}$ signals for three different calcium-binding proteins covering a range of Ca^{2+} binding strengths. We are thereby encouraged that the shift reagent method may provide a general method for separating signals from strong (slowly exchanging) and weak (rapidly exchanging) quadrupolar cation binding sites in metal NMR studies of proteins and other biological macromolecules.

Tuesday 31 July Congress Centre-first floor. Posters 133-138

Posters on Metal-Proteins and Electron Transfer

133

SPECTROSCOPIC AND KINETIC PROPERTIES OF A THERMOPHILIC BACTERIAL CYTOCHROME C OXIDASE, PS3 CYTOCHROME C_{aa}.
P. Nicholls and N. Sore, Dept. of Biological Sciences, Brock University, St. Catharines, Ontario L2S 3A1 Canada.
PS3 cytochrome c_{aa} is a three subunit enzyme containing five metal centres: haems a and a₃, two Cu atoms (A and B), and a haem c species. Like eukaryotic cytochrome aa₃, its a₃ centre reacts slowly and biphasically with cyanide in a reaction controlled by the redox state of other centres in the complex; similarly the a₃-peak of the reduced cyt. a₃ component is shifted by the binding of azide to the a₃ centre. Haem-haem interactions can thus occur in an enzyme with minimal subunit composition and do not depend upon the presence of the low molecular weight metal-free subunits. Although the c haem is located upon a 38KD subunit, its kinetic behaviour in the presence of ascorbate and excess TMPD resembles that of eukaryotic cytochrome c bound to the 'right' (I) site on eukaryotic cytochrome aa₃. Full catalytic oxidase activity is exhibited by the c_{aa} enzyme in the presence of ascorbate and TMPD and in the absence of other soluble cytochromes. We therefore regard this bound c as analogous to tightly bound eukaryotic c and not to eukaryotic c₁. When unbound into proteoliposomes the c and a haems are equally accessible to reductant and therefore on the same side of the membrane. Such proteoliposomes display both the respiratory control and proton pumping behaviour of their eukaryotic counterparts. All known major catalytic and redox functions of the oxidase system are thus retained in this 3-subunit enzyme. (Supported by Canadian NSERC grant #A0412 to P.N.).

135

LOCATION OF THE HIGHER AFFINITY COPPER SITE ON HUMAN HEMOGLOBIN BY THE USE OF THE SPIN LABEL TECHNIQUE
S.R.N. LOURO* and M. Tabak**, *Departamento de Física, Pontifícia Universidade Católica, Rio de Janeiro, RJ, Brasil
** Instituto de Física e Química de São Carlos, Universidade de São Paulo, São Carlos, Brasil
Addition of copper (II) ions to Cys 3-95 maleimide spin-labelled human hemoglobin A produces a dramatic decrease in the amplitude of the spin-label ESR spectra. This effect was analyzed in the framework of Leigh's theory which permits interspin distances to be deduced from the effect of dipolar coupling on the ESR spectra and led to an estimate of 9 Å as the distance between the label and the higher affinity copper site. Taking into account the previous results which suggest that four nitrogen atoms coordinate with copper, and that the N terminal Val 8-1 and His 8-2 residues are involved, the location of the higher affinity copper site is proposed to be at the 8₁ 8₂ interface of the hemoglobin molecule, involving the N terminal of one β subunit and the C terminal of the other.

* work partially supported by FINEP, CNPq and CAPES.

137

SPIN-LATTICE RELAXATION PROCESSES OF LOW AND HIGH SPIN STATE MINERAL IN HEMOPROTEINS
L. Kajnberg*, H.J. Kalinowski* and G. Benski**, *Department of Physics, Pontifícia Universidade Católica, **Centro Brasileiro de Pesquisas Físicas, Rio de Janeiro, Brasil
We have used the continuous wave saturation technique in ESR to study the relaxation processes of the low-spin state of met-haemoglobin and myoglobin. The experiments were taken in the temperature range from 4.2K to 25K. We have fitted saturation curves with the theoretical expression $1/P = L_{max} / (1 + P/P_{1/2})^{b/2}$ in order to obtain the saturation power $P_{1/2}$ and b, the ratio of the Lorentzian spin packet to the Gaussian envelope widths. The temperature dependence of the relaxation rate has been deduced from the $P_{1/2}$ dependence after correcting it for its dependence on the spin-spin relaxation time, which has been calculated from the peak-to-peak resonance linewidth and the b value. We have shown that relaxation in both molecules are via Resonant processes with characteristic energies of 23 cm⁻¹ and 22 cm⁻¹ for Hb and Mb respectively. We have also observed that the low-spin processes are much slower than the high spin case for these proteins, being the relaxation rates one or two orders of magnitude below the rates for the high-spin case, in the same temperature range. We also observed the rate of the high-spin state to be dependent of the g-value of the monitoring transition.

Research supported by CNPq

134

Adriamycin induces free radical formation in the mitochondrial respiratory chain.
E. Goormaghtigh, P. Pollakis, M. Delnelle, Y. Lion and J.M. Rayssac, Université Libre de Bruxelles CP 2062 Bld du Triomphe, B1050 Brussels, Belgium.
Adriamycin (ADM) is one of the most effective anthracycline glycoside antibiotic in the treatment of several types of cancer. Its clinical use is however limited by a specific cardiotoxicity. Deviation of electrons from NADPH supplemented cytochrome P450 to the anthracycline results in the formation of a semiquinone radical which reacts with O₂ to form toxic oxygen species O₂^{•-} and OH[•]. These reactions were suggested to be involved in the cardiotoxicity process of ADM till the recent finding that cardiac microsomes do not participate to such reactions (1). Using the spin-trapper DMPO combined with a flow technique, we were able to demonstrate that beef heart mitochondria, submitochondrial particles and complex I containing proteoliposomes catalyze the formation of O₂^{•-} and OH[•] species when incubated in presence of ADM and NADH. The semiquinone radical was also observed by ESR with a characteristic g value of 2.00024. Interestingly, the 5-irradiation-induced radical did not induce the formation of oxygen radical species in good correlation with its weak cardiac toxicity.
(1) Nohl H. and Jordan W. (1973) Biochem. Biophys. Res. Commun. 114, 197.

136

THE CONTRIBUTION OF TYPE I PROCESSES IN PHOTO-OXIDATION OF HUMAN HAEMOGLOBIN
H. Malak, Quantum Electronics Laboratory, A. Mickiewicz University, Grunwaldzka 6, 60-780 Poznań, Poland.
A mechanism of the conformational changes and denaturation of oxyHb induced by UV irradiation was studied in the presence of oxygen. The results obtained proved the dominating role of Type I processes in photooxidation of oxyHb. Superoxide anion radicals O₂^{•-} generated in photolysis oxyHb or in electron transfer from the excited porphyrin to oxygen, were found essential influence on the mechanism of these photo-processes. In result of the reaction between these radicals and hydrogen peroxide H₂O₂, hydroxyl radicals were formed which were found to strongly oxidize the haemoglobin. The domination of Type I processes over Type II processes generating singlet oxygen ¹O₂ in the irradiated haemoglobin decreases for pH higher than 8.5.

138

Tuesday 31 July Congress Centre-first floor. Posters 139-144

Posters on Metal-Proteins and Electron Transfer

139

140

141

142

143

144

Tuesday 31 July Congress Centre-first floor. Posters 145-150

Posters on Polysaccharides and Glycoproteins

145

CHRONOBIOPHYSICAL, RAMAN AND INFRARED STUDIES OF ACID PHOSPHATASE AGE-RELATED ALTERATIONS

J. Twardowski, A. Urbanik-Brzóska
Department of Biostructural Research, Institute of Zoology, Jagiellonian University, Cracow, Poland

The role of age in the production of acid phosphatase isoenzyme from rat liver were examined. Chromatography separation of enzyme forms showed rhythmical changes of enzyme synthesis and amount of its forms during postsynthetic modification. In rat liver the acid phosphatase is synthesised on the ribosomes of the rough endoplasmic reticulum and transported to the Golgi apparatus for packing into the lysosomes. Carbohydrate amount of this glycoprotein plays an important role in protein transport through the membrane systems. Studies of acid phosphatase heterogeneity in Raman and infrared spectroscopy were done for explanation of sugar influence on isoenzyme structure. The Raman and infrared spectra of acid phosphatase isoenzyme I are presented. Isoenzyme I is created during transport of enzyme forms through membrane system after packing into lysosomes. The infrared spectra present changes in the carbohydrate amount of this protein and its changes of enzymatic activity during aging. Parallel, Raman spectra of this isoenzyme from rats of different age present changes in protein main chain conformation. Our last results try to explain structural and physiological reasons, which explain these differences connected with age.

147

POLYSACCHARIDE CD IN THE VACUUM UV, E.S. Stevens, Dept. of Chemistry, State University of New York, Binghamton, NY, USA

CD measurements have been extended into the vacuum UV region for a series of biologically important polysaccharides including unsubstituted polysaccharides whose lowest energy electronic transition lies below 190 nm. CD spectra were obtained in solutions (to 178 nm) and gels (to 178 nm) where possible, and in films (to 165 nm). In many cases it was possible to delineate the contributions to CD from the various factors which determine the spectra, including linkage type, anomeric configuration, conformation, and intra- and intermolecular hydrogen bonding. Polysaccharides examined include α -carrageenan, agarose, galactomannan, dextran, pustulan, glucans in general, acetylated glucans, chitins, alginates, hyaluronic acid, and chondroitins. Comparison of film, gel, and solution spectra is important since the film spectra can often be correlated with results from x-ray crystallography. In chondroitins, which differ from hyaluronic acid only in configuration at C(4) of the N-acetylglucosamine residue, the VUCD approximates that expected for noninteracting monomers of glucuronic acid and N-acetylglucosamine. This we can account for in terms of the equatorial C(4) hydroxyl group of hyaluronic acid allowing for the formation of a hydrogen bond across the 1-3 linkage to the preceding pyranose ring oxygen, and, on the other hand, the axial disposition of the C(4) hydroxyl of chondroitin not allowing such a hydrogen bond. This work was supported by NIH Grant GM24262.

149

FACTORS GOVERNING THE RHEOLOGICAL ACTIVITY OF PURIFIED MUCUS GLYCOPROTEINS

D.T. Brown* and M. Litt*, School of Pharmacy, Portsmouth Polytechnic*, Dept. Bioengineering, University of Pennsylvania*, Philadelphia, Pennsylvania, USA.

Mucus gels provide protection and lubrication on many of the body's inner surfaces and chronic airway disorders such as bronchitis and secretory otitis may be characterised by apparent changes in mucus consistency and transport. In an attempt to determine the physicochemical factors which affect mucus rheology we have examined mucus glycoproteins (GP) from the human trachea, canine tracheal pouch, chronic bronchitis and secretory otitis. Glycoproteins were isolated from the above by solubilisation and then fractionation in the presence of the chaotrope, potassium thiocyanate. The resultant purified mucins were then subjected to amino acid and carbohydrate analysis and rheological activity was assessed in dilute solution by capillary viscometry and in the gel state by oscillatory shear micro-rheometry and mucociliary transport on a mucus-depleted frog palate. GPs typically displayed high limiting viscosity numbers (190 ml g⁻¹) which were sensitive to changes in ionic strength and the presence of disulphide bond reducing agents. GP gels displayed elastic moduli and transport rates which varied markedly with GP concentration, displaying an optimum concentration range for maximum mucociliary transport. In all cases, after accommodation for pH, ionic strength and GP concentration, a major determinant of rheological activity appeared to be the amount of carbohydrate in the molecule. This was found to be particularly low for otitis patients who also had cleft palate syndrome.

146

THE THREE-DIMENSIONAL STRUCTURE OF THE N-LINKED CARBOHYDRATE CHAINS OF IMMUNOGLOBULIN G FRAGMENT Fc. E.J. Sutton, D.C. Phillips and P.J. Artymus, Laboratory of Molecular Biophysics, Department of Zoology, South Parks Rd., Oxford, UK.

The conformations of the polypeptide and N-linked carbohydrate chains of the Fc fragment of rabbit immunoglobulin G have been determined by x-ray crystallography, and refined at a resolution of 2.7 Å. Chromatographic analysis of carbohydrate chains isolated from single crystals of Fc (in the laboratories of Dr. R.A. Dwek, Oxford, and Prof. Kobata, Tokyo) indicates considerable heterogeneity, which is identical to that of the Fc from which the crystals were grown. Despite this heterogeneity in chain length, the conformation of each of the two chains is clearly defined. They are, however, different from each other, particularly in the conformation of the $\alpha(1-3)$ linked branch of each chain, and contact between the two chains is asymmetric, despite the approximate two-fold axis that relates the protein domains to which each is attached. Furthermore, the two $\alpha(1-3)$ linked branches appear to differ in composition, and this 'pairing' of chains of different length within each molecule is consistent with the observed heterogeneity of the whole population. A mechanism by which this might arise is presented. Finally, the possible structural role of the carbohydrate is discussed, and the accessibility of the terminal residues to other protein molecules described.

148 ORAL PRESENTATION

ANTIFREEZE GLYCOPROTEIN ADSORPTION ONTO AN ICE SURFACE. DETECTION BY SURFACE SECOND-HARMONIC GENERATION R.A. Brown, T.S. Burcham, R.E. Feeney, and Y. Yeh, Depts. of Applied Science and Food Science and Technology, Univ. of Calif., Davis, Calif. 95616 U.S.A.

Antifreeze glycoproteins (AFGP) exhibit freezing hysteresis: The freezing temperature is less than 0°C while the melting temperature is at 0°C. Several recent studies on the mechanism of function of this protein system suggest that a likely model for function is for the antifreeze molecules to be adsorbed on the surface of the crystals. However, direct proof of the presence of adsorbed AFGP had eluded previous researchers. In the present study, enhanced surface second harmonic generation (SSHG) was observed in the presence of active AFGP solution in contact with a pure single crystal of ice. The enhancement of SSHG is a positive indication that inversion symmetry across the interface has been altered. In the present case hydrogen bonding symmetry across this ice-water interface has been broken by the presence of AFGP replacing H₂O molecules at crystal growth sites. (This work is made possible through a grant to REF (NIH GM-23817) and a minigrant to YY (NSF-SSLC) for the use of the high powered pulse laser system)

150

LECTIN-TRYPSIN INHIBITOR AS AN ANTICARCINOGEN

J.Y. Lin and L.L. Lin, Institute of Biochemistry, College of Medicine, National Taiwan University, Jen-Ai Road, Taipei, Taiwan, ROC.

Concavalin A and trypsin inhibitor isolated from *Acacia Confusa* were covalently linked by using SPDP. The Con A - trypsin inhibitor conjugate (Con A - ACTI) retains about 42% of the hemagglutinating activity present in the native ACTI and has a higher hemagglutinating activity than the native Con A. The conjugate has a greater stability to trypsin than the mixture of Con A and ACTI. The conjugate enters sarcoma 180 tumor cells whereas the free ACTI does not. A single dose of the conjugate injected i.p. into sarcoma 180-bearing noninbred N1N1H(S) white mice has a remarkable effect in increasing survival of tumor bearing mice while the mixture of an equivalent dose of free Con A and ACTI does not.

Tuesday 31 July Congress Centre-first floor. Posters 151-156

Posters on Polysaccharides and Glycoproteins

151

ELECTRON MICROSCOPY OF κ -CARRAGEENAN

B. T. Stokke, A. Elgseter, H. Grasdalen and O. Smidsrud
Division of Biophysics and Division of Marine Biochemistry,
University of Trondheim. The Norwegian Institute of
Technology, 7034 Trondheim-NTH, Norway

κ -Carrageenan, a structural polysaccharide in some red algae, is a flexible macromolecule which can undergo salt-dependent conformational transitions and gelation. We have studied κ -Carrageenan by electron microscopy using a low angle rotary shadowing preparation technique, and we find that κ -Carrageenan in the absence of salt appears clearly as a flexible macromolecule. The correlation between the apparent contour length distribution from the electron micrographs and viscosity and molecular weight data shows that 1) κ -Carrageenan has a supercoiled structure even in the absence of other salts. 2) The end-to-end distance distribution in two dimensions revealed by the electron micrographs is in accordance with average end-to-end distance estimated by the Flory-Fox theory. 3) Our analysis yields an experimental estimate of the characteristic ratio of κ -Carrageenan that is in quantitative agreement with other physical methods. RbCl is one of the most potent gel-forming salts of κ -Carrageenan. Electron micrographs of κ -Carrageenan in the presence of RbCl reveal molecular aggregates at concentrations below the gel point.

153

PHYSICAL CHEMICAL AND THERMODYNAMIC PROPERTIES OF MONOMERIC CONCANAVALIN A

G. Rialdi, E. Battistel and G. Lazzarini, Centro Studi Macromolecole C.N.R., Corso Europa 30, Genoa, Italy.

The monomeric and monovalent form of Concanavalin A was prepared and purified from the tetrameric form by UV irradiation, according to the procedure given by Tanaka et al., J. biochem., 89, 1643, (1981), partially modified. After irradiation, ConA-m was separated by affinity chromatography on Sephadex G-100 and by gel-filtration on Bio-Gel P-100. Characterization through measurement of the sedimentation coefficient, the HPLC hydrodynamic mass and electrophoresis in SDS showed that the molecular weight is in agreement with the expected theoretical value. Hemoagglutination tests showed no agglutination up to concentrations of the order of 3-4 mg/ml. Fluorescence titration analysis of $-NH_2$ groups after alkaline hydrolysis showed no major change of the extinction coefficient. ConA-m was then used to study the reaction with some pyranosides and human blood glycoproteins by calorimetry. The ΔH , ΔG and ΔS of the reaction are given and compared with equivalent reactions involving the dimeric form.

155

ORGANIZATION OF NEUTRAL GLYCOSPHINGOLIPIDS IN BILAYERS AND BIONEMBRANES. T.E. Thompson, Y. Barenholz, R. Brown, M. Correa-Freire, W.W. Young and T.W. Tillack, Departments of Biochemistry and Pathology, University of Virginia, Charlottesville, Virginia 22908 USA.

The spontaneous interbilayer transfer of glucosylceramide and asialo GM₁ between unilamellar phosphatidylcholine vesicles was examined using tritiated and pyrene-labeled glycolipids. In the temperature range 30 to 45°C, the half-times for transfer are in excess of 20 days. This is much longer than the transfer half-times determined for a variety of phospholipids under similar conditions. Differential calorimetric studies and measurements of the lateral diffusion coefficient of glucosylceramide in these systems suggest that the glycosphingolipid component is organized in gel-like domains dispersed in a continuous liquid crystalline phosphatidylcholine phase. Freeze etch electron microscopy of asialo GM₁-containing systems labeled with a ricin-60-ferritin conjugate has confirmed the phase structure and shown the average glycolipid domain to be 100-150 Å in diameter. Similar electron microscope studies carried out on sheep and human erythrocytes show the intrinsic glycosphingolipid to be similarly organized. Recent work suggests that specific glycosphingolipids serve as receptors for toxins, viruses and some peptide hormones. Alterations in the composition of lipids of this type are associated with growth, differentiation and oncogenic transformation. This domain structure must be an important determinant in the biological functions of these molecules. (Supported by NIH Grants GM-23573, GM-14628 and GM-26234.)

152 ORAL PRESENTATION

CHARACTERIZATION OF TWO ESSENTIAL TRYPTOPHANYL RESIDUES IN *ASPERGILLUS NIGER* GLUCOAMYLASE

A.J. Clarke and B. Svensson, Department of Chemistry, Carlsberg Laboratory, Copenhagen, Denmark.

N-Bromosuccinimide oxidation of glucoamylases G1 and G2 from *A. niger* (1) revealed two essential tryptophanyl residues with different functional properties. Acarbose, a pseudotetrasaccharide and potent inhibitor of the enzymes, protected both of these residues against the oxidation with the retention of enzymatic activity. In contrast with the substrates maltose, maltotriose and soluble starch and the inhibitors maltitol, gluconolactone and deoxynojirimycin the activity was lost. In the latter cases only one tryptophanyl residue had been protected against the oxidation. The roles of the two essential residues were also characterized through UV difference spectroscopy, fluorometric titration and limited proteolysis. The tryptophanyl residue protected by all of the ligands was probably involved in binding of substrate in subsite 1 (2). The second residue only protected by acarbose, is suggested to be essential in maintaining an active conformation of the enzyme. The essential tryptophanyl residues have been identified in the primary structure of the enzyme (3).

1) Svensson et al., Carlsberg Res. Commun. 47, 55-69, (1982). 2) Hiroi et al., Mol. Cell. Biochem. 51, 79-95, (1983). 3) Svensson et al., Carlsberg Res. Commun. 48, 529-544 (1983).

154

HYDRATION KINETICS OF EPITHELIAL MUCINS DURING EXOCYTOSIS

P. Verdugo and L.B. Langley, Center for Bioengineering & Dept. of Biological Structure, Univ. of Washington, Seattle WA 98195, USA.

It has been demonstrated that mucus can be swollen following a Donnan equilibrium process. We have also postulated that mucins could be secreted as densely entangled networks that undergo Donnan swelling during and/or after postexocytosis. (Nature 292, 340-42, 1981). Experiments reported here using image analysis techniques, indicate that granules of mucins, secreted by respiratory secretory cells in culture, do indeed undergo Donnan swelling during exocytosis. As in the swelling of synthetic polymer gels, the spheric volumetric expansion of exocytosed mucins follows a first order kinetics where the characteristic time (τ) demonstrates a linear relationship with the square of the radius (r^2). This evidence suggests that exocytosis of mucins could be driven by swelling of their molecular network and further support the hypothesis that, Donnan hydration could control the regulation of the rheology of epithelial mucus.

(This work was partially supported by NIH grant HL29908).

156

BIOCHEMICAL PROPERTIES OF A LECTIN FROM THE GREEN MARINE ALGA *Codium fragile* subsp. *tomentosoides*.

R.W. Loveless and D.J. Rogers, Haematology and Immunology Laboratory, Park Building, Portsmouth Polytechnic, King Henry I Street, Portsmouth, Hants., UK.

Crude aqueous extracts of *Codium fragile* contain a lectin which agglutinates human erythrocytes. The lectin is preferentially inhibited by N-acetyl-D-glucosamine (GalNAc), which has enabled a batch affinity chromatographic procedure to be developed for the purification of the lectin. GalNAc was coupled to agarose 6B using 1,4-butanediol diglycidyl ether. The lectin bound avidly to the immobilised GalNAc and could be eluted from the affinity resin with excess GalNAc. The product produced powerful haemagglutination, even in the presence of ethylenediaminetetraacetic acid. When subjected to polyacrylamide gel electrophoresis in the presence of sodium dodecyl sulphate, the lectin produced a single protein band with a molecular weight of 31,000 daltons. Isoelectric focusing demonstrated that the lectin consists of two isolectins, the major component having a pI of 3.8 and the minor component having a pI of 3.9. The properties of the lectin from *Codium fragile* are similar to those of other lectins from marine algae, but differ from lectins isolated from higher plants.

Tuesday 31 July Congress Centre-first floor. Posters 157-162

Posters on Polysaccharides and Glycoproteins

157

²³Na-NMR IN AQUEOUS SOLUTIONS OF NA-POLYURONATES.

Hans Grasdalen and Bjarne J. Kvam, Inst. of Marine Biochemistry, Univ. of Trondheim, Norway.

²³Na-NMR line widths and longitudinal relaxation were studied for aqueous solutions of sodium poly(galacturonate) and alginates as a function of polyanion concentration, degree of dissociation, and the temperature, at two distinct frequencies. The linewidth of Na⁺ in 0.128 M Na-acetate increased linearly with added Na(CH₃)₄-alginate and narrowed with increasing temperature indicating fast exchange of Na between a free and a polymer bound state with a rate exceeding the quadrupole relaxation in the latter state. The line broadening effect of poly(galacturonate) and poly(gulonate) was much larger than that of poly(mannuronate). This could be ascribed to a combination of a shorter correlation time, a smaller quadrupole coupling constant, and a smaller degree of counterion binding in solutions of poly(mannuronate). The correlation time was found to increase with decreasing concentration of polymer in salt free solutions, suggesting that it is correlated to the flexibility of the polymer chains. In dilute solutions of the polyuronates the correlation time of Na was sufficiently long to cause non-Lorentzian lines with frequency dependent widths. Electrostatic theories account satisfactory for the counterion binding. No evidence was obtained in support of a recently reported pH induced intra molecular conformational transition of poly(galacturonate).

159

158

NEUTRON SCATTERING STUDIES ON FIRST COMPONENT C1 OF HUMAN COMPLEMENT AND ITS SUBUNIT STRUCTURE

S.J. Perkins, Kennedy Institute, Bute Gardens, Hammersmith, London W6 7DW, UK.

Neutron scattering studies are reported on the subcomponents Clq and Clr₂Cls₂ of component C1 of human complement and their complex to form C1. The radius of gyration at infinite contrast are 12.8 nm (Clq), 17 nm (Clr₂Cls₂) and 12.6 nm (C1), showing that Clq and Clr₂Cls₂ have complexed with a large conformational change in one or both parts. Clq can be analysed as a flexible structure at the bend in its collagenous region, where the collagenous arm and base is of length 14.5 nm and the base-arm angle is 40-45°. Clr₂Cls₂ is analysed as a rod-like particle of length 59 nm and diameter 3.2 nm. The most successful models for the association of Clr₂Cls₂ involve the asymmetric binding of Clr₂Cls₂ to the arms and base of Clq on one side of Clq and involving 2-4 stalks of Clq.

160

161

162

Tuesday 31 July Congress Centre-first floor. Posters 163-168

Posters on Connective Tissue and Bone

163

STUDY OF THE OSTEOON AS A SINGLE PIEZOELECTRIC CRYSTAL UNDER THE EFFECT OF MECHANICAL STRESSES.

M.A. EL-MESSIERY, Dept. of Mathematics and Physics, Cairo Univ., Faculty of Engineering, Cairo EGYPT.

N. H. NOWAIRA, Faculty of Electronic Engineering, Menofia University, Menof, EGYPT.

Bone matrix exhibits electromechanical transducing abilities which persist for dead and living bones; the physics of this phenomenon is still controversial though the piezoelectric interpretation is the most acceptable argument. In this paper the collagen is taken as the source of the piezoelectricity of bone, with a crystal structure belonging to C_6 group while the hydroxy-apatite crystal is asymmetric and thus non-piezoelectric. Accordingly, a single osteon is studied and the equivalent piezoelectric moduli are obtained as a function of the moduli of the collagen crystal, the type of the osteon (dark or bright) and the wrapping angle of the fibers. The components of the polarisation vector in the cylindrical coordinates (r, θ, z) are obtained as a function of the shear stress σ such that,

$$P_r = d_1 \sigma_{\theta z}, \quad P_\theta = d_2 \sigma_{rz} \quad \text{and} \quad P_z = d_3 \sigma_{\theta z}$$

where d_1, d_2 and d_3 are the only three non-zero piezoelectric moduli of the osteon as a whole. This analysis is able to explain the observed non-linear decrease of the radial piezoelectric potential of an osteon when subjected to either tensile or compressive stresses.

165

THE MORPHOLOGY OF BONE MINERAL AS REVEALED BY SMALL-ANGLE X-RAY SCATTERING

N. Matsushima, M. Akiyama and Y. Terayama, School of Allied Health Professions, Sapporo Medical College, Chuo-ku, Sapporo 060, Japan.

Small-angle scattering pattern of oriented bone contains a strong, diffuse scattering which develops in a fan-like fashion perpendicular to the longitudinal axis of the bone. In order to explore size and shape of mineral particles in adult bone, we analyzed this anisotropic scattering based on the theory proposed first by Porod. The oriented bones from bovine femur and canine one which are regarded as a structure with cylindrically symmetrical autocorrelation function were described in terms of an ideal isotropic two-dimensional two-phase system consisting of mineral phase and organic phase. Our analysis showed that bone mineral was mostly in the form of needle-like particles with 50-60 Å diameter. The intersect distribution function which is related to the second derivative of the correlation function was directly calculated from the measured intensities and the results strongly suggested the presence of mineral with sharp edges. Also the microstructure of powdered, randomly oriented bone from bovine femur was found to be affected by grinding.

167

COMBINED OXYGEN HIGH PRESSURE AND MAGNETOTHERAPY

P. Dekleva, D. Vujanović, M. Delećin and V. Majić, Clinical Hospital Centre, Zemun, YU 9000, Yugoslavia.

Owing to the circumstance that our hospital is near the main east-west highway, we have had long experience in the worst trauma cases with multi-fractures of bones, as well as gas gangrene. Certain anaerobic infections have strong inclination to causing thromboembolic and septic emboli. However, today, with multi-ly surgical therapies, by the aid of oxygen high pressure (OHP) and antibiotics, large injuries may be cured on parenchymatous organs with more confidence. On the other hand, magnetotherapy expands the cellular possibilities. But, in magnetotherapy special precautions should be undertaken against possible side effects, as well as in OHP therapy against oxygen toxicity. The injuries are usually followed by complicated infection forms. Despite the aggressive antibiotic treatment with broad spectrum of action, clinical condition worsened with many patients. The need for antibiotic penetration into the site of infection is the most apparent in central nervous system. Infections on other body sites are more difficult to assess. The high percentage of resistant bacteria to any antibiotic action, can be overcome by the aid of OHP, partially, and generally in combined OHP and magnetotherapy. Besides, in many cases, after OHP therapy, bactericidal action of antibiotics reestablishes. In the worst stubborn bacteria resistances to antibiotics, the combined OHP and magnetotherapy, reestablish the bactericidal action of antibiotics again.

164

ON THE MECHANISMS OF STABILIZATION OF COLLAGEN TYPE STRUCTURE

N.G. Esipova, V.N. Rogulenkova, V.G. Tumanyan, M.V. Grigolava, R.A. Abagyan and Yu.A. Neyfack, Institute of Molecular Biology of the Academy of Sciences of the USSR, Vavilov Street, Moscow, USSR.

Comparative studies of collagens have been fulfilled on samples from 14 taxonomically remote species. It has been shown that X-ray patterns (positions of reflexes and their intensities) are essentially similar implying close resemblance for structures of proteins. Thus, the differences in molecular stability are entirely determined by the amino acid composition, rather than by structural differences. The interrelation between denaturation temperatures and amino acid composition has been established. The evolution process requires constancy of the hydrated water content in the samples. This, in turn, directs the necessity of fibrillogenesis in the close range of molecular denaturation conditions. The physical ground of stabilization of the molecule are discussed in connection with definite trends of collagen.

166

A SYNCHROTRON RADIATION X-RAY DIFFRACTION STUDY OF THE CRYSTALLINITY OF TENDON FIBRES.

K.H. Svendsen, M.H.J. Koch, C. Boulin, A. Gabriel, Physics Laboratory, Royal Vet. and Agricultural University, Copenhagen, Denmark and the EMBL Laboratories of Hamburg, Heidelberg and Grenoble.

The equatorial diffraction pattern of tendon collagen fibres was measured during short successive exposures at different length using a double focusing x-ray synchrotron radiation camera with film and with an area detector. Similarly, patterns from thin fibres from premature rats were recorded. The patterns unambiguously illustrate the relationship between fibre crystallinity and the age of the animal. Further, the results indicate that in the initial part of the linear region of the stiffness-versus-length curve the collagen fibres are characterized by a quasi-hexagonal arrangement of collagen molecules, whereas at the end of this region, the molecular arrangement becomes hexagonal.

168

SEPIOLITE-COLLAGEN INTERACTION

A. Martínez del Pozo, N. Olmo, M. A. Izarba and J. Gualtieri, Dpt. Biochemistry, Faculty of Sciences, Complutense Univ. Madrid, Spain.

Sepiolite is a Mg-silicate with only a minor Al component, $Mg_4Si_6O_{20}(OH)_4 \cdot 2H_2O$. This mineral has a fibrous morphology which consists of alternating ribbons forming bidimensional parallel sheets. Small groups are located at crystal edges and they are responsible for the presence of negative charge in the clay. Thus, the cation exchange capacity of sepiolite ranges from 20 to 40 meq/100 g. Type I collagen fibre (1.5 µm) interacts with sepiolite resulting in a protein-clay complex. This interaction is time-dependent. Thus, at 37°C only about 60% of the total protein present in the assay is retained. However, the retention reaches the 100% at 1 h interaction time. Characterization of the constrained protein at short periods of time indicated that this collagen appears on its monomeric form. Thus, the sepiolite treatment is useful for the preparation of collagen monomer in a good yield. Studies on the complex suggest that the collagen molecules are lined along the clay fibre. Electrostatic forces are involved in the interaction. In fact, succinyl-collagen is not retained by the sepiolite. A model for the collagen-clay complex has been elaborated based on the structural properties of both components. The biological compatibility of these complexes has been qualitatively deduced by in vitro testing with fibroblasts cultures.

Tuesday 31 July Congress Centre-first floor. Posters 169-174

Posters on Connective Tissue and Bone

169

CONFORMATIONAL CHANGES DURING COLLAGEN FIBRILLOGENESIS.
Arthur Veis and Anna M. Kucharska. Department of Oral Biology, Northwestern University, 303 E. Chicago, IL 60611
The first step in collagen fibrillogenesis requires intermolecular interactions between helical regions on one molecule with one of the non-helical telopeptide regions of a second molecule. It appears that conformational changes take place both in the telopeptides and in the helical region. The telopeptides are the only regions containing tyrosyl residues while the helical region receptor sequences contain histidyl and phenylalanyl residues. Changes in state of these residues have been studied by proton-NMR and ultraviolet fluorescence spectroscopy. The free proton-NMR spectra of $\alpha 1(\text{CBI})$ (amino-telopeptide), free $\alpha 1(\text{CBE})$ (receptor region plus carboxyl-telopeptide), and the intact collagen molecule were compared with the spectra of various interaction mixtures. Fluorescence measurements of $\alpha 1(\text{CBI})$ in trifluoroethanol (TFE)-water mixtures showed a series of transitions in the direction of more restricted environments for the tyrosyl residues at high TFE concentrations, and this agreed with the shifts in $^1\text{H-NMR}$ resonances of the $\alpha 1(\text{CBI})$ as a function of the TFE content. A comparison of ($\alpha 1(\text{CBI}) + \text{collagen}$) $^1\text{H-NMR}$ spectra at 20° and 60°C clearly shows binding related to the restriction of the tyrosyl residues. The conformation of the carboxyl-telopeptide in $\alpha 1(\text{CBE})$ is less temperature dependent and shows that $\alpha 1(\text{CBE})$ has a stable folded structure. Both telopeptide regions appear to be involved in the fibrillogenesis interactions. (Supported by NIH Grant AM13921).

171

USE OF COMPUTER GRAPHICS IN MODEL BUILDING MOLECULAR CONFORMATION AND PACKING IN COLLAGEN FIBRILS
E.Y. Jones and A. Miller, Laboratory of Molecular Biophysics, Department of Zoology, South Parks Road, Oxford, UK.
An Evans & Sutherland picture system II is being used in conjunction with the graphics program MIDAS to test proposed quasi hexagonal models for the packing of Type I Collagen in fibrils. The graphics program PRODO has been used to build a variety of side chains on to the known molecular main chain coordinates. By using such side chains in a general study information has been obtained on the spatial factors required for hydrophobic or electrostatic interactions to be possible between pairs of side chains on neighbouring collagen molecules. These findings have been applied in a three dimensional analysis by computer of the known $\alpha 1(\text{I})$ and $\alpha 2(\text{I})$ amino acid sequences for collagen to search for energetically favourable packing arrangements. Such models may then be built using the computer graphics and their predicted X-ray diffraction compared with that observed experimentally. Structure prediction and model building has also been carried out for the N terminal telopeptide region of collagen. Here while agreeing with the predicted 8 sheet structure for the $\alpha 1(\text{I})$ chain (Helseth et al. 1979), the different character of the $\alpha 2(\text{I})$ chain N terminal has been found to provide an important source of asymmetry in this region.
Reference
Helseth, D.L., Lechner, J.H. & Veis, A. (1979), Biopolymers, 18, 3005-3014.

173

THE UNIT CELL AND MOLECULAR PACKING OF CRYSTALLINE TYPE II COLLAGEN Eric E. Elkenberry and Barbara Brodsky Rutgers Medical School, Piscataway, N.J., U.S.A.
We report the unit cell parameters for the crystal structure of a Type II collagen and an interpretation of the unit cell in terms of a quasi-hexagonal arrangement of molecules. This new structure is the first reported example of a crystalline packing of any type of collagen other than the Type I collagen found in tall tendon.
The sheath of the lamprey notochord is a cartilaginous tissue which contains parallel uniform diameter cylindrical fibrils of Type II collagen. Unlike mammalian cartilage this tissue gives a strong, well-oriented x-ray diffraction pattern featuring a series of meridional Bragg reflections with a 67 nm periodicity and a complex set of equatorial diffraction maxima which show that the collagen molecules have a crystalline lateral packing within the very small (17 nm) diameter fibrils. The equatorial pattern has been indexed on the monoclinic projection of a presumed triclinic unit cell with $a = 4.1 \text{ nm}$, $b = 3.5 \text{ nm}$, $c = 67 \text{ nm}$ and $\gamma = 96^\circ$. This unit cell is consistent with a quasi-hexagonal packing of collagen molecules analogous to that deduced for the Type I collagen of tendon, but is 40% larger in volume than the tendon unit cell. The additional volume appears to occur largely along only one of the three principal axes separating the collagen molecules in the quasi-hexagonal structure. The extra glycosylation of Type II, as compared to Type I, can account for only a small part of the volume increase. The remaining volume may be occupied by water or by another substance co-crystallized with the collagen.

170

DIETARY LEAD INHIBITS AVIAN BONE FRACTURE HEALING
Milton A. Lessler and David A. Ray, Department of Physiology The Ohio State University, Columbus, Ohio 43210, USA.
We examined the effect of dietary lead poisoning on the growth and healing of bone fractures of 2 week old White Leghorn cockerels. Addition of 0.5% lead acetate (5000 ppm) to the diet markedly inhibited growth and callus reabsorption. At 14 days post-hatch 60 chicks (paired by weight) had their right radius fractured by gentle digital pressure leaving the ulna intact to act as a natural splint. The undamaged left wing of each bird served as a control. Half the chicks were fed Purina Startina Mash and the other 30 had 0.5% lead acetate added to their diet. The chicks were weighed daily, sacrificed after varying periods of time, and fracture healing was studied over 2 weeks through callus formation and bony union. Mean blood levels of lead rose above 600 g/dl within 12 hours after addition of lead to the diet and remained high during the entire experimental period. Chick growth was depressed approximately 60% in the lead-fed cockerels, but there was little observable difference in initial callus formation. There was, however, a significant delay in callus reabsorption in the lead-fed chicks. Oxygen-uptake studies of healing callus showed a tendency for elevated metabolism in samples from the lead-fed chicks. Analysis of epiphyseal (growth zone) samples indicated that they differed significantly from controls, suggesting that lead poisoning increased mineral deposition, suppressed linear bone growth and inhibited callus reabsorption after bone fracture.

172

PHOTON CORRELATION OF THE EARLY EVENTS DURING IN-VITRO COLLAGEN FIBRILLOGENESIS.
K.J. Payne, T.A. King, D.F. Holmes and K.E. Kadler.
Departments of Physics and Medical Biophysics, University of Manchester.

Photon correlation spectroscopy (PCS) is a sensitive, accurate and non-destructive technique of rapidly determining the diffusion coefficients of macromolecules in solution. We have used it to study the formation of the early aggregates of collagen. It is known that the morphology of the final fibrils and the intermediate microfibrils, is critically dependent on the way the solution is heat precipitated. Furthermore, after re-solution of the collagen the solution exhibits a thermal "memory", the mechanism of which is unknown. By comparing the scattered light from two solutions of lathyrin collagen, one possessing thermal memory, it should be possible to indicate whether the presence of stable microfibrils or a conformational change is responsible for the memory effect. The spectrometer is of advanced design, capable of heterodyning routinely. A sophisticated multi-exponential curve-fitting algorithm has been employed to analyse the correlation functions.

174

The Retention of "Propeptide-Like" Domains on Type V and Ia, 2a, 3a Collagens and the Implication on Regulation of Fibril Diameters.
Type V and Ia, 2a, 3a collagens are minor collagens which constitute a small percent of total collagen in tissues. Type V collagen was prepared from acetic acid extracts of lathyrin chick bone, crop and tendon. Cyanogen bromide peptide mapping, rotary shadowing, analysis of segment long spacing crystallites and identification of bacterial collagenase resistant domains were used to characterize a higher molecular weight form of type V collagen than that isolated from pepsin extracts. The Ia, 2a, 3a collagen chains from neutral NaCl extracts migrated more slowly on SDS-PAGE than the Ia, 2a, 3a fraction isolated from pepsin extracts and CNBr peptide mapping confirmed the identity of the NaCl extracted chains as higher molecular weight forms of Ia, 2a, 3a. Examination of the products after pepsin and bacterial collagenase digestions suggested the presence of a terminal domain similar in structure to the amino propeptide of type II collagen. In vitro fibril reconstitution experiments demonstrated that the intact forms of type V and Ia, 2a, 3a collagen present in tissues can form well defined fibrils with uniform small diameters (230 Å). A 670 Å repeat was not clearly observed, but a banded appearance was present over short segments of the fibrils. In contrast to the fibrous aggregates of these minor collagens, types I, II, and III form fibrous structures with nonuniform, large lateral dimensions which are not cylindrical. We speculate that type V and Ia, 2a, 3a collagen, unlike the major fibrous collagens, contain information which enables them to control the diameters and cylindrical shape of fibrils.

Tuesday 31 July Congress Centre-first floor. Posters 175-180

Posters on Connective Tissue and Bone

175 ORAL PRESENTATION

THERMAL STABILITY OF COLLAGEN FRAGMENTS RESULTING FROM HUMAN FIBROBLAST COLLAGENASE DEGRADATION.
C.C. Danielsen, Dept. of Connective Tissue Biology, Institute of Anatomy, University of Aarhus, DK-8000 Aarhus C, Denmark.

At temperatures well below the denaturation temperature of the tropocollagen, mammalian collagenase degrades collagen by one specific cleavage that results in two triple-helical fragments constituting the N-terminal three-fourth, TC^A , and the C-terminal one-fourth, TC^B , respectively, of the collagen molecule. The collagenase cleavage products of type-I rat skin collagen were isolated and separated by gel chromatography and recovered in the expected TC^A to TC^B mass ratio of 3 to 1. The denaturation temperature of the two collagen fragments differed only by 0.5°C and was about 5°C below that of the tropocollagen. These results were valid for collagen of different solubilities (neutral-salt-soluble, acid-soluble and pepsin-treated acid-insoluble collagen). An asymmetrical thermal 'helix to random coil' transition observed for the acid-insoluble collagen was not found for the collagenase degradation fragments of that collagen. This finding indicates a defect of the acid-insoluble tropocollagen molecule in the vicinity of the collagenase cleavage site.

177

COMPARATIVE X-RAY DIFFRACTION STUDIES OF COLLAGEN
J. Bradshaw and A. Miller, Laboratory of Molecular Biophysics, Department of Zoology, South Parks Road, Oxford, UK.

X-ray diffraction studies of collagen fibres give data which are well defined longitudinally, but cylindrically averaged axially. The longitudinal contribution to the diffraction pattern appears as a series of meridional stripes representing orders of diffraction from the 670Å repeat of the collagen fibril. The first 41 orders have been measured quantitatively and related to the structure of the molecule (Hulmes et al. 1977). The orders above number 18 are almost entirely due to the amino acid sequence of the triple helical region. This information can be used to study deletions or substitutions in the amino acid chains, and can show how other molecular species interact with the collagen molecule (White et al. 1977). Collagen is a vital structural component of connective tissue, and defects in the collagen molecule could be the cause of many connective tissue diseases. We are using diffraction data, particularly from the 18th-41st orders, to detect defects in collagen structure in connective tissue disorders. In collaboration with the Haffield Orthopaedic Centre in Oxford we are studying Osteogenesis Imperfecta and Fibrogenesis Imperfecta Ossium, and seeking the connection between molecular substitution and pathological consequence.

References

Hulmes, Miller, White & Doyle (1977) J.Mol.Biol. 110, 643-666.
White, Hulmes, Miller & Timmins (1977) Nature 266, 421-425.

179

THE DEVELOPMENT OF AN IN VITRO SYSTEM FOR THE STUDY OF PROCOLLAGEN PROCESSING.

K.F. Wheeler, D.J.S. Hulmes and J.A. Chapman, Department of Medical Biophysics, Manchester University, Manchester, England.

The aggregation of acid and neutral salt extracted collagen has been studied extensively in the past by other workers. In the present study a cell culture system has been developed in which the enzymic processing of procollagen to collagen and the resulting formation of collagen aggregates may be analysed. Chick embryo tendon fibroblasts, which secrete large quantities of procollagen, are grown in roller bottles for 24 hours. The cells are then cultured in a small volume of calcium-free medium for two hours. Thus the calcium dependent procollagen proteinases secreted by the culture into the medium are reversibly inhibited. These two enzymes are then reactivated by the addition of calcium ions. It has been found that the C-proteinase is not greatly inhibited by the exclusion of calcium from the culture medium. This suggests that it requires only a low concentration of calcium or that the calcium may be tightly bound to the enzyme. The C-proteinase activity is calcium dependent and difficult to raise above a quite low level, even in the presence of high calcium concentrations. Comparisons between the types of aggregates observed in these experiments and those seen in reconstitution experiments have been performed with the aid of electron microscopy.

176 ORAL PRESENTATION

SOLID STATE NMR STUDIES OF COLLAGEN MOLECULAR DYNAMICS
D.A. Torchia, S.K. Sarkar, Y. Hiyama, C.E. Sullivan, NIDR, NIDR, NIH, Bethesda, MD, USA.

Collagen is the major structural protein in connective tissues such as tendon and bone. In tissues, collagen molecules are assembled into fibers having high tensile strength. Intermolecular interactions between collagen molecules control fiber assembly and stability, and the purpose of our experiments is to investigate these interactions. We have labeled (a) reconstituted (uncrosslinked) collagen fibers, (b) intact rat tail tendon (crosslinked) and (c) intact rat bone with amino acids enriched at specific sites with 2H , ^{13}C or ^{15}N . NMR lineshapes are sensitive to motions having correlation times, τ , less than 10^{-8} s, and analysis of lineshapes shows that the protein backbone reorients through root mean square azimuthal angles, γ_{rms} , of 41°, 31° and 14° in uncrosslinked, cross-linked and mineralized collagen, respectively. Relaxation parameters are sensitive to much faster motions, $\tau \sim 10^{-6}$ s, and analysis of relaxation data for each sample shows that γ_{rms} is 3-4 times smaller than that found from the lineshape analysis. We also observe significant flexibility in a variety of labeled sidechains, a result which is consistent with the observed backbone mobility. It is noteworthy that we observe sidechain flexibility in mineralized samples where backbone mobility is nearly absent. We are now examining peptide nitrogen exchange rates and the effects of pH and water content on collagen flexibility.

178

CRYSTALLINITY IN COLLAGEN FIBRIL CROSS-SECTIONS VISUALISED USING A NEW IMAGE PROCESSING TECHNIQUE

D.J.S. Hulmes, D.F. Holmes & C. Cummings
Dept. Medical Biophysics, University of Manchester, UK.

We have developed a new image processing technique, context dependent anisotropic filtering (CDAF), to visualise crystalline molecular packing in electron micrographs of collagen fibril ultra-thin cross-sections. Previous work (Hulmes et al. (1981)PNAS 78, 3567) showed that the 4nm periodicity in the quasi-hexagonal packing scheme could be detected by optical diffraction of electron micrographs, but the signal to noise ratio was too low for the periodicity to be visualised directly. Isotropic bandpass filtering gives insufficient increase in signal to noise. CDAF uses autocorrelation analysis to determine the preferred orientation (if any) of the 4nm periodicity in all parts of the fibril, and then uses this information to anisotropically filter each part of the image in the appropriate direction. The technique gives a large increase in signal to noise ratio and allows the crystalline domains to be visualised easily. The technique is sensitive to regions of short range order which are not readily detected by optical diffraction. The results show that the 4nm periodicity is oriented approximately radially from the fibril centre. The lattice is distorted in some regions and there are several lattice discontinuities. It is likely that the crystalline order is restricted to only certain regions of the axial 67nm repeat.

180

ELECTRONIC STRUCTURES OF COLLAGEN MODEL POLYMERS
M. Ohsaku and A. Imamura, Department of Chemistry, Faculty of Science, San Jose University, Miyazaki, Japan

In order to investigate the relations existing between the electronic structures of collagen and its biochemical functions *in vivo*, the semi-empirical CNDO/2 SCF MO calculations were carried out on several model polymers of collagen, (Gly-Pro)n, (Gly-Hyp)n, (Ala-Pro)n, (Ala-Hyp)n, (Gly-Pro-Gly)n, (Gly-Hyp-Gly)n, (Gly-Pro-Hyp)n and (Gly-Pro-Hyp)n. Geometries of the skeleton of these polymers were assumed to be the same as those of poly(L-proline) I (cis) and II (trans) and the calculations were performed only on infinite polymers in a single chain. The calculated results show that the cis form is always more stable than the trans form for all the polymers treated. The energy difference between the cis and trans forms depends, *i.e.*, on the kind of amino acid residue, Gly or Ala, but this could not be seen in the pro or hyp residue. The flexibility or mobility of the collagen structure was attempted to explain using the obtained energy difference between the cis and trans forms of the polymers. *i.e.*, the cis-trans conversion of the collagen was discussed in connection with the energy difference. The reason why the collagen has the constitution of (Gly-Pro-Hyp)n was very briefly discussed.

Tuesday 31 July Congress Centre-first floor. Posters 181-186

Posters on Connective Tissue and Bone

181

METHODS FOR AREA AND VOLUME MEASUREMENT IN THE ANALYSIS OF TISSUE. P.F. Millington, L. Juhaz and A. Robertson, Microscopy Laboratory, Bioengineering Unit, University of Strathclyde, Glasgow, G1.

Special methods are needed for the preparation, sectioning and morphometric assessment of undecalcified bone and cartilage but it is the accurate measurement of tissue volume that is difficult to achieve. The weight of water displaced through a syphon is the method often chosen but for large specimens precision is limited to about 3%. A new, simple, rapid and accurate method using a linear magnetic transducer has been developed. A magnetic float in a side arm of the main chamber changes the output of a linear transducer. A calibrated analogue meter displays the displaced volume. A system of concentric plastic inserts is used to change the range and hence sensitivity of the apparatus. By offsetting the output voltage accuracy down to 0.1 ml can be obtained. The equipment is very stable and not significantly affected by floor or bench vibration.

A dedicated device for the direct measurement of area from T.V. images of sections or photographs has been used. These two methods facilitate the determination of tissue component areas and volumes with acceptable accuracy. Measurement of the calcified region of normal and arthritic articular cartilage from 0.6 cm thick, plastic-embedded, surface-polished sections demonstrates the use of the equipment. Neither item of equipment is expensive to construct and may be assembled in any small workshop.

183

SUBUNIT STRUCTURE AND ASSEMBLY OF THE GLOBULAR DOMAIN OF BASEMENT MEMBRANE COLLAGEN TYPE IV

Sabine Weber, Jürgen Engel, Hanna Wiedemann, Robert W. Glanville and Rupert Timpl, Biozentrum der Universität Basel and Max-Planck-Institut für Biochemie, Martinsried

Collagen IV is assembled in the basement membrane by covalent and non-covalent interactions between the end regions of the molecules. The C-terminal region is a globular domain (NC1) which is composed of six polypeptide chains. By ultracentrifugal analysis, high pressure gel permeation chromatography, light scattering and electron microscopy it was demonstrated that the hexamer dissociates into dimers ($M_r=56'000$) and monomers ($M_r=28'000$) in 8 M urea, sodium dodecylsulfate or in the pH-range of 2.5 to 4. Dimers arise from monomers by disulfide cross-links and/or formation of non-reducible cross-links. Mixtures of the subunits (monomers and dimers) or purified dimers reassembled in neutral buffer into hexamers which, however, did not acquire the full stability of native globules. Circular dichroism spectra indicated more complete refolding from acid-treated than from urea-treated material. Details of the association reaction and mode of cross-linking are investigated in view of the important problem of the assembly of basement membranes from its constituent proteins.

185

182

REGULATION OF EXPRESSION OF THE 220,000 DALTON SUBUNIT OF LAMININ.

M.E. Durkin*, S.L. Phillips*, S.M. Gardner*, and A.E. Chung, *Department of Biological Sciences, and *Department of Biochemistry, University of Pittsburgh, Pittsburgh, PA, USA.

Retinoic acid and dibutylryl cyclic adenosine monophosphate induced mouse embryonal carcinoma cells to synthesize and secrete the basement membrane glycoproteins laminin and entactin. Translation of messenger RNA from induced cells in rabbit reticulocyte lysates revealed an increase in levels of translatable messenger RNA over controls for both the 220,000 dalton subunit of laminin and entactin. DNA fragments complementary to messenger RNA derived from induced F9 cells were cloned in the plasmid pBR322. Hybridization selection procedures resulted in the isolation of a plasmid p16 that contained complementary sequences to the messenger RNA for one of the 220,000 dalton subunits of laminin. The cloned DNA fragment was used to analyze the kinetics of appearance of laminin messenger RNA during induction of F9 cells by retinoic acid and dibutylryl cyclic adenosine monophosphate. Laminin messenger RNA was first detectable at 48 hr after induction, increased by 5 to 10-fold at 72 hr and remained relatively constant thereafter.

184

BIOLOGICAL EFFECTS OF ELECTRIC AND MAGNETIC FIELD FORCES
Dr A K Rakshit

128 Harley Street, London W1, England, United Kingdom.

The arthrotic people suffer from common ailments of pain, various degrees from moderate to severe, stiffness of various joints, lack of mobility, or severe restriction of movements and poor biological function as a male/female partner. The treatment with Extremely Low Frequency (E.L.F.) and low intensity electro-magnetic irradiation of affected joints or parts of the body not only improves the symptomatology, but also the quality of life. Apart from the subjective improvements, the significant changes are noticed in the radiological appearances of the joints. In some cases, even the restoration of the pathological processes may be seen in X-ray films. It means that it is not just the arrest of an otherwise progressive disease, but the reversal of the changes in X-ray films may be seen. The scientific basis for the biological interaction of the E.L.F. non-ionising electromagnetic radiation is further discussed.

The range of E.L.F. (extremely low frequency) spectrum of frequency that I have used is between 1Hz and 50Hz (about 400 Hz impulse bundles with pulse frequency of 1Hz to 50Hz). The intensity of the pulsating magnetic field is between 5 gauss and 100 gauss. The period of application may be varied from 1-99 mins. Controlled by a pulse generator feeding a 60cm coil applicator.

186

Posters on Photosynthesis

187

THE b/f COMPLEX FROM THE CYANOBACTERIUM *SPIRULINA MAXIMA*.
González-Halphen and C. Gómez-Lojero. Departamento de Bioquímica, CINVESTAV del IPN México, D.F. México.
We have previously reported the isolation of a P700-enriched preparation from the cyanobacterium *Spirulina maxima* using a horse heart cytochrome c-Sepharose affinity column. The differential spectrum (reduced minus oxidized) of this preparation detected the presence of cytochrome f and cytochrome b. Both P700 and b/f complex could be separated by centrifugation on sucrose gradient. The partial biochemical characterization of the b/f complex is presented. Special interest has been directed towards the relationship between redox components of this cytochrome segment and the different polypeptide bands as revealed by polyacrylamide gel electrophoresis. Two different approaches were used: PAGE in the presence of Lithium Dodecyl Sulphate at low temperatures (4°C), this technique allowed direct spectroscopic identification of cytochromes eluted from the gel. Differential staining procedures were also utilized with both heated and non-heated samples in order to identify the cytochromes (with tetrazethyl-benzidine) and the iron sulphur cluster (with ortho-phenanthroline). On the other hand, denaturing gels with sodium dodecyl sulphate at room temperature yielded the polypeptide electrophoretic patterns. Some other properties of this preparation, such as quinone contents, spectroscopic features and enzymatic activities are compared with its mitochondrial analogue, the bc₁ complex.

189

DELAYED LUMINESCENCE FROM CHLOROPLASTS GENERATED BY EXTERNAL ELECTRICAL FIELD: PARTIAL CHARACTERIZATION OF ITS ORIGIN WITH EVIDENCE FOR COMPONENTS FROM PHOTOSYSTEMS I AND II.
M. Syromy, S. Malkin and R. Korenstein, Depts of Membrane and Biochemistry, Weizmann Inst. for Sci., Rehovot, Israel.
Delayed luminescence (DL) from photosynthetic membranes is a complex phenomenon, with so far only partial characterization of its origin (i.e. precursors and reaction pathways), particularly since, following preillumination, there are many ways to trigger the DL, such as an acid-base jump and application of an external electrical field. The latter phenomenon is called electrophotoluminescence or EPL, which is especially marked in blebs (swollen vesicles originating from chloroplasts under hypotonic conditions) where the natural DL can be stimulated by 3 orders of magnitude. EPL in blebs has two distinct kinetic components, rapid R and slow S, which can be experimentally separated at low pH (4.5-6). In chloroplasts only the S phase is observed. Our results are consistent with the S phase being elicited by PSII and the R phase by PSI. This attribution is predominantly substantiated by the difference in action spectrum of the two phases and their different dependence on electron acceptors and inhibitors. Besides their interest for the study of photosynthetic electron transport, these results have relevant implications concerning chloroplast membrane organization, since we previously suggested the R precursors to be located in the bleb wall (possibly resulting from stroma lamellae) and the S precursors in the patches attached to the bleb (possibly resulting from the chloroplast grana).

191

CONTROL OF THE KINETIC PROPERTIES OF MEMBRANE BOUND INORGANIC PYROPHOSPHATASE BY DIVALENT CATIONS.
I. Romero, H. Celis and A. Gómez-Fuyou, Centro de Investigaciones en Fisiología Celular, Univ. Nat. Autónoma de México, México, D.F. MÉXICO.
The relation that exists between the P_i-PP_i exchange reaction and pyrophosphate hydrolysis by the membrane bound pyrophosphatase of chromatophores of *Rhodospirillum rubrum* was studied. Optimal rates of hydrolysis are attained at 1 mM Mg²⁺ and the rate of hydrolysis correlates with the concentration of Mg-pyrophosphate, which indicates that the latter is the substrate for hydrolysis. The P_i-PP_i exchange reaction is low at concentrations of added magnesium below 1 mM but rises as the concentration of Mg²⁺ in the media is increased. The rate of P_i-PP_i exchange reaction depends on the concentration of MgHPO₄, thus indicating that this is the substrate in the exchange reaction. The optimal pH for hydrolysis is 6.5, while that for the exchange reaction is 8.0. At pH 6.5, Mg²⁺ can be replaced by Mn²⁺, Zn²⁺ and Co²⁺ in the hydrolytic reaction. Significant rates of exchange reaction can be achieved with Mn²⁺ and Zn²⁺ at concentrations below 1 mM at pH 8.0. The results indicate that the kinetic properties of membrane bound pyrophosphatase are controlled by the concentration of divalent cations. The ratio of molecules of pyrophosphate hydrolyzed to those which undergoes exchange decreases by more than an order of magnitude as the concentration of Mg²⁺ in the media increases. This can only be explained as a divalent cation induce a change in the relative rates of the steps of the catalytic cycle.

188

PARTIAL CHARACTERIZATION OF P700 COMPLEX OF THE CYANOBACTERIUM *SPIRULINA MAXIMA* ISOLATED BY DETERGENT/POLYACRYLAMIDE GEL ELECTROPHORESIS AT 4°C. C. Gómez-Lojero and B. Pérez-Gómez. Depto. de Bioquímica CINVESTAV-IPN. Apdo. Postal 14-740 México.
After incubation of thylakoidal photosynthetic membranes from *Spirulina maxima* in the presence of Lithium Dodecyl Sulphate (LDS) in ice during 10 minutes and with a 10 to 75 detergent chlorophyll ratio (w/w basis), two main protein-chlorophyll complexes were separated by LDS-PAGE at 4°C. (1). At the electrophoresis front, a brown band composed principally of carotenes and less than 15% of the total chlorophyll of the gel was observed. The green band with less mobility and more chlorophyll content (PCI) was extracted from a 7% polyacrylamide gel with a 0.1% LDS-buffer, and about 50% of the complex recovered. This PCI fraction presents a shift of 3 nm in the red wavelength absorption maximum and has a low carotenoid content compared with the intact membrane fraction. PCI is able to bleach at 700 nm in the presence of actinic light and its recolorization is accelerated by cyt c553. SDS-PAGE (11%) at room temperature shows 7 to 8 polypeptides ranging from 6 to 70 kD. It is possible to transfer PCI from 11% to 7% polyacrylamide gels with LDS, without the presence of chlorophyll in the front. It can also be rerun at 4°C on Deso-nicholate (DNC)-PAGE (2). This exchange of detergents is a methodological improvement, due to the fact that DNC is a dialyzable and mild detergent.
1.- Deleplaire, P. and Chua N.H. (1979) Proc. Natl. Acad. Sci. U.S.A. 76, 111-115.
2.- Picard, A., Acker, S., and Duranton, J. (1982) Photosynthesis Res. 3, 203-213.

190

EFFICIENCY ENHANCEMENT OF FREE ENERGY TRANSDUCTION THROUGH LOCALIZED PROTONS

O. van Kooten and W.J. Vredenberg
Gen. Foulkesweg 72
6703 BW WAGENINGEN

Transmembrane electric potential transients, measured in thylakoids, indicate the existence of localized chemiosmotic potentials at the onset of illumination. Comparison of measurements with theoretical calculations explains the transient kinetics and the efficiency of free energy transduction.

192

TRIPLET-MINUS-SINGLET ABSORBANCE DIFFERENCE SPECTRA OF THE PRIMARY DONOR OF THE GREEN PHOTOSYNTHETIC BACTERIUM *PROSTHECOCHLORIS AESTUARII*
H. Nessel, H.J. den Blanken, J.T. Dijkman, A.J. Hoff and J. Amesz, Department of Biophysics and Centre for the Study of the Excited States of Molecules, Huygens Laboratory, State University Leiden, Leiden, The Netherlands.
To obtain information on the structure of the primary donor P840 of the green bacterium *Prostheochloris aestuarii* we have applied the technique of absorbance-detected electron spin resonance in zero magnetic field (ADMR) to a photochemically active pigment-protein fraction derived from the bacterial membrane. The triplet-minus-singlet absorbance difference spectra thus obtained (at 1.2 K) show negative bands at 837 and 826 nm, a small absorbance increase at 814 nm and a band shift centered at 668 nm. The latter finding confirms the presence of B800 or a related pigment in the vicinity of the primary donor. We also determined the polarization of the two negative bands relative to the triplet axes system and found them to be practically parallel. We conclude that there is no spectral evidence for the existence of two resolved exciton bands attributable to the primary donor of *Prostheochloris aestuarii*. The method also allowed the accurate determination of the zero field splitting parameters |D| and |E| of P840, 108.3 (± 0.7) × 10⁻⁴ cm⁻¹ and 36.7 (± 0.7) × 10⁻⁴ cm⁻¹, respectively. Decay rates of 6790 (± 500) s⁻¹, 3920 (± 300) s⁻¹ and 1.75 (± 100) s⁻¹ were observed for the x, y and z triplet sublevels, respectively.

Posters on Photosynthesis

193

LOW TEMPERATURE STRESS-INDUCED INJURY IN BEAN LEAVES INVESTIGATED BY CHLOROPHYLL FLUORESCENCE IN VIVO

M.N. Tomašević, J.M. Kurepa and V.V. Urošević

Chlorophyll fluorescence technique has been used to investigate the changes in photochemical function of detached bean leaves chilled at 0°C in dark up to 36 hours. The changes due to detachment have been taken into account in order to analyse the chilling injury. Fluorescence emission kinetics at 685 nm (F685) and 735 nm (F735), as well as the fluorescence emission spectra were measured at 20°C after the chilling treatment. Significant changes were observed on the fluorescence induction curves for both wavelengths. The measured variable fluorescence (Fv) decreased almost linearly with the time of treatment. Decrease was expected and implied that PS II was more affected by this treatment than PS I. Photochemical function obtained from relevant Fv and Fp values for both wavelengths has shown decrease up to 90% of its control values. The fluorescence emission spectra have been corrected by detection system efficiency factor and the results have been analysed and compared to the known data.

195

ISOLATION OF PARTICLES CONTAINING CHLORIDE ION TRANSPORT ACTIVITY FROM THYLAKOID MEMBRANES. V. Vazbutas, Dept. of Biochem. Mount Sinai School of Medicine, New York, N.Y., USA

Thylakoid membranes are known to be permeable to a number of cations (Mg²⁺, K⁺, Na⁺) and anions (Cl⁻, Br⁻) which function as counterions during proton accumulation. It has been suggested that Cl⁻ may permeate the thylakoid membrane via a specific channel (protein(s)). The results of a search for such a channel are summarized in this report:

Particulate proteins extracted from thylakoid membranes were incorporated into phospholipid vesicle membranes and were found to stimulate Cl⁻ efflux. This stimulation was inhibited by pirenthane, an electrogenic Cl⁻ transport inhibitor. The ion transport-like activity disappeared from the extracted proteins after trypsin digestion. Cl⁻ efflux from phospholipid vesicles which contained trapped KCl and which were reconstituted with thylakoid membrane protein particles was accompanied by K⁺ efflux. Valinomycin enhanced Cl⁻ efflux only slightly. SDS-polyacrylamide gel electrophoresis showed six major polypeptides to be present in the ion-efflux active particles. In order to lend additional validity to reconstitution experiments, antiserum was raised to ion-efflux active thylakoid membrane particles. This antiserum inhibited cation driven Cl⁻ influx into intact non-energized (darkened) thylakoids by about 50%. The inhibition was proportional to antiserum concentration.

These observations support the notion that anions such as Cl⁻ permeate the thylakoid membrane at least, in part, via protein(s) and that such a protein(s) is present in the isolated particles. This work was supported by NSF Grant No. PCM 8115652.

197 ORAL PRESENTATION

SIMULATION OF THE SPECTRAL PROPERTIES NEAR THE I.R. REGION FOR REACTION CENTERS OF THE PHOTOSYNTHETIC BACTERIA AND THE POSSIBILITY OF NEW INTERMEDIATE IN PRIMARY PHOTOSYNTHESIS

A. Scherz and W.W. Parson*. Biochemistry Department, Weizmann Institute of Science, Israel and *Univ. of Washington, Seattle, USA

The oscillator strength or the lower most transition in several photosynthetic bacteria was found to be higher by a factor of 2.6 from the corresponding value for BChl (Bacteriochlorophyll) monomer in vitro. The former is also known to be optically active and is shifted by 700-1000 cm⁻¹ when compared with the Qy transition of BChl monomer. Similar phenomena are observed for dimers of BChl and BPh (bacterio- pheophytin) in Triton X-100 and LDAO respectively. They are shown to be due to intensity borrowing from Qx and Bx, y to Qy transitions. First order exciton theory that includes dipolar interactions between non degenerate states is used to simulate all the spectral features in vivo and in vitro. A special dimer structure is proposed for the primary donor and shown to be consistent with recent endor data. Excitation of the primary donor is predicted to induce absorption decrease at the lowermost transition which is 3 times higher than the integrated absorption increase. Upon oxidation, similar phenomena is expected and therefore the spectral variation around 800 nm in R. sphaeroides and 840 nm in R. viridis, includes an absorption increase that followed the cancellation of exciton interaction in P-860* or P-770*. The accompanying decrease at slightly longer wavelength must reflect the bleaching of or accessory BChl. The accessory BChl is probably modified before electron is transferred to BPh.

194

INCREASE IN BACK REACTION IN PHOTOSYSTEM II UPON CATION DEPLETION. EVIDENCE FROM Mg²⁺-INDUCED STIMULATION OF FLASH YIELD OF NADP REDUCTION IN ISOLATED PEA CHLOROPLASTS.

Salil Bose, School of Biological Sciences, Madurai Kamaraj University, Madurai 625 021. INDIA.

Effects of Mg²⁺ on the flash yield of NADP reduction have been studied in isolated chloroplasts suspended in low-cation medium. Upon addition of 5 mM MgCl₂ the flash yield increased at all intensities and frequencies of the flash. At low frequency (9 per sec) and low flash intensity the magnitude of increase was 100% which decreased to 25% as the flash intensity was increased to saturation. The magnitude of stimulation at low flash intensity remained unchanged throughout the frequency range (9 to 220 per sec) used. At saturating intensity the stimulation increased from 25% to 100% as the flash frequency was increased from 9 to 65 per sec. It is concluded that in absence of Mg²⁺ considerable back reaction occurred between the primary photoproducts resulting a decreased flash yield of NADP reduction. In presence of Mg²⁺ the back reaction is prevented resulting a stimulation in the flash yield.

196

THE CATALYTIC SITE FOR PHOTOSYNTHETIC OXYGEN EVOLUTION

G.C. Dismukes, D.A. Abramowitz, R. Danovitch and P. Mathis*, Dept. of Chemistry, Princeton University, Princeton, N.J. 08544 USA and * Serv. de Biophysique, CEN Saclay, 91191 Gif-sur-Yvette, Fr

Photosynthetic O₂ evolution is catalyzed by an enzyme (OEC) which can exist in 5 redox states S₀ to S₄ created by flash illumination. The S₂ state exhibits a multiline EPR signal due to hyperfine structure (hfs) from 2 or 4 interacting Mn ions in a mixed valence state. PSII particles enriched in the OEC exhibit Mn hfs with more resolved peaks (19-21) than in chloroplasts (17-19). Synthetic Mn₂(III,IV) complexes have only 16 major hfs peaks and do not predict the end peaks in particles. Simulations using hfs parameters for Mn₂(II,III) dimers predict the positions, but not the intensities, of all peaks. Tetranuclear clusters of Mn₂(III,III) and Mn₂(II,III) predict both intensities and positions satisfactorily. Also 1) Resolved super-hfs indicates Mn coordination by two N nuclei or possibly an I-3 nucleus (Cl or Cu). 2) Cl⁻ depletion deactivates S₁→S₀ from which 100% S₂ can be formed by 2 successive 1 e⁻ oxidations. 3) Mn²⁺ release occurs for S₃→S₂ at this Mn site. 4) S₂ multiline signal is lost upon removal of a 33kDa peripheral protein, but not upon removing proteins of 17- and 23-kDa. 5) 2-3 of the 4 Mn ions in particles are co-released with the 33kDa protein. 6) Mild extractions with chemical oxidants release the 33kDa protein containing 2 Mn in a binuclear site. 7) The manganese protein reconstitutes 30% of the original O₂ to depleted membranes. No recovery is found with the apoprotein. 8) The OEC reacts with H₂O₂ to delay O₂ by generation of •NOH which interacts magnetically with the OEC. 9) The S₂ state exhibits an IR electronic transition (ν max=400 M⁻¹cm⁻¹). This oscillates in yield every 4th flash of light and is out of phase with O₂ release by 2 flashes. This could be analogous to the intervalence electronic transition present in the mixed valence state of synthetic Mn clusters or to a Cu II and field band. USDA-CRGO, Searle Scholar, NIH-GM28789, NSF-CHE82-17920, CEN-Saclay.

198

Molecular Orbital Study of the Water Oxidation-Deprotonation Processes in Photosynthesis.

M. Kusunoki, Physics Lab., Faculty of Engineering, Meiji Univ., Kawasaki-shi, 214, Japan

The water splitting reaction in PS2 is believed to be catalyzed by a special Mn cluster involved in one of 47 kD, 43 kD and 33 kD proteins. Phenomenologically, the water-splitting enzyme system must cycle through the four stable or long-lived states S₀-S₁-S₂-S₃-S₄ before liberating one molecule of O₂ upon its successive four electron oxidation with just two water molecules. To explain this periodicity, we proposed in previous papers a "microsurface" model in which two Mn atoms form a catalytic microsurface of protein where a water dimer is absorbed to be oxidized and deprotonated step by step. In the deprotonation energetics using ab initio LCAO-MO-SCF method, we assumed that protons are released into the water layer covering the active site of protein. The effect of nonplanar ligands in the double-zeta-level calculation is estimated for some oxidation-deprotonation intermediate states of (H₂O)₂ bound to Mn(II), Mn(III) or Mn(IV). These calculations lead to a second model of molecular mechanism different from the first one proposed based on the MO calculations in the case of planar ligands. In the second model, S₁ may remain as stable as S₀ mainly due to a sign change to antiferromagnetic superexchange interaction. Further, S₂ seems to include a Mn(III,IV) cluster in agreement with the conclusion of Dismukes & Sidler. But we can not exclude the possibility that the EPR hyperfine lines may originate from non-catalytic Mn(II,III) cluster magnetically coupled with the catalytic Mn(III,III) cluster in the first model.

Tuesday 31 July Congress Centre-first floor. Posters 199-204

Posters Photosynthesis

199

A MODEL FOR THE PHOTOSYNTHETIC UNIT
M. A. R. P. and U. C. B. School of Life
Sciences, Sarsour University, Lyoti Vihar
68 01, Chisna, India.

The basic unit of the current system of the thylakoid membrane is proposed to consist of 3-4 chlorophyll, 1 carotenoid and 3-4 galactolipid molecules within a hollow β -sheet dominated protein cover. Phytol chains, galactolipids and carotenoid form a lipophilic red like core and porphyrin rings are projected like the petals of a flower. The basic units and associated proteins are proposed to be organised in a three dimensional double hemispherical array. The light harvesting protein complex forms the continuous outer most layer of the array. One hemisphere contains photosystem I and the other photosystem II. Reaction centers are at the centers of the hemispheres and on the inner side of the thylakoid membranes. The number of chlorophylls (548) in the array is assigned keeping in view the close packing of the pigments in each layer in a membrane thickness of about 100 Å. The model explains most of the experimental data and can be subjected to mathematical treatments.

201

ORIENTATION OF REDOX CENTERS IN THE CYTOCHROME b_6/c_1 COMPLEX AND BACTERIAL PHOTOSYNTHETIC REACTION CENTERS.
P. L. Tiede, P. Rich*, V. Croguet, J. Bretton
Service Biophysique, CEA/Saclay, Gif sur Yvette, France.
*Dept of Biochemistry, Univ. of Cambridge, Tennis Court Road, Cambridge, U.K.

We have been studying the organization of the redox centers within the bacterial photosynthetic reaction center (RC) and the photosynthetic and mitochondrial cytochrome b_6/c_1 complexes using optical and EPR spectroscopies on oriented membranes. These results provide a structural framework for these electron transfer reactions. With the RC, a plane formed by the Q_{xy} positions of the bacterio- Q acceptor is found to lie at an angle $\sim 60^\circ$ to the plane formed by the Q_{xy} transitions of the primary donor, the bacteriochlorophyll dimer. This indicates that the post-reaction, electron tunneling must be occurring between redox centers which are fixed by the protein to have a non-planar, and possibly perpendicular alignment. A similar orthogonal arrangement is seen for the electron tunneling complex formed between a $cyt\ b_6$ heme and the RC in $C. vinosum$. With the b_6/c_1 complex in both bacterial and mitochondrial membranes, the dichroisms of the high and low potential $cyt\ b_6$ show that these hemes are oriented nearly perpendicular to the membrane surface ($\sim 60^\circ$), while the c_1 heme shows no dichroism which may indicate a tilt near the "magic" angle of 55° with respect to the membrane surface.

203

EPR STUDIES OF THE PHOTOCHEMISTRY OF PSII.
J.-L. Zimmermann and A.W. Rutherford, Service de Biophysique,
Centre d'Etudes Nucléaires de Saclay, 91191 Gif-sur-Yvette
Cedex, France.

- A/ Oxygen-evolving enzyme.
It has been suggested that the charge storage state S_2 is associated with a multiline EPR signal attributable to a mixed valence multinuclear Mn cluster (Dismukes and Siderer, 1980). This signal has been studied in isolated PSII particles and the following results have been obtained:
1-The signal amplitude oscillates with a period of four (maxima on flashes 1 and 5). This clearly indicates an association with the S_2 state.
2-The improved resolution obtained in this study shows that more lines are present than previously reported. This may have important consequences on the model used to explain the origin of the signal.
3-Glycerol enhances the amplitude of the signal but this effect is due to a change in relaxation properties rather than an increase in spin concentration.
4-Deactivation studies indicate that acceptor side electrons are involved in recombination reactions with S_2 .
5-The relationship of the multiline signal with other donor side components is under investigation.

B/ The acceptor side.
We have obtained the following data:
-A new EPR signal associated with Q_A^- is reported.
-Herbicides acting in the region of the Q_A^- complex in PSII give rise to changes of the RC EPR signals.

200 ORAL PRESENTATION

A TECHNIQUE FOR THE RECONSTITUTION OF PHOTOSYNTHETIC OXYGEN-EVOLVING PARTICLES FROM PHORMIDIUM LAMINOSUM
A.W.D. Larkum*, J. Bowes and D.S. Bendall, Biochemistry
Department, University of Cambridge, Cambridge, U.K.

Highly resolved particles enriched in photosystem II components and light-dependent oxygen evolution have been prepared from thylakoids of *Phormidium laminosum* (Bowes, Stewart and Bendall, 1983. Biochim. Biophys. Acta. 725, 210-219). These particles have been inserted into the membranes of liposomes prepared from *Phormidium* lipids using polystyrene beads to remove detergent. When mixed in ratios of lipid to protein of 20:1 to 50:1 the technique is successful in incorporating 100 percent of the particles into proteoliposomes which sediment as a single layer on a sucrose gradient. The proteoliposomes show rates of light-dependent oxygen evolution similar to the original particles. Freeze-fracture studies show a single population of particles in the liposome membrane. The stability and effects of osmotic concentration, medium composition and ion-exchange chromatography on the proteoliposome preparations have been studied. Criteria useful in assessing the success of reconstitution will be discussed.

* On leave from School of Biological Sciences, University of Sydney, N.S.W., Australia.

202

ELECTROSTATIC INTERACTIONS IN PHOTOSYNTHETIC ELECTRON TRANSPORT SYSTEMS

T. Takabe, Dept. of Chem., Fac. of Sci. & Tech., Meijo Univ.,
Tempaku-ku, Nagoya, Japan

Chemically modified spinach plastocyanin, in which negatively charged carboxyl residues are replaced with positively charged amino residues, has been prepared to study the roles of overall and local charges on the electron transfer reactions of plastocyanin with photooxidized P700 ($P700^+$) and with reduced cytochrome f . The rate of electron transfer from reduced cytochrome f to oxidized singly substituted plastocyanin was only 30 % of the native unmodified one, and the reaction decreased further with increasing the number of modified carboxyl residues. These results indicate the importance of electrostatic interactions between the negative charges on plastocyanin and the positive charges on cytochrome f in this reaction. Since the overall charges of cytochrome f are negative at neutral pH, the positive charges on cytochrome f involved in the reaction should be localized ones. On the other hand, the rates of electron transfer from reduced singly and doubly substituted plastocyanin to $P700^+$ in the highly purified P700-chlorophyll a protein complex were almost similar to the case of native plastocyanin, which suggests that these carboxyl residues have a only minor role for the electron transfer to $P700^+$. The modification of three and four carboxyl residues drastically changed the divalent cation dependency in this reaction. These results suggest the presence of different reaction site domain, at least partially, on the plastocyanin for the reaction with $P700^+$ and with cytochrome f .

204

EXCITATION ENERGY TRANSFER FROM TRYPTOPHAN RESIDUES TO HYDROPHOBIC PROTEINS IN GREEN ALGAE
J. L. D. Larkum*, J. Bowes and D. S. Bendall, Biochemistry
Department, University of Cambridge, Cambridge, U.K.

In the highly efficient excitation energy transfer from tryptophan residues of intrinsic membrane proteins to hydrophobic fluorescent probe various states are demonstrated in chloroplast membranes under "stacked" and "unstacked" conditions. The excitation energy migration a correct estimate of lipid "viscosity" near protein can be obtained by a semiempirical formula. Absorption and fluorescence spectroscopies were used to study the incorporation and structural transitions in lipid phase. Chloroplasts in "stacked" and "unstacked" states were compared with respect to structural transitions induced by temperature and efficiency of excitation energy transfer from tryptophan residues to pyrene at the same temperature intervals. It was found that: 1/ efficiency of energy transfer was higher in "unstacked" chloroplasts; 2/ "viscosity" of lipids near proteins was higher in "stacked" chloroplasts; 3/ the structural transitions of lipid phase and efficiency of energy transfer were more sensitive to temperature changes in "unstacked" chloroplasts. The data were estimated in relation to the structural organization of chloroplast membranes.

Tuesday 31 July Congress Centre-first floor. Posters 205-210

Posters on Photosynthesis

205

ELECTRON TRANSPORT IN PHOTOSYSTEM II PARTICLES - RELATION TO POLYPEPTIDES REMOVED BY SALT TREATMENTS

L.-E. Andréasson, L.-G. Franzén, Ö. Hansson and T. Vänngård, Department of Biochemistry and Biophysics, University of Göteborg and Chalmers Institute of Technology, Göteborg, Sweden.

EPR studies of the effect of treating inside-out vesicles from thylakoids with NaCl have been carried out in this laboratory (C. Jansson et al., submitted). The work has now been extended to PS II Triton particles prepared according to R.C. Ford and M.C.W. Evans (FEBS Lett. 160 (1983) 159-164). Treatments with 1 M MgCl₂ or NaCl inhibit oxygen evolution with very little release of Mn, but the Mn multiline signal no longer can be produced. MgCl₂ removes the 18, 25 and 33 kDa polypeptides and Signal II, appears. NaCl removes only the 18 and 25 kDa polypeptides and no increase in Signal II₂ is observed. Thus, the two lighter polypeptides are not directly involved in electron transfer to Z, but in their absence only partial advancement through the S-state cycle can occur. The 33 kDa polypeptide, on the other hand, may be required for rapid electron transfer to Z.

207

SPECTRAL AND KINETIC RESOLUTION OF $Q_A^-Q_B + Q_AQ_B^-$ ELECTRON TRANSFER IN PHOTOSYSTEM II

G.H. Schatz and H.J. van Gorkom, Department of Biophysics, Huygens Laboratory, University of Leiden, The Netherlands.

Electron transfer from the primary (Q_A) to the secondary (Q_B) quinone acceptor of photosystem II (PS II) was studied in PS II particles isolated from a cyanobacterium *Synechococcus* sp. Measurements of flash-induced chlorophyll fluorescence yield and absorbance changes in the presence of 0.6 M Tris and 0.4 mM K₂Fe(CN)₆ gave the following results:
1) About 80% of Q_A formed after a flash is oxidized with a half time of about 1 ns. The remaining 20% of Q_A show a longer decay time (several 100 ns) which is dependent on Fe(CN)₆³⁻ concentration with a second order rate of $k = 1.7 \cdot 10^3 \text{ M}^{-1} \text{ s}^{-1}$ (at pH 8.3, 20 °C). In the presence of Fe(CN)₆³⁻ reoxidation of all Q_A is much slower (half time about 7 s). It is concluded that in the absence of DCMU the fast phase (1 ns) is due to the reaction $Q_AQ_B^- + Q_AQ_B$, the slow phase reflects the oxidation of $Q_AQ_B^-$ and the equilibrium constant $K = [Q_AQ_B]/[Q_AQ_B^-]$ equals 1.
2) Absorbance changes were analyzed in the ultraviolet and visible part of the spectrum. The difference spectrum associated with the fast phase consists mainly of a bleach at 470, 545 and 685 nm. It is explained as a result of an electrochromic blue shift of the pheophytin a band which is due to electron transfer from Q_A to Q_B . The slow phase accounts for most features in the visible region of the difference spectrum and is much smaller (or even opposite) to the $Q_AQ_B^-$ difference spectrum.

209

WHY ISOLATED THYLAKOIDS CANNOT BE STABILIZED?

L. Nedbal, I. Setlík, J. Masojídek, E. Setlíková, Institute of Microbiology, Czech. Acad. Sci., Prague, Czechoslovakia.

The activity of isolated thylakoids (particularly of the photosystem 2) declines much faster if they perform photochemical work than if they are stored in the dark (Rao, Hall in Photosynthesis in Relation to Model Systems (J. Barber, ed.), pp. 299-329, Elsevier (1979)). Recently we have pointed out that photosystem 2 electron transport in photosynthesizing cells may also become gradually inhibited if photosynthesis on 70S ribosomes is blocked. This phenomenon is common to all organisms with oxygenic photosynthesis, its rate is irradiance dependent and it forms also the basis of photoinhibition. The primary cause of the inhibition is the degradation of the D-protein followed by the destruction of the PS2 core. We show, now, by measurements of electron transport, fluorescence and by PAGE of chlorophyll-protein complexes, that this is also the main destruction process which inevitably accompanies the work of isolated thylakoids. Their PS2 activity cannot be stabilized by immobilization or other means since they lack the synthesis of polypeptides degraded in proportion to the rate of photochemistry.

206

MEMBRANE POTENTIAL AND ELECTRIC CAPACITANCE IN CHROMATOPHORES OF RHODOSPIRILLUM RUBRUM

L. Casadio, G. Venturoli and B.A. Melandri, Inst. of Botany University of Bologna, Bologna, Italy.

In phospholipid (PL)-enriched chromatophores, the electric capacitance of the membrane was evaluated from the ratio of the membrane potential (measured from the electrochromic carotenoid band shift elicited in the presence of antimycin by single turnover flash) to the correspondent amount of oxidized reaction center (RC). The obtained values, normalized per mg protein, increased at increasing PL-enrichment and correlated linearly with the PL to protein molar ratios of the closed vesicles obtained upon freezing and thawing of chromatophores with presonicated liposomes and characterized by a low conductivity to ions. Carotenoid signals, induced in the dark by imposing diffusion potentials of known extent with K⁺ valinomycin pulses, were unaffected by PL-enrichment at constant RC content. Energy transfer efficiency from the carotenoids to core light harvesting complexes (B875) was also unaffected even in the presence of a large PL excess. Overall, these results suggest that the RC complexes are dispersed in the bilayer upon fusion and that the carotenoids sense a delocalized light-induced transmembrane field.

208

FLUORESCENCE MECHANISMS IN CHLOROPLASTS ON SUB-NAVOSECOND TIME SCALES PROBED BY PICOSECOND PULSE PAIRS

A. Dobek, J. Deprez, N.E. Geacintov, G. Paillotin and J. Breton, Département de Biologie, Centre d'Etudes Nucleaires de Saclay 91191 Gif sur Yvette, France

Fluorescence enhancement phenomena and quenching by exciton-exciton annihilation on sub-nanosecond time scales were investigated in spinach chloroplasts utilizing picosecond laser pulse pairs (530 nm, 30 ps wide) of equal intensity, spaced apart in time by variable delays of $\Delta t = 0 - 6$ ns. In the case of open PSII reaction centers the quenching effect of excitons generated by the first pulse on the fluorescence yield of the second pulse diminishes with increasing Δt with a characteristic decorrelation time of 140 ± 60 ps. This effect is attributed to either the decay of mobile excitons in the light harvesting (LH) antenna pigment bed as these excitons migrate towards the PSII reaction centers and the associated smaller core antenna pigment pools, or to the decay of a quenching state of the reaction center (and/or core antenna) which appears following a rapid (< 140 ps) trapping of the excitons initially created in the pigment bed. The absence of a significant decay component of exciton quenchers with a lifetime comparable to the 300-600 ps intermediate phase of fluorescence decay kinetics suggests that this phase is not caused by freely mobile excitons interacting in a lake of pigments, but originates instead from smaller pigment pools to which the excitons have migrated. Consequently, bimolecular exciton annihilation in these smaller domains dominates over annihilation in the larger LH antenna pigment bed.

Partially supported by NRS Grant RCM 83-08190.

210

CONFORMATION AND ORIENTATION OF CHLOROPHYLL PROTEINS IN THE THYLAKOID MEMBRANE: CIRCULAR DICHROISM AND POLARIZED INFRARED SPECTROSCOPY OF LIGHT-HARVESTING AND PHOTOSYSTEM I COMPLEXES

E. Hildebrandt, P. Brédet, S. Durr, A.M. Bardin and J. Breton, Centre Biophysique, CNRS, Gif sur Yvette, France.

The structure and orientation of the two main protein constituents of photosynthetic membranes from green plants, the chlorophyll *a/b* complex (LHC) and the Photosystem I complex (PSI) have been investigated by UV circular dichroism (CD) and polarized infrared (IR) spectroscopy. These complexes have been reconstituted into phosphatidyl bilayer vesicles by a freeze-thaw technique and they have been compared to the intact thylakoid membrane. The native orientation of the pigments in the reconstituted complexes was characterized by monitoring the fluorescence emission, the visible CD and linear dichroism spectra. Conformational analysis of LHC and PSI indicates that 44% (in LHC) and 50% (in PSI) of the protein is α -helical. By measuring the IR dichroism of the amide bands of air-dried oriented multilayers of native and reconstituted membranes, we have estimated the degree of orientation of the α -helical chains with respect to the membrane plane. IR dichroism data demonstrate that transmembrane α -helices are present in both LHC and PSI with the helix axis tilted at less than 30° in LHC and 35° in PSI, with respect to the membrane normal. These results are consistent with a transbilayer organization of chlorophyll-protein complexes in the thylakoid membrane.

Posters on Photosynthesis

211

STUDY OF PHOTOSYSTEM I REACTIONS AT LOW TEMPERATURE.

P. Sétif, P. Mathis and T. Vanngard

Service Biophysique, CEN/Saclay, Gif sur Yvette, France.

Electron transport has been studied at 10-30K in digitonin PS1 particles, by flash absorption and EPR spectroscopies. In mildly reducing conditions, an irreversible charge separation between P700 and iron-sulfur center A is progressively induced at 10K by successive laser flashes up to a maximum which corresponds to about two thirds of the reaction centers. Heterogeneity of the rate of center A reduction is shown. In the other third of reaction centers, a reversible charge separation occurs and relaxes with a $\tau_1 = 120$ μ s. When the centers A and B are pre-reduced, the 120 μ s relaxation becomes the dominant process (70-80% of the reaction centers) and a slow relaxation ($\tau_2 = 50-400$ ms), corresponding to the recombination between P700⁺ and center X⁻ occurs in only 10-15% of the reaction centers. The partner of P700⁺ in the 120 μ s recombination is proposed to be the acceptor A₁⁻ as defined by Bonnerjee J. and Evans, M.C.W. (1983) FEBS Lett. 148, 313-316. Our data also suggest that center X is not on the electron flow from P700 to centers A or B. The existence of different relaxation phases in both redox conditions is shown to result from an heterogeneity in the processes of electron transfer to the secondary acceptors of PS I. This heterogeneity is probably due to the trapping of different conformational states during freezing but may be also related to different physiological roles.

213

ELECTROGENIC REACTIONS OF THE CHLOROPLAST CYTOCHROME b₆/f COMPLEX IN CHLOROPLASTS

R.W. Jones, M.A. Selak and I. Whitmarsh, Department of Plant Biology, University of Illinois, Urbana, Illinois, U.S.A.

We have attempted to determine the charge transfer reactions in the cytochrome b₆/f complex that give rise to the slow electrogenic step by spectroscopic measurements of the electrochromic shift at 515 nm and cytochrome b₆ and f redox changes. In these studies duroquinol was used to support photosystem I driven electron transport using single-turnover light flashes. Our data indicate that the slow electrogenic reaction is due to quinol oxidation by the cytochrome b₆/f complex. To investigate this problem we studied the effect of 2-n-nonyl-hydroxyquinoline N-oxide (NQHNO) and 2-n-heptyl-4-hydroxyquinoline N-oxide (HQNO), both of which inhibit the oxidation of cytochrome b₆ on the slow phase of the electrochromic change. The extent and kinetics of the electrochromic change were compared to a simple kinetic model. The data were fitted best by assuming that the slow electrogenic step arises from two consecutive reactions: (1) electron transfer from one cytochrome b₆ to the other, and (2) a reaction coupled to the oxidation of the cytochrome b₆ closest to the outer aqueous phase. In this model we envision NQHNO (or HQNO) having two inhibitory effects while binding at the quinone reductase site on the cytochrome b₆/f complex. First, it blocks the oxidation of the cytochrome b₆ molecule closest to the outer aqueous phase, and second, it slows electron transfer from the inner cytochrome b₆ to the outer one.

215

EFFECT OF MOLECULAR ORIENTATION ON THE RATE OF EXCITATION ENERGY TRAPPING IN THE PHOTOSYNTHETIC UNIT

Z.G. Fetisova, Moscow State University, Moscow, USSR

Operation efficiency of a planar model photosynthetic unit (PSU) is evaluated by computer calculations of the time of excitation energy trapping by reaction centers (RC). It is shown that (1) the mean value of the orientational factor for randomly oriented transition moment vectors ($\bar{\mu}$), lying in the same plane, $k^2=5/4$; (2) for partially ordered PSUs (with any lattice), in which the $\bar{\mu}$ vectors lie in the PSU plane but are randomly oriented in the plane, the rate of energy trapping by RC is doubled as compared to that for the vectors randomly oriented in three-dimensional space; (3) in optimal PSU with the square lattice all $\bar{\mu}$ vectors are parallel to the long axes of elementary PSUs (which form macroscopic multicentral PSUs through the translational symmetry); in PSUs considered such optimal orientation of these collinear vectors accelerates the energy trapping by RC at most 5-fold (as compared to that for three-dimensional random orientation of the vectors, i.e. for $k^2=2/3$); (4) operation efficiency of PSUs with the triangular (or hexagonal) lattice is the same for the optimal orientation of collinear $\bar{\mu}$ vectors and for two-dimensional random orientation of the vectors in the PSU plane; (5) operation efficiency of PSU with any lattice is tolerant to heat motion of PSU molecules both in the case of the optimal orientation of collinear $\bar{\mu}$ vectors of PSU molecules and in the case of two-dimensional random orientation of the vectors in the PSU plane.

212

EFFECT OF HERBICIDES ON ELECTRON TRANSFER BETWEEN PLASTOQUINONE MOLECULES IN PS II. STUDY BY FLASH ΔA IN THE UV.

J. Farineau and P. Mathis.

Service de Biophysique, CEN/Saclay, Gif sur Yvette, France.

Herbicides are known to block electron transfer at the level of 2 plastoquinone molecules, Q_A and Q_B, bound to PS II reaction center. This effect has been investigated by flash absorption spectroscopy around 320 nm (maximal absorption of the anion PQ⁻ in spinach chloroplasts incubated with NH₄OH and valinomycin-K⁺). We used sequences of short flashes; the material was in a flowing system at 10°C. In untreated dark-adapted material without inhibitor, a period-2 pattern of oscillations is clearly seen (with positive stable ΔA after flashes 1,3,5 and negative after flashes 2,4) which damps in about 6-8 flashes. The amplitude of the ΔA was larger when chloroplasts were incubated with ferricyanide before NH₄OH addition. These changes reflect formation and disappearance on successive flashes of PQ⁻ (as Q_B⁻), the level of Q_B (ox) being maximal in chloroplasts incubated with an strong oxidant (Mathis and Havenan, BBA, 1977, 461, 167-181). In the presence of saturating amounts of herbicides, all the ΔA are suppressed except a bleaching at 320 nm with a small amount of herbicide a period-2 pattern was evidenced (negative stable ΔA after flashes, 1,3,5 and positive after flashes 2,4). It is well observed with herbicide having a low I₅₀ for PS II activity, specially phenolic (DNOC, oinoseb) after a preillumination. It seems that about 50% of the centers are blocked before the train of flashes in state Q_A⁻, the other being in the state Q_AQ_B.

214

ENERGY TRANSFER IN FLUORESCENCE OF ANAENA AZOTICA (L. S. P. E. ALBA)

Zhen-mo Jia, Zhao-xi Fang, Ji-liang Jiao, Department of Biology, Peking University, Beijing, China

The absorption, emission and excitation spectra of *Anaena azotica* suspensions were measured. The emission spectra were measured at two different temperatures: 15-18°C and -176°C with different excitation light whose wavelengths were: 430nm, 515 nm, and 550nm. To compare those fluorescence spectra of algal suspension which were treated by the following methods: (1) heating at 60°C for 0, 4, 8, 12, 15, 20 mins., (2) adding hydroxylamine whose final concentration in algal suspensions were: 2, 5 and 8mM, (3) adding D2O to make their final concentrations in suspensions reach: 0.04, 0.08, 0.12, 0.16 and 0.20M, (4) adding 0-phenanthroline of which final concentrations in algal suspensions were: 5, 10, 15, 20, 25 μ M, (5) adding divalent cations: K₂SO₄ and Zn²⁺. All these treatments effected on the relative intensity ratio of maxima of fluorescence spectra. These maxima were: F644, F650, F695, F695, F728 at -176°C and F665, F683, F720-725 at 15-18°C.

Our data showed the route of energy transfer from phyocyanin to chlorophyll a of photosystem II. We discussed the possible relation between pigments and protein.

216

ISOLATION OF A CALCIUM BINDING PROTEIN FROM AN OXYGEN-EVOLVING PHOTOSYSTEM 2 PREPARATION

R.W. Sparrow and R.R. England, Biology Division, Preston Polytechnic, Preston, Lancashire, Great Britain.

A heat stable protein has been isolated from highly-active oxygen evolving Photosystem 2 particles, isolated from lettuce chloroplasts. This protein was found to bind to fluphenazine-Sepharose in the presence of calcium and can be eluted by substitution of calcium with EGTA. The purified protein has an estimated molecular weight of 13-15 kDa and is able to stimulate, calmodulin depleted 3':5'-cyclic nucleotide phosphodiesterase. This calcium-binding protein was shown not to be similar to proteins removed from Photosystem 2 particles, by Tris-washing.

Tuesday 31 July Congress Centre-first floor. Posters 217-222

Posters under Category 29: General

217

UNIVERSAL PATTERN OF SYSTEMIC RESPONSE OF HIGHER EUCARYOT CELLS TO THE EFFECTS OF PHYSICAL AND CHEMICAL FACTORS, I.N. Todorov, M.K. Pulatova and N.M. Emanuel, Institute of Chemical Physics, USSR Acad. Sci., Moscow, USSR.

It has been found that systemic response of liver cells to the effects of various chemical and physical factors having different nature is of universal pattern. These factors are radiation, pharmacological blockade of translation, introduction of adaptogens, antioxidants and cancerogenes. The following processes are observed as a response to the disturbances in bioenergetics, synthesis of macromolecules, detoxication system, structure of cell organelles and changes in the redox parameters of electron transfer systems (ETS): 1. activation of additional ways of energy supply, including oxidation of fatty acids and lipids by oxygenases; 2. activation of protein synthesis by mobilizing and increasing the components of the protein-synthesizing apparatus (ribosomes, mRNA and tRNA) which results in 3. additional synthesis of the enzymes of energy supply (oxygenase, ETS carriers), enzymes of protection and metabolism of biopolymer synthesis precursors. 4. The above processes bring about growth of the cell mass, which automatically switches on the DNA replication system to raise the "gene dose" per increased cell volume.

219

CALCULATION OF THE VIBRATION MODES ARISING FROM PHOSPHATE-BACKBONE IN B AND Z FORMS OF DNA. M. Ghomi, J.A. Taboury and E. Taillandier, Laboratoire de Spectroscopie Biomoléculaire, Université Paris XIII, 74, rue Marcel Cachin, 93012 Bobigny Cedex, France.

Using the Wilson GF-method the frequencies of the vibration modes of phosphate-backbone in B and Z forms of poly(dG-dC).poly(dG-dC) have been calculated. These calculations are based on a simplified valence force field which is supposed to be independent of the used conformations. It takes account of the interatomic interactions sugars and phosphate in DNA chains. In order to respect the harmonic approximation of potential field a set of non-redundant internal coordinates has been used. For this, a standard B.G. matrix product diagonalization procedure has been adopted following the local symmetry of the different constituents of DNA chains. Our dynamic model is formed by two deoxyribose molecules surrounding a phosphate group. To calculate the G matrix the geometry of GpC and CpG sequences of wrinkled B form or that of Z forms of poly(dG-dC).poly(dG-dC) has been taken into consideration. The calculated frequencies are in good agreement with the peak positions of the infrared and Raman spectra corresponding to the phosphodiester chain of the B and Z forms of the poly(dG-dC).poly(dG-dC) observed between 1400 and 600 cm^{-1} .

221

STRUCTURAL AND FUNCTIONAL CHANGES IN SYNAPTIC MEMBRANES AFTER TREATMENT WITH DIFFERENT PHOSPHOLIPASES. Kozlov Yu.P., Selishchova A.A., Brusovani V.I., Erin A.I., Prilipko L.L., Kagan V.B. Moscow State University, Moscow, U.S.S.R.

The role of phospholipids and products of their metabolism in transmembrane transfer of a signal was studied, using Ca^{2+} transport into synaptosomes. Transport of Ca^{2+} was recorded by ^{45}Ca accumulation in synaptosomes; the transmembrane potential $\Delta\psi$ was measured by fluorescence of di-8-C₁₂(5). Changes in phospholipid environment were induced by treatment with phospholipases. Under effects of phospholipases A₂, C and D, the value of $\Delta\psi$ changes significantly in a resting state, but not upon depolarization. The loss of integrity of the phospholipid bilayer induced by phospholipases A₂ and C lead to inhibition of Ca^{2+} transport. Conversely, phospholipase D increases ^{45}Ca accumulation in synaptosomes which may be due to elevated intramembrane content of phosphatidic acid, an effective ionophore of Ca^{2+} . The experimental data suggest that the inhibition of potential-dependent Ca^{2+} -channels induced by changes in the phospholipid bilayer may be compensated for by the appearance of phospholipid metabolism products, that are actively involved in the formation of Ca^{2+} permeability channels.

218

ION PERMEABILITY IN BILAYER LIPID MEMBRANES: THE SIGNIFICANCE OF THE PHASE TRANSITIONS, INDUCED BY TEMPERATURE, pH AND Ca^{2+} CHANGES. V.F. Antonov, E.V. Shevchenko, A.A. Molnar, E.T. Koszomkulov, S.A. Vosnesenskiy, E.Yu. Smirnova, A.N. Wasserman, Yu.V. Morozov, I.M. Sechenov First Moscow medical institute, B. Pirogovskaja Street, 2-6, G-435, 119436, USSR, Moscow.

Until now there have been no reports of single-ion channels in unmodified lipid membranes. We have studied the electrical conductance of planar lipid bilayer membranes made of synthetic dipalmitoylphosphatidic acid in voltage clamp conditions. Conductance fluctuations of amplitude ranged from 20 pSm to 10 nSm and duration about 1 s have been discovered at the phase transitions induced by temperature, pH and Ca^{2+} changes. The obtained data show that the appearance of ionic channels may be the result of lipid bilayer defect interactions. This would explain the dramatic increase in ion permeability observed in liposomes during phase transitions (1). We suggest that these channels could conduct the membrane ionic current in biological membranes during nerve excitation, thermo- and chemoreception and H-ATPase and Ca^{2+} -ATPase activities.

1. V.F. Antonov et al, 1980, NATURE, v.283, p.585.

220

ON THE MECHANISM OF METABOLISM PHOTOREGULATION IN THE BOTH HUMAN AND ANIMAL CELLS. V.N. Zaleskiy and N.V. Lisenkov, Department of Laser and Antitumor Effects, R.E. Kavetsky Institute for Oncology Problems, Acad. Sci. of Ukrainian S.S.R., Kiev, U.S.S.R.

The light has its activatory or inhibitory effects on the living organism's chemical reactions over all the range of wavelengths. A decrease in the number of photoacceptors results in a wavelength increase, thus, the UV-radiation is absorbed by many of the bioactive molecules and important biopolymers, while the blue-green and red light is absorbed by a less number of compounds. In an animal cell, particularly in neuron, there is a sufficient number of the photoacceptors which alter their electron states upon absorbing number of photons. This effect was shown with a use of the both spectral (electron spin resonance and atomic absorption) and enzymatic techniques in complex proteins containing chromophore groups and metals of varying valency as well as in more simple bioactive molecules (porphyrins, carotenoids, etc.). In the clinic experiments on laser acupuncture for intractable cancer pain, the laser biostimulation was shown to promote more active transformation of photon energy to nerve impulse energy. It appears that the light is able to control the different metabolic processes in the human and animal body through the specific photo-acceptor molecules.

222

THERMOTROPIC BEHAVIOUR OF BIPOLAR LIPIDS OF THERMOPHILIC ARCHAEABACTERIA

G. Paoli, A. Gliozzi, D. Pisani, M. De Rosa and A. Gambacorta. Dipartimento di Fisica, Via Dodecaneco 33, 16146, Genova, Italy

The plasma membrane of *Sulfolobus Solfataricus*, an extreme thermo acidophilic archaebacterium, is characterized by unusual bipolar lipids. Arranged in a single monolayer they are based on two C₄₀ - biphytanil residues, with up to four cyclopentane rings per chain, linked to either two glycerols (symmetric lipid) or to one glycerol and to one branched-chain inonitol (asymmetric lipid).

In this work we present a comparative calorimetric study of the symmetric and asymmetric lipid at various degrees of hydration. The thermotropic properties of the asymmetric lipid are very complex one, showing two transitions in the dry state and at least two in the hydrated one. The low enthalpies displayed by most of these transitions, might indicate lipid polymorphism associated with temperature-dependent hydrogen bonds between the inonitol polar heads. Water content is shown to play a fundamental role in determining the kind and the temperature of the transitions. The symmetric lipid exhibits a much simpler behaviour, being arranged in a lamellar structure with a single melting transition.

Tuesday 31 July Congress Centre-first floor. Posters 223-228

Posters under Category 29: General

223

A COMPARATIVE STUDY ON THE STRUCTURE & FUNCTIONS OF SOME SYMPATHOMIMETIC & ALLIED DRUG MOLECULES
N. N. Saha, Saha Institute of Nuclear Physics,
92, A. P. C. Road, Calcutta, India.

Structures of a number of drug molecules of various types were determined by us for structure-function correlation. This paper gives a comparative picture of our findings on 10 sympathomimetic amines, (1) Tyramine, (2) p-hydroxyephedrine, (3) Nor-ephedrine, (4) L-phenylephrine, (5) DL-N-ethylmorphine, (6) Phenylpropanolamine, (7) Naphazoline, (8) DL-metanephrine, (9) 3,4-dimethoxyphenethylamine and (10) DL-normetanephrine. All these molecules have in common an ethylamine sidechain connected to a benzene ring. Molecules (1)-(7) have marked sympathomimetic properties, the first six of which have the preferred conformation required for a molecule to have sympathomimetic activity, i.e. a maximally extended ethylamine sidechain normal to the benzene ring, whereas (7) Naphazoline, which is as active a drug as adrenaline, has conformation unfavourable for sympathomimetic activity, the side chain being rigid and folded. The last three molecules (8), (9) & (10) do not have any sympathomimetic property. As expected, molecules (8) & (9) do not have the preferred conformation required for drug activity, whereas molecule (10) has favourable conformation but no drug activity. It thus indicates that conformation is not the sufficient condition for drug activity.

225

SPECTRAL ANALYSIS OF THE ERYTHROCYTE FLICKERING: A SENSITIVE METHOD TO MEASURE MEMBRANE ELASTICITY AND TO DETECT SUBTLE CHANGES IN MEMBRANE STRUCTURES.

E. Sackmann, K. Wirthensohn and K. Fricke, Physik Department, Technical University München, München FRG.

The overdamped surface undulations of erythrocyte plasma membranes are determined by the bending elasticity and the curvature elastic constants can be obtained from the flickering frequency spectrum. By measuring the spectra of individual cells in a flow chamber by a direct microscopic method subtle changes in the bending elasticity caused by (1) thermally induced conformational changes, (2) by cholesterol depletion or (4) by the action of drugs are observed. Moreover, the flicker spectrum analysis provides information about alterations in the membrane elasticity caused by diseases such as diabetes. In parallel experiments we try to correlate the changes of membrane elasticity to variations in the lateral organization of the membrane proteins.

227

ZERO POINT OSCILLATIONS AND BIORITHMICS
U. Kopvillem, Quantum oceanology lab, Radio st. 7
Vladivostok 690032, USSR

We consider the possibility of the appearing of biorhythms by the influence of electromagnetic and elastic zero point motions. The general idea steps from the fact that the potential energy may transform into kinetic energy of motion or energy of coherent radiation by means of zero point fluctuations and that this process is a spontaneous transformation. The potential energy may be accumulated step by step from the energy of sunlight and chemical energy. Depending from the structure and composition of the system the spontaneous transformation will be launched rhythmically with a constant period that may be calculated precisely from quantum theory of photon and phonon avalanches. Bloch and Dicki states will appear spontaneously. The first state is not connected with macroscopic space motion of the system or inside the system but acts as a generator of characteristic signals and coherent stimulated chemical reactions. Bloch states also generate memory effects in the matter. Dicki states on the contrary give macroscopic motions. Electromagnetic and elastic solitons in biological systems are generated by zero point motions. The experimental detection of solitons in biological systems would be the confirmation of our assumption. We discuss several models of involved biological systems.

224

ANGIOTENSIN-MEDIATED CALCIUM EFFLUX FROM ADRENAL GLOMERULOSA CELLS, R. Foster, A. Rojas and E.T. Marusic, Faculty of Medicine, University of Chile, Casilla 137-D, Santiago, Chile.

Isolated bovine adrenal glomerulosa cells placed in a flow through system exhibit an increase in calcium efflux when exposed to angiotensin II (AII). Calcium in the perfusate was measured with a Radiometer F2112 Ca-selective electrode coupled to the cell perfused system. 1 min exposure to 10 nM AII produced an increase of 66.7 ± 14.8 nmole Ca/mg protein (sd, n=8) from cells perfused with medium 199 (1.3 mM Ca). Cells perfused for 45 min with calcium free medium supplemented with 50 μ M EGTA and challenged with 10 nM AII for 1 min produced 55% of the calcium efflux seen when perfused with medium 199 (1.3 mM Ca). By perfusing the cells with medium 199 (1.3 mM Ca) containing 20 μ M dantrolene we observed that the angiotensin-induced calcium efflux was inhibited in more than 90% (5.3 ± 0.8 nmole Ca/mg protein, sd, n=8). Replacing the dantrolene by normal calcium containing medium and desaturated the cells from the inhibitor for 20 min, the response was not only restored but enhanced by 35% to the one observed before perfusing with dantrolene. We suggest that the endoplasmic reticulum of this cells show (1) a high capacity of calcium accumulation and (2) a possible participation during hormone activation.

226

DETERMINATION OF (1) ELECTRON DENSITY PROFILE AND (2) FORCES BETWEEN HIGHER PLANT THYLAKOIDS BY MEANS OF SMALL-ANGLE X-RAY SCATTERING
K. Diederichs, W. Welte, W. Kreutz; Institut für Biophysik, Universität Freiburg, Albertstrasse 23 D-7800 Freiburg i. Br., FRG

The electron density profile (EDP) of spinach chloroplast grana thylakoids was evaluated by means of a least squares procedure taking into account statistical distortions of the membrane stacking period. Phase determination was performed with the help of swelling experiments. For this purpose a new dehydration device was used which made it possible to control (1) the amount of cations in contact with the sample and (2) the osmotic pressure exerted by a sucrose solution of known concentration which was in osmotic equilibrium with the sample via a semipermeable membrane. The measured curves of bragg period versus osmotic pressure at two different concentrations of the cations together with the determined EDPs showed (1) the cytoplasmic side of the thylakoid EDP (partition region) remains constant whereas the luminal part swells when the osmotic pressure is lowered and (2) the amount of swelling can be explained in terms of a long-range electrostatic repulsive force between the luminal sides of the thylakoid bilayers.

228

CONFORMATIONAL CHANGES OF POLY(dG-dC).POLY(dG-dC) - CIS Pt (NH₃)₂ Cl₂ STUDIED BY IR AND CD SPECTROSCOPY.
L. Fort, B. Hervé, J.A. Tabor, J. Liquier, T. Theophanides, E. Tatlandier, Laboratoire de Spectroscopie Biomoléculaire, Université de Paris XIII, 74, rue Marcel Cachin, 93012 Bobigny Cedex, France.

Complexes between poly(dG-dC).poly(dG-dC) and cis-Pt (NH₃)₂ Cl₂ have been investigated by IR spectroscopy and circular dichroism. For a high cis-platinum/nucleotide ratio ($r = 0.12$) corresponding to 1 cis-platinum molecule per 4 guanine bases the left-handed form of the polynucleotide is not detected by IR spectroscopy. The spectrum is consistent neither with a B nor a Z geometry, but reflects a distorted conformation. The use of specifically deuterated poly(dG-dC).poly(dG-dC) on the C8 of guanines shows that the cis-platinum binds directly on the N7 site of these bases. The binding of the cis-platinum on the bases is also evidenced by the displacement of a double bond in plane stretching vibration on the bases observed at 1600 cm⁻¹ in the complex. However CD measurements reveal an extremely weak signal of Z form when compared with the usually observed CD spectrum of poly(dG-dC).poly(dG-dC) in the same experimental conditions. For lower cis-platinum contents ($r = 0.06$; $r = 0.03$) the IR spectra of the poly(dG-dC).poly(dG-dC)-cis Pt complexes reflect the existence of right (B) or left (Z) conformations depending on the hydration of the complexes. The CD spectra reveal that these cis Pt complexes partly adopt a Z conformation in conditions in which free polymer is in a B geometry. The G-C bases between two adjacent cis-Pt perturbed sites may adopt the Z form more easily than in the case of the free polymer.

Tuesday 31 July Congress Centre-first floor. Posters 229-234

Posters under Category 29: General

229

STUDY OF THE α -CHYMOTRYPSIN ENZYMIC SITE BY USE OF 9-AMINO-ACRIDIN FLUORESCENT PROBES

A. MARTY, M. BOURDIN, M. M. DELL'AMICO, P. MAILLET.

Laboratoire de chimie organique, Université de Perpignan, Avenue de Villeneuve, PERPIGNAN, FRANCE.

Laboratoire de pharmacologie, UFR de Pharmacie, 27 Boulevard Jean Moulin, MARSEILLE, FRANCE.

The fluorescence emission light of various 9-amino-acridinic cationic derivatives (A) was quenched without any spectrum shift in the presence of α -chymotrypsin (α -CT). Moreover this quenching phenomenon became saturated at high α -CT concentration; it was reversible and was suppressed by addition of hydrocinnamic acid, a competitive inhibitor of the α -CT enzymatic activity.

So, it has been deduced that A compounds located in the protein active site, forming fluorescent complexes of which the apparent association constants (K_A) were calculated. These results made obvious that the less the A compound was soluble, the more easily it was interacting with α -CT.

So, the quantum yields and fluorescent lifetimes of A compounds in non aqueous solvents with different polarity and of A- α -CT complexes were studied.

The values obtained for complexes were close to those measured for A tetrahydrofuran solutions, indicating some hydrophobic and rather apolar character of α -CT enzymatic site.

231

ISOLATION AND IDENTIFICATION OF FLAVONOID GLYCOSIDES FROM *SALVIA TRILOBA* PLANTS

by
I. Ghali, S. Gabr, M. Saleh, and A. Abu-Ezta
Biochem. Dept. Faculty of Agriculture, Cairo University,
Giza, EGYPT
Biochem. Dept. Faculty of Agriculture, Zagazig University
EGYPT.

Salvia triloba grows in the Egyptian desert as a wild plant. The ethanolic extract of the plant was subjected to fractionation on polyamide column and the different fractions were detected by U.V. light. Each fraction was purified by chromatographic technique, and the pure product was subjected to different analyses in order to identify its structure.

Ultraviolet and mass spectrometry techniques were used to identify the structure of the isolated compounds. Demethylation, acid or enzymatic hydrolysis and alkali treatment were also used in some cases.

Fourteen flavonoid glycosides were identified from the aerial part of *Salvia triloba* plant.

233

PH SENSITIVE LIPOSOMES. ACID INDUCED FUSION AND IMPROVED CYTOPLASMIC DELIVERY. Leaf Huang, Dept. of Biochem., Univ. of Tenn., Knoxville, TN 37996-0840.

Sonicated unilamellar vesicles (SUV) consisting of dioleoyl phosphatidylethanolamine (PE) and palmitoyl homocysteine (PHC) in an (8:2) molar ratio rapidly fuse, at a pH lower than 6.5, with vesicles of various lipid composition. Fusion was monitored by a) mixing of lipids as shown by resonance energy transfer, b) gel filtration and c) electron microscopy. The presence of phosphatidylethanolamine greatly enhanced fusion, while the presence of phosphatidylcholine, cholesterol and gangliosides inhibited fusion. PHC could be replaced by a long chain fatty acid such as oleic or palmitic acid. The addition of 0.5mM Ca^{++} synergistically increased the fusion, whereas the addition of 0.5mM Mg^{++} had no effect. Fatty acid derivatized monoclonal anti-H2K^b was incorporated into reverse-phase evaporation vesicles (REV) consisting of the fusion competent PE-PHC (8:2) lipids by a modified method of Shen et al. (BBA 669(1982), 31-37). Mouse L929 cells (k haplotype) incubated with these immunoliposomes containing calcein, revealed diffused fluorescence throughout the cell indicating a release of the dye into the cytoplasm. In contrast, cells incubated with pH insensitive immunoliposomes displayed only punctate fluorescence. In control experiments, mouse A31 cells (d haplotype) were incubated with immunoliposomes and no fluorescence was observed. These results indicate that the immunoliposomes are specifically and effectively endocytosed by the target cells and the pH sensitive immunoliposomes are efficient in delivering their contents into the cytoplasm of target cells; possibly by fusing with the endosome membranes at low pH.

230

NEUTRON SCATTERING STUDIES OF WATER IN MACROMOLECULAR SYSTEMS

C.F. Hazlewood, D.B. Heidorn, H.E. Korschach, R.M. Nicklow, Baylor College of Medicine, Houston, Texas.

The microscopic structure and dynamics of water in the presence of macromolecules in water-polymer mixtures and living systems are not well-understood. Much work has been done using various experimental techniques to study the properties of water in these heterogeneous systems, yet there is no generally accepted model which describes the interaction of water with macromolecules. Quasielastic neutron scattering (QNS) is a relatively new technique that is capable of a spatial resolution of 1-10 Å and a frequency resolution of 10^3 to 10^{13} sec⁻¹ which cover the ranges of interest for diffusive water motion. The large incoherent scattering cross section of hydrogen relative to other biologically abundant nuclei also makes this technique especially suitable for the study of water dynamics. Our results for water diffusion in agarose and polyox gels and in hydrated cysts of brine shrimp (*Artemia salina*) were interpreted by using a jump-diffusion model for translational water motion and a simple Brownian rotational model and show that the translational and rotational diffusion coefficients are reduced from the values for pure water, especially in the least hydrated systems. We show that these measured values are consistent with diffusion coefficients and T_1 relaxation times measured by NMR methods.

Funding for this research was provided by the Robert A. Welch Foundation and the Office of Naval Research.

232

ACTIVITY COEFFICIENTS OF SALTS IN PROTEIN SOLUTIONS AND PHOSPHOLIPID SUSPENSIONS

M.D. Rebolras, P. Ocon and C. Acerete, Departamento de Electroquímica, Universidad Autónoma de Madrid, Madrid, Spain.

The knowledge of the chemical potentials of the components of biological solutions is of central importance for the understanding and the interpretation of the life processes taking place both in-and out-side of cellular membrane. The EMF method using ion-exchange membrane electrodes is a suitable procedure for measuring the interactions between single salts and the rest of the components present in the solutions. High accuracy is necessary for detecting the small influences of the protein or phospholipid component on the activity of the salt. The error in EMF being +0.2 mV, the relative error in the activity at $E=0$ was +0.5%. We report the determination of the mean activity coefficients of XK salts (being X=F⁻, Cl⁻, Br⁻, I⁻, NO₃⁻, SCN⁻) in concentrated protein (BSA) solutions and Cl₂Ca, MgCl₂ in mixed multilamellar phospholipid vesicles. For all the salts studied, the mean activity coefficients decreases with increasing protein concentration, being the variation quantitatively different for each salt due to specific binding of the anions on the protein molecule. Specific interactions have been shown between the Ca²⁺ and Mg²⁺ ions and the mixed multilamellar vesicles depending strongly on the dipalmitoylphosphatidylcholine (DPFC)-phosphatidylinositol (PI) ratio.

234

Diffraction and calorimetry study of structural modifications induced by γ -ray irradiation on phosphatidylcholine multilamellar liposomes.

C. Albertini^a, E. Fanelli^b, L. Guidoni^c, F. Ianzini^c, P. Mariani^d, F. Rustichelli^a, V. Viti^c.

^aIstituto di Fisica Medica, Facoltà di Medicina, Università di Ancona (Italy).

^bDipartimento di Scienze Chimiche, Università di Camerino (Italy).

^cLaboratorio di Fisica, Istituto Superiore di Sanità, Roma, (Italy)

^dSez. Fisica, Dipartimento Scienze dei Materiali e della terra, Facoltà di Ingegneria, Università di Ancona (Italy).

The behavior of synthetic lecithins, 75% weight water, has been examined in temperature ranges including the lipid phase transitions for irradiation doses between $1.6 \cdot 10^3$ and $77.8 \cdot 10^3$ Gy. Modifications in differential calorimetry scan were observed even at the lowest irradiation doses. At the highest doses similar modifications have been previously observed (1). The X-ray diffraction pattern, too, exhibits appreciable modifications at the lowest irradiation doses. Among the different obtained structural changes a general increase of the two-dimensional lamellar lattice periodicity was observed as a function of the irradiation dose.

(1) F. Ianzini, L. Guidoni, P.L. Indovina, V. Viti, G. Erriu, S. Onnis, P. Randaccio, Rad. Eff. 94, 154-166 (1978).

Tuesday 31 July Congress Centre-first floor. Posters 235-240

Posters under Category 29: General

235

ROTATIONAL AND TRANSLATIONAL SWIMMING OF HUMAN SPERMATOZOA
P. Thyberg & R. Rigler, Department of Medical Biophysics,
Karolinska Institute, Stockholm, SWEDEN

Rotational and translational swimming motion of human spermatozoa have been evaluated from autocorrelated intensity fluctuations of scattered laser light. It can be shown that Maxwellian speed distributions for both longitudinal and rotational motions can be used to describe in a consistent manner the wave vector dependence of the measured autocorrelation function. When the scattering is detected at zero degree (using crossed polarizers) the autocorrelation function is solely due to rotational motion where at angles 20° it is dominated by the longitudinal motions.

For human spermatozoa a rotational frequency of about 40 Hz was found which can be ascribed to be the rotation of the sperm head (1) whereas for the longitudinal motion an average speed of 40 $\mu\text{m/s}$ was obtained.

From comparison of the translational with the rotational swimming speed a propelling efficiency of about 10 $\mu\text{m/turn}$ is deduced. This parameter describes the linkage between the rotational and translational swimming motion and is likely to be discriminatory in the analysis of physiological sperm motions.

(1) Rigler, R. & Thyberg, P. (1984). Rotational and translational swimming of human spermatozoa: A dynamic laser light scattering study. *Cytometry* 5, 1-6.

237

THE EFFECT OF CALCIUM ANTAGONISTS ON THE INOTROPIC EFFECT OF SOME CARDIOSTIMULATIVE SUBSTANCES ON THE ISOLATED RAT RIGHT VENTRICLE OF HEART D.R. Matejević, M.R. Pavlović, V.A. Vucković and J.E. Nestorović, Institute of Physiology, Faculty of Medicine, Beograd, Yugoslavia.

Bearing in mind the well known role of calcium ions in contractility, the aim of our work was to investigate the relationship between the positive inotropic effect of db-cAMP , isoprenaline, ouabain and calcium ions. Experiments were carried out on the isolated rat right ventricle of heart, electrically stimulated, under the condition of blockade of calcium channels (verapamil), binding of calcium ions (di-Na-EDTA) and excess of calcium. We have found that change in the concentration of free extracellular calcium, as well as their transmembrane transport, strongly modified the amplitude of contractions of the investigated cardiostimulative substances. Considering that the blockade of calcium channels by verapamil insignificantly reduce the inotropic effect of ouabain in our experiments, we may suggest that in some way ouabain facilitates the entry of calcium into myofibrils. On the basis of our results it can be concluded that for the inotropic effects of examined cardiostimulative substances, an optimal concentration of extracellular calcium, as well as their unobstructed influx through the plasma membrane, are necessary.

239

PIEZOELECTRIC PROPERTIES OF HYDRATED FIBROUS PROTEINS P. Maeda, Research Institute for Polymers and Textiles, 1-1-4 Yatabe-Higashi, Tsukuba, Ibaraki Pref. 305, JAPAN

The purpose of the present study is to investigate the hydration and temperature dependence of the piezoelectric properties of fibrous proteins in the solid state, such as collagen, keratin and silk fibroin. We measured the piezoelectric constants of these fibrous proteins at $-150 \sim 150^\circ\text{C}$, relative humidity 0~75%, and 10 Hz. Some of the results are as follows: 1. The temperature dependence of the piezoelectric constant of dry collagen is similar to that of dry silk fibroin. With increasing temperature, they gradually increase up to 100°C and afterwards exhibit somewhat larger increase, while that of dry keratin exhibits no temperature dependence up to 100°C and afterwards decreases. 2. At low temperature with increasing hydration level, the piezoelectric constant of collagen increases below 8% moisture content and decreases above that content, while these behavior is quite different from that of keratin. 3. Above -50°C , the adsorbed water steeply reduces the piezoelectric constants of collagen and keratin. 4. Each of these proteins have hydration dependent piezoelectric loss peaks at around -100 and -50°C . We will report a possible molecular mechanism of the above mentioned piezoelectric behavior.

236

RESPONSE OF THE RIGHT VENTRICLE IN GUINEA-PIGS OF DIFFERENT AGE UNDER THE STIMULATION OF ALPHA AND BETA ADRENOCEPTORS, M.R. Pavlović, D.R. Matejević, J.M. Vojvodić and J.E. Nestorović, Institute of Physiology, Faculty of Medicine, Beograd, Yugoslavia.

The aim of our investigation was to represent the inotropic effect of isoprenaline and phenylephrine on the right ventricle of the heart. Experiments were carried out in vitro on adult and young guinea-pigs of three, six and nine weeks of age. The heart was removed immediately after sacrifice, the right ventricle was dissected and put in bovine electrode. Electrode was, then, placed in an oxygenated bath with Tyrode's solution. Stimulation was effected with square wave of 1 Hz frequency and intensity twice as high as that of the threshold. Contractions were transmitted via an isometric transducer (7003) into a microdynamometer (7050, Ugo Basile). After a stabilization period of 30 minutes, into the bath were added isoprenaline ($3.6 \times 10^{-7} \text{mol}$) and phenylephrine ($1 \times 10^{-6} \text{mol}$). Contractions were recorded continuously for the next 10 minutes. On the basis of our results we can conclude, that isoprenaline caused a significant positive inotropic effect both in the adult and young animals, while phenylephrine caused a slight negative inotropic effect.

238

IONIZING RADIATION EFFECTS ON PHOSPHATIDYLCHOLINE MULTILAYERS G. Erriu, M. Ladu, S. Onnis, J.H. Tang and W.K. Chang, Institute of Medical Physics, University of Cagliari, Via Della Pineta, Cagliari, Italy.

By differential scanning calorimetry (DSC) it was observed that γ -radiation induce modifications in phosphatidylcholine multilayers in presence of water excess. Actually, with the increase of the absorbed dose, the peak associated with the pretransition disappears gradually, while the peak associated with the main transition becomes wider and flatter. Fluorescence anisotropy and NMR studies, confirming the results of DSC, gave additional information on γ -radiation produced damage. The damage consists of the appearance of new molecular species and the consequent structural modification of the multilayers. The effects of high LET radiation like α particles seem quite different. Indeed, at room temperature the structural defects induced by α particles seem to be randomly distributed within the lipid matrix; while above the main transition there is some tendency to cluster. Moreover with the increase of the absorbed dose, the initial temperature of the main transition decreases while a tail towards higher temperature appears. Such broadening of lipid main transition seems to indicate the presence in the bilayers of other components different from what created by γ -radiation.

240

MOLECULAR MECHANISMS FOR THE ANTI-SICKLING ACTIVITY OF AROMATIC AMINO ACIDS AND RELATED COMPOUNDS: A PROTON NUCLEAR MAGNETIC RESONANCE INVESTIGATION. Irina M. Russu, Claudio Davvit, Allison K.-L. C. Lin, Chao-Ping Yang, and Chien Ho. Department of Biological Sciences, Carnegie-Mellon University, Pittsburgh, PA 15213, U.S.A.

Proton NMR spectroscopy has been used to investigate the interaction between sickle hemoglobin [Hb S ($\beta 6\text{Glu} \rightarrow \text{Val}$)] and several anti-sickling compounds such as p-bromobenzyl alcohol and aromatic amino acids. The binding of these compounds to Hb S and human normal adult hemoglobin (Hb A) was determined by measuring the transferred nuclear Overhauser effects (NOE) and the longitudinal relaxation rates (T_1) of their proton resonances in the Hb solutions. T_1 measurements for the C2 protons of individual surface histidyl residues of Hb and intermolecular truncated driven NOEs were used to determine the binding sites of the anti-sickling compounds to Hb S and Hb A. We have found that one binding site on Hb S for all compounds investigated is at or near the E6 mutation site. A second binding site was identified at or near the heme pockets of the α and δ chains and is present in both Hb S and Hb A. These NMR results will be discussed in terms of two molecular mechanisms for the anti-sickling activity: (i) the allosteric mechanism in which alterations in the local conformation(s) at the intermolecular contact site(s) occur as a result of binding of an anti-sickling compound to other regions on the Hb S molecule, and (ii) the competitive mechanism in which the binding of an anti-sickling compound blocks one or more of the intermolecular contact sites between the Hb S molecules in the polymer. [Supported by a research grant from the NIH (HL-24525)]

Tuesday 31 July Congress Centre-first floor. Posters 241-246

Posters under Category 29: General

241

A NEW METHOD FOR SELECTIVE SEPARATION OF FINE PARTICLES IN GRAVITATIONAL FIELD

I. Aoki and K. Shirane*. Department of Physiology and *Biophysics Laboratory, Osaka City University Medical School, Abeno-ku, Osaka, Japan.

New methods for selective separation of particulate materials in gravitational field, we have developed a rotating tilted open-column with steady flow (RSF) method by the improvement on that of a rotating tilted liquid column (RTC). Velocity of particles in the direction of the column axis (RSF velocity) depends on (1) each sedimentation velocity (V_0) at $t^\circ\text{C}$, (2) each pseudocircular locus specific to its property and (3) Poiseuille's flow. We have found that the power index (n') in RSF method is larger than that (n) in RTC one, if the column is rotated with an angular velocity ω within a suitable range of parameter $A\omega/V_0$ ($1.3 \leq A\omega/V_0 \leq 7$), where A is a radius of the column ($2 < n < n' \leq 4$). It is expected that the index n' takes the maximum value at $\theta = 0^\circ$ (θ is a tilted angle of the column to the horizontal) when ω is fixed. This method is of use for selective separation of fine particles about $10\mu\text{m}$ such as biological cells. We have separated some biological particles by this method.

243

CHIRAL DISCRIMINATION OF THE INERT METAL COMPLEXES $\text{Ru}(\text{bipy})_2^{2+}$ AND $\text{Fe}(\text{bipy})_2^{3+}$ UPON BINDING TO DNA.

T. Hård and B. Nordén, Dept. of Physical Chemistry, Chalmers Univ. of Technology, 421 96 Göteborg, Sweden.

The interactions between the metal complexes $\text{Ru}(\text{bipy})_2^{2+}$ and $\text{Fe}(\text{bipy})_2^{3+}$ and DNA have been studied by linear and circular dichroism. Two binding modes have been detected and characterized. The stronger binding gives rise to a Pfeiffer shift in the diastereomeric equilibria leading to an excess of one of the enantiomers which can be directly monitored through circular dichroism. In this way the method may be used for probing the helicity, i.e. discriminating between right- and left-handed nucleic acids. From flow linear dichroism of two charge transfer bands the orientation of the complexes was determined. The angle between the C_2 -axis of the complex and the DNA helix axis is 61° . For this orientation space-filling models show a good fit of the Δ -enantiomer in the major groove of the right-handed DNA helix. At higher binding densities another binding of lower order, probably due to a weak electrostatic association, occurs. Equilibrium analysis was carried out at 1 mM and 10 mM NaCl.

245

CIRCULAR DICHROISM FOR PROBING γ -ORIENTATION OF INTERCALATED DNA-ADDUCTS

R. Lyng¹, B. Nordén¹ and J.A. Schellman²; 1: Dept. of Physical Chem., Chalmers Univ. of Technology, S-412 96, Gothenburg, Sweden. 2: Dept. of Chem., Univ. of Oregon, Eugene, Oregon 97403, USA.

We have calculated the circular dichroism induced in an intercalated DNA-adduct chromophore by coupling with the $\pi-\pi^*$ transitions of surrounding basepairs.

The effect of lateral displacements as well as rotations in the basepair pocket has been studied.

The statistical monomeric CD-formula of Schipper, Nordén and Tjerneld is essentially confirmed, i.e. the circular dichroism is mainly determined by the γ -orientation of the chromophore.

242

THE EFFECT OF DNA SYNTHESIS INHIBITORS ON EXCISION REPAIR IN HUMAN CELLS. W. L. Carrier and J. D. Regan, Biology Division Oak Ridge National Laboratory, Oak Ridge, Tennessee 37831.

Chemical and physical agents damage DNA resulting in various deleterious effects leading to cell transformation and/or death. Studies of UV light damage to DNA has led to an understanding of the way in which damage is repaired. The steps leading to DNA repair are incision and excision of the altered base(s), DNA resynthesis and ligation. We have used agents that inhibit DNA replication to better understand the biochemical events leading to repair. Arabinofuranosyl cytosine is incorporated into repaired DNA preventing strand rejoining. The number of DNA single-strand breaks is indicative of excision repair. However, the breaks observed is related to the cell growth stage which may implicate endogenous DNA precursor pools. The ratio of dCMP to Ara-CMP incorporated into the repaired region may determine whether complete resynthesis and strand rejoining occurs. Hydroxyurea (HU) at concentrations greater than 10mM have a pronounced effect on the number of pyrimidine dimers excised over a 24 hr period and this inhibitor is more effective in quiescent cells than in log phase cells. HU is believed to act by limiting precursor pools for repair synthesis. The inhibitors are useful tools in the attempt to interfere with specific DNA repair steps and thus learn more about the mechanism of DNA excision repair.

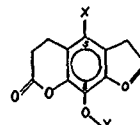
Research sponsored by the U.S. Department of Energy under contract DE-AC05-84OR21400 with the Martin Marietta Energy Systems, Inc.

244

FLOW DICHROISM STUDIES OF INTERACTIONS OF PSORALENAMES WITH DNA

B. Ygge¹, J.B. Hansen², P.E. Nielsen³, O. Buchardt² and B. Nordén¹; 1: Dept. of Physical Chem., Chalmers Univ. of Technology, S-412 96, Gothenburg, Sweden. 2: Chemical Laboratory I, the H.C. Ørsted Institute, Univ. of Copenhagen, Universitetsparken 5, DK-2100 Copenhagen Ø, Denmark. 3: Biochemical Institute B, the Panum Institute, Univ. of Copenhagen, Blegdamsvej 3, DK-2200 Copenhagen N, Denmark.

Five differently substituted aminopsoralenes have been studied utilizing flow linear dichroism and equilibrium analysis. Due to the positively charged amino groups all of these substances bind strongly to DNA. Their orientation as judged from linear dichroism shows that bulky substituents in 5 position (on the "hydrophobic" edge of the psoralene moiety) prevents intercalation. With the amino substituents in 8 position, the psoralene is oriented parallel to the plane of the DNA bases as expected for intercalation.



246

EFFECT OF CHAIN LENGTH ON THE PACKING CHARACTERISTICS OF LAMELLAR LIPID ASSEMBLIES: RAMAN SPECTROSCOPIC STUDY OF A SERIES OF n-ALKYLPHOSPHOCHOLINES.

William C. Harris,^{1,2} Gerard H. deHaas² and Ira W. Levin³; ¹National Institutes of Health, Bethesda, Md. 20205 and ²Rijksuniversiteit Utrecht, Utrecht, The Netherlands

The thermotropic behavior of a series of n-alkylphosphocholines fully hydrated multilamellar dispersions has been examined by vibrational Raman spectroscopy in both the C-H stretching ($2800-3100\text{ cm}^{-1}$) and the C-C stretching ($1000-1200\text{ cm}^{-1}$) mode regions, spectral intervals characteristic of acyl chain lateral interactions and intrachain disorder, respectively. These single chain systems, including both the even- and odd-numbered chains from C(10) to C(20), exhibited sharp lamellar to micellar transitions from -1° to 38°C . Additional polymorphic forms, whose transition temperatures were 3 to 12° below the more stable structures, were identified. Raman spectra provide clear and definitive spectral patterns enabling the subcell packing characteristics of each polymorph to be characterized. The sharp order/disorder transition observed for the lamellar to micellar change for the dispersions is interpreted in terms of high lipid cooperativity resulting from tight, lateral chain packing arrangements within the extended, interdigitated bilayers.

³On sabbatical leave from the National Science Foundation, Washington, D.C.

Tuesday 31 July Congress Centre-first floor. Posters 247-252

Posters under Category 29: General

247

DETOXIFICATION OF TITUSTOXIN (TtTX) BY IODINATION.
L.G.D. Heneine, V.N. Cardoso, J.P. Daniel and I.F. Heneine.
Dept. Physiology & Biophysics, Institute of Biological Sciences, Federal University of Minas Gerais, Belo Horizonte, MG, Brazil.

The purified toxin of *Tityus serrulatus* venom was iodinated with 1 to 4 atoms of ^{127}I per molecule by the IODO-GEN method. In some experiments an isotopic dilution with ^{125}I was done to follow incorporation. The iodinated toxin was recovered in Sephadex G-25 columns. Groups of 6 mice were injected intraperitoneally with crescent doses of the iodinated toxin. Controls with native and glycoluril treated TtTX were used. The LD_{50} is $3.4 \pm 0.6 \mu\text{g}$ per 20 g mice. The procedure did not affect the toxicity of non-iodinated TtTX. The mortality rate decreased with the number of I atoms incorporated, and in the four substituted toxin, TtTX- $^{127}\text{I}_4$, doses up to 50 μg per mice were applied weekly without lethal effects. The data indicates that iodination with more than 3 atoms per molecule detoxicates tityustoxin. Immunogenic properties are now being studied.

Supported by CNPq, Cpq-UFMG and FINEP.

249

ROTATION OF THE PROTEIN LIPOPHILIN WHEN INCORPORATED INTO MODEL MEMBRANES AS STUDIED BY ELECTRON SPIN RESONANCE.
A.I. Vistnes, Inst. of Physics, Univ. of Oslo, Oslo, Norway, J.M. Boggs, Hosp. for Sick Children, Toronto, Ontario, Canada.

Lipophilin, isolated from myelin membranes, was spin labeled and incorporated into phospholipid vesicles made from dipalmitoyl- and dimyristoyl-phosphatidyl-choline. The conventional electron spin resonance (ESR) spectrum was composite, indicating a slowly tumbling spin label and a small fraction more mobile spin labels. The presence of the two components in the spectra makes it difficult to use standard saturation transfer ESR to study the slow motion of the protein. A variety of the so-called magnetization-hysteresis ESR method (Biophys. J. 43(1983) 31) was developed to handle this situation. A new digital phase sensitive detector and new methods for data accumulation and processing were also introduced. The preliminary data indicates a very slow rotational motion of the protein (rotational correlation times in the 10^{-4} sec range). No abrupt changes in the rotation is observed when the temperature is varied through the pretransition and the main transition for the lipids. This seems to contrast lateral diffusion data for similar systems. No heavy aggregation of the protein is seen in freeze fraction electron micrographs.

251

LIPIDS WITH BRANCHED ACYL CHAINS - FUNCTION AND PACKING PROPERTIES IN BIOLOGICAL MEMBRANES

G. Lindblom¹, L. Rilfors¹, A. Wieslander² and I. Brentel¹, Dept. of Phys. Chem. and Dept. of Biochem., Univ. of Umeå, Sweden.
Several genera of bacteria have membrane lipids which contain mainly iso and anteiso methyl-branched acyl chains. In our study we have used: (1) *Bacillus regesterii*, whose lipids contain about 90 mol% branched acyl chains; (2) *Acholeplasma laidlawii*, which readily incorporates branched fatty acids (95 mol%) into its lipids. The influence of iso and anteiso acyl chains on the packing properties of membrane lipids was studied with phosphatidylethanolamine (PE) isolated from *E. regesterii* grown at different temperatures. The phase equilibria in PE-water mixtures were determined with ^{31}P NMR, ^1H NMR and polarized light microscopy. It was found that the molecular shape of the lipid is affected by the position of the methyl-branching point along the acyl chain. The difference in molecular shape, and hence in packing properties, between lipids containing iso and anteiso acyl chains, is most likely an important explanation to the temperature dependent lipid regulation mechanism observed in *E. regesterii*. The role played by the two branched fatty acids in biological membranes was further elucidated by investigating the way in which the polar head group composition in membrane lipids of *A. laidlawii* is affected by incorporation of these acids. It is concluded, that iso and anteiso acyl chains have distinctly different packing properties in a biological membrane, and that the two acids are able to fulfill the same role as straight-chain saturated and unsaturated acids, respectively, in lipid regulation mechanisms.

248

RAMAN AND RESONANCE RAMAN INVESTIGATION OF THE INTERACTION OF CYTOCHROME c WITH CARDIOLIPIN AND OTHER MODEL PHOSPHOLIPID BILAYER SYSTEMS.

J. S. Vincent and I. W. Levin, Laboratory of Chemical Physics, NIDDK, National Institutes of Health, Bethesda, MD 20205.

Cytochrome c and cardiolipin are two of the many components of the mitochondrial inner membrane which may be implicated in electron transfer reactions. In addition, cytochrome c and other agents (divalent metal cations) induce the hexagonal H_{II} phase in cardiolipin—a phase also found in lipid extracts from mitochondria. An attempt is made to characterize the interaction of cytochrome c with phospholipid systems and its induction of the H_{II} phase of cardiolipin bilayers by Raman and resonance Raman spectroscopy using both scanning monochromator, spectrographic and diode array detection techniques. Temperature profiles, using specific Raman spectral intensity ratios as indices, were determined for multilamellar DPPC dispersions interacting with ferricytochrome c at various lipid to protein ratios and pH values. At pH 4 depressions in T_m , the gel to liquid crystalline phase transition temperature, were dramatic ($>20^\circ\text{C}$), while at pH 7, the lowering of T_m was dependent upon the protein concentration. Characteristic Raman spectra of the H_{II} and lamellar bilayer phases were observed for cardiolipin complexes with cytochrome c and various metal cations.

250

SIALIC ACID SPIN LABELING OF SERUM LIPOPROTEINS
V. Nöthig-Laslo, G. Knipping and G. Jürgens
"Rudjer Bošković" Institute, Zagreb, Yugoslavia and Institute for Medical Biochemistry, University of Graz, Austria

We describe the method for selective spin labeling of sialic acid, the terminal carbohydrate moiety of serum low density lipoproteins, isolated from porcine and human plasma. Lipoproteins were oxidized with periodate under mild conditions selective for the sialic acid (L. van Leuten and G. Ashwell (1971) J. Biol. Chem. 246, 1889). The resulting aldehydes were condensed with 4-amino-2,6,6-tetramethylpiperidinooxyl followed by reduction with NaCNBH₃ (J. B. Feix and D. A. Butterfield (1980) FEBS Lett. 115, 183). The degree of labeling and the spectral lineshapes varied upon the reaction conditions. Specificity of labeling was proved by enzymatic reaction with neuraminidase. The conformational properties of the sialic acid spin labeled lipoproteins were studied with respect to various external perturbants of the lipoprotein structure.

252

MAGNETIC MEASUREMENTS, EDXRF ANALYSIS AND ELECTRON MICROSCOPY ON IRON RICH PARTICLES IN EUROPEAN EEL (*ANGUILLA ANGUILLA* L.)

M. Hanson¹, G. Wirmark², M. Ublad² and L. Strid²
¹Physics Dept. and ²Dept. of Biochemistry and Biophysics, Chalmers University of Technology, Gothenburg, Sweden.

We have investigated samples of tissue and organs of the European eel, looking for magnetic material. Magnetic susceptibility measurements showed that bone samples from the skull, the vertebral column and the pectoral girdle contain magnetic precipitates or particles as evidenced by a magnetization contribution that becomes saturated in a field of 4.4 kOe. In samples from the premaxilla the monomer block the magnetic material is localized to the periosteum and/or the meninx whereas the bone is purely diamagnetic¹. Energy dispersive X-ray fluorescence (EDXRF) analysis of the samples showed that the magnetic material is associated with iron. Tissue scraped from the ventral side of the skull roof and containing magnetic precipitates was chemically fractionated and further investigated by EDXRF and by high resolution electron microscopy. These analyses revealed that the main part of the iron is present in the form of iron rich particles. The particles, about 100-3000 Å large, have irregular shapes and are composed of two or more iron rich phases. The structures of magnetite (Fe_3O_4), hematite ($\alpha\text{-Fe}_2\text{O}_3$) and bcc iron were identified by electron diffraction².

1) M. Hanson, L. Karlsson and H. Westerberg, Comp. Biochem. Physiol. Vol. 77A, No. 2, pp. 221-224, 1984.

2) M. Hanson, G. Wirmark, M. Ublad and L. Strid, to be published in Comp. Biochem. Physiol.

Tuesday 31 July Congress Centre-first floor. Posters 253-258

Posters under Category 29: General

253

EPR STUDY OF Mn(II) BINDING TO HUMAN SERUM LOW DENSITY LIPOPROTEIN

Greta Pifat, J. Brnjac-Kraljević, Lj. Udovičić, J.N. Herak and G. Jürgens, Rudjer Bošković Institute, Bijenička c. 54, Zagreb, Yugoslavia

The mechanism of interaction between human low density lipoprotein (LDL) and certain cells within the arterial wall, could be enlightened by the characterisation of the surface of the LDL particles. The ESR technique is used to determine the capacity of LDL to bind divalent ions. The paramagnetic Mn(II) was found to be a suitable probe. Different isolation procedures of serum LDL are found to influence the LDL surface. In the preparation procedure with sodium tungstate, the LDL particles exhibit two types of binding sites. Preparation by ultracentrifuge resulted in LDL particles with only one type of Mn(II) binding sites. In the TRIS-HCl medium buffered at pH 7.4 with the ionic strength between 0.01 and 0.07 M/L the number of binding sites is about 60. Apparent binding constants strongly depend on the ionic strength of the buffer. The magnitudes of these constants are related with the use of a simple electrolyte theory. In the buffers of higher ionic strength (0.08-0.20 M/L), the Mn(II) binding parameters are different. The enhanced number (100) of binding sites could be the indication that the LDL surface structure is influenced by the ionic strength.

255

HAIR AND NAIL AS A BIOPSY MATERIAL PROGRESS AND PROSPECTS

T. Rindler, Physics Department, Faculty of Science Tanta University, Tanta, EGYPT

Instrumental neutron activation analysis has been performed on human hair and nail of the normal Egyptian student populations to define the base line levels of trace elements. The elemental abundances for 24 elements (Na, Cl, K, S, Ti, Cr, V, Mn, Fe, Co, Cu, Zn, As, Se, Br, Rb, Ag, Cd, Sb, I, La, Ce, Sm and Au) computed using a k_0 and relative procedures. The concentration of metallic elements in human hair and nail has been related to several demographic variables based on sex, diet, place of residence and pregnancy location.

257

TEMPERATURE DEPENDENCE OF THE FIBRINOGEN-FIBRIN AGGREGATION

C. Dietler, W. Känzig, Laboratorium für Festkörperphysik, ETH, CH-8093 Zürich / Switzerland

A. Hübnerli, P.W. Straub, Thrombose-Laboratorium, Medizinische Universitätsklinik, Inselspital, CH-3010 Bern/Switzerland

The aggregation process occurring in a solution of fibrinogen molecules after addition of the enzyme thrombin was studied as a function of time at different temperatures by means of static and dynamic light scattering and simultaneous determination of the released fibrinopeptide A (FPA). Light scattering gives information on the evolution of the mean molecular weight of the polymers. The FPA release gives the number of activated binding sites and thus represents the reaction coordinate determining the polymer distribution. Prior to the sol-gel transition the evolution of the polymer distribution in time is found to be independent of the temperature. The analysis of the experiments shows that there are two processes involved with opposite temperature dependence. On the one hand the rate of FPA release by the enzyme thrombin increases with increasing temperature showing that the enzymatic step is thermally activated. On the other hand the aggregation rate of the monomers decreases with increasing temperature showing that the polymerization is exothermic. The polymerization enthalpy could be extracted from the probability of bond formation as deduced from the light scattering data. Its value, -19 kcal/mole is in agreement with calorimetric data by other authors.

254

EMERGENT COLLECTIVE COMPUTATIONAL PROPERTIES IN NETWORKS OF GRADED RESPONSE NEURONS. D.W. Tank* and J.J. Hopfield*

*Department of Molecular Biophysics, AT&T Bell Laboratories, Murray Hill, NJ, USA and *California Institute of Technology, Pasadena, CA, USA.

In earlier work (J.J. Hopfield (1982) Proc. Natl. Acad. Sci. USA 79, 2554-2558) neurons were modeled as simple two-state McCulloch-Pitts threshold devices having outputs of 0 or 1. A highly interconnected network of these two-state neurons behaved as a content addressable memory (CAM). The state of the network at any time was represented by the set of neuron outputs. Stable system states were the "memories" of the CAM. Content addressable memory-recall followed relaxation of the network from an initial state which was a subpart of one of these memories. We have now performed computer simulations of networks of neurons having graded input-output relations. The goal was to make the communication and processing properties of the model neurons more "biological". The effects of discrete outputs (action potentials), membrane time constants, and sigmoidal dependence of output firing rate on membrane potential were included. Also, we have used parameters similar to those empirically determined from electrophysiological data. We find that these networks retain the capability of two-state neuronal networks to behave as a CAM. The results suggest that one collective computational task that real neuronal networks could perform is content addressable information storage with recall times of the order of tens of milliseconds.

256

ROLE OF LIPID CHAIN UNSATURATION IN MEMBRANES

J. T. Ho and N. R. Chen, Dept. of Physics, State Univ. of New York at Buffalo, Buffalo, New York, USA.

We have used laser Raman scattering to study the phase transitional properties of membranes made up of synthetic lipids containing unsaturated bonds in one or both acyl chains, as well as those which contain symmetric or asymmetric saturated chains. It was found that membranes with asymmetric saturated chains exhibit sharp phase transitions over a temperature range of less than 1°C, similar to those with symmetric saturated chains. Thus the asymmetry affects the degree of order in the chains, as was found in previous studies, but it does not affect the temperature width of the transition. On the other hand, lipids with asymmetric chains, of which one is saturated and the other one containing a -C=C- bond, exhibit a much broader phase transition over a temperature range of about 5°C. To test whether this effect is due to the asymmetry in the chains, we have also studied lipids with symmetric saturated chains, and found the same broad phase transition. Thus the occurrence of a double bond in one or both of the acyl chains of the phospholipid has a profound effect on the degree of cooperativity and phase transition of the membrane.

258

A ²H-NMR STUDY OF THE EXCHANGEABLE PROTONSITES OF GRAMICIDIN D AND S IN DPPC LIPOSOMES.

K.P. Datei, K. Pauls and M. Bloom, Dept. of Physics, Univ. of British Columbia, Vancouver, Canada.

*Dept. of Molecular Physics, Agricultural Univ., Wageningen, The Netherlands

Deuterium nuclear magnetic resonance experiments are presented of gramicidin D and S in dipalmitoylphosphatidyl choline multilamellar vesicles dispersed in ²H₂O. Invariance of the obtained ²H-NMR spectra, spin-spin (T_{2e}) and spin-lattice ($T_{1\rho}$) relaxation times of the deuterated amide bonds of gramicidin S in the liposomes indicate an interfacial location of the gramicidin S α -pleated sheet. This is in strong contrast with the dynamic structure of the amide bonds in the helical backbone of the bilayer spanning gramicidin D dimer channel, which changed at the onset of the broadened phase transition. Axial motions with a fixed axis of rotation that are fast on the ²H-NMR time scale (10^{-7} s) were experienced above the phase transition by the amide deuterons and caused the quadrupole splitting to split up in several quadrupole splittings. From the maximum quadrupole splitting (145 kHz) an angle of $\sim 10^\circ$ between the amide-nitrogen deuterium bond and the long axis of the gramicidin D channel was calculated. Spin-spin relaxation times of the deuterated amide bonds inside the gramicidin D channel showed a minimum, $T_{2e} = 50 \mu s$, at the onset of the phase transition (35°C). By the location of the T_{2e} minimum at the onset of the phase transition also preferential partitioning of the gramicidin D channel in the liquid-crystalline regions of a mixed phase bilayer was indicated.

Tuesday 31 July Congress Centre-first floor. Posters 259-264

Posters under Category 29: General

259

STRUCTURE OF BOVINE β -LACTOGLOBULIN AT 2.8 Å RESOLUTION
L. Sawyer*, M. Papiz*, A.C.T. North†, E.E. Eliopoulos† and
R. Cooper†, *Napier College, Edinburgh and †Astbury
Department of Biophysics, Leeds, UK.

Bovine β -lactoglobulin is a dimeric protein with a molecular weight of $2 \times 18,400$. In solution it undergoes a pH-dependent transition between two alternative structures. The structures of two different crystal forms, lattices Y and X crystallised on either side of the transition at pH 7.5 and pH 6.5 respectively, are currently under investigation. The lattice Y structure determined by multiple isomorphous replacement at 2.8 Å resolution reveals a mainly β -protein consisting of two twisted β -sheets with perpendicular directions, forming a deep cavity at the centre of the molecule. The lattice X structure determined by isomorphous replacement and molecular transformations is currently being examined in order to investigate the conformational differences between the two structures.

260

A DIGITAL PHASE SENSITIVE DETECTOR FOR USE IN ELECTRON
SPIN RESONANCE SPECTROSCOPY

A.I. Vistnes, D.I. Wormald, S. Isachsen, and D. Schmalbein
Inst. of Physics, Univ. of Oslo, Oslo, Norway

A digital phase sensitive detector (DPSD) has been developed to investigate slow molecular movements of proteins in biological membranes. A minicomputer connected to a modified Bruker ESR spectrometer controls the modulation and the data acquisition. The number of data acquisition per modulation period may be set to an integer number so that acquisition is carried out at the same points in every modulation period. The high phase accuracy allows compressing of the data before the Fourier transformation which then becomes very fast. The in-phase and phase-quadrature signals are recorded simultaneously and all errors due to drift are eliminated. The DPSD should be very well suited for non-linear ESR techniques such as saturation transfer ESR, magnetic saturation transfer ESR, and magnetization hysteresis ESR.

261

Calcium Buffering in Myxocella Giant Axons Investigated by Arsenazo III Injection Using Inhibitors of Calcium-Sequestering Processes. R.A. Slodin, Department of Biophysics, University of Maryland School of Medicine, Baltimore, Maryland, USA.

Previous work from this laboratory using ^{45}Ca and centrifuged isolated axoplasm samples has shown that calcium sequestration can be separated with inhibitors into two classes, one sensitive to the mitochondrial uncoupler FCCP and the other class sensitive to inhibitors of Ca^{2+} ATPase such as vanadate or quercetin. To determine the influence of these inhibitors on the kinetics of calcium sequestration in intact *Myxocella* giant axons, axons were microinjected with arsenazo III and mounted for monitoring the internal ionized calcium concentration by dual-wavelength absorption spectrophotometry. The axons injected with arsenazo III were subsequently internally dialyzed for introduction of calcium loads and inhibitors according to given dialysis-pulse schedules of 1 minute each. In control axons in the absence of inhibitors introduction of a standard calcium load by dialysis that increased the total calcium content by about 10% increased the value of $[\text{Ca}^{2+}]_i$ by about 30 nM initially followed by a return to the initial baseline within about 10 minutes. In the combined presence of FCCP, vanadate, and A23187, the same calcium load produced about the same initial rise in $[\text{Ca}^{2+}]_i$, but recovery was markedly slowed and incomplete. As the rise in $[\text{Ca}^{2+}]_i$ would have been about 1300-fold greater in the complete absence of buffering, the conclusion is that considerable residual buffering of Ca ions remains in axons with both mitochondria and SER vesicles poisoned.

262

STRUCTURE OF CAULOBACTER FLAGELLAR FILAMENT

Y. Shirakihara and S. Koyasu, Dept. of Physics and Dept. of Biophysics and Biochemistry, Faculty of Science, Univ. of Tokyo, Hongo, Tokyo, Japan.

The *Caulobacter* flagellins (flagellin A and flagellin B) are of half molecular weight of *Salmonella* flagellins. The *Caulobacter* flagellum comprises the two portions each of which is composed of either flagellin only (flagellin A: distal, flagellin B: proximal). (1) We examined the structures of two straight flagellin polymers (A-polymer and B-polymer) by image analysis to see the packing of those small flagellins. The two helical lattices (L and R) of *Salmonella* straight flagella were found in the A-polymer and B-polymer, respectively. In the proposed model of each polymer, the two conformationally different molecules appear alternately along n=1 helix and the whole molecules are placed on every intersection between n=1 helix and n=11 helix. (2) We examined the shape and the handedness of flagellar filament by EM and dark field OM and found that the helical filament of wild type *Caulobacter* is curly which has right-handed helical form. This means that *Caulobacter* swims by rotation of a flagellum in an opposite sense compared to *Salmonella* whose flagella have left-handed helical form. From these results of (1) and (2), we may conclude that flagellin B plays an important role in flagella formation because of its tendency to adopt the R-type conformation. This is supported by an observation of mutants defective in synthesis of flagellin B.

263

PHASE TRANSITIONS AND PHASE SEPARATIONS INDUCED BY CATIONIC POLYPEPTIDES IN DIPALMITOYLPHOSPHATIDYLGLYCEROL BILAYERS; A FLUORESCENCE POLARIZATION STUDY. D. Carrier*, J. Dufourcq, J.-F. Faucon and M. Pérolet*, Cntr. Rech. Paul Pascal, C.N.R.S., Talence, France and D p. Chimie, Univ. Laval, Qu bec, Canada.

The influence of lysine containing homo and copolypeptide on dipalmitoylphosphatidylglycerol (DPPG) thermotropic behavior has been studied by fluorescence polarization measurements with diphenylhexatriene as optical probe. The number of phases observed and their gel to liquid crystalline transition temperatures (T_c) proved to be the same for the lipid dispersion and for small unilamellar vesicles, although an excess of polypeptide appeared to modify the structure of these latter. Below equimolar ratio of lipid molecules to lysine residues, a single phase transition was detected (four degrees higher than for the pure lipid) and the fluid phase fluorescence polarization (P_f) was increased. Both T_c and P_f then remained constant with increasing peptide concentration. The value of T_c depended on the nature and molecular weight of the peptide, a larger shift being obtained for longer chains of polylysine. For molar ratios between ten and two lipid molecules per lysine residue, the number of phases differed according to the nature and length of the polypeptide: for example, three phases were observed with poly-D-Lys of M.W. 100 000, two with (L-Lys, L-Ala)_n and only one with a shorter poly-L-Lys (M.W. 4000). When several phases were present, the lowest T_c corresponded to that of the pure lipid. These data are compared with previous Raman spectroscopy results on a similar system.

264

FREE RADICALS IN QUINONE CONTAINING ANTITUMOR AGENTS: ELECTROCHEMICAL REDUCTION OF DIAZQUONE (NSC 182986) AND TWO ANALOGS. P.L. Gutierrez, B.M. Fox, M.M. Mossoba, and N.R. Bae*, University of Maryland Cancer Center, Division of Developmental Therapeutics, Baltimore, MD, U.S.A.

Diaziquone (AZQ) belongs to a family of antitumor agents characterized by the presence of quinone groups. In general, quinone containing antitumor agents can be reduced to their free radical anions by rat liver microsomes, rat liver nuclei, purified NADPH cytochrome C reductase, and Ehrlich ascites cells. We previously reported the activation of diaziquone and analogs RQ2 and R14 to free radicals by liver microsomes and NADPH-cytochrome C reductase. These two analogs contain chlorine atoms which substitute either the carboethoxyamino groups (RQ2) or the aziridine groups (RQ14) in the AZQ molecule. The free radicals observed for AZQ exhibited a 5 line ESR spectrum of broad unresolved lines. We investigated the diaziquone free radical formation and that of its two analogs using controlled potential electrolysis. This technique allows one to control the number of electrons involved in the reduction process as well as providing an environment free of metals, proteins and other chemicals. The lines which were unresolved in the ESR spectra of the enzymatically generated free radical became well resolved (11-line spectrum), facilitating the identification of the free radical. The addition of water to the aprotic solvents of the electrochemically generated free radical resulted in the 5 line spectra observed enzymatically. The data show that it is reasonable to study the basic structure of free radicals of quinone containing agents electrochemically and draw biologically relevant conclusions with regards to the drug activity and its free radical structure.

Tuesday 31 July Congress Centre-first floor. Posters 265-270

Posters under Category 29: General

265

Protein-Lipid Interactions at Membrane Surfaces
F. Sixl, P.J. Brophy and A. Watts
Department of Biochemistry, University of Oxford,
Oxford OX1 3QU.

Basic protein from bovine spinal cord was reconstituted into bilayers of dimyristoylphosphatidylglycerol (DMPG) and equimolar mixtures of DMPG with phosphatidylcholine (DMPC) at various protein concentrations. Both liquids were selectively deuterated at all positions of their polar head groups and their rates and amplitudes of motion characterized by ^2H - and ^{31}P -NMR. Basic protein did not perturb any part of the DMPG head group, whether in pure DMPG bilayers or in DMPG/DMPC mixtures. This was evident from the insensitivity of the ^2H NMR spectra of deuterated DMPC to the presence of protein. The interaction of basic protein with the acidic head group of the DMPG however gave rise to significant changes in the ^{31}P -quadrupole splittings, the ^{31}P -chemical shift anisotropic (CSA) and, to a smaller degree, the ^2H spin lattice relaxation times. An analysis of the data for DMPG/basic protein membranes gave the following results. Up to protein concentrations of 33 weight % the exchange of lipid molecules between the lipid-protein complex and the free lipid matrix is fast on the NMR timescale (exchange frequency $>10^5\text{ s}^{-1}$). The number of lipids interacting with basic protein in the domain was estimated to be between 15 and 28. The head groups of DMPG still have fast motion at the protein interface but are completely disordered, resulting in a common value of zero for CSA and $\Delta\chi$.

267

ECONOMIZATION IN ENERGY METABOLISM UNDER EXPANDING ADAPTIVE CAPACITY OF THE ORGANISM
M.N. Kondrashova, E.A. Kosenko and Y.G. Kaminsky
Inst. Biol. Physics, USSR Acad. Sci. Pushchino, USSR

The rabbits exposed to moderate hypoxic training were made, in some physiologic and morphologic aspects, like hares that characterized by greatly expanded adaptive capacity. Biochemical differences between hypoxia-exposed and unexposed animals were observed and expressed more after 24 hr fasting. The steady activation of energy metabolism in the adapted rabbits as seen with significant enhancement in gluconeogenesis in fasting caused increasing (rather than decreasing generally occurred) the hepatic glucose and glucose-6-phosphate levels. This activation was due to increased NAD^+/NADH ratio and poorly decreased ATP/ADP ratio in the fed rabbit liver. Such the redox and energization changes seem to determine the decrease in blood lymphocyte and liver mitochondrial succinate dehydrogenase activities that results in the lesser enhancement of mitochondrial oxygen consumption under fasting and in the accelerated formation of phosphoenolpyruvate. The reorganization described in energy metabolism explains the mechanism of "paradoxal" decrease in the requirement of trained human and animal species for oxygen and feed during the intensive muscular work (the economization phenomenon).

269

RELATION BETWEEN CALCIUM TRANSPORT BY SYNAPTOSOMES AND PYRUVATE DEHYDROGENASE ACTIVITY
R.G. Mansford and F. Castro, Gerontology Res. Ctr., NIA, NIH, Baltimore, MD U.S.A.

We have investigated the importance of Ca^{2+} transport across plasma and mitochondrial membranes in mediating the increase in the content of active pyruvate dehydrogenase (PDH) which occurs when synaptosomes are depolarized. PDH was 60 ± 3 (7), 67 ± 2 (7) and 80 ± 2 (9) % of total pyruvate dehydrogenase. In controls and in synaptosomes depolarized with 30 mM KCl and 30 μM veratridine, respectively. Measurements of intrasynaptosomal free Ca^{2+} ($[\text{Ca}^{2+}]_i$) using Quin 2 fluorescence gave values of approximately 60, 290 and 420 nM under these same conditions. Incubation with Ruthenium Red (RR), an inhibitor of mitochondrial Ca^{2+} transport, gave much lower resting values of PDH, i.e. 42 ± 2 (7) % of total, but did not prevent a small increase due to veratridine, i.e. 52 ± 1 (7) %. There was a large increase in $[\text{Ca}^{2+}]_i$ and in O_2 -uptake on adding veratridine in the presence of RR. Addition of an excess of EGTA immediately prior to veratridine only slightly diminished the response of PDH content to depolarization (76 ± 2 (8) %). Addition of ouabain also gave a diminished response (73 ± 2 (8) %). These results lend support to the idea that net transport of Ca^{2+} into the mitochondria, a consequence of a rise in $[\text{Ca}^{2+}]_i$, is important in the response of PDH content to depolarization. However, other effectors of PDH interconversion, e.g. NADH/NAD^+ and ATP/ADP ratios, are also implicated. Entry of Ca^{2+} across the plasma membrane appears not to be necessary.

266

^1H AND ^{13}C NMR STUDY OF PHOSPHOLIPID INTERACTION WITH ERGOLENE DERIVATIVES

J. Kidrič, M. Grad, S. Zagorac, and D. Hadži
Boris Kidrič Institute of Chemistry, Ljubljana, Yugoslavia

The interaction of phosphatidylcholine (PC) micelles and vesicles with ergolene derivatives (ED) methylidihydroisergate and both ergosine epimers was investigated by ^1H and ^{13}C NMR spectroscopy. Paramagnetic ions were used to label the vesicle outer layer. Considering the ^1H and ^{13}C chemical shifts of PC and ED resonances and the disappearance of the shift differences between the ^1H and ^{13}C signals of the outer and inner $-\text{N}^+(\text{Me})_3$ groups of PC after addition of ED it is concluded that ED penetrate the membrane bilayer and interact with both the inner and outer polar heads of PC. A model for the interaction between ED and PC bilayer is proposed. It is based on non specific electrostatic and hydrogen bonding forces.

268

THE STRUCTURE, PHASE SEPARATION AND INTERACTIVE FORCES OF OXIDIZED CHOLESTEROL-DIPALMITOYLPHOSPHATIDYLCHOLINE MIXTURES.
M. Pantazopoulou and L.J. Lis, Kent State University, Kent, Ohio 44242.

Oxidized sterol compounds replace some fraction of the cholesterol content in cell membranes in a number of disease states including neoplasia and atherosclerosis. We have mixed 7-keto cholesterol with dipalmitoylphosphatidylcholine (DPPC) to form multi-bilayer arrays, which are then studied using x-ray diffraction. Preliminary results show that there are two independent bilayer phases at all water contents for 9:1 mixture of DPPC and 7-keto cholesterol, and only one phase at higher water contents for 1:1 mixtures. The former mixture produces one phase with a repeat spacing of 65Å, and another with a spacing of ca. 80Å. These results indicate that 7-keto cholesterol interacts with DPPC bilayers in a manner similar to cholesterol rather than cholesterol esters. The net repulsive force between bilayers was measured as a function of separation using the osmotic pressure technique (LeNeveu et al (1976) Nature 253: 601-603). A comparison of the force decay with bilayer separation will be made between DPPC bilayers, and DPPC bilayers with cholesterol or 7-keto cholesterol.

270

Study of Sympathomimetic drugs and allied compound

By REKHA R. PAITANAYEK, J.K. DATTA GUPTA & N.N. SAHA
J & M. B. Division, Saha Institute of Nuclear Physics, Sector-1, Block-'AF', Bidhan Nagar, Calcutta-700 064, India.

Five compounds in the form of hydrochlorides, para hydroxy epedrine (OHEPH), DL-N $^{\alpha}$ -ethylnorphenylephrine (ENPE), DL-metanephrine (MNP), DL-normetanephrine (NMNP) and 3,4, Dimethoxyprenethyamine (DMPEA), have been studied, the first two compound being sympathomimetic drugs and the remaining three are sympathomimetic derivatives having no direct drug action. In first compound (OHEPH) is the substituent group at the para position of the benzene ring of epedrine and in the second compound the $(\text{C}_2\text{H}_5)_2$ group is substituted at the N-terminal position of ethylamine side chain. In other two compounds, MNP and NMNP, the $(\text{OCH}_3)_2$ is the substituent group in the meta position of benzene ring of epinephrine and norepinephrine respectively and in DMPEA, two OCH_3 groups are substituted in the para- and meta- position of benzene ring. In first two compounds, in spite of substitution the conformation remains more or less same as that of the sympathomimetic amines. In MNP and DMPEA, the side chain in each case unlike the former two, is folded and have no direct drug action. Whereas, in NMNP, the conformation of the molecule is like that of sympathomimetic drug but it has also no direct drug action.

Tuesday 31 July Congress Centre-first floor. Posters 271-276

Posters under Category 29: General

271

INFLUENCE OF ACYLCARNITINES ON PHOSPHATIDYLCHOLINE BILAYERS.
F. Van Cauwelaert, I. Maessens, W. Herremans, Interdisciplinary Research Center, K.U.Leuven Campus Kortrijk, Kortrijk, Belgium.

Some experiments suggest that accumulation of long-chain acylcarnitines in the cellular and subcellular membranes of myocardial cells may alter cardiac function. Therefore we studied the interaction between small unilamellar vesicles (SUV) of DMPC and DPPC at 37°C, 23°C and pH 6.8 with different amounts of acylcarnitines (from Hexanoyl- to palmitoylcarnitine) with steady-state fluorescence anisotropy of DPH inserted in the bilayer and light scattering at 400 nm. The permeability for Ca^{2+} -ions was also followed during the interaction.

It is observed that addition of acylcarnitines to SUV of DMPC or DPPC decreases the width of the gel to liquid crystalline phase transition in the bilayer. This effect is not observed when the added carnitine has an acyl chain length which is 2-carbon-segments shorter than the acyl chain length of the phospholipid in the bilayer. Incubation of SUV of DMPC with PCa, MCa and LCa at 37°C and 30°C did not change the light scattering. However at 23°C the SUV show a drastic increase in light scattering, starting at a DMPC acylcarnitine molar ratio of 108 with a maximum at a ratio of 20. These results suggest that the SUV are destabilized by the acylcarnitine into large structures. This was confirmed by electron microscopy. By permeability experiments with carboxyfluorescein or a Ca^{2+} -Arsenazo mixture, and also by NMR-experiments with Pr^{3+} , we did find an increase in permeability of the bilayer during the reorganization of SUV in larger structure.

273

Ca^{2+} INDUCED PHASE SEPARATIONS IN PHOSPHOLIPID MIXTURES
W. Tamura-Lis, M. Pantazopoulou, and L.J. Lis. Department of Physics, Kent State University, Kent, Ohio 44242, U.S.A.

Ca^{2+} solutions of low molarity (7 to 100 mM) have been shown by x-ray diffraction to produce phase separations in egg yolk phosphatidylcholine (EYPC) multibilayer arrays (Biochemistry (1981) 20: 1771-1777). One phase was clearly swollen with a very large bilayer separation characteristic of charged lipid systems, while the second phase swelled to the same limited extent as EYPC in pure water. We have extended this study to mixtures of homogeneous chain phosphatidylcholines (DOPC:DLPC, DMPC:DLPC, and DOPC:DMPC), egg yolk phosphatidylethanolamine mixtures of phosphatidylcholine and phosphatidylethanolamine (DOPC:DOPE), and a mixed chain phosphatidylcholine (palmitoyloleoyl PC). This data indicates that phase separations in these systems only occur in mixtures of phospholipids with dissimilar acyl chains or head group. Preliminary data from our study on mixed chain phosphatidylcholines indicate that the phase observed in EYPC with limited swelling may be due to the lipid population with mixed chains.

275

272

BIOPHYSICS OF FAST EXTENSION OF THE UPPER LIMB. M.J. Naeimi and S.A.E. Hoseini, University of Technology P.O.Box 3406 Tehran, Iran

Fast extensions of the partially stretched upper limb in a vertical plane under four load conditions (0,1,2,3 kg in hand) and various movement ranges (90° to 150°) were registered by a high speed movie camera (50 and 100 frames per second) and also by stroboscopic sampling (50 pps) on still pictures with simultaneous recording of EMG from biceps brachii and triceps brachii muscles. Movement involves elbow and shoulder joints with possible excess extension up to 45°. Displacement, speed, and acceleration of ten points from thumb (P1) to shoulder (P10) were obtained and plotted vs. time. Trajectories near P1 are smooth curves with acceleration and deceleration periods. On getting close to P10, trajectories decompose in to three phases resembling an inverted Z with distortion (). The geometrical and kinematical characteristics of three phases and their transition to the smooth trajectories near P1 depend on load, speed, and movement range. The EMG recording shows stronger correlation with these phases than with the acceleration and deceleration periods of P1. The forearm may be modeled as a system with a pair of dominant poles and two correlated inputs, i.e., elbow joint displacement and muscles' force. Patterns of input observed in these experiments is shown to eliminate overshoot and oscillatory behaviour of the system and produce a step-like output.

274

276

Wednesday 01 August

Symposia

09.30 - 12.30

Folding, Dynamics and Solvation of Macromolecules
(Part 1)

Image Reconstruction

Dissipative Structures and Pattern Formation in
Biological Systems

Affinity Group Meeting on Structure of Food
Biopolymers

Afternoon at Leisure

Apart from

13.30 - 19.00

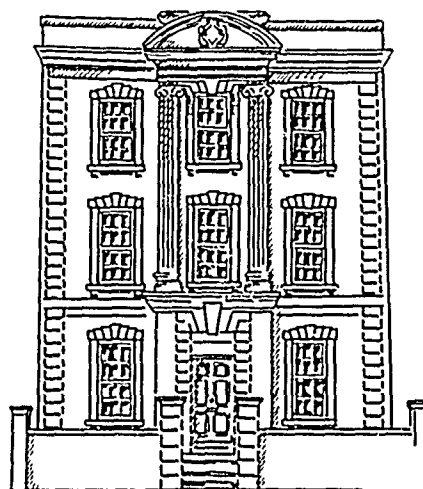
I.U.P.A.B. General Assembly

No Poster Sessions

Social Programme

Afternoon and evening activities include:

SS Great Britain
Bath
Bath and Theatre Royal in Bath - "HMS Pinafore"
Wells, Glastonbury and Sheppy's Cider Farm
Big Pit and Cardiff Castle Banquet
Royal Shakespeare Theatre - "Richard III"
Theatre Royal in Bath - "HMS Pinafore"
Chequer's Inn Cruise
Harvey's Wine Museum



Wednesday 01 August

Colston Hall Main Hall	Council House Conference Hall	Unicorn Hotel Trident Suite
09.30		
Folding, Dynamics and Solvation of Macromolecules Part (1) Co-Chairmen: M. Karplus (Harvard) D.C. Phillips (Oxford) Speakers: C. Chothia (London) T.E. Creighton (Cambridge) K. Wuthrich (Zurich) and Authors of Posters E. Duee (112) L.C. Helleman (056)	Image Reconstruction Chairman: R. Henderson (Cambridge) Speakers: J. Frank (Albany) R.A. Crowther (Cambridge) J.L. Carrascosa (Madrid) and Authors of Posters T. Wakabayashi (229) E.-M. Mandelkow (221)	Dissipative Structures and Pattern Formation in Biological Systems Chairman: G. Ivanitsky (Moscow) Speakers: E.E. Selkov (Puschino) A. Gierer (Tubingen) D. Walgraef (Brussels) and Authors of Posters Th. Plesser (233) J.-H. Xu (240)
12.30 Morning Coffee 10.50-11.10	Morning Coffee 10.50-11.10	Morning Coffee 10.50-11.10

13.30

AFTERNOON

AT

LEISURE

19.00

Timetable

Watershed
Cinema 1

Congress Centre
First Floor

09.30

Affinity Group Meeting on Structure of Food Biopolymers

Chairman: A.J. Bailey (MRI, Bristol)

Speakers: P.P. Purslow (MRI, Bristol)

A.G. Naylor (Unilever,
Colworth)

G.G. Jewell (Cadbury
Schweppes, Reading)

P.J. Frazier (Dalgety,
Cambridge)

A.M. Hermansson
(Goteborg)

Morning Coffee

10.50-11.10

12.30

**NO
POSTER
SESSIONS
TODAY**

13.30

**I.U.P.A.B.
GENERAL
ASSEMBLY**

19.00

STRUCTURE AND CONFORMATIONAL CHANGE IN PROTEINS

Cyrus Chothia

Christopher Ingold Laboratories, Department of Chemistry, University of London, London and Medical Research Council, Laboratory of Molecular Biology, Cambridge

The general principles governing the three-dimensional structure of globular proteins that have been discovered over the past few years include:

1) The interior of proteins are close packed. The shape of the surfaces of α -helices and β -sheets is determined to a first approximation by main chain conformation. As a consequence, α -helices and β -sheets usually pack in one of a small number of relative orientations.

2) The links between secondary structures tend to be short, have a topology that is right-handed and do not form knots.

3) A consequence of 1) and 2) is that protein chains often fold to give secondary structures arranged in one of a few common patterns. Thus there are families or classes of proteins that have a similar tertiary structure but no evolutionary or functional relationship.

4) The stability of protein structures arises from the reduction in the surface accessible to solvent that occurs on folding and upon intramolecular contacts. The total surface buried within proteins and the number of intramolecular hydrogen bonds is a function of molecular weight.

The understanding of the principles that govern protein structure facilitates an understanding of the way in which the structure may be changed. Many important properties of proteins, particularly those concerned with the regulation of activity, depend upon the transmission of conformational changes between widely separated sites. The approach that revealed the principles governing the structure of proteins - the computational and graphical analysis of protein atomic coordinates - is also revealing how proteins can change their structure. The analysis of different forms of insulin has given information on the relative movements of packed α -helices. The main chain of the helices moves as rigid bodies except for occasional bending (kinking) and small conformational changes in residues at the termini. The shift of one helix relative to another against which it is packed is accommodated by small conformational changes in the side chains which form their interface. Such conformational adjustments limit relative helix sheets to no more than approximately 1.5 Å. Such helix movements are of central importance in the allosteric mechanism of haemoglobin and domain closure in enzymes.

Symposium on Folding, Dynamics and Solvation of Macromolecules (Part 1)

PATHWAYS AND MECHANISMS OF PROTEIN FOLDING DETERMINED EXPERIMENTALLY
T.E. Creighton, MRC Laboratory of Molecular Biology, Hills Road, Cambridge,
England.

The number of conformations accessible to a polypeptide chain is so great, and current understanding of the physical interactions responsible for folded conformations so poor, that it is currently impossible to rationalize or to predict the mechanism, pathway, or end-product of protein folding. Experimental elucidation of the folding process is hampered by the cooperativity of the transition; the partially-folded intermediate states that define the folding pathway are usually unstable. Such unstable intermediates can accumulate transiently, but the kinetics of folding are complicated by slowly interconverted forms of the unfolded protein, resulting from slow cis-trans isomerization of peptide bonds preceding Pro residues. Nevertheless, that compact, partially folded intermediates have been frequently observed in refolding, but not in unfolding, suggests that the rate-limiting transition state in both unfolding and refolding is a high-energy distorted form of the final folded conformation. This contrasts with suggested mechanisms involving a nucleation event in the unfolded polypeptide chain, with subsequent rapid folding.

At the present time, folding pathways can be elucidated only by trapping intermediates in a stable form, using the readily controlled disulphide interaction between Cys residues. The pathway determined in this way for the small trypsin inhibitor, BPTI, showed folding to start randomly in the unfolded, reduced protein, but to converge through a relatively small number of disulphide intermediates. The disulphide coupled transition is like other folding transitions; it is cooperative, with all the intermediates transient and unstable (unless trapped), and has a rate-limiting step that is a high-energy distorted form of the native conformation. The nature of the rate-limiting step was surprising, as it involves intramolecular rearrangement of disulphide bonds between Cys residues widely separated in the folded conformation; consequently, folding does not occur by the sequential formation of the three final disulphides. Why this complex transition is the energetically most favourable pathway into and out of the folded conformation is still not known, but it probably reflects the high stability of the BPTI conformation and the high energy required to distort it. Homologues of BPTI from black mamba venom, with the same backbone conformation but lower stabilities, have the direct, sequential pathway as the most favourable.

Conformational forces that guide the disulphide pathway are being investigated by the effects on folding of altering the folding conditions and the covalent structure of the protein, and by determination of the conformational properties of the trapped intermediates.

The kinetics and thermodynamics of disulphide formation provide unique information about the free energies of the various steps in folding. Since interactions within a folded protein are intramolecular, they are most readily compared to intermolecular interactions (like those between an unfolded protein and the solvent) by the effective concentration of the two groups when intramolecular. The stabilities of the disulphides in BPTI increase enormously during folding, from effective concentrations of about 10^{-2} M in reduced BPTI up to 10^5 M in the folded conformation. This results from the entropic effect of the protein conformation bringing the Cys residues into proximity. In turn, those disulphides with the greatest stability provide the greatest stabilization to the folded conformation. These considerations are not unique to the disulphide interaction, and the concept of effective concentrations is useful in rationalizing protein conformational stability. The high effective concentrations observed in folded proteins imply that net stability is provided by intramolecular hydrogen bonds, salt-bridges, and van der Waals interactions, in addition to the hydrophobic effect. This probably explains why proteins decrease in stability with increasing temperature, whereas the hydrophobic effect alone would give the opposite tendency.

Symposium on Folding, Dynamics and Solvation of Macromolecules (Part 1)

NUCLEAR MAGNETIC RESONANCE AND DYNAMICS OF SPATIAL PROTEIN STRUCTURES

K. Wüthrich, Institut für Molekularbiologie und Biophysik, Eidgenössische Technische Hochschule-Hönggerberg, Zürich, Switzerland.

Protein conformations are the result of a multitude of weak, non-bonding interactions between different atoms of the polypeptide chain and between the polypeptide and the surrounding medium. The latter may, for example, be an aqueous solvent, ordered lipids in biological membranes, or the crystal lattice in the single crystals used for X-ray studies. With the thermal energy at ambient temperatures these non-bonding interactions may frequently be opened and reformed. In contrast to typical "inorganic" solids, where the individual atoms are covalently linked to neighbouring atoms in all directions, it is even possible that groups of weak interactions may simultaneously be severed and reformed, thus enabling larger scale thermal motions in proteins. The occurrence of "breathing motions" was discussed even before protein spatial structures could be determined by crystallographic methods.

In recent years interest in protein motility was revived after several different methods proved capable of providing characterizations of dynamic aspects of proteins at atomic resolution. One of these techniques is nuclear magnetic resonance (NMR). Two different NMR approaches capable of leading to information on dynamic aspects of proteins will be discussed. The first approach consists of studies of intramolecular rate processes in proteins at thermodynamic equilibrium. This includes quantitative measurements of ring flip frequencies, amide proton exchange rates and spin relaxation parameters. Once individual resonance assignments have been obtained, a map of the motility along the amino acid sequence can be derived, which in turn provides a map of motility across the three-dimensional structure. This will be illustrated with investigations of chemically modified analogs of the basic pancreatic trypsin inhibitor and of bull seminal inhibitor IIA.

The second approach to be discussed relates to another consequence of the intrinsic flexibility of proteins, i.e. that the conformation can readily adapt to different environments. Different environments corresponding to different equilibrium conformations can, for example, be provided by binding of substrates or effectors to a protein, so that during a reaction cycle the macromolecular structure may be constantly in the process of rearrangement towards a new equilibrium conformation. Among the growing number of protein crystal structures there are examples of different conformations for different functional states of the same protein, which are related by movements of individual functional groups of atoms or by movements of entire domains. It appears of considerable interest that such studies can be extended to non-crystalline proteins with the use of NMR.

The information content of the NMR spectra both for investigations of internal motions in proteins and for structure determination depends largely on the availability of sequence specific resonance assignments. A brief survey of the procedures used for assigning the ^1H NMR spectra of proteins with two-dimensional correlated spectroscopy (COSY) and two-dimensional nuclear Overhauser enhancement spectroscopy (NOESY) will be presented. Our strategy for NMR determination of the spatial structure of non-crystalline proteins relies further primarily on measurements, with the use of NOESY spectra, of intramolecular distance constraints between specified hydrogen atoms along the polypeptide chain. For the structural analysis of these data a distance geometry algorithm is used. As an illustration of the potentialities of this approach for studies of the conformations of a specified polypeptide chain in different non-crystalline environments, the spatial structures of the polypeptide hormone glucagon in aqueous solution and bound in the lipid-water interphase near the surface of a lipid micelle will be compared with the conformation observed in single crystals.

Wednesday 01 August Council House-Conference Hall 09.30-12.30

Symposium on Image Reconstruction

QUANTITATIVE STUDY OF MACROMOLECULAR ASSEMBLIES WITH THE AID OF CORRELATION ALIGNMENT, MULTIVARIATE IMAGE ANALYSIS, AND THREE- DIMENSIONAL RECONSTRUCTION.

J. Frank, Center for Laboratories and Research, New York State Department of Health, Albany, New York, USA.

The three-dimensional (3-D) reconstruction of the 30S ribosomal subunit of *E.coli* from hundreds of views /1-3/ and the unravelling of the architecture of the *Limulus polyphemus* hemocyanin molecule /4-6/ are examples for the combined use of new techniques of image analysis in molecular structure research. While the analysis of crystals imaged in the electron microscope /7,8/ can be based on the assumptions that a molecule (or group of molecules) occurs with identical structure and identical relative spatial arrangement on precisely defined positions of a regular lattice, the analysis of single molecules is complicated by variations in structure, and by the fact that their orientations and positions on the specimen grid are unknown. Correlation functions are used to bring the molecule views into precise superposition /9,10/ for averaging.

Due to different surface topologies and binding characteristics of macromolecular assemblies, two different data collection situations may exist: In the electron microscope, we may observe either a set of more or less defined views (such as the cross, top, bowtie, ring, and pentagonal views of the 48-meric *Limulus* hemocyanin molecule /6/), or a continuum of views (as in the case of the 30S subunit of the *E.coli* ribosome /1-3/). Both the variability of observed structure and the variability of the viewing direction (either due to small movements of the particle around an essentially stable orientation, or to its unimpeded rotation) make it necessary to group the images according to their similarities. Averaging of molecule images is a meaningful procedure only if extended over a subset that relates to the same orientation of the molecule within a narrow range. Correspondence analysis has been found very useful in achieving the grouping of molecule views without the aid of any a priori information /4,5,11,12/.

Molecules occurring randomly oriented in a continuous range of views may be sorted to form an ordered "tilt series" /13/. This interesting possibility has been recently exploited in the 3-D reconstruction of the 30S ribosomal subunit /1-3/. Molecules occurring in a few distinct views such as the various dissociation products of the *Limulus polyphemus* hemocyanin may reveal 3-D information indirectly through their rocking behavior /4-6/. Additional information (in this case, the shape of the subunit from x-ray work) is however required to obtain an unambiguous model of the structure. Theoretically, a single high-angle tilt of a specimen grid containing molecules in random (in-plane) orientations exhibiting the same view provides sufficient information for 3-D reconstruction /14/. Work along these lines is continuing in our laboratory. (This work was supported by NIH grant 1R01 GM29169)

- /1/ A. Verschoor et al., Proc. 41st Ann. Meetg. EMSA, p. 758.
- /2/ M. van Heel, Proc. 41st Proc. Ann. Meetg. EMSA, p. 460.
- /3/ A. Verschoor et al., submitted.
- /4/ M. van Heel and J. Frank, Ultramicroscopy 6 (1981) 187.
- /5/ M.M.C. Bijlholt et al., J.Mol.Biol. 161 (1982) 147.
- /6/ J. Lamy et al., Biochemistry 21 (1982) 6825.
- /7/ H.P. Erickson and A. Klug, Phil. Trans. Roy. Soc. Lond. 261 (1971) 105.
- /8/ P.N.T. Unwin and R. Henderson, J. Mol. Biol. 94 (1975) 425.
- /9/ J. Frank et al., Ultramicroscopy 3 (1978) 28; Science 214 (1981) 1353.
- /10/ J. Frank, in: Computer Processing of Electron Microscope Images, Ed. P.W. Hawkes (Springer, Berlin 1980) pp. 187-222.
- /11/ J. Frank et al., J. Mol. Biol. 161 (1982) 107.
- /12/ J. Frank and M. van Heel, J. Mol. Biol. 161 (1982) 134.
- /13/ J. Frank and M. van Heel, Proc. 10th Intl. Congr. El. Microsc., Hamburg 1982, Vol I, p.107.; M. van Heel, Proc. 41st Ann. Meetg. EMSA, p. 762.
- /14/ J. Frank and W. Goldfarb, in: Electron Microscopy at Molecular Dimensions Ed. W. Baumeister and W. Vogel (Springer, Berlin 1980), pp. 261-269.

Wednesday 01 August Council House-Conference Hall 09.30-12.30

Symposium on Image Reconstruction

THREE DIMENSIONAL RECONSTRUCTION OF SECTIONED MATERIAL

R.A. Crowther, Medical Research Council Laboratory of Molecular Biology,
Hills Road, Cambridge, U.K.

Reconstruction from serial sections is a well-established technique for analysis of cellular structure. The depth discrimination achieved is limited by the thickness of each section. In order to improve the resolution and retrieve three dimensional information about structures lying within the thickness of a given section, more powerful methods of reconstruction are needed. In general three dimensional reconstruction of the internal details of specimen structure within a plastic section requires that the section be tilted in the electron microscope and that the many different views so obtained be combined by one of the standard methods to produce a three dimensional map. Such an analysis is made difficult by the dimensional instability of plastic sections, which shrink severely in thickness on electron irradiation.

One way of overcoming the difficulty is to use colloidal gold particles as markers of the two section surfaces. Analysis of the changes in position of the gold particles in images of the tilted section by a least squares fitting procedure, permits estimation of the alteration in section thickness as a function of electron dose. If it is assumed that the section collapse occurs normal to the plane of the section, it is possible to correct for the change in thickness in the reconstruction procedure. The effect of the collapse is that the tilt angle given by the goniometer reading on the microscope over-estimates the effective tilt angle of the collapsed section relative to the uncollapsed one. Spatial frequencies in the image of the tilted collapsed section are also scaled geometrically by an amount depending on the angle of view and the degree of collapse.

An alternative approach for periodic specimens is to use a single untilted view of an oblique section, in which the various parts of the unit cell contents are displayed in a superimposed form at different points of the image. If the thickness of the oblique section were small compared with the size of details in the specimen, the unit cell contents would be serially displayed and an adequate reconstruction could be made by simply restacking successive areas of the image. In practice the section thickness is much greater than the size of features one would like to resolve and simple restacking is not sufficient. A given element of density within the unit cell will contribute to a set of image points, at each of which its density will be added to those of a varying set of neighbouring points that are contained within the section. The situation can be described mathematically by a set of linear projection equations or alternatively considered as a convolution operation in which the density within the unit cell is smeared by projection through the section thickness. Solution of the projection equations or equivalently deconvolution of the smeared densities should give a three dimensional image superior to that produced by simple restacking. The degree of improvement achievable depends on the noise level in the image but computational experiments indicate that a factor of at least four should be attainable. Since it uses a single untilted image, the method is not directly affected by the section collapse.

Symposium on Image Reconstruction

STRUCTURE OF BACTERIOPHAGE CONNECTORS.

J.L. Carrascosa. Centro de Biología Molecular (CSIC-UAM). Universidad Autónoma de Madrid. Canto Blanco. Madrid. Spain.

The head to tail connecting region of complex bacteriophages plays an important role in phage assembly and DNA encapsidation. These two processes seem to be related to one structure called "connector" that is built by several copies of one polypeptide. In recent years, there has been an accumulation of genetic, biochemical and structural information on the connector-related regions of bacteriophages T4, lambda and ϕ 29, showing striking similarities among them that suggest a close relationship structure-function on these structures.

We have studied the head to tail connecting region of bacteriophage ϕ 29. This is a small but complex *B. subtilis* phage and the viral particle is built up by only six structural proteins. The neck region of this phage was purified from assembled virions by chemical treatments. These necks were composed by two proteins (p10 and p11). Electron microscopy of these specimens revealed a circular structure (14 nm in diameter), with a hole in the center. The production of hexagonal two-dimensional arrays of ϕ 29 necks allowed to process their electron micrographs by Fourier filtering. The filtered necks were further enhanced by rotational analysis, leading to a final image that revealed an external region made by 12 morphological units, and an inner region (with 6-fold symmetry) with a hole in its center (1). These morphological features were confirmed by the analysis of a different two dimensional aggregate (tetragonal) of ϕ 29 necks (Carazo, García, Santisteban and Carrascosa, submitted for publication). At this level of resolution, the connector-related structures studied so far (besides phage ϕ 29) as the one of phage T4 (2) and phage lambda (3), present basically identical morphology. The mapping of the two structural proteins (p10 and p11) in the ϕ 29 neck was performed by two methods: a) Mild protease treatment, led to the removal of a fragment of p10, leaving p11 intact. After crystallization of each type of neck, the Fourier filtered images from the control and protease-treated necks were compared, and the difference was located at the 12-folded external region (4). b) The protein p10 was purified from *E. coli* harbouring a plasmid that contained the gene coding for this protein. Purified p10 was assembled in oligomers that looked in the electron microscope similar to the upper neck of ϕ 29. More detailed information was obtained after two-dimensional crystallization of these p10 oligomers and Fourier and rotational filtering of their electron micrographs. Purified p10 was shown to be assembled in a circular structure with 12 external morphological units, identical to the ones observed in ϕ 29 extracted necks (Carrascosa, Carazo, Ibañez and Santisteban, submitted for publication).

A more detailed view of the head to tail connecting region of this phage was obtained by three-dimensional reconstruction of ϕ 29 necks. Hexagonal two-dimensional arrays were tilted in the electron microscope and the different projections were combined using Fourier methods to obtain a three-dimensional structure to 2.2 nm resolution (Carazo, Santisteban and Carrascosa, submitted for publication). The 12 morphological units that build the external area were paired towards the center, leading to a clear rotation of the subunits. There was a conical hole inside, that was almost closed near the interaction place between p10 and p11. The inner 6-folded region is the one that must interact with DNA during the process of encapsidation (and injection). Further studies on the structure of the connector and its relation with other protein(s) are presently being carried out in our laboratory.

1. J.L. Carrascosa, E. Viñuela, N. García and A. Santisteban (1982). *J. Mol. Biol.* **154**, 311-324.
2. R.A. Driedonks, A. Engel, B. Ten Heggeler and R. van Driel (1981). *J. Mol. Biol.* **152**, 641-662.
3. J. Kochan, J.L. Carrascosa and H. Murialdo. *J. Mol. Biol.*, in press.
4. J.L. Carrascosa, J.M. Carazo and N. García (1983) *Virology* **124**, 133-143.

Symposium on Dissipative Structures and Pattern Formation in Biological Systems

DISSIPATION AGAINST DISSIPATION IN MULTIENTZYME SYSTEMS

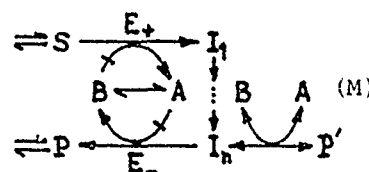
E.E. Sel'kov, Institute of Biological Physics, the USSR Academy of Sciences, Pushchino, USSR

Some multienzyme systems in the cell metabolism (CM) depend critically for their normal operation on the temporal organisation of the incompatible processes involved such as energy-dissipating futile cycles of amphibolic pathways /1,2/ or catabolic cycles (like Krebs cycle) capable of complete decomposing of anabolizable molecules. The required temporal organization is provided by the cell clock. In an evolutionary sense, the cell clock must be as ancient as the cell itself because the reproduction of cells is impossible without the clock. Therefore, the cell clock must be stoichiometric in nature. At the same time, CM contains evolutionarily younger allosteric regulations which stabilize the self-oscillations generated by the stoichiometric cell clock and render them invariant to perturbations in the environment or in the structure of CM. A high degree of invariance is attained only if the stoichiometric mechanism and the related network of allosteric regulations contain no unique (indispensable) elements.

By theoretical screening of the numerous types of self-oscillatory stoichiometric structures, we have revealed a mechanism (M) which is universal and is easy to recognize in any specific CM of pro- or eucaryotes. M represents a sequence of reactions coupled through a cofactor which has two forms, A and B ($A+B=A_0 = \text{const}$). Conversion of substrate S into end products P and P' through intermediates I_1, I_2, \dots, I_n ($n>1$) is of an autocatalytic nature (the crossed arrows $A \rightleftharpoons$ and $B \rightleftharpoons$ denote saturation of enzymes E_+ and E_- with the cofactors). In a broad range of parameter values, M can generate self-oscillations with periods from minutes (reaction $I_n \rightarrow P$ is irreversible, $P' = \text{const}$) to many hours (either $I_n \rightleftharpoons P$ or $I_n \rightleftharpoons P'$ is possible). Mechanisms of the type of M can be identified in different branches of CM. For instance, if $A=\text{NADH}$ and $B=\text{NAD}$, M is part of glycolysis ($E_+=\text{GAPDH}$, $E_-=\text{LDH}$ or $\text{ADH}+\text{PDC}$, $S=\text{GAP}$, $I_n = \text{Pyruvate}$, $P=\text{Lactate}$ or Ethanol , $P'=\text{Malate}$ or other species related to transamination reactions) or of oxidative conversion of pyruvate (S) to glutamate (P) through the unclosed Krebs cycle. In different parts of CM, B stands for different cofactors (NAD(P) , NAD(P)H , ATP , CoA , Acyl-CoA , etc.). Modifications of M with $A=\text{ATP}$, $B=\text{ADP}$ were considered in /3,4/.

The allosteric regulation based on the equilibrium ligand binding to allosteric enzymes is relatively weak because the normalized modulus of the slope of the regulatory characteristics $|S|<n$ (n being the number of binding sites). In contrast, the mechanisms of stoichiometric regulation can provide $|S| \rightarrow \infty$. This high sensitivity is achievable in M and also in the stoichiometric mechanisms of chemical modification of allosteric enzymes due to continuous energy dissipation. Thus, minute energy dissipation, which is the cost paid for the temporal organization of incompatible processes, prevents much greater dissipation in CM.

- /1/ E.E. Sel'kov, Ber. Bunsenges. Phys. Chem. 84, 1980, 399-402.
- /2/ A. Boiteux, B. Hess, E.E. Sel'kov, Curr. Topics Cell. Reg. 17, 1980, 171-203.
- /3/ E.E. Sel'kov, Eur. J. Biochem. 59, 1975, 151-157.
- /4/ J.G. Reich, E.E. Sel'kov. The Cell Energy Metabolism. Acad. Press, London, 1981.



Wednesday 01 August Unicorn Hotel-Trident Suite 09.30-12.30

Symposium on Dissipative Structures and Pattern Formation in Biological Systems

**GENERATION AND REGULATION OF BIOLOGICAL PATTERNS AND THEIR ROLE
IN NEURAL CONNECTIONS**

**A. Gierer, Max-Planck-Institut für Entwicklungsbiologie,
Tübingen, West Germany.**

Spatial order in organisms results, in part, from the development of different substructures within originally near-uniform cells, and cell sheets. Probably, the primary event is the formation of spatial concentration patterns. They can be generated by autocatalytic reactions of short range, coupled to inhibition or depletion effects of wider range. These conditions are mathematically necessary for the simplest case of two coupled reactions with diffusion, but they apply also to more complex schemes. Patterns produced in this way account for an impressive list of self-regulatory properties empirically observed in developmental biology, such as induction, inhibition, regular spacing, symmetry changes and proportion regulation.

Visible structures result from the response of cells to such primary patterns, e.g. by cell differentiation and changes of cell shapes. In embryology, structures can often be traced back to local evagination or invagination of a subarea within nearly flat cell sheets. It is likely that this is caused by local changes of cell shapes involving both membrane components and internal cytoarchitecture. Changes may result from activation of a subarea of the cell sheet interfering with cellular components. Bending moments and curvature are generated, independent of details of the mechanism if cell form corresponds to a stable steady state and if the sheet of cells is asymmetric with respect to the inside-outside-dimension of the tissue. Such asymmetry is characteristic for epithelial cell sheets.

Of particular interest is the role of spatial concentration patterns in the generation of ordered neural connections as they occur, for instance, in the projection of retinal axons onto the tectum. While several mechanisms are likely to contribute to projections, experimental evidence suggests that directional cues on the tectum encoded in graded distributions of spatial markers are essential for the primary projection. Guidance may be caused directly by forces of adhesion between axons and target tissue. This however, is only one out of many possibilities for directional guidance. Generally, any graded cue (whether related to adhesion or not), however slight, may be enhanced by metabolic processes involving autocatalysis within the growth cone of the axon, leading to directional outgrowth. For the generation of a projection by gradients, for each dimension, two antagonistic graded effects are mathematically required on the target and at least one on the tissue of axonal origin. While such mechanisms are postulated to be involved in the primary projection, there are also other effects such as direct or indirect fiber-fiber interaction, especially at later stages.

Wednesday 01 August Unicorn Hotel-Trident Suite 09.30-12.30

Symposium on Dissipative Structures and Pattern Formation in Biological Systems

PATTERN SELECTION IN REACTION DIFFUSION SYSTEMS.

D.WALGRAEF , Service de Chimie-Physique 2, Université Libre de Bruxelles, CP 231
B-1050 Bruxelles, Belgium.

Abstract.

The spontaneous appearance of spatial structures far from thermal equilibrium has long been a puzzling phenomenon both from the experimental point of view and from the theoretical point of view. Numerous questions related to pattern selection in physical, chemical and biological systems remain still unanswered. As reaction diffusion equations have been widely invoked to play an essential role in morphogenesis, differentiation, wave generation or cooperative locomotion in various biological systems, important aspects of this description which is based on the competition between chemical or biological reactions and active transport or spatial diffusion are reviewed. The interplay between linear and nonlinear contributions induces pattern selection mechanisms as well as phase singularities leading to long range desynchronisation fluctuations.

In the case of stationary spatial patterns, different planforms may be selected owing to the structure of the nonlinearities of the dynamics. Fortunately the remaining orientational degeneracy is usually removed in small isotropic systems by the effects of lateral walls. In large systems however the phase variable associated to the position and orientation of the structure obeys a diffusive dynamics. Singularities of the phase may appear spontaneously and induce topological defects and irregularities able to destroy any long range order in low dimensional systems by inducing an algebraic or even exponential decay of the spatial correlation function of the variable playing the role of order parameter in the system.

In the case of temporal oscillations, the phase dynamics is given by the Burgers equation:

$$\partial_t \phi = \mu \nabla^2 \phi + \nu (\vec{\nabla} \phi)^2 + \omega(\vec{r}, t)$$

Hence phase fluctuations may lead to concentric or spiral autowaves of activity in the medium. Their statistics are very different and spiral waves are able to desynchronize the oscillations in large low dimensional systems in agreement with experimental observations either in chemical and biological or physiological systems.

Affinity Group Meeting on Structure of Food Biopolymers

THE FRACTURE BEHAVIOUR OF COOKED MEAT
P.P. Purslow, AFRC Meat Research Institute, Langford,
Bristol, BS18 7DY, UK

Simple tensile tests have been used to investigate the basic fracture properties of cooked meat and to relate these to its structure. Observations on the manner in which this complex material fractured showed that, in a variety of test configurations, rupture started in the perimysial connective tissue, resulting initially in the separation of intact muscle fibre bundles. The tensile strength along and across the fibre direction was measured and anisotropy in strength between these two directions was found to account for the qualitative fracture behaviour of cooked meat. The basis of a fracture mechanics approach to meat fracture is outlined. An energy-based measure of toughness (work of fracture) and stress-concentration considerations (notch sensitivity) are described. Work of fracture through the perimysium was found to be low in absolute terms (0.4 - 1.8 kJm⁻²). The difficulty in propagating fracture in meat across the fibre direction is explained on the basis of the material's complete notch-insensitivity. These results imply that the muscle fibre bundle is an important level of structural organisation in relation to meat fracture. The qualitative aspects of fracture behaviour are accounted for by a model of cooked meat as a uniaxial fibrous composite of strong fibre bundles in a weak connective tissue "matrix" with poor interfacial strength between the two components.

STRUCTURE AND FAILURE IN AERATED CAKES
A.G. Naylor and M.J. Hale, Unilever Research, Colworth Laboratory, Sharnbrook, Bedford.

The formation of a domed top to aerated cakes is preferred since the top can be pressed down without changing the texture of the cake significantly. In contrast, a concave top cannot be lifted and the texture is usually unacceptable as it is more dense and has a less porous structure than a cake which is domed or flat.

Experiments have been performed to determine the causes and methods of prevention of the collapse of aerated cake structures on cooling, and the development of a physical model to explain the formation, structure and properties of aerated cakes.

Three standard formulations of cake batter were used: (1) A standard commercial formulation, containing 60% flour and 40% starch, which usually produced cakes which did not collapse too much on cooling; (2) A 100% flour formulation, which collapsed every time on cooling; (3) A 100% starch formulation, which did not collapse too much on cooling.

The baking process itself was examined by visualisation techniques to determine the behaviour of the different batters, and to observe the formation of the cake structure. The batters themselves were characterised in terms of surface tension and viscosity as a function of temperature. The structure of the cake was examined by various techniques, eg stereo microscopy, X-ray photography and permeametry. Models of its structure were derived based on network structure as used in structural engineering and foamed structures as found in foam rubbers.

CHOCOLATE CRYSTALLISATION - MOLECULAR THEORY AND PRODUCTION PRACTICE

G.G. Jewell, Cadbury Schweppes PLC, Lord Zuckerman Research Centre, The University, Whiteknights, Reading RG6 2LA, UK.

Chocolate is a complex confection in which the principal fat is cocoa butter, but it may also contain milk fat, vegetable fat and lecithins. These fats all exhibit complex polymorphic behaviour, and so it is by understanding and controlling the polymorphism that the manufacturer achieves the optimum rheological properties (important during processing) and ultimate texture and stability of his products. The critical factors are quantity, size and polymorphic form of the fat crystals and these can be studied using x-ray diffraction, differential scanning calorimetry, electron microscopy and wide line NMR. By combining these physical chemistry measurements with a precise knowledge of glyceride composition, it is possible to begin to explain the polymorphic behaviour at the molecular level in terms of crystal packing. It is evident that the main factors controlling cocoa butter crystallisation are the cis oleic acid in the 2 position and presence of predominantly C16 and C18 fatty acids. The introduction of fats with either significantly different chain lengths or trans isomers leads to eutectic mixtures and possible phase separation. Such information enables the manufacturer to select recipes and design processes for crystallisation (solidification) which ensure effective production and high quality products.

DOUGH DEVELOPMENT AND THE STRUCTURE OF BREAD
P.J. Frazier, Dalgety U.K. Limited, Group Research Lab., Research & Technology Centre, Station Rd., Cambridge, U.K.

Although comprising only 10-12% by weight of wheat flour, the unique, visco-elastic, gluten-forming proteins are fundamental to the structure of bread. Development of a continuous matrix of protein, capable of holding leavening gases and carrying all the embedded starch granules, is dependent on hydration and mixing of the flour followed by a period of time for 'maturation' of the dough. In traditional processes ideal bread structure is achieved after a long (20 min) slow-speed mix followed by a lengthy (3 h) bulk fermentation before proving and baking. Modern methods such as the Chorleywood Bread Process depend on a short (2-4 min) high-speed mix, during which a measured quantity of energy is expended on the dough, effectively replacing the maturation stage, followed only by proving and baking. Recently, using rheological techniques, the interactions between mechanical work, chemical oxidants and enzymes ('improvers') have become better understood. Specific examples of ascorbic acid, azodicarbonamide and lipoxigenase will be discussed, and it is now possible to optimise the process for flours of widely differing quality or 'strength'. Having developed the dough, the formation of an aerated crumb structure is dependent on entrained air and generation of gas by yeast. Finally, during baking, the protein is denatured but retains cohesive strength and some elasticity, and the starch gelatinises, rapidly increasing dough viscosity and setting the whole bread structure.

COMMINUTED MEAT SYSTEMS

A.M. Hermansson, SIK - The Swedish Food Institute, Gothenburg, Sweden.

During comminution structural components are released from the muscle and fat tissues, and the structure formed on comminution and subsequent heating varies depending on processing and environmental conditions. The relationships between the microstructure and physical properties such as fat- and water-holding will be discussed with regard to structural changes of the myofibrillar proteins, collagen, and the dispersed fat phase at various stages of comminution before and after heat treatment. At low degrees of comminution swelling of myofibrils contributes to the water-binding properties. At high degrees of comminution and in the presence of 2-4% sodium chloride the myofibrils disintegrate and the ability of myofibrillar proteins and collagen to form a continuous gel network on heating is of major importance for properties such as texture, fat and water-binding. In highly comminuted meat systems the state of the dispersed collagen plays a more active role than previously believed. The stability of the dispersed fat phase depends on several factors such as the properties of the continuous matrix, the dispersed fat, as well as on the surrounding wall or other types of interfacial layers and on the particle size distribution of the dispersed fat phase. The microstructure has been evaluated by means of various types of light microscopy, scanning and transmission electron microscopy.

Notes

Thursday 02 August

Symposia

09.30 - 12.30

Folding, Dynamics and Solvation of Macromolecules
(Part-2)

Photosynthesis

Medical Imaging

Affinity Group Meeting on Structure of Food
Biopolymers

14.00 - 17.00

Molecular Evolution

Metal-Proteins and Electron Transfer

Polysaccharides and Glycoproteins

Plenary Lecture

17.15 - 18.00

"Water Movement through Channels in Lipid Bilayers
and Cell Membranes"

A. Finkelstein (New York)

The American Society of General Physiologists Lecture

Poster Sessions

Cross-Bridge Mechanisms and Muscle Contraction

Cytoskeleton

Electric Field Effects in Cell Membranes

Photo and Auditory Receptors

Applications of Synchrotron Radiation

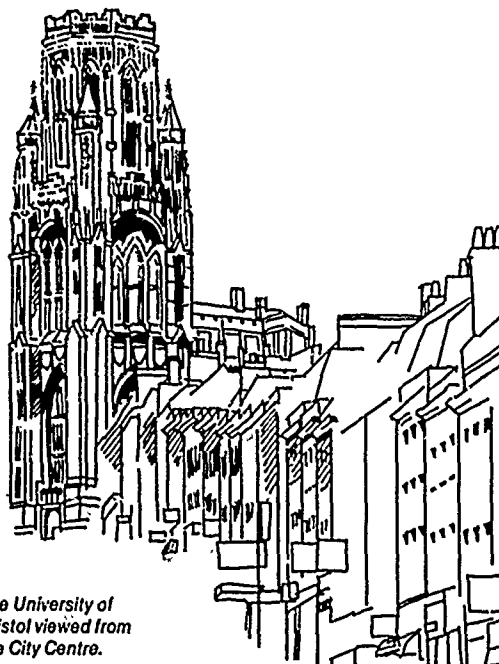
Developments in Microscopy

Image Reconstruction

Processing and Control of Visual Information

Environmental Biophysics

Education in Biophysics

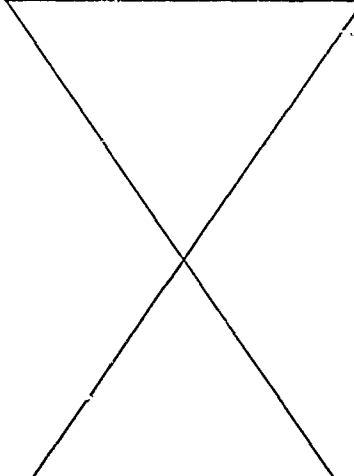


*The University of
Bristol viewed from
the City Centre.*

Thursday 02 August

Colston Hall Main Hall	Council House Conference Hall	Unicorn Hotel Trident Suite
<p>Folding, Dynamics and Solvation of Macromolecules (Part 2) Co-Chairman: M. Karplus (Harvard) D.C. Phillips (Oxford)</p> <p>Speakers: V.I. Goldanskii (Moscow) M. Karplus (Harvard) R.E. Dickerson (California) and Authors of Posters K. Yutani (152) E. Poerio (172)</p>	<p>Photosynthesis Chairman: W. Junge (Osnabrueck)</p> <p>Speakers: J. Barber (London) W.W. Parson (Washington) W. Junge (Osnabrueck) and Authors of Posters A. Scherz (197) A.W.D. Larkum (200)</p>	<p>Medical Imaging Chairman: P.C. Lauterbur (Stony Brook)</p> <p>Speakers: P.N.T. Wells (Bristol) M.E. Raichle (St. Louis) P.C. Lavtêbur (Stony Brook) and Authors of Posters S.S. Arora (279) P. Greguss (277)</p>
<p>12.30 Morning Coffee 10.50-11.10</p>	<p>Morning Coffee 10.50-11.10</p>	<p>Morning Coffee 10.50-11.10</p>

Break for Lunch (90 Minutes)

<p>14.00</p>  <p>17.00</p> <p>17.15</p>	<p>Molecular Evolution Chairman: C.C.F. Blake (Oxford) Speakers: P. Schuster (Wien) S. Ohno (California) C.C.F. Blake (Oxford) and Authors of Posters H. Liljenstrom (032) D.P. Burma (027)</p> <p>Afternoon Tea 15.20-15.40</p>	<p>Metal-Proteins and Electron Transfer Co-Chairmen: Bo. G. Malmstrom (Goteborg) C.L. Tso (Beijing)</p> <p>Speakers: R.J.P. Williams (Oxford) H.B. Gray (California) Bo. G. Malmstrom (Goteborg) and Authors of Posters C.L. Tso (128) K. Nagayama (091)</p> <p>Afternoon Tea 15.20-15.10</p>
<p>18.00</p> <p>Water Movement through Channels In Lipid Bilayers and Cell Membranes</p> <p>Plenary Lecture by A. Finkelstein (New York)</p>		

Timetable

Watershed Cinema 1	Congress Centre First Floor	
	Presenting Authors should set up their Posters before the start of Today's Symposium	09.00
		09.30
Affinity Group Meeting on Structure of Food Biopolymers	Poster Sessions	
Chairman: P.J. Lillford (Unilever, Colworth)	Cross-Bridge Mechanisms and Muscle Contraction Poster Nos: 001-078	
Speakers: R.A. Marsh (RHM Research) J. Adler-Nissen (Novo, Bagsvaerd) E.W. Evans (NIRD, Reading) E.E. McDermott (FMBRA, Chorleywood) D.J. Wright (FRI, Norwich) V.J. Morris (FRI, Norwich)	Cytoskeleton Poster Nos: 079-108	
	Electric Field Effects in Cell Membranes Poster Nos: 109-150	
	Photo and Auditory Receptors Poster Nos: 151-180	
	Applications of Synchrotron Radiation Poster Nos: 181-204	
	Developments in Microscopy Poster Nos: 205-216	
	Image Reconstruction Poster Nos: 217-234	
Morning Coffee 10.50-11.10	Processing and Control of Visual Information Poster Nos: 235-240	12.30
	Environmental Biophysics Poster Nos: 241-276	
	Education In Biophysics Poster Nos: 277-282	
		14.00
Polysaccharides and Glycoproteins		
Chairman: E.D.T. Atkins (Bristol)		
Speakers: J.F.G. Vliegenthart (Utrecht) O. Smidsrod (Trondheim) J. Montreuil (Lille) and Authors of Posters B. Svensson (152) Y. Yeh (148)	Presenting Authors should attend their Posters throughout the Afternoon Discussion Period.	
Afternoon Tea 15.20-15.40		
	Presenting Authors must take down their Posters	17.00
		17.15
		18.00

MÖSSBAUER DATA, LOW-TEMPERATURE SPECIFIC HEATS AND THE GLASS-LIKE DYNAMICAL MODEL OF BIOPOLYMERS.

V.I. Goldanskii, Institute of Chemical Physics, Kosygin Street, 4, Moscow, 117334, USSR.

Analysis of dynamical properties of biopolymers leads to the conclusion that they possess peculiar combination of properties of crystals and glasses. Using as the main characteristics of substance the presence (+) or absence (-) of the ordering (i.e. definiteness of the structure); periodicity and geometrical uniqueness of the ground state; i.e. describing the ideal crystals as (+++) and glasses as (---), one can conclude that the biopolymers which were treated formerly as (++) (aperiodic crystals) would after the revealing of quasi-degenerated conformational states (QDCS) by the X-ray dynamical analysis of protein crystals (Frauenfelder, D. Phillips) rather be denoted as (+--).

Mössbauer absorption spectroscopy is widely used for the studies of dynamical properties of biopolymers since the experiments with Fe-labelled HSA and model Fe-S proteins performed in the Institute of Chemical Physics (Doklady AN SSSR, 212, (1), 165-168, 1973). Characteristic peculiarities of Mössbauer absorption spectra studied by various groups for crystalline met-Mb and deoxy-Mb and for met-Mb in solutions at 4-300 K (abrupt strengthening of $f'(T)$ dependence at $T \geq 200$ K, appearance of broad and narrow components of spectral lines) confirm the existence of QDCS and of the transitions between these states.

Temperature dependence $f_R(T)$ of the fraction of elastic Rayleigh scattering of Mössbauer radiation (RSMR) f_R for crystals and hydrated samples of met-Mb, hydrated trypsin, HSA, and DNA is characterized by abrupt strengthening at $T \geq 200$ K for the weight content of water $h \geq 0.3$.

Hydration isotherm at room temperature demonstrates sharp decrease of $f_R(h)$ at $h > 0.1$. The overall $\langle x^2 \rangle$ value for mentioned biopolymers at $h \approx 1$ (300 K) is close to 1 \AA^2 .

Thus the RSMR data illustrate the existence of QDCS also in the hydrated samples of biopolymers. Increasing degree of hydration leads to the ordering of biopolymers (due to the hydrophobic interactions) i.e. to the definiteness of the structure and to the sharp rise of the number of QDCS (due to the weakening of intramolecular hydrogen bonds).

The strong effect of the viscous solvent on the protein dynamics is observed by the example of HSA in water-glycerol solution. Obtained data give the argument that glycerol influences the protein dynamics through the decrease of preferential hydration of a protein (and corresponding decrease of QDCS number) rather than through the increase of solvent viscosity by itself.

Analysis of data on the low-temperature specific heat of poly-L-alanine, polyglycine, dehydrated collagen and DNA manifests the considerable contribution of linear $C_p T$ term bound to the transitions between QDCS via the phonon-assisted tunneling (Anderson-W. Phillips dynamical model of glasses).

Totality of data on low-temperature specific heats and RSMR brings the evidence that the transitions between the QDCS proceed not only as thermally activated but also as tunneling processes and that the substantial role of tunneling maintains even at room temperature.

Thursday 02 August Colston Hall - Main Hall 09.30-12.30

Symposium on Folding, Dynamics and Solvation of Macromolecules (Part 2)

DYNAMICS OF MACROMOLECULES

M. Karplus, Department of Chemistry, Harvard University, Cambridge, Massachusetts
USA.

Molecular and harmonic dynamics of macromolecules are providing insights into their internal motions. Some results of dynamical studies will be presented and the relation between motion and function will be discussed.

Symposium on Folding, Dynamics and Solvation of Macromolecules (Part 2).

STABILIZATION OF THE B-HELICAL DNA STRUCTURE BY BINDING WITHIN THE MINOR GROOVE OF WATER, CATIONS, OR THE ANTITUMOR ANTIBIOTIC NETROPSIN

Mary L. Kopka, Philip Pjura, Chun Yoon, David Goodsell and Richard E. Dickerson
Molecular Biology Institute, University of California at Los Angeles,
Los Angeles, California, USA

In the x-ray crystal structure analysis of the B-helical DNA dodecamer of sequence CGCGAATTCGCG, an ordered spine of hydration extends down the minor groove in the A-T-containing center of the molecule (Figure 1). A first layer of water molecules bridges adenine N3 and thymine O2 atoms from adjacent base pairs on opposite strands of the double helix. The bases so bridged are those that are brought into closer proximity by the rotation of the helix. These first layer waters in turn are bridged by second-layer waters, giving them a local tetrahedral environment. This spine of hydration is disrupted in the G-C-containing ends of the dodecamer because of steric clash with the protruding $-NH_2$ groups of guanines. The spine of hydration is believed to play a major role in stabilizing the B helix relative to the A under high humidity conditions. No equivalent ordered water structure is observed elsewhere around the B helix, or anywhere in crystal structure analyses of the A form.

Skuratovskii and coworkers have observed in fibers of B-form DNA under high salt conditions that large monovalent cations such as Cs^+ can replace the spine of hydration with a spine of cations. This may explain the requirement of low salt for the drying-induced B-to-A transition in fibers: cations replace the spine of hydration upon drying, and continue to stabilize the B form.

In the x-ray crystal structure analysis of CGCGAATTCGCG co-crystallized with the antitumor drug netropsin, the drug molecule is observed to sit in the minor groove and displace the spine of hydration (Figure 2). Amide NH groups bridge the same bases as are bridged by the water spine, and the two cationic ends of the drug also interact with the bottom of the groove. The cytotoxic effect of netropsin presumably arises because it "glues" the B-DNA minor groove shut, preventing both transcription and translation.

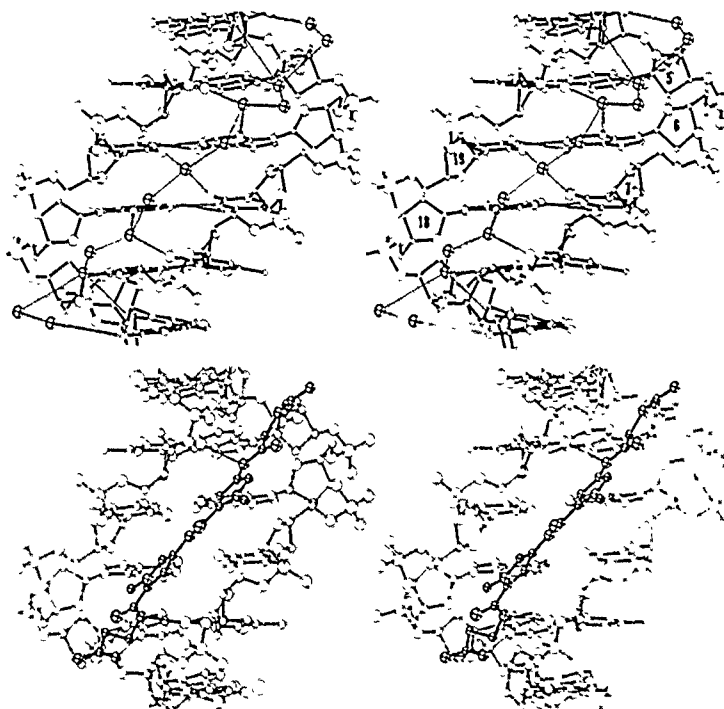


Figure 1. View into minor groove of the central six base pairs of the B-DNA helix of sequence: CGCGAATTCGCG, with the spine of hydration. (Water oxygens as crossed spheres.) Waters bridge A and T bases on opposite chains at adjacent base pairs.

Figure 2. Identical view into the minor groove of the complex of netropsin with the same dodecamer DNA. Netropsin NH bridge A and T bases as above. In both cases G is incompatible with binding because of the bulk of the N2 amine group in the minor groove.

Thursday 02 August Council House-Conference Hall 09:30-12:30

Symposium on Photosynthesis

RELATIONSHIP BETWEEN THE STRUCTURE AND FUNCTION OF PHOTOSYNTHETIC MEMBRANES

J. Barber, AFRC Photosynthesis Research Group, Department of Pure and Applied Biology, Imperial College, London, U.K.

The pigments and associated electron carriers of photosynthetic organisms are contained within the chloroplast thylakoid membranes of higher plants and algae or the chromatophore membranes of bacteria. In the former case there are two types of photochemical reaction centres, photosystem one (PS1) and two (PS2) which act in series to extract electrons and protons from H_2O and pass them to $NADP^+$ while at the same time producing ATP and molecular O_2 . In bacterial chromatophores there is only one type of reaction centre which when photoactivated does not have enough potential to oxidise H_2O but instead uses substrates such as organic acids and H_2S for their electron/proton supply. In both types of organisms, the photoproduction of NADPH or NADH and ATP is required for carbon fixation and net generation of organic molecules. However in the case of bacteria the mechanism of producing NADH varies although in all cases ATP is synthesised directly as a result of light induced electron flow. This ATP generating process involves the cooperation of four major intrinsic membrane protein complexes; the reaction centre, the light harvesting system containing many tens of pigment molecules, the cytochrome *b-c* complex and an ATP-synthetase. The precise nature of these complexes, the associated dehydrogenase and the way they interact varies between species. In O_2 evolving organisms five major protein complexes can be identified; the chlorophyll *a*/chlorophyll *b* light harvesting system (LHC) of higher plants and green algae or the phycobilisomes (PB) of red algae and cyanobacteria, the PS1 reaction centre core, the PS2 reaction centre core, the cytochrome *b₆-f* complex and an ATP-synthetase. Despite the difference between the various classes of organisms there is a remarkable functional and structural homology between the various complexes, a conclusion which also engulfs the comparative complexes involved in bacterial and mitochondrial respiration.

In the case of higher plant chloroplasts, mechanical fragmentation and considerations of surface electrical properties have indicated that there is considerable lateral separation of the intrinsic complexes along the plane of the thylakoid membrane. From these studies it has been concluded that under normal conditions, the PS2 and LHC complexes are mainly localised in appressed lamellae regions of the grana stacks while the PS1 and ATP-synthetase complexes are located in the non-appressed membranes which constitute the end granal and stromal lamellae. The position of the cytochrome *b₆-f* complex is uncertain but may be restricted to an interface region between the appressed and non-appressed membranes. There is no evidence at present to suggest that lateral separation comparable with the higher plant chloroplast exists in bacterial membranes or in the membranes of red-algae and cyanobacteria. In the case of higher plants there seems also to be a partial lateral heterogeneity in lipid composition with the appressed lamellae having higher levels of anionic and monogalactosyl lipids. However, no significant difference has been found in the fatty acid content of appressed and non-appressed membranes even though fluorescence anisotropy measurements using the hydrophobic probe, diphenylhexatriene (DPH), showed that the former membranes were less fluid than the latter. It is suggested that the different fluidity properties in the two regions are due to differences in protein to lipid ratios, a conclusion supported by studies with reconstituted systems. These various findings are pertinent to discussions concerning the lateral movement of plastoquinone (PQ) as a redox carrier between PS2 and cytochrome *b₆-f* and also for understanding the molecular mechanism of the State 1-State 2 phenomenon. The latter process regulates energy distribution between PS2 and PS1 and involves the phosphorylation of the LHC surface. It is proposed that (PQ) diffusion is rapid along the mid-plane of the lipid bilayer and that in the case of the State 1-State 2 phenomenon, the addition of electrical charges introduced onto the LHC surface by phosphorylation induces lateral migration of the complex from the appressed to the non-appressed region. With isolated thylakoids the extent of the pigment-protein movement is dependent on the cation level in the suspending medium in a way expected for a process under electrostatic control.

Thursday 02 August Council House-Conference Hall 09.30-12.30

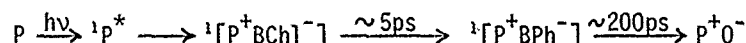
Symposium on Photosynthesis

EXCITED STATES AND ELECTRON TRANSFER IN PHOTOSYNTHETIC BACTERIAL REACTION CENTERS

W. W. Parson, Department of Biochemistry, University of Washington, Seattle, Washington 98195

Photochemical "reaction centers" have been purified from several species of photosynthetic bacteria. The pigment-protein complexes isolated from purple bacteria typically contain 3 polypeptides, 4 molecules of bacteriochlorophyll (BChl), 2 molecules of bacteriopheophytin (BPh), 2 quinones (Q), and 1 nonheme Fe. (BPh is BChl with 2 H in the center instead of Mg.) Two of the 4 BChls appear to form a "special pair" (P), which has an intense absorption band in the near infrared. Although various explanations have been offered for the intensity, position, and large circular dichroism of this band, these features can be attributed reasonably to exciton interactions between the two BChls, provided that one considers interactions between both degenerate and nondegenerate excited states of the two molecules.

When P is excited, it transfers an electron to another molecule within a few picoseconds. Measurements of the optical absorbance changes that occur after excitation under various conditions suggest that the sequence of electron-transfer steps is:



The interactions of P^+ with $BChl^-$ appear to be many orders of magnitude stronger than its interactions with BPh^- or Q^- . The chain of electron acceptors provides a reasonable explanation for the remarkable efficiency of the photosynthetic apparatus. Back-reactions between P^+ and the reduced electron acceptor will decrease abruptly as the electron moves from one acceptor to the next, because of the decreasing orbital overlap between the two radicals.

If electron transfer from BPh^- to Q is blocked, ${}^1[P^+BPh^-]$ lives for about 10 ns, before it decays by other pathways. Under these conditions, back-reactions can regenerate P^* , leading to delayed fluorescence. Measurements of the amplitude of the fluorescence provide information on the free energy gap between P^* and ${}^1[P^+BPh^-]$. The decay kinetics of the fluorescence suggest that ${}^1[P^+BPh^-]$ undergoes a series of relaxations on the time scale of 0.5 to 5 ns. The relaxations could result from nuclear movements in the electron carriers or the protein.

Thursday 02 August Council House-Conference Hall 09.30-12.30

Symposium on Photosynthesis

ELECTROCHEMICAL EVENTS AT THYLAKOID MEMBRANES

W. JUNGE, Biophysik, Fachbereich Biologie/Chemie, Universitaet Osnabrueck Osnabrueck, Germany (FRG).

Light driven electron transport in chloroplasts of green plants produces reducing power and, in addition, it electrochemically charges the thylakoid membrane. Approximately 25% of the total useful work flows via the proton motive force into the synthesis of ATP. The net pumping of protons is separated into very rapid electron transfer across the membrane in each of the two types of photochemical reaction centers. Under excitation of chloroplasts with single pulses from a pico-second laser this occurs in less than 200 ps and it charges the membrane by approximately 30-50 mV. Coupled to secondary electron transfer are protolytic reactions of the respective electron carriers with the aqueous phases. Under conditions of only linear electron transfer from water to Hill-acceptors two protons per electron are released into the thylakoid interior. This acidifies the internal space by some 0.05 pH-units. The greater part of the electrochemical energy is in the electric form. This reflects that the chemical (buffering) capacitance (some $0.1 \text{ mol H}^+/\text{mol chl} \times \text{pH}$) is much greater than the electrical one (some $0.5 \mu\text{F}/\text{cm}^2$). Under continuous illumination of chloroplasts and continuous turnover of the proton pumps other ions than protons are outwardly driven to electrically compensate proton influx. The internal pH drops by up to 3 units (under linear electron transfer) and by up to 3.8 units under cyclic electron transfer with artificial cofactors. In the steady state the electric component is negligible. The electrochemical energy is used for ATP-synthesis with a proton/ATP-stoichiometry of three. With this stoichiometry chloroplasts can sustain a phosphate potential of some 60 kJ/mol in the light.

It is still under debate whether or not protons obligatorily path via the aqueous phases on their way from the pump sources into the ATP-synthases. We found that this is so under some conditions but not so under others. We studied partial reactions of proton release during photosynthetic water oxidation. With a membrane adsorbed indicator dye, neutral red, and in a laser flash-photometer we measured pH transients in the internal phase of thylakoids with very high sensitivity (better than 10^{-4}) and at very high time resolution (better than 20 μs). The water oxidating enzyme was switched from one of its four oxidation states to the other by a series of laser flashes. The extent of proton release varied with a period of four and the velocity of the internal acidification followed closely the velocity of the respective oxidation step of the enzyme. Hence, proton release was kinetically and stoichiometrically labeled as originating from water oxidation. In freeze-thaw and swollen thylakoids we found that even the most rapid acidification steps (half-rise time 100 μs) could be quenched by notoriously hydrophilic buffers like phosphate and the internal phase behaved like an osmotically variable aqueous bulk phase. This demonstrates that swollen thylakoids, which showed high rates of photophosphorylation can function as true chemiosmotic ATP-synthasizers in line with Mitchell's claim. And there is no functionally relevant necessity to sequester protons into special domains, remote from the bulk buffering power, in order to promote ATP-synthesis (William's proposal).

However, in freshly prepared thylakoids we found various deviations from this simple behaviour: failure of the internal space to behave as an extended aqueous bulk phase - transient trapping of protons originating from water oxidation in special domains, which are different from the internal lumen - great delay for the propagation of a "proton wave" along stacked thylakoids. Closer inspection of these phenomena, which will be presented in the lecture, revealed that these deviations from orthodox chemiosmotic behaviour do not seem to matter in the steady state.

Symposium on Medical Imaging

MEDICAL ULTRASONIC IMAGING

P.N.T. Wells, Department of Medical Physics, Bristol General Hospital,
Bristol, UK

The propagation speed of ultrasound in biological soft tissues ranges from around 1480 m/s in fat to 1600 m/s in muscle and the attenuation rate is about 1 dB/(cm MHz). Pulse-echo techniques are widely used in medical diagnosis. The resolution depends on the ultrasonic wavelength which decreases with increasing frequency. The attenuation limits the penetration to about 200 wavelengths in soft tissues, so that frequencies in the range 1-15 MHz provide the optimal compromise between resolution and penetration.

The reflexions which give rise to the echoes which form the basis of most echo techniques in ultrasonic diagnosis arise from discontinuities in characteristic impedance (equal to the product of the density of the material and the speed of ultrasound within it). Moreover, the reflected ultrasound is shifted in frequency by the Doppler effect if the backscattering structures have a component of velocity in the direction of the ultrasonic beam.

Piezoelectric transducers are used to generate and detect ultrasound. Lead zirconate titanate is the most commonly used transducer material but there is growing interest in the polarised plastic polyvinylidene difluoride. In the near field, the ultrasonic beam can be focused by lenses, concave transducers, shaped mirrors or electronically controlled arrays. Arrays can also provide the capabilities of controlling the beam position and direction and of dynamically focusing the receiving beam.

Pulse echo techniques depend on measurements of echo delay times (proportional to reflector ranges), echo amplitudes (giving information about reflector characteristics) and beam directions (the azimuths and elevations of the reflectors). The dimensions of the resolution cell depend on the ultrasonic beam and pulse shapes (which vary with position) and the dynamic range of the receiving system.

Pulse echo information can be displayed as an A-scan (in which time, corresponding to distance, is on one axis and the occurrences of echoes, on the other axis), a time-position recording (depth on one axis and real time on the other), or a two-dimensional B-scan (a sectional image in the scan plane). Nowadays, the A-scan is generally used as an adjunct to other displays. Time-position (M-mode) recording has its main application in cardiology.

Instruments designed to produce two-dimensional B-scans by manual scanning of the probe over the surface of the patient ('static' scanners) or by automatic scanning through a water bath are now less popular than systems which can image in real time. Real time systems are based either on fast mechanical scanning or on electronically controlled arrays.

Two-dimensional ultrasonic images are composed of various textures which depend on the characteristics of the imaging system in addition to those of the corresponding anatomical and histological structures. Quantitative analysis of the echo signals may allow tissues to be identified.

Systems based on the Doppler effect are used to detect motion and to measure blood flow velocity. The simplest instruments employ continuous wave ultrasound and non-directionally-sensitive detectors. The most advanced use pulsed range-gated ultrasound and directionally-sensitive detectors with on-line frequency spectrum analysis. Pulsed Doppler systems are also used in combination with real-time pulse-echo imaging systems. Such instruments have applications in cardiovascular investigations.

Measurements of ultrasonic transmission are used in computed tomography to study two-dimensional distributions of speed and attenuation in accessible organs. Orthogonal transmission techniques produce useful images with incoherent ultrasound. Acoustic microscopy, using ultrasound in the 10-2000 MHz frequency range, has promising applications in the investigation of small living structures and cells.

The exposure conditions used in contemporary diagnostic systems appear to be safe.

Thursday 02 August Unicorn Hotel-Trident Suite 09.30-12.30

Symposium on Medical Imaging

QUANTITATIVE IN VIVO TISSUE AUTORADIOGRAPHY IN HUMAN SUBJECTS WITH POSITRON EMISSION TOMOGRAPHY. Marcus E. Raichle and Peter Herscovitch, Washington University (Box 8131), St. Louis, Missouri, 63110, USA

Positron emission tomography (PET) is a nuclear medicine imaging technique which produces an image of the distribution of a positron-emitting radionuclide in any desired cross-section of the human body. A PET image reconstructed from the radioactive counting data is an accurate and quantitative representation of the spatial distribution of a positron-emitting radionuclide in the chosen section. This approach is analagous to quantitative tissue autoradiography but has the added advantage of permitting in vivo studies in humans (M.E. Raichle, Ann Rev Neuroscience 6:249-267, 1983). Investigators with access to radio-pharmaceuticals labeled with these radionuclides (e.g. $H_2^{15}O$, $O^{15}O$, $C^{15}O$, ^{18}F -deoxyglucose) and a PET imaging device have employed a variety of quantitative radiotracer strategies to evaluate the relationship between the functional activity of the human brain (i.e., motor, somatosensory, auditory and visual) and local metabolism as well as the metabolic and hemodynamic correlates of disorders of human cognition (amnesia) and mood (anxiety and depression) and specific diseases such as stroke, epilepsy, and dementia. In addition, because of the sensitivity of PET to extremely low in vivo concentrations of specific radiopharmaceuticals it has been possible to design and implement tracer strategies to measure, in vivo, receptor pharmacology in the human brain.

Thursday 02 August Unicorn Hotel-Trident Suite 09.30-12.30

Symposium on Medical Imaging

NUCLEAR MAGNETIC RESONANCE IMAGING

P. C. Lauterbur, Departments of Chemistry and Radiology, State University of New York at Stony Brook, Stony Brook, New York, U.S.A.

Many atomic nuclei, including the most common isotopes of hydrogen, phosphorus, sodium and fluorine and the one percent abundant ^{13}C , have spins and magnetic moments. The interaction energies between such nuclei and the magnetic fields within practical large magnets correspond to radio frequencies. The transitions between the long-lived quantized energy levels are extremely sharp, especially in liquids, in which molecular motions average out the frequency differences caused by anisotropic local interactions. In a non-uniform magnetic field the exact resonant frequencies depend upon the local values of the field and hence on the spatial coordinates of the nuclei. Images of the nuclear distributions can be obtained by varying the non-uniformity of the magnetic field, usually by the superposition of small linear gradients on a uniform static field, and then using either projection reconstruction or phase-encoding techniques. Molecular motions modify the phase coherence of the spins and the probabilities of transitions between the energy levels, and the resulting differences in natural relaxation rates, from about 0.5 s^{-1} to 20 s^{-1} in tissues, can drastically change the signal strengths, permitting high-contrast imaging of normal and abnormal anatomy with resolutions of the order of one millimeter in hydrogen NMR images of water and fat.

The local magnetic fields are also modified slightly, by a few parts in 10^6 to 10^5 , by the effects of molecular electronic structure. These spectroscopic differences can be used to analyze tissue *in vivo* for major hydrogen, phosphorus and carbon-containing compounds, and to image their distributions in the body. Because hydrogen NMR signals from the high concentrations of protons in water and fat are relatively strong, small volumes give rise to good signal-to-noise ratios and high-resolution images, comparable to those obtained by x-ray computed tomography, are possible. Signals from nuclei at lower concentrations, such as phosphorus in ATP, phosphocreatine and inorganic phosphate, must be averaged over larger volumes, usually at least several cubic centimeters, to obtain useful spectra, but the detailed metabolic information that can be obtained compensates for the lower resolution. NMR images also contain information about flow and motion, and can be used to study the function of the cardiovascular system. Images of small objects at microscopic resolution of the order of $20\text{ }\mu\text{m}$, have also been obtained, and a variety of specialized techniques and new developments are being introduced.

Affinity Group Meeting on Structure of Food Biopolymers

STRUCTURAL PROPERTIES OF MYCOPROTEIN

R.A. Marsh, RHM Research Ltd., The Lord Rank Research Centre, High Wycombe, Bucks, U.K.

Mycoprotein is a protein and fibre-rich human food derived from fungal mycelium of a strain of *Fusarium graminearum* (Schwabe). It is grown by continuous culture fermentation on food grade substrates, and has been developed into a range of products with eating qualities similar to meat. The texture of mycoprotein is very dependent on the structural properties of the mycelium. Fungal hyphae attain a typical unbranched length of 300µ (5µ in diameter) during fermentation. After a heat shock to reduce the RNA to <2%, mycoprotein is harvested by filtration to give a buff coloured, bland flavoured product of about 30% solids. Hyphae consist of fibrous chitin-glucan cell walls, containing thermally denatured protein, and can be aligned into fibres by mechanical means. Light and electron microscopy coupled with a measurement of fibre strength using a modified Instron 1122, shows that the size and strength of mycoprotein fibres are comparable with muscle fibres in beef, but as mycoprotein contains no natural connective tissue it has chewing properties closer to chicken. NMR, Differential Scanning Calorimetry and Dynamic Rheological Spectrometry have been used to investigate properties of mycoprotein, and show it to be different from meat in water uptake, flavour binding and thermal shrinkage. This is related to the hyphal structure and the surface being carbohydrate rather than protein.

FOOD-FUNCTIONAL AND PHYSICO-CHEMICAL PROPERTIES OF WHEY

PROTEINS E.W. Evans, B.E. Brooker, K.R. Langley and D. Millard, NIRD, Shinfield, Reading, UK.

Whey protein represents a valuable and nutritious source of proteins for food use. These proteins are well characterised chemically and nutritionally and much is known about their thermal stabilities and physico-chemical properties. Fractions concentrated in particular proteins, produced by ion-exchange methods developed at NIRD, are being used to evaluate physical and physico-chemical properties of relevance to manufactured foods. Current tests for food functionality of proteins are imprecise and often meaningless; progress depends on relating functionality to physico-chemical properties. We are developing methods of measuring and determining the kinetics of gelation and the physical properties of gels, and the efficiency of formation and the stability of emulsions, produced from these fractions. Effects of physical and chemical factors, both in protein production and in the formation of model systems, on these physico-chemical properties are being assessed. An objective is to explore the extent to which these food functional properties of the globular proteins can be related to their physico-chemical properties. Another is to identify the contributions of specific proteins within a mixture, to assess whether these properties are additive or synergistic.

LEGUME PROTEINS IN FOODS - A STRUCTURE/FUNCTION APPROACH

D. J. Wright
Division of Chemistry and Biochemistry, AFRC Food Research Institute, Colney Lane, Norwich, U.K.

The various functional roles of proteins in food products have been recognised for some time and many studies have been initiated to explore the basis of this functionality. These studies have attempted, in the main, to correlate *ad hoc* measurements of protein functionality with observed physical parameters or have merely compared functional properties between proteins or raw materials. Despite all the work undertaken, we are still not in a position to say precisely what governs, for example, the foam- or emulsion-stabilising ability of proteins. The lack of real success would seem to indicate that perhaps a more radical approach is required.

Although the link between protein structure and function is indisputable, the exact relationship remains unclear. This paper will attempt to examine the importance of structure to the properties of proteins and the means by which the impact of structural variation on functional properties can be assessed, using, as examples, proteins mainly of vegetable origin.

PEPTIDE MIXTURES AS EMULSIFIERS

J. Adler-Nissen, Novo Industri A/S, Enzyme Applications R & D, Bagsvaerd, Denmark.

The emulsifying properties of food proteins are generally positively correlated with their solubility and their hydrophobicity. It has previously been shown that by partial enzymic hydrolysis improved emulsifying properties can be achieved, presumably as a result of the increase in solubility. A further separation of the iso-electric soluble fraction yields 100% soluble peptide mixtures which also exhibit emulsifying properties. 12 such soluble hydrolysates have been prepared from casein and soya protein using different enzymes and different degrees of hydrolysis. The hydrolysates are characterized by: Average peptide length, gel chromatography, TCA-solubility, partition coefficient in 2-butanol:H₂O, and amino acid composition. The emulsifying capacity of these hydrolysates shows considerable variation (from 8 to 80 g oil per g protein), and this variation is discussed in relation to the molecular weight distribution and the hydrophobic properties of the hydrolysates. The dominating determinant for the emulsifying capacity is the relative concentration of long-chain peptides which are essential for achieving good emulsifying properties.

The properties and baking performances of commercial glutens

E.E. McDermott, FMBRA, Chorleywood, Herts.

Recently, considerable interest has been shown in the use of gluten to replace, wholly or partly, the protein in bread flour normally derived from Canadian or other third country wheats in the bread grist. The reason for this interest is an economic one since such wheats carry a net import charge. These economic advantages depend heavily on the efficiency with which added gluten simulates the performance of the natural proteins present in a mixed grist flour. It is important therefore to choose, from the glutens at present available to the industry, those which give the best possible performances. As a part of a continuing study on gluten we have compared the baking performances of a number of commercial glutens and have attempted to relate these baking performances with other gluten properties. The gluten properties studied included water adsorption, rate of hydration and particle size among many others. The results showed that good glutens can be separated from the not so good glutens by means of a few simple tests. Practical aspects of gluten denaturation during the drying of wet gluten are being investigated as well as the influence of flour type on the properties of the gluten prepared from it.

GELLAN GUM - A NEW GELLING POLYSACCHARIDE

V. J. Morris
AFRC Food Research Institute, Colney Lane, Norwich, U.K.

Gellan gum is an extracellular polysaccharide produced by aerobic fermentation of the micro-organism *Pseudomonas elodea*. It shows promise as an industrial gelling agent and is currently marketed as an agar replacement for microbial growth media. Although not as yet approved for food use, food applications have been explored, and the material shows potential as a "broad spectrum" gelling agent. The polymer is anionic and gelation is sensitive to cation type and concentration as well as the acetyl content of the polymer. Physical chemical studies have provided an insight into the mechanism of gelation. Details of these studies will be presented.

Thursday 02 August Council House-Conference Hall 14.00-17.00

Symposium on Molecular Evolution

POLYNUCLEOTIDES - MOLECULES CAPABLE OF DARWINIAN EVOLUTION

P. Schuster, Institut für Theoretische Chemie und Strahlenchemie
Universität Wien, Austria

Polynucleotides form the only class of molecules which are capable of efficient self-replication. This capability is also the most important property these biopolymers have in common with intact organisms. Polynucleotide replication has been studied extensively by experimental techniques. Thereby insight was obtained into the mechanism of mutation and selection on the molecular level. Although polynucleotides are not more than a very faint reflection of the biosphere they enable us to study the two basic features of Darwin's theory of evolution: the creation of variability by mutations and the optimization of properties through selection, the conditions of which are dictated by the environment. The accuracy of the replication process sets a limit to the length of the genome. Three examples for which experimental data are available will be presented:

- (1) enzyme free template induced polyribonucleotide synthesis
- (2) replication of viral RNA by specific replicases and
- (3) procaryotic DNA replication.

We find a straight forward explanation for the maximum genome lengths observed in nature with primitive namely procaryotic organisms. Present day biochemistry is based on the complex dynamic interrelations of proteins and nucleic acids. Both classes of molecules are well understood as far as molecular structures and static properties are concerned. Our knowledge on the dynamics of the processes taking place in the living cell is still fragmentary, although rapidly improving at present. Nevertheless, the data available seem to be sufficient to construct molecular model systems which can be subjected to experimental tests. Dynamical interrelations between proteins and nucleic acids became important at the origin of translation. We shall present a dynamical model of polynucleotide-polypeptide interactions which is based on higher order autocatalytic reactions. The dynamical model called hypercycle provides a possibility to suppress competition between polynucleotides and allows to form an organized system consisting of several polynucleotides. Some predictions on the origin of the genetic code which follow from this model will be discussed.

Thursday 02 August Council House-Conference Hall. 14.00-17.00

Symposium on Molecular Evolution

NOTION OF PRIMORDIAL BUILDING BLOCKS IN CONSTRUCTION OF GENES. Susumu Ohno
Beckman Research Institute of The City of Hope, Duarte, CA 91010

Recently, a number of investigators independently arrived at the conclusion that modern polypeptide chains are composites of oligopeptidic units. I contend that the reason for the above can be traced to the very beginning of the life either on this earth or elsewhere. The important thing to remember here is that natural selection began to play the customary omnipotent role only after the creation of the first cell and not before. Thus, there had to be certain *a priori* conditions that permitted the spontaneous generation of the first cell. The base triplet coding system with sets of chain-initiator and chain-terminators must have preexisted, or else the first set of polypeptide chains produced by the prebiotic translation machinery had to represent random sampling from the astronomical 20^{100} variety of 100-amino-acid-residue-long sequences, even if the average length of original polypeptide chains were that short. In the absence of natural selection, such a collection of randomly generated amino acid sequences would have remained as such without ever resulting in the creation of the life. Under the universal coding system, on the other hand, only $(\frac{61}{64})^{100} \times (\frac{1}{64})$ fraction (0.0132%) of the

300-base-long randomly generated base sequences could have specified an 100-amino-acid residue-long polypeptide chain. The above are the very reason for believing that the first set of coding sequences that made the creation of the life possible had to be repeats of base oligomers. Provided that the number of bases in each oligomeric unit is not a multiple of 3, repeats of base oligomers are endowed with three outstanding virtues that uniquely qualify them as the primordial coding sequence. First of all, a high proportion (e.g., 59.14% of monodecameric repeats) of them are capable of specifying long periodical polypeptide chains from all three reading frames. The next, periodical polypeptide chains specified by them tend to assume either α -helical or β -sheet secondary structure. The third and probably most important of all, the coding potential of oligomeric repeats are not easily destroyed by randomly sustained base substitutions, deletions and insertions, thus, permitting accumulation with time of a sufficient variety of periodical polypeptide chains to start the life.

Even modern organisms apparently employ the above strategy for the *de novo* generation of new coding sequences. For example, anti-freeze proteins in the blood of polar fish, sporozite antigens of malarial parasites and salivary proteins of the dipteran insect *Chironomus tentans* to encase its aquatic larvae are all oligopeptidic repeats. Other coding sequences that maintain sufficient degrees of initial repetitiousness may utilize different reading frames to encode two distinctly divergent polypeptide chains, instead of one.

Symposium on Molecular Evolution

EXONS AND THE EVOLUTION OF PROTEINS

C.C.F. Blake. Laboratory of Molecular Biophysics, University of Oxford, South Parks Road, Oxford, England.

Typically, a eucaryotic gene is a mosaic of coding sequences (exons) separated by a number of non-coding regions (introns). The most influential theory to account for this structure proposes that the split-genes organisation has a number of features that facilitate the large-scale evolution of protein molecules. The most far-reaching proposal involves the assumption that exons may encode particular protein functions which can be rearranged in new combinations by DNA recombination in the intronic regions of genes. Protein functions are normally associated with structural domains, and there is increasing evidence that domains of common structure and common function are present in otherwise different protein molecules. It is important, therefore, to determine whether or not molecules of this type have evolved by the so-called "exon shuffling" mechanism.

Correlation of gene fine-structures with known tertiary structures of proteins reveals a complex situation. First, it is evident that most protein domains are encoded by a number of exons, rather than one as proposed in the hypothesis. Secondly, it is clear that a number of large protein molecules have evolved by the multiple tandem duplication of a single primordial exon and/or a small cluster of exons. Thirdly, there are examples where it is suspected that exons have been lost or gained during this process, resulting in a functional modification of the duplicated protein. However in many cases the correlation of gene structure with protein structure gives no such clear-cut results. There are possible reasons for this: first, although in some genes the exon/intron pattern is remarkably stable, in others the pattern has apparently undergone change, which current evidence suggests is due to loss rather than gain of exons; secondly, it has been proposed that splice junctions are the loci of chain growth, thus increasing the sizes of exons. Finally, there is a good correlation between exon number and chain length for a wide range of protein molecules. This could indicate that exon encoded fragments represent the fundamental building blocks of protein molecules, suggesting a role in the earliest stages of protein evolution.

The indications are that exons encode protein fragments mostly in the range of 40-50 amino acids, which are often folded in a compact form and correspond to simple units of protein supersecondary structure. These observations can be combined with the discovery that certain, probably primitive, introns appear to act as sequence dependent RNA "enzymes" that catalyse their own removal, to produce a model for the early evolution of proteins. This model envisages exons as mini-genes coding for small folded polypeptides, flanked by non-coding sequences that define the self-excision RNA "enzymes". Multiple tandem duplications of these units, perhaps with exon shuffling, could lead to longer genes of mosaic structure producing larger proto-proteins built from the fragments which are seen as supersecondary structures. The introns excise themselves from the m-RNA. Thus the exon/intron pattern could represent the early structure of protein expressing genes, and at a later stage this structure could be utilised for the larger scale evolution processes described previously. This view would require either that the procaryotes had lost all the introns from their genomes, perhaps in the cause of efficiency, or that procaryotes and eucaryotes represent separate lines of evolution.

Symposium on Metal-Proteins and Electron Transfer

THE PROPERTIES OF CYTOCHROME-c

R.J.P. Williams, G.R. Moore, M.N. Robinson and G. Williams, Inorganic Chemistry Laboratory, South Parks Road, Oxford, England

All methyl and aromatic resonances in at least one state of cytochrome c in solution have been assigned in the proton NMR spectrum. The assignment allows a discussion of the protein structure in solution since the spectral differences between the oxidised and reduced states are very largely due to the pseudo-contact shift, originating at the paramagnetic Fe(III) atom. Only at the first level of approximation (\pm approx. 1.0Å) is it true to say that the several known crystal structures (amongst themselves) and the solution structures are the same independent of oxidation state and site in the crystal. We exclude surface residues since virtually all these residues, some thirty, are mobile and only their α -carbon coordinates are well defined. [The surface of a protein has no structure and new methods need to be designed for their description generally, see below]. Against the knowledge of the general similarity of all structures we have used NMR NOE and coupling constant methods to inspect solution structure locally against that given by the crystallographic analysis. In one region of the protein from about residue 38 to about residue 59 there are several noteworthy differences between solution and crystal, between the two different molecules in the crystal, and between oxidation states both in solution and in the solid state. Because the main crystal packing interface between molecules is exactly in this region we can not tell which features of the crystal structure changes on redox reaction are packing artefacts. The NMR study shows that the region in question is the most easily deformed part of the molecule. It is the most sensitive to redox change, temperature change, chemical modification and single or multiple amino acid substitutions (i.e. the site specific mutagenesis effect). Changes are relayed more weakly to more distant parts of the molecule, probably through helices as we have shown for other proteins.

We have used chemical shift and line width studies to elucidate the mobility of the protein in the time regime of chemical reaction interest. Flip and flap rates are very variable within the body of the protein from 10 per sec to 10^6 per sec. Their activation energies can be as large as 100KJ per mole indicating that a protein may act like a viscous solvent cage. Clearly reaction mechanisms inside proteins may not be described without reference to seemingly inert residues. The major mobility is underneath the heme (see later) apart from at the termini.

Apart from conformation change and mobility an understanding of electron transfer rates demands knowledge of the site from which the electron is transferred. This site must be in a reagent associated with the mobile and ill-defined surface. We have therefore started a study of the surface using NMR probe reagents. Regions of negative, positive and neutral electrostatic potential are searched for using positive, negative, and neutral probes respectively. Reagents such as ferricyanide bind to several sites so that definition of their reaction kinetics is extremely difficult. We have discovered that Fe(III).EDTA has a very selective single site which is not the major ferricyanide site. By the use of competitive blocking of different sites we are now studying the rates of electron transfer from known surface positions.

The structural data show how access of reactants to a closed heme pocket, compare cytochrome P-450, can be through the breaking of the labile Fe-methionine bond. The lability is connected with the lability of the 40-60 section of the protein under the heme (see above). Note also that this labile region around Ile-57 is a major antigenic site. The most antigenic sites of proteins may be partially hidden in those loops of the protein which are labile. Antibody specificity is then in part connected to the specific fold energy or part of the protein.

Cytochrome c functions can not be related to structure except through the study of dynamics in solution and this may be true of many proteins where knowledge of group positions is needed to \pm 1.0Å.

LONG DISTANCE ELECTRON TRANSFER IN METALLOPROTEINS

W. B. Gray, Arthur Amos Noyes Laboratory, California Institute of Technology, Pasadena, California, USA

Recent experiments have shown that electrons can be transferred relatively rapidly (greater than 1 s^{-1}) over long distances (12-13 Å) in proteins. Work in our laboratory in this area has involved heme and blue copper proteins that have been surface-modified with electron-transfer-active ruthenium complexes. Samples with pentaammineruthenium(III) (a_5Ru^{3+}) groups attached to histidine 33 in horse heart cytochrome c, histidine 83 in *Pseudomonas aeruginosa* azurin, and histidines 12, 48, 81, and 116 in sperm whale myoglobin (Mb) have been prepared and purified. Intramolecular electron transfer from Ru^{2+} to Fe^{3+} (or Cu^{2+}) in these derivatives has been studied over a range of temperatures by flash photolysis methods. In the experiment, the surface $\text{a}_5\text{Ru}(\text{His})^{3+}$ group is reduced by electronically excited $\text{Ru}(\text{bpy})_3^{2+}$ (bpy = 2,2'-bipyridine), and in the presence of sacrificial donors (to reduce $\text{Ru}(\text{bpy})_3^{3+}$) this event is followed by intramolecular $\text{a}_5\text{Ru}(\text{His})^{2+} \rightarrow \text{Fe}^{3+}$ (or Cu^{2+}) electron transfer. The rate of $\text{a}_5\text{Ru}(\text{His-33})^{2+} \rightarrow \text{Fe}^{3+}$ electron transfer in $\text{a}_5\text{Ru}(\text{His-33})$ cytochrome c is between 20 and 40 s^{-1} over the temperature range $0 - 80^\circ\text{C}$. (Above 80°C , the protein structure changes substantially, and intramolecular electron transfer is not observed.) The rate of $\text{a}_5\text{Ru}(\text{His-83})^{2+} \rightarrow \text{Cu}^{2+}$ electron transfer in $\text{a}_5\text{Ru}(\text{His-83})$ azurin also is temperature-independent (2 s^{-1} between -10 and 55°C). Analysis of the results for $\text{a}_5\text{Ru}(\text{His-33})$ cytochrome c and $\text{a}_5\text{Ru}(\text{His-83})$ azurin suggests that the reorganizational enthalpies of the protein electron transfer sites are less than 7 kcal mol^{-1} , which accords with the view that solvation effects are minimal in these protein interiors. Unlike the results obtained for cytochrome c and azurin, the intramolecular electron transfer rate in $\text{a}_5\text{Ru}(\text{His-48})\text{Mb}$ (the closest His-48 to heme distance is 13.3 Å) is strongly dependent on temperature (k increases from 0.05 s^{-1} at 20°C to 0.5 s^{-1} at 50°C), thereby indicating that the reorganizational enthalpy of the high-spin heme is greater than 10 kcal mol^{-1} . It is likely that a substantial fraction of this activation is attributable to partial dissociation of the axial water ligand in the high-spin ferriheme. The rates of intramolecular $\text{Ru}^{2+} \rightarrow \text{Fe}^{3+}$ electron transfer in the other three a_5RuMb derivatives fall well below 0.01 s^{-1} at 25°C (the closest His-heme distances are 19 Å (His-116), 20 Å (His-81), and 22 Å (His-12)). Examination of the electron transfer properties of these three derivatives is being extended to include experiments in which the reduction potential of the heme is increased by selected variations in axial ligation. Experiments also are underway aimed at the characterization of $(\text{en})_2\text{RuL}(\text{His})$ (en = ethylenediamine; L = H_2O , OH^- , Cl^-) derivatives of cytochrome c, azurin, and myoglobin. The driving force for Ru^{2+} to Fe^{3+} (or Cu^{2+}) electron transfer should be tunable over the range $0.1 - 0.5 \text{ V}$ in these derivatives. At the higher driving forces it may be possible to obtain intramolecular electron transfer rates for myoglobin derivatives in which the ruthenium complex is 20 Å from the ferriheme.

Symposium on Metal-Proteins and Electron Transfer

METAL CENTERS AND ELECTRON TRANSFER IN CYTOCHROME c OXIDASE AND LACCASE

B.G. Malmström, Department of Biochemistry and Biophysics, University of Göteborg and Chalmers University of Technology, Göteborg, Sweden.

Cytochrome c oxidase (EC 1.9.3.1) and the blue oxidase, laccase (EC 1.10.3.1), couple one-electron transfers from reducing substrates to the four-electron reduction of O_2 to $2H_2O$. They are structurally related with some metal binding domains of apparently common evolutionary origin. In both enzymes four metal centers are present in catalytic units, which are structurally and functionally asymmetric. In the oxidized proteins, two of these centers are detectable by EPR, namely cytochrome a_3^{3+} and Cu_A^{2+} in cytochrome oxidase and types 1 and 2 Cu^{2+} in laccase. The EPR-detectable metal ions serve as the primary acceptors of electrons from reducing substrates. From these metal centers the electrons are transferred intramolecularly to the EPR-nondetectable centers, cytochrome a_3 - Cu_B and the type 3 copper ions, respectively. The EPR-nondetectable centers constitute strongly exchange-coupled metal pairs, and they are the O_2 -reducing sites of the enzymes.

The structures of the metal centers in both cytochrome oxidase and laccase have been characterized by a variety of spectroscopic techniques (optical, EPR, ENDOR, resonance Raman and EXAFS) and, to some extent, by amino acid sequence comparisons. Each center has unique structural features which favor its particular role in the catalytic process. The structures are forced upon the metal ions by the overall protein conformation through a rack mechanism, as will be discussed in some detail for type 1 (or blue) Cu^{2+} centers. The three-dimensional structures of two single-site blue proteins, plastocyanin and azurin, have been determined. The metal ligands are the side chains of two histidine, one cysteine and one methionine residues. The energies of the $d-d$ transitions in plastocyanin show that the CuN_2SS^* site is more than 70 kJ mol^{-1} ligand-field destabilized above an optimally stabilized planar Cu^{2+} site by the protein rack. The high reduction potentials and the facile outer-sphere electron transfer kinetic properties are directly related to this rack destabilization. Variations in the reduction potentials between different blue proteins can also be explained by rack-induced bonding. There is a linear relationship between ligand-field strengths and electron-transfer enthalpies. This suggests that the potentials are tuned by changes in π back bonding, which would lead to different degrees of preferential stabilization of the reduced ($Cu(I)$) state. Sulfur ligands are obvious candidates for this rack-induced π bonding. As the $S(\text{met})$ - Cu and $S(\text{cys})$ - Cu bonds are made shorter, the reduction potentials increase. ENDOR and resonance-Raman results show that the Cu - S interactions do become stronger with increasing electron-transfer enthalpies, as the model predicts.

Amino acid sequence studies indicate that the coordination structure of Cu_A in cytochrome oxidase is related to that of blue sites. They also suggest that Cu_B and type 3 Cu^{2+} in the bimetallic sites have similar structures. This is supported by EPR and ENDOR spectra, which show that in both sites there are three protein N ligands with H_2O or OH^- as the fourth ligand. The reduced bimetallic centers react rapidly with O_2 to form peroxide intermediates. These are further reduced in two consecutive one-electron reactions. The paramagnetic intermediates formed on addition of the first electron are suggested to have the following structures: $[Cu_A^{2+} - OH^- \cdots O = Fe^{4+}]$ in cytochrome oxidase and $[Cu^{2+} - O^- - Cu^{2+}]$ in laccase.

Electron-transfer in cytochrome oxidase is coupled to proton translocation from the matrix to the cytosol side of the inner mitochondrial membrane. It is suggested that this coupling involves a conformational change triggered by the reduction of cytochrome a and Cu_A and monitored as an increased rate of binding of HCN to oxidized cytochrome a_3 . The coupling process will be described as an essentially kinetic phenomenon. It is suggested that rapid electron transfer from the primary acceptors to the O_2 -reducing site can only take place in a protonated form of the oxidase.

Symposium on Polysaccharides and Glycoproteins

STRUCTURAL STUDIES ON THE CARBOHYDRATE CHAINS OF GLYCOPROTEINS.

Johannes F.G. Vliegthart and Herman van Halbeek, Department of Bio-Organic Chemistry, University of Utrecht, Croesestraat 79, Utrecht, The Netherlands

Glycoproteins represent a class of biopolymers consisting of a polypeptide backbone having one or more covalently bound carbohydrate chains. The linkage between sugar and protein can be N-glycosidically by attachment to the amide group of asparagine or O-glycosidically by attachment to the hydroxyl group of hydroxy amino acids. The carbohydrate chains exhibit a large variation in primary structure.

Several factors complicate the determination of the primary structure of the carbohydrate chains of glycoproteins. In particular the occurrence of more than one carbohydrate chain which may be N- or O-glycosidically bound to the protein, in conjunction with their natural or artificially introduced (micro)heterogeneity makes it almost impossible to analyse the carbohydrate chains at the level of the intact macromolecule. Degradation to glycopeptides, oligosaccharides or oligosaccharide-alditols is necessary.

For the analysis of the O-linked mucin type of glycoprotein carbohydrate chains, oligosaccharide-alditols obtained after alkaline borohydride degradation are very suitable. After separation and purification the oligosaccharide-alditols are amenable for structural analysis. In the past few years we have had the opportunity to demonstrate that high-resolution ^1H -NMR spectroscopy at 500 MHz, in combination with sugar analysis, is an extremely powerful method for primary structural characterization of such oligosaccharide-alditols. The structural-reporter-group concept, used to translate a ^1H -NMR spectrum of an oligosaccharide into the primary structure [1], enables to define the core, backbone and peripheral portions of the structures in a rapid and non-destructive way (e.g. [2-4]). Moreover, ^1H -NMR allows the adequate analysis of mixtures of structurally related oligosaccharide-alditols [2]. Therefore it can cope with microheterogeneity to a considerable extent. For primary structural analysis, about 20 nanomoles of compound are sufficient.

The mucin type of oligosaccharide-alditols have GalNAc-ol as the common element. It can be extended to different types of cores. A substituent can be present at position 3 and/or position 6. At C-3, β -Gal or β -GlcNAc may be found, whereas at C-6 β -GlcNAc or α -Neu5Ac can occur. By consequence 8 different core structures can in principle exist. Recently, the existence in nature of all types could be demonstrated and they were unambiguously characterized by ^1H -NMR. The structural reporter groups of GalNAc-ol reflect the substitution pattern. The backbone usually consists of β -Gal and β -GlcNAc residues linked 1 \rightarrow 3 or 1 \rightarrow 4. In one chain these both types of glycosidic linkages may occur. Immunodeterminants are often present in these carbohydrate chains. They are extensions of the backbone and occupy terminal positions in the molecule. Fuc and Neu5Ac are frequently occurring constituents of such determinants. Especially the peripheral parts of these compounds can readily be identified on the basis of the structural reporter group concept.

In case when 5 to 10 millimoles of a pure oligosaccharide-alditol can be made available, more advanced NMR techniques, e.g. two-dimensional J-resolved and correlated spectroscopy allow insight to be gained into its solution conformation. Knowledge of the spatial structure is essential to understand recognition phenomena at the molecular level.

References

- [1] J.F.G. Vliegthart, L. Dorland & H. van Halbeek (1983) Adv. Carbohydr. Chem. Biochem. 41, 209-374
- [2] H. van Halbeek, L. Dorland, J.F.G. Vliegthart, W.E. Hull, G. Lamblin, M. Lhermitte, A. Boersma & P. Roussel (1982) Eur. J. Biochem. 127, 7-20
- [3] H. van Halbeek, L. Dorland, J.F.G. Vliegthart, N.K. Kochetkov, N.P. Arbatsky & V.A. Derevitskaya (1982) Eur. J. Biochem. 127, 21-29
- [4] D. Blanchard, J.-P. Cartron, B. Fournet, J. Montreuil, H. van Halbeek & J.F.G. Vliegthart (1983) J. Biol. Chem. 258, 7691-7695

Symposium on Polysaccharides and Glycoproteins

UNIFIED MOLECULAR MECHANISM FOR GELATION IN POLYSACCHARIDE SYSTEMS

O. Smidsrød, Institute of marine biochemistry, The Norwegian Institute of Technology, Trondheim, Norway.

Many polysaccharides are potent gel formers with a wide variety of uses inside the food and pharmaceutical industries, and with large potentials for uses in modern biotechnology. With some few exceptions (e.g. agarose, galactomannans) all the gel forming polysaccharides are polyelectrolytes with chain conformations and physical properties strongly dependent on the ionic environment. Gel systems from the three polysaccharides alginate, κ -carrageenan and Gellan Gum (an extracellular polysaccharide elaborated by *Pseudomonas elodea*) have been studied by gel strength measurements, viscometry, light scattering, osmometry, polarimetry and NMR in order to get information about the gel structure. In all three cases the salt induced physical crosslinks in the gel network are due to side-by-side aggregation of stiff polymer chain sections. In alginate the stiffness is inherent in the chain due to diaxial glycosidic linkage. In κ -carrageenan a single helix with a strong tendency for association is formed prior to/or simultaneous with the chain association. In Gellan Gum chain stiffening occurs during the association reaction. All three systems show strong ion specificity in the association reaction. In alginate and κ -carrageenan this may be correlated to an ion-selective interchain sitebinding of counterions. In Gellan Gum there are no indications of site-binding of counterions inside the Group I cations, in spite of a marked ion-specific gelation with such cations. This suggests that the state of hydration of the counterions must be considered in addition to the possibilities for site-binding. Our limited knowledge of the chain conformation in the junction zones does not permit a detailed discussion of the role of the counterions in the association reaction, but it may be suggested that the degree of dehydration is different in the three polysaccharide systems.

Symposium on Polysaccharides and Glycoproteins

SPATIAL CONFORMATION AND MOLECULAR BIOLOGY OF GLYCOPROTEINS

J. Montreuil, Laboratoire de Chimie Biologique (LA CNRS 217), Université des Sciences et Techniques de Lille I, Villeneuve d'Ascq, France.

Glycoproteins, which result from the covalent linkage of a sugar moiety called *glycan* with proteins, have acquired a great importance in the 15 past years thanks to a series of discoveries demonstrating the role played by the carbohydrate moiety. In fact, we know now that glycans 1°) influence the conformation of peptide chain ; 2°) protect the protein against proteolytic attack ; 3°) diminish the immunogenicity of proteins ; 4°) are receptor sites for viruses, proteins and hormones ; 5°) regulate the catabolism of circulating proteins and determine the lifetime of proteins and cells ; 6°) control the social life of cell by intervening in intercellular adhesion and recognition and in cell-contact inhibition. In this connection, the profound modifications of the glycan structures observed in cancerous cell membranes could be a factor of cancer induction and metastatic diffusion.

Taking advantage of the knowledge of the primary structure of glycans, which will be briefly reviewed, the above points will be envisaged on the basis of the spatial conformation of glycans. Concerning the latter, we shall appreciate the evolution of ideas which, at the beginning, were speculative and resulted from the molecular model construction of the human serum transferrin biantennary glycan. A "Y-conformation" was first proposed. A few later, on the basis of X-ray diffraction, the "T-conformation" was suggested. Then, the "bird-conformation" was described which spreads the 2 antennae in opposite direction. This view was supported by computer calculations, X-ray diffraction and NMR spectroscopy.

The Y-, T- and bird-conformers are interconvertible as demonstrated by EPR of spin-labelled glycans, by using NMR techniques, including two-dimensional ¹H-nuclear Overhauser effect (NOE) experiments. The fundamental role of the mannotriose core in the conformation of glycans has been recently pointed out by Carver et al. who demonstrated by using proton NMR that the trisaccharide has two preferred conformers with variability occurring mainly at the 1,6-linkage : a linear structure, leading to the bird-conformation and a bent structure, leading to a "broken wing-conformation" in which the α -1,6-antenna is folded back along the di-N-acetylchitobiose residue of the innercore chiefly in the case of the presence of a bisecting GlcNAc residue. The bird-conformation, as well as the concept of the mobility of antennae, is in a good agreement with the reactivity of lectins by rendering accessible any specific sugar structure, and with the activity of glycosyltransferases by making attainable the substitutable hydroxyl groups, even in the case of penta-antennary structures.

On the basis of the bird-conformation of a biantennary glycan, the construction of the molecular model of tetraantennary structure leads to the so called "umbrella-conformation" in which the four antennae are disposed almost perpendicularly in the same plane and parallel to the protein surface with which they can interact and link by ionic, hydrophobic and/or hydrogen bonds.

This speculative concept has been recently confirmed by NMR and computerized hard-sphere molecular modelling and by neutron scattering study. So, tri- and tetraantennary glycans could mask large parts of the protein moiety due to the fact that each of them, in adopting an umbrella-conformation, covers an area of about 2.000 Å². So could be explained the resistance of certain glycoproteins towards proteases and their weak antigenicity, glycans acting as protective shields towards the proteases, and their weak antigenicity, glycans acting as protective shields towards the protein moiety. This view could lead to the explanation of the peculiar behaviour and resistance of metastatic cancerous cells since we know now that the membrane glycoproteins of this kind of cells are significantly enriched in tri- and tetraantennary glycans.

Reviews : 1) Montreuil J., 1980, Adv. Carbohydr. Chem. Biochem., 37, 157-223 ;

2) Montreuil J., 1982, Comprehensive Biochemistry, 19B, Part II, 1-188 ;

3) Montreuil J., 1983, Biochem. Soc. Trans., 11, 134-136.

Thursday 02 August

Colston Hall-Main Hall

17.15-18.00

Plenary Lecture by A. Finkelstein

(The American Society of General Physiologists Lecture)

WATER MOVEMENT THROUGH CHANNELS IN LIPID BILAYERS AND CELL MEMBRANES.

A. Finkelstein, Department of Physiology and Biophysics, Albert Einstein College of Medicine, Bronx, New York, U.S.A.

The only direct data on the water permeability coefficients, P_f and $P_d(H_2O)$, of "biological-like" channels comes from studies on the channels formed in planar lipid bilayer membranes by gramicidin A and the polyene antibiotics nystatin and amphotericin B. This lecture reviews these data, along with water permeability measurements on unmodified lipid bilayer membranes, and uses them to infer the magnitude of water transport through channels in plasma membranes.

In unmodified lipid bilayers, $P_f/P_d(H_2O) = 1$. Water traverses the bilayer by a solubility-diffusion mechanism; the magnitude of the water permeability coefficients, which is a function of acyl chain lengths, their degree of saturation, sterol content, and temperature, varies from a low of 2×10^{-5} cm/sec to a high of 10^{-2} cm/sec. These values span almost the entire range reported for plasma membranes.

Nystatin and amphotericin B form channels (pores) of approximately 4A radius that manifest classical sieving properties for small nonelectrolytes up to the size of glucose and in which $P_f/P_d(H_2O) \approx 3$. Interestingly, these polyenes form two types of channels which we have dubbed "single-length" and "double-length" channels. The double-length channel is formed by two "barrels" hydrogen-bonded end-to-end, with each barrel consisting of 8 to 10 nystatin (or amphotericin B) monomers arranged circumferentially as staves. The single-length channel has essentially the same structure, except that only one "barrel" spans the bilayer to form a functional channel. Apparently, there is enough flexibility in bilayer thickness for the same bilayer to accommodate both types of channels, even though they differ in length by a factor of two. Gramicidin A, in contrast to nystatin and amphotericin B, forms channels of only 2A radius that exclude urea and all other larger nonelectrolytes. Despite its smaller radius, $P_f/P_d(H_2O) \approx 6$ for the gramicidin A channel. This larger value is a consequence of single-file transport of water in the 2A radius channel: for a channel in which water undergoes this mode of transport, $P_f/P_d(H_2O) = N$, where N is the number of water molecules in the channel. N can also be determined from electrokinetic measurements (streaming potentials and electro-osmosis), because single-file transport of both ions and water imposes an obligatory coupling of the movement of all N water molecules within the channel to the transport of an ion through the channel.

Combining macroscopic water permeability measurements with single channel conductance data, one can determine P_f per channel for nystatin, amphotericin B, and gramicidin A channels. The values are in surprising agreement with those calculated from a naive application of Poiseuille's Law. Applying these results to channels in plasma membranes, I conclude that there are too few channels in most plasma membranes to provide the major pathway for water movement; by implication, most water movement across plasma membranes occurs through their lipid bilayers. An important exception is the antidiuretic hormone (ADH)-induced water permeability pathway in the luminal membrane of toad urinary bladder and cortical collecting tubules, which is formed by channels specifically permeable to water. These channels, like those formed by gramicidin A, are so narrow at some place along their length that single-file transport must occur there. Unlike gramicidin A channels, however, ADH-induced channels have an immeasurably small conductance, implying a very low permeability to ions. A comparison of water and nonelectrolyte permeability with ion permeability, for the channels considered in this lecture, illustrates the dominant role electrostatic forces play in the latter and hence the difficulty in determining channel size from single-channel conductance measurements. For example, although the radius of the amphotericin B channel is larger than that of the gramicidin A channel, its conductance is 40-fold smaller. This disparity between channel radius and ion permeability is particularly striking, since neither channel contains charged groups in its lumen.

Thursday 02 August Congress Centre-First Floor Posters 001-006

Posters on Cross-Bridge Mechanisms and Muscle Contraction

001. ORAL PRESENTATION

ANGLE OF ACTIVE SITE OF MYOSIN HEADS IN CONTRACTING MUSCLE DURING SUDDEN LENGTH CHANGE T. YANAGIDA, Department of Biophysical Engineering, Osaka University, Toyonaka, Osaka, Japan.

In muscle, myosin cross-bridges undergo a cyclic interaction with F-actin coupled with ATP hydrolysis. The sliding force is believed to be generated by the cross-bridges in the attached state but their detailed structure has not been sufficiently elucidated. Investigating the structure of working cross-bridges requires clarification of the correlation between the structural state and the chemical state of the myosin-nucleotide complex and of the dynamic structure of the cross-bridges by time-resolved measurements. This study used a fluorescent ATP analogue, N⁶-etheno-2-aza-ATP (ε-2-aza-ATP). Its fluorescence is considerably enhanced upon binding with heavy meromyosin and the enhancement is dependent of the chemical state of myosin-nucleotide complex. I show here that bound nucleotides in the intermediate state (probably, actomyosin-ε-2-aza-ADP-Pi) of the cross-bridge cycle in isometrically contracting muscle are highly oriented relative to the F-actin axis at the same angle as that in rigor with ε-2-aza-ADP and furthermore that the orientation of the bound nucleotides is not altered during sudden changes in the length of isometrically contracting muscle. The present results indicate that an orientation of the active site of the myosin head remains unchanged during the force generation.

003

ANALYSIS OF OPTICAL DIFFRACTION PATTERNS OF ISOLATED SINGLE SKELETAL MUSCLE FIBRES J.C. Hwang, Y.M. Cheung and A.F. Leung, Department of Physiology, Faculty of Medicine, University of Hong Kong, 5 Sassoon Road, Hong Kong and Department of Physics, The Chinese University of Hong Kong, Shatin, Hong Kong.

Diffractions of a normally incident laser beam by single skeletal muscle fibres of frog were projected directly onto photographic films. Individual substructures within each diffraction order were clearly resolved. The intensities of the substructures increased uniformly when the bathing solution became hypotonic and decreased again uniformly when the solution became hypertonic. However, the pattern of the substructures remain nearly constant in different solutions. The meridional intensity variations with different bathing solutions could be used to monitor the cross-sectional areas of the fibre. The equatorial intensity variations allowed estimation of the myofibrillar diameter. In experiments where the meridional intensities of different diffraction orders were measured and the myofibrillar diameters determined in different solutions but for the same illuminated spot, the intensity of each diffraction order increased nearly with the fourth power of myofibrillar diameter. The constancy of the diffraction substructure pattern in different bathing solutions and the meridional intensity variations with myofibrillar diameters rule out the existence of large discrete diffraction planes in muscle fibres but seem to favor a model in which the myofibrillar registers are randomized.

005

LIMITED TRYPTIC FRAGMENTATION OF BOVINE CARDIAC TROPONIN C. U.D. McCubbin and C.M. Kay, MRC Group in Protein Structure and Function, Department of Biochemistry, University of Alberta, Edmonton, Canada T6G 2H7.

Tryptic digestion of bovine cardiac troponin C has been carried out both in the presence and absence of Ca²⁺ (TR-C and TR-E fragments respectively). TR-C fragments (MW ~13K to 6K) resulted from a digestion time of 1 hour at an enzyme to protein ratio of 1:100 in the presence of 2mM Ca²⁺ at 23°C. A mixture of TR-E peptides (MW ~11K to 6K) was generated from a 3 minute digestion with the enzyme at a ratio of 1:500 at 23°C. The resulting peptides in both cases were purified by a combination of gel filtration, hydrophobic interaction chromatography on Phenyl Sepharose, and in some cases, by preliminary HPLC on reverse-phase supports. Purity was monitored by SDS and SDS/urea PAGE and amino acid analysis. CD and fluorescence studies monitored the ability of these peptides to bind Ca²⁺ and to interact with cardiac TN-T and TN-I. Certain of the fragments containing cysteine residues have been labelled with a thiol-specific fluorescent probe and the resulting derivatives have proved very useful in measuring Ca²⁺ affinity and the binding of cardiac TN-I and TN-T. These latter proteins have also been labelled specifically at thiol functions and the binding to the tryptic peptides monitored. Tryptic cleavage of cardiac TN-C results in a more complex mixture of peptides than is found with the skeletal protein, but here too the large peptide fragments retain many of the properties of the intact protein molecule. (Supported by Medical Research Council of Canada and Alberta Heritage Foundation for Medical Research)

002

FINE STRUCTURE OF EARTHWORM HEART MUSCLE. S.G. Pal and P.K. Dinda, Deptt. of Zoology, Calcutta University, CALCUTTA 700 019, INDIA.

On the evolutionary scale the invertebrate cardiology is hardly exhaustively surveyed and understood. The structural modulations of the various subsystems of the heart muscles of the earthworms (*Pheretima posthuma*) include the oblique striations, contractile proteins, arrangement of the Z-bodies, distribution of the tubule-vacuolar profiles, mitochondria, etc. Essentially these muscle cells are of circumferential type where the striations or bands criss-cross diagonally with swarms of mitochondria placed at the periphery. The narrow tubular systems regularly alternate with the Z-bodies along the long axis of the cell. The superficial vacuolar fields lying close to the sarcolemma are quite extensive. The contractile apparatus is formed of both thick and thin myofilaments measuring 300-400Å and 60Å in thickness respectively. The ratio between thin and thick myofilaments is about 16. The thick myofilaments taper at both ends. We have not seen a Golgi body. Glycogen particles are scarce. A marked presence of collagenous septum or partition between some of the muscle cells of *Pheretima posthuma* has been observed. Apparently these muscles are closer to those of arthropods, molluscs and echinoderms, but oversimplified.

004

MODULATION OF NET CA²⁺-LOADING VIA K-CHANNELS IN THE MEMBRANES OF SARCOPLASMIC RETICULUM R.H.A. Fink & D.G. Stephenson, Department of Zoology, La Trobe University, Melbourne, Victoria, Australia.

K⁺ selective channels have recently been found in sarcoplasmic reticulum (SR) membranes, and it has been shown that they can be blocked with 4-aminopyridine (4AP) and other substances. In mechanically skinned fibres of amphibian iliofibularis muscle (*Bufo marinus*) we used blockers of SR-K-channels as a tool to study the generally unknown physiological function of these channels. The preparations with intact SR were fully loaded at pCa 6.5 and Ca²⁺ was then released by 30 to 45mM caffeine in a solution containing 0.75 to 1mM EGTA. Experiments were performed at 0.3 and 1mM free Mg²⁺. As a relative measure of the loaded Ca²⁺ we compared peak tension (P) and the area (A) under the force transient developed by the fibres during Ca²⁺-release in the presence or absence of the blockers. Increases up to 60% for P and 80% for A were observed after loading in the presence of 4AP and other blockers. Partial substitution of K by the less permeant Na ion during loading also increased the net Ca²⁺ loaded by the SR. These results lead to the conclusion that SR-K-channels can have a modulating function on Ca²⁺ movements across SR-membranes.

Supported by NH&MRC (Australia) and ARCS.

006

HYDROPHOBIC PROTEINS AND LIPIDS IN THE MUSCLE Z-DISC B. Bullard¹, G. Sainsbury², N. Miller¹ and J. Erriman³ ¹AFRC Institute of Animal Physiology, Babraham, Cambridge U.K., ²Dept. of Zoology, Oxford, U.K., ³EMBL, Heidelberg Germany.

Two hydrophobic proteins (zeelins) make up a large proportion of the Z-disc; the capacity of zeelins to form cross links between actin filaments in the Z-disc is being investigated. The proteins have the amino acid composition of intrinsic membrane proteins and are insoluble in aqueous solutions. Micelles that are miscible with water are formed under certain conditions. The micelles are 60 nm in diameter and are made up of subunits; they are similar to structures formed by amphiphilic membrane proteins. G-actin binds to the hydrophilic surface of the micelles obscuring the subunit structure. The Z-disc has 8% lipid, the composition of which differs from the composition of myofibrillar lipid. The particular lipids in the Z-disc may be associated with the hydrophobic region of zeelins and may regulate the calcium activated protease which degrades the Z-disc. Financed by a grant from the Muscular Dystrophy Group of Great Britain.

Thursday 02 August Congress Centre-First Floor Posters 007-012

Posters on Cross-Bridge Mechanisms and Muscle Contraction

007

THE RELATION BETWEEN MYOFIBRIL DYNAMICS AND CROSS-BRIDGE MOTION. N. Berovic, R.A. Thornhill, Physics Department and Zoology Department, University of Birmingham, Birmingham, U.K.

Dynamics of myofibrils is examined by computer simulation. The myofibril is treated as a linear chain of two kinds of bodies M and A, consisting of myosin and actin filaments respectively.

The interaction potential between M and A is constructed on the basis of filament molecular structure and the anharmonicity of the potential is taken into account. If a random energy input is included in the equations of motion, the results reproduce physiological phenomena of muscle contraction. The exact treatment of the sarcomere dynamics makes it possible to establish quantitative relationship between macroscopic quantities such as force and shortening velocity, and, microscopic parameters like the cross-bridge-actin potential and rate of energy input.

We obtain a consistent interpretation of experimental data on time resolved X-ray diffraction (HUXLEY), mobility of cross-bridges (THOMAS) and stepwise shortening (POLLACK).

009

THIN FILAMENT X-RAY DIFFRACTION IN CONTRACTING FROG MUSCLE. M. Kress, H.E. Huxley, A.R. Faruqi, M.H.J. Koch and J. Hendrix MRC Lab. of Mol. Biol., Cambridge, UK and EMBL Outstation, Hamburg, FRG

Using synchrotron radiation as an high intensity X-ray source the pattern given by contracting live frog muscle can be followed with high time resolution. The so-called second actin layer line (181 Å) arises from movement of tropomyosin. We find that it reaches half its final intensity 17 ms after the stimulus, relatively independent of temperature. The changes in the equatorial reflections, which arise from movement of crossbridges towards the thin filaments, occur 14 ms later. In overstretched muscle, where thick and thin filaments no longer overlap, the reflection appears upon stimulation with similar time course and intensity as in full overlap. This indicates that tropomyosin movement in response to calcium binding to troponin is the first structural step in muscular contraction and not just a result of myosin binding. Lastly, the same intensity as in contracting muscle is seen in rigor, where tropomyosin is probably locked in the active position by the attached crossbridges. The 59 Å layer line shows about 50 % increase during contraction. This is only partly due to labelling by attaching crossbridges, as the change can precede the equatorial changes and about half the change is still present in overstretched muscle. The 51 Å layer line doubles its intensity during contraction, but shows no major change in overstretched muscle. Both 59 Å layer line and second layer line revert ahead of tension and the equatorial changes.

011

CALDESMON AND MYOSIN LIGHT CHAIN KINASE: MAJOR CALMODULIN-BINDING PROTEINS OF SMOOTH MUSCLE. M.P. Walsh and P.K. Ngai, Department of Medical Biochemistry, University of Calgary, Alberta, Canada.

Smooth muscle (chicken gizzard) contains two major calmodulin (CaM)-binding proteins which have been purified and identified as myosin light chain kinase (MLCK) and caldesmon (CaD). Their tissue concentrations were estimated to be ~4 μM and ~20 μM, respectively, by densitometric scanning of dodecyl sulphate-polyacrylamide gradient gels of tissue homogenates. Consistent with the findings of most investigators, MLCK (which catalyzes phosphorylation of the 20,000-dalton light chains of myosin) plays a central role in Ca²⁺-mediated control of smooth muscle contraction, as shown by its effect on the actin-activated myosin Mg²⁺-ATPase activity and superprecipitation in a system reconstituted from purified contractile and regulatory proteins. Myosin phosphorylation is also involved in the regulation of myosin filament assembly. MLCK and CaD both interact with F-actin; however, binding of CaD to F-actin is blocked in the presence of Ca²⁺-CaM. CaD does not inhibit the activities of MLCK or cyclic nucleotide phosphodiesterase (PDE; another CaM-dependent enzyme), suggesting it may interact with CaM at a site distinct from the MLCK- and PDE-binding site. Consistent with this finding, CaD does not affect the actin-activated myosin Mg²⁺-ATPase or superprecipitation in a reconstituted system, nor does it affect myosin filament assembly induced by myosin phosphorylation. (Supported by MRC Canada and the Alberta Heritage Foundation for Medical Research).

008

INTRACELLULAR EFFECTS OF VERAPAMIL (VP) AND DILTIAZEM (DT) ON RABBIT MYOCARDIUM. J.Y. Su, Department of Anesthesiology, University of Washington, Seattle, WA USA

The importance of intracellular VP on the Ca²⁺ channel blocking action in the heart has been reported. In this study we investigated the effects of VP and DT (tertiary amines) on intracellular sites [contractile proteins and sarcoplasmic reticulum (SR)] of the contractile process of the muscle using functionally skinned myocardial cells. Papillary muscle was isolated from rabbits. Pieces of the muscle were homogenized (sarcolemma disrupted) in relaxing solution. A fiber bundle was dissected from the homogenate and mounted on a photodiode tension transducer. The bathing solution contained 0.1 M Mg²⁺, 70 mM K⁺ + Na⁺, 2 mM MgATP²⁻, 15 mM creatine phosphate, pCa = -log [Ca²⁺] (M) = 9, 6.5-5.0 buffered with 0.05-7 mM EGTA, methanesulfonate (major anion), pH 7.00 at 23°C with indazole and μ = 0.15. High EGTA (7 mM) was used to control free [Ca²⁺] to study Ca²⁺-activated tension development of the contractile proteins. The SR in the fiber bundle was loaded with Ca²⁺, then caffeine was used to release the Ca²⁺ from the SR resulting in a tension transient. We found that VP and DT (0.1-3 μM) increased the maximal (3-20%), and the submaximal Ca²⁺-activated tension development (0.25 pCa unit left shift of the pCa-tension curve at 1 μM VP or DT) in a dose-dependent manner. Both drugs, at the same dose range, directly caused Ca²⁺ release from the SR, and decreased Ca²⁺ uptake by the SR. DT, but not VP, inhibited the caffeine-induced Ca²⁺ release from the SR. It is concluded that both drugs have similar mechanisms of action on the contractile proteins and the SR of the skinned myocardial cells. Supported by grants HL 20754 and HL 01100 (RCDA) from NIH.

010

THE SPATIAL ARRANGEMENT OF BOTH HEADS OF THE MYOSIN MOLECULE ON RELAXED TARANTULA MUSCLE THICK FILAMENTS. R. Padrón, R.A. Crowther and R. Craig. MRC Laboratory of Molecular Biology, Cambridge, U.K.

We have made a three dimensional image reconstruction from minimal dose electron micrographs of negatively stained relaxed thick filaments from the leg muscle of tarantula. Particles were selected by general visual appearance and by the strength and symmetry of their optical diffraction patterns, which extend meridionally to the 6th order of 43.5 nm, but appear to show peaks to higher radial resolution. Phase differences across the meridian indicated 4-fold rotational symmetry, so that on a given layer-line Bessel function contributions of different orders start to overlap at fairly low resolution, and must be separated computationally by combining data from different views. Independent reconstructions agree well and show more detail than the previous reconstructions of thick filaments of *Limulus* and scallop. The strongest feature is a set of long pitch (4x43.5 nm) right-handed helical ridges. There are also ridges with an axial spacing of 14.5 nm lying in planes roughly normal to the filament axis and running circumferentially. We suggest that the latter may be formed by the stacking of an S1 head from one myosin molecule on an S1 head from an axially neighbouring molecule. This interpretation must be checked by further work, but it does suggest that sufficient detail is present to make it worthwhile to undertake biochemical experiments to observe structural changes in the filaments.

012

Mechanical properties of cross-bridges in smooth muscle. N.L. Stephens, Dept. Physiol., Faculty of Med., Univ. of Manitoba, Winnipeg, Manitoba, Canada.

Abrupt load clamping of isotonically shortening airway smooth muscle showed stiffness of its series elastic component was proportional to active force, hence cross-bridge theory was applied to analysis of its contraction. During preloaded (5mN) isometric shortening, 10 mN clamps were applied. In early shortening (within 5 sec), after initial elongation, shortening redeveloped. After 5 sec no shortening redeveloped. The 5 sec point was termed transition time (TT). dP/dL studies at 4 sec and 10 sec showed the same stiffness. We concluded that at these two times the same numbers of cross-bridges were involved, those in early phase cycling at normal rate, those in late, cycling slowly. Since TT is influenced by load, the experiment was repeated using zero loads, and a zero-load velocity vs time plot obtained, analysis of which showed maximum zero-load velocity (V₀) developed 2 sec after stimulus onset. This was followed by a decline which was fitted by two exponential terms: V₀ = a e^{-k₁t} + b e^{-k₂t}. The rate constant and half-time of the rapid compartment were 0.13 ± 0.05 (SE) and 1.86 sec ± 0.21 (SE) respectively. Those for the slow compartment were 0.17 ± 0.04 (SE) and 2.36 sec ± 0.24 (SE). We speculate the rapid compartment reflects normally cycling cross-bridges while the slow represents slowly cycling bridges. The equation permits us to quantitate, for any given moment, the ratio of the two types of bridges. Thus at an average TT of 5 sec, slowly cycling bridges contributed to 90.7% ± 11.2 (SE) of the contraction.

Thursday 02 August Congress Centre-First Floor Posters 013-018

Posters on Cross-Bridge Mechanisms and Muscle Contraction

013

THEORETICAL FRAUNHOFER LIGHT DIFFRACTION PATTERNS CALCULATED FROM 3-D SARCOMERE ARRAYS IMAGED FROM RESTING HEART CELLS. K.P. Roos and A.F. Leung*, Department of Physiology, UCLA School of Medicine, Los Angeles, CA, USA, and *Department of Physics, Chinese University of Hong Kong, Shatin, Hong Kong.

Discrete sarcomere positions have been obtained throughout the volumes of calcium-tolerant resting heart cells by direct computer interfaced high-resolution optical imaging (Roos & Brady, Biophys. J., 40:233, 1982). Each sarcomere position is stored in a 3-D matrix array from which Fraunhofer light diffraction patterns have been calculated using numerical methods based on the grating equation (Leung, Comp. Prog. Biomed., 15:163, 1982). Calculated diffraction patterns demonstrate the same features observed in real resting striated muscle diffraction patterns. The main correlated features are: 1) the meridional layer line angular separation, θ , follows the grating equation; 2) the layer line intensities decrease with increasing order number ($0 < l < 2$) at normal incident angle, $\omega = 0$; 3) there are left/right intensity asymmetries in the 1st and 2nd orders at $\omega = 0$; 4) the intensity of a given layer line goes through a maximum as the incident angle ω is varied; 5) the left/right, 1st and 2nd order ω -angular separations of these maxima correspond to the calculated Bragg angle; 6) the layer line intensities decrease in the equatorial, θ , direction; 7) the angular layer line separation, θ , varies with incident angle; and 8) some fine structure exists, but cannot be attributed to specific groups of sarcomeres since the sarcomere length distribution is random. These data confirm that theoretical calculations can predict real muscle diffraction patterns and their asymmetries.

015

MEASUREMENT OF LONGITUDINAL AND TRANSVERSE STIFFNESS OF FROG SKELETAL MUSCLE IN RIGOR. Y. Tamura, I. Hatta and H. Sugi, Department of Applied Physics, Faculty of Engineering, Nagoya University, Nagoya 464, Japan.

By use of the ultrasonic pulse method, we have successfully measured the longitudinal and transverse muscle stiffness at rest and during contraction (Tamura et al., 1982). To compare the stiffness values between the activated and rigor states, the sartorius of the semitendinosus muscles of the bullfrog (*Rana catesbeiana*) were put into rigor state by the method of Mulvany (1975) and the stiffness measurements with ultrasonic waves (7MHz) were performed. The increment of the longitudinal muscle stiffness in rigor was almost the same as that in during isometric tetanus. In contrast with tetanized muscles which showed a decrease in the transverse stiffness, the transverse stiffness in rigor muscle rose to a value similar to that for the longitudinal stiffness. The longitudinal muscle stiffness of rigor muscle did not change appreciably when the force in them was varied from zero to the level of the maximum isometric force by small length stretch ($< 2\%$). These results indicate a definite difference between the cross-links in tetanized and rigor muscles.

017

THE EFFECT OF INTRACELLULAR EGTA UPON CA TRANSIENTS IN CUT SKELETAL MUSCLE FIBERS. J. Ribalet and M. Delay, Dept. of Physiology, Univ. of California at Los Angeles, Los Angeles, CA 90024, USA.

The role of intracellular Ca buffers upon the Ca economy of cut frog skeletal muscle fibers was studied in preparations diffused with either of the metallochromic Ca indicator dyes, Arsenazo III or Antipyrylazo III, as well as with concentrations of the Ca buffer EGTA varied between 1.25 and 10 mM. The resting pCa was maintained near 7, and stimulation was accomplished by voltage clamp pulse or action potential. The time constants characterizing the exponentially falling phase of the Ca signals are strongly dependent upon (EGTA) for both dyes; thus, higher EGTA levels result in faster removal of Ca from the dye. The effect of (EGTA) upon resequestration of Ca by the sarcoplasmic reticulum was studied by monitoring Ca signals elicited by two stimuli, separated by a variable time interval (Miledi et al., J. Physiol., 339:223, 1984). As the interstimulus interval is increased, the magnitude of the second Ca signal recovers to the control value in two phases, a fast phase to near 90% in about 100-200 ms, and a slower phase lasting about 1 min. Increasing (EGTA) decreases the amount of recovery in the fast phase, suggesting that part of the Ca bound by EGTA is made inaccessible to rapid uptake by the SR. However, the time constant characterizing the fast phase of recovery is relatively little affected by (EGTA); this is consistent with the hypothesis that the reuptake process involves the binding of Ca to a high affinity site before it can contribute to the SR-Ca release. (F. Mandel, Biophys. J. 45:3a, 1984).

014

WINTER AND SUMMER FROG SKELETAL MUSCLE—DIFFERENCE IN REGULATION MECHANISM OF MUSCLE CONTRACTION

S. Yoshino, Department of Physics, Nagoya University, Chikusa-ku, Nagoya, JAPAN

Frog muscle is one of the widely used materials which has been used for many kinds of breakthrough in muscle science. Tension development is the result of chemical reaction caused by the interaction between thin and thick filaments in muscle. Since the reaction is easily modified by temperature change, unfortunately for poikilothermic frogs, tension development must be modified by surrounding temperature, especially by change of seasonal average temperature in a state of nature. We report here the first observation about the difference in regulation mechanism between winter and summer frog skeletal muscle fibres by use of an electro-optical effect under sinusoidal electric field. Troponin-C on thin filament of winter frog skeletal muscle has Ca/Mg, Ca and Mg binding sites the same as rabbit skeletal muscle, but summer frog does not have Mg binding sites, only Ca and Ca/Mg binding sites. This difference caused only by cultured temperature. Temperature dependence of thin filament flexibility suggests the following facts; since muscle contractile proteins have a fully evolutionary structure, if tension development becomes larger than normal state, the thin filament breaks. Since winter frog muscle fibre in summer develops a force larger than in winter, the force would be enough to break the muscle. Then summer frog must save the force generation by changing the regulation mechanism. Frog may have the function in the evolution under the change of temperature on the earth.

016

FILAMENT ORDER IN MUSCLE FIBERS

Takashi Matsuda and Richard J. Podolsky, Lab. of Physical Biology, NIAIDK, National Institutes of Health, Bethesda, MD 20205 USA.

We have recently reported that lattice spacing and equatorial intensity I_{eq} of skinned rabbit psoas muscle fibers in relaxed state decrease sharply when pH is changed from 7.0 to 5.5, and showed that electrostatic lattice shrinkage and the thin filament lattice disorder are closely linked (Matsuda and Podolsky, 1984, Biophys. J., 45:100a). To investigate this myofibrillar lattice instability further, the lattice was compressed by the addition of Dextran T500 and the equatorial patterns were taken over a range of pH. The loss of I_{eq} was found to be an effect of pH rather than of spacing. Decrease in lattice spacing and increase in thin filament disorder both appear to be caused by decrease in filament charge. Electron microscopy was also used to visualize the filament array at various pHs. In cross sections from the low pH (5.5) relaxed fibers, the thin filaments were not visible in the A band and they clumped in the I band (Rigor fibers at pH 5.5 contained normal thin filaments at the trigonal lattice positions). The lattice spacing in micrographs of low pH fibers was about 25% less than that for pH 7 fibers. These observations are all in reasonable agreement with the X-ray data of layer line and equatorial patterns. In relaxed fibers, lattice stabilization mechanism appears to be electrostatic. On the other hand, the thin filaments in rigor fibers appear to be ordered mainly by the cross bridge.

018

OBSERVATIONS OF CROSS-BRIDGES IN STRETCHED SKELETAL MUSCLE FIBERS BY THE FREEZE-FRACTURE METHOD.

S. Suzuki and G.H. Pollack, Division of Bioengineering, WD-12, University of Washington, Seattle, Washington, USA.

Electron microscope studies by a number of investigators have suggested the possibility that the cross-bridges may form links between thick and thin filaments, comparable to M-bridges (e.g., Hoyle et al., 1973). The present work was performed to determine whether such thick-thick interconnections could be observed using the freeze-fracture, deep-etch, rotary shadowing method. Mechanically skinned fibers of frog semitendinosus muscle were stretched to decrease or eliminate the overlap between thick and thin filaments, and were then frozen rapidly in each of several physiological states using a dual jet liquid propane device. Freeze-fracture replicas were obtained with a Balzers-BAF301 freeze-etch apparatus, and examined with a JEOL 100C electron microscope. Interconnections between thick filaments were well observed in rigor fibers, and sometimes but not always observed in contracting fibers as well as in relaxed fibers. Such interconnections were rod-like, and their dimensions were about 60 Å in diameter (after subtraction of shadow thickness) and 300 - 350 Å in length. The axial periodicity of the interconnections fitted reasonably well with expectations based on X-ray diffraction. The formation of interconnections between thick filaments may arise out of chemical binding of opposed cross-bridges projecting from adjacent thick filaments, as described by Morel and Garrigos (1982). They may play a role in stabilizing the thick filament lattice.

Thursday 02 August Congress Centre-First Floor Posters 019-024

Posters on Cross-Bridge Mechanisms and Muscle Contraction

019.

LOCALIZATION OF THE ELASTIC COMPONENTS IN FROG SKINNED MUSCLE FIBERS

H. Higuchi and Y. Umazume, Department of Physiology, the Jikei University School of Medicine, Tokyo 105 Japan

Localization of the parallel elastic components (PECs) in a skinned muscle fiber was investigated by analysing the change of the resting tension during the dissociation of thick and thin filaments. Thick and thin filaments were dissociated by increasing the concentration of KCl or KI in a relaxing condition. The length of thick filaments was estimated by comparing the intensity of the first-order optical diffraction line and the results of model calculation. It was shown that the resting tension decreased nearly in proportion to the shortening of thick filaments. This suggests that the PECs bind almost uniformly to thick filaments. At a sarcomere length shorter than 4.0 μ m, the resting tension after the dissociation of thick filaments was lowered to less than 10% of an initial value. This means that the resting tension at a physiological sarcomere length may be mainly ascribed to the extension of the PECs bound to thick filaments. But, at a sarcomere length longer than 5.0 μ m, the resting tension after the dissociation of thick filaments still showed about 35% of an initial value and did not change after the dissociation of thin filaments. This suggests that there also are PECs connecting Z-lines.

021

PARTICIPATION OF LC2 LIGHT CHAIN IN THE CONFORMATION OF ESSENTIAL DOMAINS OF FAST SKELETAL MYOSIN. A POSSIBLE FILAMENT MEDIATED MECHANISM.

R. Cardinaud and M. Roux-Fromy

Service Biophysique, CHU/Geolacry, Gif sur Yvette, France.

In the presence of Mg^{2+} filament myosin is cleaved by papain according to two simultaneous patterns: (A) 200 \times 177 \times and (B) 200 \times 110 \times 90 \times . Added ATP or AMP-PNP strongly inhibits pattern A. With monomeric myosin also two simultaneous schemes are observed: b) 200 \times 110 \times 90 \times and c) 200 \times 135 \times . Nucleotides have a negligible effect on either of these two cleavage reactions. Kinetics of light chain cleavage confirm a remarkable difference in sensitivity between LC1 and LC2 with the proteolytic enzyme (R.C. 1982) Eur. J. Biochem. 122, 527). Trypsin converts LC2 to LC2' (19 kDa) very rapidly but further cleavage is strongly inhibited by Mg^{2+} in the filament and is also very slow in monomeric myosin even in the presence of EDTA. Parallel RGR studies of the N-terminal N-trimethylalanine protons reveal a striking difference in mobility of the LC1 and LC2 N-terminal residues. In the filament these protons are shown to be considerably less mobile. The selective cleavage of the LC2 N-terminus restore full mobility to the remaining LC1 N-terminus but the reverse is not observed pointing to an active interaction of the LC2 N-terminus with the filament structure. A model is proposed showing LC2 interacting with the filament shaft on its N-terminus and thereby mediating directly or indirectly a conformational change at the nucleotide binding site located at the 50K-27K junction.

023

STEPWISE SHORTENING OF MUSCLE FIBER SEGMENTS

Henk L.M. Granzier, John A. Myers, Frank V. Broczvich and Gerald H. Pollack, Division of Bioengineering and Department of Anesthesiology, University of Washington, WD-12, Seattle, WA 98195

The shortening of striated muscle has been shown to resemble a staircase; periods of high shortening velocity alternate with pauses during which there is little or no length change (Pollack et al., *Nature* 268: 757, 1977). However, it has been proposed that the appearance of steps and pauses arises out of certain optical artifacts, and that the real shortening is smooth, as predicted by the cross-bridge model.

To test this possibility we studied shortening dynamics using a method independent of the optical properties of the striations. We developed a high resolution version of a segment length measuring system; segment length is measured by detecting the position of surface markers.

Unstimulated single frog fibers were released, and 12 out of 21 showed clear steps. Four fibers were released during contraction; we observed stepwise shortening in three of the four.

We tested the possibility that artifacts caused the observed stepwise shortening; the effects of potential sources of artifact were far too small to have caused pauses in a supposed smooth shortening pattern.

We conclude that stepwise shortening is a genuine phenomenon. It implies that the basic contractile event is quantized, and that the contractile units do not operate at random, as envisioned in the cross-bridge model, but synchronously.

020

FORCE AND STIFFNESS TRANSIENTS IN FROG MUSCLE FOLLOWING RAPID STEP CHANGES IN TEMPERATURE. Barry D. Lindley and D.A. Goldthwait, Jr. Dept. of Physiology, Case Western Reserve Univ., Cleveland, Ohio USA 44106.

Toe muscles or single fibers from semitendinosus of R. pipiens, mounted in a small volume acrylic chamber within a waveguide, were activated by tetanic stimulation or by depolarization by elevated potassium in chloride-free solutions. During the peak of force development the muscles were rapidly heated by bursts of microwave energy, either at 9.4 GHz or at 2.45 GHz. Stiffness was measured by subjecting the muscle to 1000 Hz sinusoidal length displacement (0.1% of total length) and recording the resulting increment in force. Temperature jumps ranged from 2.5 K in 8 ms to 15 K in 40 ms. At maximal force (tetanus or 100 mM potassium), force increases at the temperature rises, but stiffness declines slightly. At submaximal force (e.g., 30 mM potassium), force rises quickly (time constant of 30 ms) before falling to a value lower than that at the cold temperature. The stiffness falls with the deactivation in this latter case. We conclude that the rise in temperature causes a shift of cross-bridges into the force-generating state, followed by a slower detachment, driven either by Ca-dissociation from troponin as a consequence of the T-dependence of the Tn Ca-binding or by accelerated uptake of Ca by the sarcoplasmic reticulum. (Supported by the USPHS, HL19848).

022

ENERGETICS OF Ca^{2+} BINDING TO TROPONIN SUBUNITS. H.C. CHEUNG and C.K. WANG, Graduate Program in Biophysical Science, University of Alabama in Birmingham, Birmingham, AL, USA

The binding data of Ca to troponin C labeled with iodoacetamidodansyl (TnC*) and to TnC*-TnI (troponin I) were analyzed by a nonlinear least squares procedure. It yielded two sets of Ca sites with two sites in each class. Attempts to fit the data to 4 distinct sites were unsuccessful. The binding constants for the formation of the complex TnC*-Ca were determined in the presence and absence of Ca or Mg. This interaction is endothermic and therefore entropy-driven. The various stoichiometric equilibrium constants for the two types of reactions are not independent, but related as a consequence of detailed balancing. The observed constants are in reasonable agreement with the relationship which requires 4 Ca sites divided into 2 classes. The free energy change upon binding TnI to TnC* in the presence of excess of Ca (free energy coupling) is ca. -5 kcal/mol of TnC*. This is also the free energy coupling for binding 4 Ca to TnC* in the presence of TnI. The binary protein complex is stabilized by Ca or Mg binding to the high affinity Ca/Mg sites by only -1 kcal, whereas the complex is further stabilized by Ca. -4 kcal when Ca binds to the remaining two low affinity Ca specific sites. If stabilization of troponin subunits by Ca is an important mechanism by which Ca regulates contraction in muscle, the present results would suggest that the correlation between Ca binding and Ca regulation is very good since a free energy coupling of -4 kcal corresponds to better than 50% saturation of TnC* by both TnI and Ca. (Supported in part by US NIH grant AM 25193.)

024

DIFFERENT MODES OF MASS TRANSFER IN SINGLE RELAXED AND RIGOR RAEB* PMSA* FIBERS DERIVED FROM HIGHER ORDER EQUATORIAL X-RAY DIFFRACTIONS. Leopo C. Yu* and Bernhard Brenner*

*NIH, Bethesda, MD, USA 20205; *University of Tübingen, FRG.

To investigate in greater detail the structural changes associated with crossbridge formation in relaxed rabbit psoas muscle fibers at low ionic strengths (a) (preceding abstract), we obtained higher order equatorial X-ray reflections beyond [1,1] from the relaxed and rigor states between μ 20 to 100mM with varying concentrations of Kpropionate. Axially projected two dimensional electron density maps were constructed based on intensities of five reflections ([1,0], [1,1], [2,0], [2,1] and [3,0]), with phase assignment (+, +, -, +, +). One of the main features of the density maps is that the backbone of the thick filament is resolved from the myosin heads which are mostly concentrated in a surrounding annular shell. As μ is lowered from 100mM to 20mM in the relaxed muscle, mass redistribution causes net loss most prominently in the region surrounding the thin filaments where the myosin heads are less concentrated. The part of the annular shell where myosin heads are highly concentrated shows less change. In contrast, in transition from relaxed to rigor state, the most severe net loss is in the region where the myosin heads are highly concentrated. The different characteristics of mass redistribution are unlikely to be simply due to a difference in the number of crossbridges, since the stiffness in the 20mM relaxed state is more than half that of the rigor state (Brenner, et al., PNAS, 1982). Hence, the difference in mass redistribution provides evidence that the modes of crossbridge attachment are different in these two states.

Thursday 02 August Congress Centre-First Floor Posters 025-030

Posters on Cross-Bridge Mechanisms and Muscle Contraction

025

ROTATORY FLUCTUATION OF SINGLE SARCOMERE

H. Suda, N. Imai, Department of Physics, Nagoya University, Nagoya City, JAPAN

This study is to clarify the internal structure of several constructal units, for example IZI, in a single muscle fibre through the measurements of their rotatory fluctuations or hydrodynamic resistances. The rotatory fluctuations were obtained by image analyses under the direct observations with a microscope-video-tape recording system. The rotatory diffusion constants (D_r) were obtained by tracing the time processes of the above rotatory fluctuations on the basis of the theories. The D_r -values of a relaxing or charged state of a sarcomere, of which structure is thought to have a compact form, showed a fairly good agreement with Burger's theory (about rigid cylindrical molecules). The D_r -values of other samples were remarkably smaller than the theoretical values. These facts are interpreted in terms of the inside resistance against solvent flow. On the other hand, a solvent-drained I-Z-I showed only one thirtieth of theoretical value. This small value is thought to be due to a less solvent-penetration into IZI. An IZI-HEM complex showed a larger D_r -value than that of I-Z-I. In the case of the contraction state, in spite of its compact structure as imagined, a rather smaller value was obtained. This fact can be attributed to the fact that the sample takes a loose structure appropriate to make the substrate ATP easily diffuse into the inside for splitting.

027

HYSTERESIS IN MUSCLE CALCIUM SENSITIVITY

A.M. Gordon, R.L. Coby, D.A. Martyn, and L.D. Yates
Department of Physiology and Biophysics, University of Washington, Seattle, WA 98195, USA

We previously demonstrated a hysteresis in the Ca sensitivity in membrane-disrupted barnacle muscle fibers: more steady force is produced at a given [Ca] if that [Ca] immediately follows a [Ca] that produces maximal force (stepping down), than if that same [Ca] immediately follows the relaxed state (stepping up). This hysteresis in Ca sensitivity has been hypothesized to be due to cross-bridge-dependent Ca binding. This property is not unique to barnacle muscle since hysteresis is observed in both frog semitendinosus and rabbit soleus muscle fibers in which the surface and sarcoplasmic reticulum membranes have been disrupted chemically. Though little consistent hysteresis is observed for rapid contractions in solutions with 5mM MgATP, significant hysteresis is seen for slower contractions in the 50mM MgATP, in which there is no increase in resting tension. In frog semitendinosus fibers, the midpoint of the steady force vs pCa relationship shifted by 0.12 pCa units toward increased sensitivity and the steepness decreased (Hill n value) from 3.9 to 3.2 for measurements of steady force for decreasing Ca from a maximum (stepping down) compared with increasing Ca from rest (stepping up). In rabbit soleus muscle, hysteresis was more prominent at long sarcomere lengths. Thus, other muscles show evidence of hysteresis and cross-bridge-dependent Ca sensitivity. This work was supported by a grant from the NIH, NS08384.

029

THE TWO CALCIUM-BINDING SITES OF PIG INTESTINAL CALCIUM-BINDING PROTEIN: A MULTINUCLEAR NMR STUDY

S. Forsén, T. Hofmann*, T. Drakenberg and H. Vogel, Dept. of Physical Chemistry 2, Univ. of Lund, Lund, Sweden

*Dept. of Biochemistry, Univ. of Toronto, Toronto, Canada
Pig Intestinal Calcium Binding Protein (ICaBP) is a 9000 MW protein involved in Ca^{2+} -resorption from the intestine. Amino acid sequencing and crystallographic data indicated that the protein should be able to bind two Ca^{2+} ions, one in a typical EF-hand binding site (similar to those found in parvalbumins (PV), calmodulin (CaM) and troponin C (TnC)) and a second one in a unique pseudo-EF-hand site. Using ^1H NMR we have demonstrated that binding of Cd^{2+} and Ca^{2+} induces very similar conformational changes in ICaBP. In both ^{43}Ca and ^{113}Cd NMR spectra we observed one resonance with the typical chemical shift, linewidth and T_1 of an EF-hand site. Furthermore, with both techniques we also registered a second resonance for the pseudo-EF-hand site. These had a chemical shift and linewidth which is different from that measured for any other bound Ca^{2+} or Cd^{2+} ions. Occupation of this second site influences the EF-hand site. The binding constants for the two sites differ by less than a factor of 3. Unlike for the two strong calcium-binding sites in CaM, TnC and PV Ca^{2+} -binding to the two sites appears not 100% positive cooperative. This effect is most pronounced when using Cd^{2+} . In summary, our data clearly confirm the suggested existence of one EF-hand as well as one pseudo-EF-hand for the binding of Ca^{2+} to ICaBP. Thus this protein is strikingly different from typical EF-hand proteins such as CaM, TnC or PV. Sponsored by MRC Canada and NFR Sweden.

026

EFFECT OF THE FILAMENTOUS STRUCTURE OF MYOSIN ON THE ACTOMYOSIN ATPase ACTIVITY

J.-J. Béchet and A. d'Albis, Lab. Biologie Physicochimique, Univ. Paris-Sud, Orsay, France

The ATPase activities of acto-heavy meromyosin and of acto-myosin minifilaments have been compared under the same conditions at low ATP (0.1 mM) and at several KCl concentrations. The activities which are strongly salt-dependent in both systems have been found to be similar at high (about 3.16 M) but different at lower (0.06-0.07M) ionic strength. Under this last condition, the catalytic constants k_{cat} and K_m are lower for acto-myosin minifilaments ATPase than for acto-heavy meromyosin ATPase. Furthermore any decrease in the concentration of ionic species (ATP, citrate...) at constant low ionic strength, induces an increase in the interaction strength between myosin and actin filaments, as revealed by the K_m changes. The presence of the troponin-tropomyosin complex also enhances the strength of this interaction. The organized structure of the myosin minifilaments promotes therefore the actomyosin ATPase activity.

028

ENERGY TRANSDUCTION IN MUSCLE INVOLVES PROTON-MOTIVE FORCE

M. Amin, School of Life Sciences, Jawaharlal Nehru University, New Delhi, India.

ATP hydrolysis by myosin ATPase generates a chemical potential difference for protons between the overlap region and the regions of H- and I-band. It has been shown that, if the myofilaments are assumed to conduct protons by the Grotthus-Onsager mechanism, the flux of H^+ to the M-line and the Z-disc generates a diffusion potential and brings about a 3-dimensional loop flow of the diffuse cationic layer around the myofilaments. The viscous drag of the cationic layer on the myofilaments has been estimated to be of sufficient magnitude to account for the muscular force. The energy output of the proton circuit is dependent on the mechanical constraints by means of the viscous coupling between the cationic layer and the movement of the myofilaments. The theory explains the experimental observations quantitatively and leads to Hill's equation in the first approximation. In this approach the cross-bridges serve the purpose of H^+ -generating electrodes which release H^+ into the myofilaments during Ca^{2+} mediated transient contacts with the actins but are not envisaged to act as molecular muscles.

030

THE BINDING AND HYDROLYSIS OF MgATP BY DEMEMBRATED MUSCLE FIBRES AT TEMPERATURES BELOW 0°C

R.T. Tregear, S. Kellam, and S. Heaphy, A.F.R.C. Institute of Animal Physiology, Babraham, Cambridge, U.K.

Glycerol-extracted rabbit psoas muscle fibres were brought to a temperature between 0° and -40°C in a neutral, Ca^{2+} -free, low ionic strength solution containing 50% ethylene glycol. The fibres were incubated in 100mM 3H-ATP for 30-90 min. Diffusible 3H-ATP was then briefly chased from the fibres in cold ATP and the bound nucleotide eluted in trichloroacetic acid first in the cold and then at room temperature; two-thirds of the nucleotide was eluted in the cold. The total recovered nucleotide was consistent with binding to the enzymatic sites of myosin within the fibres. At -40° most of the nucleotide recovered in the cold was ATP; the proportion rose as the temperature was raised and at 0°C most was ADP. We are currently examining the mechanical properties of the muscle fibres under these conditions, in order to determine whether hydrolysis of bound nucleotide correlates with relaxation.

Thursday 02 August Congress Centre-First Floor Posters 031-036

Posters on Cross-Bridge Mechanisms and Muscle Contraction

031

CONTRACTILE ACTIVATION IN A MUSCLE WITH SIMPLE TRANSVERSE TUBULES T. Schöner and M.F. Gilly, Hopkins Marine Station of Stanford University, Pacific Grove, CA 93950, USA

Contractile activation of scorpion skeletal muscle was studied because its ultrastructure resembles that of vertebrate striated muscle. The major difference is the transverse tubular (T)-system which consists of short, radially oriented tubules with prominent mouths. Contractile activation in scorpion (*Uroctonus mordax*) muscle fibers was characterized at 20°C using a two microelectrode voltage clamp technique. Threshold amplitude for just detectable sarcomere shortening was determined for voltage steps of different durations by microscopic observation of superficial sarcomeres in the voltage clamped segment of the fiber. The Strength-Duration curve thus obtained in Na-free, TTX-containing saline is similar to that found in TTX-poisoned frog muscle. However, threshold for long (20-50 ms) pulses is near -20 mV, substantially more positive than in frog. In Na-free saline (+TTX) containing 5 mM Ca, contractile activation is always accompanied by a voltage-dependent inward current. Both the inward current and voltage-dependent contractile activation are abolished in nominally Ca-free (no EGTA) external solutions. Cadmium (0.5 mM) blocks contractile activation and reduces or eliminates inward current. However, in cadmium-containing, Na-free solutions strong inward currents sometimes persist when contractile activity has been eliminated. Tetracaine (.5 mM) reversibly inhibits contractile activation especially with brief pulses and renders contraction impossible with a 2 ms pulse. Thus contractile activation in scorpion muscle resembles several vertebrate muscle types.

033

GEOMETRICAL CONSTRAINTS ON THE CROSS-BRIDGE ATTACHMENT

V. Starc, J. Stefan Institute and Medical Faculty, E. Kardelj University, Ljubljana, Yugoslavia

Computer modeling studies have been undertaken to investigate the possibility of the cross-bridge attachment in a three-dimensional lattice.

Three-stranded myosin filaments are considered to be made up by myosin molecules with the two heads flexibly joined to the tail that is flexibly attached to the myosin backbone. Thus, the position of any head can be described by four parameters (angles). Actin filaments are assumed to be 27/2 helices arranged in such a manner that the cross-bridge contact regions on the actin molecules define several strands around each myosin filament depending on the lattice dimension.

For the described structure with the length of five-myosin axial repeat we calculated the number of all possible cross-bridge contacts as well as the probabilities for attachment especially looking for the contacts of one myosin molecule with two different actin filaments. Further, the influence of a small axial displacement or rotation of the myosin filament on this number is investigated.

035

FLUORESCENCE ENERGY TRANSFER BETWEEN Tb^{3+} AT THE HIGH AFFINITY SITES AND LABELS IN THE REGION OF THE LOW AFFINITY SITES OF TROPONIN-C. C.-L.A. Wang, T. Tao and J. Gergely, Boston Biomed. Res. Inst., Boston, MA USA

Tb^{3+} bound at the two high affinity sites of troponin-C (TnC) can be excited either indirectly through Tyr-109 with a pulsed UV lamp, or directly with a N_2 -pumped dye-laser. The Tb^{3+} luminescence resulting from either method of excitation decays with a single lifetime of 1.3 ms, suggesting that the immediate environments of both bound Tb^{3+} ions are identical. Upon direct excitation of Tb^{3+} labeled at Met-25 with 4-nitrobenz-2-oxa-1,3-diazole (NBD) or 4-dimethylamino-phenylazobenzene (DAB) as Förster type energy transfer acceptor the luminescence decays bi-exponentially, the lifetimes being 0.76 ms and 1.40 ms for TnC^{NBD}, and 1.0 ms and 1.38 ms for TnC^{DAB}. These two lifetimes indicate that (i) only one of the two bound Tb^{3+} ions transfers energy to the label, the transfer efficiencies yielding a distance of 3.7 nm between them; and (ii) Tb^{3+} at the other site, corresponding to the component associated with the unquenched emission, is at a greater distance from the label. Indirect excitation of Tb^{3+} bound to labeled TnC results in emission with a single lifetime as with unlabeled TnC, suggesting that Tyr-109 transfers energy only to one of the Tb^{3+} ions bound at the high affinity sites. Since the luminescence of this Tb^{3+} is not quenched, the binding site at which interaction with Tyr-109 occurs is the one more distant from Met-25.

032

EXPERIMENTAL AND THEORETICAL STUDY OF LASER LIGHT DIFFRACTION BY STRIATED MUSCLE.

R.A. Thornhill, N. Berovic Department of Zoology and Department of Physics, University of Birmingham, Birmingham, B15 2TT England

The technique of laser light diffraction has not realized its full potential due to the fact that the resultant diffraction patterns are usually interpreted as if diffraction originates from a plane grating, or from a three dimensional grating in the 'kinematic' regime. Isolated muscle fibres, with their relatively large modulation of refractive index, behave in a way that requires the application of a 'dynamical' theory of Bragg diffraction. The experimentally observed features of the diffracted light intensity as a function of specimen angle, can be related to the structure of the muscle by using an almost exact treatment of the 'thick phase grating', coupled-wave theory (Kogelnik 1969, Magnusson & Gaylord 1977). This has enabled us to conclude that freshly excised, viable muscle fibres possess a high degree of order. The sarcomere lattice also has a degree of simple hexagonal order, and failure to take its three dimensional orientation into account can lead to misleading results. The degree of order decays with time and eventually disappears leaving a completely amorphous material. Kogelnik, H. (1969) Bell Syst. Tech. J. 48 2909-2947 Magnusson, R., Gaylord, T.K. (1977) J. Opt. Soc. Am. 67 1165-1170

034

X-RAY EVIDENCE FOR TWO STRUCTURAL STATES OF THE ACTOMYOSIN CROSSBRIDGE IN MUSCLE FIBERS. T. Matsuda, B. Brenner,

L.C. Yu, and R.J. Podolsky, NIADDC, NIH, Bethesda, MD, USA. Biochemical data (Chalovich & Eisenberg, JBC, 257 2432, 1982) and stiffness measurements (Brenner et al., PNAS, 79 7288, 1982) provide evidence that actomyosin-crossbridges form in relaxed skinned rabbit fibers at low ionic strength (20-50 mM). We used X-ray diffraction to obtain structural information regarding these crossbridges. At low ionic strength, the intensity of the 11 equatorial reflection in the relaxed state was close to that of the rigor state, while the intensity of the 10 reflection was about twice that of the rigor reflection, indicating that (1) substantial extra mass is associated with the thin filaments at low ionic strength, and (2) the mass distribution in low ionic strength is different from that of the rigor state. Low ionic strength crossbridges did not change the myosin-based reflections characteristic of relaxed fibers at 120 mM ionic strength (notably the 86 Å and 108 Å layer lines and the 72 Å and 143 Å meridionals) and they did not produce the additional intensity on the 59 Å actin-based layer line near the meridian that is associated with rigor crossbridges. However, they caused the 215 Å meridional reflection to decrease in intensity, as is also the case when rigor crossbridges are formed. These observations show that the structure of the low ionic strength crossbridge is significantly different from that of the rigor crossbridge, and they support the idea that contractile force may be generated by transitions between different actomyosin configurations.

036

CATION MODULATED CROSS-BRIDGE DETACHMENT FROM THE MYOSIN FILAMENT SHAFT: NEW STRUCTURAL DETAILS.

Arthur J. Renge, Department of Biochemistry, University of Leicester, Leicester LE1 7RH, U.K.

It has been suggested that the attachment/detachment of the myosin head (subfragment-1) from the filament shaft during the contraction cycle may occur through the opening/closure of the line of attachment-2 to the shaft (cf. Hargrove & co-workers). The ability of divalent cations (M^{2+}) to modulate ADP in competition in well-oriented filament preparations, i.e., the hydrolysed actin levels, lends support to hypothesis of this type (see also Renge, J. Mol. Biol. 172 43-59, 1984). Electron microscopy of such filaments using a newly defined technique, demonstrates that the cross-bridges detach from the shaft at $25^\circ C$ in buffers from pH 6 to 9.5. However the extent of such detachment with respect to the ADP is limited to apply to a region close to the ADP - ATP junction, i.e. the cross-bridge 'pools off' rather than 'lifts up'. These findings are not compatible with theories which suppose an effect of cation on the 'line of attachment-2' (cf. Hargrove & co-workers) or consider a region of ADP close to the latter to be a site for force transduction.

Evidence from other techniques confirms this view: the modest extent of the M^{2+} effect on frictional coefficient (cf. α) and recent studies by neutron scattering (cf. L. Jorgensen & J. More) imply that although a substantial change in ADP flexibility may occur, its radial (though not necessarily azimuthal) position changes only to a modest extent with changes in cation level.

Thursday 02 August Congress Centre-First Floor Posters 037-042

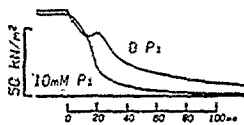
Posters on Cross-Bridge Mechanisms and Muscle Contraction

037

TENSION DEVELOPMENT AND Ca-SENSITIVITY IN SKINNED MUSCLE FIBRES OF THE FROG.
G.J.M. Stienen, T. Blangsted and B.W. Treijtel, Department of Physiology, University of Amsterdam, Eerste Const. Huygensstraat 20, 1054 BW Amsterdam, the Netherlands.
Isometric tension development at different Ca concentrations was measured in single muscle fibres of the ileofibularis muscle of the frog, skinned by a freeze-drying method. Stienen et al. *Pflügers Arch.* 397:272-276, 1983. The experiments were carried out at 20°C, pH = 7, $[Mg^{2+}] = 5 \text{ mM}$, $[ATP] = 160 \text{ mM}$. The maximum tension as a function of Ca concentration was fitted to a Hill curve by means of a least squares method; at 2.15 μM sarcomere length $K = 1.6 \mu\text{M}$, $K/[Ca^{2+}]$ for half-maximum tension) and $n = 3$. However, for $[Ca^{2+}] < K$ the calculated curve was not steep enough, while for $[Ca^{2+}] > K$ the calculated curve was too steep.
The Ca-sensitivity increased with increasing sarcomere length; at 2.7 μM , K was 1.1 μM . Additionally, it was observed that the optimal sarcomere length for tension development shifted to larger values when the Ca concentration was lowered. Osmotic compression of the fibres at 2.15 μM , by means of long chain polymers (Dextran) also caused an increase in Ca-sensitivity. At a fibre width corresponding to the width at 2.7 μM (without Dextran), K was 1.0 μM . Therefore both effects might originate from changes in spacing between the actin and myosin filaments. This suggests that the Ca-sensitivity is influenced by the electrostatic field between the filaments.

039

P_i SPEEDS ATP-INDUCED RELAXATION OF SKINNED MUSCLE FIBERS
M.G. Hibberd*, J.A. Dantzig*, Y.E. Goldman* and D.R. Trentham*
Dept. of Physiology* and Dept. of Biochemistry and Biophysics*, University of Pennsylvania, Phila., PA U.S.A.
When caged ATP is photolyzed within rabbit single skinned muscle fibers in rigor, the ATP liberated causes rapid relaxation of rigor tension (see figure). In these experiments, reattachment of a proportion of the cross-bridges detached by ATP causes a transient increase in tension and slows the final relaxation (Goldman, Hibberd, McCray & Trentham, *Nature* 300, 701-705; 1982). Addition of a steady 10 mM concentration of orthophosphate (P_i) reduces the tension rise and increases the rate of final relaxation 2-3 fold. These effects depend on P_i concentration and are detectable at 1 mM P_i . If our results are due to specific binding to the active site of myosin, P_i may increase the cross-bridge detachment rate by the reverse pathway: $A.M.ADP + P_i \rightarrow A.M.ADP.P_i \rightarrow A + H.ADP.P_i$ ($A = \text{actin}$, $M = \text{myosin}$). The apparent binding of P_i to $A.M.ADP$ in fibers suggests that P_i release is coupled to the power stroke of the cross-bridge cycle. Supported by NIH grants HL15835 and AM00745 and by NDA, BHF and AHA.



041

THE POSITION OF TROPONIN-T IN MUSCLE THIN FILAMENTS
H.J. Carr and E.J.O'Brien, MRC Cell Biophysics Unit, King's College, 26-29 Drury Lane, London WC2, England.
In the thin filaments of vertebrate skeletal muscle, two molecules of the troponin complex are bound to the actin: tropomyosin strands at intervals of 38.5 nm. Troponin-T, which binds tropomyosin-I and tropomyosin-C to tropomyosin is thought to be an elongated molecule, possibly binding to tropomyosin over more than 10 nm. In order to evaluate this model, we have compared the structure of actin:troponin-T filaments with that of actin:troponin-T:troponin-T filaments. The filaments were in the form of paracrystals induced by Mg^{2+} , and were analysed by electron microscopy and computer methods. The filaments formed arrays in which adjacent filaments were antiparallel, and in which the actin helical symmetry comprised 22 subunits in 13 turns of the left-handed genetic helix. When troponin-T was present in addition to actin and tropomyosin, the arrays were less well ordered. The order was improved if the major chymotryptic fragment, troponin-T1, was used instead of troponin-T. Average filaments were obtained by computer filtering of the electron micrographs, and 3D reconstructions generated by Fourier-Bessel transformation. In reconstructions of actin:troponin-T, a column of density at a radius of about 4 nm was assigned to tropomyosin, leaving an elongated actin monomer shape, with the longest dimension of the monomer oriented roughly perpendicular to the filament axis. In the reconstructions containing also troponin-T or troponin-T1, the column of density attributed to tropomyosin was larger, indicating the presence of a considerable part of the troponin-T molecule in that region.

038

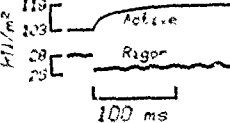
RELATIONSHIP OF FORCE POTENTIATION TO V₀, STIFFNESS AND ENERGY LIBERATION DURING SKELETAL MUSCLE CONTRACTION. D.M. Burchfield and J.A. Ball, Dept. of Physiology, The Ohio State University, Columbus, Ohio, U.S.A.
Velocity of unloaded shortening (V_0) and steady rate of energy liberation (S.R.E.L.) depend on the rate of ATP hydrolysis by cross-bridges. Experiments were designed to determine if V_0 and S.R.E.L. maintain a fixed relationship to each other when both parameters are altered. Increasing the temperature of frog semitendinosus muscle from 0 to 10°C increased peak tetanus force $45 \pm 4\%$ ($n=15$) and S.R.E.L. $462 \pm 11\%$ ($n=10$). V_0 increased $252 \pm 27\%$ ($n=9$). The increase in S.R.E.L. was significantly greater than that of V_0 , but account must be made for the increased force. Usually S.R.E.L. is divided by force, assuming that force is proportional to the number of attached cross-bridges. This point was examined by determining the ratio of peak muscle stiffness, using ramp releases, at 0 and 10°C. This ratio is 1.10 ± 0.05 ($n=7$). Thus S.R.E.L. should be normalized by stiffness. Before comparing V_0 and cross-bridge energy liberation, the temperature dependence of Ca^{2+} cycling energy liberation must be known. This was determined by measuring S.R.E.L. at a sarcomere length of 3.8 μm at 0 and 10°C, and was found to increase $569 \pm 28\%$ ($n=5$). Cross-bridge energy liberation was determined by subtracting S.R.E.L. at 3.8 μm from that at 2.4 μm . Cross-bridge energy liberation increased 350% from 0 to 10°C. This increase is greater than the increase in V_0 . This result suggests that V_0 and cross-bridge energy liberation are not two measures of the same reaction sequence. (Supported by NIH grant AM20792).

040

LENGTH-DEPENDENCE OF Ca^{2+} SENSITIVITY AND Ca^{2+} BINDING IN CARDIAC MUSCLE. Franklin Fuchs and Polly Hofmann, Dept. of Physiology, University of Pittsburgh School of Medicine, Pittsburgh, PA 15261 (USA).
The force-pCa relationship in skinned cardiac muscle bundles is shifted to a higher pCa range when the sarcomere length is reduced from optimal length to a length which lies on the ascending limb of the length-force curve (Hibberd and Jewell, 1982). A study has been undertaken to determine if this shift in Ca^{2+} sensitivity is related to a length-dependent change in Ca^{2+} -troponin affinity. With detergent-extracted canine cardiac muscle bundles half-maximal force at sarcomere length 2.2 μm was obtained at pCa 6.05. At sarcomere length 1.5 μm half-maximal force was obtained at pCa 6.2. A double isotope technique was used to measure Ca^{2+} binding to cardiac muscle bundles (in rigor) at the long and short sarcomere lengths. At the short sarcomere lengths Ca^{2+} saturation was reduced by 15-35% in the pCa 5-6 range. At higher pCa values Ca^{2+} saturation was independent of sarcomere length. These data provide evidence that Ca^{2+} binding to the low affinity (regulatory) site of cardiac troponin is sensitive to sarcomere length. This effect may provide a basis for the Frank-Starling relationship in cardiac muscle. (Supported by grants from the NIH and Western Pennsylvania Heart Association).

042

LASER TEMPERATURE JUMP STUDIES ON SKINNED MUSCLE FIBERS
J.A. Smith*, Y.E. Goldman*, M.G. Hibberd*, G.A. Liguori*, M.A. Luttmann*, and J.A. McCray*, Dept. of Physics and Atmospheric Sciences, Drexel University* and Dept. of Physiology, University of Pennsylvania*, Phila., PA U.S.A.
We have developed a new and non-destructive method for abruptly increasing the temperature (T-jump) of a contracting muscle fiber. Skinned single fibers from frog semitendinosus or rabbit psoas muscle were immersed in a trough of rigor or activating solution aligned in the beam of a holmium laser. A 200 μs , 500 mJ pulse of infrared radiation ($\lambda = 2065 \text{ nm}$) was absorbed by water ($\alpha = 37 \text{ cm}^{-1}$) so that the temperature of the solution and the muscle fiber increased by 6°C. The figure shows tension transients following a T-jump from 20° to 30°C in a frog fiber. In rigor, the T-jump caused an abrupt decrease in tension. As the trough cooled over the next 3 s rigor tension returned to its original level. When the same fiber was fully activated at 3 mM MgATP and 10 μM Ca^{2+} , the tension increased after the T-jump in at least two kinetic phases and reached a maximum value at 150 ms, after which tension decreased again as the trough cooled. The rigor tension decrease indicates thermal expansion of the contractile proteins, while the active tension increase probably reflects cross-bridge cycle kinetics. Supported by NIH grants AM26846 and AM00745 and a Drexel Research Award.



Thursday 02 August Congress Centre-First Floor Posters 043-048

Posters on Cross-Bridge Mechanisms and Muscle Contraction

043

BINDING OF ATP TO MYOSIN SF-1, ACTOMYOSIN SF-1 AND COVALENTLY CROSSLINKED ACTOMYOSIN SF-1, I.E. Barman, J.A. Biosca and F. Travers, Institut National de la Santé et de la Recherche Médicale, CNRS, Montpellier, France.

The presteady state kinetics of the binding of ATP to myosin SF-1, actomyosin SF-1 and covalently crosslinked actomyosin SF-1 were studied by the ATP chase method in a flow quench apparatus. The binding processes were slowed down with 40 % ethylene glycol as solvent at 5 mM KCl, pH 8, 15 °C. The kinetics were studied as a function of the ATP concentration. The binding of ATP was tight to all three proteins. With myosin SF-1 and actomyosin SF-1, the binding process followed an hyperbolic law with the ATP concentration. This suggests a two step binding process: a rapid equilibrium (K_a) followed by a slow conformational change (k). The values for K_a and k for the two proteins were different ($K_a = 1.15 \times 10^5 \text{ M}^{-1}$, $k = 15.6 \text{ s}^{-1}$ for myosin SF-1 and $K_a = 3.4 \times 10^4 \text{ M}^{-1}$, $k = 62.7 \text{ s}^{-1}$ for actomyosin SF-1). A two step binding process for ATP to covalently crosslinked actomyosin SF-1 could not be demonstrated: the slope of the ATP dependency curve was $3.4 \times 10^5 \text{ M}^{-1} \text{ s}^{-1}$. These results can be interpreted as showing that the conformations of the ATPase site of myosin SF-1 is modified in actomyosin SF-1 and covalently crosslinked actomyosin SF-1.

045

ELECTRON MICROSCOPIC STUDY OF ACTIN-TROPOMYOSIN-HEAVY MEROMYOSIN RIGOR COMPLEX
H. Kajiyama, Y. Shirakihara and T. Wakabayashi, Department of Physics, Faculty of Science, University of Tokyo, Bunkyo-ku, Tokyo, Japan

Since thin filament containing tropomyosin was used, electron micrographs of the longer (4-6 x 380 Å) and more straight rigor complex were obtained. Larger box size was used so that the outer region of the actin-tropomyosin-heavy meromyosin rigor complex is included in the reconstructed image. It was shown that the whisker of arrow-head has a dense turning point. The analysis of such an image of actin-tropomyosin-heavy meromyosin complex enables the observation of the shape and size of intact myosin heads in rigor state and the detailed structural analysis of linkage of two heads and myosin rod. Other than major domains, in the reconstructed image, we can see three kinds of circumferences at the radii of about 100 ± 10 , 130 ± 10 and 165 ± 10 Å. At the outer radius of about 100 Å, the above-mentioned dense region, F, G and new areas reside. The contour length of intact myosin head was about 200 Å. We are now analysing further data with respect to these fine structures and the features of major domains.

047

THE APPLICATION OF A TWO-STATE ACTIN-MYOSIN MODEL ON THE CONTRACTING LEFT VENTRICLE OF THE RABBIT. FAN van Kaam, EL de Beer and P. Schiereck, Dept. of Med. Physiology, State Univ. Utrecht, Vondellaan 24, Utrecht, The Netherlands.

Controlled volume changes are performed on isolated contracting left ventricle of a rabbit and compared with model calculations based on a two-state actin-myosin interaction model. In skeletal muscle a typical shoulder-shaped force-transient is found during a tetanus. This shoulder is simulated by a two-state actin-myosin interaction model (Van Kaam et al. 1983, J. Biomech. In press). Despite discrepancies in geometry, homogeneity, and isotropy a similar shoulder is observed during steady volume releases in contracting left ventricles (Van Kaam et al., 1983, Arch. Int. Physiol. Bioch. 91:451). The present study characterises the shoulder by means of the amplitude and the time of the volume release at which the pressure time course reveals a point of inflexion, i.e. $d^2p/dt^2 = 0$. The behaviour of the point of inflexion depends on velocity of release and is comparable with the point of inflexion shown during steady shortenings in skeletal muscle. At larger velocity, d^2p/dt^2 equals zero at larger amplitude, while the period to reach this point, is decreased. In order to fit isovolumic contraction the two-state model (Julian et al., 1974, Biophys. J. 14:576) is extended with a time-dependent activation function. The parameters of this activation function were fitted. Afterwards the calculated activation curve was used to describe the pressure curve as affected by a steady volume release. Calculations and experimental results are compared both qualitatively and quantitatively. The agreement is rather well.

044

CONFORMATIONS OF MODIFIED TROPOMYOSIN: INTERACTION STUDIES.
B. Nagy and H. Bialkowska-Nagy, Department of Neurology: Department of Pharmacology and Cell Biophysics; Department of Microbiology, University of Cincinnati Medical College, Cincinnati, Ohio USA.

Studies on the chromophoric tyrosine side chains of rabbit skeletal muscle tropomyosin with use of absorption, fluorescence and circular dichroic spectroscopy indicated significant environmental effects in the native protein. Solvent perturbation, pH and denaturation studies indicated and reconstructed coiled-coil helical pattern confirmed that in α -helical native state 10 of 12 tyrosines of the molecule have close proximity carboxyl neighbors. Fluorescence intensity increase of 2.6 fold in protonation or denaturation confirmed carboxyl quenching. Circular dichroic spectra of tyrosines in native state also changes on protonation. Since tyrosines are widely distributed along the polypeptide chain in TM, the quenched fluorescence in α -helical state can be used as an indicator for retained conformation upon extensive amino acid side chain modifications with use of succinylation or reaction with fluorescamine. Fluorescamine is the fastest and most benign reagent for the primary amine containing amino acid side chains of tropomyosin. It labels the whole surface of coiled-coil tropomyosin. Blocking the primary amines blocks tryptic digestion. Tropomyosin-actin complex hinders from fluorescamine some of the sites. Trypsin digestibility of fluorescamine labeled tropomyosin from the complex indicates side chain locations on tropomyosin surface by the interactions.

046

Structural studies of filamentous actin using X-ray fibre diffraction and Magnetic Birefringence.

A.G. Fowler*, J. Reed* and D. Suck*

*European Molecular Biology Lab. Postfach 10.2209 D-69 HD, FRG. Postfach 10.2209, D-69 HD, FRG. *Deutsches Krebs Forshungs-Zentrum. Im Neuenheimer Feld, D-69 HD, FRG.

Thin filaments purified from the scallop *Pecten maximus* adductor muscle orient reversibly in a strong magnetic field. Magnetic birefringence was employed to establish i) conditions for optimal coupling to the magnetic field, including pH, ionic strength and the formation of paracrystals ii) the magnitude of the Cotton Mouton coefficient.

Birefringence kinetics of f-actin polymerised in the magnet yields two time constants. The fast component is associated with a strong linear dichroism in the near UV; the result of interfilament 'bundling'.

X-ray diagrams of oriented f-actin gels reveal a marked absence of scattering in the range 0.5 to 0.8 nm⁻¹. This is consistent with a mobile tertiary structure for the actin monomer.

048

A REGION OF TROPONIN C CONTAINING RESIDUES 89-100 UNDERGOES FAST CONFORMATIONAL CHANGES UPON Ca^{2+} -BINDING TO SITES I AND II. Z. Grabarek, P.C. Leavis and J. Gergely., Dept. Muscle Res., Boston Biomed. Res. Inst. and Dept. Neurology, Mass General Hosp., Boston MA 02114.

Residues 89-100 of TnC (C₈₉₋₁₀₀) and 96-116 of TnI (I₉₆₋₁₁₆) interact with each other in the troponin complex (Dargatzis et al., 1982, FEBS Letters, 150:54) and are necessary for the Ca^{2+} -sensitive inhibition of actomyosin ATPase activity (Syska et al., 1976, Biochem. J. 153:375, Grabarek et al., 1981, J. Biol. Chem. 256: 13121). In order to determine whether regulatory Ca^{2+} -binding sites (I,II) or Ca^{2+} - Mg^{2+} sites (III,IV), induce changes in C₈₉₋₁₀₀ we have monitored the fluorescence of TnC labelled at Cys-98 with 1,5-IAEDANS. Titration of the labeled TnC with Ca^{2+} has shown that the probe is sensitive to binding to site III and IV with or without TnI present. We have performed stopped flow experiments on labeled TnC in the presence of Mg^{2+} . There is rapid fluorescence increase related to Ca^{2+} -binding to unoccupied sites I and II, followed by a slower phase ($k=11.4 \text{ s}^{-1}$) that represents Mg^{2+} - Ca^{2+} exchange in sites III and IV. In the presence of TnI only the fast change is detected. Thus the presence of Mg^{2+} at site III and IV permits the detection of rapid changes in the environment of Cys-98 upon Ca^{2+} -binding to the regulatory sites I and II. This rapid change may be instrumental in triggering activation of the thin filament by transferring information to TnI via a change in the contact between C₈₉₋₁₀₀ and I₉₆₋₁₁₆.

Thursday 02 August Congress Centre-Floor Posters 049-054

Posters on Cross-Bridge Mechanisms and Muscle Contraction

049

X-RAY DIFFRACTION STUDIES IN RADIALLY COMPRESSED FROG SKINNED MUSCLE FIBERS.

Y. Uemura, Department of Physiology, The Jikei University, School of Medicine, Minato-ku, Tokyo, JAPAN.

One of the interaction energies between myofilaments is electrostatic repulsive energy which is exerted by negative charges of the filaments. From the relation between osmotic compressing force exhibited by polyvinylpyrrolidone (PVP, K-30) and fiber width (D) or 1,0 lattice spacing ($d_{1,0}$), we can determine the radial stiffness (K) which would reflect the electrostatic repulsive force affected by divalent cations or pH. We studied the effects of magnesium ion (Mg) and pH on K by measuring D under the microscope and $d_{1,0}$ from equatorial reflections of X-ray diffraction patterns in single mechanically skinned fibers at 20°C (ionic strength was fixed at 0.15 M). When PVP was added, the skinned fiber shrank in D or $d_{1,0}$. Above 1 M PVP, the rate of shrinkage of D was highly proportional to that of $d_{1,0}$. In the fibers of the sarcomere length (L) of 2.5 μ m, $d_{1,0}$'s were 41.4 ± 0.7 (n=13), 38.3 ± 0.8 (8) and 41.1 ± 0.4 (3) nm in pH 7 (standard solution); Mg 1, MgATP 4, EGTA 4, PIPES 10 and KCl 90 mM, pH 6 and 30 mM Mg (pH 7) respectively. In 6 M PVP, each $d_{1,0}$ was 32.7 ± 0.2 (4), 28.8 ± 1.2 (10) and 28.6 ± 0.7 (5) nm. Below $d_{1,0}$ of 35 nm, K showed significantly smaller values in pH 6-6.5 or 10-30 mM Mg than in the standard solution. Effects of pH and Mg were also observed in the fibers of L = 4 μ m, in which $d_{1,0}$ was 37.4 ± 1.3 (15) nm in standard solution. We considered that a change in conformation of HMM can explain these changes. A provisional model is proposed, in which the effect of Mg or low pH is to decrease the rigidity of S1-S2 or S2-LMM hinge.

051

RATCHET-AND-PAWL APPROACH TO MUSCLE CONTRACTION

Neil Thomas, Physics Dept., Birmingham Univ., Birmingham 15
Shortening velocities of a few muscle lengths per second are common for unloaded frog sartorius muscles when stimulated, but stretching velocities are only a small fraction of this (provided that the stretching force is not too high).¹ This asymmetrical behaviour is also apparent in length-step experiments^{2,3}, which show a rapid recovery from a sudden release and a much slower recovery from a sudden stretch. The asymmetry can be understood in simple terms if we regard the thin filaments and myosin cross-bridges in striated muscles as a microscopic ratchet-and-pawl system. This is analysed using Feynman's approach to a thermally driven ratchet acting as a heat engine.⁴ Heat from the hot reservoir is used to represent the energy obtained from ATP in real muscle, and this phenomenological viewpoint leads to a remarkably simple explanation for the force-velocity characteristic and for the heat of shortening. Following Huxley and Simmons², we include a series elastic component for each cross-bridge to treat transients, but we go further by including the masses of the thick and thin filaments to construct a model of a whole myofibril. Finally, it is suggested that the ratchet mechanism may still operate in relaxed muscle.

1. N.A. Curtin and R.E. Davies, *Cold Spring Harbor Symp. on Quant. Biol.* 37, 619 (1972)
2. A.F. Huxley and R.M. Simmons, *Nature* 233, 533 (1971)
3. H.E. Huxley et al., *Proc. Nat. Acad. Sci.* 78, 2297 (1981)
4. R.P. Feynman, in *Feynman Lectures on Physics*, Vol. 1, Ch. 46 (Addison-Wesley 1963).

053

DIFFERENTIAL EFFECTS OF ANESTHETICS AND ALCOHOLS ON MYOCARDIAL EXCITATION-CONTRACTION COUPLING.

C. Lynch III, Dept. of Anesthesiology, Univ. of Virginia Medical Center, Charlottesville, Virginia 22908, USA

Depressant effects of local anesthetics, volatile anesthetics (isoflurane or halothane) and aliphatic alcohols, which have anesthetic properties similar to volatile agents, were studied on twitch responses and membrane action potentials (AP) of guinea pig papillary muscles. Muscles (field stimulated at: rested state, 0.1, 0.25, 0.5, 1, 2, and 3 Hz) were studied in normal Tyrode solution, or in 26 mM K Tyrode with 0.1 μ M isoproterenol, which produces slow APs and a markedly augmented, late-peaking twitch at low frequencies (rest to 0.5 Hz). The aliphatic alcohols (0.10 mM 1-octanol, 1.0 mM 1-hexanol, 3 mM 1-pentanol) and isoflurane (0.54 mM) uniformly depressed (>70%) the late-peaking tension at low frequencies and the late rate of tension development (dTL), while causing less depression (5-30%) of tension at 2-3 Hz stimulation and having little effect on the initial rate of tension development (dTI). These agents increased the AP duration at low freq., and slightly depressed the slow AP rate of rise. Lidocaine (100 μ M) and bupivacaine (10 μ M) showed a similar differential pattern and degree of contractile depression. The increase in myoplasmic Ca causing contraction at low rates of stimulation appears to be inhibited by these drugs, with little effect on excitation-contraction coupling at increased frequencies. The potency of each compound in depressing dTL was proportional to its octanol: water partition coefficient. In contrast, halothane uniformly depressed tension, dTI and dTL at all frequencies.

050

A FAST-PHYSIOLOGICAL TECHNIQUE TO DETERMINE THE FIBER TYPE WHICH CORRELATES WITH MYOSIN LIGHT CHAIN COMPLEMENTS IN SKELETAL MUSCLES. Masataka Kawai and Frederick H. Schachar, Dept. of Anatomy and Cell Biology, Columbia University, New York, N.Y., 10032, U.S.A.

Sinusoidal analysis technique was applied to single fibers from slow (SF) twitch muscles and fast (FF) twitch muscles (psoas, tibialis, EDL, diaphragm, soleus, semitendinosus) from rabbits. The difference of transient response was examined in order to find a quick physiological method to determine the fiber type. Our investigation showed that SF's complex stiffness during maximal activation is very different from that of FF. In FF complex stiffness consists of 3 characteristic exponential processes (A), (B), and (C), whereas in SF process (C) is large in magnitude, but processes (A) and (B) are strikingly small. In addition, we found that apparent rate constants are 9-27 times faster in FF compared to those of SF. Assuming that the mechanism of energy transduction is the same for both muscle types, the above results can be interpreted to mean that the intrinsic rate constants of faster reactions in the cross-bridge cycle are different by a factor of 27 between FF and SF. In order to examine if our physiological assay is consistent with known light chain complements, the same fibers were also analyzed on SDS PAGE. A 100% correlation between the physiological identification and the gel identification of fiber type was obtained. This observation justifies the use of sinusoidal analysis to determine the fiber type, and suggests the importance of light chains in cross-bridge functions.

052

CHANGES IN THE X-RAY DIFFRACTION PATTERN OF TETANIZED FROG SKELETAL MUSCLE DURING SINUSOIDAL LENGTH CHANGES, STUDIED BY SYNCHROTRON RADIATION

K. Wakabayashi, H. Tanaka, T. Kobayashi, Y. Amemiya, T. Hamanaka, S. Nishizawa, H. Sugi and T. Mitsui, Photon Factory, National Laboratory for High Energy Physics, Oho-machi, Ibaraki-Ken, Japan

To study the dynamic behaviour of the cross-bridges, sinusoidal length changes (14, 10-Hz) were applied to isometrically contracting frog sartorius muscles, and the resulting changes in the X-ray diffraction pattern were examined at 10 msec intervals, using the diffractometer made by Amemiya et al. (1983) for synchrotron radiation. Both the equatorial and meridional reflections exhibited distinct periodic changes in response to the muscle length changes. The equatorial 1,0 and 1,1 intensities changed nearly in phase and in antiphase with the length change, respectively. The above changes in the equatorial reflections were much more marked than those taking place in response to slow stretches (Sugi et al., 1977; Yagi et al., 1977; Tanaka et al., 1983) or quick length changes (Amemiya et al., 1980; Huxley et al., 1981). The meridional 143 Å intensity changed in a very characteristic manner with the length change; it decreased for both the release and stretch phases of the sinusoidal length perturbation and exhibited a maximum at the boundary from stretch to release phases. Fourier analysis of the 143 Å intensity change indicated that the second harmonics had an amplitude comparable to that of the fundamental frequency component.

054

CROSS-BRIDGE MOTION IN SKINNED FIBERS STUDIED BY OPTICAL ELIPSOMETRY, R.J. Baskin, K. Burton, M. Jones and Y. Yeh, Depts. of Zoology and Applied Science, Univ. of Calif., Davis Calif. 95616, U.S.A.

Optical ellipsometry studies of single, skinned muscle fibers conducted on the diffraction orders, have yielded spectra which are sensitive to the state of the fiber. The linearly polarized light field vector becomes elliptically polarized when collected at the diffraction orders. Under certain conditions, the ellipticity spectra exhibit differences between left and right order lines as well as between the various orders of a given side. Fibers that have been subject to extraction of myosin (0.6M KCl) retain a diffraction pattern but exhibit no depolarization of incident linearly polarized light. A significant decrease in polarization is seen in skinned fibers that are subject to an increase in pH from 7.0 to 8.15. This increase in pH results in a decrease of 30% in the depolarization angle of single fibers. Our studies show that the depolarization is caused by the myosin moiety. The major decrease in depolarization angle that we observe at pH = 8.15 is consistent with the notion that as crossbridges move out from the shaft of the thick filament, their ability to cause depolarization of the incident linearly polarized light decreases. (Yeh, Corcoran, Baskin, and Lieber, *Biophysical J.* (1983) 44, 343-351. This interpretation is also consistent with the work of Ueno and Harrington (*J. Mol. Biol.* (1981) 149, 619-640) where the decrease in the ability to crosslink S-1 and S-2 to the thick filament at pH = 8.2 suggests crossbridge movement away from the thick filament.

Thursday 02 August Congress Centre-First Floor Posters 055-060

Posters on Cross-Bridge Mechanisms and Muscle Contraction

055

A CONSIDERATION ON THE ELASTIC PROPERTIES OF THE CONTRACTILE MACHINERY IN MUSCLE

I. Hatta, Y. Tamura and H. Sugi, Dept. of Appl. Phys., Nagoya Univ., Chikusa-ku, Nagoya, Japan.

We have measured the change in the sound velocity during contraction in the semitendinosus muscles of the bullfrog (*Rana catesbeiana*), using the 7 MHz ultrasonic pulse propagation method (Tamura et al., 1982), and found from the sound velocities at rest and during contraction that the increment of the elastic stiffness constant above the resting value was $6 \times 10^7 \text{ N m}^{-2}$ during the tetanus. An analogous value can be estimated from the slope of the t_1 curve of Ford et al. (1981) using the quick release completing in 0.2 ms. The above agreement indicates that the additional elastic element appearing during the activation of the contractile machinery has almost no frequency-dispersion from kHz to MHz region. However, care should be taken for the fact that the elastic measurement with low frequency perturbations at kHz produces the change in the cross-sectional area of the muscle and therefore, makes possible to obtain Young's modulus, which is different from the spring constant directly sustaining the generated force. In this sense, we emphasize that our measurement with ultrasonic waves is the only method to give the true elastic stiffness constant.

057

CHANGES IN THE EQUATORIAL X-RAY DIFFRACTION PATTERN FROM TETANIZED FROG SKELETAL MUSCLE DURING AND AFTER A SLOW STRETCH

H. Sugi, H. Tanaka, T. Kobayashi and Y. Asanishi, Photon Factory, National Laboratory for High Energy Physics, Ohomachi, Ibaragi-ken, Japan

When a tetanized muscle is slowly stretched, the force attained after stretch is appreciably larger than the isometric force at the same muscle length, despite the reduced amount of myofibrillar overlap. The mechanism of force enhancement by stretch was studied by the time-resolved X-ray diffraction technique with intense X-ray source at the Photon Factory. The sartorius muscle of the bullfrog was isometrically tetanized, and slowly stretched at about 0.05 length/sec for 0.25 sec. This procedure was repeated 3 times without appreciable muscle fatigue, and the resulting change in the equatorial reflections was examined with a time resolution of 0.25 sec. The intensity of 1,1 reflection decreased during stretch, and then showed partial recovery after the completion of stretch; the recovery of the 1,1 intensity took place in parallel with the decay of force after stretch. Meanwhile, the 1,0 intensity showed a large scatter, and did not change significantly by stretch. These results are consistent with the idea that the force enhancement by stretch is associated with the disordering of myofibrillar lattice spacing, which results in an increase in the overall electrostatic repulsion forces within the whole filament-lattice system; the increased electrostatic repulsion forces would show up as the force increment after the completion of stretch.

059

MYOPLASMIC Ca TRANSIENTS AND SARCOPLASMIC RETICULUM Ca MOVEMENTS IN FROG SKELETAL MUSCLE FIBRES INJECTED WITH ANTIPYRYLAZO III

M. E. Quintana-Ferreira, S. M. Baylor and C. S. Hui, Departments of Physiology, University of Pennsylvania, Philadelphia, PA, and Biological Sciences, Purdue University, West Lafayette, IN, U. S. A.

The release and re-uptake of Ca ions by the s.r. was studied in intact twitch muscle fibres by injecting the metallochromic dye Antipyrilazo III into highly stretched single fibres and recording dye-related absorbance changes following action potential stimulation. The dye signal is characterized temporally and spectrally by two main isotropic components. The earlier component, due to the formation of the 1:2 dye complex, appears to be a rapid and linear monitor of the change in myoplasmic free [Ca], whereas the later component appears to reflect an increase in myoplasmic [Mg] and/or pH. In order to estimate the Ca flux (release minus uptake) between s.r. and myoplasm, the computational model described by Baylor, Chandler and Marshall (J. Physiol. 344, 625-666, 1983) for analyzing Arsenazo III Ca transients was used. The results at 16 °C indicate that Ca release and myoplasmic free [Ca] reach peak values of 35-45 $\mu\text{M/s}$ and 2-4 μM , respectively, 5-7 ms and 8-11 ms following stimulation. The computed uptake rate during the falling phase of the transient is presumed to reflect s.r. Ca pump activity and, when plotted versus [Ca], reveals a saturating sigmoid curve. The maximum uptake rate, 2.0 to 2.8 $\mu\text{M/s}$, corresponds to a pump turnover rate of 8-12 per second. Half-maximal pumping occurs at a free [Ca] 60-100 nM above resting. The sigmoidal foot of the curve may reflect a pump stoichiometry of 2 Ca ions per turnover.

056

COMPARATIVE STUDIES OF THE ACTIVE SITE STRUCTURE OF SKELETAL AND CARDIAC MYOSINS

Yoh Okamoto and Ralph G. Yount, Biochemistry/Biophysics Program and Department of Chemistry, Washington State University, Pullman, WA 99164-4630.

The active site of bovine cardiac myosin has been labeled by a photoaffinity analog of ADP, N-(4-azido,2-nitroamino)ethyl diphosphate (NANDP). MgNANDP was trapped stoichiometrically at the active site by cross-linking of SH₂ and SH₁ by a Co(II)/Co(III)phenanthroline system or by p-phenylene dimaleimide. Trapped NANDP reacted with cardiac subfragment one (SF₁) during photolysis for 2 min in a manner similar to that of skeletal SF₁ [Y. Okamoto and R.G. Yount, *Biophys. J.* (1983), 41, 298a]. Radioactivity of [³H]-NANDP was found only in the 95K-heavy chain fragment after SDS-PAGE. Limited trypsin digestion further localized the reacted NANDP to the N-terminal 25K peptide. After extensive trypsin and subtilisin BPN' digestion in the identical manner for skeletal SF₁, two major radioactive peptides, CP1 and CP2, were found at exactly identical positions in the HPLC chromatogram for NANDP-labeled peptides from skeletal SF₁. Initial sequence studies indicate NANDP reacts with a specific Trp residue adjacent to a trimethyllysine residue in both skeletal and cardiac myosins. Supported by an MDA Fellowship to Y.O. and NIH grant AM-05195 to R.G.Y.

058

STRUCTURAL CHANGES IN A S-2 MYOSIN DETECTED BY AN ENZYME-PROBE METHOD

H. Ueno and W. F. Harrington, Dept. of Biol., The Johns Hopkins Univ., Baltimore, MD, U.S.A.

We have recently developed an enzyme-probe technique to detect local conformational changes in polypeptide structure quantitatively (1). The kinetics of proteolytic digestion and the sites of cleavage in the polypeptide chain were determined by following the time-course of fragmentation on SDS-gels. Cleavage rate constants for a substrate protein are normalized by intrinsic hydrolysis rate of an enzyme for a model compound, and the normalized rate constants were compared. Using this method, we studied the cleavage of isolated rod and S-2 subfragments by three enzymes (chymotrypsin, trypsin and papain) at 5-40 °C. We found that the S-2 hinge domain showed much higher susceptibility to the enzymes than other regions of the myosin rod. Arrhenius plots showed that the hinge domain had $\Delta H^\ddagger = 10-40 \text{ kcal/mole}$, which was much lower than that in the LIM or short S-2. The hinge domain spans a region of about 200 Å near the center of the rod (2). In conjunction with previous findings (3-5), the present results strongly suggest that the hinge domain undergoes substantial melting upon activation.

Ref. Ueno & Harrington (1) *JMB*, (1984) 173, 35. (2) *JMB* (1984), submitted. (3) *PNAS* (1981) 78, 6701. (4) *JMB* (1981) 149, 619. (5) Ueno et al., (1983) *JMB* 168, 207.

060

MECHANISM OF FATIGUE IN SKELETAL MUSCLE: STUDIES WITH SKINNED FROG FIBERS

R.E. Godt, K.J. Fender & T.M. Nosek, Dept. of Physiology, Med. Coll. of Georgia, Augusta, GA, USA.

Both tetanic force and relaxation rate decrease in fatigued skeletal muscle. Recent work by Wilkie and colleagues (*Nature* 274:861, 1978; *J. Physiol.* 299:465, 1980) using NMR to study changes in intracellular conditions in fatigued frog muscles, shows that the decrease in both force and relaxation rate are correlated with the decline in free energy available from ATP, due to the large increase in the products of ATP hydrolysis (ADP & Pi). These changes could produce fatigue by affecting the sarcoplasmic reticulum (SR) and/or the contractile machinery. We determined the effects of these changes on the contractile machinery using skinned fibers from frog (*Rana temporaria*). Control solutions contained 2 mM MgATP and no ADP or Pi at pH 7 and 22 °C ("infinite" affinity for ATP hydrolysis). In solutions with ADP, Pi, and pH mimicking those reported for fatigued muscle (0.3 mM ADP, 26 mM Pi, pH 6.65; calculated affinity -43 kJ/mol), maximal calcium-activated force is decreased while relaxation rate is actually increased. A similar depression of force and acceleration of relaxation was observed, however, in similar solutions with Pi but no added ADP. Lowering pH had a small depressant effect on maximal force. These results indicate that the decrease in force associated with fatigue is primarily due to an effect on the contractile machinery of the increased intracellular Pi and not to the decrease in affinity. The decreased relaxation rate of intact fibers is likely due to effects on calcium uptake by the SR.

Thursday 02 August Congress Centre-First Floor Posters 061-066

Posters on Cross-Bridge Mechanisms and Muscle Contraction

061

A TEMPERATURE JUMP METHOD, TO BE USED IN THE STUDY OF EXCITATION-CONTRACTION COUPLING
J.W. Metselaar, J. Crezee and H.G. Goovaerts, Department of Medical Physics, Faculty of Medicine, Free University, Amsterdam, NETHERLANDS.

The action potential and the force of contraction are governed by fast processes, some of which are strongly temperature dependent. In order to study these processes and their interrelationship a method has been developed in which an isolated papillary muscle of the rabbit heart can be quickly raised in temperature. The fast increase of the muscle temperature is obtained by means of the local dissipation of heat from an alternating current of 30 MHz. The method has the advantage that the heat is developed in the muscle as well as in its immediate surroundings so that the speed of temperature increase of the whole muscle is not hindered by heat conduction. The temperature distribution and its time dependence can be measured with a small thermocouple with a short response time (< 1 ms) and a high spatial resolution. Specific features of the method are that the muscle temperature can be increased 3°C in about 15 ms, with a dissipative power of 15 W. Reliable measurement of action potential and force of contraction is possible immediately after the power pulse. The applicability of the method is demonstrated by the result that the shape of the action potential responds to the temperature jump in a few excitations and the force of contraction within one contraction.

063

EFFECT OF DIFFERENT ANIONS AND PH ON THE THERMAL STABILITY OF SKELETAL MYOSIN ROD. W.F. Stafford, Dept of Muscle Res., Boston Biomed. Res. Inst., Boston, MA, U.S.A.

The helix-coil transition of myosin rod was monitored under various ionic conditions by following the circular dichroic ellipticity at 222nm as a function of temperature. In 0.6M NaCl, 5mM phosphate, 0.1mM EDTA, pH 7.3, rod exhibited a biphasic melting curve with transitions at 45° and 53° as seen previously by Burke et al. [Biochemistry 12, 701, (1973)]. However, in 0.6M CH_3COONa , 5mM phosphate, 0.1mM EDTA, pH 7.3, the transitions occurred at 50° and 58° , respectively. The two transition temperatures, T_1 and T_2 , increased with increasing salt concentration up to about 1.0M. Above 1M, increasing [NaCl] destabilized the helix while increasing $[\text{CH}_3\text{COONa}]$ caused the helix to become more stable. Substitution of ammonium or potassium for sodium ion had no significant effect on T_1 showing that cation type is not important. These results correlated with papain digestion experiments which showed that digestion at the S2/LMM junction was faster in the presence of chloride than in the presence of acetate. The rate was dependent on chloride concentration but essentially independent of acetate concentration up to 2M. It is thought that the intracellular free chloride ion concentration is about 2-3 mM [Bolton and Vaughan-Jones, J. Physiol. 270, 801 (1977)] and that predominant anions are derived from organic acids. These results suggest that myosin rod may be more stable under physiological conditions than past solution studies have suggested. (Supported by NIH grant HL-26229)

065

LOCATION OF HIGH AFFINITY METALBINDING SITES IN MYOSIN HEAD G.G. Charkviani, Z.O. Japaridze, T.M. Eristavi and S.H. Džebadze, Department of Biophysics, Beritashvili Institute of Physiology of Georgian Academy of Sciences, Tbilisi, USSR.

Using the method of saturation curves of Kulikov and Likhstein for measuring the distances between paramagnetic Mn^{2+} and spin labels and spin labelled derivative of ATP (SL-ATP), synthesized according to Zhdanov, as a label to the ATPase sites of myosin we have found that metalbinding sites with highest affinity for the divalent cations, which are located in DTNB light chains, are at a distance of 42-45 Å from the corresponding ATPase sites. In the case of myosin with SH₂ groups labelled with iodacetamide spin-labels the distance between them and above mentioned sites is 45-50 Å. Additional purification of Zhdanov's SL-ATP gave us the possibility to establish the ability of the latter to be a substrate for myosin ($K = (6.4) \cdot 10^{-5}$ M versus $K = (3.2) \cdot 10^{-5}$ M for usual ATP). Using this purified SL-ATP and specimen of subfragment I of myosin (SI) with removed DTNB light chain we attempted to measure the distance between ATPase site of SI and another high affinity metalbinding site which appears in the presence of nucleotide. Preliminary measurements indicate that this distance is approximately half of the distance between ATPase site and metalbinding site on DTNB light chain.

062

BIOENERGETICAL INVESTIGATIONS BASED ON MECHANICAL AND RESPIRATORY PARAMETER OF CYCLIC SPORT-MOVEMENTS
A. Török, I. Ocsosvsky, Ö. Takács, G. Zombori* and F. Guba, Inst. Biochem. Univ. Med. Sci. Szeged and *Csongrad County Council T.B. Hospital-Sanatorium, Szeged-Deszk, Hungary.

The swimming, rowing, paddling in kayak or canoe generally are termed as endurance sports, the forward movement being impeded by the drag of water, of which density is several times higher than that of the air. We found that during a single cycle 130-180 N force has to be exerted in these sports. Naturally the performance is influenced by the frequency of cycles as well as the work per cycle or by the working capacity. The hardness could be judged on the basis of two biophysical parameters, i.e. the mechanical work exerted by the subjects and the time of work. According to our measurements only 0.2-0.3 KJ/kg work could be performed by untrained subjects in our kayak-canoe ergometer within 2-3 minutes, while 0.5-0.8 KJ/kg work was done by the trained ones. The total energy production of subjects was determined by respiratory parameters, too. From the latter and the mechanical work the efficiency of the organism was calculated and proved to be 12-16 per cent. The "Szeged-mechanoergometer" is suitable for this purpose and in addition it is useful for drilling the optimal rating speed in rowing sports.

064

EFFECT OF DENERVATION AND SPREADING DEGENERATION ON ACTIN STRUCTURE. I.G. Strankfeld, Y.S. Borovikov, I.E. Moskalenko, V.F. Kirillina, V.M. Lobachov, Institute of Biophysics, USSR Academy of Sciences, Pushchino; Institute of Cytology, USSR Academy of Sciences, Leningrad; Cancer Centre, USSR Academy of Medical Sciences, Moscow, USSR.

Actin from skeletal rabbit and frog muscles was studied by polarized UV-fluorescence microscopy, UV-fluorescence spectroscopy, microcalorimetry and circular dichroism. Actin in solution as well as in muscle ghost fibres were investigated after denervation and spreading degeneration. These pathological states cause some changes in fluorescence of actin. Thus, tryptophan fluorescence anisotropy in denervated ghost fibres is higher than that in control ones, while tryptophan fluorescence intensity in actin in solution is lower than that in a control one. Phalloidin and ATP decrease the anisotropy of tryptophan fluorescence in denervated fibres and increase it in intact ones. Decrease in fluorescence anisotropy of F-actin in denervated and degenerated fibres induced by the binding heavy meromyosin or myosin subfragment-1 to actin is lower than that in control actin. The character of CD-spectrum of G-actin is not changed after denervation. The increase of F-actin thermostability at 30°C is shown.

066

ON THE CHARACTERISTICS AND FUNCTION OF MUSCLE CONTRACTION OF DIGESTIVE TRACT

He Zhen-lu, Department of Biology, Jinan University, Guangzhou, China.

Through the study of the contractive motion of the pyloric sphincter and esophageal sphincter, the contraction may be divided into three-phases: the phase of elasticity, of pursing and of enclosure. This conclusion has been reached through repeated experiments, conducted under fiber-gastroscope with microtransducer, which has been designed by us. This finding is of importance in studying muscle contraction both microcosmically and macrocosmically. As an example the Chinese PSP (pyloric sphincter pressure) and the LESP (low esophageal sphincter pressure) have been measured, which broadly tally with the theoretical calculation. In this paper the muscle contraction of stomach has also been physically analysed and some new opinions suggested.

Thursday 02 August Congress Centre-First Floor Posters 067-072

Posters on Cross-Bridge Mechanisms and Muscle Contraction

067

UNDAMPED COMPLIANCE AND A RELAXATION TIME CONSTANT IN THE MICROSECOND RANGE IN THE SKINNED SKELETAL MUSCLE FIBRE OF THE FROG. T. Blangé, G.J.M. Stienen and B.W. Treijtel. Department of Physiology, University of Amsterdam, 1e Const. Huygensstraat 20, 1054 BW Amsterdam.

The tension response of isometrically contracting skinned fibres of the iliofibularis muscle of the frog to changes in length completed in 40 μ s was investigated with respect to the part during and shortly after the length change. The fibres were obtained by the freeze-drying procedure described by Stienen, Gith and Rieggs (1983). Fibre segments with a length of a few millimeters were mounted between a displacement generator and a force transducer with a resonant frequency of about 50 kHz with the fibre attached. The fibres were incubated and - between measurements - kept in relaxing solution containing 40 mM KCl, 60 mM Imidazole (pH = 7), 20 mM EGTA, 5 mM MgATP, pMg = 3, 10 mM Pcr and 50 U/ml CPK. The tension response in a fully activating Ca-buffered solution consists of a delayed increase (stretch) of decrease (shortening) in tension up to the maximum T_i , followed by relaxation towards the original isometric level. The tension recordings are analysed by frequency-analysis as well as by simulation. The analyses indicate that the elastic impedance of the activated fibre contains an undamped elasticity with a Young's modulus of between 3 and 6.10¹⁰ N/m² and a relaxation time constant of about 5 to 10 μ s. The undamped elasticity of the relaxed fibre is 5 to 10 times less, where as the relaxation time is about the same. * Pflügers Arch. 397: 272-276

069

STRUCTURAL CHANGES IN CONTRACTILE SYSTEM OF A SINGLE MUSCLE FIBRE DURING SPREADING DEGENERATION. S.A. Krolenko, V.P. Kirillina, Yu.S. Borovikov, Inst. of Cytology, Acad. of Sci. of USSR, Leningrad, USSR. Spreading degeneration was studied on isolated skeletal muscles of frog and rat using the methods of phase contrast, electron and polarized UV-fluorescence microscopy. The rate of spreading and pattern of degeneration varied depending on sarcomere length, solution conditions and selective extraction of Z-line. Wave-shaped changes in anisotropy of tryptophan fluorescence were observed far from the injury site. They are more distinctly seen in Ca²⁺-free solution. The changes reflect two different states of myosin and actin in muscle fibre similar to contraction and relaxation. Primarily, no morphological changes can be observed within the area of maximum changes of fluorescence anisotropy. Later in these sites the contraction knots appear. In Ca²⁺-free solution they usually look like narrow stripes covering several sarcomeres. Their formation is accompanied by stretching or disruption of neighbouring sarcomeres. Local contractions might also arise in highly contracted fibres or after the extraction of Z-line by urea solution. It is assumed that local contractions as well as spreading of degeneration are controlled by intracellular membranes of the fibre, rather than by surface membrane.

071

EMG QUANTITATIVE ANALYSIS OF TRICEPS MUSCLE UPON IRRADIATION BY DIFFERENT MAGNETIC FIELDS. M.I. El Gohary, E.M. El Sayed, and M.I. Sharaf, Biophysics Lab., Al Azhar Univ., Cairo, Egypt.

An action potential analyser was used to measure the EMG characteristics; generated by the triceps muscle. Three EMG parameters were investigated, (i) the integrated voltage of the muscle's electrical activity in μ V/Sec, (ii) the frequency in spikes/sec, and (iii) the amplitude of the EMG triceps muscle in μ V. The employed magnetic fields were, (a) Constant magnetic fields of intensities 500 Gauss and 10 KG, (b) pulsating magnetic field (MF) of intensity 50 G/50 Hz the exposure time for all fields used was 15 min. The results of the present work showed that; the constant field of 500 G induced a little on muscle performance ability when it was applied for a short duration, and the increase of the EMG amplitude was 25.6% on the average. While the constant MF of 10 KG increased the amplitude of the EMG by an average of 33.4%. Therefore, when the muscle is exposed to constant strong MF, its energy increases and this, in turn improves its performance ability. However, a pulsating MF of 50 G/50 Hz increased the muscle performance ability by an average of 96.2%.

068

RAMAN & FTIR STUDIES OF FAST- AND SLOW- TWITCH MUSCLE SR Ca²⁺-ATPase AND LIPID VESICLES. E. Bicknell-Brown, D. Borchman, & S. Navarro, Chemistry Dept., Wayne State Univ., Detroit, Mich and K.G. Brown, Dept. Chem. Sci., Old Dominion Univ., Norfolk, Va. USA

Both lipid extracts and purified Ca²⁺-ATPase vesicles were prepared from rabbit caudofemoralis (fast-twitch) and soleus (slow-twitch) muscles. Temperature plots of IR CH₂ stretch frequencies for lipid extracts showed that caudofemoralis SR lipids undergo three phase transitions, while soleus lipids melt gradually between -10 & 20°C. Temperature plots of Raman CH₂ stretch intensities are in agreement. Intensities of -CH₂ st. modes show that melting of unsaturated chains occurs first, at ca. -10°C. Both IR and Raman results show that soleus lipids are more rigid above -10°C than are caudofemoralis lipids.

SR Ca²⁺-ATPase vesicles were prepared by removing extrinsic proteins. Temperature IR and Raman studies of the Ca²⁺-ATPase vesicles show that those of caudofemoralis are more fluid than those of soleus.

Composition studies were carried out for both types SR, and these provide the basis for explanations for the observed differences in fluidity.

Results of Arrhenius plots are correlated with the spectroscopic results and a possible mechanism for the different rates of slow- & fast-twitch muscle relaxation is suggested.

070

FORCE-FREQUENCY RELATIONSHIP IN CANINE WORKING AND CONDUCTING VENTRICULAR TISSUES

C.-I. Lin and H.-H. Lu, Inst. of Biophysics and Dept. of Pharmacology, Nat. Defense Med. Cntr., Taipei, Taiwan, ROC.

The force-frequency relationship was studied in dog ventricular muscle and Purkinje fibers. The transmembrane potential, the contractile force and its first derivative (dF/dt) were recorded. In ventricular muscle fibers, the force and the dF/dt increased when the drive cycle length was reduced from 2000 to 333 ms (positive staircase). The force and the dF/dt declined as drive cycle length was shortened (negative staircase) in Purkinje fibers. When [Ca]_o was elevated from 2.7 to 5.4 mM, contractile force of Purkinje fibers increased but the staircase remained negative. The staircase became positive as contractile force declined at higher [Ca]_o (8.1-12.1 mM). Strophanthidin (10⁻⁷ - 10⁻⁶ M) first increased and then decreased contractile force. During the declining phase of strophanthidin inotropy the staircase became positive. During positive staircase, the contractile force of the extrasystolic beat was found to be higher than the control beats. The positive staircase was still present after the action potential duration was prolonged by amiodarone but could be reversed gradually by Ca antagonists (diltiazem and verapamil). The above findings suggest that an accumulation of [Ca]_i is responsible for the positive staircase and that the regulation of [Ca]_i is different in these two types of cardiac cells.

072

NMR STUDIES OF SOLUTION STRUCTURE OF LIGHT CHAINS. H.R. Wilson and R.J.P. Williams, Inorganic Chem. Lab., Oxford, U.K.

The phosphorylatable and alkali two light chains (PLC and A2LC) from rabbit skeletal muscle have been examined by ³¹P and ¹H nmr respectively.

Ionisation characteristics of the phosphoserine group of PLC have been compared with those of the free amino acid.

pH, temperature and nuclear Overhauser experiments with A2LC have been used to assign some of its proton spectrum, to identify interaction of residues and to indicate tertiary structure for the protein. Similarities are observed with the calcium binding protein family, including ICBP and parvalbumin whose tertiary structure are known.

Thursday 02 August Congress Centre-First Floor Posters 073-078

Posters on Cross-Bridge Mechanisms and Muscle Contraction

073

074

075

076

077

078

Thursday 02 August Congress Centre-First Floor Posters 079-084

Posters on Cytoskeleton

079 ORAL PRESENTATION

THREE DIMENSIONAL STRUCTURE OF INTERMEDIATE FILAMENTS
D.A.D. Parry, Massey University, Palmerston North, New Zealand; R.D.B. Fraser and T.P. MacRae, CSIRO, Division of Protein Chemistry, 343 Royal Parade, Parkville, Vic. 3052, Australia.

Analysis of the amino-acid sequence data for intermediate filaments reveals a centrally located helix-rich domain about 300 residues in length, with a high degree of inter-species homology, and predominantly non-helical terminal domains which vary widely in size and composition. The central domain contains four α -helical segments showing the heptapeptide repeating pattern of hydrophobic residues indicative of coil-coil rope formation, separated by short non-helical segments. Interaction studies combined with physico-chemical data suggest that the chains associate in pairs to form two-strand parallel-chain ropes in the helical segments and that the chain segments are in-register. Earlier studies suggested that these rope-like segments constitute the framework of the intermediate filament and the parameters of the surface lattice have now been derived from X-ray diffraction studies. Four polypeptide chains are associated with each lattice point and arrangements of the two-strand rope segments have been derived which are consistent with physico-chemical studies of enzymatic fragments. In addition inter-rope interactions have been investigated for different axial shifts and maxima found which lead naturally to one of the observed dimensions of the surface lattice.

081

EFFECT OF THE TIGHTLY BOUND CATION ON ACTIN POLYMERIZATION

L.C. Gershman, L.A. Selden and J.E. Estes, Res. Service, Veterans Admin. Med. Center, Albany, New York and Dept. of Physiology, Albany Medical College, Albany, New York, U.S.A.

We recently reported that exchange of actin-bound divalent cation affects the lag phase in actin polymerization (Biochemistry, in press, 1984) and that actin containing bound Mg^{++} (Mg-actin) has a critical actin concentration (CAC) about 20x smaller and a forward rate constant of polymerization about 1.5x larger than Ca^{++} -containing actin (Ca-actin) (Biochem. Biophys. Res. Comm. 116:478-485, 1983). We have extended these measurements over a wider range of divalent cation concentrations and have also studied polymerization initiated by KCl. Monomeric actin was labeled with N-pyrenyl-iodoacetamide, and the relative forward and reverse rate constants (k^+ and k^-) for Mg-actin and Ca-actin measured as a function of added $MgCl_2$, $CaCl_2$ or KCl. Graphical analyses of the data showed 1) the ratio k^+/k^- remains constant at various cation concentrations, but both the ratio k^+/k^- and the ratio CAC_{Mg}/CAC_{Ca} decreased markedly at low cation concentrations. 2) The type of external (solution) cation does not affect the rate of depolymerization, but the type of actin-bound cation does. 3) Mg-actin depolymerizes faster than Ca-actin under similar conditions; we propose that this may be due to a larger number concentration of polymers at equilibrium in Mg-actin solutions. Supported by the Veterans Administration.

083

Preparation and polymerization kinetics of skeletal muscle ADP-actin. Altaf A. Lal, Stephen L. Brenner and Edward D. Korn, Laboratory of Cell Biology, NHLBI, NIH, Bethesda, MD 20205.

ADP-actin was prepared by polymerizing about 100 μ M ATP-actin complex (5-10% pyrenyl actin) in 0.5 mM $MgCl_2$. Excess ATP was exhausted by repeated sonifications. Filamentous ADP-actin was diluted to about 25 μ M in 5 mM Tris, pH 8.0, 0.2 mM ADP, 5 mM AP_5A , 0.1 mM $CaCl_2$, 0.2 mM DTT, 0.01% sodium azide. Depolymerized actin was separated by centrifugation at 65,000 rpm for 2.5 h at 4 °C in a type 70 Ti rotor. ADP-actin isolated in this way is oligomer free and polymerization competent. The critical concentrations obtained in 1.0 mM $MgCl_2$ and 1.0 mM $MgCl_2$ + 0.1 M KCl were 8.0 μ M and 2.0 μ M respectively. Covalently cross-linked actin trimer was used to nucleate the assembly of ADP-actin. The sum of association rate constant (k^+) at the two filament ends, assuming each trimer acts as a seed were 0.8 μ M $^{-1}$ s $^{-1}$ and 0.9 μ M $^{-1}$ s $^{-1}$ in $MgCl_2$ and in $MgCl_2$ + KCl buffers respectively. The dissociation rate constants (k^-) calculated from elongation rate constants and measured critical concentrations were 6.4 s $^{-1}$ in $MgCl_2$ and 1.8 s $^{-1}$ in $MgCl_2$ + KCl. These observed rate constants were independent of trimer concentration. In 1.0 mM $MgCl_2$ spontaneous polymerization was too slow to measure and the time required for polymerization in 1 mM $MgCl_2$ + 0.1 M KCl was about 8 fold longer than for polymerization in ATP. The results of this study show that k^+ for ADP actin is about 2-6 fold smaller whereas k^- 's about 5-10 fold bigger than for ATP actin.

080

1H -NMR STUDIES OF VILLIN HEAD FRAGMENT.
G.H.M. Scott and R.J.P. Williams, Inorganic Chemistry Laboratory, Oxford, U.K.

V. Gerke, L.K. Hasterberg and K. Weber, Max-Planck Institute for Biophysical Chemistry, Göttingen, F.R.G.
The work concerns the 1H -NMR studies of the 8,800d villin headpiece fragment, which is shown to possess substantial tertiary structure in solution. Interactions are observed between three of the six phenylalanines and between the single histidine, a fourth phenylalanine and several methyl groups. These two hydrophobic regions form part of a tightly packed structure, which is believed to play an important role in the structural change in intact villin on calcium binding. Studies so far indicate that the structure of the headpiece can not be similar to other intra-cellular calcium-binding proteins we have studied.

082

THE PRESENCE OF OLIGOMERS BELOW THE CRITICAL ACTIN CONCENTRATION

J.E. Estes^{1,2}, J. Newman³, L.A. Selden¹, and L.C. Gershman^{1,2}
¹Res. Service, Veterans Admin. Med. Center, Albany, N.Y.,
²Dept. of Physiology, Albany Med. College, Albany, N.Y., and
³Dept. of Physics, Union College, Schenectady, N.Y., U.S.A.

The theoretical description of actin polymerization proposed by Oosawa and colleagues implies the presence of oligomers below the critical actin concentration. We have attempted to use the sensitive method of laser light scattering to detect this molecular species. The translational diffusion coefficient (D_{20}) for monomeric actin was determined to be $8.25 \pm 0.15 \times 10^{-7}$ cm 2 /sec at 20 μ M actin. This value dropped to $6.2 \pm 1.0 \times 10^{-7}$ cm 2 /sec within 1-2 hr after the addition of low concentrations of $MgCl_2$. The drop in D_{20} could be reversed by the addition of low concentrations of $CaCl_2$. Using sub-critical concentrations of actin labeled with N-pyrenyl-iodoacetamide, the time course of oligomerization was determined to take about 80-100 min, which is markedly longer than the time required for exchange of the actin-bound Ca^{++} for Mg^{++} (cation exchange) was measured using atomic absorption and Ca^{++} measurements. Our results indicate that it is likely that the species undergoing oligomerization is Mg-actin monomer. Supported by the Veterans Administration.

084

THE PLATELET RETICULAR NETWORK. C. Richard Zobel & H. Manuel, Dept. of Biophysical Sciences, State University of New York at Buffalo, Buffalo, NY, USA.

Studies by a number of investigators of activated platelets have revealed an extensive trabecular-like cytoskeleton whose components have been identified as ABP, α -actinin and actin by SDS-PAGE of TX-100 insoluble cell fractions.

SEM examination of spread platelets rinsed with a jet of buffer after incubation in 1 mM $ZnCl_2$ reveals an apparent reticular network encompassing the entire spread cell. In some preparations the surface meshwork is disrupted making apparent an internal trabecular cytoskeleton.

Although platelets have been reported to react with anti-serum to mammalian α -spectrin and have a 240 Kd band on SDS-gels (and thus might have an erythrocyte-like submembranous reticulum), this constituent normally occurs in the soluble fraction of TX-100 treated cells. SDS-PAGE of cells treated with $ZnCl_2$ in the presence of enzyme inhibitors shows an enhanced appearance of 255, 240, 220 and 100 Kd components in the insoluble fraction and their loss from the soluble fraction. Furthermore, membranes prepared by sucrose fractionation of platelets sonicated in $ZnCl_2$ have an enhanced 255 Kd band while the supernatant fractions from these preparations also lack 255, 240, 220 and 100 Kd constituents.

These results suggest that in addition to an internal trabecular cytoskeleton spread platelets have a surface reticular network whose appearance is enhanced in the presence of $ZnCl_2$ due to increased interactions among high mol. wt. components comprising the platelet cytoskeleton and membrane components.

Thursday 02 August Congress Centre-First Floor Posters 085-090

Posters on Cytoskeleton

085

THERMODYNAMIC STUDIES OF AN INTERACTION BETWEEN A BICYCLIC COLCHICINE DERIVATIVE AND TUBULIN OLIGOMERS. Heinz Decker and James C. Lee, Department of Biochemistry, St. Louis University School of Medicine, St. Louis, MO 63104 U.S.A.

Equilibrium binding and a thermodynamic analysis of the interaction of calf brain tubulin with the bicyclic colchicine derivative (2-benzyloxy-5-(2,3,4-trimethoxyphenyl)-2,4,6-cycloheptatrien-1-one) (MTC) were studied in 10^{-2} M sodium phosphate buffer, 10^{-4} M GTP at pH 7.0 by fluorometric and sedimentation techniques. Binding isotherms were obtained as a function of protein concentration ranging from 1×10^{-5} to 10^{-3} M tubulin dimers of 110,000 in molecular weight. At 20°C and high protein concentration the binding behavior is characterized by one binding constant, $K_1 = (5.1) \times 10^{-4}$, whereas at low-protein concentration two binding constants of $K_1 = (5.1) \times 10^{-5}$ and $K_2 = (5.4) \times 10^{-3}$ are necessary to fit the data. Results from thermodynamic studies revealed that K_2 is very dependent on temperature, whereas K_1 is not. Both K_1 and K_2 appear to be driven by a positive entropy change. The physical states of tubulin were monitored by sedimentation velocity. It was shown that tubulin dimers undergo dissociation with a dissociation constant of 5×10^{-7} M at 23°C. The binding behavior of MTC is correlated to the physical states of tubulin. (Supported by NIH Grant NS-14269 and AM-21489.)

087

DISTRIBUTION OF ACTIN IN PHYSARUM AMOEBOFLAGELLATES. M.R. Adelman, Dept. of Anatomy, USUHS, Bethesda, MD, U.S.A.

During the synchronous transformation of *P. polycephalum* amoebae into flagellate swimmers, intermediate cells - amoeboid flagellates - transiently display a novel motile domain, the ridge. This flattened cytoplasmic extension undergoes rapid undulations and contains a lamellar core of actin microfilaments. The fluorescent probe rhodamine-phalloidin has been used to characterize changes in actin distribution coincident with the formation and breakdown of the ridge. Transforming cells were briefly fixed with formaldehyde, bound to glass slides, and then permeabilized with acetone: most cells showed intense and specific fluorescence after exposure to rhodamine-phalloidin and binding was blocked by preincubation with phalloidin. Time course experiments showed that symmetrical amoeboid cells, present only in early stages of the transformation, were labeled at the periphery of pseudopod-like extensions. As the transformation proceeds, such amoeboid cells disappear and cells with flagella and broad extensions - similar to the ridge - appear. Amoeboid flagellates with a fully-formed ridge showed pronounced labeling of the ridge and of a small uroid-like patch; a weaker cortical fluorescence was also seen but the anterior (microtubule-rich) region of such cells was essentially devoid of actin. The highly elongate swimmers which dominate the population at later time points show a more uniform cortical distribution of actin; although such cells usually lack a ridge they often retain a small ridge-like concentration of actin on their dorsal aspect. (Supported by USUHS Protocol No. C07015)

089

MEMBRANE EVENTS PRIOR TO FUSION OF MYOGENIC CELLS N.V. Samosudova, U.S. Larin, V.E. Shungskaja. Institute of Problems of Information Transmission Academy of Sciences, Moscow, USSR.

It was established that a gap junctional communication formed prior to fusion during myogenesis. In the present work the interactions of plasma membranes of myogenic cells (myoblasts and myotubes) were studied by electron microscopy in the period of fusion. The breast and leg muscles of 7-8 day-old chick embryos were fixed in two ways: (1) 2.5% glutaraldehyde and 1% OsO_4 , (2) 2.5% glutaraldehyde, 1% tannic acid and 1% OsO_4 . The fixation by tannic acid revealed asymmetry of the three-lamellar plasma membrane (i.e. the external leaflet is electron denser). Two kinds of intercellular contacts are described. One of them is formed by membranes of adjacent cells arranged in parallel. The space between the external leaflets is 150 Å. They are connected by "bridges", consisting of material which is apparently localized on the membrane surface. The "bridges" are seen only after tannin-fixation. Another kind of intercellular contact has the pentalamellar structure (three dense strata separated by two light strata) and displays an undulation. These junctions often enclose elongated electron-dense bodies. The second kind of junction resembles the contacts previously seen by others (Zampighi et al., 1982, J. Cell Biol. 93:175-189).

086

NEUROPLASMIC LATTICE PARAMETERS IN SOME VERTEBRATE AND INVERTEBRATE AXONS A.J. Hodge and W.J. Adelman, Jr., Lab. of Biophysics, IRP, NINCDS, NIH, Marine Biological Lab., Woods Hole, MA, USA.

The neuroplasmic lattice in representative vertebrate axons (mouse, rat, roach) and in molluscan axons (squid, *Loligo*), as seen in electron micrographs of relatively thick ($\sim 0.2 \mu\text{m}$) sections, consists primarily of longitudinally oriented neurofilaments and neurotubules spaced about 50-70 nm apart in a roughly hexagonal array, a symmetry strongly supported by computerized nearest neighbor vectorial analysis. These filamentous elements are linked transversely by an ordered array of thin (2-4 nm diam.) cross-bridges spaced 40-50 nm apart in the axial direction as shown by (a) direct stereoscopic observation of longitudinal sections, (b) optical and electron optical autocorrelation techniques, and (c) Fourier analysis of video line signals from appropriately aligned longitudinal sections in STEM. In contrast, the axons of arthropods (lobster and *Limulus*) appear to lack neurofilaments entirely, their neuroplasmic lattices consisting of a hexagonal array of neurotubules spaced about 110 nm apart and linked by complexly coiled transverse bridges (~ 2 nm diam. when extended). Autocorrelative methods suggest a longitudinal spacing between cross-bridges of 45-50 nm in these axons, a value essentially indistinguishable from the 40-50 nm axial spacing typical of the vertebrate and molluscan axons studied thus far. The latter values appear to be consistent with the widely reported occurrence of a 19-22 nm axial periodicity in α -type keratin and other intermediate filaments.

088

CHARGE EFFECTS IN SEDIMENTATION OF INTERMEDIATE FILAMENT SUBASSEMBLIES. M. Potschka, H. Winkler, G. Wiche. Institute of Biochemistry and Institute of Theoretical Chemistry, Univ. of Vienna, Währingerstr. 17, Austria, and Max Planck Institute for Biophysical Chemistry, Göttingen, BRD.

We studied size and shape of oligomeric subassemblies by analytical ultracentrifugation to elucidate the structural organization of Intermediate Filaments. Nucleotide-free Vimentin was isolated from C6-cell cultures and purified by a novel HPLC scheme. S-values were measured down to 70 $\mu\text{g/ml}$ in Tris/HCl ($1 \leq 20 \text{ mM}$, pH 7.5-8.5). A generalized model was derived where charge effects depend on the ratio of protein concentration to ionic strength, Brønsted equilibrium of the monovalent counter ion, and the charge density of the polymer. Neglecting the secondary charge effect and assuming that the ionic strength contribution of the polymer is negligible one obtains:

$$\frac{1}{M_w} = \frac{1}{M_w} + \alpha \quad \frac{1}{S_{20,w}} = \frac{1}{S_{20,w}} + \frac{Nv \cdot fR}{1 - \beta} \alpha$$

$$\alpha = \frac{1}{2} \cdot \frac{2 \cdot \left(\frac{z_p}{M_p} \right) \cdot \left(\frac{C_p (\text{mg/ml})}{I (\text{Mol})} \right)}{\left(\frac{z_p}{M_p} \right) + 1} \quad ; \quad \beta = 10^{\text{sign}(z) \cdot (pK - \text{pH})}$$

After extrapolation to zero protein concentration to eliminate charge effects, only a small increase of oligomer size with increasing ionic strength was observed, indicating that the dominant aggregate is a tetramer in equilibrium with a sub-isodesmic distribution of larger aggregates. The observed tetramer shape $f/f_0 = 2.6$ is expected for a rod of dimensions $70 \times 2 \text{ nm}$. Absence of monomers and dimers was verified by gel permeation chromatography.

090

Butyrate-Induced Cytoskeletal Reorganization in HeLa Cells. M. M. Cassidy, S. Jahangeer, G. Yabouny, & R. C. Henneberry. George Washington University Medical Center, Washington, D.C. 20037 & NINCDS, NIH, Bethesda, MD 20205

Butyrate is a potent inducer of a variety of functional alterations in many cultured cells. These include induction of β -adrenergic receptors in HeLa cells, hormone and enzyme synthesis, metabolic modifications and shape changes. We hypothesize that restructuring of the cytoskeleton may precede the definitive expression of membrane related events. By indirect immunofluorescence microscopy using polyclonal and monoclonal antibodies, HeLa monolayers were shown to possess an extensive network of randomly arranged microtubules (MTs) which were particularly dense in the juxtanuclear region. In the presence of 5 mM butyrate for 24 h the previously reported elongate shape change was reflected in a reorganization of the MTs such that a majority were then oriented in the long axis of the cell, extending to the tips of the neurite-like processes or between them and few were seen in the vicinity of the nucleus. Essentially similar results were obtained with cells grown in chemically-defined, serum-free medium. Colchicine (2×10^{-4} M) prevented the butyrate-induced shape and MT alterations. With colchicine alone a diffuse staining pattern, due perhaps to the presence of depolymerized tubulin, was observed. Cycloheximide (10 $\mu\text{g/ml}$) had no effect on the control cells but blocked the butyrate-induced alterations in shape and MT pattern. It is concluded that the induction of β -adrenergic receptors and shape changes in HeLa cells by butyrate is associated with a dramatic reorientation of the cytoskeleton and modification of protein synthesis. (Supported in part by ONR contract N00014-79-C-0003).

Thursday 02 August Congress Centre-First Floor-Posters 091-096

Posters on Cytoskeleton

091

INTERACTION OF BLEOMYCIN WITH ERYTHROCYTE GHOST MEMBRANES

M. Bryszewski, J. Rodriguez-Paris, I.V. Chapman^{*}
Department of Biophysics University of Lodz, Lodz, Poland, ^{*} Department of Medical Biophysics, University of Dundee, Dundee, UK.

The inactivation of bleomycin during incubation with erythrocyte ghost membranes was studied. The method based on DNA-damaging activity of bleomycin was used. It is known that bleomycin causes the release of malondialdehyde (MDA) from the deoxyribose moiety of DNA which can be measured colorimetrically using thiobarbituric acid-reactivity for MDA formation. A significant decrease of the bleomycin activity/ability to damage DNA/ with the increasing erythrocyte membrane protein content was found.

Changes in erythrocyte membrane fluidity under the influence of bleomycin were also studied. The method used was the optical method using the fluorescent label pyrene, which is incorporated deep in the hydrophobic membrane region. A measure of the lateral mobility of the probe is the formation rate of excimers during the collision of an excited monomer and a monomer in the ground state. It was found that bleomycin causes a significant decrease in membrane lipid fluidity.

092

MULTIFREQUENCY PHASE FLUOROMETRIC STUDY OF TRYPTOPHAN FLUORESCENCE IN TUBULIN

Y. Engelborghs and R. Audenaert, Laboratory of Chemical and Biological Dynamics, Celestijnenlaan 200 D, B-3030 Leuven Belgium

A multifrequency phase fluorometer was constructed using a dye laser, a pockels cell and a frequency doubler. In this way excitation at 295 nm with a modulation up to 50 MHz was possible. Using phosphocellulose purified tubulin, two major life times were determined and the lifetime resolved spectra were recorded, using phase sensitive detection. These experiments were repeated with tubulin in different states of nucleotide and inhibitor binding. Tubulin with GTP, GDP on the E-site, or even an open E-site, did not show significant differences. Of the different inhibitors tested, only colchicine seemed to introduce significant alterations. Exposure of the tryptophan residues to the solvent was tested by stopped flow analysis of the reactivity of the tryptophan residues towards N-bromosuccinimide. Two fast and one slow phase of small amplitude were observed. Here again, only colchicine binding caused a significant change in the reactivity of some tryptophan residues.

093

MICROTUBULE LENGTH DISTRIBUTION IN VITRO

V. Gal and D. Trajković, Department of Biophysics School of Medicine and Institute for Biological Research, Belgrade, Yugoslavia.

The microtubule length distribution was determined by two methods: (1) electron microscopy and (2) turbidity measurements of the extent of assembly and the apparent rate constant of elongation. When assembly is induced by temperature shift from 40° to 28°C the change of length distribution with the concentration is very small in the range of 0.5 to 3.0 mg/dm³ of microtubule protein. In the same concentration range when microtubule protein is exposed to gamma radiation before assembly, one can note a significant decrease of the average length and its standard deviation in a dose dependent manner. The assembly in the presence of Ca⁺⁺ results in the formation of long microtubules. The decrease of GTP concentration also causes an increase of microtubule length. Using this approach we studied the effect of various parameters on nucleation and elongation of microtubules.

094

TAXOL EFFECTS ON CNS NEURONS AND GLIA IN ORGANOTYPIC FETAL MOUSE SPINAL CORD-DRG CULTURES

E. B. Masurovsky, E. R. Peterson, S. M. Crain and S. B. Horwitz, Depts. of Neuroscience & Molecular Pharmacology, A. Einstein Coll. Med., Bronx, N.Y., USA

Explants of fetal mouse spinal cord (SC) with attached dorsal root ganglia (DRG), which had developed 2-3 wks in organotypic culture, were exposed for up to 6 days to 1-2 μ M taxol. Morphologic analyses revealed unusual numbers, groupings and/or locations of microtubules (MT) in SC neurons and glia similar to those previously observed in the DRG cells (Neurosci., 10:491, 1983). Unlike DRG neurons which displayed abundant peripheral MT groupings, SC neurons exhibited notable variations in both numbers and loci of taxol-induced MT formations. MT-endoplasmic reticulum (ER) arrays and disrupted/dispersed Golgi complexes were seen in SC neurons, as in DRG neurons. MTs increased considerably in oligodendroglia, but rel. little in astroglia where MTs are normally sparse. However, MT-ER arrays were seen in both glial types. These data suggest that CNS cells with diverse tubulin complements and/or related factors (e.g., MAPs) may display differential MT responses to taxol. (Supported by NIH NS-08770, -14990, & -19611 and ACS CH-86)

095 ORAL PRESENTATION

THE INTERACTION OF 1,2-DIPALMITOYL-SN-GLYCERO-3-PHOSPHOSERINE MONOLAYERS WITH G-ACTIN (AIR/WATER INTERFACE). E. Llerenas and M.I. Haro. Department of Biochemistry, Centro de Investigación y Estudios Avanzados del IPN, A.P. 14-740, 07000 México, D.F., and Faculty of Psychology, UNAM, México.

Further studies on the interaction of lipid monolayers and G-actin, now with an acidic phospholipid (di-C₁₆PS), results in an even more marked rigidifying effect of the lipid structure brought about by the protein than in previous work where 1,2 dipalmitoyl-sn-glycerol-phosphocholine was tested. It can be tentatively interpreted as the protein exerting a charge-exclusion effect of the surrounding lipid from the mixed di-C₁₆ PS-G-actin monolayer. This in turn giving rise to and even more compact lipid structure. A temperature dependence programme was run out in order to estimate the sort of energy involved in the lipid/protein monolayer interaction. Enthalpy, entropy and Gibbs free energy values of the interaction (ie with and without protein) in the range of 10-20°C were as follows: $\Delta H^{\circ} = 57$ cal/mole, $\Delta S^{\circ} = 0.175$ eu and $\Delta F^{\circ} = 5.88$ cal/mole. These values would be energetically equivalent to the compression effect induced by the introduction of an extra methylene residue to each pair of the lipid chains. These and previous results point to the conclusion that whenever G-actin is within a structured lipid the latter becomes more compressed, the mechanism probably being different for each phospholipid though. The implications these results could have for the dynamics of cell membrane cytoskeleton interaction will be discussed.

096

THE MECHANISM OF MICROTUBULE ASSEMBLY IN VITRO

D.C. Clark, S.R. Martin, P.M. Bayley, E.J. Manser and P.M. Butler, Division of Physical Biochemistry, National Institute for Medical Research, Mill Hill, London NW7 1AA

The kinetics of assembly of bovine and porcine microtubule protein are biphasic over a wide range of solution conditions. The rates of the two processes are concentration independent and therefore each phase must contain a rate-limiting first order process.

We have examined the composition of the material formed in the fast phase of assembly by PAGE, EM and the wavelength dependence of turbidity, and present evidence for the formation of MAP-rich microtubules during the early stages of assembly. We infer that MAP-containing fragments play a key role in determining the kinetics of both phases of assembly and examine the implications of the redistribution of MAPs as a rationale for the slow phase elongation process.

Thursday 02 August Congress Centre-First Floor Posters 097-102

Posters on Cytoskeleton

097

INTERACTION OF GLYCERALDEHYDE-3 PHOSPHATE DEHYDROGENASE WITH BAND 3 PROTEIN OF THE RBC MEMBRANE
A.H. Beth, J.H. Park and W.E. Trommer, Dept. of Physiology, Vanderbilt Univ., Nashville, TN, U.S.A.
Several glycolytic enzymes including glyceraldehyde-3 phosphate dehydrogenase (GAPDH) bind reversibly to the cytoplasmic N-terminal domain of band 3 protein in the red blood cell (RBC) membrane. Bound GAPDH can be released by high levels of substrates or NAD⁺. We have previously shown that the relative positioning and spatial distribution of a spin labeled NAD⁺ (SL-NAD⁺) derivative bound to soluble GAPDH in various stoichiometric ratios can be determined by deconvolution of electron paramagnetic resonance (EPR) spectra. These data provided direct evidence for a ligand induced sequential binding model with random spatial addition of NAD⁺ to the tetramer subsequent to binding of the first coenzyme (J. Biol. Chem., in press). In the present report with membrane bound enzyme, band 3 interacted with one NAD binding domain of GAPDH resulting in displacement of one SL-NAD⁺. Catalytic activity was partially inhibited by binding. The 23-Kda fragment purified from band 3 interacted with two coenzyme binding domains and completely inhibited activity at pH 7. Kinetic data indicated that the 23-Kda protein was a competitive inhibitor with respect to NAD⁺. The quaternary structure of the enzyme-coenzyme complex was preserved in the membrane complex. These data provide insight into the arrangement of the cytoplasmic domain of band 3 in the RBC membrane.

099

TAXOL CHANGES THE HYDRODYNAMIC PROPERTIES OF MICROTUBULES
J. Mergh, M. Wallin and J. Deinum, Dept. of Physical Chem., Chalmers Univ. of Technol., S-421 96 Göteborg, Dept. of Zoophysiol. and Dept. of Medical Physics, Univ. of Göteborg, S-300 33 Göteborg, Sweden.
Microtubule, MT, assembly was followed and monitored by 1) the development of linear dichroism of the apparent absorbance at 350 nm upon flow orientation, the LD signal, 2) the change in absorbance at 350 nm, the turbidity and 3) the specific viscosity, SV, measured at 2 min intervals. We found that the hydrodynamic properties of MTs are changed in the presence of taxol, a drug which binds to tubulin, while the MT associated proteins, MAPs, do not seem to be of equal importance. The presence of taxol did not change the relative amount and composition of the MAPs in the MT-pellet. Although for normal MT assembly the three methods showed the same features these were different in the presence of taxol. Furthermore, these MTs were difficult to orientate, as high flow gradients were needed and the optimal LD value represented only 10% orientation in contrast to normal MTs, rapid relaxation to random orientation was found. Taxol induced MTs, assembled from purified tubulin, showed the same behaviour. Low orientability was also indicated by electron micrographs of pelleted MTs randomly orientated in the presence of taxol. A further indication for altered hydrodynamic properties is the very high SV, 4x the steady state value found with normal MTs, in the initial phase of assembly both for purified tubulin as well as for MT-proteins. Furthermore, the apparent steady state as found by turbidity does not represent a stable state as both LD and SV continued to change for a much longer time.

101

COLCHICINE SPIN PROBES AND OTHER EFFECTORS BOUND TO TUBULIN
Johanna Deinum and Per Lincoln, Dept. of Medical Physics, Univ. of Göteborg, Box 330 31, S-400 33 Göteborg, Sweden.
A spin probe (I) for the colchicine binding site on tubulin has been synthesized which inhibits microtubule assembly and competes with colchicine. From EPR-titration a non-linear Scatchard plot was found indicating that tubulin at 37°C contains more than one colchicine binding site: one high affinity binding site ($K_d \approx 20 \mu M$), consistent with the binding studies of the isolated complex and one or more low affinity site(s) (K_d approx. 200 μM).
Allosteric spin probes with varying larger chain lengths were found to have less affinity for tubulin compared to (I). From the EPR spectrum of these tubulin-bound probes it can be concluded that the high affinity colchicine binding site lies in a hydrophobic protein cleft.
No disturbance of the EPR signal of the tubulin-bound allosteric spin probe could be observed at 20°C from Mn(II) or Co(II), used for the Mg(II) resp. Zn(II) binding site, Cr(II)GTP, used for the binding site of the exchangeable GTP and the essential SH-groups labelled with a SH-group spin probe. This lack of interaction indicates that the colchicine binding site is sterically isolated from the binding site for GTP, Zn(II), Mg(II) and the two essential SH-groups.
However, in the presence of spin probe (I) the reaction rate of the SH-groups decreased to about 50%. Binding of colchicine to tubulin apparently induces a conformational change which affects the accessibility of the two most reactive SH-groups.

098

PROTEIN INTERACTIONS IN MICROTUBULE FORMATION
K.E. Foster and M.A. Rosemeyer, Department of Biochemistry, University College London, Gower Street, London WC1E 6BT, UK.
Microtubule proteins were prepared from bovine brain by assembly-disassembly cycles that provide the main component, tubulin, and microtubule-associated proteins (MAPs), which promote the polymerization of tubulin. We have investigated the factors affecting polymerization by studying the properties of tubulin in the presence and absence of MAPs using: electron microscopy; preparative ultracentrifugation as a gelling assay; analytical ultracentrifugation to detect oligomers; and electrophoresis to determine composition.
There was a correlation between the characteristic sedimentation pattern of 6 S, 19 S and 30 S components and the production of microtubules seen under the electron microscope. Our results suggest that formation of microtubules depends on the microtubule protein preparation being competent to form these particular species.
On removal of the MAPs, the property of tubulin to form aggregates other than microtubules becomes more evident. One of these associations involves the formation of a 60 S oligomer in the presence of an extraneous protein with a molecular weight of 160,000. This entity corresponds with one of the neurofilament proteins, and indicates a possible interaction between microtubules and neurofilaments.
On further purification of tubulin, it showed an association of the dimer to a tetramer, which could be the initial step for polymerization to microtubules.

100

STRUCTURE OF F-ACTIN IN SINGLE-LAYERED PARACRYSTALS
E.P. Morris, R. Mendelson and E.J.O'Brien, M.R.C. Cell Biophysics Unit, 26-29 Drury Lane, London WC2, England.
Electron microscope analysis of paracrystals of F-actin induced by Mg²⁺ has usually been complicated by the presence of superimposed layers of filaments, so that the projected appearance may represent a composite (Egelman et al 1983 J. Mol. Biol. 166 605). At lower levels of Mg²⁺ (25mM) single-layered paracrystals are obtained which appear well suited for image analysis. Optical and computer-generated diffraction patterns indicate that the filament symmetry comprises 13 subunits in 6 turns of the 5.9 nm genetic helix. The intensity of the 2nd layer-line is relatively strong, about half that of the 1st layer-line. Filtered images of the paracrystals show clearly that adjacent filaments have opposite polarity. Individual filaments in the filtered image were extracted from arrays and used for helical three-dimensional reconstruction. In the reconstructions the actin subunits have a large elongated region extending to a radius of about 4.4 nm and a smaller projection extending to about 3.5 nm. Connections along the long-pitch helices occur at lower radius.
The F-actin reconstructions are consistent with the region assigned to actin in the three-dimensional reconstructions calculated from electron micrographs of F-actin + tropomyosin by O'Brien et al (1983, in "Actin, its structure and function in muscle and non-muscle cells", Academic Press, Sydney). The binding of tropomyosin does not therefore alter the conformation of F-actin greatly. An interesting feature of the F-actin reconstructions is a thin extended region which may form part of the tropomyosin binding site.

102

CONFORMATIONAL EFFECTS OF NUCLEOTIDE BINDING TO TUBULIN
E.J. Manser and P.M. Bayley

The effect of bound nucleotide upon the conformation of tubulin has been investigated by removal of the nucleotide from the E(exchangeable) binding site on the tubulin dimer, using carefully controlled treatment with alkaline phosphatase. The conformational effects are monitored by near-UV circular dichroism, and the nucleotide hydrolysis by HPLC.
Alkaline phosphatase causes an exponential change in the near-UV CD of tubulin at a rate correlating with the loss of bound nucleotide. Subsequent addition of GTP causes a reversal of the effect. The magnitude of the spectral change is different in magnitude and kind from effects associated with modulation of tubulin conformation by MAPs. Similar effects are observed with tubulin and with microtubule protein.
The effects show that nucleotide removal causes change which, though substantial, are reversible under these conditions. The results are relevant to the role of nucleotides in promoting microtubule assembly, and also indicate the feasibility of performing quantitative substitution of nucleotides with various analogues.

Thursday 02 August Congress Centre-First Floor Posters 103-108

Posters on Cytoskeleton

103

IMMUNOCHEMICAL LOCALISATION OF 30kD MICROTUBULE ASSOCIATED PROTEIN FROM GIARDIA FLAGELLA. J.T. Clark and D.V. Holberton. Department of Zoology, University of Hull, Hull, U.K.

A method has been developed for the isolation of flagella from *Giardia lamblia* using a Percoll density gradient; flagella occupy a broad density range of 1.076-1.111 g/ml. Analysis of the proteins of purified flagella by SDS PAGE reveals the major polypeptides as tubulin and a group of proteins of about 30kD. Microtubule-associated proteins of similar M_r have been shown to be present in the cytoskeleton of *Giardia* and were called giardins (Crossley & Holberton, *J. Cell Sci.*, 59, 81-103, 1983). Flagellar giardins appear to be antigenically distinct from cytoskeletal giardins when blotted from a gel into cellulose nitrate and tested for cross-reactivity with an antibody to cytoskeletal giardin.

Some of the isolated flagella are ventral flagella which have a specialised ultrastructure, possessing a paraflagellar rod which is attached to 3 doublet tubules of the axoneme and extends to form a broad fin beneath the membrane. 1% Triton X-100 removes these rods when flagella are demembranated. When the proteins of the detergent-insoluble axonemes are examined, the giardin bands are lost whilst most other major components are retained.

Protein eluted from the major giardin band was used as an immunogen. The resulting anti-serum preferentially labelled the ventral flagella of cells examined by immunofluorescence.

105

MAPs Mediate Association of Microtubules and Neurofilaments *In Vitro*. E.J. Asanodi and R.C. Williams, Jr., Dept. of Molecular Biology, Vanderbilt University, Nashville, Tennessee, USA. Neuronal intermediate filaments (neurofilaments, abbreviated NF) prepared from brain form a viscous, sedimentable complex with microtubules under suitable conditions. [Runge, M.S. et al., *P.N.A.S.*, USA 78, 1431 (1981)]. NFs prepared from spinal cord did not. Brain NFs differ from spinal cord NFs in part by bearing proteins that resemble microtubule-associated proteins (MAPs). MAPs bound to spinal cord NFs when they were incubated together. The MAP-decorated NFs formed a viscous complex with microtubules (MTs), showing that a component of MAPs mediates association between MTs and NFs. MAP-2, prepared by a method involving heat-treatment of MT protein, did not mediate a viscosity increase. The dependence of the viscosity of NF-MT mixtures upon the concentration of MAPs displayed a maximum, suggesting that MAPs act as true cross-bridges between the two structures. Gel filtration separated the MAPs into a fraction of large Stokes' radius which was active in producing NF-MT mixtures of high viscosity, and a fraction of small Stokes' radius which was not. The peak of viscosity-inducing activity had a larger Stokes' radius than purified MAP-2, indicating that a complex of MAPs connects MTs and NFs. Electron microscope grids with adherent MAP-decorated NFs bound numerous MTs, each in apparent contact with one or more NFs. Grids prepared with untreated NFs lacked MTs. These results confirm that one or more of the MAPs mediates association between MTs and NFs. Supported by grant GM 29834 of the US NIH.

107

104

THERMODYNAMIC EVIDENCE FOR CYTOSKELETAL CONSTRAINTS ON THE α -ADRENERGIC RECEPTOR OF TURKEY ERYTHROCYTES. J. Hoebeke and A.D. Strosberg, Laboratory of Molecular Immunology, Institut Jacques Monod, 2, Place Jussieu, F-75251 PARIS Cedex 05. At temperatures below 28°C, the binding of the antagonist 1-dihydroalprenolol and the agonist 1-isoproterenol is of a hydrophobic nature in view of the positive enthalpy and entropy changes upon complex formation. Above 28°C, the receptor is present in an altered state. This is inferred from the sharp decrease in affinity for both antagonist and agonist, from the negative enthalpy changes and from the small entropy changes upon binding. Kinetic experiments suggest that the modification in the thermodynamic parameters is due to drastic changes in dissociation rates and activation energy of the dissociation reaction. The actin polymerisation inhibitor, cytochalasin D, and the microtubule inhibitor, nocodazole, induce an antagonist binding state comparable to that above 28°C, over a temperature range from 17 to 37°C. Nocodazole treated cells displayed a low affinity, a high negative enthalpy and a zero entropy change upon agonist binding. Cytochalasin D treated cells exhibited a high affinity, a higher negative enthalpy and a negative entropy change. These results suggest the different modulation of receptor affinity by the actin-spectrin network and the peri-membranar microtubules.

106

108

Thursday 02 August Congress Centre-First Floor Posters 109-114

Posters on Electric Field Effects in Cell Membranes

109

BIOPHYSICAL STUDIES ON CELLULAR MEMBRANE EXPOSED TO HIGH INTENSITY TRANSIENT ELECTRIC FIELDS

V.T. Srinivasan, K.C. George and B.B. Singh
Biology and Agriculture Division, Bhabha Atomic Research Centre, Trombay, Bombay, India

The structural changes induced in the intact membrane of rat thymocytes exposed to high voltage (upto 10 kV/cm) D.C. Pulses (0.2 and 125 μ sec.) have been monitored using fluorescent probes ANS and DEH. Whereas, the intensity of ANS fluorescence increased with the voltage indicating unfolding of the membrane at the water-lipid interphase, a slight decrease in DEH fluorescence under similar circumstances demonstrates only minor disorganization in the lipidic interiors. These effects are accompanied by permeability changes in the membrane as revealed by the release of intracellular materials or by the uptake of erythrocin B. For the short duration pulse, such changes could be reversed on incubation of cells at 37°C but the changes induced by 125 μ sec pulse appeared permanent. Furthermore, the reversible changes in the fluorescence or membrane permeability could also be made permanent on storing at ice temperature. These results on the molecular alterations and their manoeuvrability by temperature would be useful in entrapment of foreign materials e.g. drugs, in cellular systems.

111

LOW-ANGLE X-RAY DIFFRACTION STUDIES OF HUMAN ERYTHROCYTE MEMBRANES

N. Zhao*, Y. Xu*, Z. Lu*, K. Yao**, and H. Pan*. *Institute of Modern Biology and Biomedical Engineering, Tsinghua University, Beijing, China. ** Institute of Material Science, Tsinghua University, Beijing, China. + Chinese Academy of Medical Science, Beijing, China.

Reports on low angle x-ray diffraction measurements of human erythrocyte membrane structure have appeared frequently in recent literatures, but few of them deal with influence of ions on erythrocyte membranes. In this study, low angle x-ray diffraction patterns have been obtained from ordered arrays of hemoglobin-free human erythrocyte membranes by use of one dimension position-sensitive detector. The spacing corresponding to the peak of intensity was varied (depending on the humidity) from 55 Å to 65 Å which was good agreement with Stamatoff et al (1975). The effect of ions (such as Mg, Al, Cu, Zn, Se, Pb et al) on the structure of erythrocyte membranes has been investigated. From the change of diffraction patterns, we found that some kind of ions, for example Se, presumably could bind with membranes. The influence of some traditional Chinese medicines on the structure of human erythrocyte membranes was also studied. It is interesting to find that some traditional Chinese medicines (such as *Ilex pubescens*) for angina pectoris have obvious effect on human erythrocyte membrane structure.

113

STUDIES OF INTERACTIONS IN PROTEIN-LIPID LAMELLAE SYSTEM USING THE AUTOCORRELATION FUNCTION APPROACH - THE EXAMPLE OF NERVE MYELIN

M.K. Ghazizadeh, Noqchi Memorial Institute for Medical Research, Univ. of Ghana, Legon.

In studying protein-lipid and lipid-lipid interactions in bio-membranes and model membrane systems, the methods of biochemical analysis of membrane components and phase transition phenomena have been widely used. The autocorrelation function has been applied mainly in determining the electron density distribution of a membrane pair. Since myelin lipids and proteins contain charged and uncharged groups which interact, the autocorrelation function of a unit cell offers in principle a basis for studying protein-lipid, lipid-lipid and protein-protein interactions in the lamellar system. Using the autocorrelation (generalized Patterson) function of normal, swollen and CaO_4 -fixed myelin samples, we identify qualitatively in analogy to a potential function areas of the function related to electrostatic, hydrophobic and dispersion interactions. This qualitative description of the autocorrelation function in terms of interactions between membrane constituents agrees in principle with the generally assumed distribution of basic and hydrophobic proteins and lipids in the electron density profile of the unit cell.

110

THE EFFECT OF THE ALTERATION OF SKIN SURFACE CHARGE ON THE GROWTH OF Sarcoma SA-180 IN MICE.

J.Jaskowski, H.Zawadzki, J.Witkowski and J.Lukowicz

Institute of Medical Biology, Medical School, Gdansk, Poland.

In the course of the studies on the role of surface charge in various physiological and pathological processes we studied the influence of surface charge on the growth of experimental tumor.

Experiments were done on 60 mice with sarcoma SA-180 implanted into tails. The skin surface charge was measured on the basis of the fluorescence of 1,8-aniline-naphthalene sulfonate (ANS). The measurements were done immediately after tumor implantation and next each other day for 20 days. One half of mice received biguanide (BGD), which was applied on that area of skin, where the tumor was implanted. BGD was used in order to decrease the negative charge of the skin. The second group of mice served as a control.

Statistically significant inhibition of tumor growth was observed in the case of BGD-treated animals.

112

THE EFFECT OF VARIOUS IONS ON THE PHASE TRANSITIONAL PARAMETERS OF LIPID-WATER SYSTEMS

F. Tölg, I.P. Sugár and S. Györgyi, Inst. of Biophysics, Semmelweis Med. Univ., Budapest, Hungary

The temperature and enthalpy of the phase transitions of some phospholipid - electrolyte systems were determined by using differential scanning calorimetry. The investigated lipids were synthetic dipalmitoyl-phosphatidylcholine and dipalmitoyl-phosphatidyl-ethanolamine and the salts were the chlorides, nitrates, perchlorates of the alkali cations. There is no difference between the cations in respect to the effect on the main phase transition (at 41.5°C for DPPC and 63.0°C for DPPG) in contrary to the anions. The chlorides increased the main transition temperature while the nitrates and perchlorates did not. The effects could be interpreted by assuming the formation of H-bonds between the polar heads of lipid molecules. These results are discussed in the frame of Landau's phenomenological theory on the base of Priest's model for pure lecithin-water system. It seems that there is difference between the cations in respect to the effect on the pretransition of lecithin. The behaviour of Li^+ is quite prominent, while among the others the $\text{Na} > \text{K} > \text{Rb} > \text{Cs}$ sequence can be established.

114

HYDRATION CONTRIBUTION TO ION-ION AND ION-MEMBRANE INTERACTIONS

R. Podgornik and B. Žekš, Institute "Jožef Stefan" Jamova 39, 61000 Ljubljana, YU

A generalized version of a recent model of the hydration force was used to investigate the interaction between membranes and ions in water. By taking into account the variations in polarization as well as in density due to the presence of Bjerrum defects in ice we have extended the model of the hydration force in water to the case of local variations in water density which is more closely connected to the conditions met in real water solutions. The density and polarization profile of water was compared to the Monte Carlo simulations and satisfactory qualitative agreement was found. The hydration contribution to the Born energy was evaluated in connection with the transport of ions through membranes. The influence of hydration on ion-ion and ion-membrane interaction was treated in the frame of proposed model. We emphasize the importance of hydration for interactions in biological systems.

Thursday 02 August Congress Centre-First Floor Posters 115-120

Posters on Electric Field Effects in Cell Membranes

115

EFFECT OF MEMBRANE COMPOSITION ON APPARENT POTENTIAL MEASURED BY FLUORESCENT CYANINE DYE
M. Deloers, J.P. Servais, F. de Laveleye and E. Willfert, Biocentrals Lab., Dept. Biochemistry, UCB Pharma S.A., B-1060 Brussels, Belgium.

Egg yolk phosphatidyl choline liposomes containing variable amounts of phosphatidyl ethanolamine, phosphatidyl inositol or phosphatidyl serine induced important variations in the fluorescence of 3,3'-dipropylthiobarbituric acid. The variations of fluorescence are probably due to changes in electrostatic interaction between lipids and the fluorophore by increasing or decreasing the amount of sorbed dye. The fluorescence response is not correlated to the membrane fluidity as measured by diphenyl hexatriene polarization when the membrane contains no cholesterol. Increasing cholesterol concentration in the valinomycin containing liposome membrane, decreased the apparent membrane potential due to high potassium content and prevented dye sorption to the membrane. Although a discontinuity in the apparent potential occurred at 30 mol % cholesterol, it could not be correlated with changes in microviscosity as measured by DPH polarization.

These results indicate that great care should be taken when correlating rapid variations of fluorescence to potential changes when induced by ligands in some cell types.

We suggest that changes in phospholipid metabolism (turnover, phosphatidyl inositol cycle) might well explain fluorescent changes when monitoring the fluorescence of the dye molecules sorbed to biological membranes.

117

THE EFFECT OF THE ALTERATION OF SKIN SURFACE CHARGE ON THE HEALING OF BURN WOUNDS.

J. Jaskowski

Institute of Medical Biology, Medical School, Gdansk, Poland.

We found previously that the alteration of surface charge of cultured cells affected transport processes in cell membranes. In this investigation we determined the influence of membrane transport stimulation on the healing of burn wounds in clinical practice. The experiments were carried out on 30 patients with 2nd grade burns of the upper limbs. Skin surface charge was measured on the basis of the fluorescence of 1,8-aniline-naphthalene sulfonate (ANS). The burns resulted in an immediate decrease of the negative charge of the wounded skin. The wounds were exposed daily for 3 hours on negative air ion cloud (artificially generated) in order to reverse this decrease of skin negative surface charge. The persistent increase of the negative charge accompanied the morphologically observed healing of the wound. The latter process was completed by 10 days, what was considerably shorter time than in the case of control wounds that were not irradiated with air ions.

119

INTERACTION OF Z-BUTYLIDENEPHTHALIDE WITH K AND Ca ANTAGONISTS IN FIELD-STIMULATED MOUSE VAS DEFERENS
Y.C. Ko and L.C. Lin, Department of Pharmacology, Taipei Medical College and Department of Chemistry National Taiwan University, Taipei, Taiwan, R.O.C.

Z-butylidenephthalide (Z-Bdph), as well as Ca antagonists used, such as asipaminol, diltiazem and verapamil, but not phosphodiesterase inhibitors (PDEI) potentiated the field stimulation-induced twitch response of mouse vas deferens in a dose dependent manner. The Bdph-induced potentiation was not affected by atropine, propranolol, atenolol, yohimbine, prazosin or phenoxybenzamine (1-3 μ M). But the potentiation was blocked by a high dose of phenoxybenzamine (25 μ M), owing to its non-specific property. This blocking effect was more apparently observed in a low calcium medium, whereas not observed in a high one. Asipaminol or diltiazem, at a maximal but not at a half maximal concentration, blocked the twitch potentiation caused by Z-Bdph. In contrast, Z-Bdph at a half maximal concentration blocked those induced by asipaminol or diltiazem. While verapamil and Z-Bdph did not block each other. However, K channel blockers, such as tetraethylammonium and 4-aminopyridine, could augment the twitch potentiation caused by Z-Bdph. These results suggest that the Bdph-induced twitch potentiation may be via K and Ca channel but not via cholinergic or adrenergic pathway, and that the mode of action of Z-Bdph may be different from those of Ca antagonists and PDEI.

116

CRYOPROTECTION OF LIPID BILAYER VESICLES BY STABILIZATION OF WATER STRUCTURE. G. Strauss, A. Ebneter, and C. Leski, Dept. of Chemistry, Rutgers University, New Brunswick, N.J., U.S.A.

Structural changes during freezing and thawing of liposomes of phosphatidyl serine were investigated in presence of salts, carbohydrates, and water-soluble polymers. Small unilamellar vesicles were made by sonication. Freezing to -70° and subsequent thawing resulted in fusion of vesicles, leakage of solutes from vesicle interiors, and take-up of arylphiles from external solution. Size increases were measured by dynamic light scattering. Solute redistributions were monitored by fluorescence methods. KCl, NaCl, and LiCl below 0.1 M slightly increased the degree of fusion and membrane disruption during freeze-thawing, whereas MgCl₂ and sucrose greatly diminished the extent of freeze-damage. Polyethylene glycol, polyvinylpyrrolidone, and polyvinyl alcohol at 1 - 2% by weight were cryoprotective. Higher concentrations of polyethylene glycol caused aggregation. The results demonstrate that the extent of membrane fusion depends on the degree of disruption of membrane-coordinated water. The disruptive effect of alkali metal ions correlates with their known disruption by electrostrictive hydration. The cryoprotective action of tetraethylammonium ion is in line with its hydrophobic, structure-stabilizing hydration. The dual effect of polymers can be related to prevention of freezing and dehydrating action at low and high concentrations, respectively.

118

CHANGES OF THE TRANSPORTING ACTIVITY OF MEMBRANE Na,K-ATPase OF L₁₂₁₀ CELLS INDUCED BY AIR IONS.

J. Witkowski, J. Jaskowski and A. Mysliwski

Institute of Medical Biology, Medical School, Gdansk, Poland.

The influence of artificially generated air ion cloud to the cation transporting activity of the membrane Na,K-ATPase of mouse leukaemia L₁₂₁₀ cells was investigated by means of the measurement of ouabain-sensitive transport of ⁸⁶Rb cations into these cells. As shown, both negative and positive air ion application resulted in the diminution of ouabain-sensitive Rb⁺ transport (in the case of negative ions it was statistically significant). For the explanation of the phenomenon observed, the influence of air ions on the total membrane charge of treated cells was investigated using 1,8-aniline-naphthalene-sulfonate (ANS) as a probe. Microphotometric measurement of the ANS fluorescence of individual cells was done for determination of relative changes of charge. As shown, negative air ions caused significant increase and positive ones - decrease of the fluorescence of ANS incorporated into the membranes of treated cells. In the light of above, the paradoxical answer of Na,K-ATPase to air ions of both signs could be explained only with regard to its function as regulator of bursting of action potential.

120

TIME DEPENDENCE OF ELECTRIC BIREFRINGENCE SIGNALS OBSERVED DURING APPLICATION OF THE PULSE. Nancy C. Stellwagen, Department of Biochemistry, University of Iowa, Iowa City, Iowa 52242.

The electric birefringence of aqueous solutions of a variety of small electrolytes has been studied as a function of concentration, electric field strength and pulse length. Since the solute molecules are small, the transient behavior of the birefringence signal at the beginning and end of the pulse reflects the time constant of the detecting system, as expected. However, the amplitude of the birefringence, instead of reaching a constant steady state value during the pulse, oscillates sinusoidally when very long pulses are applied to the solution. The oscillations appear to be superimposed on the constant steady state birefringence. The frequency of the oscillations is proportional to the solute concentration and to the square of the applied field strength. The frequency also depends upon the size of the electrolyte ion, with smaller ions causing higher frequency oscillations than larger ions at a given concentration and electric field strength. Similar effects are observed with dipolar solutes in aqueous solution. (Supported by NIH research grant GM 29690).

Thursday 02 August Congress Centre-First Floor Posters 121-126

Posters on Electric Field Effects in Cell Membranes

121

MAGNETO-ELECTRO-FUSION OF HUMAN ERYTHROCYTES
I. Kramer, K. Vienken, J. Vienken and U. Zimmermann, Arbeitsgruppe Membranforschung am Institut für Medizin, Kernforschungsanlage Jülich GmbH, Postfach, Jülich, F.R.G.

The technique to collect cells dielectrophoretically to establish the close membrane contact needed for fusion by an electric field pulse is well known. Besides this technique another way of collecting the cells was tried: cells - in this case human erythrocytes - were made magnetic by incubating them in a Fe_3O_4 - suspension and then the "magnetic" cells were collected in an inhomogeneous, static magnetic field. Thus close contact between the cells could be gained and the fusion was triggered by an electric field pulse of short duration. Fusion products of two or three cells were frequent; giant cells made of hundreds of cells formed if cell suspensions of high densities were used. The advantage of collecting cells in static, inhomogeneous magnetic fields is that, rather conductive media (conductivity up to $3 \cdot 10^{-2} \Omega^{-1} \text{cm}^{-1}$) can be used which provide better physiological conditions.

123

ELECTRIC PULSE-INDUCED CELL FUSION BETWEEN HUMAN LYMPHOBLASTS AND MOUSE LYMPHOMA CELLS. Hiroko Hama-Inaba*, Takako Ohno -Shosaku** and Yasunobu Okada**, *Division of Genetics, National Institute of Radiological Sciences, Chiba 260, and **Department of Physiology, Faculty of Medicine, Kyoto University, Kyoto 606, Japan.

Somatic cell hybrids between human and mouse cells have great potential in genetic and biochemical studies of genetic disorders, such as Fanconi's anemia. We applied a technique of electric pulse-induced cell fusion (electrofusion) to obtain hybrids between human normal lymphoblasts (HSC93) and mouse leukemic lymphoblasts (HKN151), a mitomycin C-sensitive mutant of L5178Y cells, which carry similar phenotype to Fanconi's anemia cells. After the cells were brought into contact under dielectrophoresis with an alternative electric field (0.8 kV/cm, 100 kHz), cell fusion was induced by two electric pulses (3 and 5 kV/cm, 10 μ s) to the cell suspension consisting of both cell types. Cell treatment with proteolytic enzymes and the application of free Ca ions to extracellular solutions were found to improve the fusion yield and cell viability. Pretreatment of mouse lymphoma cells with neuraminidase did not affect cell fusion and cell viability. In contrast, human lymphoblasts treated with neuraminidase were brought into closer contact under dielectrophoresis and fused with higher probabilities than those without neuraminidase pretreatment. Using human lymphoblasts stained with Janus Green and mouse lymphoma cells with Neutral Red, it was found that about 40% of fused cells was the desired cell combination, that is, human to mouse.

125

INFLUENCE OF MEMBRANE POTENTIAL, SURFACE CHARGE AND POLYLYSINE ON THE INTERFACIAL STABILITY OF MEMBRANES.

W.T. Coakley, F.A. Doulah and D. Tilley, Department of Microbiology, University College, Cardiff, U.K.

Surface wave growth on erythrocytes heated at 1.0°C/s through the denaturation temperature of the cytoskeleton protein, spectrin, has been recorded by video microscopy. Cell morphology altered within 1.0s either by development of a surface wave on the cell rim and the pinching of vesicles from the crests of the growing wave or by a rounding of the cell into a sphere with an internalized dimple which immediately developed a surface wave and internalized membrane. The percentage of cells fragmenting by either mode depended on both zeta potential and on cell membrane potential. When these potentials were varied independently a 1.0mV increase in the membrane potential altered the fragmentation pattern by an amount similar to that affected by a 1.0mV decrease in the zeta potential modulus.

Electron and light microscopy of erythrocytes agglutinated by polylysine at 37°C show a regular periodicity of contact points between the cells consistent with the growth of surface waves at the membrane-water interfaces as the cells approach each other. The distance between contact points varied only from 0.8-1.3 μm over a molecular weight range of 4,000-210,000 daltons and a concentration range of 2-2,000 $\mu\text{g/ml}$. The incidence of spatially periodic agglutination fell sharply when the polycation length was less than the glycocalyx thickness. Polycations with small effects on zeta potential required a large concentration for agglutination.

122

CHARACTERISTICS OF ELECTRICALLY INDUCED AQUEOUS PORES IN THE ERYTHROCYTE MEMBRANE

K. Schwister, B. Deuticke, Department of Physiology, Medical Faculty, RWTH Aachen, D-5100 Aachen, F.R.G.

The leaks formed in human erythrocytes subjected to short ($\tau = 1-40 \mu\text{s}$) pulses of high voltage (2-20 kV/cm) were studied with respect to the conditions of their formation, their permselectivity and their resealing properties by measuring a) net and tracer fluxes of various solutes in osmotically protected cells and b) rates of colloid-osmotic lysis under various conditions. The induced permeability P is constant at 0°C for hours. It depends exponentially on the breakdown voltage E_b ($P/P_0 = \exp. (a - E_b)$). The slope a is a function of τ and E_b . The leak permeability has an activation energy of 15 - 25 kJ/mole indicative of diffusion through an aqueous pathway. Somewhat different equivalent pore radii emerge from measurements with different probes: 0.6 - 0.8 nm from tracer fluxes of polyols ($M_w < 0.36 \text{ kD}$); 0.8 - 1.9 nm from osmotic protection studies with polyethylene glycols ($M_w 0.2 - 3.3 \text{ kD}$). The leaks discriminate small ions in the sequence of their free solution mobility. They reseal by a non-mono-exponential, highly temperature-dependent process. $t/2$ values for resealing (after 6 kV/cm breakdown) range from 0.2 (37°C) to 45 min (10°C). A break in the Arrhenius diagram for resealing indicates changes in rate limiting steps. Electrically induced leaks in the erythrocyte membrane thus differ in many aspects from electrically induced leaks in artificial lipid membranes.

Supported by the Deutsche Forschungsgemeinschaft, SFB 160/C3

124

THE EFFECTS OF ELECTRIC CURRENT ON A TUMOROUS TISSUE

B. Bolouri and M. L. Pancoe, Department of Biophysics, Talleghani Medical School, Tehran, Iran; College of Human Medicine, University of Wyoming, Laramie, Wyo., U. S. A.

This research investigates the effect of steady direct electric current on a sarcoma type cancerous tissue. Inoculated male mice while keeping the negative electrode in contact with tumor growth region, were placed in a constant current path for various densities and length of time during the course of tumor growth. Samples of impaired test tumors were fixed for light and electron microscopy to compare with those of controls. It was indicated that optimal values of 0.05 (mA) / (cm² - min) has marked effect on reducing tumor size and altering the organizational growth pattern of tumor tissue mainly by impairing vascularization of tumor mass, dislocating fatty cells within the tumor, blocking metastasis by inhibiting formation of tumor emboli, reducing the size of cancerous cell nuclei, and creating cytoplasmic vacuolation. Further investigation is being carried out to study ultrastructural changes at the membrane level for cultured cells.

126

ELECTRON TRANSFER REACTIONS IN MODIFIED BILAYER LIPID MEMBRANES AS STUDIED BY CYCLIC VOLTAMMETRY. H. Ti Tien, Membrane Biophysics Lab, Department of Physiology, Michigan State University, East Lansing, MI 48824 (USA)

Insofar as the transduction of foodstuff into electrical and/or chemical free energy is concerned, a type of energy-transducing membrane system has been evolved in nature, namely, the cristae membrane of the mitochondrion. Ideally, a great deal of bioelectrochemistry of this membrane system can be learned from electrical measurements by placing electrodes across such a membrane, such as has been done for the nerve membrane of squid axon. Unfortunately, such an approach is not yet feasible for most organelle membranes, owing to their tiny size. Therefore, bilayer lipid membranes (BLM) appear to offer the most useful system with which to investigate energy conversion processes and redox reactions (See Bilayer Lipid Membranes (BLM): Theory & Practice, Dekker, Inc., New York). As a means of studying transmembrane redox reactions, we have applied cyclic voltammetry to the BLM system (Biophys. J., 45, 167a, 1984). The present studies examined TCNQ-containing BLM in the presence of a variety of redox couples. Voltammograms obtained clearly indicate that redox reactions are occurring at the interfaces of the BLM with electrons moving transversely across the TCNQ-doped BLM. Cyclic voltammetry is a powerful technique for detecting and characterizing coupled redox reactions at the membrane/solution interface and its application to membrane bioenergetics will be discussed.

[Supported by NIH GM 14971].

Thursday 02 August Congress Centre-First Floor Posters 127-132

Posters on Electric Field Effects in Cell Membranes

127

KINETIC STUDY OF ULTRA-WEAK LIGHT EMISSION FROM PLANT TISSUE, M. Jeremić, Ž. Vučinić, Č. Radenović, D. Fidler and M. Střbac, Institute of Physical Chemistry, Faculty of Science, University of Belgrade and Maize Research Institute, Belgrade, Yugoslavia.

Ultra-weak light emission (ULE) of plant and animal tissue is chemiluminescence which originates from redox reactions in living system. It is believed that free radicals, like OH^\cdot , O_2^\cdot , and singlet oxygen play major role in production of ULE. Since KMnO_4 and H_2O_2 can create those radicals, we investigated their influence on the intensity and rate of ULE from maize root. It was found that the intensity of ULE increased linearly with increasing H_2O_2 and KMnO_4 concentration up to some limiting concentration. Further increase of H_2O_2 concentration had no influence on ULE contrary to KMnO_4 , where ULE decreased. Kinetic study showed that three different first order reactions create total light emission. The rate constants for H_2O_2 are: $k_1 = 2.5 \cdot 10^{-4} \text{ s}^{-1}$, $k_2 = 4.6 \cdot 10^{-3} \text{ s}^{-1}$ and $k_3 = 5 \cdot 10^{-4} \text{ s}^{-1}$. Treatment of the sample by ascorbic acid eliminated the fastest reaction while two others remained unchanged. The rate constants for reaction with KMnO_4 are: $k_1 = 7.7 \cdot 10^{-4} \text{ s}^{-1}$, $k_2 = 2.3 \cdot 10^{-2} \text{ s}^{-1}$ and $k_3 = 4.0 \cdot 10^{-3} \text{ s}^{-1}$. The influence of temperature was studied too.

129

RESPONSE OF C3H/10T1/2 FIBROBLASTS TO AN EXTERNAL ELECTRIC FIELD - REORIENTATION, CON A RECEPTOR AND INTRAMEMBRANOUS PARTICLE DISTRIBUTION AND CYTOSKELETON REORGANIZATION. Sek-Ken Hui, Wei-Ping Yang and Edward K. Onuma, Biophysics Department, Roswell Park Memorial Institute, Buffalo, New York 14263, U.S.A.

C3H/10T1/2 mouse embryo fibroblasts were stimulated by a steady electric field ranging up to 15 V/cm. The cells became spindle shape and orientated with their long axes perpendicular to the field direction. Correlative fluorescence and scanning electron microscopy revealed no difference in the density of Con A-gold microsphere labels on either side of the cell. The density of intramembranous particles on the E-face of the plasma membrane was 54% higher on the anode side than on the cathode side of the cell. Membrane potential measured by carbocyanine dyes diminished uniformly and reversibly with electric field stimulation. The immunofluorescence labelled microfilament bundles were disrupted after 30 minutes of 10 V/cm stimulation. The cell sensitivity to electric field-induced reorientation and cell shape changes was reduced by pretreatment with Con A, and to a lesser extent, with succinyl Con A or WGA. Con A pretreatment alone also reduced the prominence of microfilament bundles. It is possible that the generally flat 10T1/2 cells retract and realign in order to minimize the disruption of their membrane potential. The Con A binding-mediated receptor-cytoskeletal linkage temporarily immobilizes the cell and inhibits subsequent field-induced shape changes.

131 ORAL PRESENTATION

THE ELECTRODICHROISM OF PURPLE MEMBRANE SALT CONCENTRATION DEPENDENCE

E. Papp and G. Fricsovszky, Department of Atomic Physics, Eötvös University, 1088 Budapest, Puskin st. 5/7 Hungary

The dichroism of purple membrane suspension was measured in dc and ac electric fields. From these measurements three parameters can be obtained: the permanent dipole moment, μ , the electrical polarizability, α , and the retinal angle δ . The functional dependence of the dichroism on the electric field is analyzed. There is a small decrease ($\sim 2^\circ$) in retinal angle going from dark adapted to the light adapted form. No measurable difference in μ , α and δ was found under the photo cycle.

The dichroism was measured in two different salt solutions (KCl and CaCl_2) in the range 0-10 mM. The retinal angle increases from 64° to 68° with increasing ionic strength going through a minimum. This is attributed to the changing (decreasing) inner electric field in the membrane. The polarizability, α , consists of two parts. One component is related to the polarization of the purple membrane and the second component to the ionic cloud. The second component decreases with ion concentration approximately as κ^{-3} (κ is the Debye parameter) in agreement with a model calculation for the polarization of the ionic cloud. The origin of the slightly ionic strength dependent permanent dipole moment is not well understood.

128

LIGHT SCATTERING STUDIES OF MAGNETIC FIELD EFFECTS ON THE SUB, LOWER AND MAIN TRANSITIONS IN MODEL MEMBRANES A.S. Monem, B.H. Blott, L.F. Braganza and D. Melville, Department of Physics, Southampton University, Southampton, U.K.

We have extended our recent study of the main and pre-transitions in one and two-component multilamellar lipid vesicle suspensions to an investigation of the sub-transition in similar systems. It is shown that turbidity measurements provide a simple method of studying the sub-transition and we have investigated the effect of magnetic fields on this phase change. We have found that the change in light scattering at T_s is enhanced by applied magnetic fields of about 1 Tesla. The magnitude of the field enhancement is similar to that observed at the lower and main transitions.

The study is being extended to investigate the angular distribution of light scattering to provide more detailed information on the nature of these magnetic field effects.

130

THE EFFECT OF ELECTRIC FIELD DURATION ON THE ACTIVATION ENERGY FOR IONIC CONDUCTANCE ACROSS MEMBRANES M.A. Dinno, Biophysics Laboratory, Department of Physics, University of Mississippi, University, MS 38677, USA.

Studies of ion transport across biological membranes often rely on the measurements of electrophysiological parameters of the membrane under investigation. One of these parameters is the ionic conductance (G). In its measurement as $\Delta I/\Delta V$, an RC-like behavior is usually observed. This behavior could be explained by changes in charge density across the electrolyte/membrane interface, polarization emfs, etc. However, its effect on ion transport kinetics is not very clear. In this investigation, the activation energy E_a for ion conductance across the frog gastric mucosa was studied with current pulses of different durations (t). It was found that E_a obtained from Arrhenius plots ($\ln(\Delta I/\Delta V)_t$ vs. $1/t$) was significantly reduced with longer pulse durations. $E_a^{100\text{ms}} = 14 \pm 0.8 \text{ kcal/mole}$ compared to $E_a^{100\text{sec}} = 7 \pm 1.7 \text{ kcal/mole}$. The addition of agents that alter ion transport characteristics manifested asymmetric ionic conductances (rectification) in the presence of hyperpolarizing vs. depolarizing fields of long duration. Thus, different activation energies were determined. These results help in understanding some of the underlying mechanisms for the effects of small currents on the rate of biological processes (Supported by ONR N00014-77-1-0663)

132

ELECTRICAL HEMOLYSIS AND RESEALING OF RED BLOOD CELLS FROM DIFFERENT MAMMALIAN SPECIES

P.C. Mangal and Kusum Grover, Department of Biophysics, Panjab University, Chandigarh 160 014, India.

The effect of external electric field on the red blood cell membrane of six mammalian species has been studied in terms of hemolysis and resealing characteristics of these cells. The pulse height ($V = 10 \mu\text{s}$) for the onset of hemolysis in monkey, sheep, rat, rabbit, mouse and human erythrocytes is found to be 3.0, 3.6, 3.1, 3.0, 3.0 and 3.0 kV/cm respectively. Taking into consideration the mean diameter of the red blood cells of the different species and using Laplace equation, the breakdown potential across these cells comes to be 1.90, 1.80, 1.60, 1.40, 1.46 and 1.66 volts respectively. It is different for different species indicating that the breakdown potential, in addition to the diameter, depends on other properties like dielectric constant and intrinsic elastic constant of the membrane which are likely to be different for different species. The voltage for 50% hemolysis is found to be 4.95, 5.2, 4.3, 4.5, 4.0 and 3.95 kV/cm for monkey, sheep, rat, rabbit, mouse and human erythrocytes respectively. Graphical analysis of the data shows that the rate of hemolysis is maximum for monkey and minimum for rat erythrocytes. The resealing has been studied at 15 hrs after pulsing and it is observed that sealing is 100% in all the species except in monkey erythrocytes where the maximum loss hemoglobin is found to be about 10%. These results are discussed in terms of the electro-mechanical model.

Thursday 02 August Congress Centre-First Floor Posters 133-138

Posters on Electric Field Effects in Cell Membranes

133

ENERGETIC EVALUATION OF GRAVISMOTIC MEMBRANE SYSTEM

S. Przestalski, M. Kargol, Department of Physics and Biophysics, Agricultural University, Wrocław and Department of Physics, Technical University, Kielce, Poland.

A multilamellar model, forming the basis of the gravismotic hypothesis of water transport in the xylem tracheal elements, can be analyzed and evaluated with respect to energy by using the method introduced by one of us. For a single gravismotic system driving water against external pressure ΔP , one can determine energetic efficiency of the gravismotic process

$$\eta = \frac{M_u}{M_u + M_r} = \frac{L}{L + L_0}$$

where M_u expresses useful power, M_r - dissipated power in the pores of the membranes, $L = L_1 L_2 / (L_1 + L_2)$, $L_0 = I_V \Delta P$, L_1, L_2 - filtration coefficients of both membranes, respectively, I_V - volume flux. The obtained expression allows a detailed analysis of energetic potential of the given gravismotic system.

135

IONIC CONTROL OF MAMMALIAN CELL ELECTROFUSION

Blangero C. Teissie J., Biochimie et Génétique cellulaires du C.N.R.S., 31062 Toulouse, France

Electrofusion is a very effective method to obtain cell hybridization. During the last few years, our laboratory has developed an original technique under conditions where the contact between cells is spontaneous. DC electric pulses are applied directly to a culture growing in monolayers on a culture flask. When the density is high enough, contact occurs between the cells giving the so-called contact inhibition. The advantages are that the cells are not treated by any exogenous agent and that the pulsing medium is buffered and contains ions. Its ionic content appears critical for electrofusion. An increase in monovalent ion content (Na^+ , K^+ , choline, Li^+) induces a strong decrease in the fusion yield. This effect is less pronounced with Li^+ than with the other ions. Mg^{++} , when present at low concentration (less than 5 mM), is a promoter but prevents fusion at higher concentration. Ca^{++} inhibits fusion. These effects are not due to a change in the cell surface electric charge as shown by microelectrophoresis experiments. We propose that the interactions between cells are modulated by the ionic content of the medium. The behaviour of Mg^{++} is explained by a bridging effect leading to a closer contact between cells. At high ionic strength, however, the intercellular contact is looser due to the electrostatic character of the interactions. These changes would prevent intercellular membrane mixing following electroporation.

137

THE ROLE OF Ca BOUND TO THE INNER SARCOLEMMA SURFACE IN CARDIAC EXCITATION-CONTRACTION COUPLING. D.M. Bers and P. Mansier, Division of Biomedical Sciences, University of California, Riverside, CA 92521. USA.

Ca binding sites on the internal surface of cardiac sarcolemma (SL) could be involved in cardiac E-C Coupling in two basic ways: 1) They could provide a source of Ca which can be released in response to membrane depolarization to activate contraction (Lüthmann and Peters, Prog. Pharmacol., 21, 1979). 2) They could buffer the increase of $[\text{Ca}]$ produced by Ca influx and SR Ca release. These possibilities have been directly evaluated by the measurement of Ca binding to isolated cardiac sarcolemmal vesicles which are primarily inside out. Ca binding was measured as functions of $[\text{Ca}]$ (100 nM - 100 μM), pH (6.7 - 8.0) and membrane potential (E_m -40 to +40 mV generated by $[\text{K}]$ gradients and valinomycin). At pH 7.4, $[\text{Ca}]$ = 125 nM changing E_m by 30 mV in the direction analogous to action potential depolarization changes Ca binding from 1.06 ± 0.13 to 0.96 ± 0.03 nmoles/mg protein (1 nmol/mg SL protein $\sim 1.7 \mu\text{mole/kg}$ wet myocardium). This would have no significant effect on contractile activation. When $[\text{Ca}]$ is increased from 125 nM to 5 μM with E_m = 0 bound Ca increases from 0.90 ± 0.05 to 2.21 ± 0.13 nmol/mg and is still relatively unaffected by E_m . Thus, Ca binding to these internal sites would provide some, but only weak buffering of $[\text{Ca}]$, during a cardiac twitch. These high affinity Ca binding sites do not appear to be potential dependent and it is unlikely that depolarization during the cardiac action potential causes Ca to be released from the internal sarcolemmal surface. More likely is that these binding sites weakly buffer myoplasmic $[\text{Ca}]$ transients.

134

DIELECTRIC STUDY OF INTERNAL MOTION IN LECITHIN HEAD GROUP BY TIME DOMAIN REFLECTOMETRY

Y. Shimoto, M. Inaba, R. Ozawa, S. Yagihara and S. Masuno, Lab. of Physics, Fac. of Gen. Education, Shova Univ., Shinjuku-ku, Tokyo 142, Japan* and Dept. of Physics, Fac. of Science, Tokai Univ., Hiratsuka-shi, Kanagawa 259-12, Japan.

Dielectric relaxation measurements over a frequency range from 1 MHz to 10 GHz were performed on dipalmitoyl phosphatidylcholine (DPPC), egg lecithin, phosphatidyl ethanolamine, and sphingomyelin in chloroform solution at 25°C by using a time domain reflectometry (TDR) method. Three relaxation processes were found in DPPC, egg lecithin and phosphatidyl ethanolamine, but two relaxation processes were found in sphingomyelin. The first relaxation peak observed in DPPC at about 0.1 GHz can be attributed to an over-all rotation of lecithin molecule. The relaxation time estimated from the over-all rotation of ellipsoidal molecule, size of which is nearly the same as lecithin molecule, agrees well with the observed one. The second relaxation peak at about 0.5 GHz can be due to motion of the flexible zwitterions in the lecithin head group. The third peak at about 3 GHz can be assigned to an orientation of ester group in the head group. These results suggest strongly that internal motions in the head group occur even in the lipid membrane.

136

PULSE IMPEDANCE METHOD FOR DETERMINATION OF THE CONDUCTIVITY AND THE CAPACITY OF ERYTHROCYTES MEMBRANE M.S. Markov, D.L. Abadzieva, Department of Biophysics, Biological Faculty, Sofia University, Blvd. D. Tzankov 8, Sofia 1000, Bulgaria

The pulse impedance method has been applied for determination of the passive electric properties of the living cells. A comparison between classical method of Cole-Cole and pulse impedance method has been made. The equivalent circuit of some different by their complexity biological systems have been constructed. Passive electric properties (conductivity and capacity) of human red blood cell membrane have been determined in norme and under the influence of physical and chemical factors.

It has been established that under constant magnetic influence both capacity and conductivity were changed depending on the value of magnetic induction.

Protamin and Heparin (applied) as chemical factors also leads to changes in investigated parameters. The changes were more significant when Protamin was applied.

138

NEGATIVE HYDROAIRION EFFECTS ON STATE OF MITOCHONDRIA AND STRUCTURE OF WATER

M.N. Kondrashova, E.V. Grigorenko, A.V. Temnov, A.M. Babitsky, E.B. Okon, A.A. Platonov*, I. Protasevich*, N.G. Esipova*, Inst. Biol. Physics, Acad. of Sci. USSR, Pushchino, *Inst. Molecular Biol., Acad. of Sci. USSR, Moscow, USSR

The influence of light negative hydroairions, i.e. $-\text{OH}$ separated from H^+ on isolated mitochondria (M) was investigated. The wonderful and unique effect was revealed consisting in rapid reversion of damage of M during storage (aging) or its prevention. It is due to support the natural ability of M to form associations connected with improvement of ADP phosphorylation and of Ca^{++} output. The latter induces membrane hyperpolarisation and rise of restoration processes, which may provide hydroairion therapeutic activity. The effects observed are explained by decrease of high local positive membrane charges typical of pathology. $-\text{OH}$ effects are revealed distinctly in M isolated by our mild method providing conservation of natural ability of M to form association in cell (natural M). Effect of $-\text{OH}$ flow is reproduced by the action of water previously saturated with $-\text{OH}$ in buffer. $-\text{OH}$ induce cooperative formation of structures in water connected with decrease of free positive ions. It may be concluded from alkaline shift of nonbuffered water, increase of its calorific capacity and decrease of surface tension.

Thursday 02 August Congress Centre-First Floor Posters 139-144

Posters on Electric Field Effects in Cell Membranes

139 ORAL PRESENTATION

CONDUCTANCE AND CAPACITY OF THE XENOPUS EGG MEMBRANE DURING ACTIVATION

A. Peres and G. Bernardini, Dip. Fisiologia e Biochimica Generali and Dip. Biologia, Università di Milano, Via Celoria, 26, I-20133 Milano.

We have voltage-clamped *Xenopus* eggs to measure the membrane capacity and ionic conductances during activation. Two currents develop after pricking or 10 μ M A23187 in 1/10 Ringer: an inward current carried by Cl^- and an outward current (mostly carried by Na^+) which develops when the membrane potential is over about +20 mV. Both currents disappear after 3 to 4 min though with different time courses. The membrane capacity of the unactivated eggs ranges between 50 and 60 nF; during activation, it increases by about 60 % and then slowly declines towards the initial value. Electron microscopy observations show that this time course parallels the cortical granule exocytosis and the related changes in membrane area. Simultaneous measurements of conductance and capacity show that the capacity time course is delayed with respect to that of the Cl^- conductance. Experiments on CO_2 treated eggs show that, upon activation, no capacity changes occur while the Cl^- current develops normally. These results are against the possibility that the Cl^- channels are introduced into the surface membrane by means of cortical granule exocytosis. Comparison between the capacity changes and the outward, voltage-dependent, current is under study.

141

Permeation and transport of alkali metal ions in human erythrocyte membrane in normal and homozygous β -thalassemic state - A. Bonincontro*, C. Cametti*, A. Rosi*, L. Sportelli*. *Dept. of Phys. Univ. Rome - †Inst. Sup. Sanità, Rome - ‡Dept. of Phys. Univ. Cosenza.

The permeation and the transport of alkali metal ions across membranes of human normal and β -thalassemic erythrocyte cells have been studied by means of radiowave conductivity measurements. The model employed accounts for the hydrophobic region of the aliphatic hydrocarbon chains and for the polar head region of the membrane. The permeation of the cations line-up in the series $\text{Na}^+ > \text{Cs}^+ > \text{Li}^+ > \text{K}^+$ and $\text{Ca}^{2+} > \text{Na}^+ > \text{Li}^+ > \text{K}^+$ for normal and pathological membranes respectively, indicating lipid-polar group interactions with a partial decrease of the transmembrane protein concentration in the pathological state. These indications are further supported by ESR measurements performed on the same samples. No differences for the polarity and fluidity of the membrane at the two penetration levels of 5 and 16 NSA spin-labels are observed. On the contrary internal microviscosity measured by means of tetramine is affected by the different cations used, showing significant differences in normal and β -thalassemic erythrocytes.

143

GEL-LIPID DOMAIN AS A SOLITON ON THE PHASE SEPARATION OF LIPID BILAYER MEMBRANE.

A.S. Pasynkov, A.V. Alekseev, Radiospectroscopy Laboratory, Pacific Oceanological Institute, Far Eastern Science Centre, USSR Academy of Sciences Radio Street, Vladivostok, USSR.

The sine-Gordon and ϕ^4 field models of order parameter on the phase separation gel-liquid crystal of lipid bilayer membrane have been used to investigate gel-lipid domain dynamics. The models of lipid bilayer having solitary waves (soliton) solutions are discussed in details. The interaction of gel-lipid domains with the protein molecules of membrane as well as the external driving electrical field is investigated within the scope of many-soliton nonsingular perturbation theory. The membrane proteins trap such solitons with the creation of gel-lipid region around the protein sites. Our models predict the existence of the high value of the spontaneous electrical polarization $P_s \sim 10^{-6}$ q/sm² in these regions. The conformational modification of proteins, for example enzymes, causes the redistribution of domain density around the protein sites with the electromagnetic radiation of domain group in the frequency band $\gamma \sim 10^3 - 10^6$ Hz. Within the scope of nonlinear membrane models we are now extending these domain effects for the mechanisms of ionic transport across biological membranes, energy transfer between the proteins of membrane and intercellular interaction.

140

ELECTRO-OPTIC STUDIES OF THE ELECTRIC FIELD EFFECT ON MEMBRANE PROTEINS

S.P. Stoylov, Department of Physics and Biophysics at the Medical Academy, 1431 Sofia and Institute of Physical Chemistry, Bulgarian Academy of Sciences, 1040 Sofia, Bulgaria

The potential of electro-optic methods for studying the effect of electric fields on the dynamics of membrane proteins are illustrated on the example of the bacteriorhodopsin and the rhodopsin respectively in purple membrane fragments and disc membranes. Results obtained in the author's laboratory in Sofia and from other authors are presented. Possibilities for future broader studies in this field are considered.

142

ELECTROKINETICS AT STRUCTURED SURFACES

E. Donath, and A. Voigt, Department of Biophysics, Humboldt-University, Berlin, GDR

Assuming a spatially distributed fixed charge and allowing for an electroosmotic flow through this layer the electrokinetic properties of a structured interface are calculated both in an analytical form within the linearized Poisson-Boltzmann approximation and numerically. For a model of charge distribution realizing the minimum of the free interfacial electric energy analytically the nonlinear solution both for the basic electrokinetic values and for the surface conductivity are presented, thus allowing the interpretation of streaming potential measurements as well. Comparing this theoretical results with experiments the electrostatic interfacial properties of the human erythrocyte and the glass surface are evaluated.

Preliminary papers have been published in Bioelectrochem. & Bioenerg. 2, 31 and J. theor. Biol. 101, 569.

144

DETECTION OF CELL SWELLING BY OPTICAL TUNNEL EFFECT

M. Baringelli, G. Bonazzola, G. Ciocchetti, E. Conte, A. De Marco, G. Monticelli and A. Trabucco, Istituto di Fisica Superiore, Corso M.D'Azeglio 46, Torino, Italy.

The optical tunnel effect allows the measurement of distances between two media separated by an optically less dense medium. Variations of distance by fractions of a nanometer can be detected. A general theory of the effect has been developed in order to design different experimental setups for biophysical applications. An optimum agreement has been achieved between theoretical and experimental data. A first attempt to detect the swelling of cells in suitable biological samples has been performed.

Thursday 02 August Congress Centre-First Floor Posters 145-150

Posters on Electric Field Effects in Cell Membranes

145

146

147

148

149

150

Thursday 02 August Congress Centre-First Floor Posters 151-156

Posters on Photo and Auditory Receptors

151

CONTROL OF ROS CYTOPLASMIC Ca^{2+} BY cGMP.
John S. George and Mark W. Bitensky, Life Sciences Division, Los Alamos National Laboratory, Los Alamos, New Mexico 87545 USA
Cytoplasmic Ca^{2+} activity (Ca_i) appears to modulate the Na^+ dark current of the vertebrate rod, but mechanisms controlling Ca_i are not well understood. We have studied Ca^{2+} metabolism in preparations of isolated, concentrated rod outer segments (ROS) with leaky plasma membranes, using Ca^{2+} and pH electrodes to monitor ion activities and measuring Ca partition between particles and suspending aqueous medium. Mitochondrial Ca^{2+} transport was inhibited with ruthenium red or with actinomycin and oligomycin. In the dark, ROS disks take up Ca^{2+} by an ATP dependent process. This uptake is associated with a rise in suspension pH, i.e. protons also disappear from the medium. Both Ca^{2+} uptake and alkalization are stimulated by cGMP in the presence of ATP. Dinitrophenol inhibits ATP-dependent Ca^{2+} uptake by disks and releases sequestered Ca^{2+} . Light releases Ca^{2+} from dark adapted, preloaded disks - thousands of ions per second per bleached rhodopsin at low light levels. A weak continuous light typically releases more Ca^{2+} than a much more intense flash. Much or all of this Ca^{2+} release may depend on the hydrolysis of cGMP. Under conditions of low ATP, or when phosphodiesterase (PDE) is active (e.g. in the light) addition of cGMP causes a fall in pH and release of Ca^{2+} . Stimulating PDE in the presence of cGMP with Gpp(NHppG) or protamine also provokes Ca^{2+} release. Thus high cGMP levels stimulate Ca^{2+} uptake while cGMP hydrolysis releases disk Ca^{2+} by another mechanism. Our data suggest the possibility that both processes may operate by exchange of Ca^{2+} for H^+ across the disk membrane.

153

EFFECTS OF VARYING THE REFRACTIVE INDEX ON THE SPHERICAL ABERRATION OF THE EYE (COMPUTER SIMULATION)
M.A. El Mesiery and E. El Karamany, Dept. of Mathematics and Physics, Faculty of Engineering, Cairo University, Egypt.
The formation of images on the retina of the human eye is usually believed to be associated with spherical aberration. This conclusion comes from schematic and reduced eye models. In this paper, this belief is questioned by taking into consideration the fact that the refractive index n of the eye lens varies from 1.41 in the innermost layer to 1.386 at the outermost layer. The function describing n throughout the lens is taken as
$$n(x) = 1.386 + \beta [1 - \exp(-\alpha x)]$$
where x is the distance taken from the centre of the lens, α and β are arbitrary constants. The lens itself is subdivided into 300 concentric layers each of which has its own n . Ray tracing calculations were followed to obtain the image of an object situated at a fixed distance. Since these calculations are formidable, computer modelling is adopted. A model of the eye and the object is produced to simulate the image formation on the retina. The results show that spherical aberration can be minimized to a negligible limit when optimum values of α and β are considered. Moreover, the image of a straight line object is formed as a curved line on the retina and inverted by 180 degrees. The magnification factor of the eye as a whole was found to be 0.6.

155

CELLULAR MECHANISMS MEDIATING RETINAL HORIZONTAL CELL COUPLING. M. Lauffer and R. Salas, Neurophysiology Lab., Inst. Venezolano de Investigaciones Cientificas, Caracas, Venezuela.
The electrical coupling between horizontal cells of the teleost retina is modulated by dopamine, which is present in, and liberated from, interplexiform amacrine cells. The cellular mechanisms mediating the changes in coupling were investigated by means of intracellular iontophoretic injection of H^+ , cAMP, Ca^{2+} , EDTA, EGTA and cAMP. Triplets of microelectrodes were used to record voltages in two neighboring horizontal cells of the isolated and perfused retina of *Eggeria plumieri*, to inject the agents, and to pass current pulses in order to evaluate membrane (R_m) and coupling (R_c) resistances. The resistances were computed using a model of an hexagonal planar resistive network, either directly or from a cell matrix. Control injections were made with KCl, Tris base, polarity inversion, injection and recording from the same cell, and using three independent micropipettes. Intracellular pH reduction using different proton sources leads to cell uncoupling; R_m increases slightly, up to 2 times, R_c increases markedly, 4 to 20 times more than R_m , and the coupling ratio falls markedly. Injection of cAMP also uncouples horizontal cells; R_m is barely changed but R_c increases 3 to 6 times. While no effects of intracellular Ca^{2+} injection were observed, both chelators increased coupling through a marked reduction of R_c with practically null effects on R_m . The effectiveness of electrical coupling between horizontal cells appears to depend upon intracellular pH, Ca^{2+} and cAMP.

152

INFRARED SPECTROSCOPIC STUDIES ON BACTERIORHODOPSIN CHROMOPHORE MODELS
R. Stružinský, S. Hilgard, A. Kotyk, Faculty of Science, Charles University, Hlavova 2030, Prague, Czechoslovakia.
Bacteriorhodopsin chromophore analogues resembling spectrally the ground and the K states of the photocycle were prepared by the reaction of retinal with diphenylamine or indole derivatives (indoline, indole, 3-methylindole). The prepared compounds reproduce well the absorption spectra of intermediates of the bacteriorhodopsin photocycle and provide a suitable model for the study of charge delocalization induced on the nitrogen atom. The greatest changes in the IR spectra are found in regions characteristic for N-H, C=N and aldehyde group vibrations. The N-H and aldehyde group vibrations are missing in the reaction product, the C=C vibrations is shifted to lower wavenumbers by 40 cm^{-1} and a new band characteristic for the presence of a C=N⁺ structure evolves in the 1620 cm^{-1} region. The synthesized products are stable only under acidic conditions. An overlap of the two connected double-bond conjugated systems is manifested in a downward shift of the C=C vibration as well as in the downward shift of the C=N⁺ vibration compared with compounds where the C=N⁺ structure is not a part of the conjugated or aromatic moiety.

154

RECONSTITUTION OF ION CHANNELS FROM PHOTORECEPTOR MEMBRANES INTO PLANAR BILAYERS
W. Hanke & S. Kaupp, Lehrstuhl f. Zellphysiologie, Univ. Bochum and § FB Biologie, Abt. Biophysik, Univ. Osnabrück
Two different channels from bovine rod outer segments have been incorporated into planar lipid bilayers and analyzed by current fluctuations through single channels. One type of channel ("sodium channel") has a unit conductance $\Lambda = 20$ pS and is highly selective for Na^+ over K^+ (~10:1). The other channel ("cationic channel") has a unit conductance $\Lambda = 120$ pS and the selectivity for Na^+ over K^+ is 2:1. Both channels are not permeable to Cl^- . The opening and closing events of both channels occur in "bursts". The cationic channel is rapidly activated (<100 ms) by changing the transmembrane potential from 0 mV to a more negative value (-50 mV) and inactivated within 5 sec at low concentrations of Ca^{2+} (1 μM). The activation-inactivation behaviour is highly dependent on the concentration of free calcium in the medium and the transmembrane voltage. The channel does not inactivate after an activating voltage jump in a medium that contains 2 mM calcium. The mean open time within a burst is voltage dependent ($\tau = 55$ ms at $V = -50$ mV). This channel is also permeable to Ca^{2+} ions (30 pS at 75 mM Ca^{2+}). Most likely the cationic channel originates from the disk membrane. The properties of these two channels in the reconstitution experiments are compared with ionic conductances that have been studied by other techniques in vertebrate rods.

156

SPECTROSCOPIC PROBING OF ELECTRIC POTENTIALS ON THE PURPLE MEMBRANE
B. Ehrenberg, Z. Meiri, Y. Ben-Zion and L.M. Loew
Dept. of Physics, Bar-Ilan University, Ramat-Gan, Israel, and
Dept. of Chemistry, SUNY at Binghamton, N.Y., U.S.A.
Fluorescence and resonance Raman spectroscopies of two dye molecules were employed to study components of the electric potential profile across the purple membrane from *Halobacterium halobium*. A benzothiazole styryl dye (BW-638), whose resonance Raman spectrum is sensitive to its aggregation, can monitor the Debye layer adjacent to the surface of the membrane where charged side chains of the bacteriorhodopsin protein molecule are exposed. Our results, which comply with the Gouy-Chapman theory, show that the surface charge density on the membranes is $4.4 \cdot 10^{-4}$ charges/ \AA^2 , and it increases by 20% during the photochemical conversion of the pigment to the M species. We found that the charges are located at the cytoplasmic side of the membrane and amount to 2 charges per pigment molecule. The removal of the retinal chromophore does not change the surface charge density, thus secondary chromophore-protein interactions do not extend to the surface. Due to trans-membranal proton pumping during the photochemical cycle of bacteriorhodopsin, a cross membrane potential develops. Using a fast responding styryl dye indicator (RH-160), we could follow the evolution of the potential in a flash photometric experiment by monitoring the fluorescence intensity of the dye. The formation half time of 30 μs is faster than the formation of the M intermediate. Thus deprotonation of the Schiff base bond in the protein which precedes formation of M could be the trigger for proton transport.

Thursday 02 August Congress Centre-First Floor Posters 157-162

Posters on Photo and Auditory Receptors

157

FLUORESCENCE OF EUGLENA PHOTORECEPTOR PIGMENTS: AN "IN VIVO" MICROSPETROSCOPIC STUDY
F. Gnetti, G. Colombetti, F. Lenzi, C.N.R. Istituto di Biofisica, Via S. Lorenzo 26, Pisa, Italy and M. Quaglia, E. Polacco and E. Campani, GNEQP and Istituto di Fisica Università, P.zza Torricelli, Pisa, Italy.

We have developed a tunable dye-laser-microspectrofluorometer, in order to investigate the spectroscopic properties of the photoreceptor pigments of the green unicellular flagellate *Euglena*. The "in vivo" fluorescence excitation spectrum has been determined and is reported. The fluorescence quantum yield has been measured. The results show that flavins are the photoreceptor pigments in *Euglena* and that the primary molecular photoreactions occur at a high rate starting, most probably, from the first excited singlet state.

159

AN ALLOSTERIC MODEL FOR BACTERIAL CHEMORECEPTOR PROTEINS: ROLE OF MULTIPLE METHYLATION S. Asakura & H. Honda, Inst. of Mol. Biol., Sch. of Sci., Nagoya Univ., Nagoya, Japan
To explain bacterial excitation and adaptation during chemotaxis, we propose a model for receptor proteins (MCP's) in light of evidence that they are multiply methylated in a preferred order. The model consists of the following assumptions. 1. The receptor protein is in rapid equilibrium between two conformations, S and T, and the equilibrium shifts towards the T form as the number of methyl groups increases. 2. Attractants bind to the S form, repellents bind to the T form, and both classes of ligand shift the S/T equilibrium. 3. The S form accepts methyl groups in an order, while the T form releases them in the reverse order. These reactions are slow, and changes in the number of methyl groups lag behind shifts in the S/T equilibrium. 4. The frequency of bacterial tumbling is a monotonically increasing function of the T fraction of the receptor. This model shows that, if the receptor satisfies two sets of conditions imposed on its equilibrium and kinetic constants, it can maintain the steady-state T fraction virtually constant over a wide range of ligand concentration, allowing the cells to adapt. A stepwise change in concentration leads to a rapid change in the T fraction (excitation), followed by a slow relaxation (adaptation). Computer simulations have been made of the whole response process, employing the receptor with 6 methylation sites/molecule and assuming simple sets of parameters. The results show that multiple methylation of the receptor is necessary for the cells to respond sensitively to environmental changes, and to adapt.

161

CHANGES OF FLAGELLAR BEATING FREQUENCIES OF PHOTOTACTIC MICROORGANISMS IN RESPONSE TO LIGHT FLASHES.
F. Angelini, C. Ascoli, C. Frediani and D. Petracchi, Istituto di Biofisica, C.N.R., Via S. Lorenzo 26, Pisa, Italy.
Light scattered from optically not spherical microorganisms is anisotropically distributed around the incident beam and its intensity depends on the cell body orientation. Flagellar beating induces vibrations of the cell body; therefore the light scattered from a swimming microorganism results to be modulated at the flagellar beating frequency. The spectral analysis of the photocurrent elicited by the light scattered from a population allow us to measure the flagellar beating frequency distribution. This technique was firstly used with a laser as light source (Ascoli et al., Biophys. J. 24, 585, 1978); here an ordinary infrared source is used with an experimental set up which takes advantage of the anisotropic scattering. Transient changes of flagellar beating frequency in response to flashes of white light are measured in samples of *Haematoxylon pluvialis*. An increase in flagellar beating frequency occurs when the dose (light intensity x flash duration) is sufficient. The reciprocity between light intensity and flash duration holds for durations not exceeding 60 ÷ 100 ms. For lower doses a bimodal distribution of flagellar beating frequency is observed. No effect is observed for very low flashes nor for red light; green light on the contrary is effective in determining the increase of flagellar beating frequency. A detailed analysis of spectra allows us to determine characteristic times of the phenomenon and to draw out suggestions about the mechanism of sensory transduction in *Haematoxylon pluvialis*.

158

SURFACE PRESSURE, SURFACE POTENTIAL AND ELLIPSOIDAL MEASUREMENTS OF ROD OUTER SEGMENT DISC MEMBRANE COMPONENTS AT NITROGEN-WATER INTERFACE.
C. Salesse, D. Ducharme, R.M. Leblanc and F. Boucher, Centre de recherche en photobiophysique, Université du Québec à Trois-Rivières, Trois-Rivières, Québec, Canada.
Surface and ellipsometric measurements of rod outer segment (ROS) disc membrane components and intact discal membranes at nitrogen-water interface have been performed to model the photoreceptor membrane and to investigate the rhodopsin-phospholipid interactions. The surface pressure isotherms of PE_{ROS} , PC_{ROS} and PS_{ROS} showed that a large variation in the percentage of polyunsaturated fatty acids from one phospholipid to the other (36-80%) yielded a little variation in the corresponding apparent limiting area (72-75 Å² per molecule). Furthermore, we found that the ellipsometric and surface potential isotherms of these ROS phospholipids were similar. Therefore, the film thickness and the dipole moment of each ROS-phospholipid present a similar behavior during the surface pressure measurements. The analysis of these isotherms reveals that ROS disc membranes must be highly fluid and allow molecular movements. Besides this, the discal membrane compression and decompression isotherms showed a large hysteresis effect which can be explained in terms of rhodopsin-phospholipid interaction since no such effect is observed with the phospholipids alone neither with the whole ROS disc lipid extract or with purified rhodopsin in Triton X-100. We are now extending our work to look at the pure rhodopsin and rhodopsin mixed with each ROS phospholipid.

160

FREE EXTRACELLULAR (Ca²⁺) AT PHOTORECEPTOR LEVEL MEASURED WITH CALCIUM-SELECTIVE ELECTRODES EQUALS THAT IN THE VITREOUS IN FROG AND CARP EYES
K. Kaila and J. Voipio, Dept. Zoology, Div. Physiology, University of Helsinki, Helsinki, Finland.
The extracellular Ca²⁺ concentration is known to have a strong influence on the function of photoreceptors, but there is no information available on the (Ca²⁺)_e in the subretinal space surrounding the receptors in vivo. In this context it is of interest that the subretinal space is distally bounded by the retinal pigment epithelium (RPE), an ion-transporting "tight" epithelium. Single- and double-barreled Ca²⁺-selective electrodes containing the neutral ligand ETH 1001 in a PVC-jelled sensor were constructed to measure the subretinal (Ca²⁺)_e in opened excised eyes of frogs and carps. The results obtained with the single-barreled electrodes were interpreted on the basis of parallel recordings made with conventional KCl-filled microelectrodes. The tips of the electrodes were localized by voltage drops related to current pulses (15-20 nA, 400 ms) passed radially through the preparation by means of macroelectrodes, using the high-resistance RPE as a landmark. The results indicated a subretinal Ca²⁺ concentration very close or identical to that prevailing in the vitreous, 1.0 - 1.1 mM (n=28) in the frog retina and 1.2 - 1.4 mM (n=22) in the carp.

162

STUDIES OF LONG-LIVED PHOTOPRODUCTS OF FROG RHODOPSIN. K. AZUMA AND M. AZUMA, Dept., Biol., Osaka Med. Coll., Takatsuki, Osaka and *Dept. Health Sci., Osaka Kyoiku Univ., Tennoji-ku, Osaka, Japan
Long-lived photoproducts of frog rhodopsin (Rh) in isolated retina and digitonin solution have been investigated by spectroscopy and their chromophores have been analyzed by high-pressure liquid chromatography. By irradiation (>560 nm) at 3°C, metarhodopsin III (MIII) and a photoproduct analogous to MIII are formed, whose chromophores are determined as all-trans and 7-cis retinal respectively. The latter photoproduct (7-cis photoproduct) decays more slowly (t_{1/2} = 50 min at 22°C) than M.II (t_{1/2} = 15 min) does. The formation of 7-cis photoproduct is derived from the photoisomerization of lumirhodopsin (L) and metarhodopsin I (MI), but the efficiency of isomerization to 7-cis is better in MI than in L. The λ_{max} of 7-cis photoproduct at -20°C is 455 nm and its maximum absorbance is 1.1 times as large as that of rhodopsin. This photoproduct exhibits positive CD ([θ]₂₂₂ = 73,000 at λ = 222 nm) which is larger than that of Rh ([θ]₂₂₂ = 61,000). The examination of absorption spectra of Rh intermediates has shown that absorption peaks of L, MI and MIII are at 522, 482 and 475 nm respectively.

Thursday 02 August Congress Centre-First Floor Posters 163-168

Posters on Photo and Auditory Receptors

163

Ca²⁺ RELEASED BY CYCLIC GMP FROM DISKS OF BOVINE ROD OUTER SEGMENTS. The Ca²⁺ release occurs rapidly (10-20 sec) at a high stoichiometry (10.000-15.000 Ca²⁺ ions/disk). The K_{1/2} value for cyclic GMP is 80 µM. The maximum amplitude of the Ca²⁺ responses elicited by cyclic GMP or 8-brc-GMP are of similar magnitude; other analogues of cyclic GMP are ineffective. A Ca²⁺ gradient across the disk membrane is a necessary condition for the release to occur. If this Ca²⁺ gradient is dissipated by the ionophore A23187 no Ca²⁺ release is observed after addition of cyclic GMP. The Ca²⁺ release is inhibited by organic and inorganic Ca²⁺ blocking agents. L-cis-Diltiazem inhibits the release at micromolar concentrations; D-cis-Diltiazem is without effect. The efficiency to inhibit the cyclic GMP-stimulated Ca²⁺ release decreases in the following order:

L-cis-Diltiazem > PN 205-033 > (+)Fenylamin > D-600

Nifedipine and Nimodipine are ineffective. The Ca²⁺ release is also inhibited by 5 µM Ca²⁺. The above results suggest that cyclic GMP regulates an ion transport system in the disk membrane but does not affect directly the redistribution of Ca²⁺ bound to the surface of the disk membrane and free Ca²⁺.

165

FLUORESCENCE MICROSCOPY OF BLEPHARISMA JAPONICUM PIGMENTS

F. Lenci, G. Colombetti, R. Matteoni, C.N.R. Istituto di Fisica, Via S. Lorenzo 26, Pisa, Italy and E. Polacco, M. Quaglia, Istituto di Fisica Università, P.zza Torricelli 2, Pisa, Italy.

Fluorescence excitation spectra of the red pigment of the ciliated protozoan *Blepharisma japonicum* have been determined in single intact cells, in cold-extracted granules and ethanol extracted pigments. Measurements have been performed by means of a tunable dye-laser, coupled to a suitable modified microscope.

All the spectra are similar to each other and to the absorption spectrum of the red pigment "in vitro". Fluorescence quantum yields have been determined for cold-extracted and ethanol extracted pigments: the results indicate that in the former case the yield is 4.5×10^{-3} and in the latter 1.6×10^{-2} .

"In vivo" measurements also show the pigment is homogeneously distributed along the cell body.

A rough action spectrum indicates the red pigment as the photoreceptor pigment for the step-up photophobic reaction.

167

BIPHASIC PHOTORESPONSES AND SENSITIVITY REDUCTION OBSERVED WHEN RETINAL RODS ARE OXIDIZED

K. Donner, S.O. Hemilä and A. Koskelainen, Laboratory of Physics, Helsinki University of Technology Espoo, Finland.

We recorded the aspartate-isolated receptor potential from the dark-adapted frog retina. A normal photoreponse is seen as a vitreous-negative deflection (time to peak a few seconds at 12°C). However, in some retinas, at the beginning of the perfusion a small positive deflection (time to peak one second or less) preceded the negative one in responses to low-intensity stimuli. As we thought this could be due to the rising level of oxidation caused by the perfusion with aerated Ringer, we then studied the effects of switching from aerated to deoxygenated Ringer and back. Introducing deoxygenated Ringer at least doubled sensitivity without much changing the maximum response. Re-introducing aerated Ringer did indeed transiently (first 10 minutes) produce the biphasic photoreponses involving an initial positive wave and depressed sensitivity by some 0.5 log units. The initial positive wave cannot be due to the activation of voltage-dependent channels, nor to glial currents, as it preceded the photoreponse proper. Adding to the Ringer sodium ascorbate (0.1 mM), which may work as either an oxidant or an anti-oxidant, gave results highly similar to those of aeration, but only after a 10 min. delay.

164

PORPHYRIN PRODUCTION AND INACTIVATION OF *P. ACNES* BACTERIA.

A. Johnsson, B. Kjeldstad and S. Sandberg. Dept of Physics, Univ of Trondheim, N-7055 Dragvoll, Norway.

Propionibacterium acnes (*P. acnes*) belong to the bacterial inhabitants of the skin and take part in the acne disease. Porphyrin production by bacteria grown on Eagles basal medium was studied by fluorometry and HPLC. The relative amount of proto- and coproporphyrin was changed with pH in the range of 5.3 to 7.2 and time of incubation. Emission spectra from the bacteria in PBS had peaks at 612 and 635 nm.

Inactivation of the bacteria was studied by measuring their colony formation. Inactivation was oxygen dependent. D₂O caused an increased inactivation as compared with normal water. Singlet oxygen is likely to be involved in these mechanisms. A preliminary action spectrum of the inactivation shows a peak in the 410 nm region. This indicates that porphyrins produced by the bacteria take part in the destruction mechanisms.

166

CURRENT SOURCES AND SINKS OF LOCAL ERG COMPONENTS IN PRIMATE

R.G.M. Heynon and D. van Norren, Institute for Perception TNO Kampweg 5, Soesterberg, The Netherlands.

The local electroretinogram (LERG) was recorded in vivo in the macaque eye. Extracellular voltage changes evoked by light flashes were recorded with a bipolar microelectrode (tip distance 30 µm) at various depths in the retina. A principal component analysis was used to extract isolated components from different parts of the LERG. The photoreceptor component was isolated from two 20 ms time windows following, respectively, stimulus on and off. Current pulses, passed through the eye wall from an electrode behind the eye to an electrode in the vitreous, yielded voltage effects from which the local resistivity as a function of retinal depth was calculated. Combination of light evoked voltages and resistivities yielded local currents in the extracellular space. The receptor component has a current source at the outer segments level and a sink in the outer nuclear layer. The b-wave has a current source around 40% and a sink around 55% depth. Our b-wave results contradict the existing models in that there is no additional b-wave source in the most proximal 10% of the primate retina.

168

SPECTRAL SENSITIVITY OF THE PHOTOMECHANICAL RESPONSE OF THE CRUSTACEAN DISTAL PIGMENT CELLS

J.L. Cortés and H. Aré-chiga, Department of Physiology and Biophysics, CINVESTAV, Mexico, D.F.

The compound eye of crustaceans contains a set of non-visual shielding pigments, the position of which depends on the intensity of illumination. One of such pigments is contained in dark granules located in cells extending from the cornea to the base of retinula cells. It hence its denomination as distal retinal pigment. Under illumination, the pigment granules expand within the cell. The photomechanical response is mediated by the release of a neurohormone from the eyestalk. There is no information about the photoreceptor mediating this reflex. In this report we characterize the spectral sensitivity of the response, as an initial step in the study of the pigment(s) mediating the phototransduction stage of the reflex. The experiments were conducted in adult specimens of the crayfish *Procambarus clarkii* of either sex. The illumination was provided with a Bausch & Lomb monochromator, and calibrated filters. The position of the distal pigment in the retina was determined micrometrically. Threshold for eliciting the pigment migration ranged from 10^{11} to 10^{13} quanta cm⁻² s⁻¹, depending on the state of light adaptation. Two peaks of sensitivity were found, one at 580 nm, and the other at 480 nm. The first one with a lower threshold. Preadaptation to red light, suppressed the first peak without significant changes of that at 480 nm. Adaptation to blue light produced the opposite result. The photoreceptors driving the response are extra-retinal.

Thursday 02 August Congress Centre-First Floor Posters 169-174

Posters on Photo and Auditory Receptors

169

EFFECT OF PRESSURE ON PHOTOCHEMISTRY OF THREE RETINOID PIGMENTS (BR, HR, TR) IN *HALOBACTERIUM HALOBIIUM*
M. Tsuda, Y. Terayama. Department of Physics, Sapporo Medical College, Sapporo 060, Japan

The cytoplasmic membranes of *Halobacterium halobium* contain at least three retinal pigments, i.e., bacteriorhodopsin (BR), halorhodopsin (HR), and third rhodopsin like pigment (TR)^{1,2}. The rate and amplitude of the photo-transients of BR, HR, and TR were measured under various conditions of pressure, temperature, salts and detergents. Increasing pressure and decreasing temperature diminished the amplitudes of phototransient of TR but did not affect so much that of HR. The recovery of TR was accelerated but that of BR was retarded upon increasing pressure. HR was insensitive to pressure. Pressure effect of photocycle of SR³ in F1X3 mutant (provided by Dr. Spudich) was very similar to TR. Thus TR and SR could be the same pigment. The amplitude of phototransient of HR decreased in decreasing concentration of NaCl, but that of TR was not influenced in the range of 4 M to 100 mM NaCl. The amplitude of the photo-transient of the BR⁺ mutant and the magnitude of the photo-induced membrane potential were measured in various salt solutions. The results suggest HR is a light driven halogen pump and TR is not electrogenic.

1). Tsuda, M. et al., Biochem. Biophys. Res. Commun., 108, 970 (1982). 2). Hazemoto, N., et al., Biophys. J., 44, 59 (1983). 3). Bogomolny, R.A. and Spudich, J.L., Proc. Natl. Acad. Sci. USA, 79, 6250 (1982).

171

SYNTHETIC MODELS OF BIOLOGICAL PHOTORECEPTORS.
PHOTOREGULATION OF POLYPEPTIDE CONFORMATION

O. Pieroni, A. Fissi, J.L. Houben and F. Ciardelli, CNR - Inst. of Biophysics; Centre of Stereoregulated and Optically Active Macromolecules. Inst. of Industrial Organic Chemistry, University of Pisa, Pisa, Italy.

Photoresponsive polypeptides, which undergo reversible variations of conformation upon exposure to light or dark conditions, have been prepared by introducing photochromic azobenzene groups into the side chains of poly(L-glutamic acid). The extent and the kind of the photo-behaviour depend on azo content and solvent conditions under which irradiation is carried out. The maximum of the light-induced effects is achieved when the system is in a labile folded structure. The pK for the ionization of the unmodified COOH groups, and the conformational transition curves of the dark-adapted samples (trans-azo) were found to be different from those of the irradiated ones (cis-azo). So the trans-to-cis photo-isomerization produces a higher ionization degree of the COOH side chains, amplifying the first light effect and causing the unfolding of the polypeptide. The mechanism could be operative also in the case of naturally occurring photoreceptors, where the photoexcitation of a photochromic molecule seems to induce conformational changes of the attached protein matrix.

173

QUANTITATIVE ELECTRON PROBE ANALYSIS (EPMA) OF PRUG RETINAL ROES. B. Walz & A.P. Soslyo, Pennsylvania Muscle Institute, Univ. of Pennsylvania, Philadelphia, PA, USA 19104

The elemental composition of retinal rods was determined with EPMA (Soslyo, A.P. & Shuman, H., Ultramicroscopy 8:219 1982; Kitzawa, T. et al. Ultramicroscopy 11:251, 1983; Soslyo A.P. et al. these Proceedings) of dry cryosections of shock frozen, dark adapted and illuminated (5 min), *a. pipiens* retinas in 0.16M Ca²⁺ Ringer. Elemental composition was determined in the outer segments (OS), inner segments (IS), and in mitochondria. The results (in nmol/kg dry wt SEM) are shown in the Table.

	n	Na	Mg	P	S	Cl	K	Ca
DARK								
OS	81	70.3	14.2	597.11	408.8	55.2	127.2	0.4±0.1
IS	28	127.5	6.74	634.22	368.11	120.5	326.10	3.6±0.4
MITO	44	61.2	43.1	550.12	413.8	44.2	253.8	0.0±0.2
LIGHT								
OS	44	29.2	12.1	589.13	418.8	45.2	174.5	0.4±0.2
IS	27	46.5	50.2	595.17	374.12	104.5	414.14	3.6±0.6
MITO	40	21.2	36.1	501.10	397.7	35.2	257.8	0.4±0.2

In Na-free solution the [Na] in the OS was reduced to 3 nmol/kg (n=34) and total [Ca] was unchanged. We conclude that 1) there is a significant (OS P<0.05, IS P<0.01) reduction in rod [Ca] after 5 min illumination; 2) the Ca content of ROS (~0.1/Rhodopsin) is at the lower limit of published values (Cauts & Cone, EBA 463:194, 1977) and is not detectably changed by light; 3) the K/Na ratio in rods is increased and mitochondrial Na is decreased by light. The very small (P<0.05) change in mitochondrial Ca is compatible with Na-induced Ca release in the dark. Supp. by HL15835 to the Penna. Mus. Inst. and Deutsche Forschungsgemeinschaft (Va 463/2-2) to B.W.

170

EFFECTS OF CALCIUM-FREE SOLUTIONS AND COBALT IONS ON LIGHT-INDUCED pH_i CHANGES IN *BALANUS* PHOTORECEPTORS.
D. Erne and H.M. Brown, Dept. Physiol., Univ. Utah, Salt Lake City, UT, USA.

Illumination of some invertebrate photoreceptors has been shown to initiate an inward Ca²⁺ current. Additionally, Ca²⁺ released from intracellular Ca²⁺ pools is a likely source of an increase in intracellular Ca²⁺. A subsequent intracellular Ca-H exchange could contribute to the decrease of pH_i seen under these conditions. In an attempt to distinguish between these two processes we have recorded light-induced intracellular pH_i changes in barnacle photoreceptors in the absence of extracellular Ca²⁺ as well as in the presence of Ca²⁺ channel blocking Co²⁺ ions. Intracellular pH_i was assessed using neutral carrier based liquid membrane microelectrodes (D. Ammann et al., Anal. Chem. 53, 2267 (1981)). Experiments in the absence of external Ca²⁺ (1mM EGTA) showed a light induced pH_i decrease and recovery in the dark similar to the control experiments. This suggests that the influx of Ca²⁺ is not primarily responsible for the acidification of the cytoplasm but rather some intracellular mechanism triggered by illumination. Reducing extracellular Ca²⁺ from 20mM to 10mM or adding up to 30mM CoCl₂ increased the light induced acidification in the steady-state by a factor of 2 to 5. The recovery in the dark is remarkably slower under these conditions. A Co²⁺ induced inhibition of the pH_i recovery after acidification could account for both the increased acidification in light and the longer time constant of the recovery in the dark. NEI EY00762.

172 ORAL PRESENTATION

THE ULTRAVIOLET FLUORESCENCE-AND INTRAMOLECULAR ENERGY TRANSFER OF PURPLE MEMBRANE

J.L. Chang, Z.P. Feng and P.L. Zhou, Biophysics Div Dept. of Biology, Fudan Univ., Shanghai, China

The ultraviolet fluorescence spectra of purple membrane fragments were measured. The PM samples were saturated with and without ether, in either case the protein fluorescence of the PM samples irradiated with orange light were lower than the control one. The intensities of UV fluorescence of PM and apo-membrane were similar, but the quantum yield of UV fluorescence of bacteriorhodopsin was twice as large as the natural purple membrane. This result illustrated that the protein fluorescence was quenched by the chromophore of PM. The conversion of the dark-adapted PM into light-adapted PM was catalyzed by irradiation of UV light at 280nm. The photobleaching of PM was also catalyzed by the UV light at 280nm in the presence of hydroxylamine. By measuring the action spectrum of photobleaching of PM irradiated with 280nm, we showed that the action spectrum of photobleaching of PM coincided with the absorption spectrum of PM in the UV region. All the results showed that the energy absorbed by protein had transferred to retinal.

174 ORAL PRESENTATION

IONIC SELECTIVITY OF THE TOAD ROD OUTER SEGMENT MEMBRANE
B.J. Nunn, P.A. McNaughton and A.L. Hodgkin, Physiological Laboratory, Downing Street, Cambridge, U.K.

The effects of rapid ionic changes on the light-sensitive current of rods were investigated by transferring a rod, held in a suction pipette, across the boundary between two flowing solutions. The relative permeabilities of monovalent cations through the light-sensitive channel are Li:Na:K:Rb:Cs = 1.4:1.0:8.0:6.0:1.5; choline, TMA and TEA are impermeant. Ca²⁺ can carry a substantial current in some circumstances, but can also rapidly block a current carried by another ion. No ion apart from Na⁺ can maintain appreciable current continuously in the presence of 1 mM-Ca; this is probably because no other cation can replace Na in the Na:Ca exchange which normally holds [Ca]_i at a low level.

The rate at which channels close in low [Na]_o or high [Ca]_o is accelerated by weak background lights and slowed by IBMX, which inhibits the hydrolysis of cyclic GMP.

After a period in Li containing 1 mM-Ca the light-sensitive channels remain closed for a second or two when Na_o is restored. Reducing Ca in the Li solution from 1 to 0.1 mM accelerates the recovery on restoring Na, but, surprisingly, has little effect on the time constant with which current declines in Li.

Although our results suggest that Ca is involved in transduction, they seem quantitatively more consistent with an inhibitory effect of Ca_i on the production of cyclic GMP than with a direct action of Ca_i on light-sensitive channels.

Thursday 02 August Congress Centre-First Floor Posters 175-180

Posters on Photo and Auditory Receptors

175

STEPPED RECOVERY OF THE PHOTOCURRENT OF MONKEY RODS.
J.L. Schnapf, B.J. Nunn, and D.A. Baylor, Department of Neurobiology, Stanford University, Stanford, CA, USA.
Photocurrent was recorded from single rods of *Macaca fascicularis* with a suction electrode. The photocurrent evoked by a bright flash showed a long tail consisting of the superposition of step-like outward currents. Individual events seen after bleaching 200-1000 rhodopsin molecules displayed quantized amplitudes of 1-2 pA, transition times of 0.2 sec, and widely varying durations which sometimes exceeded 30 sec. The duration and mean number of events increased with increasing flash strength. Events lasted longest when elicited by light at the tip of the outer segment, and were never observed during the saturating photocurrent, indicating that they result from local blockage of the light sensitive conductance.

A speculative model is that bleaching of a rhodopsin can trigger the steady point injection of Ca^{++} into the rod cytoplasm, blocking the dark current along a 1-2 μ m length of outer segment. Experiments with plane-polarized light indicate that absorption of light in the discs, not the surface membrane, initiates the events.

After very bright light, prominent current fluctuations result from the superposition of many step events, giving a possible basis for the "equivalent background" observed psychophysically.

177

ELECTROPHYSIOLOGY OF THE COLOR RECEPTORS IN THE FRAYING MANTIS

Nelson A. Zabala, Dpto. Biología de organismos, Univ. "Simón Bolívar", Caracas, Venezuela.

Corneal field ERG (Ruck, 1961, J.G. Physiol. 44: 606) of the mantis (*Stagmatoptera biocellata*) compound eye (CE) shows different wave length (WL) responses in different eye areas. In the antero-internal area it shows WL sensitivity curves with two maximum peaks, one in 420 nm and another one in 516 nm. The relation of these two peaks change with light or dark adaptation, showing a Purkinje shift. In the rest of the CE areas the only peak detected was the one corresponding to 516 nm, and the Purkinje shift can not be detected. Using intracellular recording of the reticular cells of the mantis CE, two types of wave length sensitivity cells were found. The more frequent were ones with maximum sensitivity WL in 516 nm, and the less frequent were ones with maximum sensitivity WL in 420 nm. The 516 nm cells were found in all the CE but in AI CE area was found 420 nm cells too. Because the AI area of the mantis CE has been proposed for form and distance detection, thus it is possible to assume that mantis has dichromatic color vision for these eye functions.

179

176

Ca^{2+} BUFFER CAPACITY IN BALANUS PHOTORECEPTORS FROM ARSENIZO III MEASUREMENTS.

H.M. Brown and B. Rydqvist, Depts. Physiol., Univ. Utah, Salt Lake City, UT, USA; Karolinska Inst., Stockholm, Sweden.

Light-induced intracellular Ca^{2+} and pH changes have been measured in *Balanus* photoreceptor cells with ion-selective electrodes. This raises the question of the interdependence of these changes and implications for photoreceptor function. Arsenazo III (AIII) exhibits large changes in extinction at 620 nm for pH changes and at 650 nm for Ca^{2+} changes. This property of the dye was utilized for simultaneous measurement of intracellular pH (pH_i) and free Ca^{2+} changes (Ca^{2+}_i). The Ca^{2+} buffer capacity of the cell ($1-\Delta Ca^{2+}_i / \Delta Ca^{2+}_{load} \times 100$) was estimated in the dark by acidifying Cs/EGTA injected cells with CO_2 equilibrated salines or by exposing the cell to light. A Ca^{2+} load could be computed from the pH dependence of K_D^{AIII}. The buffer capacity was about 95% and was independent of the mode of ΔpH , i.e. light or CO_2 . The situation in cells injected exclusively with AIII proved to be different. For a given ΔCa^{2+}_i , the light-induced pH was considerably smaller than the CO_2 induced change (0.05 vs. 0.5). These observations suggest 1) these photoreceptor cells have an inherently low Ca^{2+} buffer capacity compared to some other nerve cells (e.g. squid axon can buffer 99.9% of a Ca^{2+} load) and 2) that the Ca^{2+} buffer capacity is further diminished during light. Supported by NEI EY00762.

178

180

Thursday 02 August Congress Centre-First Floor Posters 181-186

Posters on Applications of Synchrotron Radiation

181

LOCAL STRUCTURE OF Fe SITES IN FOETAL HAEMOGLOBIN BY XANES

A. Congiu-Castellano, A. Bianconi, E. Burattini, M. Castagnola, M. Dell'Arciccia, P.J. Durham, A. Giovannelli, Dipartimento di Fisica, Università di Roma "La Sapienza", Roma, Italy.

Iron X-ray Absorption Near Edge Structure (XANES) spectra of human foetal (F) and adult (A) deoxy haemoglobin (Hb) measured at the Frascati synchrotron radiation facility reveal the different geometrical structure of the Fe-porphyrin complexes in the two proteins. The difference of the Fe-site structure between the foetal and adult deoxy Hb is related with the different affinity for oxygen of the two forms of haemoglobin.

The k-XANES spectra are interpreted by multiple-scattering XANES theory which show a good agreement with experimental data. The agreement between the experiment and theory allows us to assign the iron XANES spectra to multiple scattering of the excited photoelectron in the continuum within a cluster of 30 neighbour atoms. The effect of the increasing Fe-displacement out of the porphyrin plane predicted by XANES calculations is in agreement with the observed variation of experimental XANES spectra going from deoxy HbA to deoxy HbF.

182

SYNCHROTRON RADIATION X-RAY SCATTERING DURING THE INITIAL STAGES OF IN VITRO COLLAGEN SELF-ASSEMBLY. G. Sanoz and A. L. Ormosy, Dept. of Orthopaedics, Mount Sinai School of Medicine, New York, N.Y., U.S.A.; J. Bordes and M. H. J. Koch, European Mol. Biol. Lab., Hbrburg, F.R.G.

In order to obtain information on the structure of the early supramolecular collagen assemblies the temporal course of fibril formation was monitored by synchrotron radiation X-ray scattering. Following a temperature jump from 4°C to 32°C, which induced collagen polymerization, a continuous increase in the scattering intensity was detected with no discernible lag phase. Parallel turbidimetric experiments under the same conditions revealed a lag phase of ca. 90 sec. A direct correlation was found between the temperature and both the rate of increase of scattering intensity and the final intensity, which indicate early aggregate formation. Only partial aggregate reversal occurred by lowering the temperature. In contrast prevention of Schiff base mediated intermolecular crosslinks, by reduction with sodium borohydride, led to complete aggregate reversal upon cooling. From these results and modelling based on Guinier plots of the scattering intensity we conclude that early aggregates crosslink irreversibly upon assembly and appear to correspond to 5-crossed subfibrils previously proposed by others. (Supported in part by NATO grant #953-82, American Heart Association grant #82-946, The American Diabetes Association and the Milton Petrie Fund).

183

SUBTLE STRUCTURAL CHANGES AT THE Fe SITE OF HAEM-PROTEINS AND PROTEIN FUNCTION DETECTED BY XANES USING SYNCHROTRON RADIATION

A. Bianconi, E. Burattini, M. Cerdonio, A. Congiu-Castellano, M. Dell'Arciccia, P. Durham, A. Giovannelli, C. Marcelli, S. Morante, Dipartimento di Fisica, Università di Roma "La Sapienza", Roma, Italy.

The new experimental method XANES (X-ray Absorption Near Edge Structure) using synchrotron radiation, has given new insight on the relationship between local structure of Fe site in haemoglobin and the affinity for oxygen binding. In spite of long standing interest in this problem, the solution has not yet been reached because of the lack of experimental methods sensitive to very small structural changes involving subtle distortions of the local structure in proteins in solution close to the "in vivo" situation. XANES is a direct probe of the local atomic structure around the Fe atom within ~5 Å giving bonding angles and the geometry of a cluster of 30 atoms including the porphyrin plane and the proximal histidine.

We have studied 1) the variation of Fe-displacement from the porphyrin plane in the deoxy haem proteins in the T form with different O₂ affinity, 2) the Fe-displacement in deoxy myoglobin, 3) bonding angles of molecules O₂, CO, CN bound to Fe in protoporphyrins, myoglobin, haemoglobin and carp haemoglobin, 4) the R to T transition of carp haemoglobin, 5) the Fe effective charge variation upon O₂ binding.

184

EXAFS STUDY OF ARTHROPATHIC DEPOSITS

J. E. HARRIES*, S. HASNAIN* & J. S. SHAH*
H. R. Mills Physics Laboratory, University of Bristol, U.K.
Daresbury Laboratory, U.K.

Diseases of the joints and periarthritic tissues are often associated with pathological deposits. Deposition of hydroxyapatite (HAP) occurs in articular hyaline cartilage and intra-articular fibro-cartilage pads in attacks of acute synovitis and osteoarthritis. Periarthritic deposits occur in acute calcific periarthritis, tissues. Subcutaneous deposits are common in systemic sclerosis and can cause painful ulceration of the skin.

EXAFS spectra of the deposits from subcutaneous and periarthritic tissues were compared with the EXAFS of bone mineral. The pathological crystalline deposits showed a different EXAFS spectrum and confirmed the findings from the previous infra red spectral studies (Shah, 1983) that the deposits are not pure hydroxyapatite.

Infra-red spectra and x-ray powder diffraction indicated the presence of CO₃ in the pathological specimens. Therefore EXAFS of synthetically prepared carbonate apatite were also obtained. From the studies so far, it can be concluded that both the crystallinity and the presence of carbonate ions influence the spectra of hydroxyapatite.

REFERENCES

Shah, J. S. (1983). Application of Physical Methods in the investigation of crystal related arthropathies. *Ann. Rheum. Dis.* 22 suppl. 100.

185

ANGULAR RESOLVED XANES SPECTRA USING SYNCHROTRON RADIATION OF HbCO SINGLE CRYSTALS

A. Bianconi, S. Hasnain, P. Durham, A. Congiu-Castellano, M. Dell'Arciccia, S.E. Phillips, M. Perutz, Dipartimento di Fisica, Università di Roma "La Sapienza", Roma, Italy and Daresbury Laboratory, Warrington, U.K.

The first angular resolved XANES (X-ray Absorption Near Edge Structure) experiment on single crystal myoglobin CO is reported. We have measured the XANES spectra with the photon electric field parallel (perpendicular) to the *a* axis *E* // *a*, (*E* ⊥ *a*) of monoclinic P2₁ crystals. The XANES spectra in the two polarizations are quite different. The data are in agreement with multiple scattering XANES calculations which predict a strong resonance in the photoelectron scattering in direction of CO molecule. The comparison with spectra of HbCO in solution gives the physical assignment to their weak spectral features. We show that this new method can give unique information of molecule bonding geometry in haem-proteins.

186

SEQUENCE DEPENDENT EMISSIONS IN DINUCLEOSIDES PHOSPHATES BY SYNCHROTRON EXCITED TIME-RESOLVED EMISSION.

J.P. Ballini⁽¹⁾, M. Daniels⁽²⁾ and P. Vigny⁽¹⁾, ⁽¹⁾Institut Curie and Université Paris VI, Paris, France, Université Paris-Sud Orsay, France and ⁽²⁾Oregon State University, Corvallis, U.S.A.

The luminescence equipment built at Orsay, which combines the Lure synchrotron source with a spectrofluorometer using a fast single photon counting detection operating in the nanosecond range, has been used to analyse the complex room temperature weak emissions of dinucleosides phosphates. Time-resolved spectroscopy allowed us to discriminate the arrival of early (0 to 2.96 ns) intermediate (2.96 to 6.04 ns) and late (6.04 ns to 53.35 ns) emitted photons following the excitation and to record the various components separately. In the special case of nucleic acids components, we have to discriminate between picosecond range and nanosecond range, and this time resolved spectroscopy is suitable. Different sequences of dinucleotides like ApT and TpA, ApC and CpA have been studied, and show three components which peaks respectively at about 330, 400 and 460 nm. The intermediate one at 400 nm, attributed to stacked bases, is more intense in ApT or ApC sequences than in TpA or CpA ones. This may be due to either increased fractional stacking or increased quantum efficiency or both, for the pur-pyr sequence relative to the pyr-pur one.

Thursday 02 August Congress Centre-First Floor Posters 187-192

Posters on Applications of Synchrotron Radiation

187

X-RAY ANALYSIS OF THE KINETICS OF E. coli LIPID AND MEMBRANE STRUCTURAL TRANSITIONS

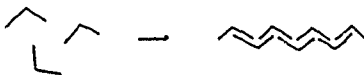
J.L. Ranck, L. Letellier, E. Shechter, B. Krop, P. Pernot and A. Tardieu, Lab. des Biomembranes, Univ. Paris-Sud, Orsa and Centre de Génétique Moléculaire, Gif sur Yvette, France

Synchrotron Radiation was used to follow the time course of the transitions, induced by temperature jump, in E. coli membranes and lipid extracts isolated from a fatty auxotroph grown with different fatty acids. We measured the relaxation times associated with the phase transitions as well as with the conformational transitions of the hydrocarbon chains and observed different behaviour as a function of chemical composition. Relaxation times of 1 to 2 sec. were found at a hexagonal to lamellar transition and within a lamellar phase whose parameters display important variations with temperature when the conformational transition takes place. No delay was observed for a phase transition where large lipid or water diffusion was not needed. We have shown that phase transitions and conformational transitions are to a large extent not coupled and that the relaxation times corresponding to the latter transition could be related to the size of the ordered domains. In all cases, the order-disorder transition is more rapid than the disorder-order transition. Finally the relaxation times associated with the disorder-order transition in the membrane and in the lipid extracts were found to be strongly correlated, indicating that the proteins do not play a role in this transition.

189 ORAL PRESENTATION

FIBRINOGEN-FIBRIN CONVERSION MECHANISM MONITORED BY STOPPED-FLOW X-RAY SCATTERING METHOD
H. Kihara¹, K. Toji¹, T. S. Kuchii¹, S. Saigo², M. Matsuda³, C. Nakamizawa⁴, Y. Anemitsu⁴, K. Wakabayashi⁵, T. Nagamatsu⁶ and T. Furuno⁷
1) Jichi Medical School, 2) KEK, 3) Osaka University, 4) UNISOKU Co. Ltd., 5) Phys. Chem. Research Inst. at Wako

Conversion of fibrinogen to fibrin by attack of thrombin was monitored by stopped-flow x-ray scattering method. In 50 mM Tris-Cl (pH 7.5) with 0.5 M NaCl, fibrinogen (10 mg/ml, final) was mixed with thrombin (100 unit, final). X-ray scattering pattern was monitored with one-dimensional PSPC. Total scattered intensity increased with half-time of 8 sec. After 20 sec, it shows no detectable changes through 10 min. On the contrary of it, light-scattering shows huge increase even after several minutes. Fibrin solution in the cell changed to gel after the experiment. Analysis was done with one-dimensional rod approximation. The result shows that diameter becomes larger from 88 Å to 143 Å (1.6 fold). The result would be explainable with the mechanism shown in Figure 1.



191 ORAL PRESENTATION

TIME RESOLVED FLUORESCENCE STUDY OF A 23187 INTERACTIONS WITH SARCOPLASMIC RETICULUM VESICLES USING SYNCHROTRON RADIATION

J.C. Brochon, L. U. R. E. (Synchrotron Radiation Lab.) Univ. Paris-Sud, Bat. 209C, ORSAY, D. Bréthes, J. Chevallier BORDEAUX, B. Arris, ORSAY, FRANCE

An analysis of interactions between the calcium ionophore A 23187 and the Ca²⁺-dependent ATPase of sarcoplasmic reticulum from skeletal muscle has been done by fluorimetry in the nanosecond range using synchrotron radiation. The emission of the ionophore can be described by a single decay time of 8.4, 8.3, and 7.6 nanoseconds in ethanol, chloroform and cyclohexane respectively. In aqueous medium the response is heterogeneous and drastically modified according to pH. The relative contribution of the shortest decay time (τ₁ = 0.8 nsec) to the whole fluorescence emission increases from pH 4.1 to pH 9.1 and can be attributed to the non protonated form of the ionophore. Addition of calcium has no effect on this decay.

When excited at 280 or 295 nm the fluorescence emission of the sarcoplasmic reticulum vesicles is heterogeneous, mainly due to tryptophanyl groups of the Ca²⁺-dependent ATPase. When this biological membrane preparation is excited at 295 nm in the presence of A 23187, one measures an emission at 448 nm due to energy transfer between the tryptophanyl residues and the ionophore, showing a relatively close interaction between this molecule and the Ca²⁺-dependent ATPase. The fluorescence anisotropy decay of A 23187 incorporated in the membrane can be described by two correlation times. By comparison with what is obtained with liposomes made by phospholipid extraction from S.R., the smaller correlation time τ₁ may be related to the mobility of the ionophore in the lipid bilayer. The longer correlation time, τ₂, may indicate that some ionophore molecules are located near the Ca²⁺-dependent ATPase in a more disordered phospholipid environment.

In addition a review of the various applications of Synchrotron Radiation for pulsed fluorimetry studies of biological systems is presented.

188

STRUCTURE OF MANGANESE SUPEROXIDE DISMUTASE

C.C.F. Blake and M.W. Parker, Laboratory of Molecular Biophysics, Department of Zoology, Oxford, U.K.

Superoxide Dismutase acts as the first line of defense against oxygen toxicity by catalysing the dismutation of superoxide radicals to dioxygen and hydrogen peroxide. To date two of the three classes of the enzyme have had crystal structures determined. We have determined the three dimensional structure of the third class - manganese superoxide dismutase from *B. stearothermophilus*. The enzyme crystallised in space group P2₁2₁2 with the dimer in the asymmetric unit and cell dimensions of a = 72.4 to 74.7 Å, b = 111.1 Å and c = 51.1 Å. Diffractometer data to 6 Å was collected for native, three heavy atom derivatives and a manganese free crystal. An electron density map has been calculated based on phases from the heavy atom data and the manganese sites determined from a difference Fourier with the Manganese-free data. A structural comparison with the other types of SOD will be presented.

190

Construction and Performance of a Multifrequency Cross-Correlation Phase Fluorometer Using Synchrotron Radiation. E. Gratton, D.M. Jaramon, N. Rosato and G. Weber, Depts. of Physics and Biochemistry, Univ. of Illinois at Urbana and Dept. of Pharmacology, Univ. of TX Hlth. Sci. Center at Dallas.

A cross-correlation phase and modulation fluorometer using the synchrotron radiation facility at the ADONE-Frascati electron storage ring was recently constructed and tested. The instrument utilized the large series of equally spaced harmonic frequencies available in the frequency domain from the high repetition rate pulsed source. The signal intensity does not decrease substantially at the highest harmonic frequencies utilized. The cross-correlation technique in conjunction with the high repetition rate pulsed light source permits one to isolate one harmonic frequency from the adjacent frequencies with high precision. Two coupled frequency synthesizers are used to generate the cross-correlation frequency required for the analysis of the phase delay and modulation ratio; one synthesizer drives the radiofrequency cavity of the storage ring and the other modulates the response of the photomultiplier. The system's performance of the instrument with respect to absolute accuracy, reproducibility and sensitivity has been experimentally determined. These results indicate the superiority of the cross-correlation phase techniques coupled with synchrotron radiation over conventional lifetime instrumentation. The samples investigated included NADH, tryptophan (at different pH conditions and at various excitation and emission wavelengths) bis-TNS, bis-TNS and various proteins. Experiments on energy transfer between tyrosine and tryptophan in BSA and with bis-ANS absorbed to BSA were also performed.

192

OVERSHOOT ASSEMBLY OF TUBULIN STUDIED BY TIME-RESOLVED X-RAY SCATTERING. E. Mandelkow, E.-N. Mandelkow, W. Renner and J. Bercas, Max-Planck-Institut für medizinische Forschung, Abt. Biophysik, D-6900 Heidelberg, FRG, and Daresbury Laboratory, Warrington WA4 4AD, U.K.

Microtubule assembly consists of several phases; during the pre-nucleation stage storage aggregates break down into tubulin oligomers and subunits; these re-associate in several steps during the nucleation phase, followed by the elongation phase. Nucleation and growth may be considered as a two-dimensional process, constrained to the surface of a cylinder. This implies that assembly is non-helical even though the product has a near-helical structure. The overall process may be described in terms of the theory of helical nucleation-condensation, but there are several additional features. As an example, we have studied the relationship between overshoot assembly and polymorphism. With strictly helical assembly, successful nucleation events lead to polymers of identical structure. They may have a non-equilibrium length distribution which slowly relaxes towards equilibrium. By contrast, non-helical assembly combined with kinetic overshoot may lead to a variety of structures. TNC, represent a non-equilibrium length- and width-distribution but are not assembly intermediates. Kinetic overshoot has been observed by X-ray scattering using synchrotron radiation, and the structures generated during that phase have been studied by electron microscopy. Consequences for a general assembly scheme for tubulin will be described.

1) Osawa, F. (1970). J. theor. Biol. 27, 69.
2) Mandelkow, E., Mandelkow, E.-N. & Bercas, J. (1983). TIBS 8, 144.

Thursday 02 August Congress Centre-First Floor Posters 193-198

Posters on Applications of Synchrotron Radiation

193

X-RAY ABSORPTION AND REDOX STUDIES OF MYOGLOBIN DERIVATIVES: THE RELATIONSHIP BETWEEN FE-LIGAND DISTANCES AND MID-POINT POTENTIAL. L. Garcia-Inguera¹, L. Powers², and B. Chance.
1- Monsanto Co., St. Louis, MO, 2- Bell Laboratories, Murray Hill, NJ, 3- Univ. Pennsylvania, Philadelphia, PA, USA.

Extended X-ray absorption fine structure (EXAFS) and X-ray edge spectra of several myoglobin derivatives have been measured along with corresponding oxidation-reduction mid-point potential. The multiple scattering region (XANES) in the spectra distinguishes high-spin from low-spin ferric hemes at approximately 7155 eV and 7180 eV. High-spin ferric hemes (such as fluoride or formate derivatives) show 7155 eV/7180 eV ratios of 1.44; whereas, low-spin ferric hemes (such as azide or cyanide derivatives) show ratios of 0.67-0.69. Myoglobin-imidazole derivative has a 7155 eV/7180 eV ratio of 1.10 indicating a mixed spin-state. Differences in spin-state are observed in the Fe-L, Fe-histidine, and Fe-N(porphyrin) atomic distances. The mid-point redox potentials of myoglobin derivatives are dependent on ligand concentration as well as the type of ligand bound. Mid-point potentials were measured at each ligand concentration from 0 to 0.150 Molar. At 0.020 M ligand concentration, the E_m values for formate, fluoride, azide, and cyanide derivatives were: 0.024, -0.003, -0.115 and -0.145 volts, respectively. The study shows that the shortening of the Fe-histidine and Fe-ligand distances in the heme core lowers the mid-point redox potential of the myoglobin compound, thus, inhibiting the electron transfer capability of the heme.

195

LOW RESOLUTION STRUCTURE DETERMINATION OF β -LACTAMASE I FROM *B. CEREUS*

B. Samraoui, B.J. Sutton, R.J. Todd and D.C. Phillips, Laboratory of Molecular Biophysics, Department of Zoology, South Parks Road, Oxford, UK.

β -lactamase I from *Bacillus cereus* 569 crystallises in space group C2 with cell dimensions $a = 143.9 \text{ \AA}$, $b = 35.8 \text{ \AA}$, $c = 52.7 \text{ \AA}$ and $\beta = 97.0^\circ$, consistent with one molecule of molecular weight 28,000 per asymmetric unit. Complete data sets from native crystals and three derivatives ($K_2Pt(C_2O_4)_2$, $Sm(ClO_4)_3$ and $MelHgCl$) have been collected to a resolution of 2.5 \AA using synchrotron radiation at L.U.R.E. (Orsay) and Daresbury Laboratory for the first three data sets. The phases derived from these heavy atom derivatives were used to calculate a low (5 \AA) resolution electron density map. The contrast between the α helix and the solvent is good, allowing much of the boundary of the molecule to be defined. The 2.5 \AA resolution map proved to be less readily interpretable in detail, and efforts are being made to improve the quality of the higher resolution phases. A three-dimensional data set to 2.5 \AA was also collected at Daresbury Laboratory for the substrate analogue 6- β -bromopenicillanic acid, which binds and irreversibly inactivates the enzyme.

197

X-ray diffraction study of tomato strain of tobacco mosaic virus using synchrotron radiation.

M. Taniguchi¹, Y. Amezawa², K. Wakabayashi³, T. Taniguchi⁴, N. Hara¹, S. Mituzawa¹, Y. Sato², and Y. Kamiya³.

1) Department of Physics, Faculty of Science, Nagoya University, Nagoya; 2) Photon Factory, National Laboratory for High Energy Physics, Tsukuba-City, Ibaragi; 3) Department of Biophysical Engineering, Faculty of Engineering Science, Osaka University, Toyonaka, Osaka; 4) Plant Pathology Laboratory, Faculty of Agriculture, Nagoya Univ.; 5) Department of General Education, Faculty of Engineering, Toyota Technological Institute, Nagoya (Japan).

The tomato strain of tobacco mosaic virus (TMV-T) is significantly different for serological properties and amino acid compositions from the ordinary strain (TMV-OM). It is of interest whether or not the molecular structure is the same as that of TMV-OM. X-ray diffraction using synchrotron radiation can provide powerful information about protein conformation. Oriented gels of TMV-T were used for the experiments of small-angle X-ray diffraction at the Photon Factory. The image processing system has been developed using two dimensional Fast Fourier Transformation. The results indicate that the helix pitch of its protein subunit for TMV-T is 23 \AA and the number of subunits in the three-turn repeat (69 \AA) is almost same as in the ordinary strain. However, a new set of near-meridional reflections with a 34 \AA period were observed in the diffraction pattern of TMV-T. Thus the prohibited reflections occur on the 2nd and 4th layer-lines of the 69 \AA period.

194

ACUTE CHANGES IN CNS BLOOD VESSEL MORPHOLOGY AFTER HIGH-ENERGY HELIUM ION IRRADIATION
Z. Karpfel, L. Tkadleček, Š. Viklická, and B.S. Fedorenko, Inst. of Biophysics, Czechoslovak Acad. Sci., Brno, Czechoslovakia, and Inst. of Med. and Biol. Problems, Ministry of Health, Dubna, U.S.S.R.

Wistar rats were irradiated with 4 GeV/nucleon helium ions produced by means of a synchrophasotron of the Joint Inst. for Nuclear Research, Dubna, with a dose of 2 or 4 Gy. After 4 to 9 hours or three days a perfusion fixation was performed and cerebral cortex sections were investigated under light and electron microscopes. Most vessels in the sections showed no signs of damage. In some cases there was a dilated perivascular space; a comparison of its occurrence in irradiated and control animals showed a statistically significant increase in frequency of the phenomenon at a shorter interval after irradiation with the larger dose. Morphological analysis at electron microscope level showed that the main locality of damage was the border of the perivascular foot of the astrocytes, which exhibited various degrees of oedema. The discussion stresses the peculiarities of the interaction of high-energy helium ions with living tissue, particularly the heterogeneity of the distribution of absorbed energy.

196

EXPERIMENTAL PROBLEMS IN TIME RESOLVED X-RAY MEASUREMENTS FROM MUSCLE

A.R. Faruqi, MRC Laboratory of Molecular Biology, Hills Road, Cambridge, CB2 2QH.

Time resolved X-ray diffraction measurements from muscle is a powerful technique for eliciting dynamical structural information regarding the molecular details of the contraction mechanism. The development of high intensity synchrotron sources and faster methods of data collection have made some of these measurements possible. We describe a data acquisition system, based on a high count rate multiwire detector, for recording time resolved data to millisecond time resolution, in conjunction with rapid mechanical transients. This allows one to perform experiments in which, for instance, a contracting muscle is shortened very rapidly and the changes observed in the diffraction pattern. The rate constants of the underlying chemical reactions require that the measurements be done with about 1 millisecond sampling time. Special interactive graphics software has been developed to analyze the large quantities of data from typical experiments and extract parameters such as intensity, spacings, etc. as accurately as possible.

198

SUBSTRATE-COFACTOR INTERACTIONS FOR GLYCOGEN PHOSPHORYLASE B: A BINDING STUDY IN THE CRYSTAL WITH HEPTENITOL AND HEPTULOSE-2-PHOSPHATE

P.J. McLaughlin, D.I. Stuart, H.W. Klein, N.G. Oikonomakos and L.N. Johnson, Lab. of Molecular Biophysics, Zoology Dept., South Parks Road, Oxford OX1 3PS, U.K.

The role of the co-factor pyridoxal phosphate in glycogen phosphorylase b, an enzyme which catalyses the phosphorylation of glycogen to yield glucose-1-phosphate, has been shown to involve the 5'phosphate group possibly as an acid base or an electrophile. However binding studies in the crystal have demonstrated that the phosphate of the product glucose-1-phosphate is too far away from the co-factor phosphate to yield any structural information about how they might occur.

Recent work (Klein et al. To be published) has shown that phosphorylase in the presence of inorganic phosphate will catalyse the conversion of heptenitol to heptulose-2-phosphate. The latter compound is a dead end product and the most potent inhibitor known for phosphorylase ($K_i = 24 \mu\text{M}$). Its binding of heptenitol to crystals of phosphorylase b has been studied at 3 \AA resolution. A crystal was then incubated with heptenitol and inorganic phosphate in the presence of activators, AMP and oligosaccharide and data to 3 \AA spacing collected in 2.5 h with the Daresbury S.R.S. A difference Fourier synthesis revealed that the product, heptulose 2-phosphate, had been formed. Its glucose moiety is located in a similar position to that of heptenitol and glucose-1-phosphate, but its phosphate oxygen is only 2.7 \AA from the co-factor phosphate oxygen, and it is assumed that there is a hydrogen bond between them.

Thursday 02 August Congress Centre-First Floor Posters 199-204

Posters on Applications of Synchrotron Radiation

199

BINDING OF THE OXIDISED CO-ENZYME NADP⁺ TO 6-PHOSPHO-GLUCONATE DEHYDROGENASE

M.J. Adams, S. Gover, K.C.M. Pelly and R.W. Pickersgill, Laboratory of Molecular Biophysics, Department of Zoology, South Parks Road, Oxford, UK.

The binding of the oxidised co-enzyme NADP⁺ to 6-phosphogluconate dehydrogenase (6-PGDH) is being studied at high resolution. A data set extending to 2.7 Å resolution, collected using the Daresbury synchrotron X-ray source, is being processed. Optimal soaking conditions for the crystals were found to be 5 mM NADP⁺ for 24 hours. Preliminary results at 4 Å resolution, using the same soaking conditions, have yielded a difference Fourier which suggests that the mode of binding of NADP⁺ to 6-PGDH is different from that of NAD⁺ in the NAD⁺ dependent dehydrogenases such as lactate dehydrogenase and glyceraldehyde phosphate dehydrogenase. While the adenine portion of NAD⁺ has usually been described as binding in a hydrophobic pocket, the binding site of NADP⁺ is considerably more hydrophilic, the adenine moiety having hydrophobic groups on only one face. It is also probable that the coenzyme conformation itself is different in 6-PGDH from that found in the NAD⁺ enzymes.

The high resolution data should allow a detailed description of the binding of the coenzyme. The implications of the difference in binding will be discussed.

201

SIMULTANEOUS BINDING OF SUBSTRATES TO GLYCOGEN PHOSPHORYLASE b: AN X-RAY CRYSTALLOGRAPHIC ANALYSIS OF THE INTERACTIONS BETWEEN BINDING SITES.

J. Hajdu, M.S.P. Sansom, Y.S. Babu, P.J. McLaughlin, D.I. Stuart & L.N. Johnson: Laboratory of Molecular Biophysics, University of Oxford, Oxford, OX1 3PS, U.K.

To probe interactions between the catalytic, nucleotide, and glycogen storage sites of phosphorylase, we have examined the simultaneous binding of glucose-1-phosphate (G-1-P) and maltotriose to the enzyme. Catalysis was demonstrated to take place in the crystal. The usual problem with cracking of crystals during the catalytic reaction was overcome by choosing equilibrium conditions in which only short chain oligosaccharide products form. Having reached chemical equilibrium, 3 dimensional data to 2.6 Å resolution were collected by the oscillation method using the Synchrotron Radiation Source at Daresbury Laboratory. Analysis and model building on an Evans & Sutherland Picture System II showed the oligosaccharide bound to the glycogen storage site, G-1-P bound weakly at the catalytic site, and phosphate (formed in the reaction) bound at the nucleotide binding site. The modes of binding are somewhat different from those observed in separate binding studies of individual substrates. Implications of these findings in a possible mechanism of the catalytic reaction will be discussed.

203

SMALL ANGLE X-RAY SCATTERING STUDIES OF PARVALBUMIN IN SOLUTION

S.R. Hubbard, S. Doniach, K.O. Hodgson, Departments of Applied Physics and Chemistry, Stanford University, Stanford, California, USA.

Small angle X-ray scattering (SAXS) measurements have been made on solutions of the calcium-binding protein parvalbumin. Data have been collected at the Stanford Synchrotron Radiation Laboratory (SSRL) on the metal-free protein and the protein with two bound Ca(II). There is a measurable decrease in the radius of gyration, on the order of 1 Å, in going from the metal-free to the Ca(II)-loaded protein. At larger scattering angles, out to $s = 0.09 \text{ Å}^{-1}$ ($s = 2\sin(\theta/2)/\lambda$), the scattering curves are virtually the same for the two protein forms. To compare the structures in solution and in the crystalline state, we are calculating the theoretical SAXS curve using the atomic coordinates derived from X-ray crystallography. The electron density of the solvent is taken into account utilizing a "cube" method to estimate the excluded volume of the molecule. The approach is similar to that used by Pavlov and Fedorov¹.

¹M.Yu. Pavlov, B.A. Fedorov, *Biopolymers*, 22, 1507 (1983).

200

STUDY OF CONFORMATIONAL CHANGES OF ENZYMES BY POLARISED PULSED FLUORIMETRY USING SYNCHROTRON RADIATION.

F. Mérola, J.-C. Brochon, IURE, Univ. Paris-Sud, Orsay, France

Wheat germ Hexokinase II is a monomeric enzyme endowed with hysteretic (anomalous) properties. At pH 8.5, the free enzyme has been shown to exist under two catalytically different, interconvertible forms. The equilibrium between these forms is shifted by catalysis or temperature. At pH 6.9, in addition to the "anomalous" transition above, another equilibrium has been postulated from kinetic studies, between two forms of the binary complex Enzyme-Glucose. This would explain the regulatory properties toward a second substrate, MgATP, appearing at low pH. This last feature is shared by Yeast and Wheat germ Hexokinases. A hysteretic mechanism has also been proposed for the Yeast enzyme.

Polarised pulsed fluorimetry studies using the Photon Counting technique have been performed on Wheat germ Hexokinase, at various temperatures and pH. The fluorescence decays of Tryptophyl residues have been measured with an excitation at 300 nm. The fluorescence anisotropy decay measurements lasted typically 30 minutes. At pH 8.5, we found that the "anomalous" transition itself does not involve large structural changes in the protein. At low pH, a temperature-dependent transition of the Enzyme-Glucose complex can be detected. Flexibilities between large domains of the structure appear when the temperature is raised from -1°C to 30°C. Full standard activity is retained during this structural change, which could be related to the one postulated from kinetic studies.

202

CRYSTALLOGRAPHIC STUDIES OF MUNG BEAM TRYPSIN INHIBITOR AND ITS COMPLEXES WITH TRYPSIN

Guang-da Lin, Rong-guang Zhang, You-wei Yan, *Dong-cai Liang, Cheng-wu Chi, Wei-zhong Tang, Fu-long Tan, Tien-chin Tsao, Shanghai Institute of Biochemistry and *Institute of Biophysics, Chinese Academy of Sciences

Mung bean trypsin inhibitor has earlier been isolated, purified and the primary structure elucidated in Shanghai Institute of Biochemistry. It is a Bowman-Birk type inhibitor consisting of 72 amino acid residues. The structure can be cleaved into two active domains with Lys-Ser and Arg-Ser as the respective active center. This inhibitor has been crystallized in two crystalline forms. One is tetragonal with unit cell of symmetry P4₁22 (or P4₃22) and dimensions a = b = 49.2 Å, c = 158.1 Å, each asymmetric unit containing three molecules (n = 3). Another is orthorhombic with unit cell of symmetry P2₁2₁2 and dimensions a = 39.6 Å, b = 57.2 Å, c = 52.0 Å, n = 2. Two crystalline forms of the complex of this inhibitor with porcine trypsin at a molar ratio of 1 : 2 were obtained. One of them is tetragonal with unit cell symmetry I422 and dimensions a = b = 112.4 Å, c = 113.4 Å, n = 1. The crystal of the complex of Lys-Ser active domain with bovine trypsin is orthorhombic with unit cell of symmetry P2₁2₁2 and dimensions a = 62.9 Å, b = 63.4 Å, c = 69.7 Å, n = 1.

204

Thursday 02 August Congress Centre-First Floor Posters 205-210

Posters on Developments in Microscopy

205 ORAL PRESENTATION

HIGH RESOLUTION SLIT-SCAN ANALYSIS OF TWO PARAMETERS IN A FLOW CYTOMETER

H.-Ul. Meier and W.G. Eisert
Arbeitsgruppe Cytoometrie der Gesellschaft fuer Strahlen- und Umweltforschung
Herrnhäuser Str. 2, D - 3000 Hannover 21,
West Germany

A flow cytometric system taking up to 64 measurements along the axis of each individual cell in a scanning mode is introduced. Up to 15,000 particles per sec. orientated in a single file, pass an illuminating slit with dimensions of less than one by forty microns. Two independent parameters may be recorded simultaneously. Fluorescence light of two wavelengths, the axial light loss and the scattered light are accessible parameters at a time. Using fast photomultipliers and diodes, the ultrafast analog-to-digital conversion combined with high speed cache memories provides 64 digitized data per channel for each particle. Data are transferred into a minicomputer by direct memory access. Advantages and limitations of high speed slit scanning versus conventional flow cytometry are discussed using biological samples.

207

OPTICAL MICROSCOPY USING SCHLIEN TECHNIQUES OF DYNAMIC EFFECTS IN BIOLOGICAL AND MODEL CELLS

H. Colbeck, B.M. Blott, L.F. Braganza, D. Melville and F. Paul,
Department of Physics, Southampton University, Highfield,
Southampton, UK.

The microscopic examination of biological materials is conventionally performed either by fixing and staining cells, in order to develop contrast, or by using some form of interference optics. Such techniques are necessary because in general, biological components are not significant amplitude objects in aqueous solutions. Interference systems such as the Zernike phase contrast microscope or the Nomarski (polarizing) system can be expensive and complicated however and staining has the disadvantage of introducing changes into the biological material being studied.

We have developed a microscope system, which is straightforward to use, capable of observing time varying effects in a number of biological systems. The method is based on the Schlieren principle where phase gradient info is present in the object is converted into amplitude variations in the image plane. Of particular interest are morphological changes and/or orientation effects in synthetic lipid vesicles under the influence of magnetic field at various temperatures. Other applications of the technique have been the observation of red blood cell motion and the rupture of black lipid membranes.

209

X-RAY ANALYSIS OF CELL FLUID FROM STRIATED MUSCLE: CALCIUM AND MAGNESIUM. David Maughan, Department of Physiology & Biophysics, University of Vermont, Burlington, Vermont USA

Microsampling and X-ray spectroscopic methods were used to measure the freely diffusible fraction of total intracellular calcium and magnesium in freshly isolated frog semitendinosus muscles. Single fiber segments were manually skinned under oil and 0.2 nl droplets of isosmotic sucrose solution were placed on each fiber and allowed to equilibrate with the cell fluid. The time constant for the uptake of Ca was 10.1 min (prominent slow component); of Mg, 0.8 min. X-ray spectroscopic analysis of droplets from 11 relaxed fibers yielded mean extrapolated equilibrium values of 1.0 mM [Ca] and 5.8 mM [Mg]. X-ray spectroscopic analysis of whole muscle extracts yielded, after correction for extracellular fluid, 3.2 mM [Ca] and 13.8 mM [Mg]. Thus, about one-third of the total intracellular Ca and about one-half of the total intracellular Mg is freely diffusible and equilibrates with a microdrop. These diffusible fractions include the important regulatory ions Ca^{2+} and Mg^{2+} and their ionic complexes (mostly Ca-parvalbumin and Mg-ATP). Non-diffusible fractions include counterions restricted to the vicinity of fixed anionic charges on structural proteins and ions incorporated into fixed proteins and organelles. Supported by NBREM (Harvard), C. Lechene, Director.

206

LIGHT SCATTERING CHANGES ASSOCIATED WITH SECRETION AT THE NERVE TERMINALS OF A MAMMALIAN NEUROHYPOPHYSIS.

A.L. Olsaid, H. Gainer and B.M. Salzberg. University of Pennsylvania (Philadelphia) and N.I.H. (Bethesda), U.S.A.

We have found changes in the opacity of the unstained mouse (CD-1) neurohypophysis, following membrane potential changes known to trigger the release of peptide hormones. These optical signals, recorded without signal averaging as transmitted intensity changes in the image plane of a compound microscope, reflect variations in large angle light scattering rather than absorbance, as indicated by their very weak wavelength dependence. The magnitude of these signals depends upon the frequency of stimulation and the $[Ca^{2+}]_o$; it decreases in the presence of Ca^{2+} antagonists and it is enhanced by known secretagogues. These observations strongly suggest a correspondence between the optical changes and the secretory activity. Identification of the event(s) responsible for the opacity changes must await precise measurement of light scattering per se. However, the weak wavelength dependence of these signals contrasted with the strong wavelength dependence of the extrinsic absorption signal provided by linear potentiometric probes (e.g. merocyanines), permits one to monitor simultaneously, in a stained preparation, the secretory events and the local membrane potential changes that regulate them. Supported by USPHS grant NS 16824.

208

SURFACE ARCHITECTURE OF THE LARGE INTESTINE IN SUCKLING RATS. A SCANNING ELECTRON MICROSCOPIC STUDY

R. Šegović-Mihailović, Lj. Radunović, Dj. Polić, S. Susić, S. Osmanović and Lj. Ljumezi, Institute of Physiology, Faculty of Medicine, Belgrade, Yugoslavia.

The surface characteristics of the rat large intestinal mucosal epithelia within 15 days of suckling under postprandial condition and after fasting were studied by scanning electron microscopy. A wide range of variation in mucosal surface structure is seen in caecum, colon and rectum depending mostly on the age and sex of suckling rats. Some individual differences in surface patterns, probably due to the modeling activity of the muscularis mucosae is also observed. The most striking observation is the existence of villi in the colon during the first week of postnatal life which are not present later on. The fasting affects the size and shape of these villi and increases the loss of surface epithelial cells in all parts of the large intestine. Ultrastructural cytological analysis shows that in suckling rats the microvilli of absorptive cells are thinner and more closely packed than those in the adult animal. Besides the numerous goblet cells, the presence of tuft cells has been noticed, particularly in 15 days old rats.

210

MORPHOLOGY OF GASTROINTESTINAL CELL LOSS IN LACTATING AND SUCKLING RATS. A SCANNING ELECTRON MICROSCOPIC ANALYSIS

S. Susić, Dj. Polić, S. Osmanović, E. Ljumezi, Lj. Radunović and R. Šegović-Mihailović, Institute of Physiology, Faculty of Medicine, Belgrade, Yugoslavia.

The gastrointestinal mucosa (GIM) is characterized by high rates of surface epithelial cell/SEC/ loss. However, little is known about the detachment of SEC from epithelial sheet. We have used scanning electron microscopy to study the modes of cell loss from rat GIM within 15 days of lactation and suckling under postprandial condition and during 3 days of fasting. Our studies suggest that there are at least two distinct modes of cell loss from this mucosal epithelium: extrusion and degeneration in situ. In postprandial rats, both lactating and suckling, SEC loss occurred primarily via extrusion of individual cells and only rarely by degeneration in situ. Some differences in the intensity of extrusive process in different functional parts of GIM have been noticed. The influence of duration of lactation and age of suckling animals also has been observed. Exposure to fasting results in an increase in the incidence of extrusive cell loss and also in the incidence of degeneration in situ of isolated SEC or even groups of SEC, particularly after 3 days fasting.

Thursday 02 August Congress Centre-First Floor Posters 211-216

Posters on Developments in Microscopy

211

CRITERIA FOR IN SITU IDENTIFICATION OF PEPTIDE SYNTHESIS IN CELLS. G.C. Budd, B. Pansky, B. Cordell and A. Das, Medical College of Ohio, Toledo, OH 43699, U.S.A. and California Biotechnology, Inc., Palo Alto, CA 94303, U.S.A.

Immunocytochemistry is an accepted method for localizing intracellular peptides provided that the antisera are specific for the peptide in question. Localization may not, however, be synonymous with synthesis. Identification of sites of specific peptide synthesis requires attention to other criteria in addition to localization of antigenic determinants including: a) localization of mRNA *in situ* with a labeled cDNA probe that is specific for the peptide in question; b) synthesis of a specific labeled product in tissue culture by the cells of interest; c) identification of a specific clone in a cDNA library obtained from the cells or tissue of interest; d) sequence analysis of the specific cDNA clone or labeled peptide product. Using immunocytochemistry with anti insulin antisera we have localized inulin or insulin-like immunoreactivity in the brain, anterior pituitary cells and in cells of the retina. In addition we have localized specific radioactivity in the cytoplasm of certain anterior pituitary cells following *in situ* hybridization with P-32 and H-3 labeled rat insulin cDNA. These data, coupled with the observation that primary cultures of anterior pituitary cells, when provided with labeled amino acids, can synthesize a labeled peptide resembling insulin, provide evidence in accordance with the criteria outlined above, that insulin or a highly homologous peptide can be synthesized by anterior pituitary cells. Identification of a clone in a rat pituitary cDNA library and sequencing analysis, which are in progress, should provide definitive evidence.

213

OBJECTIVE ASSESSMENT OF CELLULAR PARAMETERS WITH THE AID OF COMPUTERIZED DIGITAL MICROSCOPY

P. Coltellì, P.A. Benedetti, V. Evangelista and P. Gualtieri, Istituto di Biofisica CNR Pisa (Italy)

The performance of instrumentation in the quantitative optical analysis of microscopical specimens is being progressively improved with the use of the computer and modern techniques for image acquisition and processing. A system is described, which performs various spectroscopical and structural measurement on living and fixed cells such as absorption and fluorescence spectrometry, studies of kinetics, optical density integration, morphometry, etc. The apparatus includes a moving-condenser scanning device, a photoarray detector and a chalnicon camera sensor for versatile data acquisition. High-efficiency detection of faint images and spectra is being introduced with the aid of electronic multichannel spectrometry. Spatial scanning and other relevant optical conditions are under computer control during the measurement. Application oriented programs drive the experiments and perform data processing, by means of specifically developed algorithms and display procedures.

215

212 ORAL PRESENTATION

FURTHER STUDIES OF URINARY BLADDER HEXAGONAL MEMBRANES FRACTURED AT NEAR LIQUID HELIUM TEMPERATURES.

J. David Robertson and Florence B. Stubbs, Duke University School of Medicine, Durham N.C., U.S.A.

Our laboratory has established that 120 Å globular particles seen in hexagonal arrays in the EF faces in the luminal membranes of mammalian urinary bladder membranes represent plastic deformation artifacts. (Robertson, J.D. and Vergara, J., 1980, J. Cell Biol. 86:514). The globular particle arrays are sometimes replaced by a smooth hexagonal pattern if fractured under liquid N₂. This led us to try fracturing in the low Kelvin temperature range using liquid He. We obtained specimens that, in some cases, displayed apparent EF patterns that were very much like previously observed external etch (ES) faces. These faces were almost exactly complementary to PF faces. We considered the possibility that they were in fact ES faces but rejected this on several grounds, including the fact that the replication was done under normally zero etch conditions. These findings were reported briefly (Proc. 10th Int. Cong. on Elec. Microsc., Hamburg, August 17-24, 1982.) Subsequent study of membranes labeled before fracture with TMV and of complementary replicas have convinced us that these faces previously interpreted as EF faces are, after all, external membrane surfaces. Supported by GM28224 and PCM 8113764.

214

216

Thursday 02 August Congress Centre-First Floor Posters 217-222

Posters on Image Reconstruction

217

STRUCTURAL ORGANIZATION OF PHAGE INFECTIONING APPARATUS

G.R. Ivanitsky, A.A. Deev, I.M. Edintsov, A.A. Khushainov, A.S. Kunisky, M.A. Tayganov, O.D. Veprintseva, Inst. of Biol. Physics, USSR Acad. Sci., Pushchino, USSR

Structural organization of basic elements of phage tail was studied using the methods of electron microscopy, diffraction analysis, optical and digital filtration and three-dimensional reconstruction. On the basis of diffraction analysis of the phage tail (phage H-17 *Bac.mycoides*) at extended and contracted states the difference in the parameters of helix package of the sheath subunits was revealed. Distribution of electron density of the structural sections determined by direct methods of three-dimensional reconstruction revealed the alterations in the form of the sheath subunits in the process of contraction. The analysis of abnormal (aberrant forms of T4 phage) showed that lack of modification of the protein gene product 12 as well as the bands of baseplate with a core induces the aberrant contraction. Structure and mechanism of infection of phages with uncontractile tail were studied on phage Mo-2 *Corynebacterium glutamicum*. Reconstruction of the platform and distal part of the baseplate of phage T4 in the intact, normally reorganized and aberrant forms elucidates the mechanism of its functioning.

219

LASER FOURIER IMAGING OF LIVING REACTION

Shozo Ishizaka and Toshiyuki Urano, Institute of Biological Sciences, University of Tsukuba, Ibaraki, Japan.

The chemical gradient about the structure in living system has been imaged by a specially designed Laser Fourier Transfer. The structural change, the diffusion of reactants and products, and also the diffusion of reaction heat fluctuate the electric susceptibility in the system. The distribution of the fluctuation diffracts the incident light of laser beam. Then, the chemical gradient about the bio-structure has been optically Fourier transferred to the diffraction pattern. In the Fourier domain on frequency and wave vector, the chemical gradient detected by the Laser Fourier Transfer has been simply algebraic correlated with the experimentally periodic stimulation. Although, in the pictorial time-space, the cause-effect relationship is complicated in the convolution of the stimulation. It is found that the Laser Fourier Transfer can be applied to the image processing on the living system. During chemical reaction, the diffusion of reactants and products, the diffusivity of reaction heat, and also the structural change can be analyzed by means of the relation between the phase shift and frequency, respectively.

221 ORAL PRESENTATION

IMAGE RECONSTRUCTION OF UNSTAINED FROZEN-HYDRATED MICROTUBULES. E.-M. Mandelkow and E. Mandelkow, Max-Planck-Institut für medizinische Forschung, Abt. Biophysik, D-6900 Heidelberg, FRG.

Microtubules rapidly frozen in vitreous ice have been studied by cryo-electron microscopy^{1,2}. Their structure is compared with that of negatively stained microtubules and X-ray specimens. Optical diffraction patterns of ice-embedded microtubules and X-ray patterns are consistent with each other, as are the reconstructions derived from them. In ice the resolution is limited to 2-3 nm because of low contrast and the small number of unit cells diffracting coherently. Partial denaturation leads first to a collapse of the cylindrical shape, later to loss of substructure, whereas with negatively stained specimens the substructure is reasonably well preserved in spite of flattening. Frozen-hydrated particles reveal a supertwist of period 5-6 nm, present in tubules with 13 or 14 protofilaments. Microtubules rapidly frozen during disassembly suggest that tubulin oligomers, in addition to subunits, break away from the ends. Moreover, disassembly may proceed from within the microtubules, indicating that the mechanism of endwise disassembly is not the only one possible.

Dubochet, J., Lepault, J., Freeman, R., Berriman, J. & Homo, J.-G. (1982). *J. Microsc.* 128, 219.
Milligan, R.A., Brisson, A. & Unwin, P.N.T. (1984). *Ultramicroscopy* 13, in press.

218

THE SIZE AND SHAPE OF THE HEMOGLOBIN OF MACROBDELLA DECORA. O. H. Kapp, A. V. Crewe, M. G. Mainwaring, and S. N. Vinogradov. * Enrico Fermi Institute, University of Chicago, Chicago, IL 60637 and #Department of Biochemistry, Wayne State University School of Medicine, Detroit, MI 48201.

The hemoglobin of the annelid leech *Macrobdella decora* was examined by SDS PAGE, gel filtration, and field emission scanning transmission electron microscopy (STEM). SDS PAGE of the unreduced hemoglobin shows it to possess one subunit of $M_r = 13$ Kd and three subunits of intermediate size ($M_r = 25,000 - 35,000$). This SDS PAGE pattern differs from the SDS PAGE patterns of most oligochaete and polychaete hemoglobins in that it contains no band corresponding to the generally ubiquitous 50,000 subunit. Negatively stained preparations of the hemoglobin were examined in the STEM operated in the dark field mode. The molecule displays the characteristic two-tiered hexagonal appearance found in other annelid extracellular hemoglobins. Dimensions of 310×205 Å were obtained from the computer summed and averaged images. Using an IBM 4341 and a program written in APL2 inexact 3D reconstruction was attempted using three orientations. The subsequent model corresponded closely in gross structure to a model of *Lumbricus* obtained using a similar algorithm. Supported in part by grants HL-25952 (to SNV) and from the Department of Energy (to AVC).

220

A NEW IMAGE PROCESSING SYSTEM FOR STEM IMAGES.

G. R. McNamara, O. H. Kapp, T. A. Barrett, P. E. Mooney, J. Ximen, and A. V. Crewe. Enrico Fermi Institute, University of Chicago, Chicago, IL.

We are developing a menu-driven image processing system for analysis of digital images from our existing STEM and for future use with our 0.5 Å STEM presently under construction. The system runs on an IBM 4341 mainframe (16 Mbytes RAM, 4 Gbytes disc) and employs a Mathews $\Omega 400$ display generator to provide high resolution (768 x 1024 pixels) black and white and color displays. This system, which is operated through a combination of mouse-driven cursor and command menus, presently incorporates routines for summing and averaging, fast Fourier and Walsh transforms, various filtering methods, correlation techniques, as well as a three-dimensional reconstruction algorithm⁽¹⁾ for biological objects. We have used this system to perform a stochastic 3D reconstruction of the giant hemoglobin of *Lumbricus terrestris* using only three projection orientations. The model suggests the presence of large gaps between adjacent 1/12th subunits of opposite tiers.

(1) A. V. Crewe and D. A. Crewe, *Ultramicroscopy*, (In Press). Supported by a grant from the Department of Energy. We thank IBM and Mathews Corporations for assistance.

222

A MODEL FITTING ALGORITHM.

Joan Aymami, Juan A. Subirana, Unidad de Química Macromolecular del CSIC, Barcelona, Spain and Joachim Frank, New York State Dept. of Health Albany, New York, USA

We have developed a method for fitting a mass or electron density distribution experimentally obtained with a model containing a given number of identical subunits. We feel this method may be of general interest in different areas of Structural Biology.

Essentially the method consists of minimizing the difference Fourier between the model and the experimental distribution using a least-squares method, with the three-dimensional shift components of the subunits as fitting parameters. We have written a program to solve this problem for a model consisting of spheres, which can be used within the SPIDER package of computer programs (Frank et al., *Ultramicroscopy* 6, 343, 1981) in the analysis of three-dimensional mass density distributions reconstructed from electron micrographs.

We have used this program with excellent results for determining the arrangement of nucleosomes consistent with a three-dimensional distribution of stain density which was obtained from a tilt series of electron micrographs of chromatin fibers.

Thursday 02 August Congress Centre-First Floor Posters 223-228

Posters on Image Reconstruction

223

STRUCTURE OF (Na⁺,K⁺)-ATPase DETERMINED BY ELECTRON MICROSCOPY AND IMAGE PROCESSING

H. Mohraz, C.A. Rinder, H.V. Simpson and P.R. Smith, Dept. of Cell Biology, NYU School of Medicine, New York, NY, USA

Membrane-bound (Na⁺,K⁺)-ATPase forms two-dimensional crystals in buffer solutions containing NaVO₃, Na₂VO₄ or K₂HPO₄. Two types of crystalline arrays have been observed. One form has an $\alpha\beta$ monomer ($a=5.9\text{nm}$, $b=5.6\text{nm}$, $\delta=70^\circ$), and the other an $(\alpha\beta)_2$ dimer ($a=16.1\text{nm}$, $b=5.5\text{nm}$, $\delta=66^\circ$) per unit cell. Computer-filtered images of negatively stained sheets show an asymmetrical mass distribution for the molecule consisting of a large 'body' with a less massive 'hook' extending from it. A limited digestion of the enzyme by trypsin leads to the cleavage of the α subunit into a membrane-bound fragment of 77,000 daltons. The digested enzyme has been crystallized ($a=5.6\text{nm}$, $b=4.3\text{nm}$, $\delta=66^\circ$) and the comparison of its mass distribution with that of the whole enzyme allows the identification of the α subunit with the 'body' region in the filtered image.

Work is in progress on the three-dimensional reconstruction of the mass distribution from tilted views of the crystalline arrays. Tilt series have been recorded from negatively stained sheets at tilt angles up to 60° . Preliminary results from the filtrations indicate that there is consistent recovery of high-resolution information up to the maximum tilt, allowing computation of the structure to a resolution of at least 22Å .

225

STRUCTURAL STUDIES ON CRYSTALLINE 50S RIBOSOMAL PARTICLES. K. Leonard(a), T. Arad(a), H.G. Wittmann(b) and A. Yonath(c)

(a)European Molecular Biology Laboratory (EMBL), Heidelberg (b) M.P.I. fuer Molekulare Genetik, Berlin-Dahlem, Germany (c)Weizmann Inst. for Science, Rehovot, Israel.

Several 3-D crystal forms for *B. stearothermophilus* 50S ribosomal particles have been obtained by vapour diffusion using organic solvents (1). Single crystal X-ray diffraction studies show that crystalline diffraction is present to at least 1.2nm . For these crystals, which are too large to study directly by electron microscopy, we have information at low-resolution on the 3-D structure and crystal packing from image analysis of epon-embedded thin sections (2).

Single-layer crystals of 50S ribosomal particles which can be visualised directly in the electron microscope have now been obtained. These are suitable for study by negative staining and, by optical diffraction, have a maximum resolution of about 3.0nm . The unit cell dimensions are $14.5 \pm 0.3\text{nm} \times 31.1 \pm 1.4\text{nm}$, $\gamma = 89 \pm 2.6^\circ$.

We have now carried out a 3-dimensional image reconstruction of these crystals by combining tilted images, including tilt angles to $\pm 60^\circ$. Features of the 3-D model can be identified with the low resolution surface structures which have been described previously for the 50S subunit. 1. Yonath A., Tesche B., Lorenz S., Mussig J., Erdmann V.A., Wittmann H.G., Febs Letters, (1983) 154,15-23. 2. Leonard K.R., Arad T., Tesche B., Erdmann V.A., Wittmann H.G., Yonath A., in "Electron Microscopy 1982", Int. Congress in Electron Microscopy, Hamburg, Vol. 3, 9-15.

227

STRUCTURE OF THE Ca²⁺ TRANSPORT ATPase OF SARCOPLASMIC RETICULUM IN THE PRESENCE OF VANADATE IONS, Kenneth Taylor¹, Laszlo Dux² and Anthony Martonosi³, Dept. Anat., Duke Univ. Med. Ctr., Durham, N.C. 27710; ¹Ingt. Biochem., Medical School, Univ. of Szeged, Hungary; ²Dept. Biochem., SUNY Upstate Medical Center, Syracuse, N.Y. 13210.

Crystalline tubules formed from skeletal muscle sarcoplasmic reticulum membranes after treatment with vanadate have been used to determine the structure of the Ca²⁺ transport ATPase. In projection the density map of crystalline tubules negatively stained with uranyl acetate and flattened onto a carbon support film, shows ribbons of Ca²⁺-ATPase dimers that form right-handed helical tracks around the surface of the cylinder. The projection symmetry is P2, establishing that the crystals are made up of dimers of the enzyme (J. Mol. Biol. 174, 193-204, 1984).

We have recently extended the projected structure to a 3-dimensional density map that shows primarily the cytoplasmic part of the molecule. No density was observed protruding into the luminal space of the cylinders, despite the accessibility of this region to negative stain. The Ca²⁺-ATPase molecules project 50-60Å above the cytoplasmic surface of the membrane bilayer. The bonding of Ca²⁺-ATPase molecules to form the dimer creates a bridge over a trough of negative stain on the cytoplasmic side of the membrane. The bonding of dimers into dimer-chains occurs through a lobe on the Ca²⁺-ATPase molecule extending along the "a" axis of the crystal. The center of this connection is located some 20-30 Å above the surface of the bilayer. This research was supported by NIH grants GM 30598, AM 26545 and grants from the MDA.

224

STRUCTURAL STUDIES OF 2-DIMENSIONAL CRYSTALS OF ALGAL CELL WALL GLYCOPROTEINS AND PHOTOSYSTEM II

P.J. Shaw, G.J. Hills and J.A. Kenwood, Department of Cell Biology, John Innes Institute, Colney Lane, Norwich, U.K.

The Volvocian green algae possess crystalline cell walls composed of hydroxyproline-rich glycoproteins similar to the primary cell wall glycoproteins of higher plants. Electron microscopy and computer image processing have been used to determine the crystal structure cell wall of *Chlorogonium elongatum* in three dimensions to a resolution of 2.0nm . The structure is composed of heterologous dimers. Each subunit of the dimer comprises a long, thin spacer domain and a large globular domain which is the site of the intra- and inter-dimer interactions. There are also sites of inter-subunit interactions at the opposite ends of the rod domains. We suggest that the rods are composed predominantly of glycosylated polyproline helix, as has been suggested for higher plant cell wall glycoproteins and has been shown for the cell wall glycoprotein of *Chlamydomonas reinhardtii*, which is closely related to *Chlorogonium*.

The barley mutant *viridis-2503* entirely lacks photosystem II. Regular arrays of particles, thought to be photosystem II are frequently seen in the grana of this mutant, and we are using image processing of negatively stained membranes to study the structure of these arrays.

(1) Hiller, R.G., Moller, B.L., Hoyer-Hansen, G. (1980). Carlsberg Res. Comm. 45, 315-328.

226

LASER FOURIER MOLPHOMETRY ON CELL SURFACE WITH MICRO SPHERES BOUND BY MEANS OF ANTIGEN-ANTIBODY REACTION TO SPECIFIC SITES.

T.Havashi, F.Igarashi, H.Masago and S.Ishizaka, Inst. of Biological Sciences, University of Tsukuba, Sakura-mura, Ibaragi, Japan.

It is a problem to detect distribution of the specific sites on the cell membrane that has too small number to find them fluorescently. Now it is reported that the distribution of highly refractive micro spheres of poly-styrene with the same size bound to the cell surface by means of the antigen-antibody reaction to specific sites should be measured. The distribution of micro spheres was illuminated in a plane parallel beam of LASER, the diffraction pattern of each micro sphere were concentric about optical axis. The difference of the incidental phase and scattered path length dependent on the position of each micro sphere causes to the interference fringes on diffraction pattern. The interference fringes were photographed and also computer-simulated. The orientation of each micro sphere extracted from the center of interference fringes, and the distance between each micro sphere obtained from a interval of the interference fringes. It is found that the distribution of specific sites on cell surface could be measured by LASER Fourier Molphometry on the spacing of micro spheres bound by mean of the antigen-antibody reaction.

228

COMPUTER AVERAGING OF E. COLI 70S MONOSOMES

A. Verschoor, J. Frank, and T. Wagenknecht, Center for Laboratories and Research, New York State Department of Health, Albany, NY 12201 USA.

Although the 70S monosome is essentially globular, one projection (or narrow range of projections) seen in electron micrographs, the overlap view, is amenable to image averaging, due to its distinctive features and the more or less stable position of the particle on the grid. 100 individual overlap images obtained from 5 micrographs (0.5% UA stain, single-carbon preparation) were aligned using correlation techniques. Because of the variability in the precise angle of view, the aligned images were grouped by multivariate statistical analysis, and averaging was done only over more homogeneous subsets.

The averages clearly showed the characteristic features of the overlap view: the main, strongly stain-excluding portion of the projected particle corresponds to the 30S subunit lying in a slanted position (that we previously [1] termed the broad view) directly against the grid. The 50S subunit fits on top of it, on the side facing away from the grid. Because the staining is (intentionally) one-sided, most of the 50S subunit is not contrasted and is thus 'invisible'; typically its L7/L12 stalk and portions of its head and the edge of the body below the stalk can be seen.

Supported by NIH grant 1 R01 GM 29169.

Reference

1. A.Verschoor et al. (1983) Proc. 41 Ann. Mtr. ENSA pp 758-9

Thursday 02 August Congress Centre-First Floor Posters 229-234

Posters on Image Reconstruction

229 ORAL PRESENTATION

PROPOSAL OF THE NEW MODE OF ACTIN-MYOSIN INTERACTION AND THE MYOSIN BINDING SITES ON THE MUSCLE THIN FILAMENTS
T. Wakabayashi, C. Toyoshima, A. Tomiooka and M. Tokunaga,
Department of Physics, Faculty of Science, University of Tokyo, Bunkyo-ku, Tokyo 113, Japan.

Localization of actin monomer in the thin filament decorated with myosin S1 was determined by comparing the improved three-dimensional image reconstituted from the electron micrographs of actin-tropomyosin-troponin-Ca filaments which are straight over the stretch of about 4,000 Å and compared with that of actin-tropomyosin-myosin S1 complex. The resolution of the former became about 15 Å both in axial and radial direction and is comparable with that of the latter. This improvement made it easier and more unambiguous to interpret the model of actin-tropomyosin-S1. It was shown that both A and B domains (defined in ref.1) are a part of the thin filament. Detailed similarity of the density distribution, especially the existence of the low density region in the middle of actin monomer in both models, supports this new interpretation. S1 binds mainly to the upper right half of the outer side of actin monomer shown in the Plate VII(b) or in the bottom of the Plate VI(a) of ref.2, though the strongest interaction seems to occur at the middle of the outer side of actin monomer. This interpretation also shows that the z-band direction is upward in the Plate VI(a) of ref.2. It is interesting that the subdomain B2 (defined in ref.3) can be interpreted as tropomyosin. Since this subdomain seems to interact with the tip of myosin S1, actin-myosin interaction can be sensitive to the position of tropomyosin.

REFERENCES (1) Wakabayashi & Toyoshima (1981) J. Biochem. 90, 697. (2) Wakabayashi et al. (1975) J. Mol. Biol. 93, 477. (3) Wakabayashi et al. (1983) ACTIN: Structure and Function in Muscle and Non-Muscle Cells, pp.27, Academic Press.

231

STRUCTURAL COMPARISON OF NATIVE AND LIPID-DEPLETED PURPLE MEMBRANE R.M. Glaeser, J. Jubb and R. Henderson, MRC Lab. of Molecular Biology, Hills Road, Cambridge, U.K.

Electron diffraction and high resolution (low dose) imaging have been used to obtain the projected structure of purple membrane after partial removal of lipids by extraction with 5 to 10 percent sodium deoxycholate (DOC). DOC extraction results in a shrinkage of the lattice of glucose embedded purple membrane from 62.4 Å to 57.3 Å. Only a very small change occurs in the visible absorption spectrum, but there are large changes in the diffraction spot intensities. Comparison of the Fourier maps of native and DOC-extracted membranes shows that the structure of the protein monomers and of the protein-protein contacts within trimers is not measurably altered after lipid depletion. The decrease in lattice parameter is accounted for completely by removal of a boundary layer of lipid (between trimers) which is one molecule wide. The positions of two remaining pairs of lipid molecules (i.e. four moles of lipid per mole of bR) are clearly shown in the map of DOC-extracted purple membrane. A comparison of the native and DOC-extracted structures suggests that at least part of the boundary layer of lipid in the native membrane must be crystallographically ordered, since long range order is established across a protein-lipid-protein interface and there are no protein-protein contacts between trimers. However, the positions of ordered lipid molecules within the native membrane cannot be assigned uniquely, unlike the case of the DOC-extracted membrane.

233

230

Electron Microscopy of DNA Binding Proteins. W. Chiu, H. A. Cohen, R. A. Grant, M. F. Schmid, I. W. Jeng, and D. Rankert, Dept. of Biochemistry and Dept. of Molecular and Cellular Biology, Univ. of Arizona, Tucson, AZ 85721.

We have studied the 3-dimensional structure of T4 DNA helix destabilizing protein (gp32*1) and of RecA protein by electron microscopy coupled with computer processing techniques. Gp32*1 binds cooperatively to single stranded DNA and can substitute for gp32 in an in vitro replication system. Gp32*1 crystallizes as thin platelets at low ionic strength. The low resolution 3-D reconstruction of gp32*1 crystal shows the molecule to have an elongated shape with an axial ratio of 4:1. We have made a tentative assignment of the domain of the molecule that binds to single stranded DNA. The projected density map of ice embedded gp32*1 crystal shows details beyond 0.8 nm with an average figure of merit in phases of 0.8. The interpretation of this map requires a complete determination of its 3D structure. RecA protein has a DNA-dependent ATPase activity and is involved in recombination in *E. coli*. RecA is associated with a protease activity which cleaves the LexA repressor, allowing expression of the SOS genes involved in DNA repair in *E. coli*. RecA protein tends to form helical filaments under proper buffer conditions in the presence of ATP/S. We have determined the helical parameters of this specimen and are completing a low resolution 3-D reconstruction of this filament. A more detailed structure of the RecA monomer requires microscope data to higher resolution.

232

234

Thursday 02 August Congress Centre-First Floor Posters 235-240

Posters on Processing and Control of Visual Information

235 ORAL PRESENTATION

CIRCADIAN RHYTHM GENERATION IN A NEURAL NETWORK CONTROLLED BY ENVIRONMENTAL CYCLE: Shuji Endo, Department of Technology, Fukuoka University of Education, Munakata-shi, Fukuoka-ken, Japan, Yohsuke Kinouchi and Tsuyuki Ushita, Faculty of Engineering, Tokushima University, Tokushima-shi, Japan.

It is well known that the life body has a rhythm of about 24-hours in period, i.e., circadian rhythm. Since the rhythm keeps its period constant under the the environment of no time cue and has the property of re-entrainment, it is considered as an endogenous and autonomous rhythm.

Biological and mathematical models have been proposed to analyze the mechanical of circadian rhythm generation. However, they have some difficulties such as too short period and no corresponding real organization.

In recent neurophysiological research, the neural population, e.g., the lobe, the pineal gland and the suprachiasmatic nucleus, has been found as a pacemaker of circadian rhythm. Therefore a neural network model which is able to generate circadian rhythm under the control of periodic environment is proposed.

Analysis and computer simulation show that the model has some important properties of circadian rhythm such as entrainment to the periodic environment and operation following the Aschoff's rule.

236 ORAL PRESENTATION

A POSSIBLE MATHEMATICAL MODEL OF VISUAL PROCESSING OF VISUAL INFORMATION

Wang Yun-liu and Fan Zho-hua, Inst. of Biophysics, Academia Sinica, Peking, China.

If visual system is considered as a system of processing image information, the kernel function plays important role in describing this system. We suggest that two-dimension Gabor functions are suitable for mathematical expression of image early processing system in vision. Gabor functions can take two forms. One is in polar coordinate:

$$G(r) = A \cos(2\pi r \theta) \exp(-(r/\sigma)^2)$$

Another is in Descartes coordinate:

$$G(x, y) = A \cos(2\pi f_1 x + \theta_1) \cos(2\pi f_2 y + \theta_2) \exp(-(x/\sigma_1)^2 - (y/\sigma_2)^2)$$

In the case of kernel function getting first form $G(r)$, Kuffler's and other's on-, off-center RF and multi annulate RF can be represented qualitatively. In the second form, when parameters of $G(x, y)$ are selected properly, Hubel-Miesel's RF and some others can be represented. Furthermore, considering the temporal factor of the visual system, the results simulated with this model are consistent with responses of single cell in visual system to moving patterns.

237

FRAME FOR A THEORY OF ELECTRICAL SIGNAL PROCESSING IN VERTEBRATE RETINA. R. Moreno Diaz, Dep. of Cybernetics, Univ. College and Univ. Politécnica, P.O. BOX 550 Las Palmas de Gran Canaria, Canary Islands, Spain.

Only recorded electrical signals are considered to be the substrate of information processing and communication of retinal cells; a low level code based on the shape of slow potentials and/or the instantaneous frequency of firing is assumed. According to the proposed frame, the retina is considered as a layered processor. Outer layers (horizontal, bipolar and outer amacrine cells) provide with variously delayed and laterally translated versions of the signals given by photoreceptors. Nonlinearities are assumed to be local at these stages. The resulting signals generate an "space-time" input space to inner layers, where ganglia sample the information directly or via amacrine cells. Processing there takes place according to a generalization of the centre-periphery structure, where centre and periphery correspond to volumes, concentric or not, within the input space. Processing in each volume can be assumed to be quasi-linear, whereas the interaction between signals from the volumes follows a nonlinear or even an algorithmic rule. When the action of peripheral volumes is low, simple behaviour of retinal ganglia results. Specialization and colour coding, even in the cases of very high specialization (i.e. frog's retina) are then consequences of said interaction.

238

AMPLITUDE OF CONSECUTIVE VEPs ACCORDING TO THE INTERVAL OF TIME BETWEEN STIMULUS. Díaz-Calavia E.J., David-Hilner M.S. and Fernandez del Moral R. Dept. of Biophysics, Fac. of Medicine, Universidad de Navarra, SPAIN.

Adult cats with chronic electrodes implanted in area 17 were used.

We studied VEP using two identical consecutive flashes. The relationship between the amplitude of the two VEPs and the interval of time between the two stimulus was analyzed.

Being
 A_2 = Amplitude 2nd VEP
 A_1 = Amplitude 1st VEP
 We found that the relationship

$$\left(\frac{A_2}{A_1} \right) \text{ follows the next equation: } \left(\frac{A_2}{A_1} \right) b^{-t} = c$$

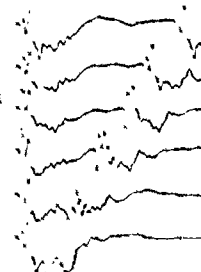
$$r = 0.99; p > 0.99$$

b and c are constants

t = time in ms

b, c such that

$$A_2 \neq A_1 \text{ for } t > 0.8 \text{ s.}$$



239

KINETIC ANALYSIS OF THE PHOTOCONVERSION PROCESSES IN VISUAL PIGMENTS BY PICOSECOND SPECTROSCOPY. J.M. Puchert, R.R. Alfano, Institute of Physics, A.Mickiewicz University, Poznań, Poland, Institute for Ultrafast Spectroscopy and Lasers, City College of New York, USA.

Absorption and fluorescence relaxation kinetics from squid rhodopsin and 7-membered artificial visual pigment were studied with single picosecond pulse excitation. The transition of rhodopsin to bathorhodopsin occurs on the picosecond time scale and is found to form after rhodopsin or isorhodopsin photolysis within the time resolution /about 6 ps/ of the equipment at room temperature with apparently parallel bathorhodopsin production. Kinetic analysis indicated not only that the 11-cis to trans isomerization of the retinal moiety is a crucial primary event in the photolysis of rhodopsin but is also established that this isomerization must occur on the picosecond time scale or faster.

240

Thursday 02 August Congress Centre-First Floor. Posters 241-246

Posters on Environmental Biophysics

241

EFFECTS OF ZINC IONS ON THE NEUROMUSCULAR TRANSMISSION IN FETUS, NEONATUS AND ADULT ANIMALS
 Marija Keser-Stanković, D. Stanković and M. Nekeš
 Institute of Physiology and Pathophysiology, Medical Faculty University of Sarajevo, Yugoslavia.
 Investigations of the effects of Zn^{2+} on neuromuscular transmission in fetuses, neonates and adult mice, rats and guinea-pigs were done. As a convenient model system the isolated innervated organs stomach, esophagus, urinary bladder and ductus deferens were used. Electrical stimulations were performed by means of HSE Stimulator II using the pulses of 5-10 mA and 1 msec at 10-20 Hz each minute. Recording microdynamometer 7050 have been used for muscle contraction registrations. Results have shown that application of Zinc ions at 10^{-6} mol and higher concentrations causes the reversible increased response to the nerve stimulation in fetus stomach and urinary bladder, while in neonates at the same concentration it induces reversible inhibition of the transmission in esophagus and urinary bladder, and in stomach it induces increased contractions and turgor at 10^{-6} mol. In adult animals the effects of Zn^{2+} at 10^{-6} mol as temporary increased responses to the stimulation in all four organs used. There were no differences in type of reaction between different species.
 The study was financially supported by Republican Research Council Grant.

243

EFFECTS OF LOW-INTENSITY MILLIMETER WAVE RADIATION ON BIOLOGICAL SYSTEMS
 F. Kremer, C. Koschnitzke, A. Poglitsch, L. Santo, P. Quick, D. Sperber, L. Genzel, Max-Planck-Institut für Festkörperforschung, Stuttgart, Fed. Rep. Germany
 Our previous observation of a non-thermal influence of mm-wave radiation on the puffing of giant chromosomes of the midge *Acutopus lucidus* is now extended on the frequency range between 40 GHz and 80 GHz (power density ≤ 6 mW/cm²). The effect is manifested as a reduction in size of a specific puff that expresses genes for a secretory protein. The experiments were carried out blind and the effect could be established to a level of significance of $P \leq 0.5\%$.
 In another set of experiments, roots of cress seedlings were irradiated. The root growth was measured with a computer controlled optical system, capable of continuously measuring the position of the growing roots with an accuracy of $\pm 5 \mu m$. Irradiating the roots at $24 \pm 0.5^\circ C$ with mm-waves of a power density as low as 2 mW/cm² resulted in a 30% decline of the growth rate within 2 min. The microwave-induced temperature increase was less than $0.2^\circ C$. The effect strongly depends on the polarization of the microwaves. In additional experiments the seedlings were irradiated with infrared radiation (wavelength: $> 2 \mu m$). A similar decrease of the growth rate was found. This indicates that the observed effects are of thermal origin although the irradiation-induced temperature increase is small on a physiological scale.

245

THE EFFECT OF TEMPERATURE ON THE ELECTRICAL POTENTIAL DIFFERENCE ACROSS THE GASTRIC MUCOSA IN EVISCERATED RAT STOMACH
 A. Szlachetka, A. Frączek, Department of Biophysics, Medical Academy, Kraków, Poland.
 The electrical potential difference (PD) between the inner and the outer sides of gastric wall is maintained by electrogenic ionic pumps responsible for the ionic concentrations gradients across the mucosa. The lumen of the stomach is always negatively charged. Any agent affecting distribution of ions changes value of PD. The aim of our studies was to explain the influence of stomach temperature on PD. The experiments were performed in anesthetized rats. The eviscerated stomach was dipped in physiological saline which was cooled after every 60 min gradually by 5 deg from 35 to $15^\circ C$. The initial value of PD at $35^\circ C$ was 32.3 ± 1.2 mV. After each change of temperature PD stabilized on a new, lower level within about 50 min. The final value of PD at $15^\circ C$ was 15.9 ± 1.2 mV. All changes of PD were statistically significant. For the investigated range of temperature a linear relation between PD and temperature was obtained and it might be described by the equation:
 $PD = 0.5 + 1.044 \cdot t$, t - temperature in $^\circ C$; correlation coefficient $r = 0.999$. The changes of PD upon temperature were reversible. The direct elevation of temperature from $15^\circ C$ to $35^\circ C$ resulted in reversal increase of PD to its initial value. The obtained results suggest that decreasing yield of active transport in lower temperature is the main factor responsible for observed effects.

242

PARTIAL SUPPRESSION OF UV-SENSITIVITY BY PLASMIDS IN HAEMOPHILUS INFLUENZAE
 R.P. Kanade and N.K. Notani, Biology and Agriculture Division, Bhabha Atomic Research Centre, Bombay-400085, India.
 Plasmid RSP0885 and a chimeric plasmid-pd7 (consisting of RSP0885 and a splice of *H. influenzae* chromosomal DNA) are shown to suppress UV-sensitivity of several strains of *H. influenzae* containing them. On the other hand, pJ1-8, a plasmid derived from pd7 but which has suffered a spontaneous deletion in a region of RSP0885 does not ameliorate the UV-sensitivity of these strains. A chimeric plasmid pJ1-8N19 consisting of pJ1-8 and a splice of chromosomal DNA bearing *nov*^r (novobiocin-resistance) marker also does not confer any resistance on the host-strain. Only in a recombination-deficient strain *rec*⁻, both groups of plasmids impart some additional resistance. Higher survival, however, is unaccompanied by any significant increase in mutagenicity by UV irradiation. Plasmids isolated from UV-irradiated cells harboring pd7 or pJ1-8N19 and plated for genetic transformation showed that pd7 is repaired to a considerable extent regardless of the host strain but pJ1-8N19 is repaired efficiently only in excision-proficient strains.

244

BIOLOGICAL INFORMATION AND COMMUNICATION SYSTEM MODEL OF ECOSYSTEMS
 Masahiro Tanaka, Department of Physics, Osaka Medical College, Takatsuki, Osaka 569, JAPAN

What is information for living organisms? An answer to this question is given on a physical basis and a contrast between genetic information and sensory information is stressed with a relation to information theory. A simple model of environments of living organisms is investigated on the basis of communication system model proposed by the author and a cost of information transmission is taken into consideration through capacity-cost theory. It is shown that channel capacity of information theory can be interpreted as an environmental index measuring a mildness of the environment, and furthermore that a large diversity of genetic information needs a large capacity of the environment. In addition, a definition of life in terms of information is proposed and a unified view on life processes is suggested.

246

BIOLOGICAL EFFECTS OF DISTURBED GEOMAGNETIC FIELD
 D.M. Mikhov, Institute of Neurology, Psychiatry and Neurosurgery, Sofia, Bulgaria.
 For a period of six consecutive years 1968-1973 we studied the effects of the geomagnetic disturbances on the death-rate in persons with cerebrovascular disease and ischemic heart disease, in children up to the age of 1 year and adults above 80, in persons with stomach cancer and in persons with childbirth injuries and difficult labour. It was made an attempt to evaluate the influence of the various geomagnetic variations over the mortality. For that purpose we used a method of the least squares, the Gauss method for solution of large system of linear equations and a heuristic method. For the first time, it was discovered that the various geomagnetic variations have a diverse biological significance. It turned out that the dependence between the different geomagnetic fluctuations and the biological effect has a resonance character. However, the geomagnetic disturbances standing in the middle of the range of all geomagnetic variations exert a biological influence which is much more considerable in comparison with the effect of the adjacent slower or quicker changes of the geomagnetic field.

Thursday 02 August Congress Centre-First Floor Posters 247-252

Posters on Environmental Biophysics

247

HUMAN BLADDER: A PRELIMINARY STUDY ON VISCOELASTICITY AND ON STRUCTURAL ORGANIZATION OF MACROMOLECULAR COMPONENTS.

G. Albertini*, A. Bigli*, S. Melone*, G. Mazzonigro*, M. Polito*, A. Ripasanti*, M. Roveri*, F. Rustichelli*

- * Istituto di Fisica Medica - Università di Ancona - Italy
- * Istituto Chimico - Università di Bologna - Italy
- * Istituto di Patologia dell'Apparato Urinario - Università di Ancona - Italy
- * Dipart. Scienze Materiali e Terra - Univ. di Ancona - Italy

Visco-elastic properties of human bladder are studied from a theoretical and an experimental point of view. Experimentally, cystometric measurement are performed on human bladders. From a theoretical point of view a biophysical model is developed, based on Maxwell and Hooke elements, in order to evaluate the data of the cystometric measurement. The structural organization in the bladder of various macromolecular components of interstitial and fibrocellular nature is also investigated by X-ray diffraction techniques, in order to derive a correlation between viscoelasticity and structure. In particular the preliminary results are presented on collagen fibre distribution and orientation in the bladder wall.

249

INFLUENCE OF ALUMINUM ON PRIMARY MAIZE ROOTS

V. Lazić, V. Furtula, M. Denić, Č. Radenović
Maize Research Institute "Zemun Polje" Belgrade
1) Institute of physical chemistry, faculty of science, Belgrade.

Growth of plants on acid soils is often reduced owing to the toxic effect of high aluminium concentrations. We have investigated the effect of Al on the growth of primary maize roots. Al content in the root of two genotypes different in response to Al, possible influence of Al on the plasma membrane ATP-ase activity and protein profiles of plasma membrane fractions of these genotypes. It was shown that Al reduces root growth of some investigated genotypes. There is no correlation between Al content in the root and the effect on root growth. ATP-ase activity in plasma membranes from roots grown in media with Al was 16% lower in comparison with control plants. Electrophoretic analysis of protein solubilized from isolated membranes from treated and control plants have shown variation in polypeptide composition.

251

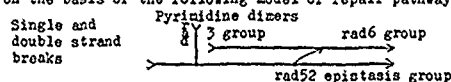
VARIATIONS IN UV AND BLEOMYCIN SENSITIVITY IN AGED CULTURES OF YEAST. E. Nunes, L. Candrova, D. Keszenman, S. Calvo and E. Barrios. Dept. Biophysics. Sch. Med. Montevideo - URUGUAY.

Diploid *Saccharomyces cerevisiae* populations at the stationary phase of growth were submitted to different incubation periods in YED under different concentrations of α -tocopherol and their UV and bleomycin sensitivities, survival fractions and repair abilities were measured. Following are the main observations: 1) Intermediate incubation periods (30-60 days): 1.1-A continuous increase in UV and bleomycin sensitivities as measured by survival curves with a decrease in the mean lethal dose and in repair abilities which become similar to that of the rad 6 sensitive mutants. 1.2-In the presence of α -tocopherol in the incubation medium (15-30 μ g/ml⁻¹), the radio resistance is similar to that of early stationary cells. 1.3-The exposure to UV light plus bleomycin determines a SOS survival curve type, that indicates the selection of an inducible type of DNA repair. 2) For very long incubation periods (500-600 days): massive mutation of survivors with very high UV and bleomycin resistance. These findings are consistent with the three main theories of aging processes at the cellular level, namely: decrease of repair abilities (1.1), stochastic free radical damage (1.2) and error catastrophe in the transmission of genetic information (2).

248

EFFECT OF BLEOMYCIN ON RADIATION SENSITIVE HAPLOID MUTANTS OF *SACCHAROMYCES CEREVISIAE*. D. Keszenman and E. Nunes, Dept. Biophysics. Sch. Med. Montevideo. URUGUAY.

The effect of Bleomycin, an antitumor antibiotic, which causes single and double strand breaks in DNA, on the kinetics of population growth and on survival curves of haploid wild type and radiosensitive strains of *S. cerevisiae* was analysed. Strains N123 (wild type), rad3, rad18 and rad52 were used. Growth kinetics is significantly modified by the drug added at 7.5 μ g/ml to YED batch cultures of the four strains at 30°C, being rad52 the most sensitive one, showing no proliferation. Survival curves to different Bleomycin concentrations (0.75-45 μ g/ml) of these strains exhibit two components and they can be described by the following mathematical model: $S = A(\exp(-C/C_0)) + [1 - (1 - \exp(-C/C_0))]^N$, where S: survival fraction, C: Bleomycin concentration, C_0 , C_{01} , C_{02} and N: sensitivity parameters of the two components, A: fraction of cells without Bleomycin and ρ : the probability of DNA repair. Under our experimental conditions mutations of rad18 and rad52 genes determine slightly changes in the shape of survival curves. The rad3 mutant has wild type resistance. Taking into account the effect of Bleomycin at the molecular level and previous results on the UV and X-rays sensitivity of yeast, we discuss results on the basis of the following model of repair pathways.



250

MEMBRANE EFFECT OF HEAVY METALS IN MOLLUSCAN CNS

J. Salánki and Katalin S.-Róssa, Balaton Limnological Research Institute of the Hungarian Academy of Sciences, H-8237 Tihany, Hungary

Environmental pollution with heavy metals causes damage of living functions in animals. Investigations carried out in acute and chronic experiments on central neurons of the pond snail *Lymnaea stagnalis* and land snail *Helix pomatia* revealed that various heavy metals (Hg, Cd, Cu, Pb) influence differently both resting and action potential generation and the responsiveness of neuronal membranes to bioactive substances (acetylcholine, serotonin, dopamine). Selective blocking effect of some metal ions can be interpreted on the basis of specificity of postsynaptic receptor structures responsible for the transmitter action and/or of ion channels involved in the excitatory processes. The heavy metal effect was not uniform on different type of neurones, suggesting that pollutants can modify various functions in a different degree. The results show that testing on nerve cell membranes can serve as a useful method and model in investigating the effect of sublethal environmental contamination.

252

ENTROPY BUDGETS OF PLANT LEAVES

I. Aoki, Department of Physics, Osaka Medical School, Takatsuki-shi, Osaka, Japan.

Entropy flows into or out of leaves due to (1) solar radiation, (2) infrared radiation, (3) convection and (4) transpiration are theoretically calculated based on the values of corresponding energy flows. Net entropy flow into leaves becomes non-positive. On the assumption that entropy in leaves is in a steady state, the amount of the entropy production in leaves is given and turns out to be non-negative. Non-negativity of the entropy production in leaves shows that the Second Law of Thermodynamics is certainly valid in plant leaves. The entropy productions on nights become zero irrespective of leaf orientation in nyctinastic leaves and of leaf temperatures. The entropy production is a linear function of the solar energy absorbed by plant surface through the origin. Degree of the linearity for deciduous leaves is same as that for conifer branches. The linearity of the entropy production on the absorbed solar energy suggests that the entropy production in leaves will be almost due to biochemical reactions of substances engaged in photosynthesis or due to those induced by onset of photosynthesis.

Thursday 02 August Congress Centre-First Floor Posters 253-258

Posters on Environmental Biophysics

253

SPECTROSCOPIC STUDY OF POLLUTANTS IN THE ENVIRONMENT OF SOME EGYPTIAN FACTORIES

F.M. Abdel Kerim, M.A. Moharram and N. Abdel Hakim, Spectroscopy Lab., National Research Centre, Cairo, Egypt.

This work includes estimation of organic and inorganic compounds present in three types of trade wastes. These wastes are textile and dyeing wastes; soaps, insecticides and fertilizer mixed wastes; electronic and metal wastes. The spectroscopic techniques used were ultraviolet and infrared absorption spectrophotometry. It was concluded that textile and dyeing wastes consist mainly of diazophenol phenyl cyanide, chromium amine complexes, sulphate, carbonate and silicate compounds. The mixed wastes contain aliphatic hydrocarbon, nitrate, carbonate and phosphate. Electronic and metal wastes contain sulphonamide, oxalate, zinc and chromium nitrate and carbonate.

254

TECHNOGENIC CONTAMINATION OF SOIL AND PLANTS BY WASTE WATER FROM KAHKHA CHEMICAL FACTORY (EGYPT).

Fakhry A.A., Basily A.B., Higazy H.E. & El-Anany F.A. (NRC)

Results of atomic emission and absorption spectroscopic analyses for more than 20 elements in samples of waste water soil and plant (*Eichhornia Crassipes*) collected from places adjacent to the drainage pipeline terminal of KAHKHA Chemical Factory are discussed. The samples were collected in such a sequence so that they represent an artificially man-made biogeochemical cycle. The result of analyses figures out the appearance of conspicuously high anomalous concentrations for most of the elements under investigation in both soil and plant samples. On the other hand, the content of these elements in water samples down-stream was found to be noticeably lower. The elements distribution shows a remarkably sharp decrease with distance away from the source of contamination. This presumably indicates the presence of these elements mostly in the form of weakly mobile compounds which are readily under the new prevailing physicochemical conditions of the drainage canal-either deposited on soil or absorbed gradually by plants growing in the vicinity of the pipe-line terminal. This distribution pattern reveals the presence of a highly contaminated but fortunately rather limited area around the mouth of the pipeline terminal, thanks to the low mobility of the compounds and the absorbing ability of the plant (*Eichhornia Crassipes*).

255

ESR MODEL OF RESONANT MICROWAVE BIOLOGICAL EFFECTS

F. Keilmann

Max-Planck-Institut für Festkörperforschung, 7 Stuttgart 80 Fed. Rep. Germany

Sharp resonances in a yet unexplained nonthermal biological sensitivity to microwaves have recently been demonstrated [1]. In this experiment the growth rate of yeast cultures is studied under the influence of weak millimeter wave irradiation. The results prove weak effects (10%) at fixed frequencies (e.g. 41782 MHz) with a saturation behaviour characterized by low intensity thresholds (1 mW/cm²).

Here I discuss a model for explaining these effects by resonant pumping of magnetic sublevels in triplet molecules. The model requires (i) the existence of molecules with relatively large zero-field-splitting matching the resonance, (ii) the existence of a nonthermal population and (iii) a sublevel-selective chemical reactivity in these molecules.

[1] W. Grundler and F. Keilmann, Phys. Rev. Lett. **51**, 1214 (1983).

256

ISOLATION AND IDENTIFICATION THE STRUCTURE OF FLAVONOID GLYCOSIDES IN SALVIA TRILOBA PLANTS.

Y. Ghali, S. Gabr, N. Saleh and A. Abu-Fyta, Department of Biochemistry, Faculty of Agriculture, Zagazig University, Zagazig, Egypt.

Salvia triloba is grown in Egypt as a desert wild plant. The ethanolic extract of the plant was subjected to fractionation on the polyamide column. The fractions were detected on the column using the U.V. light. Each fraction was reprecipitated for purification, and the resulted pure compounds were affected separately by several tools to confirm the structure of these glycosides and their corresponding aglycones. Ultraviolet spectrum and mass spectrum analysis were used for detecting the structure of each pure isolated glycoside and its aglycone. Also, the methods of demethylation, acid and enzymatic hydrolysis were used. The alkaline fusion of glycoside was carried for identification of the phenolics and phenol carboxylic acids. Alkaline hydrogen peroxide oxidation of glycosides was used in order to split the sugar molecule from p-cumaric acid. Fourteen flavonoid glycosides were isolated and identified from the aerial part of *Salvia triloba* L. fil (labiatea) plants. These glycosides concluded different derivatives of apigenin, luteolin and chryseriol.

257

EFFECTS OF MANGANESE IONS ON THE BIOELECTRICAL ACTIVITY OF ISOLATED NERVES

M. Hakeš, A. Janakosmanović, M. Kaser-Stanković and M. Drecun, Institute of Physiology and Biochemistry Medical Faculty University of Sarajevo Yugoslavia

Investigations of the effects of Manganese ions on threshold excitation and compound action potential of isolated frog sciatic nerve were performed. Experiments were performed in two groups of isolated nerves. In the first series isolated nerves were exposed to the action of 5 mmol Mn²⁺ for 30 minutes, while the second one served as control. Being extracellular recording technique measurements were made just before and immediately after the exposure to Manganese ions, and after six successive time intervals following transference of the nerves into saline again during experimental period of 120 minutes. Results have shown that Manganese ions induce significant increase of the threshold voltage, while the changes in latency, amplitude and duration of the compound action potential were not significant.

(The study was financially supported by the Republican Research Council Grant)

258

EFFECTS OF DIFFERENT REPETITION RATE AND PULSE WIDTH ON THE LEVEL OF SEROTONIN IN RAT BRAIN AFTER WING REVEALED 2450 MHz MICROWAVE IRRADIATION

A. Janakosmanović, A. Javrić, M. Hakeš, and M. Drecun, Institute of Physiology and Biochemistry Medical Faculty University of Sarajevo, Yugoslavia

Albino 6 days old rats were exposed to either 100 cycles/s and pulse width 2 microsec or 200 cycles/s and pulse width 1 microsec of 2450 MHz microwave irradiation in a waveguide system. After 14 days Pulse Signal Source Model 40K as a source of irradiation was used. Control of repetition rate and pulse width was continuously performed by means of Oscilloscope. Using a Microwave Dose Rate Integrator it was possible to calculate average of single and total absorbed energy. The average of total absorbed energy was 82.7 J/g for 100 cycles/s and 91.9 J/g for 200 cycles/s. Irradiated as well as control animals were sacrificed by decapitation the brain was quickly removed in liquid nitrogen and pulverized. The content of serotonin was estimated according to electrochromatographic method of Pullar.

Compared to its control group repetitive pulsed 2450 MHz microwave irradiation resulted in decrease of serotonin level by 37% and 28% depending on repetition rate and pulse width used. (The study was supported by US-Yugoslav Joint Bio- and Research Grant No 02-007-3)

Thursday 02 August Congress Centre-First Floor Posters 259-264

Posters on Environmental Biophysics

259 ORAL PRESENTATION

RESPONSES OF SINGLE HERBST CORPUSCLES TO VIBRATION AND CENTRAL PROJECTIONS OF THEIR AFFERENT FIBRES IN SPINAL CORD OF THE PIGEON.

Jun-Xian Shen and Zhi-Hui Xu, Lehrstuhl für Allgemeine Zoologie, Ruhr-Univ. Bochum, F.R.G.
Herbst corpuscles are found to be sensitive to weak vibrational stimuli by recording action potentials from single corpuscles in situ on the tibia. Horseradish peroxidase (HRP) techniques have been also used to investigate projections of the afferent fibres of Herbst corpuscles in the spinal cord. We have demonstrated that Herbst corpuscles are rapidly adapting mechanoreceptors having frequency-following characteristics. They respond with a regular 1:1 fashion to supra-threshold stimuli at a frequency range of 400-4000 Hz. The lowest threshold amplitude is 0.3 μ m (peak to peak) at 600-800 Hz. The similar ranges of best frequencies could be determined from 400 to 1,000 Hz showing "bandpass-filter" property. Using HRP we have found that the axons of Herbst corpuscles bifurcate into ascending and descending branches extending in rostro-caudal direction and their collaterals curve along the medial edge of the head of the dorsal horn, branch and terminate mainly in the medial area of lamina IV in the lumbosacral spinal cord in the pigeon (*Columba livia*).

261

A MOLECULAR FRACTION METHOD FOR MEASURING PERSONNEL RADIATION DOSES

M.A. Fadel, W.A. Khalil, R.R. Krodja, E. Sheta and H.S. Abd El-Baset, Biophysics Department, Faculty of Science, Cairo University, Giza, Egypt.

This work represents a development in fast and albedo neutrons and gamma ray dosimetry, using cellulose nitrate, as a tissue equivalent material, in which radiation damage was registered.

The changes in molecular fractions of the polymer was measured, after irradiation with neutron fluences from 252Cf in the range $10^5 - 10^{10}$ n/cm² and gamma doses in the range $10^{-4} - 10^{-1}$ Gy through the use of gel filtration chromatography. Effects of, irradiation on phantom, phantom to dosimeter distance, phantom thickness and storage at extreme environmental condition were studied on the detector response and readout. The results showed that, main chain scission followed by formation of new molecular configurations are the predominant effect of radiation on the polymer. Empirical formulae for calculating the neutron fluences and gamma doses from the measured changes in molecular fractions were given.

263

THE CHARACTERISTICS OF PISCINE GLYCERALDEHYDE-3-PHOSPHATE DEHYDROGENASE AFTER ACCLIMATION TO 5°C OR 15°C.

Michael A. Phelan and Irving Gray, Department of Biology, Georgetown University, Washington, D.C. U.S.A.

The rainbow trout (*Salmo gairdnerii*) has developed a response to changing environment which adjusts its biochemical processes to meet its needs. The biochemical modification to a single change, termed acclimation, has been studied at the kinetic and molecular level. In earlier studies we had demonstrated alterations in NAD⁺ binding, U.V. absorption and antigenicity. The present study has examined the kinetic and physical chemical parameters and structural characteristics of G3PDH from the lateral muscle of trout acclimated to 5°C and 15°C. No differences were found in the Km's, isoelectric patterns, amino acid composition or tryptic digest peptide maps of the enzyme isolate. However, the Km of the "cold" enzyme determined at 7°C is about one-half that of the "warm" enzyme. The V_{max} of the "warm" enzyme is greater at all assay temperatures. The K_a is smaller for the 5°C acclimated enzyme at 7°C but increases with temperature so that at 17°C there is no difference. The ΔG^\ddagger of both enzymes is the same but the E_a and thus the ΔH^\ddagger of the "cold" is greater than the "warm" enzyme. The ΔS^\ddagger is found to have a smaller negative value for the "cold" enzyme. It is concluded that the changed "milieu interieur" of the cold acclimated fish causes an altered but thermodynamically stable configuration of the same primary sequence which requires a greater change in enthalpy with a consequent lesser degree of negative entropy for the formation of the enzyme-substrate complex. (*Indicates the parameter for the activation step)

260

OCCCLUSION CONDITIONING IN PRESERVING CIRCULATORY DISTURBANCES DURING ANTIORTHOSTASIS

Y.G. Zorbas, V.G. Andreyev, Med. Exptl. Lab., Faculté de Med., Univ. de Clermont, 63001 Clermont-Ferrand, France.

The effect of occlusion conditioning in diverting blood from the head during antiorthostasis (AO) was tested on 14 physically healthy men ranging in age from 17-22 years. They were divided into three groups. In the 1st group of 4 men all four limbs were occluded for 30 min by a pressure of 70 mm Hg beginning on the 16th min of AO at an angle of -30°, the 2d group were occluded periodically for 3-h and 50 min only the lower limbs by a graded pressure of 60-30 mm Hg beginning one hour after the exposure to AO (-15°) and the 3d group none of the four limbs were occluded and served as control. Electrocardiograms (EKG), rheograms (RG) and rheoencephalograms (REG) were recorded. The obtained results were processed statistically. In the 1st and to a greater extent the 2d group of men occlusion tests diminished unpleasant sensations, and they reduced cerebral blood flow to the level that corresponded to horizontal position (0°). It was concluded that both occlusion modes attenuated the adverse reactions of men following redistribution of blood to the head during the exposure to antiorthostatic position (head-down) and aided in normalization of intracranial hemodynamics.

262 ORAL PRESENTATION

MODELS FOR MICRONUCLEI

A. Norman, M. Pincus, H. Callisen, and J. C. Mitchell, Departments of Radiation Oncology and Radiological Sciences, University of California, Los Angeles, California, USA

The frequency of micronuclei (MN) in peripheral blood lymphocytes provides a useful measure of chromosome damage in human populations. In order to learn more about the mechanisms of MN production we have measured the yield and DNA content of MN in lymphocytes that had been exposed to graded doses of ⁶⁰Co gamma rays. The yields of MN with radiation dose exhibit a typical hockey-stick shape. This is consistent with a model in which the DNA repair processes are highly efficient but are saturated at radiation doses above 10 rads. Some 70% of the MN have DNA content between 0.5 and 4% of that in the diploid nucleus. Their DNA distribution is consistent with an origin from acentric chromosome fragments that are produced by the random breakage and rejoining of chromosomes. The DNA distributions are not sensitive to lymphocyte culture times ranging from 48 to 76 hours. This implies that the MN with DNA content in the range of 4 to 20% of the diploid DNA, arise from mitotic non-disjunction and other mitotic errors rather than from the reduplication of acentric chromosome fragments.

264

PHOTOTACTIC RESPONSES IN WILD TYPE AND STIGMALESS MUTANTS OF EUGLENA GRACILIS

V. Passarelli, F. Lanci, M.R. Di Lena, G. Colombetti, L. Barsanti, C.N.R. Istituto di Biofisica, Via S. Lorenzo 26, Pisa, Italy.

By means of a computer-aided videorecording system, negative phototaxis in the flagellate *Euglena gracilis* has been investigated, both in wild type and in stigmaless mutants. The analysis of the movement parameters shows that the two types of cells are both negatively phototactic but exhibit different degrees of orientation with respect to the light stimulus direction. In fact the swimming paths of green cells are more directional than those of the mutants, whose orientation is impaired. These results may be explained in terms of a shading mechanism, in which the cell stigma plays an important role.

Thursday 02 August Congress Centre-First Floor Posters 265-270

Posters on Environmental Biophysics

265

EFFICIENCY OF BIOMASS TRANSFER IN MODEL ECOSYSTEMS

A. Porati and M.I. Granero-Porati, Dipartimento di Fisica, Università di Parma, Via d'Azeglio 85, Parma, ITALIA

Computer simulation has been used to test the feasibility and stability of model ecosystems described by Generalized Lotka-Volterra Equations (GLVE). In particular the analysis has been focused on the relation between topology of ecosystems and their biomass conversion efficiency. The temporal behaviour of the biomass M_i of the species, is described by the following GLVE:

$$\dot{M}_i = b_i M_i - \sum_{j=1}^n a_{ij} M_i M_j \quad (i=1, \dots, n)$$

Defining the efficiency of biomass transfer ϵ as follows:

$\epsilon = \sum_{i=1}^n \epsilon_i$ (the i -th species preys on the j -th one) we were interested in the analysis of ecosystems represented, in the language of Graph Theory, by "Trees", for which we know that every feasible ecosystem is also asymptotically stable. We constructed many thousand of Random Matrices for various values of ϵ and for various topological structures. The results indicate a different behaviour between single alimentary chains and other kinds of "trees": in the first case, the percentage of homeostatic (feasible and stable) systems increases as ϵ increases, while in the second case the behaviour is completely inverted, as, for example, in the case of many preys and one predator.

267 ORAL PRESENTATION

A NEW TYPE OF FAST NEUTRON DOSIMETER FOR PERSONAL USE

M.A. Fadel, A.M. Nassar, A.A. El-Sayed and M.G. Osiris, Biophysics Department, Faculty of Science, Cairo University, Cairo, Egypt.

A fast neutron dosimeter for measuring neutron fluences in the range $10^4 - 10^{11}$ n/cm² through measurements of the induced changes in d.c. resistivity or dielectric properties of lithium-alumino-borate glass are described.

The d.c. resistivity, $\rho_{d.c.}$ ($\approx 10^9$ ohm.cm) of the dosimeter increased upon irradiation with fission neutrons. Our results showed that, irradiating the glass dosimeter with 2.88×10^8 n/cm² caused a 430% increase in $\rho_{d.c.}$. The dielectric constant, ϵ' , measured in the frequency independent region (270 - 340 KHz), which lies between the dipole and atomic resonance peaks, increased progressively with fission neutron fluences in the range $10^4 - 10^9$ n/cm². An increase of 13.16% in ϵ' have been estimated after irradiation with 2.70×10^8 n/cm².

Moreover, no measurable fading in the induced radiation effects have been noticed when the dosimeter was shelf stored at room temperature for one week. Concerning $\rho_{d.c.}$ a formula had been suggested to correct the dosimeter readout when stored at 62 °C for periods greater than 24 hours. However, no measurable fade in the radiation induced changes in ϵ' at the frequency independent region was noticed when the dosimeter was shelf stored for periods up to 120 hours at 60 °C.

Gamma irradiation up to 0.5 Mrad showed no measurable effects on the measured electric properties.

269

ELECTROSTATIC EFFECTS AND COMPLEXATION OF PENTACHLOROPHENOL DUE TO ITS PRESENCE IN LECITHIN BILAYERS AND MONOLAYERS.

P. Smejtek, W. Barstad, A. Levinson and K. Hsu, Departments of Physics and Chemistry, Environmental Science and Resources Program, Portland State University, Portland, Oregon, U.S.A.

Biological effects of pentachlorophenol (PCP) a widely used pesticide, are primarily related to its ability to induce hydrogen ion transfer in lipid matrix of biomembranes. We summarize results of our studies on (1) changes of electrostatic potential distribution across the aqueous phase/lecithin array interface in monolayers, liposomes and planar bilayer membranes due to the presence of pentachlorophenol; (2) partition of neutral and ionized form of PCP into membranes and model solvents; (3) spectroscopic evidence for the existence of negatively charged dimer implicated in the transfer of hydrogen ions across lipid membrane. The changes of electric potential distribution across the lipid array/water interface were obtained from measurements of (a) electrophoretic mobility of liposomes, (b) surface potential of lipid monolayers and (c) conductivity of lipid membranes induced by lipophilic probe ions. The experimental results are compared with the predictions of Langmuir-Stern-Grahame models of adsorption assuming either homogeneous or discrete charge distribution at the adsorption plane. We present spectroscopic evidence for the existence of AHA⁻ complex formed between the neutral, HA, and ionized, A⁻, species of pentachlorophenol. This complex is essential for understanding the mechanism of pentachlorophenol-induced hydrogen ion permeability in lipid membranes.

Research supported by NIH grant 5R01 ES 00937-09.

266 ORAL PRESENTATION

THE RELEVANCE OF $\delta^{13}C$ VARIATIONS IN TREE LEAVES FOR ASSESSING THE CONTRIBUTION OF SOIL RESPIRED CO_2 TO THE TOTAL ASSIMILATION OF LEAVES

G.H. Schleser and R. Jayasekera, Inst. f. Chemie 2, Kernforschungsanlage Jülich GmbH, 5170 Jülich, F.R. of Germany

$\delta^{13}C$ values in leaves of forest trees show significant differences not only as a function of tree height but also as a function of the state of development of leaves, i.e. the growing season. $\delta^{13}C$ differences of up to 5 ‰ have been observed from bottom to top of a forest beech while seasonal variations show differences of up to 2 ‰. A model for the ^{13}C fractionation during CO_2 assimilation shows that $\delta^{13}C$ values of leaves basically depend on two factors: a) The source of ^{13}C , namely ^{13}C of atmospheric CO_2 and b) the physiological status of leaves, given by the ratio of internal over external CO_2 concentration of leaves (C_i/C_a) and the respiratory coefficient, defined as total respiration over gross photosynthesis. According to this model the seasonal $\delta^{13}C$ trend should mainly be due to changes of the respiratory coefficient, while the vertical $\delta^{13}C$ differences should primarily depend on the assimilated amount of soil CO_2 in the lower forest strata and the differences of C_i/C_a between top and bottom of the canopy. The contribution of soil respired CO_2 to total assimilation of leaves in the lower forest strata has been estimated to vary between 14 and 19 % depending on the time of the growing season, i.e. the CO_2 flux out of the soil.

268

THERMODYNAMIC APPROACH TOWARDS THE ADHESION OF ORAL BACTERIA TO TOOTH ENAMEL SURFACES. H.J. Busscher, A.W.J. van Pelt, H.P. de Jong and J. Arends, Laboratory for Materia Technica, Univ. of Groningen, Ant. Deusinglaan 1, 9713 AV Groningen, Holland.

Adhesion of bacteria to tooth surfaces is the main cause of one of the world's most wide spread diseases: dental caries. With the aim of reducing bacterial adhesion to tooth surfaces, a study has been carried out to develop a model, predicting bacterial adhesion to surfaces. Basic to the model, are relations between SURFACE CHARACTERISTICS and BACTERIAL ADHESION.

The SURFACE CHARACTERISATION parameter of interest with respect to adhesion, is the surface free energy γ . Using contact angle measurements with liquids of known surface free energy, the solid surface free energy γ_s can be calculated. γ_s data have been obtained for polymers, ionic crystals and human enamel, treated with various fluorides and after salivary protein adsorption. Aminfluoride e.g., was found to reduce γ_s from 84 to 54 erg/cm². This reduction in γ_s increases the interfacial free energy of adhesion ΔF_{adh} of most oral bacterial which is on theoretical grounds expected to reduce bacterial adhesion.

In order to quantify BACTERIAL ADHESION *S. sanguis* cells were adhered during one hour adhesion experiments onto various surfaces with γ_s ranging from 22 to 141 erg/cm². Subsequently the number of bacteria adhered per cm² n_a was counted using S.E.M.. Negative correlations between n_a and γ_s were obtained in adhesion from bacterial suspensions of varying bacterial concentrations ($10^5 - 10^7$ cm⁻³). Although this result is opposite to expectations, based on calculations of ΔF_{adh} , the observation made, that the bacteria are more loosely bound to the low energy surfaces, is in agreement with these expectations.

270

SPECTROSCOPIC STUDIES OF BENZO(A)PYRENE-7,8-DIHYDRODIOL-9,10-EPOXIDES COVALENTLY BOUND TO NATURAL OR SYNTHETIC NUCLEIC ACIDS

A. Gräslund^a, P.-O. Lycksell^a, A. Ehrenberg^a, B.-M. Olsson^a, B. Jernström and B. Nordén^b, ^aDept. of Biophysics, Univ. of Stockholm, Stockholm, ^bDept. of Forensic Medicine, Karolinska Inst., Stockholm, ^cDept. of Physical Chemistry, Chalmers Univ. of Technology, Göteborg, Sweden.

Benzo(a)pyrene-7,8-dihydrodiol-9,10-epoxides (BPDE) are among the most active and reactive intermediates in the metabolism of the chemical carcinogen BP. The spectroscopic properties of the covalent adducts between (+)-anti-BPDE (or its less carcinogenic stereoisomers) and calf thymus DNA, poly d(GC)-poly d(GC) or poly d(AT)-poly d(AT) have been studied, mainly with fluorescence and linear dichroism techniques. - The spectroscopic properties of the complexes as well as their fluorescence lifetimes display a marked heterogeneity. Two major classes of complexes with different spectral and steric properties have been characterized. One class (I) has typical characteristics of an intercalated complex. The other class (II) exhibits a smaller shift towards longer wavelengths of its light absorption and less quenching of its fluorescence by the nucleic acid. The molecular plane of the carcinogen forms <55° angle with the DNA helix axis. - Class II complexes are predominant for (+)- and (-)-anti-BPDE in complex with both DNA and poly d(GC)-poly d(GC). Class I complexes are observed coexisting with class II for the less carcinogenic BPDE's in complex with DNA. Also the (-)-anti-BPDE bound to poly d(AT)-poly d(AT) exhibits a class I complex, but the binding is unstable

Thursday 02 August Congress Centre-First Floor Posters 271-276

Posters on Environmental Biophysics

271

FOLIAGE TEMPERATURE MEASUREMENTS OVER AN OAK CANOPY
R. Valentini, B. Schirone and G. Scarascia, Istituto Biologico
Selvicolturale, Università della Tuscia, Via Riello, Viterbo,
Italy.

Foliage temperature measurements were collected over an oak (*Quercus Cerris* L.) canopy near POTENZA in southern Italy, in order to investigate the energy exchanges between the canopy and the atmosphere. Foliage temperatures were measured by means of an I.R. thermometer in the 8-14 wavelength band from a tower 4 m. high above the canopy. Air temperature and humidity were contemporaneously measured at two levels (2 m. spaced) above the canopy. Only cloudless days were considered. Large positive gradients between foliage and air temperature were found during the day. At the sunrise and the sunset gradients are small or negative as shown by the behaviour of sensible heat which was measured by the Bowen ratio technique. Temperature gradients at the two levels above the canopy are much smaller than the ones between foliage and air. Under the assumption of null divergence fluxes, this behaviour can be explained by higher water vapour and heat diffusion resistances between leaves and the atmosphere than the ones between the two levels in the air above the canopy. We are now looking for a relation between foliage temperature and stomatal resistance for sunlit leaves.

273

VARIATIONS OF PHOTOSYNTHETIC ELECTRON TRANSPORT RATE ASSOCIATED WITH PLANT TOLERANCE TO Ca^{2+} AND Pb^{2+} .
E. Hilary Evans, S.M. Keskin and R. Cotton, Biology Division,
Preston Polytechnic, Preston, Lancs., U.K.

We have previously shown that Ca^{2+} added to the preparation buffer stimulates electron transport in lettuce chloroplasts. This effect is only observed in uncoupled barley chloroplasts, but Ca^{2+} protects against ageing. The effect depends on whether barley is grown on low Ca^{2+} (serpentine) or high Ca^{2+} (calcareous) soils, being most marked in the former case. However, *Agrostis* sp. collected from serpentine soils gives chloroplasts with high electron transport rates, unstimulated by Ca^{2+} , suggesting that the plant adapts to bind Ca^{2+} tightly to the chloroplast membrane. Conversely, *Agrostis* sp. collected from calcareous soil gives chloroplasts with lower electron transport rates, stimulated by Ca^{2+} . In addition, this plant is more susceptible to inhibition by Pb^{2+} . We propose that, in both these cases, there is a genetic alteration to a Ca^{2+} -binding protein in Photosystem 2 which also affects the Pb^{2+} -binding site.

275

THE EFFECT OF THE HYPOXIC HYPOTHESIS ON THE ELECTRICAL IMPEDANCE OF THE STRIATED MUSCLE IN CATS. J. Bilski, J. Michalski, H. Diolen, J. Myliński, Department of Biophysics,
Institute of Physiology, Medical Academy,
Kraków, Poland.

In the experiments performed in anaesthetized, decapitated cats kept in a low pressure chamber, the electrical impedance of the striated muscle at six different frequencies within the range 10 - 5.10⁵ Hz by the A.C. bridge method was determined. Nickel needle electrodes with a 0.4 mm gap were inserted in the muscle of the hind limb. The pressure in the chamber was gradually reduced during 3 hours from normal to a value corresponding to an altitude of 10,000 m above sea level, that is ca. 20 kPa. The absolute impedance value increased in proportion to the intensity of hypoxia in all frequencies tested, reaching maximum at 20 kPa. Under this pressure the greatest increase in impedance was observed at the frequency of 10 kHz /25%. When animals were breathing oxygen at the same simulated altitudes the increase of impedance was inhibited. Our study shows that hypobaric hypoxia causes a marked increase in the electrical impedance of the rat striated muscle.

272

NMR ANALYSIS OF RADIATION-MODIFIED PRODUCTS IN DNA MODEL COMPOUNDS. Charles A. Belfi and Harold C. Box, Department of Biophysics, Roswell Park Memorial Institute, 666 Elm Street, Buffalo, New York, USA.

Aqueous solutions of dinucleoside monophosphates have been subjected to ionizing radiation in the presence of various mediators including H_2O_2 , O_2 and electron affinity sensitizers. Products were isolated using C18 reverse phase HPLC. Individual products have been characterized by ¹H and ³¹P NMR spectroscopy. In H_2O saturated solutions of dTpa, for example, several products containing modified thymine are observed. C1s and trans glycols exhibit methyl proton chemical shifts of between 0.41 and 0.58 PPM upfield compared with dTpa. The H6 thymine resonance in the glycol products is consistently shifted 2.4 PPM upfield. These chemical shifts are consonant with those observed in glycol modified monomers as reported by Cadet and Teoule. The 5- and 6-hydroxydihydrothymine products are also observed. The latter are particularly easy to identify from their ¹H NMR spectra by virtue of spin-spin splitting of the methyl resonance into a doublet pattern. Other major products result from crosslinking and depurination. As expected, the HPLC profile of products changes profoundly when the irradiation is carried out on oxygen saturated solutions.

(1) J. Cadet and R. Teoule, Bull. Soc. Chim., France 3, 885 (1975); J. Cadet, R. Ducloux and R. Teoule, Tetrahedron 33, 1603 (1977).

274 ORAL PRESENTATION

EFFECTS OF X-IRRADIATION OF SINGLE CRYSTALS OF RIBONUCLEASE A
S.K. Burley, G.A. Petsko and D. Ringe, Chemistry Department,
Massachusetts Institute of Technology, Cambridge, Massachusetts,
United States of America.

Radiation damage of biomolecules is an important yet poorly understood phenomenon. We have studied X-radiation damage of ribonuclease A by high-resolution X-ray crystallography. Structural changes induced by irradiation with 10 Mrad were restricted to a few specific sites in the enzyme. All the disulphide bridges were opened and oxygen atoms appear to have been added to each sulphur atom. The four methionine residues appear to have been changed to methionine sulfoxides. The aromatic side chains also showed evidence of chemical modification. Despite the scission of the disulphide bridges, there was no major conformational change suggestive of general unfolding of the enzyme.



3-D electron density difference map of radiation damaged and native RNase A ($\rho_{\text{damaged}} - \rho_{\text{native}}$) calculated at 1.5 Å. The +ve and -ve differences are shown as lines and points, respectively. The refined structure of native RNase A is shown as a stick figure. The S-S bond between cyst65 and cyst72. -ve density is visible at the S-S bond. Large, lobate +ve density features surround each sulphur. The positions of the lobes are consistent with the addition of oxygen atoms to the cyste sulphurs.

276

Thursday 02 August Congress Centre-First Floor Posters 277-282

Posters on Education in Biophysics

277

EFFECT OF PHASE TRANSITION OF PHOSPHOLIPIDS ON NADH DEHYDROGENASE FROM BACTERIA
A. Kotani, S.M. Shu, M. Hisae, T. Sekiguchi, N. Koyama and Y. Nosoh, Laboratory of Natural Products Chemistry, Tokyo Institute of Technology, Yokohama, Kanagawa 227, *Shino Test Laboratories, Sagamihara, Kanagawa 229, Japan

Membrane-bound NADH dehydrogenase was solubilized and purified from *Bacillus subtilis*. The enzyme consisted of two subunits, and contained about 70 moles of phospholipids/subunit. The purified enzyme and the enzyme bound to phospholipid-liposome exhibited discontinuous Arrhenius plots having two break points at 10° and 30°C, where liposome showed phase transition. The enzyme having about 10 moles of phospholipids prepared by detergent treatment exhibited a continuous Arrhenius plot. Similar discontinuous Arrhenius plot was observed with the enzyme purified from alkalophilic *Bacillus* which contains no phospholipids. The secondary structure of the de-phospholipid *B. subtilis* enzyme changed on binding with phospholipids or liposome. The structure of the de-phospholipid enzyme exhibited no change with temperature, but the purified and liposome-bound enzymes exhibited considerable change in secondary structure at phase transition temperatures.

279

THE PROTEIN DATA BANK^a
Thomas F. Koetzle, Enrique E. Abola and Frances C. Bernstein, Chemistry Department, Brookhaven National Laboratory, Upton, New York, USA

The Protein Data Bank (P. C. Bernstein, T. F. Koetzle, G. J. B. Williams, E. F. Meyer Jr., M. D. Brice, J. R. Rodgers, O. Kennard, T. Shimanouchi and H. Tasumi, J. Mol. Biol. (1977) 112, 535) is a computerized archival database for structural data on biological macromolecules. The Bank presently contains approximately 250 sets of atomic coordinate data for proteins, nucleic acids, virus and polysaccharide structures. Structure factor data have been deposited for some studies, and bibliographic citations are included for structures when atomic coordinates are not yet available. Data are distributed upon request from Brookhaven and distribution centers in Cambridge, UK; Osaka, Japan; and Melbourne, Australia. A number of computer programs have been developed to enable users to extract information from the file.

^aWork supported by the US National Science Foundation and US National Institutes of Health and carried out under contract with the US Department of Energy.

278

PURPLE MEMBRANE FRAGMENTS FROM HALOBACTERIUM HALOBIVM AS A MODEL SYSTEM IN BIOPHYSICAL EDUCATION PROCESS

S.P. Stoyov, N.G. Popdimirova, M.R. Kantcheva, Department of Physics and Biophysics at the Medical Academy of Sofia, Bulgaria

In order to present biophysical properties of membrane structure and functions, bioelectrical properties, active transport especially, light driven proton pumping, photobiology et c., the purple membrane fragments of *H. Halobium* as a model system are proposed. The significance of some relevant parameters - electric surface charge density, dipole moment, dielectric properties, electrooptic behaviour, effective for the protein and lipid phase organization and functional activity are discussed. The present model system can successfully serve as a starting point and joining line for the understanding a great number of biophysical fact and in such a way could be a good basis for the biophysical education which could be if necessary profolized for medicals, physics, agriculture biology and other students.

280

THERMODYNAMIC EQUILIBRIUM: A NEW APPROACH.

C. Tanford, Dept. of Physiology, Duke Univ. Med. Cntr. Durham, N. C., USA.

The concept of thermodynamic equilibrium is under-utilized in the teaching of Biophysics. One reason for this is that biochemists have tended to limit equilibrium considerations to isolated chemical reactions. New insight is gained if we focus instead on the equilibrium state of an entire system, in which many different individual reactions are possible. One conclusion that emerges is that enzymes, transport catalysts, etc., dramatically alter the equilibrium state of a complex system, in contrast to the more familiar fact that they leave the equilibrium state of an isolated reaction unchanged. Once this is recognized, it follows that many biophysical processes can be represented as a succession of different equilibrium states. There is great benefit in using this approach for a basic understanding of physiological function. (1) Quantitative calculations of equilibrium states are easily made and (being independent of the pathway to equilibrium) do not require complex kinetic schemes. (2) The critical role played by protein catalysts is emphasized when a new phenomenon is first introduced. This creates an immediate natural bridge between phenomenology and protein structure and function, i.e., a focus on the area of biophysical science that we must in any case increasingly turn to for major progress in the future. (Supported by the National Science Foundation.)

281

282

Notes

Notes

Friday 03 August

Symposia

09.30 - 12.30

Electrostatic Effects in Protein Function

Photo and Auditory Receptors

Applications of Synchrotron Radiation

Rheology of Cell Membrane

14.00 - 17.00

Electric Field Effects in Cell Membranes

Developments in Microscopy

Environmental Biophysics

Plenary Lecture

17.15 - 18.00

"Energetics of Protein Structure"

P.L. Privalov (Puschino)

followed by

Closing Ceremony

Poster Sessions

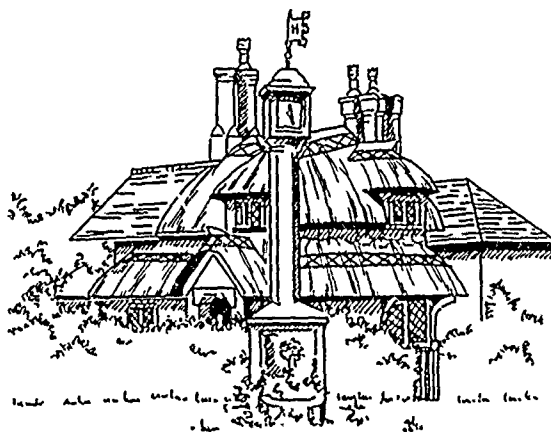
Chemical and Electrical Regulation of Ion Channels

Mechanisms of Transport across Membranes

Food Biophysics

NMR in-Vivo

Medical Imaging



*Blaise Hamlet, a picturesque village
owned by the National Trust.*

Friday 03 August

	Colston Hall Main Hall	Council House Conference Hall	Unicorn Hotel Trident Suite
09.30	<p>Electrostatic Effects in Protein Function</p> <p>Chairman: F.M. Richards (Yale)</p> <p>Speakers: F.M. Richards (Yale) H.J.C. Berendsen (Groningen) A. Wada (Tokyo) and Authors of Posters A. Warshel (207) D.J. Barlow (208)</p>	<p>Photo and Auditory Receptors</p> <p>Chairman: A.L. Hodgkin (Cambridge)</p> <p>Speakers: D.A. Baylor (Stanford) R. Fettiplace (Cambridge) H. Kuhn (Julich) and Authors of Posters J.-J. Cheng (172) B.J. Nunn (174)</p>	<p>Applications of Synchrotron Radiation</p> <p>Chairman: R. Fourme (Orsay)</p> <p>Speakers: R. Fourme (Orsay) S.S. Hasnain (Daresbury) G. Schmahl (Gottingen) and Authors of Posters H. Kihara (189) J.C. Brochon (191)</p>
12.30	<p>Morning Coffee</p> <p>10.50-11.10</p>	<p>Morning Coffee</p> <p>10.50-11.10</p>	<p>Morning Coffee</p> <p>10.50-11.10</p>

Break for Lunch (90 Minutes)

<div data-bbox="247 1256 664 1793" style="position: relative; height: 638px;"> <div data-bbox="247 1256 664 1793" style="position: absolute; top: 0; left: 0; width: 100%; height: 100%; border: 1px solid black; transform: rotate(45deg); transform-origin: center;"></div> </div>	<div data-bbox="687 1319 1004 1363">Electric Field Effects in Cell Membranes</div> <div data-bbox="687 1388 936 1408">Chairman: R. Glaser (Berlin)</div> <div data-bbox="687 1428 994 1580">Speakers: R. Glaser (Berlin) U. Zimmerman (Julich) L.A. Jaffe (Connecticut) and Authors of Posters A. Peres (139) E. Papp (131)</div> <div data-bbox="687 1716 1004 1737"> <div data-bbox="687 1716 802 1737">Afternoon Tea</div> <div data-bbox="903 1716 1004 1737">15.20-15.40</div> </div>	<div data-bbox="1050 1319 1356 1344">Developments in Microscopy</div> <div data-bbox="1050 1365 1348 1388">Chairman: E. Kellenberger (Basel)</div> <div data-bbox="1050 1406 1364 1587">Speakers: E. Kellenberger (Basel) AP. Somlyo (Philadelphia) H. Rohrer (IBM, Ruschlikon) and Authors of Posters H.-UL. Weier (205) J.D. Robertson (212)</div> <div data-bbox="1050 1716 1364 1737"> <div data-bbox="1050 1716 1166 1737">Afternoon Tea</div> <div data-bbox="1262 1716 1364 1737">15.20-15.40</div> </div>
<div data-bbox="335 1807 627 1886"> Energetics of Protein Structure Plenary Lecture by P.L. Privalov (Puschino) </div> <div data-bbox="335 1936 513 1964"> Closing Ceremony </div>		

Timetable

Watershed Cinema 1	Congress Centre First Floor	
	Presenting Authors should set up their Posters before the start of Today's Symposia	09.00
Rheology of Cell Membrane Chairman: R. Skalak (New York) Speakers: R. Skalak (New York) M.P. Sheetz (Connecticut) J.N. Israelachvili (Canberra) and Authors of Posters Y. Shimoyama (258) L.K. Tamm (265)	Poster Sessions Chemical and Electrical Regulation of Ion Channels Poster Nos: 001-102 Mechanisms of Transport Across Membranes Poster Nos: 103-246 Food Biophysics Poster Nos: 247-264 NMR in Vivo Poster Nos: 265-276 Medical Imaging Poster Nos: 277-282	09.30
Morning Coffee		12.30
Environmental Biophysics Chairman: M. Baltscheffsky (Stockholm) Speakers: G.R. Williams (Toronto) G.H. Kohlmaier (Frankfurt) and Authors of Posters W.G. Osiris (267) A. Norman (262) J-X. Shen (259) S.K. Burley (274) G.H. Schleser (266)	Presenting Authors should attend their Posters throughout the Afternoon Discussion Period.	14.00
Afternoon Tea		17.00
	Presenting Authors must take down their Posters	17.15
		18.00
		18.20

Symposium on Electrostatic Effects in Protein Function

ELECTROSTATIC INTERACTIONS BETWEEN IONIZABLE GROUPS. MODIFICATION OF THE EFFECTIVE DIELECTRIC CONSTANT BY SOLVENT ACCESSIBILITY.

Frederic M. Richards Department of Molecular Biophysics and Biochemistry, Yale University, New Haven, CT, U.S.A.

Over the last decade Gurd, Matthew, Shire, Friend and their colleagues have developed and extended the original Tanford and Kirkwood (T-K) formalism for the interactions between pairs of charges at or near a dielectric interface. Following the original work in the early '50s, further developments have had to await the appearance of high resolution X-ray structures of proteins. In addition to providing the 3D coordinates of the charges the structural data also defines the access to the solvent of the charged atoms through the procedure of Lee and Richards. Gurd et al. have used such data in an iterative algorithm which estimates the electrostatic interactions between specific functional groups and allows direct comparison with experimental data. The T-K work factor for a given charge pair is modified by the mean static accessibility of the two groups. The basic idea is that a charge fully surrounded by solvent will have maximum shielding by counterions and thus contribute less to any given interaction than a charge with less exposure.

A set of intrinsic pK values, and the implied self potentials are chosen for the various groups from the behavior of fully solvated, non-perturbed, small molecules. The X-ray structure of the protein and the algorithm of Gurd et al. then provide estimates of the pK shifts for each group under the influence of all other groups. The critical tests are then the comparison of calculated and observed effects of both pK and ionic strength. The pK shifts weighted by the net charge of each group yield the overall electrostatic stability of the protein.

For a series of myoglobins there is remarkable agreement between the calculated and observed pK shifts for specific His residues. The calculated pH dependence of the stability of various proteins bears no simple relation to the isoelectric point and corresponds well to the observed onset of acid and alkaline denaturation. Regions of high electric field near the protein identify possible specific ion binding sites. These are populated according to the Boltzmann distribution and fed into the iteration along with the protein charges. The binding constants are evaluated. The electrostatic contribution to the association of two proteins being "checked" can be estimated. The ion binding and stability of different forms of DNA can be calculated by the same general procedures.

The remarkable agreement between prediction and experiment is perhaps unexpected. The theory assumes that the "static" X-ray structure can be used while substantial motion, and thus fluctuating accessibility is clearly occurring and may change with solvent conditions. The T-K factors are based on a spherical particle with a smooth surface, and uniform dielectric media with a sharp interface are assumed. No account is taken of the effects of partial charges in the protein and the fixed moments that result from their uneven distribution. There must be some cancellation of the errors associated with these assumptions to permit the degree of correlation actually found.

Much of the recent work of J.B. Matthew was supported by the National Institute of General Medical Sciences under grant GM-22778 (F.M. Richards, principal investigator).

Symposium on Electrostatic Effects in Protein Function

THE EFFECTS OF LONG RANGE ELECTROSTATIC FORCES AND THEIR COMPUTATION IN MOLECULAR DYNAMICS

H.J.C.Berendsen, W.G.J.Hol and E.Egberts, Chemical Laboratories of the University of Groningen, Nijenborgh 16, Groningen, the Netherlands

A contribution of the Biomolecular Structure Centre (BIOS)

A survey will be given of the principal sources for long-range electrostatic interactions in proteins and other biomolecular systems, their functional role and the various methods of computation of electric interactions suitable for molecular dynamics simulations.

Whereas charges are normally either screened by the high dielectric constant and the ionic strength of the solvent, or are compensated at short range by countercharges, correlated dipoles produce long-range electrostatic fields. Sources for correlated dipoles are principally alpha-helices in proteins, although also double layer charges in membranes have important long-range fields. A linear array of correlated dipoles acts as a separated charge pair in a hydrophobic environment, producing strong electric fields. An alpha-helix is approximately equivalent to a positive charge of one half electron at the aminoterminal and a negative charge of one half electron at the carboxyl terminal.

The effects of helix fields include binding of substrates, stability of conformations, facilitation of proton transfer, stabilization of reaction intermediates and modification of redox potentials and acid dissociation constants.

The computation of long-range electrostatic interactions is complicated by the presence of a high-dielectric constant medium, and conventional methods using a cut-off radius of less than 10 Angstrom fail to produce accurate results. For molecular dynamics computations it is required to use efficient and accurate methods to compute long-range forces; one method uses the evaluation of correlated long-range forces only every 10 or 20 steps. The use of distance dependent dielectric constants leads to incorrect results and is not advised for accurate evaluation of the effects of solvent polarization. Available methods to compute the electric fields will be reviewed.

The computation of long-range forces in a bilayer membrane has been realized through the use of an analytical extension of the field outside a cut-off radius. A molecular dynamics simulation using this field has been carried out. The results give insight into the polarization of water molecules near a charged membrane and the dielectric behaviour of the solvent.

Symposium on Electrostatic Effects in Protein Function

CORRELATION BETWEEN STRUCTURES OF ELECTROSTATIC POTENTIAL SURFACE AND PROTEIN FUNCTIONS.

A. Wada¹⁾, H. Nakamura²⁾ and T. Sakamoto¹⁾, Department of Physics¹⁾, Faculty of Science, and Department of Applied Physics²⁾, Faculty of Engineering, the University of Tokyo, Tokyo, Japan

We would like to discuss the protein structure and function in terms of electrostatic effects. The effects are unique among the many interactions because of their long range nature, which sometime extend over the whole protein molecules.

The electrostatic field in and around globular proteins is produced by two types of charges: the ionic charges and partial atomic charges. The ionic ones are located only in the side chains of ionizable amino acids, while all the atoms in a protein have the charge of the latter type, the amount of which is derived from the Mulliken population analysis of molecular orbital calculation.

These charges produce a unique electrostatic field pattern corresponding to the characteristic secondary and tertiary structures of each of the globular protein. For instance, in the secondary structure level, an electrostatic macrodipole is generated in the α -helix as a collective property of the partial atomic charges which are involved in such an ordered backbone conformation. In this case, we can substitute atomic partial charges of all atoms of the α -helix by two virtual charges ($+e/2$ and $-e/2$) at the α -helix termini.

Statistical analysis on the distribution of the distances separating the ionic charges of ionizable groups and the virtual charges at the termini of the α -helices indicates that a charge in the protein is surrounded, on average, by charges of opposite sign; sometimes they construct more tightly bound ion-pairs. This type of charge distribution provides locally closed electronic lines of force within a protein and contributes to stabilize its compact structure.

In contrast to this general and averaged picture of charge distribution, evidence of the clustering of charges of the same sign is often observed in a protein, especially at its functional site. In this case the electric lines of force, i.e. electrostatic potential, extend into the solvent in that particular region. Even if such charge clustering acts to destabilize the local protein conformation, it acts to guide a charged substrate to the active site and to stabilize the active complex; such mechanism will expand the collision diameter greatly.

During the long history of the evolution of life, living organisms have accumulated a great deal of advantageous characteristics for maintaining their existence into genetic information by the mechanism of natural selection. In this regard, the study of the electrostatic role in the protein functions gives us a new insight into how such physical quantity is utilized, sometime contradictorily as mentioned above, to produce effective protein functions.

In this context, we examined correlations between the structure of the electrostatic field and biological functions in many proteins the structures of which are known with angstrom resolution. Remarkable correlations are found and can be displayed graphically in color. The examinations are made on the embarrassing problem which comes from the fact that the protein is imbedded in a high dielectric medium, water. The difficulties there are in assigning a shielding factor for charges in the protein (i.e. the evaluation of the effective internal dielectric constant in a macroscopic scheme), and in the technical problem for calculating the electric field in or outside of the non-spherical and rugged dielectric boundary of the protein surface.

Symposium on Photo and Auditory Receptors

VISUAL TRANSDUCTION IN PRIMATE PHOTORECEPTORS

D.A. Baylor, B.J. Nunn and J.L. Schnapf

Neurobiology Department, Stanford Medical School, Stanford, CA, USA

The ultimate limits on many features of visual performance probably derive from characteristics of the transduction mechanism in the photoreceptors. Nevertheless, little is known about the light-evoked electrical signals of primate rods and cones. We have used suction electrodes to record photocurrents from single outer segments in pieces of retina from the monkey *Macaca fascicularis*, whose photoreceptors are thought to be similar to those of man.

In rods a flash of light causes a graded suppression of an inward dark current up to 35 pA in amplitude. A single photoisomerization gives a response about 0.7 pA in peak amplitude, and a flash causing 30 isomerizations evokes a half-saturating response. The waveform of the response to a dim flash resembles the impulse response of a series of 6 first order delays with time constants of roughly 40 msec.

Desensitization of rods by steady background light results mainly from saturation of the light-sensitive conductance of the outer segment. Comparison of the behavior with that of the human scotopic system suggests that saturation of rod vision is caused by the saturation in the outer segment, while the mechanism responsible for Weber's law is located central to the outer segments.

In complete darkness the rods give occasional spontaneous signals resembling responses to single photons. The estimated frequency of occurrence of these events is about 0.006 sec^{-1} , and they probably account for the "dark light" measured in human psychophysical experiments. A second component of the dark noise consists of a continuously-present current fluctuation of rms amplitude about 0.15 pA. It is not yet clear how this component of the noise is suppressed by the rod system so that only photoisomerizations are registered. After bright light the recovery of the photocurrent is marked by quantized step-like events during which the dark current is apparently blocked over a length of roughly $1 \mu\text{m}$ on the outer segment. Superposition of these events may contribute to the desensitization of rod vision that follows bleaching.

The rod spectral sensitivity is fitted by the Dartnall nomogram for a rhodopsin of maximal absorption at 491 nm and is in good agreement with the human scotopic visibility curve after corrections for absorption in the lens and self-screening.

Cones give graded outward photocurrents with an underswing on the recovery phase. The spectral sensitivities measured from several red-sensitive and green-sensitive cones are in good agreement with estimates of the respective pigment absorptions of human cones as derived from color-matching experiments. The long wavelength decline of the red cone sensitivity is more rapid than that of the green. This gives a simple basis for the perceived "yellowing" of monochromatic lights of increasing wavelength at the red end of the visible spectrum.

(supported by grant EY01543, USPH)

Symposium on Photo and Auditory Receptors

MECHANOELECTRICAL TRANSDUCTION IN TURTLE HAIR CELLS

R. Fettiplace and A.C. Crawford, Physiological Laboratory, Cambridge, U.K.

Hair cells, which are the sensory receptors of the cochlea, transduce acoustic energy into electrical signals, and, by filtering these signals, may also contribute to the cochlea's frequency selectivity. The mechanically sensitive component of each hair cell consists of about 100 stereocilia, packed with actin filaments and protruding from the hair cell's apical surface. The purpose of the experiments to be described was to obtain information about the mechanical properties of the ciliary bundles.

The experiments were performed on isolated basilar papillae, removed from the inner ear of the turtle, and separated from the gelatinous tectorial membrane that normally envelopes the cilia. Intracellular recordings in this preparation showed that the hair cells were able to transduce imposed deflexions of their ciliary bundles into changes in membrane potential, and did so in a frequency selective manner. The cells could generate receptor potentials of 1 mV for bundle displacements of a few nanometres towards the kinocilium.

The mechanical stiffness of the ciliary bundles was measured by bending them with the tip of a fine flexible glass fibre of known compliance. The base of the fibre was driven by a piezoelectric element and the subsequent motion of the tip, placed on the bundle, was detected by a pair of photodiodes on which the magnified image of the fibre was focussed. The experiments suggested that the ciliary bundles can pivot about their base, and the torque opposing rotation was estimated as about 2×10^{-9} Newtons/radian for small displacements towards or away from the kinocilium.

When the flexible fibre was used to deliver force steps to the tip of the ciliary bundle, the membrane potential of the hair cell underwent a damped oscillation. The oscillation, reflecting the tuning of the hair cell, varied in frequency from about 20 to 350 Hz among different cells. The range of characteristic frequencies, and inferred sharpness of tuning are comparable to the values of these parameters measured in the intact turtle cochlea. Since in the present experiments, the stimuli were delivered directly to the ciliary bundles, it seems likely that the properties of individual hair cells are the major determinants of this cochlea's frequency selectivity.

Symposium on Photo and Auditory Receptors

ACTIVATION OF PHOTORECEPTOR ENZYMES BY LIGHT

Hermann Kühn

Institut für Neurobiologie der KFA Jülich, W. Germany

Rhodopsin is the photosensitive protein in rod cell outer segments of the vertebrate retina. It is an integral membrane protein embedded in densely packed stacks of disk membranes, most of which are separate from the surrounding plasma membrane. Absorption of a photon by rhodopsin leads to local changes in the concentration of cytoplasmic soluble substances which are thought to transmit the signal by diffusion to the plasma membrane; as a result, the Na^+ ion permeability of the plasma membrane is decreased. Evidence is high that both Ca^{++} ions and cyclic GMP have key functions in this process of internal signal transmission. Neither the relationship between the light-dependent metabolisms of Ca^{++} and cyclic GMP, nor the controlling mechanisms of plasma membrane permeability, are yet understood. On the other hand, it has become rather clear in recent years how a photoexcited rhodopsin (R^*) molecule communicates the message of photon absorption to its environment in the cell: it interacts with proteins peripherally associated with the disk membrane, and thereby triggers the amplified activation of the enzyme system that degrades cyclic GMP. I will discuss the molecular mechanism by which R^* activates these enzymes.

Light absorption causes rapid (psec) cis-trans isomerization of rhodopsin's chromophore (11-cis retinal), followed by a series of protein conformational changes that occur not only in the hydrophobic chromophore binding center, but also at the cytoplasmic-exposed surface of rhodopsin. Such surface-conformational changes are recognized by at least two enzymes: a GTP-binding protein (G-protein, also called GTPase or transducin), which mediates activation of cyclic GMP phosphodiesterase, and a protein kinase which, in the presence of ATP and independently of cyclic nucleotides and Ca^{++} , specifically phosphorylates photobleached rhodopsin. Sedimentation studies show that these two enzymes, and a third protein (48 kd protein), bind to photobleached disk membranes under conditions in which they would be soluble in the dark.

The G-protein consists of three subunits G_α (37 kd), G_β (35 kd), and G_γ (6 kd). Binding of the G-protein to R^* enables the exchange of GTP for previously bound GDP on the G_α -subunit. In the absence of GTP, the complex formed between R^* and G-protein, $\text{R}^*\text{-G}(\text{GDP})$, is stable for many minutes. If GTP is present, it rapidly displaces the bound GDP, leading to dissociation of the protein complex into R^* , $\text{G}_\alpha(\text{GTP})$, and $\text{G}_{\beta\gamma}$. The time course of these protein interactions - binding of $\text{G}(\text{GDP})$ to R^* , and dissociation of $\text{G}_\alpha(\text{GTP})$ from R^* - has been measured by taking advantage of specific, accompanying changes in light-scattering intensity ("binding signal", "dissociation signal"). It is in the range of tens of milliseconds. One R^* molecule can serially interact with several hundred G-protein molecules and thereby catalyze their nucleotide exchange. $\text{G}_\alpha(\text{GTP})$ activates the cyclic GMP phosphodiesterase by removing an inhibitory subunit from it. The photon signal is thus amplified in two stages: one photon leads to activation of several hundred phosphodiesterase molecules, each of which hydrolyzes about 1000 molecules of cyclic GMP per second. The activating capacity of $\text{G}_\alpha(\text{GTP})$ is slowly terminated by its intrinsic GTPase activity.

Recent experiments with purified G-protein and purified, lipid-free rhodopsin in detergent solution have shown that the light-induced binding of G-protein to R^* , and the subsequent nucleotide exchange, take place even in the absence of membranes.

Symposium on Applications of Synchrotron Radiation

MACROMOLECULAR CRYSTALLOGRAPHY USING SYNCHROTRON RADIATION

R. Fourme, LURE, CNRS-Université Paris-Sud, Orsay, France.

Abstract.

Macromolecular crystallography is highly dependent on the state of available technology. In particular, the advent of bright and tuneable synchrotron radiation sources (SR) in several countries has changed both quantitatively and qualitatively the collection of diffraction data; further, new orientations have been stimulated and sociological changes have been induced in this field, at least in some countries such as France and UK.

(i) Brightness: When using the standard data collection method (rotation camera) and the presently available bending magnet SR sources, exposure times are reduced by about two orders of magnitude when compared to a rotating anode tube and, in most cases, radiation damage for a given dose is lower for the higher dose rate. It is then possible, in a significant number of cases, to measure more accurate data to a higher resolution. This is a breakthrough for complex structures, molecular assemblies and/or unusually small samples. Experimental constraints such as low temperature are relaxed when using SR; this is of concern for studies of molecular vibrations at various temperatures through an analysis of temperature factors or in substrate-binding experiments. Finally, kinetic experiments on a sub-millisecond time-scale are in progress. A systematic investigation of the radiation damage with even brighter SR sources such as wigglers has been undertaken, possibly combined with very low temperature operation.

(ii) Tunability: One application of tunability is the use of short wavelengths, in the range 0.6-1 Å, in order to reduce absorption effects. Another application is related to optimised anomalous dispersion at one or several wavelengths, either to locate metal cofactors or to solve the phase problem. As an example, we will describe an experiment performed at LURE on a single crystal of a Tb-labelled parvalbumin; using data measured with an electronic area detector at three wavelengths close to the LIII absorption edge of Tb, an electron density map has been calculated.

SR sources stimulate innovations in instrumentation, such as monochromators, beam monitors, data acquisition systems and electronic area detectors. Up to now, the high brightness has been used in some respects to counter balance inefficiencies of films. The latest electronic detectors may give a new chance to conventional X-ray sources in high resolution data collection and they are adequate for anomalous scattering experiments with SR sources. But processing the tremendous flow of information which is potentially available in a focused beam diffraction experiment with a bending magnet SR source or, a fortiori, a wiggler source is yet an unsolved problem.

Finally, we discuss "sociological" changes which have been induced or accelerated by SR sources in connection with the concentration and sharing of advanced and/or expensive instruments at SR facilities.

Symposium on Applications of Synchrotron Radiation

EXAFS AND XANES : APPLICATION TO BIOLOGICALLY INTERESTING SYSTEMS

S S Hasnain, Daresbury Laboratory, Warrington WA4 4AD, Cheshire, England.

Extended x-ray absorption fine structure (EXAFS) and x-ray absorption near edge structure (XANES) have been increasingly used to investigate the environment of a specific atom (eg Fe in Haemoglobin) in a biological system. Various aspects of the technique will be briefly reviewed. Examples are chosen to illustrate some of the strengths and limitations of the technique. Results are presented on type 2 copper proteins, Cu-Zn superoxide dismutase and dopamine β -monooxygenase, where direct structural information is obtained for the catalytic site.

For example, the copper and zinc K-edge-EXAFS have been measured for the metal sites of oxidised and reduced bovine superoxide dismutase in aqueous solution. Detailed analysis of the spectra indicates that the copper site of the enzyme changes upon reduction and is most probably coordinated to three imidazole groups at a shorter distance $\text{Cu-N}(\alpha) = 0.194\text{nm}$ (1.94\AA) in the reduced form compared to a coordination of four imidazoles at 0.199nm (1.99\AA) and an oxygen atom from solvent water at 0.224nm (2.24\AA), in the oxidised form. Examination of the edge, near edge structure and EXAFS of the zinc sites indicates that the stereochemical changes at copper which accompany reduction introduce minimal perturbation on the stereochemistry at zinc.

EXAFS results on the studies of calcium in bone, milk and arthropathic deposits are presented illustrating the advantage of the technique for probing subtle changes in amorphous biological systems. Polarisation dependence of the XANES is shown for a myoglobin and carbonyl bound single crystal to illustrate the potential of obtaining detailed geometrical information of the ligands around the Fe atom.

Symposium on Application of Synchrotron Radiation

X-RAY MICROSCOPY

G. Schmahl, Forschungsgruppe Röntgenmikroskopie, Universität Göttingen, Geismarlandstraße 11, Göttingen, Fed. Rep. of Germany

X-ray microscopy fills a gap between optical and electron microscopy. Using soft x-rays a higher resolution than with visible light can be obtained. In comparison to electron microscopy thick, wet, unstained specimens can be examined using a natural contrast mechanism caused by an order of magnitude difference between the absorption coefficients for water and e.g. protein in the soft x-ray region between 2,3 nm and 4,4 nm.

X-ray microscopy was started with considerable enthusiasm in the 1950's. This initial enthusiasm, however, slowed down after it became evident that the achievement of high resolution and short exposure time was beset with considerable experimental difficulties. The renewal of interest in x-ray microscopy is caused by the development of intense soft x-ray sources, the use of high resolution x-ray resists for contact x-ray microscopy (x-ray microradiography) and the development of improved x-ray optics.

X-ray contact microscopy experiments have shown /1/ that in living specimens features of about 10 nm can be detected with soft x-rays. This high resolution, however, can be obtained with this method only for very thin layers of about 50 nm which are in direct contact to the recording medium. For imaging of thicker specimens, e.g. mammalian cells, x-ray optical elements, i.e. x-ray lenses or x-ray mirrors are necessary.

During the last years an x-ray microscope has been developed at the University of Göttingen based on the development of condenser zone plates and high resolution micro zone plates as x-ray lenses. The x-ray microscope had been installed up to spring 1982 at the ACO electron storage ring in Paris/Orsay. Since spring 1983 an improved version of the microscope is established at the BESSY electron storage ring in Berlin. The x-ray optical and mechanical set up of the system is described in /2/. X-ray microscopy experiments of biological specimens with a resolution of 50 nm and exposure times of a few seconds have been performed using this microscope with synchrotron radiation of the storage ring in the wavelength region between 2,3 nm and 4,5 nm.

Scanning x-ray microscopes, i.e. systems in which the object is scanned through a small x-ray spot, are under development in several laboratories /3/ because of the advantageously reduced radiation dose of such systems compared with imaging x-ray microscopes.

For further work in x-ray microscopy for biological and medical applications the following points are most important: (1) Close cooperation between biologists and physicists in performing biological research programs, (2) development of improved x-ray lenses, namely lenses with higher resolution and higher diffraction efficiencies, (3) use of improved x-ray sources, as e.g. undulators in electron or positron storage rings and the development of intense pulsed laboratory sources for soft x-rays.

1 B.J.Panessa-Warren, in "X-Ray Microscopy", Eds.G.Schmahl and D. Rudolph, Springer Series in Optical Sciences Vol.43 (1984),p.268; R.Feder et al,ibid.,p.279; P.C.Cheng et al,ibid.,p.285

2 D.Rudolph et al,ibid.,p.192

3.H.Rarback et al,ibid.,p.203; B.Niemann,ibid.,p.217;E.Spiller,ibid p.226

Symposium on Rheology of Cell Membrane

RHEOLOGY OF RED BLOOD CELL MEMBRANE

R. Skalak, Bioengineering Institute, Department of Civil Engineering and Engineering Mechanics, Columbia University, New York, New York, U.S.A.

The red blood cell membrane is modelled as a thin viscoelastic shell. Depending on the type of stress and strain applied, the properties of membrane elasticity, viscosity, bending stiffness or plastic behavior may be predominant. An important feature of the membrane elasticity is that the elastic modulus associated with changes of area is about four orders of magnitude greater than the modulus of elasticity associated with shear deformations at constant area. Because of this feature the motions of the red blood cell membrane take place at essentially constant area under most circumstances. The membrane fractures if the areal strain is greater than about two or three percent. Due to the low shear modulus large deformations are possible at low shear stresses at constant area. These moduli are measured by micropipette experiments. The bending stiffness gives the red blood cell its normal smooth biconcave disk shape. The bending stiffness is due to a combined action of the lipid bilayer and the cytoskeleton. It is important only under relatively small stresses. It is essential to the computation of the shapes of red blood cells during osmotic sphering and in rouleau formation. At high stresses the membrane tensions predominate and the influence of viscosity may be important under rapid motions such as the sudden entrance of a red cell into a capillary. The plastic deformation of the membrane leads to permanent deformations. The plasticity can lead to formation of very long thin tethers. The relatively constant area of the red blood cell membrane is considered to be a reflection of the structure of the lipid bilayer of the membrane. The membrane elasticity in shear is primarily due to the network of protein macromolecules on the endoface of the membrane. This cytoskeleton evolved continuously during a prolonged deformation. This results in a fading memory behavior in which the preferred configuration of the membrane from which elastic strains are measured may not coincide with the initial stress free configuration. The model incorporating evolving preferred configuration reproduces the observed behavior in which the time constants of transient deformation are different in the loading and recovery phases of pipette experiments. This model also predicts that in tank-treading motions the elastic strains gradually decrease and the primary influence of the membrane is its viscous behavior during a steady tank-treading motion. For capillary flow, a model of an elastic membrane with constant surface area but neglecting bending stresses is found to give realistic results for the shapes and apparent viscosities in the microcirculation. Rouleau formation is studied with a model including bending resistance and a surface energy of adhesion. The final state is found by the minimization of a total potential energy including the strain energy (free energy) of the membrane and the surface adhesion energy. The model computation allows an estimate of the adhesion surface energy to be derived from the known properties and experimental observation of the red blood cell shapes in rouleaux.

REFERENCES

1. Skalak, R., A. Tözeren, R.P. Zarda, and S. Chien. 1973. Strain energy function of red blood cell membranes. *Biophys. J.* 13:245-264.
2. Tözeren, A., R. Skalak, B. Fedorciw, K.L.P. Sung, and S. Chien. 1984. Constitutive Equations of Erythrocyte Membrane Incorporating Evolving Preferred Configuration. *Biophys. J.* 45:541-549.
3. Evans, E.A., and R. Skalak. 1980. *Mechanics and thermodynamics of biomembranes*. CRC Press, Boca Raton, FL. 129-141.
4. Fischer, T.M., and P. Schmid-Schönbein. 1977. Tank tread motion of red cell membranes in viscometric flow: behavior of intracellular and extracellular markers (with film). *Blood Cells*. 3:351-365.

Symposium on Rheology of Cell Membrane

MEMBRANE CYTOSKELETON DYNAMICS

M.P. Sheetz, Department of Physiology, University of Connecticut Health Center, Farmington, Connecticut. USA 06032.

The rheological properties of membranes result from the specific organization of the membrane components and the rate of making and breaking (i.e. dynamics) of associations between components. In the erythrocyte, the plasma membrane is composed of two primary structural elements; the lipid bilayer and the membrane cytoskeleton or shell. Because the lipids are in a fluid state, the bilayer provides little resistance to mechanical shear; however, the continuity of the bilayer and the asymmetry of the bilayer surfaces make it possible to produce membrane bending forces by asymmetric changes in bilayer surface area (Bilayer Couple hypothesis (1)). The shear elasticity properties of the erythrocyte are believed to be determined primarily by the nature of the membrane skeleton. We submit that rapid deformations (<10 sec) sample the existing organization of the skeleton whereas under prolonged deformations (>1 min) rearrangements in the membrane skeleton occur to produce the fading memory of previous morphology. Because of the high concentration of the major membrane skeletal components, spectrin, actin and band 4.1, at the cytoplasmic surface, they are largely associated (>99% based on measured K_a 's) and alterations in association constants will most dramatically affect the dynamics of spectrin-spectrin and spectrin-actin associations. We have evidence that the lateral diffusion rate of membrane glycoproteins (primarily the anion channel, band 3) like membrane plasticity is related to the dynamics of skeletal associations (2). Control of lateral diffusion has been explained by a matrix model (3) in which the spectrin-actin network forms physical corals which fence in membrane glycoproteins and lateral diffusion of glycoproteins requires the breaking of the links which form the fence. It has been found that soluble polyanions will dissociate spectrin from actin and will increase glycoprotein lateral diffusion rates (2). The highly anionic lipid, triphosphoinositide, can also increase membrane skeleton dynamics in the red cell. These findings suggest a role for polyanionic metabolites in regulating membrane skeleton dynamics and membrane rheological properties as well (4). Indeed recent findings of Chasis et al (Blood 60: 23a (1982)) do show an increased fragmentation of erythrocyte membranes under shear in the presence of the endogenous polyanion, 2,3-diphosphoglycerate. Because of the presence of other spectrins and actins in membrane skeletons of other cells, it is possible that the mechanisms of control of membrane skeleton dynamics in the erythrocyte may be generally applied to control glycoprotein lateral mobility and membrane rheological properties in other cells.

REFERENCES

1. Sheetz, M.P. and S.J. Singer. 1974. Biological membranes as bilayer couples. A mechanism of drug-erythrocyte interactions. Proc. Natl. Acad. Sci. USA 22: 4457-4461.
2. Schindler, M., D.E. Koppel, and M.P. Sheetz. 1980. Modulation of membrane protein lateral mobility by polyphosphates and polyanions. Proc. Natl. Acad. Sci. USA 77: 1457-1461.
3. Koppel, D.E., M.P. Sheetz, and M. Schindler. 1981. Matrix control of protein diffusion in biological membranes. Proc. Natl. Acad. Sci. USA 78: 3576-3580.
4. Sheetz, M.P. 1983. Membrane skeletal dynamics: role in modulation of red cell deformability, mobility of transmembrane proteins, and shape. Semin. Hematol 20: 175-188.

Symposium on Rheology of Cell Membrane

MEASUREMENT AND ANALYSIS OF FORCES AT MEMBRANES AND SURFACES

J.N. Israelachvili, Department of Applied Mathematics, Research School of Physical Sciences, Australian National University, Canberra, Australia.

We review experimental measurements of the four major forces that occur between colloidal and bio-colloidal surfaces, such as lipid bilayers and biological membranes, in aqueous solutions. These are (i) attractive *van der Waals* forces, (ii) repulsive *electrostatic* (*double-layer*) forces, (iii) *hydration* (or *solvation*) forces which arise from the ordering (structuring) of water molecules around hydrophilic or hydrophobic surface groups (these forces can be repulsive or attractive), and (iv) repulsive *steric* forces which arise from the thermal motions of hydrated surface groups. Sufficient experimental data is now available from direct measurements of these forces to allow for some reliable estimates to be made of their magnitude and range, and the conditions under which one or other of these forces will dominate.

The attractive van der Waals force between bilayers and membranes is long-range (effective out to 15nm), but this force is weak and largely nonspecific. Van der Waals forces can cause membranes to come together and adhere weakly, but the strong tight adhesion and fusion of membranes is almost certainly brought about by other, stronger and more specific, interactions.

The repulsive electrostatic double-layer force between highly charged membrane surfaces in high salt — corresponding to physiological conditions can stabilize the van der Waals force at aqueous separations of 3-5nm. However, biological membrane surfaces are rarely highly charged, especially in the presence of divalent cations; and the most common lipids in both animal and plant membranes are themselves uncharged (these being the zwitterionic phosphatidyl cholines and ethanolamines in animals, and the nonionic mono- and di-galactosyldiglycerides in plants).

There is now clear evidence that there are additional strongly specific short-range (< 3nm) repulsive hydration forces between surfaces, especially between surfactant and lipid bilayer surfaces. These forces arise from the energy needed to dehydrate hydrophilic surface groups. Hydration forces can be *intrinsic* to a surface, e.g. in the case of the uncharged lipids mentioned above, or they can be *regulated*, e.g. by changing the pH and/or exchanging the cations adsorbed onto surfaces — the more hydrated the bound ions the stronger the hydration force. Hydration forces are particularly important in regulating the short-range interactions of biological membranes, e.g. their adhesion and stacking (as occurs in plant thylakoid membranes).

At very short distances, below 1nm, hydration forces can be oscillatory, having energy minima at discrete separations corresponding to integral numbers of water molecules, though the thermal motions of fluid membranes and their surface groups (e.g. lipid head-groups) can smear out the oscillatory component, resulting in a purely monotonic repulsive force law. Further, between two hydrophobic surfaces the hydration force is attractive. This *hydrophobic interaction* is much stronger than, but of comparable range to, the van der Waals interaction.

It is proposed that at distances below 2-3nm the major forces between bilayers and membranes are the repulsive hydration and attractive hydrophobic forces (rather than the double-layer and van der Waals forces). But it is still not clear how these two interactions operate simultaneously when hydrophilic and hydrophobic groups are in close proximity (as occurs at membrane surfaces).

Finally, it is well to note that the same forces mentioned above also govern the physical properties of *isolated* bilayers and membranes, e.g. they determine head-group areas of lipid molecules. Consequently, there is an intimate correlation (interdependence) between inter-membrane and intra-membrane interactions.

Symposium on Electric Field Effects in Cell Membranes

THE REGULATORY ROLE OF ELECTRIC MEMBRANE FIELD-CALCULATIONS
AND MODEL EXPERIMENTS ON ERYTHROCYTES

R. Glaser, Bereich Biophysik, Sektion Biologie,
Humboldt-University, Berlin GDR

The structure of the membrane electric field is determined by the double layers on both sides as well as by the transmembrane phase potential difference inside-out. Even under physiological conditions potential differences up to 100 mV may occur producing considerable field strength. The field, of course, is not only spread in the direction perpendicular to the membrane area but exhibits a complicated three-dimensional function. As a first approach however we analysed the situation only in one dimension. For human erythrocytes, being the most simple and most intensively investigated cell, the following charge distribution was considered: Hemoglobin charges as well as charges of slowly exchangeable ions in the inside bulk phase, fixed charges of the spectrin layer, negative charges of the phosphatidylserine head-groups in the inner lipid leaflet, dissociated carboxyl groups of the neuraminic acids in the outer surface coat of the cell (glycocalyx). For the distribution of the fixed charges in the glycocalyx as well as in the spectrine layer a rectangular function $\rho(x)$ is considered. For this charge distribution the POISSON-BOLTZMANN-equation is formulated and solved by iteration avoiding linearization. Additionally it is taken into consideration that the charges of hemoglobin strongly depend on pH. Therefore this model is connected with the occurrence of stationary ionic states in erythrocytes under special conditions. This theoretical background enables us to define more or less realistic electrostatic conditions of erythrocytes in definite experimental situations.

Experiments were undertaken to check the calculated conditions and to follow the influence of field strength and local potentials on various membranal functions. We chose the variation of the potential by changing the outside ionic strength as well as pH-value. In solutions of decreasing ionic strength the transmembrane potential increases strongly. Changing the membrane permeability using ionophores like nystatine or amphotericine, in case of lowered ionic strength, such conditions could be obtained where the transmembrane potential strongly depends on the outside pH. It could be shown that the shape transformation, the passive potassium transport and the active sodium transport are functions of the transmembrane potential.

The interpretation of these experiments leads to the conclusion that the electric field may influence membrane functions in quite distinct ways. The passive transport processes are strongly dependent on local concentrations in the electric double layers. Transport-proteins are influenced additionally directly by the electric field strength. Complicated feedback mechanisms are to be considered, especially in view of the dynamical structure of the glycocalyx, which is determined by the electrostatic interaction of its own fixed charges. It seems that the human red blood cell as the simplest and most investigated cell is a useful model for studying this question.

Symposium on Electric Field Effects in Cell Membranes

ELECTRIC FIELD-INDUCED CELL FUSION

U. Zimmermann, Lehrstuhl für Biotechnologie der Universität Würzburg,
Röntgenring 11, Würzburg, FRG.

In 1978 electric-field-mediated fusion was discovered for the first time. Exposure of cell suspension to electric fields of appropriate geometry, magnitude, and frequency can be used to induce cell fusion. Specifically, the application of high-frequency, inhomogeneous field to a cell suspension causes the cells to drift in the direction of the field-inducing electrodes and to form cell chains parallel to the direction of the field. Exposure of the chains to a field pulse of very high intensity (kV/cm) and very short duration (microseconds) causes reversible electrical breakdown of adjoining membrane surfaces and large localized increases in permeability in the breakdown area. Cytoplasm exchange between the adjoining cells may then lead to fusion. Such electrically-induced cell fusion has been applied successfully to a variety of cell types including plant protoplasts, yeast cells, Friend cells and liposomes, and has been used to produce giant cells from as many as one thousand erythrocytes. Electric field-induced preparation of both animal and human hybridomas and yeast hybrids has also been achieved and has been found to exhibit efficiency several orders of magnitude better than traditional chemical- and virus-induced fusion procedures. Other advantages of the method include the ability to monitor the process beneath a microscope, to preselect the number and type of cells to be fused, and to control the dynamics of the fusion process by selection of electrical conditions determined to be least traumatic to the cells being treated.

Symposium on Electric Field Effects in Cell Membranes

CONTROL OF SPERM EGG FUSION BY MEMBRANE POTENTIAL: PATCH RECORDING DURING ACTIVATION OF *RANA PIPIENS* EGGS. L.A. Jaffe, R.T. Kado and L.F. Muncy, Department of Physiology, University of Connecticut Health Center, Farmington, Connecticut U.S.A., and Laboratoire de Neurobiologie Cellulaire, Centre National de Recherche Scientifique, Gif-sur-Yvette, FRANCE.

At fertilization, a single sperm nucleus must combine with the egg nucleus to preserve the normal genetic complement of the new individual; participation of more than one sperm nucleus leads to death of the embryo. In order to prevent polyspermy, some species use an electrical mechanism. At fertilization, the egg membrane potential shifts from a negative to a transiently positive level. The positive potential prevents additional sperm from fusing with the egg membrane.

We have been investigating the ionic mechanism of the fertilization potential in the egg of the frog, *Rana pipiens*. For the 20 minute period during which the egg's membrane potential is positive (about +15 mV) the egg membrane is permeable to chloride and potassium ions; the conductance is maximum during the first three minutes (see N.L. Cross and R.P. Elinson, 1980, *Develop. Biol.* 75, 187-198, and L.C. Schlichter and L.A. Jaffe, 1984, *Biophys. J.* 45, 23a). In the present study, we investigated the distribution of the chloride and potassium channels on the egg surface. We used patch electrodes to record current from localized regions of the egg membrane (pipet tip diameter = 1-10 μ m). The jelly and vitelline envelope of the egg were removed mechanically after a few minutes treatment with protease. Seal resistances of up to one gigohm were obtained. Because fertilization of naked eggs is difficult, we artificially activated the eggs, which results in an activation potential. Previous work (Schlichter and Jaffe, 1984) has shown that artificial activation produces conductance changes very similar to those at fertilization.

In most experiments, the bath solution contained 10% Ringers, which includes 12 mM Cl^- and .2 mM K^+ , and the patch pipet contained .5 mM Cl^- and .2 mM K^+ . Under these conditions, the chloride conductance produces an inward current, while the potassium conductance produces an outward current. In some patches, both currents are seen, with an outward current initially and an inward current superimposed. In a given patch, the current appears 10 seconds to three minutes after the rise of the activation potential. It is largest for a period of several seconds, but a smaller current sometimes persists for minutes. The potassium current can be blocked with 10 mM TEA; usually the remaining current is almost entirely inward.

By recording simultaneously with two patch electrodes, we determined that the activation-induced chloride and potassium conductances appear first in the animal region of the egg and then in the vegetal region. The delay between the current recorded from a patch in the animal region and another patch in the vegetal region is one to two minutes. With two electrodes close together, the activation-induced currents occur at about the same time.

In small patches (about 1 μ m tip diameter), we see single channel openings and closings which produce the potassium current. The single potassium channel conductance, in 10% Ringers, is about 30 to 40 picosiemens. Channel opening is voltage-dependent, becoming more probable as the membrane is depolarized. These channels can also be seen in the unfertilized egg, but their probability of being open, at a given potential, increases greatly after fertilization.

Supported by USPHS grant HD14939 to L.A. Jaffe, and a grant from the Philippe Foundation to R.T. Kado.

Symposium on Developments in Microscopy

A SHORT REVIEW OF NEW METHODS OF ELECTRON MICROSCOPY OF BIOLOGICAL MATERIAL
E. Kellenberger, Department of Microbiology, Biozentrum of the University of
Basel, Basel, Switzerland.

The imaging of biological structures is not limited by the resolving power of modern instruments but related to the specimen preparation. The limitations are the following (i) distortions due to collapses due to surface tensions and thermal agitation. (ii) Distortions (or denaturations) and precipitations induced by organic liquids, (iii) completely unknown location of heavy metal stains and finally, (iv) the electron beam induced destruction during observation.

(i) Collapses can become reduced by partial or complete embedding. Here the observation of thin layers of frozen hydrated particle suspensions, when still in ice and in absence of a supporting film has given outstanding results at the EMBL (1). (iii) Stain location can become studied by a new imaging mode, the Z- or ratio contrast, which allows high contrast with unstained material and which minimizes the influence of the surface relief e.g. on thin sections (2).

Cryo-methods become successfully developed: besides the frozen hydrated suspensions, frozen hydrated cryosections made at the EMBL produced new informations (3) in agreement with cryosubstitution and low temperature resin embeddings. The latter which however allow higher resolutions by being thinner, and obviously on section cytochemical labeling is possible.

The envelopes of *E. coli* show a periplasmic gel of regular thickness inbetween inner and outer membrane (4); the nucleoids are much less confined than assumed previously. Their shape is modified by chloramphenicol, but it is no longer dependent on the salt concentration of the growth medium (5). With virus related particles we demonstrate morphological alterations due to the embedding procedures. With septate junctions we show that staining does not occur on the hydrophobic part of transmembrane proteins (2).

We will speculate on potential further improvements by using cryolenses, where the specimen is held at temperatures near 10°K.

References:

- (1) Adrian, M., Dubochet, J., Lepault, J. and McDowell, A.W. (1984) *Nature* **308**, 32-36
- (2) Carlemalm, E. and Kellenberger (1982) *The EMBO Journal* **1**, 63-67
- (3) Dubochet, J., McDowell, A.W., Menge, B., Schmid, E.N. and Lickfeld, K.G. (1983) *J. Bacteriol.* **155**, 381-390
- (4) Hobot, J., Carlemalm, E. and Kellenberger, E.: The periplasmic gel: a new concept resulting from the reinvestigation of bacterial cell envelope ultrastructure by new methods. *J. Bacteriol.*, submitted
- (5) Hobot, J., Villiger, W., Escaig, J., Maeder, M., Ryter, A. and Kellenberger, E.: The organisation of the bacterial nucleoid and DNA fine structure as observed by freeze-substitution under different environmental conditions. *J. Bacteriol.*, to be submitted.

Symposium on Developments in Microscopy

ANALYTICAL ELECTRON MICROSCOPY IN BIOLOGY. A.P. Somlyo, Avril V. Somlyo and H. Shuman, Penn. Mus. Inst., Univ. of Pa. School of Med., Phila., PA U.S.A.

Principles and applications of electron optical methods suitable for determining the subcellular distribution of elements and for obtaining elemental images will be reviewed. Electron probe X-ray microanalysis (EPMA) utilizes the production of X-rays having energies characteristic of the elements irradiated by a focussed electron beam. In ultrathin cryosections of rapidly frozen tissues, the elemental content of cell organelles can be measured with EPMA with a sensitivity (for Ca) better than 1mmol/kg dry wt. and a spatial resolution of $\sim 50\text{nm}$ (1,2). Studies of frog skeletal muscle showed that the sarcoplasmic reticulum (SR) is not in ionic communication with the extracellular space and that, during both tetanus (3) and caffeine contracture (4), the release of Ca from the terminal cisternae (TC) of the SR is associated with an uptake of Mg and K into the TC. The post-tetanic return of Ca from the cytoplasm to the TC was shown to have a $t_{1/2}$ of 1sec, similar to the off-rate of Ca from parvalbumin, and to be followed by a delayed release of Mg from the TC. EPMA also demonstrated that mitochondria in situ do not accumulate Ca^{2+} at physiological $[\text{Ca}]$ ($< 5 \times 10^{-6}\text{M}$) (5), and has been used to study epithelial cell electrolytes (2,6). Recently, EPMA was used to determine the effects of illumination on the ionic composition of the outer and inner segments and of mitochondria in retinal rods (Walz et al. these Proc.), and to show the release of Ca from the SR in smooth muscle.

X-ray maps showing elemental distribution to a resolution of 8.7nm can be generated by recording the characteristic X-rays in a two-dimensional array while the electron beam is scanned over the specimen (1). The distribution of various elements (Na, K, Mg, Ca) in muscle and in bacterial spores has been determined in this fashion (1).

Electron energy loss spectroscopy (EELS) involves the detection of the energy spectrum of electrons that have lost energy as the result of inelastic interactions with the specimen. Advantages of EELS over EPMA include the ease of analyzing elements having low atomic numbers (e.g.: C,N,O), larger signals due to better detection efficiency and the utilization of larger (outer shell) ionization cross-sections, and the availability of information about chemical states (1). Disadvantages include problems due to plural electron scattering and a large background due to plasmon and carbon K shell scattering. The detection sensitivity of EELS for Ca at high resolution is better than that of EPMA.

Images showing the distribution of characteristic elements can be generated with EELS either in a conventional transmission electron microscopy (CTEM) mode (e.g. Fe in ferritin, P in ribosomes, 1), or by collecting the loss electrons for each pixel of a rastered (STEM) image. Accurate subtraction of the usually large background is essential for both methods. Chromatic aberrations, in the filtered CTEM, and probe size in STEM mode are technical limits on resolution. The physical limit to resolution due to delocalization of the inelastic scattering event is estimated to be $\sim 1\text{nm}$ for 100eV loss at 100keV (7). Images of Ca distribution obtained by collecting parallel spectra (C through N) pixel-by-pixel to form EELS-STEM will be demonstrated. The ultimate resolution attainable in analytical electron microscopy will be determined by radiation damage. Low dose EELS imaging is conceptually feasible, but may prove technically difficult, due to the much lower cross-sections for inelastic than elastic scattering. In any event, the visualization of elemental distribution in cells and organelles with EPMA and EELS will represent a major application of electron microscopy to biology.

Supported by HL15835 to Pa. Mus. Inst. & Trg Gr. 07499. 1) Somlyo, A.P. & Shuman, H. *Ultramicroscopy* 8: 219, 1982; 2) Hall, T.A. & Gupta, B.L. *Quar. Rev. Biophys.* 16: 279, 1983; 3) Somlyo, A.V., Gonzalez-Serratos, H., Shuman, H., McClellan, G. & Somlyo, A.P. *J. Cell Biol.* 90: 577, 1981; 4) Yoshioka, T. & Somlyo, A.P. *Biophys. J.* 45: 319a, 1984; 5) Somlyo, A.P., Somlyo, A.V., Shuman, H., Scarpa, A., Endo, M., and Inesi, G. In: *Calcium Phosphate Transport Across Biomembranes*. F. Bronner & M. Peterlik, eds. Academic Press, NY, 87, 1981; 6) Civan, M.M. *Epithelial Ions & Transport*. 1983; 7) Bourdillon, A.J. et al. *Phil. Mag A* 44: 1335, 1981.

Friday 03 August **Unicorn Hotel-Trident Suite** **14.00-17.00**

Symposium on Developments in Microscopy

SCANNING TUNNELING MICROSCOPY

Prof. H. Rohrer, Dr. Gross, C. Binnic, I.B.M. Zurich Research Laboratory,
Saunerstr. 4, CH-8803 Ruschlikon, SWITZERLAND.

Scanning Tunneling Microscopy is a novel method for real space three-dimensional imaging of surfaces on an atomic scale. The method so far has been applied to structural imaging of surfaces, in particular surface reconstruction. Extension to chemical imaging is very promising and the possibility to apply the method to biological matter is presently explored. Our first example is DNA.

Symposium on Environmental Biophysics

SIMPLE MODELS OF BIOGEOCHEMICAL CYCLES

G. R. Williams, Department of Biochemistry, Scarborough Campus, University of Toronto, Canada M1C 1A4.

Most modelling of biogeochemical systems has aimed at simulation and has therefore had to incorporate as much of the complexity of the modelled system as possible. If the purpose of modelling is characterization it is more useful to start with the simplest possible generalized scheme with the minimum number of parameters. The simplest conceivable model would have two compartments (nutrient and biota) but for most purposes it is necessary to introduce a "dead-organic" pool through which at least some of the nutrient is regenerated. For a "closed" system (e.g., a global model) a fourth "abiotic" pool is introduced but "open" three-compartment systems can be represented as subsets of the four-compartment system if the abiotic pool is given dimensions sufficiently large that it approximates a constant environmental source and/or sink. Even a minimal four-compartment system needs five constants for the characterization of its steady-state. Three of these are algebraic combinations of the rate-constants governing the flow of a given chemical element between the abiotic, nutrient, "dead organic" pools and the biota. The remaining two are the "Michaelis constant" for nutrient and the "carrying capacity" of the system (a measure of the restriction of biotic growth by non-modelled factors). Many multi-box models ignore these latter two and assume either first- or second-order relationships. The simple model makes it possible to test easily the consequences of assuming these limiting cases. Sensitivity analysis is employed to show the quantitative effect of perturbation of any given rate-constant. It is thus possible to construct a taxonomy of eco-systems based on their responsiveness to disturbance. For most eco-systems the data are not available to permit such characterization and the virtue of simplification is that it makes clear the sort of information that is needed for impact assessment.

Another major advantage of ultra-simple models is that they are isomorphous for different elements and it becomes possible to consider the interactions between biogeochemical cycles. Two such four-compartment cycles may be coupled either by mass-action effects (Liebig's law) or by strict stoichiometry (Redfield ratios). If the rate-equations are written in such a way that the growth rate of the biota is a function of both nutrient pools, the coupling exhibits positive feed-back and time-dependent solutions can exhibit complex oscillatory behaviour, the amplitude and phase of which is determined by the same five constants that govern the steady-state plus cross-coupling coefficients ("Michaelis constants" for the alternate nutrient). The principal factor restraining such oscillations is however the strictness of the stoichiometry between the elements making up biomass. The constancy of these proportions is currently the subject of considerable discussion among ecologists. This analysis demonstrates that the issue is of major theoretical importance.

Symposium on Environmental Biophysics

THE MAUNA LOA ATMOSPHERIC CO₂ RECORD IN CONNECTION WITH MAN'S IMPACT ON THE TERRESTRIAL VEGETATION

G.H. Kohlmaier, Institut für Physikalische und Theoretische Chemie, Universität Frankfurt, Robert-Mayer-Straße 11, Frankfurt am Main, FRG

Despite of the clearing of virgin tropical forests of $11.3 \cdot 10^6$ ha/a (Lanly, FAO) or even higher clearing rates (Myers) and despite of the negative effects of acid precipitation over Europe and the Eastern United States and Canada the amplitude of the seasonal cycle of atmospheric CO₂, believed to be mainly caused by the photosynthesis/respiration patterns of the terrestrial vegetation, has been increasing over the past 25 years by approximately 16%, indicating an increased seasonal net ecosystem production. Part of this increase in the amplitude of the seasonal cycle may be due to a CO₂ stimulation effect in connection with other anthropogenically released nutrients like N, S or PO₄³⁻. However, models of the changing seasonal net ecosystem production/net ecosystem respiration cycle as a function of human impacts show, that these fertilization effects alone cannot account for the observed amplitude increase. Other effects to be considered include afforestation and regrowth in the temperate and boreal forests, increased agricultural production in the temperate and tropical zones, conversion of tropical and subtropical forests into cropland and pasture as well as selective logging and small changes in oceanic productivity. The seasonal cycle, however, could have been also changed by the increased use of fossil fuels affecting the seasonal amplitude by the difference in summer/winter atmospheric transport across the equator, or by different summer/winter use of the fossil fuels itself.

Simulation models based on national forest inventories and remote sensing data have been developed to describe the net CO₂ exchange between atmosphere and terrestrial biota during the Mauna Loa period between 1958 and 1983. In particular, a regional model for the tropics and the subtropics has been designed pointing out the differences between Tropical Latin America, Tropical Africa and Tropical Asia in shifting cultivation practices, conversion of forest to agricultural land, selective tree logging and use of wood and litter as fuel and fertilizer. A model for the temperate and the boreal zone emphasizes features such as regrowth of younger forests to the climax state, of abandoned agricultural lands to woodlands as well as the fertilization through anthropogenically released nutrients.

Plenary Lecture by P.L. Privalov

ENERGETICS OF PROTEIN STRUCTURE

P. L. PrivalovInstitute of Protein Research, Academy of Sciences of the USSR,
Pushchino, Moscow Region, USSR

Our conception of protein structure is based mainly on the information obtained from two independent sources: chemical studies of the amino acid sequence in protein polypeptide chains (primary structure of protein) and crystallographic studies of the three-dimensional arrangement of these residues in native protein (tertiary structure of protein). However to connect these two levels of protein organization and to understand the mechanism of transformation of linear information contained in the sequence into a three-dimensional one, we need independent information, principally undeducible from the first two, on the energy grounds of this transformation, i.e. on the energy grounds of the unique arrangement of groups in native protein notwithstanding the dissipative action of thermal motion. This information can be obtained by studying the energy of disordering the arrangement of protein groups at an increase in thermal motion intensity. Experimentally this can be done by the scanning microcalorimetric technique designated specially for this purpose.

Studies on various proteins and their fragments show that at temperature increase the native protein structure disrupts stepwise, absorbing discrete energy portions. The energy discreteness of protein reflects the structural discreteness of these macromolecular systems which present a set of more or less independent, but quite definite, cooperative subsystems. The subdivision into structural subunits, i.e. domains, and the extremal cooperativity of the subunits appears to be a general principle of structural organization of proteins, which seems to have an evolutionary, functional and physical basis.

Physically, the discreteness of protein structure proceeds from the necessity of cooperation of many weak secondary interactions to withstand against thermal motion at physiological temperature and of limitations imposed on their cooperation. For heterogeneous polymers extensive cooperation is principally improbable and can be realized only in the case of some exceptional sequences of limited length which can fold into unique compact structures. The compact packing of groups into clusters with the separation of the water phase seems to be essential for cooperation which is unlike to be a simple summation of all the possible efforts. However, the mechanism of cooperation is still obscure.

The cooperative unit of proteins usually includes from 50 to 200 amino acid residues. Thus, a small protein can consist of a single cooperative domain while a large protein can consist of several domains. The interaction between the domains varies to a very broad extent from positive to negative values, manifesting a tendency of domains to attach or to reject each other. In some cases domain interaction changes significantly at modification of protein, e.g. at activation of proteolytic enzymes, indicating that the subdivision into domains can be important for protein functioning.

The discreteness of protein structure caused by the physical limitation on the cooperative domains suggests that protein evolution has proceeded by the joining of domains, i.e. by the joining of sufficiently long peptides capable of forming a compact and stable structure. This concept is supported by the finding of long homologous regions in protein sequences and the establishment of the fact that these regions usually form distinct domains in proteins. One can imagine that the joining of long peptides can occur by the multiplication and crosslinking of genes. In this connection the discovery of discreteness in the organization of eukaryote genes, i.e. an alternation of the coding and non-coding regions, was most intriguing. A comparison of known genes with the respective proteins reveals in some cases a striking resemblance in their discrete organization showing that the coding region of a gene (exon) might correspond to the cooperative structural unit of protein, the domain.

Friday 03 August Congress Centre-First Floor Posters 001-006

Posters on Chemical and Electrical Regulation of Ion Channels

001

AN ALLOSTERIC MODEL FOR ELECTRICALLY EXCITABLE SODIUM CHANNELS
T. Kunitawa and J. Otsuka, Dept. of Applied Biol. Sci., Sci. Univ. of Tokyo, Chiba 278, Japan.

An allosteric model of Monod-Wyman-Changeux (1965) type for electrically excitable sodium channels is developed to give a physical counterpart to electrophysiological data. In this model it is assumed that the sodium conductance is regulated by the quaternary conformation of a multi-subunit protein encompassing the sodium channel and that the gating current originates from the tertiary conformation change of the subunit carrying an electric dipole moment or electric charge; the accumulation of the tertiary conformation changes in one of quaternary conformations induces the quaternary conformational transition and the sigmoidal dependence of the sodium conductance on the voltage is explained by this conformational transition. The model quantitatively explains the correlation between the normalized sodium conductance and the fraction of electric charges transferred by the gating current. Properties of the gating current, charge immobilization and difference between the ON and OFF kinetics at the same membrane potential, are also explained by the tertiary conformation change occurring in the respective quaternary conformations. The voltage-dependent binding of the scorpion toxin to the sodium channel and the slowing of inactivation suggests that this toxin exhibits a preferential binding to one of the quaternary conformations.

003

BRIEF CLOSINGS OF GRAMICIDIN A CHANNELS IN CHO MEMBRANES.
A. Ring, Dept. of Physiology and Med. Biophysics, Univ. of Illinois, U.S.A.

Recordings of gramicidin A single channel events were found to exhibit brief (0.5-5 msec) closings, so called flickers or bursts when examined at high resolution. The similarity of the gramicidin flickers to those of biological channels reinforces the hypothesis that the gramicidin channel may serve as a general model for channel gating as well as ionic conduction. At high activities of HCl, transitions to subconductance (miniature) states were observed. The average duration I_{off} and interval between I_{off} flickers was evaluated by fitting exponentials to the histogram distribution of the time intervals. The fit requires at least two exponential, the slower however of small amplitude. Also, a fit to I_{off} was attempted giving $\alpha 1.7$. The concentration and voltage dependence was examined for CsCl and HCl and a procedure was developed. It was found that I_{off} , I_{on} and I_{off}/I_{on} all decrease with voltage. The results are related to the "simple" model, in which the stability of the channel is determined by its coordination in the lipid environment, and it is concluded that the generalization of flickers for biological channels may involve the interaction of conformational change of channel gating and membrane lipid reorganization. The field dependence is interpreted as a charge displacement of 2em, in agreement with recent studies on the "loss of conduction" of the gramicidin dimer by a "slow" dissociation of the monomers.

005

EFFECT OF "ALLIUM ON THE LIPID PACKAGED GRAMICIDIN A TRANSMEMBRANE CHANNEL.

E. Casali, L. Pasotti, C. Farruggia, M.B. Ferrari, G. Sartori, L. Pasquali-Renchetti, Inst. Mol. Chemist., Univ. Parma, V.le Cavour 14, Parma, Italy, *Inst. Gen. Pathol., Univ. Modena, via Campi 105, Modena, Italy.

Peating at length Gramicidin A with lysophosphatidylcholine results in the assembly of multilayer liposomes where the channels are organized in row of aggregates (1). Furthermore it has been demonstrated that Trp residues play an important role during the assembly of the supermolecularly organized system (2,3). The hypothesis has been put forward that such aggregates are formed by clustering of channels (4). Recently, it has been observed that a slight excess of Ca^{2+} with respect to channel concentration alters the conductivity of the channel. We have investigated therefore if the observed functional modification can be due to an alteration of the mode of assembly of the channel. It shows that in the presence of Ca^{2+} the membranes undergo noticeable structural modifications. Dynamic fluorescence measurements seem to indicate that also Trp-Trp interactions are somewhat altered.

REFERENCE

- 1) Pasquali-Renchetti L., et al., 1983, BioScience Reports, 3, 127-133.
- 2) Cavatorta P., et al., 1982, BBA, 689, 113-120.
- 3) Pasotti L., et al., 1983, in Structure and Function of Membrane Proteins (Quagliariello E., Paladini F. Eds), 3-10, Elsevier Science Publishers.
- 4) Spindl A., et al., 1983, BBA, 732, 58-68.

002

BLOCKING EFFECT OF INTERNAL SODIUM IONS ON THE POTASSIUM CHANNELS IN SNAIL NEURONES

L.S. Magura and N.B. Prevarskaya, Bogomoletz Inst. of Physiology, Ukrainian Acad. of Sci., Kiev, U.S.S.R.

The effects of internal Na^+ ions on a noninactivating delayed outward current and a transient outward current were studied in voltage clamp experiments by using internally perfused nerve cell bodies from snails *Helix pomatia*. These outward currents are carried predominantly by K^+ ions. Internal concentration of K^+ was 75 mM. Internal Na^+ in concentration of 50 mM inhibited the noninactivating delayed outward current. This effect of Na^+ showed no significant voltage dependence. The holding potential was set to -100 mV in order to remove inactivation of the transient outward current. The normally linear instantaneous I-V relationship for the transient outward current was transformed by internal Na^+ (10-50 mM) into an L-shaped. Voltage-dependent block of the transient outward current channels by Na^+ produced a region of negative slope in the I-V plot over a restricted range of voltages - roughly between +40 - +80 mV. The voltage dependence may imply that the binding site is within the membrane field. The block occurred at more positive voltage when external K^+ concentration was increased. At high transmembrane voltages (≥ 80 mV) a second region of increasing current was observed. It was suggested that at high voltage Na^+ not only enters the K channels but can pass through with relative ease.

004

SINGLE-CHANNEL RECORDING OF THE Na^+ CHANNEL PROTEIN ISOLATED FROM *Electrophorus electricus* RECONSTITUTED IN PHOSPHOLIPID VESICLES; R.L. Rosenberg, S.A. Tomiko & M.S. Agnew, Dept. Physiol., Yale Univ. Sch. of Med., New Haven, CT, U.S.A.

[3H]-TTX has been used to follow isolation of the Na^+ channel protein from the main organ of electric eel. It is formed from a large glycopeptide of Mr 260,000, with no evidence for smaller peptide subunits. Amino acid and carbohydrate analyses revealed that 29 wt% of the peptide is carbohydrate, a result confirmed by enzymatic deglycosylation. When reconstituted into phospholipid vesicles, the protein mediates neurotoxin-modulated radiotracer ion flux. These studies indicated the presence of the ion channel itself, and functional sites for binding of (1) TTX and STX (saxitoxin), (2) alkaloid neurotoxins including veratridine and batrachotoxin, and (3) local anesthetics, including dibucaine, tetracaine, and QX-222. In studies reported here, the liposomes have been enlarged in a freeze-thaw cycle to 10-50 μ m for patch-clamp recording. In excised patches, in the absence of neurotoxins, voltage-dependent events were observed, with single channel conductances of 11 pS, mean open times of 1.9 msec, permeation selectivity for sodium ($P_{Na}/P_K \approx 7$), and extended first latencies of opening. Currents averaged from many traces exhibited the voltage-activation followed by inactivation characteristic of macroscopic sodium currents of native membranes under voltage-clamp. We propose that the large glycopeptide may represent the entire sodium channel functional unit, including voltage-sensing elements, the ion channel, and sites for drug and neurotoxin interaction.

006

THE GATING CHARGES OF THE VOLTAGE-DEPENDENT CHANNEL, VDCC, CHANGE THEIR ACCESSIBILITY DEPENDING ON THE CONFORMATIONAL STATE OF THE PROTEIN.

Marco Colombari & Charles Doring, Labs. of Cell Biology, Dept. Zoology, Univ. of Maryland, College Park, MD.

The amino-group reagent, succinic anhydride, was used to probe the location of the gating charges of the channel-former from the outer mitochondrial membrane, VDCC. When succinic anhydride was added to a planar phospholipid bilayer containing VDCC channels in the open state, the resulting modified channels lost their ability to close in response to an applied electric field (40 mV transmembrane potential). This result is consistent with the modification of gating charges by the anhydride resulting in channels which could no longer respond to the applied field. However, if the anhydride was added while the channels were maintained in a closed conformation by means of an applied field, the ability of the anhydride to modify VDCC's voltage-gating mechanism depended on 1) the direction of the field, and 2) which of the two aqueous compartments contained the anhydride. The modification occurred preferentially when the anhydride was added to the negative side of the membrane irrespective of the direction of the field. Therefore when the field was reversed, the gating charges became more accessible from the opposite side of the membrane. One set of gating charges seemed to be responsible for channel closure at both positive and negative fields. (Supported by NIH grant GM28450)

Friday 03 August Congress Centre-First Floor Posters 007-012

Posters on Chemical and Electrical Regulation of Ion Channels

007

PHOSPHATIDIC ACID REGULATES THE ACTIVITY OF CHANNEL-FORMING IONOPHORES. A ^1H -NMR STUDY USING PHOSPHOLIPID MEMBRANES

J.A. Yeiro, G.R.A. Hunt and I.C. Jones. Department of Science, The Polytechnic of Wales, Pontypridd, Mid Glam, CF37 1DL, UK.

^1H -NMR techniques have been used to investigate the regulation of ion channels by phosphatidic acid which is a proposed active metabolite in the phosphatidylinositol (PI) effect. Unilamellar phospholipid membranes composed of egg yolk phosphatidylcholine or dipalmitoyl phosphatidylcholine were formed by sonication of the lipid in $^2\text{H}_2\text{O}$ (10 mole % cholesterol was included when using nystatin). Vesicles containing 3 or 5 mole % egg yolk phosphatidic acid (PA) were also prepared. Following incubation with the peptide ionophores alamethicin 30 and melittin and the polyene antibiotic nystatin, ^1H -NMR spectroscopy of the vesicles was used to monitor transport of the lanthanide paramagnetic probe ion Pr^{3+} across the vesicular bilayer. Phosphatidate-containing vesicles alone showed no ionophore activity. Comparison of the ionophore-mediated transport rates in the control vesicles with those containing phosphatidate showed that PA promotes the efficiency of the ion channels formed by melittin and nystatin, but inhibits the alamethicin 30 channels. Further, the spectra reveal that the presence of PA introduces alternative mechanisms of ion transport, depending on the particular phosphatidylcholine and ionophore used.

These results suggest that in the PI effect the role of PA is not to act directly as an ionophore, but as a regulator of ion transporting channels in membranes.

009

STRUCTURE OF GRAMICIDIN A CHANNEL RECOMBINED IN A SINGLE LIPID COMPONENT AS DETERMINED BY ^2H NMR.

L.M. Strenk, J.W. Doane and P.W. Westerman, Northeastern Ohio Universities College of Medicine, Rootstown, Ohio, USA and Liquid Crystal Institute and Department of Physics, Kent State University, Kent, Ohio, USA

Aqueous multilamellar dispersions of gramicidin A recombined with dimyristoylphosphatidylcholine (DMPC), which is specifically ^2H -labelled on the glycerol backbone, choline head group, or hydrocarbon chains, have been examined by ^2H NMR. Analysis of motionally-averaged quadrupole splittings indicate that incorporation of gramicidin A into DMPC bilayers reduces orientational ordering of the choline moiety and changes the conformation of the glycerol backbone. Our results suggest that the gramicidin A ion channel resulting from NH_2 -terminus to NH_2 -terminus dimerization of single-stranded β -helices, extends only across the hydrophobic portion of the bilayer. Hydrogen bond interactions between donor groups at the C-terminus of each polypeptide chain and hydrogen-bond acceptor groups on DMPC are proposed. In general, we find ^2H quadrupole splittings from the glycerol backbone and choline moiety of DMPC to be very sensitive to, and specific of the chemical nature of substances which are incorporated into the lipid bilayer. Fatty acids, dimyristin, other phospholipids, cholesterol and several general anesthetics have been shown to significantly influence peptide-lipid interactions in DMPC-gramicidin A bilayers.

011

MOLECULAR STRUCTURE AND DYNAMICS OF THE NEURONAL Na^+ CHANNEL. Kimon Angelides, T. Nutter, L. Elmer, and B. O'Brien, Dept. Biochemistry, Univ. Florida, Gainesville, FLA, USA

In excitable cells the action potential is produced by transient changes in the membrane permeability to Na^+ and K^+ ions controlled by intrinsic channels. We have prepared biologically active fluorescent and photo-fluorescent derivatives of the neurotoxins TTX, BTX, Lqg, and Csx II to map the molecular structure of the Na^+ channel by fluorescence energy transfer, to monitor the conformational transitions during conduction, and to visualize channel distribution and mobility. Energy transfer between channel receptor sites yield these distances: TTX-Csx 33A, Csx-Lqg 22A, TTX-Lqg 35A, and BTX-Lqg 37A. Activation by BTX increases the TTX-Lqg distance by 7A and indicates that conformational changes in the channel are effected over significant distances (37A). Energy transfer between TTX sites shows that Na^+ channels are within 50-70A and suggest that in nerve channels may occur as oligomers. In synaptosomes clustering of Na^+ channels has been observed by electron microscopy using immunogold complexes. Radiation inactivation of Na^+ channels show independent functional unit sizes for the TTX, Lqg, and Csx receptors of 220KD, 263KD, and 45KD; the BTX receptor shows target sizes of 287KD and 45KD, the ratio depending upon the state of channel activation. Electron microscopy of purified channels show rod-shaped cylinders of 40x100A with ribbon-like helices, and under certain conditions hole-shaped particles of 30A diameter. In peripheral nerve fluorescent Lqg and anti-channel IgG show specific staining at nodes which upon demyelination diffuse to ~15 μm along the axon.

008

SINGLE CHANNEL CURRENTS IN THE EMBRYONIC CELLS OF THE NEWT (*TRITURUS VULGARIS*)

T.O. Jälonen and A. Talo, Department of Biology, University of Turku, Turku, Finland.

The patch clamp technique was used to study the single channel currents in the cells of the newt (*Triturus vulgaris*). The cells of morula, blastula or gastrula stage embryos were isolated mechanically in Holtfreter-solution. No enzymatic treatment was necessary for obtaining giga-seals.

Various different channel types were found: (1) Channels with small amplitude (0.5-2.0pA), small conductance, and long open and closed times (possibly Na^+ -channels); (2) Small amplitude channels, which open in two-step mode with fast flickering closures and conductance of about 20-25pS (possibly Cl^- -channels); (3) Cation-channels with very short open times and conductances of about 75pS and 240pS; (4) Other channel types with relatively long open times and conductances of 35, 50, 90, 130, 160 and over 200 pS. Most of these seem to be non-selective cation-channels. Future studies would reveal more of the nature of these channels and their role in the ionic regulation of developmental phenomena.

010

SINGLE Na^+ AND Ca^{2+} CHANNELS IN VERTEBRATE SENSORY NEURONS.

E. Corbione and H.D. Lux, Max-Planck-Institut für Psychiatrie, Piar-39-Martinsried, F.R.G.

Unitary Na^+ and Ca^{2+} current events were recorded from outside-out patches of cultured dorsal root ganglion cells of chick and rat. Na^+ currents were studied in Ca^{2+} -depleted external and Ca^{2+} -containing internal solutions. They appeared in the form of discrete inward going unitary events at potentials between -50 and -10 mV from a holding of -90 mV. They revealed typical voltage-dependent activation and inactivation kinetics with mean open times (m.o.t.) of 2 to 3 ms at -40 mV and an average amplitude (\bar{y}) of 11.5 \pm 2 pS at 12°C. The currents were eliminated by micromolar additions of TTX. Time-dependent inactivation was strongly reduced when the patch pipette contained 0.1 mg/ml of pronase or 50 μM nitro-bromacetamide.

Two types of Ca^{2+} channels were identified in isolated patches in Na^+ -free media, containing Choline and μM TTX. Both channels were blocked by external Ni^{2+} or Cd^{2+} . One type had kinetic features similar to those of previously described Ca^{2+} channels (m.o.t. 0.8 ms at -40 mV, \bar{y} 4.5 pS). It showed slow and incomplete inactivation. A second type was already activated at potentials of -50 mV and had higher probability to be open at more negative holding potentials (-100 to -120 mV). Openings of this channel lasted 4 to 6 ms on the average and its conductance was 9.5 pS. Inactivation was also faster and more complete than that of the common Ca^{2+} channel. The occasional failure of occurrence of one of the two types of events suggests different Ca^{2+} channels entities rather than different states of one channel.

012

TEA^+ BLOCK OF POTASSIUM CHANNELS IN FROG SKELETAL MUSCLE

A.E. Spruce, N.B. Standen, P.R. Stanfield & T.A. Ward, Department of Physiology, University of Leicester, Leicester, LE1 7RH, U.K.

We have studied the effect of TEA^+ on unitary currents through delayed rectifier K-channels in sarcolemmal vesicles formed in 120mM KCl solution. Single channel currents were reduced by TEA^+ in the external (recording pipette) solution which contained 2.5mM KCl and 120mM NaCl+TEACl. From the currents measured in different TEA^+ concentrations, dose-response curves were drawn. The results were best fitted assuming binding of one TEA^+ to a channel and a dissociation constant (K_d) of 5.6mM at 0mV. The reduction in current was attributed to the TEA^+ blocking reaction being too fast to resolve (low pass filter, 3dB down at 1kHz). In a sequential reaction scheme where TEA^+ can block only the open channel, halving the unitary current (i) by TEA^+ should be associated with a doubling of the mean open time (t). Our results did not suggest this type of relationship (at 0mV, 0 TEA^+ , \bar{f} = 1.29 \pm 0.05pA(n=11), τ = 4.49 \pm 0.59ms(n=7); 10mM TEA^+ , \bar{f} = 0.51 \pm 0.06pA(n=6), τ = 5.35 \pm 1.13ms(n=6)), though the small current level in 10mM TEA^+ caused difficulty in identifying closings. In an attempt to determine whether TEA^+ blocking caused increased noise in the open level, we calculated open minus the baseline variance of the data points in records but, in fact, found little difference between 0 TEA^+ and Ringer, at 0mV (10 TEA^+ , 0.007 \pm 0.001pA; 0 TEA^+ , 0.011 \pm 0.002pA).

1 N.B. Standen, et al. (1984). J. Physiol. 346, 61P.

Friday 03 August Congress Centre-First Floor Posters 013-018

Posters on Chemical and Electrical Regulation of Ion Channels

013

GABA-SENSITIVITY IN OOCYTES

S. Dolci and F. Eusebi, Istituto di Istologia ed Embriologia Generale, via Scarpa 14, Università di Roma.

It has been recently shown that the membrane surface of amphibian and mammalian oocytes carries receptors for various neurotransmitters (Kusano et al., J. Physiol. 328, 143 (1983); Eusebi et al. J. Physiol. 346, 321 (1984)). We show here the presence of a chemical sensitivity to gamma-aminobutyric acid (GABA) in mouse and human oocytes using electrophysiological techniques. GABA was applied by pressure in the bathing medium while recording either membrane potential or membrane current. The ovarian oocytes studied were sensitive to GABA, which usually hyperpolarized the membrane, with a decrease followed by an increase of membrane conductance, with threshold concentration as low as 10^{-6} M. The early phase of GABA-potential with decreased conductance was Ca- and Cl-dependent and reversed at -17 mV; the potential accompanied by a decreased conductance was Cl-dependent and reversed at -39 mV. Mouse and human metaphase II oocytes responded to GABA in a way which resembles ovarian oocytes. In contrast, zygotes were insensitive to GABA at a concentration of 10^{-6} M. These findings support the hypothesis that GABA is a possible neuromodulatory agent in the follicles. This work has been supported by a NATO Grant 387/82.

015

DOES SUPERNORMAL CONDUCTION OCCUR IN THE IN-VIVO SQUID AXON?

A. Blumsohn and D.R.L. Scriven, Dept. of Physiology, University of the Witwatersrand Medical School, Johannesburg.

Squid axons in-vivo show behaviour consistent with a leak conductance of the order of $1 \mu S$, [Moore and Cole (1960) J. Gen. Physiol. 43, 961-970], a value less than one-hundredth of that found in the isolated axon. We have examined the effect of reducing the leak conductance to its in-vivo value on the activity dependent velocity variations shown by the Hodgkin-Huxley cable equations. Such an axon shows subnormal velocity for small interspike intervals, but shows no superexcitable range. A comparison of the simulated isolated and in-vivo axons showed that the large leak conductance of the isolated axon results in an oscillatory return of the n and h parameters towards their resting states after the action potential. Excitation during the periods when the h parameter is super-activated results in a greater influx of sodium and hence a greater conduction velocity. The n and h parameters of the simulated in-vivo axon show a monotonic return to their resting values, and thus this axon shows no supernormal period. We therefore suggest that the phenomenon of supernormality is a feature of the isolated squid axon and does not occur in-vivo.

017

DISTINCTION BETWEEN DIPOLAR AND INDUCTIVE EFFECTS OF SUBSTITUTED PHENYLALANINE SIDE CHAINS IN MODULATING THE SINGLE-CHANNEL CONDUCTANCES OF GRAMICIDIN A ANALOGUES

Roger E. Koeppe II, University of Arkansas, Fayetteville, Arkansas, USA; Olaf S. Andersen and Jean-Luc Hazet, Cornell University Medical College, New York, New York, USA.

The single-channel activity of gramicidin A can be changed by replacing the N-terminal formyl-L-Val with other formyl-L-amino acids of varying polarities. For example, replacing Val with Phe decreases the conductance 6-fold, and likewise F-Phe at the N-terminal yields a lower conductance than does Phe. Based on the currently accepted β -helical model for the structure of the channel, these side chains are not in direct contact with the passing ions, but exert their effects at distances some 6-10 Å from the ions. The modulation of conductance could be due primarily to electrostatic ion-dipole interactions ("through space"), or alternatively to electron withdrawing (or donating) effects which could influence the electronegativity of a peptide carbonyl oxygen ("through bonds"). We have addressed this question by measuring the single-channel conductances of gramicidin A analogues having p-hydroxy- (3.9 pS), p-methoxy- (10.5), unsubstituted (10.2), p-fluoro- (5.8), and m-fluoro-Phe (6.2) as the N-terminal (formyl-) amino acid. The Hammett sigma parameters for the five different ring substituents are: -0.37, -0.27, 0.00, +0.06 and +0.34, respectively. The results indicate that there is no correlation between the observed conductance and the electron-withdrawing properties of the phenyl substituent. Therefore, inductive effects are less important than ion-dipole interactions in modulating the gramicidin A conductance.

014 ORAL PRESENTATION

METABOLIC DEPENDENCE OF CALCIUM CHANNEL FUNCTION IN THE SOMATIC MEMBRANE OF NERVE CELL

P.G. Kostyuk, N.S. Veselovsky, P.A. Doroshenko, A.E. Martynuk, S.A. Fedulova and Y.M. Shuba, Bogomoletz Institute of Physiology, Ukrainian Acad. of Sci., Kiev, U.S.S.R.

Changes in the function of potential-dependent calcium channels have been studied on isolated intracellularly perfused neurons of rat dorsal root ganglia and of snail ganglia during various interferences in the cytoplasmic processes. The perfusion of nerve cells by saline solution, per se, results in a progressive decrease of calcium currents which is largely accelerated by an increase in the intracellular ionized calcium content. The study of single channel behavior shows that the reason for such a decrease is switching off a portion of channels from the function without affecting the unitary conductance. Intracellular introduction of exogenous cAMP together with ATP and Mg ions considerably restores the function of the channels. cGMP has no such an effect. Restoring effect can also be achieved by the introduction of the catalytic subunit of protein kinase isolated from bovine heart muscle together with ATP (but without cAMP). The described effects are preserved if Ba ions are the current carrier in the channels. Along with metabolically-dependent channels, there exists a population of calcium channels slightly sensitive to cytoplasmic disturbances.

016

DISTRIBUTION OF CALCIUM CHANNELS IN A CILIATE

J.W. Deitmer, Abt. Biologie, Ruhr-Universität, D-4630 Bochum, Federal Republic of Germany.

Action potentials and voltage-dependent membrane currents were investigated in the freshwater ciliate *Stylonychia mytilus*, using two intracellular microelectrodes. The action potential contains two components, and the inward current-voltage relationship has two maxima, one at -45 mV and another at -17 mV, suggesting two types of voltage-dependent inward currents (J.W. Deitmer, J. Physiol. in press). Both types of inward currents are blocked when Ca is replaced by Mg, Co or Mn, or after addition of Cd, but are present when Ca is replaced by Ba or Sr. This indicates that these inward currents flow through Ca channels in the membrane. When the cell released its membranelle band, or when the anterior part of the cell was severed, the second component of the action potential and the maximum of the inward current-voltage relationship at -45 mV disappeared. This suggests that the two Ca currents are separable by their localization in the membrane: the Ca current with its peak at -45 mV appears to be restricted to the membrane of the membranelle band. The presence of two voltage-dependent Ca currents may be functionally related to the independent motor control of different ciliary organelles in this unicellular organism.

Supported by the DFG, SFB 114, TP A5

018

MUTATIONS OF TWO GENES ALTER DIFFERENT COMPONENTS OF POTASSIUM CURRENTS IN DROSOPHILA

Chun-Fang Wu, Dept. of Zoology, Univ. of Iowa, Iowa City, Iowa and Barry Ganetzky, Dept. of Genetics, Univ. of Wisconsin, Madison, Wisconsin.

Mutations that alter excitable membranes provide one means to probe the function and molecular identity of ion channels. This approach is especially useful for the study of channels, e.g., potassium channels, which lack specific, high-affinity toxins that facilitate biochemical analysis. In *Drosophila*, previous analysis of several behavioral mutants suggested altered membrane currents. We used two-microelectrode voltage clamp techniques to measure membrane currents in larval segmental muscle fibers that are identifiable and meet isopotential conditions. Among different mutants examined, *Shaker* mutations affect transient potassium current (I_T), but not delayed rectification potassium current (I_D) or Ca current. For several alleles, I_T was completely eliminated. In other alleles, I_T showed different I-V characteristics of activation but normal kinetic and steady state properties of inactivation. I_D was normal for all alleles studied as indicated by I-V characteristics, reversal potential and tail current kinetics. Mutations of another gene *egg* were found to affect both I_T and I_D . In certain alleles, I_D was reduced to a greater extent than I_T , while the converse is true in other alleles. We are currently using patch clamp techniques to study single channel potassium currents in the nerve membrane of cultured larval CNS neurons. We have characterized, in normal neurons, single channel currents with stationary properties corresponding to I_T . Studies of mutant neurons are in progress.

Friday 03 August Congress Centre-First Floor Posters 019-024

Posters on Chemical and Electrical Regulation of Ion Channels

019

COMPARATIVE ANALYSES OF THE EFFECTS OF DIVALENT IONS AND TEA ON RETZIUS NERVE MEMBRANES OF LEECH Bogdan B. Beleslin, Dept. of Patho-Physiology, Medical Faculty, Belgrade, Yugoslavia.

Unbuffered Ca Ringer which pH was between 4 to 5.6 obtained by replacing sodium with calcium and omitting phosphate buffer in the presence of 10 or 25 mM/l tetraethylammonium (TEA) ions caused a significant increase of coupling resistance in Retzius nerve cell of leech (*Haemaphysalis sanguisuga*). Comparative analyses showed that the changes in effective input resistance depended on its initial values and pH of the external medium. If the input resistance was higher the drop was lower. The same effect was obtained with less acidic external fluid. Addition of TEA to the normal leech Ringer was less effective on cell to cell communication. Enriched Mg Ringer with 25 mM Li, was followed with an increase of coupling resistance with a drop of effective input resistance. The present experiments showed that Retzius nerve cells uncoupling is difficult to obtain without an increase of conductance of "free" membrane, indicating at the same time that the effects of divalent ions and TEA are rather non specific on coupling.

(Supported by the Research Council of Serbia)

021

PHALLOLYSIN, A MUSHROOM TOXIN, FORMS ION CHANNELS IN PLANAR LIPID BILAYERS WHICH ARE GATED BY PROTONS AND VOLTAGE H.U. Wilsen, H. Faulstich and G. Boehm, Dept. Cell Physiology, Ruhr-Universität Bochum, Postfach 102140, D-4630 Bochum, W-Germany

Phallolysin, a water soluble protein of *M. 34000* produced by the mushroom *Amanita phalloides*, causes lysis of various mammalian cell types. Lysis was suggested to be initiated by the formation of ion permeable membrane channels. We therefore studied the interaction of phallolysin with virtually solvent-free lipid bilayers. In the presence of low phallolysin concentrations (10-100 nM) single channel current fluctuations were observed. Gating kinetics showed a pronounced voltage, pH and lipid dependence. The correlation between voltage and (cis-side) proton concentration reveals the equivalence of a pH change of one unit to a corresponding voltage change of 130 mV. A quantitative analysis of the channel properties was carried out on the basis of a three state model (closed, open, inactive).

023

IONIC PROCESS IN PHOTOMOTILE RESPONSES OF BLEPHARISMA JAPONICUM

G.Colombetti, F.Lenci, V.Passarelli, C.N.R. Istituto di Biofisica, Via S.Lorenzo 26, Pisa, Italy and E.Barone, R.Nobili, Istituto Zoologia Università, Via Volta 4, Pisa, Italy.

The ciliated protozoan *Blepharisma japonicum* exhibits light controlled behaviour in the form of an "avoiding" reaction i.e. when the cells are illuminated they stop and swim backward for some seconds, then resume forward swimming in a randomly chosen direction. This behaviour may be regulated by varying the external cation concentrations or by blocking specific ionic processes. An increase in external K^+ concentrations causes spontaneous backward swimming and stops the light response; this effect may be reversed by adding external Ca^{++} so to keep constant the $[K^+]/[Ca^{++}]$ ratio. Protonophores and the Ca^{++} channel blocking agent Ruthenium-red block selectively the light reaction, thus showing the importance of K^+ and Ca^{++} conductivity in the light response of the cells.

020

KINETICS OF ENDPLATE ACETYLCHOLINE RECEPTOR CHANNELS AT REDUCED TEMPERATURE. V.E. Dionne, Department of Medicine, University of California, San Diego, USA

The activation kinetics of endplate-type acetylcholine receptor (AChR) channels at garter snake neuromuscular junctions were examined at reduced temperature using single-channel recording methods. The purpose was to determine whether, for synaptic channels, any of the kinetic complexities which have been reported for nonsynaptic [S.M. Sine and J.H. Steinbach (1984) *Biophys. J.* 45:175] and perijunctional [D. Colquhoun and B. Sakmann (1981) *Nature* 294:446] AChR channels could be detected using the improved resolution brought about by thermally slowing the kinetic processes. Studies have been conducted between 12 and 22°C with the cells bathed in a HEPES (5 mM) buffered saline at pH 7.2 containing (mM): 159 NaCl, 2.15 KCl, 1 CaCl₂, 4.2 MgCl₂. Pipettes contained the same solution and included .25 to 1 μ M acetylcholine chloride. Bandwidth was 2.5 KHz. At 22°C endplate AChR channel activation was described formally by a sequential three-state model with two closed and one open-channel state: C1-C2-O. Reducing the temperature caused the conductance of the channels to decrease and the lifetimes of the closed-activated state (C2) and the open state to increase as expected, but produced no qualitative change in AChR activation kinetics; e.g., open channels showed no increase in flickering at lowered temperature. Synaptic AChR channels appear to be kinetically distinct from nonsynaptic channels.

022

DIFFERENCE IN ASSOCIATION OF THALLOUS ION WITH GRAMICIDIN A AND GRAMICIDIN B IN LYSOPHOSPHATIDYL CHOLINE MICELLES DETERMINED BY TL-205 NMR. William L. Whaley*, Dikoma Shungu*, James F. Hinton*, Roger E. Koeppe*, and Francis S. Millett. University of Arkansas, Fayetteville, AR 72701.

TL-205 NMR spectroscopy is a useful probe for investigating the binding of monovalent cations to proteins. Tl(I) functions similarly to K^+ in several biochemical systems. Gramicidin A (A) and Gramicidin B (B) are pentadecapeptides which differ only at residue 11, where L-Phe is present in B and L-Trp is present in A. Both A and B form dimeric channels which span lipid bilayer membranes. These channels are selective for monovalent cations including Tl(I) and Ag(I). The single channel conductance of B is only .65 that of A. The explanation for this difference is not clearly understood. We have monitored the effects of L-lysophosphatidylcholine-packaged A and B on the TL-205 chemical shift. Preparations similar to ours have previously been shown to be a mixture of micelle and vesicle structures with incorporated pentadecapeptide. The shifts in the TL-205 resonance frequency induced by A in the phospholipid-packaged system were about 3-fold greater than the shifts induced by B under identical conditions. Measurements of the gramicidin-induced chemical shift both as a function of Tl(I) concentration and temperature indicate that the ion association constant for B is smaller than that for A. (Supported in part by NSF grant PCM-83-00065 and NIH NS-16449.)

024

MATHEMATICAL THEORY OF MACROSCOPIC VOLTAGE CLAMP CURRENTS. D.M. Easton, Department of Biological Science, The Florida State University, Tallahassee, Florida, U.S.A.

The recruitment of specific ion conductance channel activity in squid axon membrane under voltage clamp is conveniently predicted by a simple equation based on Gompertz kinetics. The current carried by a specific ion is the product of 2 processes that proceed exponentially in opposite directions, each at a different rate that decreases exponentially. The rate coefficients of the opposing processes change in like fashion with respect to V , and therefore yield simple ratios with respect to one another. A λ step sets r_0 , the initial rate of change of the current with time, and k , the rate at which r changes with time, in both processes. The voltage clamp currents $I_k(t)$ and $I_{Na}(t)$, the current $I(V)$, as $t \rightarrow \infty$ for either Na^+ or K^+ , and $I_p(V)$, the peak Na^+ current, are all predicted from simple derived expressions using these constants. The equation is the same for Na^+ or K^+ currents, and "inactivation" is in either of these instances removed or produced by a change in the ratio of the "initial" time rate (r_0) over the rate of change (k) of that rate. All the parameters are rationally defined and no arbitrary constants are required in the theory, which seems capable of modelling a large array of voltage clamp behaviors manifested as the summed activity of the conductance channels of the excitable membrane.

Friday 03 August Congress Centre-First Floor Posters 025-030

Posters on Chemical and Electrical Regulation of Ion Channels

025

RAPID BLOCK AND RELIEF OF BLOCK IN CURRENTS THROUGH SINGLE Ca-ACTIVATED K CHANNELS. G. Yellen, Section of Molecular Neurobiology, Yale Univ. Sch. of Medicine, New Haven, CT USA

Currents through individual Ca-activated K channels from chromaffin cells show many brief interruptions (flickers) when small amounts of Na are added to the solution bathing the intracellular face of the channel. The properties of the flicker are explained by a model for voltage-dependent channel blockade. The rate constants for this blockade process can be measured by a new method for analysing rapid kinetic processes, amplitude distribution analysis.

This new method of analysis yields blocking and unblocking time constants in the microsecond time range. The rate constants for Na block depend on Na concentration in the expected way: the entry rate increases linearly with concentration, and the exit rate is independent of concentration. The entry rate also shows a remarkably high voltage dependence.

Adding permeant ions such as K to the external bath relieves the block produced by internal Na. This relief occurs entirely through an effect on the exit rate of Na, with no effect on the entry rate. Thus, a competitive model cannot account for the relief. Instead, it seems that relieving ions expel the blocking ion from the channel by some sort of "knock-out" mechanism.

027

EFFECTS OF WATER MOVEMENT ON F-H SPACE AND VOLTAGE CLAMP UNIFORMITY IN THE SQUID GIANT AXON.

R.E. Taylor, J.R. Stimers and F. Bezanilla, Laboratory of Biophysics, NINDS, NIH Bethesda, MD, USA and Department of Physiology, UCLA, Los Angeles, CA, USA.

Using a simplified model for the space between the nerve membrane of the squid giant axon and the Schwann cells (the F-H space) and the clefts between these cells we consider the effects of changes in the osmolarity of the external solution on the longitudinal resistance of the F-H space. We conclude that an outward movement of water will increase the volume of the F-H space with concentration slightly less than the external solution. Example: For 980 mOsm inside and 1100 mOsm outside F-H space concentration is 1079 mOsm with a pressure of 2.61 cm of water. Transient Schwann cell volume changes would be expected for hypertonic external solutions but experimental results are similar for reduced internal osmolarity. These results have been reported (Stimers, Bezanilla and Taylor). Biophysical Journal 45, 13a(1984), that the slow component of the capacity transient is reduced, as is the rising phase of the gating current. It was concluded that the F-H space is expanded by the osmotic gradient, the longitudinal resistance is decreased and the spatial uniformity of the voltage clamp is improved. Supported by USPHS Grant #GM30376 and NIH Fellowship to JRS.

029

GATING AND TETRODOTOXIN (TTX) BLOCK OF BATRACHOTOXIN- (BTX) MODIFIED SODIUM CHANNELS IN IPAD BILAYERS. K.M. Green, L.B. Weiss, O.S. Andersen, Dept. Physiol., Cornell Univ. Med. Coll., 1300 York Ave, New York, N.Y. 10021 U.S.A.

Voltage-dependent, BTX-modified sodium channels from canine forebrain synaptosomes were incorporated into neutral phospholipid bilayers. Single channel gating was studied as fractional open time as a function of membrane potential (V). The apparent gating charge was ~ 4 elementary charges, and the midpoint potential ($V_{1/2}$) varied between -75 and -95 mV in 0.5 M NaCl. Decreases in [NaCl] resulted in a shift of $V_{1/2}$ to more negative potentials consistent with changes in surface potentials at the protein/water interface. When TTX was added to the 'extracellular' aqueous phase, very long lasting blocks of the channels were observed. The degree of this TTX-induced block was estimated from the fractional closed time which exhibited a simple saturating behavior as a function of [TTX] at all V 's studied. The [TTX] for 50% block (K_d) was found to have a V -dependence of 60-70% and vary with [Na]. The unblock rate constant was independent of [Na], while the rate constant for block varied as $(1 + [Na]/K_{Na})^{-1}$; $K_{Na} \sim 20$ mM. The STX-induced block exhibited a similar V - and [Na]-dependence despite a different net charge of TTX (+1) and STX (+2). If TTX and STX bind to the same site in the sodium channel, the V -dependence of the block cannot reflect the electrical distance between the extracellular aqueous phase and the binding site. The V -dependence of the toxin-induced block may result from a V -dependent conformational change of the channel protein.

026

DIFFERENCES IN FIRING ADAPTATION DURING CONSTANT AND INTERMITTENT STIMULATION

S. Gestblom and W. Grampp, Department of Physiology and Biophysics, University of Lund, Lund, Sweden.

Firing adaptation in slowly and rapidly adapting stretch receptor neurones of lobster have been analyzed by means of a dynamical computer model based on intracellular voltage and current recordings as well as measurements of intracellular ion concentrations. The proposed model specifically accounts for the different modes of adaptation displayed by the two receptors during constant stimulation implying that in its rapidly adapting form the model invariably stops firing despite maintained stimulation, whereas in its slowly adapting form it only reduces its firing frequency to lower but finite stationary levels. In further investigations employing intermittent stimulation giving rise to impulse firing in bursts it was found that the degree of adaptation was much reduced in slowly, but also in rapidly adapting cells which, in fact lost their inability to maintain impulse firing during prolonged periods of stimulation. Since the computer model could also account for these functional modifications it was used in a further analysis indicating that some of the adaptive mechanisms, whose effects are especially pronounced in the rapidly adapting receptor, may have protective functions serving to shut off the firing activity in conditions of excessively strong and/or prolonged constant stimulation.

028

MICROSCOPIC AND MACROSCOPIC DIFFERENCES IN Na CONDUCTANCE KINETICS IN SQUID AXON. H.M. Fishman, Department of Physiology and Biophysics, University of Texas Medical Branch, Galveston, Texas, USA.

An important assumption in modeling Na channel kinetics is that relaxation times determined for a single channel are the same as those from measurements on a large population of channels. To test this assumption, internal axial-electrode voltage clamp measurements were made on squid axons which were internally perfused with a Cs (no K) perfusate to eliminate K channel conduction. Na currents elicited by step clamps were analyzed in the steady state (0.3 to 12 sec) in two ways under the same conditions of measurement and in the same axon. The linear complex admittance, determined by FFT of the response to synchronized, Fourier-synthesized pseudorandom perturbations (1 mV) superposed on step clamps, was fitted by a Hodgkin-Huxley type expression for the admittance to obtain two natural frequencies; one for Na inactivation, $f_1 = (2\pi\tau_1)^{-1}$, and the other for Na activation, $f_2 = (2\pi\tau_2)^{-1}$. The power spectrum of fluctuations was fitted by a double Lorentzian function to obtain two corner frequencies, ν_1 and ν_2 , corresponding to the two natural frequencies from an admittance fit at the same membrane potential. In three axons the comparison, for a depolarization range of 50 mV from holding potential (-60 mV), yielded ν 's that exceeded the corresponding f 's by as much as 10 times. Thus it appears that, for Na channels in squid axons, microscopic and macroscopic kinetic parameters are different.

030

MEMBRANE DYNAMICS ASSOCIATED WITH EXCITABILITY AS REVEALED BY THE FLUORESCENT PROBE PYRENE. H. Duclouier, J.P. Desmaziers and D. Georgescauld, Centre de Recherches Paul Pascal (CNRS), 33405 Talence, France.

The influence of membrane lipid composition and the involvement of membrane dynamics or fluidity in the process of membrane excitation is still a controversial matter. In order to investigate the eventual interactions between the membrane lipids and the ionic channels, pike and garfish olfactory nerves and Myxicola giant axons were labelled with pyrene, a hydrophobic fluorescent probe, specific for the hydrocarbon core of the membrane. The excited dimer (excimer) formation is controlled by diffusion and thus sensitive to fluidity changes. When stimulated, the labelled nervous trunks responded with a transient decrease for the monomer emission associated with a transient decrease for the excimer emission. This first set of results is indicative of a small membrane rigidification (relative change of the order of 10^{-3} - 10^{-4}) associated with membrane excitation. In addition, comparison with fluorescence signals from fibers labelled with ANS (a strictly potential-dependent probe) showed that the pyrene signal developed slightly earlier than the propagating action potential. Voltage-clamp analysis on pyrene-labelled Myxicola giant axons demonstrate the lack of direct effect of electric field changes upon the emission properties of the probe. Only depolarizing steps induced fluorescence signals suggesting that the membrane rigidification is not involving the bulk of the lipid bilayer but could be rather restricted to the immediate vicinity of the ionic channels.

Friday 03 August Congress Centre-First Floor Posters 031-036

Posters on Chemical and Electrical Regulation of Ion Channels

031

TRANSITIONS BETWEEN THE DIFFERENT CONFORMATIONAL STATES OF SODIUM CHANNELS

K. Nagy and D. Hof, I. Physiology, Univ. Saarland, Homburg/Saar, FRG

Single sodium channels were studied in cell-attached patches in neuroblastoma cells, NIE 115 at 10 °C. Prepulses of different height and length preceded 40 ms test pulses to (-10)-(+30) mV (relative to RP). Results indicate that depolarizations do not necessarily induce transitions from the closed state to the open or to the inactivated state. The probability of staying in the closed state could reach 0.4 at +30 mV. At pulse potentials smaller than 20 mV (relative to RP) a periodicity in the first delay histogram was observed indicating the existence of more than one closed state before the open one. At 20 mV the inactivation time constant calculated from the decaying phase of the averaged current records was 8.5 ms, which is different from the value of 18.1 ms obtained from the prepulse experiments. The explanation for the difference could be that the time constant of the current decay reflects transitions in the activation pathway and from open to inactivated state, while in calculation of the time constant from the prepulse experiments the closed-inactivated transitions are also included.

033

NICOTINIC RECEPTOR CHANNELS ACTIVATED BY RAPID PERFUSION OF AGONISTS. J.P. Dilger, R. Brett and P.R. Adams, Department of Neurobiology and Behavior, State University of New York, Stony Brook, NY USA.

We recently described a technique for reversibly applying a known concentration jump to an excised membrane patch within 100 msec (Biophys. J. 45, 386a (1984)). This technique has now been modified to allow concentration changes to be made within 15 msec. We are using this method to apply agonists to outside-out patches obtained from cultured BC3H1 cells containing nicotinic receptor channels. After an outside-out patch is obtained, it is moved into a small hole in a segment of tubing which dips into the culture dish. Control solution normally flows through the tubing and around the tip of the patch electrode, which is placed in the center of the flow. A solenoid-driven pinch valve, upstream from the hole, is used to switch between control solution and agonist-containing solution at selected intervals. Using this approach, we are able to change the solution bathing an outside-out patch rapidly enough to activate most of the channels in the patch before desensitization begins. Desensitization processes with time constants of about 100 msec are observed when either 100 μ M ACh or 1 μ M carbachol is applied to the receptors. We are using nonstationary fluctuation analysis to calculate the open channel probability and the number of channels in the patch. Patches with as many as 200 channels have been obtained.

035

CAN PLASMA MEMBRANE-ASSOCIATED MICROFILAMENTS CONTROL ION FLUXES?

J.E. Friedman, O.E. Harish, K. Rosenheck & A. Oplatka
The Weizmann Institute of Science, Rehovot 76 100 Israel

Ion fluxes through channels in plasma membranes are associated with the stimulation of receptors. Movements of the latter have been linked to cytoskeletal elements. We therefore investigated the possibility that microfilaments might modulate cell response to stimuli by affecting ion fluxes. The effects of actin-specific reagents on secretion, membrane potential and ion fluxes (Ca^{2+} , Rb^+ , Na^+) have been examined, employing adrenal medulla chromaffin cells fused with liposomes containing DNase-I or heavy meromyosin (HMM). Both reagents caused depolarization of non-stimulated cells, elevation of Ca^{2+} influx (for both non-stimulated and acetylcholine-stimulated cells) and an increase in catecholamine secretion (for non-stimulated cells). HMM was found to induce a rise in the rate and extent of Na^+ influx and a decrease in Rb^+ efflux. The introduction of N-ethylmaleimide-poisoned HMM led to hyperpolarization and reduction in secretion. In view of these results, we propose the possibility that actin, with or without myosin, may control the functioning of ion channels by a fine tuning mechanism. Since cellular actomyosin is sensitive to Ca^{2+} we may conclude that the mechanochemical reactivity of actomyosin in cells is self-regulated, probably via a negative feedback mechanism. Surprisingly enough, relatively high concentrations of HMM (and apparently also DNase-I) added to the cells from the outside caused an increase in basal secretion and marked changes in Ca^{2+} uptake. We wonder whether certain circumstances (e.g. stimulation, cell damage during preparation) might not expose the tips of membrane-bound filaments.

032

SHAPE AND DIPOLE MOMENT OF SYNTHETIC MODELS OF ALAMETHICIN.

V. Rizzo & G. Schwarz, Department of Biophysical Chemistry, Biocenter, University of Basel, Switzerland. K.P. Voges & G. Jung, Institute of Organic Chemistry, University of Tübingen, FRG.

The peptides Boc-(Ala-Aib-Ala-Aib-Ala)_n-OMe, n=2 and n=4, have been synthesized as models of the pore-maker alamethicin. Dielectric dispersion measurements in n-octanol, a solvent which approximates the hydrophobic membrane environment, provide a sensitive determination of the shape and dipole moment of these molecules. Information on the conformation and the aggregation state of the peptides in n-octanol is obtained independently from circular dichroism and ultracentrifuge measurements. For the longer peptide (20 residues) the results compare very well with values previously determined for alamethicin, a peptide with the same number of residues, in n-octanol: the molecule is significantly helical and can be approximated with a prolate ellipsoid with axes of 32 Å and 12 Å, and a dipole moment of about 75 Debye. On the other hand, the average dipole moment determined for the decapeptide (~45 D at 25°C) is larger than expected and increases significantly with decreasing temperature. This behaviour is rationalized in terms of aggregation and conformational variability.

034

PATCH-CLAMP STUDIES OF DELAYED RECTIFIER POTASSIUM CHANNELS IN VESICLES OF MUSCLE MEMBRANE.

A. E. Spruce, N. B. Standen, P. R. Stanfield and T. A. Ward, Department of Physiology, University of Leicester, Leicester, U.K.

We have used a patch-clamp to record unitary currents from delayed rectifier K channels in vesicles of sarcolemma formed by enzyme treatment (collagenase then protease) of frog skeletal muscle immersed in 120mM-KCl solution. Channels were activated by depolarizing steps of membrane potential and their behaviour appeared essentially the same in vesicles as in intact muscle. The reversal potential for the currents varied with external $[\text{K}^+]$. This variation could be fitted by assuming that the channel selected between Na^+ and K^+ with $P_{\text{Na}}/P_{\text{K}} = 0.01$. At -20mV the single-channel chord conductance was 14.7 ± 0.5 pS (n = 8) in 2.5mM- K^+ external solution and was about doubled when $[\text{K}]_o$ was raised to 120mM. In patches with several channels the probability of observing any given number of channels open against time fitted the binomial distribution, suggesting that the channels behave independently. Channel open times were distributed as a single exponential implying a single open state, whereas closed times could be fitted by the sum of at least two exponentials. In 60mM- K^+ external solution, the mean open time was 3.5 ± 0.6 ms (n = 5) at +40mV. With 60mM- Rb^+ external solution and 120mM- Rb^+ internal solution the mean open time was increased at all potentials, being 12.8 ± 2.2 ms (n = 6) at +40mV. The chord conductance was reduced by Rb^+ . Thus both channel kinetics and conductance may be affected by the permeant ion.

036

GATING OF SINGLE SODIUM CHANNELS

R. Horn and C.A. Vandenberg, Department of Physiology, UCLA Medical School, Los Angeles, CA 90024, U.S.A.

Outside-out patch and whole-cell recordings of Na channel currents were obtained from GH3 cells in the presence of CsF at 9°C. Patch recordings revealed that individual channels open and close several times during a single depolarizing test pulse, especially to potentials more hyperpolarized than -30 mV. We estimated rate constants for a general model with 5 states (3 closed, 1 open, 1 closed-inactivated) using a maximum likelihood method (Horn, Lange, 1983, Biophys. J. 43: 207). Inactivation could occur from any state in this model. B, the rate constant for inactivating from the open state, increased with depolarization (e-fold/13 mV), in agreement with results obtained using N-bromosuccinimide (Horn et al., 1984, Biophys. J. 45:323). The closing rate constant, on the other hand, increased with hyperpolarization. Our analysis suggests that macroscopic inactivation derives its voltage dependence from both the activation process and B. The estimated rate constants provided excellent estimates of the open time, closed time and first-latency densities, the time course of averaged currents, the autocovariance, and the distribution of number of channel openings per record. Statistically acceptable models (compared by likelihood ratio tests) required inactivation to occur from the open state and at least one of the closed states. The Hodgkin-Huxley and strictly-coupled models were statistically eliminated at the 0.1% level.

Friday 03 August Congress Centre-First Floor Posters 037-042

Posters on Chemical and Electrical Regulation of Ion Channels

037

CONFORMATIONS AND SINGLE CHANNELS OF NATURAL AND SYNTHETIC LINEAR GRAMICIDINS
F. Heitz*, C. Gavach* and Y. Trudelle**, *Laboratoire Physicochimie des Systèmes Polyphasés BP 5051, F34033 Montpellier and **Centre de Biophysique Moléculaire F45045 Orléans.

On the basis of NMR and IR data, it is shown that Gramicidin A and its 9,11,13,15-destryptophyl-phenylalanine synthetic analog (Gramicidin M) adopt in chloroform the same conformation which is based on a heterogeneous helical structure: antiparallel double-helix terminated by two α -helices at the C-terminal ends of the dimer. Although it does not correspond to the active form (additions of Cs ions generate strong modifications in the CD spectrum involving an inversion of the ellipticity around 220 nm) this finding corroborates all the observations which indicate that under identical conditions, both Gramicidins adopt identical conformations. This points out the role of the side-chains on the energy profile of the channel and therefore on the single channel behaviour. Indeed, while the binding is the determining step for Gramicidin A, for the synthetic analog which shows a non linear I-V curve, the translocation step is the determining process.

039

GMI MICELLES MODIFY THE TRANSPORT PROPERTIES OF THE IONOPHORE GRAMICIDIN D IN ARTIFICIAL PLANAR BILAYERS.

F. GAMBALE, C. MARCHETTI, C. USAI, M. ROBELLO AND A. GORIO, Istituto di Cibernetica e Biofisica, Corso Mazzini 20, Camogli (Genova), Italy.

We have analyzed the effects induced in different phospholipid planar bilayers by monosialoganglioside micelles containing the ionophore gramicidin D. The membrane conductance increases after the addition of GMI micelles at various ionophore/ganglioside ratios. We have estimated that this fact may be ascribed to gramicidin molecules which incorporate into the bilayer together with gangliosides. In presence of micelles the mean lifetime and the amplitude of the gramicidin single-channel do not present relevant modifications when dioleoylphosphatidylcholine or phosphatidylserine were used to form the bilayer. Calcium proved to trigger the interaction between phosphatidylethanolamine membranes and GMI micelles containing gramicidin. In this case the ionic pore presents a longer lifetime and a lower amplitude with respect to pure gramicidin. We suggest that different properties developed by gramicidin may depend on structural organization of gangliosides when incorporated into the phospholipid membranes.

041

VOLTAGE-SENSITIVE IONIC MECHANISMS IN THE SOMAL AND DENDRITIC MEMBRANES OF CULTURED CEREBELLAR PURKINJE NEURONS. D.L. Grwl, Division of Preclinical Neuroscience and Endocrinology, Scripps Clinic and Research Foundation, La Jolla, CA 92037 USA.

Vertebrate cerebellar Purkinje neurons (PNs) display complex patterns of activity thought to arise from voltage-sensitive ionic mechanisms regionally segregated in the somal vs. dendritic membrane. In intracellular recordings from the somal or dendritic region, Na^+ , Ca^{++} or K^+ channel blockers significantly altered the characteristic patterns of spontaneous or current evoked activity, suggesting the presence of a variety of ionic mechanisms. Single channel recordings were used to identify the ionic mechanisms and their distribution across the neuronal surface. In the somal region unitary currents mediated by several types of ion channels were observed, including at least 3 types of voltage-sensitive K^+ channels, identified by their single channel conductance (~100, 40, 20 pS), voltage sensitivity and sensitivity to TEA. Voltage-sensitive K^+ channels, including a Ca^{++} activated K^+ channel, were also observed in single channel recordings from the dendritic region of PNs. In both regions, K^+ channel activity was associated with the falling phase of action potentials. These data suggest that Ca^{++} and K^+ mediated electrical events occur in both the somal and dendritic region of PNs and that K^+ channels function in the repolarizing phase of the action potential, which appear to be generated in both regions. (Supported by NIAAA 06420)

038

A Na^+ CONDUCTING CHANNEL OBSERVED IN THE ABSENCE OF EXTERNAL Ca^{++} . R. Levi and L. J. DeFelice, Emory University School of Medicine, Department of Anatomy, Atlanta, Georgia USA

We studied inward currents during spontaneous action potentials, in cell-attached patches on ventricular cells from 7-day chick embryo. The preparation was bathed in (mM) 3.5 K/100 Na/1.5 Ca (HEPES pH 7.3, room temperature). The patch pipette contained 133 or 200mM Na and either 5mM EGTA or 3mM EDTA, giving free Ca^{++} concentrations less than 10^{-8} M. We observed large, voltage-activated, inward patch currents. This channel was not blocked by TTX (10^{-5} g/l) and was distinguishable from fast Na^+ channels when present. The conductance of this channel, measured by plotting action current against action potential, is approximately 90 pS (200mM Na) and the reversal potential is in good agreement with a Na^+ channel. We never observed this channel in the absence of Ca^{++} chelating agents. We speculate that this channel may be a modification, due to the low Ca^{++} condition or the presence of chelating agents, of the Ca^{++} channel responsible for part of the slow inward current (Kostyuk & Krishtal J. Physiol. 270: 569, 1977).

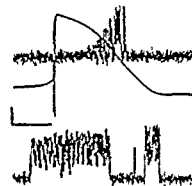


Fig. 1: 200mM Na, 3mM EDTA; Scales: 2.5 pA or 25 mV; 300 msec (top), 25 msec (bottom). Inward current is up. Supported by P01-HL27385.

040

HYPERPOLARIZATION INDUCED MEMBRANE CURRENT IN RECEPTOR NEURONES

A. Edman, S. Gestrelus and W. Grampp, Department of Physiology and Biophysics, University of Lund, Lund, Sweden.

In lobster stretch receptor neurones a slow inward membrane current is activated by membrane hyperpolarization beyond resting voltage levels. The current, which under normal circumstances is mainly carried by Na^+ , is effectively blocked by Cs^+ in 1-2 mM concentration. The current activation, which is more pronounced in slowly than in rapidly adapting receptors, is characterized by a sigmoidal voltage dependence of its stationary value and a bell-shaped voltage dependence of its relaxation time in a voltage range from about -60 to about -100 mV. The kinetic data are consistent with the current passing through membrane channels whose permeability and gating properties can be shown to be dependent on e.g. temperature and ionic composition of the extracellular solution. The functional significance of the current is still not quite obvious. Because of its kinetic properties it can not affect maintained impulse firing. It does, however, shorten post-tetanic hyperpolarization and may, in this way, contribute to a fast restoration of the cell's excitability to resting values.

042

A SMALL CONDUCTANCE K^+ -DEPENDENT CHANNEL IN CULTURED HUMAN MONOCYTES. C. Ince(1), B. Van Duyn(2), D.L. Ypey(2) & P.C.J. Leijh (1). Dept. of Infectious Diseases(1) and Dept. of Physiology(2), University of Leiden, Leiden, The Netherlands.

Recently we reported the presence of single channel activity in cultured human monocytes. These channels 1) are large conductance (130pS) K^+ channels, 2) activate at patch potentials more positive than +30mV, 3) are responsible for the hyperpolarizing response measured in mononuclear phagocytes and 4) are probably $\text{K}^+(\text{Ca}^{2+})$ channels. A second group of K^+ dependent channels was also found. Current voltage characteristics were measured in the cell attached patch mode with different patch electrode fillings. The peak of the impalement transient upon microelectrode entry was used to correct for membrane potential. Whole cell current clamp measurements in combination with microelectrode impalements showed the peak potential to be an accurate (10%) estimate of the membrane potential of such high resistance cells (20G Ω). Analysis of amplitude histograms and activation kinetics of these channels showed that 1) they are K^+ dependent, 2) have a mean conductance of 32pS, 3) activate at patch potentials less negative than -40mV, 4) show bursting kinetics (short and long bursts), 5) are not the $\text{K}^+(\text{Ca}^{2+})$ channels associated with the hyperpolarizing response, and 6) show outward rectifying properties. It is suggested that these channels are the same delayed outward rectifier K^+ channels recently reported for cultured mouse peritoneal macrophages and human T-lymphocytes.

Friday 03 August Congress Centre-First Floor Posters 043-048

Posters on Chemical and Electrical Regulation of Ion Channels

043

HOW MANY K^+ -CHANNEL POPULATIONS DO EXIST IN THE FROG NODAL MEMBRANE?

R.J. Van den Berg and G. De Bruin, Department of Physiology, State University of Leiden, The Netherlands.

Recently for the frog node of Ranvier the existence of two populations of Hodgkin-Huxley (H.H.) K^+ -channels has been proposed. The results of voltage jump experiments and fluctuation measurements -with corrections for the effects of K^+ -accumulation-, however, contradict this hypothesis.

Activation and deactivation of the K^+ -conductance could be well fitted according to 2 populations of K^+ -channels with H.H.-kinetics. However, the time constants obtained from deactivation differed considerably from the time constants obtained from the activation kinetics. This is inconsistent with the hypothesis.

The spectral density of the K^+ -current fluctuations measured during 500 ms depolarizing pulses contain 2 Lorentzians. Their cutoff frequencies did not agree with the ones predicted by stochastic interpretations of the two postulated types of H.H.- K^+ -channels.

Instead of different populations of H.H.- K^+ -channels we propose the existence of a single population with complex kinetic properties.

045 ORAL PRESENTATION

PRESSURE DEPENDENCE OF SODIUM GATING CURRENTS IN SQUID AXONS. F. Conti, I. Inoue, F. Kukita and W. Stühmer, Ist. Cibernetica e Biofisica, C.N.R. Corso Mazzini, 16032 Camogli, Italy.

Gating currents, I_g , were measured in squid axons at hyperbaric pressures, P , up to 60 MPa. I_g became gradually slower and decreased in amplitude with increasing P . By appropriate time and amplitude scaling, I_g records at P could be made to superimpose with those at normal pressure. The scaling factors were roughly independent of membrane potential. The time factor increased exponentially with pressure as if all the Na channel opening steps which produce detectable charge movements had the same activation volume, $\Delta V \sim 17 \text{ cm}^3/\text{mole}$. This value is roughly one half of that describing the pressure effect on sodium current activation, suggesting that some late opening step has a large activation volume without producing significant I_g contributions. A reversible decrease with pressure of the total gating charge associated with any step depolarization was also observed. The decrease was about 30% at 60 MPa, and it reminded the phenomenon described by Matteson and Armstrong, of Na channels becoming sleepy at low temperatures.

047

INACTIVATION OF SINGLE CALCIUM CHANNELS IN CARDIAC MYOCYTES. A. Cavalié, D. Pelzer and W. Trautwein. Dept. Physiol. 2, Univ. Saarland, Homburg, F.R.G.

Currents through single calcium channels in the membrane of isolated guinea pig ventricular cells were recorded by the patch-clamp technique in the cell-attached configuration using barium (90 mM) as charge carrier (Cavalié et al., Pflügers Arch. 398: 284, 1983). Calcium channel activity occurred as brief unitary current pulses grouped into bursts. This gating behaviour related to calcium channel activation could be explained by a sequential model in which two shut states precede the open state of the channel. However, long observation periods indicated that bursts were further grouped into clusters separated by long shut intervals, which can be attributed to the existence of an inactivated state. The mean cluster lifetime correlated well with the rate for the declining phase of the ensemble mean current, since clusters appeared usually once per depolarization and entrance into the inactivated state was rarely followed by reopenings. Some test pulses of each ensemble did not elicit channel activity at all ("blanks"). The number of "blanks" per ensemble increased by depolarizing the potential preceding clamp pulses to a constant potential. Vice versa, the probability of the calcium channel being available to open decreased in a sigmoidal manner with the conditioning depolarization providing a possible measure for the steady-state occupancy of the inactivated state.

044

DETERMINATION OF THE SURFACE CHARGE OF THE ANOMALOUS RECTIFIER CHANNEL (IK1) OF AVIAN CARDIAC CELLS USING SINGLE CHANNEL CONDUCTANCE MEASUREMENTS. M.J. Kell and L.J. DeFelice, Anatomy Department, Emory University, Atlanta, GA, USA.

Using single channel techniques, we have determined the electrical environment surrounding the anomalous rectifier channel in embryonic avian cardiac cells. The surface potential calculated from single-channel conductance measurements is about -40 mV (in 100 mM $K^+/33 \text{ mM Na}^+$). The surface charge density is estimated to be about $-1e/\text{nm}^2$. This value is equivalent to the surface charge near other K^+ channels studied with macroscopic methods. Surface charge is calculated using a model based on discrete charges in well-separated channel proteins of specified size. This model fits existing data for Na and K channels in nerve membranes better than the Gouy-Chapman-Stern model. The discrete model collapses to the infinite, uniformly charged sheet for a large number of charged sites and large membrane area. The anomalous rectifier is composed of at least five, distinct conductance substates which are not generally interconverting. The open state probability of these substates is about 90% and is voltage-independent, independent of external K^+ , and does not block with 10 mM Ba^{++} in the pipette.

046

A POSSIBLE BASIS FOR ION SELECTIVITY IN Ca CHANNELS. W. Almers, E.W. McCleskey & P.T. Palade. Dept. Physiology & Biophysics, U. of Washington, Seattle, WA 98195, U.S.A.

Experiments on frog skeletal muscle fibres voltage-clamped with the vaseline-gap technique show that, as in other tissues, Ca channels with external Ca are selectively permeable to Ca^{++} and not to Na^+ or K^+ . But when external Ca^{++} is removed, Ca channels become permeable to Li^+ , Na^+ , K^+ , Rb^+ and Cs^+ . Ba^{++} and Mg^{++} are also much more permeant when Ca is absent. Exclusion of monovalent cations is restored by external Ca binding to a single class of sites with $K_D = 0.7 \mu\text{M}$. Other divalent cations act similarly, but require higher concentrations. Evidently Ca channels are innately unselective and obtain their ability to reject cations other than Ca only by binding Ca at high affinity. Our data can be explained quantitatively if the Ca channel is an aqueous "single-file" pore containing two binding sites, to which a permeating ion must bind in succession. Ions in the pore cannot pass one another, but may dislodge each other by electrostatic repulsion. The empty pore is permeable to many cations. In ion mixtures, the pore will be occupied by the ion with the highest affinity, namely Ca^{++} . In a Ca occupied pore, only another high-affinity ion such as Ca^{++} will occupy the site sufficiently long to dislodge the resident ion, thereby generating Ca flux. Hence, the ion selectivity of Ca channels stems from the specific and high affinity of the site to Ca. With diffusion-limited access of Ca^{++} to the pore, the model predicts single Ca channel currents as observed in other tissues. Supported by USPHS grant AM-17803.

048

FLUORESCENCE QUENCHING STUDIES OF FAST ION PERMEATION THROUGH CHANNELS IN SARCOPLASMIC RETICULUM VESICLES

M. Kasai, K. Nunogaki, M. Tanifuji, and M. Sokabe, Dept. Biophys. Engineer., Fac. Engineer. Sci., Osaka Univ., Toyonaka, Osaka, Japan and Dept. Behavioral, Fac. Human Sci., Osaka Univ., Suita, Osaka, Japan.

Channel properties of sarcoplasmic reticulum (SR) membrane were studied mainly by two methods: the electrical method and the fluorescence quenching method. Single channel conductances of SR membrane incorporated into planar phospholipid bilayer membrane were determined. In 0.1 M solutions, they were 160 pS, 80 pS, 180 pS, and 180 pS for K^+ , Tl^+ , Cl^- , and I^- , respectively. Fast influx of ions through the vesicle membrane was studied by the fluorescence quenching technique. Pyrenetetrasulfonate (PTS) were incorporated inside the vesicles. After the mixing with the solution containing $TlNO_3$, the quenching process of PTS fluorescence caused by Tl^+ influx was followed by the stopped flow method. The quenching curves were analysed graphically by using a microcomputer. Four components with different time constants were obtained. An example of the distribution of the permeation times is as follows: 4.6 msec 31%, 62 msec 21%, 2.6 sec 33%, and slower component. Similarly, influx of I^- was determined by using KI instead of $TlNO_3$. Tl^+ and I^- were considered to permeate through the cation and anion channels, respectively. If we assume that each vesicle has one channel obtained electrically, the permeation times are expected to be 2.4 msec for Tl^+ and 1.1 msec for I^- . These values are consistent with the fastest components obtained by the fluorescence quenching method.

Friday 03 August Congress Centre-First Floor Posters 049-054

Posters on Chemical and Electrical Regulation of Ion Channels

049

A POSSIBLE MECHANISM OF SODIUM ACTIVATION GATING IN SQUID GIANT AXONS

Gen Matsumoto, Electrotechnical Laboratory, Tsukuba Science City, Ibaraki 305, Japan.

We found that both time and voltage dependence of the rise of the sodium conductance in squid giant axons were well approximated in terms of the triple power of the running integrals of the colchicine-sensitive component of the asymmetry current. In spite of this, the colchicine-sensitive component had a definite rising phase and did not follow first-order kinetics as Hodgkin and Huxley (1952) predicted. In order to overcome this apparent inconsistency we calculated the probability of sodium channels being open in the following two cases: One is the case that the gate has only two states but that transition velocities between open and closed states of the gate depend on not only membrane potential but also time after a potential step is applied. The other is the one that the gate has a number of states continuously and that the membrane model proposed by Matsumoto (J. theor. Biol., 1984) is rigidly applied. We found both of them could explain the experiments quite well. Further, we found the modifications on the Hodgkin-Huxley model of the sodium activation gate introduced in the former case were consistent with the membrane model by Matsumoto (1984).

051

EFFECTS OF CATECHOLAMINES ON CA CONDUCTANCE IN CULTURED DORSAL ROOT AND SYMPATHETIC NEURONS OF CHICK

C. Marchetti, E. Carbone and H.D. Lux, Max Planck Institut für Psychiatrie, Planegg-Martinsried b. München F.R.G.

The effects of dopamine and norepinephrine on whole cell and unitary Ca currents of chick sensory and sympathetic neurons were investigated using the patch-clamp technique. Cells were bathed in a solution containing (mM): 120 Na, 5 Ca, 2 Mg and 3 mM TTX. The internal medium contained (mM): 130 Cs, 20 TEA and 5 Ca-EGTA buffer (free $Ca_{i0} = 5 \cdot 10^{-6}$ M). In both preparations, Ca inward currents reached maximal amplitude between -5 and +5 mV membrane potential. At +10 mV, the peak was attained within 10 ms and then the current slowly inactivated. Catecholamines, externally applied by pressure ejection at a concentration of 10 to 100 μ M, affected mostly the rising phase of this current and depressed the later phase to a minor extent. In the presence of the drugs, the Ca current reached a peak at almost 100 ms and showed no sign of inactivation. The action of the drugs was fast and fully reversible within seconds.

Single channel recordings were performed in outside-out patches under similar conditions and also in a Na-free bath solution. Inactivation kinetics were determined by sample averaging. Two types of Ca channels were identified: one of smaller amplitude (4.5 pS) and slow inactivation and another of larger amplitude (9.5 pS) and fast inactivation. The frequency of opening of the fast inactivating channel was strongly reduced by dopamine. We suggest that catecholamines prevent specifically the voltage dependent activation of this channel.

053

CAPTURE OF MAST CELL DEGRANULATION EVENTS BY THE PATCH CLAMP TECHNIQUE. J.M. FERNANDEZ and L. NEHER, Department of Membrane Biophysics, Max-Planck-Institut für biophysikalische Chemie, D-3400 Göttingen, West Germany.

The membrane capacitance of Rat Peritoneal Mast Cells was continually monitored using the patch clamp technique in whole cell recording mode. When cells were dialyzed with solutions containing high free Ca^{2+} concentrations ($> 0.5 \mu$ M), cells degranulated, (observed under Nomarsky optics). Concomitant with these morphological changes we measured large increases in the cell membrane capacitance from about 4-6 pF in the normal cell and up to 35 pF in degranulated cells; we interpret this as a large increase of the cell membrane area. This capacitance increase proceeded in a stepwise fashion. The distribution of capacitance step sizes is well predicted by the observed distribution of secretory granule diameter described by Helander and Bloom (1974, J. Microsc. 100:315). Thus the capacitance steps probably correspond to the fusion of single secretory granules with the plasma membrane (exocytosis).

Frequently, step decreases of capacitance were also observed. Their size distribution was similar to that observed for step increases, probably corresponding to the process of endocytosis.

For both, step increase and decrease of capacitance, some very large steps were observed, that cannot be explained as the fusion or retrieval of a single secretory vesicle but probably correspond to "sequential exocytosis", the fusion of several granules prior to their fusion to the plasma membrane.

Partially supported by an Alexander von Humboldt-fellowship to J.M.F.

050

PROPERTIES OF BATRACHOTOXIN-MODIFIED SODIUM CHANNELS IN VARIANT NEUROBLASTOMA CELLS.

L-Y.M. Huang, Marine Biomedical Institute, The University of Texas Medical Branch, Galveston, Texas, U.S.A.

The gating properties of batrachotoxin-modified sodium channels was studied in cultured neuroblastoma C9 cells, using patch clamp and whole cell recording techniques. Sodium channels in this cell line could not be activated by depolarization. After the addition of batrachotoxin, the sodium channels could be activated when the membrane potential was stepped from a holding potential to a level more positive than -80 mV. The concentration of batrachotoxin required to activate these sodium channels in C9 cells was about 1.5-2 fold higher than those found in the neuroblastoma NG108-15 cell. The batrachotoxin-activated sodium current of C9 cells did not inactivate.

The single sodium channel conductance was about 12 pS. The histogram of open state dwell time could be fit by single exponential. The mean open time increases with depolarization. The properties of batrachotoxin-activated sodium channel in C9 were similar to those in neuroblastoma NG108-15 cells. (Supported by NIH NS19352-02)

052

ANALYSIS OF REFRACTORY PROCESS IN EXCITABLE MEMBRANE USING HODGKIN-HUXLEY NERVE EQUATION

S. Higashino, Department of Communication Engineering, Faculty of Engineering, Tokai University, Hiratsuka, Kanagawa-ken, Japan.

Hodgkin-Huxley nerve equation consists of four ordinary differential equations. Using electronic computer, voltage-current (V-I) characteristics of the membrane, the relation between time and V, m, n, h ($T-V, m, n, h$), and the relation between V and m, n, h ($V-m, n, h$) were investigated. In the characteristics of $V-I, V-m, V-n$ and $V-h$, a state switching over to relative refractory period from absolute refractory period was clarified. In other words, on curves of the above mentioned characteristics, a state shifting from the subthreshold response in the absolute refractory period to the action potential in the relative refractory period was made clear by changing gradually the time duration between the first and second pulses of the stimulating current. Especially, the change of curves in the before and after the threshold is very interesting. This shows the process that the operating point shifts from the stable point to the unstable point in the V-I characteristics.

054

PARALLEL SLOWING OF NA ACTIVATION AND INACTIVATION DELAY BY ZN L. Goldman, G.A. Ebert and R. Chandler, Dept. of Physiol., School of Med., Univ. of Maryland, Baltimore, MD. 21201.

Inactivation in *Myxicola* Na channels develops with a delay indicating a precursor process (Goldman and Kenyon, J. Gen. Physiol. 80:83, 1982). The precursor process is kinetically similar to Na activation. The potential dependency of its time constant is the same as Na activation and when resolvable the delay time constant is just τ_m . We report that external Zn slows the time to half maximum g_{Na} ($t_{1/2}$) and inactivation delay in a parallel way (1.6-fold in 5 mM Zn). If the change in $t_{1/2}$ were due entirely to surface potential effects, τ_c should have slowed 2-fold while only 10% was seen. In Zn, peak I_{Na} following brief conditioning always increased over the unconditioned value. Without Zn, brief conditioning pulses produced no change or a slight decrease. Without Zn delay decays as a simple exponential. In Zn delay develops as two exponentials plus a third process complete by 200 μ s of conditioning at -22 mV, as expected if three sequential processes precede inactivation. Na activation in *Myxicola* also develops as three processes, one very rapid. These effects are consistent with the suggestion (Cilly and Armstrong, J. Gen. Physiol. 79:935, 1982) that Zn stabilizes resting state(s) occupancies and weights more heavily transitions preceding channel opening. g_{Na} time course in Zn is accurately reconstructed with a five state sequential coupled model using the time constants fitted to the inactivation delay time course, providing clear evidence that some fraction of Na channels conduct before they can inactivate. Supported by USPHS Grant NS-07734.

Friday 03 August Congress Centre-First Floor Posters 055-060

Posters on Chemical and Electrical Regulation of Ion Channels

055

RECONSTRUCTING THE CARDIAC ACTION POTENTIAL FROM SINGLE-CHANNEL CURRENTS. L. J. DeFelice and R. Levi, Anatomy Dept. Emory University School of Medicine, Atlanta, Georgia USA

We are studying voltage-activated channels in cell-attached patches during spontaneous beating. If one channel, e.g., the fast Na channel, is in the patch, the ensemble average taken over many beats $\langle i_{Na}(t) \rangle$ is proportional to the macroscopic Na current during the action potential. The proportionality constant is the density of Na channels (N_{Na}). For two Na channels, the proportionality constant is $N_{Na}/2$, etc. $\langle i(t) \rangle$ can be found for each type of channel, and these are related to the whole-cell, membrane action potential $V(t)$ by

$$V(t) = \frac{N_{Na}}{C} \int_0^t \langle i_{Na}(u) \rangle du + \frac{N_K}{C} \int_0^t \langle i_K(u) \rangle du + \dots$$

C is the specific membrane capacitance. N values can be adjusted to fit $V(t)$. To measure N, whole-cell data are required. The time course of $\langle i(t) \rangle$ is model-independent; it contains the voltage- and time-dependent probability of the channel states. Since $\langle i(t) \rangle$ can also be calculated from kinetic models based on steady-state or voltage-step relaxation experiments, it can be used to test the effect of other parameters, such as changes in ion concentration. We have measured $\langle i(t) \rangle$ for the fast Na channel and for a plateau K channel (Biophys. J. 45: 308a) in embryonic chick ventricle, and we have reconstructed their contribution to the cardiac action potential. The slow-inward current and the anomalous rectifier are under study. Supported by P01HL-27385

057

INTRACELLULAR Ca^{2+} IN CLONAL ANTERIOR PITUITARY CELLS MEASURED WITH QUIN 2. P. Gangola, G. G. Schofield, and H. C. Pant, Laboratory of Preclinical Studies, National Institute on Alcohol Abuse & Alcoholism, Rockville, MD 20852, USA.

Intracellular calcium concentration $[Ca^{2+}]_i$ in clonal AtT-20/D-16 mouse anterior pituitary tumor cells was measured with the fluorescent calcium indicator Quin 2. Cells ($2-4 \times 10^6$ cells/ml) were loaded with Quin 2 by incubation with acetoxymethyl ester derivative (Quin 2/AM), which was subsequently hydrolyzed and trapped inside the cells. The fluorescence signal measured from these cells in the solution containing 145 mM NaCl, 5 mM KCl, 0.8 mM $MgCl_2$, 20 mM glucose, 10 mM HEPES (pH 7.0) and varying concentrations of calcium chloride $[Ca^{2+}]_o$ (0.01-1.0 mM) corresponded to an intracellular calcium $[Ca^{2+}]_i$ of 0.074-0.173 μ M. When 50 mM NaCl was replaced by 50 mM KCl (high K^+) in the above cell suspension the fluorescence signal corresponded to an intracellular calcium of 0.074-0.400 μ M. There was a large increase (0.240 μ M) in $[Ca^{2+}]_i$ in these cells in high K^+ containing 1.0 mM $CaCl_2$ solution; however, the $[Ca^{2+}]_i$ increase was not significant in lower (0.01 mM) external calcium concentration $[Ca^{2+}]_o$. The level of $[Ca^{2+}]_i$ also increased when cells were depolarized by addition of veratridine (10 μ M); this effect was completely reversed by the addition of tetrodotoxin (1.0 μ M). These results suggest that the calcium regulation in AtT-20/D-16 cells can be studied with Quin 2.

059

SODIUM CHANNELS IN NERVE MEMBRANE VESICLES AND IN RECONSTITUTED PROTEOLIPOSOMES

Ana M. Correa, Gloria M. Villegas and R. Villegas, Instituto Internacional de Estudios Avanzados (IDEA), Apartado 17606, Caracas 1015A, Venezuela.

Na^+ influx into lobster nerve plasma membrane vesicles was measured in the presence of veratridine (VER), anesone toxin II (ATX), VER plus ATX, and of tetrodotoxin (TTX). The effect of the toxins was studied with the vesicles prepared in 0.3 M KPI, 1 mM NaPI, 2 mM $MgSO_4$, pH 7.4, and diluted 20-fold in 0.3 M choline PI, 1 mM NaPI, 2 mM $MgSO_4$, pH 7.4, containing ^{22}Na and the toxins. VER and ATX stimulated the influx with K_m 's of 20 μ M and 0.1 μ M respectively. The addition of 40 μ M ATX diminished the K_m for VER to 2 μ M. TTX blocked the influx stimulated by VER, ATX, and VER plus ATX with K_m 's of 27, 13 and 28 nM respectively. The outwardly oriented K^+ gradient was required to observe the effect of VER and ATX. The effect of VER and ATX were diminished by increasing the external K^+ ; 50% decrease of the ATX effect was obtained with 51 mM K^+ . Proteoliposomes prepared with nerve membrane treated with 0.5% Na cholate plus 30 mM octylglucoside and reconstituted into soybean liposomes by freeze-thaw-sonication responded to VER ($K_m = 50 \mu$ M) and to TTX ($K_m = 13$ nM). ATX only stimulated the influx into the proteoliposomes at high concentrations ($>1 \mu$ M) and in the presence of VER. The K^+ gradient was required. No effect was observed with up to 10 μ M ATX in absence of VER. TTX blocked the effect of VER plus ATX ($K_m = 14$ nM). Reconstitution with fractions of membrane particles obtained by detergent are being carried out. *On leave of absence from IVIC.

056

MEMBRANE POTENTIALS AND REACTION RATES

J. Boock and H. Wennerstrom, Department of Biochemistry, Arrhenius Laboratory, University of Stockholm, S-106 91 Stockholm, Sweden

The kinetic coefficients, whether in a conventional molecular scheme or in a general non-equilibrium thermodynamic formulation, in general carry a potential dependence. Obviously, the kinetic coefficient can be considered constant over a sufficiently narrow range of potentials, but in many applications it appears that this range is too narrow for the approximation to be useful. This potential dependence has largely been neglected in quantitative models of free energy translocating systems. Based on conventional molecular kinetics we analyze the particular kinetic features of a chemical transformation involving transport of ions across a membrane. We show that membrane potentials change the kinetic coefficients in a way that is dependent on the structural organization of the enzyme system. There is consequently a relation between control behavior and the spatial enzyme organization in the membrane. We also find that under certain conditions the rate is independently dependent on the electrical and dph components of the proton motive force.

058

MODULATION OF GRAMICIDIN A CHANNEL LIFETIME BY VOLTAGE AND BLOCKING DEPENDENT ION OCCUPANCY.

A. Ring and J. Sandblom, Dept. Physiology and Med. Biophysics University of Uppsala, Sweden.

The gramicidin A channel lifetime has been measured for 90% hexadecane synthetic bilayer membranes and various electrolyte concentrations of Li, K, Cs and HCl. The effect of blocking agents, osmotic pressure and voltage dependence of asymmetric solutions has been investigated and the results evaluated using simple barrier-site models of ionic conduction. The relation of channel lifetime to membrane properties (surface tension) was examined. The surface tension was measured using laser reflections from the pressure induced curvature of the bilayer membrane. The lifetime is correlated to the cation occupancy of the channel and the results suggest that increasing occupancy increases the channel stability (lifetime). The lifetime increases with increasing ion activity reaching a maximum at about 1M. In contrast the surface tension remains essentially constant up to about 1M then decreasing for higher concentrations. Osmotic pressure increases the channel stability at low ionic strengths and divalent blocking agents reduce the lifetime at low and high ionic strengths. Also, in asymmetric solutions, e.g. HCl-KCl, the channel lifetime is strongly voltage dependent approaching the lifetime corresponding to the specific ion (H⁺ or K⁺) being driven into the channel for +/- voltages applied across the membrane.

060

CARDIOTOXIN-INDUCED CHANNELS IN LIPID BILAYER MEMBRANES. E. Diaz and J. Sandblom, Dept. of Physiology and Medical Biophysics, Univ. of Uppsala, Uppsala, Sweden.

The effect of Cardiotoxin (CTX) and Phospholipase (PLA) from the Haind Cobra (*Naja naja siamensis*) venom was studied in planar lipid bilayers. When either CTX, fraction II or IV, and/or PLA A2: A1 are added to the solution on one or both sides of a lipid bilayer membrane the conductance changes in discrete steps forming the following types of channels: (a) short-life channels which can last from less than one second to a few minutes; (b) long-life channels which open and remain in this state for some minutes or even hours. The channels are anion selective and their conductances vary between 10 to 240 pS in 0.1M KCl and 10 to 4000 pS in 1M KCl. The smallest values in each case are associated with PLA-induced channels. The long-life channels present a flicker process. The frequency of occurrence of the channels increases in the presence of PLA. Addition of Ca to the bathing solution enhances even more CTX-effect: a further increase in channel frequency appearance is observed, the channel duration is augmented, the flicker process is more frequent and the flickers are longer.

Friday 03 August Congress Centre-First Floor Posters 061-066

Posters on Chemical and Electrical Regulation of Ion Channels

061

MICROSCOPIC DISTURBANCES OF THE CARDIAC IMPULSE SPREAD AT HIGH DRIVING FREQUENCIES

E. Hofer, H. Windisch and H.A. Tritthart, Inst. für Med. Physik und Biophysik, Universität Graz, Harrachgasse 21, A8010 Graz, Austria

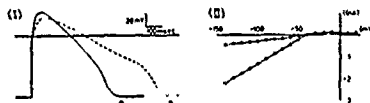
We have performed measurements of action potentials and conduction velocities in guinea pig and rabbit papillary muscles and Purkinje-fibers in microscopic areas. Continuous and save propagation was observed in Papillary-muscles within a preparation dependent frequency range (6-16Hz). Above this range spontaneous changes of the paths of excitation occurred in a beat to beat like manner, leading to exorbitant changes of conduction time in microscopic areas. Similar results were obtained in Purkinje-fibers, but the uppermost excitation frequency was limited to about 6Hz due to a 2:1 block. These results indicate, that macroscopic disturbances in impulse conduction associated with high excitation frequencies (ventricular arrhythmias) are likely caused by severe microscopic discontinuities of propagation.

062

DIFFERENTIAL EFFECTS OF pH_i AND pH_o ON THE INWARDLY RECTIFYING POTASSIUM CURRENT IN HEART CELLS FROM BULLFROG ATRIUM

K. Kanai and W. Giles, Department of Medical Physiology, The University of Calgary, Faculty of Medicine, Calgary, Canada.

An intracellular single suction microelectrode technique has been used to record the inwardly rectifying K^+ current, i_{K1} , in single myocytes obtained from bullfrog atrium by an enzyme dispersion method. The inhibition of i_{K1} by ΔpH in the acid direction has been studied; and an attempt has been made to determine whether ΔpH_i or ΔpH_o is more effective. Our results consistently show that when a Na-acetate buffered Ringers is used to change both intra- and extracellular pH from control (7.4) to acid (6.0) values: (I) the action potential is prolonged, (II) i_{K1} (recorded in 25 mM K^+ Ringers) is significantly inhibited ($80\% \pm 5\%$, s.e., $n=3$). In contrast, when only pH_o is changed to pH 6.0 (K-biphthalate Ringers) i_{K1} is reduced very little ($7\% \pm 4\%$, s.e., $n=3$). These data suggest that pH modulates i_{K1} in cardiac myocytes by a mechanism similar to that originally described by Moody and Hagiwara (1982) in starfish oocytes.



063

ON THE MECHANISMS OF POST-STIMULUS HYPERPOLARIZATION IN RETZIUS NERVE CELLS OF LEECH

S.Š. Ošanović and B.B. Beleslin, Inst. of Pathological Physiol. Med. Fac. Belgrade, Yugoslavia.

Excessive firing in Retzius nerve cells of leech, *Haemaphysalis sanguisuga*, was followed with a strong membrane hyperpolarization. With a sufficient long train of impulses post-stimulus hyperpolarization (PSH) consisted of two different phases. During the early part of PSH a decrease of input resistance, by about 30%, was obtained. The activation of the late phase with prolonged depolarizing trains (more than 10s) was strongly dependent on passive membrane properties and occurred on exponential or sigmoid manner. In K-free saline the early part of PSH was augmented, in contrast to the late one, which was completely blocked. At the same time, a drop of input resistance, with size similar to that observed in normal saline, has been registered. Replacement of all extracellular Na^+ with TRIS had a similar effects. Raising of extracellular Ca^{2+} concentration the size and duration of PSH moderately increased without change of resistance decrease pattern in the early phase. Application of strong inward current immediately after depolarizing stimulus reversed direction of PSH. The present results suggest two different mechanisms responsible for PSH genesis: 1) a prolonged increase in membrane conductance to K^+ , which contributes the early phase, and 2) activation of an electrogenic sodium pump, responsible for the late phase of PSH.

064

A METHOD FOR DETERMINATION OF THE SODIUM AND POTASSIUM CURRENT DURING ACTION POTENTIAL FROM FROG MUSCLE FIBRES

N.A. Trayanova, A.A. Gydikov, Central Laboratory of Biophysics, Bulgarian Academy of Sciences, Acad.G.Bontchev str., Bl.21, Sofia 1113, Bulgaria

Experimentally recorded action potentials (AP) were digitally processed to obtain I_{Na} and I_K currents. First the total ionic current I_t was calculated from the cable equation, the time derivatives of the AP being obtained by means of the Fourier transform method. Considering the facts that: (1) the conductivity g_{Na} is a function within the class of the unimodal stable distributions and (2) I_t begins later than I_{Na} , g_{Na} is calculated for the whole duration of the AP. I_{Na} can be obtained from the data for g_{Na} and I_t is the difference $I_t - I_{Na}$.

065

THE MONOMER-TETRAMER EQUILIBRIUM OF MELITTIN IN LIPID MEMBRANES. A POSSIBLE MECHANISM FOR PORE FORMATION.

Horst Vogel, Biocenter, University of Basel

Fluorescence energy transfer measurements on membrane incorporated melittin show that the polypeptide aggregates as tetramers. The aggregated melittin molecules traverse the lipid bilayer in form of α -helical rods, as concluded from Raman and infrared spectra. Because one side of a melittin helix surface is strongly hydrophobic and the other more hydrophilic, the tetramers could act as pores of permeation of hydrophilic substances through the membrane. The monomer-tetramer equilibrium in the bilayer can be modulated e.g. by the physical state of the lipids. Transitions between the monomeric and the tetrameric form in the bilayer may be the origin of the opening and closing of pores. Binding of melittin from aqueous solution to lipid membranes is reflected by a change of its tryptophan fluorescence. A fast (msec) and a slow (sec) process are observed, interpreted as a fast absorption of the polypeptide to the membrane surface, followed by a slower concerted aggregation/incorporation process of the melittin molecules into the lipid bilayer. The half-time t of the slow process depends on pH; at pH4 $t=300$ sec, at pH8 $t=10$ sec. The time course of melittin incorporation into membranes is determined by a protonatable group with an apparent $pK=6.5$, probably the amino terminus of the peptide.

066

AN ATP-DEPLETION CURRENT IN CHICK EMBRYO VENTRICLE CELLS THAT RESEMBLES THE INSULIN-ACTIVATED BACKGROUND CURRENT

R.L. DeHaan, R.K. Aver, Jr. and R. Fischmeister, Anatomy Dept. Emory University School of Medicine, Atlanta, Georgia USA

The background current was measured from single 12-14 um 7-day embryonic chick ventricle cells, with patch-electrodes in the whole-cell clamp configuration. The I/V relation was dependent on the concentration of ATP in the electrode internal perfusion solution (IPS). When the IPS contained 5mM ATP, the I/V curve was roughly linear from -90mV to 0mV, and had a mean slope conductance of 336 pS ($N=4$). The zero current point (resting potential) was -34mV. With IPS lacking ATP, cells rested at -86mV (near E_K); the slope of the linear portion of the I/V curve (-90mV to -10mV) was 1232 pS ($N=8$), and between +20 and +60mV it was negative. The ATP-depletion activated background current measured here resembles that in adult mammalian cardiac cells (Noma; Bechem and Pott). It is also similar to the insulin-activated background current in embryonic cells that occurs in the presence of intracellular ATP (Fischmeister et al., Biophys. J. 41: 75a). With IPS lacking ATP, the increase in net outward current occurred in less than three min after the membrane patch was disrupted; within about 30 min the current irreversibly declined to a low level. We postulate that upon depletion of intracellular ATP the open-state probability of insulin-regulated K-channels increases to a maximum after which the channels become non-functional. (Supported by NIH P01 HL-27385 and R01 HL-16567 to RLD). Permanent address: Lab. de Physiol. Cell. Cardiaque, INSERM U-241, Univ. de Paris-XI, 91405, France

Friday 03 August Congress Centre-First Floor Posters 067-072

Posters on Chemical and Electrical Regulation of Ion Channels

067

ON THE IONIC REGULATION OF THE ELECTRICAL AND MECHANICAL ACTIVITIES IN HUMAN AND GUINEA-PIG URETER.
M.Ch. Michailov, D. Martin, H. Grindler-Greimel, A. Petter*, B. Rattet*, Ch. Faltermayr and E. Elsasser**. Inst. Biol., GSF-Neuherberg; *Inst. Pharmacol., University Munich; **Urolog. Klinik, Krkh. Barmherz. Br. Munich, FRG.

The electrical (intracellular recording) and mechanical (isotonic) activities of human (surgical material) and guinea-pig (g.p.) ureter preparations were studied in McEwen solution. The membrane potential (MP) was -35 to -60 mV. MP of g.p. ureter fluctuated periodically due to superimposition of second and minute rhythms, i.e. the normal electrical pattern consisted of two types: (1) regular single spike activity and (2) regular bursts of spike discharges of varying sizes. Increase of $[K^+]$ or decrease of $[Ca^{++}]$ changed the spike- in a burst-activity; at a "critical ratio" of $[K^+]:[Ca^{++}]$ bursts with a plateau phase appeared. Frequency (v) and duration (t) of the bursts (b) are mathematical functions of the ionic concentrations:

$$v_b = f\left(\frac{1}{[Na^+]}, \frac{1}{[K^+]}, \frac{1}{[Ca^{++}]}\right); t_b = g\left(\frac{1}{[Na^+]}, \frac{1}{[K^+]}, \frac{1}{[Ca^{++}]}\right).$$

$BaCl_2$, $MgCl_2$, $MnCl_2$ have more complicated effects on the bursts than the named ions. The spontaneous mechanical activity of all preparations is influenced by ions in a similar way as the bursts. The influence of T⁺ and X-rays on the ureter was also studied. The ionic dependence of the ureter and detrusor activities (Proc. Int. Union Physiol. Sci. (1980), 14, 580; Beitr. Urol. (1984), 3, 183, Karger Basel) will be compared.

069

ANALYSIS OF THE DELAYED OUTWARD CURRENT WHEN SUBSTITUTING Ba^{++} FOR Ca^{++} IN HELIX POMATIA NEURONS
G. Monticelli, Dipartimento di Fisiologia e Biochimica Generali, Università degli Studi, via Celoria, 26, 20133 Milano, Italy.

The present research is concerned with the study of the ionic currents in some neurons of the *Helix pomatia* subesophageal ganglia when Ca is replaced by Ba . The cells were impaled with two microelectrodes and voltage-clamped by means of a conventional type electronic circuit. The replacement of the external Ca with an equimolar concentration of Ba resulted in a decrease of the total delayed outward current as the membrane potential was made more positive. The action of barium was voltage dependent. The net outward current during repeated voltage-clamp pulses has been studied too. Responses to repetitive activation with 100 ms repolarization intervals were recorded to analyze the deficit in net outward charge transfer under voltage-clamp. In normal saline this deficit in net charge transfer has been related to the inward flow of Ca ions occurring at high depolarizations and obscured by the outward current of potassium. Divalent cation Ba^{++} produced a reversible decrease of delayed outward current and it seems that both the voltage-dependent and Ca -dependent components of the delayed K^+ current are affected by this ion.

071

INTERACTION BETWEEN IONS AND WATER INSIDE THE GRAMICIDIN A CHANNEL: I. METHOD FOR MEASURING SMALL FLUXES. F.C. Franca and Joaquin Procopio, Department of Physiology and Biophysics, Institute of Biomedical Sciences, University of São Paulo, São Paulo, Brazil.

The antibiotic gramicidin A, when incorporated into planar lipid bilayer, forms ideally cationic selective channels. The transport of ions and water through these channels is believed to occur in a single-file manner. The aim of our work is to study the interactions between ions and water inside this channel. The first part of the work consists in measuring n, the number of water molecules that an ion carries as it passes through the channel. For that purpose we have made electroosmotic experiments. In this way we apply a current through the membrane and measure the associated volume flux. This flux is of the order of 10^{-9} L. To measure it we built a chamber made of a high precision thermometer with one of its extremities enlarged. This extremity forms a reservoir that communicates with the exterior through a small circular hole (about 1 mm diameter). At the other extremity we connect a 100 µl Hamilton syringe filled with colored mineral oil making an interface with the solution (0.1M KCl) in the graduated part of the thermometer. As the thermometer is closed the volume flux will cause the membrane to bulge; this is corrected with the syringe. We can read the volume variations by observing the oil-solution interface in the graduated zone of the thermometer. For an azolectin (2.51 in n-decane) membrane we obtained $n = 13.36 \pm 1.71$ (SE) (27). These results are preliminary and not corrected for unstirred layers or surface charges effects in the membrane.

068

PROPERTIES OF NEW SODIUM CHANNELS EXPRESSED IN TONIC MUSCLE FIBRES AFTER DENERVATION J. Zachar, D. Zacharová, M. Henček and G.A. Nasledov, Centre of Physiological Sciences, Slovak Academy of Sciences, Bratislava, Czechoslovakia.

Membrane currents in denervated slow /tonic/ muscle fibres of the frog were analysed by means of the vaseline-gap voltage clamp method. Sodium conductances as function of both time and voltage were found to be described quantitatively by the Hodgkin-Huxley model for the sodium channel in twitch fibres of the same muscle. Parameters of the kinetic model differ from those in twitch fibres by values of the rate constants only. The sodium channels in normal and denervated twitch fibres differ in the rate of inactivation, which is enhanced after denervation $/T = 4.6$ ms as against $T = 8$ ms in normal fibres/. The new sodium channels are TTX sensitive and show the ionic selectivity $/Na^+ : Li^+ : NH_4^+ : K^+ = 1:0.88:0.23:0.012/$ which can be compared to that in denervated twitch muscle fibres, i.e. $1:0.91:0.14:0.082$. These results support the hypothesis that sodium channels formed in denervated tonic muscle fibres are of the same genetic origin as Na channels expressed under physiological conditions.

070

ANOMALOUS REACTANCE OF POTASSIUM CHANNELS OF CHARA CORALLINA
F. Homblé, A. Jenard, H. Hurwitz, Dept. Thermodynamique Electrochimique, C.P.160, Univ. Libre de Bruxelles, Av. F. Roosevelt 50, B-1050 Bruxelles, Belgium.

Investigations of membrane potential response to a constant current pulse have been performed in *Chara corallina* cells at various current intensities, external chemical compositions and temperatures. The membrane potential response to a constant current pulse displays an overshoot which has been attributed to a time variant conductance of the potassium channels of *Chara* (1). The relative amplitude of the overshoot and its oscillation increase with the current. This behaviour appears for both inward and outward currents and precedes always the action potential. Frequencies temperature dependence yields an activation energy comparable to that of the potassium channels transfer (36 ± 2 kJ mol⁻¹) for temperatures above 15°C. The overshoot is relatively unaffected by 10 mM $CaCl_2$, $MgCl_2$ or 30 mM Sorbitol. However it disappears when potassium channels are opened with 15 mM KCl. These results are consistent with our previous conclusion (1) according to which the overshoot results from a time variant conductance of potassium channels.

(1) F. Homblé, A. Jenard (1984) J. Exp. Bot. (in press)

072

TITYUS SCORPIO TOXIN MODIFIES NA CHANNELS IN FROG NERVE
W. Vogel and P. Jonas, Physiol. Inst. Univ. Aulw-g, D-6300 Gießen, W.-Germany

The effect of α -toxin of the South American scorpion *Tityus serrulatus* (Tityx) on excitable membranes was studied by current and voltage clamp experiments with single nerve fibres of *Xenopus laevis*. The effects of externally applied Tityx appear at concentrations higher than about 100 nM, 0.1 or 0.2% of bovine albumin added. Under current clamp conditions, 700 nM Tityx depolarized the nerve membrane by 25 mV, induced repetitive and spontaneous activity with a frequency of $60 s^{-1}$, prolonged action potentials by about factor 4, and continuously decreased their amplitudes. The initial state of hyperexcitability was followed by a state of complete inexcitability. Under voltage clamp conditions, Tityx reduced the Na peak current, slowed down Na current inactivation (development of as well as recovery from inactivation) and shifted the current-voltage relations towards negative potentials. The steady-state inactivation curve, obtained with 50 ms prepulses, decreased in steepness, but remained unshifted. In 550 nM Tityx, Na peak current was reduced to 50% within 4 minutes and further decreased to 10% after 15 minutes. All effects of Tityx were reversible. The recovery of Na peak current was only partial and slower than its decrease. Tityx thus modifies activation of Na channels somehow similar to Centruroides sculpturatus IV scorpion toxin (Neves et al., 1982, Pflügers Arch. 393, 56-62). The important difference is that Tityx action does not need a directly preceding depolarization.

Friday 03 August Congress Centre-First Floor Posters 073-078

Posters on Chemical and Electrical Regulation of Ion Channels

073

KINETICS OF LUCENSOMYCIN BINDING TO HUMAN ERYTHROCYTE GHOSTS.

C. Salerno, C. Crifò, E. Capozzo and R. Strom - CNR Centre for Molecular Biology, Rome; Inst. of Biochemistry and Dept. of Biopathology, University of Rome "La Sapienza", Rome, Italy.

When the polyaromatic lucensomycin (2-30 μ M) was rapidly mixed with human erythrocyte ghosts (20-200 μ M in cholesterol), two consecutive exponential processes of similar amplitude were detected by monitoring the polyene absorbance at 320 nm.

The time-courses of both processes were independent of the polyene concentration. The apparent first-order rate constant of the faster event was a linear function of the membrane concentration; for the second process the apparent first-order rate constant approached a limiting value of $2s^{-1}$ in the presence of a large excess of the ligand. The absorbance change of the overall phenomenon was a hyperbolic function of the membrane concentration ($K=10 \mu$ M). Cholesterol-depleted membranes were unable to induce any change in polyene absorbance; if reconstituted with exogenous cholesterol, the absorbance changes upon mixing with lucensomycin were almost identical to those observed with native membranes.

Lowering of the protein content of the ghosts to 70% of their original value by digestion with proteinase K did not modify their affinity for the polyene. The kinetics of binding presented however, besides the same two exponential events observed with native membranes, a third very slow ($t_{1/2} = 10$ s) process, the presence of which was more evident at high polyene concentrations.

075

ELECTRO-, THERMO- AND X-RAY-INDUCED REACTIONS IN ISOLATED HUMAN AND GUINEA-PIG PYELOURETER AND DETRUSOR.

D. Martin, E. Neu, I. Prechter, K. Tempel*, F. Zettler**, H. Ch. Michailov. Inst. Biol., GSF-Neuherberg; *Inst. Pharmacol., Univ. Munich; **Inst. Zool., Univ. Munich, FRG.

Electrostimulation (ES), changes in temperature (T^*) and X-rays induced changes in the spontaneous phasic contractions (SPC) (isotonic recording) of preparations from human and guinea-pig (g.p.) pyelon, ureter and detrusor. ES of 10 Hz, 0.3 ms pulse and 3 s series duration inhibited or blocked the SPC of human pyelon without visible changes in frequency and basal tone; after ES of 100 Hz, 0.3 ms, 3 s the frequency of contractions and the tone increased. The pyelon of g.p. reacted to ES of 10 Hz by augmentation of the SPC-amplitudes without changes in frequency and tone; ES of 100 Hz induced an initial inhibition of SPC-amplitudes followed by an increase of frequency and tone. Human and g.p. ureter reacted with regular contractions to ES (10, 100 Hz) without changes in SPC and tone. Cooling ($37^{\circ}C$ to $25^{\circ}C$) reversibly blocked the SPC of pyelon and ureter, but had no effect on the tone changes after ES; X-rays (10-20 Gy) stimulated or blocked the SPC in these organs. The SPC of detrusor were inhibited by ES, cooling and X-rays. It can be concluded that reactions evoked by electro-, thermo- and X-ray-stimuli, furthermore, the influence of ions and drugs on these reactions, can be used for an analysis of the regulation of oscillating biophysical processes which control the rhythmic electrical and mechanical activity of these organs.

077

MEMBRANE POTENTIAL DEPENDENCY OF ACTIVATION DELAY IN GIANT AXONS OF THE SQUID

Y. Pichon, Y. Lomet and M. Paternostre, D/Partement de Biophysique, Laboratoire de Neurobiologie Cellulaire CNRS, Gif sur Yvette, France.

Special programs have been used to analyse the effects of membrane potential on the delay which separates the typically sigmoidal time course of activation of the potassium and sodium currents from the beginning of step depolarizations. Current traces were recorded under voltage-clamp conditions, digitized and stored on tape. These traces were then analysed on the basis of the Hodgkin and Huxley (1952) model assuming constant exponents (4 for n and 3 for m). A least square fit of the linearized current traces corrected for instantaneous DC components was used to calculate the time constant of activation and the activation delay. For a membrane held at -60 mV and stepped during 20 msec at -80 mV before application of the test pulse, the delay, which is negative for small depolarizations, reverses polarity around -30 mV, reaches a peak value between -20 and 0 mV, then slowly decreases for larger depolarizations. The curve relating activation delays to prepulse potentials changes polarity between -60 and -40 mV. It is steeper for depolarizing prepulses. These results support the existing evidence that electrically silent conformational changes precede activation of the ionic conductance in the axonal membrane. Hodgkin A.L. and Huxley A.F. (1952) - J. Physiol., London, 117, 500-544.

* Experiments were performed at the Station Biologique, 2-29211 Plozeff, France.

074

BLOCKAGE OF SODIUM AND POTASSIUM CHANNELS BY THE ANTIEPILEPTIC DRUG VALPROATE. Van Erp, M.G. and Van Dongen, A.H.J. Laboratory of Physiology, State University of Leiden, The Netherlands.

Valproate is a drug whose application has increased rapidly during last years because of its strong antiepileptic action and relatively small side effects. Until now, effects on GABA-ergic synaptic transmission have been claimed as its main mechanism of action. Other antiepileptic drugs (Phenytoin, Phenobarbital, Ethosuximide, Carbamazepine, Diazepam) have been shown to selectively block sodium channels. Therefore we investigated the effects of Valproate on both sodium and potassium channels. Single myelinated nerve fibres isolated from Ischiatic nerve of *Xenopus laevis* were voltage clamped using a modified Nonner clamp. Valproate (0.2-2 mM) was shown to block both sodium and potassium channels in a poorly reversible way. Hyperpolarizing prepulses (0.5-10 sec.) partly restored the amplitude of the potassium current. Due to removal of inactivation this effect was less clear on sodium channel blockage and remains to be studied in detail. Where blockage of sodium channels seems to be a general feature of all antiepileptic drugs investigated so far, blockage of potassium channels appears to be a unique property of Valproate. This may explain its special status among the antiepileptic drugs.

076

SPECTROPHOTOMETRIC PROPERTIES OF POTENTIAL SENSITIVE DYES BOUND TO HEART MUSCLE TISSUE

M. Müller, H. Windisch and H.A. Tritthart, Inst. für Med. Physik und Biophysik, Universität Graz, Harrachgasse 21, A8010 Graz, Austria

A new equipment was developed for detection of electrical properties of membranes of heart muscle cells by means of potential sensitive dyes (RH237, RH160 and RH270). It allowed measurements with higher resolution in time (5 kHz) and space (excitation spots down to 5 μ m) than described so far. Additionally the phototoxic side effects as well as photobleaching could be minimized by using a Pockels cell as an optical shutter for the exciting laser beam. We observed large changes in fluorescent light during the action potential (RH237 up to 10%, RH160 and RH270 up to 6% each, dyes synthesized by A. Grinvald). This equipment combined with an optical multichannel analyzer (OMA) could also be used for measurements of fluorescent spectra. When bound to the membrane, the fluorescent spectra of all three mentioned dyes showed a characteristic shift of the peak wave length to shorter regions compared with the spectra in aqueous or alcoholic solutions. The spectrophotometric features of these new potential sensitive dyes are attractive for photometric measurements of excitation.

078

APICAL-MEMBRANE POTASSIUM CHANNELS OF MAMMALIAN CORTICAL COLLECTING TUBULE. M. Hunter, A.G. Lopes, E.L. Boulpaep and G. Giebisch, Yale Univ. Sch. Med., New Haven, CT, USA.

The distal nephron and cortical collecting tubule are the predominant sites of potassium secretion by the kidney. Microelectrode studies have indicated the presence of a barium-sensitive potassium conductance in the apical membranes of the principal cells of the latter segment. Using the patch-clamp technique we have identified potassium-selective channels in the apical membranes of rabbit cortical collecting tubules.

Tubules were dissected from the kidneys of New Zealand White rabbits and the luminal surface exposed by ripping the tubule lengthwise. The apical membrane could then be approached with a fire-polished pipette and giga-seals were generally obtained spontaneously. Although when present the channel could be seen opening and closing spontaneously, we have not studied the channel while cell-attached. The pipette was then withdrawn from the cell forming an inside-out patch.

The channel has a slope conductance of around 100 pS with 75 mM potassium in the pipette and 15 mM potassium in the bath. It is selective for potassium over sodium with a selectivity ratio of 10:1. Decreasing the calcium concentration at the cytoplasmic face of the channel resulted in a decreased open-probability. The open probability is reduced to zero at calcium concentrations less than 10^{-6} M. The channel is also reversibly inhibited by Ba^{++} (applied to the cytoplasmic face) in a dose-dependent fashion, with a K_i around 100 μ M.

Friday 03 August Congress Centre-First Floor Posters 079-084

Posters on Chemical and Electrical Regulation of Ion Channels

079

ISOLATION OF PLASMA MEMBRANE FROM COLLAGENASE DISAGGREGATED GUINEA PIG CARDIAC MUSCLE CELLS
W. Schreibleyner, G. Zernig, K. Radl and H.A. Tritthart, Inst. Med. Phys. Biophys., Univ. Graz, Harrachgasse, A-8010 Graz, Austria.

Membrane fragments were isolated for reconstitution experiments in monolayer derived artificial bilayer membranes and the electrical properties of ionic channels studied. High connective tissue content often results in low yield membrane preparations. We have overcome this problem by perfusing the isolated heart in a Langendorff system with a collagenase (100 i.u./ml), 25 μ M Ca^{2+} containing Krebs-Ringer buffer. The subcellular fragments were separated from the isolated cells by centrifugation and further fractionated on a discontinuous sucrose density gradient. Total yield of the plasma membrane marker enzyme 5'-Nucleotidase was 9% and enrichment was about 20fold in the material collected from the top of the 0.6M sucrose solution. Contamination by mitochondrial membranes was less than 1% as tested by cytochrome-c-oxidase activity. Our approach offers (1) high yield together with (2) high purity of the plasma membrane preparation and (3) direct comparison of patch clamp data from native membranes with reconstituted membranes by setting both cells and membrane fragments to the same enzymatic treatment.

081

PHORBOL ESTER ENHANCES AN INWARD CURRENT IN THE BAG CELL NEURONS OF APLYSIA. L.K. Kaczmarek, J.A. Strong, and S.V. DeRiemer, Dept. of Pharmacology, Yale Univ. Sch. of Med., Cedar St. New Haven, CT 06510, USA.

Phorbol esters have been shown to activate the calcium-phospholipid dependent protein kinase (Protein Kinase C) in a variety of types of cells including the bag cell neurons in the abdominal ganglion of *Aplysia*. The action potentials of the bag cell neurons undergo profound changes in their shape following brief electrical stimulation of an afferent input from the head ganglia. We have now investigated the effects of the phorbol ester, 12-O-tetradecanoylphorbol-13-acetate (TPA) on isolated bag cell neurons, maintained in cell culture. We have found that TPA produces increases in the height of action potentials evoked by depolarizing current pulses. TPA also increases the tendency of these cells to fire repetitively on depolarization. The effects of TPA on ionic currents were examined using the whole-cell patch clamp method. Isolated cells, pre-exposed to 100nM TPA, were found to have significantly greater peak inward current than untreated controls. Preliminary experiments suggest that this enhanced current is carried, at least in part, by calcium ions.

083

THE DEPENDENCE OF THE ELECTRICAL PROPERTIES OF THE HEMOCYANIN CHANNEL ON A FIXED NEGATIVE CHARGE ON IT
G. Menestrina and C. Porcelluzzi, Dipartimento di Fisica, Povo, Trento, ITALY

Membrana crenulata hemocyanin incorporates into phospholipid planar bilayer membranes forming ionic channels with fixed orientation with respect to the side of addition, cis side. These channels have several conductance states but can be kept in the most conductive one, called "open". The conductance of the open state, which is cation selective, depends both on the applied voltage, positive voltages (cis negative) decrease it, and on the ionic composition of the medium, it saturates at increasing salt concentrations. It was suggested that saturation and selectivity were due to a negative fixed charge on the channel. Since protons are known to neutralize hemocyanin negative charge, we have examined the effects of varying the pH on the properties of the pore. Lowering the pH symmetrically on both sides decreases the maximal conductance of the open state and shifts its non-linear current-voltage curve towards negative voltages. The same behaviour was observed both in KCl and in K_2SO_4 solutions, both at high and low ionic strength and with membranes of different surface charge. The selectivity of the channel was independent of pH with K_2SO_4 but not with KCl, being lost at pH 4.5. All these findings are consistent with the idea that the channel bears a negative charge influencing the ionic pathway.

080

MULTIPLE SITE OPTICAL RECORDINGS OF ACTION POTENTIALS IN "WORKING" GUINEA PIG HEARTS G. Salama and R. Loebardi, Univ. of Pittsburgh, Dept. of Physiol., Pittsburgh, PA, USA.

Guinea pig hearts were perfused in a "working" heart apparatus in Ringer's containing 10 μ M of a voltage-sensitive dye. Action potentials were simultaneously recorded from 124 regions of the heart through the fluorescence and/or absorption changes of the dye bound to the sarcolemma. Light from tungsten-halogen lamps was passed through interference filters and illuminated the heart uniformly. Fluorescent or scattered light formed an image of the heart on 12 x 12 photodiode array. Outputs from 124 elements of the array were amplified, AC coupled using a 3s time constant to preserve the shape of the action potentials, then stored in a PD 11/23 for subsequent analysis. Signals from each diode were sampled every 0.6 msec for 2 to 4 sec. Software was developed to locate the upstroke of action potentials, determine delays between action potential in various regions of the heart, and draw a map of propagation pathways. Changes in patterns of propagation were correlated with the local metabolic state of the heart measured through NADH fluorescence. Propranolol (1 mg/ml) prolonged the plateau by 1.4 x and reduced atrio-ventricular conduction. Verapamil (4 μ g/ml) produced a very slight drop in the plateau but a dramatic reduction of atrio-ventricular conduction. Patterns of electrical activity provide a complete picture of cardiac excitation under normal and arrhythmic states, and point out how anoxia or local injuries alter propagation pathways. Supported by AHA 82 1231 and the Western Pennsylvania Heart Association.

082

CA LOADING AND CA CHANNEL INACTIVATION IN HELIX NEURONES

T. J. Ward, Department of Physiology, University of Leicester Leicester, U.K.

There is now considerable evidence to suggest that the inactivation of the potential dependent calcium current in many tissues is mediated by the $[\text{Ca}]_i$. Ion sensitive micro-electrodes were used to monitor $[\text{Ca}]_i$ and periodic brief depolarisations applied to the voltage clamped neurones to measure the Ca current amplitude. The mean resting $[\text{Ca}]_i$ was $0.266 \pm 0.024 \mu\text{M}$ ($n=8$). Neurones were loaded using long depolarisations in 25mM Ca^{2+} Ringer and then the recovery of both $[\text{Ca}]_i$ and current amplitude monitored. The normal rate of recovery from the Ca loading was too rapid for the ion sensitive electrode to follow. However, the application of CCMp to block mitochondrial sequestration of Ca^{2+} slowed the recovery sufficiently to allow continuous accurate measurement with the ion sensitive electrode. In this case the recovery was followed from a $[\text{Ca}]_i$ value of 3.3 μM and correlated with the current amplitude, both sets of data giving exponential recoveries with time constants of approximately 1.5 minutes. It was possible to construct a dose response curve for the reduction of current amplitude plotted against $[\text{Ca}]_i$. The maximum current amplitude for the cell was calculated assuming that the Ca current at the resting $[\text{Ca}]_i$ represented 0.76 of the maximum current seen after EGTA injection to lower $[\text{Ca}]_i$. The subsequent plot of current reduction against $[\text{Ca}]_i$ gave a good fit to a theoretical curve constructed assuming 1:1 binding with a binding constant of 0.48 μM .

084

IONIC CURRENTS IN AN ISOLATED SMOOTH MUSCLE CELL. P. G. Stein and P. A. V. Anderson, C. V. Whitney Laboratory and Dept. of Physiology, University of Florida, USA

Conventional 2-electrode voltage clamping methods were used to investigate the currents composing the action potential in large smooth muscle cells isolated from the oenophore *Membranipora*. The passive properties were first examined to establish conditions necessary for adequate space clamping. Total membrane current (I) appears similar to that seen in many excitable cells -- a transient inward I appearing at levels of membrane potential positive to the resting potential (-60 mV) followed by an outward I which peaks between 150 and 200 msec. and then decays to a steady state after 9-10 seconds. The early inward I is responsible for the rising phase of the action potential and is a TTX-insensitive, composite $\text{Na}^+/\text{Ca}^{2+}$ I through a single channel type which can be partially blocked by 200 μM D-600 or verapamil and totally blocked by 2 mM Cd^{2+} . Reduction in external Na^+ or Ca^{2+} appropriately diminishes the inward I . Depolarization is mediated by 4 currents: 1) a Ca^{2+} -activated K^+ conductance (g_{KCa}) which has a time constant of activation (τ_a) of 45 msec. and a τ of inactivation (τ_i) of 1-2 sec. 2) a rapid, voltage-activated gK^+ with a τ_a of 5 msec., which inactivates with time (τ_i 45-50 msec) and at holding potentials above -40 mV . 3) a slower voltage-activated gK^+ which does not inactivate with time or voltage (τ_i 10-50 msec). 4) a voltage-activated gCl^- . These findings suggest fundamental similarities with vertebrate smooth muscle. (Funded by the Whitehall Foundation and PHS F32 GM09920-01).

Friday 03 August Congress Centre-First Floor Posters 085-090

Posters on Chemical and Electrical Regulation of Ion Channels

085

CHEMICAL MODIFICATION OF GATING MECHANISM IN SODIUM CHANNEL. G.N. Mozhayeva, A.P. Naumov, E.D. Nosyreva. Institute of Cytology, USSR Academy of Sciences, Leningrad, USSR.

In order to approach to the chemical nature of "mobile" gating charges in Na channel parameters of channel activation and inactivation have been studied in the nodal membrane treated with some carboxyl group reagents: water-soluble carbodiimides (WRC) and Woodward's reagent K (WRK). 1-ethyl-3-(3-dimethylaminopropyl)carbodiimide and cyclohexyl-3-(2-morpholinoethyl)carbodiimide metho-4-toluene sulfonate (50-100 mM, pH 4.5-5.5) irreversibly slowed kinetics and reduced the steepness of voltage-dependence of channel activation and inactivation, membrane potential (E_m) being -80 ± 100 mV. The effective charge of activation (Z_{eff}) determined from limiting logarithmic slope of voltage dependence of the fractional number of open channels was decreased by the factor 1.8. Analogous treatment at $E_m = 0$ mV did not change Z_{eff} . WRC were noneffective at normal pH. WRK (10-100 mM, pH 5.0-6.5) induced slowing activation kinetics without changes in Z_{eff} . The data allow to suggest that gating charges are presented (partly or entirely) by carboxyl groups, located on the external surface when channels are closed and noninactivated.

087

PHOTOMETRIC MEASUREMENTS OF THE RISING PHASE OF CARDIAC ACTION POTENTIALS

H. Windisch, W. Muller, H.A. Tritthart, H. Hagauer and R. MacLeod, Inst. für Med. Physik und Biophysik, Universität Graz, Harrachgasse 21, A8010 Graz, Austria

We have measured the rising phases of cardiac action potentials, using some new potential sensitive dyes (RH237, RH160, RH270), synthesized by A. Grinvald. After the usual staining procedure atrial and ventricular strips of guinea pig and rat heart were mounted under a microscope objective (40x) in a bath superfused with normal Tyrode's solution. A new built optical system was used for the excitation of the stained preparation as well as for the detection of the fluorescent light with high time and spatial resolution (120 ns, 10 μ m). The electrical signals obtained were digitalized and transferred to a minicomputer for further data analysis. The detected rising phases obtained with spot sizes below 50 μ m generally showed the usual shape but durations significantly shorter than those obtained with conventional glass-microelectrodes under identical experimental conditions. These photometric results of excitation onset likely indicate the superiority of cell-potential measurements without electrical interference.

089

086

AMILORIDE-SENSITIVE FRAGMENT OF THE Na-SELECTIVE TRANSMEMBRANE STRUCTURES B.I. Bessonov, S.V. Butsk, M.B. Chernousova, Joint Panel of Biophysics, Pacific Oceanological Institute Far Eastern Science Centre USSR Acad.Sci., Vladivostok 7, Radio Street, 690032, USSR.

External surface of the *Rana ridibunda* skin being bathed by solution contained (10 mM NaCl, 2 mM MgCl₂, 1 mM ATP, pH=7.2) hydrolyzed ATP (2.6 mM P_i /cm²h). Internal surface was bathed by the Ringer, pH=7.2. Amiloride (10 mM) inhibited this hydrolysis at mean to 50% from the initial level. Also, Amiloride inhibited Na⁺, K⁺-ATPase (1400 mM P_i /mg h) from the pig kidney ($K_{0.5} = 110$ mM) obtained by the Jorgensen method (Ann. N.Y. Acad. Sci. 242:36, 1974, see also BBA, 433, N3:531, 1976). These data are in agreement with the hypothesis, that Na⁺ channels of the external frog skin surface may be localized within Na⁺, K⁺-ATPase of the basolateral cell membranes of the outer Stratum granulosum or inner Stratum corneum layers (Rep. USSR Acad. Sci., 268, N2:478, 1983), with the nonspecific permeability of the apical cell membranes. The alternative is the common or similar fragment in Na⁺, K⁺-ATPase and in Na-selective unexcitable and excitable cell membranes. For the later the inhibition of the sodium conductance by Amiloride is demonstrated as well (Proceed. Meet. USSR-Switzerland, Tashkent, USSR: 191, 1983, see also Amer. J. Physiol., 242, N3:2131, 1978).

088

090

Friday 03 August Congress Centre-First Floor Posters 091-096

Posters on Chemical and Electrical Regulation of Ion Channels

091

092

093

094

095

096

Friday 03 August - Congress Centre-First Floor Posters 097-102

Posters on Chemical and Electrical Regulation of Ion Channels

097

098

099

100

101

102

Friday 03 August Congress Centre-First Floor Posters 103-108

Posters on Mechanisms of Transport Across Membranes

103

ENERGETICS AND BIOELECTROGENESIS OF EXCITABLE MEMBRANES

V. Vasilescu, Euzenia Chiriac-Kovács, Eva Katona and Sonia Herman
Medical Faculty, Department of Biophysics,
Bucharest, ROMANIA

Carrying on our previous studies of D₂O action on the structure and function of excitable systems, deuteration effects on the bioelectrogenesis processes in the nerve fibre, heart and retina and also those on the excitation-energy coupling in these systems were investigated. Thus the cellular ATP pools appear to be substantially decreased in the deuterated systems in function. Under D₂O and temperature influence the retina ON-response latency remains almost unchanged, but the retina OFF-response latency is very much affected. D₂O is observed also to prevent rhodopsin molecules to aggregate. Possible role of this aggregation process in triggering of the retina OFF-response is suggested by data analysis. By correlating the results obtained from experiments performed on nerve, heart and retina, the importance of certain general phenomena occurring in the early stages of bioelectrogenesis and substantially altered by deuteration is emphasized.

105

MAGNESIUM IS BOTH AN INHIBITOR AND A NECESSARY CO-LIGAND FOR PHOSPHORYLATION FROM P_i OF SARCOPLASMIC RETICULUM ATPase

Ph. Champell, F. Guillaud, and M.P. Gingold, Service de Biophysique, CEN Saclay, 91191 Gif-sur-Yvette Cedex, FRANCE.

Magnesium-dependent phosphorylation from P_i of Sarco-plasmic Reticulum (SR) ATPase has been shown to be pH-dependent in usual buffers; this dependence vanished in the presence of dimethylsulfoxide (DMSO). We recently studied the effect of DMSO on SR membranes, and found that in its presence, the (Mg.P_i) complex was the true substrate for ATPase phosphorylation, and magnesium was no longer depleting the substrate-reactive (E) ATPase conformation. On the basis of these results, we propose here a new reaction scheme to account for phosphoenzyme formation in the absence of solvent, implying that the (Mg.P_i) complex is a substrate for this reaction whereas Mg²⁺ itself acts as an inhibitor of full phosphorylation.

This communication shows how the scheme suggested reconciles the results in the literature for equilibrium and kinetic experiments. In addition we present both equilibrium and kinetic data which lend positive support to our suggestion. In particular we show that at pH 7, the enzyme's sensitivity to magnesium is such that phosphorylation is slower when phosphate is added to SR membranes preincubated with magnesium than when magnesium is added to SR membranes preincubated with phosphate.

107

CONCERNING THE MODULATORY ACTION OF 5-HYDROXYTRYPTAMINE ON SODIUM EFFLUX: THE BARNACLE MUSCLE FIBER AS A MODEL SYSTEM.

E. Edward Bittar, G. Chambers and K. Ueno, Department of Physiology, University of Wisconsin, Madison, WI, USA.

The Na efflux into 10 mM-Mg²⁺-ASW from unpoisoned and ouabain-poisoned barnacle fibers is stimulated by external application of 5-HT in a concentration as low as 10⁻⁹M. The kinetics of the response resemble those seen following cAMP or Ca²⁺ injection viz. the response develops rapidly but begins to decay 20 mins later. As a rule, barnacle fibers are always sensitive to injected cAMP or Ca²⁺ but the same is not true when 5-HT is applied externally. However, insensitive fibers can be rendered sensitive by preinjecting Gpp(NH)p into them. The fact that sensitive fibers preinjected with Gpp(NH)p often show sustained stimulation of the Na efflux suggests that desensitization is a reversible process. Decay of the 5-HT response may also be due to the presence of a brisk cAMP-PDE system. This is suggested by experiments involving the use of the xanthine derivatives 1-propyl-3-methyl-7-(5-hydroxyhexyl)-xanthine (PMX) and 1-isozamyl-3-isobutylxanthine (IAX) which selectively inhibit high Km and low Km cAMP-PDE systems. That 5-HT interacts with a receptor is suggested by the fact that cyproheptadine abolishes the 5-HT response. Methysergide is without effect. The possibility that 5-HT action involves activation of Ca²⁺ channels is excluded by evidence that the Ca²⁺ antagonists verapamil, Cd²⁺ and MB-4101 are ineffective. Evidence is available that preinjection of PKI or Mg²⁺ reduces the response to 5-HT. This is in line with the view that 5-HT action involves activation of cAMP-protein kinase by newly formed cAMP.

104

INFLUENCE OF MEMBRANE CURVATURE ON INCORPORATION OF COENZYME Q 10 INTO SONICATED LIPOSOMES.

L. Michaelis and M.J. Moore, Department of Biochemistry, University of Hull, Cottingham Road, Hull, UK.

It is well known that ubiquinone 50 (Coenzyme Q 10 = CoQ 10) is present in many tissues and is an essential component of mitochondrial electron transfer. The proton NMR spectra of ultrasonic irradiated phosphatidyl choline vesicles containing CoQ 10 exhibit two distinct resonances of the methoxy groups (at 3.98 and 3.82 ppm). The two peaks were found to be inversely related to sonication time. After short sonication the number of large liposomes dominates and the low field peak is large, whereas after prolonged sonication the number of small liposomes dominates with the high field peak increased. A second resonance at 1.58/1.52 ppm (the precise origin of this resonance is still under investigation) behaves in the same way. It can be concluded that there are two different locations in the membrane which depend upon the curvature of the bilayer. Lanthanide induced pseudocontact shift (Eu³⁺, Pr³⁺) did not affect the resonances of oxidised and reduced CoQ 10. This suggests that both forms of the enzyme are incorporated into the fatty acyl chain region (beyond C 2) of the membrane.

106

A FLUORESCENT OXONOL DYE FOR MEASUREMENTS OF MEMBRANE POTENTIALS IN CULTURED MAMMALIAN CELLS

Thomas Bräuner, Reto J. Strasser and Dieter F. Hölser, Biolog. Inst., Abt. Biophysik und Bioenergetik, Univ. Stuttgart, Ulmerstr. 227, 7000 Stuttgart 60, FRG.

Monolayers of BCR/ABL-k and L cells were stained with a voltage-sensitive fluorescent probe, the membrane permeant, negatively charged oxonol dye diBA-C₁₂-(3)⁻. Measurements of cytoplasmic fluorescence (signals with a photomultiplier adapted to an epifluorescence illumination microscope) were compared to simultaneous glass microelectrode recordings of membrane potentials. Polyethyleneglycol-induced cell fusion provided giant cells (homokaryons) in which the inserted electrodes for voltage clamp experiments did not interfere with the cytoplasmic area for the fluorescence measurement. Over a range of -25 mV to -90 mV the relative intracellular fluorescence signal linearly decreased with increasing potential difference. Stepwise voltage changes induced by current injection resulted in slow fluorescence responses with an average signal size of about 1% per mV. Multiparameter analysis of the fluorescence response curves revealed a first order reaction with a steady state different from zero. The rate constants ranged from 0.1/min to 0.8/min. The velocity of the fluorescence change and consequently the rate constants depended on the cell size and the magnitude of the voltage step. The highest rate constants were obtained with small cells and large voltage steps. A mechanism for the voltage-sensitive reaction of the examined oxonol dye is proposed.

108

MULTIPLE STATES OF BILIRUBIN IN ERYTHROCYTE, LIVER AND MODEL MEMBRANES. V. Glushko, Department of Biochemistry, Temple University School of Medicine Philadelphia, PA, USA.

Free unconjugated bilirubin is readily incorporated into membranes at physiological conditions. The interaction of bilirubin with erythrocyte ghosts (EG) and liver plasma membranes (LPM) resulted in the appearance of fluorescence at 520 to 570 nm. Free in solution, bilirubin absorbs at 438 nm with minimal fluorescence. However, when in EG, LPM or micelles, bilirubin fluoresces in the range of 500 to 570 nm with maximum excitation at 440 to 470 nm. The appearance of fluorescence follows complex kinetics with an initial rapid increase followed by a slower enhancement process. EG and micelles with high cholesterol content showed the greatest enhancement and the longest delay in reaching equilibrium. Although maximum bilirubin fluorescence from LPM was achieved within 30 minutes, it was less than 30% as intense as that from EG after one hour. In both cases, essentially all of the bilirubin was bound to the membranes within 2 minutes. Reducing excitation from 500 nm to 420 nm resulted in a red shift in the emission maximum from 530 to 570 nm, indicative of heterogeneous photophysical transitions. This effect was most pronounced in EG and cholesterol loaded micelles. Disruption of membrane organization tended to reduce the degree of heterogeneity. Consequently, when membrane bound, bilirubin appears to exist in multiple states; the transition from one state to another may depend on mobility, polarity, and accessibility to the aqueous phase.

Friday 03 August Congress Centre-First Floor Posters 109-114

Posters on Mechanisms of Transport Across Membranes

109

PARACRYSTALLINE DISTORTIONS IN BIOLOGICAL MEMBRANES.

E. López-Cabarcos, P. Sanz del Hoyo
Dpto. de Físico-Química y Técnicas Instrumentales.
Facultad de Farmacia. Madrid - 3. S P A I N .

The theory of paracrystals offers an appropriate way of understanding the structure and properties of all "meso-structures" lying between fluid and crystalline states. The atomic or molecular lattices of these structures consist of lattice bricks with statistically varying shapes. The growth of the distance fluctuation between lattice elements is proportional to the square root of their separation.

Paracrystals obey the so called α^* -law. Typical values of $\alpha^* = 0.15$ are obtained for synthetic polymers and catalyst. In biopolymers and biomembranes a downfall of the α^* -value to 0.05 is observed. This fact may be understood by the occurrence of complex bricks within their macrolattices. The results obtained with the purple membrane of *Halobacterium Halobium* and the erythrocyte ghost membrane are discussed.

111

ATPase INHIBITOR PROTEIN MAY INCREASE THE SYNTHETIC ACTIVITY OF THE ENZYME.

M. Gavilanes. Centro de Investigaciones en Fisiología Celular, University of Mexico. Dept. de Bioquímica. Fac. de Medicina, University of Mexico, Mexico, D.F. MEXICO.

The natural ATPase inhibitor protein of the mitochondrial ATPase of Pullman and Monroy has been suggested to preserve ATP, since apparently the main effect of the inhibitor protein is to inhibit hydrolysis. However, these effects have been described when optimal conditions for ATP hydrolysis or for ATP synthesis prevail. In the present work, the effect of the inhibitor protein on ATP synthesis at low and high concentrations of ATP was explored in submitochondrial particles devoid and reconstituted with inhibitor protein. It has been found that when ATP synthesis is measured under conditions where ATP concentrations are in the mM range, the synthetic pattern is not modified by the ATPase inhibitor protein. However, when ATP synthesis is monitored in conditions where ATP concentrations are in the μ M range, the ATPase inhibitor protein can modulate the activity of the ATP synthase, giving as a result a conservation in the flow of energy.

113

BINDING OF FLUORESCIN DERIVATIVES TO THE $(Ca^{2+}-Mg^{2+})$ -ATPase OF SARCOPLASMIC RETICULUM. B.L. Levinson and A.G. Lee, Department of Biochemistry, University of Southampton, Bassett Crescent East, Southampton, U.K.

Fluorescein and its tetrabromo- (eosin) and tetraiodo- (erythrosin) derivatives bind to the purified $(Ca^{2+}-Mg^{2+})$ -ATPase, with binding constants in the micromolar range. In all cases this binding enhances the fluorescence yield. The increase is seven-fold for erythrosin, while more modest changes are obtained for the other probes. Binding is also accompanied by a red shift in both excitation and emission spectra. Binding parameters can be obtained by fitting the fluorescence data from a set of simple titrations, using a weighted, non-linear least-squares routine, and incorporating a correction for inner-filter effect. Excellent fits are obtained, showing one binding site per ATPase monomer, and for erythrosin, $K_d = 0.6$ micromolar. These probes also inhibit the Ca^{2+} -dependent ATPase activity in the same concentration range. They thus belong to the very small class of water-soluble inhibitors of the ATPase. Analysis of the precise nature of the inhibition is made difficult by the complex kinetics of the enzyme, but the inhibition is only partly reversible by ATP, suggesting some form of mixed inhibition. Further computer modelling of the kinetics is underway. The results are generally consistent with the previous observation that fluorescein isothiocyanate reacts with a unique site on the ATPase, thought to be the ATP binding site. These probes may prove to be useful in studies on the conformation and aggregation state of the ATPase.

(Supported by the Muscular Dystrophy Association.)

110

CALCIUM TRANSPORT ACROSS PHOSPHATIDYLCHOLINE VESICLES.

L. Blay, R.B. Stern, T-C. Wu and R. Bittman, Yeshiva University, New York and Queens College of CUNY, Flushing, NY, U.S.A.

Calcium transport across egg phosphatidylcholine (PC) vesicles mediated by the antibiotics A23187, its methyl ester ($CH_3A23187$) and X537A was studied by following the absorbance change at 650 nm of the calcium sensitive dye arsenazo III. Efflux studies were conducted by adding the dye to the external medium of the Ca^{2+} -trapping vesicles whereas for influx studies arsenazo III was trapped in the vesicles and the Ca^{2+} was added to their outer medium. The order of initial rates of Ca^{2+} release from vesicles was $A23187 > X537A > CH_3A23187$. The initial rates of Ca^{2+} efflux from PC and PC-cholesterol vesicles were measured as a function of $[A23187]$. Cholesterol (26 mol %) induced a 50% rate reduction. The log-log plot of rate vs $[A23187]$ gave a slope of approximately 2, indicating a second-order dependence on $[ionophore]$. A first-order dependence of the rate of Ca^{2+} efflux on $[CH_3A23187]$ was observed. The initial rate of Ca^{2+} influx into PC vesicles in the presence of A23187 was first order in $[Ca^{2+}]$. These results imply that one Ca^{2+} moves with two A23187 molecules, consistent with the existence of a 2:1 A23187: Ca^{2+} complex. The ionophore-mediated transport of Ca^{2+} across lipid bilayers depends on the composition of the vesicles, the concentration of the ion and the nature and the concentration of the ionophore.

(Supported by ONR contract N000E-K0437)

112

VOLTAGE DEPENDENCE OF THE CURRENT PRODUCED BY BACKWARD-RUNNING SODIUM PUMP IN SQUID GIANT AXONS.

R.F. Rakowski and P. De Weer, Marine Biological Laboratory, Woods Hole, Massachusetts, USA.

The effect of membrane potential on the magnitude of the current produced by electrogenic sodium transport in the reverse direction was investigated in voltage-clamped, internally dialyzed squid giant axons. The direction of sodium transport was reversed by bathing the axons in K^+ -free seawater and internally dialyzing them with Na^+ -free solution containing 5 mM ADP, 5 mM P_i , and no ATP. Reverse electrogenic pumping was demonstrated by three criteria: (1) a ouabain-sensitive ^{22}Na influx was observed ($[Na]_i = 0$), (2) the pump current was abolished in Na^+ -free seawater, and (3) addition of H_2DTG inhibited ^{42}K efflux into K^+ -free seawater. Reverse sodium pump current ($-0.15 \pm 0.02 \mu A/cm^2$ s.s.m., $n=32$, $V = -58 \pm 2$ mV, $T=17^\circ C$, was measured from the change in holding current produced by the addition of the cardiotonic steroids dihydrodigitoxigenin (H_2DTG) or ouabain to the bathing fluid. These steroids had no effect on passive membrane conductance. Hyperpolarization decreased the absolute magnitude of the pump current by about 50% per 15 mV, while depolarization increased it by a similar amount. The direction of the change in pump current is opposite to that expected from the change in thermodynamic driving force. There is, therefore, a region of negative slope conductance in the current-voltage diagram of the reversed sodium pump.

Supported by NIH grants NS11223 and NS19393.

114

RESPONSE OF ISOLATED SEA URCHIN SPERM HEAD PLASMA MEMBRANES TO EGG JELLY. J. García-Soto, L. de la Torre, I. Vargas and A. Darszon, Dept. of Biochem., CINVESTAV-IPN, México City.

We are interested in the components involved in the changes in plasma membrane ion permeability which accompany the sperm acrosome reaction induced by egg jelly. We have shown that sperm plasma membranes preferentially isolated from the flagella change their permeability to Ca^{2+} and Na^+ in response to egg jelly (Darszon et al., Biophys. J. 41: 90a). Since in sea urchin sperm (*Strongylocentrotus purpuratus*) the acrosome reaction occurs in the head we have begun the isolation and characterization of plasma membrane fragments derived from it. The isolation is based on the method of Jacobson (BBA 471:331) using positively charged beads. The SDS band pattern of the isolated head membranes differs from that found with flagellar plasma membranes. This might reflect differences in their composition, although possible contamination from organelles is being studied. Surface labeling with ^{125}I indicates a 2.5 fold enrichment of specific activity in the isolated head membranes with respect to whole sperm. Isolated head membranes sonicated in the presence of soybean phospholipid liposomes respond to jelly with a species specific increase in Ca^{2+} and Na^+ uptake. In addition, as in whole sperm, Ca^{2+} uptake is blocked by nisoldipine, a specific inhibitor of Ca^{2+} channel function.

Friday 03 August Congress Centre-First Floor Posters 115-120

Posters on Mechanisms of Transport Across Membranes

115

MOLECULAR CONFORMATION AND GATING PROCESS OF SODIUM CHANNELS IN EXCITABLE MEMBRANES

Guo-Zhu He and Wen-Xiu Yang, Department of Physics, Nankai University, Tianjin, P.R. China

A model of specific molecular conformation for sodium channel protein in excitable membranes is proposed. The spaces between some α -helices of a spanning membrane protein are supposed to be sodium channels. The polar and charged amino acid side chains extend into these spaces and constitute active or inactivating gates. Transitions of these side chains from one conformation to another form gating current and cause the channel to appear in a closed or open state. Based on polarization and statistical theories, expressions for the steady and kinetic state of conformation changing process of the side chains are derived. Numerical calculations made by using these expressions may fit fairly well with various measurements of nerve axons. Moreover, the schemes about the interactions between some chemicals and receptors in sodium channel are discussed and inferred some specific types of amino acid side chains. The general rule about the effect of depolarizing pulse procedure on the movement of gating charges has also been studied.

117

INCREASE OF THE FLUIDITY OF THE LIPID BILAYER OF THE INNER MITOCHONDRIAL MEMBRANE BY SUCCINATE AND PHENYLSUCCINATE: A STUDY BY EPR AND FLUORESCENCE

Christine Mutet, Guy Duportail, Gérard Crémel and Albert Maisman - Centre de Neurochimie du CNRS - 5, rue Blaise Pascal - 67084 Strasbourg Cedex - France.

It has been shown by electron paramagnetic resonance and fluorescence experiments that succinate and phenylsuccinate, which induce a protein movement from the inner membrane of mitochondria towards the intermembrane space and the inner matrix, also induce an increase of fluidity of its lipidic domains.

The spin-labels used were esters of fatty acids bearing a doxyl moiety either at the polar head (CDTAB) or at the 5th (5NMS), 12th (12NMS) or 16th (16NMS) carbon position of the chain. A significant increase of fluidity after incubation with succinate or phenylsuccinate was observed when membranes were probed with CDTAB, 5NMS, 12NMS, but not with 16NMS.

With the fluorophores diphenylhexatriene (DPH) and trimethyl ammonium diphenylhexatriene (TMA-DPH), the fluorescence anisotropy decreased after incubation of mitoplasts in presence of succinate. The increase of fluidity seemed more pronounced near the bilayer surface.

These results lead us to think that these modifications are related to a membrane reorganization involving *inter alia* the lipid matrix.

119

SIMILARITY BETWEEN THE EFFECT OF CHANGES IN THE SURFACE POTENTIAL OF YEAST UPON CATION TRANSPORT KINETICS AND UPON BINDING OF A CATION TO THE YEAST CELL MEMBRANE

G.W.F.H. Borst-Pauwels, A.P.R. Theuvsen, W.M.H. van de Wijn-gaard and J.W. van de Rijke, Lab. of Chemical Cytology, University of Nijmegen, Toernooiveld, Nijmegen, The Netherlands

Changes in the surface potential of the yeast cell may have a great effect upon the kinetics of uptake of both mono valent cations and divalent cations into the yeast (1,2). The K_m of Rb^+ uptake increases on reducing the surface potential (3) and the kinetics of Sr^{2+} and Ca^{2+} uptake shift from that of a diffusion process to apparent saturation kinetics (4). The primary factor involved in these effects is the decrease in the interfacial cation concentration near the yeast cell membrane caused by reduction of the negative surface potential (1). A second factor which may be involved is the concomitant change in the gradient of the electrical potential within the membrane which will be expected on reducing the surface potential at the outside of the cell membrane. We will now show that binding of an organic cation (9-aminoacridine) to the yeast cell membrane is affected in a similar way, as uptake of Rb^+ into the yeast on reducing the surface potential. This indicates that the expected changes in the electrical gradients within the cell membrane do not attribute much to the kinetics of ion transport and that the effects found are mainly due to changes in the cation concentrations near the membrane surface.

1. A.P.R. Theuvsen et al. (1976) *J. Theor. Biol.* 57, 313-329.
2. G.W.F.H. Borst-Pauwels et al. (1984) *Physiol. Plant.* 60, 86-91.
3. A.P.R. Theuvsen et al. (1983) *BBA* 734, 62-69.
4. G.W.F.H. Borst-Pauwels et al. (1984) *in press*

116

EFFECT OF SOME NEW CROWN ETHERS ON THE STRUCTURE AND ION PERMEABILITY OF MODEL MEMBRANES

J. Cserrháti¹, L. Szegyi², F. Tölgyesi², S. Agai³ and L. Tóke³

¹Plant Protection Inst. of Hung. Acad. Sci.,
²Semmelweis Medical Univ., Inst. of Biophys.,
³Techn. Univ. of Budapest, Dept. of Org. Chem. Techn., Budapest, Hungary

The influence of some new crown ethers on the K^+ and Rb^+ efflux of membranes was studied on dipalmitoyl-phosphatidyl-choline (DPPC) liposomes. To correlate the permeability increase to the physico-chemical parameters of the investigated crown ethers their lipophilicity was determined by reversed-phase thin-layer chromatography, their effect on the phase transition temperature of DPPC was measured by differential scanning calorimetry. Some derivatives enhanced considerably the permeability of DPPC liposomes. The increase was higher for K^+ than for Rb^+ proving the highly selective bonding of K^+ . No correlation was found between lipophilicity and permeability increase, however crown ethers showing extremely high or low lipophilicities hardly influenced the permeability. Crown ethers enhancing more strongly the permeability of DPPC liposomes lowered the phase transition temperature of DPPC indicating their structure damaging effect.

118

DISCRIMINATION BY EPR AND FLUORESCENCE PROTEIN LABELS BETWEEN TWO STATES OF ORGANIZATION OF THE INNER MITOCHONDRIAL MEMBRANES

Serge Hurstel, Christine Mutet, Gérard Crémel and Albert Maisman - Centre de Neurochimie du CNRS - 5, rue Blaise Pascal - 67084 Strasbourg Cedex - France.

The movement of proteins between the different compartments of rat liver mitochondria can be triggered by some movement effectors (e.g. succinate). Proteins of the inner membrane were labeled on their thiol-groups with a fluorescent probe: pyrene-iodoacetamide (PIA). The marked modification of PIA emission spectra observed before and after incubation in presence of succinate was studied. The difference of these spectra, which depend on membranar integrity, indicates a modification of the SH labeled environment and suggests a membranar reorganization. Identification of the labeled proteins by electrophoresis showed their great diversity in molecular weight. Fluorescence quenching in the two states lead us to assume a model of independent types quenching (static and dynamic) to explain the down-curved Stern-Volmer plots. No discrimination between the two states was possible with cesium and iodine. However, succinate treated mitoplasts are more sensitive to acrylamide. Experiments with spin-label thiol-reagents confirmed the existence of these two membranar states.

120

FLUORESCENCE ENERGY TRANSFER BETWEEN MEMBRANE PROTEINS AND A23187

A. Hyono, S. Kuriyama and M. Masui, Osaka City University Medical School, Asahi-machi, Abeno-ku, Osaka, Japan

When tryptophan residues of the membrane proteins of intact cells and isolated outer and cytoplasmic membranes of a moderately halophilic bacterium were excited at 279 nm, the tryptophan emission was observed at 330 nm. However, adding calcium ionophore, A23187, to the suspensions of the cells and the both membranes, the ionophore emission at 430 nm appeared. As increasing A23187 in those suspensions, the ionophore emission increased on exciting membrane tryptophan, that is, the fluorescence energy was transferred from tryptophan to the ionophore. The critical distances between the ionophore and the tryptophan residues of both isolated membranes were given by Förster equation (52 Å), while the critical distance in the intact cell membranes was further than in the isolated membranes. All these critical distances are longer than the radii of membrane proteins, so that the ionophore is thought to be rather separated from the membrane proteins and be situated in the membrane lipid bilayers. Those are the usual relations between membrane proteins and the ionophore. On the other hand, only 50 per cent or less of the tryptophan residues can participate in the fluorescence energy transfer.

Friday 03 August - Congress Centre-First Floor Posters 121-126

Posters on Mechanisms of Transport Across Membranes

121

EFFECT OF PROTEIN CROSSLINKING ON WATER AND IONIC TRANSPORT THROUGH FROG SKIN

D. G. Mărgineanu and Constanța Rucăreanu, Membrane Biophysics Group, Institute of Biological Sciences, Bucharest, Romania.

The active transport of Na^+ , as expressed by the short-circuit current, is gradually inhibited when glutaraldehyde (GA) is present in the Ringer solution on the serosal face of the skin, even at 0.01% (w/v) concentration. The inhibition is roughly exponential, with time constants around 30 min. It seems to be partly due to the inhibition by GA of the tissular oxygen consumption which is halved by 0.10% GA. Higher concentrations, up to 1.0%, significantly increase the transepithelial diffusional permeability of water, and also produce even more pronounced increments in the diffusional permeabilities for Na and K. All these data are consistent with the image of GA cross-linking between the free amino (and other reactive) groups on the proteins. This probably results in the severe modification of every functional protein aggregate, thus inactivating the transport ATP-ases, but also causes a stabilization of protein hydrophilic membrane domains making the water and the small ions to penetrate easier.

123

PROTON-HYDROXIDE PERMEABILITY OF MEMBRANES. D.W. Deamer, Dept. of Zoology, University of California, Davis, CA

Most investigators agree that proton/hydroxide permeability of model and biological membranes is orders of magnitude greater than expected. Several recent observations are pertinent to possible mechanisms. Elamrani and Blume (BBA 727, 22) showed that proton-hydroxide permeation increased two orders of magnitude when lipid bilayer membranes underwent a phase transition, similar to the increase in water permeability under the same conditions. Blume (Biochem. 22, 5436) has demonstrated an unexpectedly high molar heat capacity of hydrated lipid systems which may result from "hydrophobic hydration" of non-polar regions. Gutknecht (Biophys. J. 45, 64a) found that proton/hydroxide conductance in planar lipid membranes is markedly decreased when water activity is reduced by glycerol addition. Significantly, proton-hydroxide conductance varied only ten-fold over pH ranges of 10 pH units. These findings suggest that both protons and hydroxide ions are conducted and that water is involved in the transport process. Nagle and Morawitz (PNAS 75, 298) proposed that proton equivalents may be conducted along hydrogen-bonded "proton wires" in membranes, and Nichols and Deamer (PNAS 77, 2038) suggested that if water were organized as hydrogen-bonded strands within transient defects in the bilayer, wire-like conductance would provide a proton permeation mechanism not available to other ions. We are testing this hypothesis by measuring changes in relative permeabilities of proton-hydroxide and other ions when hydrated defects are introduced into lipid bilayer membranes.

125

Cl^- TRANSPORT IN APICAL PLASMA MEMBRANE VESICLES ISOLATED FROM BOVINE TRACHEAL EPITHELIUM.

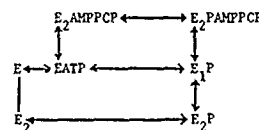
J.E. Langridge-Smith and W.P. Dubinsky, Dept. of Zoology, Univ. of Edinburgh, West Mains Road, Edinburgh, Scotland, U.K. and Dept. of Physiology and Cell Biology, Univ. of Texas, Houston, Texas, U.S.A.

Cl^- transport across the luminal border of bovine tracheal epithelium has been investigated using a highly purified preparation of apical plasma membrane vesicles. Transport of Cl^- into an intravesicular space was demonstrated by 1) a linear inverse correlation between the extent of Cl^- uptake and medium osmolality and 2) complete release of accumulated Cl^- in the presence of detergent. The rate of Cl^- uptake was highly temperature-sensitive and was enhanced by exchange diffusion, suggesting a mediated transport mechanism. Transport of Cl^- was not affected by the "loop" diuretic, bumetanide or by the stilbene-derivative anion exchange inhibitors, SITS and DIDS. In the presence of the impermeant cation tetramethylammonium (TMA^+), uptake of Cl^- was minimal; transport was stimulated equally by the substitution of either K^+ or Na^+ for TMA^+ . Addition of valinomycin to the K^+ medium further enhanced Cl^- uptake, while anionophore reduced Na^+ -stimulated Cl^- uptake towards the minimal level observed with TMA^+ . We conclude: 1) the vesicle membrane has a finite permeability to both Na^+ and K^+ ; 2) the membrane permeability to the medium counterion determines the rate of Cl^- uptake; 3) Cl^- transport is not specifically coupled with either Na^+ or K^+ ; and, finally 4) Cl^- crosses the tracheal luminal membrane via an electrogenic transport mechanism.

122

MECHANISM OF ALLOSTERIC REGULATION OF SARCOPLASMIC RETICULUM: STUDIES WITH CONVENTIONAL AND PHOTOAFFINITY ANALOGS OF ATP. F. Norman Briggs and Michael B. Cable, Department of Physiology and Biophysics, Virginia Commonwealth University, Richmond, VA.

The ATP analog adenylyl methylene diphosphate (AMPPCP) at 25, 50 and 100 μM concentrations: 1) stimulated the ATPase activity of the Ca, Mg-ATPase; 2) competitively inhibited the velocity of EP formation; 3) inhibited the ATPase activity of the monomeric form of Ca, Mg-ATPase; and 4) like ATP stimulated the rate of EP decomposition. These results can be explained by assuming either 1) active site interactions in an oligomer or 2) that AMPPCP binds to the active site after ADP departs and stimulates the following partial reactions. The observed stoichiometric relation between the photoincorporation of 3'-O-(4-benzoyl) benzoic adenosine triphosphate into the Ca, Mg-ATPase and ATPase activity is compatible only with the second alternative which is shown below:



124

STRUCTURAL, MECHANISTIC AND KINETIC ASPECTS OF VALINOMYCIN AND SYNTHETIC CYCLIC(Pro-Gly); MEDIATED TRANSMEMBRANE ION-TRANSPORT. K.R.K. Easwaran and M.B. Sankaram, Molecular Biophysics Unit, Indian Institute of Science, Bangalore 560 012, India.

Detailed investigations on the solution conformation of valinomycin complexes with a variety of alkali and alkaline earth cations gave very interesting and novel conformations for the complex. In particular, the observation of 2:1 (ion-sandwich) type complexes indicates that a relay carrier mechanism might be operative for valinomycin mediated cation transport under certain conditions. Results on the location of valinomycin in lipid vesicles showed that valinomycin is located predominantly in the head group region in DPPC vesicles and penetrates the hydrophobic core in DMPC vesicles. ^{31}P and ^1H NMR studies on the kinetics of Pr^{3+} transport across DPPC and DMPC vesicles mediated by valinomycin and synthetic cyclic peptide cyclo(pro-gly)₃ showed that valinomycin does not transport Pr^{3+} across vesicles while cyclo(pro-gly)₃ does forming a hexameric pore. These results are explained in terms of preferential stoichiometry of their cation complexes, size of the cation complex and relative rate for the various steps during the transport.

126

PHYSICAL PATHWAYS OF RECEPTOR-MEDIATED ENDOCYTOSIS: POST-INTERNALIZATION DYNAMICS OF LDL-CONTAINING VESICLES

D. Gross and W.W. Webb, School of Applied and Engineering Physics, Clark Hall, Cornell University, Ithaca, NY, USA.

Single molecules of the fluorescent analog diI-LDL (Barak and Webb, J. Cell Biol. 20:595, 1981) are visible by fluorescence microscopy. We have studied the intracellular dynamics of initially receptor-bound diI-LDL contained in endocytotic vesicles of living human fibroblasts from the time of initial internalization to final transport to the perinuclear lysosomal compartment. Real time image intensified digital video microscopy (Gross and Webb, Biophys. J. 41:215a, 1983) enables detection in real time and analysis of the dynamics of molecular positions and fluorescence intensities of diI-LDL containing structures.

The internal vesicles containing diI-LDL are strikingly motile; pairs of associated vesicles remote from the perinuclear region are often seen to rotate and oscillate about a mutual center of motion. Occasionally a pair is observed to fuse after vigorous oscillation -- the single vesicle which results continues to show high mobility for a time after the fusion. Single vesicles on fast unidirectional saltatory pathways move at about 1/2 $\mu\text{m}/\text{sec}$, but fast unidirectional transport of vesicle pairs is not observed. Short lived (5 min) linear arrays of discrete vesicles are observed far from the nucleus while smaller circular or arced arrays are often seen near the nucleus. We demonstrate that the transport of LDL-containing vesicles is blocked near the plasma membrane by the calmodulin-blocking drug trifluoperazine. Supported by NSF grant AT-01404.

Friday 03 August Congress Centre-First Floor Posters 127-132

Posters on Mechanisms of Transport Across Membranes

127

³¹P NMR AS A TOOL FOR MONITORING DETERGENT SOLUBILIZATION OF SARCOPLASMIC RETICULUM MEMBRANES
M. Roux and P. Chappell

Service de Biophysique, CEN/Saclay, Gif sur Yvette, France
Sarcoplasmic reticulum vesicles were solubilized stepwise by the nonionic detergent octaethyleneglycol-monododecylether (C₁₂E₈). ³¹P NMR enabled the extent of phospholipid solubilization to be monitored by following the conversion of the broad resonance peak characterizing the phospholipids inserted in the bilayer to the narrow resonance signal characterizing phospholipids inserted into a mixed micelle. When 0.25 g C₁₂E₈/g protein was added, no peak characteristic of solubilized phospholipid appeared. For higher detergent concentrations the spectrum shows the superposition of new peaks characteristic of phospholipids in mixed micelles. Comparison with standard lipids solubilized under the same conditions allowed assignment of the peaks to phosphatidylcholine, phosphatidylethanolamine and phosphatidylinositol. Solubilization was virtually complete for 1.5-2g detergent/g protein, a proportion commonly used for ATPase solubilization. High levels of C₁₂E₈ gave spectra with enough resolution to allow quantification of the percentage of each individual phospholipid. The values measured were in good agreement with previous analyses of SR phospholipids. Although the method allows to monitor the extent of solubilization of individual phospholipid classes, there was no evidence of either preferential solubilization or retention of a specific class of phospholipids.

129

CHLORIDE TRANSPORT AND ACCUMULATION IN ISOLATED HUMAN NEUTROPHILS

L. Simchovitz and P. De Weer, Departments of Medicine and Physiology and Biophysics, Washington University School of Medicine, St. Louis, Missouri, USA.

Chloride movements in human neutrophils were studied by chemical analysis and with ³⁶Cl. Neutrophils bathed in 148 mM-Cl media accumulate Cl to ~80 meq/liter cell water, four times higher than the expected passive distribution (resting potential ~53 mV). Accumulation is caused by a metabolism-dependent mechanism which is independent of Na₀, has a K_{0.5}(Cl) = 5 mM and V_{max} = 0.25 meq/liter cell water.min, and is inhibited by ethacrynate (K_i = 50 μM), furosemide (K_i = 50 μM), and α-cyano-4-hydroxycinnamate (CHC; K_i = 1.7 mM). Net diffusion from the cell occurs through a low-permeability pathway (P_{Cl} = 4 × 10⁻⁹ cm/s; g_{Cl} = 1 μS/cm²) that shows evidence of single-filing: the flux ratio vs. V_m plot is steeper than predicted by Ussing's equation, and one-way passive efflux is inhibited by external Cl. The bulk (~70%) of the one-way ³⁶Cl fluxes in steady-state cells represents electrically silent Cl:Cl exchange mediated by a carrier insensitive to disulfonic stilbenes but competitively inhibited by CHC, which will carry other anions including p-aminobiphenylate (PAH). In cells with [Cl]_i = 80 mM, the carrier exhibits V_{max} = 1.2 meq/liter.min, K_m(Cl) = 5 mM, K_m(PAH) = 45 mM, K_i(CHC) = 0.3 mM. The three mechanisms: active transport, electrodiffusion, and carrier-mediated exchange, account for the total one-way fluxes observed. Supported by the Veterans Administration and NIH grant NS11223.

131

EVIDENCE FOR A TWO-FOLD (C₂) AXIS OF SYMMETRY RELATING SUBUNITS OF THE HUMAN ERYTHROCYTE ANION EXCHANGE CHANNEL, J. V. Staros, Vanderbilt University, Dept. of Biochemistry, School of Medicine, Nashville, TN 37232, U.S.A.

The anion exchange channel (band 3) is responsible for HCO₃⁻:Cl⁻ exchange across the erythrocyte membrane and thus for the transport of CO₂ (as HCO₃⁻) by the erythrocytes to the lungs. This structure is composed of two or more band 3 subunits, each of which is a transmembrane glycoprotein, the polypeptide portion of which traverses the membrane several times. We have reacted our new membrane-impermeant cross-linkers with intact human erythrocytes and have found that cross-links thus introduced into the extracytoplasmic domain of the anion exchange channel result in a high yield of dimers of band 3 subunits and in no detectable higher oligomers. Treatment of unmodified erythrocytes with chymotrypsin results in a single cleavage of the band 3 polypeptide in the extracytoplasmic domain, yielding two fragments of distinct M_r. Successive treatment of intact erythrocytes with a membrane-impermeant cross-linker followed by chymotrypsin yields cross-linked chymotryptic fragments of band 3. All of the interfragment cross-links identified are between unlike fragments, whether the cross-links are intersubunit or intrasubunit. These data are consistent with a "closed" dimer of band 3 subunits related by a two-fold (C₂) symmetry axis normal to the plane of the membrane but not with other models in which four equivalent subunits are related by a C₄ axis or in which band 3 subunits associate into "open" front-to-back dimers and higher oligomers. [Supported by NIH grants AM31820 and AM25489.]

128

POTASSIUM AND OUABAIN-SENSITIVE ENERGY UTILIZATION BY CRAYFISH GIANT AXONS. E.M. Lieberman and J. Pascarella, Physiol. Eas' Carolina U. Sch. Med., Greenville, NC U.S.A.

Axons equilibrated in various [K]₀ maintain [K]_i constant, adjusting Na:K transport "coupling" in compensation for differing electrochemical gradients (Lieberman (1,2)). This observation led to the hypothesis that high energy phosphate utilization, V(P), should directly vary with the product of the Na and K electrochemical gradients and ionic conductances, not with the absolute [K]₀. This study was undertaken to directly measure steady-state V of ATP and Arginine Phosphate (ARG-P) by axons under the influence of [K]₀ and Ouabain (3). [K]₀ did not influence total V(P) of the axon. For [K]₀ between 0.5 and 21.6 mM V(P) averaged 52.8 ± 4.7 %/hr. (n=44) of the initial [ATP+ARG-P]. Unlike total V(P) the ouabain-sensitive component is markedly influenced by [K]₀. Following equilibration of the axon in 0.5 mM K ouabain poisoning decreases V(P) to 8%/hr, i.e. 85% of the energy consumed by the cell is used for Na:K exchange transport. For 1.35 mM K V(P) after ouabain poisoning is 18%/hr.; at 5.4 mM K, 29%/hr.; at 13.5 mM K, 31%/hr. The pattern of V(P) as a function of [K]₀ is similar to its effect on the sum of the Na and K electrochemical gradients (2). The data are consistent with the hypothesis that the transport system of cells, in the steady-state, responds to the electrochemical gradient against which it transports ions and not necessarily to the absolute [K]₀. (1) Europ. J. Physiol. 366: 195 (1976); (2) EJP 378: 243 (1979); (3) Anal. Biochem. 134: 413 (1983). Supported by NSF INT 8117183 and ARO DAAG29-82-K-0182.

130

MECHANISTIC STUDIES ON THE ANION ERYTHROCYTE TRANSPORT PROTEIN, BAND-3

R.J. Pace, Research School of Chemistry, Australian National University, Canberra, A.C.T. Australia.

³⁵Cl NMR, Transverse T₂ relaxation, has been used to study substrate binding to the protein in washed membranes and detergent solubilised form. At least two residues (lysine and arginine) have been identified as contributing to anion binding. Reaction of leaky red cell membranes with lysine specific reagents (1 fluoro-2,4 dinitro-benzene, 4,4'-diisothiocyanato-stilbene-2,2'-disulphonate (DIDS)) or the arginine reagent, 1,2, cyclo-hexanedione completely eliminates high affinity transport related chloride binding. The lysine site is accessible to the non permeable DIDS reagent only from the outside. Studies on sealed systems have shown that the arginine site is accessible mainly from the inside. To examine the possible involvement of internal salt bridges in the transport mechanism, the effects of the soluble carbodiimide EDC (1-ethyl-3-(3-dimethylaminopropyl) carbodiimide) on Cl⁻ binding were determined. EDC treatment does not affect Cl⁻ binding but EDC plus exogenous amines create a new class of Cl⁻ binding sites. Gel patterns suggest that any internal crosslinking induced by EDC is occurring within either of the two major membrane spanning fragments of the monomer protein.

132

THE USE OF ¹H AND ³¹P-NMR TO INVESTIGATE THE PERMEABILITY MECHANISMS INDUCED BY PHOSPHOLIPASE AND BILE SALTS IN PHOSPHOLIPID LIPOSOMAL MEMBRANES.

G.R.A. Hunt, I.C. Jones, J. Evans and C. L. Lockyer, Department of Science, The Polytechnic of Wales, Pontypridd CF37 1DL, UK.

The increasing use of liposomes as drug delivery systems by the oral and intravenous route indicates a need for the development of biophysical methods to study the interaction of the liposomal membranes with physiological fluids. The principal challenge to the integrity of phospholipid vesicular membranes in the digestive tract is the presence of phospholipase enzymes and the bile salts. We have therefore used ¹H and ³¹P-NMR spectroscopy of unilamellar phospholipid vesicles to study their permeability to the probe ions Dy³⁺ and Pr³⁺ induced by pancreatic phospholipase A₂ and the bile salts glycocholate and glycodeoxycholate. The ¹H-NMR spectra of vesicles demonstrates a marked synergism in the combined effects of these digestive agents and indicate that the products of enzyme hydrolysis (lyso lipid and fatty acids) are involved in the permeability mechanism. Experiments using ³¹P-NMR reveal in detail the role of transmembrane lipid exchange and the bile salts in producing transport mechanisms across the liposomal bilayer.

These results will be discussed in terms of the advantages of the use of NMR techniques in the future design of liposomes and in our understanding of the interaction of bile salts with cell membranes lining the digestive tract.

Friday 03 August Congress Centre-First Floor Posters 133-138

Posters on Mechanisms of Transport Across Membranes

133

THE METASTABILITY OF BACTERIORHODOPSIN: A MECHANISM FOR PHOTOINDUCED TRANSLOCATION OF PROTONS IN THE PURPLE MEMBRANE
J.E. Draheim, N.J. Gibson, S.C. Hartzel and J.Y. Cassin, Department of Microbiology, The Ohio State University, Columbus, Ohio 43210, U.S.A.

Solid-state protonic semiconductor models may appear at first glance to be the most attractive means of explaining the phenomenon of photoinduced vectorial proton translocation in the purple membrane, since this membrane seems to be void of permanent transmembrane channels and its sole protein, bacteriorhodopsin, is highly helical in structure. However, recently Cassin and coworkers have shown that this protein is structurally metastable and undergoes reversible large-scale global structural changes during the photocycle.* Two important consequences of these changes are (1) crystal lattice distortions of the membrane, and (2) a net tilting of the polypeptide segments of the protein away from the membrane normal. These structural deformations should encourage the formation of pulsating transmembrane channels normal to the membrane plane and provide the driving force and direction for active proton translocation. Clearly, deformation models of this kind provide a much more universal means for active transport in membranes than the solid state ones, since they possess the potential for the translocation of other ions than protons as well as small molecules.

* Draheim, J.E., N.J. Gibson, and J.Y. Cassin. 1983. Photochem. Photobiol. 37:554.

135

INTERACTIONS BETWEEN MONOVALENT AND DIVALENT CATIONS IN ACTIVATING THE Na,K-ATPase. Joseph D. Robinson, Dept. Pharmacology, SUNY Upstate Medical Center, Syracuse, NY, USA

For the K-phosphatase activity catalyzed by the Na,K-ATPase, divalent cations are required and added K markedly stimulates. With 3mM Mg activity in the absence of added K is only 2% of that with 10mM K, and declines as Mg is increased. With either 1mM Mn alone or 1mM Ca plus 3mM Mg activity in the absence of added K is 10-15% of that with 3mM Mg and 10mM K, but also declines at higher Mn or Ca concentrations. The $K_{0.5}$ for K as activator is increased by all 3 divalent cations. With 10mM K, Na inhibits. The $K_{0.5}$ is decreased (compared to that with 3mM Mg) by adding 1mM Ca but increased when 1mM Mn is substituted for Mg. Oligomycin inhibits activity with 3mM Mg plus 1mM Ca in the absence of K, and also activity with Mn in the absence of K. These data are interpreted as: activity depends on the E_2 form of the enzyme; the E_2/E_1 ratio is increased by Mg or Mn and decreased by Ca through occupancy of divalent cation (DC) sites; activity also requires occupancy of monovalent cation (MC) sites at which K stimulates optimally, Mn and Ca less well, Mg and Na poorly if at all. Thus Ca stimulates at the MC but inhibits at the DC sites, and augments Na-inhibition by favoring E_2 ; Mn stimulates at both and diminishes Na-inhibition by favoring E_2 , but why it also inhibits at higher concentrations is unclear. (Supported by USPHS grant NS05430.)

137

CALCIUM FLUXES ACROSS MEMBRANES OF HUMAN NEUTROPHILS OBSERVED WITH QUIN-2.
V.von Lischner, Theodor Kocher Institute, University of Berne, CH.

Neutrophils are known for their capability to kill invading microorganisms by phagocytoses and enzyme secretion. Their stimulation is closely linked to changes in cytosolic calcium. Human neutrophils have been prepared from blood by centrifugation in a percol gradient. Quin-2, a fluorescent calcium chelator, penetrates the neutrophils in its esterified form and is trapped there after hydrolysis by esterases. The fluorescence change accompanying hydrolysis inside the cell reflects the esterase activity and the cell loading process. The calcium fluxes into and out of the cytosol are also monitored by the quin-2 fluorescence change. We have calculated the competing effects of cytosolic calcium binding sites with the chelator quin-2. Measurements of the calcium fluxes for different degrees of quin-2 loading and at various internal calcium levels, allowed us to determine the concentrations of cytosolic calcium binding sites and an average binding constant for calcium inside the cytosol.

134

FURTHER EVIDENCE FOR THE PHOTOINDUCED POLYPEPTIDE TILTING PHENOMENON IN THE BACTERIORHODOPSIN OF THE PURPLE MEMBRANE
N.J. Gibson and J.Y. Cassin, Department of Microbiology, The Ohio State University, Columbus, Ohio, USA

Comparative circular dichroism spectra of oriented films of bleached and crosslinked-then-bleached purple membrane were studied in order to better understand the role played by tertiary structure changes in the photocycle of the bacteriorhodopsin of the purple membrane. Cassin and coworkers have previously used this oriented film technique to study the bleached and the photointermediate M-412 states of the purple membrane.* These studies have strongly indicated the possibility of photoinduced net tilting of the helical polypeptide segments of the bacteriorhodopsin away from the membrane normal. The results of the present study are in accord with enhancement of the tilting phenomenon after crosslinking. Furthermore, it has been shown previously that the proton translocation efficiency is increased after crosslinking. Therefore two conclusions can be drawn from these findings: (1) the protein is more delicately metastable than previously suspected and (2) tilting of the polypeptide segments is an essential feature of the photocycle. This supports the pulsating channel model proposed by Cassin and coworkers for the photoinduced proton translocation process of this membrane.**

* Luccio, D.D. and Cassin, J.Y., Biophys. J. 26, 427 (1979)

** Draheim, J.E., Gibson, N.J. and Cassin, J.Y., Photochem. Photobiol. 37, 554 (1983)

136

ELECTRICAL AND MECHANICAL EVENTS RELATED TO THE DESENSITIZATION OF THE ISOLATED GUINEA-PIG TAENIA COLI TO ANGIOTENSIN II. S.I. Shimuta, A.T. Ferreira, R.P. Markus*, A.C.M. Paiva and T.B. Paiva. Department of Biophysics and *Department of Pharmacology, Escola Paulista de Medicina, São Paulo, S.P., Brazil.

Angiotensin II (AII) and its analogues containing a guanido group in the position 2 side chain and a protonated N-terminal amino group (such as AII and Sar¹-AII) induced desensitization in the taenia coli. The phenomenon was characterized by lack of full relaxation after removal of the agonist, and decreased (or abolished) response to the second administration 5 min after. Simultaneous electrical recording (double sucrose gap) showed that the prolonged contraction was due to depolarization which persisted after removal of the agonist. During this phase the electronic potential was diminished indicating increased membrane conductance. By reducing Na concentration of the medium a fast relaxation was observed upon removal of the agonist with full repolarization. Nevertheless a new addition of Sar¹-AII did not induce depolarization or contraction. We concluded that, in the taenia coli the mechanism responsible for desensitization is related to alterations in the receptor or in the receptor-operated ionic channels and is not dependent on membrane potential.

138

THE EFFECT OF MELITTIN ON THE ROTATION OF BACTERIORHODOPSIN IN DMPC VESICLES.

K.S. Hu, M.J. Dufton, R.J. Cherry, Department of Chemistry, University of Essex, Wivenhoe Park, Colchester, Essex, U.K.

Rotational diffusion measured by the technique of flash-induced transient linear dichroism. In the presence of melittin, a 26-residue peptide from bee venom, a dose-dependent loss of rotational mobility was detected. In the case of acetylated melittin, the effect is less than with native melittin. With succinylated melittin, the loss of rotational mobility can be found only at relatively high concentration.

A mechanism is proposed in which melittin is anchored in the membrane by its hydrophobic N-terminus, while its cationic C-terminal moiety binds to negatively charged residues on bacteriorhodopsin molecules. This leads to protein-protein aggregation and hence loss of mobility. Alternatively, melittin could induce protein aggregation indirectly by changing the physical state of the lipids. This seems less likely in view of the weak effect of succinylated melittin compared with native melittin.

Friday 03 August Congress Centre-First Floor Posters 139-144

Posters on Mechanisms of Transport Across Membranes

139

PHOSPHOLIPASE D PRODUCES INCREASED CELL SURFACE Ca^{2+} -BINDING AND POSITIVE INOTROPY IN RAT HEART. J.M. Burt, T.L. Rich and G.A. Langer. Dept. of Physiology, University of California, Los Angeles, Calif., USA.

Sarcolemmal anionic phospholipids represent potential Ca^{2+} -binding sites which may be important in cardiac contractility. If anionic phospholipid Ca^{2+} -binding does influence cardiac contractility, then an increase in the number of anionic phospholipid sites in the sarcolemma may lead to increased Ca^{2+} -binding and an inotropic response. To test this hypothesis we treated cultured neonatal rat myocardial cells with phospholipase D (PLD), an enzyme which converts membrane phospholipids to phosphatidic acid. We then compared cellular ^{45}Ca uptake and binding and cell contractility from before PLD treatment to that occurring after treatment. PLD treatment (37°C , 30min) resulted in an increase of 39% in Ca -uptake or 1.6 ± 0.3 nmole/kg dry weight. As observed in untreated cells, 78% of the exchangeable Ca remained La^{3+} displaceable. The quantity of Ca displaced by Polymyxin B, a drug which displaces Ca preferentially from anionic phospholipid sites, increased by 85% following PLD treatment. Electrical activity of the cells following PLD treatment was not altered. In ventricular strips of neonatal rat muscle, measurement of contractility revealed a 1.7 - 2.5 fold increase in contractile activation as a result of PLD treatment. Similar effects were observed in the cultured cells. Thus PLD treatment, which is expected to increase the quantity of negatively charged phosphatidic acid in the membrane, resulted in an 85% increase of anionic phospholipid-bound Ca and concomitantly resulted in a significant increase in contractility. Supported by: USPHS grants: HL28599-01, the Castera Endowment and Am. Heart Assoc. Greater Los Angeles Affiliate grant 652-F2.

141

RECONSTITUTION OF Na,K,Cl -COTRANSPORTER AND A BARIUM SENSITIVE K-CHANNEL FROM LUMINAL MEMBRANES OF RABBIT OUTER RENAL MEDULLA

Charles E. Burnham, Peter L. Jørgensen* and Steven J.D. Karlsh, Biochemistry Department, Weizmann Institute of Science, Rehovot 76100, Israel and *Institute of Physiology, Aarhus University, 8000 Aarhus C, Denmark.

Potassium (^{86}Rb) fluxes have been measured in crude membrane fractions from outer renal medulla. By measuring uptake of ^{86}Rb against a large opposing chemical gradient of K^{+} -ions the isotope was accumulated allowing a very sensitive detection of either channel or carrier mediated transport processes. Three cation transport systems were detected: a) the furosemide inhibited Na,K,Cl -cotransporter, b) the barium inhibitable K-channel and c) the ouabain sensitive Na,K -pump. After centrifugation on metrizamide gradients, fractions enriched in luminal membrane vesicles containing the Na,K,Cl -cotransporter and K-channel and basolateral membrane vesicles containing the Na,K -pump were separated from the bulk of contaminant protein. In the luminal vesicles, potassium (^{86}Rb) transport through the Na,K,Cl -cotransporter was stimulated by sodium and inhibited by bumetanide.

For reconstitution, luminal membranes were solubilized by octylglucoside with soybean lipid and passed over Sephadex columns thus forming phospholipid vesicles. In these vesicles furosemide or barium inhibitable ^{86}Rb -fluxes were detected suggesting that both the Na,K,Cl -cotransporter and the K-channel had been reconstituted in a functional state.

143

The Structure of Gramicidin Transmembrane Channel, B.A. Wallace, Department of Biochemistry, Columbia University, New York, N.Y., USA.

Spectroscopic and diffraction studies of gramicidin A have provided information its conformation and organization and on structural changes in the molecule which accompany cation binding. NMR spectroscopy (PNAS 76, 4230 1979) provided the first direct physical evidence that the channel conformation in phospholipids an N-to-N terminal dimer of helices. Circular dichroism spectroscopy (Biochemistry 20, 5754 1981) demonstrated that its structure in bilayers is different than its structure in a variety of organic solvents. Ion binding also affects the membrane-bound and organic solvent forms of the molecule differently (Biopolymers 22, 397 1983). In membranes, the dimer is insensitive to monovalent cations, whereas in organic solvents, the cations apparently stabilize a helical conformation of opposite hand and different pitch from that which predominates in solution. Crystals of a gramicidin/ Cs^{+} complex have been prepared (Ann. N.Y. Acad. Sci., in press). A 1.8 Å map has been calculated using single wavelength anomalous scattering for phasing. This map reveals the helical structure of the molecule and the cation-binding sites (Wallace and Hendrickson, unpublished results). Co-crystals of gramicidin and lipid have also been prepared which diffract to high resolution and have the gramicidin in its membrane-bound channel conformation, as shown by Raman spectroscopy (Biopolymers 22, 397 1983). Data collection on this crystal form is currently underway. Supported by NSF PCM 80-20063, 82-15109, and NIH CH 27312.

140

SYNTHESIS AND CONFORMATIONAL STUDY OF $\text{Boc-L-Leu(L-Leu-Gly)}_5\text{.OBz}$ IN SOLUTION AND IN SOLID STATE

M. D'Alagni and M. Manigrasso, Centro Studio Chimica Recettori e delle Molecole Biologicamente Attive, C.N.R., Roma and Dipartimento di Chimica, Università di Roma "La Sapienza", Roma P.le A. Moro, n.5, Italy

A sequence of glycine residues alternated with non polar amino acid residues is invariably present in the middle portion of the polypeptide chain of some membrane proteins of organisms very distant in the evolutive scale. This has stimulated the interest in the synthesis and conformational study of $\text{Boc-L-Leu(L-Leu-Gly)}_5\text{.OBz}$. The undeca-peptide synthesis was accomplished via DCCD method. The conformational study of the oligopeptides was carried out using circular dichroism, uv and ir spectra. The conformation in solution was examined in trifluoroethanol (TFE), hexafluoroisopropanol (HFIP), hexafluoroacetone trihydrate (HFA) and methanol (MeOH). CD and uv spectra in TFE showed a change from unordered to β structure with increasing peptide length. The onset of β structure was found between the pentamer and the hexamer. In HFA all the oligopeptides are essentially in an unordered conformation whereas in MeOH the formation of associated species is favoured. Finally, CD evidences revealed in TFE - water solution the binding of Ca^{2+} to epta-peptide and undeca-peptide with the occurrence of a contemporaneous conformational change.

142

RELATIONSHIP BETWEEN CATALYTIC ACTIVITY, STABILITY, PHOSPHOLIPID CONTENT AND AGGREGATIONAL STATE OF SOLUBILIZED Ca^{2+} -ATPase OF SARCOPLASMIC RETICULUM.

D.B. McIntosh and D. Ross, MRC Biomechanics Research Unit/Department of Chemical Pathology, University of Cape Town Medical School, Cape Town, South Africa.

The effect of increasing concentrations of Triton X-100 on catalytic activity, stability, phospholipid content and aggregational state of solubilized Ca^{2+} -ATPase of sarcoplasmic reticulum has been investigated. In the 0.1 to 0.25% (w/v) range at fixed solubilized ATPase concentration (0.4 mg protein/ml) Triton X-100 activated ATP hydrolysis two fold. Higher concentrations of the detergent resulted in 50% inhibition. Thermal inactivation of catalytic activity in excess EGTA at 25°C was monophasic and first order at all concentrations of detergent. The rate constant for inactivation increased sigmoidally to a maximum value at 2% Triton X-100. The aggregational state of the solubilized ATPase was assessed by glutaraldehyde crosslinking and by ultracentrifugation. Both methods indicated that the solubilized enzyme changed from an aggregate to a monomer in the 0.1 to 0.25% Triton X-100 range. The phospholipid content changed from about 50 to 20 mol phospholipid/mol ATPase; higher detergent concentrations displaced all the phospholipid. These results indicate that Triton X-100 cannot substitute for phospholipids in maintaining a stable native structure of the ATPase and suggest that protein-protein interactions inhibit catalytic activity.

144

THE EFFECT OF POLYMERIZATION ON THE PERMEABILITY OF BLACK LIPID MEMBRANES

R. Benz*, W. Prass and H. Ringsdorf, Institut für Organische Chemie, Johannes Gutenberg-Universität Mainz FRG and *Fakultät für Biologie, Universität Konstanz FRG

Polymerization of lipids has been reported to increase the stability of monolayers as well as of liposomes. However, attempts to polymerize black membranes have resulted only in the destruction of the membranes.

We now describe the polymerization of a lipid containing a butadiene moiety as the polymerizable group. In this case polymerization in the black membrane yields membranes displaying increased stability.

To prove that polymerization had occurred the kinetics of dipicrylamine transport across the membrane was investigated using the charge pulse technique. By this method it could be shown that the transportation rate constant had decreased by a factor of about 20 towards the end of the polymerization. The reduction in the diffusion rate can be explained by the inability of the lipophilic ion to bypass the barrier created from covalently linked fatty acid in the hydrophobic part of the polymerized membrane.

Friday 03 August Congress Centre-First Floor Posters 145-150

Posters on Mechanisms of Transport Across Membranes

145

CHARGE TRANSPORT IN BILAYERS STUDIED IN THE TIME AND FREQUENCY DOMAINS.

A.D. Pickar, M.C. Brown, K.L. Cox, J. Hobbs and P. Smejtek. Department of Physics, Portland State University, Portland, Oregon.

Mechanisms of charge transport in lipid bilayer membranes have been investigated in a series of coordinated studies of dynamical electrical behavior in both the time and frequency domains. The experimental methods include voltage-step spectroscopy, charge-pulse relaxation spectroscopy, and alternating current admittance spectroscopy. Transport systems which have been studied include lipophilic ions, monomeric alkali ion carriers, and dimeric protonophoretic carriers in both monoglyceride and egg-phosphatidylcholine membranes. Equivalent R-C circuits used to represent results are not unique; certain alternative representations are preferred on the basis of physical models, but not because of the fit of the admittance spectra to experimental results. The high frequency region of the spectra are dominated by charging effects, which can be influenced by structural changes due to adsorbed substances. For alkali ion carriers differences between rate constants derived from charge-pulse and alternating current admittance observations may be attributed to non-specific membrane relaxations. For the protonophore pentachlorophenol the interpretation of the spectra requires consideration of adsorption isotherms obtained in auxiliary experiments.

147

COMPARATIVE STUDIES OF MEMBRANOUS AND SOLUBILIZED ADENOSINE TRIPHOSPHATASE OF SARCOPLASMIC RETICULUM

O.B. Martins and L. de Meis - Department of Biochemistry, Institute of Biomedical Sciences, Federal University of Rio de Janeiro, Rio de Janeiro, Brazil.

The aim of this study was to characterize the Ca^{2+} -ATPase of sarcoplasmic reticulum in both native and soluble forms. Thus the effects of the anionic detergents Triton X-100, Lubrol PX, C_{12}E_8 and Tween 20 on the ATPase were studied. The forward reaction (NTP hydrolysis) of the catalytic cycle of ATPase was stimulated in the solubilized enzyme. On the other hand, the backward reaction (NTP synthesis), observed with native ATPase in the absence of a calcium gradient, was fully inhibited by enzyme solubilization. Interaction of the enzyme with membrane lipids appears to be required for ATP synthesis but not for hydrolytic activity. The partial reaction involved in ATP synthesis (phosphorylation by P_i , calcium binding and the transfer of acyl phosphate to ADP) were studied. The results suggest that the vectorial performance of Ca^{2+} -ATPase is promoted by a rapid transition from the enzyme form that binds calcium with low affinity to the form that binds with high affinity.

149

VOLTAGE DEPENDENCE OF Na^+/K^+ PUMP CURRENT IN INTERNALLY DIA-LYZED CELLS FROM GUINEA PIG VENTRICLE.

D.C. Gadsby and A. Noma, Nat. Inst. for Physiological Sci., Okazaki, Japan.

Enzymatically isolated cells were voltage clamped and internally dialyzed using a patch pipette (tip diam. 4-5 μm ; resistance $< 1 \text{ M}\Omega$) and were superfused at 36°C with 5-20 mM K Tyrode's solution. Channel currents were minimized by adding 0.9 mM Ba, 1 mM Cs and 0.1 mM Cd to external solutions, by substituting Cs for all but 11 mM K and adding 20 mM TEA to pipette (internal) solutions, and by using a holding potential of -40 mV to inactivate Na channels. Internal solutions also contained 5 mM creatine phosphate plus 10 mM ATP to fuel the pump, 100 mM aspartate, and 5 mM EGTA. On suddenly raising pipette $[\text{Na}]$ from 1 mM to 30-50 mM, the holding current at -40 mV shifted outward reaching a new steady level within $< 2 \text{ min}$. Most of this outward current was rapidly (1-2 min), and reversibly, abolished by external ouabain (10 μM) or strophanthidin (50-100 μM). Current-voltage relationships (between -140 mV and +40 mV; 300 msec pulses at 0.125 Hz) obtained with high pipette $[\text{Na}]$ before, during, and after Na^+/K^+ pump inhibition with ouabain or strophanthidin, revealed that pump-induced outward current was greater at more positive potentials, and smaller at more negative potentials, than at -40 mV. At 0 mV, such strongly activated pump current averaged $190 \pm 60 \text{ pA/cell}$ ($\pm \text{SD}$, $n=8$) equivalent to $3 \pm 1 \text{ } \mu\text{A/cm}^2$ visible cell surface, and over the diastolic range of membrane potentials (-50 to -100 mV), it contributed approximately $20 \pm 9 \text{ pA/cm}^2$ surface to the membrane slope conductance.

146

THE pH-STAT TECHNIQUE APPLIED TO RAT PROXIMAL TUBULE.

G. Malnic, M. Mello Aires, A.C. Cassola, A.G. Lopes and G. Glebisch. Depts. of Physiology, Inst. Ciências Biológicas, Univ. São Paulo, Brasil, and Yale Univ. School of Medicine, New Haven, USA.

The pH-stat technique has been used to measure H-ion fluxes at constant mucosal pH in gastric mucosa and turtle bladder. In renal tubule, H fluxes have not been measured at constant luminal pH, although luminal buffer load is important for the definition of H transport. We have fixed luminal pH in oil-blocked luminal fluid columns by injecting, by means of an electronic pH-clamp, OH^- via an antimony microelectrode or H^+ via a 1M HCl-filled Ling-Gerard microelectrode, and measuring pH by a double-barrelled Sb/reference electrode. Due to ion injection at a point source, pH falls exponentially with distance even in a small blocked segment. Therefore, a treatment analogous to cable analysis was applied, where pH was used for voltage and ion flow for current. A length constant of $15.9 \pm 1.28 \text{ (n=13) } \mu\text{m}$ was obtained during OH^- injection, and of $15.5 \pm 1.00 \text{ (n=4) } \mu\text{m}$ during H^+ injection. Since it was difficult to obtain absolute fluxes per unit area of epithelium under these conditions, effective conductances ($\text{EC} = \text{current/pH}$) were measured in paired conditions at a fixed distance between injectors, and measuring electrodes. When tubules were perfused in sequence with control and 10^{-4} M acetazolamide containing solutions, using OH^- current EC fell to $0.45 \pm 0.046 \text{ (7) of controls}$, indicating, as in bladder studies, a fall in "active" H conductance. When H-ions were injected, no reduction of EC was found, suggesting that the limiting factor for H flux is cellular H-ion generation.

148

CASTRATION EFFECT ON THE ELECTRIC PROPERTIES OF SMOOTH MUSCLE CELL'S MEMBRANE OF LONGITUDINAL LAYER OF GUINEA-PIG VAS DEFERENS. A.T. Ferreira*, R.P. Markus** and A.J. Lapa**.

*Department of Biophysics and **Department of Pharmacology, Escola Paulista de Medicina, São Paulo, S.P., Brazil.

A partial depolarization of the smooth muscle cells was observed in guinea-pig vas deferens after castration. It was recorded an increase in the amplitude and a delay in the repolarization time of the spontaneous junction potentials of these organs, that suggest changes in the membrane electrical properties of these cells. Since the resting membrane potential depend mainly on K^+ and Na^+ we looked for a relationships between castration and changes in the intracellular concentrations of these ions ($[\text{K}]_i$ and $[\text{Na}]_i$) and/or changes in the membrane permeabilities to Na^+ and K^+ (P_{Na} and P_{K}). Isotonic solutions with constant sum of $\text{NaCl} + \text{KCl}$ have been used to increase the $[\text{K}]_o$ and the resting potentials were recorded through intracellular microelectrodes. The $[\text{K}]_i$ and the $[\text{Na}]_i$ have been estimated from the total ion content, the extracellular space and the dry weight/wet weight ratio. These concentrations did not change with castration or with changes in $[\text{K}]_o$ and $[\text{Na}]_o$. On other hand, the $\text{P}_{\text{Na}}/\text{P}_{\text{K}}$ ratio, obtained from Goldman-Hodgkin-Katz equation, doubles in the castrated animals.

150

ROLE OF THE SODIUM ION ON THE DIPHASIC RESPONSE OF THE SMOOTH MUSCLE TO AGONISTS. V.L.A. Nouailhetas, S.I. Shimuta, A.T. Ferreira, A.C.M. Paiva and T.B. Paiva, Department of Biophysics, Escola Paulista de Medicina, São Paulo, S.P., Brazil.

The phasic/tonic ratio (P/T) of the guinea-pig ileum's responses after a short contact with high doses of acetylcholine (ACh -5.5 μM) or histamine (Hist -2 μM) were 3.0 ± 0.2 and 2.4 ± 0.1 , respectively. A smaller P/T (nearly 1.5) was obtained when: a) near-maximal doses were used; b) after a prolonged contact with high doses; c) after short contact with high doses in the presence of low $[\text{Na}^+]$ (120 mM). The effect of further reduction of $[\text{Na}^+]$ to 80 mM was studied on the isometric responses to those agonists as well as on the membrane potential (sucrose gap). Weak hyperpolarization (3-4 mV) and partial inhibition of the phasic component occurred. After 30 min the membrane was depolarized and the contraction presented a full phasic component and a P/T of 1.6 ± 0.1 for ACh and 1.2 ± 0.1 for Hist. Reduction of $[\text{Na}^+]$ during a short or a prolonged contact with high doses determined contraction or relaxation respectively, but relaxation was always obtained with near-maximal doses. These results indicate that both components are modulated by external Na^+ , the phasic one being potential-dependent. Only high doses seems to trigger a Na^+ -sensitive mechanism which is responsible for the transient high P/T.

Friday 03 August Congress Centre-First Floor Posters 151-156

Posters on Mechanisms of Transport Across Membranes

151

THE MECHANISM FOR THE FUSION OF PHOSPHOLIPID VESICLES TO PLANAR BILAYER MEMBRANES. F.S. Cohen, M.H. Akabas, A. Finkelstein. Rush Medical College, Department of Physiology, Chicago, Illinois, U.S.A.; Albert Einstein College of Medicine, Depts. of Physiology and Neurosciences, Bronx, New York, U.S.A.

In order to experimentally model the biological process of exocytosis, we have been studying the fusion of phospholipid vesicles to planar bilayer membranes. There are two experimentally distinguishable steps in the fusion process. In the first, a very tight and close association between the vesicles and planar membrane is formed. If the vesicular and/or planar membranes contain negatively charged lipids, divalent cations are needed for the formation of this association. Once this association is formed, divalent cations are not needed to maintain the state. Vesicles made from neutral lipids and planar membranes formed from the neutral lipid phosphatidylethanolamine, however, form this tight association in the absence of divalent cations. This association between vesicle and planar membrane is not a point contact but rather is an adhesion of a substantial fraction of the vesicle with the bilayer. In the second step, the actual fusion of vesicular and planar membranes occurs. The driving force for this step is osmotic swelling of those vesicles which are in association with the planar membrane. The molecular rearrangements that occur when two membranes fuse into one are greatly facilitated if the membranes are fluid.

153

ELECTRICAL AND CHEMICAL PROPERTIES OF AN ENZYME MODEL OF $\text{Na}^+/\text{Ca}^{++}$ EXCHANGE

J.M. Kootsey and E.A. Johnson, Department of Physiology, Duke University Medical Center, Durham, NC, USA

An enzyme model of $\text{Na}^+/\text{Ca}^{++}$ exchange was studied in which random binding of three Na^+ and one Ca^{++} are required on opposing sides of a membrane before a conformational change can occur translating the binding sites to the opposite sides of the membrane (a simultaneous mechanism). A similar (return) translocation step is also permitted if all the sites are empty. None of the other states of binding permit such translocating conformational changes. The resulting reaction scheme has 22 reaction steps involving 16 enzyme intermediates. The voltage dependence of the equilibrium constant for the overall reaction required by the 3:1 Na:Ca stoichiometry was obtained by multiplying and dividing, respectively, the forward and backward rate constants of one or the other translocation steps by $\exp(FV/2RT)$. With reasonable values for the membrane density of such enzyme and an upper limit for the rate constants of both translocational steps of 100,000/sec, the behavior of the enzyme is compatible with a wide range of data from different experimental preparations: isolated cardiac sarcolemmal vesicles, squid giant axon, and cardiac muscle. Contrary to expectation, such behavior was obtainable with the same binding constant for Ca^{++} on both sides of the membrane (106/M), similar symmetry also being assumed for the Na^+ binding constant ($\sim 10/\text{M}$). Supported in part by USPHS grants RR-01693 and HL-12157.

155

MECHANISM OF BLOCKING EFFECT OF LOCAL ANAESTHETICS IN EXCITABLE MEMBRANES

J. Tigyí, K. Hildeg and T. Lakatos, Biophysical Institute of Medical University, Pécs, Hungary

Previous studies of our laboratory [1] have shown that spin-labelled local anaesthetics (LA) like procaine, procaine amide etc. are useful tools for investigating the mechanism of the nerve conduction. Other studies [2] used N ethylmaleimide cleared up some details of the role of membrane proteins. Present work aimed to explore the changes of the lipid phase of membrane under the effect of LAs.

According to the general concept the LAs eliminate the ability of axons to generate and conduct action potentials by blocking the sodium current. There are three main possibilities concerning the mechanism of blocking processes:

1. LAs are bound to specific receptors /channel proteins/
2. LAs are localised on the membrane surface.
3. LA molecules are inserted into the lipid phase. Experiments were performed on non myelinated nerve of crayfish with spin-labelled LA and spin-labelled stearic acids to find out which of the possibilities mentioned above can be considered as the most probable one. As it is shown by ESR spectra, no strong immobilization of the spin-labelled LA occurs, as it may be expected in the case of a specific receptor. On the other hand experiments with sodium ascorbate reduction excluded the possibility Nr. 2. i.e. the LA molecules do not seem to lie on the membrane surface. Very likely, the LA molecules are immersed into the lipid region of the membrane.

1. Tigyí J., Lakatos T.: Studia Biophys. 81 /1980/ 15-26
2. Gróf P., Belágyi J.: Biochem. Biophys. Acta 734/1983/319-328

152

LONG RANGE ELECTRONIC PHASE COHERENCE IN THE BACTERIORHODOPSIN MACROMOLECULE AND ITS POSSIBLE OCCURRENCE IN BIOLOGICAL SYSTEMS.

A.D. Clark, L.J. Dunne & E.J. Brandas, Physics Department, Guy's Hospital Medical School, London Bridge, London, UK.

We have recently suggested that the protein from the purple membrane of *Halobacterium Halobium*, Bacteriorhodopsin may exhibit long range phase coherence (1). The protein contains a retinal chromophore, which is believed to have at least four tryptophan residues in close proximity so this shows a marked similarity to the hypothetical structure for a molecular superconductor proposed by Little in 1964 (2). This treatment enables us to explain many of the surprising experimental results obtained with bacteriorhodopsin such as a photocycle ratio of two protons pumped per light induced photocycle (3) and also a greatly enhanced static electrical polarisability (4).

1. L.J. Dunne, A.D. Clark, & E.J. Brandas, Submitted to Accounts of Chemical Research.
2. W.A. Little, Phys. Rev. 134, A1416 (1964).
3. L.J. Dunne, A.D. Clark & E.J. Brandas, Chem. Phys. Lett. 97, 573 (1983).
4. L.J. Dunne, E.J. Brandas & A.D. Clark, Chem. Phys. Lett. 104, 431 (1984).

154

TIME COURSE OF MINERALOCORTICOID EFFECTS ON THE RENAL CORTICAL COLLECTING DUCT Na-K-ATPase. R.G. O'Neill and R.A. Hayhurst, Dept. of Physiology & Cell Biology, Univ. of Texas Medical School, Houston, Texas, USA 77030

Rabbits with intact adrenals were maintained on either control diet (normal Na and K content) or high Na, low K diet (to suppress endogenous plasma aldosterone levels) and then treated daily with the mineralocorticoid deoxycorticosterone acetate (DOCA, 2 mg/kg/day, i.m.) for 0 (no DOCA) to 4 days. Segments of CCD were isolated from the kidney, and the Na-K-ATPase activity estimated as the ouabain-sensitive rate of ATP hydrolysis at 37°C using a microassay in which the appearance of ADP was enzymatically coupled to a highly fluorescent form of ADP for quantitation. DOCA treatment caused a significant increase (*, P<0.05) in Na-K-ATPase activity after 2 or more days of treatment.

	DOCA Treatment, days			
	0 (none)	1	2	3-4
Control (n)	13(9)	23(5)	30(5)*	35(4)*
High Na, low K (n)	17(6)	14(6)	—	30(10)*

This is likely a mineralocorticoid action since treatment with dexamethasone (0.5 mg/kg day, i.m.) alone for 3-4 days had no effect. Further, DOCA treatment for 1 day has been shown (Sanson and O'Neill, unpub. obs.) to cause a doubling in the Na conductance of the luminal cell membrane. Hence, it is concluded that elevation of mineralocorticoid levels causes an increase in Na-K-ATPase activity after a latent period of 1 day, but that this is most likely secondary to an increase in Na entry at the luminal membrane.

156

WATER PERMEABILITY OF DIMYRISTOYL PHOSPHATIDYLCHOLINE SURFACE BILAYERS. L. Ginsberg and N.L. Gershfeld, NIADDK, NIH, Bethesda, MD, USA, 20205.

Dispersions of dimyristoyl phosphatidylcholine (DMPC) in water at 29° have been reported to form a film at the equilibrium air/water surface with a molecular density equal to that of a lipid bilayer (N.L. Gershfeld and K. Tajima, Nature 279, 708 (1979)). At temperatures above and below 29° the surface density, as measured by radio-tracers, falls continuously with temperature to monolayer values. In the present study, the water permeability of the DMPC surface films has been obtained by measuring the rate of water evaporation from DMPC dispersions at temperatures where the surface concentration exceeds that of a monolayer. Evaporation rates did not deviate from those for the lipid-free systems throughout the entire temperature range examined (20-35), except at 29° where a barrier to evaporation was detected. At this temperature the rate of evaporation from DMPC dispersions decreases approximately 50% from that for pure water. Our results are consistent with a model in which a bilayer coexists with liquid expanded monolayer over the entire temperature interval where surface concentrations exceed monolayer densities. The narrow temperature interval of evaporation resistance at 29.0.1° where surface concentration correlates with bilayer density, is the result of a large specific resistance ratio of 10⁵ for bilayer to monolayer.

*Present address: The Middlesex Hospital Medical School, London, England.

Friday 03 August Congress Centre-First Floor Posters 157-162

Posters on Mechanisms of Transport Across Membranes

157

VESICLE FORMATION BY SALT-OUT METHOD AND ITS APPLICATION TO THE RECONSTITUTION OF SARCOPLASMIC RETICULUM T. Taguchi and M. Kasai, Dept. Biophysical Engineering, Faculty of Engineering Science, Osaka Univ. Toyonaka, Osaka, Japan

It was found that the addition of salt such as KCl into a solution containing lipid (asolcerin) and a non-ionic surfactant, Triton X-114, led to the formation of closed membrane vesicles. The vesicles were separated from Triton X-114 by hydrophobic interaction chromatography. Electron microscopy revealed that the mean diameter of the vesicles was $110 \text{ nm} \pm 69 \text{ nm(SD)}$. Measurement of osmotic volume change showed that the permeability of the vesicle was very low to salts, sugar and amphoteric ion, but very high to glycerol, ethyleneglycol and water. It was possible to form vesicles by salting-out with another non-ionic surfactant, Triton X-100 under a certain condition. Vesicle formation by this method is very useful for reconstitution of transport systems in biological membrane because of its advantages: completion within a short time; high yield; and the possibility of utilizing samples in non-ionic surfactant solution. When we applied the method to the reconstitution of sarcoplasmic reticulum, Ca^{2+} -ATPase was incorporated into the reconstituted vesicles and was enzymatically active in the membrane.

159

SPECTROSCOPIC STUDIES OF INTERACTION OF AN AIB PEPTIDE EXTRACTED FROM TRICHODERMA SP WITH MODEL MEMBRANES. T. Le Doan, S. Rebuffat, M. El Hajji and B. Bodo, Laboratoire de Biophysique et Laboratoire de Chimie Appliquée, Muséum National d'Histoire Naturelle, 61 Rue Buffon, F-75005 Paris.

The main component of a family of antibiotic peptides has been extracted from the fungus *Trichoderma* SP. It presents antifungal activity and acts as inhibitor of vegetal transpiration (measured on barley shoots) suggesting it can act on biological membrane permeability.

The amino acid composition shows that the molecule contains 75% of non-polar residues with a predominance of α -amino isobutyric acid (Aib) residues. The N-terminal residue (Aib) is acetylated and the C-terminal group is the amino alcohol tryptophanol. This unique aromatic residue was used as intrinsic fluorescence marker for the study of the interaction of the peptide with phosphatidylcholine vesicles. In the presence of vesicles, the tryptophan fluorescence maximum was shifted to shorter wavelengths and the fluorescence quantum yield increased. These emission changes are related to the binding of the peptide to the vesicles, the chromophore being in a more hydrophobic environment. At the ratio of phospholipid/peptide = 150, the peptide molecules are considered to exist only at the bound state. Polarization and fluorescence quenching by I^- measurements confirm the embedment in the bilayer rather than a surface binding of the peptide.

161

Effect of Substrate Composition on Phospholipase A₂ Reaction. J.B. Massey, H.S. She, A.M. Gotto, Jr., and H.J. Pownall. Baylor College of Medicine, Houston, TX.

The factors that regulate the activity of *C. adamanteus*, bee, melaleuca, and porcine pancreas phospholipase A₂ have been studied. The substrates contained 1,2-dimyristoyl-sn-glycero-3-phosphocholine (DMPC) or 1,2-O-tetradecyl-sn-glycero-3-phosphocholine (DNPC-ether). The physical properties of reassembled lipoproteins (R-HDL) and single bilayer vesicles are unchanged when DMPC is replaced by DNPC-ether. R-HDL composed of DMPC-ether and apoprotein A-I or A-II and vesicles were used to determine the maximum hydrolysis rate (V_{max}), the kinetic binding constant (K_M) and the dissociation constant (K_D). A hydrolyzable radiolabeled or fluorescent phosphatidylcholine (PC) (2 mole %) was included to determine K_M and V_{max} under these conditions the reaction goes to completion, is first order, exhibits substrate saturation, and produces no change in the macromolecular structure of the substrate. K_D was determined by equilibrium gel filtration. V_{max} values for hydrolysis of R-HDL by the enzymes from bee and *C. adamanteus* were 2 to 3 orders of magnitude greater than for vesicles. Substitution of R-HDL for vesicles decreased K_M and K_D by an order of magnitude. Decreasing the acyl chain length and increasing the unsaturation of the hydrolyzable PC within the same lipid microenvironment gave increased enzyme activity that was independent of macromolecular structure. These results demonstrate that the microenvironment and macromolecular arrangement of phospholipids is a determinant in the kinetics and thermodynamics of lipolysis.

158

ARSENATE REPLACES PHOSPHATE AND SUPPORTS SODIUM PUMP-MEDIATED K:K EXCHANGE IN HUMAN RED BLOOD CELLS

L.J. Kenney and J.H. Kaplan, Department of Physiology, University of Pennsylvania, Philadelphia, Pa, USA.

When red cell ghosts are prepared in the absence of intracellular Na, Na:K exchange cannot take place and a ouabain-sensitive K:K exchange occurs via the sodium pump. This exchange of intracellular for extracellular K has a 1:1 stoichiometry and requires P_i and a nucleotide such as ADP. We find that arsenate will support K:K exchange in the presence of 2 mM ADP and in the absence of phosphate. The curve relating arsenate concentration to ouabain-sensitive K:K exchange shows biphasic activation (like P_i) with stimulation in the 0-1 mM range and inhibition at higher arsenate concentrations. Arsenate activates the exchange with a higher apparent affinity than P_i and inhibits to a greater extent than P_i . The basis of the activation probably occurs via arsenylation of the sodium pump protein. While increased external K (Rb) stimulates the rate of K:K exchange, the activation by arsenate remains biphasic, in contrast to previous reports where P_i inhibition is relieved by high external K. (LJK is supported by Training Grant 5T-32-GM07229, JHK is supported by NIH HL 30315 and is a recipient of RCDA K04-HL01092).

160

PERMEATION OF SOLUTES THROUGH PURE PHOSPHOLIPID B LAYERS J.S. Brashall, Department of Microbiology & Immunology, University of California, Los Angeles, California, U.S.A.

Using fluorescent anionic dyes such as carboxyfluorescein as model solutes it is shown that the forces allowing such solutes to be retained within sealed lipid vesicles, against a large concentration gradient, can be primarily electrostatic in nature. At temperatures distant from that of the ordered-fluid lipid phase transition a small number of the anionic dye molecules trapped within the lipid vesicles are capable of traversing the lipid bilayer and establishing an electrical diffusion potential across the membrane. Further solute movement can then only occur with the concomitant permeation of ions which restore electrical balance. A significant flux of dye can be triggered by a) increasing the permeability of the membrane to ions (for example by the addition of ionophores such as gramicidin, or by allowing the lipid to approach a phase transition) b) adding lipophilic counterions such as tetraphenylborate or dimethylophenol to the system. Because the permeation of the dye become tightly coupled to the movement of the counterions, the dye can serve as a convenient reporter of ionic flux across the bilayer. This experimental approach has been used to study the relationship between acyl chain length and the relative permeation rates of several ions through bilayers composed from an homologous series of lecithins. The studies have been conducted over a wide range of temperatures, and reveal striking differences in the behavior of saturated and unsaturated phospholipids.

162

PROPERTIES OF BACTERIAL LIPOPEPTIDES. EFFECTS ON THE PERMEABILITY OF BLM. CONFORMATIONS IN SOLUTION.

R. Naget-Dana, P. Marion, M. Genest and M. Ptak, Centre de Biophysique Moléculaire (CNRS) et Université d'Orléans, 45045 Orléans cedex, France.
F. Peypoux and G. Michel, Laboratoire de Biochimie Microbienne, Université Lyon 1, 69622 Villeurbanne cedex, France.

Several lipopeptides (Iturins and Bacillomycins) extracted from different strains of *Enterobacter* contain a cyclic heptapeptide and a lateral aliphatic chain. They have antifungal properties and strongly interact with membranes. They modify the permeability of BLM by forming pores. In a first step, Iturin A was specially studied by different methods. An analysis of the lifetime and amplitude and of the time evolution of the channels was achieved for BLM of egg lecithin + PL. The presence of cholesterol inhibits the formation of discrete conducting structures and induces a general increase of the conductance. A conformational analysis of Iturin A was undertaken by using 2D-NMR and energy calculations. Most of the relevant NMR parameters were collected which allow to elaborate a model of conformation for the minimization of intramolecular energy. A rather rigid structure was thus obtained in which hydrogen bonds stabilize the peptide cycle and the polar side chains. The aliphatic and P- side chains could play a special role in interacting with the environment. A preliminary discussion of possible structure-activity relationship is presented on the basis of data obtained in these different approaches.

Friday 03 August Congress Centre-First Floor Posters 163-168

Posters on Mechanisms of Transport Across Membranes

163

DATA CONCERNING THE ELECTRONIC, PROTONIC AND MOLECULAR MECHANISMS OF THE INTERACTIONS BETWEEN SOME LOCAL ANAESTHETICS AND EXCITABLE MEMBRANES

Micra Tripa, V. M. Sahini^{*} and V. Vasilescu
Department of Biophysics, Faculty of Medicine, Bucharest, ROMANIA
^{*} Physical Chemistry Laboratory, Polytechnic Institute, Bucharest, ROMANIA

The informations about the nature and structure of the ionic channels in neuro-membranes can be obtained by studying the interaction between the local anaesthetic substances and excitable membranes. We have correlated our previous studies concerning some molecular characteristics - aromatic nitrogen charge and the distance between the aromatic nitrogen and the secondary nitrogen - of the local anaesthetics Procaine, Lidocaine, Tetracaine and Benzocaine with the modifications induced by them on the action potential of the peripheral nerve, on the nerve ATP pool and on some enzymes involved in nerve energetic processes. The obtained data confirm the existence of an excitation-energy coupling, which is unspecific, although it exists between some structures highly specialized. The understanding of the coupling mechanisms offers also a biophysical base which could elucidate the molecular mechanisms of the local anaesthesia.

165

CONFORMATION AND STABILITY OF THE ANION TRANSPORT PROTEIN OF HUMAN ERYTHROCYTE MEMBRANES

R.A.F. Reithmeier, K. Oikawa and D.M. Lieberman, Dept. of Biochemistry, Univ. of Alberta, Edmonton, Alberta, Canada.

The conformation and stability of Band 3, the anion transport protein of human erythrocyte membranes, and its constituent proteolytic subfragments was studied by circular dichroism. Band 3, in the membrane or after solubilization by non-ionic detergents, had an α -helical content of 40%. Loss of α -helical content by denaturation with guanidine hydrochloride occurred in two phases. The carboxyl-terminal, membrane-associated domain ($M_r=55,000$) of Band 3 contained 55% α -helix and was resistant to denaturation. The amino-terminal cytoplasmic domain ($M_r=41,000$) contained 30% α -helix and was sensitive to guanidine hydrochloride. Irreversible heat denaturation of Band 3 occurred with half-maximal change in $\theta_{222.5}$ at 48°. Covalent attachment of the anion transport inhibitor, 4,4'-diisothiocyanostilbene-2,2'-disulfonate to Band 3 had little effect on the circular dichroism spectra of Band 3 or the membrane-associated domain but resulted in stabilization of Band 3 to heat denaturation (half-maximal change in $\theta_{222.5}$ at 61°). Circular dichroism studies of membranes, digested with proteolytic enzymes and stripped of extrinsic fragments, revealed that the portions of red cell membrane proteins that are embedded in the lipid bilayer contain a high (55-70%) content of α -helix. A model for the organization of Band 3 in the membrane is presented. (Supported by the Medical Research Council of Canada and Alberta Heritage Foundation for Medical Research)

167

ACETYLCHOLINE RECEPTOR: A VOLTAGE-DEPENDENT REGULATORY SITE
K. Takeyasu, S. Shiono and G.P. Hess, Biochemistry, 270 Clark Hall, Cornell University, Ithaca N.Y. 14853 U.S.A.

Acetylcholine (ACh) receptor-controlled ion flux in membrane vesicles prepared from the electroplex of *Torpedo californica* was investigated under voltage-clamped conditions using a quench-flow technique with a time resolution of 5 ms. Two rate coefficients were measured over a 1000-fold concentration range: J_{ACh} , the rate coefficient for ion translocation by the active state of the receptor in the absence of inactivation (desensitization); α , the rate coefficient for the fast inactivation of the receptor by ACh. (1) At low ACh concentrations the value of J_{ACh} and α increased with increasing concentrations. (2) J_{ACh} decreased at high ACh concentrations. In contrast α did not show a decrease. (3) When the transmembrane potential of the vesicle membrane is changed to more negative values the value of K_d (the dissociation constant for binding of ACh to the regulatory site) decreases drastically while K_i (the dissociation constant for binding of ACh to the receptor before inactivation) remains constant. (4) A local anesthetic, procaine, did not affect the binding of ACh to the regulatory site. These results can be explained by a simple model where the functioning of the receptor is regulated by binding of ACh to a voltage-dependent regulatory site, a site that is distinct from the sites responsible for receptor activation and inactivation and from the local anesthetic site. The biological significance of the voltage-dependent regulatory site of the receptor may be that it allows the receptor-controlled transmission of signals to be variable and adjustable by changes in the resting potential.

164 ORAL PRESENTATION

PATCH-CLAMP INVESTIGATIONS IN RENAL PROXIMAL TUBULES

H. Gogelein and R. Greger, Max-Planck-Institut für Biophysik Kennedyallee 70, 6000 Frankfurt/Main 70, FRG

A method is described which enables single ionic channel recordings from proximal tubules of rabbit kidney. Isolated tubule segments were cannulated on one side and the tubule was perfused. The other end of the tubule was freely accessible. After treatment with 0.5 g/l collagenase for 5 min at room temperature, the open end was torn with a glass pipette as to expose clean lateral surfaces. With this method lateral cell membranes (BLM) can be approached by a patch electrode. Furthermore it was possible to insert the electrode through the open end into the tubule lumen and to bring it into contact with the brush border membrane (BBM). Both with ELM and with BBM seals of > 10 G Ω were possible. At the BLM a K^+ selective channel was observed in cell excised patches. The channel appeared in bursts and showed fast transitions (< 10 ms) to the closed state. The single channel conductance was approximately 40 pS. With KCl-Ringers solution on both sides, the channel could be blocked by 20 mM TEA⁺ in the bathing medium. In addition to this K^+ selective channel, another channel of as yet unidentified selectivity was observed in BLM. This channel has a conductance of approximately 20 pS and, opposite to the K^+ channel, does not show flickering. The kinetics of this channel is voltage dependent. For BBM a K^+ selective channel which could be blocked by 5 mM Barium ions was identified.

166

ANOMALIES IN CHEMIOSMOTIC SOLUTE TRANSPORT: A REDOX REGULATION CAN SOLVE THE DISCREPANCIES

K.J. Hellinger, M.G.L. Elferink, J.M. van Dijk and W.N. Konings, Department of Microbiology, University of Groningen Kerklaan 30, 9751 NN Haren, The Netherlands.

The rate and extent of solute transport in bacteria is not uniquely dependent on the magnitude of the proton motive force, as would be expected on basis of the chemiosmotic hypothesis. In contrast, particularly in phototrophic bacteria like *Rhodospirillum rubrum*, the maximal rate of solute uptake in intact cells at a constant magnitude of the proton motive force, varies at least hundred-fold with the rate of cyclic electron transfer. This is true not only for transport via solute carriers that are endogenously present in this bacterium, but also for transport of lactose via the M-protein from *Escherichia coli* after transfer of this transport system to the phototrophic bacterium via genetic manipulation (1).

Also the rate of linear electron transfer similarly regulates the rate of solute uptake in these two bacteria, both in intact cells and in isolated cytoplasmic membrane vesicles (2). Furthermore, this regulation can also be demonstrated for solute uptake via sodium transport (i.e. thiomethylgalactoside uptake via the melibiose transport system from *E. coli*). We therefore conclude that these deviations from the chemiosmotic hypothesis cannot be explained by local chemiosmotic interactions. Our working hypothesis is that the redox state of a component in the membrane regulates the activity of solute transport systems.

1. Elferink M.G.L. et al. 1983. FEBS Lett. 164: 185-190

168

VITAMIN C AND CANCER

W. Lohmann, H. Sapper, D. Holz, D. Pagel, K. Beinbauer, J. Winzenburg, and P.Z. Tian, Institut für Biophysik der Universität, Leihgesterner Weg 217, D-6300 Giessen, FRG.

Recently we could show that blood and its constituents obtained from patients with an acute lymphatic leukemia exhibit an electron spin resonance signal at $g = 2.005$. This signal could be assigned to the ascorbyl radical. It is formed by the interaction between the anionic ascorbyl entity and Na^+ or K^+ . The radical has a cyclic side-chain structure presumably formed by the hydrogen bond $C(3)-O \cdots HO-C(6)$ (≈ 2.7 kJ). This special structure enables ascorbate to form an electroneutral complex with Na^+ , probably due to a 1:1 stoichiometry. Iso-ascorbate, the biologically less effective C(5)-enantiomer of ascorbate, seems to prefer a complexation with K^+ ions with a side chain ring exhibiting different bond angles as in the case of Na^+ complexation. The corresponding radicals exist in their highest concentration at physiological pH and temperature. They can be reduced by red. glutathione without changing their electroneutral bicyclic structure. These findings which occur concomitantly with changes in the vitamin C concentration in the case of certain types of cancer, suggest vitamin C dependent modifications in the Na^+/K^+ transport across membranes, in the membrane GSH concentration and in the intracellular pH. Detailed investigations are in progress at present.

This work was supported in part by grants from BMFT and the Fonds der Chemical Industry.

^{*} On leave of absence from Academia Sinica, Institute of Biophysics, Peking, China.

Friday 03 August Congress Centre-First Floor Posters 169-174

Posters on Mechanisms of Transport Across Membranes

169

TOWARDS THE 3D-STRUCTURE OF THE INTEGRAL MEMBRANE PROTEIN MATRIX PORIN FROM *E. COLI*.

J.A. Jenkins, R. Karlsson, and R.M. Garavito, Biozentrum, University of Basel, Klingelbergstrasse 70, CH-4056 Basel, Switzerland.

Crystals of matrix porin can be reproducibly grown from mixtures of β -octyl glucoside and octyl polyoxyethylenes ($C_{8}EO_x$, $x = 6-11$) by increasing the concentrations of PEG 2000 and NaCl, without detergent phase separation. The P_4 crystals diffract to 2.8 Å at -15°C. Using synchrotron radiation, we have collected a complete 4 Å dataset at room temperature ($R_{\text{sym}} = 9.6\%$) and a partial (~60%) dataset at -15°C. The 4 Å dataset has allowed us to locate a single 3-fold noncrystallographic axis and an independent 2-fold axis relating the two trimers in the asymmetric unit. The coincidence of the molecular 3-fold axes sets strong constraints on the possible packings. Within a narrow range of detergent concentrations good crystals can be grown by dialysis. Heavy atoms can be dialysed into these crystals. Small intensity differences were observed with 16 mM KAu(CN)₂ and larger changes with 5 mM K₂PtCl₆ and KAuCl₄. We are now analysing a dataset from crystals soaked in the platinum complex.

171

KINETICS OF OSMOTIC WATER TRANSPORT IN SICKLE CELLS. G.T. Craescu* and R. Cassoly*. *Unité INSERM U-91, H. Mondor, Créteil, France and *Inst. Biologie Physico-chimique, Paris, France.

The results of stopped-flow studies on kinetics of osmotic water transport in sickle cells as compared to normal erythrocytes are presented. The inward osmotic water permeability is similar in sickle cells and normal red blood cells. In contrast, outward water flux is significantly (~38%) decreased in sickle cells. Deoxygenation does not modify the water influx in either types of cells but considerably accelerates the rate of water efflux in sickle cells. No significant variation of water transport kinetics was observed in density separated cell fractions of either types. The results may be explained by differences in hemoglobin membrane interactions and not by the direct consequence of changes in the intrinsic properties of the membrane.

173

RAPID RELEASE OF OCCLUDED ⁴²K AND ⁸⁶Rb FROM THE NA PUMP. B. Forbush III, Yale Univ. Sch. Med., New Haven, CT, USA.

The rate of release of tightly bound ⁴²K (or ⁸⁶Rb) from Na,K-ATPase was examined with 15 ms time resolution using a rapid filtration apparatus (Forbush, *Biochem. J.*, 155, 76A, 1983). In the presence of 100 mM Na₂ATP, 0.3 mM free Mg²⁺, 25 mM imidazole, pH 7.2 at 20°C, ⁴²K was released from the occluded state with a rate constant of $\sim 46 \text{ s}^{-1}$ and ⁸⁶Rb was released with a rate constant of $\sim 19 \text{ s}^{-1}$. In one experiment the ⁴²K rate constant was 22, 46, 71, and $> 160 \text{ s}^{-1}$ at 15°C, 20°C, 25°C and 37°C respectively. Generally the time courses are best fit by a double exponential (with $k_1/k_2 \sim 4$). The release of either cation is stimulated by ATP with a $K_{1/2}$ of 0.4 mM and by ADP with a $K_{1/2}$ of $\sim 1.5 \text{ mM}$. In the presence of ATP, free Mg²⁺ is stimulatory below 300 μM , presumably by formation of MgATP and it is inhibitory at higher concentrations; with ADP, Mg²⁺ is only inhibitory (75% inhibition at 3 mM free Mg²⁺). In the presence of Na Mg²⁺, the rate of de-occlusion is $\sim 6 \text{ s}^{-1}$ for either ⁴²K or ⁸⁶Rb; however when the Mg²⁺ dissociation medium contains K⁺ ($K_{1/2} \sim 0.1 \text{ mM}$) or Rb⁺ but not Na⁺ the time course is very markedly biphasic, with a second phase rate constant $\sim 1 \text{ s}^{-1}$. Stabilization by KP_i is in agreement with recent observations of I.M. Glynn and D.E. Richards (*J. Physiol.*, in press). By including ⁸⁶Rb in the dissociation medium for $< 1 \text{ s}$, following occlusion of unlabeled Rb, it is found that the cations responsible for stabilization are themselves occluded. The results are quantitatively consistent with the occluded state as an intermediate in the normal cycle of the Na⁺ pump, and with non-identity of multiple K⁺ sites.

170

EFFECTS OF L-ASPARTATE ON CELLULAR Na⁺, K⁺ AND Cl⁻ ACTIVITIES IN RETZIUS NERVE CELLS OF THE LEECH

D. Čemerikić, V. Nedeljkov and B. Beleslin, Dept. of Path. Physiology, Med. Faculty, Beograd, Yugoslavia.

Effects of 10^{-2} M aspartate were studied on cellular activities of potassium (K^+), sodium (Na^+), and chloride (Cl^-) in Retzius nerve cell of horse leech (*Haemopsis sanguisuga*). Cellular ion activities were determined with selective micro-electrodes using liquid ion exchangers for K^+ , Na^+ and Cl^- . At resting membrane potential of $-42.8 \pm 1.89 \text{ mV}$, (K^+)_i was $83 \pm 4.9 \text{ mM}$, (Na^+)_i was $7 \pm 1.0 \text{ mM}$ and (Cl^-)_i was $7.8 \pm 0.63 \text{ mM}$. Application of L-aspartate (10^{-2} M) for 3 minutes depolarized membrane potential by $15.5 \pm 1.3 \text{ mV}$. After recovery membrane potential transiently hyperpolarized by $-6.2 \pm 0.77 \text{ mV}$. Exposure to L-aspartate decreased (K^+)_i by $10.6 \pm 2.04 \text{ mM}$, increased (Na^+)_i by $9.12 \pm 2.33 \text{ mM}$ and increased (Cl^-)_i by $20.6 \pm 1.6 \text{ mM}$ with complete recovery. In Na-free Ringer (Tris-Cl substitution) depolarizing effect of L-aspartate on membrane potential was significantly reduced to $5 \pm 1.2 \text{ mV}$, without change in (Na^+)_i which decreased in Tris-Ringer to $1.96 \pm 0.51 \text{ mM}$. The data suggest that L-aspartate increases membrane permeability to Na^+ with subsequent influx of Na^+ into the cell, while K^+ and Cl^- seems to be passively redistributed.

(Supported by the Research Council of Serbia)

172

DIPHTHERIA TOXIN TRANSPORT ACROSS MEMBRANES: EVIDENCE FOR THE ROLE OF A PORE.

R.L. Kagan, P. Boquet, and M. Moynihan, Dept. of Psychiatry, Univ. of Calif. at Los Angeles, USA, Dept. de Microbiologie, Institut Pasteur, Paris, France, and Dept. of Plant Breeding, Cornell Univ. Ithaca, N.Y., USA.

The cytotoxic action of diphtheria toxin (MW 62,000) requires that its enzymatic A fragment (MW 22,000) traverse a membrane in order to inactivate its biologic target, elongation factor 2. It has been suggested previously that a large aqueous pore formed by the B45 (MW 23,000) portion of diphtheria toxin is involved in the transport of fragment A across the membrane. We show that when diphtheria toxin or CRM 45 (a mutant toxin, MW 45,000) consisting of a normal A fragment plus B45) is exposed to lipid vesicles under conditions which permit pore formation, a significant fraction (10-30%) of the fragment A enzymatic activity becomes protected from the action of extravesicular protease. This protection occurs only in the presence of vesicles made with a lipid composition that allows pore formation. Fragment A alone is not protected. The results suggest that the B45 pore can mediate the transport of fragment A across a lipid bilayer membrane.

174

KINETICS OF THE ELECTROGENIC PROTON PUMP OF NEUROSPORA

D. Sanders and C.L. Slayman, Department of Physiology, Yale University School of Medicine, New Haven, CT, USA

The steady-state current-voltage (I-V) relation of the *Neurospora* plasma membrane can be dissected with a reaction kinetic model to reveal the activity of the primary electrogenic proton pump. Pump current was found to be considerably more sensitive to lowering of intracellular pH than to equivalent changes in extracellular pH, even though the shift in pump reversal potential in each case agrees closely with the theoretical value of 59 mV/pH unit. The contrasting kinetic effects of extra- and intracellular pH can be accommodated by a single 4-state carrier model in which $[H^+]_o$, $[H^+]_i$, and membrane potential all act on different, discrete reactions. The reaction constants derived from fitting the model to the I-V data yield notably low apparent pK 's for H^+ binding: 2.9 and 5.4 for the external and internal sites, respectively. The following testable predictions also emerge from the model. (1) Alkaline shifts of extracellular pH from the control value of 5.8 should have no discernable effect on the membrane I-V relation between -300 and 0 mV. (2) Raising intracellular pH should result in a decrease in pump short circuit current in approximate proportion to the change in $[H^+]_i$. Both predictions were verified experimentally. A third prediction concerning the pH sensitivity of *in vitro* pump activity (as an ATPase) is in accord with experimental data above pH 7 (where activity falls as a function of increasing pH) but not below pH 7 (where the model predicts a more acid pH optimum than is found). The latter discrepancy could be due to acid inactivation of isolated enzyme.

Friday 03 August Congress Centre-First Floor Posters 175-180

Posters on Mechanisms of Transport Across Membranes

175

APICAL MEMBRANE POTASSIUM PERMEABILITY IN SURFACE CELLS OF RABBIT DESCENDING COLON. N.K. Wills and W. Clauss. Dept. of Physiology, Yale Univ. School of Medicine, New Haven, Ct. 06510, U.S.A.

The rabbit descending colon possesses two oppositely directed active K^+ transport systems: an absorptive system and a secretory one (Wills and Biagi, J. Memb. Biol. 64:195). The present study investigated the possible participation of surface cells in active K^+ transport by assessing the K^+ permeability of these cells using conventional and K^+ -sensitive intracellular microelectrodes. To determine whether K^+ uptake can occur across the apical membrane, cells were initially depleted of K^+ by bathing the epithelium with K^+ -free solutions containing $10^{-4}M$ ouabain. Under these conditions intracellular potassium activity (a_iK) fell to less than 5 ± 1.7 mM. After restoration of K^+ to the mucosal bath, a_iK increased to 17 ± 2.1 mM ($n=6$), a value larger than predicted by passive distribution. Alternatively, a mucosal solution which contained 143 mM K^+ and no Na^+ , led to an almost complete recovery of the basolateral membrane potential (-45 ± 2.6 mV) within 20 minutes, indicating restoration of intracellular K^+ levels. We conclude that surface epithelial cells are permeable to K^+ and possess an active uptake transport mechanism for this ion in their apical membranes. Consequently, surface cells may play an important role in the mediation of active K^+ transport across the colon.

177

LIPID DISTRIBUTION IN SPIN LABELED SR AS DETERMINED BY PARAMAGNETIC BROADENING AGENTS. C. Coan, Physiology Dept., U. of the Pacific Dental School, San Francisco, CA. U.S.A.

The distribution of a stearic acid spin probe between the inner and outer leaflets of the SR bilayer is determined by the accessibility of the probe to Ni^{2+} -EDTA, a spin broadening agent. The spin probe used contains the spin moiety on the 4th carbon from the carbonyl group, and is known to incorporate into SR with the spin moiety at the membrane-solvent interfaces. Ni^{2+} -EDTA does not penetrate SR vesicles, and thus the fraction of spin probes exposed on the exterior interface can be determined directly by titration. We find this fraction to be 35%. On the other hand, when Mg^{2+} is allowed to freely enter the vesicles by use of the ionophore X-537A, all spin probe signal is reduced, indicating that all probes are on either the inner or the outer interface. Controls indicate that the probe is evenly distributed among the fluid lipids in the bilayer, suggesting a 35% outer to 65% inner asymmetry. This is in accordance with observed ATPase asymmetry favoring location of the enzyme on the vesicular exterior.

EGTA and Ca^{2+} do not compete with EDTA for Ni^{2+} and thus we have been able to probe the effect of ligand binding to the ATPase. We find a 5% increase in the protected fraction of spin probe on enzyme phosphorylation with P_i , indicating a change in the macromolecular conformation which affects the lipid phase at this step in the enzymatic cycle.

179

GASTRIC ELECTROGENIC TRANSPORT SYSTEMS AND THE PROTON PUMP. M. S. Rehm, G. Carrasquer, and M. Schwartz, Depts of Medicine and Physics, Univ. of Louisville, Louisville, KY, USA

Studies on the H-K ATPase in vesicles indicate that the H pump is electroneutral while studies on intact tissues (e.g., the in vitro frog mucosa) indicate that it is electrogenic (EG). Inhibition of H secretion usually results in an increase in R (resistance) and PD which supports EG concept. Pertinent to interpretation of ΔR are 1) change in area of the lumen-facing membrane (LFM) per se gives no change in R and 2) pathways parallel to the acid secreting cells (ASC) have a high R (e.g., 2000 ohm cm^2) while the R via the ASC is low. Ba on the serosal side does not change H rate but increases R (e.g., 100 to 800 ohm cm^2) by blocking the K pathway of serosal membrane (SM). Inhibition of H secretion by SCN or omeprazole in presence of Ba decreases R (e.g., 800 to 300 ohm cm^2). During secretion, the R of LFM < 100 ohm cm^2 , hence, above decrease in R (in Ba) is due to the decrease in R of SM. Prominent in the ΔR is a decrease in R of the EG NaCl symport in SM. In absence of Ba (normal K conductance of SM) a small decrease in R of SM is expected. Hence, inhibition of acid secretion produces an increase in R of LFM. As predicted by the EG theory the PD is inverted in Cl-free media (serosal becomes negative) and inhibition of H rate in both Cl and Cl-free media increases PD. Others use a model with a K diffusion potential from cell to lumen to account for both the inverted PD and change in PD with inhibition of H secretion. With high K on the lumen side (106 mM) inhibition gives typical ΔPD thereby negating the above model. NSF support.

176

HYDROLYSIS OF EPITHELIAL Na^+ CHANNELS BY AN ENDOGENOUS URINARY TRACT ENZYME. S.A. Lewis, W.P. Alles. Dept. of Physiol. Yale Med. Sch. New Haven, CT 06510.

During an expansion/contraction cycle of the rabbit urinary bladder, vesicles are moved into and out of the apical membrane to accommodate changes in urine volume. Na^+ channel density is greater in the vesicles than the apical membrane, indicating a loss of channels once vesicles have fused into the apical membrane. Such a loss could be by aging or enzymatic hydrolysis. Mammalian urine (as well as amphibian and reptilian urine), is known to contain urokinase, a proteolytic enzyme secreted by distal segments of the kidney. Addition of human urokinase to the mucosal solution of the bladder resulted, over a 2 hour period, in a 63% reduction in amiloride sensitive current. When amiloride was in the mucosal solution, urokinase caused only an 11% reduction in amiloride sensitive current indicating amiloride protects the channel. Urokinase has multiple sites of action which results in channels that are: 1) amiloride sensitive but poorly selective, 2) loss of selectivity and amiloride binding, and 3) as in 1) but unstable in the membrane. Aldosterone stimulates Na^+ transport by activation of quiescent channels in the apical membrane. These quiescent channels seem to be susceptible to urokinase hydrolysis. Such endogenous enzymes might be another factor which regulates ion transport across epithelia.

178

THERMODYNAMIC PROPERTIES AND MOLECULAR STRUCTURES OF TRIPHOSPHOINOSITIDE AND ITS ASSEMBLY

Y. Nakata, Y. Takano, S. Yabuki, T. Takizawa and K. Hayashi, Faculty of General Studies, Gunma University, Maebashi, Gunma, Japan.

In order to clarify the molecular basis of nerve excitation, the thermodynamic properties and molecular structures of Triphosphoinositide (TPI) and its assembly were investigated by three methods. (1) The conformation of the head group of a TPI molecule was studied by semi-empirical energy calculation. It is predicted that a stable conformation of the head group looks very similar to the structure of Glycerylphosphorylethanolamine (GPE) found in its crystalline state. (2) The molecular organization of TPI/water system was studied by using X-ray diffraction method. The repeat distance of the lamellar structure increases from 60 to 120 Å with the change of water content from 0 to 40%. In the presence of Ca^{2+} , the repeat distance remains almost 50 Å independent of water content. (3) The interaction between TPI molecules and Ca^{2+} ions were also studied by calorimetric method. The mixing enthalpy per mole of TPI is always positive at any concentration of $CaCl_2$. This result indicates that water molecules penetrate not only between lamellae of TPI molecules but also into their hydrophobic interiors. It is suggested that TPI molecules may play a role of an ionic channel in excitable membranes when Ca^{2+} ions are released.

180

LIGHT SCATTERING CHANGES DURING THE PHOTOCYCLE OF BACTERIORHODOPSIN

J. Czégé, Institute of Biophysics, Biological Research Center, Hungarian Academy of Sciences, Szeged, Hungary

Spectroscopic measurements on purple membrane suspension are disturbed by the light scattering of the particles. Systematic study of the scattered light leads to the result that the scattering changes during the photocycle, and this change depends on the flash polarization, pH, and the solvent viscosity. A theoretical model is given to explain the experimental data. The model asserts that the purple membranes are bent and, during the photocycle, the degree of bending varies which is caused by the conformational change of the bacteriorhodopsin molecules.

Friday 03 August Congress Centre-First Floor Posters 181-186

Posters on Mechanisms of Transport Across Membranes

181

CONDUCTOMETRIC MEASUREMENTS OF ION SHIFTS DURING SUGAR TRANSPORT IN YEAST

A. Kotyk, Institute of Microbiology, Czechoslovak Academy of Sciences, 142 20 Prague, Czechoslovakia

Yeast suspension conductivity was measured at 6.0 Hz when the cells do not contribute to the measured values. Hydrogen ion movement into cells in symport with organic nutrient molecules could be demonstrated more convincingly than by following pH changes (greater sensitivity even at low pH, virtually no dead time of the measuring device). In the yeast *Rhodotorula glutinis* uptake of nonmetabolizable monosaccharides was accompanied by a minute alkalinization of the medium but by a pronounced relative decrease in conductivity although it was clear that H^+ ions symported with the sugar were not accompanied by chloride or other anions to maintain electroneutrality but rather exchanged for intracellular cations, especially K^+ . In baker's yeast *Saccharomyces cerevisiae* no changes in either pH or conductivity were observed on adding monosaccharides (D-xylose, D-arabinose, D-galactose), in keeping with their being transported by a mediated diffusion system not involving any H^+ or other ion shifts. Addition of metabolizable monosaccharides (D-glucose, D-fructose) caused a transient increase in conductivity (50 s at 25 °C), followed by a pronounced drop (2 - 4 min) and finally by a prolonged increase, lasting for 1 - 3 h, depending on cell and sugar concentration. Only this last part was related to an increase in H^+ concentration, the pronounced drop being apparently due to a massive inflow of K^+ (and Cl^-) from the medium into cells.

183

BINDING OF PHORBOL ESTERS TO HUMAN BLOOD CELLS

S. Pečar, M. Nemec, M. Schara and E. Hecker^{*}
J. Stefan Inst., E. Kardelj University of Ljubljana, Yugoslavia, ^{*}Inst. for Biochemistry, DKFZ, Heidelberg, FR Germany.

Phorbol esters are potent irritant and tumor promoters especially 12-O-tetradecanoylphorbol-20-O-acetate (TPA). The fatty acid at position 12 of the phorbol moiety was replaced by spin labeled fatty acids to get spin labeled TPA analogs. They had irritant and tumor promotion activity. These molecules were used to study the binding properties of TPA analogs to human blood cells membranes. The partition coefficient were measured by the method of successive cell washing. Larger values for the partition coefficient - membrane/buffer solution were found for leucocytes as for erythrocytes. Also the anchoring of the phorbol moiety to the membrane surface was separated from the binding related to the hydrophobicity of the fatty acid residues.

185

DIRECT EVIDENCE OF POST-ALBERS MECHANISM IN Na^+ , K^+ DEPENDENT ATP HYDROLYSIS.

K. Taniguchi, K. Suzuki, D. Kai, K. Tomita and S. Iida, Department of Pharmacology, School of Dentistry, Hokkaido University, Sapporo Japan.

The addition of ATP with K^+ in the presence of 0.43 mM Mg^{2+} and 0.64 M Na^+ to pig kidney Na^+ , K^+ -ATPase modified with N-[p-(2-Benzimidazolyl)phenyl]maleimide (J. Biochem. 88, 609, 1980) induced a transient decrease ($t_{1/2}=0.01$ s) in the fluorescence followed by a slow increase ($t_{1/2}=0.07$ s) to give a higher steady level than a level observed (J. Biol. Chem. 258, 6927, 1983) without K^+ . The addition induced a transient increase ($t_{1/2}=0.02$ s) in the amount of phosphoenzyme, followed by a slow decrease ($t_{1/2}=0.07$ s), but the addition without K^+ induced a monophasic increase ($t_{1/2}=0.02$ s). The addition of ATP in the presence of 1 mM Ca^{2+} with 2 M Na^+ induced monophasic decrease ($t_{1/2}=0.1$ s) in the fluorescence with much slower increase ($t_{1/2}=0.8$ s) in the amount of phosphoenzyme. Simultaneous presence of ATP, Na^+ and Mg^{2+} or Ca^{2+} was prerequisite to above dynamic changes. The data indicated the formation of a dephosphoenzyme (ES^*) which contains divalent cation, ATP and Na^+ preceding the formation of ADP-sensitive phosphoenzyme. The relative fluorescence intensity of phospho and dephosphoenzymes and the amount of phosphoenzyme (J. Biol. Chem. 257, 10659, 1982) permitted the simulation using the reaction mechanism including ES^* , ADP-sensitive phosphoenzyme, K^+ -sensitive phosphoenzyme and K^+ bound enzyme. The simulation gave a good fit to the experimental data which show that ATP is hydrolysed through above intermediates in sequence in the presence of both Na^+ and K^+ .

182

pH HOMEOSTASIS OF A FACULTATIVELY ALKALOPHILIC BACILLUS

N. Koyama, Y. Ishikawa and Y. Nosoh, Laboratory of Natural Products Chemistry, Tokyo Institute of Technology, Yokohama, Kanagawa 227, Japan

A facultatively alkalophilic *Bacillus* grows in the range of pH 7.0 to 10.5, and exhibits almost the same growth rate over a pH range from 7.5 to 10.2. When the culture pH changed from 10.2 to 7.5, the growth of the bacteria stopped, but the addition of 5 mM KCl to the culture recovered the growth. When 5 mM KCl was added at pH 7.5 to the bacteria grown at pH 10.2, H^+ efflux accompanied by K^+ influx were observed. The internal pH of the bacteria suspended in buffer containing 40 mM NaCl increased from 6.8 to 8.9 on changing the external pH from 7.5 to 10.0 in the absence of KCl. In this external pH range with 5 mM KCl, the internal pH changed from 8.3 to 9.3, and the internal pH was higher or lower than the external pH below or above pH 8.4 (external), respectively. The ΔpH (acid interior) of membrane vesicles measured by fluorescence change of aminoacridine was almost constant up to pH 8 (external) and rapidly increased above pH 8 in the presence of 50 mM NaCl. In the presence of 50 mM KCl, the pH change was small. The following mechanism of pH homeostasis for the bacteria was suggested; the internal pH may probably be increased by K^+ above pH 8 (external) and decreased by Na^+ above pH 8.

184

THE EFFECT OF METABOLIC DEPLETION ON THE MODES OF OPERATION OF THE FUROSEMIDE-SENSITIVE Na^+ , K^+ - Cl^- CO-TRANSPORT IN HUMAN ERYTHROCYTES. G. DAGHER^{*}, C. BRUGHARA, M. CANESSA

^{*}INSERM U7, Necker Hospital, Paris, France
Dept of Physiology, Harvard Medical School, Boston MA02115.

Red blood cells from 3 subjects were metabolically depleted by starvation (12-15 hrs). Cation content was then modified with nystatin. ATP depletion (70 μ moles/l.cell) induced (i) a decrease (60 \pm 22 %) in the maximal velocity of the furosemide-sensitive (F-S) Na^+ and K^+ efflux into choline or Na^+ media without alteration of the affinity for internal Na^+ , (ii) a decrease (70 \pm 21 %) in the F-S Na^+ and K^+ influx (Nad 125, Ko 20 mM) into cells containing 20 μ moles/l.cell of Na^+ . Thus the net Na^+ efflux and the net K^+ efflux were reduced by 65 \pm 25 %. The affinity for external K^+ to inhibit Na^+ efflux was markedly increased and the Ko-stimulated Na^+ influx and the Na^+ -stimulated K^+ influx was reduced by 65 \pm 25 % after ATP depletion.

The trans-inhibition of the F-S Na^+ efflux by Na^+ and Ko and the cis-stimulation of the K^+ efflux by Na^+ is similar in percentage in control and metabolically depleted cells. This observed decrease in Na^+ and K^+ efflux was not consequent to the increased of GSSH levels and could be reversed by increasing ATP back to normal levels.

These results suggest that metabolic depletion reduced the turnover rate of the Na^+ , K^+ -cotransport system.

186

ADVANTAGES OF NUTRIENT TISSUE CULTURE MEDIUM IN THE STUDY OF RAT INTESTINAL TRANSPORT. P.T.BEALL, Basic Pharmaceuticals research, CIBA-Geigy, Ardsley, New York, 10502, USA

In studies of rat jejunal transporting epithelium, nutrient medium such as Leibovitz L-15 tissue culture medium (GIBCO), is superior to classical balanced Ringer's solutions at three levels of experimentation. L-15 medium contains a mixture of amino acids, vitamins, and cofactors, galactose as an energy source, and a buffer system in equilibrium with air. (A) For IN SITU open loop perfusions of rat jejunum, Ringer's solutions, even those containing Ca^{++} , Mg^{++} , AND DEXTROSE, support water absorption in the 0.2 \pm 0.1 ml/min/gm dry tissue range. L-15 routinely supports 0.4 \pm 0.1 ml/min/gm levels for up to four hours. (B) IN VITRO preparations of jejunum in Ussing chambers with L-15 support stable values of tissue resistance, short circuit current, and sodium flux for up to four hours compared to a constantly declining value in Ringer's. (C) ISOLATED ENTEROCYTES maintain 85% trypan blue dye exclusion for three hrs. in L-15 bubbled with 10% O_2 , compared to 30% viability of cells in Ringer's. It appears that intestinal enterocytes function better in medium which mimics the nutritional contents of the lumen rather than in solutions mimicking the blood serum. Partially supported by the Office of Naval Research.

Friday 03 August Congress Centre-First Floor Posters 187-192

Posters on Mechanisms of Transport Across Membranes

187

STUDIES OF MONOCLONAL ANTIBODY EFFECTS ON LAMB

Na^+/K^+ -ATPase FUNCTION. William J. Ball, Jr., Dept. of Pharmacology and Cell Biophysics, Univ. of Cincinnati College of Medicine, Cincinnati, Ohio 45267 U.S.A.

Monoclonal antibodies can serve as unique probes of specific regions of membrane bound enzymes. Several monoclonal antibodies have been prepared against the purified lamb kidney (medulla) Na^+/K^+ -ATPase. Binding studies using an ELISA type of surface adsorption assay have shown these antibodies to be sensitive to some conformational changes and species variations in this enzyme (Ball et al., *BBA* 719, 413, 1982). In addition, two of these antibodies have been found to inhibit the ATPase activity by altering ATP binding to the enzymes even though they bind to different antigenic regions of the catalytic subunit. These two antibodies also alter ATP-mediated increases in the enzyme affinity for the cardiac glycoside ouabain. Antibody M7-PB-E9 in the presence of Mg^{2+} can stimulate the rate of ouabain binding to the enzyme. It appears to cause an "ATP-like" conformational change in the enzyme. Thus, specific mechanisms for antibody effects on different parameters of enzyme function besides its catalytic activity can be studied using monoclonal antibodies. (Supported by NIH grant HL-24941 and the American Heart Association.)

188

THE GRAMICIDIN A CHANNEL: THE ENERGY PROFILE FOR Na^+ IN A HEAD-TO-HEAD β_3 DIMER. POSSIBLE ROLE OF THE ETHANOLAMINE END. C. Etchebest and A. Pullman, Institut de Biologie Physico-Chimique, 13 rue Pierre et Marie Curie, 75005 Paris, France.

The energy profile for Na^+ was first computed assuming the channel formed by the sole backbone, introducing all the terms in the theory of intermolecular interactions. The effect of allowing the ion to reach its successive optimal positions shows the presence of a series of energy minima. The presence of a second ion lowers the central barrier for the first one and facilitates its progression and exit. The energy profile for double occupancy indicates two symmetrical minima at about 13 Å from the center.

The effect of the ethanolamine end was then investigated for single occupancy computing the total inter- and intra-molecular terms in the energy of the system gramicidin- Na^+ , allowing the ethanolamine end to adopt its most favourable conformations during the progression of the cation in the channel. The resulting deepening and displacements of the minima will be discussed.

189

THE DEPOLARIZED POTASSIUM CURRENTS AND THE TIME DELAY

Chun Chiang, Institute of Physics, Academia Sinica, Nankang, Taipei, Taiwan, R.O.C.

An equation with five exponential terms is shown to be able to fit the depolarized potassium current in nerve membrane with different initial conditions. This equation has molecular basis and was derived with the assumption that the potassium ions are transported under the combined forces (applied electric force, dipole force of the membrane matrix, diffusional force, friction force) via the Newton's second law. It points out that the initial phase of potassium current may take different form according to different initial conditions and the usual concept that potassium conductance have a time delay may be misleading. Unlike the Hodgkin-Huxley equation which can only fit the latter part of the transient current, this equation with a given set of time constant may fit the whole range of the current for different initial conditions.

190

A NEW APPROACH USING SATURATION TRANSFER-ELECTRON PARAMAGNETIC RESONANCE IN ANALYSIS OF MEMBRANE PROTEINS - CRYOPROTECTANT INTERACTIONS.

M.A. Nunes, Lab. of Molecular Biophysics, Institute of Biomedical Sciences, USP-05508, São Paulo, SP, Brazil.

Glycerol and dimethyl sulfoxide (Me₂SO) at concentrations of 10% (v/v) in phosphate buffered saline (PBS) solution, seem to induce protein conformational changes of maleimide spin labeled ghosts submitted to temperature lowering (ranging from +20°C to -20°C). Burying of protein -SH groups was observed, but during phase transition a minimization of protein conformational changes seems to occur, via a mechanism that cannot be considered to be the same for both cryoprotective agents (d'Avila Nunes, submitted). Using ST-EPR and careful spectral analysis, the behavior of C/C vs. temperature suggests significant differences between control and experimental groups, with larger motional freedom for spin labels of the control group. During phase transition, amplitude attenuation of C/C variations was observed when glycerol or Me₂SO was present. Analysis of line width (ΔH) of maleimide spin label (MSL) spectra (MSL in PBS solution) during temperature lowering from +20°C to -90°C shows a linear increase of ΔH , with rotational correlation times ranging from 4×10^{-11} to 2×10^{-10} s. At -15°C an inflexion point of ΔH vs. temperature was detected, with 43% increase of ΔH . At -25°C an abrupt slope change suggests phase transition. However, for temperatures in the range of -35°C to -90°C there is a line width decrease, suggesting that MSL could be rotating inside a clathrate cage.

Research supported by FAPESP, CNPq and FINEP.

191

CONDUCTIVE AND NEUTRAL K FLUXES ACROSS THE BASOLATERAL MEMBRANE OF A SODIUM TRANSPORTING EPITHELIUM. Thomas C. Cox, Department of Physiology, Southern Illinois University School of Medicine, Carbondale, Illinois, USA

Most models for ion transport across Na transporting epithelia predict that the short circuit current (I_{sc}) will be equal to net K flux through conductive pathways in the basolateral membrane if the tissue has been pretreated with ouabain. If the tissue is bathed in K-free Ringer, K loss from the cells can be measured as the increase in K concentration in the bathing solution. Isolated epithelia of frog skin (*Rana pipiens*) were bathed in K-free, Cl-free (0.1 mM ouabain) sulfate Ringer and continuously short circuited. The basolateral solution was collected at 2 minute intervals and assayed for K by flame photometry. The collected K was converted to microamps (IK) and compared directly with the average I_{sc} for the 2 minute interval. I_{sc} declined with time after the ouabain treatment so that IK could be plotted versus I_{sc} . IK was tightly correlated with I_{sc} and appeared linear with average slope of $0.95 \pm .07$ and intercept of $3.0 \pm .5$ (13). Addition of 0.1 mM amiloride to the apical solution moved IK and I_{sc} along the same line. In addition, preliminary experiments in Cl Ringer suggest that 0.2 mM bumetanide decreased the elevation of the IK versus I_{sc} line. The nonzero intercept may represent the value of a neutral K flux. Assuming that under these conditions no significant portion of I_{sc} is carried across the basolateral membrane by ions other than K, this approach provides a powerful way to distinguish drug effects on neutral and conductive K fluxes.

192 ORAL PRESENTATION

23. Na^+ -NMR MEASUREMENT OF INTRACELLULAR SODIUM IN RABBIT RENAL PROXIMAL TUBULE--THE KINETICS OF NET Na^+ FLUXES

H.J. Avison, T. Ogino, S.R. Gullans, G. Giebisch and R.G. Shulman, Departments of Molecular Biophysics & Biochemistry and Physiology, Yale University, New Haven, CT 06510.

Using ^{23}Na -NMR we have been able to resolve the intra- and extracellular Na^+ pools in rabbit renal cortical tubule suspensions. The tubules were isolated by collagenase infusion of rabbit kidneys, then washed and purified in Ringer's solution. A final wash was performed in a modified Ringer's solution containing the shift reagent dysprosium triphosphate and 2mM Ca^{2+} . ^{23}Na NMR spectra were obtained using a Bruker WM 360 wide bore spectrometer with a 20 mm probe tuned to 94.26 MHz. In tubules incubated with the shift reagent Ringer, cellular ATP was slightly depleted with respect to controls (7.4 ± 0.1 vs. 8.3 ± 0.2 nmol ATP/mg protein), however the respiration rates were identical (26.1 ± 1.1 nmol O_2 /mg protein-min shift reagent). The intracellular Na^+ pool was 100% NMR visible, and its size was $185 (\pm 10)$ nmoles/mg protein, or 45 ± 5 mM. Addition of 10^{-3}M ouabain caused an initial rapid increase in Na^+ ($+43 \pm 2\%$ in 2 1/2 minutes) followed by a slower rise ($+100\%$ 30 min after addition). Nystatin (0.4 mg/ml) results in a 4-fold increase in Na^+ in 10 minutes. We have also observed a rapid K^+ -dependent reduction in Na^+ following addition of K^+ to K^+ -depleted tubules suspended in K^+ free Ringer. The Na^+ depletion could be analyzed with 5s time resolution, and we find that Na^+ reaches a new steady state value ~ 100 s following the K^+ addition.

Friday 03 August Congress Centre-First Floor Posters 193-198

Posters on Mechanisms of Transport Across Membranes

193

ACIDIC AMINO ACID TRANSPORT IN HALOBACTERIUM HALOBIVM: PARTIAL PURIFICATION AND RECONSTITUTION OF THE ASPARTATE TRANSPORT SYSTEM

R.V. Greene and R.E. MacDonald, Northern Regional Research Center, U.S. Department of Agriculture, Peoria, Illinois, USA and Department of Biochemistry, Cell and Molecular Biology, Cornell University, Ithaca, New York, USA.

Membrane vesicles of *Halobacterium halobium* R1H₁₀ bind to an aspartic acid-agarose affinity column. After disruption of the bound vesicles by low ionic strength, a protein fraction is eluted from the column with 2.5% cholate in 3 M NaCl. When this fraction is reconstituted with soybean lipids to form proteoliposomes, the proteoliposomes exhibit active aspartate accumulation. Aspartate transport in the reconstituted system is driven by a chemical sodium gradient (out > in), exhibits sensitivity to an electrical potential, and is specific for L-aspartate. These characteristics are consistent with observations on aspartate transport in intact membrane vesicles of *H. halobium*. Initial aspartate transport rates in the reconstituted system are enhanced about 10-fold over the native system. The system developed should be useful in future purification schemes and studies of the molecular details of membrane transport.

195

INFLUENCE OF THE PERDEUTERIATION ON TRANSITION PHASES OF H TETRADECANOIC ACID USED AS A PROBE

O. Bouloussa and M. Dupeyron, Laboratoire de Chimie Physique L.A. 176, 11, rue Pierre et Marie Curie, F-75231 Paris Cedex 05.

Specifically labelled or perdeuterated fatty acids and phospholipids have been used as molecular probes for determining, by using ²H-N.M.R., the ordering of aliphatic chains in more or less complex biological membranes. Very few is known about the effect of hydrogen substitution on the intrinsic conformational properties of aliphatic chains. One approach is to study the monolayer properties of hydrogenated and perdeuterated compounds by measurement of surface pressure and potential in order to get some precise information about an eventual perturbation due to perdeuterated probes on various phase transitions.

We establish that the substitution of ¹H by ²H has the same effect than a temperature increase of about 5°. This is consistent with the results of Petersen et al. who showed by D.S.C. that deuteration causes the same temperature shift with phosphatidyl choline bilayers. Besides, binary mixtures of these acid. don't obey the additivity rule. That indicates some interactions between the two chains which will be discussed.

197

INTERACTION OF MEMBRANE COMPARTMENTED ATP WITH THE Na/K PUMP OF HUMAN RED BLOOD CELL GHOSTS. David G. Shoemaker and Joseph F. Heffman, Dept. of Physiology, Yale Univ. Sch. Med., New Haven, CT., U.S.A.

Previous studies have shown that a membrane pool of ATP is used by the Na/K pump in preference to bulk solution ATP. The amount of ATP bound to hemoglobin-free, frozen-thawed porous ghosts was $1.5 \pm 0.7 \times 10^{-11}$ moles ATP/mg membrane protein, and did not differ when ghosts were prepared from cells energy depleted by incubation for 24 hrs @ 37° in the absence of substrate. Preincubation of porous ghosts in the presence of 1.5mM ATP or the substrates required to synthesize ATP via the membrane bound phosphoglycerate kinase (PGK), followed by exhaustive washing to remove bulk ATP, resulted, respectively, in $3.2 \pm 0.3 \times 10^{-10}$ and $2.6 \pm 1.1 \times 10^{-10}$ moles ATP/mg memb. prot. While preloading the membrane pool with ATP (either from bulk ATP or by synthesis from substrates of membrane bound PGK or pyruvate kinase) inhibits formation of the Na dependent EP of the Na₂K-ATPase from bulk [³²P]ATP, this pool ATP did not support [³H]ouabain binding in contrast to bulk ATP. Preincubation of porous ghosts with bulk 8-azido-[α-³²P]ATP followed by exhaustive washing before UV photolysis, resulted in incorporation of label into PAGE bands 2, 5, and 6. However, preincubation with both the photolabel and 1.5mM ATP markedly decreased the level of label incorporated into band 5, known to be actin. Low salt actin extracted porous ghosts, shown to have normal Na₂K-ATPase activity, still formed Na dependent EP after pretreatment with bulk ATP, indicating that these membranes were devoid of pool ATP. (Supported by NIH Grants HL-09906 and AM-17433)

194

FTP-Tb AS AN ANALOGUE OF ATP-Mg COMPLEX: USE AS A REPORTER OF TOPOLOGY OF ATPase ACTIVE SITES.

J.J. LACAPERE*, M. RONJAT*, J.P. DUFOUR* and Y. DUPOIN*.

* Biophysique, CEN, Saclay, France; * EMC, CEN, Grenoble, France; * Enzymologie, Univ. Louvain la Neuve, Belgique.

Formycin Tri Phosphate is an analogue of ATP (λ_{ex} = 305 nm and λ_{em} = 345 nm). It forms tight complexes with lanthanides, particularly with Terbium (K_{ass} = 10⁶ M⁻¹). This association can easily be measured by exciting FTP at 305 nm and observation of Terbium emission lines at 490, 545, 590 and 620 nm. Spectroscopic measurements and analysis following Forster's theory indicate a near distance of 3.3 ± 0.5 Å between Terbium and the chromophore center of FTP. Enhancement of fluorescence of Terbium in D₂O indicates that binding of Tb³⁺ to FTP involves 3 + 0.5 coordination bonds and that 5.5 ± 0.5 water molecules remain in the primary hydration shell of Terbium.

FTP-Tb binding was tested on SR Ca-ATPase and on Yeast H⁺-ATPase. In both cases association of the complex is strong (K_{ass} ≈ 10⁶ M⁻¹) and results in an important enhancement of Terbium emission. This enhancement is mostly due to a change in polarity around the FTP-Tb complex as well as to a change in hydration of Terbium.

196

EFFECT OF DIETARY K ON RAT RED CELL CATION FLUXES: A POSSIBLE ROLE FOR COTRANSPORT IN MAINTAINING CELL VOLUME

M.A. Milanick and J.F. Hoffman, Dept. of Physiology, Yale University School of Medicine, New Haven, CT, USA

Sprague-Dawley rats supported on a low K diet for 8 weeks were found to have a 2 fold decrease in plasma K (K_p), from 4mM to 2 mM, a slightly elevated red cell Na, and nearly equal red cell volumes (shrunk < 20 %) as compared to control animals. Rats fed a high K diet for 8 weeks had a slightly elevated K_p and nearly equal red cell Na content and red cell volumes compared to control animals. The red cell transport parameters of the rats on a high K diet and normal K diet were nearly indistinguishable. The red cells from hypokalemic rats had a 2 fold greater bumetanide-sensitive ⁴²K influx and only slightly higher pump and leak fluxes. For all three types of red cells, the osmolality of the flux medium and bumetanide-sensitive transport rate were inversely correlated. However, neither the difference in cell volume nor in cell Na completely accounted for the elevated bumetanide-sensitive fluxes in the red cells from the hypokalemic rat suggesting that the cotransport of cations was altered by the diet. The steady state pump/leak model predicts that a fall in K_p will lead to a greatly altered cell volume if pump and leak fluxes are unchanged. Thus we extended the steady state model to include cation cotransport pathways. This model predicts that cells in low K_p and with higher net cotransport fluxes can have the same volume as normal cells. (This work was supported by NIH grants HL-09906 and AM-06896c.)

198

INSERTION OF A PEPTIDE OF DIPHTHERIA TOXIN FRAGMENT B IN A LIPID LAYER.

V. Cabiaux and J.M. Ruyschaert, Lab. of Micromolec. at Interfaces, Brussels University Bd Triomph 1050 Brussels, Belgium.

Diphtheria toxin (DT) is a protein which must cross a membrane barrier to reach its target in the cytoplasm. The mechanism of translocation remains largely unknown. DT interacts strongly with lipid bilayers at low pH. Deleers et al. (1) have shown that Cbl = a cyanogen peptide of fragment B is able to induce pores formation at low pH. This peptide contains a hydrophobic domain that strongly resembles the transverse lipid associating domain of intrinsic membrane proteins. The pH dependency could be due to the presence of a cluster of prolines in the C-terminal region of Cbl. We present here evidence that Cbl is able to insert into a lipid layer. We have studied the change in spectral properties of the only Trp of Cbl. In the presence of small unilamellar vesicles made with egg phosphatidylcholine, Trp exhibits a blue shift from 350 nm to 338 nm and a four fold increase in its fluorescence emission. These modifications could be explained by the passage of Trp from a polar medium to an apolar medium which could be constituted by the lipid bilayer. This passage might play a role in the translocation process but the complete knowledge of this mechanism requires further investigations.

1. M. Deleers, H. Beugnier, P. Falgaue, V. Cabiaux and J.M. Ruyschaert, FEBS Lett. 160 82-86 (1983).

Friday 03 August Congress Centre-First Floor Posters 199-204

Posters on Mechanisms of Transport Across Membranes

199

INTRACELLULAR pH TOPOGRAPHY AND TRANSMEMBRANE pH PROFILE: DETERMINATION BY A FLUORESCENT PROBE

Jan Slávik, Dept. Cell Physiol., Inst. Microbiol., Czechoslovak Acad. Sci., Prague-Krč, Czechoslovakia

A new fluorescent probe technique based on computerized microscope fluorometry (Sávik, FEBS Lett. 156, 227) was applied to the yeast *Saccharomyces*. It gives the "map" of the pH inside the cell and its immediate surroundings with 0.1 pH unit and 200 nm resolution.

The cytoplasmic pH of cells in water was 6.7-7.5 in the center, decreasing to 6.0 toward the periphery of the cell. This heterogeneity was diminished in cells in weak buffers and disappeared in strong buffers. It was absent in starved cells and in antimycin-treated cells. Dead cells showed a uniform alkaline pH.

In water, the pH profile across the cell membrane showed diffuse pH transition, extending 1-2 μ m on both sides, with no clean Δ pH across the membrane itself. In stronger buffers the "unstirred layer" outside the cell was narrower or non-existent. Intracellular pH adjusts itself to an abrupt external pH change in about 10-20 min.

All results fully confirm the data of the "average" cell pH.

201

GABA RECEPTOR AND PROTON ATP-ase IN PLANAR LIPID MEMBRANE.

M.P. Borisova, O.V. Kolomytkin, V.I. Kusnetsov. Ins. of Biol. Physics, USSR Acad. Sci., Pushchino, USSR.

Two different methods worked out by H. Schindler et al. (1978) and Ch. Miller, E. Racker (1976) was tested for incorporation of synaptic GABA receptor and H⁺-ATP-ase into a planar bilayer membrane. The model membrane containing the receptor was chemosensitive to GABA, while the other neurotransmitters did not influence it. Single channels fluctuations of 20 pS in conductance and 10 ms life time were observed in the presence of GABA.

Measurements of transmembrane currents at voltage clamp condition showed that conductance of ATP-ase containing membrane was low. Addition of 1 mM ATP did not increase the conductance, but caused generation of stationary transmembrane current flowing from the chamber compartment with ATP. This current could be compensated for by application of membrane voltage of 130-230 mV. The results obtained indicate that incorporated ATP-ase works as a proton pump.

Therefore, membrane complexes different in structure and function such as GABA receptor and H⁺-ATP-ase can be successfully incorporated into a planar lipid bilayer.

203

FEATURES OF SQUID GIANT AXON MEMBRANES AS REVEALED BY FREEZE-FRACTURE REPLICAS G.M. Villegas*, N.J. Lane, F. Sánchez and J. Villegas*, Instituto Internacional de Estudios Avanzados (IDEA), Apartado 17606, Caracas 1015-A, Venezuela and Department of Zoology, University of Cambridge, U.K.

Giant stellar nerve fibers of squid *Sepioteuthis sepioidea* were frozen in Freon¹¹ after prefixation with glutaraldehyde and cryoprotection with glycerol. Platinum-Carbon replicas, obtained with a Balzers-510 freeze-etching unit, were examined with a Siemens 101 or a Philips 400 STEM electron microscope. The Schwann cell layer is characterized by the presence of numerous superimposed membrane faces corresponding to the channel (cleft) walls. P and E faces display complementary endo or exocytotic images. Besides, numerous small cross-fractured cytoplasmic portions which might correspond to interdigitations or capitate projections of adjacent cells are often observed. At the axon-Schwann cell interface there appear regions with many endo-exocytotic pits and also, at some other sites larger craters or pits resembling those observed in chemical synapses. Ridge-like profiles, extended up to 10 μ m long, and formed by rows of particles have also been observed at the same axon-Schwann interface. Although their functional significance is still unknown, these structures may be related to axon-glia coupling and intercellular exchange of substances. Furthermore, the ridge-like arrangements may represent either zones of mechanical attachment or specialized sites such as the structural complexes of the axolemma previously described.

* On leave of absence from Instituto Venezolano de Investigaciones Científicas (IVIC), Caracas.

200

ALTERNATIVE PATHWAYS FOR ATP HYDROLYSIS CARRIED OUT BY THE (Na,K)ATPase. PEDEMONTE C.H. and BEAUGE L., Instituto M.y M. Ferreyra, CC 389, Cordoba, Argentina.

Inhibitory effects of Mg²⁺ and Pi on the stimulation of the ATPase activity by Na⁺, K⁺ and ATP are consistent with a model where Mg²⁺ acts both as a "product" and as a dead-end inhibitor. The first follows Mg²⁺ interaction with the enzyme in the E₂ occluded state, whereas the second would occur upon formation of an enzyme-Mg complex with the enzyme in an E₁ state (as observed from trypsin inactivation studies). The enzyme activity was more sensitive to Mg²⁺ inhibition in the presence of Na⁺ and K⁺ (Na,K-ATPase) than in the presence of Na⁺ alone either at high (Na,K-ATPase) or low (Na,K-ATPase) Na⁺ concentration. Using congeners of K⁺ that form complexes of different stability with the dephosphoenzyme, it was observed that Mg²⁺ inhibition was potentiated and the K_{0.5} for ATP activation was lower when the dephosphorylating cation forms a tighter complex with the dephosphoenzyme. Mg²⁺ inhibition was reduced when ATP concentrations were increased beyond those needed to saturate its high affinity site. The present model is consistent with the formation of a Mg²⁺-phosphoenzyme complex insensitive to K⁺ that appears as an intermediate in the Na-ATPase activity found in the absence of external Na⁺ and K⁺. In addition, these experiments provide kinetic evidence indicating that ATP accelerates disocclusion but has no effect on the E₂-E₁ transformation itself, and that the affinity of the enzyme for the nucleotide is determined not by the E₂ state but by the "degree" of occlusion of the dephosphorylating cation.

202

ARREST AND REVERSAL OF THE ELECTROGENIC SODIUM PUMP UNDER VOLTAGE CLAMP.

Philippe Béné and Luca Turin, CNRS Station Zoologique La Darse Villefranche/Mer, France.

Single blastomeres isolated from the vegetal half of 64-cell stage *Xenopus* embryos have unusually low and linear membrane conductance (typically 10-20 nS), particularly if extracellular pH is made slightly acid (6.5). Under these conditions, the unstimulated electrogenic sodium pump can contribute as much as 70-80 % to membrane potential in the steady-state, i.e. without sodium loading (Turin, L. 1984 in *Electrogenic Transport*, Blaustein & Lieberman Eds, Raven Press, NYC). We have studied the pump current/voltage relation under voltage clamp by stepping membrane potential 2 mV at a time from 0 to -150 mV in 15 seconds. The pump is inhibited by removal of extracellular potassium or addition of 10 μ M ouabain. Pump current varies from cell to cell and the resolution of our measurements is of the order of 100 pA. The cells used in this study had pump currents at 0 mV ranging between 250 and 1200 pA, allowing clear separation of I/V relations with and without pump. The results revealed some unexpected features of the pump current/voltage relation. Firstly, it is linear in the range of voltage studied, and intersects the zero current axis at a potential which varies from cell to cell and lies between -110 and -160 mV (the latter extrapolated). Secondly, the current reverses past this potential without change in slope. Thirdly, removal of external sodium suppresses the slope of the pump I/V relation (pump conductance) and turns the pump into an ideal current source over the voltage range considered. This in itself is not surprising in view of the pump's lightened workload, but pump current under Na-free conditions is lower than the maximal current under normal conditions, and decreases with time, suggesting that external Na has kinetic as well as thermodynamic effects on the pump. We are presently studying pump behaviour under step voltage relaxations from "reversal" potential to determine whether there is accumulation of pumps in a particular voltage-dependent step of the pump cycle, or whether the constant slope of the pump I/V relation is due to passive ion diffusion through the active pump. (This work is supported by the CNRS under its Action Thématique Programme "Conversion de l'Energie dans les Membranes Biologiques").

204

EVIDENCE FOR TWO MODES OF CL⁻ AND K⁺ TRANSPORT ACROSS THE BASOLATERAL CELL MEMBRANE OF THE DILUTING SEGMENT OF THE AMPHIBIA KIDNEY. M.B. Cuggino, Dept. of Physiol., The Johns Hopkins Univ. School of Medicine, Baltimore, MD, USA.

Basolateral membrane potentials (V_b) and cell volume were measured simultaneously to determine the mechanism of Cl⁻ and K⁺ transport across the basolateral cell membrane of *Amphiuma* diluting segments. The cells are heterogeneous in regard to potassium and chloride transport. The evidence is as follows: 1) increasing basolateral K⁺ to 98mM or decreasing Cl⁻ to 16mM depolarizes V_b by 58mV and 33mV respectively in one cell type (Group I) and by only 62mV and 43mV, respectively, in another (Group II); 2) raising basolateral K⁺ to 98mM in Cl⁻ free solutions increases the depolarization of V_b to 84mV in Group I cells without a change in Group II cells, 62mV; and 3) the ratio of apical to basolateral resistances is greater than 10³ in Group I cells and 1.3-0.3 in Group II cells. Thus, two cell types are present, a Group I cell with a highly K⁺ and Cl⁻ conductive basolateral membrane and a Group II cell with low basolateral conductances. As expected, Group I cells swell at a rate of 195 μ m³/s in response to an increase in basolateral K⁺ to 98mM. This swelling is inhibited by chloride removal. Surprisingly, however, is that K⁺ induced swelling also occurs in Group II cells at 111 μ m³/s. This swelling is also inhibited by chloride removal indicating that K⁺ movement in those cells may involve K⁺/Cl⁻ cotransport. Thus K⁺ and Cl⁻ movement across the basolateral cell membrane is heterogeneous, with one cell type exhibiting primarily conductive transport while in a second transport is electroneutral.

Friday 03 August Congress Centre-First Floor Posters 205-210

Posters on Mechanisms of Transport Across Membranes

205

INVOLVEMENT OF ENVELOPE-BOUND Ca^{++} IN THE TRANSIENT DEPOLARIZATION OF F.coli MEMBRANE TRIGGERED BY PHAGE ADSORPTION:
L.Letellier, B.Labedan and P.Boulangier, Lab. des Biomembranes and Inst. de Microbiologie, Univ. Paris Sud, Orsay, France.

Adsorption of phages T4 and T5 to F.coli outer membrane triggers the emission of a signal transmitted to the inner membrane, which calls for its depolarization. These $\Delta\psi$ changes were shown to be independent of the nature of the phage and DNA injection process. In the case of T4, a specific requirement for envelope-bound Ca^{++} was found. Indeed, addition of EGTA prevents the $\Delta\psi$ changes. This Ca^{++} remains accessible to the chelator only as a consequence of phage adsorption and remains in this state during the depolarization and repolarization. The $\Delta\psi$ changes occur again if Ca^{++} is added after addition of EGTA. The same concentration of EGTA prevents the $\Delta\psi$ changes whatever the multiplicity of infection, suggesting that phage adsorption triggers both a conformational change of membrane components, the number of which reflects the number of phages and the liberation of a definite amount of Ca^{++} . This Ca^{++} would in turn indirectly induce the $\Delta\psi$ changes.

Using a fluorescent Ca^{++} chelator (Quin 2) we have shown that about .5 nmol Ca^{++} /mg dry weight was liberated during this process. Finally, using starved cells which show a release of respiratory control upon addition of uncouplers, we have demonstrated that the depolarization of the inner membrane induced by addition of different phages (T4, T5, BF23) was correlated with an entry of protons in the cytoplasm.

207

INFLUENCE OF VINBLASTINE INFUSION ON HUMAN SOFT TISSUE SARCOMA TUMOR CELLS - EPR STUDY
M.Sentjurc*, M.Auersperg*, and M.Schara*, *J.Stefan Institute, Ljubljana, Yugoslavia; **Institute of Oncology, Ljubljana, Yugoslavia

Human soft tissue sarcoma biopsies were taken from a case of recurrent large exofitting sarcoma in the buttock before and after intravenous and intraarterial infusion of vinblastine (VLB). The tissue samples were incubated with the spin probe, palmitic acid methyl ester spin labeled analog MeFASL(10,3), which dissolves in the tissue cell membranes. The electron paramagnetic resonance (EPR) spectra were taken for the samples removed from the tumor at various stages of treatment. It was found that VLB perturbs the fluidity of the membrane which relaxes back to the equilibrium state within 40 hours. The equilibrium value of the cell membrane fluidity decreases after several treatments of the patient with VLB. An unusual increase of the EPR signal intensity with time after incubation of tissue with the spin probe was observed, probably due to an oxidative process in this sarcoma tissue.

209

NMR STUDIES OF WATER DIFFUSION IN RED BLOOD CELLS AND GHOSTS. Ch. Tanca, V.I.Pop, Victoria Borza Ann Oregon and Adriana Todiriu, Department of Cell Biology, Faculty of Medicine, "E.L. Ibram" Institute, Cluj-Napoca, ROMANIA.

Previously developed NMR methods for following water diffusion (D) in erythrocytes have been used to comparatively study the effects of inhibitors and of chemical modifications of membranes on D in both erythrocytes and resealed ghosts. A longer relaxation time in ghosts, corresponding to a decreased exchange time of water was noticed in ghosts. We found that only mercurials (such as p-chloromercuribenzenesulfonate, PCMB) inhibited the D . A significant effect of PCMB requires several minutes of incubation at 37°C. This corresponds to the location in the membrane interior of the SH groups involved in D across human erythrocytes. Other sulfhydryl reagents, inhibitors of other transport processes or exposure of erythrocytes to trypsin (which digests glycophorin) or cyanotrypsin (which digests band 3 protein) neither inhibit the D nor hamper the inhibitory action of mercurials. In contrast, exposure of erythrocytes to papain does hamper the inhibitory effect of subsequent incubation with PCMB. Taking into account the degradation of band 3 protein by papain we suggest that the binding site for PCMB playing a role in the inhibition of D is located in this protein.

206

EFFECTS OF Ca^{++} -RINGER ON CELLULAR Na^{+} AND K^{+} ACTIVITIES IN RETZIUS NERVE CELLS OF THE LEECH
V.Nedeljkovic, D.Cemerikic and B.Beleslin, Department of Pathophysiology, Dr.Subotica 1/II, 11000 Belgrade, Yugoslavia.

Intracellular potassium (K^{+})_i and sodium, (Na^{+})_i, activities in Retzius nerve cells of horse leech (*Haemopsis sanguisuga*) determined with ion selective microelectrodes using a liquid ion exchangers, at resting membrane potential of -36.75 ± 7.11 mV were 90 ± 13 mV and 5.52 ± 0.79 mV respectively. Calculated equilibrium potential for both ions, was 69 mV for Na^{+} and -86 mV for K^{+} , indicating active distribution of both ions across the cell membrane, probably mediated by a Na^{+} - K^{+} exchange pump. Exposure to buffered Ca^{++} -Ringer (complete substitution of Na^{+} with Ca^{++} , Tris-Cl added to pH 7.2), for 10 minutes, hyperpolarized membrane potential by -18.3 ± 1.45 mV, induced a large and rapid fall in (Na^{+})_i to 1.77 ± 0.49 mV, without any change in (K^{+})_i. Exposure to unbuffered Ca^{++} -Ringer (pH = 4), for 3 minutes, produced similar rapid clearing of (Na^{+})_i, indicating that is insensitive to external pH. As (K^{+})_i remained constant during exposure to Ca^{++} -Ringer this could, indicate that a rapid clearing of cellular Na^{+} seems to be through postulated $\text{Na}^{+}/\text{Ca}^{++}$ exchange mechanism in the cell membrane.

(Supported by the Research Council of Serbia).

208

STUDY BY ^{31}P -NMR OF THE PERMEABILITY INDUCED BY IONOPHORES ON PHOSPHOLIPIDIC LARGE UNILAMELLAR VESICLES.
M. Hervé, M. Roux, S. Tran-Dinh, C. Gary-Bober*, *Service de Biophysique, Département de Biologie, C.E.N. Saclay 91191 Gif/Yvette France, U.E.R. de Médecine et Biologie Humaine, Université Paris XIII France.

^{31}P -NMR enable to monitor the pH inside vesicles, owing to the presence of a pH-dependent probe - the orthophosphate ion - (in the intravesicular medium). On this basis, the cationic permeability induced by ionophores can be studied by the proton-cation exchange method. In the present study, the permeabilization induced by two types of ionophores has been studied: mobile carrier (valinomycin) and channel forming ionophores (gramicidin and amphotericin B). The mode of action of these two types of ionophores appears different. Upon the introduction in the vesicular suspension of a mobile carrier such as valinomycin, the totality of the vesicles population is immediately permeabilized: the evolution of the chemical shift of the internal PO_4^{3-} signal enables to follow the kinetic of proton transport. In the case of channel forming gramicidin and amphotericin B, two distinct vesicle populations are observed: one of which reach equilibrium too rapidly to allow the kinetic of transport, and the other one is not permeabilized or only in the long run. These results make possible the interpretation of the kinetic of proton flux measured by the use of a glass electrode in the suspension medium.

210

COUPLING BETWEEN HEAT AND MATTER FLUXES IN BIOLOGICAL MEMBRANES

D.C. Mita, A. D'Acunzio, *P. Canciglia and F.S. Gaeta, International Institute of Genetics and Biophysics, CNR, Via Marconi 10, 80125 Naples, Italy, *Institute of General Physiology, Faculty of Sciences, Via dei Verdi 85, 98100 Messina, Italy.

A few years ago we advanced the working hypothesis that heat fluxes of metabolic origin are coupled with biological membrane transport in living cells. In this context we have studied the initial uptake rate of sulphate in the marine alga *Valonia utricularis* in function of its concentration in the outer medium. The rationale of this research is based on the fact that the resulting behaviour is indicative of the mechanism controlling the transport. We have found a characteristic pattern different from the one expected for a diffusive process as well as from the saturation trend exhibited by carrier-mediated transport but identical to the one found in non-isothermal membrane transport of electrolytes in artificial systems. These results are indicative of a common physical basis for both forms of transport, thus confirming our hypothesis.

Friday 03 August Congress Centre-First Floor Posters 211-216

Posters on Mechanisms of Transport Across Membranes

211

DIFFERENTIAL EFFECTS OF CIS- AND TRANS-UNSATURATED FATTY ACIDS ON MEMBRANE FUNCTION: VIRAL MEMBRANE FUSION. R.C. MacDonald, R.I. MacDonald, & V. Dalle Ore, Dept. Biochem., Mol. Biol. & Cell Biol., Northwestern Univ., Evanston, IL, USA

Fatty acids affect diverse functions of biological membranes. Their effect on the Sendai virus membrane, as measured by viral hemolytic activity, is to reduce the ability of the virus to fuse with a target membrane. Iso-stearic and cis-unsaturated fatty acids completely inhibited hemolysis at a few micrograms/ml. Saturated, normal fatty acids were partially inhibitory only at concentrations several times greater. Trans-unsaturated fatty acids were virtually noninhibitory. The differential activities of the fatty acids are due to their different surface activities; inhibition was directly related to equilibrium surface pressures at the air-water interface; inhibitory fatty acids have equilibrium surface pressures nearly as large (within 1-2 dyn/cm) as those of phospholipids, which means that such fatty acids are able to efficiently penetrate the lipid bilayer of the virus. Thus, as predicted theoretically, the inhibitory activity of a fatty acid such as oleate or isostearate parallels its lowering of surface tension at concentrations up to the critical micelle concentration. At the C.M.C., inhibition jumps abruptly, and this portion of the inhibition must depend upon the formation of micelles rather than bilayer penetration and is ascribed to the formation of a belt of fatty acid around an exposed hydrophobic region of a protein. Unbranched saturated and trans-unsaturated acids exhibit surface pressures too low for penetration of lipid bilayers, hence their small effects.

213

FUSION OF UNILAMELLAR LIPID VESICLES CONTAINING HEMOCYANIN CHANNELS WITH PLANAR BILAYERS

F. Pasquali, G. Menestrina and R. Antolini, Dipartimento di Fisica, Povo, Trento, Italy.

Large unilamellar vesicles were prepared by detergent removal from micelles containing octylglucoside or deoxycholate and a mixture of phosphatidylcholine, phosphatidylethanolamine and phosphatidylserine. Liposomes were then interacted with Megathura Crenulata hemocyanin, a well studied channel former. Volume changes induced by osmotic jumps and revealed measuring the light scattering indicated that the permeability of the liposomes was increased by the protein within few hours. The resulting proteoliposomes were purified by centrifugation and then incubated on one side of a planar bilayer. Strong current increases were observed when fusogenic conditions were used i.e. in presence of divalent cations in solution, negative lipids in the host membrane and after the instauration of an osmotic gradient through the vesicles' walls. Such increase is due to the transfer of the ionic channels from the proteoliposomes to the planar bilayer. Studying the effects of Ba²⁺ on the electrical properties of the channel we could confirm that the protein is always inserted into a hydrophobic medium during this process as required by the fusion hypothesis.

215

ACTIVITY ELUTION CHROMATOGRAPHY IN THE MICROGRAM RANGE OF SOLUBILIZED SARCOPLASMIC RETICULUM ATPase.

J.L. Silva and S. Verjovski-Almeida, Depto. de Bioquímica, ICB UFRJ, Rio de Janeiro, Brasil

The calcium dependent ATPase of sarcoplasmic reticulum is a membrane protein, obtained in the microsomal fraction from skeletal muscle. It was found that C₁₂E₈ solubilized ATPase self-associated from a monomer to a dimer in the concentration range of 2 to 50 µg/ml as measured by chromatography when following tryptophan fluorescence intensity or radioactivity of iodine labeled ATPase of the eluted fractions. However difficulties in the measurements arise from background fluorescence in one case and radioactive phospholipids in the other. In order to have a more specific and sensitive method we measured the ATPase activity continuously on the eluted samples. A sephacryl column was used and a reactive mixture was added to the effluent and allowed to react in a loop for 6 minutes before entering the flow cuvette of a photometer. The mixtures contained NADH, ATP, phosphoenolpyruvate and the coupling enzymes (pyruvate kinase and lactic dehydrogenase). The decrease in NADH absorbance was monitored, and it was proportional to ATP utilization by the ATPase. The elution positions of solubilized ATPase were thus determined from the peaks in ATPase activity of the effluents. Decreasing the applied protein concentration from 100 to 1 µg/ml, there was no change in the elution position of the peak and it was observed a decrease in the enzymatic specific activity. These data seem to indicate that the solubilized monomer has a much lower activity than the dimeric form.

Supported by: CNPq, FINEP and MDA

212

Na TRANSPORT ABNORMALITIES IN ERYTHROCYTES FROM ESSENTIAL HYPERTENSIVE PATIENTS.

R. Garay, C. Nazaret, G. Dagher, J. Diez, M. Price, E. Deschamps de Patisette, G. Juin & P. Braquet, INSERM U7/CHRS LA 318, Hôpital Necker, Paris 75015 and IHR, 17 av. Descartes, Le Plessis-Robinson, France.

A detailed kinetic analysis of the interaction of internal Na with different erythrocyte Na transport systems has permitted the distinction of different subgroups of essential hypertensive patients: 1) Pump - hypertensives: with low apparent pump affinity for internal Na and high maximal pump rate; 2) Co - hypertensives: with low cotransport affinity for internal Na; 3) Counter - hypertensives: showing low countertransport affinity for internal Na and high maximal rate of the Na:Li countertransport system and 4) Leak + hypertensives: characterized by an increased passive Na permeability.

A study of the apparent affinity of the Na,K cotransport system for external K has permitted to divide the Co - hypertensives into three subgroups (symmetric, asymmetric and antisymmetric) according to the presence of low, normal or high K affinity.

A study of the antihypertensive effect of cicletanide on 45 essential hypertensive patients indicated that the antihypertensive efficiency of this compound depends, among others, on the subgroup to which the hypertensive belongs.

214

SYNERGISM IN THE TRANSPORT OF CATIONS ACROSS LIPIDIC VESICLES J. Grandjean, P. Laszlo, Institut de Chimie Organique et de Biochimie B6, Université de Liège, S-4000 Liège, Belgium.

Phosphorus-31 nuclear magnetic resonance has been used to investigate Pr³⁺ and Mn²⁺ transports mediated by carbocyclic ionophores across phosphatidylcholine vesicles. The cation influx is markedly increased when two carriers are incorporated together into the lipidic phase. This observation looks quite general if at least one ionophore carries the cation as a 2/1 species (ionophore/cation): a hybrid complex is involved in this synergism. We have postulated that an enhancement of the H⁺ countertransport, coming from the ΔpK between the two carboxylic moieties within the complex, could be responsible for this synergistic effect. Transport experiments in the presence of both one ionophore and one fatty acid have been also performed. The cation inward rate is also enhanced. Kinetic studies have been made with lauric acid-lasalocid A mixtures. The transport rate is first order in fatty acid and second order in ionophore. It suggests that a neutral complex is involved in the transport process. We are now performing complementary experiments to confirm our conclusions.

216

CONFORMATIONAL CHANGES IN THE PROLINE/Na-COTRANSPORTER OF INTESTINAL BRUSH BORDERS B.E. Peerce & E.M. Wright. Physiol. Dept., UCLA, Los Angeles, CA 90024.

Brush border membrane vesicles were isolated by Ca precipitation and treated with KSCN to remove core material. These vesicles contain a Na/L-proline carrier with a K_m of 392 ± 12 µM and a V_{max} of 3.8 nmoles/mg sec. Na⁺-dependent, alanine insensitive proline uptake (i.e., uptake via the imino carrier) is irreversibly inhibited by fluorescein isothiocyanate (FITC), phenylisothiocyanate (PITC) and N-acetylimidazole. The carrier may be protected against FITC inhibition by Na and proline, and against N-acetylimidazole by Na alone. We studied the effect of ions on the fluorescence of FITC conjugated to the carrier. Na, but not K, Rb, Cs, Li or choline, induced a quenching of FITC fluorescence. N-acetylimidazole inhibits the Na dependent quench. Hill plots of the quench versus Na concentration suggests two classes of Na binding sites. SDS polyacrylamide gel electrophoresis indicates a major FITC binding protein of approximately 100 K daltons whose FITC binding is substrate sensitive. We conclude from this data that sodium induces a conformation change in a 100,000 dalton peptide, which may be the proline carrier.

Supported by AM 19567 & NS 09666.

Friday 03 August Congress Centre-First Floor Posters 217-222

Posters on Mechanisms of Transport Across Membranes

217

ANALYSIS OF THE RESPONSE TO PULSES OF DEPOLARIZING CURRENT IN NEURONS OF LYMNAEA STAGNALIS

M. Barbi, S. Chillemi and S. Lucia, Istituto di Biofisica, C.N.R., Via S. Lorenzo 26, Pisa, Italy

Long-lasting pulses of depolarizing current injected into the soma of neurons of the suboesophageal ganglia of *L. stagnalis* elicit a slowly adapting discharge of action potentials followed, at the end of the stimulus, by a "post-tetanic" hyperpolarization (PTH). PTH declines from a peak of up to 20 mV amplitude to zero in time intervals ranging from some seconds to tens of seconds; it is clearly related to the adaptation of the discharge. In principle, both phenomena can be accounted for either by an increase of the Ca-activated K conductance during the discharge, or by the activity of an electrogenic Na/K pump whose rate is raised through the Na-influx associated with the action potentials. In fact, our experimental results suggest that both processes play a role in determining the features of the investigated response. This experimental evidence has been obtained by standard separation techniques: measurement of the membrane conductance during PTH, Na substitution with Li in the external solution, pump block by strophanthidin, superfusion with Ca-free solution, loading of cells with Na by microiontophoresis.

219

MODES OF OPERATIONS AND STOICHIOMETRY OF FUROSEMIDE-SENSITIVE Na AND K FLUXES IN HUMAN RED CELLS

M. CANESSA and C. BRUGNARA
Department of Physiology and Biophysics, Harvard Medical School, Boston, Mass 02115

Six modes of Na and K transport can be inhibited by furosemide, in the presence of 0.1 mM ouabain in human red cells. Experimental evidence will be provided for inward and outward transport of Na-K pairs, K-K exchange and Na-Na exchange and uncoupled Na and K efflux.

The modes of operation depend from the relative ratio of Na and K concentrations at both sides of the membrane which determine coupling interactions such as cis and trans stimulation and trans-inhibition between furosemide-sensitive (FS) Na and K fluxes. A minimal model for a reaction scheme of a Na-K cotransport system can account for these interactions and the variable stoichiometric ratio between FS Na and K fluxes.

At the physiological range of external and internal Na and K concentrations the transport reaction has an stoichiometry of $2 \text{ Na}_o + 3 \text{ K}_i = 2 \text{ Na}_i + 3 \text{ K}_o$ with an apparent equilibrium constant of 17 and of 3 for an electroneutral coupling to chloride movements. The apparent equilibrium constant of the Na-K cotransport reaction predicts that in cells with high chloride ratio, the system will perform net Na extrusion at physiological Na and K concentration. In cells with low chloride content, the transport reaction will be operating in the inward direction as an inward chloride pump and/or accumulating K.

221

RADIATION PROTECTION FACTOR(S) OF HUMAN ERYTHROCYTES: A BIOPHYSICAL STUDY. M.A.S. Al-Shaickly and H.A. Al-Jouboury, Department of Biology, College of Science, University of Baghdad, Adhania, Baghdad, IRAQ.

10% V/V intact human erythrocytes (1×10^6 cells/ml), washed and suspended in sucrose tris buffer, were irradiated with ^{60}Co gamma and ultraviolet (254nm) radiations. The amount of potassium efflux (K_{eff}) and the percentage haemolysis (H), which were taken as parameters of the radiation response, were directly related to the given doses of radiation. Washed erythrocytes, suspended in supernatant extracted from blood samples irradiated to a sub haemolytic dose of gamma radiation, showed a reduced response to both types of radiation. Extent of reduction (protection) vary with the dilution of the supernatant. Maximum reduction in response to ultraviolet radiation are 85% and 40%, to gamma radiation 93% and 46%, as measured by K_{eff} and H respectively. Content analysis of extracted supernatant revealed the existence of low and high molecular weight proteins and divalent ions. The role of each was evaluated and a possible mechanism of lipid photoperoxidation-retention; and hence protection was inferred.

218

THE REMOTOR MUSCLE OF THE LOBSTER ANTENNA: CHARACTERIZATION OF ITS SARCOPLASMIC RETICULUM AND SKINNED FIBER EXPERIMENTS

M. Villaz, M. Ronjat, Y. Chapron and Y. Dupont

Lab. Biol. Moléculaire et Cellulaire, Dept de Recherche Fondamentale, Grenoble, France.

The synchronous remotor muscle of the lobster second antenna is known to produce rapid and weak contraction and to have an extraordinarily profuse sarcoplasmic reticulum (SR). (1) Vesicles of this SR have been prepared. They contain one major protein, the 100 KD M.W. Ca^{++} ATPase (95% of the amount in protein). The Ca^{++} -activated ATPase and Ca^{++} transport have been measured. The activity is high, more than 4 $\mu\text{moles/mg protein/min}$, and the coupling ratio is 2. There is no detectable passive Ca^{++} permeability and no Ca^{++} independent Mg^{++} ATPase activity. The Ca^{++} binding has been measured on these vesicles, which amounts to 8 nmoles/mg protein with a dissociation constant 10^{-6} M. (2) The intact remotor muscle was preincubated for hours in a Ringer containing peroxylase-glutaraldehyde ^{3}H ouabain. After homogenization, fractionation was performed on a sucrose gradient. 15% of the proteins were contained in an heavy band showing peroxylase activity and containing Ca^{++} ATPase. This band represents fragments enriched in contact membranes between SR and tubules. It is unlabelled with ^{3}H -ouabain, indicating the absence of Na-K ATPase in that area contrary to the known fast vertebrate muscles. (3) Skinned fiber experiments have been performed. Contractions in the range of the milligramme have been measured on a single split fiber. They reveal a classical behaviour of the remotor regarding the sensitivity to caffeine in the release of calcium.

220

CALMODULIN AND ITS ROLE ON THE $\text{ATP} \rightarrow \text{Pi}$ EXCHANGE REACTION AND Pi DEPENDENT PHOSPHORYLATION OF THE CARDIAC SARCOLEMMA ($\text{Ca}^{2+} + \text{Mg}^{2+}$)-ATPase. Jaime Mas-Oliva. Departamento de Bioenergética, Centro de Investigaciones en Fisiología Celular, Universidad Nacional Autónoma de México. AP 70-600 04510 México, D.F.

It has been demonstrated that calmodulin stimulates in a calcium dependent way the ATP hydrolysis as well as the $\text{ATP} \rightarrow \text{Pi}$ exchange reaction carried out by the sarcolemmal (1) and the red cell (2) ($\text{Ca}^{2+} + \text{Mg}^{2+}$)-ATPase.

The modulation of the ATPase reaction cycle was controlled by high and low affinity sites for calcium asymmetrically located on the enzyme.

A calmodulin like effect performed by trypsin was observed for the $\text{ATP} \rightarrow \text{Pi}$ exchange reaction catalyzed by the ($\text{Ca}^{2+} + \text{Mg}^{2+}$)-ATPase of intact sarcolemma. In contrast, when calmodulin depleted sarcolemmal vesicles were employed trypsin importantly decreased the exchange reaction or synthesis of ATP.

It has been also observed that together with the modulation of calmodulin upon the overall reaction sequence of the enzyme, the Pi -dependent phosphorylation of the ATPase showed to be inhibited by calmodulin. This Pi -dependent phosphorylation of the sarcolemmal ($\text{Ca}^{2+} + \text{Mg}^{2+}$)-ATPase was observed to be modified depending on the water-organic solvent mixture employed in the incubation medium. Supported by CONACYT Grant IC5A00A-001872. 1) Mas-Oliva, J., de Meis, L. and Inesi, G. Biochemistry (1983) 22,5822. 2) Mas-Oliva, J. Biochim. Biophys. Acta (submitted).

222

MOLECULAR MECHANISMS OF ELECTRON TRANSPORT IN BIOLOGICAL MEMBRANES

A.B. Rubin, Department of Biology, Moscow State University, USSR.

Studies of photosynthetic membranes and their fragments by advanced spectroscopic techniques (kinetic absorption and luminescence analyses, ESR, NMR, Mossbauer absorption and Rayleigh scattering spectroscopy) and an analysis of the obtained experimental data by applying specially developed theoretical approaches made it possible to obtain for the first time quantitative relationships between the efficiency of individual electron-transport processes of photosynthesis and structural/dynamic parameters of the systems investigated (chloroplasts, bacterial chromatophores, isolated reaction centers).

It is shown that the role of biological membrane-bound macromolecules is not restricted to the formation of static equilibrium configurations, but includes dynamic configurational changes, both spontaneous and induced, through which configurations favorable for electron-exchange interactions are produced.

Friday 03 August Congress Centre-First Floor Posters 223-228

Posters on Mechanisms of Transport Across Membranes

223

Two distinct classes of ATP binding sites in Sarcoplasmic Reticulum Ca-ATPase revealed by fluorescence of TNP-ATP. Dupont, Y., Pougeois, R., Ronjat, M. and Verjovsky-Almeida, S., GPEC, Centre d'Etudes Nucléaire, Grenoble, France
*Department of Biochemistry, UFRJ, Rio de Janeiro, Brazil.

2',3'-O-(2,4,6-trinitrophenyl) adenosine 5' triphosphate (TNP-ATP) binds with high affinity to the SR Ca-ATPase ($K_d = 50$ to 150 nM). The number of binding sites which was found (around 7 nmol/mg) is compatible with one single site per 110 kDalton. Competition between TNP-ATP and ATP was measured in the absence of calcium by following the TNP-ATP fluorescence. It was found that TNP-ATP and ATP competitively bind to two classes of sites of equal concentrations (3.5 nmol/mg). ATP dissociation constants were evaluated from the amplitude of the chase of TNP-ATP by ATP. In the absence of Mg^{2+} (independently of pH) or at acid pH (independently of Mg^{2+} concentration) the nucleotide sites behave like one single family of sites of intermediate affinity ($K_d = 20$ μ M). They become splitted into two classes of sites of high (2 μ M) and low affinity (> 500 μ M) at pH values higher than neutral and in the presence of Mg^{2+} . The calcium activated ATP hydrolysis shows a complex sensitivity to these derivatives with one inhibitory and one activating component, the latter being specific of TNP-ATP (or TNP-AMPPNP) but absent for TNP-ADP. Each of these components is in competition with ATP. This demonstrates that the two ATP sites are interacting, the hydrolytic activity of the high affinity ATP binding site being activated by ATP (or TNP-ATP) binding in the low affinity ATP binding site.

225

WATER AND PROTON PERMEABILITIES ACROSS MEMBRANES. Pitterich, H. and Lawaczek, R., Inst. of Phys. Chem., Univ. of Würzburg, Marcusstr. 9/11, D-8700 Würzburg

Passive proton translocation across membranes may be coupled to the existence of intralamellar "water-wires". We have therefore studied the permeation of water and protons, both under identical conditions, across lecithin bilayers and erythrocyte ghost membranes.

The water permeation was measured by our probe free method as the D_{2O}/H_2O exchange relaxation rate. The technique (Biophys. J. 45:491 (1984)) is based on the different indices of refraction of H_2O and D_2O . The proton permeation is monitored by intracellular pH dependent probe molecules in the same set of experiments in which the water permeation is measured; the reduction of an induced pH asymmetry across the membranes is followed. The fluorescence or absorption signal is first converted to a proton concentration before permeability coefficients are calculated.

For lecithin vesicles below the phase transition temperature (T_c) the permeation of protons and of H_2O/D_2O is equivalent. Both processes become faster above T_c . Membranes of erythrocyte ghosts are significantly more permeable to water molecules than to protons. The results for lecithin bilayers are consistent with a Grothus-like mechanism, especially in the ordered state. However, the low proton permeabilities compared with the high values for water in membranes of erythrocyte ghosts do not favor longlived and/or ordered "water-wires" as proton channels in biological membranes.

227

DISCONTINUOUS TEMPERATURE DEPENDENCE OF WATER TRANSPORT IN GIANT ALGAL CELLS

R. Srećić, P.B. Andjus, and D. Vučelić, Institute of General and Physical Chemistry Belgrade University; Department of Physical Chemistry, Faculty of Natural Sciences and Mathematics, Belgrade University, Studentski trg, Belgrade, Yugoslavia

A new NMR method was applied to the measurement of water efflux (half-time, $T_{1/2}$) in giant intermodal cells of Chara gymnophylla. The method is based on the dynamical suppression of intracellular 1H signal using a $(\pi-\tau-\pi/2-T)$ pulse sequence and D_2O as the extracellular fluid, with dextrane magnetite as the relaxation agent. Thus, only the extracellular 1H signal rise has been monitored. A detailed exploration of the $T_{1/2}$ temperature dependence revealed a temperature independent region between $19-29^\circ C$ ($T_{1/2} = 22.9 \pm 0.6$ s) and two distinct peaks at $12^\circ C$ (115 ± 14 s) and $30^\circ C$ (154 ± 8 s). Measurements of D_2O efflux by means of an analogous experimental procedure showed no large discontinuities with temperature. It has been shown that abrupt changes of $T_{1/2}$ with temperature disappear in the presence of 10 or 100 mM KCl , while this thermal behaviour remains unaffected by 1 mM KCl . Temperature dependence of the resting potential in *C. gymnophylla* cells showed also abrupt depolarising changes at 15 and $30^\circ C$. The exposure of cells to D_2O elicits an action potential followed by depolarisation; in contrast, such changes do not occur when "deuterated" cells are returned to APW. Although our temperature dependence studies reveal a close connection between water transport and membrane potential (as well as protoplasmic streaming above $30^\circ C$), the mechanism of the described thermal behaviour of water transport remains to be elucidated.

224

CONJOINT ENHANCEMENT OF LEAK PERMEABILITY AND TRANSBILAYER MOBILITY OF PHOSPHOLIPIDS IN CHEMICALLY OR PHYSICALLY PERTURBED ERYTHROCYTE MEMBRANES

B. Deuticke, C.W.M. Haest, K.B. Heller, Department of Physiology, RWTH Aachen, Pauwelsstraße, D-5100 Aachen, F.R.G.

Biological membranes as a rule form a tight seal against uncontrolled dissipative fluxes of ions and polar solutes and maintain a low transverse mobility of phospholipids (PL). Both barrier properties are not a mere consequence of the nature of the membrane constituents. Reconstituted lipid/protein membranes in many cases exhibit a high leak permeability and transverse mobility of PL. We have now demonstrated that conjoint increases of leak permeability and transbilayer mobility of PL occur in erythrocytes subjected to membrane perturbations by (a) oxidative stress [diamide, periodate, t-butylhydroperoxide] or (b) dielectric breakdown ($4-12$ kV/cm, $0^\circ C$). These treatments produce leaks reversible by reducing agents (a) or $37^\circ C$ incubation (b). The leaks have the properties of aqueous pores with apparent radii of $0.5 - 0.8$ nm, and a low Q_{10} of permeability ($1.1 - 1.3$). They discriminate ions according to hydrated radii and charge. Transbilayer mobility (flip) of PL, probed by labelled analogues, increases markedly (>100 -fold) in parallel with leak formation, the Q_{10} of enhanced flip being lower than that of the normal flip. Close parallels between the properties of the leaks and the flip sites suggest the same perturbation of the lipid domain or lipid/protein interfaces to be responsible for the two phenomena.

Supported by the Deutsche Forschungsgemeinschaft (SFB 160/C3)

226

INFLUENCE OF MEMBRANE POTENTIAL AND LIPID COMPOSITION ON PASSIVE ION TRANSPORT OF ERYTHROCYTES

I. Bernhardt, A. Erdmann and R. Glaser, Department of Biophysics, Humboldt-University, Berlin, GDR

The dependence of the rate constant of Rb^{+} -86 efflux of erythrocytes of various mammalian species on extracellular cation concentration was measured. At low ionic strengths Rb^{+} efflux increases strongly e.g. in human erythrocytes whereas bovine erythrocytes show no significant increase under the same condition. The transmembrane potential (measurement of Cl-36 distribution) as well as surface potential (measurement of electrophoretic mobility) are similar for both species. Therefore the membrane potential difference is not solely responsible for the increase of the Rb^{+} efflux in solution of low ionic strength. Erythrocytes from newborn calves show the same increase of the rate constant of Rb^{+} efflux in solution of low ionic strength as human erythrocytes. The increase depends on the age of the calves and correlates with the content of arachidonic acid (decreases with age) and linoleic acid (increases with age). Investigations with Furosemide, Quinine and without external potassium have proved that the increase of Rb^{+} efflux at low ionic strengths can not be explained on the basis of the Ca^{2+} -stimulated $K^{+}(Rb^{+})$ efflux and/or the Na^{+}, K^{+} co-transport mechanism.

228

Friday 03 August Congress Centre-First Floor Posters 229-234

Posters on Mechanisms of Transport Across Membranes

229

230

231

232

233

234

Friday 03 August Congress Centre-First Floor Posters 235-240

Posters on Mechanisms of Transport Across Membranes

235

236

237

238

239

240

Friday 03 August Congress Centre-First Floor Posters 241-246

Posters on Mechanisms of Transport Across Membranes

241

242

243

244

245

246

311

Friday 03 August Congress Centre-First Floor Posters 247-252

Posters on Food Biophysics

247

QUATERNARY STRUCTURES OF 11S GLOBULINS FROM SOYA AND PEA
M J Miles, V J Morris, D J Wright
AFRC Food Research Institute, Colney Lane, Norwich, UK.
C Nave

SERC Daresbury Laboratory, Daresbury, Warrington, UK.

Proteins extracted from soya beans and peas can be used as protein sources in human nutrition. The production of foods based on these proteins depends on the functional properties of the proteins. Many functional properties of globular proteins are determined by their three-dimensional structure. Small-angle X-ray scattering (SAXS) studies from dilute solutions of 11S globulins from soya and pea have been used to gain information on their quaternary structures. Parameters such as radius of gyration and molecular weight can be derived directly from the scattering curves, but more detailed information has been obtained by comparison of the details of the experimental scattering curves with scattering curves calculated for various models taken together with the corresponding measured and calculated values of the sedimentation and diffusion coefficients. Most measurements have been made using a conventional X-ray generator and a Kratky camera, however, recent measurements using the high-intensity Daresbury synchrotron source have revealed further details in the scattering curve at high angles. This improved resolution appears to stem from reduced aggregation and/or denaturation of the proteins resulting from the much reduced exposure times.

249

STRUCTURE FORMATION/GELATION OF AQUEOUS DISPERSIONS
G.J. Brownsey, AFRC Food Research Institute, Colney Lane, Norwich, U.K.

The network structure supported by thermally and chemically set polysaccharide gels is investigated by a range of compressive and shear techniques. This rheological characterisation of alginates and carrageenan has been extended to synthetic dispersions of microcrystalline cellulose as used in low calorie foods. The dispersions display many of the properties of the pre-gel state. They are both shear and shear rate dependent. The temporal viscoelastic response obeys power law relationship, with a critical concentration of 0.7%. Above this value, yield values are concentration dependent and the dynamic response inversely proportional to shear rate. Theories of cooperative flow and that of elastic floc formation indicate a weak structure whose development is shear history dependent. The gelled state is characterised by a frequency dependent modulus with creep and stress relaxation studies determining a variable coordination number in flow.

251

ON THE STATE OF WATER IN MAIZE SEED EMBRYO
G. Bačić, R. Srejić and S. Ratković, Dept. Phys. Chem., Faculty of Sciences, University of Belgrade and Maize Research Institute, Zemun - Belgrade, Yugoslavia.

Several physicochemical techniques (NMR, DSC, TGA, IR) were applied to seeds of the two genotypes of maize (M64A + and M64A 0₂) equilibrated at several relative humidities (RH = 0-0.65) in order to define the state of water in the seed embryo. The experiments suggest the presence of at least three types of water. The main fraction of water (I), which is in communication with environment (RH dependent), can be easily exchanged with D₂O or removed by standard drying at 378 K. NMR spin-spin relaxation time (T₂) of this water is positively correlated to its amount. All techniques applied have proved the existence of some additional fractions of water (II and III) which are not removed by conventional drying (e.g. two additional peaks in DTA and TGA). This water is not dependent of RH and differs for two genotypes. The experiments with defatted embryos proved that none of water fractions can be associated with lipids. The proton NMR signal of fractions II and III interferes with the signal of solid matrix (T₂ = 7 μs) and can be discriminated by successive drying at temperatures above 443 K. This water is most probably tightly bound to macromolecules (proteins, carbohydrates) and is "responsible" for seed viability.

248

GELATION AND RETROGRADATION OF STARCH
M J Miles, V J Morris, P D Orford, S G Ring
AFRC Food Research Institute, Colney Lane, Norwich, UK.

Starch is the major storage polysaccharide of higher plants where it occurs as starch granules. Two polysaccharides called amylose and amylopectin may be extracted from the granules. The roles played by these two polymers in the gelation and retrogradation of starch has been examined by biophysical methods. The formation of an opaque thermo-irreversible gel has been shown to be dominated by the gelation of amylose. The 'amylopectin granules' are considered to act as porous fillers reinforcing the amylose gel network. Long term storage results in an increase in 'stiffness' of the gels. This thermo-reversible change has been shown to involve crystallisation of amylopectin within the granules. Such crystallisation is believed to increase the rigidity of the granules enhancing reinforcement of the amylose gel.

250

THE INTERACTION OF CALCIUM PHOSPHATE AND PHOSPHOPROTEIN IN BOVINE CASEIN MICELLES. C. Holt and D.T. Davies, The Hannah Research Institute, Ayr, KA6 5HL.

Although mM calcium ion concentrations can cause casein to aggregate extensively, in the native casein micelle, calcium phosphate also occurs and could act as a cementing agent. Indeed, it has been suggested, from an EMAS study of micellar calcium phosphate, that the phosphate moiety of the phosphoserine residues in the caseins are incorporated in the calcium phosphate lattice, so anchoring the caseins in the micelle.

To examine the relative importance of calcium ion concentration and calcium phosphate-phosphoprotein interactions in maintaining micelle structure, milk was dialyzed against various buffers. When buffers with a range of free calcium ion concentrations, but saturated with calcium phosphate and having a constant pH, free magnesium ion concentration, ionic strength and osmotic pressure were used, micelles were found to dissociate to only a limited degree even at the lowest free calcium ion concentration studied (0.6mM). With a phosphate-free buffer, however, micelles dissociated progressively, even though the free calcium ion concentration was held at 7mM, once the micellar calcium phosphate was reduced to about 60% of its initial value. Moreover, the K- and B-caseins dissociated more readily than the more highly phosphorylated α₂-casein, which in turn dissociated more readily than the most highly phosphorylated α₂-caseins. It appears therefore that the calcium phosphate-phosphoprotein interaction is more important than free calcium ion concentration in maintaining micelle structure.

252

SALT INDUCED STRUCTURAL CHANGES IN MEAT
P. Wilding, N. Hedges and P.J. Lillford, Unilever Research, Colworth House, Sharnbrook, Bedford, UK.

The effect of hypertonic salt solutions on meat fibres has been studied as a function of post-mortem storage. Rabbit longissimus dorsi fibres (after about 20 hours post mortem storage at 4°C), were found to swell in hypertonic salt solutions to 2 to 3 times their original diameter. This swelling occurred in the fibre transverse plane only. X-ray diffraction shows swelling occurs by a combination of an increase in the myofibrillar lattice spacing, and a loss of myofibrillar order. Fibre swelling is highly cooperative. At pHs below the meat pI, hypertonic salt solutions induce fibre shrinkage.

Post-mortem storage had a pronounced effect on the response of meat fibre to either 0.25M KI or 0.64M KI.

The post-mortem time course of response shows a peak at 18-35 hours bounded by period of minimal or zero response. We propose that the collagenous endomyosial sheath acts as a restraint to myofibril swelling and that the characteristics of post-mortem swelling are a balance of the myofibrillar propensity to swell and the constraint of the endomyosium.

Friday 03 August Congress Centre-First Floor Posters 253-258

Posters on Food Biophysics

253

A STUDY OF DILATATION AND ACOUSTIC PROPAGATION IN CRYSTALLISING OILS,
M.J.W. Povey, Procter Department of Food Science,
University of Leeds, Leeds, UK.

The derivation of the relationship between acoustic and volume dilatations presented here is based on studies of seismic propagation by Kuster and Toksoz, who include in their theory acoustic propagation in a fluid matrix containing solid inclusions, as a special case. The relationship takes the form

$$(1-\alpha v/v^*)^2 = (1-\epsilon K)(1+\epsilon R)/(1-\epsilon R)$$

where I call the quantity $\alpha v/v^*$, the acoustic dilatation: v^* is the effective acoustic velocity; $\alpha v/v^* = v/v^* - v$ where v is the compressional wave velocity in the liquid matrix; ϵ is the volume fraction of solid; R and K are dimensionless quantities which depend on the densities and compressibilities, respectively, of both phases. The relationship holds in the long wavelength limit and has been verified experimentally for a range of oils and tristearin, diluted with triolein. The solid content never exceeded 15%. 5 MHz, pulsed ultrasonics were used to measure acoustic velocity and dilatometry was used to determine ϵ . I anticipate that this theory may permit the application of acoustics to the measurement of solid content and compressibilities in crystallising systems such as oils and am presently extending this work to solid contents exceeding 15% and the study of phase transformations in crystallising triglyceride mixtures. Extension of this method to a solid matrix containing gaseous inclusions is also being studied.

255

A TURBIDIMETRIC METHOD FOR THE DETERMINATION OF THE REFRACTIVE INDEX OF CASEIN MICELLES M.C.A. Griffin and W.G. Griffin, NIRD, Shinfield, Reading, UK, and EMRI, Brunel University, Runnymede, Egham, UK.

A contrast variation method which is derived from Rayleigh-Gans-Debye theory for determining the refractive index of colloidal particles by turbidimetry is examined. It is found numerically to apply to Mie particles in the range $|\alpha - 1| < 0.40$. Experiments using polystyrene latices of various sizes and colloidal silica show that approximate turbidities measured in a conventional spectrophotometer suffice to give a true estimate of the particle refractive index. Measurement of the refractive index of casein micelles of bovine milk by this method gives a value of 1.570 ± 0.005 . This will have application in the interpretation of light scattering studies on the structure of the casein micelle.

257

THE INFLUENCE OF PROCESSING ON THE STRUCTURE OF MAIZE
P E Brenner, P Richmond and A C Smith, Food Res. Inst., Colney Lane, Norwich, UK.

The extrusion cooking process has rapidly developed in recent years for the continuous cooking of a wide range of food materials, particularly cereals. The cooking extruder subjects the material to a complex history which depends on the path traversed by each food element. In a typical extruder the material undergoes high temperatures (up to 200°C) high pressures (up to 2000 p.s.i.) and ill-defined high, transient local stresses, strains and strain rates in a time of 30-90 seconds. In a typical process the cereal is conveyed as a solid powder which is transformed into a viscous dough. The viscous dough may be expanded on exit from the extruder die as a result of the release of superheated water. The structural transformations in maize and maize starch are examined as a function of passage down the extruder barrel using scanning electron microscopy. The aqueous dispersion rheology of raw, semi-cooked and extruded maize is examined under a number of extrusion conditions. The viscosity is examined as a function of shear rate and of heat treatment of the dispersion. While the raw maize dispersion exhibits a transition from shear thickening to shear thinning behaviour on heat treatment the extruded maize dispersion is almost Newtonian before and after heat treatment. The results are interpreted in terms of starch gelatinisation and breakdown and also solubility phenomena. The results of these experiments provide an insight into the interaction of extruded cereals and starches with water as appropriate to the production of instant foods.

254

COMPARISON OF THE RHEOLOGICAL PROPERTIES OF AQUEOUS DISPERSIONS OF STARCH GRANULES FROM WHEAT AND MAIZE.

S.G. Waight, P. Bowler, R.A. Marsh and D.A. Jarvis, Biomolecular Sciences Department, RHM Research Ltd., High Wycombe, Bucks. U.K.

The rheological properties of aqueous dispersions of wheat and maize starches were studied using a range of measuring techniques. Gelatinisation (the loss of molecular order within the granule and subsequent dissolution/dispersion of granules in water) was investigated with an oscillatory shear rheometer using parallel plate configuration. Retrogradation of gelatinised, cooled dispersions was studied by measuring the changes in shear modulus (G) using a pulse shearometer, and gel strengths were measured using a compression test.

The rheological properties exhibited by wheat and maize starches during gelatinisation suggest that maize starch is more fully dispersed than wheat starch under the test conditions. Differences in the extents and rates of retrogradation measured by shear modulus and gel compression studies also support this interpretation.

256

NONINVASIVE PHOSPHORUS-31 NMR STUDIES OF METABOLITES IN MEAT,
P. Lundberg and H.J. Vogel, Dept. Physical Chemistry 2, Univ. of Lund, Sweden and S. Fabiansson, E. Tornberg and H. Ruderus, Swedish Meat Research Institute, Kävlinge, Sweden.

The metabolism of phosphorylated compounds in meat samples from cow, pig and lamb was studied noninvasively by ^{31}P NMR during 10 hours after slaughter. During post mortem metabolism phosphocreatine and ATP disappeared. Sugarphosphates (mainly glucose-6-P, fructose-6-P and glyceral-3-P) remained relatively constant and inorganic phosphate (P_i) was continuously formed. The intracellular pH as deduced from the chemical shifts of P_i and G-6-P decreased from 7 to 5.7.

The ATP content plotted as a function of pH showed a linear relationship. When the NMR results were compared with those obtained using routine methods for determining pH and metabolism levels a good quantitative agreement was found. The rate of post mortem metabolism decreased in the following order pig > lamb > cow. Bovine samples frozen in liquid N_2 15 min. after slaughter displayed a 10 times faster post mortem metabolism during thawing. Moreover, low-voltage electrical stimulation of bovine samples resulted in a somewhat increased rate as compared to controls. We conclude that noninvasive ^{31}P NMR provides a useful complement to existing methods for studying post mortem metabolism in samples from slaughter carcasses.

258

PARTICLE SIZE DISTRIBUTIONS IN SOYA BEAN OIL EMULSIONS
M.M. Robins and A.R. Mackie, AFRC Food Research Institute, Colney Lane, Norwich, Norfolk, UK.

Droplet size distributions of 25% soya bean oil emulsions containing emulsifier (Tween 60) and stabiliser (propylene glycol alginate) have been measured using a Malvern 2300 Pulse Particle Sizer. Initially a comparison was made between the Malvern sizer and a Coulter Counter TALL. Four emulsions were measured by both techniques with particle sizes ranging from 0.5 to 10 μm . The distributions obtained from the two instruments were not significantly different. Experiments were carried out on two emulsions, containing 0.5% and 0.05% Tween 60, in addition to 1% propylene glycol alginate. The emulsions were produced on a laboratory scale two-stage valve homogeniser, at total pressures 1000, 3000 and 5000 psi, with one or two passes at each pressure. The initial mean volume/surface diameter of the droplets depended on (pressure) $^{-0.6}$ only at the higher emulsifier concentration. At 0.05% Tween 60 the particle size increased with pressure. These emulsions were unstable, and the change in size distribution over a period of 3 months was measured. The emulsions containing 0.5% Tween 60 showed little change in particle size over this period.

Friday 03 August Congress Centre-First Floor Posters 259-264

Posters on Food Biophysics

259

STRUCTURE OF CONCENTRATED WHEAT STARCH GELS
D.A.Jarvis, I.S.Besford and R.A.Marsh, The
Lord Rank Research Centre, Lincoln Road,
High Wycombe, Bucks, HP12 3QR, England.
Combined measurements of crystallinity and
gel modulus have been made on concentrated wheat
starch gels (starch concentration varying
between 38% and 54%) to provide information about
the structural changes which occur on ageing.
DSC was used to follow the development of
crystallinity, and a mechanical spectrometer was
used to measure the increase in shear modulus.
Storage temperatures of 4°C and 21°C were
considered.

Results obtained show that for a given gel
the rate of increase in gel modulus is different
from the rate of development of crystallinity.
The dependence of gel modulus on starch concen-
tration is also found to be different from that
of crystallinity. These results are considered
in terms of a structural model for concentrated
starch gels.

Results on the effect of storage temperature
demonstrate that the structure which develops in
a gel stored at 4°C is different from that
which develops at 21°C.

260

261

262

263

264

Friday 03 August Congress Centre-First Floor Posters 265-270

Posters on NMR in Vivo

265

³¹P-NMR OF CANINE SALIVARY GLAND M. Murakami, H. Mori, T. Nakahara, Y. Imai, Y. Seo* and H. Watari** Dept. Physiol., Osaka Med. Coll., Takatsuki 569, Japan, *Dept. Physiol., Kyoto Pref. Univ. Med., Kyoto 604, Japan and **Dept. of Mol. Physiol., Natl. Inst. Physiol. Sci., Kazaki 444, Japan. Canine submandibular glands secrete large amounts of saliva after chorda stimulation and simultaneously heat production is elevated. In order to study the kinetics of phosphorus compounds in epithelial transport, we applied the topical magnetic resonance (TMR) to living canine submandibular gland and the conventional NMR to the extracted one which was set in a NMR sample tube (30 mm diameter) with perfusion by Ringer solution. Phosphorus compounds in the gland were assigned, and phosphorus compounds and pH were determined during anoxia resulting from stopping the flow of blood to the gland or the perfusion fluid, and also during secretion induced by acetylcholine. When the blood flow or the perfusion of the gland was stopped, the tissue contents of ATP and creatine phosphate decreased and that of ADP increased, and tissue pH decrease. Restarting blood flow or perfusion after 10 minutes of anoxia led to recoveries of the tissue content of the phosphorus compounds and tissue pH to normal. Acetylcholine administration (10^{-6} M in perfusate or blood) induced secretion of saliva, decreased the level of creatine phosphate. When Na ion was replaced by Li ion in perfusate a little salivation was observed.

267 ORAL PRESENTATION

³¹P ROTATING FRAME NMR IMAGING USING TWO SURFACE COILS A. Haase, Max-Planck-Institut für biophysikalische Chemie POSTfach 2841, D-3400 Göttingen, W.-Germany.

Rotating frame imaging (RFI) can be easily modified to allow chemical shift imaging. The technique has been applied using the natural radio-frequency gradients of a surface coil (1). Applications of this method for in vivo NMR studies are limited due to the three-dimensional radio-frequency gradient of a surface coil (2). Using two surface coils, the problem can be solved. Two orientations of the coils have been investigated in detail:

a) Two coplanar surface coils with one large surface coil transmitter and one small surface coil receiver. With this arrangement one-dimensional "imaging" of high-resolution NMR-spectra is possible.

b) Two orthogonal surface coils with both coils as transmitters and one coil as receiver. The technique is a two-dimensional chemical shift imaging technique. The corresponding multiple-coil NMR probe has to be magnetically decoupled. A new decoupling scheme will be presented in detail. Both methods have been demonstrated on phantoms, containing inorganic phosphate, phosphocreatine and ATP.

(1) A. Haase, C. Malloy, G.K. Radda, J. Magn. Res. **55**, 164 (1983)

(2) A. Haase, W. Hönke, J. Frahm, J. Magn. Res. **56**, 401 (1984)

269

INFLUENCE OF MANGANOUS ION ON ³¹P NMR SPECTRA OF HUMAN ERYTHROCYTE SUSPENSIONS. A. Omachi, Dept. of Physiology and Biophysics, Univ. of Illinois at Chicago, P.O. Box 6998, Chicago, IL 60680, U.S.A.

The influence of increasing MnCl₂ concentration on the broadening of extra- and intracellular ³¹P NMR signals of erythrocyte (RBC) suspensions was investigated. When spectra of 0.164 KCl solutions containing 10mM methyl phosphonate (MeP) and 5mM P_i were acquired with the one-pulse method, MeP and P_i signals were no longer evident at 10^{-4} and 10^{-3} M MnCl₂, respectively. With a spin-echo technique, MeP and P_i signals disappeared at 10^{-5} and 10^{-4} M MnCl₂. The same results with respect to MeP were obtained with a deoxygenated RBC suspension in Ringer's medium. Thus, a slightly lower concentration of paramagnetic relaxation agent eliminates extracellular MeP signals recorded with the spin-echo procedure, allowing a little longer period of observation of intracellular signals before significant amounts of Mn²⁺ enter the cells. The areas of 2,3-diphosphoglycerate (DPG) signals obtained with the spin-echo method were markedly reduced after 60 min of incubation with 10^{-4} and 10^{-3} M MnCl₂ no significant change was observed in the one-pulse experiment. This difference is ascribed to the spin-echo results being associated with free DPG molecules, whereas the one-pulse data relates to the entire DPG population, including a significant portion bound to deoxyhemoglobin in these experiments. 10^{-4} M MnCl₂ with spin-echo recording appears useful in monitoring intracellular RBC signals, as noted by a linear rise of MeP signals in the absence of significant change in DPG.

266

NMR STUDIES OF THE PROTEOLIPID (OCCD-BINDING PROTEIN) OF E. COLI

J. Boyd, J.A. Carver, I.D. Campbell, P.T. Jones and M.F. Moody; Biochemistry Department, Oxford University, U.K. and European Molecular Biology Laboratory, Heidelberg, W.Germany.

The proteolipid subunit of the ATP synthase complex is soluble in chloroform-methanol. Using new methods for handling this protein, satisfactory ¹H spectra have been obtained, and the effects of varying solvent composition, pH, salt concentration (LiCl), water content and temperature have been investigated. Several amino-acid residues have been assigned from these experiments, and from COSY and NOESY spectra. Many of the NH groups appear to form part of alpha-helices. Lanthanide shift probes have given some preliminary information about proximity relationships.

268

PARAMETERS INFLUENCING PCr/P_i VALUES IN NORMAL AND GENETICALLY DEFICIENT HUMANS

J. S. Leigh, Jr. and B. Chance Dept. of Biochemistry/Biophysics, Univ. of Penna, Phila., PA 19104

³¹P NMR of arms and limbs (1) has identified limits to the "phosphate potential" (PCr/P_i) between >10 at rest (state 4) down to approx. 1 in exercise and more recently to 0.2 in steady state exercise of a highly trained athlete. Simple equations describe the whole work-rate P_i/PCr profile. Profiles of lower slope and maxima are characteristic of untrained conditions. Further performance degradation occurs in peripheral vascular disease. In the latter case evaluation of oxidative metabolism is made directly by recovery times following a maximal exercise bout with maximal recovery times of 10-20 min due to limited oxygen delivery to tissue. Here a good correlation of NMR recovery times and severity of disease as evaluated by doppler flow and angiography is obtained. In cases of genetic disease, for example cytochrome b deficiency of skeletal tissue, recovery times of 20 min were observed suggesting that a 20 min recovery time in a skeletal tissue is near the survival limit. In the cytochrome b deficient case, bypass of the deficient site by menadione and ascorbate caused a 10-20 fold decrease of recovery time with remarkable increases of functional activity (2).

1) Chance, B et al (1981) FNAS (USA) 78:6714-6718

2) Eleff, S. et al (1982) PNAS (USA) (in press, 6/84)

Grant Support: HL31934

270 ORAL PRESENTATION

NMR RELAXATION OF SODIUM AND POTASSIUM IONS IN LIVING SYSTEMS G. Navon and H. Shinar, Department of Chemistry, Tel-Aviv University, 69978 Ramat Aviv, Israel

NMR relaxation rates of Na⁺ and K⁺ ions in mammalian and avian erythrocytes were investigated using recently discovered NMR shift reagents for these ions. As expected, the decay curves of the transverse magnetizations could be separated into two components, while the longitudinal magnetizations decayed as single exponents. Typical values for T₂-23 relaxation times in human and dog erythrocytes are T₁=25ms, T₂=21ms and T₂ρ=6ms. They are independent of storage time in spite of the concomitant increase of the intracellular Na⁺/K⁺ ratio. Very similar values of the relaxation times were obtained in dog erythrocytes which contain high concentrations of Na⁺ ions. The temperature dependencies of the relaxation times indicate fast exchange between free and bound ions. K-39 relaxation times are quite similar to those of Na-23. By investigating the separate contributions to relaxation of the different intracellular components we may presently eliminate the binding to the inner side of the erythrocyte membrane and the binding to hemoglobin as significant sources of relaxation. In avian erythrocytes, which are known to contain nuclei, the relaxation times of sodium are significantly shorter than those in mammalian erythrocytes and increase with storage. Our preliminary measurements in serum points to serum albumin as the major source of sodium relaxation. The elucidation of the relaxation mechanisms of alkali metal ions in living systems may provide a new probe for following normal and pathological states of living cells.

Friday 03 August Congress Centre-First Floor Posters 271-276

Posters on NMR in Vivo

271

¹³C NMR AS DIAGNOSTIC TOOL FOR THE CHARACTERIZATION OF ENZYMIC BLOCKS IN MUTANTS OF THE FUNGUS *ASPERGILLUS NIDULANS*. C. Dijkema, H.G.M. Kester and J. Visser. Dept. of Molecular Physics and Genetics of the Agricultural University, Wageningen, the Netherlands.

Mutants of the filamentous fungus *A. nidulans* with wellknown or less defined genetic defects in their carbohydrate metabolism, have been compared with the wild-type, grown under identical conditions. In the case of the *pdh-C* mutant (defective in the α -component of the pyruvate dehydrogenase complex), the contrast in ¹³C label distribution with wild-type after incubation with ¹³C-enriched glucose is very obvious, even for very low substrate levels. The ¹³C label predominantly enters into alanine via transamination of the accumulated pyruvate; no enrichment in TCA-cycle related compounds is observed. In the case of the *pyc*-mutant (defective in pyruvate carboxylase activity), the contrast with wild-type is less pronounced at least for low substrate levels and short incubation times. For longer incubation times and higher substrate levels, the contrast becomes more pronounced as shown by exhaustion of the pools of TCA-cycle related compounds in the case of the *pyc*-mutant. The *pppA* mutant (defective in the EMP-pathway, lacking transaldolase activity) can be grown on glucose. Under those conditions there is no contrast with the wild-type. However, upon incubation of the mycelium with xylose, xylitol can still be observed as an intermediate, both in wild-type and mutant, but in the mutant a still unknown compound is accumulated which is not further metabolized. The nature of this compound is under investigation.

273

31-P NMR STUDY ON FRIEND ERYTHROLEUKEMIA CELLS (FLC) IN VITRO AND IN VIVO. F. Podo, G. Carpinelli, M. Di Vito, E. Proietti, S. Gessani and F. Belardelli, Istituto Superiore di Sanità, Rome, Italy.

A 31-P NMR study was carried out on FLC induced to undergo erythroid differentiation *in vitro*. Significant levels of glycerophosphorylcholine (GPC), glycerophosphorylethanolamine (GPE) and phosphorylcholine (PhC) were identified in untreated cells and their PCA extracts. In FLC treated 4 days with either dimethylsulfoxide (DMSO) or hexamethylenbisacetamide (HMB), the intracellular concentration of PhC was markedly increased and that of GPC reduced, HMB being more effective in producing this effect. 31-P NMR analysis of freshly dissected tumors determined by s.c. inoculation of FLC in syngenic mice, showed that during tumor growth: 1) GPC and GPE levels and the ratio GPC/PhC significantly increase; 2) the intracellular pH decreases. Preliminary studies on tumors treated *in vivo* with either X-rays or interferon (IFN) indicated that during IFN-induced regression of the tumors the levels of GPC and PhC are markedly decreased and the intracellular pH is maintained at physiological values. Such effects are not found in tumors treated with X-rays. Although the biochemical role of GPC and PhC is still unclear, their modulations observed during either erythroid differentiation or tumor growth or regression suggest the hypothesis that these events involve modifications of the regulatory mechanisms controlling biosynthesis and catabolism of phospholipids.

275

272

31P Creatine Phosphate in Disassociated Fetal Rat Brain and N1E 115 Neuroblastoma Cells; P. Glynn, S. Ogawa, and T.M. Lee, AT&T Bell Laboratories; R. Chappell, Hunter College, NY; Z. Ahmed, Univ. of Iowa.

ATP and creatine phosphate levels have been studied in disassociated rat brain cells and undifferentiated neuroblastoma N1E 115 cells using NMR spectroscopy. No detectable creatine phosphate was found in N1E 115 cells grown in DMEM plus 10% FBS, although there were high levels of ATP. Disassociated rat brain cells from 16-day fetuses cultured for 30 days *in vitro* with completely defined medium yielded 70% neuronal cells which showed only a small amount of creatine phosphate. In comparison, the levels in perfused and intact brains consistently show values in the same range of ATP concentration under normal aerobic conditions. When the medium for both cell systems was supplemented with 10mM creatine, the phosphocreatine levels rose to better than twice the level of ATP. When they were subsequently subjected to ischemic shock the ATP levels remained constant until the phosphocreatine vanished, and then they decreased. In intact brain experiments it has not been possible to assign the source of phosphocreatine to a cell type but the experiments on cultured cells demonstrate the existence of phosphocreatine in neuronal-type cells and show phosphocreatine level to be a good monitor of the energy state of the cells.

274

276

Friday 03 August Congress Centre-First Floor Posters 277-282

Posters on Medical Imaging

277 ORAL PRESENTATION

A NEW IMAGING BLOCK FOR BODY CAVITIES

P. Greguss, Applied Biophysics Lab., Technical University Budapest, Krusper u. 2-4, Budapest, Hungary

Biological and/or medical images, when not represented as cross sections or projections, are in general guided by a display system, called Central Convergent Perspective (CCP), used because it can fool the eye of the observer by creating the sensation of depth. In this paper a new system of perspective, the Flat Cylinder Perspective (FCP) will be developed; it will be argued it captures more adequately than CCP the range and geometric nature of a cylindrical image volumesuch as of a body cavity. The unique feature of FCP images is that it develops the totality of the surrounding visual space at once, in contrast to a CCP image which does it only successively in discrete chunks. As a consequence, the ringshaped FCP image has a horizontal viewing angle of 360°, while the width of the ring is equal to the vertical viewing angle of the imaging block. Radial lines in the annular image represent vertical field angles, and the concentric rings represent varying horizontal field angles at constant vertical field angles. Our imaging block, capable of producing in real time FCP images, consists of aspheric refracting and reflecting surfaces, and can be miniaturized to a degree suitable for endoscopic purposes. Its resolution is comparable to that of conventional endoscopes.

279 ORAL PRESENTATION

ALGORITHMIC ANALYSIS AND VISUAL TEMPORAL PRESENTATION OF ON-LINE INTRAPARTUM DATA

S.S.Arora, R.J. Parsons, and I.D. Cooke, Department of Obstetrics and Gynaecology, Univ. of Sheffield, U.K.

On-line real time analysis of the fetal heart rate (FHR) and the intrauterine pressure (IUP) signals of parturient women was achieved on PDP-8 computer. Various algorithms for data acquisition, storing, filtering, analysing, condensing, display and archiving were developed in assembly language compatible with RLS-8 system. Seven hypotheses were formulated in order to correlate fetal heart function in utero to neonatal outcome measured in terms of Apgar score. Linear and multiple regression analysis of the data with Variance and F-distribution techniques revealed the utility of such analysis. Fetal hypoxic insults due to uterine contractions can be quantified by FHR decelerations. FHR patterns during labour exhibit the fetal tissue oxygenation reserves. Fetal distress becomes predictable. Three dimensional plots between the basal heart rate, deceleration areas and the duration in labour were demonstrative of such portraiture in the critical obstetrical situations. A novel display based on Lissajous patterns was achieved for deriving a temporal relationship between FHR and IUP signals acquired. It was reckoned an information rich, easy clinical utility. Further simulation studies are attempted.

281

278

ENZYMATIC ACTIVITY OF *E. histolytica*

E. Jimenez-Cardoso, E. Recinos and J. Kumate, Lab. Immunoparasitology, Hospital Infantil de México, México, D.F. Div. Inmunología, IMSS Centro Médico Nacional México, D.F.

If we take into consideration that México is one of the countries where amebiasis is one of the most important health problems, the enzymatic study of the different strains of *E. histolytica* offers a special interest for us. Since the basal lamina of the intestinal epithelium is made up of collagen, the different collagenolytic activity of the strains studied will indicate degrees of pathogenicity. The collagenase activity in these strains of *E. histolytica* was investigated; two of them were obtained from asymptomatic carriers and the third from a patient with amebic colitis; the purpose was to determine, if there were any differences present that would allow their classification according to their enzymatic activity.

Method.- The percentage of hydrolysis on type I and III collagen obtained from small intestine was measured applying the method modified by Rodking, where the results showed differences at short periods of incubation. Likewise, the collagenolytic activity of the three strains was measured with respect to number of trophozoites where a direct relationship of hydrolysis resulted with respect to this parameter. Besides, the hydrolysis products obtained from the three strains were determined showing quite important differences that suggest an explanation to the different degree of pathogenicity present in them.

280

282

Notes

A – Z Index of Presenting Authors

Aasa R.	131	Blomberg C.	55	Chuaqui C. A.	76	Donner K.	225
Abd El-Baset M. S	130	Blumenthal R.	59	Chung A. E.	145	Duchohier H.	275
Abdel Kerim F. M	240	Boelens R.	71	Church A. K.	132	Duee E.	60
Adams P. A.	134	Boffi A.	46	Claessens F.	118	Dupont Y.	308
Adelman M. R.	212	Bolouri B.	218	Clark A. D.	296		
Adler-Nissen J.	187	Bolscher B. G. J	135	Clark D. C.	213		
Agnew W. S.	271	Book J.	280	Clark J. T.	215		
Ahlstrom P.	50	Borst-Pauwels G. W. F.	290	Clauwaert J.	126		
Aihara K.	80	Bose S.	147	Clore G. M.	121	E	
Al-Sharckly M -AS.	307	Bouloussa O.	303	Coakley W. T.	218	Easton D. M.	274
Albertini G.	239	Bourdeaux M.	153	Coan C.	300	Easwaran K. R. K.	291
Allewell N.	68	Box H. C.	243	Coe E. L.	59	Eberle H. I.	126
Almers W.	278	Bradshaw J.	144	Coe T. J.	77	Ebert G.	57
Alvaggi M.	135	Bramhall J. S.	297	Cohen F. S.	296	Edman A.	277
Amin M.	202	Braun W.	62	Colbeck H.	232	Ehrenberg B.	223
Anbar M.	106	Brauner T.	288	Coletta M.	85	Eikenberry E. F.	143
Andjus P. R.	308	Braunlin W. H.	136	Colombello G.	274	Eisenberg H.	44
Angelides K.	172	Bray R. P.	54	Colombini M.	271	Eisinger J.	87
Antonov V. F.	251	Briggs F. N.	291	Coltelli P.	233	El Gohary M. I.	209
Aoki I.	239	Brill A. S.	59	Complani M.	57	El Messierey M. A.	223
Aoki I.	155	Brochon J. C.	229	Congiu-Castellano A.	228	Eliopoulos E. E.	158
chiga H	225	Broek D.	143	Conti F.	278	Elliott G. F.	75
Arnott S.	26	Brown D. T.	139	Cooke R.	105	Einumr T.	157
Arora S. S.	317	Brown H. M.	226	Cooper S.	61	Endo S.	237
Artymuk P. J	68	Brownsey G. J.	312	Correia M.	84	Engel J.	41
Asakura S.	224	Brunoni M.	52	Cox T. C.	302	Engelborghs Y.	213
Ascenzi P.	70	Bruschi M.	135	Craescu C. T.	299	Eras S.	66
Ascoli F.	52	Bryszewska M.	213	Crane-Robinson C.	43	Erru G.	154
Atkins E. D. T.	102	Buchert J. M.	237	Creighton T. E.	165	Esipova N. G.	142
Avison M. J	302	Budd G. C.	233	Crowthor R. A.	168	Eskelsen S.	86
Ayamami J.	234	Bullard B.	198	Cserhati T.	290	Espel E.	45
Azuma K.	224	Burattini E.	228	Cuniberti C.	125	Estes J. E.	211
		Burchfield D. M	204	Cupane A.	63	Etchebest C.	302
		Burley S. K.	243	Czege J.	300	Evans E. H.	243
		Burma D. P.	46			Evans E. W.	187
		Burnham C. E.	294			Evans P. A.	60
B		Burt J. M.	294			Evans S. T.	61
		Busscher H. J	242	D			
Bacic G.	312			D'Alagni M.	294		
Balasubramanian D	44			Dadlez M.	50	F	
Balbi C.	45			Dagher G.	301		
Baldwin R. L.	67			Dalglish D. G.	102	Fadel M. A.	241
Ball Jr. W. J	302	C		Dalvit C.	53	Fakhry A. A.	240
Ballini J. P.	228			Dalzoppo D.	60	Fanneau J.	150
Banerjee A.	117	Cabiaux V.	303	Danfelsen C. C.	144	Farmer M. C.	134
Barber J.	181	Caiafa P.	42	Darszon A.	289	Faruqi A. R.	230
Barbi M.	307	Campos J. L.	129	Datema K. P.	157	Feeney J.	77
Barlow D. J.	76	Canessa M.	307	Davies R. J. H.	120	Fetelson J.	66
Barman T. E.	205	Capel M. S.	125	De Felice L. J.	280	Felsenfeld G.	99
Baskin R. J	206	Carbone E.	272	De Haan R. L.	281	Fernandez J. M.	279
Baum J.	58	Cardinaud R.	201	De Meis L.	95	Ferreira A. T.	295
Baylor D. A.	253	Carrascosa J. L.	169	De Mello P.	43	Ferrone F. A.	57
Beall P. T.	301	Carnier D.	158	De Weer P.	292	Fetsova Z. G.	150
Beatlie D. S.	136	Carnier W. L.	155	Deamer D. W.	291	Fettplace R.	254
Bechet J. J	202	Casadrio R.	149	Debrunner P. G.	130	Fink A. L.	60
Beddell C. R.	77	Casali E.	271	Decker H.	212	Fink R. H. A.	198
Belleslin B. B.	274	Casas-Finet J. R.	124	Deinum J.	214	Finkelstein A.	197
Bellelli A.	46	Cassidy M. M.	212	Detimer J. W.	273	Fisher M. T.	49
Benbasat J. A.	115	Cavalie A.	278	Dekleva N.	142	Fishman H. M.	275
Benga Gh.	305	Cavatorta P.	115	Delay M.	200	Fontana A.	54
Beratan D. N	136	Cavazza B.	44	Deleers M.	217	Forbush III B.	299
Berendsen H. J. C	251	Cemenikic D.	299	Delapierre M.	75	Forsen S.	202
Bernhardt I.	308	Champeil P.	288	Demiroglou A.	49	Forsyth V. T.	121
Berovic N.	199	Chance B.	131	Demsar F.	50	Fort L.	152
Berriman J. A.	129	Chandani B.	66	Deuticke B.	308	Foster R.	152
Bers D. M	220	Charkviani G. G.	208	Diaz E.	280	Fourme R.	256
Borthel-Colominas C	78	Charney E.	119	Diaz-Calavia E. J	237	Fowler A. G.	205
Bertrand E.	125	Chay T. R.	82	Dickerson E. E.	130	Franca F. C.	282
Bessonov B. I.	285	Chazin W. J.	64	Dickinson E.	102	Frank J.	167
Beth A. H.	214	Chazotte B.	133	Diedenchs K.	152	Franks F.	39
Bezanilla F.	21	Cheng J. J.	226	Dietler G.	157		63
Bianconi A.	228	Cheung H. C.	201	Dijkema G.	316	Frazier P. J.	173
Bicknell-Brown E.	209	Cheung S.	126	Dilger J. P.	276	Friedani C.	224
Bilski R.	243	Chiancone E.	52	Dinno M. A.	219	Frey M.	133
Bittar E. E.	288	Chiang C.	302	Dionne V. z.	274	Friedman J. E.	276
Blake C. C. F	190	Chirien-Kovacs E.	288	Dismukes G. C.	147	Fuchs F.	204
Blake R. D.	47	Chignell C. F.	131	Doglia S.	81	Fujiyoshi Y.	127
Blange T.	209	Chiu W.	236	Dolci S.	273	Fuller W.	122
Blanschard J. M. V.	102	Chothia C.	164	Donath E.	221		
Blau L.	289	Christoph G. W	60				

G		Hama-Inaba H.	218	Jacrot B.	79	Krolenko S. A.	209
Gabr S.	240	Hamaguchi K.	52		112	Kruse J.	79
Gadsby D. C.	295	Hammond S. J.	63	Jaffe L. A.	264	Kuhn H.	255
Gal V.	213	Hansford R. G.	159	Jalcnen T. O.	272	Kunisawa T.	271
Gambale F.	277	Hanson M.	156	Jamakovsmanovic A.	240	Kuriyan J.	71
Garay R.	306	Hard T.	155	Jarvis D. A.	314	Kurtz P. J.	85
Garcia-Inguez L.	230	Harries J. E.	228	Jaskowski J.	217	Kusumi A.	86
Gary-Bobo C.	305	Harris W. C.	155	Jenkins J. A.	299	Kusunoki M.	147
Gause jr. G. G.	48	Hartsef S. C.	293	Jennissen H. P.	53	Kuwata K.	64
Gavilanes M.	289	Hashimoto M.	220	Jeremic M.	219		
Gbordzoe M. K.	216	Hasnain S. S.	257	Jernigan R. L.	72		
Geacintov N. E.	149	Hatta I.	207	Jewell G. G.	173		
George J. S.	223	Hayashi T.	235	Jezowska-		L	
Gershfeld N. L.	296	Haydock C.	57	Trzebiatowska B.	132		
Gershman L. C.	211	Hazlewood C. F.	153	Jimenez-Cardoso E.	317	La Mar G. N.	63
Gerstman B. S.	75	He G. Z.	290	Johnsson A.	225	Lacapere J. J.	303
Gestrelus S.	275	He Z. L.	208	Jones E. Y.	143	Lacombe C.	84
Ghali Y.	153	Heitz F.	277	Jones R. W.	150	Ladislav A.	46
Ghetti F.	224	Helene C.	124	Joshi V. P.	116	Laigle A.	116
Ghomi M.	151	Hellems L.	51	Julesz B.	38	Lai A. A.	211
Giacometti G. M.	51	Hellingwerf K. J.	298	Jung F.	135	Land E. H.	114
Gibbons I. R.	97	Heneine I. F.	156	Junge W.	183	Langridge-Smith J. E.	291
Gibson N. J.	293	Henis Y. I.	87			Larkum A. W. D.	148
Giege R.	34	Henry G. D.	61			Larsson-	
Gierer A.	171	Hermansson A. -M.	173			Raznikiewicz M.	77
Gill S. J.	67	Herve M.	305	K		Laufer M.	223
Ginsburg A.	71	Hess G. P.	298			Laugaa P.	125
Girardet J. L.	42	Hibberd M. G.	204	Kaczmarek L. K.	284	Laustnat G.	83
Glaeser R. M.	236	Higashino S.	279	Kagan B. L.	299	Lauterbur P. C.	186
Glaser R.	262	Higuchi H.	201	Kaila K.	224	Lawaczcek R.	308
Glushko V.	288	Hinton J. F.	274	Kaijyama H.	205	Lazic V.	239
Glynn I. M.	94	Hinz H. -J.	121	Kalinowski H. J.	130	Le Doan T.	297
Glynn P.	316	Hisae N.	244	Kaminsky Y. G.	159	Lecomte J. T. J.	63
Go N.	58	Ho J. T.	157	Kanai K.	281	Leibl W.	56
Godt R. E.	207	Hodge A. J.	212	Kanehisa M.	47	Leigh Jr J. S.	315
Gogelein H.	298	Hoebcke J.	215	Kantcheva M. R.	244	Lenci F.	225
Goldanski V. I.	53	Hofer E.	281	Kapp O. H.	234	Leng M.	118
	178	Hofrichter J.	52	Kappl R.	62	Leonard K.	235
Goldman A.	56	Holt C.	312	Kaptein R.	35	Lessier M. A.	143
Goldman L.	279	Hombie F.	282	Karlsson R.	133	Letellier L.	305
Goldman Y. E.	104	Hopkins R. C.	119	Karpfel Z.	230	Leupin W.	116
Gomez-Lojero C. C.	146	Horn R.	276	Karplus M.	179	Levi R.	277
Gonzalez-Halphen D.	146	Howell P. L.	68	Kasai M.	278	Levinson B. L.	289
Goormaghtigh E.	137	Hu K. S.	293	Kaupp U. B.	223	Lewis M. L.	85
Gordon A. M.	202	Huang L.	153	Kawai K.	65	Lewis S. A.	300
Grabarek Z.	205	Huang L. Y. M.	279	Kawai M.	206	Lewit-Bentley A.	128
Grandjean J.	306	Huat P.	130	Kayushin L. P.	132	Lieberman E. M.	292
Granero-Porati M. I.	46	Hubbard S. R.	231	Kelderling T. A.	66	Liljenstrom H.	47
Granzler H. L. M.	201	Hudson B. D.	76	Keilmann F.	240	Lin C. I.	209
Grasdalen H.	141	Hul S. W.	219	Kell M. J.	278	Lin G. D.	231
Graslund A.	242	Hulmes D. J. S.	144	Kellenberger E.	265	Lin J. Y.	139
Gray D. M.	118	Hunt G. R. A.	292	Kennard O.	56	Lin K. C.	86
Gray H. B.	192	Hunter M.	283	Kenney L. J.	297	Lindblom G.	156
Gray I.	241	Hurstel S.	290	Keser-Stankovic M.	238	Lindley B. D.	201
Green N. M.	61	Huxley H. E.	103	Keszenman D.	239	Lipscomb J. D.	133
Green W. N.	275	Hwang J. C.	198	Kida K.	66	Lis L. J.	160
Greene R. V.	303	Hyono A.	290	Kidokoro S.	65	Littlechild J. A.	127
Greenstock C. L.	70			Kidric J.	159	Llerenas E.	213
Greguss P.	317			Kihara H.	229	Lohmann W.	298
Greve J.	43			Klein B. K.	120	Lopez-Cabarcos E.	289
Griffin M. C. A.	313	I		Kneale G. G.	128	Louro S. R. W.	137
Grigera J. R.	56	Ianzini F.	84	Ko W. C.	217	Loveless R. W.	140
Grigorenko E. V.	220	Ikai A.	47	Koch K. W.	225	Lu Z.	216
Gronenborn A. M.	122	Ince C.	277	Koeppel II R. E.	273	Lundberg P.	313
Gross D.	291	Inouyo H.	65	Koetzle T. F.	244	Lynch III C.	206
Gruol D. L.	277	Isachsen S.	158	Kohlma.er G. H.	269	Lyng R.	155
Guggino W. B.	304	Ishizaka S.	234	Kolaskar A. S.	55		
Gutierrez P. L.	158	Koller Th.	100	Kolfer Th.	100		
Gydikov A. A.	281	Israelachvili J. N.	261	Kolomytkin O. V.	304		
		Ito M.	37	Kootsey J. M.	296	M	
		Ivanitsky G. R.	78	Kopvillem U.	152		
			234	Korn A. P.	127	Mabbutt B. C.	70
		Ivanov A.	148	Kostyuk P. G.	273	MacDonald R. C.	306
H		Ivanov V. I.	29	Kotlyk A.	301	MacDonald R. I.	83
				Kovarsky V. A.	80	Macgregor Jr. R. B.	124
Haas E.	63			Kozlov Y. P.	151	Maeda H.	154
Haase A.	315	J		Kramer I.	218	Magura I. S.	271
Hagerman P. J.	121			Kremer F.	238	Mahendrasingam A.	121
Hajdu J.	231			Kress M.	89	Maiti M.	115
Hallam L. R.	122	Jameson D. M.	229	Krinsky V. I.	191	Malumder K.	11

Malak H.	137	N		Pavlic M. R.	55	Rodriguez R.	46
Maleev V. Ya.	119			Pavlovic M. R.	154	Roe J. H.	125
Malmstrom B. G.	193	Nabedryk E.	149	Payne K. J.	143	Rogers N. K.	75
Malnic G.	295	Nagaoka S.	65	Pecar S.	301	Rohrer H.	267
Mandelkow E.	229	Nagayama K.	130	Pedemonte C. H.	304	Romero I.	146
Mandelkow E. M.	234	Nagy B.	205	Peerce B. E.	306	Roos K. P.	200
Mangal P. C.	219	Nagy K.	276	Pelly K. C. M.	231	Rosemeyer M. A.	214
Mani R. S.	68	Nahvi M. J.	160	Peres A.	221	Rosenberg N. L.	44
Manser E. J.	214	Nakamura H.	75	Perkins S. J.	141	Rosi A.	221
Marchetti C.	279	Nakamura T. J.	54	Pessen H.	57	Ross-Murphy S. B.	102
Margineanu D. G.	291	Nakas M.	240	Petersson L.	134	Rousseau D. L.	134
Maringelli M.	221	Nakata K.	127	Pfeil W.	69	Roux M.	292
Markov M. S.	220	Nakata Y.	300	Pichon Y.	283	Rowe A. J.	203
Markus M.	80	Nakaya S.	54	Pickar A. D.	295	Rubin A. B.	307
Marsh R. A.	187	Nall B. T.	64	Pieroni O.	226	Russu I. M.	154
	313	Nascimento O. R.	69	Pifat G.	157	Rustichelli F.	153
Martin D.	283	Navon G.	315	Pinkney M.	127	Ruterjans H.	125
Martinez del Pozo A.	142	Naylor A. G.	173	Plesser Th.	80	Rydgqvist B.	227
Martins O. B.	295	Nedbal L.	149	Poddar R. K.	115		
Martonosi A.	235	Nedeljkov V.	305	Podgornik R.	216		
Mas-Oliva J.	307	Neumann J. M.	120	Podo F.	316		
Mascarenhas S.	107	Nicholls P.	137	Podolsky R. J.	203	S	
Masotti L.	83	Nikandrov V. N.	66	Poerio E.	70	Sachse J. H.	87
Massey J. B.	297	Nishikawa K.	47	Poglitsch A.	53	Sackmann E.	152
Masurovsky E. B.	213	Norby J. G.	108	Poole P. L.	68	Saha N. N.	152
Matejevic D. R.	154	Nordenskiold L.	50	Popot J. L.	51	Sakmann B.	16
Matsuda T.	200	Nordh J.	214	Porali A.	242	Salama G.	284
Matsumoto G.	279	Norman A.	241	Post C. B.	61	Salanki J.	239
Matsushima N.	142	North A. C. T.	109	Potschka M.	212	Sallesse C.	224
Matthew J. B.	126	Ntsoh Y.	301	Poulsen F. M.	59	Samosudova N. V.	212
Matthews B. W.	33	Notani N. K.	238	Povey M. J. W.	313	Samraoui B.	230
Maughan D.	232	Nothig-Laslo V.	156	Powers L.	130	Sandblom J.	280
McCray J. A.	204	Nouailhetas V. L. A.	295	Prass W.	294	Sanders D.	299
McCubbin W. D.	198	Nowaira N. H.	142	Preteasa E. A.	49	Sanderson M. R.	127
McDermott E. E.	187	Nunes E.	239	Preston B. N.	81	Sanyal N. K.	116
McGavin S.	118	Nunes M. A.	302	Privalov P. L.	270	Sasmto T.	72
McIntosh D. B.	294	Nunn B. J.	226	Prosser V.	116	Satterlee J. D.	132
McLaughlin P. J.	230			Przestalski S.	220	Savage H.	50
McNamara G. R.	234			Ptak M.	297	Schaefer J.	24
Mendelsohn R.	87			Purslow P. P.	173	Schatz G. H.	149
Menestrina G.	284	O				Schauer P.	42
Merola F.	231					Scheek R. M.	71
Metselaar J. W.	208	O'Brien E. J.	204	Q		Scheraga H. A.	70
Michaelis L.	288	O'Neil R. G.	296			Scherz A.	147
Michailov M. Ch.	282	Obaid A. L.	232	Quinta-Ferreira M. E.	207	Scheuer T.	203
Mikhov D. M.	238	Offer G. W.	30			Schleser G. H.	242
Mikkelsen A.	87	Ogata H.	52	R		Schmahl G.	258
Milanick M. A.	303	Ogura S.	67			Schnapl J. L.	227
Miles M. J.	312	Ohno S.	189			Schnarr M.	126
Miller A.	39	Ohsaku M.	144			Schoot B. M.	120
Millington P. F.	145	Okamoto Y.	207			Schreibmayer W.	284
Mill's P.	120	Omachi A.	315			Schuster P.	188
Mishra R. K.	81	Onuchic J. N.	136			Schwister K.	218
Mita D. G.	305	Oslis W. G.	242			Scott G. M. M.	211
Mitchinson C.	62	Osmanovic S. S.	281			Scriven D. R. L.	273
Mitraki A.	58	Ostashevsky J. Y.	62			Seeman N. C.	121
Mitsui T.	206	Otsuka J.	129			Segawa S.	53
Miyazawa S.	56					Segovic-Mihailovic R.	232
Mizraji E.	129	P				Selkov E. E.	170
Mohan R.	76					Sellers P.	133
Mohraz M.	235	Pace R. J.	292			Sentjurc M.	305
Monaselidze J. R.	42	Padron R.	199			Setif P.	150
Monen A. S.	219	Pain R. H.	70			Shaeffer J. R.	56
Montenay-Garestier T.	126	Pal S. G.	198			Shafer R. H.	119
Monticelli G.	282	Palmieri F.	93			Shakke Z.	27
Montreuil J.	196	Pant H. C.	280			Shalitin C.	44
Moody M. F.	315	Pantazopoulou M.	159			Shaw P. J.	235
Moran F.	64	Paoli G.	151			Sheetz M. P.	260
Moreno Diaz R.	237	Papp E.	219			Shelnblatt M.	55
Morikawa K.	128	Parker M. W.	229			Shelling J. G.	134
Morris E. P.	214	Parkhurst L. J.	131			Shelnuitt J. A.	132
Morris V. J.	187	Parry D. A. D.	211			Shen J. X.	241
Mozhayeva G. N.	285	Parson W. W.	182			Sherman W. V.	67
Mrevlishvili G. M.	49	Pasquali F.	306			Shi Y. Y.	63
Muhamad M. A.	81	Passarelli V.	241			Shigemi J.	64
Muller U. R.	115	Pasynkov A. S.	221			Shimizu T.	134
Muller W.	283	Patel D. J.	28			Shimoyama Y.	84
Murakami M.	315	Pattanayek R. R.	159			Shimuta S. I.	293
Muszkat K. A.	49						
Mutet C.	290						

Shin Y. A.	115	Takeda Y.	117	Vincent J. S.	156	Yeagle P. L.	86
Shirakihara Y.	158	Tamm L. K.	86	Vincze J.	47	Yeh Y.	139
Shoemaker D G	303	Tamura Y	200	Vistnes A. I.	156	Yellen G.	275
Shoham M	135	Tanaka M.	238	Vliegenthart J. F. G.	194	Yew F. H	43
Shulman R. G.	23	Tanaka Y.	51	Vogel H.	281	Ygge B	155
Sigworth F. J.	22	Tanford C.	244	Vogel W.	282	Yoshino S.	200
Silva J. L.	306	Taniguchi K.	301	Von Tscharner V.	293	Yu L. C	201
Simonovic B.	51	Taniguchi M.	230	Vovelle F	43	Yutani K.	67
Simons K	113	Tank D W.	157	Vucelic V.	51		
Singh B B	216	Tanner M. J. A.	92				
Sixl F.	159	Tardieu A.	229				
Sizer P. J.	78	Tauc P.	55				
Sjodin R. A.	158	Taylor R. E	275				
Skalak R.	259	Taylor W. R	58				
Slavik J	304	Teeter M M	58				
Smejtek P.	242	Teissie J.	220				
Smidsrod O	195	Terner J.	131				
Smith A. C.	313	Thakur A. R	116				
Smith J	69	Thomas N.	206				
Sogami M.	64	Thompson T. E.	140				
Somiylo A. P	266	Thornhill R. A.	203				
Somorjai R. L.	61	Thyberg P.	154				
Soto M. A.	48	Ti Tien H.	218				
Sparrow R. W	150	Tiede D. M	148				
Spohn K. H.	50	Tigyri J.	296				
Spruce A. E.	272	Timasheff S. N	98				
Stafford W. F	208	Timmins P. A.	78				
Standen N. B	276	Todorov I. N.	151				
Starc V.	203	Tolgyesi F.	216				
Staros J. V	292	Tomasevic M. N	147				
Staynov D.	45	Torchia D. A.	144				
Stein P. G.	284	Tornberg E.	102				
Stellwagen E.	62	Torok A.	208				
Stellwagen N. C	217	Traub W.	40				
Stephens N. L.	199	Trefiletti V.	45				
Stern M. S.	54	Tregear R. T.	202				
Stevens C. F	20	Tripsa M.	298				
Stevens E. S	139	Tsou C. L.	136				
Stienen G. J. M	204	Tsuda M.	226				
Stockwell J.	69	Tuchsen E.	71				
Stokke B. T.	140	Turin L.	304				
Stoylov S. P.	221						
Strankfeld I. G	208						
Strassburger W	59						
Strauss G.	217						
Strazhevskaya N. B	42						
Strom R.	283						
Struzinsky R	223						
Stuart D. I.	68						
Stubbs M. T	79						
Su J. Y.	199						
Suarez G.	228						
Subirana J. A.	44						
Suck D.	128						
Suda H.	202						
Sugi H.	207						
Susi H.	69						
Sussman F.	77						
Sutton B. J	139						
Suyama A.	118						
Suzic S.	232						
Suzuki S.	200						
Svendsen K. H	142						
Svensson B.	140						
Sybesma C.	110						
Sykes B. D	135						
Symons M.	146						
Szabo A.	54						
Szabo A. G.	85						
Szlachcic A.	238						
						</	

OYEZ SCIENTIFIC AND TECHNICAL SERVICES LTD

MEETINGS AND NEWSLETTERS

FIRST EUROPEAN SEMINAR & EXHIBITION ON COMPUTER-AIDED MOLECULAR DESIGN 18th/19th October 1984, London

The design of molecular structures has been revolutionised by recent advances in computer graphics. Organised in association with the Molecular Graphics Society, this seminar will review the state of the art in design principles and update delegates in contemporary hardware and software. The meeting is aimed at research workers in biochemistry, biophysics, chemistry, crystallography, molecular biology, pharmaceutical research, polymer science and quantum chemistry, and hardware and software suppliers.

EXHIBITION: Delegates will receive hands-on experience from a number of exhibitors using a VAX 750 computer to demonstrate their software systems.

FEES: A special reduced rate will be available for academics.

For further details, please complete the form below.

BIOTECHNOLOGY BULLETIN REPORTS

Two BIOTECHNOLOGY BULLETIN REPORTS are published each month, providing up-to-date, in-depth analysis of the activities and future plans of those who operate at the cutting edge of biotechnology.

Based on personal interviews with key personnel, BIOTECHNOLOGY BULLETIN REPORTS offer a well-researched, reliable assessment of a leading company, research organisation or research topic. Read by many leading European, Japanese and US companies, our Reports give essential briefing in the fast-changing field of Biotechnology.

Subscription Rate: £48 per year (24 Reports), post free.

For further details, please complete the form below.

BIOTECHNOLOGY BULLETIN

An essential information source covering the key developments in one of the world's most rapidly emerging technologies.

Biotechnology is an intensely competitive field — but the potential rewards are enormous for those who can keep abreast of the opportunities as they arise. BIOTECHNOLOGY BULLETIN is an established and authoritative newsletter providing up-to-the-minute information for anyone in the field — whether involved in research, production, investment, marketing or regulation. Published every month throughout the year, BIOTECHNOLOGY BULLETIN presents a thorough briefing on developments at home and abroad. Succinct, itemised features cover new products and processes, investment potential, Government policies, company briefs, market news and R & D developments.

Subscription Rate: £90 per year, post free.

For further details, please complete the form below.

INTERNATIONAL CONFERENCE ON INVESTMENT IN BIOTECHNOLOGY 1st/2nd November 1984, London

This conference will focus on how investment has gone into biotechnology in the last few years and where the best opportunities are for investment over the next few years. An international panel of speakers ranging from venture capital companies, multi-nationals, specialist biotechnology companies to engineering contractors from the USA, UK, Australia, Sweden and Denmark will lead the conference, designed for investors, bankers, scientists and financial analysts.

For further details, please complete the form below.

For further details on any of the above please tick the appropriate box and return the completed form to

Oyez Scientific & Technical Services Ltd., Bath House, 56 Holborn Viaduct, London EC1A 2EX, UK.
(Tel: 01-236 4080)

☐ First European Seminar & Exhibition on Computer-Aided Molecular Design

☐ International Conference on Investment in Biotechnology

☐ Biotechnology Bulletin

☐ Biotechnology Bulletin Reports

Name

Position

Organisation

Address

Satellite Meetings In Bristol

In Vivo Biochemistry Workshop

Saturday 04 August

Organisers

B. Chance
Dept. of Biochemistry and Biophysics
University of Pennsylvania
Philadelphia
USA

D.R. Wilkie
Dept. of Physiology
University College London
Gower Street
London
United Kingdom

Venue

Holiday Inn
Lower Castle Street
Bristol
United Kingdom

Registration

Fees: There will be no registration fee.

Morning coffee, afternoon tea and a light lunch will be provided.

Procedure: To be advised. Details will be published on the notice board on the ground floor of the Congress Centre.

Programme

An informal meeting on Magnetic Resonance Techniques applied to the study of intact organs of humans and animals. A panel of speakers will be selected for a series of 20 minute presentations. Voluntary contributions, either as posters or oral presentations will be welcomed and fitted into the programme as may be possible. Details of the programme will be published on the notice board in the Congress Centre when the list of participants is known.

09.30 - 10.00

Morning coffee and introductions

10.00 - 13.00

Exercise Performance Evaluation by Phosphorous NMR, Vascular Disease and Studies of Genetic Deficiencies with Developments of Therapies using Phosphorous NMR

Chairman: B. Chance (Pennsylvania)

Speakers: To be selected.

14.00 - 17.00

Studies of Neonates and Animal Models, with particular emphasis on Carbon and Sodium Studies as well as Phosphorous, and Technological Aspects of In Vivo NMR such as signal to noise ratio, probe design and data analysis

Chairman: D.R. Wilkie (London)

Speakers: To be selected.

Satellite Meetings In Bristol

Symposium on New Methods in X-Ray Absorption, Scattering and Diffraction for Applications in Structural Biology.

**Sunday 05 August
and
Monday 06 August**

Organiser

H.D. Bartunik
European Molecular Biology Laboratory
c/o Desy
Notkestrasse 85
2000 Hamburg 52
F.R.G.

Registration

Fees: Delegates £20.00, Students and Postdoctoral workers £10.00. The fees include tea and coffee, lunch on Sunday and Monday and the Symposium dinner on Sunday 05 August. Procedure: To be advised. Details will be published on the notice board on the ground floor of the Congress Centre

Programme:

Sunday 05 August

09 00 - 12 00

X-Ray Absorption

Chairman: B Chance (Pennsylvania)
Speakers: L Powers (A T & T Bell)
A Bianconi (Roma)
J Penner-Hahn (Stanford)
B Chance (Pennsylvania)
D Mills (Cornell)
A Fontaine (Paris)

13 00 - 15 00

Low-Temperature and Time-Resolved Crystallography

Chairman: G.A. Petsko (MIT)
Speakers: H.D. Bartunik (EMBL, Hamburg)
G.A. Petsko (MIT)
K. Moffat (Cornell)

15 15 - 16 30

Time-Resolved Solution Scattering and Fiber Diffraction

Chairman: J. Bordas (Daresbury)
Speakers: J. Bordas (Daresbury)
E. Mandelkow (MPI, Heidelberg)
Y. Maeda (EMBL, Hamburg)
M. Mody (EMBL, Heidelberg)

20 30 - 22 00

Contributed Papers/Poster Discussion

Monday 06 August

09 00 - 10 30

Anomalous Scattering and Diffraction

Chairman: W.A. Hendrickson (Washington)
Speakers: W.A. Hendrickson (Washington)
R. Fourme (Paris)
Z.R. Korszun (Pennsylvania)
H.B. Stuhmann (Mainz)
J.K. Blaisie (Pennsylvania)

11 15 - 12 00 and 13 00 - 16 00

Intense X-Ray Sources / High Count Detection Systems

Chairman: H.E. Huxley (MRC, Cambridge)
Speakers: K.C. Holmes (MPI, Heidelberg)
R.D. Frankel (Rochester)
J.C. Phillips (Brookhaven)
B. Chance (Pennsylvania)
H.E. Huxley (MRC, Cambridge)
V.W. Arndt (MRC, Cambridge)
J. Hendrix (EMBL, Hamburg)
C. Boulton (EMBL, Heidelberg)
G.C. Nicolae (EMBL, Hamburg)

Accommodation

Special arrangements have been made with the Holiday Inn for those attending these meetings, and details of these financially advantageous arrangements can be obtained from the organisers

Further Information

Delegates, who are interested in receiving further information about either Satellite Meeting, should

- 1 Study the notice board and message boxes on the ground floor of the Congress Centre for further details
- 2 Leave their name and telephone number/address while in Bristol with the Congress Scientific Secretariat, in order that they can, if necessary, be contacted by the Organisers of these Satellite Meetings
- 3 Leave a message in the message boxes for one of the Organisers

Congress Exhibitors

Congress Centre - Ground Floor

Monday 30 July - Friday 03 August

09.00 - 17.30

Stand No. 01

Marconi Avionics Limited

Applied Physics Division
Elstree Way
Borehamwood
Hertfordshire WD6 1RX
United Kingdom
Telephone (01) 953 2030
Telex: 22777
Contact John C. Holben

Marconi Avionics has been manufacturing the Elliott range of Rotating Anode Generators for almost twenty years. These generators are used widely in the field of bio-medical research and have achieved a degree of reliability unthought of in the early days of rotating anodes. The current range starts with the GX20, a relatively low cost instrument for microfocus work with a maximum power of 4kW and includes the GX13 which provides 27kW/mm², the highest specific intensity available from a laboratory instrument, and the GX21 which will deliver 15kW into a 10mm x 0.5mm focus.

A Small Angle Scattering Camera is also manufactured which consists of a general purpose camera stand with the choice of three different configurations of X-ray optics offering various angular resolutions. The Small Angle Scattering Camera is complemented by a Linear Position Sensitive Detector which may be used to obtain rapid diffraction profiles in place of the conventional film.

Another item of interest is that there are a number of successful installations operating where the power of the GX21 Rotating Anode Generator has been combined with the sophistication of the Enraf Nonius CAD4 Diffractometer for rapid solution of biological structures. In this area of growing interest, the system is supported by the combined efforts of Marconi Avionics and Enraf Nonius.

Stand No. 02

Nature

Macmillan Journals Limited
Brunel Road
Houndmills
Basingstoke
Hampshire RG21 2XS
United Kingdom
Telephone. (0256) 29242
Telex: 858493
Contact Felicity Parker

For more than a century, Nature has maintained an unrivalled reputation for the speedy publication of new discoveries and "firsts" and it has retained its independence throughout without the support of a society or wider scientific organisation.

Since the very first issue in 1869, the journal has been filled with reports from eminent scientists: in the early years Hooker, Lodge, Fitzgerald and Darwin, and in our own century Chadwick, von Braun, Raman, Baltimore, Watson and Weissman.

Biophysics has always been at the forefront of Nature's articles and editorials. Many of the most important articles on protein structure and muscle, the most significant advances in techniques of image reconstruction (some contributed by Aaron Klug), and many of the key papers on single channel recording from cells (first discovered by B. Sakmann) have been and continue to be published in Nature.

With all this and Nature's special subscription offer to personal subscribers, you surely can't afford not to be a regular reader of the world's leading science weekly.

Come to Stand No. 02 for a free copy, and see for yourself!

Stand No. 03

Bristol Economic Development Board

Council House
College Green
Bristol BS1 5TR
United Kingdom
Telephone: (0272) 291620
Telex: 449714 BRIEDO G
Contact Mike West

Bristol is the regional capital of the south west of England and is one of the most prosperous and thriving cities in the UK. Historically a major seaport and one of the world's great centres for trade and commerce, the twentieth century, and in particular the 1980's, has seen the city developing to keep ahead of the changes in science and technology.

The local economy in Bristol is broad-based. Bristol's approach to all its activities, whether industrial, scientific, cultural, or social, is dynamic.

The city is proud of its heritage. Once the second city in the country, Bristol has an historic legacy and tradition of exploration and of welcoming new ideas and visitors.

It is for this reason that Bristol is equally proud to welcome the 8th International Biophysics Congress to the United Kingdom, and to the city in particular.

Bristol is at the forefront of new developments. It is a city without parallel. Easy communications, whether by road, rail, sea or air make it accessible to all parts of the world.

Equally within the city itself the University, Polytechnic and Colleges carry on the traditions of supplying the region with a skilled workforce well versed in the demands of high technology industry.

The City of Bristol welcomes you and wishes all delegates to the Congress an enjoyable stay in our fine city.

Stand No. 04

MicroCal Inc.

29 Cottage Street
Amherst
Massachusetts 01002 U.S.A.
Telephone 413 549 4641
Contact Linda Witmer

MicroCal is the world's largest supplier of ultrasensitive scanning calorimeters designed specifically to meet the demanding requirements of researchers studying thermal transitions of proteins, polynucleotides, lipids, membranes and other biological materials. The new MC-2 Scanning Calorimeter offers many important advantages over our earlier MC-1 instrument including its much higher sensitivity, greater ease of operation, and option of manual or computerized models. The differential design utilizes matched 1.3 ml cells of the total-fill type with access only through external filling ports. Scan rates are selectable from 10 deg/hr to 90 deg/hr over the temperature range from -20 C to +110 C. The thermopile-driven feedback system provides differential power with a noise level of only 5 microcal/deg and baseline repeatability of 25 microcal/deg.

Utilizing the DA-2 interface-software option in conjunction with an IBM-PC, the MC-2 is converted to digital operation. While maintaining automatic control of the instrument, MicroCal's software provides for visual display of data, dynamic filtering, automatic calibration of the power axis, baseline subtraction, data normalization and manipulation, data storage, ΔH and ΔC_p determinations, curve fitting, deconvolution of overlapping transitions, and continuous-line hardcopy.

Congress Exhibitors

Congress Centre - Ground Floor

Monday 30 July - Friday 03 August

09.00 - 17.30

Stand No. 05

Elsevier Science Publishers B.V.
Biomedical Division
P.O. Box 1527
1000 BM Amsterdam
The Netherlands
Telephone: 020 5803 547
Telex: 18582
Contact: Phyllis Bruin

Elsevier Science Publishers is one of the leading publishers of books, journals and review magazines in the life sciences. Our latest addition to this list is the Journal of Biotechnology which will provide a medium for the rapid publication of full articles and short communications of results obtained from research or various aspects of biotechnology. Other products featured on the Elsevier stand include Biochimica et Biophysica Acta, one of the world's largest biochemical and biophysical journals, Biophysical Chemistry, an international journal devoted to the physical chemistry of biological phenomena, Chemistry and Physics of Lipids, Biophysics, Bio-Engineering and Medical Instrumentation, Advances in Biophysics. Sample copies of these and other Elsevier journals can be requested at our stand.

Stand No. 06

Academic Press Inc.
Orlando
Florida 32887
U.S.A.
Telephone: 305 345 4100
Telex: 568364 ACP ORL
Contact: Kathy Swigart

Academic Press is a leading international publisher of books and journals in the Life and the Medical Sciences, the Physical and the Social Behavioural Sciences.

Academic Press publish over 300 books each year and produce 180 journals worldwide. Grune and Stratton is the rapidly growing medical imprint.

Stand No. 07

Wisepress Book Exhibitions
4 Ashford House
39 High Street
Wimbledon Village
London SW19 5BZ
United Kingdom
Telephone: (01) 947 0927
Contact: Penelope Head

George's Booksellers
89 Park Street
Bristol BS1 5PW
United Kingdom
Telephone: (0272) 276602

Wisepress Book Exhibitions in cooperation with George's Booksellers of Bristol are pleased to present an exhibition of current books and journals concerned with biophysics and related disciplines. All the titles on display can be purchased during the Congress and, if you wish, posted to your home address. A number of publishing houses taking part in the book exhibition have editors and representatives present at the Congress and they can be contacted at the stand.

Stand No. 08

Robbie Charles Duff-Scott
The Flat
82 Alma Road
Clifton
Bristol BS8 2DJ
United Kingdom
Telephone: (0272) 827743
Contact: Robbie Charles Duff-Scott

The artist was born on 1st July 1959 in Bristol. He was educated at Clifton College and then at York University where he read English and Related Literature. He has exhibited works in Bath, at the Royal West of England Academy in Bristol and at the National Portrait Gallery in London.

If the paintings can be labelled with any critical term it is that of romanticism. The works attempt to appeal to our emotions by analogies buried memories and 'the sublime effect of darkness'. The predominance of dark shadows in many of the portraits is a debt to two much admired painters Rembrandt and Caravaggio.

All the portraits are of people Scott is familiar with. The mood of the pictures is grave but they are not intended as images of despair. They are an attempt to show people as sympathetic, warm, lonely but never ridiculous or worthy of dislike. This last credo will dictate the future direction of Scott's painting.

Prints and original works can be purchased during the Congress and despatched to your home.

Stand No. 09

Avon County Council
Planning Department/Economic Development Unit
Avon House North
St James Barton
Bristol BS99 7EU
United Kingdom
Telephone: (0272) 290777
Contact: Bob Williams

Biotechnology has entered a new commercial phase involving multinational grants and small scale start-ups. The County of Avon is in an ideal position to encourage both, with its attractive location and abundant support services.

Success depends more than ever before on close links with academic advance. Within Avon, the University of Bristol has research facilities and projects in its Departments of Biochemistry, Microbiology, Pharmacology and Pathology. Bath University operates South Western Industrial Research Ltd which undertakes contract work in engineering, biology, pharmacy and chemistry. The national Meat Research Institute is based at Langford. Medical services and research in the County's fifty hospitals are of national significance.

Avon lies in the rail/motorway corridor extending westwards from London through Heathrow airport. Already a centre of the British chemical and aviation industries, Avon recently has attracted such high technology enterprises as the Inmos silicon chip company's research, design and administrative HQ and Hewlett Packard's European R&D Centre and production plant for computer peripherals. The Aztec West science park houses ICL, Geac, Digital, Systime and Benson Electronics. British Aerospace has a key satellite development unit in the County.

Congress Exhibitors

Monday 30 July - Friday 03 August

Stand No. 10

The British Biophysical Society

The Society Treasurer
Biophysics Laboratory
Portsmouth Polytechnic
St. Michael's Building
White Swan Road
Portsmouth PO1 2DT
United Kingdom
Telephone: (0705) 827681
Contact: Dr. Henry Rattle

For over 25 years the BBS has provided a unique forum for discussion of the application of physical principles to biological problems. The regular Spring and Winter meetings have been held on topics as diverse as trigger processes in biology, gels and gelation, and low temperature transmission electron microscopy, and are designed to appeal to scientists in academia, industry and medicine. In addition to these main meetings, the Society encourages the organisation of one-day discussion meetings on specialist topics, to which it may make a modest financial contribution. The current membership includes biologists, physicists, chemists, physiologists and biochemists as well as biophysicists and molecular biologists. The Society has always been aware of the importance of biophysics education in the U.K., and continues to pay particular attention to course and career guidance in the subject. It publishes a guide to biophysics courses in the U.K. and also a regularly-updated booklet "Why Biophysics" which is distributed to schools and colleges throughout the country.

The annual subscription of £4 (£2 for bona-fide students) provides reduced registration fees for all Society meetings. Further financial assistance is often available for postgraduates and post-doctoral workers to attend these meetings. A society newsletter is issued several times each year, and carries news and comments as well as announcements of meetings and job vacancies.

Membership application forms are available at the Society's stand at the IUPAB conference, or may be obtained directly from the Society Treasurer. Communications for the Committee should be sent c/o The Biochemical Society, 7 Warwick Court, High Holborn, London.

Stand No. 11

Butterworths

Borough Green
Sevenoaks
Kent TN15 8PH
United Kingdom
Telephone: (0732) 884567
Telex: 95678
Contact: Graham Marshall

Butterworths publish a range of journals and books of interest to Biophysicists and others working in related disciplines.

Key journals include the *International Journal of Biological Macromolecules*. This journal was established to aid communication between the many disciplines involved in all aspects of the structure, function and interaction of biological macromolecules and assemblies.

Biomaterials provides for studies in the physics, chemistry and engineering of materials, diffusion, surfaces and colloids, tissue and blood interactions, toxicology, carcinogenicity, implant design and evaluation.

Cell Biochemistry and Function is the international journal of the function and interaction of cells and organelles, the influence of disease, drugs and other chemicals.

Congress Centre - Ground Floor

09.00 - 17.30

Image and Vision Computing meets the need of researchers and engineers in the growing field of computer-based imaging and vision processing.

The *Journal of Molecular Graphics* assists researchers in using computers to visualize, manipulate and interact with molecular models.

Polymer is the leading international journal for the science and technology of all polymeric materials. *Polymer Communications*, is a new supplement devoted to the rapid publication of short communications.

Vaccine is the international journal for those engaged in the production and use of vaccines.

The Butterworth stand will display and carry stock of the following books:

Handbook of Microscopy;

Eukaryotic Genes;

Polysaccharides in Food;

Electron Transfer Reactions;

Radioisotope Laboratory Techniques.

Stand No. 12

Hi-Tech Scientific Limited

Brunel Road
Salisbury
SP2 7PU
United Kingdom
Telephone: (0722) 20322
Telex: 477877 HITECH G
Contact: David Mitchell

Hi-Tech Scientific Limited are the world's leading manufacturers of Rapid Chemical Kinetic apparatus.

The range of apparatus is continually subject to development to keep ahead in this exciting and rapidly developing field. Hi-Tech Scientific being such a small and versatile company can easily adapt the 'standard' range to manufacture specialist equipment to the individual requirements of the customer.

The product range includes a comprehensive choice of research systems comprising of, the SF-3L support unit with precision thermostating; a choice of 4 modules, either the standard stopped-flow unit, the cryobiochemical stopped-flow unit, the versatile multi-mixing module or the temperature-jump unit, a complete spectrophotometer unit with UV/VIS light sources, monochromator and photomultiplier, all integrated to the Hi-Tech computerised data acquisition and processing unit.

A teaching series is also available covering the three essential kinetic techniques of, stopped-flow, temperature-jump and flash photolysis. Recently introduced is the new and ingenious SFA-11, stopped-flow accessory, which enables previously impractical kinetic experiments to be performed on an existing UV/VIS spectrophotometer or fluorometer.

Recent developments adding to the existing Hi-Tech range are, a high pressure stopped-flow module (capable of up to 1000 bars), a conductivity attachment, or a self contained conductivity unit, a quench flow module and, under development, a rapid scanning monochromator.

Congress Exhibitors

Congress Centre - Ground Floor

Monday 30 July - Friday 03 August

09.00 - 17.30

Stand No. 13

Bio-Logic
Zirst
Chemin Des Prèles
38240
Meylan
France
Telephone: (76) 41 04 72
Contact:
Yves Dupont

Bio-Logic is a young company born in 1983. Located in the suburbs of Grenoble it has a very strong connection with the public research centers of the alpine city. This allows Bio-Logic to benefit from years of experience in high-technology instrumentation and basic research in the following fields
Electrophysiology: Bio-Logic offers the latest developments in the design of micro-probes for intracellular measurements and clamping or of Patch-Clamp technique.

Research Spectrophotometer/fluorimeter: Derived from a laboratory research instrument. Completely modular to match the needs of the user, it offers the highest available stability and sensitivity in light detection.

Rapid Kinetics Systems: The Bio-Logic Stopped-Flow module is the most advanced on the market, syringes are driven by microprocessor controlled stepping-motors. This module has been developed to be fitted with the Bio-Logic Spectrophotometer/fluorimeter, it may be easily adapted for other observation systems.

Rapid Filtration System: A unique patented system which allows filtration to be performed down to the millisecond time scale, an important breakthrough in membrane research and rapid kinetics

Stand No. 14

GCA Corporation
Precision Scientific Group
3737 West Cortland Street
Chicago
Illinois 60647
U.S.A.
Telephone: 312 227 2668
Telex: 4330120
Contact: R. Rhine

The Zimmermann Cell Fusion System on display, electrically fuses cells, including hybridomas for monoclonal antibody production and cells or plant genetics, yeast transformations and other biotechnology and cell research applications. With the Zimmermann Cell Fusion System, cells are exposed to a low level electrical field, orienting the cells end to end. Alignment voltages can be varied from zero to 40 volts at a frequency of 10KHz to 5MHz. The Zimmermann Cell Fusion technique, also called electrofusion, is a patented biotechnology process developed by Dr. Zimmermann and sold under an exclusive license by GCA/Precision Scientific Group worldwide, except for continental Europe

Stand No. 15

Oxford Research Systems Limited
Nuffield Way
Abingdon
Oxfordshire
OX14 1RY
United Kingdom
Telephone: (0235) 32421
Telex: 83356 ORS G
Contact: Randal Rue

Oxford Research Systems is a Company specialising in the development, manufacture, and support of scientific instruments for research in biology and medicine using Nuclear Magnetic Resonance.

In cooperation with the Biochemistry Department of Oxford University, Oxford Research Systems built the first in-vivo NMR spectrometer which was commissioned in 1980. The technique allows the non-invasive chemical study of selected tissues within animals and humans.

The main product is a versatile biomedical NMR spectrometer called BIOSPEC. It is a multi-purpose in-vivo instrument that allows NMR images and chemical spectra to be obtained in the same patient examination

BIOSPEC uses a wide range of horizontal superconducting magnets with diameters between 150mm and 1000mm and field strengths between 1.5 Tesla and 7 Tesla

Oxford Research Systems is now part of Bruker, a European Company that has 25 years experience in NMR spectrometers. Local support is assured through a world wide network of subsidiaries.

The scientists and engineers working at Oxford Research Systems are proud to be providing the instrumentation for the exciting research work in biomedical NMR at many centres including Oxford, London, Yale, California and Detroit

The Congress Centre at a Glance

General

Congress Centre

(City Docks Centre)

Canon's Road

Bristol

will be open

SUNDAY 29 JULY 08.30 hours - 19.00 hours

MONDAY through THURSDAY 08.30 hours - 21.00 hours

FRIDAY 03 AUGUST 08.30 hours - 17.30 hours

These times coincide with the first arrival and last departure, each day, of the Congress shuttle coach service.

Congress Coach Stop

is at the Congress Centre's main entrance on Canon's Road

Car Park on Anchor Road

costs £1.00 per day.

Car Park adjacent to the Congress Centre

is for permit holders only.

Walking to the Symposia Venues

The most picturesque route is along the quayside to the city centre, rather than along Canon's Road.

Congress Secretariat

Registration and Information Desks will be open

SUNDAY through FRIDAY 09.00 hours - 17.30 hours

Congress Exhibition

will be open

MONDAY through FRIDAY 09.00 hours - 17.30 hours

Stand No.

01	Congress Exhibitors
02	Marconi Avionics Limited
03	Nature
04	Bristol Economic Development Board
05	MicroCal Inc
06	Elsevier Science Publishers B.V.
07	Academic Press Inc.
08	Wisepress Book Exhibitions/
09	George's Booksellers
10	Robbie Charles Duff-Scott
11	Avon County Council
12	The British Biophysical Society
13	Butterworths
14	Hi-Tech Scientific Limited
15	Bio-Logic
	GCA Corporation
	Oxford Research Systems Limited

First Floor

Congress Scientific Secretariat

will be open

SUNDAY through FRIDAY 09.00 hours - 17.30 hours

Poster Session Areas

for Posters 001 - 282 on Monday, Tuesday, Thursday and Friday.

Restaurant and Bar

will be open

SUNDAY through FRIDAY 10.00 hours - 17.30 hours

serving tea, coffee and soft drinks. A licence to serve beer and wine throughout this period has been granted by the Justices of the Peace. Light Lunches and speciality afternoon teas will be available.

Toilets

Ground Floor

I.U.P.A.B. Secretariat

will be open at times to be advised - delegates are asked to check the Noticeboard marked "I.U.P.A.B. Announcements." Outside published opening hours, delegates who need to make urgent contact with the Secretary General of I.U.P.A.B. may leave a message with the Congress Secretariat.

Lounge and Quayside Bars

will both be open

SUNDAY 29 JULY 08.30 hours - 19.00 hours

MONDAY through THURSDAY 08.30 hours - 21.00 hours

FRIDAY 03 AUGUST 08.30 hours - 17.30 hours

These times coincide with the opening times of the Congress Centre and with the first arrival and last departure, each day, of the Congress shuttle coach service. The bars will serve tea, coffee and soft drinks throughout these periods, and the Justices of the Peace have granted a licence to operate a full bar service from 10.00 hours every morning until the Congress Centre closes each evening

Fruit and Ice Cream Stall

Message Boxes and Noticeboards

Delegates are encouraged to leave messages in the message boxes and also to routinely check for announcements.

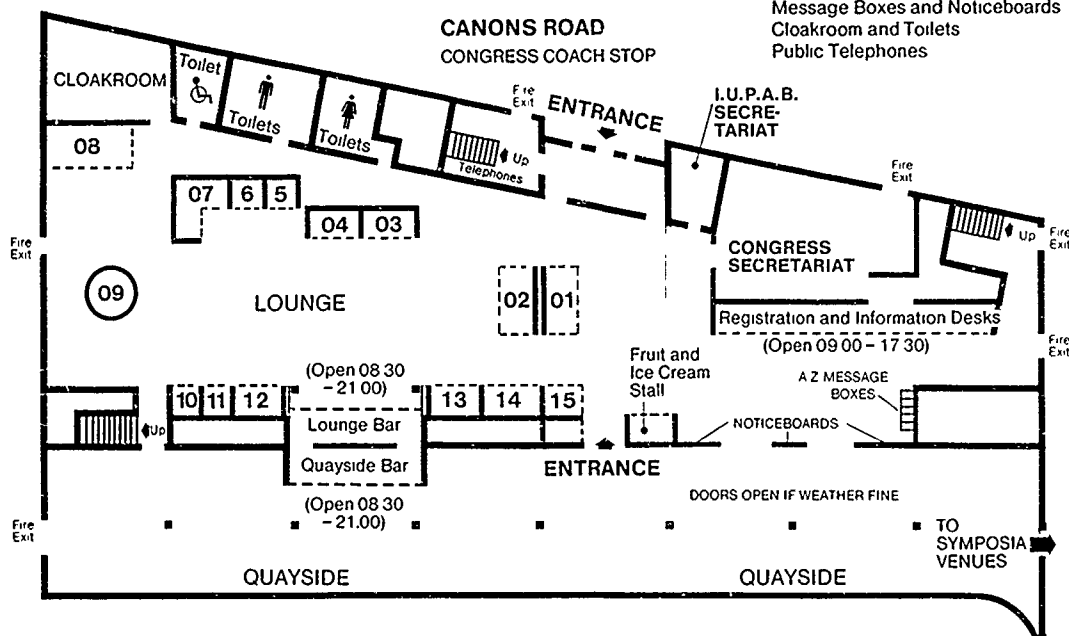
Cloakroom and Toilets

Public Telephones

for outgoing telephone calls only, including flight reconfirmations.

CONGRESS CENTRE
(CITY DOCKS CENTRE) CANONS ROAD, BRISTOL

GROUND FLOOR
I.U.P.A.B. Secretariat
Congress Secretariat
Congress Exhibition
Lounge and Quayside Bars
Fruit and Ice Cream Stall
Message Boxes and Noticeboards
Cloakroom and Toilets
Public Telephones



"FLOATING HARBOUR"

FIRST FLOOR
Congress Scientific Secretariat
Poster Session Areas
Restaurant and Bar
Toilets

